DOE/BC/14434-13
Distribution Category UC-122

DEPOSITIONAL SEQUENCE ANALYSIS AND SEDIMENTOLOGIC MODELING FOR IMPROVED PREDICTION OF PENNSYLVANIAN RESERVOIRS

FINAL REPORT

By
W. Lynn Watney

December 1994

Work Performed Under Contract No. DE-FG22-90BC14434

Prepared for
U.S. Department of Energy
Assistant Secretary for Fossil Energy

Chandra Nautiyal, Project Manager
Bartlesville Project Office
P.O. Box 1398
Bartlesville, OK 74005

Prepared by
Kansas Geological Survey
1930 Constant Avenue, Campus West
Lawrence, KS 66047

MASTER

DISTRIBUTION OF THIS DOCUMENT IS UNLIMITED

DISCLAIMER

This report was prepared as an account of work sponsored by an agency of the United States Government. Neither the United States Government nor any agency thereof, nor any of their employees, make any warranty, express or implied, or assumes any legal liability or responsibility for the accuracy, completeness, or usefulness of any information, apparatus, product, or process disclosed, or represents that its use would not infringe privately owned rights. Reference herein to any specific commercial product, process, or service by trade name, trademark, manufacturer, or otherwise does not necessarily constitute or imply its endorsement, recommendation, or favoring by the United States Government or any agency thereof. The views and opinions of authors expressed herein do not necessarily state or reflect those of the United States Government or any agency thereof.

DISCLAIMER

Portions of this document may be illegible in electronic image products. Images are produced from the best available original document.

TABLE OF CONTENTS

LIST OF FIGURES ix

ABSTRACT 1

EXECUTIVE SUMMARY 2

INTRODUCTION 3
- Significance to DOE Research Plan 3
- Statement of Problem 4
- Research Approach 4
- Summary of Results 5
- Rationale for Study of Lansing-Kansas City Carbonate Reservoirs 9

STRATIGRAPHY OF THE RESERVOIR INTERVAL 12
- Introduction 12
- General Characteristics of Upper Pennsylvanian (Missourian) Stratigraphy 14
  - Pennsylvanian Cyclothems 14
  - Sequence Stratigraphic Components in Pennsylvanian Cyclothems 14
    - Orders of Cycles 15

REGIONAL GEOLOGIC FRAMEWORK 15
- Introduction 15
- Regional Sequence Stratigraphy of the Middle and Upper Pennsylvanian 18
  - Middle to Upper Pennsylvanian Paleogeography 18
  - Evidence of 3rd-Order Depositional Sequences 19
  - Summary of Findings 19
  - Discussion 20
- Stratal Architecture of the Pennsylvanian Kansas Shelf -- A Record of Basement Reactivation 23
  - Longer-term Stratigraphic Intervals 24
    - Base Pennsylvanian to Excello Shale 24
    - Base Pennsylvanian to Base Swope Sequence 24
    - Marmaton 3rd-Order Cycle Excello Shale to Nuyaka Creek Shale 26

Kansas City 3rd-Order Cycle Nuyaka Creek Shale to Muncie Creek Shale 27
Lansing 3rd-Order Cycle 28
Top Lansing to Heebner Shale 29
Lansing to Haskell Isopach 30
Haskell Limestone to Heebner Shale Isopach 30
Fourth-Order Sequences 31
Pleasanton Sequence 32
Hertha Sequence 33
Swope Sequence 34
Dennis Sequence 36
Cherryvale Sequence 38
Dewey Sequence 39
Evidence for Relief on Shelf During Deposition of 4th-Order Sequence 39
Relative Sea Level Curve for Pennsylvanian 40

SUBTASK 1. FIELD SCREENING AND RESERVOIR ANALOGUE IDENTIFICATION 42
1.A. Field Selection 42
Cahoj Field 44
Pen Field 47
Summary of Reservoir Properties 50
Dennis Sequence 50
Cherryvale Sequence 51
Reservoir Parameters 52
Victory Field 53
1.B. Near-surface and Surface Reservoir Analogue Selection 56

SUBTASK 2. DEPOSITIONAL SEQUENCE CHARACTERIZATION 57
2.A. Near-surface and Surface Reservoir Analogues 57
2.A.1. Hertha, Swope, and Dennis Limestone Project 58
Introduction 58
Regional Analog Study 59
Methodology 59
Regional Stratigraphy and Depositional History of Sequences 59
Overview of Depositional Sequences 59
Hertha Sequence 60
Bethany Falls Sequence 62

Mound Valley Sequences 64
Lower Winterset Sequence 65
Detailed Study 67
Methodology 67
Geological Setting 67
Characteristics of Porous Grainstones Within Depositional Sequences 68
Hertha Sequence 68
Bethany Falls and Mound Valley Sequence 68
Lower Winterset Sequence 71
Conclusions 72
2.A.2. Drum Limestone Project 74
Introduction 74
Methodology 75
Outline of Major Stratigraphic Units 75
Drum Limestone Facies Descriptions 76
Depositional Environments and Sea Level History 78
High Resolution Seismic Stratigraphy 80
Introduction 80
Field Procedures 80
Data Processing 81
Modeling and Interpretation 81
Summary and Conclusions 83
Porosity Evolution In Drum Oolite Facies 83
Introduction 84
Description and General Stratigraphy of Cements 84
Paragenetic Sequence of the Drum Oolite 85
Discussion 87
Summary 89
2.B. Regional Stratigraphic Correlation and Mapping Linking Near-surface and Surface Sites With Western Kansas 91
Introduction 91
Methodology 91
2.B.1. Regional Cross Section and Pre-Permian Structural/Stratigraphic Database . . . 91
Introduction 91
Discussion 94

Cross section A-H 94
Cross section D-D' 97
Cross section G-G', G'-G" 98
2.B.2. Regionalized Classification of Mapped Sequence Stratigraphic Data 100
Overview 100
Methodology 101
Results 102
Conclusions 106

SUBTASK 3. CORRELATION METHODS 107
3.A. Biostratigraphic Analysis 108
3.B. Gamma Ray Spectrolog Analysis 108
Recognition of Depositional Sequences and Genetic Units 109
Time-series Analysis of Th/U Ratio 113
Summary of Findings 113
Discussion 114
SUBTASK 4. SUBSIDENCE PATTERNS/RATES 118
4.A. Subsidence Modeling 119
4.B. Fischer Accommodation Plots 122
4.C. Basement Mapping 123

SUBTASK 5. COMPUTER MODELING 126
5.A. Database Development 126
5.B. Stratigraphic Simulation Modeling 127
Introduction 127
Development Background 130
Modeling in 1-D and 2-D 130
2-D Modeling Results 131
Parameter Definition 132
Differentiation of Temporally-Distinct Stratigraphic Units 132
Estimates of the Subsidence Across the Upper Pennsylvanian Western Kansas Shelf 133
Elevation of the Pennsylvanian Shelf and Magnitude of Sea-Level Change 133
Magnitude of Sea-Level Change 134
Characteristics of Pennsylvanian Eustacy 134

Sea-Level History Estimated From Quaternary Analogues 134
Sediment Accumulation Rates From Recent and Quaternary Analogues 135
Inverse Methods 136
Spatial Fourier Analysis 136
Inversion of Facies Thickness to Time - the General Problem 137
Linear Inversion 138
Two-Dimensional Stratigraphic Simulation Modeling -- Parameter Selection 139
Two-Dimensional Modeling -- Oolites on Shelf Break, Bethany Falls Analog Area, Southeast Kansas 140
High Resolution Two-Dimensional Modeling 141
Forward Modeling of 3rd- and 4th-Order Cycles Using the 1-D Model 143
Two-Dimensional Modeling of 2nd- Through 5th-Order Cycles 145
5.C. Three-Dimensional Computer Modeling in Victory Field 147

SUBTASK 6. RESERVOIR DEVELOPMENT, PREDICTION, AND PLAY POTENTIAL -- VICTORY FIELD STUDY AND COMPARISON TO CAHOJ AND PEN FIELDS 151
Overview 151
Introduction 153
Structure 153
Stratigraphy 154
Oil/Gas Production 157
Wireline Analysis - The "Super" Pickett Crossplot 158
Drill Stem Test Analysis 166
Reservoir Evaluation 168
Maximum Gamma-Ray 170
Diagenesis of Reservoir Rocks in Victory Field 170
Methods of Diagenetic Study 171
Stratigraphy of the Bethany Falls Limestone in Victory Field 171
Diagenesis of Reservoir Rocks in Victory Field 172
Study of Drill Cuttings in Victory Field 173
Conclusion of Diagenetic Study 174

SUBTASK 7. TECHNOLOGY TRANSFER 175
Introduction 175
Published Articles 176
Published Abstracts 177
Open-File Reports 178
Conference and Meeting Participation 179

SUMMARY 179

REFERENCES CITED 183

APPENDIX A. CYCLOTHEM CONCEPT 196
Middle (Transgressive) Limestone 196
Core Shale 196
Upper (Regressive) Limestone 197
Outside Shale 198
Causal Mechanisms for Cyclothem Development 199

APPENDIX B. SEQUENCE STRATIGRAPHIC COMPONENTS IN UPPER PENNSYLVANIAN CYCLOTHEMS 201
Introduction 201
Formal Definitions 201
Sequence Stratigraphic Components (Genetic Units) of Pennsylvanian Cyclothems 203
Flooding Unit 203
Condensed Section 205
Late Highstand Stratal Unit 208
Lowstand Siliciclastics 209
Paleosols and Other Evidence For Subaerial Exposure 209

APPENDIX C. OUTCROP DESCRIPTIONS FROM DRUM LIMESTONE STUDY 212

APPENDIX D. DETERMINATION OF PERMEABILITY FROM DRILL STEM TESTS . . . . . .

LIST OF FIGURES

Figure I.1. Stratigraphic section of Middle and Upper Pennsylvanian in Kansas adapted from Heckel (1991).
Figure I.2. Wells penetrating and producing from the Lansing-Kansas City (LKC) in Kansas.
Figure I.3. Distribution of single pay leases from LKC by cumulative production (by Beene and Wong, Kansas Geological Survey, 1992).
Figure I.4. Cumulative frequency distribution of production of single pay leases producing from LKC in Kansas during the period 1965 to present.
Figure I.5. Depth of perforated interval below the top of the Lansing Group for wells producing from LKC.
Figure I.6. a) Preliminary map showing oil fields in Kansas that have had no reported production for 1989 and 1990 (considered abandoned). (prep. by G. Ross, Ks. Geol. Survey, 1992). b) Number of oil fields abandoned in Kansas by year (from D. Beene, 1992).
Figure I.7. Crude oil production plots for leases on the Central Kansas uplift showing performance of new leases added each year since 1970 compared to performance of leases placed on production before 1970.
Figure I.8. Detailed stratigraphic chart for Lansing-Kansas City in Kansas including formal stratigraphic nomenclature and sequence stratigraphic information.
Figure I.9. Wireline log/core of portion of Hertha through Dennis formations from southeastern Kansas with identification of cyclothem components.
Figure I.10. Basic Kansas cyclothem characterizing carbonate-dominated strata in the northern Midcontinent shelf (from Heckel, 1977).
Figure I.11. Project map.
Figure I.12. Late Carboniferous paleogeography showing global siting of Kansas lying north of an active tectonic zone (including Ouachita mountains).
Figure I.13. Basement structure of the Midcontinent (from Rascoe and Adler, 1983).
Figure I.14. Subsidence plot of basement versus time for well in Hugoton embayment in southwest Kansas accompanied by coastal onlap curve of Vail et al. (1977).
Figure I.15. Wells used in backstripped (decompaction) subsidence analysis.
Figure I.16. Basement depth vs. time plot for six wells (shown on map in Figure I.15) using backstripping technique.
Figure I.17. South-to-north regional structural cross section D-D' prepared from well logs.
Figure I.18. Lithofacies map of Marmaton Group (modified from Rascoe, 1962).
Figure I.19. Lithofacies and paleogeography of Missourian in the Midcontinent showing average conditions during this period.
Figure I.20. Dominant lithofacies of interval from Dewey to Hertha formation in Kansas City Group for southwestern Kansas and western Oklahoma (from Rascoe, 1962).
Figure I.21. Lithofacies map of interval from Stanton Limestone through Iola Limestone showing southern carbonate margin for this interval and previous Kansas City section.
Figure I.22. Well log from Amoco Cox #A-4 in Victory field, Haskell County, Kansas for the interval including the Heebner Shale to the Excello Shale interval.
Figure I.23. Fischer plots for selected wells located in western Kansas.
Figure I.24. South-to-north regional stratigraphic cross section datumed on the Heebner Shale for the Middle and Upper Pennsylvanian interval running approximately 125 miles (200 km) from northern Oklahoma to central Kansas Figure I.25. North-to-south stratigraphic cross section datumed on Heebner Shale for the stratigraphic interval from the base of the Pennsylvanian to the top of the Oread Limestone.
Figure I.26. A portion of the original published wireline log section from Lukert (1948) showing framework correlations.
Figure I.27. Generalized Precambrian basement map of Kansas prepared by D. Baars.

Figure I.28. Digitized contoured surface of "basement" in Kansas including configuration of Precambrian to the north and Cambro-Ordovician Arbuckle Group, overlying basement, in southern Kansas.
Figure I.29. Geology of the Precambrian surface based on combined lithologic, age, and magnetic and gravity signatures (from Yarger, 1983, after Bickford et al., 1981).
Figure I.30. Lineaments derived from magnetic maps from Yarger (1983).
Figure I.31. Isopach of base of Pennsylvanian to base of Excello Shale from regional stratigraphic databases.
Figure I.32. Isopach of base of Pennsylvanian to base of the Swope cycle (K Zone) from linked regional stratigraphic databases.
Figure I.33. Isopach map of the total Morrow in the Anadarko and southern Hugoton Embayment (Swanson, 1979).
Figure I.34. Structural cross section of interval from Heebner Shale to base of Pennsylvanian.

Figure I.35. Structural cross section of interval from Heebner Shale to base of Pennsylvanian.
Figure I.36. Structural cross section of interval from Heebner Shale to base of Pennsylvanian.
Figure I.37. Structural contour map on the top of the Lansing Group. Countour interval is 100 feet.
Figure I.38. Isopach of the Marmaton 3rd-order sequence (Excello Shale to Nuyaka Creek Shale) from regional stratigraphic databases.
Figure I.39. Wireline log (GR-porosity) stratigraphic and structural cross sections along southern edge of Central Kansas Uplift for lowermost Pennsylvanian onlap over basal Pennsylvanian unconformity.
Figure I.40. Isopach of Nuyaka Creek Shale to the Muncie Creek Shale from regional stratigraphic databases.
Figure I.41. Isopach of base of Swope (K zone) sequence to base of Muncie Creek Shale from regional stratigraphic databases.
Figure I.42. Isopach of base Muncie Creek to top of Lansing from regional stratigraphic databases.
Figure I.43. Isopach of top of Lansing to base of Heebner Shale from regional stratigraphic databases.
Figure I.44. Isopach of top of Lansing to base of Haskell Limestone (commonly correlated and recognized as Iatan in subsurface) from regional stratigraphic databases.
Figure I.45. Isopach of base of Haskell Limestone (commonly referred to as Iatan in subsurface) to base of Heebner Shale from regional stratigraphic databases.
Figure I.46. Regional south-to-north stratigraphic cross section extending from Oklahoma line to 50 mi. south of Kansas City.
Figure I.47. South-to-north stratigraphic cross section from eastern Oklahoma to north of the Kansas state line for the uppermost Desmoinesian and lower Missourian siliciclastic-rich section derived from Ouachita Mountains.
Figure I.48. Base of Nuyaka Creek Shale to base of Hertha (L zone)(Pleasanton sequence) from linked regional stratigraphic databases.
Figure I.49. Isopach of Sniabar sequence from linked regional stratigraphic databases.
Figure I.50. Isopach of Swope sequence from linked regional stratigraphic databases.
Figure I.51. Isopach of Bethany Falls Limestone in surface and near-surface analog area in southeast Kansas.
Figure I.52. Isopach of Mound Valley Limestone in surface and near-surface analog area in southeast Kansas.
Figure I.53. Isopach of Ladore Shale in surface and near-surface analog area in southeast Kansas.
Figure I.54. Isopach of Galesburg Shale in surface and near-surface analog area in southeast Kansas.
Figure I.55. Isochore map of the thickness of porous carbonate above 8% percent porosity in the Swope sequence (Bethany Falls Limestone) from linked regional stratigraphic databases.
Figure I.56. Hand contoured isochore map of the thickness of porous carbonate in the Swope sequence (Bethany Falls Limestone).
Figure I.57. Isopach of the Dennis sequence from linked regional stratigraphic databases.
Figure I.58. Isopach of the Canville Limestone in the analog area in eastern Kansas.
Figure I.59. Isopach of the interval from the Nuyaka Creek Shale to the Stark Shale.
Figure I.60. Isochore of thickness of porous carbonate in Dennis sequence (Winterset Limestone) with porosity in excess of 8% from linked regional stratigraphic databases.
Figure I.61. South-to-north stratigraphic cross section of Dewey, Cherryvale, and Dennis sequences based on core descriptions including the Amoco #A-4 Cox well on the south end of the section.
Figure I.62. Isopach of the Cherryvale sequence from linked regional stratigraphic databases.
Figure I.63. Isochore map of thickness of porous carbonate in the Cherryvale sequence (Westerville or Drum limestone equivalents) from linked regional stratigraphic databases.
Figure I.64. Isopach of thickness of the Dewey sequence from linked regional stratigraphic databases.
Figure I.65. Isochore map of thickness of porous carbonate in excess of 8% in the Dewey sequence (Cement City Limestone) from linked regional stratigraphic databases.
Figure I.66. Relative changes in coastal onlap for Middle and Upper Carboniferous modified from Ross and Ross (1987).
Figure I.67. Relative sea level chart for Midcontinent region for this study and Youle (1992).

Figure 1.A.1. Map showing leases producing oil and gas from the Missourian (LKC) in Kansas with location of Cahoj, Pen, and Victory fields.
Figure 1.A.2. Structure contour map of the top of Lansing Group in the Cahoj field area from Watney et al., 1992.
Figure 1.A.3. Map of Cahoj field area showing completion dates on wells.
Figure 1.A.4. Combination well log, core analysis, and rock description for continuously cored well, Skelly #1 Bartosovsky located in Section 9-T.1S., R.34W.

Figure 1.A.5. Structural wireline log cross section indexed in Figure 1.A.2 showing LKC interval with subsurface letter nomenclature applied to zones (from Watney et al., 1992).
Figure 1.A.6. Porosity-permeability cross plots for (A) Skelly Bartosovsky #1 (Sec. 9, T.1S., R.34W) in Cahoj field compared with (B) Conoco Adell L-KC Unit #409 (Sec. 2, T.6S, R.27W) in Sheridan County.

Figure 1.A.7. Log-log plot of induction resistivity vs. shale-corrected sonic porosity for porous zones of Skelly Bartosovsky #1.
Figure 1.A.8. Map of perforated wells by zone for upper zones in LKC for same six township areas shown in Figure 1.A.2.
Figure 1.A.9. Map of perforated wells by zone for lower zones in LKC.
Figure 1.A.10. Two maps are shown for the same Graham County area. Map a): Dot shows location of Pen field on hand-drawn structure map of Precambrian basement (from Cole, 1976); b) Computer drawn map of isopach interval from base of Pennsylvanian to base Swope sequence.
Figure 1.A.11. Production status and completion dates for wells in Pen field.
Figure 1.A.12. Structure contour map of the top of the J zone (Winterset Limestone of the Dennis sequence) at Pen field.
Figure 1.A.13. Isopach map of the grainstone interval of the I zone (from Phares, 1991).
Figure 1.A.14. Isopach map of the grainstone interval of the J zone (from Phares, 1991).
Figure 1.A.15. Gamma ray neutron-density log of Bethell #5 located in SW SW Sec. 17, T.6S., R.22W.
Figure 1.A.16. Stratigraphic wireline log cross section indexed in Figure 1.A.14.
Figure 1.A.17. Base map of Victory field, Haskell County, Kansas.
Figure 1.A.18 (a). Gamma ray neutron-density porosity log of Amoco Cox #A-4 well from Victory field.
Figure 1.A.18 (b). Continuation of Figure 1.A.18 (a).
Figure 1.A.19. Structure contour map of base of Canville Limestone immediately overlying Bethany Falls reservoir.
Figure 1.A.20. Thickness of porous carbonate (>8%) in Bethany Falls Limestone in the Victory field area.
Figure 1.A.21. Thickness of porous carbonate (>8%) in Dewey Limestone in the Victory field area.
Figure 1.A.22. Porosity-permeability cross plot for Iatan Limestone from the Amoco Cox #A-4 core.
Figure 1.A.23. Porosity-permeability cross plot for Bethany Falls Limestone from the Amoco Cox #A-4 core.
Figure 1.A.24. Log and core analysis profile through the Iatan reservoir. Pay is fine intergranular porosity.
Figure 1.A.25. Log and core analysis profile through the Bethany Falls reservoir. Pay is oomoldic porosity.

Figure 2.A.1.1. Map of Kansas showing the locations of the regional and detailed study areas examined in the analog study.
Figure 2.A.1.2. North-south core cross-section of the study interval just west of the outcrop belt in eastern Kansas.
Figure 2.A.1.3. Isopach map of the Pleasanton interval across the regional study area.
Figure 2.A.1.4. Cross section showing the four depositional sequences in the study interval along the southeastern margin of the Pleasanton platform.
Figure 2.A.1.5 West-to-east cross section of the Hertha sequence across the east flank of the Pleasanton slope.
Figure 2.A.1.6 North-south cross section of the Hertha sequence.
Figure 2.A.1.7. Core slab photos of Sniabar and Middle Creek limestones.
Figure 2.A.1.8. Isopach map of the interval from the base of the Mound City black shale to the top of the Middle Creek Limestone.
Figure 2.A.1.9. Map of the southern part of the study area showing the locations of the Pleasanton platform and the Sniabar bank complex.
Figure 2.A.1.10. North-south core cross section showing the Bethany Falls sequence.
Figure 2.A.1.11. West-east cross section showing the Bethany Falls and Mound City sequences along the east flank of the Pleasanton slope.
Figure 2.A.1.12. Slab photos of the Bethany Falls Limestone.
Figure 2.A.1.13. Core slab and photomicrograph photos of Bethany Falls Limestone (grainstone).
Figure 2.A.1.14. Map showing the general area of occurrence of oolitic grainstone in the Bethany Falls Limestone.
Figure 2.A.1.15. North-south core cross section showing the basinally restricted Mound Valley sequence.
Figure 2.A.1.16. Map showing the occurrence of thick Mound Valley Limestone just basinward of the underlying Sniabar bank complex.
Figure 2.A.1.17. North-south core cross section showing lower Winterset sequence.
Figure 2.A.1.18. West-east core cross section showing lower Winterset sequence across east flank of the Pleasanton platform.
Figure 2.A.1.19. Map showing occurrences of >10 ft (3 m) of porous carbonate in the Winterset Limestone portion of the lower Winterset sequence.
Figure 2.A.1.20. Map of detailed study area showing locations of >10 ft (2 m) of porosity development (large dots) in lower Winterset sequence overlain on an isopach of the Nuyaka Creek black shale-to-Stark black shale interval.
Figure 2.A.1.21. Core slab photos of Winterset Limestone.
Figure 2.A.1.22. West-east core cross section showing oolitic grainstones within Bethany Falls, Mound Valley, and lower Winterset sequences.
Figure 2.A.1.23. Isopach map of the interval from the base of the Nuyaka Creek black shale to the base of the Mound City black shale in the datailed study area.

Figure 2.A.1.24. Isopach map of the interval from the Mound City black shale facies to the top of the Sniabar Limestone in the detailed study area.
Figure 2.A.1.25. Core slab photos of Bethany Falls Limestone.Figure 2.A.1.26. Thickness of the Bethany Falls Limestone overlain on the thickness of the underlying Nuyaka Creek black shale to Hushpuckney black shale interval.
Figure 2.A.1.27. Cross section of closely spaced cores that shows the thinning of porous oolities within the Bethany Falls and Mound Valley sequences just west of outcrop belt.
Figure 2.A.1.28. Core slab photos and photomicrographs of Bethany Falls Limestone.
Figure 2.A.1.29. Carbon and oxygen isotopic values of selected samples of the upper part of the Bethany Falls and the Mound Valley depositional sequences in the KGS Woodward #2 core.
Figure 2.A.1.30. Carbon and oxygen isotopic values of selected samples of the upper part of the Bethany Falls and the Mound Valley depositional sequences in the KGS Woodward #3 core.
Figure 2.A.1.31. Plot showing the porosity and permeability values for the Bethany Falls and Mound Valley oolities in the Woodward transect cores.
Figure 2.A.1.32. Porosity and permeability values and estimated grain size ranges within the Bethany Falls and Mound Valley limestones, KGS #3 Woodward core.
Figure 2.B.1.1. Base map for project showing location of regional cross sections.
Figure 2.B.1.2. West-to-east regional structural cross section A-H prepared from wireline logs.
Figure 2.B.1.3. South-to-north regional structural cross section D-D' prepared from wireline logs.
Figure 2.B.1.4. West-to-east regional structural cross section G-G' prepared from wireline logs.
Figure 2.B.1.5. West-to-east regional structural cross section G'-G" prepared from wireline logs.
Figure 2.B.1.6. Key to abbreviations used in cross sections.
Figure 2.B.2.1. Three-class regionalization for 9 Pennsylvanian interval thicknesses listed in text.
Figure 2.B.2.2. Six-class regionalization for 9 Pennsylvanian interval thicknesses.
Figure 2.B.2.3. Subsidence curves for 6 areas classified in Figure 2.B.2.2.
Figure 2.B.2.4. Probability of correct classification for 6-class regionalization.
Figure 2.B.2.5. Northwest-to-southeast structural cross section along Central Kansas uplift utilizing 10 stratigraphic horizons used in regionalization.
Figure 2.B.2.6. Southwest-to-northeast structural cross section from the Hugoton embayment unto the Central Kansas uplift utilizing 10 stratigraphic horizons used in regionalization.
Figure 3.A.1. Gamma ray, uranium, thorium, potassium log for Amoco #1 Rebecca Bounds core from Section 17, T.18S.R42W, Greeley County, Kansas.
Figure 3.B.1. Thorium vs. alumina percent for various aluminosilicates (from Hassan et al., 1976).
Figure 3.B.2. Gamma ray and Th/U ratio plotted for Amoco Cox #A-4 core in Victory field showing facies vs. log response.
Figure 3.B.3. Uranium vs. organic carbon in sedimentary rocks (from Levanthal, 1981).
Figure 3.B.4. Gamma ray, Th/U ratio, and two Fourier harmonics of Th/U ratio for Amoco Cox #A-4 core for interval from Heebner Shale to Excello Shale.
Figure 3.B.5. Power spectrum obtained from Fourier analysis of Th/U ratio from Amoco Cox #A-4.
Figure 3.B.6. Oil fields map of Kansas with locations of wells used in expanded Th/U ratio analysis.
Figure 3.B.7(a). Power spectra for Th/U ratio data for six wells identified on the map in Figure 3.B.6.
Figure 3.B.7(b). Continuation of power spectra from Figure 3.B.7(a).
Figure 3.B.8. Plot of harmonic number (cycle) for major peaks vs. thickness of cycles for seven wells distributed across the Kansas shelf.
Figure 3.B.9(a). Cross sections linking wells used in the Th/U analysis presented as logs of the gamma ray, original Th and U concentrations, the Th/U ratios, and the 3rd- and 4th-order harmonics.
Figure 3.B.9(b). Continuation of Figure 3.B.9(a).
Figure 4.A.1. Oil fields map of Kansas showing wells used in backstripping (decompaction) subsidence analysis.
Figure 4.A.2. Basement depth vs. time plot for six wells using backstripping.
Figure 4.A.3. Subsidence rates in m/ka (meters/1000 years) vs. age of strata.
Figure 4.A.4. Same as Figure 4.A.3.
Figure 4.B.1. Fischer accommodation plots for wells in western Kansas.

Figure 5.A.1. DOE project database management program.
Figure 5.A.2. DOE project databases and data sets.
Figure 5.A.3. Computer Operations in DOE Project.
Figure 5.A.4. Structure Diagram of DOE.EDT.
Figure 5.A.5. Database form.
Figure 5.B.1. Flow chart showing logic of quantitative model.
Figure 5.B.2. (a) Conceptual model of Quaternary coastal sedimentation in the Pacific region responding to two cycles of eustatic rise (from Carter et al., 1986).

Figure 5.B.2. (b) Conceptual model of Lansing-Kansas City carbonate shelf cycle.
Figure 5.B.3. Quaternary-age oxygen isotope record for two deep sea cores obtained from the Caribbean (Denton and Hughes, 1983).
Figure 5.B.4. Subsidence and sediment accumulation (Schlager, 1981).
Figure 5.B.5. Carbonate sediment accumulation rate vs. water depth used in 2-D model.
Figure 5.B.6. Conceptual model graphically depicting processes influencing development of an 4th-order sequences.
Figure 5.B.7. Facies classification used in "gamma" inverse modeling procedure.
Figure 5.B.8. Menu screen showing choices when running the 2-D model.
Figure 5.B.9. Curve/profile shown at large scale.
Figure 5.B.10. Screen showing profile selected with reduced version in upper left hand corner of screen.
Figure 5.B.11. Example screen of finished model run.
Figure 5.B.12. Diagrammatic well log cross section of the Bethany Falls from southeastern Kansas analog area.
Figure 5.B.13. Two-dimensional stratigraphic simulation developed around sedimentation of the Swope sequence on an inclined slope.
Figure 5.B.14. Close-up of stratigraphic simulation of oolitic grainstones developed along the slope as a result of three minor sea level oscillations during overall fall in sea level.
Figure 5.B.15. Two-dimensional model of Hertha and Swope sequences deposited over Pleasanton shelf-to-basin setting in eastern Kansas analog area.
Figure 5.B.16. High-resolution output of the two-dimensional model produced by storing pixel information on facies and replotting the information as full stratigraphic columns.
Figure 5.B.17. One-dimensional stratigraphic model showing interaction of 4th- and 3rd-order sea-level change.
Figure 5.B.18. One-dimensional model at mid-shelf position with same sea level curve, decreased initial surface elevation, increased subsidence, and sediment accumulation rate producing noticeably thicker cycles.
Figure 5.B.19. One-dimensional model at lower shelf position.
Figure 5.B.20. Lower shelf 1-D model where position has been drowned during a 3rd-order sea level rise of 20 m.
Figure 5.B.21. Lower shelf scenario where decreased sediment accumulation rate and lower subsidence result in a progressive rise in the sediment surface elevation through the course of the model run.
Figure 5.B.22. Repeat of Figure I.24 for comparison with longer-term 2-D modeling runs.
Figure 5.B.23. Sea-level curve used in long-term 2-D computer simulation.
Figure 5.B.24. Large time and distance 2-D simulation model run to test sea-level curve in Figure 5.B.23 utilizing 2nd-, 3rd-, and 4th-order cyclicity.
Figure 5.B.25. Selected stratigraphic columns generated along profile in Figure 5.B.24. Lines connect 3rd-order sequence boundaries.
Figure 5.B.26. Four additional stratigraphic simulation scenarios for same initial shelf profile, varying one parameter while holding other parameters constant.
Figure 5.C.1. Index map of Victory field showing wells included in digitizing.
Figure 5.C.2. Southeast-to-northwest computer-constructed gamma ray cross section between wells as labeled on base map in Figure 5.C.1.
Figure 5.C.3. Southwest-to-northeast structural cross section showing sonic porosity between Will #3 and James #2 wells indexed in Figure 5.C.1.
Figure 5.C.4. Southwest-to-northeast structural cross section showing sonic porosity between William #2 and James #B1 wells indexed in Figure 5.C.1.
Figure 5.C.5. 3-D panel looking northwest showing elevation of cells in the Bethany Falls interval.
Figure 5.C.6. 3-D panel showing layer numbers for the Bethany Falls interval.
Figure 5.C.7. 3-D panel, again looking northwest, showing the gamma ray for the Bethany Falls Limestone interval.
Figure 5.C.8. 3-D panel with same orientation as above displaying density porosity for the Bethany Falls Limestone.
Figure 5.C.9. 3-D panel of density porosity in the Bethany Falls Limestone filtered to show only porosity above 20%.
Figure 5.C.10. Two parallel southeast-to-northwest structural cross sections showing density porosity in the Bethany Falls Limestone. Sections are indexed on map in Figure 5.C.1.
Figure 5.C.11. Water saturation calculated with cementation exponent of 2.2 for Bethany Falls Limestone filtered with density porosity cutoff of 25%.
Figure 5.C.12. Conventional well log cross section in the same location as the cross section in Figure 5.C.11.
Figure 5.C.13. 3-D panel of calculated bulk water volume (BVW) for the Bethany Falls Limestone using sonic porosity, filtered at 10% sonic porosity cutoff.
Figure 5.C.14. 3-D panel of calculated BVW for Bethany Falls Limestone using sonic porosity, filtered at 16% sonic porosity.
Figure 5.C.15. Slice map of density porosity in view looking northwest showing layer from the lower porosity zone lapping up onto higher portion of field.
Figure 5.C.16. Slice map of density porosity for the layer from the uppermost porosity in the Bethany Falls Limestone in view looking northwest.
Figure 5.C.17. Geobody of connected volume of the Bethany Falls reservoir using density porosity with 25% cutoff.

Figure 6.1. Structure map of the K-zone (Swope sequence) in the northern portion of the Hugoton Embayment in western Kansas showing very low dips.
Figure 6.2. Structure map of the Heebner Shale in the Victory-Northeast Lemon Fields.
Figure 6.3. Structure map of the Iatan Limestone.
Figure 6.4. Structure map of the Paola Limestone.
Figure 6.5. Structure map of the Canville Limestone.
Figure 6.6. Structure map of the Middle Creek Limestone.
Figure 6.7. Structure map of the Nuyaka Creek Shale.
Figure 6.8. Structure map of the Excello Shale.
Figure 6.9. 'Type-section' log Victory-Northeast Lemon Fields (4050-4500'), Amoco A-4 Cox (Sec. 8-T30N-R33W).
Figure 6.10. Type-section log Victory-Northeast Lemon Fields (4500-4950'), Amoco A-4 Cox (Sec. 8-T30N-R33W).
Figure 6.11. West-east gamma ray-density log cross section from Wea Shale of Cherryvale sequence to Nuyaka Creek Shale.
Figure 6.12. North-south gamma ray-density log cross section from Wea Shale of Cherryvale sequence to Nuyaka Creek Shale.
Figure 6.13. Isopach of Excello-Nuyaka Creek interval (Marmaton Group).
Figure 6.14. Isopach of Nuyaka Creek-Hushpuckney interval (L and M sequences).
Figure 6.15. Exline Limestone. Feet of porosity greater than 8%.
Figure 6.16. Isopach of the Hertha sequence (L).
Figure 6.17. Isopach of the Sniabar Limestone illustrating southeast-northwest trending oolitic shoals.
Figure 6.18. Sniabar Limestone. Feet of porosity greater than 8%.
Figure 6.19. Sniabar Limestone. Porosity feet 8% cutoff.
Figure 6.20. Sniabar Limestone. Porosity feet 16% cutoff.
Figure 6.21. Isopach Swope sequence (K).
Figure 6.22. Isopach Bethany Falls Limestone illustrating southeast-northwest trending oolite shoals with 30-40 feet of buildup.
Figure 6.23. Average porosity Bethany Falls Limestone.
Figure 6.24. Bethany Falls Limestone. Feet of porosity greater than 8%.
Figure 6.25. Bethany Falls Limestone. Porosity feet 8% cutoff.
Figure 6.26. Bethany Falls Limestone. Porosity feet 16% cutoff.
Figure 6.27. Isopach Galesburg Shale to Quivera Shale (I and J sequences).
Figure 6.28. Isopach Dewey sequence (H).
Figure 6.29. Dewey Limestone. Feet of porosity greater than 8%.
Figure 6.30. Isopach of Iola sequence (G).
Figure 6.31. Isopach Iatan Limestone to Lane Shale (B through F sequences).
Figure 6.32. Stanton Limestone. Feet of porosity greater than 8%.
Figure 6.33. Iatan Limestone. Feet of porosity greater than 8%.
Figure 6.34. Mississippian limestone production.
Figure 6.35. Pennsylvanian Morrow sandstone production.
Figure 6.36. Pennsylvanian Marmaton limestone production.
Figure 6.37. Lansing-Kansas City limestone lease production decline curves in the Victory Field.
Figure 6.38. Lansing-Kansas City limestone lease production decline curves in the Victory Field.
Figure 6.39. Lansing-Kansas City limestone lease production decline curves in the Victory Field.
Figure 6.40. Lansing-Kansas City limestone lease production decline curves in the Victory Field.
Figure 6.41. Lansing-Kansas City limestone lease production decline curves in the Victory Field.
Figure 6.42. Lansing-Kansas City limestone lease production decline curves in the Northeast Lemon Field.
Figure 6.43. Lansing-Kansas City limestone lease production decline curves in the Northeast Lemon Field.
Figure 6.44. Lansing-Kansas City limestone lease production decline curves in the Northeast Lemon Field.
Figure 6.45. Iatan Limestone production decline curve from the Mesa #7 Huxman, Victory Field.
Figure 6.46. Stanton Limestone production decline curve from the Mesa #3-12 Dudley, Victory Field.
Figure 6.47. Principles of Pickett (resistivity vs. porosity) crossplot.
Figure 6.48. Plot of water saturation (Sw) versus porosity (phi) to determine bulk water volume (BVW) hyperbolic curves on a linear plot.
Figure 6.49. Cumulative frequency plots of irreducible bulk volume water (or Buckle's number) for carbonate reservoirs.
Figure 6.50. Location of irreducible bulk volume water trend on Pickett plot.
Figure 6.51. Pickett plot of limestone zone data from a well from south Texas indexed with water and irreducible bulk volume water lines (data from Fertl, 1979).
Figure 6.52. "Super" Pickett crossplot of Bethany Falls Limestone, Victory Field, Amoco #A-4 Cox.
Figure 6.53. Log of Amoco #A-4 Cox in Bethany Falls and Sniabar Limestone intervals.
Figure 6.54. "Super" Pickett crossplot Bethany Falls Limestone, Victory Field, Mesa #1-14 Leathers well.

Figure 6.55. Log Mesa #1-14 Leathers, Bethany Falls and Sniabar Limestones.
Figure 6.56. "Super" Pickett crossplot, Sniabar Limestone, Northeast Lemon Field, Amoco #1-A Brennan.
Figure 6.57. Log of Amoco #1-A Brennan in the Bethany Falls and Sniabar Limestones.
Figure 6.59. Log of Ensign #1-31 Thunderbird in the Iatan and Stanton Limestones, Victory Field.
Figure 6.58. "Super" Pickett crossplot in the Iatan and Stanton Limestones, Victory Field, Ensign #1-31 Thunderbird.
Figure 6.60. Pickett plot for Mobil University 1535.
Figure 6.61. Sniabar Limestone potential producing area in the Victory-Northeast Lemon Fields.
Figure 6.62. Bethany Falls Limestone potential producing area in the Victory Field area.
Figure 6.63. Dewey Limestone potential producing area in Victory field.
Figure 6.64. Stanton Limestone potential producing area in the Victory Field area.
Figure 6.65. Pickett crossplot, multi-reservoirs, Cahoj Field.
Figure 6.66. "Super" Pickett crossplot J zone, Pen Field, Pan Canadian #3 and #4 Bethell.
Figure 6.67. Maximum gamma ray in Hushpuckney Shale.
Figure 6.68. Maximum gamma ray in Stark Shale.
Figure 6.69. Maximum gamma ray in Muncie Creek Shale.
Figure 6.70. Stratigraphic description of the Bethany Falls Limestone in Victory Field.
Figure 6.71. Stratigraphic distribution of diagenetic aspects of the grainstone in the Bethany Falls Limestone at the Blair 'C' No. 2 well.
Figure 6.72. Stratigraphic distribution of diagenetic aspects of grainstone in the Bethany Falls Limestone at the Cox No. A-4 well.
Figure 6.73. Stratigraphic distribution of diagenetic aspects of grainstone in the Bethany Falls Limestone at the Thompson 'E' No. 2 well.
Figure 6.74. Porosity evolution of grainstone in the Bethany Falls Limestone, Victory Field.
Figure 6.75. Bethany Falls photomicrographs of thin sections (4x). Cities Service #C-2 Blair, Sec. 29-T30S-R33W.
Figure 6.76. Distribution of effective porosity in the Bethany Falls Limestone.
Figure 6.77. Distribution of effective porosity in the Dewey Limestone.
Figure 6.78. Comparison of petrographic studies of thin sections of cuttings versus assessments of pore fabrics using low power, reflected light microscopy.
Figure 6.79. Distribution of petrographically defined effective porosity in the Bethany Falls Limestone.

ABSTRACT

Reservoirs in the Lansing-Kansas City limestone result from complex interactions among paleotopography (deposition, concurrent structural deformation), sea level, and diagenesis. Analysis of reservoirs and surface and near-surface analogs has led to developing a "strandline grainstone model" in which relative sea-level stabilized during regressions, resulting in accumulation of multiple grainstone buildups along depositional strike. Resulting stratigraphy in these carbonate units are generally predictable correlating to inferred topographic elevation along the shelf. Primary porosity in these grainstones was modified by early meteoric diagenesis which laterally and vertically compartmentalized these reservoirs. Effective permeability in oolitic grainstone was radically changed through time eventually controlled by early meteoric leaching to form oomolds and interparticle cements. Continued leaching and later burial crushing of the oomoldic fabric led to a patchy permeability within the original oolitic grainstone facies. This model is a valuable predictive tool for 1) locating favorable reservoirs for exploration, and 2) anticipating internal properties of the reservoir for field development.

Reservoirs in the Lansing-Kansas City limestones are developed in both oolitic and bioclastic grainstones, however, re-analysis of oomoldic reservoirs provides the greatest opportunity for developing bypassed oil. A new technique, the "Super" Pickett crossplot (formation resistivity vs. porosity) and its use in an integrated petrophysical characterization, has been developed to evaluate extractable oil remaining in these reservoirs. This technique makes use of the limited data common to older Lansing-Kansas City fields to generate a number of important reservoir parameters such as irreducible water saturation, estimates of pore size and type, percent effective porosity, information about the presence of a transition zone (if present), and an estimate of the permeability of the zone. The manual method in combination with 3-D visualization and modeling can help to target production limiting heterogeneities in these complex reservoirs and moreover compute critical parameters for the field such as bulk volume water. Application of this technique indicates that from 6-9 million barrels of Lansing-Kansas City oil remain behind pipe in the Victory-Northeast Lemon Fields.

Regionally significant, shelf-wide repetitive stacking patterns of 4th-order sequences are developed in 3rd-order sequence sets. The recognized patterns in the mid and upper Pennsylvanian apparently resulted from interactions of basin configuration, subsidence, eustacy, and sedimentation. Simulation modeling provides the means to test the interaction of these parameters revealing likely causal mechanisms. Recognition of this cycle hierarchy presents additional constraints to describing and predicting the character of 4th-order cycles (cyclothem-scale sedimentation) on the shelf in Kansas. The envelope of resolution of deterministic modeling is improving as interdisciplinary studies, such as this one, are completed. Petroleum geologists are challenged to quantify inferred processes to aid in developing rationale geologically consistent models of sedimentation so that acceptable levels of prediction can be obtained.

EXECUTIVE SUMMARY

This grant allowed the Kansas Geological Survey to conduct research, resource characterization, and technology development and transfer designed to enhance the domestic supply of fossil fuels. The interdisciplinary data obtained in the research was used to resolve specific problems in high-resolution correlation of strata and to quantify the mechanisms responsible for the observed stratigraphy. The data obtained in this study resulted in better constrained solutions to ancillary, but important, problems such as validation of subsequence correlation, subsidence patterns, sedimentation rates, sea-level changes and establishing relationships between the development of sedimentary sequences and basement structure. The geoscientific information, including data from field studies, surface and near-surface reservoir analogues, and regional database development, were used to construct geologic process-based computer simulation models. These models are tailored to specific depositional sequences and used to improve prediction of reservoir characteristics.

The focus of the study on depositional sequence development and modeling of Upper Pennsylvanian Kansas City Group carbonate reservoirs addressed a high priority geologic class of reservoirs, shelf carbonates as identified by DOE in the Implementation Plan of the Oil Research Program. As indicated in this report, this reservoir class has a high potential for incremental oil recovery both in exploration (stratigraphic traps) and development (complex reservoir heterogeneity). Furthermore, many fields representing significant resources in this reservoir class are in a position to be abandoned if an understanding of the heterogeneities can not be assessed and actions taken to improve recovery. The research reported helps to constrain geologic interpretations of the Lansing-Kansas City reservoirs and serves as a general model for high frequency Paleozoic reservoirs for the ultimate use in improving their characterization and prediction.

The objectives of this research were to: 1) assist producers in locating and producing petroleum not currently being produced because of technological problems or the inability to identify details of reservoir compartmentalization, 2) to decrease risk in field development, and 3) accelerate the retrieval and analysis of baseline geoscience information for initial reservoir description.

Technologies are demonstrated here including very high resolution seismic reflection profiling (>400 hz), new logging suites such as GR spectralog, strategic shallow coring in near-surface analog areas, new approaches to analyzing old logging suites, quantifying geologic process data coupled with geologic computer simulation. These technologies are used to develop improved models of stratal architecture, lithofacies and diagenesis to reduce associated uncertainties and risks in exploring for and developing complex reservoir rocks. PC, mainframe, and workstation were used to display and process large amounts of local and regional subsurface geologic data compiled in this study. Abundant well and sample information in Kansas provide critical information for using these technologies and evaluating reservoirs for improved oil recovery. Concepts and

methods developed here can be applied by independent operators to other comparable reservoirs with resources available to them.

The products of this research consist of digital data sets, descriptions, interpretations, and recommendations and methodology to address Upper Pennsylvanian reservoirs in Kansas. The information provided by our research will help the independent operator to retool for the uncertain future.

INTRODUCTION

Significance to DOE Research Plan

Quantification in geology is rapidly evolving due to substantial increases in speed and graphics capability along with decreased cost of personal computers and workstations. Quantification is coupled with the development of new concepts and methods in interpreting stratigraphy, namely depositional sequence analysis. Improved stratigraphic resolution using sequence stratigraphic concepts and methods coupled with cost effective computer processing have made feasible research in geologic simulation modeling for reconstructing geologic observations. However, many problems such as constraining variables for modeling, improving understanding of complex processes, and defining limits to geologic interpretations restrict the resolution of deterministic modeling. This research provides fundamental concepts and parameters for modeling, model development and testing for improved characterization of Upper Pennsylvanian Kansas City Group depositional sequences. It also addresses pragmatic aspects of more precise reservoir characterization for use in improving oil recovery.

Prediction of reservoir parameters can be improved through application of careful reservoir characterization and quantitative modeling as described in this study. The deterministic modeling approach based on integrated, multi-scale description advocated in this study can probably be coupled with stochastic methods to model small-scale variations in the reservoir below the limit of determinism. Deterministic procedures are limited due to insufficient subsurface information and detailed knowledge of processes. Integrated geologic studies with field, analog, regional description and interpretation coupled with geologic simulation models should improve predictions and decrease risks in drilling and application of improved recovery techniques in these reservoirs. This result should be applicable to extension drilling in field development and for trend definition in exploration where analysis of subtle stratigraphic controls is needed.

The study identifies parameters needed to improve geologic interpretation, quantitative and qualitative. The level of application of this approach by independents will vary according to their resources. All will benefit by this accelerated effort to characterize Pennsylvanian depositional sequences by providing a foundation to make more precise and accurate geologic interpretations.

Statement of Problem

There is a general lack of ability to accurately predict reservoir heterogeneity at all scales. In part, the problem stems from limited sampling and spacing of wells in a field and distances between control along plays and regional trends. Engineering data such as pressure testing and performance analysis can be used to constrain elements of heterogeneity at the interwell scale and seismic data (where available) is also useful in defining facies, stratal units, and structure at multiple scales. Three-dimensional visualization is vastly improving exploration and development ventures. Engineering and seismic data have limited resolving power, but complement other subsurface information. Geologic analysis can help to constrain possible solutions obtained through an integrated approach.

The role of regional controls on stratigraphy and sedimentation and application to problems of reservoir characterization are still in the stage of proving their value. Base-level control, e.g., magnitude and rates of change in relative sea level, affects accommodation space for sedimentation and thus impact facies characteristics. Base-level changes in the Pennsylvanian are believed to have been a significant, attributed by most workers to glacioeustacy and tectonic subsidence linked to nearby foreland basin subsidence. Their impact on facies distribution and early diagenetic overprinting needs to be established.

Research Approach

Many advances have been made in sedimentary geology that have yet to be fully incorporated and tested in oil-field-scale applications. These include: 1) use of integrated (multiscale) depositional sequence analysis to develop the high-resolution time stratigraphy needed for more precise correlations and quantitative modeling; 2) application of methods such as time-series analysis to develop an improved understanding of the larger-scale stratal packages that include the hydrocarbon reservoirs and; 3) utilization of very high resolution seismic methods for characterization of analog stratigraphy; and 4) application of new well log procedures to enhance characterization of reservoirs.

An interdisciplinary study of the Lansing and Kansas City groups was undertaken in order to develop a quantitative understanding of the processes responsible for depositional sequences that include important oil and gas reservoirs. The concepts and methods of sequence stratigraphy are used to define and interpret the three-dimensional depositional framework of the Kansas City Group. Separate studies of oil fields in central and western Kansas are linked through regional mapping to near-surface and surface analogs investigations in southeastern Kansas. Geologic simulation modeling is used to integrate quantitative estimates of controls on sedimentation to produce reconstructions of these reservoir-bearing strata.

Analog studies of oolitic grainstone and phylloid algal carbonate units in the Kansas City Group in southeastern Kansas include outcrop descriptions, coring and wireline logging, high-resolution seismic reflection surveys, and porosity-permeability and stable carbon and oxygen isotopic analyses of cores. The analog studies permitted construction of field- and interfield-scale, three-dimensional descriptions of complex stratal geometries in units that contain reservoir-quality rock. Seismic surveys and existing often dense well control were used to locate core holes in strategic parts of the reservoir analog area. Seismic resolutions of 1 meter vertically and 5 meters horizontally were obtained.

Regional mapping including a total of nearly 5000 points is used to extend the results from the field studies to the analog sites and to interpret the regional controls that affected sedimentation. Regional cross sections correlating pre-Permian strata link eastern and western Kansas. The result of the succession of isopach mapping of temporally distinct depositional sequences is essentially a frame-by-frame view of the geologic evolution of these hydrocarbon reservoirs.

Computer modeling includes: 1) 3-D visualization and analysis of reservoir characteristics using the graphic workstation; and 2) one- and two-dimensional stratigraphic simulation modeling to reconstruct 11 different depth and energy controlled carbonate facies for various orders of cyclicity and various scales from regional long-term to short-term field scale. Stratigraphic simulation modeling incorporates subsidence, sea-level change, depositional profile and slope parameters, that have been estimated for the region of this investigation.

Stratigraphic modeling has focused on refining processes to re-create the cycles of sedimentation that typify the Upper Pennsylvanian studied here including multi-scale cyclicity. The successful transfer of reservoir characterization techniques to other reservoirs requires knowledge of the processes that formed the reservoir and modeling may eventually be an important vehicle. Quantitative simulation modeling provides the only means to integrate major controlling processes as a dynamic system. Modeling provides the means to study the dynamic interaction of processes and, in turn, refine our view of what is important for synthesis (prediction) of reservoir characteristics.

Summary of Results

Findings include:

1) Reservoir-Scale Heterogeneities -- Multi-scale (vertical and horizontal) reservoir heterogeneity is closely related to temporally distinct episodes of sedimentation interrupted by hiatuses in sedimentation represented by bounding surfaces. Bounding surfaces are created by non-deposition, submarine and subaerial erosion, and sediment dissolution from subaerial exposure. Grainstones host most of the volumetrically significant porous reservoir rock in the Lansing-Kansas City. The distribution and

thicknesses of grainstones are believed to be controlled by widely changing sea level interacting with local conditions including depositional or structurally induced topography (elevation, orientation, and amount of slope). Local topography coupled with residence time of high-energy shallow water (strandline) conditions appears to be important as to where reservoir rock is developed. Early meteoric diagenesis, particularly pervasive dissolution of oomolds, and later cementation and dissolution events in the Kansas City Group appears to have been responsible for significant redistribution and occlusion of primary pore space. An example described later in this report is the marked heterogeneities of grainstone reservoirs in the Iatan, Stanton, Dewey, Bethany Falls, and Sniabar in Victory field.

The reservoir characteristics, e.g. grain type, size, and sorting of carbonate grainstones, particularly oolites, vary within a single field in association with large-scale stratal sequence architecture affecting cyclothem (4th-order) scale reservoir development and patterns of minor stratigraphic cycles (stacking, thickness, and lateral extent), depositional processes, and early and late diagenesis. Each cycle has its own distinct characteristics. Two end-member groups of grainstone reservoirs are distinguished in this investigation, oolite with varying oomoldic and vuggy porosity and grainstone reservoirs with varied-sized interparticle pore space. A key technique to describing the pores and fluid content has been the "Super" Pickett crossplot. The "Super" Pickett crossplot provides a quick means to determine parameters of effective pay -- bulk water volume, irreducible water saturation, porosity and water saturation cutoffs. It is advantageous to have complete modern log suites, but any resistivity and porosity logs can provide useful information. This makes the "Super" Pickett plot especially useful in the older reservoirs of the Midcontinent. Validation of correlations to reservoir and fluid types obtained from this plot were empirically developed from over 1500 plots from 300 wells in the Victory field area. Production data and core or cuttings sample description were used to establish relationships of results to well performance and an improved understanding of pore fabric including permeable and productive intervals. Reservoir characteristics critical to evaluating bypassed oil and improved oil recovery options were obtained from these plots. An integrated program using "Super" Pickett crossplot, called the Petrofacies Analysis Project, has become a new research area developed from this project.

2) Reservoir-Scale Paleotopography -- Structural deformation concurrent with deposition has influenced sedimentation regionally and locally. Topography associated with concurrent structural deformation at the field-scale operated in concert with any preceding depositional topography to affect elevation and slope and, in turn, contribute to local sediment accommodation and depositional profile. These factors combined to influence location, depositional and diagenetic facies, and stratal character of the reservoir. Basement heterogeneities reveal recurring structural deformation varying in character due to orientation

and extent of inferred stress fields resulting from nearby foreland basin development. The regional configuration of the shelf was strongly influenced by combined tectonically driven subsidence patterns, eustacy, and sedimentation. The configuration of the shelf was basically reset at the initiation of each 3rd-order cycle.

Structural deformation (fracturing, folding, faulting) following deposition contributing to trapping and closure, influencing the nature of oil migration and charging in the field and reservoir. The hydrocarbon charging pattern and fill-up, or lack thereof, are also critical factors in Lansing-Kansas City reservoirs, variable probably because of complex patterns of reservoir connectedness.

3) Cycle Hierarchy and Predictive Stratigraphy -- A hierarchy of sedimentary cycles have been documented including long-term (1 Ma, >300 ft. thick) stratal stacking patterns along prominent shelf margin and from correlatable time series trends of the Th/U ratios in equivalent interior shelfal deposits. Stratal changes are more subtle and complex on the shelf and appear to relate to local conditions and residence time in shallow water. Thus, thickness is not expected to closely serve as a proxy of accommodation space.

Small-scale cycles are less than several meters thick, representing 4th- and 5th-order (0.1-1. and 0.01-0.1 million years, Ma). These cycles correspond to regionally correlable depositional sequences and more localized, perhaps autogenic parasequences. Small-scale cycles occurring within depositional sequences strongly influence porosity and permeability through facies dislocation and diagenetic changes. Large, 3rd-order sequence sets contain sets of five to seven-4th-order cycles.

Formal stratigraphic groups and subgroups correspond to these 3rd-order sequence sets indicative of major adjustments to the stratigraphic pattern and shelf configuration due to large-scale changes in sea level resulting from eustacy and subsidence. Higher order sequences undergo progressive changes within these 3rd-order sequence sets. These patterns are useful in correlating geological events between different fields and analog sites occupying different shelf settings and producing stratigraphic interval. These changes may eventually be correlated to specific reservoir properties. These results also suggest an important deterministic contribution to relative sea-level history.

4) Inverse Modeling for Parameter Definition -- Time-series (Fourier) analyses of Th/U ratios derived from natural gamma ray logs of twenty Middle and Upper Pennsylvanian depositional sequences (upper Cherokee, Marmaton, and Lansing-Kansas City groups) situated over the State of Kansas reveal both long- and short-term (3rd- and 4th-order) sedimentary sequences. The very high-frequency fifth-order

cycles can not be resolved. The stratal signatures correlate closely with patterns of landward and basinward stepping carbonate and siliciclastic events that are well-preserved along the shelf margin in southern Kansas and northern Oklahoma. Accordingly, this stratigraphic signal is interpreted to reflect regional relative sea-level history, a critical variable for successful stratigraphic simulation modeling. Other time series may provide an improved means to define this stratigraphic signal and eventually provide the means to "tune" the stratigraphic section. Local departures from the trend could be recognized to produce a clearer distinction of local and regional controls. This approach is analogous to the methods of handling del-O^{18} data obtained from deep sea sediment cores. The cause(s) (subsidence or eustacy or some combination of both) for the 3rd-order sequence sets will not be definitely known until inter-basinal correlations are accomplished. Forward models are used to combine best estimates of parameters to produce observed stratal geometries for 3rd- and 4th-order cycles. Parameters include shelf elevation and subsidence, eustasy, and sediment accumulation rate.

Other inverse methods were examined to derive sediment accumulation rates for depth-based, log-derived depositional facies. The gamma method (Bond et al., 1991) was used to estimate accumulation rate by converting the stratigraphic-depth section to time. The goal was to develop tailored sea-level curves using the stratigraphic information for input into forward modeling.

5) Stratigraphic Simulation of Pennsylvanian Cyclic Sedimentation -- A 2-D forward stratigraphic model was developed that runs on an IBM-compatible personal computer. The simulations are specialized in that input and output are focused on parameters deemed important in describing Pennsylvanian depositional cycles observed in the Midcontinent. Eleven carbonate facies, condensed sections, and subaerial surfaces are generated in solid color sections. Carbonate facies are based on water depth and energy level, the latter derived from the angle of the depositional slope. Synthetic, high-resolution stratigraphic columns can be generated along the modeled profile based on a detailed matrix of facies attributes for each model run. A major objective of modeling is to be able to test and experiment with data to develop an improved geologic interpretation in order to predict details of the reservoirs and associated strata.

6) Three-Dimensional Reservoir Visualization and Modeling -- Three-dimensional computer visualization and modeling of reservoir properties in Victory field provided a means to systematically examine the complex characteristics of the Bethany Falls oolitic grainstone reservoir. The model provided the ability to test scenarios of deposition via how the stratigraphic model is constructed. The best correlation of petrophysical data within the carbonate reservoir was found to be a layered model in the carbonate reservoir where layers parallel the base of the unit. The buildups of the oolite, occurring

at the top of the unit forms new layers with limited lateral extent. This coincides to generally isopachous deposition in the lower subtidally deposited lower section of the reservoir and localized bar-shaped facies development in the shoal-water oolite facies.

Images can be filtered based on critical cutoffs of reservoir attributes that are included in a particular model. Attributes can be any mathematically relationship of numerical data that is originally input. Three-dimensional views of the reservoir provide the means to quickly and effectively assess reservoir compartments in the combined perspective of structure, petrofacies, and stratigraphic changes. Visualization also provides a powerful means to grasp the implications of stratal architecture (onlap and offlap relationships) on reservoir performance.

7) Technology Transfer -- Oral and written papers have been prepared throughout the course of the project. Oral presentations have taken place in conferences, workshops, and field trips including onsite reviews to local geological society. Numerous publications have resulted from this work. Key elements developed in this project that have been directly transferred to the independent producer include:

a. Methodology for establishing reservoir parameters using data common to older fields -- "Super Pickett Plot"

b. Robust, multi-scaled sequence stratigraphy model and methodology for defining high-resolution paleogeographic framework for Pennsylvanian reservoirs

c. Computer simulation permitting experimentation with processes to help understand the reservoir system.

Rationale for Study of Lansing-Kansas City Carbonate Reservoirs

The Lansing-Kansas City (LKC) is a dominant reservoir interval in Kansas containing a dozen productive limestone reservoirs with many indications of considerable remaining potential (Fig. I.1). The Lansing-Kansas City is estimated to have contributed between 1 and 2 billion barrels of oil in Kansas. The Pennsylvanian Lansing-Kansas City Groups currently produce in over 8100 wells, 18% of the active oil wells in Kansas, representing 4839 leases. These active leases have produced nearly half a billion barrels (Figures I.2 and I.3). Average cumulative lease production is 98,214 barrels (Figure I.4). All intervals of the Lansing-Kansas City contribute to production as evidenced by the depth of perforations below the top of Lansing (Figure I.5). The producing wells can be grouped into several producing areas in the State: a) the Central Kansas uplift, b) the western Kansas shelf with numerous exploration and development opportunities, and c) widely scattered production from across the southern portion of the State.

The number of leases that have produced from the Lansing-Kansas City in Kansas for at least 5 years since 1965 is second only to the Mississippian. However, many Lansing-Kansas City fields in Kansas are nearing their economic limit (DOE, 1989; DOE/BC-89/6/SP, Abandonment rates of the known domestic oil resources, Bartlesville, Oklahoma, 39 p.). This DOE report estimates that over 50% of Kansas' fields will be abandoned by the year 2000 at current conditions (Figure I.6).

The need to study these reservoirs is critical because of abandonment rates that threaten loss of access to the remaining potential of these fields. The availability of geologic data (surface exposures, cuttings, wireline logs) is excellent for a mature, Lansing-Kansas City producing province. The database provides the means to reveal important aspects about the three-dimensional stratigraphic framework of a shelf-to-basin setting that is important to developing predictive geologic models of these reservoirs. The database is also amenable to application of some of the latest concepts and technologies, e.g., sequence stratigraphy, high resolution seismics, petrofacies analysis, and stratigraphic simulation providing a unique opportunity for geologic re-appraisal of the Lansing-Kansas City reservoir interval with important implications to further petroleum activity in this area.

The Lansing-Kansas City reservoirs consist of discontinuous layers and pods of phylloid algal carbonate buildups (biostromal), grainstone shoals, and occasional quartz sandstones. Variable stratigraphic, depositional, and diagenetic processes and subtle structural deformation create marked complexities in reservoir development and hydrocarbon trapping. Multiple pays are common in many fields in western Kansas. Commingling of pays and testing over several zones creates difficulties in assessing the contribution of production from individual zones. Furthermore, production is reported by lease. Together, analysis of the areal or stratigraphic distribution of production is difficult. Conventional means of analyzing these reservoirs is nearly impossible. Other techniques are needed to analyze data that is available -- older well logs, cuttings, some cores, and original completion data.

In general, oil recovery from the Lansing-Kansas City is limited, even though the interval has contributed a substantial amount of oil as a whole reservoir system. The Lansing-Kansas City reservoirs usually produce by solution gas drive in northern and central Kansas with recoveries of less than 20% OOIP (Randy Koedel, personal com.). Gas caps are common in these reservoirs in southern Kansas. Waterflooding varies in its effectiveness and mobile oil likely remains in the more heterogeneous reservoirs where waterflood performance has been poor. The giant billion-barrel Hall-Gurney field, the largest LKC field in Kansas, is one example of a major field on the Central Kansas uplift that has realized a poor overall waterflood response. Estimated oil recovery is only 19% of OOIP (Poyser, 1987). The poor recovery is attributed to several factors: 1) complex reservoir heterogeneity (areal continuity, high permeability streaks, vertical conformance); 2) lack of a natural reservoir drive (except for solution gas); and 3) commingled production from multiple limestone reservoirs with

contrasting permeability. If reservoir heterogeneities were better defined and recovery technologies more closely tailored to these heterogeneities, the potential exists for significant improvements to oil recovery.

A comparison of production statistics on field development and exploration produce some interesting results. Drilling of extension wells in both old and new fields has provided a majority of the increased oil production during the boom development in the early 1980's. A comparison of pre-1970 leases and later development in the Central Kansas uplift indicates that most of the incremental oil realized during the early 1980's drilling and production boom comes from new leases rather than from new activity in older leases (Figure I.7) (Watney et al., 1989). Combined production from the older leases show a steady decline suggesting that a substantial opportunity remains to improve this recovery.

The potential impact of this study becomes even more apparent when examining additional statistics. At least one-fifth of Kansas' estimated 2.4 billion barrels of unswept mobile oil (BPO/Toris data base) and 8.7 billion barrels of residual (immobile) oil remain in existing Pennsylvanian reservoirs. These reservoirs are also estimated to contain over 23% of the 17 billion barrels of original-oil-in-place.

A large potential exists for exploration in Lansing-Kansas City as well as field re-development. Fields producing from the Lansing and Kansas City Groups are commonly found on structural highs because these reservoirs have been primarily structurally oriented exploration targets based on seismic, corehole, or subsurface mapped anomalies. Many of these structures were also positive paleotopographic features that affected reservoir development, either through localization of favorable depositional environments (such as grainstone shoals or phylloid algal buildups), or through early diagenesis related to subaerial exposure (Watney and Ebanks, 1978; DuBois, 1985; Ebanks and Watney, 1985; Watney, 1980, 1984; Watney and French, 1988; Watney, Stephens, and Wong, 1992). The potential remains to find additional oil and gas associated with subtler stratigraphically related traps that are not current structural highs. Improving our understanding of effective pay cutoff would prove useful in assessing reservoir seals and stratigraphic traps. Establishing facets of multi-scale heterogeneities are critical to evaluating stratigraphic traps and reservoir compartments off structure whether in a field, extension opportunity, or a rank wildcat.

Opportunities are afforded now to: 1) resolve details of reservoir heterogeneities for use in understanding and predicting performance of zones and evaluating bypassed production.; 2) model stratigraphic zonation to improve understanding of reservoir framework; 3) define new methodologies using commonly available data to more efficiently and accurately define reservoir attributes critical to evaluating performance; and 4) select analog and field studies to test and experiment with ideas in better constrained systems.

STRATIGRAPHY OF THE RESERVOIR INTERVAL

by

W.L. Watney, J. Youle, J. French, H. Feldman, E. Franseen, A. Verma,
J.C. Wong, T. Gerhard, G. Stevenson, D. Baars, T. Meham

Introduction

The Lansing and Kansas City groups are part of the Missourian Stage, Upper Pennsylvanian (Figure I.1). These groups are informally combined and referred to as the Lansing-Kansas City (LKC). This interval contains 10 separate cyclic successions of alternating transgressive-regressive limestone-shale cycles each up to 80 ft (24 m) thick (Figure I.8, a,b,c). The shales serve as sealing strata in addition to being associated with tight intervals that often occur within the upper portions of the limestone reservoir units. These successions are inferred to have been deposited during rapid rises and falls of sea level, which resulted in their lithologic heterogeneity and abrupt facies changes. Within thicker carbonate units of the Lansing-Kansas City, multiple producing horizons are common.

The LKC carbonate reservoirs are part of unconformity-bounded cyclothems (cycles of sedimentation) and essentially, closely correspond to depositional sequences on the shelf. Each carbonate-dominated cycle is an individual unconformity-bounded package that ranges from 25 ft (7.6 m) to over 100 ft (30 m) in thickness (Figures I.9 and I.10). The cycles typically consist of a basal transgressive limestone less than 10 ft (3 m) thick that is overlain by a marine black shale normally less than 3 ft (1 m) thick. This marine shale, referred to as the "core shale," is overlain by an upper, generally regressive limestone that is up to 90 ft (27.4 m) thick. The cycle is capped by another shale, the "outside shale" that varies in thickness from inches to 10's of feet. The shale can contain a succession of shelf sandstones and shales or as is often in the lower LKC composed of a thin (<5 ft, 1.5 m) paleosol.

Cyclothems depending on how they are defined are commonly separated from bounding strata by surfaces that are commonly associated with paleosols and diagenetic and textural features indicative of subaerial weathering (Watney and Ebanks, 1978; Watney, 1980; Prather, 1981; Schutter and Heckel, 1985; Goebel et al., 1989; Watney et al., 1989). Variations in thickness, areal extent, and lithofacies in typical cyclothems suggest varying degrees of marine inundation of the craton (Heckel, 1980, 1984, 1986; Watney, 1984, Watney, et al., 1989). Additional omission surfaces including paleosols interstratified within these Pennsylvanian cyclothemic successions on the shelf that define subcyclothemic sequences and parasequences. The smaller-scale (high frequency) stratal packages are important components of the reservoir description.

Minor cycles are characterized by shifts in facies delimited by bounding surfaces which are commonly associated with a tight streaks or zones as will be described later (French and Watney, 1992). These and other thin, tight horizons subdivide carbonate grainstone reservoirs, interrupting their vertical conformance. Minor cycles can themselves be bounded by subaerial exposure surfaces making them sequences in their own right. However, regional correlations of the minor cycles is equivocal, limiting the classification of these as depositional sequences.

Depositional sequences are used in the text and are equivalent to zonal designation used in the field studies. This is one of several orders of cyclicity recognized in these strata ranging from 5th-order to 3rd-order, from short to long duration. This cycle hierarchy follows that of Goldhammer et al. (1991) and is modified in Table I.1. The ranges of time included in each cycle category varies with different workers, albeit similar. The conventional stratigraphic and sequence stratigraphic nomenclature are provided in Figure I.8 (Watney et al., 1989). The stratigraphic section shown here includes what are termed 3rd-order sequences which represent bundles of smaller-scale cyclothems or (depositional sequence or 4th-order cycle). Third-order sequences have not been previously associated with these rocks.

Table I.1: CYCLE ORDERS (modified after Goldhammer et al., 1993)

Cycle Order	Duration (Ma)	Amplitude (meters)	Rise/Fall rates (m/ka)	Sequence terminology (Goldhammer et al., 1993)
1st order	>100		<0.01	
2nd order	10-100	50-100	0.01-0.03	Supersequence
3rd order	1-10	50-100	0.01-0.1	Sequence
4th order	0.1-1	1-150	0.4-5	Sequence, cycle, cyclothem
5th order	0.01-0.1	1-150	0.6-7	Parasequence, cycle

General Characteristics of Upper Pennsylvanian (Missourian) Stratigraphy

Upper Pennsylvanian (Missourian) strata of the midcontinent United States are characterized by thin cyclical successions of variable percentages of carbonate and siliciclastic rocks, with thicknesses of less than 10 ft (3 m) to in excess of 150 ft (50 m). Cycles of sedimentation or cyclothems developed on shelf areas of the midcontinent generally are thin with widespread transgressive basal lithofacies overlain by thicker regressive strata (Figures I.9 and I.10, Heckel, 1977).

Pennsylvanian Cyclothems

In the midcontinent, the upper limestones serve as the primary reservoir-bearing stratum. The primary reservoir rock is carbonate grainstone that in most cases was deposited late in the period of overall relative sea-level fall. This is evidenced by an overall upward transition from relatively deep-water deposits such as the black shale through open-shelf wackestones into the high-energy, shallow-water oolitic lithofacies with exceptions. Subaerial exposure features are common at or near the top of the regressive carbonate or peritidal lithofacies that cap the grainstone. The regressive limestone ranges from a single shallowing-upward unit to a complex set of thinner, small-scale (minor) unconformity-bounded cycles. Pennsylvanian cyclothems are discussed in more detail in Appendix A.

Sequence Stratigraphic Components in Pennsylvanian Cyclothems

Cyclothems are defined and constrained by lithofacies successions while depositional sequences are constrained by internal and bounding surfaces. The depositional sequences readily accommodate facies variation, but are often difficult to define precisely and carry through the subsurface. Alternatively, cyclothems and their usual widespread lithofacies provide a pragmatic reference in regions that have limited rock information such as in the subsurface. Pennsylvanian cyclothems are discussed in greater detail in Appendix A.

The cyclothem model is limited in its ability to encompass marked variation in lithofacies that occur vertically or laterally as conditions change -- siliciclastics, changes in elevation, and accommodation on shelf. Examples of these complexities are expressed in the analog sites along the lower shelf where sediment accommodation space varies considerably. For more accurate and precise reconstructions of the paleogeographic setting, temporal distinction is essential to accommodate changes in lithofacies. The element of time in stratigraphy is introduced through distinction of stratal elements bounded by regional unconformities. This is the basis for the sequence stratigraphic approach to Midcontinent cyclothems. Lithofacies change radically between unconformities, deviating from typical and ideal successions. This facies variation is given more latitude as genetic units within sequences, e.g., flooding, condensed, late-highstand, lowstand, etc. The smallest scale

unconformity-bounded unit that is readily mappable in these strata is at the scale of the cyclothem. Details about sequence stratigraphy as applied to these Pennsylvanian strata are provided in Appendix B.

Orders of Cycles

The depositional sequence is the fundamental unit of sequence stratigraphy defined as a genetically related succession of strata bounded by unconformity surfaces and their correlative conformities (Mitchum, 1977). The sequence boundaries are identified by an abrupt basinward shift in facies or change in parasequence stacking patterns (Van Wagoner, et al., 1990). Van Wagoner (1985) defines parasequence as "a relatively conformable succession of genetically related beds bounded by marine-flooding surfaces and their correlative surfaces". Parasequences stack into sets that delineate systems tracts within a depositional sequence. Sequence sets are groups of sequences that stack into similar progradational, aggradational, or retrogradational motifs and are analogous to systems tracts within a single depositional sequence (Mitchum and Van Wagoner, 1991). A composite sequence consists of lowstand, transgressive, and highstand sequence sets (Mitchum and Van Wagoner, 1991).

Although most sequence stratigraphers agree that the depositional sequence is the "fundamental unit of sequence stratigraphy" (Vail, et al., 1991), they disagree on its scaler properties. Vail et al. (1991) refer to the depositional sequence as a third-order cycle that ranges from 0.5 to 3 Ma in duration; however Mitchum and Van Wagoner (1991) and others (e.g., Posamentier et al., 1992) believe the sequence is scale independent.

For the purposes of this report a non-scaler sequence stratigraphic terminology is used. Despite estimated durations of between 0.25 and 0.5 Ma for the Pennsylvanian sequences, they possess all of the components of third-order depositional sequences even though they are 4th-order scale in time. Furthermore, like cyclothems, these sequences serve as the fundamental stratigraphic unit in the Pennsylvanian. They are regionally correlative and capable of supplying temporally distinct stratigraphic frameworks for paleogeographic reconstructions and can be used to establish detailed facies relationships.

REGIONAL GEOLOGIC FRAMEWORK

Introduction

The study focused on the Missourian Upper Pennsylvanian Lansing-Kansas City carbonate reservoirs and covers most of the state of Kansas (Figure I.11). The regional studies provide a structural and stratigraphic framework linking the oil field areas and field study sites in western Kansas with the near surface/surface analog sites in the eastern part of the state. Regional framework also provides rationale for the correlation of the two distinct areas. The regional study provided information on the evolving nature of the Pennsylvanian shelf as affected by

structural deformation and sea-level change. Additional details of the regional study are discussed in later sections.

During the Middle and Upper Pennsylvanian the large supercontinent Pangea was in the final stages of formation. The Ouachita Mountains bordering the Midcontinent on the southeast formed along a portion of a suture zone created by the collision and thrusting of Laurasia and Gondwana (Figures I.12 and I.13). Timing of orogenic deformation was diachronous along the length of the Ouachita orogen. Broad, active patterns of subsidence on the upper Midcontinent developed in proximity to active foreland basins including the Arkoma and Anadarko basins. Subsidence was also accompanied by more restricted uplifts, occurred on the craton during this collision creating a relatively high sediment accommodation potential during the Pennsylvanian over broad reaches of the Midcontinent (Houseknecht and Kacena, 1983; Kluth and Coney, 1981a,b; Thomas, 1985).

The distribution of uplifts and basins on the craton is notable in that most are oriented at a high angle to the orogenic belt. The prominent Amarillo-Wichita uplift (Oklahoma), Nemaha uplift (Kansas), and Central Basin Platform (Texas) all occupy locations corresponding to the axes of lower Paleozoic basins (Ham and Wilson, 1967) which, in turn, formed above, or adjacent to, relict Cambrian or Proterozoic crustal features (Keller et al., 1983). The crustal heterogeneities include structures and composition differences related to different terranes and structural provinces such as the MRS. Smaller scale heterogeneities appear to be closely tied to the occurrence of many existing fields. For example, structurally induced topography concurrent with sedimentation appears to have occurred due to episodic structural reactivation (differential subsidence) along basement heterogeneities (Baars and Watney, 1991).

Clastics derived from the Ouachita thrust belt began filling the Arkoma foreland basin during the Atokan, nearly filling this basin to the carbonate platform that bordered the basin to the north in southern Kansas during the Missourian (Figure I.13) (Houseknecht and Kacena, 1983). In contrast, the southern margin of the western Kansas shelf along the Anadarko basin remained unfilled and deep until the Virgilian. This lack of filling was apparently due to limited sediment supply from local clastic sources, rapid subsidence to limit carbonate shelf progradation to the north, and greater distance from competent clastic sources, namely the Ouachita Mountains (Ham and Wilson, 1967; Rascoe and Adler, 1983; and Kumar and Slatt, 1984).

Development of the Anadarko basin, apparently caused significant subsidence along the western Kansas shelf. The Anadarko basin is a hybrid foreland basin that partially owes its subsidence to overthrusting of crustal blocks now exposed in the Wichita Mountains in western Oklahoma. Uplift of the Amarillo-Wichita-Arbuckle mountains beginning in the Early Pennsylvanian (Atokan) coincides with the onset of significant subsidence and definition of the Anadarko basin (Brewer et al., 1983). Some eight to nine kilometers (5-6 miles) of northward

thrusting in the Wichita Mountains are indicated by deep-reflection seismic profiling (Brewer et al., 1983). Thrusting is attributed to the plate collision along the Ouachitas, perhaps ultimately linking with tectonic events in the Arkoma basin. Periods of uplift and clastic-dominated cycles deposited along the mountain front is recorded as major episodes of conglomerate progradation covering portions of the southern Anadarko basin (Ham and Wilson, 1967; Dutton, 1982). These episodes appear to have each lasted several million years apparently responsible for considerable subsidence in the basin and adjoining shelves.

During Missourian and Virgilian (Late Pennsylvanian) the Anadarko basin was at its maximum development; subsidence was estimated to have exceeded 2 m/Ka (Dickinson and Yarborough, 1979). Major subsidence in the western Anadarko basin is recognized by sediment-starved conditions in an area situated immediately south of the western Kansas shelf (Galloway et al., 1977; Rascoe and Adler, 1983; Kumar and Slatt, 1984). Eastern limits of the basin in proximity to the Ouachita Mountains received episodic influx of tectonically derived siliciclastic sediments similar to the Arkoma basin. Estimated relief across the shelf margin in the Anadarko basin during the Late Pennsylvanian was estimated up to 1100 ft. (335 m) (Kumar and Slatt, 1984).

The fidelity of the Pennsylvanian stratigraphic record is high in Kansas due to relatively high rates of subsidence. Shelf strata were able to preserve considerable evidence for significant base-level change including a strong influence on reservoir development. Forty-five to 75 percent of the Paleozoic sedimentary column is Permo-Pennsylvanian in Kansas, even though this interval represents only 23 percent of Paleozoic time (Figure I.14). Backstripped subsidence modeling in our study suggests that subsidence varied between 0.015 m/ka (meters/thousand years) to 0.035 m/ka from locations distal (north) to proximal (south) to the active Anadarko and Arkoma basins (Figures I.15 and I.16). This differential subsidence played an important role in creating and maintaining topographic relief across the shelf. In the south, high rates of subsidence often led to sediment starvation that was able to persist through multiple 4th-order (cyclothemic-scale) sedimentary cycles. The average subsidence values arrived do not indicate what was probable variable rates of subsidence due to episodic thrusting typifying foreland basin development. Episodic thrusting resulted in pulses of rapid downwarp followed by longer periods of slower subsidence, each typically lasting several millions of years (Quilan and Boumont, 1986). The precise duration of these episodes is not well known, but may be related to the development of the 3rd-order sequences described later.

While, in general, subsidence rates increased basinward across the State of Kansas during the Pennsylvanian, crustal heterogeneities on the shelf led to localized abrupt changes in subsidence rates. These abrupt changes in subsidence influenced sediment accommodation and reservoir development. Regionalization analysis, a spatial analysis technique, operating on interval thickness data provided a consistent means to recognize areas of more uniform thickness variation and was used to delimit boundaries delimiting abrupt changes in stratigraphy. The

boundaries generally correspond closely to apparent basement heterogeneity as defined by magnetic, gravity, geochronology, and basement composition. Basement heterogeneities include regional Pre-cambrian terranes and MRS fault boundaries. Details of the regionalization analysis are presented later.

In general, precursors to current structural provinces including the Hugoton embayment, Pratt anticline, Central Kansas uplift, Sedgwick basin, Nemaha uplift, and the Cherokee basin. These and associated basement heterogeneities interacted with likely changing stress patterns resulting in modifications to the patterns and orientation of reactivation. This structural deformation apparently led to notable differences in elevation, slope and configuration of the shelf as represented by the changing character of the Pennsylvanian depositional sequence to be described later. These changes in shelf configuration along with changes in sediment supply affected the character of the shelf margin bordering the foreland basins, siliciclastic distribution, and general thickness and patterns of strata that will be described in more detail below.

Mapping of small- to large-scale depositional sequences over the region suggests that magnitudes of relief on the shelf was up to several hundred feet (10's to 100 meters). Cycles of increased relief followed by filling in of this topography is recognized, usually within the span of several depositional sequences. This relief occurred in conjunction with reorganization of the shelf established through probably a combination of subsidence, eustacy, and sedimentation associated with 3rd-order sedimentary cycles. The resultant changes to the shelf configuration appear to be systematic and resultant stratal stacking patterns have significant implications to reservoir development. These cycles of changing shelf configuration and relief and sediment infilling are not obvious when looking at regional, large-interval structural cross sections or large-interval isopach maps (Figure I.17). Nor can they be easily recognized when examining stratigraphy at local sites. The relatively small temporal changes are dwarfed by the long accommodation change created by combined subsidence and sea-level history (Figure I.14).

Regional Sequence Stratigraphy of Middle and Upper Pennsylvanian

Middle to Upper Pennsylvanian Paleogeography

The regional discussion continues with a review of the evolution of the shelf setting beginning in the Desmoinesian Marmaton Group through the end of the Lansing-Kansas City interval (Figure I.1). The southern shelf margin of the late Desmoinesian Marmaton Group, underlying the Lansing-Kansas City, extends generally west to east across central Oklahoma (Figure I.18). The prominent shelf margin is a constructive carbonate bank with local relief on the banks in excess of 100 ft (30 m). To the north a broad shelf was the site of widespread deposition of thin, carbonate-dominated cycles. Locally, the entire Marmaton Group laps out over what are inferred to be the higher reaches of the Central Kansas uplift and Nemaha uplift, suggesting a lower relative sea level than the overlying Lansing-Kansas City (Figure I.18).

The Lansing-Kansas City thins from nearly 1000 ft (305 m) of carbonate deposits along the northern shelf margin in Texas County in the Oklahoma Panhandle to 60 ft (18 m) in Wheeler County, Texas over a distance of only 20 miles (32 km) (Figure I.19). Siliciclastic mud and locally, allodapic (shallow sediments redeposited into deep water) carbonates shed from adjoining shallow shelves, accumulated in the generally sediment-starved basin. The rate of thinning is approximately 50 ft/mi (9.4 m/Km) into the starved basin during the Missourian. Seismic stratigraphy and subsurface studies suggest that relief across the shelf was up to of 1100 ft. (335 m) (Kumar and Slatt, 1984). The sediment surface in the interior of the Anadarko basin was apparently too deep for carbonate accumulation.

The Lansing-Kansas City thins to 185 ft (56 m) from the shelf margin onto the Central Kansas uplift. These Late Pennsylvanian strata progressively onlap and eventually covered the uplift as relative sea level rose. Thinning of cycles is common as is the increase in proportion of shallow-water carbonate facies over the Central Kansas uplift.

Facies and thickness maps of the lower Missourian Kansas City Group (Dewey, Cherryvale, Dennis, Swope, and Hertha formations) indicate a prominent rotation and northward shift (backstepping) of up to 62 mi (100 km) of the carbonate shelf margin compared to the underlying Marmaton Group (Figure I.20). This relatively abrupt backstepping led to formation of a basinal setting over what had earlier been a carbonate shelf. A lithofacies map of the succeeding Lansing Group (including Stanton, Plattsburg, Wyandotte, and Iola formations) indicates another 31 mi (50 km) of northward backstepping of the carbonate shelf margin (Figure I.21). As other investigations of this study demonstrate, the change in the shelf configuration was not gradual, but appears to have occurred abruptly at the time the boundaries of the stratigraphic groups developed.

Evidence for 3rd-Order Depositional Sequences

The abrupt changes in the shelf configuration and the stratigraphy are classified as 3rd-order cycles (Table I.1). Implications of this adjustment while profound at the regional scale appear to be just as important to the development and character of reservoirs within the succession of small-scale cycles that comprise each 3rd-order cycle. Stratigraphic and shelf reorganization is reflected by stacking geometry of 4th-order cycles along the shelf margin, regional patterns of thickness and facies distribution obtained through mapping, accommodation history from Fischer plots, and time-series analysis of Th/U ratio profiles. All of these data are consistent in the patterns that they reveal about the 3rd-order cyclicity.

Summary of Findings

Third- (1-10 Ma) and 4th-order (.1-1 Ma) sequences are recognized in these Middle and Upper Pennsylvanian strata. Fourth-order cycles average 33 ft (10 m) thick and are unconformity-bounded depositional sequences that

include significant petroleum reservoirs, while 3rd-order sequences are sets of 5 to 7 of these sequences. Third-order sequences are recognized by significant landward shifts (up to 50 mi [80 km]) in stratal stacking patterns along shelf margins and stratal variation of Th/U ratios. Third-order Atokan (lower Middle Pennsylvanian) sequences show gradual deepening, in contrast to the more abrupt deepening typical of later Pennsylvanian cycles. The stratal pattern in the late Middle and Late Pennsylvanian 3rd-order sequences are characterized by initial retrogradation (a transgressive sequence set) followed by lateral and vertical accretion (highstand sequence set).

While the 3rd-order sea-level changes are easiest to discern in stacking patterns along shelf margins, third-order sequences can be recognized in the interior of the shelf through time-series analysis of wireline-log-derived depth profiles of thorium/uranium (Th/U) ratios. Th/U ratios can be used to recognize varying redox conditions and inferred water-depth variations (Figure I.22). Bases of the 3rd-order cycles indicate more intense reducing conditions, while the upper portions show greater oxidation and associated leaching (thorium enrichment, uranium loss). The consistency of the 3rd-order cyclicity in the Th/U profile across this region is made more clear using Fourier analysis. Accommodation profiles (Fischer plots) also suggest the presence of the 3rd-order cycles (Figure I.23).

Reservoir development on the shelf is closely related to the relative occurrences of each 4th-order cycle in the 3rd-order cycle sets. Fourth-order cycles in the lower portions of the 3rd-order cycles are generally associated with increased magnitude of depositional topography and greater overall thickness. This tends to result in greater lateral thickness and facies variation in the carbonate grainstones. The varying spacial distribution of accommodation can lead to isolated occurrences of grainstone development such as buildups on the flanks of topographic highs, e.g., Sniabar and Bethany Falls in Victory and Northeast Lemon fields to be described later.

Lansing-Kansas City grainstones are commonly oolitic and are diagenetically unstable due apparently to their initial aragonite mineralogy. The oolitic grainstone are excellent reservoirs in many places; however, early diagenesis related to subaerial exposure can severely modify porosity distribution. Subaerial exposure while commonly the last stage of each 4th-order cycle, tends to be more intense in the upper portions of the 3rd-order cycles. In addition, 5th-order cycles within the reservoir lithofacies can be terminated by their own subaerially exposed bounding surfaces and each cycle affected by its own distinctive early diagenesis.

Discussion

Two north-south cross sections are shown from similar locations in southern Kansas and northern Oklahoma, one a gamma ray wireline log cross section based on wells each with suites of gamma ray, neutron, and density logs. Another cross section is modified from an older published section (Lukert, 1947). The original older

cross section established many of the regional markers that were "fleshed out" as a new modified version benefitting from additional well control and use of modern log suites. Furthermore, a stratigraphic model based on stratal relationships developed in the nearsurface and surface analog studies in southeast Kansas was employed to strengthen the choice of correlations. The sections reveal details about the shelf-to-basin transition that have important implications about sea-level history (Figures I.24 and I.25). These regional sections are approximately 125 mi (200 km) long are indexed on the paleogeographic map (Figure I.19). The cross sections reveal the stacking pattern of Middle and Upper Pennsylvanian strata along a profile extending from south-central Kansas into northern Oklahoma. The stratal interval extends from the base of the Pennsylvanian to the Heebner Shale. Thickness ranges from 900 ft (274 m) thick on the north to nearly 1800 ft (548 m) on the south. Both stratigraphic cross sections use the Virgilian Heebner Shale as a datum.

Major flooding surfaces and stratigraphic dislocations delimit stratigraphic bundles, each including from five to seven 4th-order cycles (cyclothems). These bundles are recognized as 3rd-order sequences. Major flooding events correspond to the Excello Shale, Nuyaka Creek Shale, Muncie Creek Shale, and the Heebner Shale. Each of the 3rd-order sequences range from 300 ft (90 m) to in excess of 500 ft (150 m) thick. Each major flooding event results in initial landward (backstepping) shift of lithologic units, suggesting relative sea-level rise. Following initial landward stepping, succeeding 4th-order cycles of each 3rd-order sequence undergo overall lateral, basinward accretion along the shelf margin. Each 4th-order cycle undergoes apparent high magnitude, rapid deepening to introduce sediment starvation and shallowing events that extend to subaerial exposure without affecting the overall pattern of progressive change. The 3rd-order sequences coincide closely with formal stratigraphic groups (Figure I.1) reflecting a reorganization of the shelf. The flooding events initiating the 3rd-order sequences acted much the same way as Galloway's condensed section, controlling the depositional sequences recognized in Cenozoic Gulf Coast strata. Likewise, these 3rd-order cycles are seismically resolvable units and reflect fundamental sequences equivalent by definition to Vail's depositional sequence.

The stratal geometries observed on the dip-oriented cross sections are used to estimate a relative sea-level history that affected the Middle and Upper Pennsylvanian in this shelfal region. During deposition of the Marmaton Group a broad, rather uniform carbonate shelf extended through the line of section. The shelf margin of the Marmaton Group lies 50 mi (80 km) beyond the southern end of the cross sections. In contrast, during accumulation of the Kansas City Group, a shelf margin crossed the line of section. This abrupt landward shift of the carbonate shelf margin is interpreted as drowning of the lower portion of the shelf proximal to the active Arkoma and Anadarko basins. Sediment starvation and presumed basinal conditions existed along the southern portion of this cross section during the Pleasanton and lower portion of the Kansas City 3rd-order cycle between the Nuyaka Creek and Muncie Creek Shale flooding events. Studies utilizing core and outcrop investigations and mapping from wireline logs to the east along the outcrop belt (Sniabar, Swope, and Dennis analog study,

work by Bennison, 1989, and regional mapping, e.g., Pleasanton isopach) indicate that this sediment starvation extended eastward along strike covering large portions of southeastern Kansas and northeastern Oklahoma. During this time early in the 3rd-order cycle siliciclastics did not reach the lower shelf.

Siliciclastics of the Galesburg and Layton intervals episodically appear during the mid and later portions of the Kansas City 3rd-order sequence infilling the lower shelf areas that were previously sediment starved. Work in the analog study areas support the lowstand setting in that the Galesburg section is equivalent to an extended period of subaerial exposure across the higher reaches of the shelf in central and northern Kansas. In addition, isolated occurrences of valley incision are noted in the Galesburg interval on the shelf including that extending through the underlying Bethany Falls Limestone (Bob Slamel, personal communication).

The cross sections also reveal that significant landward (northward) backstepping (43 mi, 70 km) of the carbonate shelf margin occurred at the Muncie Creek Shale horizon, the beginning of the Lansing 3rd-order sequence succeeding the Kansas City 3rd-order sequence (Figure I.1). The carbonate margin along the lower shelf retreated to central Kansas in the Sedgwick and Cherokee basins. This carbonate margin slowly accreted laterally southward during successive 4th-order cycles similar to that of the underlying 3rd-order cycle. Depositional topography along this front is estimated to be on the order of 300 ft (91 m). According to wireline-log correlations, the major episode of siliciclastic sedimentation that filled the space created beyond the shelf margin and lower shelf did not occur until the Stalnaker event, equivalent to the siliciclastic interval in the Lawrence Shale immediately below the Haskell Limestone including the Tongonoxie Sandstone. Correlation markers extending from the shelf originating from individual 4th-order cycles and appear to downlap into the basin (Figures I.24 and I.25). These correlations have been carried successfully into the third dimension across the study area in Kansas.

Based on analog sites that were selectively core drilled and examined in outcrop the shelf margin is comprised of an amalgamated carbonate bank complex. Basinward beyond the bank the area apparently was sediment starved during times when water depths exceeded the photic zone, eliminating significant carbonate production. Furthermore, the area was too distant from significant clastic influx. Meanwhile, subsidence meanwhile continued over the course of this 3rd-order event, further enhancing the topographic relief along the carbonate shelf-to-basin framework (five - 4th-order cycles, 300 ka duration, with subsidence of 0.035 m/ka = 52 meters). As longer-term sea level progressively fell, progradation of siliciclastics was reorganized and eventually returned to the area filling in the space in front of the carbonate banks.

Regional studies indicate that siliciclastics from the Ouachita episodically prograded into the area from the southeast (Wanless and Wright, 1978). However, significant siliciclastics were supplied from the north during

accumulation of the Douglas Group at the close of the Lansing 3rd-order sequence. Recent studies by Archer et al. (in press) have described large (200 ft [61 m] deep by in excess of 20-miles [32 km]-wide) incised valleys that have been cut into pre-Haskell Limestone strata in the Douglas Group in northeastern Kansas. These valleys run southward through eastern Kansas and exit across the shelf margin in southeastern Kansas. Sediment was apparently bypassed through these valleys to reach a regional base level at that time, apparently beyond the shelf margin, accumulating to become what is called the Stalnaker Sandstone and associated lowstand siliciclastics. These siliciclastic sediments have been described as deltaic (Walton and Griffith, 1985) and estuarine (Archer, et al., 1992). The coarsening-upward succession of the broad Stalnaker in the basin is consistent with a progressive lowering of relative sea level resulting ultimately in bypassing and incision of the upper shelf. This pattern of abrupt inundation of the shelf, carbonate progradation, eventual clastic influx, and incised valley formation is very similar to that observed in the Kansas City 3rd-order sequence.

What was once the shelf-to-basin transition was nearly filled in by the time of Haskell Limestone deposition (Figures I.24 and I.25). The Heebner Shale, the datum of the cross section, is overlain by cyclothemic carbonates and siliciclastics representing shelf deposition in the region once part of the basin. The shelf setting of Virgilian persists through the remaining record of the Upper Pennsylvanian that is preserved here while basinal conditions shifted to the west toward the Anadarko basin. This suggests that the subsidence rates in the Arkoma basin diminished such that the depth of the sediment surface did not exceed the photic zone, whereas the depths did in the Anadarko basin. This is consistent with the evidence for the migration of the orogenic activity to the Marathon Mountains in southwestern U.S. by the lower Permian (Rascoe and Adler, 1983).

The proximity to foreland basin subsidence and basement structural and compositional heterogeneities apparently led to differential subsidence patterns. These trends and patterns in stratal thicknesses are described in the following section.

Stratal Architecture of the Pennsylvanian Kansas Shelf -- A Record of Basement Reactivation

Regional stratigraphic patterns in Kansas are revealed through a series of maps and cross sections derived from the regional database developed in this project. The information links the analog site studies in eastern Kansas with the oil field region in central and western Kansas.

The basement rocks were remapped over large areas of Kansas this project to establish the basis for structural interpretation. Previous published map of the Precambrian in Kansas is by Cole (1976). The revised Precambrian (Figure I.27) and combination Precambrian basement and top Arbuckle (Cambrian-Ordovician) (Figure I.28) maps represent substantial variations from previous interpretations in that faulting is readily

utilized. Most of the faults are high angle and are not cut by wells; fault throw is commonly less than several hundred feet and consequently can be easily mapped as folding. Many of the interpreted faults coincide with lineaments on the potential fields geophysical maps of Kansas which in turn closely delimit basement compositional and structural patterns (Figures I.29 and I.30).

Longer-term Stratigraphic Intervals

First, larger-interval isopachs are used to show the evolution of the shelf shortly before, during, and following the Lansing-Kansas City to illustrate longer-term patterns and changes to the shelf between near surface and surface analogs inn the east and field areas in the west. The intervals chosen for mapping closely follow the boundaries of the 3rd-order sequences. This section is then followed by a discussion of regional characteristics of the 4th-order cycles that comprise the 3rd-order Kansas City sequence.

Base of Pennsylvanian to Excello Shale

Only the central Kansas portion of the database is mapped (Figure I.31). Pennsylvanian strata included in the isopach interval are primarily the Lower Desmoinesian Cherokee Group comprised of siliciclastic-dominated 4th-order scale cycles (Figure I.25). Lower portions in thicker reaches of this interval include Atokan and possibly Morrow aged deposits including areas such as the Forest City basin in northeastern Kansas (Peppers et al, 1993). The map readily delimits the pre-Pennsylvanian uplifts -- Nemaha uplift, Central Kansas uplift, and the Pratt anticline through substantial thinning or lapout. Thickening is greatest east of the Nemaha uplift in the Cherokee basin. The area of the Sedgwick basin is moderately thick and separated from the Salina basin by a narrow east-west trending saddle extending through McPherson County. The base of Pennsylvanian is a unconformity surface developed over broad reaches of the craton during a time of lowered sea level. While sea level was low the craton became tectonically active with notable uplifts including the Sierra Grande uplift in northeast New Mexico and southeastern Colorado, the Central Kansas uplift, and the Nemaha uplift. The northeasterly trends of the thickening and thinning correspond closely with the orientation of structural and compositional variations in the Midcontinent Rift System (MRS), a 1.1 billion year old incipient rift (Figure I.29). The position of the Sedgwick and Salina basin as mapped here closely correspond to axial region of the MRS suggesting reactivation of the older structure as tectonic forces were introduced in the Late Paleozoic.

Base Pennsylvanian to Base Swope Sequence

The map area is extended using the base of Swope to base of Pennsylvanian. Prominent northwest trends and secondary northeast trends in thickening and thinning are apparent (Figure I.33). The interval closely parallels changes in the southern Pratt and Nemaha anticlines and Cherokee basin as seen on preceding map. A structural saddle separates the Sedgwick basin from the Salina basin centered in Marion County. The southern border of the saddle crossing Marion and McPherson counties trends west-northwest to a junction with the Central Kansas

uplift forming a prominent 90-degree bend. This bend coincides with the location where the uplift extends to the southwest. This feature is common on many of the interval isopachs. The west-northwest-trending lineament crossing Marion and McPherson counties closely parallels a basement fault and potential field lineament (Figures I.27-I.30).

In the western portion of the map, several abrupt changes in thickness occur along northwest-trending lineaments that parallel the Central Kansas Uplift. These trends do not appear to follow obvious basement heterogeneities. The prominent thickening of the interval in the southwest portion of the map is the eastern edge of a large, lower Pennsylvanian embayment. During the early Pennsylvanian (Morrow) the embayment was an interior seaway that extended northward from the resurging Anadarko basin (Figure I.33, Swanson, 1979). The Morrow and Atokan strata are limited to this embayment due to a lower stand of sea level and higher elevations of the surrounding region (Youle et al. 1994).

Morrow sediments were derived from surrounding uplands including the Central Kansas uplift, southeastern Wyoming, and the Sierra Grande Uplift in southeast Colorado and northeast New Mexico (Figure I.33, Swanson, 1979). The isopach of the Morrow strata and the locations of marine facies in this interval, as identified by Swanson (1979), suggest that active subsidence and consequent lower elevation of the depositional surface extended along the axis of the Anadarko basin and into the embayment alongside the eastern border of the Sierra Grande uplift (Figures I.33, Swanson, 1979). The northwest trend of the eastern edge of the embayment with thicker strata and greater sediment accommodation may be related to subsidence associated with movement (along high angle reverse faults) of the Sierra Grande uplift. The location of the abrupt increases in thickness, e.g., along the 400-ft contour in the southwestern portion of the map borders the broad "plateau" to east and coincides closely to the subcrop of the underlying Meramec Ste. Genevieve Limestone (Figure I.32).

A series of east-west structural cross sections constructed from structural elevation grids of the various mapped datums (Figures I.34-I.37) illustrate this abrupt and stepwise thickening of the early Pennsylvanian strata toward the Sierra Grande uplift. Strata succeeding the early Pennsylvanian thicken off of the Central Kansas uplift, but no where near the pronounced fashion of the earlier Pennsylvanian. In contrast brief, pronounced subsidence of the embayment, north-south cross sections reveal more gradual and consistent thickening of Pennsylvanian strata to the south toward the Anadarko basin in western Kansas.

Farther east, the cross sections reveal the location of abrupt thickening bordering the eastern side of the Central Kansas uplift. Also abrupt thickening of the lower Pennsylvanian is noted in the western margin of the Forest City basin.

Marmaton 3rd-order cycle -- Excello Shale to Nuyaka Creek Shale

The interval isopach from the Excello Shale to the Nuyaka Creek Shale, encompasses the carbonate-dominated, upper Desmoinesian Marmaton Group. The map covers south-central and eastern portion of Kansas and ranges in thickness from zero to 410 ft (125 m) (Figure I.38). The mapped area was all part of the shelf region during the Marmaton with the shelf margin residing in central Oklahoma (Figure I.18). Greatest thickness is in southeastern Kansas in the Cherokee Basin in closest proximity to the Arkoma basin where presumably greater accommodation was being created by higher subsidence in conjunction with continued foreland basin development. This pattern of gradual thickening toward the Arkoma basin contrasts with the isopach of the underlying Pennsylvanian interval (base Pennsylvanian to Excello) where thickness of the early Pennsylvanian was abruptly thicker adjacent to the Nemaha uplift. This early uplift and inferred relief along the Nemaha, Central Kansas, and Sierra Grande uplifts suggests a broad, consistent pattern of abrupt initial structural activity oblique to the foreland basin followed by gradual downwarping that extended progressively landward through time from the foreland basin.

Secondary (local) trends of thickness change often parallel earlier defined regional trends. For example, an area of abrupt northwesterly-trending thinning occurs immediately southwest of Kansas City. This structural feature lies adjacent to the Bolivar-Mansfield tectonic zone (Berendsen and Blair, 1991). Major thinning of 40 ft (12 m) occurred adjacent to the surface location of the Worden fault (Merriam, 1962). The Nemaha and Central Kansas uplifts are clearly denoted by areas of marked isopach thinning. The eastern border of the Central Kansas uplift, Nemaha uplift, and a linear-trending isopach pattern in the Sedgwick basin all trend northeasterly and overlie lineaments associated with the MRS. The northern extent of the linear trending isopachs in the Sedgwick basin terminates, roughly at the intersection with the Fall River tectonic zone (Berendsen and Blair, 1990) and corresponds to a saddle-shaped thinning on the other isopachs. This is also the general location of the terrane boundary between the granite basement to the north and younger rhyolite-granite terrane to the south (Figure I.29).

Portions of the Marmaton Group, represented by this 3rd-order sequence isopach thin and eventually lap out over the Central Kansas uplift (Figure I.18). Correlations from the database indicate that the lower 4th-order cycles in the Marmaton Group (e.g., Ft. Scott to Pawnee) cycles are more completely developed over the uplift with all of the cycle components than the younger Marmaton cycles (Figure I.39). The upper 4th-order cycles (Altamont and Lenapah) appear to thin and loose character against the underlying more uniform and continuous cycles of the Marmaton. The more uniform succession in the Kansas City 3rd-order sequence follows initiated by the Nuyaka Creek Shale. It appears that the regressive carbonates of the lower 4th-order cycles (e.g., Ft. Scott and Pawnee) were deposited during relatively higher sea level. This high to low trend in sea level for this 3rd-order cycle is paralleled by: 1) the presence of lower, thicker, more extensive radioactive black shales of the

Excello, Little Osage, and Anna and 2) generally lower Th/U ratios (more reducing conditions) for these lower cycles, the topic of later discussion. Previously discussed results indicate that the Marmaton 3rd-order sequence, dominated by marine carbonates, laps out higher on the shelf than the underlying Cherokee Group, indicating overall higher relative sea level than the Cherokee Group. The succeeding Kansas City 3rd-order sequence finally covers the uplift completely suggesting an even higher relative sea level.

Kansas City 3rd-Order Cycle -- Nuyaka Creek Shale to Muncie Creek Shale

The succeeding 3rd-order cycle, the Kansas City cycle extends from the Nuyaka Creek Shale to the Muncie Creek Shale. The Nuyaka Creek Shale forms the base of this interval and is the marine flooding event to first cover most of the higher reaches of the Central Kansas Uplift that had remained exposed since at least the beginning of the Pennsylvanian. The patterns of thinning also follows that of the isopach of the Marmaton 3rd-order cycle with more gradual thinning toward the Arkoma and Anadarko basins (Figures I.40 and I.41). The overall thickness of this interval is greater than the Marmaton 3rd-order. Since their durations are similar, accommodation during the Kansas City 3rd-order was greater either due to eustatic rise in sea level or increased subsidence.

Shelf areas that have equivalent thicknesses run generally east-west along the southern border of the state with a re-entrant in the Sedgwick basin, suggesting a localized sag over the old MRS (Figure I.41). Northwesterly-trending thinning continues to persistent over the Central Kansas uplift.

Thinning is more restricted to the Central Kansas uplift whereas the Pratt anticline appears to be less positive than it was earlier in the preceding interval. The southern edge of the more positive Central Kansas uplift forms an northeast trend coinciding with a prominent basement fault and potential fields lineament, both thought to be associated with the MRS. In contrast, the lineament is vaguely noticeable on the base Pennsylvanian to Base Excello Shale (Figure I.30). Interval isopachs of the overlying stratigraphic intervals indicate that this lineament also became a flexural hinge zone. Together these suggest the selective reactivation of basement weaknesses, perhaps related to changing orientation and magnitude of the tectonic stress field that apparently was affecting this area during the Pennsylvanian.

In southwestern Kansas a prominent northwesterly-trending thick extends over a nine-county area, covering a significant part of the Hugoton Embayment. This area of doubled interval thickness forms a rhombic-shaped embayment defined by a conjugate sets of northeasterly- and northwesterly-trending borders. The east-central northwest trending edge of this thick corresponds closely to the line of abrupt thickening of the interval from the base of Pennsylvanian to base K zone. The far eastern edge borders the Pratt anticline while the western limit of this thickened area borders the structural feature called the Cimmaron arch, an extension of the Sierra Grande

uplift. The northern border of this subsiding area is not clearly aligned with any obvious basement heterogeneity. The increased accommodation appears to be linked to subsidence of the nearby Anadarko basin. The pattern of thickening represents a significant modification of the shelf compared to the earlier Pennsylvanian.

Lansing 3rd-order Cycle -- Muncie Creek Shale to Haskell Limestone. Several interval isopachs are included here to show the changes that occur in this 3rd-order cycle. The interval isopach from the Muncie Creek Shale to the top of Lansing (lower 2/3rd of the Lansing 3rd-order sequence) reveals distinctive regional changes in the thickness patterns (Figure I.42). In the east the border of the thinner region of the Central Kansas uplift follows the same northeast trend as before, but continues northeastward until reaching McPherson County where it turns and becomes perpendicular to the southeast some 50 mi (80 km). The trend borders the eastern edge of the Forest City basin. The sag (thick) that existed in the northern Sedgwick basin no longer exists. The positive (thin) area previously inn the Cherokee basin became part of a composite thick increasing to the south. The thickening continues, but abruptly ends inn south-central and southeastern Kansas with an arching trend of rapid thinning farther southwest occurring over a distance of 2-3 mi (3-5 km). This abrupt thinning is caused by the abrupt termination of the Lansing Group carbonate units to the south. Cross section previously shown (I.24-I.25) illustrate the downlap of these carbonate units into sediment starved basinal units of the Lansing 3rd-order cycle. Only the lower portion of the Kansas City cycle was sediment starved along a more isolated portion of the lower shelf in southeastern Kansas. This will be described in more detail in the next section.

The siliciclastics abutting the carbonate units on the south were deposited later on the downlapped surface. Effectively, the lower shelf was drowned in that carbonate accumulation could no longer occur while subsidence continued uncompensated for by any significant sedimentation. The massive carbonate lithofacies thick appears to be a classic rimming carbonate bank "buildup" where conditions were well suited for carbonate accumulation. Samples indicate that this bank is comprised of lime mud-rich phylloid algal and open marine wackestone facies. These characteristics suggests that the bank built along a clear water, open marine shelf margin rather than along a siliciclastic wedge. The drowning of the previous carbonate bank may be due to increased subsidence or eustatic rise. However, the changing pattern of the thickness and close tie of these patterns to pre-existing structural elements suggests that differential subsidence is at least partly responsible for the drowning and reconfiguration of the carbonate-dominated shelf. Subsidence analysis in this area of sediment starvation indicates that this region underwent maximum subsidence in the state during the Pennsylvanian (0.035 m/ka). Even though the section notably thickens to the southwest, the shelf-to-basin transition was not developed there, presumably because subsidence was less (0.03 m/ka).

Also in western Kansas the positive shelfal setting situated over the Central Kansas uplift extends westward during this interval indicating changing sediment accommodation patterns. The extent of this thinning over such a broad region suggests some component of tectonic uplift, possibly related to development of a foreland basin peripheral bulge.

Another prominent change observed on this interval isopach is a parallel northeasterly trending lineament bisects the Central Kansas uplift. The presence of this lineament and associated spatial changes represents a marked contrast compared to the lower Pennsylvanian isopachs. This lineament is associated with a major southwest extension of thinning along the Central Kansas uplift. This lineament is situated 50 miles (80 km) northwest and parallel to the southeastern edge of the Central Kansas uplift. The lineament forms the northern edge of the Central Kansas uplift that is characterized by prominent northeast-trending faults that parallel the MRS. Again, reactivation of basement heterogeneities is indicated.

Top Lansing to Heebner Shale. The interval isopach from top of Lansing to Heebner represents the uppermost portion of the Lansing 3rd-order sequence (Figure I.43). Further evolution of the shelf configuration is noted, most prominently a northeast-trending flexural hinge bisecting the Central Kansas uplift. The southerly positive (thinned) area of this uplift is no longer present, but is absorbed into the west end of a broad area of increasingly thick (and presumably subsiding) region bordering the Arkoma and Anadarko basins. This southerly dipping hinge zone overlies and parallels a set of underlying northeasterly trending basement faults. Farther north the Central Kansas uplift is no longer delimited as an isolated positive (thin) area, but rather there is a very broad, thin region covering much of western Kansas as described previously. In effect, the northwest-trending embayment that once existed in western Kansas during the lower Pennsylvanian is no longer active. Subsidence patterns have effectively rotated from that position to a location now facing the Arkoma and Anadarko basins to the south.

North of the hinge zone on the positive shelf in western Kansas, the Douglas Group siliciclastics that form the majority of the interval are very thin and carbonates and clearly marine strata included such as the Iatan and Haskell limestones are also very thin. In addition, cores from this broad, thin region in northwest Kansas indicate that the Douglas Group is comprised of oxidized red shales. This evidence suggests less sediment accommodation space and more emergence; either the area was structurally uplifted or sea level fell. The regional cross sections shown earlier indicate lateral accretion of the carbonate margin followed by substantial infilling of the basin by siliciclastics by the end of the Lansing 3rd-order cycle. Also redox profiles from Th/U ratios on the shelf indicate more oxidizing conditions and thus more emergence for the later part of the Lansing 3rd-order sequence throughout Kansas well beyond this particular area suggesting loss of sediment accommodation space. Reduction in accommodation is at least shelf wide. The clastic-dominated deposition in

the Douglas although significant in thickness was restricted to the mid and lower shelf regions of southern and eastern Kansas. This suggests that the region was possibly lower elevation than to the northwest. These clastics were sourced from both the northeastern shelf (a cratonic source) and from the southeast from the Ouachita front. The competent southeastern sediment source represents the initial stage of long-term sediment progradation across the Arkoma basin (Wanless and Wright, 1978).

The Douglas Group is currently included in base of the Virgilian Stage of the Upper Pennsylvanian. It is divided into a lower Stranger Formation and an overlying Lawrence Formation. The Haskell Limestone, located at the base of the Lawrence Formation, is a significant regional marker that extends from eastern Kansas to the western part of the state and into adjoining Nebraska and Oklahoma. The Missourian-Virgilian boundary is currently recognized at the top of the South Bend Limestone (currently in the Stanton Formation of the Lansing Group) in Kansas, Nebraska, and Iowa, but is placed at the base of the Tonganoxie Sandstone in Missouri. New conodont and ammonoid information suggest that the Missourian-Virgilian boundary may actually be located in the Douglas Group. The only faunal change in the interval between the Eudora Shale (Stanton Limestone) and the Heebner Shale (Oread Limestone) occurs in the thin dark marine shale called the Little Pawnee Shale associated (as the core shale) with the Haskell Limestone. This change has been recognized throughout the Mid-Continent, Texas, and Illinois. The Little Pawnee shale contains the first appearance of the distinctive idiognathodid conodont Streptogathodus zethus (Heckel and Watney, 1991). Boardman and Heckel (1989) proposed that the base of the Virgilian Stage be placed at the base of the Haskell Limestone. This boundary is consistent with major stratal changes as described herein.

Lansing to Haskell Isopach. Although the mapped areas of the Lansing to Haskell isopach is restricted to central Kansas, it reveals the extremely thin and uniform region in north-central and northwestern Kansas (Figure I.44). In contrast, the northwest-trending eastern edge of this thin abruptly abuts a broad thickened region overlying the northern Sedgwick basin. This northwest trend parallels the eastern faulted margin of the Central Kansas uplift as it was developed during the early Pennsylvanian. The broad, attenuated interval to the west suggests reduced accommodation. This loss in accommodation may have occurred through eustatic lowstand late in the Lansing 3rd-order sequence as suggested by stratal geometries depicted in the cross sections (Figures I.24 and I.25).

The reduced sediment accommodation and probable sea level lowstand during the Haskell Limestone interval is strengthened by evidence of pronounced incised valleys with dimensions of up to 140 ft (43 m) deep x 15 mi (24 km) wide crossing eastern Kansas unto the lower shelf in southeast Kansas (Linn, 1950; Winchell, 1957; Sanders, 1959; Archer et al., in press).

Haskell Limestone to Heebner Shale. The isopach of the interval from Haskell to Heebner accounts for all of the notable southerly thickening developed in the Lansing to Heebner isopach (Figure I.45). The implications are that downwarping of the shelf along this hinge occurred rather abruptly during the time this interval was deposited coinciding with the beginning of the next 3rd-order sequence. Significant increase in accommodation on the upper shelf did not occur until after Heebner Shale deposition, suggesting the onset of the overlying 3rd-order sequence was longer term including the post Haskell to Heebner interval.

Fourth-Order Sequences

Each of the 3rd-order cycles discussed to this point include generally five or six 4th-order cycles. This section examines stratal composition and architecture and distribution of six successive 4th-order cycles that comprise the Kansas City 3rd-order cycle. Strata include Pleasanton and Kansas City groups and lowermost Lansing Group. This succession illustrates the evolution of the shelf during a single 3rd-order cycle and is used to demonstrate analogous shelf conditions between the outcrop in eastern Kansas and the producing region in central and western Kansas. These fourth-order cycles are the basic correlatable stratigraphic mapping units of Lansing-Kansas City petroleum reservoirs. They are easily recognized and correlated on wireline logs and observable in surface exposures. The 3rd-order cycles on the other hand are not easily established on the wireline logs and are never fully exposed in surface exposures.

Figure I.46 depicts the Pleasanton, Hertha, Swope, and Dennis sequences (4th-order cycles) along a cross section extending from near Kansas City, Missouri to near Coffeyville, in extreme southeastern Kansas. The datum of the stratigraphic section is the Nuyaka Creek Shale, the base of the 3rd-order Kansas City sequence. This datum coincides with a major 3rd-order boundary distinguished by an overstepping of the Kansas City cycle over the Marmaton 3rd-order sequence (Figure I.23). The Pleasanton, Hertha, and lower Swope sequences undergo sediment starvation in the northern Arkoma basin as depicted on the southern part of the cross section in Figure I.46. These stratal geometries were validated with strategic coring and use of surface exposures. Sediment-starved sequences are represented by a succession of thin (< 2 m) organic-rich marine shales without significant intervening carbonates. The carbonates in each starved sequence downlap into the basin in an updip position. This sediment starved interval extends approximately 75 mi (120 km) southward into Oklahoma (Figure I.47). Farther south these sequences thicken substantially as siliciclastic-dominated successions introduced from the Ouachita front (Bennison in Watney et al., 1989; Bennison, 1985). The axis of the depositional basin lie in the sediment-starved area between clastic southern wedge and the carbonate shelf to the north in Kansas. The result is that the continuous dark marine to black radioactive shales representing condensed sections (connected by continuous lines on the cross section), including the Mound City and Hushpuckney shales, converge in a basinward direction due to the loss of the intervening strata. In contrast, subaerial exposure surfaces and paleosols are developed at the tops of the sequences across the northern shelf. These terminate before reaching

the lower portion of the sediment starved shelf and depositional basin (not seen in core or surface exposures) placing constraints on the lowest elevation of subaerial exposure. In the Marmaton Group, carbonate platform deposits and subaerial surfaces were developed southward across the entire lower shelf area in northern Oklahoma indicating a lower stand in relative sea level or that subsidence increased markedly during the Missourian lowering the depositional surface.

The other aspect of this shelf-to-basin transition is that while early 4th-order cycles (Pleasanton, Hertha, and early Swope) are sediment starved, sediment aggrades and progrades into the basin and fills it over the duration of several successive cycles. This infilling was accomplished in the lower Kansas City Group with the accumulation of siliciclastics in the upper Swope sequence and lower Dennis sequence. These siliciclastics are limited to these lower shelf areas and are interpreted to represent lowstand in sea level, i.e., accommodation was lacking in the higher shelf. The equivalent of these siliciclastics on the upper shelf are thin shales containing paleosols. The upper sequence boundary of the Swope is a paleosol that extends through the lowstand siliciclastics and into the thin shales on the shelf. The upper Swope sequence also contains a thin but widespread marine limestone on the lower shelf that onlaps the overlying Bethany Falls limestone of the Swope at intermediate elevations on the shelf. Apparently, during lowstand a minor marine inundation resulted in deposition of this limestone. The terminating paleosol onlaps onto an underlying paleosol developed on the Bethany Falls limestone along the intermediate shelf elevations where the upper limestone laps out. This indicates that sea level fell at least twice in association with this sequence.

A series of isopach maps of the depositional sequences in Kansas are presented in the order of deposition (Figures I.49 through I.64) (Pleasanton, Hertha, Swope, Dennis, Cherryvale, and Dewey). The succession of maps and cross sections depict the progressive stages of aggradation and progradation on the Kansas shelf during the Kansas City 3rd-order cycle.

Pleasanton Sequence. The upper, northern shelf in eastern Kansas depicted in the top half of the cross section (Figure I.48) contains a 150+ ft (46+ m) thick deltaic and shallow marine shelf shale and sandstone succession comprising the Pleasanton sequence. The Pleasanton thickens up to 200 ft (61 m) forming a broad clastic apron in eastern Kansas (Figure I.48). The southern edge of this unit thins abruptly over 1-2 mi (1.6-3.2 km) in Neosho and Bourbon counties in and near the outcrop as illustrated in the cross section. Locations south of the clastic wedge (less than 30 ft thick) are have been documented as sites of sediment starvation and anoxia attributed to deeper shelf setting most distant from clastic influx and too deep for carbonate accumulation. These stratal relationships along the southern edge of the clastic thick are further substantiated with closely spaced logs and cores. This slope extends westward 120 mi (193 km) along the edge of this clastic wedge. The

southern edge of the Pleasanton changes in thickness at the rate of 20 ft/mi (3.8 m/km), over 20 times the average rates on the shelf.

This inferred steep margin has salients and embayments suggesting morphologic features like deltaic protrusions. The general appearance resembles the general character of the delta-dominated Gulf Coast shelf margin comprised of multiple episodes of deltaic progradation in association with late Pleistocene and Holocene sea-level changes.

The western margin of the Pleasanton clastic wedge coincides with the position of the Nemaha uplift suggesting onlap onto this area of structural change. The rate of thinning here is much more gradual. Farther west the thinning of the interval is even more prominent, locally missing over the Central Kansas uplift. On the lower shelf in southwestern Kansas a marine limestone locally thickens to become a correlable unit, reflecting increasing accommodation without siliciclastic influx.

The thick clastic wedge continues to the outcrop in western Missouri while it thins northward into southwestern Iowa. The source of the clastics is indicated from eastern Missouri (Ozark uplift?) (Howe, 1982).

Hertha Sequence. A prominent feature seen in a map of this sequence is the large continuous east-west, oriented interval thick located adjacent to the steep southern margin of the Pleasanton sequence. The linear thick is a carbonate bank in the Sniabar limestone member within the Hertha sequence. Thickness ranges up to 100 ft (30 m) thick situated as an amalgomated unit along the slope created by the Pleasanton clastic wedge. The mound contains predominately mud-dominated phylloid algal mound facies (bioclastic wackestone) (Figure I.49). The Hertha bank is accreted to the entire 120 mi. (190 km) long margin of the Pleasanton clastic wedge. Two culminations of the bank occur, one in Wilson County and another along the western margin in Sumner and Kingman counties. A local northeasterly elongated bank is developed in Sumner County, a site located immediately west of the Nemaha uplift.

The lateral accretion of the Hertha carbonate bank in southern Kansas extended the shelf over 19 mi (30 km) basinward beyond the base of the Pleasanton slope overstepping the condensed section (Mound City Shale) of the Hertha sequence. This amounts to an effective progradation rate of 0.1-0.05 mi/ka (0.16 to 0.08 km/ka). The rate depends on the sequence duration ranging from 200 ka minimally or 400 ka maximally (Heckel, 1986). Maximum carbonate production apparently occurred along the seaward margin of the slope break where increased accommodation space was available along with favorable environmental conditions such as nutrient supply (Figure I.49). The development of this bank (internal stratal architecture) is described in the section on analog studies and is also modeled by computer simulation.

The basinal equivalent lithofacies of the carbonate bank based on strategic coring and log correlation in southern Wilson County appears to be a thin (<2 ft) dark, organic-rich, argillaceous wackestone with crinoids, brachiopods, spirorbids, and encrusting forams. No evidence of subaerial exposure was recognized in this lower shelf (basinal) position.

In western Kansas the Sniabar Limestone of the Hertha sequence is characterized by locally thick oolitic grainstone bar deposition. The patterns of both broad northeast and northwest trending sequence thicks in this region follow, in part, previously documented trends in shelf configuration and structure. A northwest trend flanks the western edge of the Central Kansas uplift and Pratt anticline. One of the thick trends passes adjacent to Victory field, the site of detailed field study, and through nearby Northeast Lemon field. The Sniabar Limestone consisting of a thick oolitic grainstone is a prolific producing unit in Northeast Lemon field. The northeasterly trend along which this thick coincides with the location of a later flexural hinge developed during the Haskell to Heebner interval. Perhaps an early episode of structural movement occurred.

The Hertha sequence thins across the Central Kansas uplift. The interval is also very thin overlying the thick Pleasanton clastics in the Kansas City area in eastern Kansas. Surface exposures of the Sniabar Limestone in this mid shelf area typically reveal complex, multiple episodes of subaerial exposure including a significant paleosol that caps the sequence (Elm Branch Shale).

Swope Sequence. The Swope sequence overlying the Hertha is relatively thick and contains a complex stratigraphy in the analog area in southeastern Kansas. The Swope sequence is the focus of the detailed analog study in southeastern Kansas and field investigation at Victory (Figure I.50). The regional isopach of the sequence presents a pattern of broad thinning of the upper shelf rimmed by thick areas to the south and west. Similar thicknesses coincide closely with similar stratigraphy and facies composition as detailed site studies will later show. For example, the stratigraphic character and lithofacies of the Swope sequence in the analog area in southeastern Kansas is very similar to areas in southwestern Kansas. The two isolated northeast-trending thicks in central Kansas parallel pre-existing magnetic lineaments of the Precambrian Midcontinent Rift System in the area of the Sedgwick basin. The pattern and location suggests more accommodation space was available over the old rift with local variation in elevation (subsidence) along old basement heterogeneities.

The Bethany Falls Limestone of the Swope sequence has been described on the upper shelf as a simple regressive shallow-water carbonate where sediment accommodation is limited, e.g., Kansas City area and the Central Kansas uplift. In this study, the Bethany Falls Limestone is shown to contain at least two distinctive regressive limestones containing multiple subaerial exposure surfaces along lower reaches of the shelf. A Swope sequence thick rims the Sniabar Limestone bank margin in southern Kansas, including pods of oolitic grainstone

(Figure I.51). The Mound Valley Limestone, recognized because of its mappability in southern Kansas, overlies the Bethany Falls Limestone. The Mound Valley Limestone, up to 35 ft (11 m) thick, is apparently a minor marine cycle in the Swope sequence that is restricted to the lowermost shelf. This limestone is separated from the Bethany Falls by the Ladore Shale (Figure I.53). The Ladore Shale can be up to 70 ft (21 m) thick on the lower portions of the shelf. The Galesburg Shale overlies the Mound Valley Limestone. This shale contains a regionally significant paleosol identified as the sequence boundary. A thin, but very widespread coal, the flooding unit of the overlying sequence initiates the next sequence (Figures I.46 and I.54).

Northward, the paleosol in the Galesburg Shale merges with the top of the Mound Valley and eventually the paleosols at the top of the Bethany Falls Limestone when the Mound Valley Limestone laps out (Figure I.46). The Galesburg Shale while in excess of 170 ft (52 m) thick in the basin thins to under 3 ft (1 m) on the upper shelf. The Bethany Falls on the upper shelf (Kansas City area and Central Kansas uplift) (Figure I.50) contains substantial evidence of subaerial weathering (microkarst, deep weathering profiles, shale infilling). The paleosols observed in the sequence higher on the shelf typically show multiple events, e.g., microkarst followed by laminated calcrete.

The Swope cycle developed in the analog area provides critical information to reveal what appears to be a complex sea-level history that makes up individual sequences. The extensive coring program at the Woodward transect described later integrates the regional and local (reservoir-scale) characteristics that develop the relevancy of this work to reservoir prediction. Separate grainstones shingle the depositional slope at the Bourbon County analog site, each apparently temporally distinct, some unconformity bounded, and, in some cases, with different diagenetic histories. This has significant ramifications for reservoir prediction, namely lateral and vertical continuity of grainstones and diagenetic compartmentalization.

Victory field in Haskell County lies at a similar shelf elevation to the analog site in Bourbon County as interpreted from the regional isopach of the sequence (Figure I.50). The Bethany Falls Limestone contains three stacked oolites that crest and flank the structure in Victory field, relationships similar to that observed at the near-surface analog site. This will be described in more detail in a later section.

The availability of siliciclastics during low stand in southeastern Kansas lead to greater stratigraphic complexity (high fidelity) of the Swope cycle (Figure I.46). The accumulation of lithologic units comprising the upper portion of the Swope sequence in southeastern Kansas resulted in further lateral accretion of the shelf margin some 20 mi. (32 km) from the original slope associated with the Hertha sequence (Figures I.50). The thicker, basinward portion of the Galesburg Shale is interpreted as a lowstand deposit infilling the lowermost reaches of the shelf. This relationship is shown to persist to the west (Figures I.24 and I.25).

An isopach map of the porous carbonate in the Swope cycle is primarily a reflection of the distribution of grainstone (Figure I.55). Simple patterns of porosity distribution are recognized that correlate well with the overall thickness of the sequence and inferred shelf configuration. The broad thinning of regional porosity over the Central Kansas uplift and western Kansas shelf parallels the thin nature of the overall cycle (Figure I.50). Grainstones are present, but are thin to moderate thickness. The thinning on the upper shelf is rimmed by isolated and coalesced lobate thicks of porous carbonate which extend southward across the lower shelf. Cores and cuttings from these thick porous intervals indicate oolitic grainstone similar to that in Victory field. The porous carbonate wraps around the upper shelf with thickest lobes in southwestern Kansas and surrounding the Central Kansas uplift.

A hand-contoured version of the porosity map in western Kansas simplifies the patterns and delineates large lobes of oolite (each around 5 x 20 mi, 8 km x 32 km) that rim the shelf (Figure I.56). The heavy lines on this map are 4th-order trend surface contours fit to the thickness of porous carbonate. Where the rate of thickening of the cycle is greatest, the oolite lobes are thickest forming a ramp (including the Victory field area) extending across southern Kansas. Much of the thickening of this sequence is contributed by the oolite and associated shoal water deposits.

The southwestern mapped is shaped like a broad embayment (Figure I.50). Similarly the area in the Sedgwick basin is a narrow re-entrant into the platform. These apparent topographic embayments may have helped to accentuate tidal current action aiding in deposition of the thick oolites. Thickness in excess of 50 ft. (15 m) of porosity and grainstone perhaps reflects the stacking of a succession of minor marine cycles as documented from the reservoir analog area in southeast Kansas and at Victory field.

Dennis Sequence. The thickness of the Dennis sequence in Kansas illustrates a lower shelf (thick), mid shelf (moderately thin), and upper shelf (thin) settings (Figure I.57). Thicknesses over the mid shelf region east of the Central Kansas uplift are greater than that of the Swope sequence while areas west of the uplift indicated more thinning in the Dennis sequence. The analog site in southeastern Kansas and at Victory field both lie on the lower shelf. A large carbonate buildup developed in the analog area extends west intermittently to the Pratt anticline and into the southwestern part of the state. Cores in the analog area indicate that the buildup consists of interbeds of oolitic grainstone and bioclastic phylloid algal wackestone. Sediment starved conditions are confined to the lowermost shelf in extreme southeastern Kansas.

The Canville Limestone (flooding unit) and the Stark Shale (condensed section), and Winterset Limestone (late highstand regressive carbonate) comprise the Dennis sequence. The upper portion of the lowstand Galesburg Shale also is included in this genetic package on the lower shelf in southeast Kansas. The sequence boundary is

imbedded in this clastic unit delimited by an extensive paleosol. This bounding surface is succeeded by deposits initially indicative of gradual inundation with coal and estuarine lithofacies.

Even though this sequence is part of the 3rd-order Kansas City cycle of longer-term relative sea level change, a modest rise in baselevel is noted in eastern Kansas based on cross sections and maps (Figures I.46 and I.57). The evidence is sediment starvation returning to the extreme lower reaches of the shelf in southeastern Kansas in a location when thick lowstand siliciclastics had previously filled the basinal area. These data indicate moderate landward backstepping of the Dennis carbonate margin to the site of the underlying Hertha bank area, approximately 20 mi (32 km). The drowning of the carbonate shelf may be attributed to renewed subsidence or eustatic rise, but additional regional information would be needed to make this distinction. A corresponding backstep of the siliciclastic flysch sediment wedge in eastern Oklahoma is noted by Bennison (Figure I.47). This increased accommodation if due to foreland basin subsidence was not closely followed by clastic progradation into the basin.

The Canville Limestone is a basal unit of the Dennis sequence thought to be associated with initial marine flooding of the shelf. An isopach map of the Canville Limestone (flooding unit of the Dennis sequence) in southeastern Kansas reveals a narrow linear carbonate buildup that parallels and lies immediately basinward of the superjacent Winterset Limestone buildup of the Dennis sequence. The lithology of this Canville carbonate buildup is primarily phylloid algal wackestone. Although the flooding is inferred to have been rapid due to a usually thin or missing Canville Limestone, the buildup suggests a reduced rate of rise or stillstand during the overall rapid flooding of the shelf.

The location of this buildup coincides with the southern edge of the Mound Valley Limestone buildup. This position represents a slight backstep from the position of the Swope sequence shelf margin. Furthermore, this clearly defined linear trend cross-cuts thick subjacent clastic facies of the Galesburg Shale that filled in the lower shelf.

The isopach map of porous carbonate in the Dennis cycle coupled with core and sample information again indicate thicker oolitic grainstones rim the western Kansas shelf (Figure I.60). The northern limit of these thick grainstone lobes do not occur as high on the shelf as in the Swope sequence, suggesting that the backstepping event noted in eastern Kansas may not have occurred in this part of the shelf or that the flexure of the shelf or previous progradation limited the extent of the ramp inferred to have developed where oolite was deposited. Increased subsidence could have occurred in the east adjacent to the Arkoma basin and not in and locally adjacent to the Anadarko basin.

The northern-most updip edge of the porous carbonate is a series of moderately thick landward-oriented lobes rimming the upper shelf. Further south a set of thicker porous lobes forms another rim paralleling the first (Figure I.60). Only thinner, scattered grainstones occupy the northern shelf such as at Pen and Cahoj field where the Winterset is a primary pay zone. The southwestern thick porous carbonate is particularly thick around the embayment previously described.

Multiple zones of grainstone are characteristic of the Winterset Limestone of the Dennis sequence across the entire shelf resembling the Swope sequence along the lower shelf. The multicycle behavior in the Dennis is quite apparent along the upper shelf, e.g., Pen and Cahoj fields (Figure I.61).

Cherryvale Sequence. The Dennis sequence is overlain by two additional 4th-order sequences (Cherryvale and Dewey) completing the 3rd-order Kansas City sequence. Lateral accretion and filling of the lower shelf margin continued during the Cherryvale sequence indicated by evidence of continued broadening of the area of thinning and inferred reduced accommodation space on the northern shelf (Figure I.62). The sequence is generally thinner than the Swope and Dennis. Marked thinning of this sequence extends through much of western Kansas, particularly southward across the Central Kansas uplift.

The marine deposits of the Cherryvale sequence lap out along the extreme northwestern portion of the shelf. Furthermore, there is no condensed section (marine shale) developed through most areas on the shelf. Both lines of evidence are consistent with lowered relative sea level (Figure I.62). North of the pinchout of the Cherryvale marine interval only a thick paleosol is noted between the Dennis and Dewey sequences in a core from Cahoj field. No significant erosion in indicated.

The Montgomery County Drum Limestone (part of Cherryvale sequence) analog area, described in more detail later, resides along the extreme lower shelf margin where accommodation is believed to have been considerably more significant. Furthermore, local topography and appreciable slope led to notable lateral accretion in this lower shelf setting. The thick oolite described in this analog area developed along the forward edge of the shelf margin. Sites analogous to this site are restricted to the lower shelf in western Kansas.

The isopach of porous carbonate in the Cherryvale sequence shows broad northwesterly and northeasterly trends of moderate thicknesses of porous carbonate over the shelf. Grainstones are still prevalent in the Cherryvale as in the lower cycles, but are thinner. Even though the rim of the shelf is now displaced basinward into southern Kansas (Figure I.63) the thicker grainstones are still scattered across the shelf and are locally quite productive. This may be due to the generally lower sea level (suggested by the updip lapout and loss of the condensed section) coupled with a sequence dominated by numerous small-scale cycles creating multiple episodes of shoal-

water conditions at a particular position on the shelf (Figure I.61). Local topography would play an important part in development of these grainstones. Thick porous carbonate is again found on the eastern flank of the Central Kansas uplift in the Sedgwick basin overlying the Midcontinent Rift System where the sequence is generally thick. Some of the porous areas are not accompanied by overall thickening of the sequence suggesting compensating thickening and thinning of stratal units in the sequence or lateral facies change without notable buildups or topographic expression.

Dewey Sequence. The Dewey sequence is located at the top of the 3rd-order Kansas City sequence and is associated with multiple evidence for lower sea-level conditions associated with the close of the 3rd-order sequence. The rather broad, uniformly thin nature of the sequence suggests a platform settings exhibiting limited accommodation space (Figure I.64). The most positive location on the shelf (greatest thinning of sequence) occurs along the southern Central Kansas uplift and Pratt anticline continuing this site of thinning in the underlying Cherryvale sequence. This represents the most southerly position of the positive area since the Middle Pennsylvanian. Progressive lateral accretion and infilling by the series of underlying cycles reduced and eliminated the inferred ramp along the southern shelf suggesting static or falling baselevel. The renewal of the southern position of the Central Kansas uplift suggests structural rejuvination. The rather level platform expression of the shelf and limited accommodation upon it suggests that regional relief was limited. This is supported by the limited occurrence of grainstones compared to the underlying sequences (Sniabar, Swope, Dennis, and Cherryvale) and the common development of isolated, but often very broad biostromal phylloid algal banks typifying the Dewey cycle on the upper shelf in western Kansas (Figures I.61 and I.65)(Watney, 1985; 1987). Locally, relief was sufficient to produce thin, sporadic local grainstone buildups such as in parts of Victory field.

Outside shales that lie below and above the Dewey sequence, namely the Nellie Bly and Chanute shales, are thick basin infilling shales in southeast Kansas analogous to the Galesburg Shale beneath the Dennis sequence. These intervals contain prominent incised valleys often filled by very coarse limestone conglomerate suggesting lowstand conditions and erosion of the shelf. This evidence suggests a long-term trend to increasing loss of accommodation and more significant lowstand closing the 3rd-order Kansas City sequence.

Evidence of Relief on Shelf During Deposition of 4th-Order Sequence. Individual sequences show considerable thinning over the northern shelf and uplift areas. Corresponding changes in facies and diagenesis support an interpretation of higher elevation of the shelf including:

1. loss of black shales over the crest of the Central Kansas uplift in all cycles. Where the condensed sections are lacking, very thin phosphatic and skeletal lag deposits locally occur at the flooding

surfaces. Also flooding and regressive carbonates exhibit no marked interruption of sedimentation between them, e.g. Cherryvale sequence. The Dennis and Dewey sequences and the underlying Swope sequence all contain widespread black shales, each of which is locally missing over the Central Kansas uplift, and all of which grade to gray shale northward.

2. shallow-water carbonate facies are more frequent and often occupy a greater proportion of the cycles over the Central Kansas uplift and upper shelf;

3. evidence for more intensified and multiple episodes of subaerial exposure across the upper shelf.

4. The lower portions of the late high-stand carbonates (Swope, Dennis) on the lower southwestern Kansas shelf contain dark, silty, pyritic, organic-rich carbonate lithologies. Dysoxic fauna are present. The Th/U ratios are lowest in any facies in these intervals indicating more reducing conditions. This is consistent with lower shelf conditions where the change from deposition of condensed section to carbonate may have alternated back and forth analogous to paleosols and marine position on the high shelf.

Northward, and even higher on the shelf in southern Nebraska along the transcontinental arch, solution karst is very common and red oxidized siltstones and silty carbonates are common (Rascoe and Adler, 1983; Watney, 1980). Also, mixed-clast carbonate pebble conglomerates and thick paleosols attest to significant weathering and local erosion of the carbonates on the upper shelf in southwestern Nebraska (Watney, 1980; Dubois, 1885; Prather, 1983).

Southwestern Kansas did not receive significant clastic influx because of the persistently deep adjoining Anadarko basin and the long distance from the minor clastic influx to the north and to the west (Cimmaron arch). Due to a lower shelf elevation, greater accommodation space was available for marine sediment leading to thicker deposits recording greater fidelity of sedimentary events. Due to the ramped shelf early in the 3rd-order Kansas City sequence, thick and extensive oolite deposits accreted along the broad slope over southwestern Kansas, (covering approximately 16,000 mi^2 [41,000 Km^2]). Accommodation was probably provided by a combination of subsidence and eustacy, modified by sediment accumulation and local depositional topography.

Relative Sea Level Curve for the Pennsylvanian

Ross and Ross (1987) produced a relative sea-level (coastal onlap) curve for the Pennsylvanian (Figure I.59). A similar diagrammatic relative sea-level curve was developed for summary purposes for the Midcontinent

Pennsylvanian based on evidence provided by the cross sections, regional mapping, and Th/U ratios (Figure I.60). The sea-level curve reflects the 3rd- and 4th-order sequences recognized from the Atokan through the early Virgilian. The letter scheme in the lower portion of the Pennsylvania were assigned by Youle (1992). Onlap and downlap, 5th-order cycles, and 4th-order Desmoinesian and Atokan sequences developed along the eastern margin of the Hugoton embayment are described by Youle et al., in press.

The rhythm of the sea-level history is apparent, even from this diagrammatic treatment. The cause and effect are still in question. The diagram reveals a 2nd-order cycle (10's millions of years) with a long-term change in sea level initiated with the Pennsylvanian. Third-order cycles are distinguished by the bundling of sets of 4th-order cycles. The boundaries of the higher 3rd-order sequences are identified by flooding units (Excello, Nuyaka Creek, Muncie Creek, and Heebner shales).

SUBTASK 1. FIELD SCREENING AND RESERVOIR ANALOGUE IDENTIFICATION

by W.L. Watney and W. Guy

1.A. Field Selection

The objective of this subtask is to assess the variations and trends in reservoir character of the Lansing-Kansas City carbonates at different geologic settings in Kansas in order to establish the range in variability and to select fields that represent this variability for further study. Selection of fields was based on their location in contrasting geologic settings, including shelf position and current structural setting as discerned from the regional investigation. Structural provinces in the producing area include the Central Kansas Uplift, Hugoton Embayment, Pratt Anticline, and the Sedgwick Basin (Figure I.27). The shelf setting varies from an upper shelf location in northern Kansas (most distant from the Anadarko and Arkoma basins) to a lower shelf position in southern Kansas recognized as variations in sediment accommodation and paleotopography as inferred from facies mapping and interval isopaching, e.g., base Swope Sequence (K zone) to Muncie Creek Shale interval isopach (Figure I.34). Reservoir development and stratal architecture are compared in selected fields located in these contrasting locations. The focus of the new field investigation was in Victory field, located on the lower, southern shelf in the Hugoton Embayment. Victory field was compared with Cahoj and Pen fields located on the upper, northern shelf on the Central Kansas Uplift (Figure 1.A.1). Table 1.A.1 lists several Lansing-Kansas City fields and basic parameters that have been studied at KU in the recent past.

TABLE 1.A.1. SELECTED LANSING-KANSAS CITY FIELDS

FIELD	DISC	ACRES	CUM. BBLS	RES. ENERGY	NO. OF PAY ZONES
1. Cahoj, Rawlins Co.	6/59	2960	7,724,863	pressure depletion	9
NE Cahoj	8/70		872,811		
W Cahoj	4/62		785,000		
2. Adell, Sheridan Co	5/44	1200	8,558,104	solution gas	5+
3. Pen, Graham Co	5/85	680	583,618	solution gas	2
4. Max, Stafford Co	5/38	2400	13,039,902	solution gas	3+
5. Collier Flats, Com Co	7/70	2560	995,191	solution gas	1
6. Victory, Haskell Co	12/60	6550	10,892,000	solution gas+ minor water drive	5
7. Hall-Gurney, Russell	5/31	49160	148,889,912	solution gas?	5+
8. Wilson Creek	1/67	1760	7,573,970	solution gas ?	1

The primary reservoir type represented in this study is carbonate grainstone. The size and shape of individual carbonate grainstone bodies are highly variable and are difficult to define in producing fields due to the well spacing and limited sampling. Results from this project suggest that simple circular grainstone pods with dimensions of approximately one mile are a composite of several grainstone units formed by multiple events. This will be apparent in the ensuing discussions.

The grainstones reservoirs and analogs mapped to date using available subsurface data suggest a range of overall dimensions (Table 1.A.2). As shown in this study, these pods are separated into individual flow compartments because of depositional, diagenetic, and structural controls.

TABLE 1.A.2. OVERALL DIMENSIONS OF SELECTED GRAINSTONE RESERVOIRS IN WESTERN KANSAS

Field/Analog Area	Maximum Thickness	Areal Dimensions
Cahoj -- Dennis	15 feet maximum	3 X 2 miles
Pen -- Drum, Dennis	14 feet maximum	1.5 X 0.75 miles
Adell --	5 feet maximum	1.5 X 1 miles
Max -- Swope	16 feet maximum	1 X 0.5 miles
Collier Flats -- Swope	8 feet maximum	1.25 X 0.5 miles
Victory -- Swope	40 feet maximum	5 X 1.5 miles
Kansas City area -- Dennis	13 feet maximum	0.75 X 0.2 miles
Bourbon County -- Swope	30 feet maximum	7 X 2 miles
Montgomery County -- Drum	60 feet maximum	12 X 3 miles

In general, post depositional diagenesis can introduce significant heterogeneity. Meteoric freshwater diagenesis during subaerial exposure has been recognized as an important process in porosity and permeability development in Lansing-Kansas City carbonate rocks (Watney and Ebanks, 1978; Watney, 1980; Watney and French, 1988). Subaerial exposure has been attributed to prolonged periods of emergence of the western Kansas shelf at the close of each depositional cycle; diagnostic evidence for this is abundant in the rocks. Original depositional fabrics such as layering and cross bedding and the associated porosity- permeability framework are often heavily altered, leading to either enhancement of overall porosity or reduction or occlusion of porosity. The intensity of subaerial exposure appears to vary across the shelf in western Kansas, from moderate levels on the lower shelf in southern Kansas to extreme levels of alteration on the upper shelf (Watney, 1980; 1985).

Cahoj field

The basic geologic characteristics of the reservoirs in Cahoj field, an upper shelf field, were compared with those in Victory field, a lower shelf field (Figure 1.A.2). In particular, the super-Pickett plot developed in the study of Victory field was applied to the producing zones in Cahoj field in order to further classify the reservoir types.

Cahoj field is located on the higher portion of the upper Kansas Shelf as maps in previous section indicate. The geologic database includes several cores and varied wireline logs suites. Production is commingled and reservoir quality varies significantly among the commingled zones. Pay zones are generally thin, under 10-feet thick, typical of the upper shelf. Previous studies have provided a baseline from which to compare with Victory field (Watney, 1980; Watney et al., 1992). Major problems associated with this field are: delimiting reservoir quality in commingled zones, characterizing nature of effective pay and remaining oil in place, and designing waterfloods tailored to specific zones.

The Cahoj field was discovered in 1959. Cahoj field is developed on the crestal closure associated with a large northeast-southwest trending anticline (Figure 1.A.2). Most of the production is limited to the crestal areas of the field although later production has moved downdip to find combination structural-stratigraphic trapping. The field complex as defined here encompasses six officially defined fields covering a total of 2960 acres. Initial drilling was based on a seismic structural high. Production peaked quickly only two years after its discovery in 1961; rapid production decline ensued, typical of pressure depletion reservoirs. Production continued to decline until 1969 when infill and extension drilling accompanied a waterflood program (Figure 1.A.3). Three waterflood operations, including the last one initiated in 1974, account for over 90% of the present production. Production in 1985 equaled that of 1968, just before waterflooding and infill drilling began. Over nine million barrels of oil have been produced. Sixty wells of the total of 184 wells drilled are still producing.

Nine stacked Lansing-Kansas City carbonate reservoirs produce from field (Figure 1.A.4). In addition, the overlying Oread Limestone of the Virgilian and a siltstone/sandstone (B zone) produce locally within Cahoj field. A stratigraphic section based on a continuously cored well identifies the producing intervals using the subsurface letter nomenclature (Figure 1.A.5). The J zone (Dennis Limestone) is the major producing interval in the field. These carbonate reservoirs consist of very thin (several feet thick), discontinuous porous units ranging from grainstone to moldic and vuggy phylloid algal and bioclastic wackestone (Watney, 1980; Ebanks and Watney, 1985). Reservoirs are separated by thin, but widely continuous shales that effectively isolate them. The thinness of the pay zones is a common feature to the upper shelf setting. Reservoir rocks vary widely in quality. Porosities range from 8% to 22% and permeabilities from 0.1 md to several Darcies. Figures 1.A.6 and

1.A.7 include permeablity-porosity crossplot and conventional Pickett plot of resistivity and porosity for LKC zones. A reservoir summary is included in Table 1.A.3.

A map locating producing wells by zone that is perforated (Figures 1.A.8 and 1.A.9) reveals a complex spatial pattern. The J zone (Dennis) has two different statigraphic levels of reservoir development. This multi-tiered reservoir is analogous to the J zone in Pen field and many other fields in western Kansas. Lateral porosity variations and barriers to flow typify the J zone in Cahoj field are suggested by these maps. The patchy reservoir development ranging up to 10 contingous productive wells is similar to the continuity suggested at other fields, e.g., Pen field. Production occurs on both structurally high and flanking positions (Figure 1.A.2). The vertically commingled, laterally discontinuous production presents significant problems for efficient primary recovery and especially improved oil recovery activities such as waterflooding due to variations in intra-zone porosity and permeability.

TABLE 1.A.3. RESERVOIR SUMMARY FOR CAHOJ FIELD

Field Name:	Cahoj
Geographic Location:	Rawlins County, Kansas
Geologic Setting:	Flank of Cambridge Arch, northern Hugoton Embayment
Discovery Date:	1959
Initial Production: (Discovery Well)	528 BOPD
Reservoir Drive:	Pressure Depletion/waterflood
Nature of Trap:	Anticlinal trap with isolated closures and multiple pays exhibiting variable porosity development across structure
Reservoir Rocks:	
Age:	Upper Pennsylvanian, Missourian
Stratigraphic Units:	11 of 12 units in the Lansing-Kansas City groups
Lithology:	all limestone reservoirs except one quartz sandstone/siltstone
Depositional Environment:	shallow, agitated marine shelf
Productive Facies:	bioclastic grainstone, leached packstones and wackestones

Entrapping Facies:	shale and tight limestone facies
Diagenesis/Porosity:	early meteoric freshwater dissolution and cementation andlater stage calcite spar cementation; lesser microgranular dolomitization of mud
Petrophysics:	
Pore Type(s):	(1) between particle; (2) molds; (3) vugs; and (4) intercrystalline porosity
Porosity:	Averaging 15 percent
Permeability:	Averaging 10 md
Fractures:	not noted

Reservoir Dimensions:

Depth:	3950 feet
Thickness:	0-10 feet
Areal Dimensions:	8.7 miles x 2.6 miles
Productive area:	2980 acres

Fluid data:

Original Reservoir Pressure:	1305+
Saturations:	water 30% +-
API Gravity:	30 to 38 degrees
Gas-Oil Ratio:	unavailable
Water salinity:	65,000 mg/l but variable
Water resistivity:	0.07 ohm-m at 110 degrees F
Other:	paraffinic-napthenic oil

Production Data:

Oil and/or Gas in Place:	unknown
Ultimate Recovery:	unknown
Cumulative Production:	9,825,981 bbls. (1992)
Current Annual Production:	104,125 (1992)

Well data:

Maximum Number of Producing Wells:	184
Current No. of Producing	

Wells: 60

Well Spacing: 40 acres reduced to 20 acres in areas under waterflood

Remarks: Data based on field complex including Cahoj, Cahoj West, Cahoj East, Cahoj NE, Cahoj NW, Cahoj South

---

Discussion of the results comparing Cahoj and Victory fields is found in Subtask 6.

Pen field

Pen field resides on the upper shelf on the prominent Central Kansas uplift (Figure 1.A.10.). Grainstone reservoir development is compared with that in Victory field, a lower shelf field. The Super-Pickett plot developed in the study of five Lansing-Kansas City reservoirs in Victory field was applied to the J zone in Pen field to further characterize reservoir conditions and to compare to those conditions found in Victory field.

Pen field is located in Graham County, Kansas on the southern edge of the Cambridge arch (Figures 1.A.10 and I.50). A basement structural contour map (Figure 1.A.10 (a), closeup of basement from Cole, 1976) and isopach map for the interval from the base Pennsylvanian to base Swope (Figure 1.A.10 [b]) indicate at updip edge of a southwestward facing slope being filled during the Pennsylvanian. The area of Graham County is the site of many LKC fields, reservoir grainstones developed on an inferred broad southwest (basinward) facing ramp along the edge of the Central Kansas Uplift. Pen field as mapped includes portions of sections 17, 18, 19, and 20 of T. 6 S., R. 22 W. The field was discovered in 1985 on a small subtle anticlinal closure located on the northern flank of the heavily drilled Central Kansas Uplift (Figures 1.A.11 and 1.A.12). The structural configuration on the top of the Dennis cycle indicates slightly over 10 feet of closure. After discovery in May 1985, the field was fully developed on 40-acre spacing by March 1988, with seventeen producing wells and eight dry holes. Water injection began in November 1990 after four producers were converted to injectors.

The field was selected for comparison even though it is small, because of the baseline geological and engineering work that has already been done on the field and the abundance of cores, wireline logs, and excellent production and test records (Phares, 1991; Gould, 1991, 1993; Phares et al., 1992). While Pen field is small, the characteristics of the reservoir are thought to be representative of other fields along the northern end of the Central Kansas uplift -- thin pay in carbonate grainstone pods with subtle lateral changes in reservoir quality and porosity pinchouts (Figures 1.A.13 and 1.A.14).

The Pen field has two major pay zones, the Cherryvale (I) and the Dennis (J) in the Kansas City Group (Figure 1.A.15). The Swope (K) and Sniabar (L) are also locally productive. Reservoirs are separate and distinctive, each warranting a separate analysis. Porous limestone consists of lobe-shaped bodies of carbonate skeletal grainstone and oolitic grainstone ranging in thickness up to 6 feet (Phares, 1991). Initial geologic and engineering data indicate that reservoir properties are quite uniform within each of these lobate reservoirs. The Cherryvale and Dennis reservoirs appear to be isolated except where connected by the boreholes. Diagenetic alteration in this field is mainly the result of early freshwater dissolution of grains and dolomite cementation. Neither late stage cementation or dissolution are of any consequence in this field (Phares, 1991).

The primary reservoir rock is an oolitic grainstone in the Dennis (J zone). Two stratigraphically distinct grainstones are developed in the Dennis, similar to that observed in other areas of Kansas. The upper grainstone is the thickest reservoir unit, ranging from zero around the edges of the field up to 6 feet thick in the southern portion of the field. This unit appears as a pod of porosity about 1.5 miles long by 0.75 miles wide. This thick is offset from the present day subtle structural crest of the field (Figure 1.A.14).

An extraordinary amount of information is available and has been already compiled on the field due to geologic and engineering examinations by TORP-supported students (e.g., Phares, 1991; Gould, 1991) and by continuous monitoring of a new waterflood (Koedell, in press). The dataset includes production records with monthly barrel tests, cores from the productive interval in eight producing wells and three dry holes, modern wireline logs, including neutron-density porosity logs to help evaluate the carbonate lithologies, and drillstem tests of the reservoir unit in almost every well.

A summary of the reservoirs in Pen field is included in Table 1.A.4.

TABLE 1.A.4. RESERVOIR SUMMARY FOR PEN FIELD

Field Name:	Pen
Geographic Location:	Graham County, Kansas
Geologic Setting:	Northern edge of Central Kansas uplift
Discovery Date:	May 1985
Initial Production: (Discovery Well)	60 BOPD, no water
Reservoir Drive:	Solution gas/waterflood
Nature of Trap:	Low relief anticlinal trap
Reservoir Rocks:	
Age:	Upper Pennsylvanian, Missourian

Stratigraphic Units:	Dennis (J zone) and Drum (I zone) primarily; also D, K, and L zones in the Lansing- Kansas City groups
Lithology:	Limestone
Depositional Environment:	Shallow, agitated marine shelf
Productive Facies:	Lower skeletal peloid grainstone to upper oolitic grainstone; northerly facies lacks ooids, but contains peloids, skeletal grains and intraclasts; locally cross bedded
Entrapping Facies:	Shale and tight limestone facies
Diagenesis/Porosity:	Early meteoric freshwater dissolution
Petrophysics:	Neutron-density porosity, induction resistivity, gamma ray
Pore Type(s):	Mostly between particle pores with moderate cement reduction; abundant skeletal molds as oomolds, few vugs
Porosity:	Core porosity ranges from 2 to 29 percent; cutoff 8 percent
Permeability:	50 md, cut-off 1 md
Fractures:	Not noted
Reservoir Dimensions:	
Depth:	3700 feet
Thickness:	6 feet, thickest in south
Areal Dimensions:	0.5 miles by 1.75 miles
Productive area:	1000 acres
Fluid data:	
Original Reservoir Pressure:	1350 psi
Saturations:	Oil 27.2 to 44.0%
API Gravity:	37 to 41 degrees
Gas-Oil Ratio:	59 SCF/STB
Water salinity:	52,381 chlorides
Water resistivity:	Rw= 0.08 ohm-m @ Fm. Depth
Other:	
Production Data:	
Oil and/or Gas in Place:	1.9-2.8 MMSTB
Ultimate Recovery:	Unknown

Cumulative Production:	827,602 bbls.
Current Annual Production:	43,984 bbls. (1992)

Well data:	
Maximum Number of Producing Wells:	25
Current No. of Producing Wells:	7
Well Spacing:	40 acres
Stimulation:	Acidized
Remarks:	Production is commingled

Summary of Reservoir Properties

The Pen field represents a combination structural-stratigraphic trap. Structure is very subtle with the reservoir grainstone forming pods, apparently related to the presence of a small penecontemporaneous structure. Five zones are productive in parts of the field. The main producing zones are oolitic or skeletal grainstone lenses in the Dennis and Cherryvale zones that range up to 6 feet thick. The Plattsburg, Swope, and Sniabar zones are productive in some wells but the zones are either small isolated reservoirs or have low permeability (<5 md) (Gould et al., 1992). The Dennis sequence is the only interval which produces throughout the field.

Dennis Sequence. A thin (7 to 11 inches), dense lower transgressive (flooding) limestone forms the base of the cycle followed by a thin (1 to 6 inches) lower marine shale (Stark Shale member of the Dennis cycle). The lower shale (condensed section), the Stark Shale, in the Pen field contrasts with much of the rest of the state because of its thinness, insignificant organic carbon and lack of phosphate. This condition is common on the central portion of the Central Kansas Uplift. This evidence together with the abundant silt content and plentiful brachiopod fauna in the marine shale suggests accumulation under more open and shallower marine conditions relative to other areas of the shelf surrounding the Central Kansas Uplift.

The reservoir unit in the Dennis sequence is a late highstand regressive carbonate (Winterset Limestone) containing two distinct limestone beds (Figure 1.A.16). Total thickness ranges from 9 to 13.5 feet. The lower bed is a shallowing-upward mud-rich limestone cycle capped by a thin (5 to 14 inches) grainstone-packstone (Phares, 1991). This lower grainstone is not a good reservoir unit.

The main reservoir is a grainstone developed in the upper limestone bed (and shallowing-upward minor cycle) of the Winterset Limestone. This reservoir unit is referred to as the alpha grainstone. The alpha grainstone is

the most extensive of the reservoirs developed in Pen field forming a pod that covers essentially the entire field area roughly 2.5 mi^2 (Figure 1.A.14).

A thin muddy facies caps the limestone separating it from the overlying upper shale that terminates the cycle. The capping unit ranges from 0 to 2 feet thick consisting of mixed carbonate lithologies. Importantly, microkarst, root molds, rhizoliths, and autoclastic breccia are common in this unit, features considered diagnostic of subaerial exposure. The upper shale ranging from 2 to 9 feet thick consists of color-mottled maroon and red to green silty, unfossiliferous shale containing indicators of paleosol development including slickensides (ped surfaces) and rhizoliths. Other evidence of subaerial weathering is suggested by blackened, faceted carbonate clasts scattered in this shale.

The J zone alpha grainstone (upper zone of carbonate reservoir) is typified by interparticle porosity supplemented by molds and a few vugs. Locally, packstone facies are intermixed with an oolitic grainstone facies. Local cross stratification is observed in several cores. Stylolites and microstylolitic solution seams developed every 2 to 4 inches (5-10 cm) are abundant in the grainstone in one half of the cored wells. The other cored wells reveal solution seams spaced every 2 to 3 feet (Phares, 1991). A few vertical fractures have been observed in the cores, ranging from completely cemented to open with minor cementation.

Oomoldic porosity and marine cement occluding the interparticle pore space are particularly abundant in the southwest sector of the Dennis reservoir (Figure 1.A.14). Higher bottom hole pressure maintained in this southwestern sector of the J zone grainstone pod suggests that this area is isolated from the remainder of the field.

The Winterset Limestone in Pen field accumulated under shallow marine conditions ranging from quite open marine to shallow agitated and shallow slightly restricted marine conditions. The Dennis sequence culminated in subaerial exposure as evidenced by abundant rhizoliths, root molds, microkarst, and autoclastic breccia, best developed in the capping bed.

This type of grainstone reservoir and porosity development exhibited by the alpha grainstone closely resembles that developed in other Lansing-Kansas City reservoirs on the Central Kansas uplift. While differences exist among the other reservoirs in thickness, the pod shape is the usual appearance in map view (Watney, 1980; French and Watney, 1988).

Cherryvale Sequence. The Cherryvale sequence is thinner than the Dennis ranging from 8 to 13.5 ft (2.5-4 m) thick. The carbonate unit in the sequence contains both transgressive and regressive components, ranging in

thickness from 2.5 to nearly 8 ft (0.75-2.5 m). Pen field is near the landward terminus of the marine portion of this cycle. The cycle deviates from the normal cyclothemic succession in that it has no lower shale, a feature common in this sequence at other sites in northern and central Kansas including at the analog site in southeastern Kansas (Figure 1.A.15). The lower transgressive limestone lies in contact with a shallowing-upward, upper limestone. The lower limestone includes 0 to 3 ft (.9 m) grainstone with grains commonly coated by Osagia, typical of transgressive carbonates. The grainstone is missing in three of the cored wells, but is difficult to distinguish in wells that are not cored. The composite transgressive-regressive limestone is heavily brecciated and fissured in proximity to its upper surface with resulting connected pore space occluded by sediment resembling the overlying shale (Phares, 1991). Root molds, rhizocretions, and carbonate glaebules and circumgranular cracking are diagnostic of intense subaerial exposure that followed carbonate accumulation. The cycle is capped by the upper shale containing slickensides, mixed carbonate pebble conglomerates, and blackened faceted carbonate clasts in a predominately red silty matrix. This example of more intense weathering is common along the upper shelf.

The composite limestone contains grain-supported reservoir facies in the lower part of the unit giving way to mud-supported non-reservoir facies at the top of the zone. Oolitic grainstone is present, but Osagia-coated grains and micrite-coated grainstones are most common. Moldic porosity is infrequently observed in the cores as the result of lack of oolites and abundant skeletal grains that were resistant to meteoric diagenesis. Most pore space that is developed is interparticle in the lower grainstone.

Reservoir Parameters

Reservoir development is primarily associated with preservation of primary interparticle porosity in the carbonate grainstones of the Dennis and Cherryvale. Table 1.A.4 summarizes reservoir parameters in Pen field. Early meteoric freshwater diagenesis immediately following deposition of the grainstones enhanced primary porosity through dissolution of ooid carbonate grains and development of solution pipes and fissures. Carbonate cements and shale infilling reduced porosity, occluding porosity in some areas of the Dennis (southwestern part of field). Scattered karstic features probably form barriers or conduits to fluid flow. Further evidence for barriers and conduits is needed from fluid flow and testing.

Correlations of reservoir properties were examined by Phares (1991). Porosity in the J zone alpha grainstone (Dennis) derived from cores and neutron-density logs closely agree, particularly when a three-foot average is applied to the core-derived porosity. Permeability obtained from core measurements varies proportionately and predictably with porosity. Moreover, water saturation varies closely with porosity indicating capillarity is related to the rock fabric rather than to height of oil column or presence of a transition saturation zone. In contrast, permeability derived from cores correlates poorly with permeability secured from drill stem test (DST) results.

Clear explanations for this discrepancy do not presently exist. Phares (1991) concluded that the rock properties show significant lateral variation in the Pen field such that values of porosity, permeability, and water saturation are only accurate in the vicinity of the well-bore.

Estimated original-oil-in-place (OOIP) for all zones is 2.584 MM barrels. Correlation exists between estimates of original-oil-in-place on a 40-acre grid and individual well performance. The J alpha grainstone accounts for 66% of the estimated OOIP while the Cherryvale accounts for 10.4%, the Swope at 9.1%, and the Sniabar at 12.7% (Phares, 1991). The Swope and Sniabar have limited production for several reasons. The Swope is only completed in three of 11 wells that have indicated pay. The Sniabar tested uneconomic or pay was too thin to complete in the other wells. The Sniabar is completed in only two wells of 11 that indicate pay. The Sniabar grainstone is spatially very disconnected and drainage areas are concluded to be very small (Phares, 1991). Comparisons of Pen and Victory fields are made in Subtask 6.

Victory Field

The Lansing-Kansas City reservoirs noticeably thicken south of Cahoj and Pen field off of the Central Kansas uplift into the Hugoton embayment. There has been and continue to be modest exploration and development in the mid-shelf area in west central Kansas. Production dates back to the late 1950's and early 1960's. Individual Lansing-Kansas City reservoirs in the mid and lower shelf areas are thicker, sometimes markedly, as compared to the upper shelf and uplift regions. Even though overall reservoirs are thicker, previous work indicates that lateral variations in reservoir quality continue at both field and interwell scales. In addition, these thicker cycles in the south contain internal stratigraphic units that appear to impede fluid flow.

Victory field is discussed in considerably more depth in Subtask 6. A introduction to Victory field to support its selection for detailed investigation is presented here. Victory field is located on the lower southwestern shelf in Kansas (Figures 1.A.1 and 1.A.17, containing both skeletal grainstones with more uniform porosity and highly variable oolitic grainstone reservoirs). An extensive set of analyses were conducted including: 1) petrographic analyses of cores and cuttings from 33 wells for major pays in the LKC, 2) 47 wellsdigitized within the interval between the Dennis to Pleasanton sequences to provide for 3-D visualization and modeling of petrophysical data, and 3) over 350 wells cross plotted in 5 different carbonate reservoir units using the new "Super" Pickett plot of porosity vs. resistivity and conventional reservoir analysis for fluid saturation. This information was compared with available production and well test data. All sequences were correlated and datums entered into a computer database for the field.

Victory was selected for detailed study because of its lower shelf position, contrasting with locations of the Cahoj and Pen fields, abundance of subsurface data, and the complex and wide ranging nature of the reservoirs

in the field. The study of such a complex field with this breadth of variability can be more easily used to generalize from application to other less complex reservoirs, perhaps rescaled to the thickness and extent of reservoir pods. The appropriateness of scaling to other sized reservoirs is part of what is assessed here. Victory field has both old and modern wireline log suites, cores, samples, and some lease production and test information. The oomoldic porosity common to many Lansing-Kansas City (Stanton, Dewey, Bethany Falls, and Sniabar) reservoirs in Victory field is abundant in other LKC fields across the southern half of the shelf. The oomoldic porosity is also the primary pore type observed at the analog sites in southeastern Kansas. An enduring problem in Lansing-Kansas City oomoldic reservoirs is distinguishing effective pay, pore characteristics, and fluid saturations using commonly available well data.

Victory field was discovered in 1960 as part of a large anticlinal play. Five zones in the Lansing-Kansas City (Figure 1.A.18) produce with minor contributions from Marmaton, Morrow, and St. Louis. Cumulative production is slightly over 11.3 million barrels of oil. Seventy-eight oil wells and 34 gas wells currently produce on an acreage of 2,340 acres.

Victory is located at a prominent structural nose (Figure 1.A.19). Within the producing area the thickness of the Iatan reservoir ranges from 10 to 27 ft (3-8 m), the Dewey from 0 to 17 ft (5 m), and the Swope from 0 to 47 ft (14 m). The Iatan has the best reservoir quality rock--interparticle porosity and uniform thickness, while the Swope offers some of the most complex rock spanning scales of significant microscopic to field-scale heterogeneities. The thickness of porous carbonate relates very closely to occurrence of grainstone as it did in Pen field and contrasts in its occurrence in the field, e.g., on and near the crest of the structure for the Bethany Falls (Figure 1.A.20) and along the edges of the current structure in the Dewey (Figure 1.A.21).

Porosity in the Amoco Cox #A-4 core varies from 9 to 33%. Average permeability for the Iatan is 399 md, Dewey is not available, and Swope is 84 md. These differences are exhibited in Ø-K depth profiles and cross plots (Figures 1.A.23 through 1.A.25).

Lithologies vary from a carbonate skeletal grainstone with finer interparticle and moldic pores in the Iatan (B) zone to oomoldic and vuggy carbonate rock in the Stanton (C), Dewey (H), Swope (K), and Sniabar (L) zones. The "K" zone contains an oolitic reservoir with highly variable oil production, thickness and effective porosity development. While the porosity remains high, effective porosity varies significantly. This is common for oomoldic reservoir rocks where interooid porosity is now occluded with calcite or dolomite cement.

The problem of evaluating this field for improving oil recovery is focused on defining and mapping effective pay in the zones mentioned above utilizing available data to recognize effective cutoffs of porosity, water

saturation, and bulk water volume. Also transition zones and lateral compartments in these zones are recognized to develop an overall geologic framework to evaluate further improved oil recovery activities such as testing pay behind pipe and initiating waterflooding.

The approach has been to analyze the wireline logs, cores, cuttings, production and test information to provide independent evidence for conclusions reached. Methods such as development of the "Super" Pickett plot and use of 3-D visualized digitized wireline log data are new approaches that aid in the discrimination of reservoir heterogeneities and opportunities to recover bypassed oil. The effectiveness of the log analysis approach is that it utilizes available resistivity and porosity log suites regardless of vintage. Table 1.A.5 is a reservoir summary of Victory field.

TABLE 1.A.5. RESERVOIR SUMMARY OF VICTORY FIELD

Field Name:	Victory
Geographic Location:	Haskell County, Kansas
Geologic Setting:	Hugoton Embayment
Discovery Date:	November, 1960
Initial Production: (Discovery Well)	192 BOPD
Reservoir Drive:	Iatan: water; Swope: depleted gas cap and solution gas
Nature of Trap:	Iatan: structural; Swope: combination structural/stratigraphic/diagenetic
Reservoir Rocks:	
Age:	Upper Pennsylvanian, Missourian; Desmoinesian, Morrowan, Meramecian
Stratigraphic Units:	Iatan, Dewey, Swope, and Sniabar of Lansing-Kansas City; Morrow, Mississippian
Lithology:	limestone and sandstone (Morrow)
Depositional Environment:	shallow, agitated marine shelf
Productive Facies:	oolitic grainstone (Swope and Sniabar); moldic skeletal grainstone (Iatan)
Entrapping Facies:	shale and tight limestone facies
Diagenesis/Porosity:	early meteoric freshwater dissolution
Petrophysics:	
Pore Type(s):	moldic, vuggy, between particle
Porosity:	Iatan: 10 to 30%, average 15%; Swope: 9 to 33%, average 22%

Permeability:	Iatan: 0.01 to 790 md, average 399 md; Swope: 0.06 to 386 md, average 84 md
Fractures:	small discontinuous fractures common in core. Fracture density unknown

Reservoir Dimensions:

Depth:	4100 to 4700 feet
Thickness:	Iatan: 10 to 27 feet; Swope: 0 to 45 feet;
Areal Dimensions:	4.0 miles X 6.0 miles (irregular)
Productive area:	2340 acres

Fluid data:

Original Reservoir Pressure:	1370 psi +-
Saturations:	water 20 to 50%
API Gravity:	38 degrees
Gas-Oil Ratio:	varies
Water salinity:	127,000 mg/l chlorides
Water resistivity:	R_w= 0.03 ohm-m at 113 degrees F
Other:	

Production Data:

Oil and/or Gas in Place:	unknown
Ultimate Recovery:	unknown
Cumulative Production:	11,322,053 STB (1992)
Current Annual Production:	225,939 STB (1992)
	2,382,852 MCF (1991)

Well data:

Maximum Number of Producing Wells:	88 oil, 31 gas
Well Spacing:	40 acres
Stimulation:	acidized

Remarks: production is commingled

1.B. Near-surface and Surface Reservoir Analogue Selection

Near-surface and surface analogues to Lansing-Kansas City reservoirs were selected along the outcrop belt in eastern and southeastern Kansas, in order to study equivalent-age cycles in similar shelf settings to those in the subsurface of western Kansas. The near-surface and surface sites provide additional and more detailed geological information because of surface exposures, targeted coring, and high-resolution seismic information.

Regional mapping and reconnaissance of outcrops of the lower Kansas City and Pleasanton Group were initial steps to defining analog sites. A summary of sequence development was provided earlier in this report. The mapping of the Kansas City and Pleasanton groups in eastern Kansas initially covered 18,000 mi^2 and some 800 wells including an area of up to 50 mi (80 km) distant from the outcrop. A similar database and mapping program extended westward through the course of this project to include much of western Kansas as described earlier. This stratigraphic analysis provides the regional sequence stratigraphic framework from which to compare and contrast eastern Kansas shallow and outcrop analog sites with fields in western Kansas.

The sites and stratigraphic intervals selected were based on the local development of common reservoir rocks equivalent to those from producing intervals in western Kansas. Sites were selected such that additional geologic and geophysical data could be obtained to permit detailed sequence stratigraphic interpretations. Two projects were selected: 1) the Hertha, Swope, and Dennis limestone study and 2) the Drum Limestone study.

These units contain oolitic grainstones that are similar to the actual reservoir facies in coeval strata to the west. An extensive set of cores, seismic data, and porosity-permeability data from the cores have been acquired to improve understanding of the stratigraphic architecture, spatial distribution, and selected internal characteristics of these grainstone analogs for use in developing more precise and accurate interpretations of reservoirs in western Kansas.

SUBTASK 2. DEPOSITIONAL SEQUENCE CHARACTERIZATION

2.A. Near-surface and Surface Reservoir Analogues

The Hertha, Swope, Dennis, Cherryvale, and Drum limestones (equivalent to the L, K, J, I, and H zones in the subsurface) are good reservoirs in western Kansas including all three fields selected for further analysis. The units crop out in eastern Kansas and are penetrated by literally thousands of boreholes near the outcrop drilled in search for "deeper" (Cherokee) oil and gas targets. The regional study in eastern Kansas identified reservoir analogue facies including oolitic and bioclastic grainstone units and phylloid algal banks. Previous work along surface exposures of the Lansing-Kansas City groups in the northern Midcontinent established a general shelf-to-basin depositional framework extending from southwestern Iowa to northern Oklahoma (Heckel, 1974; Heckel, 1980).

The five limestones of interest are noted to contain reservoir-equivalent facies analogous to those found in central and western Kansas. Facies include oolitic and skeletal grainstones and phylloid algal facies. Facies and stratigraphy vary along the outcrop in a similar way to the shelf-to-basin setting in the subsurface to the west. Regional mapping linking the outcrop with the western limits of the study (350-400 miles distant) confirms that these shelf settings are very similar (see section Regional Geologic Framework). Two near-surface and surface sites were selected for detailed analysis. The Hertha, Swope, and Dennis projects developed in southeastern Kansas included mid to lower shelf settings where oolitic grainstones in the Swope and Dennis were studied extensively. The area of detailed study in Bourbon County is most similar and analogous to Victory field area in southwestern Kansas. The composition and thickness of the stratigraphic interval in these two areas (350 miles apart) is very similar (Figure I.43). Surface/near surface analog studies were concentrated in two areas: 1) the Dennis-Swope-Hertha project area, and 2) the Drum Limestone Project area.

2.A.1. Hertha, Swope, and Dennis Limestone Project

by John French

Introduction

The Hertha, Swope, and Dennis limestones are typical lower Missourian cyclothems in much of the area where they crop out in eastern Kansas. These units can be readily correlated westward into the deeper subsurface where they contain important oil and gas reservoirs. The physical correlations are facilitated by the ubiquitous presence of radioactive black shales near the base of each of these units that are easily recognized and traced on well logs; many of the shales contain diagnostic conodont faunas that allow for accurate biostratigraphic correlation as well.

This portion of the project has been divided into two parts:

1) A regional study of these units that focusses on thickness trends, lithofacies distribution, depositional history, and depositional-sequence architecture in an approximately 11,000 mi^2 (28,500 km^2) area of eastern Kansas (Fig. 2.A.1.1);

2) A more detailed examination of the Swope (including the Mound Valley) and to a lesser extent the Dennis in a roughly 500 mi^2 (1300 km^2) area in east-central Kansas (Fig. 2.A.1.1) that concentrates on the occurrence of porous oolitic grainstones similar to those that make up oil and gas reservoirs in the same interval in the western subsurface.

Major objectives of the regional study include:

1) An overall characterization of the depositional sequences that make up this succession of cyclothems in eastern Kansas. This includes the recognition of sequence boundaries (i.e. subaerial

exposure surfaces), the description of lithofacies patterns and thickness trends within each depositional sequence, and determining the relative sea-level history of this succession;

2) Obtaining a better understanding of the areal distribution and characteristics of porous ooid- and ooid-skeletal-grainstone units that occur in the Bethany Falls, Mound Valley, and Winterset limestones;

3) Characterization of the shelf-slope-basin transition in the Sniabar Limestone Member of the Hertha Limestone, which ranges in thickness from less than 1 foot to over 90 feet across the study area. The abrupt southward thinning of this bank complex has affected the overlying Swope sequence, which thickens and changes facies basinward;

4) The development of a generalized depositional model for these lower Missourian strata that can be applied in areas of central and western Kansas where these units occur in the deeper subsurface, and where much less lithologic control is available.

Objectives of the more detailed study include:

1) Descriptions of the Bethany Falls, Mound Valley, and Winterset limestones, which contain relatively thick, porous oolitic grainstones in the detailed study area;

2) Characterization of these oolitic grainstone units, including their stratigraphic relationships within each depositional sequence, the geometry of individual oolitic units, and the porosity and permeability of selected examples;

3) Determining the possible controls on the deposition of these oolitic, reservoir-quality lithologies.

Regional Analog Study

Methodology. A grid of preliminary cross-sections was prepared to facilitate correlations and mapping. Over 700 wells were then used to construct interval isopach maps. These maps were used to determine the locations of cores that were obtained to provide specific regional lithologic information about the study interval.

Regional Stratigraphy and Depositional History of Sequences -- Overview of Depositional Sequences. Three dominant, probably fourth-order depositional sequences (most likely 100 ka to 400 ka (Heckel, 1986)) (the Hertha, Bethany Falls, and lower Winterset), and one basinally restricted, either fourth- or fifth-order depositional sequence (the Mound Valley), were delineated (Fig. 2.A.1.2) (the sequences have been named for the dominant limestone formation or member in each). In most places, each depositional sequence is bounded

above and below by surfaces or lithofacies indicative of subaerial exposure, such as paleosols, rooted zones, or coal/underclay couplets. Above the basal subaerial unconformity in each depositional sequence is a marine shale or limestone that is generally less than 10 ft (3 m) thick, except in the southern portion of the study area, where a sandstone and/or shale unit up to 60 ft (20 m) thick occurs in some sequences. This unit is succeeded upward in the dominant sequences by a widespread, organic-rich, phosphatic black shale usually less than 1 m thick. These shales are readily recognizable on gamma-ray logs throughout the area, and have proven to be instrumental in establishing correlations both within this study area and between this area and central and western Kansas. In general, this black shale passes upward through a thin (< 3 ft/1 m) gray shale into an upward-shallowing carbonate unit that can range from a feather-edge to almost 90 ft (27 m) in thickness. It is the upper part of this unit that contains cross-bedded, high-energy oolitic grainstones and packstones very similar to those that occur as oil and gas reservoirs in the subsurface. In the northern part of the study area it is this upper carbonate that is capped by the upper, subaerial sequence boundary; farther south a siliciclastic package as thick as 45-60 ft (15-20 m) may occur between the uppermost carbonate and the subaerial unconformity.

A key factor that controlled the overall makeup of these four depositional sequences was the presence of a shale-dominated siliciclastic wedge that generally thinned from north to south across the study area. This unit, dominated in terms of thickness by the Pleasanton Group, can be mapped between two laterally extensive black shales, the Nuyaka Creek and the Mound City Shale members of the Hertha Formation (Fig. 2.A.1.3). The thick and relatively flat northern area is herein termed the "Pleasanton platform". Isopach maps of intervals just below the Nuyaka Creek indicate only gradual thickening to the south, strongly suggesting that there was minimal topography prior to Nuyaka Creek deposition. Present Pleasanton thicknesses indicate paleoslopes of up to 60 ft/mi (about 12 m/km). This slope especially affected the Hertha sequence, which was essentially deposited directly on the Pleasanton slope (e.g Fig. 2.A.1.2). The additional accommodation present in a downslope direction was gradually reduced as successive depositional sequences were deposited, until the lower Winterset sequence more or less blanketed the area (subject to local irregularities in the depositional surface) except to the south, where it appears to pinch out (Fig. 2.A.1.2).

Hertha Sequence. The Hertha sequence is the lowermost depositional sequence in the study interval. In updip positions (this and future references to updip and downdip refer to the inferred depositional dip that existed during sedimentation, and not to any present or past structural features) it rests on a subaerial exposure surface that was developed on top of the Critzer Limestone (Figs. 2.A.1.2, 2.A.1.4, 2.A.1.5, 2.A.1.6). Downdip, evidence of exposure is lost, and the base of the Hertha sequence is simply picked at the top of the Critzer or,

where the Critzer is absent, it is arbitrarily placed at the top of a paleosol associated with the underlying South Mound Shale.

The Hertha sequence consists of the Mound City Shale and Sniabar Limestone members of the Hertha Limestone (Fig. I.8, 2.A.1.5, 2.A.1.6). The Mound City is largely a gray to dark-gray marine shale that contains some thin (< 3 ft/1 m) calcareous units and an organic-rich, platy, phosphatic, radioactive interval typical of the core shales (Heckel and Baesemann, 1975) found in these lower Missourian cyclothems. The Mound City ranges in thickness from about 2 ft (0.6 m) in updip positions to over 70 ft (21 m) on the lower Pleasanton slope in northern Bourbon County (Figs. 2.A.1.4, 2.A.1.5). The Sniabar Limestone Member comprises the upper portion of the Hertha sequence. It ranges from about 3 ft (1 m) to almost 90 ft (27 m) in thickness. The Sniabar is dominantly a fossiliferous lime wackestone and packstone that contains a diverse biota dominated by brachiopods, phylloid algae, bryozoans, and encrusting foraminifera (Figs.2.A.1.7A, B). In some places there is a zone of skeletal grainstone a few inches to several feet thick at the top of the unit. In almost every core and outcrop in the study area the Sniabar is capped by a subaerial exposure surface that exhibits features such as laminated crusts and root tubules (Fig. 2.A.1.7C). This widespread surface marks the upper boundary of the Hertha sequence.

Especially noteworthy within the Hertha sequence is the presence of a relatively thick Sniabar Limestone Member in the south-central part of the study area (Figs. 2.A.1.6, 2.A.1.8). This thickening is associated with the southward thinning of the Pleasanton interval, such that accommodation was much greater south of the Pleasanton platform during Sniabar deposition than it was across the top of the platform. This thick Sniabar, informally termed the Sniabar bank complex, is up to almost 90 ft (27 m) thick and 20 mi (32 km) across (Figs. 2.A.1.8, 2.A.1.9), and pinches out abruptly to the south over a distance of less than 2 mi (3.2 km), forming a significant pre-Bethany Falls slope. The bank is arcuate in plan view, with an north-south-trending embayment up to about 25 mi (40 km) across associated with it (Figs. 2.A.1.6, 2.A.1.8). To the northeast of this bank complex, the Hertha sequence has a different character; there the thinning of the Pleasanton is associated with thick Mound City Shale instead of Sniabar Limestone (see Figs. 2.A.1.4, 2.A.1.5).

The Hertha sequence is a transgressive-regressive midcontinent cyclothem. It lacks the transgressive limestone that typifies many of these cyclothems, with the lower portion of the Mound City Shale representing the initial marine inundation. The organic-rich, radioactive portion of the Mound City likely represents abrupt deepening, culminating in the deepest water (see Heckel, 1991). The Sniabar represents mainly low- to moderate-energy, open-shelf, normal-marine sedimentation during relative sea-level fall that ended in widespread subaerial exposure. In places, higher-energy grainstones developed late in Sniabar deposition, most likely as falling wave-base encountered the depositional surface just prior to exposure. Significantly, very little porosity developed in

these dominantly skeletal grainstones in the Sniabar in southeastern Kansas, in contrast to the oolitic grainstones that were deposited in similar positions within the overlying depositional sequences and within the Sniabar itself in western Kansas.

Bethany Falls Sequence. The Bethany Falls sequence overlies the Hertha sequence (Fig. 2.A.1.2). It rests on the subaerial-exposure surface that marks the top of the Sniabar Limestone except in areas south of the Sniabar bank complex (discussed above), where the sequence rests apparently conformably on the southern feather-edge of the Sniabar (Fig. 2.A.1.10). The upper sequence boundary is in most places a well-developed subaerial-exposure surface that occurs at the top of either the Bethany Falls Limestone or the lower Ladore Shale.

This sequence consists of (in ascending order) the Elm Branch Shale, the Middle Creek Limestone, Hushpuckney Shale, and Bethany Falls Limestone members of the Swope Limestone, and the lower portion of the Ladore Shale (Figs. I.8, 2.A.1.10, 2.A.1.11) (note that all of these units are not necessarily present at a given location). The sequence ranges in thickness from about 20 ft (6 m) to over 70 ft (>20 m) (Fig. 2.A.1.2). In the northern and central portions of the study area north of the Sniabar bank complex the Bethany Falls sequence is dominated by carbonates, with the Bethany Falls generally comprising 70% to 80% of the unit (Figs. 2.A.1.10, 2.A.1.11). South of the Sniabar bank complex the sequence becomes dominated by shale in many places, with the lower Ladore Shale making up the majority of the sequence (e.g. Fig. 2.A.1.10).

Throughout most of the study area the Elm Branch Shale consists of about 1 to 10 ft (0.3 to 3 m) of slightly to moderately fossiliferous gray shale and associated thin, argillaceous limestones. In places the Elm Branch is absent, and the overlying Middle Creek Limestone rests directly on the Sniabar. This is particularly common where the Sniabar is relatively thick. In the southern part of the area the Elm Branch is over 20 ft (6 m) thick, and thicknesses as great as 40 ft (12 m) have been reported by Heckel (personal communication). Overlying the Elm Branch is the Middle Creek Limestone. It is typically made up of dense, dark-gray-to-brown fossiliferous lime wackestone less than 3 ft (1 m) thick that has abrupt lower and upper contacts. The Middle Creek is in turn overlain by the Hushpuckney Shale, which ranges from less than 1 ft (0.3 m) to (in a few places) almost 40 ft (12 m) in thickness. The Hushpuckney is a gray marine shale that sandwiches a thin (less than 3 ft/1 m), black, organic-rich, phosphatic, radioactive interval that persists across the entire study area and which can be readily correlated into the western Kansas subsurface; this is another core shale analogous to the Mound City Shale of the Hertha sequence discussed above. Where the Hushpuckney is thinnest, such as across the thickest parts of the Pleasanton platform, this black facies tends to persist at the expense of the gray shale. The only exception to this is over the crest of the Sniabar bank, where the Hushpuckney is gray throughout. The upper

gray facies of the Hushpuckney typically grades upward through a calcareous interval into the base of the Bethany Falls Limestone.

Across most of the study area the Bethany Falls sequence is capped by the Bethany Falls Limestone, which is generally between 15 and 35 ft (4.6 to 10.7 m) thick. It is a bipartite unit in most places, consisting of diversely fossiliferous lime wackestone and packstone in its lower part (Figs. 2.A.1.12A, B) that is sharply overlain by generally cross-stratified and very porous (porosities up to 35%) ooid- or ooid-skeletal lime grainstone and packstone (Figs. 2.A.1.12C, 13A, B). Porosity in these oolitic lithologies is dominantly oomoldic (Fig. 2.A.1.13C), although some interparticle porosity does occur. The lower, muddy carbonate is the more persistent lithofacies, occurring virtually everywhere that the Bethany Falls is found. The oolitic unit varies greatly in thickness, being absent in some locations and up to almost 20 ft (6 m) thick in others (Figs. 2.A.1.10, 2.A.1.11). The relatively thick oolites occur almost exclusively in the northeastern part of the study area, in association with the eastern margin of the Pleasanton platform (Fig. 2.A.1.14). In places the grainstones contain thin (< 4 ft/1.2 m) zones of skeletal-peloidal packstone. These oolites will be discussed more fully in the following section that describes the detailed portion of this study. In most places north of the Sniabar bank complex the top of the Bethany Falls is marked by features such as laminated crusts, rhizoliths, solution pipes, and gray-green, unfossiliferous blocky mudstones that have been interpreted as paleosols (e.g. Watney et al., 1989). These are interpreted as evidence of subaerial exposure and mark the top of the Bethany Falls sequence.

In the southern part of the study area (south of the Sniabar bank complex) the Bethany Falls virtually pinches out locally, especially in the extreme southern part of the area (Figs. 2.A.1.10, I.44). In such locations the upper part of the sequence consists of the lower Ladore Shale, which is up to roughly 70 ft (24 m) thick and is for the most part a gray-green shale that contains scattered marine fossils. A rooted blocky mudstone overlain by a thin coaly zone within the Ladore separates the informally designated lower and upper parts of the unit, and is considered to be the boundary of the upper Bethany Falls sequence.

Like the underlying Hertha sequence, the Bethany Falls sequence is interpreted to represent a cycle of rise and fall of relative sea level. The marine Elm Branch and Middle Creek reflect the inundation of the subaerially exposed Sniabar surface, with proximal Elm Branch siliciclastics giving way to the clear-water marine carbonates as the waters deepened and siliciclastics were trapped shoreward. The inundation culminated in deposition of the black, phosphatic, organic-rich facies of the Hushpuckney, which may reflect water depths as great as 650 ft or more (200+ m) (e.g. Heckel, 1990, 1991). Because deposition of the Bethany Falls sequence above the Hushpuckney ended in subaerial exposure and because that part of the sequence is over an order of magnitude thinner than these potential maximum water depths represented by the Hushpuckney, deposition of the upper part of the sequence (i.e. the Bethany Falls Limestone and the lower Ladore Shale) most likely

occurred during relative sea-level fall. As relative sea level fell, deposition of the anoxic black muds of the present Hushpuckney core facies gave way first to calcareous gray muds and then to the open-shelf marine carbonates that comprise the lower Bethany Falls Limestone. Higher-energy nearshore conditions prevailed late in the deposition of the sequence, especially to the northeast along the eastward- and southeastward-dipping Pleasanton slope. These conditions resulted in deposition of the oolitic grainstones and packstones that typify the top of the sequence in those areas. To the south, lower Ladore muds prograded into the area, probably from the south (Nimmer, 1992), prior to the final lowering of sea level and subsequent subaerial exposure. Meteoric waters introduced during this exposure probably created most of the oomoldic porosity within the upper Bethany Falls (Heckel, 1983). The thin, muddier carbonates that occur locally within the oolites may reflect multiple depositional events during sea-level fall, perhaps due to small-scale relative rises and falls that could be regional phenomena.

Mound Valley Sequence. The Mound Valley sequence overlies the subaerial-exposure surface that marks the top of the Bethany Falls sequence, and is capped by an equally well-developed exposure surface that occurs either at the top of the Mound Valley Limestone, or within or at the top of the Galesburg Shale (Figs. 2.A.1.11, 2.A.1.15).

In the northern portion of the study area the Mound Valley sequence consists of only the Mound Valley Limestone, whereas to the south the sequence contains the upper Ladore Shale below the Mound Valley and the lower Galesburg Shale above it (Figs. 2.A.1.11, 2.A.1.15). In extreme southern parts of the area the Mound Valley pinches out and the sequence is a wholly siliciclastic succession in which the Galesburg cannot be differentiated from the Ladore. While the other three depositional sequences considered in this study occur across the entire area, the Mound Valley sequence is restricted to the southern part of it (Fig. 2.A.1.16). Unfortunately, the fact that the sequence boundaries are in most places marked by paleosol/coal couplets precludes mapping the sequence in the subsurface, because these units cannot be picked on the unscaled gamma-ray-neutron logs that make up 95 % or more of the database in eastern Kansas.

The Mound Valley Limestone ranges up to about 35 ft (10 m) thick and pinches out both northward and southward. This unit is thickest just south of the Sniabar bank complex (Fig. 2.A.1.16). To the north near its updip limit is a variably porous ooid-skeletal grainstone. Farther south the unit consists of a lower, diversely fossiliferous lime wackestone and packstone that is capped by a usually porous oolitic grainstone that in places is up to about 15 ft (4.6 m) thick; south and west of roughly the location of the Heilman core (see Figs. 2.A.1.15, 2.A.1.16) the oolite pinches out and the Mound Valley includes only the wackestone/packstone facies.

As the Mound Valley sequence thickens southward of the Pleasanton platform and Sniabar bank complex it becomes a three-part unit that includes the upper Ladore and lower Galesburg shales as well as the Mound Valley Limestone (Fig. 2.A.1.15). The upper Ladore is a gray-green marine shale similar to the lower Ladore (see above). The lower Galesburg Shale is a complex siliciclastic unit that typically is a sandy shale and mudstone in its lower part overlain by a slightly to very argillaceous, fine-grained sandstone (Fig. 2.A.1.15). Its maximum observed thickness in core is 55 ft (16.8 m). The most common sedimentary structures in the sandstone are plane and ripple laminae and various features indicative of soft-sediment-deformation, such as ball-and-pillow and flame structures. Intervals typified by hummocky cross-stratification are present, as are burrowed units. Marine body fossils are rare but do occur. The lower Galesburg is capped by a rooted blocky mudstone that is interpreted to be a paleosol reflecting subaerial exposure; it forms the upper boundary of the Mound Valley sequence. This blocky mudstone is overlain by a thin (< 1 ft/0.3 m) coal at all locations examined.

Like the underlying Hertha and Bethany Falls sequences, the Mound Valley sequence represents a cycle of relative sea-level rise and fall. The major difference between this unit and those that underlie (and overlie) it is that the Mound Valley sequence does not contain a black, purportedly deep-water core shale. This and the fact that the sequence is basinally restricted suggest that the relative sea-level event responsible for deposition of the Mound Valley sequence was of lesser magnitude than were those that resulted in deposition of both the underlying Hertha and Bethany Falls sequences and the overlying lower Winterset sequence (see below). The relatively simple upper Ladore represents the initial Mound Valley inundation, which probably reached maximum water depths during deposition of the wackestone/packstone facies of the Mound Valley Limestone. At that time the siliciclastic sediments that make up both the Ladore and Galesburg were ponded on floodplains and in nearshore environments, allowing carbonate deposition on an open marine shelf. In the northern part of the study area falling relative sea-level resulted in shallow-water, high-energy oolite deposition followed by subaerial exposure and porosity generation via meteoric leaching of the unstable ooids, while farther south and lower on the shelf siliciclastics reached the area prior to subaerial exposure, precluding shallow-water carbonate sedimentation. In areas removed from such siliciclastic intrusion the Mound Valley sequence could contain reservoir-quality carbonates across a much broader area of the shelf.

Lower Winterset Sequence. The lower Winterset sequence overlies the Mound Valley sequence in the southern portion of the study area; north of the Mound Valley pinchout the lower Winterset sequence rests directly on the Bethany Falls sequence (Fig. 2.A.1.2). Across most of the study area the upper sequence boundary is a variably developed subaerial-exposure surface that occurs within the Winterset Limestone Member of the Dennis Limestone. South of the Sniabar bank complex this surface apparently becomes a conformity, and

the upper sequence boundary is tentatively assigned to the top of the Winterset Limestone (Fig. 2.A.1.17). This may be incorrect, but without closely spaced core control in the area of this change the exact relationships will be difficult to unravel.

In most of the study area north of about Township 27 South the lower Winterset sequence is made up of (in ascending order) the Canville Limestone, Stark Shale, and lower Winterset members of the Dennis Limestone (Figs. 2.A.1.17, 2.A.1.18). Farther south the upper Galesburg shale forms the base of the sequence (Fig. 2.A.1.17). The same relationships exist in the east-central part of the area as the lower Winterset sequence occurs progressively farther down the Pleasanton slope (Fig. 2.A.1.18). As with the underlying Mound Valley sequence, the lower boundary is virtually impossible to pick on the available well logs, precluding effective mapping of the sequence.

The upper Galesburg shale is generally a fining-upward siliciclastic unit that consists of fine-grained, in places calcareous, sandstone at the base that grades upward into slightly sandy, typically calcareous shale below a gradational contact with the Canville Limestone. Common sedimentary structures include plane and ripple laminae; soft-sediment deformation features are present but are not as common as in the lower Galesburg. Thin coaly zones and layers of mud chips also occur. Its maximum observed thickness in core is 43 ft (13.1 m). The overlying Canville Limestone is a fossiliferous lime wackestone and packstone that contains large and distinctive phylloid algae. It ranges up to almost 30 ft (9 m) in thickness, but more typically is less than 3 ft (1 m) thick, and it pinches out to the north. Above the Canville is the black, phosphatic, organic-rich, radioactive Stark Shale. The Stark is another core shale very similar to the Hushpuckney Shale within the underlying Bethany Falls sequence. Gradationally overlying the Stark is the lower Winterset Limestone, which ranges in thickness from less than 10 ft (3 m) in the extreme southern part of the area to perhaps as much as 50 ft (15 m) on the eastern flank of the Pleasanton platform (Figs. 2.A.1.17, 2.A.1.18). The lower Winterset is mainly a diversely fossiliferous lime wackestone and packstone containing a biota dominated by brachiopods, fenestrate bryozoa, phylloid algae, and echinoderms (Figs. 2.A.1.21A, B). In a few locations an ooid-skeletal grainstone as much as 25 ft (7.6 m) thick occurs in the upper part of the unit (Figs. 2.A.1.17, 2.A.1.18, 2.A.1.19, 2.A.1.20, 2.A.1.21C, D). In at least one small area this grainstone pinches out in a north-south direction over less than a mile (Fig.2.A.1.22). This unit will be considered in more detail in the next section.

The lower Winterset sequence is interpreted to be another well-developed transgressive-regressive deposit reflecting a cycle of relative sea-level rise and fall. The upper Galesburg shale likely represents the initial phase of deepening during the inundation of the formerly exposed Mound Valley/Bethany Falls upper surface. During the early part of this marine incursion, southerly sourced (Stermer, 1992) siliciclastics apparently were able to prograde partially across the study area before a more rapid sea-level rise halted their northward march. The

deepening-upward nature of the upper Galesburg is suggested by its becoming progressively more fine-grained and calcareous upward, and by its upward transition into the fully marine Canville Limestone. The Canville represents open-shelf carbonate deposition that preceded the maximum water depths that prevailed during Stark Shale deposition; in that regard the Canville-Stark couplet is analogous to the underlying Middle Creek-Hushpuckney in the Bethany Falls sequence. As with the Bethany Falls sequence, relative sea-level almost certainly was falling overall during lower Winterset deposition. The open-shelf, muddy carbonates of the lower Winterset were deposited first; at certain shelf positions and for other reasons that will be considered more fully in the next section, ooid and ooid-skeletal grainstones developed during the late stages of lower Winterset deposition, which was terminated when sea level fell below the depositional interface.

Detailed Study

In order to more fully understand the oolitic grainstones that occur in the Bethany Falls, Mound Valley, and lower Winterset sequences, an approximately 500 mi^2 (1300 km^2) region in the east-central part of the study area was selected for a more detailed study of these units (Fig. 2.A.1.1). This region was chosen because it is the area of best development of these reservoir-quality lithologies in these three depositional sequences. The goals of this part of the study were to characterize these grainstone units in terms of occurrence, depositional controls, and porosity distribution.

Methodology. Detailed isopach maps were constructed for both the units of interest and for the underlying interval, and porosity trends were plotted on these maps. This data set was used to determine the locations of three relatively closely spaced core transects. These cores were slabbed and described, and selected intervals were sampled for porosity and permeability and stable isotope analyses.

Geologic Setting. This study area is located along the eastern flank of the Pleasanton platform (described in the preceding section). Isopach maps of the (conservatively) decompacted Nuyaka-Creek-to-Mound-City interval (Fig. 2.A.1.23) suggest that at least 175 ft (53 m) of topography existed across a distance of about 20 mi (32 km) (Fig. 2.A.1.23). The inference that this thick-to-thin transition in the Pleasanton interval represents true depositional topography is based largely on the observation that intervals just below the Nuyaka Creek tend to be of constant thickness, suggesting that they were laid down on an essentially flat surface.

Even this slope of only about 0.1 m/km was enough to exert a significant influence on the deposition of these units. For example, the Hertha sequence ranges from a simple carbonate-dominated unit only 10 ft (3 m) thick to a multicyclic, mixed siliciclastic-carbonate unit over 90 ft (about 27 m) thick about 15 mi (24 km) to the southeast, about 110 ft (33.5 m) down depositional dip (Fig. 2.A.1.5).

Characterization of Porous Grainstones Within Depositional Sequences. ***Hertha Sequence***. The Hertha sequence contains no reservoir-like carbonate grainstones in this area. Cross sections and isopach maps show this interval to be a basinward- (i.e. down the Pleasanton slope) thickening wedge that becomes progressively more shale-dominated in that direction (Figs. 2.A.1.5, 2.A.1.24).

Bethany Falls and Mound Valley Sequences. These sequences contain the best-developed oolitic, reservoir-type grainstones in the area. In places along the Pleasanton slope the grainstones, which occur in the upper part of the Bethany Falls Limestone and comprise virtually the entire Mound Valley Limestone, attain thicknesses of up to 16 ft (almost 5 m) in the Bethany Falls and 9 ft (2.7 m) in the Mound Valley. These lithologies consist mainly of cross-stratified, ooid- and ooid-skeletal grainstone with one or two ooid-bioclast-peloid packstone intervals (Figs. 2.A.1.12C, 13, 25A-D). North and west across the top of the Pleasanton platform the Mound Valley pinches out, and the porous interval in the upper Bethany Falls (inferred to reflect most of the ooid grainstone interval by analogy with the cored and logged locations) is rarely more than about 5 ft (1,5 m) thick. Within the detailed study area, there tends to be a 1:1 correlation between thick Bethany Falls Limestone and the presence of the oolitic grainstone. An isopach map of the Bethany Falls Limestone with occurrences of porosity plotted on it (Fig. 2.A.1.26) shows this relationship. Thick Bethany Falls tends to occur as elongate, generally northwest-southeast-trending areas about 1 to 2 mi (1.6 to 3.2 km) wide and at least 9 mi (14.5 km) long; these trends are essentially normal to the strike of the Pleasanton paleoslope (Fig. 2.A.1.26).

These oolitic lenses that trend normal to an underlying depositional slope resemble the tidally influenced oolitic sand bars that occur on the modern Great Bahama Bank (Ball, 1967), although the individual modern sand belts are narrower. This may be due to a coalescence of the ancient bars through time, or may reflect the lack of closely spaced control needed to resolve all the oolitic buildups that may be present. Some of the best-developed oolitic bars occur in association with a slight embayment in the Pleasanton slope that is evident in an isopach map of the decompacted Nuyaka Creek to Hushpuckney interval (Fig.2.A.1.26). Such an embayment could have focussed tidal currents, resulting in deposition of the high-energy grainstone bars.

The best development of porous oolitic carbonate in the Bethany Falls sequence occurs in the central portion of individual bars. In these settings up to 14 ft (4.3 m) of porous grainstone and packstone (porosities as high as 34%) are locally present, with the total thickness of grainstone almost 20 ft (6 m). Porous oolite in the Mound Valley sequence is thickest where it overlies one of the best-developed bars in the Swope sequence. Interbar areas are essentially devoid of porous lithologies .

A six-core, 1/2-mi-long transect from near the center to the edge of one grainstone buildup (Fig. 2.A.1.27) shows these relationships. At least two stacked oolitic grainstones are present in this particular bar, with the upper one apparently not extending as far shelfward (eastward) on the bar crest. The six cores were taken at 20 acre (or less) offsets.

Fig. 2.A.1.27 is a cross section comprised of graphic core descriptions of the six wells. A paleosol and inferred sequence boundary separate the two oolites in the southernmost core, defining what are probably the Mound Valley Limestone above and the Bethany Falls Limestone below. The Mound Valley is a minor marine cycle that laps out updip along the shelf in southeastern Kansas and thickens into a nonporous algal wackestone in a downdip direction. The Mound Valley and Bethany Falls limestones were deposited during different sea-level events. It is possible that the upper porous oolite is within the Bethany Falls, with the Mound Valley missing over the high created by the stacking of the two oolites. This lateral onlap of porous grainstone appears to be an excellent analog to the truncation of effective porosity in the Bethany Falls Limestone along the lower flanks of Victory field, described earlier.

The northernmost cores in the transect (keeping in mind that separation is less than 20-acre spacing) indicate a more subtle division of the two oolites due to loss of the paleosol and thinning of the upper oolite. Petrographic examination reveals that there are significant differences in grain composition and diagenesis, with variable development of effective porosity, in these two oolites (figs. 2.A.1.28A-D). Even though they are in close vertical proximity their diagenetic histories are considerably different.

Oxygen and carbon stable isotope profiles are available for two of the cores (the Woodward #2 and Woodward #3) in the Woodward transect (Figs. 2.A.1.29, 2.A.1.30). Two oolites separated by a thin, nonporous, finer-grained interval occur in both cores, but in the Woodward #3 there is no paleosol separating the oolites as there is less than 1000 ft (305 m) to the south in the Woodward #2. An important question concerns whether there is any indication that a period of subaerial exposure preceded deposition of the upper oolite in the Woodward #3; evidence of such exposure would suggest that the two oolites were deposited during different sea-level events, rather than as a stacked couplet of oolite that merely represented the migration of individual bars within one related complex. The isotopic data reveal unmistakable negative shifts in the carbon isotope profiles immediately below the paleosol in Woodward #2 and below the muddy, finer-grained zone in Woodward #3. If fact, the shift in Woodward #3 is one of the better examples. In addition, the oxygen isotope profile shows a slight positive shift beneath the finer-grained zone.

The significance of these relationships is that the muddy zone immediately overlies a subaerial-exposure surface which is very likely a sequence boundary that reflects a sea-level fall, subaerial exposure, and subsequent sea-

level rise. The lower oolite was subjected to different early and late diagenetic conditions than was the overlying oolite. Moreover, this bounding surface appears to be associated with an impermeable zone that is relatively widespread. Because the two oolites appear to have experienced very different diagenetic histories, the zone probably has been a barrier to fluid flow throughout the history of these units at this location. It would be an effective lateral seal in other areas unless fractured.

These isotopic profiles are accompanied by detailed comparisons of depositional and diagenetic facies in thin section and polished slabs, and with porosity and permeability analyses. Observations and hypotheses regarding the distribution of porosity and permeability in the Bethany Falls/Mound Valley limestones in the KGS Woodward #3 core are as follows:

1) Porosity is dominantly oomoldic. There is little primary porosity left in these rocks, and it is common for the oomoldic porosity to have been reduced or occluded by calcspar. More on porosity follows.

2) Permeability is positively correlated with porosity. There appears to be a jump in permeability from sub-1-md values to higher values at about 20% porosity (Fig. 2.A.1.31). This is seen in other cores as well, including the Woodward #4 (The porosity cutoff separating effective and non effective porosity in the Bethany Falls Limestone in Victory field is around 16%).

3) Porosity and permeability are positively correlated with average grain size and sorting (Fig. 2.A.1.32). Intervals characterized by relatively coarse, well-sorted grains (dominantly ooids but with some skeletal grains as well) tend to have porosities >20%, with correspondingly high permeabilities.

4) Near the base of the lower oolite there are zones of relatively coarse, well-sorted grainstone (Fig. 2.A.1.32), but many of the oomoldic pores have been occluded by baroque dolomite and silica cements. These cements are much less common in other zones.

5) The proportion of neomorphosed ooids seems to be relatively high in the finer-grained grainstones, indicating the possibility that fluid flow was much less dynamic in those lithofacies as compared to the coarser, better-sorted sediments. Higher rates of flow of fresh water may have resulted in more wholesale dissolution of ooids in the coarser lithofacies.

6) The most porous units are cross-stratified grainstones that are in general less than a meter thick. Significant differences in porosity and permeability occur over distances of as little as a few millimeters

at boundaries between coarse- and fine-grained bedsets, such as at about 77 ft in the core (Fig. 2.A.1.27A).

The stratigraphic complexity within the Bethany Falls/probable Mound Valley grainstone succession in this near-surface analog is an example of the heterogeneity that might be encountered in actual reservoirs in the coeval K-zone in the western Kansas subsurface.

Lower Winterset Sequence. Highly porous ooid and ooid-skeletal grainstones also occur in the upper Lower Winterset Limestone along the east flank of the Pleasanton platform (Fig. 2.A.1.19). Because the Winterset Limestone is the uppermost resistant unit in the eastern part of this area, it is commonly partially to totally eroded, and therefore the data density for this unit is not as great as for the underlying sequences. Nevertheless, it is possible to make some inferences regarding the distribution and possible depositional controls on these grainstones, which correspond to the J-zone reservoir lithologies in the western subsurface.

There are at least four areas within the detailed study area where porosity zones in the upper part of the lower Winterset Limestone are greater that 10 ft (3 m) thick (Figs. 2.A.1.19, 2.A.1.20). In the southernmost area of porosity development there are wells that have almost 40 ft (12 m) of porosity at this stratigraphic horizon. Two of the core transects (the Mitchelson and Womelsdorf transects) (Figs. 2.A.1.18, 2.A.1.22) include cores that recovered part or all of this porous zone. Especially noteworthy is the limited distribution of the porous upper Lower winterset oolite that occurs along the western edge of Township 25 South/Range 21 East (Figs. 2.A.1.20, 2.A.1.22). At this location 25 ft (7.6 m) of mostly porous ooid-skeletal grainstone pinches out both north and south across about 1 mile (1.6 km) in both directions (Fig. 2.A.1.22). A log about 1.5 mi (2.4 km) to the southwest indicates that the porosity trend extends in that direction (Fig. 2.A.1.20.

A map of the interval from the Nuyaka Creek Shale to the radioactive portion of the Stark Shale (which is the black, organic-rich core shale just below the base of the lower Winterset Limestone) reveals that all four areas of lower winterset porosity development occur in association with subtle, elongate thins in the Nuyaka Creek-to-Stark interval (Fig. 2.A.1.20). Again inferring that this interval isopach represents the topography that existed during lower Winterset deposition (see discussion above regarding the Bethany Falls grainstones), it appears that the lower Winterset oolites were deposited within subtle embayments in the depositional surface. Such embayments in the Pleasanton slope would have been ideal places for the focussing of tidal currents, which are, by analogy with modern carbonate settings, commonly associated with oolite deposition (e.g. Halley et al., 1983). If this is the case, then the configuration of the pre-existing depositional surface, both at a large and

small scale, is a very powerful predictive tool for both locating such porous, oolitic zones and for determining the geometries of known occurrences.

Conclusions

The most important observations and inferences related to this study of the lower Missourian reservoir analogs include:

- Three major depositional sequences (the Hertha, Bethany Falls, and lower Winterset) can be identified throughout the study area, with one depositional sequence (the Mound Valley) occurring only in the southern part of the area. The major depositional sequences record widespread cycles of marine inundation and withdrawal, with the Mound Valley sequence reflecting a less areally extensive relative sea-level rise.

- Porous oolitic grainstones are common in the Bethany Falls, Mound Valley, and lower Winterset sequences. They occur at and near the top of each sequence, having been deposited in relatively shallow-water, high-energy settings that developed just prior to the subaerial exposure that terminated marine deposition in each sequence.

- Grainstone deposition in some sequences appears to be related to locally high depositional slopes, and more specifically to subtle embayments and other topographic features associated with those slopes. In the oil and gas plays in the deeper subsurface, mapping of structure **and** the thickness of the interval underlying the zone of interest may prove useful, both for exploration and production. In particular, selective mapping of genetically significant and temporally distinct units significantly aided in elucidating the geologic framework and paleogeography to improve making predictions of reservoir properties.

- Grainstone bodies appear to represent large lobate bars that are elongate perpendicular to the strike of the shelf, radiating away from the axis of an embayment. Bars vary considerably in size and are difficult to accurately define the lower limits due to limited subsurface control or large surface exposures. However, dimensions appear to range from 1 mi. x 2 or 3 miles to over 5 mi. x 10 mi.

- Porous grainstones commonly contain laterally persistent, relatively non-porous and impermeable lithofacies such as skeletal-peloidal lime packstones and wackestones that may be related to regional events such as minor episodes of relative sea-level change. Non-porous lithofacies may be inches thick, but appear to continue for 1000's of feet or more. In some cases these units may act as barriers to fluid flow, especially vertically. Within known reservoirs, consideration of such barriers could be critical to the effective production of hydrocarbons, particularly in terms of secondary and tertiary recovery. While thin intervening

barriers disrupt the reservoir facies stratigraphic subdivision also carries changes in the facies of the primary reservoir facies. The stacked reservoir facies such as the oolitic grainstone are alike in a general sense, but vary in grain size and pore fabric due to differences in deposition and diagenesis. Although subtle, these changes can have a significant affect on the flow properties, particularly fluid displacement. Pore fabric and their interpretation in the near-surface and surface analogue sites closely resemble their analogs in producing fields, e.g., Victory field as will be described later. Thus, knowledge grained in each situation is believed to be transferrable.

- The porosities and permeabilities of the grainstones themselves vary considerably. Permeability can vary by three orders of magnitude for similar levels of porosity. For example, in one area the oolitic grainstones that occur in the upper Bethany Falls Limestone have porosities in the 15% to 30% range and permeabilities generally between 1 and 10 md (and as high as 178 md); in contrast, the immediately overlying Mound Valley Limestone tends to have only slightly lower porosities, but virtually no permeable intervals.

- The porosity history appears to be analogous to that in Victory field, where original pores are eliminated early after deposition, oolitic grains are dissolved to form oomolds or vugs when dissolution is more extensive. When the weakened moldic fabric is buried and the moldic pore fabric can be crushed to give very irregular pores. Burial cements can occlude some or all if this porosity or late-stage dissolution can further modify the porosity distribution. The vuggy pores provide the effective (permeable) porosity. The net result is a bimodal pore system ranging from permeable to non-permeable. A threshold level of porosity is needed to make the rock permeable because the pores need to be sufficiently abundant to be connected or to be sufficiently weakened to be susceptible to crushing.

- The oolitic lobate bars host the porosity thus providing some constraints to location of porosity. The strong diagenetic modification is closely tied to early meteoric water percolation through the grainstone. Internal subaerial exposure in the midst of the oolite is the Woodward transect points to multiple episodes of water infiltration. The initial exposure event in the Bethany Falls capping the lower oolite in the transect apparently was more substantial leading to greater modification beyond initial cementation of the interparticle pores.

- Similarly, the shingled genetically and texturally distinct oolite layers delimited in dip sections have contrasting properties due to varying depositional and diagenetic history. Even though these units are thin and juxtaposed, the intervals are temporally distinct and associated with swings in relative sea-level history. If correlatable, it would be possible to reconstruct detailed paleogeography providing a template for locating

petrographic and petrophysical information. This may in turn help to recognize distinct patterns possibly related to changes in accommodation, elevation and slope of the shelf.

2.A.2. Drum Limestone Project

by H. Feldman, E.K. Franseen, R. Miller, N. Anderson

Introduction

The Drum Limestone has been investigated as a potential surface analog for oolitic reservoirs in the Lansing Kansas-City Groups in central and western Kansas. The study area in Montgomery County, Kansas was chosen because the Drum Limestone contains a well-developed oolite that can be studied in outcrops and well-logs, and a complete depositional shelf to basin transect can be observed along the outcrop belt. Major controls on oolite deposition appear to include pre-Drum depositional topography, sea-level history, shelf margin currents, and possibly local structural elements. Pre-Drum topography was controlled by thickness changes in underlying units and possible tectonic movements. In the oolite facies, the Drum has high porosity and low permeability similar to many Lansing-Kansas City Group reservoirs and apparently has an overall similar diagenetic history with the reservoirs.

The Drum Limestone is part of the Missourian (Upper Pennsylvanian) Kansas City Group (Fig. 2.A.2.1) which is characterized by alternating limestones, many of which are oolitic, and siliciclastic units. During Kansas City Group deposition, eastern Kansas was the site of shallow water to terrestrial settings on a tectonically stable shelf. Siliciclastic wedges prograded to the south and southwest from Missouri. The Anadarko and Arkoma basins in southern Kansas, Oklahoma, and Arkansas were rapidly subsiding and dominated by siliciclastic deposition. Major siliciclastic wedges prograded from the south keeping pace with subsidence and spilling over to the carbonate shelf in Kansas. The study area is near the southern limit of carbonate deposition at the broad boundary between the slowly subsiding shelf to the north and the more rapidly subsiding basin to the south.

The primary goals of this project were to develop a predictive model of oolite accumulation and porosity development applicable to Lansing-Kansas City Group oolitic petroleum reservoirs by studying the outcrops and shallow subsurface of the Drum Limestone in Montgomery County. Subtasks within the Drum Limestone outcrop analog study were to determine the sedimentologic and general diagenetic history of the Drum oolite body, to determine the relationship between facies and geometry of the Drum Limestone and facies and geometry of underlying and overlying units, and to determine the possible role of tectonism and sea-level fluctuations as controlling factors in depositional history of the Drum Limestone and associated strata. Also investigated were possible causes of reservoir heterogeneities that would affect fluid flow within the porous zones of the oolite.

Methodology

The initial phase of this study was mapping of the Drum Limestone. The Drum Limestone was mapped along the outcrop belt from northernmost Montgomery County southward to the edge of the oolite (Appendix I). In the subsurface the Drum Limestone and related units were mapped with geophysical logs from oil wells. This mapping extended from Township 30 S southward to the Kansas border, and from Range 13 E eastward to the outcrop belt (Range 16 and 17 E). Mapping data was supplemented with 9 cores. Seven cores were taken along a depositional shelf-to-basin transect southwest of Independence. Two cores were taken along the outcrop belt. Gamma ray-neutron logs were acquired for all cores. Three high-resolution seismic lines were acquired southeast of Independence along the coring transect. These data provided additional information on the geometry of the Drum Limestone and related units. Petrographic data were obtained from thin sections taken from outcrop and core samples.

Outline of Major Stratigraphic Units

The study interval in Montgomery County represents a departure from the more typical expression of Missourian cyclothems (sensu Heckel, 1977). The Drum Limestone can be traced from northeastern Kansas (where it is generally correlated with the Westerville Limestone) to southeastern Kansas where it pinches-out. The Drum limestone is characteristic of many regressive limestones of Heckel (1977) in that it is laterally continuous, thick, contains oolites, and has evidence of exposure. Yet in the study area the Drum Limestone is different from classic regressive limestones in that it is not associated with a core shale, and it is overlain and underlain by siliciclastic facies instead of shale facies that are normally characteristic of "outside" shales.

The stratigraphic units focused on in this study extend from the Mound Valley Limestone to the sandstones and shales of uncertain affinity immediately above the Drum Limestone. The Mound Valley Limestone is generally a wackestone to packstone that is thickest in the northern part of the study area (up to 25 ft thick [7.6 m]) and gradually thins southward to a pinch-out (Fig. 2.A.2.2). The overlying Galesburg Shale consists of sandstone, shale, and coal. The source of this sediment is from the south (Stermer, 1992) and the Galesburg thickens dramatically southward to approximately 150 ft (45.7 m) (Fig. 2.A.2.3). However, unlike underlying units, the Galesburg does not thicken gradually but has a complex pattern of thick and thin areas. The cause of this is not clear, but some of the thick and thin patterns are parallel to northeast- and northwest-trending basement structures. This may suggest that Galesburg deposition was responding to basement faults.

The Dennis Limestone, overlying the Galesburg Shale, from base to top consists of the thin (generally under 5 ft [1.5 m]) transgressive Canville Limestone (Fig. 2.A.2.4), the Stark Shale, a fissile black, platy shale, and the thick, regressive Winterset Limestone (Fig. 2.A.2.5). During Winterset deposition a shelf edge was established in southern Wilson County, a few miles north of the Montgomery County border. The Winterset Limestone

thins from nearly 100 ft (30.5 m) thick in central Wilson County to under 10 to 15 ft (1.5 m) in central Montgomery County.

The Cherryvale Shale, overlies the Winterset Limestone, and apparently filled in topographic low areas left after Winterset deposition, and extended the depositional shelf edge further to the south (Fig. 2.A.2.6). The general morphology of the Cherryvale Shale in the study area suggests a primary delta lobe that was prograding to the southwest from eastern Montgomery County, and a minor lobe in west-central Montgomery County. The Cherryvale consist of unfossiliferous, gray shale with siderite bands and concretions, and does not contain a succession of facies characteristic of deltas, therefore it is difficult to interpret the exact environment of deposition for the Cherryvale Shale.

The Drum Limestone overlies the Cherryvale Shale. The thickness and facies patterns of the Drum Limestone were apparently responding to depositional topography left after Cherryvale Shale deposition stopped (Fig. 2.A.2.7). This topography resulted in a relatively flat depositional shelf in central and northern Montgomery County where the Drum is generally thin. A depositional shelf edge was created at the southern edge of the Cherryvale Shale. The Drum Limestone thickens dramatically south of the shelf edge, and then thins basinward.

Drum Limestone Facies Descriptions

Interbedded limestone and shale facies: The lower part of the Drum Limestone in most places along the outcrop belt in the study area consists of alternating beds of limestone and shale. Limestone beds range from 1 to 7 inches (3 to 17 cm) thick (Fig. 2.A.2.8, 9). Where this facies is thickest in southern Montgomery County, the shale interbeds gradually thicken downwards through the facies from thin (approximately 0.1 inch or 2.5 mm) clay drapes near the top to over 5 inches (25 cm) thick near the base. Upper and lower boundaries of beds appear gradational. Average thickness of shale beds near the middle of the facies is 4 inches (12 cm). Most limestone beds are composed of laminated mudstone. Laminations are distinct on weathered surfaces, but, in thin section are indistinct, rarely observable as slight changes in crystal size, or are represented by laminae of quartz silt. In addition to the common irregularly spaced, horizontal laminations, there are small (1 inch or 2.5 cm long) cut and fill structures as well as rare, possible ripples. In the southern portion of the study area bioturbation increases upwards: laminations become more disturbed by burrows, mudstone-filled burrows extend down into shale interbeds, and pellets become more abundant. Some beds are composed of peloidal packstone to grainstone. Cross beds up to 10 inches (25 cm) thick are also present. Rare tabulate corals are the only fossils that have been observed in this facies.

Intraclastic grainstone to packstone facies: This facies consists of flat pebbles composed of medium-crystalline spar (probably neomorphosed mudstone) and shale clasts rich in quartz silt. Pebbles range in length up to 1.2

inches (31 mm) long and are up to 0.2 inches (5 mm) thick. Most pebbles are 0.2 to 0.4 inches (5 to 10 mm) long and 0.08 to 0.1 inches (2 to 3 mm) thick. Fossils within this facies include brachiopods, bivalves, gastropods, bryozoans, and echinoderms. Most fossils are broken and abraded. Other allochems include oolites, coated grains, and peloids. Many of the pebbles have oolitic coatings as well. North of the Heartland Cement Quarry this facies consistently occurs as a thin bed generally 2 to 3 inches (5 to 7.5 cm) thick, but ranging up to 9.5 inches (24 cm thick) at the base of the interbedded limestone and shale facies and apparently forms a continuous bed at the base of the Drum Limestone (Fig. 2.A.2.7-B). This particular bed is rarely cross-bedded and is distinguished from other occurrences of the facies because it contains foraminifers encrusting the pebbles. At one outcrop where the contact between the Drum Limestone and underlying Cherryvale Shale can be traced for several meters, the bed of intraclastic grainstone to packstone rests unconformably on the Cherryvale. At the Heartland Cement Quarry and in the White #1 core, the interbedded limestone and shale facies grades downward into the Cherryvale Shale, and a bed of the intraclastic grainstone to packstone facies (with encrusting foraminifers) occurs in the middle of the interbedded limestone and shale facies. The intraclastic grainstone to packstone facies occurs sporadically at the base of the bryozoan, stromatolitic wackestone to boundstone facies and skeletal, oolite grainstone facies as well.

Bryozoan, stromatolitic wackestone to boundstone facies: This facies consists of fossiliferous wackestone with an abundant and diverse fossil assemblage consisting of large fenestrate bryozoans, encrusting bryozoans, brachiopods, crinoid plates, and gastropods. Some of the fenestrate bryozoan colonies are complete and are over 20 cm long. The bryozoan stromatolitic wackestone to boundstone facies thickens gradually from 2 ft (0.6 m) in northern Montgomery County to 4 ft (1.2 m) east of Independence, and then thins to a feather edge near Independence. This facies is absent in the Heartland Cement Quarry. In the northern-most outcrops in Montgomery County this facies contains well-developed, steep-sided, elongate stromatolites (Fig. 2.A.2.10). Based on observations from overturned blocks, the stromatolites are arranged in parallel rows, and aligned asymmetrically in one direction, suggesting deposition in response to waves or currents probably in very shallow water. Near the southern terminus of the bryozoan stromatolitic wackestone to boundstone facies there are boundstone mounds constructed of stromatolites and encrusting fistuliporoid bryozoans. Oncolites that nucleated on fossil debris are common in some exposures, suggesting high energy conditions. Ooids are a rare component of this facies.

Skeletal oolitic grainstone facies: The skeletal oolitic grainstone facies is thickest immediately south and southwest of the edge of the Cherryvale clastic wedge. The facies is best exposed in the Heartland Cement Quarry where it is approximately 50 ft (15.2 m) thick (Fig. 2.A.2.11). Petrographic observations reveal that the composition ranges from nearly pure, well-sorted oolite, to poorly sorted oolitic fossiliferous grainstone and a

small amount of packstone. Fossils are abundant and diverse, including fenestrate bryozoans, echinoderm ossicles, brachiopods, ramose bryozoans, gastropods, bivalves, rugose corals, tabulate corals, and cephalopods.

The main body of the oolite is well exposed in the mile-long (1.6 km) highwall of the Heartland Cement quarry and consists of thick (3 to 4 ft, 1 to 1.3 m) tabular, planar cross beds at the base of the oolite and grade upwards to thinner, trough cross beds at the top. Current orientations are predominantly to the southwest with a minor mode to the northeast (Hamblin, 1969) (Fig. 2.A.2.12). There is also an increase in shale content upward in the uppermost 10 ft (3.05 m) of the Drum Limestone in the quarry. Troughs are separated by shale drapes, that grade upward into isolated troughs surrounded by shale.

Northward the skeletal oolite grainstone facies is thin (generally under 20 ft [6.1 m]) on the Cherryvale shelf where the oolite overlies the bryozoan stromatolitic wackestone to boundstone facies. The contact between the two facies in that area is sharp and erosional. In most outcrops there is clear evidence of erosion of the bryozoan stromatolitic wackestone to boundstone facies after lithification. In one exposure (Lib-5, see Appendix I) it appears that paleosol features developed on the bryozoan stromatolitic wackestone to boundstone facies and were later buried by the skeletal oolite grainstone facies. The skeletal oolite grainstone facies thins northward to a pinch-out.

South of Independence the skeletal oolite grainstone facies rests on the interbedded shale and limestone facies. The skeletal oolite grainstone facies thins southward to a pinch-out approximately 4 miles south of Independence along the outcrop belt. In the subsurface this facies pinches out within a mile of the edge of the Cherryvale shelf.

Depositional Environments and Sea Level History

The wide range of lithofacies and thicknesses of the units considered in this study indicate that there was significant sea floor topography prior to Drum Limestone deposition. The lowest unit studied, the Mound Valley Limestone which generally thickens northward. This is followed by the Galesburg Shale that is thickest in the southern part of the study area, but otherwise displays a complex series of thick lobes of shale. The origins of these features are not clear, however there is no obvious pre-Galesburg incisement, and this unit probably represents deltaic or fluvial deposition (Stermer, 1992). One notable pattern is the tendency for thick and thin zones of Galesburg to be northeast trending, and parallel to basement structural trends in this area. The overlying Dennis Limestone also shows a pronounced northeast-trending pattern of isopach lines, but there is no clear relationship between the thickness of Dennis Limestone and Galesburg Shale, however, the there is a thin area of Galesburg Shale directly below the thickest Drum Limestone in the area of the seismic lines and coring transects (Fig. 2.A.2.13, 14, 15).

The overlying Cherryvale Shale forms a delta lobe that prograded to the south and west (Fig. 2.A.2.14). The Cherryvale Shale apparently filled in a low area just south of the Dennis buildup and extended the depositional shelf edge further southward (Fig. 2.A.2.15). Thus, the northern edge of the Cherryvale Shale lobe does not represent a depositional shelf edge; only the western and southern edges likely represent delta shelf edges. The contact between the Cherryvale Shale and Drum Limestone is exposed at several locations, but only at Lib-5, where it be traced for several 10's of ft, is the erosional nature of the contact be exposed (Fig. 2.A.2.8-B). The origin of this contact remains enigmatic; there is little relief associated with the surface on the Cherryvale lobe based on subsurface analysis, and no evidence of subaerial exposure has been observed. The contact may represent a ravinement surface. North of the quarry this surface is overlain by an apparently deepening upward sequence of facies starting with an intraclastic fossiliferous limestone. This limestone may represent deposition during transgression. Local scouring and/or channeling in lower Drum beds suggests relatively shallow-marine conditions. Above the lowest limestone bed in the Drum is the interbedded limestone and shale facies. The paucity of bioturbation, fossils, and current structures all suggest a relatively deeper, quiet-water marine environment. Basinward (to the south) the interbedded limestone and shale facies thickens, and rests conformably on the Cherryvale Shale. Near the center of the facies is an intraclastic grainstone with abundant foraminifers. This bed may be the basinward extensions of the lowest limestone in the shelf position. Thus, the erosional surface on the Cherryvale shelf may be represented by continuous deposition in the basin.

On the shelf, the bryozoan stromatolitic wackestone to boundstone facies overlies the interbedded limestone and shale facies. The predominance of stromatolites, abundant and diverse fossils, and general low energy conditions, all suggest shallow-water, protected lagoonal deposits. The upper contact of the bryozoan stromatolitic wackestone to boundstone facies is sharp and was eroded after lithification. Features such as autobrecciation, laminated crusts, iron staining and circumgranular cracking at LIB-4 suggest subaerial exposure, and thus the bryozoan, stromatolitic wackestone to boundstone facies represents a shallowing upward trend capped at least locally by a probable subaerial exposure surface. However, it is not known yet if this exposure surface represents a relative drop in sea level or was caused by autogenic processes.

Overlying the erosional and possible subaerial exposure surface is cross bedded oolite deposited upon transgression of the sea over the previously exposed shelf and renewed shallow-water marine deposition. The oolite is thin over the shelf probably in response to limited accommodation space. As the Cherryvale thins to the south and west, the oolite thickens up to 65 ft (19.8 m). The ooids were probably being generated at the break in slope and transported seaward by tidal currents. Upward thinning of cross-bed units may suggest shallowing and filling of accommodation space. Carbonate deposition was halted by renewed influx of siliciclastic detritus.

High Resolution Seismic Stratigraphy

Introduction. A high-resolution seismic-reflection study was conducted in the Drum Limestone study area in an effort to image geometric changes within Missourian stage strata at depths of up to 350 ft (106.7 m). These features are significant from both a geologic and geophysical perspective. Three seismic lines were acquired. Line 1 is a transect across the center of the thickest oolite, from a thin shelf limestone to the north, to the limestone pinch-out to the south over a distance of 1 mile (Fig. 2.A.2.17). A coring transect and well-log control were used to model the line prior to data acquisition. Lines 2 and 3 are also transects across the shelf edge, but in a position where the oolite is not well developed (Fig. 2.A.2.17). The geometry of the Drum Limestone was not known in the area of line 2 prior to data acquisition. Line 2 is at the southern end of this line and was intended to image the dramatic thickness changes in the Galesburg Shale through Drum Limestone.

This study highlights the geophysical aspects of quantifying practical thin-bed resolution. The data were acquired and processed to focus on a distinct shallow high-resolution seismic reflection at approximately 65 ms within the Galesburg Shale where the shale thins from 63 ft (19 m) to 23 ft (7 m).

The thin-bed resolving power of the CDP seismic-reflection technique is dependent upon the dominant frequency of the recorded reflection wavelet (Widess, 1973). Increasing the dominant frequency of recorded reflection signal involves: (1) generating a high-frequency source pulse, (2) sensing the signal with receivers with high voltage output, low noise, and a flat frequency response over the desired high frequencies, (3) recording the signal digitally on a seismograph with a large instantaneous dynamic range and electronically quiet analog filter and gain capabilities, and (4) optimizing the spread interval and receiver spacing for the target of interest (Knapp and Steeples, 1986). Criteria for resolving converging thin-bed sequences relies on observations of interference as evidenced by distortion of reflection waveforms (Ricker, 1953).

Practical resolution limits are dependent not only on recorded reflection frequencies but also on wavelet characteristics and noise. Zero phase wavelets possess the highest resolving potential (Knapp, 1990). A known theoretical wavelet can be phase-filtered to zero phase. Successful application of deconvolution requires a statistically large number of unique reflection wavelets and data with a large signal-to-noise ratio (Yilmaz, 1987). Shallow high-resolution reflection data sets rarely have more than four to six reflections and are notoriously noisy (Steeples and Miller, 1990). Practical optimization of shallow high-resolution data sets by phase filtering to zero phase is generally not possible.

Field Procedures. The selected low-cut filters have a 18 dB/octave rolloff from their indicated -3 dB point. Production lines were acquired with 100 Hz analog low-cut and 500 Hz analog high-cut filters. The 1024

samples recorded per trace were at a 1/2 ms sampling interval. The dynamic range of the seismograph was more than adequate to record high-quality reflection information in the presence of source-generated and cultural noise at this site.

A series of walkaway-noise tests was conducted prior to acquisition of the production seismic lines. The spectral and total energy characteristics of the downhole .50-cal. seismic source made it the source of choice at this site for this geologic target. The receiver array consisted of three 40-Hz geophones equally spaced over approximately 3 ft (0.9 m) and centered on each station. The receiver array was designed in an attempt to attenuate some of the source-generated noise (Steeples and Miller, 1990). Analysis of the noise tests allows acquisition parameters and equipment to be optimized for the site conditions.

The nominal 12-fold CDP production line (line 2) and 24-fold CDP production lines (lines 1 & 3) were acquired using an end-on source/receiver geometry. Analysis of the walkaway data allowed determination of an optimum source-to-nearest-receiver offset of 55.8 ft (17 m) and source-to-farthest-receiver offset of 246 ft (75 m). A large component of direct and refracted wave energy inhibited closer source-to-receiver offsets. Near vertically incident recording minimizes normal move-out corrections and the associated stretch allowing a higher frequency, less distorted reflection wavelet to be recorded (Miller et al. 1990). The target reflector for line 2 is approximately 246.1 ft (75 m) deep which is within the optimum recording offset as evidenced by the walkaway- noise tests and general rules of thumb (Knapp and Steeples, 1986).

Data Processing. The CDP data were processed at the Kansas Geological Survey (KGS) using a proprietary set of algorithms developed by the KGS (Eavesdropper). Extreme care was used during the editing process to ensure removal of all non-seismic energy that could either be misinterpreted as reflections on stacked data or that hampered interpretations of real reflection events. Velocity analysis incorporated iterative constant velocity stacking with detailed 1/5 wavelength surface-consistent statics to improve both accuracy of velocity corrections and time/depth conversion on interpreted cross sections. The main distinctions between the shallow high-resolution processing flow used on this data and most routine petroleum sequences relate to conservative use and application of correlation statics, precision required during velocity and spectral analysis, extra care during muting operations, and lack of deconvolution.

Modeling and Interpretation. As an aid to the interpretation of the seismic lines geologic cross-sections (Figs. 2.A.2.18, 19), corresponding two-dimensional geologic models and synthetic seismograms were generated for lines 1 and 2 (Figs. 2.A.2.20, 21). The geologic cross-sections are structurally consistent with well control from the Clarkson #2 core (Fig. 2.A.2.19) at trace 494 on line 2 (Fig. 2.A.2.22). The velocities and densities incorporated into the models are consistent with the lithologies encountered in the Clarkson core, check shot

survey data at the same well site, and stacking velocity control. The cross-sections in Figs. 2.A.2.20 and 21 are presented as reasonable representations of that portion of the subsurface imaged by the seismic control and illustrate some of the geometric details which characterize the Missourian stage strata in the study area.

The two-dimensional synthetic seismograms (Figs. 2.A.2.20, 21) were generated for the geologic models using Geophysical Micro-Computer Ltd. diffraction modeling software. A 5 ms, zero-phase, normal-polarity Ricker wavelet was used. The more prominent events on the synthetic seismograms have been labeled in order to facilitate comparisons between the geologic models, synthetic seismograms and seismic lines (Figs. 2.A.2.22, 23).

A comparison of the geologic model and the synthetic seismogram for line 2 indicates that tops of the Mound Valley Limestone, Winterset Limestone, unnamed sandstone and a limestone in the upper Nellie Bly(?) Formation, and the base of the unnamed sandstone are manifested as relatively high-amplitude peaks on the synthetic seismogram (Fig. 2.A.2.20). The base of the interpreted channel-fill, in contrast, is represented as a moderate-amplitude trough. Low-amplitude diffractions originate at the edges of these truncated horizons. The complexity of the central part of the synthetic seismogram is increased as a result of the non-vertical incident reflections from the base of the channel which collectively produce the observed classic "bow-tie" effect beneath the base of the channel.

The interpreted seismic line 2 is presented as Fig. 2.A.2.22A. The labelled events were identified on the basis of the synthetic seismogram. The time-depths to the respective horizons are consistent with subsurface control at the Clarkson #2 well site, stacking velocities and check shot survey control. The high degree of correlation between the geologic model, synthetic seismogram and seismic line support the seismic interpretations presented.

As anticipated from the analysis of the synthetic seismogram, the tops of the Mound Valley Limestone, Winterset Limestone, unnamed sandstone and a limestone in the upper Nellie Bly(?) Formation, and the base of the unnamed sandstone correspond to relatively high-amplitude peaks on the seismic line. The Mound Valley Limestone, Winterset Limestone, unnamed sandstone and Nellie Bly(?) Formation events appear to be correlatable across the seismic line. In contrast, the reflections from the top and base of the unnamed sandstone unit, as correlated, are truncated by an interpreted deeply incised and infilled channel. The base of the interpreted channel fill is correlated as a moderate-amplitude trough. The polarity of this event, and the subtle negative drape across the channel along the Nellie Bly(?) event, suggests that the channel fill is composed predominantly of compacted shales. This thesis has not been independently confirmed by drilling.

One striking feature on seismic line 2 is the dramatic thinning of the Galesburg shale to the north (Fig. 2.A.2.22; at about 65 ms, between the Dennis and Mound Valley Limestones). This is consistent with core and well log data (Fig. 2.A.2.19) and interpreted as confirmation of either the local depositional thinning or erosional thinning of the Galesburg Shale.

Also of significance is the apparent absence of the Drum Limestone along the entirety of seismic line 2. (The absence of Drum Limestone at trace 494 has been confirmed by the Clarkson core.) Our preferred interpretation is that the Drum Limestone was not deposited in this part of the study area. Based on outcrop and shallow well control, we interpret the Drum Limestone to have been deposited as several(?) lobes elongated perpendicular to the edge of the Cherryvale delta. In our opinion, the example seismic line was shot between Drum Limestone lobes, in an area that received only shale deposition (Fig. 2.A.2.17).

Analysis of cores and well logs in the study area suggests that the unnamed sandstone within the Nellie Bly(?) Formation rests unconformably on lower older units. The irregularity of this reflector on the seismic line and the interpreted channel are further evidence of the erosional nature of the lower contact and basal portion of the Nellie Bly(?) Formation.

The seismic line illustrates that stratigraphic complexity of the upper Nellie Bly(?) and overlying units indicated by lack of lateral continuity of events shallower than approximately 45 ms (Fig. 2.A.2.22). This complexity is suggested in the geologic cross section by our inability to correlate the Quivira Shale(?) north of the Clarkson #2 core (Fig. 2.A.2.19). A shale-filled channel is hypothesized as a partial explanation for the lack of continuity of shallow reflectors based on the similarity of the seismic line and synthetic model data. Channeling in the Nellie Bly(?) Formation may explain the lateral discontinuity of thin limestone and sandstone beds shown on the well logs in Fig. 2.A.2.19.

Summary and Conclusions. A 12-fold and 2 24-fold high-resolution seismic lines were obtained along an two transects in central Montgomery County, Kansas. The interval from the Mound Valley Limestone to the Quivira Shale(?) was imaged. Ground truth was based on cores and well logs. These data in addition to interpretation of the seismic line were used to construct simplified geologic models. The models were used to construct a synthetic seismic section. The synthetic sections agree well with the original seismic sections. This technique revealed outcrop-scale features in the rocks, including one small channel in the Nellie Bly(?) Formation not previously suspected.

Porosity Evolution in Drum Oolite Facies

Introduction. A petrographic study of diagenetic characteristics was conducted on selected samples from the skeletal, oolite facies of the Drum Limestone from the Heartland Cement Quarry. This facies was focused on because of its apparent similarity to known reservoir facies in the subsurface of Kansas. Twenty-eight, 2 inch by 3 inch thin sections were studied using the thin section staining techniques described by Dickson (1965) and standard plain light petrography to determine the different diagenetic features and events and their spatial distribution. Our observations indicate a complex history and spatial distribution of post-depositional diagenetic events that affected the Drum skeletal, oolite facies in the Heartland Cement Quarry. The descriptions and discussion below focus on our initial results of the porosity and cement history for these rocks.

Description and General Stratigraphy of Cements. Isopachous bladed calcite (Cement A): Forms isopachous fringes up to 80 m thick (Fig. 2.A.2.24 A). This cement is rare, but most common in the lower 30 ft (9.1 m) of the Drum Limestone. The isopachous bladed calcite typically occurs in patches as fringes on adjacent grains. No cements were observed to have precipitated prior to this cement. The isopachous bladed calcite cement is overlain by the medium crystalline, equant clear calcite cement.

Isopachous cloudy, bladed to equant calcite (Cement B): Coarse, equant to bladed, crystals (up to 500 m long) of cloudy calcite is abundant in the upper part (upper 1/4) of the skeletal oolite grainstone facies in the Heartland Cement Quarry where it fills nearly all (>95%) of original void space (Fig. 2.A.2.24 B, C). The cement decreases in abundance downward, where it occurs primarily in large shelter pores. Locally, the cloudiness appears to be the remnant ghost structure of an originally fibrous cement. In these areas, coarse crystals are probably a replacement of an isopachous, fibrous, botryoidal aragonite(?) cement. The cloudy, originally fibrous, cement occurs as isopachous crusts and as uneven coatings on allochems. The isopachous morphology is most obvious in shelter voids where the original pore diameter is much greater than cement thickness. In intraparticle voids this cement (cement B) is manifest as an medium- to coarse-crystalline equant, cloudy, pore-filling calcite cement. In large pores alternating zones of turbid and less turbid cement are apparent. Cement B was not observed in contact with the isopachous bladed calcite cement and they could have been precipitated at essentially the same time. Cement B is overlain by coarse, clear, equant calcite (cement D) and medium-crystalline, equant, clear calcite cements (cement E).

Syntaxial calcite (Cement C): Large (up to 400 m) clear crystals in optical continuity with echinoderm grains occur throughout the skeletal oolite facies, but are most common in the upper 1/4 of the oolite. This cement does not occur on echinoderm grains with oolitic coatings or micrite rims. Interference with the growth of cloudy, isopachous cement suggests they were precipitated simultaneously.

Coarse-crystalline, clear, equant calcite (Cement D): Large (up to 400 m) clear, equant calcite crystals overlie the isopachous cloudy cement (cement B) in large voids that were not completely filled by the isopachous cloudy calcite cement (Fig. 2.A.2.24 B). Most crystals of coarse clear equant calcite are in optical continuity with the underlying crystals of cloudy calcite.

Medium-crystalline, clear, equant, calcite (Cement E): Cement composed of small (average approximately 100 m) equant calcite crystals is the most common cement in the skeletal oolite grainstone facies in the Heartland Cement Co. Quarry, and fills most original void space in the lower 3/4 of the Drum Limestone in the Heartland Cement Quarry (Fig. 2.A.2.24 D). It clearly overlies the isopachous bladed calcite (cement A), but its relationship to the coarse, cloudy isopachous calcite (cement B) is not clear. Downward through the Drum Limestone in the quarry (and even within individual thin sections) there is a gradual change from coarse turbid and clear calcite to medium equant calcite suggesting that this cement may, in part, be a product of neomorphism.

Coarse, equant, clear, ferroan calcite (Cement F): Composed of coarse (up to 300 m) equant crystals with sweeping extinction (Fig. 2.A.2.24 E). This cement has only been observed in interparticle pores in the uppermost 10 ft (3 m) of Drum Limestone where other cements are absent, and the sediment has been highly compacted. In addition some grains have been neomorphosed to ferroan calcite. Ferroan dolomite fills molds in rock supported by this cement, and therefore probably was precipitated after the ferroan calcite.

Baroque ferroan dolomite (Cement G): Medium to coarsely crystalline with sweeping extinction; stains blue with potassium ferricyanide (Fig. 2.A.2.24 C). The dolomite is the last pore-filling cement occurring stratigraphically above the coarse, clear calcite (cement D) and the coarse, clear, ferroan cements (cement F). The dolomite occurs in many secondary pores throughout the skeletal oolite grainstone facies and also occurs locally as a replacement of grains and previous cements.

Paragenetic Sequence of the Drum Oolite. A generalized paragenetic sequence and spatial distribution of diagenetic features has been determined for the skeletal oolite facies. It appears from initial observations that this general sequence and distribution can vary significantly over very short lateral and vertical distances. However, the sequence of events and distribution patterns presented herein are useful in a general understanding of heterogeneities within a potential reservoir facies, comparing the Drum sequence and features to similar facies that are reservoirs, and they form a good foundation on which to conduct further, more detailed diagenetic studies.

The relative timing of diagenetic events within the skeletal oolite facies is as follows:

1) Precipitation of isopachous bladed (probably originally as fibrous, botryoidal aragonite) and bladed-to-equant marine cements shortly after oolite deposition (cements A, B).
2) Precipitation of syntaxial cement overgrowths (cement C) locally on crinoid fragments, possibly concomitant precipitation with cements A and B.
3) Initiation of early compaction that ends prior to precipitation of cement F.
4) Selective dissolution of aragonitic allochems (e.g. ooids, mollusc fragments); early marine isopachous cements (cements A and B) were not affected by dissolution.
5) Replacement of cements A, B and C?, and allochems, and cement precipitation in primary and secondary pores by medium- and coarse-crystalline, clear, equant calcite (cements D and E).
6) Selective precipitation and replacement by ferroan calcite (cement F).
7) Selective precipitation and replacement by ferroan baroque dolomite (cement G).
8) Late stage compaction and dissolution.

In addition to the above general paragenetic sequence of events for the skeletal oolite facies of the Drum Limestone exposed in the Heartland Cement Quarry, this facies can be further divided into three general diagenetic facies based on a vertical distribution pattern of dominant diagenetic features described above. These three diagenetic facies are as follows:

Diagenetic Facies 1: The upper most few feet (from the top of the oolite down to a maximum of 10 ft [3 m]) are highly compacted, lack early cements, and contain abundant late cement (cements F and G) (Fig. 2.A.2.24 E).

Diagenetic Facies 2: The rest of the upper third (down to approximately 25 ft [7.6 m] below the top of the skeletal oolite grainstone) is dominated by the isopachous cloudy calcite cement (cement B), and is not compacted (Fig. 2.A.2.24 B, C).

Diagenetic Facies 3: The lower two thirds of the skeletal oolite grainstone is cemented dominantly by the medium- and coarse-crystalline equant calcite (cements D and E), and is not compacted (Fig. 2.A.2.24 D).

Diagenetic facies 1 (the uppermost facies) is characterized by highly compacted sediment (pressure solution along grain-to-grain contacts is common, many grains are cracked, and oolitic coatings are spalled off of grains) and coarse ferroan calcite cement (cement F) with minor amounts of ferroan dolomite cement (cement G) within rare oomolds. The high degree of compaction of this facies is consistent with the lack of early cements. Samples from this diagenetic facies have been recovered as low as just below the lowest shale within the upper part of the Drum Limestone. In the Heartland Cement Quarry core only the upper 2 or 3 ft (1 m) of Drum are within this diagenetic facies. Ooids and fossils are generally well-preserved, however ooids have been

neomorphosed to ferroan and nonferroan calcite. Crystals within ooids generally follow the concentric laminations, but some cut across laminations.

Diagenetic Facies 2 (the middle facies) occurs immediately below the zone of compacted grainstone of diagenetic facies 1. The contact between these two facies is sharp. Diagenetic facies 2 consists of approximately 10 - 20 ft (3 - 6 m) of uncompacted grainstone in which the most pervasive cement is cloudy isopachous calcite (cement B). Due to the extreme thickness of this cement (approximately 500 m), the isopachous morphology can only be observed in large shelter voids below fossils (Fig. 2.A.2.24 B, C). The cement was likely originally fibrous and has been subsequently neomorphosed to a bladed to equant morphology. Overlying the isopachous calcite is clear equant calcite (cements D and E) and then ferroan dolomite cement (cement G). Ooids are well preserved with many thin concentric layers that are along crystal contacts or are preserved as ghost structures within crystals. Porosity generally decreases downward in diagenetic facies 2. Primary porosity is currently present only in the largest pores that were not completely filled with cement (Fig. 2.A.2.25 A). Most remaining porosity is moldic. Originally, aragonite allochems such as ooids and molluscs were selectively dissolved (Fig. 2.A.2.25 C, D). Other allochems such as brachiopods, echinoderms, and bryozoans are well-preserved. Most pores are isolated molds so permeability is low.

The boundary between diagenetic facies 2 and diagenetic facies 3 (the lowest facies) is gradational with the isopachous bladed to equant calcite cement (cement B) characteristic of diagenetic facies 2 becoming less common and medium- to coarse-crystalline equant calcite (cement D and E), characteristic of diagenetic facies 3, becoming the primary cements. As these latter cements becomes more abundant downward, the nature of neomorphism in ooids changes from relatively large crystals with crystal boundaries that follow ooid laminations to ooids that are neomorphosed to calcite crystals similar in morphology to the medium-crystalline equant calcite cement. The medium-crystalline equant cement may therefore represent, in part, a product of neomorphism. As is the case in diagenetic facies 2, permeability is generally low, but is locally increased by two factors: degree of dissolution and crushing of molds (Fig. 2.A.2.25 C). Degree of dissolution generally increases downward in diagenetic facies 2 and 3, but also ranges widely within a single thin section. Dissolution may have been affected by the permeability of the sediment after early cementation. Where dissolution is maximized, intergranular cements are partly dissolved, producing pore throats between adjacent molds. Permeability is also maximized in cm-thick zones of collapsed oomolds. These zones occur preferentially along the bases of beds where grain size was apparently small, and sorting was good.

Discussion. The contrast in cementation history between the upper (diagenetic facies 1) and lower part (diagenetic facies 2 and 3) of the Drum Limestone in the Heartland Cement Quarry may be the cause of several factors including early marine cement distribution with the resultant porosity and permeability trends, variability

in effects of early compaction and selective dissolution, and possibly the level of an relatively early, ancient meteoric water table.

It appears the early marine cements (cements A, B, and C) precipitated in the lower 3/4 of the Drum Limestone prevented significant early compaction of these rocks in contrast to the upper 10 ft (3 m) of the Drum Limestone in which these early marine cements are absent and the rocks experienced significant early compaction. Although the original depositional facies were essentially the same, the lack of marine cements in the upper part may indicate changing environments and/or change in relative sea level that would have prevented marine cement precipitation in these rocks. The increase in shale in the upper part may indicate a relative rise in sea level.

Early dissolution, replacement fabrics and precipitation of medium- to coarse-crystalline clear, equant cement (cements D and E), probably reflecting a fresh water, phreatic environment, affected only the lower 3/4 of the Drum Limestone facies and not the upper 1/4. This may reflect differences in porosity/permeability due to early compaction essentially making the upper 1/4 rocks an aquitard to the early meteoric waters. Additionally the shale lenses and seams in the upper 1/4 of the oolite may have reduced permeability. The aquitard hypothesis seems unlikely because of the extensive replacement and cementation by later ferroan calcite and dolomite (cements F and G) that occurred in the upper 1/4 Drum rocks likely in an anoxic(?) burial environment. Alternatively, the distribution of early dissolution and precipitation of cements D and E may reflect an ancient water table; the upper limit of the water table occurred at the sharp boundary between the lower 3/4 (diagenetic facies 2 and 3) and upper 1/4 (diagenetic facies 1). However, no features suggestive of a vadose environment (e.g. meniscus cements, pendant cement fabrics, vadose silt) nor of subaerial exposure have been identified to date in the upper 1/4 Drum rocks to substantiate this hypothesis. A third alternative is that cements A,B,C,D and E were all precipitated prior to the deposition of the upper 1/4 of Drum oolite. This would suggest that there was a depositional hiatus and incursion of a fresh water lens likely tied into a relative sea level drop prior the deposition of the upper 1/4 of Drum oolite. The upper 1/4 of Drum oolite facies would have been deposited during the subsequent transgression. However, to date, no erosional truncation surface, subaerial exposure features, nor transgressive lags have been recognized at the boundary between the lower 3/4 and upper 1/4 of Drum in outcrop, handsample, or thin section. Similarly, no observations have been made from thin sections, to date, of truncation of cements A,B,C,D or E at this boundary nor of inclusion of any of these cements in clasts in the upper 1/4 Drum oolite that would support a depositional break between the lower 3/4 and upper 1/4 of Drum oolite.

It is clear that much detailed diagenetic and geochemical work will be necessary to further document the paragenetic sequence and understand the processes and environments important in the diagenetic evolution of the

Drum oolite facies of the Heartland Cement Quarry. At this stage of the study, it appears likely that much of the cementation and porosity creation/occlusion is related to early marine cements and to meteoric cements likely tied into a relative sea level drop during or shortly after deposition of the Drum skeletal, oolite facies. A relative sea level drop just after Drum oolite facies deposition may be supported by evidence from outcrop, core, well logs and high resolution seismic data that indicates the upper Drum Limestone experienced, at least locally, significant erosion possibly due to shallower marine conditions related to a relative fall in sea level.

The diagenetic history of the Drum oolite is very similar to the diagenetic history of the oolitic reservoir in the Swope Sequence of the Victory Field. The primary difference is that the Victory Field lacks the cement that occur in large shelter voids beneath fossils in the Drum, such as cements B and D. Thin sections of well-sorted oolite from the Drum Limestone at the Heartland Cement Co. Quarry are indistinguishable from thin sections from cores and cuttings of reservoir facies in the Victory Field. This suggests patterns of porosity zones observed on Drum oolite outcrops may be useful for developing models of fluid flow in Lansing-Kansas City Group oolitic petroleum reservoirs.

Summary

An integrated study incorporating sedimentologic, stratigraphic, diagenetic, and high resolution seismic data was conducted on the Drum Limestone in Montgomery County, a potential surface and shallow subsurface analog for oolitic reservoirs in the Lansing and Kansas City groups in central and western Kansas. The goals of the project were to determine the sedimentologic and general diagenetic history of the Drum skeletal oolite facies, to determine the facies and geometry relationships of the Drum Limestone with associated strata and to determine the controlling factors for deposition and diagenesis of the Drum Limestone.

The Drum Limestone in Montgomery County was deposited on a surface with pre-existing topography that resulted from deposition of underlying units, chiefly the Dennis Limestone and Cherryvale Shale. A broad, flat shelf existed to the north. Near Independence there was a shelf edge that corresponded to the southern edge of a major lobe of the Cherryvale delta. Drum Limestone deposition consisted of four facies from base to top: 1) A thin (generally less than 1 ft [0.3 m]) intraclastic limestone that was deposited during transgression; 2) a deeper water, sparsely fossiliferous interbedded shale and laminated limestone; 3) fossiliferous wackestone, packstone, and stromatolites that were deposited in shallow-water, normal marine to restricted conditions; and 4) cross-bedded skeletal oolite grainstone deposited in shallow-water marine conditions. The contact between the fossiliferous wackestone to packstone and grainstone is sharp, and may have been locally subaerially exposed. Basinward of the depositional shelf edge the oolite thickens from under 20 ft (6.1 m) on the shelf, to 50 ft (15.2 m), and then thins southward to a pinch-out. The fossiliferous packstone to wackestone has not be observed basinward of the depositional shelf edge. The interbedded shale and carbonate mudstone thickens basinward,

and the upper part becomes increasingly bioturbated likely indicating increasing oxygenated conditions associated with shallowing at the end of Drum deposition. Locally, upper Drum strata were eroded possibly as a result of a relative lowering of sea level.

High resolution seismic studies were conducted to study geometries and test correlations of Drum and associated strata in the subsurface. The seismic data and synthetic modeling confirmed most observations from outcrop, core and well log data. The seismic data proved most useful for detecting local and overall thickening and thinning patterns in some strata and for detecting outcrop-scale significant erosion of Drum and post-Drum strata.

A petrographic study of diagenetic characteristics was conducted on samples of the Drum skeletal oolite grainstone facies from the Heartland Cement Quarry because of the similarity of this facies to known reservoir facies in the subsurface of Kansas. A complex history of cementation, dissolution and compaction affected this facies and resulted in a variable distribution of diagenetic features.

Despite the spatial distribution complexities, the skeletal oolite grainstone facies can be divided into three general diagenetic facies based on vertical distribution pattern of dominant diagenetic features. The upper zone (consisting of up to 10 ft [3 m] of Drum Limestone) lacks early cements, is significantly compacted, and contains only late ferroan calcite and dolomite cements and replacement fabrics. The middle and lower zones were relatively unaffected by early compaction due to cementation by early marine and meteoric phreatic cements. Moldic porosity generally increases downward through the upper most 15 ft (4.6 m) of Drum Limestone. Permeability is greatest where oomolds have collapsed. A reservoir model based on the Drum Limestone would indicate that fluid would flow along the zones of collapsed oomolds which occur primarily along bedding contacts. These zones would form conduits of fluid flow, potentially leaving large amounts of bypassed oil.

Several hypotheses could explain the paragenetic sequence and spatial distribution of diagenetic features. It appears likely that much of the cementation and porosity evolution is related to early marine cements and meteoric cements related to a relative sea level fall during or shortly after Drum skeletal oolitic facies deposition.

The integrated methods used in this study have resulted in a better understanding of depositional and diagenetic features associated with the Drum Limestone and a better understanding of potential reservoir characteristics and heterogeneities within the Drum skeletal oolite grainstone facies. The methods demonstrated in this study should prove useful in the study of similar, potential and actual reservoir facies.

2.B. Regional Stratigraphic Correlation and Mapping Linking Near-surface and Surface Sites with Western Kansas

By W.L. Watney and G. Stevenson

Introduction

Principal results of this work were presented in the initial discussion of the regional geology. Additional supporting information on the regional study are provided in this section.

The objective of the database was to establish a regional sequence-stratigraphic framework extending from the reservoir analog areas of southeastern Kansas to the region of significant Lansing-Kansas City oil fields in central and western Kansas. Some 5,000 total wells are included. Goals of the regional mapping and cross section construction include: 1) to infer nature of the changing configuration of the shelf, its accommodation history (perhaps distinguishing subsidence and sea-level change), 2) to understand the influence of basement structure and heterogeneity sedimentation patterns and reservoir development, and 3) as constraints or parameters and results of computer simulation modeling.

Methodology

Wireline log correlations of major markers in the pre-Permian interval were completed and are used to construct regional cross sections. Detailed stratigraphic correlations in the Middle and Upper Pennsylvanian were placed into a regional database. Results from analysis of outcrop and shallow coreholes assisted in establishing correlations in the deeper subsurface to the west along the shelf-to-basin and carbonate-siliciclastic transition. Mapping of individual 3rd- and 4th-order sequences across the shelf provides a high resolution temporal framework from which to reconstruct changing shelf configuration and controls for use in defining analogous locations on the shelf (e.g., having similar elevation, slope, and stratigraphy). Biostratigraphic information was used to confirm the physical correlations of 4th-order sequences in the Middle and Upper Pennsylvanian extending between outcrop and extreme western Kansas (400 miles).

A multivariate statistical method called regionalization was performed, helping to establish the correlations of the stratigraphic variation with basement structure and heterogeneities.

2.B.1. Regional Cross Section and Pre-Permian Structural/stratigraphic Database

Introduction

Eleven (11) regional structural cross-sections were constructed from available well logs and lithologic control to provide the framework for subsurface correlations and the regional database in central and western Kansas.

These regional cross sections were prepared at a scale of 1"=100 feet vertical and 1"=8 miles horizontal for a vertical exaggeration of 422 times. Cross sections run from surface to Precambrian basement. The wireline logs of choice were generally gamma ray-induction logs. Correlations were also based on the lithologic descriptions of sample logs commonly available for wells in Kansas. In some areas the Precambrian and Arbuckle datums were estimated from maps (Cole, 1976, and Baars, in prep.).

Cross-sections are labeled A-A' through K-K'. Locations of the cross sections are found on the state map in Figure 2.B.1.1. Total length of all of these sections is over 1740 miles. Most significantly, the sections tie the Pennsylvanian outcrops in the eastern part of the state to the subsurface. The relationships between basement heterogeneity, structural reactivation, and sedimentation is illustrated by the localized thickness changes where suspected faults are present. The cross sections provide the framework for a pre-Permian regional structure/stratigraphic database (Gene.base) that was linked to other datasets used to generate the regional maps.

Several of the cross sections are presented here as "stick" sections (Figures 2.B.1.2 to 2.B.1.5) to summarize structural and stratigraphic relationships at a scale that is more manageable for this report (actual log sections are 10's of feet in length). The stratigraphic key to the symbols used on these cross sections is provided in Figure 2.B.1.6. Actual log sections are available for examination and reproduction as open file reports of the Kansas Geological Survey. Convention, format, and scale are the same for all of the stick sections presented here.

Log datums range in degree of "confidence" due to a number of parameters including:

1. log quality
2. log type
3. geologic variability
    a) tops within a variable lithology are difficult to correlate
    b) tops above/below consistent lithology are easy to correlate
    c) tops based on LS/Sh or SS/Sh boundaries are very tenuous when they merge to LS/LS or SS/SS boundaries
    d) easiest picks are top/base of black shales (condensed sections "core shales"); however, many are not regionally continuous because they are too thin to resolve or they pinch out laterally
    e) tops are difficult to correlate when separating cyclic sedimentary packages that have identical lithologies above/below log pick
    f) picks are difficult when section expands dramatically or attenuated--due to fault omission, onlap, offlap, etc.

g) some picks may be readily discernable in samples but have no particular log definition (e.g. Miss carbonates).

Logs have been correlated on a regional basis, from top/Penn. to basement (where available). These picks probably contain mistakes at the local level that would be resolvable with additional control. However, the dataset represents one of the best public domain databases for regional correlation in the Pennsylvanian of Kansas. Additional detailed correlations and cross sections were made for the sequence database (Lynn.base). A separate log file exists for both databases. Logs are marked with tops and include completion information. Table 2.B.1.1 describes information on reliability of correlations in cross sections.

Table 2.B.1.1. Reliability of correlations in cross sections.

Grading System of Well Data

strong	1. High degree of correlatability - 90% or greater are within agreement
moderate	2. Moderately high 80% - locally correlates--but problems when extended regionally
weak	3. Low 70% - highly variable and probably should not be used.

Datums with excellent reliability:

Heebner
Hushpuckney
Top Cherokee
Top Mississippian carbonates (but not ages)
Arbuckle (subregionally)

Datums of limited extent:

Pennsylvanian sandstones - SE/4 of state

Datums that are moderately reliable:

T/Penn.
Wabaunsee (locally very difficult)
Root (locally very difficult)
Douglas
Lansing
Kansas City

Muncie Creek (base Iola)

Marmaton

Atoka

St. Genevieve (locally difficult)

St. Louis (locally difficult)

Osage (locally difficult)

Kinderhook (locally difficult)

Viola

Simpson

Arbuckle

Precambrian

Datums difficult to correlate:

Topeka

base Kansas City, "base Hertha", Mound City Shale

Morrow

Chester

Pennsylvanian basal conglomerate

Discussion

The following is a review of key elements on each of the cross sections. Certain features are identified on the cross section at the appropriate well and depth by an asterisk (*). An asterisk and well number noted below is the key to these features.

Cross section A-H (Figure 2.B.1.2). Cross section A-H is 250-miles-long, oriented west-to-east running from the Kansas/Colorado border to the south end of the NW-SE trending Central Kansas uplift and NE-SW trending Pratt anticline.

* Well #1 - The Amoco Rebecca Bounds #1 well. This well was continuously cored. Total core footage is 5425 running from the Cretaceous to the Uppermost Ordovician. Black shales and flooding units were sampled from this core in September, 1990 for biostratigraphic analysis at the Amoco Research Center. Permission was given and arrangements made by Dr. Robert Scott. Our appreciation is extended to him and his staff. Results of the biostratigraphic analysis, described separately in this report, helped to resolve some discrepancies between the log correlations here and those previous

works, particularly Heebner Shale and top Lansing, confirm Haskell Limestone, Nuyaka Creek with the physical log correlations described here.

-- Lansing top correlates to Lansing top to east, north and south but is appreciably lower than previously correlated (Biostratigraphic data confirms this). "False Lansing" top is actually Douglas equivalent --Haskell Limestone. See original cross-section C'-C" for best example of Lansing correlation problem.

-- Pennsylvanian basal Morrow disconformably overlies lower Chesterian St. Genevieve Ls.

* Well #4

-- Very thin Simpson 5452-5459 (7') overlies Arbuckle, whereas Viola disconformably overlies Arbuckle in well #1.

-- Well located on one of Cole's (1976) "bullseye" basement anomalies. Shown here to be possible horst block to account for drastic dip reversals necessary if left unfaulted.

-- Note thinned St. Genevieve and St. Louis relative to well #1, but thicker Osage, Kinderhook and Viola section.

* Basement fault between wells #6 and #7. Fault defines eastern limit of St. Genevieve and Morrow. Well #7 has a much thinner Atokan interval disconformably overlying Meramecian St. Louis Ls.

* Well #11. Another Cole (1976) bullseye basement anomaly-confirmed by well penetrating Precambrian at 5230' (-2937), and shown as horst block.

-- Note Arbuckle to basement thickness in this well is 261' compared to approximately 700' in wells on either side.

-- fault shown between wells 10 & 11 defines eastern limit of Atokan age rocks.

-- wells 11 & 12 mark the easternmost occurrence of Meramecian age rocks. Here, Cherokee disconformably overlies Meramec.

* Well #13. E. limit of Meramec. Cherokee disconformably overlies Osagian carbonates.

-- Note thinning in Marmaton section as compared to that shown in well #12 immediately to west.

-- Relative thick Arbuckle, Simpson, Viola and Kinderhook in wells 13-16 as compared to thins in flanking wells suggest that this block was low in Cambrian, Ordovician, Devonian and Kinderhook time, but reversed motion in Osage time and again positive in Marmaton time.

-- Block faults shown in cross-section between wells #10 & 17 are a series of "half-grabens" caused by overall basement extensional faulting in Precambrian time.

* From well #17 to #22 - crosses the southern end of the Central Kansas uplift

-- Numerous periods of uplift and down-faulting are demonstrated in the various cross-sections constructed--and in the well log database.

* -- Well #17 demonstrates post-Arbuckle uplift--in that Simpson disconformably overlies PreC. Also shows Mississippian rejuvenation--Cherokee disconformably overlies Kinderhook.

* Wells 18 & 19 -- Note presence of thick Arbuckle compared to well #17, suggesting a paleo-graben during Simpson deposition. However, it was a positive feature following Viola deposition and continued high through at least Missourian time, Hertha disconformably overlying Marmaton which in turn, disconformably overlies Viola.

-- Wells 20-21. This relationship of Marmaton disconformably overlying Viola still present, but a very thin Pleasanton preserved, and thickens eastward.

-- Wells 21 to 26. Series of "half-grabens" on east flank of Central Kansas uplift showing progressive preservation of pre-Penn. units as transect extends eastward. (Marmaton disconformably on Kinderhook in well 22, then Marmaton over Osage in wells 23, 24 and 25, and finally Cherokee disconformably overlying Osage in well #26.

-- Note overall eastward thickening in all pre-Missourian rock units except Viola--where the opposite is true--it thins eastward (not sure where eastern limit of Viola lies, but east of Nemaha, Kinderhook overlies Arbuckle).

-- Most notable aspect in post-Desmoinesian rocks is the occurrence of siliciclastic wedge occurring in Douglas Group (Ireland and/or Tonganoxie sandstones).

-- Note also the rapid thickening of Lansing Group. Farther east the Lansing shelf carbonates change facies to the Stalnaker siliciclastics (see eastern portion of cross-section G'-G").

The pre-Missourian tectonic history shows numerous episodes of block faulting in cross section A-H. Each fault block demonstrates varying rates of collapse, and periodic episodes of quiescence, or uplift, relative to bounding fault blocks. This apparent "oscillation" of the basement does not require alternating regional compression and extension (transtension and transpression) but can be accommodated entirely by extensional (divergent) intracontinental wrench faults driven by the recurrent north-south compression of the North American craton (Baars and Watney, 1991).

Although apparently much more subtle during the Missourian and Virgilian deposition, it is seriously doubted that this long-term history of recurrent basement faulting was "turned-off" during this time. Reactivation of basement block-faulting is considered to be a significant factor in controlling the distribution and characteristics

of the Pennsylvanian cyclothems, and should be incorporated in any effort to understand the stratigraphic relationships of the region (as discussed throughout the text). Eustasy, while important in generating Pennsylvanian cyclothems, is not the only element at work.

Cross section D-D' (Figure 2.B.1.3). A 200-mile-long, south-to-north cross-section extending from the Oklahoma/Kansas border near the northern flank of the Anadarko basin, crossing Victory field to the northeast corner of Graham County through Pen field located on the northern portion of the Central Kansas uplift and Cambridge Arch. The section is essentially a dip section running from the lower to the upper shelf. Most strata including the Kansas City Group reveal marked attenuation onto the upper shelf.

* Wells 1-10 demonstrate the stratigraphic relationships of the pre-Pennsylvanian interval in the Hugoton embayment.
  - -- Note the omission of unnamed Chester rocks on the Victory structure (Well #5, location of one of the field studies) and the updip limit of unnamed Chester between wells #10 & #11. Note also the marked thinning of Early Pennsylvanian Morrowan strata and the updip limits near well #13 (this well ties A-A').
  - -- Well #13 is also updip limit of St. Genevieve
  - -- Note a thin Atoka interval between wells #13 and #16

* At well #17, Cherokee disconformably overlies Meramec
  - -- Note Marmaton "thin" corresponds to basement structure between wells 12 and 17.

* Wells 17 to 22. Note updip (northeast) thinning of pre-Pennsylvanian section and the updip limit of Meramec rocks occurring between wells #19 & 20. Well #17 also is located in the vicinity of a significant shelf flexure developed during the Missourian (oriented perpendicular to the section). A basement terrain boundary is interpreted to coincide with this zone of flexure (Yarger, 1983) (see discussion on regionalization in next section).

* Well #20. Kinderhook strata disconformably overlie Simpson. Viola is present in flanking wells.

The omission of Viola in well #20 suggests that this area was structurally high during or immediately following Viola deposition. The site was relatively structurally quiet through the lower Mississippian but again became a positive site during post-Osage time (the Cherokee Group rests unconformably on Osage rocks). The area then subsided through late Desmoinesian (Marmaton thick) and once again became a subtle positive location during Missourian.

* 23-28 (located on the Central Kansas uplift). Wells show a progressive northward thinning of Arbuckle through Marmaton stratigraphic units.

* Wells 23-24. Updip limit of pre-Penn to post-Arbuckle interval. (includes truncation of Simpson, Viola, and all Mississippian strata). Cherokee disconformably overlies Arbuckle in well #24.

* Wells 25-26.
  -- Updip limit of Cherokee

* Wells 27-28.
  -- Updip limit of Marmaton with Missourian strata resting on Cambrian Reagan sandstone.

Cross section G-G', G-G" (Figures 2.B.1.4 and 2.B.1.5). A 380-mile-long, west-to-east cross section beginning at the Colorado border and extending to the Missourian outcrop belt in southeastern Kansas. The line of section crosses the Hugoton embayment, Central Kansas and Nemaha uplifts.

* Wells 3, 4, 5 -- faults shown correspond to basement faults and rapid changes in basement gradient as mapped by Cole (1976). Note omission of unnamed Chester in Well #3.

* Well 13 -- the depth to basement is greatest in this vicinity; occurring at an estimated subsea elevation of -6500'. Although this would appear to be the deepest part of the Hugoton embayment in Kansas, the greatest thickness of Lower Pennsylvanian Morrowan rocks occurs farther west, near well #8.

* Well 8 -- the thickest pre-Missourian Pennsylvanian interval occurs in this vicinity (wells 7, 8, 9) and thins rapidly eastward.

* Well 15 -- eastern limit of Morrow.

* Well 17 -- fault shown immediately west of this well defines eastern limit of all rocks of Chester age (both unnamed interval and St. Genevieve Ls.). At this location, Atoka disconformably overlies Meramec.

* Well 20 -- Note rapid thinning (truncation) of Meramec rocks between wells 17 and 20. In a distance of approximately 30 miles, Meramecian age strata change from over 600 ft. in thickness in well 17 to zero in well 20.

-- Atokan strata also thin and/or truncated to east and are missing in well 20, such that a very thin Cherokee section disconformably overlies Osage strata.

-- Although deep pre-Mississippian penetrations are scarce in this vicinity, note the relatively thick Viola-Simpson interval compared to similar interval to west or east. This thick pre-Carboniferous section suggests that in early Paleozoic time, the area between wells 17 and 20 was structurally low, allowing a thicker section to be preserved.

-- Wells 19 and 20 are the westernmost wells to show a Quindaro shale marker. While present to the west, it is less obvious on well logs and is of less use for correlation purposes. However, to the east, the Quindaro shale marker is most useful, particularly in delineating the age equivalent siliciclastic units of the Lansing, Douglas, and Kansas City groups.

* Well 21 -- Cherokee disconformably overlies thin Kinderhook strata.

* Well 22 -- Marmaton disconformably overlies thin Osage. Note much thicker Kinderhook interval than in well 21.

* Wells 24 to 33 -- Cherokee disconformably on Osage.

Well 25 -- Westernmost limit of Stalnaker Ss. Note that siliciclastic unit lies below the Iatan Ls. (brown lime).

Three distinctly different siliciclastic units are shown on cross-section from this location (well 25) eastward to end of line (well 42). These siliciclastic units have been mistakenly mapped as time-correlative units by other workers, but the correlations provided on this cross-section and H-H' demonstrate the following:

1) The Layton Ss lies below the Layton LS, and radioactive shale.
2) Log correlations demonstrate the Haskell LS separates the older Stalnaker Sandstone from the overlying Ireland/Tonganoxie sandstones. Therefore, the Stalnaker is Lansing equivalent while the Ireland/Tonganoxie are Douglas equivalent.

* East of Well 35 Pennsylvanian strata outcrop-Virgil from Well 35 to 40 and Missourian strata east of well 40.

Common practice is to confirm subsurface correlations through comparison to outcrop exposures. In the case of the siliciclastic units mentioned above, and possibly carbonate examples as well, a case can be made that the subsurface correlations may help delineate stacked depositional intervals of similar lithologies (e.g., Tonganoxie sandstones indistinguishable from Stalnaker sandstones).

* Well 42 ties directly into the Drum limestone near-surface and outcrop reservoir analogue research area.

Note the drastic jump in depth-to-basement immediately west and east of this block. Note also that Osage rocks disconformably overlie Arbuckle indicating at least one period of pre-Pennsylvanian uplift.

2.B.2. Regionalized Classification of Mapped Sequence Stratigraphic Data

--Conducted in collaboration with J. Harff, J.C. Davis, J. Bohling, and J.C. Wong

Overview

Isopachs of major Pennsylvanian stratigraphic intervals were presented and interpreted in Regional Geologic Framework. Datums from selected area in the database were analyzed using a multivariate statistical method in order to objectively characterize areas where multiple interval isopachs undergo similar changes.

Analysis of such large stratigraphic data sets to define patterns, trends, and correlations among layers of strata has provided significant challenges. Pattern recognition, for instance in establishing the influence of recurrent structural movement, includes simultaneous analysis of potentially many mappable datums. Physical overlay of maps for visual trend and pattern identification often works, but much information can be missed or is unnecessarily biased using the manual approach. With digital data it is possible to "electronically overlay" the mapped datums to extract correlations, associations, and patterns from which to make interpretations. The procedure described below is scale independent.

The following is a synopsis of the multivariate spatial modeling summarized from a manuscript prepared for publication (Watney et al., 1993). The research is done in collaboration with Dr. J. Harff at the Institute for Baltic Sea Research, Wanemunde, Germany, and Dr. John Davis, Kansas Geological Survey.

Clear spatial patterns and trends from the analysis of the Pennsylvanian thickness data suggest areas of homogeneous structural deformation. The results are potentially useful in defining analogous sites for reservoirs on the shelf. The fields occupying specific areas may have similar properties associated with these patterns and trends in thickness, e.g., fracturing affecting reservoir quality, oil migration and reservoir charging.

Some of lineaments identified here reflecting areas of recurring changes in thickness patterns serve as sites of flexural hinging of shelf influencing deposition. Other influences have yet to be defined.

Methodology

Regionalized classification is an consistent, quantitative statistical procedure. Boreholes are clustered into a heirarchial classification based on correlations of mapped variables. Compact groups are formed in variable space that simultaneously delineate contiguous geographic subareas. The approach effectively subdivides a basin or an oil field into homogeneous subareas, where variables that are compared behave in a similar manner. The reliability of the regionalization is expressed by a Bayes-probability that forms the basis of the mapping.

The nature of the regionalized subareas obtained in this procedure depends on the variables used. The results may not correspond to conventional classifications. The use of complex variables may make the results of this procedure difficult to interpret. For example, regionalization conducted on a series of formation tops would distinguish subareas of similar structural variation. A regionalization based on geologic variables correlating to oil production would define regions of similar oil potential. Regionalization based on isopachs such as in this example delineate subareas with similar thickness and depositional history.

The regionalized classification procedure involves two steps: 1) typification, where actual observations from each well, individual isopach thickness in this case, are grouped into a heirarchy of clusters on the basis of mutual similarity; 2) regionalization, where every possible map locality is assigned to a region based on probability functions relating the mapped characteristics of every locality to each other. The statistical procedure is described in detail in (Harff and Davis, 1992; Watney et al., 1993).

In the typification procedure of this example, a set of geological observations, is assumed to be composed of K multivariate normal distributions having a common covariance structure. Heirarchial agglomerative clustering around group centroids, using Mahalonbis' distance as a similarity measure, leads to successive approximations of the underlying set of distributions. The true number of constituent distributions is approximated when the ratio of within-group to between-group variances is minimized. Then the clusters are simultaneously as compact and as distinct as possible. Multivariate discriminant analysis is used to calculate the intergroup distances and Bayesian classification probabilities.

The geological variables are interpolated over the study area using an optimal spatial estimator, in this case, kriging. A regular set of grid nodes is calculated. At every grid node, K-multivariate Mahalonbis' distances are calculated to each of the K-centroids. The probability that the grid node belongs to a specific cluster is calculated for each of the k clusters, using the Bayesian probability functions. Because the mapped variables are

spatially continuous, the probability functions will also be continuous functions. Each grid node is assigned to the class having the highest probability.

Results

The example includes nine interval thickness variables from the Pennsylvanian and Permian interval and thicknesses of four depositional sequences in the Kansas City Group from a portion of the dataset overlying the Central Kansas Uplift and western Kansas shelf. The dataset used in this region includes 2112 wells and 350 oil fields.

The thicknesses of large stratigraphic intervals are expressed in Variables 1-5:

Variable	Interval
1	Top of Stone Corral Formation (Lower Permian) to top of Heebner Shale (Upper Pennsylvanian)
2	Top of Heebner Shale to top of Lansing Group
3	Top of Lansing Group to base of Iola Limestone (G-zone)
4	Base of Iola limestone (G-zone) to base of the Swope Limestone (K-zone)
5	Base of Swope Limestone (K-zone) to basal Pennsylvanian unconformity

The thicknesses of individual 4th-order cycles in the Upper Pennsylvanian Kansas City Group are expressed in Variables 6-9.

Variable	Interval
6	Thickness of Dewey Limestone (H-zone)
7	Thickness of Cherryvale Formation (I-zone)
8	Thickness of Dennis Limestone (J-zone)
9	Thickness of Swope Limestone (K-zone)

The objective is to identify homogeneous subareas where thickness changes among these 9 thickness variables are similar.

The wells were grouped using the hierarchical clustering. An initial classification into three clusters distinguishes major broad, homogeneous structure elements of the shelf, including: the Central Kansas uplift; the northern part of the shelf that is farthest from the Anadarko basin; and the shelf closest to the Anadarko basin (Figure 2.B.2.1). A six-class regionalization subdivides these three major structural regions (Figure 2.b.2.2). The differences in thicknesses of the nine stratigraphic intervals between these regions can be thought of as differences in sediment accommodation space resulting from subsidence and sea-level change. Locations classified within the same region underwent similar changes in sediment accommodation space.

The changes in accommodation space within each of the six regions is represented by separate subsidence curves (age vs. depth), constructed using the estimated means of the nine thickness variables for each class (Figure 2.B.2.3). Each class, representing a specific contiguous area, has a separate average thicknesses for each of the stratigraphic intervals. Subsidence curves were constructed by plotting successive interval thicknesses for each class vs. the age of each interval. No corrections for compaction were applied to these particular subsidence curves. The objective was to examine general trends in thickness change and general subsidence among six regions. Because of the differences in scale, subsidence curves are constructed separately for the large stratigraphic interval and individual depositional sequences.

Pennsylvanian sediments were first deposited on the basal Pennsylvanian unconformity in Regions 6 and 5, located in the south adjacent to the Anadarko basin. Regions 5 and 6 exhibit the most sustained subsidence during the time from the basal Pennsylvanian to Lower Permian Stone Corral deposition, spanning some 60 Ma. This subsidence can be attributed to proximity to the tectonically active Anadarko basin. During deposition of the Kansas City Group, subsidence was greatest in Region 6 adjoining the western portion of the Anadarko basin. Significant subsidence in the western Anadarko basin during the upper Pennsylvanian is suggested by: evidence of sediment starvation; deep water (>1100 ft) with considerable shelf relief; and turbidite deposition in the western part of the Anadarko basin (Dickinson and Yarborough, 1976; Kumar and Slatt, 1984). However, the subsidence rate in Region 6 diminished below that in several other regions during the time of deposition of the Heebner to Stone Corral interval. Nevertheless, cumulative subsidence was greatest in Region 6. A cratonic salt basin developed in central and southern Kansas over the locations of Regions 3, 4, and 5 during the Leonardian Permian, immediately beneath the Stone Corral datum, reflecting the eastward displacement of subsidence at this time (Watney *et al.*, 1988).

Region 2 is a broad area in west-central Kansas immediately west of the Central Kansas uplift. The area initially was a low shelf that became filled with older Pennsylvanian strata. Subsidence in Region 2 prior to deposition of the Kansas City Group exceeded that in areas on the Central Kansas uplift, including Regions 1, 3, and 4. However, subsidence rates in Region 2 were similar to that on the Central Kansas uplift and upper shelf during deposition of the Kansas City Group. Region 2 experienced lower subsidence rates during the time of the youngest Heebner to Stone Corral interval, resulting in a cumulative subsidence intermediate between the upper and lower shelf areas.

Region 1, the upper shelf and the Cambridge arch in the northern portion of the Central Kansas uplift, has undergone the least amount of subsidence. Pennsylvanian sedimentation began earlier in Region 1 than in Regions 3 and 4 on the Central Kansas uplift, reflecting an early western downwarp associated with a long, narrow embayment that developed in westernmost Kansas and adjoining Colorado during lower Pennsylvanian Morrowan and Atokan time. Minimal subsidence in Region 1 is consistent with its position as most distant from the Anadarko basin. Region 3, located on the northern portion of the Central Kansas uplift, is characterized by only slightly greater subsidence rates than Region 1 during the deposition of the interval from the base of the Pennsylvanian to the top of the Heebner Shale. However, subsidence in Region 3 accelerated significantly during the time of Heebner to Stone Corral deposition.

Thicknesses of individual depositional sequences in the Kansas City Group (Figure 2.B.2.3) represent very short intervals of geologic time (250 Ka to 500 Ka). Thicknesses of strata deposited during these shorter time intervals were probably a function of changes in accommodation space caused by both subsidence and global sea-level changes. Sediment accommodation space generally increased from the northern part of the uplift region and upper shelf that is most distant from the Anadarko basin (Region 1) to the southern portion of the Central Kansas uplift (Region 4). This trend continues southwestward into Region 6 toward the western part of the Anadarko basin, which was the most tectonically active.

The probability of correct classification of the wells was calculated as a space-dependent Bayesian probability. The map for the probability of correct classification of all six regions is displayed as_Figure 2.B.2.4). The central parts of the homogeneous regions are marked by high probabilities, reflecting more definitive classifications than in the zones of transition from one homogeneous region to another. In these zones, the probability of correct classification drops rapidly, forming "probability valleys." These may be interpreted as regions of tectonic instability characterized by fracturing, faulting, and folding as seen on the basement configuration map (Figure I.27) and as inferred from gravity and magnetic potential field maps (Yarger, 1983; Baars and Watney, 1991). Cross sections (Figures 2.B.2.5 and 2.B.2.6) illustrate the changing structural styles

in the different regions. Thickness and attitude of strata and basement heterogeneities coincide closely with class areas of thickness data.

Most of the boundaries and locations of the six regions correspond to recognizable elements of the Precambrian basement; these are especially apparent on the cross sections (Figs. 2.B.1.3 and 2.B.1.4):

1) The boundary between Regions 3 and 4, which divides the Central Kansas uplift, corresponds to the western edge of a basement area crossed by faults associated with the Keweenawan (1.1 billion year old) Midcontinent rift system.
2) The boundary between Regions 4 and 5 corresponds to the southwestern end of an area of rifted basement rocks.
3) The northernmost boundaries along Regions 5 and 2 correspond to a Precambrian terrain boundary defined by potential field mapping and differences in basement geochronology (Yarger, 1983). Regions 2, 5, and 6 are south of this boundary and underwent greater subsidence during deposition of the Kansas City Group than did the area north of the boundary. This boundary is also the axis of an inferred southward flexure of the shelf, characterized by abruptly thickened trends in oolitic grainstone in sequences of the Kansas City Group (Watney, 1985).
4) The boundary between Regions 2 and 6 is not well defined from basement mapping because of the absence of subsurface control used in this part of the investigation.

Fundamental heterogeneities in the basement rocks consist of lateral contrasts in age, composition, and structure. The characteristics of the variables that define the six regions can be attributed to a combination of differential structural deformation between the basement elements and lateral heterogeneities.

Region 4 contains the highest percentage of productive oil wells (20% of the wells in the database) of all the regions. The percentage is 7% in Region 1, 8% in Region 2, 14% in Region 3, 2% in Region 5, and 10% in Region 6. Region 4 probably has a higher percentage of productive wells because:

1) The area was predominantly a sustained positive site during deposition of Upper Pennsylvanian strata, leading to subaerial exposure during the later stages of each depositional sequence in the Lansing Kansas City. Criteria diagnostic of subaerial exposure are common in sequences in Region 4, accompanied by nontectonic fracturing and dissolution of carbonate.
2) Region 4 includes the southern part of the Central Kansas uplift and represents the first major uplift beyond the northern edge of the Anadarko basin, the probable source of much of the oil that accumulated on the western Kansas shelf (Schmoker, 1986). Oil migrating out of the basin would encounter this uplift as one of the first major structural traps.

3) Structural flexure associated with development of the southern margin of the Central Kansas uplift was concurrent with sedimentation of Kansas City strata, providing favorable sites for high energy carbonate accumulation (Watney, 1984, 1985). Updip pinchouts of primary intergranular porosity associated with these grainstones added to the potential for trapping hydrocarbons.
4) The Precambrian basement beneath the area of Region 4 is characterized by numerous intersecting conjugate faults at the intersection of the NW SE-trending Central Kansas uplift and the NE SW-trending Midcontinent rift system (Baars and Watney,1991). Changing stress patterns from southern orogenic systems would likely lead to formation of fractures in overlying strata during the intermittent reactivation of faults in this area. Fracturing facilitates oil and gas migration and formation of reservoirs. The NW SE structure cross section (Figure 2.B.2.5) shows the clear association of thickness and structural changes in this zone of basement faulting.
5) The positive structural location resulted in thinning of shales deposited prior to Lansing Kansas City time, causing a closer proximity or juxtaposition of successive limestones and unconformities. This configuration produced greater opportunities for vertical oil migration. Most of the oil can be geochemically correlated with source rocks in the underlying Mississippian-Devonian Chattanooga (Woodford) Shale.

Conclusions

Regionalization can be regarded as a mathematical expression and computer implementation of traditional methods of geological mapping and interpretation applied to the structural component of basin analysis. The subsidence behavior of subunits in a basin during different time steps can be constructed from data on stratigraphic thicknesses. These multivariate data, derived from well records, are used for regionalization. Thicknesses of large stratigraphic intervals are assumed to be proportional to subsidence. Thickness variations in nine successive Pennsylvanian and Permian stratigraphic intervals are sufficient to define six coherent regions, forming geologically distinctive areas that reflect basement heterogeneity, anisotropy and proximity to orogenic activity. The pattern of subsidence within each region is regular but distinctive from adjoining regions, reflecting changes in rates and locations of directed tectonic stress that originated primarily in the south as the Anadarko basin developed.

Typification of wells based on these variables distinguishes different characteristic subsidence (sea-level rise) curves. Regionalization of western Kansas based on this typification expresses the regional differences in subsidence history and delineates major structures. Each of the homogeneous regions can also be judged on the basis of favorability for petroleum accumulation, reflecting the formation of traps, reservoirs, and hydrocarbon migration pathways. The map of probability of correct classification (regionalization) shows linear zones of transitions from one homogeneous region to another. These transitions are marked by low classification proba-

bilities that may be due to local instability, corresponding to faults and folds. The regions reflect oil productivity and can be used for risk assessment in exploration.

The correlation to tectonic grain and stress fields may also have implications regarding application and design of improved recovery methods, e.g., fracture length, openness, frequency, and orientation for horizontal well assessment; stimulation design, injection well placement.

SUBTASK 3. CORRELATION METHODS

The objective of this subtask is to develop and test methods for establishing temporal correlations and patterns of stratal packages independent from initial log correlations.

Promising methods to obtain new perspectives on stratal correlation include the use of geochemical (isotopes, trace elements, fluid inclusions) analyses to obtain chemical stratigraphic profiles. These data can serve to establish correlations as well as provide more information about processes to help in refining interpretations of stratal variation in depositional and diagenetic environments. Biostratigraphic methods are being refined to aid in correlating individual depositional sequences previously below the resolution of conventional methods.

Two approaches are being used in this program to substantiate physical correlation and stratal patterns:

1) conodont biostratigraphy to correlate individual depositional sequences,
2) Th/U ratios from natural gamma spectrologs to define a chemical stratigraphic succession to aid in recognizing stratal patterns and possibly sea-level change.

This subtask sought to further resolve time and spatial relationships of strata to assist in the quantification of processes and provide more precise geologic reconstructions between eastern and western Kansas. Regional physical correlations of depositional sequences, condensed sections, and marker beds were established through an intersecting set of wireline log cross sections. These cross sections were described in section 2.B.1. The grid of wireline log correlations were verified at intersections with other cross sections. Correlations were extended to other wells to form a database for mapping. Conodont biostratigraphy was used to confirm correlations. The correlation was extended using Th/U ratio and time-series analysis to examine longer-term trends in stratigraphic data.

3.A. Biostratigraphic Analysis

Conducted in Collaboration with L. Lambert and P.H. Heckel

The Upper Pennsylvanian marine depositional sequences are known to be widespread across the Midcontinent through physical correlation along outcrops (over some 500 km). However, long distance and particularly interbasinal correlations have not been possible until recently because the time durations of the depositional sequences (50 to 500 ka) was shorter than resolution of accepted biostratigraphic data. Current investigations of Boardman and Heckel (1989) on independent comparisons of ammonoid, conodont, fusulinid, and coral groups have established correlations between 13 major Virgilian and Missourian depositional sequences in the eastern shelf of the Midland basin and the northern midcontinent. Correlations reflect synchronous marine inundation in both areas. Foraminiferal, ammonoid, and conodont zones have also been used by Ross and Ross (1987) to extend correlations of similar Pennsylvanian marine inundations globally. Biostratigraphic analysis ties this dataset to the global framework.

A set of samples for biostratigraphic analysis were collected from the Amoco #1 Rebecca Bounds core located in Sec. 17-T18S-R42W in Greeley County, Kansas. Additional samples were taken from selected marine shales from cores at scattered sites across western and central Kansas. The samples from the Amoco #1 Rebecca Bounds are from black shales and flooding units of Virgilian through mid Desmoinesian Pennsylvanian age spanning an interval from 3950 to 4700 feet. Samples were analyzed at University of Iowa by L. Lambert and P.H. Heckel. These core samples were broken down with chemical reagents to concentrate the microscopic conodont remains (platforms resembling jaws and teeth) for identification. The cored well had been logged with the latest suite of tools and was subsequently used for both subsidence and Th/U studies. The results of the biostratigraphic analysis are shown by the assigned stratigraphic units in a wireline log of the Rebecca Bounds well (Figure 3.A.1).

3.B. Gamma Ray Spectrolog Analysis

Conducted in Collaboration with J. Doveton, A. Verma, J.C. Wong, R. Black

Wireline logs are the most common form of subsurface information and provide a continuous and usually quantitative record of the stratigraphy. Conventional wireline log interpretation provides information about the lithologies, pore space, fluid types and saturation. Wireline logs can also provide fundamental information about the depositional sequences once they are calibrated with cores.

Because of the continuous record over usually large stratigraphic intervals, wireline logs permit examination of many scales of stratigraphic variation in the rock record that have little opportunity in otherwise being resolved. These changes resolved with well logs can be chemical in nature and go unnoticed via any other common means of description and analysis. For these reasons, wireline logs are very important if not essential in stratigraphic

modeling (Doveton, 1991). New logging tools are capable of detecting fundamental rock properties such as mineralogy, elemental composition, and aspects of texture and stratification (Serra, 1985; Doveton, 1986).

The advantage of the continuous recording of well logs is offset by limited resolution, generally one or two feet. However, selected tools such as the electromagnetic propagation tool, high-resolution dipmeter, and various micro-resistivity logs have resolutions down to inches. The numerical data that logs provide is easily incorporated into statistical and mathematical methods for reduction, trend analysis, and testing.

The logging tools most commonly run in boreholes in Kansas include gamma ray, neutron, density, and resistivity. These logs provide basic lithologic information and permit physical correlation. An increasing number of operators particularly in western Kansas are running the spectral gamma ray tool. This log was used here to improve depositional sequence correlation and enhance interpretations.

The gamma ray spectrolog was examined in three phases: 1) to evaluate the use of this tool in recognizing and characterizing depositional sequences and component genetic units and 2) to investigate the nature of short- and long-term periodicity exhibited by wireline logs, and 3) to help decipher the responsible processes for this periodicity.

Recognition of depositional sequences and genetic units

Natural gamma-ray spectral logs measure the concentrations of the three most common occurring radioactive elements--potassium, thorium, and uranium. Elemental concentrations are determined from emission spectra by using a pulse-height window filter to divide the spectra, and to calibrate detectors against standards (Hurst, 1990). An application of the log is to use the Th/U ratio as an indicator of redox potential. Uranium has an insoluble 4^+ state that is fixed under reducing conditions, but can be mobilized into solution under oxidizing conditions in the 6^+ state. In contrast, thorium, which is geochemically associated with uranium, has a single insoluble 4^+ state and is unaffected by redox reactions. Thorium can be concentrated through chemical leaching since surface conditions can lead to formation of inert oxides. Properties of thorium are very similar to aluminum. The Th/U ratio has been found to be an indicator of redox potential of the environment of deposition (Adams and Weaver, 1958; Almoussli, 1987; Doveton, 1992).

Thorium concentration is associated with common silicate minerals. It can be concentrated as thorium oxide during surface weathering as chemical leaching intensifies. The greater the intensity of leaching the higher the thorium content (Figure 3.B.1). Bauxite (aluminum oxide one) is an example where thorium concentrations are very high.

The initial step in this investigation was to investigate the aspects of the Th/U ratio:

1) to use multivariate criteria to establish the use of the gamma ray-neutron-density and gamma ray spectral log information for recognition of lithofacies or genetic stratigraphic units comprising the depositional sequences
2) to evaluate thorium-uranium ratios as quantitative indicators of depositional environments and diagenetic events;

The time-series analysis of the Th/U ratio was analyzed in the second phase of this activity.

The genetic components of a depositional sequence are listed in Table 3.B.1 and shown in a log of the Th/U ratio for the Dennis and Swope sequences in Figure 3.B.2. The concentrations of Th and U appear to the be result of both deposition and diagenesis. The distinction of these mechanisms is not easy.

Table 3.B.1 . Genetic components of the depositional sequence.

Peritidal carbonates
Subtidal carbonates
Deeper-water subtidal carbonates
Paleosols
Condensed section
Flooding unit

A vertical profile of a depositional sequence generally contains a predictable succession of genetic units: flooding unit, condensed section, late-highstand or shallowing-upward carbonate units, and possibly a paleosol (Figure 3.B.2). One or more minor cycles or parasequences often punctuate these depositional sequences. Because the flooding unit is usually thin, the minor cycles are most often observed in the late-highstand unit. The minor cycles are usually several feet thick and are composed of a flooding surface succeeded by relatively deeper-water lithofacies followed by a shallowing-upward succession.

The Amoco #A-4 Cox well in Victory field in Haskell County, Kansas was used in the initial analysis because the well was cored through the entire Lansing-Kansas City (900 ft.) and adjacent strata. The well also has a complete suite of well logs that were used in this investigation. The gamma ray-neutron-density tool distinguishes the basic lithologies in the Lansing-Kansas City which are dominated by limestone with minor shale interbeds. The very high uranium content of the darker-colored marine shales (condensed sections) is very prominent. The relationship of uranium to organic carbon content in sedimentary rocks is well established (Figure 3.B.3). The thorium:uranium ratio for the marine shales ranges consistently between 0.1 and 1.5

suggesting uranium fixation and reducing conditions. Lowest ratios consistently occur in the lowermost regressive carbonate immediately overlying the condensed section.

Thorium-uranium ratios above 7 are considered to represent oxidizing conditions (Adams and Weaver, 1958). However, this ratio rarely exceeds 7 in the Cox well Lansing-Kansas City. Paleosols and some thin flooding units have ratios in excess of 2, and have definitive oxidized properties observed in cores (Figure 3.B.2). Thus, the threshold of the Th/U ratio for oxidizing conditions is reduced in this stratigraphic interval. Paleosols also have Th/U ratios that are indicative of neutral or slightly reducing conditions. These rocks are gray in color, suggesting reducing conditions.

The distinction of subaerial exposure and paleosols is critical to locating unconformities, and is essential and fundamental to interpreting depositional sequences. However, the thinness and variable character and preservation and Th/U ratios of the paleosols coupled with the resolution of thin beds present problems in resolving this important genetic unit.

Carbonate units exhibit features indicative of accumulation in shallow, oxygenated water and evidence for subaerial exposure. In these cases Th/U ratios range between oxidizing to reducing. Diagenetic overprinting apparently can significantly influence this ratio, e.g., depositing reduced calcite cements or possibly slight uranium enrichment in conjunction with a redox. The lower portion of the late-highstand carbonate unit consistently has a lower Th/U ratio because carbonate lithology has little thorium while pyrite and marine organic matter present in this carbonate preferentially concentrate uranium. The organic matter and reducing conditions may also reflect greater preservation of organic material and retention of associated uranium because of isolation from oxidation associated with the subaerial exposure event at the tops of these 4th-order sequences.

Examples of this ratio and corresponding lithofacies and genetic units are provided from the Cherryvale (I), Dennis (J), and the Swope (K) sequences in the Amoco #A-4 Cox well located in Victory field (Table 3.B.2).

Table 3.B.2. Core sample description and corresponding Th/U ratio in the Amoco #A-4 Cox well from Victory field. Sample numbers correspond to that shown along left margin in Figure 45.

lithofacies	Th/U ratio
1) I-zone flooding unit, dark, pyritic marine lime packstone	Low
2) J-zone peritidal oolitic grainstone	High

4)	J-zone lower highstand unit, dark, organic-rich, sparse infauna (small crinoids, Zoophycus)	Low
6)	K-zone gray/brown mottled, shaley siltstone, paleosol with abundant rhizoliths	High
7)	K-zone peritidal oolite grainstone, cut by gray cherty veins	Low
8)	K-zone dark crinoidal mudstone (deeper subtidal) with extensive mottling and brecciation (diagenetic overprint, probably subaerial exposure)	Intermediate
10)	K-zone flooding unit with lithoclast of underlying paleosol	High
11)	L-zone gray shaley siltstone, paleosol with caliche and rhizoliths	High

Table 3.B.2 indicates that flooding units can have both low or high Th/U ratios depending on the extent of reworking of paleosol clasts versus reducing dark-gray matrix.

A statistical test was done to determine the relationship of Th/U ratio to lithology. Principal component analysis, an unsupervised statistical method, was used to define correlations between the responses of various logging tools used in the Amoco A-4 Cox well. The object is to identify a small number of factors to represent relationships among sets of interrelated variables. Terrastation^{tm} software was used to perform the analysis from the Lansing-Kansas City interval of the Amoco #A-4 Cox well (900 feet). Logs included the gamma ray, neutron (ØN), density, resistivity, and Th/U ratio. Sampling was every 0.5 feet. The specific variables selected for principal component analysis are rhomma and umma, both lithologic indices calculated from the density and neutron logs; gamma ray, a shale indicator; neutron porosity; and the Th/U ratio, an apparent redox index.

Four factors were calculated from the principal component analysis. An eigenvalue is calculated that represents the total variance explained by each factor. Nearly half of the variance is explained by the first factor, with the remaining variation evenly distributed among the next three (Table 3.B.3).

Table 3.B.3. Discriminant Function Analysis

	Eigenvalue	PC1	PC2	PC3
RHOMMA	2.26	45.22	.45	-.27
UMMA	.99	19.71	.49	-.29
GR	.76	15.18	.51	-.17
ØN	.63	2.60	.43	-.43
LOG (Th/U)	.36	7.29	.32	+.79

Depth interval: 4125-4791 feet in #A-4 Cox well.

The first principal component (PC1) represents the coefficients used to express the standardized variables in terms of the first principal component vector. PC1 is a shale indicator, as inferred from the covariation with the gamma ray. PC1 reflects the variation of lithologies in this succession, primarily limestone and shale. PC3 shows a strong loading associated with the Th/U ratio. The negative loadings for the other variables suggest that PC3 is unrelated to lithology, i.e., is independent. This is consistent with observations of the rock where values of the ratio can be the same for different lithologies. The strong correlation with PC3 probably corresponds with the conditions measured by the ratio.

Time Series Analysis of Th/U Ratio

Summary of Findings

The means to extract relative sea-level curves from strata in cratonic settings is hampered by the lack of shelf margins and significant depositional relief. The use of stacking pattern of strata on the shelf to discern changes in accommodation have inherit problems due to what are believed to be broad but tin temporally deposited facies tracts. The means to obtain small-scale correlations is unavailable with the subsurface data that is generally available. Moreover, patterns of stratal distribution at a small scale can be highly variable and limit longer-distance correlation. Accordingly, the use of simple vertical trends in thickness alone is not an adequate means to discern sediment accommodation.

Time-series analysis of the Th/U ratio appears to provide the means to distinguish changes in redox conditions that in turn seems to be related to sediment accommodation. This inverse method of extracting information on sea level from the stratigraphic record has the potential to sharpening the information going into the stratigraphic simulation models.

Continuous profiles of Th/U ratios denoting redox conditions obtained from natural gamma ray logs are here used to recognize and characterize several consistent and correlable orders of cyclicity. The smallest cycle consistently recognized and correlated is a fourth-order, 50 to 60 ft. (16 to 20 m) thick (0.1-1 m.y.) cycle corresponding to unconformity-bounded depositional sequences. A third-order 300 ft. (100 m) (1-10 m.y.) cycle is also noted, recognized as a asymmetric trend (usually sharply bounded) of more reducing to more oxidizing conditions. Each 3rd-order cycle correlates with a separate landward and basinward stepping sequence set developed along the shelf margin bordering the Anadarko basin, substantiating the significance of this cycle.

The 4th-order cycles have durations that are in the rhealm of glacio-eustacy while the 3rd-order cycles are long enough to be related to foreland basin tectonism. The 3rd-order cycles are correlatable across Kansas spanning over 80,000 square miles (207,000 km^2) of the shelf, suggesting region-wide processes are responsible for their formation, possibly active foreland basin flexure or eustacy.

Discussion

The time-series analysis was initially performed on the Th/U ratio using the 1100-foot stratigraphic interval of the Amoco Cox #A-4 well including the Marmaton, Pleasanton, Lansing-Kansas City, and Douglas Groups. The Th/U response can be represented by the sum of regular sinusoids of different amplitudes, wavelength, and starting position. Spectral gamma logs were digitized and a Fourier analysis was performed using Terrasciences Terrastation^{tm} log analysis package. The analysis follows the procedures outlined by Davis (1986). A total of seven wells were digitized and included in this analysis. Fourier analysis was to fit a series of sine waves to establish the cyclic record in the Th/U ratio profiles. Rather than examine the lithologic repetition that is clearly observed from gamma ray and neutron-density logs, the objective is to examine the variation in the redox condition of the strata, shown earlier to be statistically independent of their lithology, as an indicator of any trends in cyclicity related to the redox conditions.

First Th/U data from Amoco Cox A-4 well (Figure 3.B.4) was subjected to spectral analysis. This well provided a good control site because of the continuous core. The power spectrum indicated two prominent harmonics in the digitized 1100-ft interval between the Excello and Heebner Shales, including a long-wavelength sine wave of 363 ft. (3rd-order scale) and shorter wavelength 57 feet (4th-order scale) cycle (Figure 3.B.5). A long-term harmonic (approximately 363 feet) accounts for approximately one-third of the variation.

This sinusoid encompasses 5 to 7 4th-order depositional sequences. The time represented by this cycle interval is on the order of 1.5 to 2 million years corresponding in time to the 3rd-order cycle of Goldhammer et al. (1993). Time duration is based on ages of the stratigraphic groups encompassed by the 3rd-order cycles using a geologic time chart.

Another 20% of the variation is explained by the short-period harmonic of 57 feet. This sinusoid corresponds with the thickness of the 4th-order cycles. These small-scale sequences are clearly defined in the lithologic domain and are easily distinguished on the raw Th/U curve. Scales of cyclicity smaller than this are not seen because of possible systematic errors in measurement as beds approach the limits of precision of the gamma ray spectral tool. Furthermore, Fourier analysis and the use of sine waves used to fit these unconformity-bounded cycles may not be as appropriate as other time-series methods and may introduce error of their own (Doveton, in press).

Approximately half of the variation of the Th/U ratio profile is explained by the 3rd- and 4th-order sinusoids. When sinusoids representing these two harmonics are combined the resulting curve is distinctively asymmetric (Figure 3.B.4) with 3rd-order cycles consisting of 5 to 7 fourth-order cycles. Third-order cycles are separated by abrupt negative shifts in the ratio. These boundaries coincide closely with the formal lithostratigraphic group boundaries, i.e., changes in sedimentary and lithologic assemblages. These boundaries are picked at the position of maximum shift. In all cases this boundary coincides with prominent radioactive marine shale markers (condensed sections) including the Oakley Shale, Excello Shale, Nuyaka Creek Shale, Muncie Creek Shale, and the Heebner Shale.

The long-period cycles encompass the intervals from the Excello to Nuyaka Creek Shale, Nuyaka Creek to Muncie Creek Shale, and Muncie Creek to Heebner Shale, corresponding to the Marmaton, Kansas City, and Lansing 3rd-order sequences defined earlier in the discussion of the shelf margin stacking patterns. The Th/U ratio abruptly decreases at the base of these intervals to lower redox conditions and generally increases gradually up through the interval to higher redox conditions. The progressive change in the redox conditions through each long-term cycle is caused by concurrent and consistent changes, particularly in the deeper water carbonate and the paleosols. Although there is little physical evidence of difference in character, the deeper water carbonates are less reducing and the paleosols are more oxidized and leached upward in the 3rd-order cycle. The implication is that with reduced accommodation, the deeper water carbonate is deposited in increasingly shallower, more oxidizing conditions. Alternatively, this sediment has come in contact with increasing amounts of oxygenated groundwater that might precolatge through the sediment during subaerial exposure. Similarly, the higher Th/U ratio of the paleosols suggests more oxygenated conditions accompanied by more leaching. This

may reflect a trend of increasing duration or intensity of the weathering process moving to the top of the 3rd-order cycle.

The spectral analysis was extended to six additional Th/U profiles at scattered shelf locations across Kansas encompassing range of lithologic successions: 1) SW shelf-thick carbonates, 2) CKU-attenuated carbonates 3) eastern Kansas siliciclastic/carbonates (Figure 3.B.6). The results of the Fourier analysis are expressed first as the raw power spectrums for seven wells (Figure 3.B.7 (a) and (b)). A plot of the thicknesses of the spectral peaks for each well shows a very close correspondence in thickness and arbitrary cycle number between wells in spite of the changes in lithofacies (Figure 3.B.8). The 4th-order harmonics are very similar in thickness while the 3rd-order cycles vary more in thickness with shelf position, i.e. longer-term accommodation. The thinnest 3rd-order cycles group together on the plot and are all from eastern Kansas while the thicker cycles are all from western Kansas sites. The logs of the gamma ray, original Th and U concentrations, the Th/U ratios, and the 3rd- and 4th-order harmonics are presented in a cross section with correlation lines connecting the boundaries of the 3rd-order cycles [Figures 3.B.9 (a) and 3.B.9(b)]. Redox trends readily distinguish the 3rd-order cycles sequences.

The Th/U patterns persists across the shelf even though accommodation and elevation of the shelf varies and relative proportions of carbonate and siliciclastics change. Regardless of the relative contribution of diagenesis or original deposition contribution, this consistent stratigraphic pattern is seen. The two processes appear to act in concert to reinforce the other; reducing marine environments result in reducing diagenetic environments while shallow marine and emergent conditions tend to be more oxidizing.

As described in greater detail in a previous section regional stratigraphic data supports the following regular patterns for the 4th- and 3rd-order cycles:

1) the Kansas shelf evolved from a ramp to a platform configuration during the Kansas City 3rd-order sequence (including Pleasanton to Dewey 4th-order cycles as with 4th-order cycles generally evolving from thick, rather widespread grainstones across the shelf early in the 3rd-order cycle (Swope and Dennis cycles) to extensive low relief mud mounds, more intense subaerial exposure, and limited grainstone development late in the 3rd-order (e.g. Dewey cycle).

2) Sediment accommodation generally shifted basinward later in the 3rd-order sequence including the tendency for more lowstand deposits while the shelf areas appear to have undergone more substantial emergence reflected by incised valley formation, and more oxidized and weathered upper shelves.

3) Landward backstepping and drowning of shelf coinciding with the lower 3rd-order boundaries such as the inundations following the (Nuyaka Creek), Dewey (Muncie Creek), and Douglas Group (Heebner) (Figures I.24 and I.25).

The Th/U response is not due to simple variation of a single facies or genetic unit, but rather is related to independent, but parallel changes in at least two facies components deposited at contrasting times and inferred sea-level conditions. The ratio increases in the upper portion of each 3rd-order sequence, i.e., becomes more oxidizing, independent of facies (e.g., subtidal carbonate facies, paleosols, uppermost regressive facies). Fourth-order cycles with highest ratios occur immediately beneath the Nuyaka Creek (end of Desmoinesian), at the top of the Dewey Limestone beneath the Muncie Creek Shale, and in the Douglas Group beneath the Heebner Shale (around the end of the Missourian). These cycles mark the end of the 3rd-order sequences.

One or more carbonate units located at the beginning of the 3rd-order are generally thicker than succeeding cycles. This implies increased sediment accommodation and more prolonged periods of marine deposition early in the 3rd-order cycles. This is consistent with the initial stages of 3rd-order sequence development from the Th/U ratio indicating more reducing conditions and probably more substantial inundation. The thicknesses depend, in part, on the shelf location. In addition, the shelf deposits at the beginning of the 3rd-order sequence are displaced landward. Intervals that have notably thicker marine sections and exhibit landward displaced shelf sedimentation at the base of these third-order sequences include:

1) the Ft. Scott Limestone above the Excello Shale (database construction indicate that this cycle maintains thickness farther onto shelf and reaches farther unto Central Kansas uplift than later Marmaton cycles);

2) the thick, predominately marine Pleasanton clastic wedge (approx. 200 ft thick) on the mid shelf in eastern Kansas and western Missouri and the impressive carbonate bank development in the overlying Sniabar Limestone along the basinward margin of the Pleasanton depositional slope, both overlying the Nuyaka Creek Shale;

3) the very thick Iola Limestone over the western Kansas shelf superjacent to the Muncie Creek Shale (bank margin displaced northward in eastern Kansas from Oklahoma border to near Chanute Kansas (70 mi.); thick extensive, very phosphatic marine shale at base of Iola cycle with phosphate showing anomalous rare earth element distribution possibly suggesting enhanced sediment starvation, Kidder, 1992);

4) and the regionally thick Oread Limestone overlying the regionally extensive and thick radioactive marine shale, the Heebner Shale. On lower shelf settings, in southern Kansas the Heebner Shale is overlain by the black shale of the next four Th-order cycle (Queen Hill Shale) indicating drowning of the lower shelf.

Conclusions

The Th/U ratio is indicative of redox conditions. The 3rd- and 4th-order cycles recognized here are believed to represent oscillations of marine inundation, based on corroborating stratigraphic evidence.

Is this 3rd-order sequence one derived from eustatic rise or from tectonic subsidence? What is the magnitude of these changes? Subsidence is addressed in the next section. A rise in global sea level characterizes the early to mid Pennsylvanian worldwide. Vail et al. (1977) defined a global coastal onlap curve for the Phanerozoic that shows a 2nd-order sea level rise during the early to mid Pennsylvanian. This corresponds to a major North American transgression associated with the Absaroka cratonic sequence of Sloss (1963). Ross and Ross (1987) and Heckel (1986) define more detailed relative sea-level curves for the Pennsylvanian (Figures I.59). Both agree with the general rise in sea level during the Pennsylvanian. Third-order sequences are regional in extent and appear to correspond to 3rd-order seismic sequences defined by Sarg (personal comm.) in the Midland basin. These cycles are at the scale of time and thickness defined as the primary depositional sequence of seismic stratigraphy (Vail et al., 1991). Fourth-order cycles have been correlated interbasinally and are attributed to the waxing and wanning of continental glaciers. Simulation modeling to test scenarios of 3rd-order cyclicity are addressed in a later section.

These results extend the analysis of the natural gamma ray logging to modeling geologic processes of strata deposited on epeirogenic settings and likely have application to other shelf deposits.

SUBTASK 4. SUBSIDENCE PATTERNS/RATES

By W. Lynn Watney

The objectives of this subtask are to:

1) refine subsidence rates and general patterns that are responsible, in part, for the shelf configuration;

2) establish the relationship of subsidence to basement heterogeneity and tectonism that occurred during the Pennsylvanian.

The reservoirs and near-surface analogues reside on platforms, ramps, and in shelf-margin settings that were developed due to the interaction of basin subsidence, eustatic sea-level change, and sediment accumulation. The section on regional sequence stratigraphy indicates that relative sea-level changes exert a major control on development of Pennsylvanian reservoirs, influencing stratal thicknesses and geometries, occurrence of favorable reservoir facies, and extent of diagenetic overprinting associated with subaerial exposure.

Subsidence and sediment compaction coupled with eustatic sea-level change create space for sediment accumulation (accommodation) and must be evaluated in terms of rates, magnitudes, and durations. In addition, the spatial and temporal variations of subsidence need to be placed in perspective of the tectonic forces and the heterogeneity and structure of the basement in order to help assemble patterns and trends.

Flexural foreland basin subsidence occurred during the Pennsylvanian in response to the Ouachita orogeny and concurrent Wichita-Arbuckle thrusting leading to formation of the Arkoma and Anadarko basins. The basic tectonic framework was previously described, and subsidence processes associated with foreland basin development are addressed by Quinlan and Boumont (1986).

4.A. Subsidence Modeling

Subsidence modeling (one-dimensional backstripping with decompaction) was performed on six wells using an algorithm incorporating average lithologies within stratigraphic intervals listed in Table 4.A.1. Further subdivision of the column is not warranted due to the limited resolution of geologic age.

The rates, the time-series trend, the magnitude, and the spatial variation of subsidence appear to be linked to foreland basin development in the Anadarko and Arkoma basins. Subsidence rates increasing in proximity to these basins, each the convex-up shape of the time-depth plots is characteristic of foreland basin development (Quinlan and Boumont, 1986). Subsidence rates in Kansas during the Pennsylvanian and early Permian were very rapid compared to the rest of the Phanerozoic. Substantial increases in accommodation produced the Permo-Pennsylvanian domination of the stratigraphic column in Kansas (Figures I.14 and I.17). Other implications of increased subsidence is increased fidelity of the Pennsylvanian-Permian record as reflected in preservation of stratigraphic detail.

General subsidence pattern for the Midcontinent during the Upper Pennsylvanian (Missourian) shows greatest rates focused around the Anadarko basin with rates diminishing northward across Kansas. The resultant map from the regionalization analysis of Pennsylvanian thickness data established six broad areas of more coherent thickening or subsidence (Figure 2.B.2.2). Subsidence curves for the interval from early Pennsylvanian to

lowermost Permian for these six areas using no decompaction indicate different rates of subsidence for these six regions. However, all of the curves are convex upward, typical of foreland basin settings (Figure 2.B.2.3).

Figure 4.A.1 identifies names and locations of six wells that were used to determine subsidence using a one-dimensional decompaction algorithm (backstripping). The wells are from contrasting structural sites including various class areas established from regionalization analysis, and locations from the Central Kansas uplift and the Anadarko, Sedgwick, and Cherokee basins. The stratigraphic divisions and time assigned to their boundaries used in the model are shown in Table 4.A.1. Ages assigned are derived from Klein (1990).

Table 4.A.1. Stratigraphic datums and ages used in subsidence analysis.

Strat. Tops	Age (Ma)
Stone Corral	270
Neva	300
(top Pennsylvanian)	
Topeka 302	
Haskell	303
(top Virgilian)	
Kansas City	304.5
(Muncie Creek)	
Marmaton	306
(Nuyaka Creek)	
Cherokee	308
(Excello)	
Atokan 310	
Morrow	314
base of Morrow	316

Figure 4.A.2 is a depth-age representation of subsidence with compaction. The concave-up shapes of the curves are essentially the same as those in Figure 2.B.2.3. Figures 4.A.3 and 4.A.4 depict subsidence rate versus time. The first data point in the subsidence rate plot is not valid. Subsequent points indicate that subsidence rates during the depositional interval containing the Lansing-Kansas City Group reservoirs between 306 (date given for Nuyaka Creek horizon) and 303 Ma (date given for Haskell horizon) range over a narrow set of values. The patterns and ranges of subsidence rates by geologic area include:

Southern Cherokee basin (Batton well) --
a stable subsidence rate of -0.037 m/ky through the duration of the interval

Sedgwick basin (Hiebert well) --
rate increasing from -0.025 to -0.035 m/ky

lower Hugoton shelf nearest the Anadarko basin in edge of Class #5 (Mai well) --
a very stable -0.03 m/ky

mid Hugoton shelf adjacent to Victory field in Class #6 (Orth well) --
initial increase then slowing of rate from -0.025 to -0.035 to -0.027 m/ky

higher Hugoton shelf position in Class #2 (Bounds well) --
steady to slowing rate from -0.021 to -0.017 m/ky

on Central Kansas uplift near Pen field in Class 3 (Marshall well) --
relatively slow rate of -0.016 m/ka

The Bounds and Marshall wells are the same ones that were analyzed using the time-series analysis of the Th/U ratios. The stratigraphic boundaries of the 3rd-order sequences recognized from spectral analysis of the log Th/U data coincide with the boundaries of the time increments used in this subsidence analysis. The reliability of the age dates precludes reducing the time interval of the analysis any further.

The 3rd-order sequences are generally characterized by more rapid deepening and gradual shallowing. Cross sections across the shelf-to-basin hinge in southeastern Kansas indicate that the succession of 3rd-order sequences during the early to mid upper Pennsylvanian define backstepping stratigraphic successions. This pattern is interpreted as the result of increasing inundation of the shelf through time, and could occur by an increasing subsidence rate. Such is the case for the Hiebert well in the Sedgwick basin where subsidence rate

increases from -0.025 m/ky for the late Desmoinesian to -0.035 m/ky by the end of the Missourian. However, the subsidence rate in the Batton well in the Cherokee basin remains steady. Subsidence rates in the Orth and Mai wells are rather steady through this interval of time. Any apparent close relationship between subsidence and the 3rd-order remains equivocal.

The rates of subsidence and average sediment accumulation rates converge as longer intervals of time (millions of years) are considered. At shorter times such as the duration of 3rd- and 4th-order cycles, 1 to 10 Ma and 0.1 to 1 Ma, respectively, hiatuses or breaks in sedimentation become increasingly important and impose a limit below which the durations of cycles can not yet be estimated accurately. The significance of any subsidence calculations at these scales is suspect, and the lower acceptable limit for calculating subsidence rates is probably that which is used here.

4.B. Fischer Accommodation Plots

by W. Lynn Watney

The Fischer plot is used to depict accommodation history at individual locations, i.e., a one-dimensional model. The plot depicts time against elevation for the 4th-order cycles in the interval from the Excello Shale to the Heeber Shale. Each 4th-order cycle was plotted for wells used in the subsidence analysis. Each cycle is represented by a triangle, with the bottom side exhibiting a negative slope equal to subsidence. Subsidence varies according to that which was calculated for each site. The horizontal distance of the triangle is equal to the duration of the cycle, set here as a constant of 350 ka. The vertical side of the triangle is the measured thickness of the cycle. The hypotenuse connects the point at time zero before subsidence began and connects vertical line segment representing thickness. The hypotenuse is essentially an estimate of the relative elevation of the depositional surface. All of the wells are combined onto one chart (Figure 4.B.1).

The 3rd-order sequences are generally discernable as abrupt changes in elevation of the depositional surface and accordant changes in thickness of 4th-order cycles. The abrupt changes in accommodation in the mid to upper Pennsylvanian as suggested by these plots are mainly increases, but also show no change or decreasing elevations. However, the interpolation is complicated by evidence that each 4th-order cycle is characterized by excess accommodation. The thickness of a particular 4th-order cycle is a function of accommodation (related to subsidence rate, eustacy, and elevation of shelf) and, importantly, the time spent in shallow water in the photic zone when carbonate sediment accumulated. The longer the time in the shallow water, the thicker the carbonate deposit. A rapid rise and fall in sea level for whatever reason would leave little time for deposition while a staggered fall in sea level would result in more prolonged, perhaps episodic shallow-water deposition.

The longer-term 2nd-order (10-100 Ma) cycle is also discernable on the Fischer plots, indicated by the overall increase in accommodation that occurs throughout most of the time period that is charted. Estimates of this sea-level change based on these charts is roughly between 75 to 180 ft. (25 to 60 m) from the Excello to the Heebner Shale. This rise in sea level is consistent with other work (Vail et al., 1977; Haq et al., 1987; and Ross and Ross, 1987). The higher shelf positions such as at the Marshall well on the crest of the Central Kansas uplift were not flooded until the early Missourian. Once submerged, only a minor increase in accommodation is noted relative to the other locations.

While stacking geometries along the shelf margin and Th/U ratios both suggest abrupt deepening followed by more gradual shallowing during the 3rd-order cycles, the trends revealed by the Fischer plots are not as clearly developed. The changes in thickness and accordant elevation changes associated with the Excello (Ex) to the Nuyaka Creek (Nc) interval does not change in the 3 wells that contain this section. The wells are all located over 100 mi. inland from the shelf margin in central Oklahoma. The 4th-order cycles of this interval are thin and are not highly variable in thickness. In contrast, the Nuyaka Creek (Nc) to Muncie Creek (Mc) interval varies from a loss or little change early in this cycle to little to significant gain in elevation latter in the cycle. The early cycles of the 3rd-order cycle are thinner along the lower shelf, but correspond to overall increased accommodation as suggested by drowning and backstepping of strata along the lower shelf. In contrast, sites on the upper shelf showed a steady gain in elevation through this 3rd-order cycle suggesting accommodation was not significantly reduced during the early 4th-order cycles. These upper shelf areas are probably higher elevation and underwent less subsidence.

A fall in relative sea level was apparently needed on the lower shelf to provide greater time in the photic zone to produce both thicker carbonate deposits and 4th-order cycles. The abrupt thickening of cycles on the lower shelf such as at the Cox A-4 well location probably represents a catch-up phase in accumulation in a shallow-water setting following a time of reduced sedimentation during prolonged deeper water. Shallow-water accumulation was enhanced due to increased depositional slope created by a combination of increasing subsidence toward the basin and reduced sedimentation. The resultant ramp encouraged formation of oolite shoals that were developed extensively across the lower shelf in the early cycles. Local depositional topography developed as mobile sand shoals attempted to fill in the available space. In contrast, the upper shelf sites show a steady increase in thickness, perhaps reflecting the longer-term second-order rise in sea level. The ramp setting was nearly eliminated at the end of this 3rd-order cycle probably through a combination of sediment progradation coupled with the inferred long-term fall in relative sea level.

The Muncie Creek Shale to Haskell Limestone interval exhibits a initial thickening to a notable loss in thickness at the end of this 3rd-order cycle in all areas of the shelf. Early 4th-order cycles keep up with a rise in sea level

and then undergo notable loss of accommodation space, more so than previous 3rd-order cycles. Indications from the shelf margin stacking patterns and regional mapping of the Haskell to top Lansing interval also indicates accommodation space is considerably reduced at the close of this 3rd-order cycle across the Kansas shelf. In particular, loss of accommodation space is noted in central and western Kansas because it appears that central and western Kansas were over 100 ft (33 m) higher in elevation as suggested by interval isopachs between the top of the Lansing Group and the Haskell Limestone.

The variations in the topography on the shelf and the location of the shelf margin inferred from thickness maps indicate that tectonism is a primary causal mechanism. Furthermore, these strata are the products of a complex interaction between tectonics, eustacy, and sedimentation; the former two changing the potential sediment accommodation space through the domains of time and space. The complex interaction of these mechanisms can be examined through simulation modeling.

These complex changing patterns in relative sea-level are inferred to have significantly impacted the character of petroleum reservoirs, the stratal packaging most evidently affected. Integrated techniques such as the use of chemical and sequence stratigraphy can resolve these patterns. Challenges are now to define the resolution of the techniques for use in predicting increasingly finer detail of the reservoir.

4.C. Basement Mapping

by D. Baars and W.L. Watney

A Precambrian basement database was prepared in order to update the surface configuration map of the Precambrian. An extensive set of basement penetrations were identified using the Petroleum Information Well History Control System information as "seed" files. The resulting configuration map was digitized from hand-contoured postings made on 1:125,000 bases, 1 x 2 degree maps of the state. Figure I.28 shows a portion of the basement configuration map for Kansas. Significant revisions were made original mapping.

The details of the new basement map were previously presented. The map clearly shows the prominent Hugoton embayment, Central Kansas uplift, Sedgwick basin, Nemaha uplift, and the Cherokee basin (Figure I.27). The prominent northeasterly trending grain in the central portion of the state corresponds with the location of the underlying 1.1 Ga (billion years) Midcontinent Rift System. The width of the rift influenced area extends over 200 miles east-west along the Oklahoma border to 75 miles east-west at the Nebraska border. Many subtle northeast-trending lineaments are seen in the central part of the state corresponding to distinct magnetic lineaments. Many of the structural elements of the rift were apparently reactivated in the Phanerozoic as faults, anticlines, synclines, and hingelines (see previous discussion on regional cross sections and regional geology). The positive correlation of the boundaries of the regionalized areas described earlier closely

corresponds with boundaries between changes in composition and deep-seated structural elements. The structural expression of a particular basement heterogeneity varies according to its orientation and that of the stress field existing at a particular time.

SUBTASK 5. COMPUTER MODELING

by W.L. Watney, J.A. French, J.C. Wong, A. Verma, R. Black, and B. Guy

Acknowledgment

T. Gerhard,--dB develop, J. French 2-D computer model; J.C. Wong 1-D computer model and 3-D model programming; A. Verma--database management, 3-D model building; B. Guy, geological knowledge, verify data integrity

5.A. Database Development

Database development is an integral and essential activity of this research. The data structure consists primarily of well information -- completion data, stratigraphic datums, attributes of depositional sequences, digitized wireline logs and statistical results from operating on stratigraphic, sequence, or wireline log information. In addition, files were prepared on lease and field production data for field studies and regional play assessment. Finally, parameter information used in sedimentary modeling occupies additional files. Host computers for this data development and editing include PC's, minicomputer, and workstation. Integration of databases on regional, oil field, and near surface/surface site studies and file transfers between databases are an integral part of the data management system established for the project. Features such as being able to combine information from several files is important for certain types of data manipulation, e.g., integrating site study data with regional information or combined regional datasets for statewide mapping. Files remain separate for ease in editing and maintaining unique information exclusive to a particular dataset.

The procedures to build, edit, and combine these databases were accomplished through a series of utility programs written on the minicomputer. Frequently used maps or other graphics were built and generated in an efficient process where repetitive steps were automated or flowcharted for a logical implementation. Data entry, error checking, editing, preview of plots and final plot generation are current features in the database management and mapping system. These are described in a series of charts (Figures 5.A.1 through 5.A.5).

Database management programs were developed for several datasets: 1) basement, 2) pre-Permian, 3) sequence, 4) oil field, and 5) southeast Kansas reservoir analogues. A flow chart in Figure 5.A.3 summarizes the procedures and logic used to develop this database management system.

The basic methodology used in subsurface database development once the geologic data is collected is to use the management program to find the matching well in a "seed" well file maintained on the mini computer (Data General MV20000). Once the match is found the API number, completion information, and the latitude-longitude coordinates are extracted from the "seed." The next step is to enter the geologic data to complete the

file. During data entry the program checks for "out-of-bounds" values to minimize errors introduced during keyboard entry. Once the data is entered, mapping and error checking can begin through additional automated procedures.

The minicomputer is interfaced via a PC using a terminal emulation program. Database access is accomplished via menu-based commands. Editing, addition of new records, and printout generation are handled through this interface. Total well count with the combined datasets is over 5000.

Gridding, map, trend-surface analysis, transect, and automatic cross sections were made using Surface III mapping software. Elevation grid files of datums from Victory field were saved for later input to a workstation (Silicon Graphics Personal IRIS) for use in 3-D visualization.

Cartographic database for Kansas was developed by the Kansas Geological Survey. Final plotting was done using several devices including color and black and white postscript printers, Calcomp electrostatic color plotter, and pen plotter.

Wireline logs for 82 wells were hand digitized using a tablet and Terrastation^{tm} software on a PC. Fourier analysis and well plots were done using the same software. ASCII files of the log data were transferred to the workstation for use in 3-D visualization.

5.B. Stratigraphic Simulation Modeling

Introduction

Currently, stratigraphic simulation modeling is not a primary vehicle to predict reservoir characteristics, but it is serving as an increasingly important tool in viewing, testing or experimenting on interaction of processes that control reservoir development. Simulation modeling in the geosciences began over 20 years ago. Harbaugh and Bonham-Carter (1970) and Schwarzacher (1975) are classic references summarizing accomplishments of that time. However, computer modeling has been greatly enhanced in recent years due to interactive computing and improved graphic display (Cross, 1988; Franseen et al., 1991). Improvements in computing coupled with our ability to acquire more precise and accurate information to constrain results, have made modeling increasingly more practical.

Geologic modeling has advanced in several directions. Simulation (or forward, process-response) modeling includes basin, sedimentation, and stratigraphic types. These models are forward in the sense that they utilize process information inferred from the sedimentary record to recreate observed geology. Many of these models are deterministic because they arrive at identical results given the same input variables. Other models are based

on stochastic methods which introduce the element of chance into getting a particular response. Deterministic modeling results are limited by the lack of geologic data to accurately constrain the solution (i.e. the solution is non unique), or there is a lack of sufficient understanding of the processes to recognize them and properly account for them. The latter problem leads to oversimplified solutions and results can be of trivial or limited practical value (Table 5.B.1.).

TABLE 5.B.1. PROS AND CONS REGARDING PROCESSED BASED (SIMULATION) GEOLOGIC MODELING

Pros:

1. New quantitative information exists on geological processes; modeling itself drives geological approach toward quantification
2. Ability to adapt the model to local conditions to aid in portability
3. Provide the means to experiment, refine model, and build upon efforts; model offers insights into nature of reservoir development.

Cons:

1. Experimental, lacking sufficient process information in most areas
2. Commonly appropriate and relevant quantitative observations are limited
3. Limited ability to currently model random or very localized processes that may significantly affect observed reservoir characteristics, storms, earthquakes, floods
4. Errors or incompleteness in interpretation of processes.

Alternatively, stochastic modeling, particularly as used in geologic reservoir modeling introduces variability, commonly conditioned (or constrained) by available information. The results are based on extending known spatial characteristics through extrapolation or interpolation. As the dataset is better constrained the spatial model can be refined. However, there is a limitation in that there are always multiple realizations (outcomes) that are defined by nonphysical (statistical) functions. The statistical model does not learn directly through improved geologic interpretation. Rather, the new data are incorporated through an improved statistical function. The lack of tie to processes between improved statistical versions does not facilitate adapting the model to a new geologic setting, having to rely instead on conditioning (matching existing control) the data (Table 5.B.2.).

TABLE 5.B.2. PROS AND CONS REGARDING STOCHASTIC MODELING

Pros

1. Ability to experiment for optimization
2. Ability to constrain or condition model
3. Quick and objective predictions of reservoir properties.

Cons

1. Rock system may not meet statistical assumptions.
2. No inherit basis for portability -- lack robustness without correlation to geological processes/products.
3. Application to appropriate models needs to be established for varied geological conditions.

A geologic simulation model that does a good job at reconstructing the observed geology can be improved as the processes are better understood. The simulation model may ultimately become a significant predictive tool of reservoir character because of its ability to be tailored to specific basin, depositional system, and local characteristics.

Geoscientists have yet to establish the limitations in simulation modeling. On the contrary, results to date from this study and those of many of our international colleagues point toward a significant potential for obtaining practical results for simulating models at scales small enough to be useful in characterizing reservoirs by the oil industry. If the models are properly constrained with accurate and precise parameters, the simulations will likely have significant predictive capabilities. Development of inverse methods for improved parameter definition are critical to this end. A combination of deterministic and stochastic modeling may offer the best answers for modeling small-scale features that are below the resolution of determinism.

Until simulation modeling parameters (process data) are more fully developed for various stratigraphic intervals and basin and shelf settings that harbor petroleum reservoirs, existing conventional approaches to geologic interpretation must continue to be used to characterize and predict reservoir properties, including stochastic modeling. Parameter definition for simulation modeling is a complex task that involves the assessment of data at both regional and local levels, as is being done in this project. Our approach to extracting time-related process information is founded on sequence-stratigraphic analysis and the definition of temporally distinct stratigraphic units.

Recent models are producing increasingly more sophisticated and realistic results that incorporate more complex information. There is no unique approach in this early stage of development. It is extremely important that workers stay abreast of developments, in part, by actively communicating with groups who are making

contributions in both model development and parameter definition. An example of our efforts during the course of the project include editing a book entitled, "Sedimentary Modeling: Computer Simulations and Methods for Improved Parameter Definition" published in 1991 by the Kansas Geological Survey (Franseen et al., 1991). The book contains basic elements and latest advances regarding sedimentary modeling and approaches to parameter definition and serves as a means of helping transfer this technology. The volume brings together the results of individuals working at the forefront of simulation modeling.

Development background

The development of the stratigraphic simulation model is an inductive simulation approach. Several avenues of research were pursued simultaneously to quantify and model the geologic processes responsible for reservoir development, including:

1) collection of regional- and local-scale data for refined, integrated stratigraphic interpretation;
2) quantitative definition of parameters for stratigraphic modeling:
   a) identification, description, correlation, mapping and interpretation of geometriesof temporally distinct genetic units (depositional sequences);
   b) compaction and subsidence analysis;
   c) time-series analysis of logs and lithologic data;
   d) inverse modeling to derive independent estimates of timing and rates of sediment accumulation;
3) integration of parameters through process of informed constrained synthesis of this geologic system;
4) simulation of observed geology and prediction of characteristics between control at regional and local scales.

Modeling in 1-D and 2-D

Our initial geologic simulation model was implemented on a personal computer using one-dimensional output, i.e., limited to a single stratigraphic succession at one location. This 1-D model incorporated parameters derived from characterization of Upper Pennsylvanian Missourian depositional sequences as well as data on sedimentation and stratigraphy derived from Quaternary and Recent analogues (Watney, et al., 1991).

The second phase of the modeling was followed by a two-dimensional development (French and Watney, 1990). The implementation and refinements of the 2-D model were made to simulate various geologic observations as they became known through the course of the project. The extension of this model to 3-D was attempted but, was not successful due to limitations in the lack of constraints on geological processes operating in 3-D.

2-D Modeling Results

Characteristics of the 2-D model will be summarized briefly. The model simulates carbonate sedimentation (facies) according to a depth and energy levels (slope). A flow chart of the logic used on the 2-D model is included in Figure 5.B.1. Three examples of the modeling results are described: 1) oolite in the Bethany Falls Limestone analog, 2) high-resolution stratigraphy, and 3) combined 2nd - 5th-order cycle modeling. The 2-D model generates up to 11 different carbonate facies, including carbonate skeletal grainstone and oolite, the most abundant reservoir type in the Missourian carbonate-dominated depositional sequences. These carbonate depositional facies are controlled primarily by variations in water depth, energy level, loci of sediment redistribution (updip oolitic facies), and presence of seaward barrier to dampen currents and waves. Deposition is significantly affected by rate of relative sea-level rise (subsidence + eustasy) without the need to modify accumulation rates. Sediments are also slowly eroded during subaerial exposure. The current program carries 200 lines of code written in Turbo Pascal for the PC.

Both a solid color 2-D image of the deposit is generated as well as detailed stratigraphic profiles from user selected sites on the modeled shelf. Output is to the computer screen with hard copy obtained via screen capture. Input parameters include subsidence rates, eustatic sea-level change, and initial depositional topography. Sediment accumulation rates are inferred from modern sediment analogues. Subsidence can be varied across the area that is being modeled. A eustatic sea level curve can be drawn using the keyboard, read from a file, or generated through the use of Milankovitch orbital parameters. The initial shelf configuration on which deposition takes place can be drawn on the screen or input from a file based on information interpreted from mapping and facies analysis.

The horizontal and vertical scale can be changed for successive runs to maximize the screen image and improve visualization. Parameters that can be varied include the time duration of individual runs and the vertical exaggeration of the output. Smaller areas of the output can be selected and expanded to full screen by drawing a box around the area of interest and repeating the run. The second screen is then filled with the boxed in area.

Run length can be varied, within two basic scales: 1) 100,000 to perhaps 2 million years; 2) longer term, 5+ million years, for 3rd-order sequence modeling. Time steps vary with run length; shorter runs are composed of shorter time steps. At each time step during a model run, a pixel of a given "facies" is "deposited." Model runs typically vary from 3.5 minutes to 5 minutes on a 386-33 IBM-compatible computer; super VGA graphics are preferred.

The basic stratigraphic unit that is recreated via the modeling is the depositional sequence. All of the primary types of genetic units that comprise these depositional sequences can be produced, including flooding units,

condensed sections, late-highstand units with complex internal stratigraphy, high-energy oolitic grainstone buildups, and subaerial exposure surfaces. Lowstand, transgressive, and highstand systems tracts can be developed under the proper conditions. Geometries common to observed geology are produced including progradation of late highstand genetic units with toplap and downlap. Time lines can be included at user-selected intervals to identify where the depositional surface was at various times during development of the deposit.

Parameter Definition

The parameters that are used in this model are derived from Pennsylvanian strata in the Midcontinent, Quaternary stratigraphic records, and processes inferred from the modern environments. Quaternary coastal sedimentary cycles are similar in geometry and facies succession to Pennsylvanian shelf cycles in the Midcontinent (Figure 5.B.2) (Carter et al., 1986).

Parameters used in modeling the Pennsylvanian cycles are categorized into five groups. These parameters are listed and briefly discussed:

I) Characterization and interpretation of temporally-distinct stratigraphic units;

II) Estimates of subsidence across Kansas shelf during the Upper Pennsylvanian;

III) Estimates of elevation across the Pennsylvanian shelf and magnitude of sea-level change;

IV) Characteristics of Pennsylvanian eustacy;

V) Sea-level history estimated from Quaternary analogues;

VI) Sediment accumulation rates from Recent and Quaternary analogues

Differentiation of Temporally-Distinct Stratigraphic Units. Delimiting temporally-distinct depositional units (depositional sequences) bounded by unconformities is essential to resolving time and rate-dependent parameters from these strata. Depositional sequences also provide more precise paleogeographic and lithofacies reconstructions that can be used in estimating model parameters such as water depth and sediment accumulation rates. Regional, temporally significant depositional sequences range from a few meters to 30 meters in thickness.

Estimates of the Subsidence Across the Upper Pennsylvanian Kansas Shelf. During the Pennsylvanian subsidence increased progressively southward across Kansas from less than 0.015 m/ka on the north to in excess of 0.035 m/ka in the extreme southern part of Kansas. Subsidence also varied locally on the shelf due to basement heterogeneity. Regionalization analysis has shown that linear discontinuities in the basement are common and important features on the shelf. Regional mapping has demonstrated that differential subsidence on some of these basement elements results in hinges and abrupt contact between ramp and platform setting of shelf or sites of shelf-to-basin transition (basin defined as region of lower elevation below zone of effective carbonate sedimentation).

Elevation of the Pennsylvanian Shelf and Magnitude of Sea-level Change. Cycles which show notable thickening toward the Anadarko basin are inferred to have been deposited on a sloping shelf based on several lines of evidence as previously discussed. Higher elevation of the upper (northern) shelf is supported independently through recognition of:

1) loss of the widespread black, organic-rich marine shales over the upper shelf and prominent uplifts;
2) a greater proportion of shallow-water carbonate facies in each cycle over upper shelf and uplifts;
3) evidence for sustained and relatively intense periods of subaerial exposure and oxidation across the upper shelf, e.g., deep karstification and extensive autobrecciation (DuBois, 1985); red paleosols with multiple episodes of soil formation (Watney, 1980; Prather, 1985).

In more basinward shelf areas where the rate of thickening is greatest, cycles exhibit regional accumulations of thick (up to 83 ft, 25 m) oolitic grainstone deposits, supporting the interpretation of widespread ramp conditions rimming the Anadarko basin. In contrast, cycles that exhibit no regional thickening trends on the shelf tend to be dominated by scattered micritic carbonate buildups with only local oolite development associated with local, minor relief.

The minimum regional relief across the approximately 280 mi (450- km) wide Pennsylvanian shelf during times of ramp development is estimated by the range in thickness of an individual cycle, approximately 83 ft (25 m). Ramp setting suggested by increased thickness gradient along restricted portion of the shelf. Trend-surface mapping of the sequence thickness was used to refine this estimate of slope (Watney, 1985).

In southeast Kansas the depositional topography is in excess of 200 ft (60 m) as inferred from the thickness of a single depositional sequence (Pleasanton). Decompaction of shales could increase this relief up to at least 300 ft (90 m). The Mound City Shale drapes across this topography (formed by the thinning of the underlying Pleasanton), overlying a flooding unit which lies on a surface that appears to be subaerially exposed, at least at the higher elevations.

Magnitude of sea-level change. The estimate of relative sea-level change is closely linked to estimates of relief across the shelf. The maximum lateral extent of these inundations is some 280 mi (450 km) north of the Anadarko basin. The magnitude of the change in sea level would be constrained by the maximum elevation on this shelf reached by the shoreline, and the lowest elevation that was subaerially exposed. Marine waters apparently covered the entire shelf during the inundations associated with the major cycles northward, beyond where data is available in southwestern Nebraska (Rascoe and Adler, 1983). Thus, no upper shoreline has been identified for the major cycles. Less extensive marine cycles, e.g., Cherryvale, laps out on the upper shelf and provide an example of the lithofacies and stratigraphic framework associated with the shoreward onlap of a cycle. Estimated maximum water depth encountered in a cycle at the most northerly data site is roughly 65 ft (20 m) including the gray marine shale (condensed section).

Sea level fell to expose the lowermost reaches of the shelf in western Kansas for all cycles of the Kansas City Group based on evidence of subaerial exposure seen in cores. In contrast, subaerial exposure is not observed in all cycles at the lowest elevations of the shelf in southeast Kansas.

Characteristics of Pennsylvanian Eustacy. Upper Pennsylvanian sedimentary cycles are widespread on many the shelf areas around the world (Veevers and Powell, 1987; Ross and Ross, 1987). The duration of these cycles has been estimated to be about 20 ka to 400 ka (Heckel, 1991). The 4th-order cycles likely ranged between 200 ka and 400 ka utilizing numbers of cycles developed over the Missourian (Heckel, 1986). Current investigations by Boardman and Heckel (1989) utilize independent comparisons of ammonoid, conodont, fusulinid, and coral groups to provide correlations between 13 major Virgilian and Missourian cycles in the eastern shelf of the Midland basin and the northern Midcontinent. Regional correlations confirm high frequency, synchronous marine inundations in both areas. Foraminiferal, ammonoid, and conodont zones have also been used by Ross and Ross (1987) to extend correlations of similar Pennsylvanian marine inundations globally.

Both Boardman and Heckel (1989) and Ross and Ross (1987) attribute these sea-level fluctuations to late Paleozoic continental glaciation. Glacial-eustatic control of these Pennsylvanian cycles has also been invoked by many previous workers (e.g. Wanless and Shepherd, 1936; Wanless and Cannon, 1966; Crowell and Frakes, 1975; Heckel, 1977; Crowell, 1978; Heckel, 1986; Crowley et al., 1987; Veevers and Powell, 1987). The durations of these cycles fall in the range of the earth's orbital parameters which control insulation and, in turn, influence the waxing and wanning of glaciation.

Sea-level History Estimated From Quaternary Analogues. Workers such as Broecker and Van Donk (1970), Imbrie and Imbrie (1980), Matthews (1984), and Williams (1988) have determined that the del-^{18}O curves of planktonic foraminifera from deep sea cores of Pleistocene-age closely coincide to changes in volume of glacial

ice. As the lighter oxygen isotope is tied up in building glaciers, the ^{18}O increases in ocean water. A 0.11 per mil change in ^{18}O has been equated to about a 33 ft (10 m) change in sea level (Williams, 1988) (Figure 5.B.3).

Asymmetric, high-frequency (100 ka), high amplitude (330 ft, 100+ m) sea-level fluctuations characterize the late Pleistocene (<850,000 year BP). Eustatic cycles typically begin with a rapid sea-level rise followed by slow, staggered falls (Figure 5.B.3). This pattern is thought to be a common feature of ice retreat and advance (Broecker and Van Donk, 1970) and is used here as a proxy for the basic shape of the Pennsylvanian eustatic curve. The rates of rise during the last half-million years range from 2.5 to 10 m/ka whereas the rates of fall in sea level during these cycles was generally less than 1 m/ka (Figure 5.B.3). Such great rates and magnitudes of sea-level change make glacial-eustacy a predominant mechanism that can significantly modulate and displace sediment accumulation.

Sediment Accumulation Rates From Recent and Quaternary Analogues. Based on an extensive literature review, Schindel (1980) compared rates of sedimentation with constancy of sedimentation for several contrasting carbonate and siliciclastic depositional systems. Both rates of sediment accumulation and constancy of sedimentation vary by orders of magnitude within a depositional system. However, studies of Holocene shallow marine carbonate sedimentation suggest a smaller range in carbonate accumulation rates. Tidalites and oolites have a potential accumulation rate of +/- 1 m/ka (Schlager, 1981) (Figure 5.B.4). Reef growth ranges from less than 1 m/ka to greater than 10 m/ka. The average growth potential of a carbonate platform is around 1 m/ka (Schlager, 1981). It is likely that multiple hiatuses are developed in the sediment package and the effective aggradation rate is reduced by these times of non deposition.

Carbonate sediment accumulation rate decreases with greater depths down to the base of the euphotic zone (Figure 5.B.5). Integrated conceptual model in Figure 5.B.6 shows the relationships of parameters associated with building a stratigraphic model of a Pennsylvanian depositional sequence. Significant carbonate sedimentation is limited to times when the photic zone intercepts the seafloor. During the Pennsylvanian there were no significant planktonic carbonate producers like nanoplankton. As a result when the photic zone left the bottom, it became sediment starved. For thick carbonate accumulations such as large algal mounds or thick oolitic shoals, the shelf was probably in the photic zone for extended times. Rapid rise due to glacioeustacy was generally great enough (2-10 m/Ka) to have exceeded sediment accumulation rate, consequently drowning the site temporarily until sea level again fell. Buildups would be most likely along shelf elevations where adequate time in photic zone was realized. The strike-oriented trends of oolite on the shelf in the Swope and Dennis sequences suggest possible sites where the strandline may have resided over a longer time. This is referred to as the "strandline" sedimentation model (Figure 5.B.6.).

Inverse Methods by R. Black. Inverse modeling was investigated to assist in estimating accumulation rates based on stratigraphic record.

Preliminary analysis and evaluation of the "gamma" method was conducted by Ross Black, Department of Geology, Kansas University. The gamma method of Bond and Caimans (1991) was applied to the facies succession defined from 890 feet of core from the top of the Desmoinesian Marmaton Group to the top of the Lansing Group in the Amoco Cox #A-4 well in Haskell County, Kansas (Figure 5.B.7). The gamma method provides a means of viewing a geological column as a time series that can be analyzed in terms of sedimentary cyclicity. Application of the method entails detailed logging of individual facies occurrences by depth in a core or measured section, converting the stratigraphic unit (facies) thicknesses to equivalent geologic time, and finally doing Fourier analysis of the resulting time series.

The conversion of stratigraphic thickness to geologic time is the heart of the gamma method. The gamma term calculated during the analysis is the conversion coefficient multiplied by the facies thickness to convert it to time. This conversion is theoretically quite simple. In reality, however, the conversion can become a very difficult non-linear inverse problem, dependent on the data set available for the inversion. Because of the potential difficulties in calculating the conversion coefficients, an initial Fourier analysis was also performed on the facies data as a function of depth for comparison with the time series results.

A simple test of the method was attempted utilizing the data set taken from a single core that penetrates 15 Pennsylvanian depositional sequences in western Kansas. The facies data were tabulated from core samples of the Cox #4 well reposited at the Kansas Geological Survey. Each facies was assigned an identifying rank qualitatively linking the facies to relative water depth. Facies rank was plotted versus depth from the top of the cored interval.

Spatial Fourier Analysis. In order to facilitate Fourier analysis, the facies rank sequence (Figure 5.B.7) was resampled at a regular depth interval. The facies were resampled at an interval of 0.1 m to insure adequate sampling of the thinnest of facies units in the data set. Spectra calculated on these depth series are functions of spatial frequency (cycles/m). Conversion from depth to time is considered in a later section (after conversion to time the Fourier spectra are functions of true time frequency).

Amplitude spectra were calculated for the resampled facies using two independent 'canned' fast Fourier transform (FFT) subroutines. The spectra calculated with the two routines were identical, indicating that, although the program coding was completely different, both routines use the same theoretical development, the

Cooley-Tukey algorithm (Claerbout, 1976). Neither plot showed any spectral peaks of obvious significance. Both plots displayed an exponential decline in amplitude with spatial frequency.

Inversion of Facies Thickness to Time - The General Problem. The total time required to deposit the j'th sedimentary cycle is:

$$t_j = {}_i(T_{ij}\ {}_i) \qquad (1)$$

where T_{ij} is total thickness of an individual facies type 'i' within the cycle and ${}_i$ is the thickness to time conversion coefficient for facies 'i'. The coefficient 'i' is expressed in units of depositional time/unit thickness (i.e. k.y./m). Equation 1 assumes that each facies type has a consistent depositional rate from cycle to cycle within the sedimentary package. This is probably a valid assumption since the individual facies are interpreted in terms of unique depositional environments and associated energy regimes.

Equation 1 is valid for the j'th cycle within the sedimentary column. Assuming there are 'm' such cycles equation 1 can be rewritten as the multiplication of a matrix and a vector. The resulting equation:

$$\begin{matrix} T11\ T12....TT1n & & 1 & & t1 \\ T21\ T22....T2n & & 2 & & t2 \\ . \quad . \quad . \quad . & & . & & . \\ . \quad . \quad . \quad . & & . & & . \\ . \quad . \quad . \quad . & & . & & . \\ Tm1\ Tm2....Tmm & & n & & tm \end{matrix}$$

is the general form of the simple linear problem. Each row of the T matrix represents a set of cumulative facies thicknesses for a given sedimentary cycle. Each column of the matrix represents the set of thicknesses for a given facies across all the cycles sampled.

Since absolute age control is normally not available at each cycle boundary, a further assumption must be made to make use of equation 1. This assumption is that the time period represented by each t_j is approximately the same. Also, since even the mean duration time of the cyclothemic deposits is not well known, the time entries for the cycles are usually simply normalized to one (i.e. the basic time unit is one cycle period, whatever that

may be). The unit cycle period can then simply be scaled to comply with any assumptions made in later analyses. Using this assumption equation 1 can be rewritten in matrix and vector notation as:

$$\mathbf{T} = \mathbf{t} \qquad (2)$$

where **T** is an m by n dimensional matrix containing the facies thicknesses, and **t** is an n dimensional vector of unknown coefficients. The m dimensional vector **t** consists of entries of one in each component location.

Equation 2 would appear to define a very simple linear problem that could be solved using standard linear inversion methods. Several techniques were used to solve this problem using the small data set from the Cox #4 well described above. Results of the analysis indicate that many pitfalls surround applications of inverse theory to geological data consisting of interpreted rank information.

Linear Inversion. The least-squares solution to the standard overdetermined linear inverse problem (equation 2) is given by (Menke, 1989):

$$= (\mathbf{T}^T\mathbf{T})^{-1}\mathbf{T}^T\mathbf{t} \qquad (3)$$

This type of solution is convenient because several ancillary calculations can be made from the results to check the resolution and variance of the solution.

The least-squares problem of equation 2 was solved for the Cox #4 data set using equation 3. The results indicate that there are some problems in directly applying a least-squares technique to this data set. The most obvious problem is that there are negative coefficients. This is, of course, physically impossible unless erosion is the dominant mechanism acting in this depositional system. Upon analysis of the resolution matrices (Menke, 1989) it was determined that, although the problem probably is slightly overdetermined, the data are inconsistent enough that the generalized inverse matrix is nearly singular, and also, the global minimum in the function they describe truly is in the negative half-space along certain parameter axes.

Three possible solutions to these problems were attempted. First, the data set was reparameterized. Three of the ten existing facies types were grouped together to reduce the number of unknown parameters to eight. Secondly, a damping factor was added to the generalized inverse matrix. Such a damping should be subjectively fine tuned to provide 'optimum' results in some sense. In this first cut attempt, however, only a single, very small, damping factor was added to the matrix. The results for both the original and reparameterized data sets were encouraging, although there was still one parameter with a negative coefficient.

The third method used to improve the solution to the problem was the use of parametric constraints. This simply means that the output coefficients were forced to be positive by redefinition of the problem.

Simple linear least-squares techniques do not allow these types of constraints to be added to a problem, so the problem was redesigned as a non-linear, iterative procedure. A black-box approach was attempted first using a commercial statistical software package. This package provided both simplex and quasi-Newton general non-linear modeling algorithms. The quasi-Newton algorithm was chosen after testing indicated it was slower but more stable when run on this data set. The algorithm iteratively steps toward the area in parameter space where the error function is a minimum. The desired solution is at this minimum. The constraints are supplied as large steps or walls in the error function. When the algorithm steps into one of these walls the next step is forced away from the wall. The results of the black box non-linear analysis indicate that the main problem is that there is a range of five orders of magnitude in the parameters. This is probably not physically reasonable. One parameter indicates that there was a depositional rate of nearly 100,000 m/m.y.

The second constrained, non-linear algorithm involved use of a simple reparameterization of the problem to solve for the square root of g. In this way the final solution was forced to be positive since it was the square of the non-linear algorithm' output. Results of using this algorithm are by far the most encouraging. Further work needs to be done, but the parameters are now positive and more realistic in their range of values.

The basic findings of the work are that the more sophisticated inversion algorithms help the results and that the problem of inverting for depositional rate is poorly posed with ten parameters to be estimated and only fifteen equations on which to base the estimate.

Two-Dimensional Stratigraphic Simulation Modeling -- Parameter Selection. The following is a brief description of a run of the 2-D model, showing the user-selectable options as examples of different input parameters.

The first screen (not shown) prompts for a menu number; this refers to one of the menus that contains options for sea-level curves and depositional profiles. Two menus, each having nine profiles and nine sea-level curves is shown (Figure 5.B.8.). Menus can be customized by individual users to include preferred curves. When one of the menus is selected, a screen showing the choices available on that menu is displayed (e.g. Figure 5.B.8). Combinations of sea-level curve and depositional profile may be selected. Once the selections are made, the curve/profile combination is displayed at a larger scale (e.g. Figure 5.B.9), and the user may then decide 1) to choose a different combination by returning to one of the available menus, 2) keep the chosen combination but offset the sea-level curve vertically relative to the profile, or 3) keep the selected configuration.

Once the configuration is accepted, the next screen appears (e.g. Figure 5.B.10). This screen displays the selected profile, along with reduced versions of that profile overlain with the selected sea-level curve in the upper left-hand corner. The user is prompted for information on the interval between time lines (if desired), maximum and minimum subsidence rates (in m/ka), and length of run (in ka). After those choices are entered, the run begins. An 'x' marks the current eustatic position on the curve in the upper left corner, and blue tic marks show the relative sea-level position on the large profile. A key showing the colors used to designate each "facies", as well as other information, is displayed along the bottom of the screen (Figure 5.B.11). Pertinent information, including the length of the run, the amount of time into the run, subsidence rates, the length of individual time steps, and the instantaneous rate of relative sea-level rise, is displayed at the top right-center of the screen.

Two-Dimensional Modeling -- Oolites on Shelf Break, Bethany Falls Analog Area, Southeast Kansas. The southeast flank of the Pleasanton siliciclastic platform is a pronounced depositional slope (Figure I.52). At least three sets of strike-oriented oolite buildups were deposited in the Bethany Falls Limestone along this slope. The available data suggests that the oolites onlap landward and downlap basinward. In some locations several of the oolites form a shingled stack of oolites representing separate episodes of accumulation. The bounding surfaces separating the oolites may be subaerially exposed. The bases of the oolites contain thin flooding units of shallow subtidal carbonate. A similar stack of oolites is suggested at Victory field based on results of 3-D visualization. However, the topography there is much more subdued. Similarity of stacking patterns at similar inferred shelf elevations coupled with characteristics of facies and bounding surfaces suggest regional sea-level fluctuation is the cause.

The model run closely approximates the depositional topography along a dip-oriented wireline log cross section (Figure 5.B.12). The regional N-S run shows position of oolite on a shelf margin where depositional slope is prominent. An actual example of the Swope Sequence containing oolite from the Woodward analog area in Bourbon County is compared with a generated column along a slope equivalent to that interpreted at the Woodward site (Figure 5.B.13). Another model run shows more detail of oolite generated on slope (Figure 5.B.14). Multiple oolites are generated at different sea-level events, i.e., the strandline model. The computer model output resembles the wireline log cross section. This model output includes optional time lines showing the toplap-downlap relationships in the oolite and contemporaneous facies.

High resolution Two-Dimensional Modeling. A high-resolution data file can be generated during the model run, capturing pixel information. The size of the file is limited by the available RAM. These files include information from each time step across the entire two-dimensional model "area", including facies and thickness

information as well as temporal data, such that the duration of the hiatuses and the relative ages of unconformities can be captured.

This intermediate file is used to output a series of high-resolution stratigraphic columns showing the succession of facies and surfaces generated at shelf positions chosen by the user from the 2-D output. The stratigraphic columns are output in a separate window from the 2-D model run using Windows version 3.1 utilities. The software permits viewing of multiple windows and greatly increases the utility of the model. The windows can be easily and freely manipulated in this environment. A 486-33 or 50 Mhz CPU with at least a 128 kb cache memory is recommended because runs can be cut from over two hours on a 386-25 to less than 30 minutes. Each parameter saved (e.g. facies type and the age of each increment of strata) takes over 2 Megabytes of memory, so a great deal of memory is needed in order to create large RAM disks.

The screen output can be captured as a bit-mapped image for printing on a black and white laser or dot matrix printer. A commercial screen capture program was used in the examples provided here. The captured graphic can also be converted to pcx format for input into Corel Draw™ for additional labeling and color selection. The graphic can then be printed to a color postscript laser printer using Corel Draw™.

An example output from the 2-D simulation program is shown in Figures 5.B.15 and 5.B.16. Included is the 2-D image of two 4th-order marine carbonate-dominated sequence deposited along a sloping depositional surface modeled after the Swope analog area eastern Kansas. A color screen image was converted to gray tones for reproduction in this report. This transformation reduced the contrast between some of the component facies. Color copies of the output are available upon request from the Kansas Geological Survey.

The parameters used to build the model run that is illustrated here include:

1) two cycles of rise and fall of sea level with a range of 100 meters characterized by rapid deepening and gradual shallowing, patterned after late Quaternary eustatic fluctuations;
2) depositional slope estimated from isopach data with a relief of 100 meters;
3) sediment accumulation rates determined by water depth and slope of depositional surface;
4) subsidence of -0.02 m/ky at right and -0.2 m/ky at left;
5) the depth at which carbonates accumulated was set at 35 meters.

The two cycles that are displayed are distinguished by the black stratum (the marine shale) deposited at the base of each cycle. The high-energy facies (lighter colors) occur along the two breaks in slope on the shelf. The subaerial surfaces (sequence boundaries) representing emergence of the shelf are denoted by thin white lines.

Figure 5.B.16 shows detailed stratigraphic columns developed along eight different positions of the shelf. The numbers on the base of the columns correspond to shelf position from Figure 5.B.15. The black facies is the marine shale developed at the base of each 4th-order cycle in this example. The lines were added to emphasize the correlation of the two cycles.

Considerable lateral variation occurs within both cycles resulting from the interaction of shelf elevation and slope. The lower cycle is very thin across the upper shelf (positions 300, 450, and 600 in Figure 5.B.16), much like the observed 4th-order cycles, e.g., the Sniabar Limestone. The stack of facies on the upper shelf is a simple shallowing-upward set. The sea-level curve for the first cycle fell steadily with no stillstands during carbonate accumulation on the upper shelf; consequently little variation in thickness is noted.

Limited thickness of high-energy carbonate sediments (lighter colored, dotted pattern) are deposited in the lower cycle on the basinward slope of the upper shelf (position 270 in Figure 5.B.16). Carbonate deposition on the middle shelf occurs later while the upper shelf is subaerially exposed. The duration of sedimentation on the middle shelf is extended during the lower cycle and consequently a thick bank of carbonates was deposited (positions 140 and 210). The complex stratigraphic succession in the carbonate bank of the lower cycle is due to short-period sea-level oscillations. The thickness, shelf setting, and internal stratigraphy are very similar to that observed in the Sniabar bank in southeastern Kansas.

The lowermost shelf on the left side of Figure 5.B.16 experienced limited carbonate sedimentation during the first cycle. Low-shelf or basinal settings usually show no evidence of subaerial exposure. Rather, the basin and low shelf are the sites of sediment-starved conditions typified by accumulation of dark marine shale (black facies in stratigraphic column #30 in Figure 5.B.16). Reduced sedimentation rates over most of the cycle in this low shelf, resulted in preservation of depositional topography in front of the carbonate bank. This relief continues until either subsidence rate declines to permit more progradation of siliciclastics or carbonates or until sea-level falls enough to bring the low shelf area into the photic zone, permitting relatively rapid carbonate production. Again, these facies and geometries are analogous to those observed for the Sniabar Limestone in southeastern Kansas.

The upper 4th-order sequence developed in response to an asymmetric sea-level fluctuation, where the overall sea-level fall was characterized by several smaller-scale fluctuations. These oscillations occurred when shallow-water conditions developed on the upper shelf. The result is that this upper cycle is significantly thicker than the lower one and exhibits intervals of short-term deepening and shallowing (minor cycles) (columns #300, 450, and 600, Figure 5.B.16). The edge of the upper shelf is the site of high-energy grainstone deposition in the

upper cycle. The section is similar to the underlying cycle at this position, but it is thicker, reflecting longer periods of sedimentation due to a slower fall in sea level.

In contrast to the lower cycle, the upper cycle is much thinner on the middle shelf (#140 and 210). This is due to a rapidly falling sea level during the upper cycle. The condensed section is also very thick, indicating a longer period of sediment starvation on the middle shelf. Finally, only limited carbonate sedimentation occurred on the lower shelf due to the elevation and resultant deeper water. The low shelf had lost more elevation due to longer periods of slow sedimentation, and consequently the location was sediment starved. The character of this upper cycle is very analogous to that observed in the Bethany Falls Limestone.

Forward Modeling of 3rd- and 4th-Order Cycles Using the 1-D Model. One- and two-dimensional simulation (forward) modeling of 3rd- and 4th-order sequences was done using parameters that are currently the best available estimates. The goal of this modeling is to establish the most likely scenarios of 3rd-order sequence development based on best estimate of parameters derived from this investigation. Initially, parameters reflecting upper-, mid-, and lower-shelf locations were incorporated into the 1-D model using values consistent with previous interpretations of the configuration of the Upper Pennsylvanian paleotopography in western Kansas. Elevations of the shelf sites were estimated as previously described. Subsidence rates are derived from the backstripping analysis described in an earlier section. Sediment accumulation rate varies at rates that are low in comparison with recent sedimentation rates. The depth of the photic zone, above which primary carbonate production takes place, is set at 100 ft (30 m), which is a moderate depth compared to modern extremes of 50 ft (15 m) to 500 ft (150 m).

The input parameters for this 1-D modeling include:

- sediment accumulation rate -- 0.1 and 0.2 m/ky
- subsidence rate (upper, middle, lower shelf) -- -0.015, -0.03, -0.04 m/ky
- initial sediment surface elevations (upper, middle, lower shelf) relative to sea level -- -35, -60, -90 meters

The 4th-order sea level curve closely resemble the late Pleistocene sea-level signature proxied by del-O18. The period of the 4th-order cycle was set at approximately 350 ka, 3.5 times longer than the Pleistocene (Fischer, 1981). The amplitude of sea-level change used to create the 4th-order cycle was set at 100 meters, a value similar to the Pleistocene range of glacio-eustacy.

The 3rd-order cycle was imposed on the shorter 4th-order cycle by adding an abrupt rise in sea level of between 65 ft (20 m) to 83 ft (25 m) at the end of five 4th-order cycles. This rise was followed by a slow linear decline in the 3rd-order sea level back to the original level. The sea-level curve, sediment surface, and water depth are graphically output in the 1-D model as seen in Figures 5.B.17 through 5.B.20.

The modeling reveals distinct changes in sediment response among the three shelf positions. Third-order sequences on the upper shelf are thin because marine sedimentation occurs only during limited intervals of marine inundation when the sea-level signature is a simple rise and fall. Between sedimentation events, the upper shelf was subaerially exposed for relatively long periods of time. Fourth-order cycles are thicker at the beginning of the 3th-order sequence than they are at the end of the 3rd-order sequence. The 4th-order cycles are more prone to exhibit small-scale sea-level events near the base of 3rd-order sequences.

The mid-shelf site is situated at a lower elevation than the upper shelf; at these locations marine sedimentation associated with the 4th-order cycles occurs over longer periods and the sea-level signature is more complex than at higher positions on the shelf. Again, 4th-order cycles are thicker near the base of the 3rd-order sequences.

At lower-shelf positions, cycles develop that tend to be thicker than at either of the other shelf positions due to longer periods of marine sedimentation. Note that the elevation of the sediment surface declined over the course of three separate 3rd-order sequences even though sedimentation was relatively more continuous on the lower shelf. This was due to differential subsidence with only partial compensation by sedimentation, leading to enhanced topographic relief.

Figure 5.B.20 illustrates what can happen on the lower shelf when subsidence is increased from -0.04 to -0.05 m/ky with other variables held constant. The sediment surface elevation begins to decrease more quickly during the first 3rd-order sequence. Sea level abruptly increases at the beginning of the second 3rd-order sequence and this lower shelf location is subsequently drowned. Even during a later fall in sea level during the next 4th-order cycle, the sediment surface has declined significantly and the site remains sediment starved. Subsidence continues, uncompensated for by sedimentation. The site continues to be sediment starved and the sediment surface subsides even further. The site that was once part of a shelf that had undergone active shallow-water sedimentation became a basin. This could be reversed if subsidence diminished allowing sediment to prograde back into the area, or if sea-level fell to a greater extent to again put the area into the photic zone. A small reduction in subsidence rates and increase in rate of sediment accumulation resulted in thickened 4th order sequences and actual increase in shelf elevation at this same shelf position (Figure 5.B.21).

This 1-D simulation model only roughly approximates these processes, but it presents a reasonable, quantitative scenario of the response of a carbonate shelf to two orders of cyclicity and furthermore demonstrates how the interaction can lead to retrogradation of the carbonate shelf margin. Rapid subsidence coupled with fluctuating sea level and resulting episodic sediment production are the ingredients for drowning the shelf. Although the large rates and magnitudes of eustatic sea-level change interpreted for the Pennsylvanian appear to have produced the dominant signature seen in the sedimentary record, subsidence is critical to sediment preservation. Changes in subsidence rates can lead to significant modifications, such as the transformation from a shelf to basinal setting.

Another summary observation is that the fidelity of the sedimentary record is diminished on the upper shelf due to its elevation and the low rate of subsidence. In effect, the upper shelf "sees" a very simple sea-level curve, whereas the opposite tends to be true on the lower shelves. The recognition of the details of stratigraphic packaging, including details regarding the completeness of the stratigraphic record at different shelf locations, is critical to our understanding of reservoir architecture.

The 3rd-order sequences have been linked with backstepping carbonate margins during the Upper Pennsylvanian (Figure 5.B.22). Accordingly, the modeling would be more realistic if the 3rd-order sequences were tied to a longer term, 2nd-order sea-level rise. Independent evidence supports a 2nd-order longer-term cycle of sea-level rise during the Pennsylvanian (Sloss, 1963; Vail et al., 1977; Ross and Ross, 1987; Haq et al., 1987). This 2nd-order cycle is incorporated into the 2-D model run that follows.

Two-Dimensional Modeling of 2nd- Through 5th-Order Cycles. The two-dimensional computer simulation was modified to handle longer time runs in excess of 3 million years and to include more than 15-4th-order cycles. This model was developed to examine the interaction of parameters to generate 2nd-, 3rd-, and 4th, and 5th-order cycles. The north-south regional cross section of Figure 5.B.22 was chosen for comparison to simulation results. Relative sea-level change is estimated from the stratal record as previously discussed including shelf margin stratal geometry, time-series analysis of Th/U profiles, and Fischer plots (Figure 5.B.23). The magnitude of 4th-order sea level change was estimated as previously described. The range of sea-level change associated with 3rd-order cyclicity is estimated at 66 ft (20 m) based on the distance that the carbonate shelf was drowned and the associated relief over this distance. Landward backstepping of the carbonate shelf margin were 62 mi (100 km) and 31 mi (50 km) for the Kansas City and Lansing 3rd-order sequences.

A 2nd-order cycle is also inferred from the record. The magnitude of change in sea level estimate from the Fischer plots is 230 ft (70 m) which is in the range offered by Goldhammer et al. (1993). Other workers also

recognize the rising leg of the 2nd-order cycle extending from early to late Pennsylvanian (Vail et al., 1977; Haq et al., 1987; Ross and Ross, 1987).

Various experiments were made to examine the sensitivity of the parameters (Figures 5.B.24 through 5.B.26). The experiments suggest that even with steadily increasing subsidence along an initial ramped shelf with extremely low slope, drowning of the lower shelf occurs at the beginning of the 3rd-order sequences. The first drowning is the largest backstepping event of 40 mi (65 km) and is similar to the 62 mi (100 km) backstep observed at the end of the Marmaton 3rd-order sequence. Internal 4th-order cycles reveal an upward trend of shallower facies in each cycle and basinward stepping subaerial exposure surfaces reaching farther down the shelf.

The subaerial surfaces are shingled (toplap) with lower surfaces extending down into 4th-order cycles until reaching conformity. This development is the expression of the minor 5th-order cyclicity. The 5th-order cycle leads to repeated shallowing-upward events, some culminating in subaerial exposure. An optimum location on the shelf occurs where thickness and fidelity of the rock record is maximized due to shelf elevation and residence time of sea level in shallow water. In contrast, the fidelity of the sedimentary record is reduced both basinward and landward. This is a graphic expression of the "strandline" model described earlier where time in photic zone is needed for thicker shallow water carbonates to accumulate. This is linked to those elevations of the shelf where residence time is greatest.

The Marmaton-like shelf margin in the model would be comparable to a position in central Oklahoma along the edges of both the Anadarko and Arkoma basins (Figure I.18). As observed in the Marmaton 3rd-order, the simulated cycle sequence apparently does not undergo significant basinward lateral accretion due to the steady rise in long-term sea level. The second 3rd-order sequence is characterized by a relatively steep carbonate shelf margin (~15 m/km) (actual slope in model is up to 30 m/km). A consistent pattern of backstepping and forward stepping is noted in the bank margin in the 3rd-order sequence as expressed in the facies and subaerial exposure surfaces associated with the internal 4th-order cycles. The margin steepens late in the 3rd-order cycle producing a massive, rapidly deposited, high-energy oolite facies before the shelf is again drowned.

As interpreted from the field data the shelf margin of the Kansas City 3rd-order sequence along the southern Kansas border undergoes initial reduced sedimentation and minor drowning followed by lateral accretion. This is observed in the model except that in the partial filling of the lower drowned shelf by siliciclastics coming primarily from the Ouachita front to the south is not incorporated.

In the model the simulated Lansing 3rd-order sequence did not step back as significantly as the previous 3rd-order cycle corresponding to what is observed. The decline in the rate of 2nd-order sea level rise is probably an important factor in this development. The deeper water facies and subaerial surfaces are displaced landward early in the cycle, but step forward again toward the basin later in the cycle. The basinward edge of shelf margin of the observed Lansing 3rd-order sequence is relatively steep (up to 30 m/km) where the massive carbonate section of amalgomated 4th-order cycles is over 300 ft (100 m) thick. The space created by missing carbonate deposition and sustained subsidence on the lower shelf was filled later during lowstand siliciclastics of the (observed) Stalnaker.

Detailed stratigraphic columns were generated for selected sites on the 2-D model providing added resolution of the facies succession and surfaces generated in the model run (Figure 5.B.24). The selection of the location of the columns is user selected.

Modeling is important because it demonstrates the changing fidelity of the stratigraphic section at different shelf positions and sea-level conditions. These are simply experiments and many scenarios are possible, but the parameters are constrained by independent methods. The estimates of parameters provide a good rendition of actual conditions. The "strandline" sedimentation model for shallow-water carbonate accumulation is supported by this modeling.

5.C. Three-dimensional Computer Modeling in Victory Field

Wireline log data in Victory field contain critical information for recognition of bypassed oil and evaluation of improved oil recovery potential. The dominant porosity type of pore found in the Lansing-Kansas City reservoirs in Victory field is oomoldic. Detailed discussion of this pore system and its characterization are found in Subtask 6. A brief summary is provided here. The pore space is complex at all scales and 3-D visualization has proven to be a useful tool to help characterize these heterogeneities. The oomoldic pores are initially isolated, but are connected through processes of dissolution and collapse of this pore network. Locally, these pores are occluded by late-stage cements which adds further complexity (see description of Victory field). Effective pay was recognized for this pore system using the "Super" Pickett plots, typically high porosity cutoff (>16%) and low water saturation (<20%). This is expressed as a relatively low bulk water volume (porosity x water saturation). The wells in which these cutoffs are met and have reservoir thickness over 3 feet are displayed on a set of maps for each of the zones examined (Figures 6.61 through 6.64). Other zones were treated similarly, but with varying cutoffs according to the nature of the plots and the pore types (see later discussion on selection of pay cutoffs). Three-dimensional modeling as described was used to supplement existing analysis to further isolate specific reservoir volumes where additional oil may reside.

A 7.5 square mile area was selected from Victory field for 3-D visualization and modeling (Figure 5.C.1). Forty-seven wells were digitized from this area representing over 50,000 feet of log traces from an interval extending from the Nuyaka Creek Shale to the mid Dennis sequence. Log types used included gamma ray, sonic, neutron and density porosity, and induction resistivity. The area resides at the northern part of Victory field encompassing one of the two large oolite lobes developed in the Bethany Falls Limestone. The particular objectives were to:

1) examine stratigraphic variation of the petrophysical properties.
2) calculate variables including water saturation, sonic minus density porosity to show interparticle and total porosity, bulk water volume (S_w x porosity), and visual display of an empirical estimate of separated vug porosity developed by Lucia (1987).
3) apply filters to target areas of the field with specific reservoir properties.
4) systematically examine pattern of attributes in the modeled reservoir volume to assess controls and perhaps enhanced views of areas to be targeted for additional oil recovery.

Stratamodel software was used, a three-dimensional visualization and modeling program running on a Silicon Graphics Personal IRIS. Stratamodel is a stratigraphic geocellular modeling program that can display various well attribute information interpolated into 3-D as surfaces, panels, cross sections, and solids.

Computer elevation grids of key stratigraphic surfaces from Victory field were read into the program. These datums serve as event surfaces, in this case divisions between depositional sequences and genetic units that comprise them (flooding units, condensed sections, late-highstand regressive carbonates, and paleosols). The list of elevation grids read into Stratamodel are listed in Table 5.C.1.

TABLE 5.C.1. LIST OF ELEVATION GRIDS READ INTO STRATAMODEL.

Mid Winterset Limestone

top Stark Shale

top Canville Limestone

top Bethany Falls Limestone

top Hushpuckney Shale

top Middle Creek Limestone

top Ladore Shale

top Sniabar-Limestone

top Mound City Shale

top Critzer Limestone

top Nuyaka Creek Shale

Additional layers are generated within these packages for use in interpolating log attributes. The layering template can be selected that most closely fits the internal stratigraphic framework:

1) onlap -- layers parallel the upper event boundary;
2) offlap -- layers parallel an inclined internal surface that is assigned to approximate progradation;
3) truncation -- layers of equal thickness parallel the lower event boundary where thickening and thinning of interval is accomplished by adding or truncating layers at the top event surface, e.g., upper surface is an unconformity
4) proportional -- layers are a constant number in interval, each varying in thickness in proportion to overall thickness

The regressive limestones were best treated by truncation while the shales and flooding units were assigned layers that onlap.

The layers define the correlation template for interpolation between the wells. The incremental distances of the grids (x and y distance, 300 ft. in Victory) of the event surfaces define two of the dimensions of cells that subdivide the layers. The cells are as thick as each of the layers (two feet in the case of the carbonate reservoirs in Victory field). Each cell retains the values of the attributes assigned by interpolation from the wells. The grid size (60 x 60) and layers (739) determine the size of the model that is manipulated by Stratamodel. The total number of cells in the Victory field model is 2.6 million.

Digitized well data, sampled every 0.5 foot, was read into Stratamodel. The program reassigns (averages) the vertical well data to values for each layer, e.g., into 2-foot layers. The values of the attributes in the layers are then interpolated using a weighted distance function, analogous to the surface gridding procedure. The search radius and other parameters can be selected to conform with that of the imported grids.

An attribute model was built from Victory field log data transforming the raw log values to new variables using equations and comparisons and usually involving multiple logs. An option called geobody was also used to determine the amount of connectedness between cells that met certain criteria, e.g., cutoff values of porosity and water saturation.

The visualization and modeling conducted for Victory field well log data included construction of a series of cross sections between wells to be able to relate back to the original data and more easily compare results with the other analyses of the wells (Figures 5.C.2 and 5.C.4). Panels of multiple, regularly intersecting cross sections were generated that served as a primary means for visualization of 3-D properties (Figures 5.C. through 5.C.9).

While working on the computer, models can be rotated and brought closer or farther away. Attributes are selected for display and color values assigned (scaled or given default values). The power of this tool comes when attributes are filtered to be able to isolate specific intervals, layers, areas, or attributes in a certain range.

This 3-D modeling confirmed and displayed the 3-D extent of the areas in the Bethany Falls Limestone that are targeted as sites of potential bypassed oil using "Super" Pickett plot (Figures 6.61 through 6.64). In addition, it has provided an enhanced stratigraphic view of the Bethany Falls indicating the complicated nature of the layering in this reservoir. The filtering option allowed isolating a portion of the reservoir that appears to contain effective pay, located slightly down structure on the southeast flank of the modeling area (Figures 5.C.9 through 5.C.11). The area is not currently developed. Three separate porous layers in the Bethany Falls Limestone are observed in the model. The distribution of the porous layers are oolite as confirmed by cuttings. The lower porous layer laps out onto the structure, the middle layer passes over the crest of the structure, and the top porous layer onlaps again on the flank of the structure, suggesting a rise and fall of base level. This onlap/offlap relationship closely parallels observations in the analog sites in southeastern Kansas. Apparently, the subdued topography influenced the distribution of the oolite events. The same porosity variation is only vaguely seen when examining the same area using conventional wireline log cross sections (Figure 5.C.12). The log cross section follows the same line of section and uses the same well logs that were interpolated and displayed using the modeling in Figures 5.C.10 and 5.C.11. In particular, the porosity pinchout is not readily discerned because of the high porosity cutoff.

Porous reservoir developed at the structurally higher producing area and lower area on the flank of the structure to the southeast are separated by a region where porosity is below the effective porosity cutoff apparently forming a seal, trapping the oil in a downdip position. The lower flank position of potential pay was first recognized when examining favorable bulk volume water (porosity X water saturation) using the "Super" Pickett plots described in detail in Subtask 6 (Figures 5.C.13 and 5.C.14). The areas of favorable bulk volume water from this model compare closely with areas defined from crossplot analysis. This off structure pay is analogous to the development of flanking effective pay in the underlying Sniabar Limestone reservoir in nearby Northeast Lemon field. The implications for similar traps and compartments in other fields or wildcat locations beyond existing fields and in new pays is significant. In general, stratigraphic compartmentalization coupled with diagenetic overprinting is very important in defining the location of remaining reservoir development and reservoir continuity.

Slices through the individual layers of the reservoir further illustrate the lateral onlap/offlap relationships of the porosity in the oolite layers (Figures 5.C.15 and 5.C.16). Cells that were connected were used to define a geobody. The surface of this resulting volume is displayed in Figure 5.C.17. It reveals the basic tripartite division of the reservoir created by the layering and should be an important element in considerations in enhanced recovery efforts.

Lateral and vertical heterogeneities are many in the Lansing-Kansas City including multiple cycles, subzones and layers within the cycles. Each cycle and possibly each subcycle can have different reservoir properties due to separate, temporally distinct depositional environments (grain type) and diagenesis. Three-dimensional modeling is expensive at the front end in terms of preparing data, but the ease in examining the reservoir drawing inferences, and communicating to other collaborators is greatly facilitated. The modeling provides an excellent vehicle to communicate the nature of reservoir heterogeneity and can be helpful in later design of recovery methods. Also this software permits the geologic model to be transferred directly to a reservoir simulator (e.g. VIP).

SUBTASK 6. RESERVOIR DEVELOPMENT, PREDICTION, AND PLAY POTENTIAL--VICTORY FIELD STUDY AND COMPARISON TO CAHOJ AND PEN FIELDS

by W. Guy and R. Carlson

Overview

The major objectives of the field studies are 1) to geologically characterize Lansing-Kansas City reservoirs as they occur in the various settings, 2) to define processes which led to the development of reservoirs and the

depositional sequences that contain them; 3) to compare and contrast reservoir development with reservoir analog areas and other fields; 4) to develop procedures that can effectively and efficiently characterize complex carbonate reservoirs in older mature fields to evaluate potential for bypassed oil and opportunities for improved oil recovery, and 5) apply knowledge of reservoir to develop a quantitative stratigraphic model that incorporates as many reservoir characteristics as practical.

The major focus of the field study subtask was placed on Victory field. Characterization of Victory field provides a good example of many of the complexities of a reservoir system. The Lansing-Kansas City reservoirs are complex carbonates consisting of stacked reservoirs with contrasting reservoir types, porosity pinchouts and lateral changes in reservoir quality, strong diagenetic overprinting, and the predominance of oomoldic, vuggy pores that are difficult to evaluate for effective pay. In addition, the production is commingled, production is aggregated by lease, and reservoir energy is varied ranging from water drive, gas cap depletion, and solution gas. These complexities resemble those encountered in other fields.

Tasks included establishing a data base of attributes of the Lansing-Kansas City reservoirs in Victory field. Well logs were stratigraphically correlated based on analysis of a continuously cored well in the field (the Cox #A-4) and use of the regional cross-section framework. Depositional sequences and component genetic units were identified. Working cross sections were prepared.

The second phase of this study of Victory field consisted of characterization of the reservoir units. This was initiated based on interpretation of wireline logs, drill stem tests, and core analysis. Gamma ray, neutron, density, and sonic logs are generally available, but some of the original wells drilled in the 1960's have only spontaneous potential and resistivity logs. Water saturation (Sw), minimum effective porosity, pore type, cementation factor (-m), resistivity index (I), irreducible water saturation (Swi) and movable oil were some of the variables sought though a series of analyses being conducted. Preparation and interpretation of porosity-resistivity (Pickett) cross plots, Horner plots, porosity-permeability plot, resistivity (R_{xo}/R_t:R_{mf}/R_w) ratio and moveable oil plots were completed. Capillary pressure data were sought, but were unavailable at the time of reporting.

A third phase of this project involved mapping the 3-D distribution of reservoir properties, depositional sequences and components, stratigraphic datums, and structure. The objectives were to ascertain trends, patterns, and anisotropy in reservoir development and related stratigraphic and structural variables in order to establish covariation and to determine how reservoir-quality rocks developed. The results of this phase were described in Subtask 5.C.

The fourth and final phase of this project included:

1) the correlation of reservoir parameters obtained to date with lease and well production;
2) the integration of results from the various analog studies;
3) the comparison of reservoir parameters with other analog and other fields
4) drawing relationships about geological processes responsible for reservoir development
5) defining optimum procedures for evaluation.

Introduction

The Victory Field, Township 29 and 30 South-Range 33 and 34 West, Haskell County, Kansas, was discovered in 1960 using subsurface data along a very low relief southeast plunging anticline. The producing reservoirs include the Toronto (Virgilian) limestone at 4000 feet, the Lansing-Kansas City (Missourian) limestones at 4100-4700 feet, a Marmaton (Desmoinesian) limestone at 4700 feet, a Morrowan sandstone at 5200 feet and the St. Louis (Meramecian) limestone at 5400 feet. Accumulative production to date is 11.3 million barrels of oil and 360 billion cubic feet of gas (Petroleum Information, 1992; Dwights 1992).

The Northeast Lemon Field, Township 29 South, Range 33 West, Haskell County, Kansas, produces from Lansing-Kansas City limestones, a Marmaton limestone, the Morrow sandstone, and the St. Louis limestone. To-date accumulative production is 1.8 million barrels of oil and 11 billion cubic feet of gas (Petroleum Information, 1992; Dwights, 1992).

This study of reservoir development and prediction is limited to the Missourian Lansing-Kansas City limestones between 4100-4700 feet and is primarily concerned with the five principal producing reservoirs in the two fields: the Sniabar Limestone (Hertha) at 4650 feet, the Bethany Falls Limestone (Swope) at 4600 feet, the Dewey Limestone at 4400 feet, the Stanton limestone at 4200 feet and the Iatan limestone at 4100 feet.

The Victory and Northeast Lemon Fields were chosen for the Lansing-Kansas City reservoir study because of their multiple pay zones (5), a variety of pore types, available core of the entire Lansing-Kansas City (Amoco #4 Cox, Section 8-T30S-R33W), a significant number of wells (300±), and relatively good wireline logs throughout the study area. Previous reservoir studies of the Victory Field area have been by Watney and French (1988), Aufmuth (1966), and Brown (1962).

Structure

The Victory-Northeast Lemon Fields are located on the northwest flank of the Hugoton Embayment of the Anadarko Basin. Regional dip in the Pennsylvanian is to the southeast at about 25 feet per mile (1/4 degree±) (Figure 6.1). Structural maps on multiple horizons from the Heebner Shale to the Excello Shale (4000-4900

feet) are very similar (Figures 6.2-6.8), and show that the Victory Field is located on a very low relief southeast plunging anticline with dips up to 50-60 feet per mile (1/2 degree). The Eubanks Field area to the north is also along this low relief anticline, but little to no structural closure is evident in the area. The nearby Northeast Lemon Field is on a lower structural flat that trends east-west. No faulting is known in the area except for possible faulting associated with a strong northwest-southeast linearity in Section 36-T30S-R34W and for the anomalous trend of the Northeast Lemon structure. The structural attitude of the area is probably basement controlled and movement has been consistent over a great period of time.

Stratigraphy

The Lansing-Kansas City limestone in western Kansas consists of at least ten depositional sequences along an east-west shoreline across the entire state of Kansas between the deeper basin to the south and the continental area to the north (Figures 6.9-6.10). All of these sequences consist of shallowing upward packages that are predominantly limestone. Each sequence consists of a basal thin (4'±) transgressive limestone followed by a thin (2-4'±) marine shale which is then overlain by a thick or (40'±) regressive shallowing-upward limestone that contains the oil and gas producing horizon. The top of the regressive limestone represents a sub-aerial event. Overlying the regressive limestone is a thin regressive gray shale of variable thickness (0-6'). The cyclical nature of these sequences indicates a regional periodic change of sea level due to glaciation and/or tectonics.

Three sequences are well documented in this report: the Hertha, the Swope, and the Dewey (Figure 6.9, 6.10, 6.11, and 6.12). The Hertha sequence has the Mound City Shale (marine), the Sniabar limestone reservoir (regressive) and the overlying Elm Branch Shale (regressive). The Swope sequence has the basal Middle Creek Limestone (transgressive), the Hushpuckney Shale (marine), the Bethany Falls Limestone reservoir (regressive) and the capping Galesburg Shale (regressive). The Dewey sequence has the Nellie Bly Limestone (transgressive) and the Quivira Shale (marine) at the base, the Dewey Limestone reservoir (regressive), and the Chanute Shale (regressive) on the top. All three of the above regressive limestones produce economic oil/gas in the Victory and Northeast Lemon Fields.

The two sequences at the top of the Lansing Group in the Victory and NE Lemon Fields; the Iatan and Stanton; produce oil/gas, but do not show the characteristic depositional sequence. They consist of about 40 feet of regressive limestone with both an underlying and overlying regressive shale. No measurable marine shale is evident in their depositional sequence (Figure 6.9).

Porosity development normally occurs at the top of the thick shallowing upward limestones beneath the regressive shale by diagenetic processes related to the subaerial exposure surface. The Iatan limestone also has a well developed porous unit in the lower half that is distinctly separated from the porous interval at the upper

surface of the sequence. Development of this "extra" porous unit may likely indicate a minor fluctuation in sea level.

Interval isopach mapping begins at the top of the Cherokee Group (Pennsylvanian), which is the base of the marine Excello Shale (Figure 6.10). An isopach of the interval from the Excello Shale upward to the base of the marine Nuyaka Shale, which includes the Marmaton Group, varies only from 160-200 feet in thickness in the Victory-Northeast Lemon Field area (Figure 6.13).

An isopach of the overlying interval from the Nuyaka Shale to the marine Hushpuckney Shale varies in thickness from 90-130 feet (Figure 6.14). This interval includes the Pleasanton Group as well as the Hertha sequence. The thicker section at the northeast corner of the study results from a well-developed oolite grainstone shoal in the Sniabar member of the Hertha sequence. The marine Mound City Shale that typically separates the Hertha sequence from the Pleasanton Group is very poorly developed in the study area and difficult to map in detail.

Immediately below the base of the Kansas City Group in the Northeast Lemon producing area is a thick development of the Exline Limestone (Pleasanton Group). The limestone interval is 50-60 feet in thickness, and has an unusually thick (20'±) highly porous unit (Figure 6.15). Throughout most of the Victory-Northeast Lemon Fields area, the Exline Limestone has little to no porosity, and is not productive in the area of this study.

The basal sequence of the Kansas City Group (Figure 6.16) is the Hertha, which is typically about 40-50 feet in thickness, but varies from 30-70 feet. The sequence is composed of a thin transgressive limestone overlain by the Mound City Shale, which is overlain by the thicker regressive Sniabar Limestone and the regressive Ladore Shale (Figure 6.10). The Sniabar Limestone is from 10-50 feet in thickness. It is a shallowing upward oolitic, but slightly bioclastic, grainstone deposited in southeast-northwest trending oolitic grainstone pods that are interpreted as isolated shoals. These shoal developments are typically 30-40 feet thick, one mile wide, and 2-3 miles in length (Figure 6.19). The porosity, which can approach 30% and averages 20-22%, is best developed on the crests of the shoals (Figure 6.18). The best developed porosity, as well as the most prolific oil production in the area occurs in the Northeast Lemon Field where over 30 feet of better than 8% porosity occurs. Figures 6.19 and 6.20 show the porosity feet at an 8% porosity cutoff and a 16% porosity cutoff. Comparison of the two figures indicates that the porosity is relatively consistent. Total volume of the porous grainstone is somewhat reduced with the higher porosity cutoff. The producing Sniabar grainstone averages 20% porosity.

Overlying the Hertha sequence is the Swope sequence, which includes the transgressive Middle Creek Limestone, the marine Hushpuckney Shale, the regressive Bethany Falls Limestone and the regressive Galesburg Shale (Figure 6.10). The Swope sequence varies from 40-70 feet in thickness with significant thinning occurring to the south and east in the Victory Field area (Figure 6.21). The Bethany Falls Limestone, which is the most significant portion of the sequence, varies from 20-60 feet in thickness (Figure 6.22). It was deposited in similar manner to the underlying Sniabar Limestone as southeast trending oolitic pods with a width of 1-2 miles and a length of 3-4 miles. Again, these oolitic pods are interpreted as part of a shoal complex. The Sniabar and Bethany Falls shoals are offset from each other in the Victory Field area, that is, a thick Bethany Falls overlies a thin Sniabar. The porous development occurs in the top 20± feet of the shoal and averages about 20% in porosity (Figure 6.23). The porosity over 8% occurs over a broader area than just the top of the more restricted shoals (Figure 6.24). Comparison of the porosity feet maps in Figures 6.25 and 6.26, shows that the reservoir has near consistent porosity of over 16% (actually about 20%).

The Dennis and Cherryvale sequences overly the Swope. The basal member of the Dennis sequence is the transgressive Canville Limestone whose base is the top of the Galesburg Shale which is then overlain by the marine Stark Shale (Figures 6.9 and 6.10). The Stark Shale is overlain by a thick dominantly regressive limestone of 150-180 feet that represents both the Dennis and the Cherryvale sequences elsewhere in the Anadarko Basin. They are separated by the Wea Shale, which in the Victory Field area is difficult to select in samples, cores, or wireline logs. The lithology is a light colored occasionally oolitic limestone with scattered oomoldic porosity. No oil or gas production has been found in these reservoirs in the Victory-Northeast Lemon Fields area. The isopach interval that depicts this interval is the Galesburg Shale to Quivira Shale (Figure 6.27).

The Dewey sequence consists of a thin basal transgressive Nellie Bly limestone which is overlain by the marine Quivira Shale, the regressive Dewey Limestone, and a regressive shale (Figure 6.9). The sequence is 20-50 feet in thickness and is dominated by the regressive Dewey Limestone (Figure 6.28). An anomalous thickening is observed in the southeast portion of the study area to almost double the anticipated sequence thickness. The Dewey Limestone is similar to the Bethany Falls and Sniabar Limestones in that it is typically an oolitic grainstone with oomoldic porosity. Spatially, its porosity development is more like the Sniabar Limestone in that it is erratic, but its thickness rarely exceeds 10 feet, except for the thick lobe in the southeast part of the study area where the porosity thickness is slightly over 30 feet (Figure 6.29).

Overlying the Dewey sequence is the Iola sequence composed of the transgressive Paola Limestone, the marine Muncie Creek Shale, the regressive Raytown oolitic grainstone, and the regressive Lane Shale (Figure 6.9). The thickness is approximately 100 feet (Figure 6.30). The Iola sequence is readily apparent on wireline logs

by its very thick (50± feet) spatially consistent interval of oomoldic porosity. No oil/gas production is known from this section in the Victory-Northeast Lemon Fields area.

The interval from the top of the Iola sequence (or Lane Shale) to the top of the Iatan sequence (top of the Lansing Group) consists of at least five sequences (Figure 6.9). The total thickness varies from 150-180 feet with the isopach trends being in a northwest-southeast direction (Figure 6.31). The four depositional components of a typical Pennsylvanian Midcontinent sequence are not easily recognized in these intervals. The lower three sequences are the Wyandotte, lower Plattsburg, and upper Plattsburg in ascending order. The two uppermost sequences (Iatan and Stanton), show significant porosity development.

The Stanton sequence is a regressive limestone and is about 40-50 feet in thickness (Figure 6.9). It is dominantly an oolitic grainstone with good to excellent oomoldic porosity. The thickness of the porous unit varies from 10-40 feet (Figure 6.32).

The uppermost sequence in the Lansing Group is the Iatan, which is a bioclastic slightly oolitic limestone with good intercrystalline-intergranular porosity (Figure 6.9). Two separate porosity developments occur within the Iatan sequence. One zone is within the top 20 feet of the interval while the second interval is within the basal 10 feet. Both intervals are oil/gas productive over most of the Victory Field (Figure 6.33). Reservoir beds with over 8% porosity vary from 10-40 feet with 20 feet being a good average thickness.

Oil/Gas Production

The Victory and Northeast Lemon Fields produce oil and gas from the St. Louis (Mississippian) (Figure 6.34), a Morrow sand (Pennsylvanian) (Figure 6.35), a Marmaton limestone (Desmoinesian) (Figure 6.36), three limestones in the Kansas City Group (Missourian) two limestones in the Lansing Group (Missourian), and the shallow Permian limestones in the extensive Hugoton Gas Field.

For purposes of this report, the Victory Field includes all production in T30S-R33W and the southwest quarter of T29S-R33W, the Northeast Lemon Field includes the production in Sections 13, 14, 22-26, and 36 in T.29S-R33W. The Cutter Field in T31S-R34W and the Koenig Field is in sections 13, 14-T29S-34W.

The Victory Field has 92 current oil/gas producers from pre-Permian reservoirs. Since production is reported to the state only by leases and most wells in the field have commingled production from various zones it is difficult to determine what each reservoir contributes to the total production. The Victory Field has produced 11.3 million barrels of oil and 360 billion cubic feet of gas (as of 12/92). The large majority of this

accumulative production has come from the Lansing-Kansas City limestone reservoirs. The Iatan reservoir at 4100 feet is believed to be the largest contributor.

The Northeast Lemon Field currently has 28 oil/gas producers from the pre-Permian reservoirs. To date the Northeast Lemon Field has produced 1.8 million barrels of oil and 11 billion cubic feet of gas (12/92). The dominant producing horizon is the Sniabar Limestone.

Oil production decline curves indicate that most of the production is solution-gas drive as indicated by the early rapid rate of decline until the wells reach the bubble point (Figures 6.37-6.46). However, a few leases might indicate a water drive of some degree since the production decline is very slight (Figures 6.45 and 6.46).

The evaluation of the Lansing-Kansas City reservoirs is somewhat difficult because of the heterogeneity of the individual reservoirs. The determination of the effective porosity and permeability is necessary to evaluate the individual reservoir.

Reservoir evaluation of the Lansing-Kansas City limestones was done by the review and calculations of drillstem tests, wireline logs, and production testing.

Wireline Analysis - The "Super" Pickett Crossplot

Fifty years after they were introduced, the Archie equations remain the keystone of log analysis of potential oil and gas zones. The equations can be drawn as lines on the well-known Pickett resistivity-porosity plot for the interpretation of well logs. The position of crossplotted zones gives estimates of water saturation that have been used for decisions concerning potential pay zones in innumerable wells.

In more recent years, there has been a much clearer understanding of the role of pore size and geometry in the determination of reservoir characteristics. This knowledge has come from geological studies of the relation between rock textures and the depositional and diagenetic history of the rock, as well as engineering studies of productivity as related to porosity, water saturation, and rock type. These new insights have gone a long way to the explanation as to why some zones that appear to be wet have significant production, while other, supposedly good pay zones, produce only water.

When George Pickett introduced his plot, he emphasized that it should not be used simply as a graphical substitute for estimations that could be done on a calculator. Instead, it was to be a means for pattern recognition, so that trends and separations within the clouds of crossplotted points could be related to pay zone discrimination and reservoir structure. The newer concepts of textural controls on productivity can be evaluated

immediately on the Pickett plot and used in the distinction of potential pay. Contour lines of bulk volume water may be plotted directly as cut-off boundaries for immediate decisions concerning testing or abandonment. Some interpretations of permeability are also possible in favorable situations.

The basic method for the plot that bears his name was described by Pickett (1966). In a later paper, Pickett (1973) described in detail the pattern recognition properties of the plot which made it a particularly powerful method for log interpretation. If anything, the mathematics of the Pickett plot are simpler than those of the Hingle plot (Hingle,1959), and is another transformation of the Archie equation:

$$S_w^n = aR_w / \phi^m R_t$$

Rearranging the Archie equation and substituting the resistivity index, I, gives:

$$R_t = aR_w I/\phi$$

Taking logarithms, the equation becomes:

$$\log R_t = \log (aR_w) - \log I - m \log \phi$$

which describes a family of parallel lines for different resistivity index values whose slope is the negative of the cementation exponent (-m). When the resistivity index, I, is unity, the line is the water line (Sw=100%) with an intercept equal to a*Rw. Other water saturation lines are displaced to the upper right-hand corner and are drawn as lines parallel to the water line and with resistivities which are the water line resistivities multiplied by the index at common values of porosity. In common with most visual methods, these concepts are more obvious when sketched out graphically, as in Figure 6.47.

Pickett (1973) emphasized that this crossplot method was a powerful pattern recognition technique. He demonstrated that the process involves the recognition and analysis of a complex variety of geometrical trends and patterns. These are the consequence of geological and reservoir engineering properties, as well as logging tool characteristics. For a relatively homogeneous reservoir, water zones will be differentiated as a upper-left corner- lower-right corner-limiting trend with hydrocarbon zones displaced to the upper-right-hand corner (Figure 6.47). The water line can be established by eye, or numerically by using line-fitting techniques of regression analysis.

Pickett (1973) also recognized that reservoir zones at irreducible water saturation (Sw_i) should tend to lie on a steeper linear trend, whose intercept with the water line (Sw=100%) reflected the grain- or pore-size. This is because of a general inverse relationship between irreducible water saturation and porosity that was noted by several early authors, including Archie (1952). They correctly attributed differences in the curvilinear trends to differences in reservoir pore sizes (Figure 6.48). This is because irreducible water saturation is controlled by surface tension at the internal surfaces and capillary pressure. While zones at irreducible water saturation in a moderately homogeneous reservoir should lie on a common curve, transition zones will be displaced to higher values of bulk water volume (f*Swi) The distinction is important, because it determines which zones should produce water-free oil or gas, and which should produce water or water-cut hydrocarbon. Computations of bulk volume water (BVW) are therefore a critical additional step in log analysis for the assessment of producibility, as pointed out by Morris and Biggs (1967), Asquith (1985), and others.

Buckles (1965) made an extensive numerical analysis of reservoir measurements and concluded that the quadrilateral hyperbolic function:

$$\phi Sw_i = C$$

was a good first-order approximation to real field data. Low values of C reflected large average pore sizes, high values were linked with finer pores, as a direct consequence of a control by internal surface area. Buckles (1965) reasoned that the form of the empirical relationship was to be expected, because the specific surface area was proportional to the reciprocal of the grain size, and that this was in turn, approximately linearly related to porosity

The quantity C, is simply the irreducible bulk volume water (BVW) which will be effectively a constant, provided that there is a limited range in pore size. Zones with comparable pore size that have higher values of bulk water volume should be water-cut or totally water-bearing. When computed for a field or reservoir, the characteristic value is often known as the Buckles number (especially if it is computed as the product of porosity and water saturation in percentages, rather than fractional amounts). Ranges of field values are shown plotted as cumulative frequency curves in Figure 6.49 for sandstones (using data from Bond, 1978) and carbonate reservoirs with vugular and intercrystalline/intergranular porosities (based on data from Chilingar et al , 1972). Carbonate reservoirs dominated by fracture porosities showed an erratic range of Buckles numbers. Morris and Biggs (1967) point out that is to be expected because of the very minor contribution of fracture porosity to bulk volume Otherwise, the data show systematic trends that reflect distinctions in internal surface area, and provide values that are useful in the following analysis.

The hyperbolic relationship of :

$$fSw_i = C$$

can be linearized to :

$$log\ Sw_i = log\ C - log\ \emptyset$$

Substituting the Archie equation solution for water saturation and rearranging, the relationship becomes :

$$\log Rt = \log (aRw) - n \log C - (n-m) \log \emptyset$$

which describes a line on the Pickett plot with a slope of (n-m) and an intersection with the water line at a porosity corresponding to the water line.

Greengold (1986) was the first to describe the systematic graphic properties of the irreducible bulk volume water on the Pickett plot. When the cementation factor (-m) and the saturation exponent (n) equal 2, zones at irreducible water saturation should follow a line parallel to the porosity axis (Figure 6.50). Otherwise, the lines will be inclined according to whether the saturation exponent is greater or less than the cementation factor. The parameters that determine the BVW line give a powerful new means to extend the function of the Pickett plot beyond its traditional roles of cementation exponent and formation water resistivity. If the irreducibly saturated zones form a coherent trend, then the saturation exponent can be estimated directly from the plot for water saturation calculations, while the producibility will be indicated for any zone. These ideas are explored in the following example.

Resistivity and porosity values from a limestone section in south Texas (taken from Fertl, 1979) are shown located on a Pickett plot in Figure 6.51. The visual fit of a water line (Ro, Sw=100%) to the extreme points has a slope whose estimate of the cementation exponent is close to a value of 2, and a water resistivity intercept of 0.025 ohm-meters (assuming the parameter a to be unity). If there is a single irreducible bulk water trend, it should be located as a high resistivity boundary to the potential hydrocarbon zones. The irreducible trend marked on Figure 6.51 gives a saturation exponent which is, again, close to 2 and a Buckles number of about 400 (or 0.04, in fractional terms). All of these parameter estimates are good functional numbers for a limestone reservoir with intergranular and/or intercrystalline porosities.

The Pickett crossplot (1972, 1973) technique for evaluation of oil and gas reservoirs has been modified to become almost a complete reservoir analysis. It is a technique of pattern recognition requiring porosity and formation resistivity (Rt) values from wireline surveys of almost any age and type.

The "Super" Pickett crossplot will visually determine the approximate values of formation water saturation (Sw), cementation factor (-m), bulk volume water (BVW), effective porosity (Ø), saturation exponent (n), resistivity index (I), zones at irreducible water saturation (Sw_i), and even the permeability (K) when a recognizable transition zone occurs.

The crossplot is plotted on log-log graph paper (3 x 3 or 3 x 2 cycle) with the porosity plotted on the vertical axis and the formation resistivity plotted on the horizontal axis (Figure 6.47). The Super Pickett crossplot requires that you connect the consecutive individual porosity-resistivity data points (dot to dot) to ultimately show the crossplot pattern arranged by depth through the zone of interest. An occasional half-arrow alongside the plot will remind you of the down section direction of the plot (Figure 6.52).

If Sw=100% and m and Rw are constant, a line (Ro) will be determined by using the minimum porosity-resistivity data points and the intercept where the Ø=100% (when I=1) at aRw (a is assumed to be 1). That is, the intercept of the Ro (Sw=100%) line with a slope (-m) with the 100% porosity line at aRw. At a formation water saturation of Sw=10% and a porosity of 100%, the intercept will always be 100 times (I=100) the formation water resistivity (Rw) when the saturation exponent (n) equals 2. The intervening Sw values can then be determined mathematically using the resistivity index (I) or by the use of a logarithmic scale. The water saturation lines will all be parallel with the logarithmic spacing being related to the saturation exponent (n) (Figure 6.52).

Upon completion of the Pickett crossplot, one constructs the Buckles number or Bulk Volume Water (BVW) lines by using the Sw=100% and Sw=10% lines (Greengold, 1986). For example, Ø=.04 times Sw=1.00 gives BVW=.04 and Ø=.40 times Sw=.10 gives BVW=0.04. Connecting the values of significant BVW will give you a set of lines separated logarithmically whose slope will be dependent upon the cementation factor (-m) and the saturation exponent (n). By mathematical coincidence when n=m=2 (Archie, 1952), which are the most widely accepted average values in carbonate log interpretation, the BVW value lines will be vertical. Bulk volume water plots have customarily been plots of Ø vs. Sw on normal graph paper forming a series of hyperbolic curves, which are difficult to coordinate with Pickett crossplots (Figure 49) (Morris and Biggs, 1967).

Fertl and Vercellino (1978) and Asquith (1982, 1985) compared the grain size (or pore size) of carbonates to bulk water volume and carbonate type of porosity to bulk volume water in Table 6.1. Asquith believes that

economic carbonate reservoirs should have a BVW of .04 or less. A carbonate with a higher BVW value would either be wet or have very low permeabilities (Asquith, 1985). As will be discussed later, this number is a great general point for reservoir evaluation, but unfortunately it does not apply to all textures and pore geometries.

TABLE 6.1

BULK VOLUME WATER AT IRREDUCIBLE WATER SATURATION AS A FUNCTION OF GRAIN SIZE (PORE SIZE) AND TYPE OF CARBONATE POROSITY

(modified after Asquith, 1982).

Grain Size (millimeters)		**Bulk Volume Water (BVW)**
coarse	1.0 to 0.5 mm	0.02 to 0.025
medium	0.5 to 0.25 mm	0.025 to 0.035
fine	0.25 to 0.125 mm	0.035 to 0.05
very fine	0.125 to 0.0625 mm	0.05 to 0.07
silt	<0.0625 mm	0.07 to 0.09

(after Fertl and Vercellino, 1978)

Carbonate Porosity	**Bulk Volume Water (BVW)**
Vuggy	0.005 to 0.015
Vuggy & Intercrystalline (intergranular)	0.015 to 0.025
Intercrystalline (intergranular)	0.025 to 0.04
Chalky	0.05

If we use the "Super" Pickett crossplot technique in a relatively thick (>6 feet) reservoir that is within the transition zone (oil/gas to formation water), the porosity can remain relatively constant while the resistivity decreases progressively with each foot of penetration. Using Tixier s equations (1949)

$$K = C\,(a * 2.3/\delta w - \delta hc)^2 \qquad \text{where } a = \Delta R/\Delta D * 1/R_o$$

C = constant

δw - density water

δhc = density hydrocarbon

R_o = resistivity of reservoir when 100% water saturated

we can estimate the average permeability of the reservoir. The technique is primarily an indication of the resistivity gradient. A more permeable reservoir will have a thinner transition zone.

When using the Pickett crossplot, any one porosity tool can be used, but the more porosity tools available, the greater the value of the analysis. A Density-Neutron combination is an excellent combination (Figures 6.54, 6.56). If a sonic log is available in conjunction with either a neutron or density (or both) log, an additional significant interpretation can be made. The density or neutron logs primarily read the total porosity of the reservoir, while the sonic log does not ordinarily see the vugs or moldic porosity. Thus, if we construct overlying Pickett crossplots using Rt vs. sonic porosity and Rt vs. density or neutron porosity, a separation in the crossplots will indicate moldic or vugular porosity. The amount of separation is a numerical indication of the amount of moldic or vugular porosity (Figures 6.54, 6.56).

The Amoco #4 Cox (NE SW sec. 8, T. 30 S., R. 33 W.) was analyzed in the Bethany Falls Limestone (Figures 6.52 and 6.53). The prospective reservoir from 4,590 to 4,600 feet is an oolitic grainstone with oomoldic porosity. The "Super" Pickett crossplot indicates an average porosity of 20%; a significant transition zone (Rt from 30± ohm-m to 6±ohm-m); a formation water saturation (Sw) of 13 to 30%; a BVW of from .03 to .06; and a cementation factor (-m) of 2.0. The average permeability of this interval is 105 millidarcies by core analysis and 149 millidarcies by the resistivity gradient method. Perforations from 4,591 to 4,600 feet yielded 248 MCFG, 10 barrels of oil, and a minor amount of saltwater. Analysis of the Super Pickett crossplot indicates that nearly water-free gas production should occur where the BVW is less than .05 (Buckles 500) and the Sw is less than 22%.

The Mesa #1 14 Leathers (SE NE sec. 14, T. 30 S., R. 34 W.) was also analyzed in the Bethany Falls Limestone (Figures 6.54 and 6.55). The prospective reservoir from 4,560 to 4,580 feet is an oolitic grainstone with oomoldic porosity. The "Super" Pickett crossplot indicates an average density-neutron porosity of 24%; an average sonic porosity of 20%; a long transition zone (Rt from 35±ohm-m to 3± ohm-m); a formation water saturation (Sw) of 15-45%; a BVW of from .03 to 0.1; and a cementation factor (-m) of 2.1. The average permeability by a Horner plot of a drill stem test is 52 millidarcies (ISIP), 217 millidarcies (FSIP). A drill stem test of almost the complete Bethany Falls zone recovered 2,681 feet of gas-cut saltwater and found 4,590 feet of gas in the pipe. Analysis of the "Super" Pickett crossplot indicates that the water-free gas pay is where the

BVW is less than .05 and the Sw is less than 20%. The separation of the crossplots indicates that the total porosity is about 24% of which about 4% is effective porosity. The service company computer log is shown which illustrates the same values as determined by the Pickett crossplot, but at a much higher cost to the operator.

The Amoco #1 A Brennan (SE SW sec. 24, T. 29 S., R. 33 W.) was analyzed in the Sniabar Limestone (Figures 6.56 and 6.57). The prospective reservoir from 4,550 to 4,570 feet is also an oolitic grainstone with oomoldic porosity. This Super Pickett crossplot indicates an average neutron-density porosity of 20 to 29%; an average sonic porosity of 13 to 18%; a long transition zone (Rt from 20± ohm-m to 4± ohm-m); a formation water saturation (Sw) from 21 to 30%; a BVW of from .04 to 0.1; and a cementation factor (-m) of 2.2. The separation of the porosity logs indicates that the total porosity is 20% in the upper part and 29% in the lower part while the effective porosity is about 5 to 6% in the upper part and 9% in the lower part. The well was completed for 126 barrels of oil, 71 MCF gas, and 1,919 barrels of water per day from the entire porous interval. Analysis of the crossplot would indicate that the oil zone is the upper zone where the BVW is less than .05 and the Sw is less 25%. The lower zone has a BVW greater than .06 even though the Sw remains at about 30%, and is definitely water wet.

The Ensign #1-31 Thunderbird well in the Victory Field (sec. 31-T30S-R33W) is an excellent example of a "Super" Pickett cross-plot that illustrates the ability to determine texture and type of porosity (Figures 6.58, 6.59). The data points to the left are from the Iatan limestone from 4093-4128 feet. The reservoir in this zone is a bioclastic limestone with intercrystalline-intergranular porosity, water saturation (Sw) 60%, porosity (Ø) 10 to 18%, and bulk water volume (BVW) 8%. The data points to the right are from the underlying Stanton Limestone from 4138-4178 feet. This reservoir is an oolitic grainstone with good-excellent oomoldic porosity, water saturation (Sw) 12 to 20%, porosity (Ø) 15 to 30%, and bulk water saturation (BVW) .04. Both zones are capable of production. The crossplot shows that the Iatan has finer pores, while the Stanton has larger vugs and oomoldic porosity. Figure 6.60 is a cross plot from the Grayburg formation (Permian) Dune Field in west Texas that illustrates the relationship between water saturation and rock or pore type (adapted from Bebout, 1987). Thin sections verify that the intergranular porosity between larger grains have lower water saturation (Sw) and a lower bulk water volume (BVW). The intercrystalline porosity has the smallest pore sizes and the higher water saturation. A very similar condition occurs in the Lansing-Kansas City Limestones with the oomoldic porosity having the largest pores, the lowest water saturation (Sw), and the lowest bulk water volume (BVW). The bioclastic limestones typically had finer pores, higher water saturations (Sw), and higher bulk water volumes (BVW).

Drill Stem Test Analysis

The drill stem test has been used to evaluate the Lansing-Kansas City limestone reservoirs since the 1940's. Originally, the operators were primarily interested in only the recoveries, but as the tests evolved from a single flow period and shut-in to multiple flows and shut-ins in the 1950s, a more complete reservoir evaluation became possible. A well run drill stem test is in reality a temporary well completion.

The available information determines what type of analysis can be done. The evaluation parameter that is normally desired is permeability (K), but the damage ratio (DR), anticipated production (A), transmissibility (Kh/m), radius of investigation, and potentiometric surface can be estimated from a well-run test.

The highest quality analysis is obtained when the test consists of at least two flow periods and at least two shut-in periods of sufficient length of time to accurately determine the static pressure. One must also have the incremental time vs. pressure data in order to make a Horner plot to better determine the static pressure, which is the unknown, but critical factor in the determination of permeability (Halliburton).

If a test having two shut-ins and two flow periods, is run, but the time vs. pressure charts are not available, a so-called limited data analysis can be made using only scout data. The accuracy is not as good as when you can do a Horner plot, but it is a good evaluation tool. However, it requires that the final shut-in pressure be less than the initial shut-in pressure (Earlougher, et al., 1967).

If you have only scout information on an older drill stem test with only a single flow period and a single shut-in period, you can still determine permeability by the use of a technique developed by Carel Otte (1954). The accuracy is not as good as when you have the time vs. pressure data on a multi-shut-in test, but has been found to be very reliable. This technique is attached to this report since it has not been published (Appendix D).

Early in the study of the Victory and Northeast Lemon Fields, it was hoped that a sufficient number of drill stem tests could be analyzed for permeability in order to map the fluid paths in the individual reservoirs. However, industry unwillingness to share this data made it impossible. Thus, just isolated scattered permeability measurements were made.

TABLE 6.2.

DRILL STEM TEST PERMEABILITY

VICTORY FIELD BETHANY FALLS LIMESTONE

S-T-R	Location	Interval Ft.	Por >8%	PERM (md)	No. SIP
4-30-33	NW SW	4598-4640	10	0.3	2
5-30-33	NE SE	4538-4618	14	152	2
5-30-33	SW NW	4618-46	12	5.8	1
6-30-33	SE SE	4616-20	2±	2.6	2
6-30-33	NW NE	4620-26	2±	106	2
7-30-33	SW SW	4568-4604	16?	14.7	1
17-30-33	SW NE	4601-17	10	21.8±	1
28-30-33	NW SE	4633-75	6±	10.9	1
29-30-33	SE SW	4579-88	9	12.5	1
29-30-33	NW SW	4565-77	11	12.5	2
29-30-33	NW SW	4575-97	22	4.0	1
31-30-33	SE SE	4581-88	7	3.0	1
31-30-33	NW SE	4576-88	4	15.4	1
31-30-33	SE NE	4578-86	2	62.5	1
31-30-33	NW NE	4568-80	10	2.4	1
31-30-33	SE NW	4575-85	5	17.5	1
31-30-33	NW NW	4534-55	17	0.02	1
31-30-33	NW NW	4556-77	3	0.6	1
32-30-33	NW NW	4560-77	0±	55.8	1
32-30-33	NW NW	4575-87	5	11.6	1
32-30-33	SE SW	4585-95	7	7.7	1
32-30-33	SE NW	4580-4600	16	5.1	2
12-30-34	N/2 SE NE	4595-4625	15±	9.3?	1
14-30-34	E/2 SE	4567-91	12	1.6	1
14-30-34	N/2 NE SE	4556-90	18	24.7	1
23-30-34	NE SW	4550-4601	10±	4.1	1
25-30-34	SE SE	4577-86	9	5.6	1
26-30-34	SE NE	4586-4629	10±	182	2
34-30-34	NE SE	4579-4600	8±	3.6	1
36-30-34	SW SW NE	4594-4651	8±	7.9	1

Reservoir Evaluation

The "Super" Pickett resistivity-porosity crossplot was judged to be the best method of evaluation of the Lansing-Kansas oil/gas producing reservoirs. Two significantly different oil/gas reservoirs are present in the Lansing-Kansas City limestones in the Victory-Northeast Lemon Fields. They are the oolitic grainstone with oomoldic porosity and the bioclastic grainstone with intercrystalline-intergranular porosity. Both types have very different petrophysical characteristics:

	Oolitic Grainstone	Bioclastic Grainstone
Porosity	20-30%	8-15%
Water Saturation	18-22%	50-60%
Bulk Volume Water	.02-.05	.04-.08
Porosity Cut-off 16%		8%
Water Sat. Cut-off	22%	50%
Bulk Volume Water Cut-off	.045	.08

Figures 6.61, 6.62, 6.63, and 6.64 are maps constructed from "Super" Pickett cross plots using the above cutoffs where over 3 feet of oil/gas pay exists. These maps of the Sniabar, Bethany Falls, Dewey and Stanton reservoirs illustrate that significant oil/gas is yet to be produced in the Victory and Northeast Lemon Fields from zones yet to be perforated. A conservative estimate is that from 6-9 million barrels of oil/gas equivalent remain behind pipe from the Lansing-Kansas reservoirs in the Victory-Northeast Lemon Fields.

Figure 6.65 is a Pickett crossplot taken from Watney (1980) for the Cahoj Field in Rawlins County, which produces from multi-zones in the Lansing-Kansas City Limestones. Added to Watney's crossplot are a few additional water saturation values (Sw) and the bulk volume water (BVW) lines. The J and H reservoirs are centered around Sw = 30%, Ø=20%, and BVW=.05. These same values in the Victory Field would be oil productive. As indicated on Figure 6.65, these zones recovered 3360 and 1800 feet of oil, respectively, on drillstem tests.

Another use of the "Super" Pickett crossplot is to see the subtle reservoir differences seen in the same field and reservoir, but in a different well. In Figure 6.66 are two "Super" Pickett crossplots from different wells in the Pen Field, Graham County, which primarily produce from the same J formation.

	#3 Bethell	#4 Bethell
Porosity	10%	16%
Sw	60%	18-30%
BVW	.055-.07	.026-.05
Completion	29 BO/D 12% W	110 BO/D N.W.

The data indicates that the reservoir in the #4 Bethell has larger pores than the #3 Bethel. However, the #3 Bethell is still productive even with higher BVW and Sw because it has finer pores and will therefore have a lower porosity (Ø) cutoff and a higher water saturation (Sw) cutoff. This type of information would be extremely valuable in field development and water flooding.

The "Super" Pickett crossplot has two characteristics that, when present, are very illustrative of specific reservoir conditions. If the plot has a consistent formation water resistivity (Rw), a nearly constant porosity (Ø), and a decreasing formation resistivity (Rt), a gas/oil-water transition is present. A high resistivity gradient (Rt/feet) indicates a short transition zone which indicates a better permeability. A low resistivity gradient will have a lower permeability.

The bulk water volume (ØxSw) indicates "irreducible water saturation" which theoretically should indicate a water-free producing interval. Thus, if on the "Super" Pickett crossplot, a series of continuous data points follow a trend of the BVW values, that footage is at irreducible water saturation. Since the BVW values in the "Super" Pickett crossplot are near vertical when the cementation (m) and saturation (n) exponents are approximately 2, the irreducible water saturation is evident when the formation resistivity (Rt) and the formation water resistivity (Rw) are nearly constant, and the porosity (Ø) and formation water saturation (Sw) are variable in a reciprocal manner. That is, as the porosity (Ø) increases, the water saturation (Sw) decreases.

The "Super" Pickett crossplot is also a visual aid in determining effective porosity in a reservoir. Blakeman (1989) in his paper on bimodal porosity using capillary, core, and log data, has inferred that water wet reservoirs have two parts. Microporosity is that which does not contribute to permeability, whereas the remaining macroporosity controls permeability and relative permeability. Therefore, permeability is better related to macroporosity than to total porosity. Blakeman's study indicates that the BVW (or Buckles) value and the minimum interstitial water saturation values are approximately the same. Time and pressure <u>can</u> reduce water saturations to less than the minimum interstatial water saturation, but for practical purposes they are the same. On the "Super" Pickett crossplots in the Victory and Northeast Lemon Fields, the porosity below the Ro or Sw=100% line is considered microporosity, the porosity from the Sw=100% line to the sonic log cross plot is

the macroporosity (intercrystalline or intergranular), and the porosity between the sonic and the neutron or density log cross plot is the secondary porosity. The sum of these three porosity units is the total porosity.

Maximum Gamma-Ray

The maximum Gamma-Ray values (A.P.I. units) were read and placed in the Victory Field database for the marine Muncie Creek, Quivira, Stark, Hushpuckney, Mound City and Anna Shales. The Muncie Creek, Stark, and Hushpuckney intervals are illustrated (Figures 6.67, 6.68, 6.69) to see if any relationship exists between the high radioactive content, which is principally due to uranium, and structure, topography, or depositional thickness. The Gamma-Ray readings are extremely variable, but no valid relationship exists in the Victory-Northeast Lemon Fields.

An interesting Gamma-Ray anomaly occurs at the very top of many of the regressive carbonate reservoirs in the Lansing-Kansas City limestones. This is especially noticed in the top of the Bethany Falls and Sniabar reservoirs in the Victory-Northeast Lemon Fields (Figure 6.53). This anomaly is a variable, but noticeable, decrease in the Gamma Ray units, making the reservoir to appear "cleaner," when in reality it is a decrease in uranium (Natural Gamma Ray Log-Amoco #4 Cox, Sec. 8-T30S-R33W). The anomaly only occurs at the very top of coarsening upward sequences and is related to porosity. Post-depositional transfers of uranium occur during leaching and dissolution of carbonates (Serra, et al., 1980). Chung and Swart (1990) measured concentrations of uranium in the Bahamas which indicated a "paleo" water table between the vadose (0.2 ppm uranium) and the phreatic (1.5-2.5 ppm uranium). The anomaly in the Victory Field area can be mapped throughout the area. It is not coincident in thickness with the thickness of the good-excellent oomoldic porosity in the Bethany Falls and Sniabar grainstone, but only represents the upper portion. The effect of this diagenetic overprinting on the on the Th/U ratio described earlier would be to strengthen trend to more oxygenated at the top of the cycle.

Diagenesis of Reservoir Rocks in Victory Field

by R. Carlson

Diagenetic studies of reservoir rocks in Victory Field were undertaken to accomplish three primary objectives: 1) to describe the nature and distribution of pore fabrics, 2) interpret the history of pore evolution, and 3) devise petrographic methods of assessing and mapping areas of effective porosity in oil field development projects. Most of the attention in this diagenetic study has been given to the Swope sequence (Bethany Falls Limestone - K- zone) in Victory Field. Additional studies of the Dewey Limestone (H - zone), Stanton Limestone (C - zone), and Iatan Limestone (B - zone) sequences were conducted to compare the porosity types of different reservoir units in Victory Field. Porosity fabric in the Swope, Dewey, and Stanton grainstones is primarily oomoldic. These rocks are highly porous but can have low permeabilities due to limited connections between

pores. The Iatan, on the other hand, is a skeletal grainstone with abundant interparticle porosity that is much more permeable than the other reservoir rocks studied.

Methods of diagenetic study

Cuttings from many of the wells in Victory Field are available at the Kansas Geological Survey's Sample Library in Wichita. In addition, two nearly complete cores (Cox no. 4 and Thompson 'E' no. 2) and two partial cores (Blair 'C' no. 2 and Conover 'D' no. 2) were available for study at the core library at the Kansas Geological Survey (KGS) in Lawrence.

Cuttings and polished slabs from the cores were studied with binocular microscope to discern depositional fabrics and macroscale diagenetic textures. Some thin sections of the above cores were available at the KGS in Lawrence, and additional thin sections of the cores were acquired for petrographic analysis (69 total). Sixty-one thin sections from the reservoir intervals were point counted (500 points) to estimate the volume and stratigraphic distribution of different porosity types and the volume and types of cements occluding the pore space. Cuttings from 30 wells in Victory Field were studied and thin sections of selected cuttings of reservoir grainstone were obtained and point counted to check the validity and consistency of observations and interpretations derived from low-power, microscopic studies and, furthermore, evaluate the utility of cuttings in the overall scheme of defining reservoir parameters. Wireline logs are often unavailable in the Lansing-Kansas City fields on the Central Kansas Uplift. Aside from logs and well testing, cuttings are the only indicator of reservoir quality that may exist for many of the wells in an old field. Cuttings have further utility by serving as a means to acquire capillary pressure information.

Stratigraphy of the Bethany Falls Limestone in Victory Field

The most complete core of the Bethany Falls was from the Cox no. 4 well which was studied in detail to characterize depositional and diagenetic fabrics (Figure 6.70). The uppermost Bethany Falls in Victory Field consists of argillaceous, rhizolith-rich, lime mudstone that is sharply overlain by light-gray, calcareous shale of the Stark member. Well-developed rhizoliths at the top of the Bethany Falls indicate the occurrence of a subaerial exposure event separating deposition of the Bethany Falls from deposition of the overlying Stark Shale. The lime mudstone at the top of the Bethany Falls grades downward to poorly cemented, ooid packstone. A sharp lower contact separates the ooid packstone from highly-porous ooid grainstone beneath it. The grainstone is consistently oolitic, except for the very base, and generally has abundant oomoldic porosity. At the very base of the grainstone, the fabric becomes more skeletal and less oolitic and grades downward, over a few inches, from echinoderm grainstone to echinoderm packstone. The basal grainstone/packstone contains reworked clasts from the underlying beds and makes a sharp, stylolitic, lower contact with lime mudstone below. The uppermost one foot of the lime mudstone contains areas with a soil-like granular fabric and possible

rhizolith structures. This suggests that the break between muddy rocks in the lower half of the Bethany Falls and the porous grainstones above is marked by a surface of subaerial exposure. Beneath the lime mudstone the Bethany Falls consists of skeletal wackestone with subdued mottling that is in turn underlain by lime mudstone with well-developed mottling. Within the upper part of this lime mudstone interval some mottles have angular forms that resemble an autoclastic breccia and some horizons have a granular fabric. The definition of angularity in the mottling increases downward to become a well-developed autoclastic breccia fabric. The development of autoclastic breccia is interpreted to be the result of subaerial exposure, either at the top of the lime mudstone mid-way in the Bethany Falls, or if that horizon was not subaerially exposed, then due to the well-developed subaerial exposure surface at the top of the Bethany Falls. The lowermost strata in the Bethany Falls consist of laminated lime mudstone whose lamination occurs as broadly-wavy (due to compaction?), fine laminae that are sometimes accentuated by finely-crystalline pyrite.

Diagenesis of Reservoir Rocks in Victory Field

Point counts of the thin sections were made to quantify several lithologic and diagenetic aspects of the reservoir rocks with much attention given toward determining the amount and stratigraphic distribution of effective and noneffective porosity (Tables 6.3 and 6.4). Effective porosity was defined as connected moldic, interparticle, fracture, and vuggy porosity. Noneffective porosity was defined as isolated moldic and isolated intraparticle porosity. Oomoldic porosity dominates the Bethany Falls grainstone and commonly accounts for 20 to 30 percent of the total porosity evident in thin section. In some wells, such as the Blair 'C' no. 2, the porosity is fairly uniform throughout (Figure 6.71), whereas in others, such as the Cox no. 4 and Thompson 'E' no. 2, there are one to two foot thick zones within the grainstone where late cements occlude the bulk of secondary pore space (Figures 6.72 and 6.73). Core coverage in the Conover 'D' no. 2 well was too limited to make similar assessments. Based on the cores available, the upper one foot of the Bethany Falls appears to have less effective porosity than much of the reservoir rock beneath it. In the Cox and Thompson wells the highest effective porosities occur below well-cemented intervals in the upper part of the lower half of the grainstone. Thus, in addition to poor connectivity of the oomoldic pore fabric, the reservoir may be compartmentalized by tight zones within it. Pore fabrics in the Dewey and Stanton Limestones are similar to those in the Bethany Falls (Tables 6.3-6.6). The skeletal grainstone of the Iatan Limestone is primarily interparticle and, as evidenced by its widespread production history, its pore system is much more homogeneous and interconnected than the oomoldic pore fabrics.

Abundant caliche nodules, rhizoliths and desiccation cracks at the top of the Bethany Falls provide evidence of an early subaerial exposure event. Meteoric waters introduced to the carbonate sediment during subaerial exposure resulted in three diagenetic stages that affected the porosity (Figure 6.74). Stage 1 was the growth of uniformly distributed equant calcite cement on the ooid grains. In many cases the equant calcite completely

occludes the interparticle space. Early cementation was followed by dissolution of most oolitic grains (stage 2). Cessation of meteoric diagenesis at this stage results in a rock that has high porosity but very low permeability. Effective porosity was achieved by stage 3, wherein the walls of the ooids were dissolved leading to the creation of better connected pores. During burial, equant calcite precipitated on the inner walls of some oomolds (stage 4). Precipitation of the intramoldic cements armored the molds, further diminishing pore connectivity. Oomolds where intramoldic cements did not form are commonly sightly crushed together (Figure 6.75a,b), an action which furthers the amount of pore connections (stage 5). The final cements to precipitate (stage 6) were ferroan calcite followed by baroque dolomite (Figure 6.75c) followed by very minor amounts of quartz. Complete occlusion of oomolds is commonly achieved by the precipitation of ferroan calcite and baroque dolomite. High effective porosities are achieved through high total porosities accompanied by abundant pore connections and a lack of late cements. A similar sequence of diagenetic events appears to have affected the oolitic grainstone of the Dewey and Stanton Limestones.

Study of Drill Cuttings in Victory Field

Previous studies of thin sections from Swope cores in Victory Field revealed that late cements in oomoldic pores can occlude a significant porosity and, therefore, must contribute to reducing the amount of effective porosity. Examination of the well cuttings reveal that these late cements can be discerned under low-power, reflected light studies with a binocular microscope. As such, it is possible to differentiate three classes of grainstone cuttings based on the abundance of porosity and the presence of cements within secondary porosity:

Type A: Nonporous oolitic grainstone with abundant late cement occluding secondary pore space.

Type B: Partially porous oolitic grainstone with secondary porosity partly occluded by late cement.

Type C: Fully porous oolitic grainstone lacking late cement within secondary pores.

The percent of Type C grainstone can then be considered as an index of effective porosity. A map of the distribution of effective porosity in the Bethany Falls can then be obtained by contouring the percent of the Type C grainstone. To attempt this, 30 wells were studied (Table 6.7). Chips of oolitic grainstone were picked from the cuttings, each chip counted as one of the above types, and the total of each type recorded as a percent (Table 6.8). A similar exercise was performed from cuttings from the Drum limestone (Table 6.9). The percent of Type C grainstone was then contoured and overlain on isopach and porosity feet maps derived from electric logs (Figures 6.76 and 6.77). These maps show good correspondence with highs in the percent of Type-C grainstone mimicking the distribution of thick buildups and thick sections of log porosity. Productive areas in

Victory Field are outlined by contours greater than or equal to 40 percent Type C grainstone and, thus, the percent of Type C cuttings appears to be a good index of the effective porosity.

To assess the success of the cuttings examination, 40 thin sections of cuttings, from 20 wells, were prepared. Point counts were made of the relative percents of isolated oomoldic, connected oomoldic, and interparticle porosity; and the distribution of calcite, dolomite and quartz cements in interparticle versus moldic pore space (Table 6.10).

Comparison of these point counts with the percent of Type C cuttings were made (Table 6.11) and regression equations were calculated for three variables on Type C percent: a) total porosity, b) connected porosity, and c) cement in moldic porosity (Figure 6.78). Regression equations for percent total porosity on percent Type C cuttings and connected porosity on percent Type C cuttings have significant R-squared values at 80% and 90% probability level, respectively, and show that the visual assessment of Type-C grainstone from the well cuttings was successful.

There is some correlation (at the 50% level) between the amount of cement in moldic pore space and the percent of Type C (fully porous) grainstone. The porous grainstone may also be related to grain crushing (Figure 6.75a,b) that is commonly observed in thin sections from cores, but is not apparent in binocular examination of cuttings.

Comparisons of the cuttings versus thin section examination showed that they agreed 15 out of 22 times (68 percent agreement). The cuttings examination correctly predicted high effective porosities in 6 out of 9 wells and correctly predicted low effective porosities in 5 of 7 wells.

The percent connected porosity from thin section point counts was mapped and overlain on an isopach map of the Swope (Figure 6.79), for comparison with the earlier map based on percent Type C grainstone (Figure 6.76). These maps have a good correspondence in delineating the areas of highest and lowest effective porosities and show that well sample examination is a useful exercise for evaluating the distribution of effective porosity.

Conclusions of the Diagenetic Study

Porosity in the Bethany Falls, Dewey, and Stanton limestones is mostly secondary in origin, having resulted from the dissolution of ooid grains by meteoric waters during early subaerial exposure. Initially, oomoldic porosity was poorly connected, but may have become well connected through extensive dissolution or by minor crushing of the thin-walled oomolds to join one to another. During burial, oomolds commonly became partly or fully filled by late cements of calcite and/or baroque dolomite. The extent of cement within the oomolds then

becomes a limiting factor in the amount of effective porosity. Cements in oomoldic pores can be recognized in well cuttings. The percent of the more porous chips can be used as an index of the effective porosity. A high index of effective porosity in well cuttings defines areas of production in the Bethany Falls and Drum limestones in Victory field. Such an index can be used to explore for areas of greatest reservoir potential in other areas where similar reservoir conditions exist.

In general, thicker grainstones in the Bethany Falls Limestone preferentially develop areas of permeable rock. The thicker grainstone may originally develop a larger meteoric freshwater lens. Relief on the sediment body and perhaps thicker and more continuous beds of oolite may facilitate greater freshwater circulation through the body leading to greater flushing and dissolution of carbonate. Mapping the thickness of the porous facies appears to provide a reliable indicator of where effective reservoir quality rock may be located. Once these sites are found, log analysis, namely the "Super" Pickett crossplot, provides the means to discern the effective and saturated pay.

SUBTASK 7. TECHNOLOGY TRANSFER

Introduction

Information was conveyed to petroleum operators about this project during numerous opportunities in the past three years including:

1) presentations at international meetings -- AAPG, SEG, DOE/NIPER Reservoir Characterization Conference,
2) presentations at regional meetings -- arranged a core workshop and field trip associated with AAPG Midcontinent meeting in Wichita in 1991, co-convene Reservoir Description Workshop held in Wichita in February 1993,
3) onsite visits and presentations in Lawrence -- Kansas Geological Society technical meetings in September 1992,
4) informal visits with geologists and engineers inquiring about project, e.g., applications of "Super" Pickett plots, stratigraphic problems, waterflood problems,
5) submission of articles for publication.

In addition interest was shown by the general geological community interested in cyclothemic sedimentation and the work being conducted, in part stemming from this research:

1) Predictive stratigraphic analysis group of the U.S Geological Survey organized by Blaine Cecil with over 80 attendees from across U.S. (led field trip and presented paper),

2) Pangea conference in May 1992 with 85 attendees from worldwide held in Lawrence organized by G. dev. Klein (led field trip, presented paper, chaired committee on resources of Pangea).

Published Articles

Baars, D.L., and Watney, W.L., 1991, Paleotectonic control of reservoir facies: in Sedimentary Modeling: Computer Simulations and Methods for Improved Parameter Definition, Kansas Geological Survey Bulletin 233, p. 253-262.

Coveney, R.M., Jr., Watney, W.L., and Maples, C.G., 1991, Contrasting depositional models for Pennsylvanian black shale discerned from molybdenum abundances: Geology, v. 19, p. 147-150.

Feldman, H.R., Franseen, E.K., Miller, R.D., and Anderson, in press, Geometry and Stratigraphic Relationships of the Drum Oolite and Related Units, Missourian, Southwestern Kansas: Reservoir Description Workshop-Application of Underutilized Technologies, February 16-17, 1993, Wichita, Kansas.

Feldman, H.R., and Franseen, E.K., 1991, Stratigraphy and depositional history of the Drum Limestone and associated strata (Pennsylvanian) in the Independence, Kansas area -- A field trip guidebook and road log: Mid-Continent Section AAPG Meeting, Wichita, 30p.

Franseen, E.K., Feldman, H.R., Anderson, N.L., and Miller, R.D., in press, Depositional and Stratigraphic Analysis of Kansas City Group Strata Utilizing High-Resolution Seismic Imaging, Montgomery County, Kansas: in Anderson, N.L., Hedke, D. et al., eds., Geophysical Atlas of Kansas, Kansas Geological Survey Special Publication.

Franseen, E.K., Watney, W.L., Kendall, C.J., Ross, W., Editors, 1991, Sedimentary Modeling: Computer Simulations and Methods for Improved Parameter Definition: Kansas Geological Survey, Bulletin 233, 524 p.

French, J.A., and Watney, W.L., 1993, Integrated field, analog, and shelf scale geologic modeling of oolitic grainstone reservoirs in the Upper Pennsylvanian Kansas City Group in Kansas (USA): in, Linville, B., ed., Reservoir Characterization III, Third International Reservoir Characterization Technical Conference Proceedings, PenWell Books, Tulsa, 982-993.

Miller, R.A., Anderson, N.L., Franseen, E.K., and Feldman, H.R., in review, Practical Vertical Resolution Limits of CDP Data Targeting Reflectors Less Than 125 m Deep Near Independence, Kansas: Geophysics.

Watney, W.L., Wong, J.C., and French, J.A., 1991, Computer simulation of Upper Pennsylvanian (Missourian) carbonate-dominated cycles in western Kansas (United States), in Sedimentary Modeling: Computer Simulations and Methods for Improved Parameter Definition, Kansas Geological Survey, Bulletin 233, p. 415-430.

Watney, W.L. and Heckel, P.H., in review, Revisions of nomenclature and classification of strata in the Marmaton, Pleasanton, and Kansas City groups; in, Baars, D.L., ed., Revision of Kansas stratigraphy, Kansas Geological Survey.

Watney, W.L., Wong, J.C., and French, J.A., 1991, Computer simulation of Upper Pennsylvanian (Missourian) carbonate-dominated cycles in western Kansas, in Sedimentary Modeling: Computer Simulations and Methods for Improved Parameter Definition, Kansas Geological Survey, Bulletin 233, p. 415-430.

Watney, W.L., Stephens, B., and Wong, J.C., 1992, Cahoj field, in Foster, N.H. and Beaumont, E.A., eds., Petroleum Reservoirs--Structural Traps, Treatise of Petroleum Geology, American Association of Petroleum Geologists, p. 239-273.

Watney, W.L., Harff, J., Davis, J.C., Bohling, G., and Wong, J.C., 1993, Controls on petroleum accumulation in Upper Pennsylvanian cyclic shelf carbonates in western Kansas, USA, as interpreted from space modeling and multivariate techniques: Proceedings of COGEODATA-IAMG Symposium on Computerized Basin Analysis for Prognosis of Energy and Mineral Resources, Pergamon Press, p. 215-237.

Published Abstracts

Baars, D.L., 1990, Conjugate basement rift zones in Kansas, Midcontinent U.S.A.: 9th International Conference on Basement Tectonics Program and Abstracts, Canberra, Australia, p. 24.

Feldman, H.R., Franseen, E.K., Miller, R.D., and Anderson, N.L., 1992, Analysis of Carbonate and Siliciclastic Strata at a Depositional Shelf Edge Utilizing High-Resolution Reflection Seismic Imaging, Pennsylvanian, SE Kansas: 1992 AAPG-SEPM Annual Convention, Official Program, p. 40.

French, J.A., 1992 (b), Quantitative modeling of Pennsylvanian cyclothems: Implications for understanding relative sea-level histories: Abstracts With Programs, North-Central Section GSA, p. 15.

French, J.A., Feldman, H.R., Watney, W.L., and Franseen, E.K., 1992, Stratigraphic architecture and facies distribution of upper Middle Carboniferous cyclic depositional sequences (cyclothems), southeastern Kansas, U.S.A., Abstracts with Programs, North-Central Section GSA, p. 15.

French, J.A., and Watney, W.L., 1990, Computer modeling of Mid-Continent cyclothems and its application in the prediction of hydrocarbon reservoirs: American Association of Petroleum Geologists, Bulletin, v. 74, p. 657. (Annual Meeting of AAPG-SEPM, San Francisco)

French, J.A., and Watney, W.L., 1991, Description and quantitative modeling of oolitic reservoir analogs within the lower Kansas City Group (Pennsylvanian), southeastern Kansas: American Association of Petroleum Geologists Bulletin, v. 75 (8), p. 1394.

French, J.A., Watney, W.L., Wong, J.C., and Guy, W.J., Jr., 1991, Integrated field, analog, and shelf-scale geologic modeling of oolitic grainstone reservoirs in the Upper Pennsylvanian Kansas City Group in Kansas (USA): Third International Reservoir Characterization Technical Conference, Preprints, Vol., 2, DOE CONF-911125/NIPER-558/2, p. 3RC-76 to 3RC-81.

Guy, W.J., and Watney, W.L., 1992, Victory field study, Haskell County, Kansas--An interdisciplinary reservoir characterization: American Association of Petroleum Geologists Bulletin, v. 76, p. 1276.

Guy, W.J., Watney, W.L., Carlson, R., in press, The Lansing-Kansas City (Upper Pennsylvania) Limestones in the Hugoton Embayment (Western Kansas)--An Independent's Exploration Target, American Association of Petroleum Geologists Bulletin.

Harff, J., Davis, J.C., Watney, L., Bohling, G., and Wong, J.C., in press, Regionalization of the western Kansas shelf based on stratigraphic data from wells (abs.): American Association of Petroleum Geologists Bulletin.

Heckel, P.H., Barrick, J.E., Boardman, D.R., Watney, W.L., and Weibel, C.P., 1991, Biostratigraphic correlation of eustatic cyclothems (basic Pennsylvanian sequence units) from Midcontinent to Texas and Illinois: AAPG Bulletin, v.

Lambert, L., Heckel, P.H., Watney, W.L., Stevenson, G.M., Barrick, J.E., and Boardman, D.R., 1991, Precision correlation of Kansas Pennsylvanian cyclothems emphasizing wireline logs and conodonts in a sequence stratigraphic framework: American Association of Petroleum Geologists, Bulletin, v. 75, p. 616.

Miller, R.D., Feldman, H.R., Franseen, E.K., Keiswetter, D.A., and Steeples, D.W., 1992, Practical Vertical Resolution Limits of CDP Seismic-Reflection Data Targeting Reflectors Less Than 250 m Deep Near Independence, Kansas (expanded abstract): 1992 Society of Exploration Geophysicists Annual International Meeting, Technical Program, p. 374-377.

Watney, W.L., French, J.A., Wong, J.C., Feldman, H.R., Franseen, E.K., and Guy, W.J., 1992, Sequence stratigraphy and stratigraphic modeling for improved understanding of midcontinent reservoirs: American Association of Petroleum Geologists Bulletin, v. 76, p. 1289.

Watney, W.L., Baars, D.L., Stevenson, G., French, J.A., Wong, J.C., Lambert, L., and Harff, J., 1991, Regional structure and stratigraphic framework in Kansas and relationship to oil and gas accumulation: American Association of Petroleum Geologists Bulletin, v. 75 (8), p. 1400.

Watney, W.L., Doveton, J.H., French, J.A., and Collins, D.R., 1990, Petrophysical characterization of Upper Pennsylvanian depositional sequences in western Kansas: Geological Society of America, Abstracts With Programs, v. 22, no. 1, p. 35.

Watney, W.L., 1991, Reservoir characterization in the Midcontinent: Official Program, 1991 Annual Meeting, Interstate Oil and Gas Compact Commission, New Orleans, p. 6.

Open-File Reports

Feldman, H.R., and Franseen, E.K., 1991, Stratigraphy and Depositional History of the Drum Limestone and Associated Strata (Pennsylvanian) in the Independence, Kansas, Area-A Field Trip Guidebook and Road Log: Kansas Geological Survey Open-File Report 91-45, 29 p.

Miller, R.D., Feldman, H.R., Franseen, E.K., Knapp, R., and Black, R.A., 1991, Practical Vertical Resolution Limits of CDP Seismic-Reflection Data Targeting Reflectors Less Than 125 m Deep Near Independence, Kansas: Kansas Geological Survey Open-File Report 91-36, 12 p.

Watney, W.L., 1992, Upper Pennsylvanian (Virgilian and Missourian) cyclothems in the Lawrence, Kansas Area: Part II Field Trip, Project Pangea Workshop--Getting It and Holding It All Together, 25 p.

Watney, W.L., West, R., Maples, C., Denham, P., 1991, Upper Pennsylvanian (Virgilian and Missourian) Cyclothems in the Lawrence, Kansas Area: for Midcontinent meeting of Predictive Stratigraphic Analysis (PSA) Workshop -- C.B. Cecil and N.J. Edgar, program planners: Kansas Geological Survey Open-File Report 91-22, 128 p.

Watney, W.L., in review, Geological aspects of waterflooding workshop, Technology Transfer Project.

Watney, W.L., Walton, A.W., Caldwell, C.D., and Dubois, M.K., eds., 1991, Midcontinent Core Workshop -- Integrated Studies of Petroleum Reservoirs in the Midcontinent, Midcontinent Section Meeting, Wichita, Ks, Sept. 22, Kansas Geological Survey, Open-File 91-52, 172 p. (10 papers, 14 authors, all papers reviewed)

Watney, L., French, J., Guy, B., Carlson, R., and Wong, J., 1993, Geological characterization of oolitic grainstone reservoirs in the Upper Pennsylvanian Lansing-Kansas City Groups in Victory field and near-surface analog in Kansas: Reservoir Description Workshop -- Application of Underutilized Technologies, Kansas Geological Survey, Open-File Report 93-5, p. 145-174.

Conference and Meeting Participation

Co-Leader, field trip for Project Pangea Workshop (Global Sedimentary Geology Program), 80 international participants, Lawrence, Kansas, May 28, 1992.

Co-Chairman, Resources Working Group, Project Pangea Workshop, Lawrence, May 23-28, 1992.

Co-Convene, (Chair) Reservoir Description Workshop--Application of Underutilized Technologies, Wichita, February 16-17.

"Integration of Sedimentologic, Stratigraphic and High Resolution Seismic Data in the Drum Limestone Project of Southeast Kansas"; and "Overview to DOE project" to the Kansas Geological Survey Advisory Council, May 9, 1992.

"The Drum Limestone Project in Southeast Kansas"; to the University of Kansas Geology Department Geology Associates Advisory Board, October 9, 1992.

DOE project review to technical session of Kansas Geological Society in Lawrence, September 29, 1992.

SUMMARY

Integration of results from Victory Field study, near-surface and surface analog sites, field comparisons, and regional framework

1. There are two dominant types of oil/gas reservoirs in the Lansing-Kansas City limestones -- oolitic grainstones with both oomoldic and vuggy porosity and bioclastic limestone with intergranular and intercrystalline porosity. Each reservoir has its own unique petrophysical characteristics. The determination of effective porosity in the complex pore structure of the oomoldic grainstones presents the greatest challenge and opportunity for developing bypassed oil in existing fields.

2. Reservoirs in the Victory-Northeast Lemon Fields resulted from complex inter-related structural, stratigraphic, and diagenetic processes. Individual limestone reservoirs are commonly multi-layered and exhibit offlap and onlap relationships of these layers to inferred paleotopography. This topography, inferred from mapping of individual depositional sequences, may or may not coincide to the current structural configuration. Lateral and vertical reservoir compartments are also related to the effects of early meteoric diagenesis, vastly

changing the original pore systems in the oolitic grainstones. This diagenesis follows the same path of dissolution and cementation in both the analog and field areas.

3. The Victory Field oolitic grainstone shoals trend northwest-southeast and generally appear here to be best developed on a very subtle positive feature that apparently exhibited slight topographic relief during deposition of the oolite. Stratal geometries of the Bethany Falls Limestone at Victory Field are almost identical to those in the near-surface analog site in southeastern Kansas.

4. A "strandline grainstone model" of reservoir development is proposed based on integrated regional and local mapping of depositional sequences. A strong correlation appears to exist between the stratal geometries of grainstones developed along depositional strike at similar inferred elevations on the shelf. The accumulation of these buildups is believed to require greater residence time of shoal-water conditions through stillstand in sea level. Modeling results suggest average rates of sea level change during a 4th-order cycle were too fast to permit significant carbonate sedimentation. Parallel grainstone belts that rim the shelf suggest multiple stillstands of the strandline as sea level fell during the late highstand regressive carbonate. Grainstone lobes and pods are also thicker and more numerous in embayments where apparently energy is focused. The "strandline" model is a valuable predictive tool for: 1) locating favorable reservoirs for exploration and 2) anticipating internal properties of the reservoir in field development.

5. We have developed an accurate, practical, cost efficient technique for evaluating and understanding Lansing-Kansas City oil/gas reservoirs, the "Super" Pickett crossplot -- formation resistivity (R_t) vs. porosity (Ø). This technique is supported by over 1400 plots verified with production data. Most importantly, the procedure can help establish pore type, effective porosity, and water saturation cutoffs. The crossplot may be the only available means to characterize the properties of reservoirs where there are only older wireline logs, no cores, commingled and lease-aggregated production, and no separate production tests of separate zones. These limited data are common to Lansing-Kansas City fields and other fields in the U.S.

6. The least understood and underutilized petrophysical information is bulk volume water (BVW) and its companion attributes, capillarity and relative permeability. The bulk volume water (Sw x porosity) is critical to defining pay in complex carbonate reservoirs. The key is to establish the irreducible water saturation. A graphical depiction ("Super" Pickett crossplots) of the potential pay section can be done in a cost-effective and expeditious manner to obtain a number of important reservoir parameters, including irreducible water saturation, estimates of pore size and type, percent effective porosity, information about presence of a transition zone, and, if the latter is present, an estimate of the permeability in the zone. This information can be derived from a minimal amount of well-log information.

7. By using the "Super" Pickett crossplot in combination with 3-D visualization, it is estimated that from 6-9 million barrels of Lansing-Kansas City oil remain behind pipe in the Victory-Northeast Lemon Fields. Crossplotting other wells in other fields indicates that many leases need to be re-examined for bypassed oil associated with both primary and waterflood operations.

8. Application of the "Super" Pickett crossplots has demonstrated that the minimum porosity for an oomoldic Lansing-Kansas City reservoir to be effective is about 16% whereas a minimum porosity for reservoir with intergranular-intercrystalline porosity is about 8%. These cutoffs are substantiated by log analysis, thin sections, and point-counting. We believe that the 8% cutoff reservoirs which are readily evaluated through conventional methods have been recognized and probably fully developed in most fields, e.g. Iatan in Victory field. However, many of the high-porosity-cutoff pore types are behind pipe and should be re-evaluated. The waterflooding efficiency should vary among these contrasting reservoir types, an objective of ongoing investigation. Commingled zones should be re-evaluated individually to determine if each zone has been fully flooded.

9. Three-dimensional visualization can be combined with new techniques (e.g., "Super" Pickett crossplots) to re-examine the limited older data set from such fields as Victory. Three-dimensional modeling provides the means to see the heterogeneity such as layering and pinchouts, expedite calculation of key reservoir parameters, facilitate communication among geologists and engineers, and accelerate the transformation of the geologic model for use in reservoir simulation. The net result is to help identify additional oil.

10. Cross-shelf comparison between Victory, Cahoj and Pen Fields.

a. The Pen and Cahoj Fields are located higher on the western Kansas shelf than the Victory-Northeast Lemon Fields and reservoir analog sites in southeastern Kansas. Although they are thinner, basic reservoir properties are similar to those in Victory Field as indicated from cores, sample, and use of the "Super" Pickett crossplot.

b. The extreme heterogeneity in the oomoldic reservoirs exists primarily on the lower shelf where thick oolite bodies are developed. Findings from both the analog studies and Victory Field indicate that early meteoric diagenesis was very important and was controlled, in part, by layering, grain size, and thickness of the oolite. For example, the thicker portions of the Bethany Falls oolite in Victory Field apparently had much more extensive dissolution, leading to more widespread grain collapse and improved permeability. The intercrystalline porosity between the oolites and oomolds in the oolitic grainstone reservoirs is not usually effective. Effective permeability and porosity is dependent upon

crushing of the oomolds. This same characteristics is noted in the analog sites in southeast Kansas. The basic pore type and connectedness can be estimated through analysis of sample cuttings.

c. In general, both the grain size and pore size within the Lansing-Kansas City reservoirs are larger in the Victory-Northeast Lemon Fields area than to the north. The larger pore size indicated by low irreducible water saturation is probably reflecting the collapsed ooid fabric commonly seen in the petrographic examination of cores and cuttings.

d. Although structure is important in all three fields, the stratigraphy and diagenesis are of equal or greater importance to oil and gas entrapment. This conclusion is also supported by work in the analog study areas.

11. Toward improved predictive modeling of the petroleum reservoirs --

a. Recognition and detailed mapping of individual depositional sequences provide the means to decipher local paleotopography and regional paleogeography. The stacking of successive 4th-order sequences in 3rd-order sets on the shelf and shelf margin indicates a rhythm, regularity, and predictability of facies patterns. Regional (global) processes (i.e., subsidence, eustacy, and sedimentation) are acting on a local scale, controlling many of the details of the stratal architecture, facies, and diagenesis.

b. Simulation modeling has provided the means to test the interaction of these parameters in an attempt to model the dynamically changing conditions during the Pennsylvanian. The approach toward quantification of these parameters and the ability to integrate effects can only help us move toward more robust, deterministic predictive models of reservoirs (based on processes) that are needed to add "ground truth"--to integrate with current, geologically less well-constrained, stochastic models. Ideally, the two modeling approaches will soon be integrated using geostatistics at scales where observations are limited, (e.g., well-to-well spacing).

c. The envelope of resolution of deterministic modeling will improve as more interdisciplinary, quantitative studies of the variables controlling sedimentation are advanced (involving climate, basin, sea level change, etc.). Petroleum geology is challenged to grasp this information for use in quantitatively resolving reservoir characteristics.

REFERENCES CITED

Adams, J.A.S., and Weaver, C.E., 1958, Thorium to uranium ratios as indications of sedimentary processes: Example of concept of geochemical facies: American Association of Petroleum Geologists Bulletin, v. 42, p. 387-430.

Adey, W.H., Macintyre, I.G., Stuckenrath, R., and Dill, R.F., 1977, Relict barrier reef system of St. Croix its implications with respect to late Cenozoic coral reef development in the western Atlantic: Proceedings of Third International Coral Reef Symposium, v. 2, p. 15-21.

Almoussli, M.O., 1987, The application of the gamma ray spectrolog to the analysis of the Chase Group (Gearyean Stage, Lower Permian) in Stevens County, Kansas, Unpublished M.S. Thesis, Wichita State University, 142 p.

Archer, A.W., Lanier, W.P., and Feldman, H.R., 1992, Documentation of tidal influence with fluvial to estuarine transitions, Douglas Group, Virgilian, northeastern Kansas: Geological Society of America, Abstracts With Programs, v. 24, p. 2.

Archer, A.W., Lanier, W.P., and Feldman, H.R., in press, Fluvio-estuarine facies within incised paleovalley fills, Douglas Group (Stephanian; Upper Carboniferous) of Kansas, U.S.A. in Boyd, R., Zaitlin, B.A., and Dalrymple (eds.), SEPM Special Publication 51, Incised Valley Systems: Origin and Sedimentary Sequences.

Archie, G.E., 1952, Classification of reservoir rocks and petrophysical considerations: American Association of Petroleum Geologists, Bulletin, v. 36, no. 2, p. 278-298.

Asquith, G.B., 1985, Handbook of log evaluation techniques for carbonate reservoirs: American Association of Petroleum Geologists, Methods in Exploration Series, no. 5, 47 p.

Asquith, G.B., 1982, Basic well log analysis for geologists: American Association of Petroleum Geologists, Methods in Exploration Series, no. 3, 216 p.

Aufmuth, R.E., 1966, The Lansing, Kansas City, and Marmaton groups (Pennsylvanian) of the Lemon-Victory oil and gas field (Haskell County, Kansas): Miami University (Ohio), Masters Thesis.

Baars, D.L., and Watney, W.L., 1991, Paleotectonic control of reservoir facies: in, Franseen, E.K., Watney, W.L., Kendall, C.G.St.C., and Ross, W., eds.: Sedimentary Modeling: Computer Simulations and methods for improved parameter definition: Kansas Geological Survey Bulletin 233, p. 253-262.

Bebout, D.G., et al., 1987, Characterization of the Grayburg reservoir, University of Texas, Lands, Dune Field, Crane County, Texas, Bureau of Economic Geology, Report Investigation 168, 98 pp.

Berendsen, P. and Blair, K.P., 1991, Interpretive subcrop map of the Precambrian basement in the Joplin 1 x 2 quadrangle: Kansas Geological Survey, Subsurface Geology Series 14, 10 p.

Bickford, M.E., Harrower, K.L., Nussbaum, R.L., Thomas, J.J., Nelson, B.K., and Hoppe, W.J., 1981, Rb-Sr and U-Pb geochronology and distribution of rock types in the Precambrian basement of Missouri and Kansas: Geological Society of America, Bulletin, Part 1, v. 92, p. 323-341.

Blakeman, E.R., 1989, Application of bimodal porosity concepts to the development of log interpretation models: SPE No. 19575, p. 25-38.

Boardman, D.R., II, and Heckel, P.H., 1989, Glacial-eustatic sea- level curve for early Late Pennsylvanian sequence in north- central Texas and biostratigraphic correlation with curve for midcontinent North America; Geology, v. 17, p. 802-805.

Boardman, D.R., II, Mapes, R.H., Yancey, T.E., and Malinky, J.M., 1984, A new model for depth-related allogenic community succession within North American Pennsylvanian cyclothems and implications on the black-shale problem: Tulsa Geological Society ,Special Publication 2, p. 141-182.

Boardman, D.R., II, and Malinky, J.N., 1985, Glacial-eustatic control of Virgilian cyclothems in north-central Texas: Southwest Section, American Association of Petroleum Geologists, Transactions, p. 13-23.

Bond, D.C., 1978, Determination of residual oil saturation: Interstate Oil Compact Commission Report, Oklahoma City, 217 p.

Brewer, J.A., Good, R., Oliver, J.E., Brown, L.D., and Haufman, S., 1983, COCORP profiling across the southern Oklahoma aulacogen--overthrusting of the Wichita Mountains and compression within the Anadarko Basin: Geology, v. 11, p. 109-114.

Brezinski, D.K., 1984, Faunal diversity and community composition as indicators of episodic transgression in the Mauch Chunk Formation (Chesterian) of southwestern Pennsylvania: in Busch,

Brown, H.A., 1962, Preliminary Investigation of Lansing-Kansas City carbonate reservoirs of western Kansas: Pan American Petroleum, Kansas Geological Survey, Open-file report.

Brown, L.F., 1972, Virgil Lower Wolfcamp repetitive depositional environments in north-central Texas; in, Cyclic Sedimentation in the Permian Basin, 2nd ed., Elam, J.C., and Chuber, S., eds.: West Texas Geological Society, p. 41-54.

Brown,L.F., 1989, A sequence-stratigraphic and systems-trace model for the Virgilian and Wolfcampian Series, eastern shelf and adjacent Midland basin, Texas; in, Boardman, D.R., Barrick, J.E., Cocke, J., Nestell, M.K., Middle and Late Pennsylvanian Chronostratigraphic Boundaries in North-central Texas Glacial-Eustatic Events, Biostratigraphy, and Paleoecology, Part II: Contributed Papers, Texas Tech University, Studies in Geology 2, p. 35-62.

Buckles, R.S., 1965, Correlating and averaging connate water saturation data: Journal of Canadian Petroleum Technology, p. 42-52.

Busch, R.M., and Brezinski, D.K., 1984, Stratigraphic analysis of Carboniferous rocks in southwestern Pennsylvania using a hierarchy of transgressive-regressive units a guidebook: Eastern Section Meeting of the American Association of Petroleum Geologists, 104 p.

Busch, R.M., and Rollins, H.B., 1984, Correlation of Carboniferous strata using a hierarchy of transgressive-regressive units: Geology, v. 12, p. 471-474.

Calvert, S.E., Vogel, J.S., and Southon, J.R., 1987, Carbon accumulation rates and the origin of the Holocene sapropel in the Black Sea: Geology, v. 15, p. 918-921.

Carter, R.M., Carter, L., and Johnson, D.P., 1986, Submergent shorelines in the SW Pacific -- evidence for an episodic postglacial transgression: Sedimentology, v. 33, p. 629-649.

Cecil, C.B., 1990, Paleoclimate controls on stratigraphic repetition of chemical and siliciclastic rocks: Geology, v. 18, p. 533-536.

Cecil, C.B., Stanton, R.W., Neuzil, S.G., Dulong, F.T., Ruppert, L.F., and Pierce, B.S., 1985, Paleoclimate controls on Late Paleozoic sedimentation and peat formation in the central Appalachian Basin: International Journal of Coal Geology, v. 5, p. 195-230.

Chilingar, G.V., Mannon, R.W., and Rieke, H.H., III (eds.), 1972, Oil and gas production from carbonate rocks: American Elsevier, New York, 408 p.

Cole, V.B., 1976, Configuration of the top of the Precambrian rocks in Kansas: Kansas Geological Survey, Map M-7.

Coveney, R.M., Jr., and Martin, S.P., 1983, Molybdenum and other heavy metals of the Mecca quarry and Logan quarry shales: Economic Geology, v. 78, p. 132-149.

Coveney, R.M., Jr., Watney, W.L., and Maples, C.G., 1989, Rates and durations for accumulation of Pennsylvanian black shales in the Midwestern U.S.; in, Franseen, E.K., and Watney, W.L., eds.: Sedimentary Modeling Computer Simulation of Depositional Sequences, Kansas Geological Survey Subsurface Series, v. 12.

Cross, T.A., 1989, Quantitative Dynamic Stratigraphy: Prentice-Hall, Englewood Cliffs, New Jersey, 625 p.

Crowell, J.C., 1978, Gondwanan glaciation, cyclothems, continental positioning, and climate change: American Journal of Science, v. 278, p. 1,345-1,372.

Crowell, J.C., and Frakes, L.A., 1975, The late Paleozoic glaciation; *in*, Campbell, K.S.W., ed., Gondwana Geology: Canberra, Australia National University Press, p. 313-331.

Crowley, T.J., Mengel, J.G., and Short, D.A., 1987, Gondwanaland's seasonal cycle: Nature, v. 329 (Oct. 29), p. 803-807.

Davis, J.C., 1986, Statistics and data analysis in geology, 2nd Ed., John Wiley and Sons, New York, 646 p.

Demaison, G.J., and Moore, G.T., 1980, Anoxic environments and oil source bed genesis: American Association of Petroleum Geologists, Bulletin, v. 64, p. 1,179-1,209.

Denton, G.H., and Hughes, T.J., 1983, Malankovitch theory of ice ages hypothesis of ice-sheet linkage between regional insolation and global climate: Quaternary Research, v. 20, p. 125-144.

Dickinson, W.R., and Yarborough, H., 1979, Plate tectonics and hydrocarbon accumulation: American Association of Petroleum Geologists, Continuing Education Case Notes Series 1, 150 p.

Dickinson, W.R., and Yarborough, H., 1979, Plat tectonics and hydrocarbon accumulation: American Association of Petroleum Geologists, Continuing Education Case Notes Series 1, 150 p.

Dickson, J.A.D., 1965, A modified staining technique for carbonates in thin section: Nature, No. 4971, p. 587.

DOE, 1989; DOE/BC-89/6/S, Abandonment rates of the known domestic oil resources, Bartlesville, Oklahoma, 39 p.

Donaldson, A.C., 1974, Pennsylvanian sedimentation of central Appalachians: Geological Society of America, Special Publication 148, p. 47-78.

Donovan, D.T., and Jones, E.J.W., 1979, Causes of world-wide changes in sea level: Journal of the Geological Society, London, v. 136, p. 187-192.

Doveton, J.H., 1991, Lithofacies and geochemical facies profiles from nuclear wireline logs: New subsurface templates for sedimentary modeling: in, Franseen, E.K., Watney, W.L., Kendall, C.G.St.C., and Ross, W., eds.: Sedimentary Modeling: Computer Simulations and methods for improved parameter definition: Kansas Geological Survey, Bulletin 233, p. 101-110.

Doveton, J.H., 1986, Log Analysis of Subsurface Geology, Wiley Interscience, New York, 273 p.

Doveton, J.H., 1992, Reading rocks from wireline logs: Kansas Geological Survey, Open-File Report.

Dubois, M.K., 1985, Application of cores in development of an exploration strategy for the Lansing Kansas City E Zone, Hitchcock County, Nebraska: Kansas Geological Survey, Subsurface Geology Series 6, Core Studies in Kansas, p. 120-144.

Duff, P. McL. D., and Walton, E.K., 1962, Statistical basis for cyclothems a quantitative study of the sedimentary succession in the east Pennine coal fields: Sedimentology, v. 1, p. 235- 255.

Dwights, 1992, Natural Gas Well Production Histories, December.

Earlougher, R.C., Jr., 1977, Drill stem testing: Advances in well test analysis, SPE Monograph Series, Chapter 8, p. 90-104.

Ebanks, W.J., Jr., and Watney, W.L., 1985, Geology of Upper Pennsylvanian carbonate oil reservoirs, Happy and Seberger fields, northwestern Kansas; in, Roehl, P.O., and Choquette, P.W., eds., Carbonate Petroleum Reservoirs--A Casebook: Springer-Verlag, New York, Inc., p. 241-250.

Feldman, H.R., and Franseen, E.K., 1991, Stratigraphy and depositional history of the Drum Limestone and associated strata (Pennsylvanian) in the Independence, Kansas, area: A field trip guidebook and road log: Kansas Geological Survey Open-File Report 91-45, 29 p.

Feldman, H.R., Franseen, E.K., Miller, R.D., and Anderson, N.L., 1992, Analysis of Carbonate and Siliciclastic Strata at a Depositional Shelf Edge Utilizing High-Resolution Reflection Seismic Imaging, Pennsylvanian, SE Kansas: 1992 AAPG-SEPM Annual Convention, Official Program, p. 40.

Feldman, H.R., and Franseen, E.K., 1991, Stratigraphy and Depositional History of the Drum Limestone and Associated Strata (Pennsylvanian) in the Independence, Kansas, Area-A Field Trip Guidebook and Road Log: Kansas Geological Survey Open-File Report 91-45, 29 p.

Feldman, H.R., Franseen, E.K., Miller, R.D., and Anderson, in press, Geometry and Stratigraphic Relationships of the Drum Oolite and Related Units, Missourian, Southwestern Kansas: Reservoir Description Workshop-Application of Underutilize Technologies, February 16-17, 1993, Wichita, Kansas.

Ferm, J.C., 1975, Pennsylvanian cyclothems of the Appalachian Plateau; a retrospective view; in, E.D. McKee and E.J. Crosby, eds., Paleotectonic Investigations of the Pennsylvanian System in the United States Part II, Interpretative Summary and Special Features of the Pennsylvanian System: U.S. Geological Survey, Professional Paper 853, p. 57-64.

Fertl, W.H., 1979, Hingle crossplot speeds long-interval evaluation: Oil and Gas Journal, p.114-118.

Fertl, W.H., and Vercellino, 1978, Predict water cut from well logs, in practical log analysis, Part 4: Oil and Gas Journal

Fischer, A.G., 1964, The Lofer cyclothems of the Alpine Triassic, in, Merriam, D.F., ed., Symposium on Cyclic Sedimentation: Kansas Geological Survey, Bulletin 169, p. 107-149.

Franseen, E.K., Feldman, H.R., Anderson, N.L., and Miller, R.D., in press, Depositional and Stratigraphic Analysis of Kansas City Group Strata Utilizing High-Resolution Seismic Imaging, Montgomery County, Kansas: in Anderson, N.L., Hedke, D. et al., eds., Geophysical Atlas of Kansas, Kansas Geological Survey Special Publication.

French, J.A., Feldman, H.R., Watney, W.L., and Franseen E.K., 1992, Stratigraphic architecture and facies distribution of upper Middle Carboniferous cyclic depositional sequences (cyclothems), southeastern Kansas, USA: Geological Society of America, Abstracts with Programs, v. 24, no. 4, p. 15.

French, J.A. and Watney, W.L., 1993, Integrated field, analog, and shelf-scale geologic modeling of oolitic grainstone reservoirs in the upper Pennsylvanian Kansas City Group in Kansas: in, Lineville, B., ed., Reservoir Characterization III, PennWell Books, Tulsa, OK, p. 983-993.

Galloway, W.E., and Brown, L.F., 1973, Depositional systems and shelf-slope relations on cratonic basin margin, uppermost Pennsylvanian of north-central Texas: American Association of Petroleum Geologists, Bulletin, v. 57, p. 1,185-1,218.

Galloway, W.E., Yancey, M.S., and Whipple, A.P., 1977, Seismic stratigraphic model of depositional platform margin, eastern Anadarko basin, Oklahoma: American Association of Petroleum Geologists, Bulletin, v. 61, p. 1,437-1,447.

Goebel, K.A., Bettis, E.A., III, and Heckel, P.H., 1989, Upper Pennsylvanian paleosol in Stranger Shale and underlying Iatan Limestone, southwestern Iowa: Journal of Sedimentary Petrology, v. 59, , no. 2, p. 224-232.

Goldhammer, R.K., Lehmann, P.J., and Dunn, P.A., 1993, The origin of high-frequency platform carbonate cycles and third-order sequences (Lower Ordovician El Paso Group, West Texas): Constraints from outcrop data and stratigraphic modeling: Journal of Sedimentary Petrology, v. 63, p. 318-359.

Goldhammer, R.K., Oswald, E.J., Dunn, P.A., 1991, Hierarchy of stratigraphic forcing: Example from Middle Pennsylvanian shelf carbonates of the Paradox basin: in, Franseen, E.K., Watney, W.L., Kendall, C.G.St.C., and Ross, W., eds.: Sedimentary Modeling: Computer Simulations and methods for improved parameter definition: Kansas Geological Survey, Bulletin 233, p. 361-413.

Goldstein, R.H., Anderson, J.E., and Bowman, M.W., 1991, Diagenetic responses to sea-level change: Integration of field, stable isotope, paleosol, paleokarst, fluid inclusion, and cement stratigraphy research to determine history and magnitude of sea-level fluctuation: in, Franseen, E.K., Watney, W.L., Kendall, C.G.St.C., and Ross, W., eds.: Sedimentary Modeling: Computer Simulations and methods for improved parameter definition: Kansas Geological Survey, Bulletin 233, p. 139-162.

Gonzalez Bonorino, F., and Terruggi, M.E., 1952, Lexico sedimentologico: Instituto Nacional de Investigaciones de Ciencias Naturales, Buenos Aires, Publicaciones de extension cultural y didactica, no. 6, 164 p.

Gould, G.E., Green, D.W., Willhite, G.P., Phares, R.A., Walton, A.W., 1993, Reservoir description and modeling of the Pen field, Graham County, Kansas: in, Lineville, B., ed., Reservoir Characterization III, PennWell Books, Tulsa, OK, p. 715-744.

Gould, G.E., 1991, Geostatistical study and reservoir simulation of the Pen field, Graham County, Kansas: unpublished M.S. Thesis, 142 p.

Greengold, G.E., 1986, The graphical representation of bulk volume water on the Pickett crossplot: The Log Analyst, v. 27, no. 3, p. 21-25.

Guy, W.J. and Doveton, J., 1992, New interpretation strategies for predicting oil productivity using extensions of classic log analysis techniques: Reservoir Description Workshop: Application of Underutilized Technologies, Energy Research Center, Lawrence, KS, p. 51-72.

Halley, R. B., Harris, P. M., and Hine, A. C., 1983, Bank margin environment, *in* Scholle, P. A., Bebout, D. G., and Moore, C. H., eds., Carbonate Depositional Environments: A.A.P.G. Memoir 33, p. 463-506.

Halliburton Services, various service manuals on drill stem testing.

Hallock, P. and Schlager, W., 1986, Nutrient excess and the demise of coral reefs and carbonate platforms: Palaios, v. 1, p. 389-398.

Ham, W.E., and Wilson, J.L., 1967, Epeirogeny and orogeny in the central United States: American Journal of Science, v. 265, p. 332-407.

Hamblin, W.K., 1969, Marine paleocurrent directions in limestones of the Kansas City Group (Upper Pennsylvanian) in eastern Kansas: Kansas Geological Survey, Bulletin 194, pt. 2, 25 p.

Harff, J., and Davis, J, 1990, Regionalization in geology by multivariate classification: Mathematical Geology, v. 22, p. 573-588.

Hassan, M. and Combaz, A., 1976, Fundamentals of the differential gamma log-interpretation technique: in, Transactions of the SPWLA 17th Annual Logging Symposium, Paper H.

Hatch, J.R., and Leventhal, J.S., 1985, Organic and trace-element geochemical evidence of depositional and post-depositional processes for midcontinent Middle and Upper Pennsylvanian organic-matter-rich rocks; *in*, Watney, W.L., Kaesler, R.I., and Newell, K.D., eds., Recent Interpretation of Late Paleozoic Cyclothems: Midcontinent Section, Society of Economic Paleontologists and Mineralogists, Proceedings Third Annual Meeting and Field Conference, p. 267-268.

Hatch, J.R., and Leventhal, J.S., 1992, Relationship between inferred redox potential of depositional environment and geochemistry of the Upper Pennsylvanian (Missourian) Stark Shale Member of the Dennis Limestone, Wabaunsee County, Kansas, U.S.A.: Chemical Geology, v. 99, p. 65-82.

Heckel, P. H., and Baesemann, J. F., 1975, Environmental interpretation of conodont distribution in Upper Pennsylvanian (Missourian) megacyclothems in eastern Kansas: Am. Assoc. Petroleum Geologists Bull., v. 59, p. 486-509.

Heckel, P.H., 1977, Origin of phosphatic black-shale facies in Pennsylvanian cyclothems of midcontinent North America: American Association of Petroleum Geologists, Bulletin, v. 61, p. 1,045- 1,068.

Heckel, P.H., 1980, Paleogeography of eustatic model for deposition of Midcontinent Upper Pennsylvanian cyclothems; in, Fouch, T.D., and Magathan, E.R., eds., Paleozoic Paleogeography of the West-central United States: Rocky Mountain Section, Mountain Paleogeography Symposium 1, p. 197-216.

Heckel, P. H., 1983, Diagenetic model for carbonate rocks in Midcontinent Pennsylvanian eustatic cyclothems: Journal Sedimentary Petrology, v. 53, p. 733-759.

Heckel, P.H., 1984, Changing concepts of midcontinent Pennsylvanian cyclothems: IX International Carboniferous Congress 1979, Compte Rendu, v. 3, p. 535-553.

Heckel, P.H., 1985, Current view of midcontinent Pennsylvanian cyclothems; *in*, Watney, W.L.,

Heckel, P. H., 1986, Sea-level curve for Pennsylvanian eustatic marine transgressive-regressive depositional cycles along midcontinent outcrop belt, North America: Geology, v. 14, p. 330-334.

Heckel, P. H., 1990, Evidence for global (glacial-eustatic) control over upper Carboniferous (Pennsylvanian) cyclothems in midcontinent North America: in Hardman, R. F. P., and Brooks, J. (eds), Tectonic events responsible for Britain's oil and gas reserves, Geological Society Special Publication 55, p. 35-47.

Heckel, P.H., 1991, Thin widespread Pennsylvanian black shales of Midcontinent North America: a record of cyclic succession of widespread pycnoclines in a fluctuating epeiric sea: in, Tyson, R.V. and Pearson, T.H., eds., Modern and Ancient Continental Shelf Anoxia: Geological Society Special Publication No. 58, p. 259-273.

Hingle, A.T., 1959, The use of logs in exploration problems: Society of Exploration Geophysicists, 29th Annual Meeting.

Hite, R.J., 1978, Possible genetic relationships between evaporites, phosphorites, and iron-rich sediments: The Mountain Geologist, v. 14, no. 3, p. 97-107.

Houseknecht, D.W., and Kacena, J.A., 1983, Tectonic and sedimentary evolution of the Arkoma foreland basin; in, Houseknecht, D.W., ed., Tectonic-sedimentary Evolution of the Arkoma Basin: Society of Economic Paleontologists and Mineralogists, Midcontinent Section, v. 1, p. 3-33.

Howe, W.B., 1982, Stratigraphy of the Pleasanton Group, Pennsylvanian System in Missouri, Missouri Department of Natural Resources, Division of Geology and Land Survey, Open-File Report Series 82-10-GI, 112 p.

Hsui, A.T., 1991, Subside -- A basin subsidence analysis program for IBM PC.

Hurst, A., 1990, Natural gamma-ray spectrometry in hydrocarbon-bearing sandstones from the Norwegian continental shelf: in, Hurst, A., Lovell, M.A., and Morton, A.C., eds., Geological Applications of Well Logs, Geological Society of London, Special Publication 48, p. 211-222.

Kaesler, R.L., and Newell, K.D., eds., Recent Interpretations of Late Paleozoic Cyclothems: Proceedings for the 3rd Annual Meeting and Field Conference, Midcontinent Section Society of Economic Paleontologists and Mineralogists, p. 1-22.

Keller, G.R., et al., 1983, The role of rifting in the tectonic development of the midcontinent USA: Tectonophysics, v. 94, p. 391-412.

Kidder, D.L., 1985, Petrology and origin of phosphate nodules from the midcontinent Pennsylvanian epicontinental sea: Journal of Sedimentary Petrology, v. 55, p. 809-816.

Klein, G. deV., 1990, Pennsylvanian time scales and cycle periods: Geology, v. 18, p. 455-457.

Klein, G. deV., and Willard, D.A., 1989, Origin of the Pennsylvanian coal-bearing cyclothems of North America: Geology, v. 17, p. 152- 155.

Kluth C.F., and Coney, P.J., 1981a, Plate tectonics of the ancestral Rocky Mountains: Geology, v. 49, p. 10-15.

Kluth, C.F., and Coney, P.J., 1981b, Reply to comments on plate tectonics of the ancestral Rocky Mountains: Geology, v. 9, p. 388-389.

Knapp, R.W., and Steeples, D.W., 1986, High-resolution common depth point seismic-reflection profiling: field acquisition parameter design: Geophysics, 51, 283-294.

Knapp, R.W., 1990, Vertical resolution of thick beds, thin beds, and thin-bed cyclothems: Geophysics, 55, 1183-1190.

Koedell, R., 1992, Waterflood case history, Pen Lansing Kansas City Unit: Advanced Waterflood Shortcourse Manual, KU Energy Research Center, Barton County Community College, p. 109-130.

Kumar, Naresh, and Slatt, R.M., 1984, Submarine-fan and slope facies of Tonkawa (Missourian-Virgilian) sandstone in deep Anadarko basin: American Association of Petroleum Geologists, Bulletin, v. 689, p. 1,839-1,856.

Leventhal, J.S., 1981, Pyrolysis gas chromatopography--mass spectrometry to characterize organic matter and its relationship to uranium content of Appalachian Devonian black shales: Geochemical et Cosmo Chemica Acta, v. 45, p. 883-889.

Lins, T.W., 1950, Origin and environment of the Tonganoxie Sandstone in northeastern Kansas: Kansas Geological Survey, Bulletin 86, pt. 5, p. 105-140.

Loutit, T.S., Hardenbol, J., Vail, P.R., and Baum, G.R., 1988, Condensed sections the key to age determinations and correlations of continental margin sequences; *in*, Wilgus et al., eds., Sea- level Changes An Integrated Approach: Society of Economic Paleontologists and Mineralogists, Special Publication No. 42, p. 183-213.

Lucia, F.J., and Conti, R.D., 1987, Rock fabric, permeability, and log relationships in an upward shoaling, vuggy carbonate sequence: Geological Circular 87-5, Bureau of Economic Geology, University of Texas, 22 p.

Maples, C.G., 1986, Enhanced paleoecological and paleoenvironmental interpretations result from analysis of early diagenetic concretions in Pennsylvanian shales: Palaios, v. 1, p. 512-516.

Mathews, C.S. and Russell, D.G., 1967, Drillstem test pressure analysis: pressure buildup and flow tests in wells, SPE Monograph Series, Chapter 9, p. 84-91.

Merrill, G.K., 1973, Pennsylvanian conodont paleoecology: Geological Society of America, Special Paper 141, p. 239-274.

Miller, R.D., Steeples, D.W., and Myers, P.B., 1990, Shallow seismic- reflection survey across the Meers fault, Oklahoma: Geological Society America Bulletin, v. 102, 18-25.

Miller, R.A., Anderson, N.L., Franseen, E.K., and Feldman, H.R., in review, Practical Vertical Resolution Limits of CDP Data Targeting Reflectors Less Than 125 m Deep Near Independence, Kansas: Geophysics.

Miller, R.D., Feldman, H.R., Franseen, E.K., Knapp, R., and Black, R.A., 1991, Practical Vertical Resolution Limits of CDP Seismic-Reflection Data Targeting Reflectors Less Than 125 m Deep Near Independence, Kansas: Kansas Geological Survey Open-File Report 91-36, 12 p.

Miller, R.D., Feldman, H.R., Franseen, E.K., Keiswetter, D.A., and Steeples, D.W., 1992, Practical Vertical Resolution Limits of CDP Seismic-Reflection Data Targeting Reflectors Less Than 250 m Deep Near Independence, Kansas (expanded abstract): 1992 Society of Exploration Geophysicists Annual International Meeting, Technical Program, p. 374-377.

Mitchum, R.M., 1977, Seismic stratigraphy and global changes of sea level, Part 1: Glossary of terms used in seismic stratigraphy, in, Payton, C.E., ed., Seismic Stratigraphy-Applications to Hydrocarbon Exploration: American Association of Petroleum Geologists, Memoir 26, p. 53-62.

Mitchum, R.M. and Van Wagoner, J.C., 1991, High-frequency sequences and their stacking patterns: sequence stratigraphic evidence for high-frequency eustatic cycles: Sedimentary Geology: v. 70, p. 131-160.

Moore, R.C., 1949, Divisions of the Pennsylvanian system in Kansas: Kansas Geological Survey, Bulletin 83, p. 1-203.

Moore, R.C., 1936, Stratigraphic classification of the Pennsylvanian rocks of Kansas: Kansas Geological Survey, Bulletin 22, p. 1- 256.

Morris, R.L., and Biggs, W.P., 1967, Using log-derived values of water saturation and porosity: Transactions, SPWLA, 8th Annual Logging Symposium, Paper X, 26 p.

Neumann, A.C., and Macintyre, I., 1985, Reef response to sea-level rise keep up, catch up or give up: Proceedings of the Fifth International Coral Reef Congress, Tahiti, v. 3, p. 105-110.

Nimmer, P. L., 1992, The petrology and depositional environments of the Upper Pennsylvanian (Missourian) Ladore Shale in southeastern Kansas and adjacent Oklahoma: unpublished Master's thesis, University of Iowa, 131 p.

Otte, Carel, 1954±, Determination of permeability from drill stem tests: Research Report, The Pure Oil Company.

Parrish, J.T., 1982, Upwelling and petroleum source beds, with reference to Paleozoic: American Association of Petroleum Geologists, Bulletin, v. 66, no. 6, p. 750-774.

Peppers, R.A., Howe, W.B., and Deason, K., 1993, Palynological zonation and physical stratigraphy of pre-Desmoinesian strata along a subsurface cross section in northwestern Missouri: Geological Society of America, Abstracts with Programs, North-Central Section, v. 25, p. 72.

Petroleum Information Corporation, 1992, Kansas crude production report (Western), December.

Phares, R.A., 1991, Characterization and Reservoir performance of the Lansing-Kansas City "I" and "J" zones (Upper Pennsylvanian) in the Pen Oil Field, Graham County, Kansas: M.S. Thesis, University of Kansas, 445 p.

Pickett, G.R., 1968, A review of current techniques for determination of water saturation from logs: Journal of Petroleum Technology, p. 1425-1433

Pickett, G.R., 1973, Pattern recognition as a means of formation evaluation: The Log Analyst, v. 14, no. 4, p. 3-11

Posamentier, H.W., Allen, G.P., and James, D.P., 1992, High-resolution sequence stratigraphy -- The East Coulee delta: Journal of Sedimentary Petrology, v. 62, p. 310-317.

Prather, B.E., 1981, Petrology and diagenesis of the D-Zone megacyclothem of the Lansing-Kansas City groups, Hitchcock County, Nebraska: M.S. thesis, University of New Orleans, 97 p.

Prather, B.E., 1981, Petrology and diagenesis of the D-Zone megacyclothem of the Lansing Kansas City groups, Hitchcock County, Nebraska: M.S. thesis, University of New Orleans, 97 p.

Quinlan, G.M., and Beaumont, C., 1984, Appalachian thrusting, lithospheric flexure, and the Paleozoic stratigraphy of the eastern interior of North America: Canadian Journal of Earth Sciences, v. 21, p. 973-996.

Rascoe, B., Jr., 1962, Regional stratigraphic analysis of Pennsylvanian and Permian rocks in western Mid-Continent, Colorado, Kansas, Oklahoma, Texas: American Association of Petroleum Geologists, Bulletin, v. 46, p. 1345-1363.

Rascoe, B., Jr., and Adler, F.J., 1983, Permo-Carboniferous hydrocarbon accumulations, midcontinent, U.S.A.: American Association of Petroleum Geologists, Bulletin, v. 67, p. 979-1,001.

Raymer, L.L., Hunt, E.R., and Gardner, 1980, An improved sonic transit time-to-porosity transform: Transactions, SPWLA, 21st Annual Logging Symposium, Paper P, 13 p.

Retallack, G.J., 1988, Field recognition of paleosols; *in*, Reinhardt, J., Sigleo, W.R., eds., Paleosols and Weathering through Geologic Time Principals and Applications: Geological Society of America, Special Paper 216, p. 1-20.

Ricker, N., 1953, Wavelet contraction, wavelet expansion, and the control of seismic resolution: Geophysics, 18, 769-792.

Ross, C.A., and Ross, J.R.P., 1987, Late Paleozoic sea levels and depositional sequences: Cushman Foundation for Foraminiferal Research, Special Publication 24, p. 137-168.

Rossignol Strick, M., 1982, Petroleum origin heavy rain, river plume, ocean stratification: American Association of Petroleum Geologists, Bulletin, v. 66, p. 625-626.

Scandal, D.E., 1980, Microstratigraphic sampling and the limits of paleontologic resolution: Paleobiology, v. 6, no. 4, p. 408- 426.

Schmoker, J.W., 1986, Oil generation in the Anadarko basin, Oklahoma and Texas: modeling using Lopatin's method: Oklahoma Geological Survey Special Publication 86-3, 40 p.

Scholle, P.A., Arthur, M.A., Ekdale, A.A., 1983, Pelagic environments; *in*, Scholle, P.A., Bebout, D.G., and Moore, C.H., Carbonate Depositional Environments: American Association of Petroleum Geologists, Memoir 33, p. 620-691.

Schutter, S.R., and Heckel, P.H., 1985, Missourian (early Late Pennsylvanian) climate in Midcontinent North America: International Journal of Coal Geology, v. 5, p. 111-140.

Sanders, D.T., 1959, Sandstones of the Douglas and Pedee groups in northeastern Kansas: Kansas Geological Survey, Bulletin 134, pt. 3, p. 125-159.

Schlager, W., 1981, The paradox of drowned reefs and carbonate platforms: Geological Society of America, Bulletin, v. 92, p. 197-211.

Schutter, S.R., and Heckel, P.H., 1985, Missourian (early Late Pennsylvanian) climate in Midcontinent North America: International Journal of Coal Geology, v. 5, p. 111-140.

Scotese, C.R., and Golonka, J., 1992, Paleogeographic Atlas, PALEOMAP Project, Dept. of Geol., Univ. of Texas, Arlington, TX

Serra, O., 1985, Sedimentary environments from wireline logs: Schlumberger, 211 p.

Sloss, L.L., 1963, Sequences in cratonic interior of North America: Geological Society of America, Bulletin, v. 74, p. 93-114.

Steeples, D.W., and Miller, R.D., 1990, Seismic-reflection methods applied to engineering, environmental, and ground-water problems: Society Exploration Geophysicists volumes on Geotechnical and Environmental Geophysics, Stan Ward, ed., Vol. 1: Review and Tutorial, 1-30.

Stermer, E. G., 1992, Depositional environments and diagenesis of sandstones in the Galesburg Shale, southeastern Kansas and northeastern Oklahoma: unpublished Master's thesis, University of Iowa, 170 p.

Swann, D.H., 1964, Late Mississippian rhythmic sediments of Mississippi Valley: American Association of Petroleum Geologists, Bulletin, v. 48, p. 637-658.

Thomas, W.A., 1985, The Appalachian-Ouachita connection--Paleozoic orogenic belt at the southern margin of North America: Annual Review of Earth Planetary Science, v. 13, p. 175-199.

Tixier, M.P., 1949, Evaluation of permeability from electric log resistivity gradients: Oil and Gas Journal, 5 p.

Vail, P.R., 1987, Part 1 Seismic stratigraphy interpretation procedure Key definitions of sequence stratigraphy; *in*, Bally, A.W., ed., Atlas of Seismic Stratigraphy: American Association of Petroleum Geologists, Studies in Geology 27, v. 1, p. 1-10.

Vail et al., 1977, Seismic stratigraphy and global changes in sea level, in Payton, C.E., ed., Seismic Stratigraphy -- Applications to Hydrocarbon Exploration: American Association of Petroleum Geologists, Memoir 26, p. 49-212.

Vail, P.R., Audemard, F., Bowman, S.A., Eisner, P.N., and Perez-Cruz, C., 1991, The stratigraphic signatures of tectonics, eustacy, and sedimentation -- an overview: in, Einsele, G., Rieken, W., Seilacher, A., eds., Cycles and Events in Stratigraphy, Springer-Verlag, New York, p. 617-659.

Van Wagoner, J.C., 1985, Reservoir facies distribution as controlled by sea-level change, abs.: Society of Economic Paleontologists and Mineralogists Mid-Year Meeting, Golden, Colorado, Aug. 11-14, p. 91-92.

Van Wagoner, J.C., Mitchum, R.M., Jr., Posamentier, H.W., and Vail, P.R., 1987, Part 2 Key definitions of sequence stratigraphy; *in*, Bally, A.W., ed., Atlas of Seismic Stratigraphy: American Association of Petroleum Geologists, Studies in Geology 27, v. 1, p. 11-14.

Van Wagoner, J.C., Mitchum, R.M., Campion, K.M., and Rahmanian, V..D., 1990, Siliciclastic sequence stratigraphy in well logs, cores, and outcrops: Concepts for high-resolution correlation of time and facies: American Association of Petroleum Geologists, Methods in Exploration Series, No. 7, 55 p.

Veevers, J.J., and Powell, C.McA., 1987, Late Paleozoic glacial episodes in Gondwanaland reflected in transgressive-regressive depositional sequences in Euramerica: Geological Society of America, Bulletin, v. 98, p. 475-487.

Walton, A.W., and Griffith, G., 1985, Deltaic deposition of the Tongonoxie or "Stalnaker" sandstone (Stranger Formation, Virgilian), TXO Robinson Core, Harper County, Kansas: Core Studies in Kansas, Kansas Geological Survey, Subsurface Geology Series 6, p. 145-160.

Wanless, H.R., 1964, Local and regional factors in Pennsylvanian cyclic sedimentation: Kansas Geological Survey, Bulletin 169, v. 2, p. 593-606.

Wanless, H.R., and Cannon, J.R., 1966, Late Paleozoic glaciation: Earth-Science Review, v. 1, p. 247-286.

Wanless, H.R., and Wright, C.R., 1978, Paleoenvironmental maps of Pennsylvanian rocks, Illinois Basin and northern Midcontinent region: Geological Society of America MC-23, 165 figures.

Wanless, H.R., 1979, Limestone response to stress pressure solution and dolomitization: Journal of Sedimentary Petrology, v. 49, p. 437-462.

Wanless, H.R., and Shepard, F.P., 1936, Sea level and climatic changes related to late Paleozoic cycles: Geological Society of America, Bulletin, v. 47, no. 8, p. 1,177-1,206.

Wanless, H.R., and Wright, C.R., 1978, Paleoenvironmental maps of Pennsylvanian rocks, Illinois Basin and northern Midcontinent region: Geological Society of America, MC-23.

Watney, W.L., 1980, Cyclic sedimentation of the Lansing and Kansas City Groups (Missourian) in northwestern Kansas and southwestern Nebraska--a guide for petroleum exploration: Kansas Geological Survey, Bulletin 220, 72 p.

Watney, W.L., 1984, Recognition of favorable reservoir trends in Upper Pennsylvanian cyclic carbonates in western Kansas; in, Hyne, N.J., ed., Limestones of the Midcontinent: Tulsa Geological Society, Special Publication No. 2, p. 201-246.

Watney, W.L., 1985, Resolving controls on epeiric sedimentation using trend-surface analysis: Mathematical Geology, v. 17, p. 427-454.

Watney, W.L., and Ebanks, W.J., Jr., 1978, Early subaerial exposure and freshwater diagenesis of the Upper Pennsylvanian cyclic sediments in northern Kansas and southern Nebraska (abs.): American Association of Petroleum Geologists, Bulletin, v. 62, p. 570-571.

Watney, W.L., and French, J., 1988, Characterization of carbonate reservoirs in the Lansing Kansas City groups (Upper Pennsylvanian) in Victory field, Haskell County, Kansas; in, Goolsby, S.M., and Longman, M.W., eds., Occurrence and Petrophysical Properties of Carbonate Reservoirs in the Rocky Mountain Region: 1988 Carbonate Symposium, Rocky Mountain Association of Geologists, p. 27-46.

Watney, W. L., French, J. A., and Franseen, E. K., 1989, Sequence-stratigraphic interpretations and modeling of cyclothems: Kansas Geological Survey and Kansas Geological Society guidebook for the 41st annual field trip, 211p.

Watney, W.L., Wong, J.C., and French, J.A., 1991, Computer simulation of Upper Pennsylvanian (Missourian) carbonate-dominated cycles in western Kansas: in, Franseen, E.K., Watney, W.L., Kendall, C.G.St.C., and Ross, W., eds.: Sedimentary Modeling: Computer Simulations and methods for improved parameter definition: Kansas Geological Survey, Bulletin 233, p. 415-430.

Watney, W.L., Stephens, B., and Wong, J.C., 1992, Cahoj field -- U.S.A. Anadarko Basin, Kansas: Foster, N.H., and Beaumont, E.A., comp., Structural Traps VI, Treatise of Petroleum Geology, Atlas of Oil and Gas Fields, American Association of Petroleum Geologists, Tulsa, p. 239-273.

Watney, W.L., Harff, J., Davis, J.C., Wong, J.C., and Bohling, G., 1993, Controls on petroleum accumulation in Upper Pennsylvanian cyclic shelf carbonates in western Kansas, USA, as interpreted from space modeling and multivariate techniques: Harff, J., and Merriam, D.F., eds., Proceedings of COGEODATA-IAMG Symposium on Computerized Basin Analysis for Prognosis of Energy and Mineral Resources, Pergamon Press, p. 215-237.

Widess, M.B., 1973, How thin is a thin bed? Geophysics, 38, 1176-1180.

Winchell, R.L., 1957, Relationship of the Lansing Group and Tonganoxie ("Stalnaker") Sandstone in south-central Kansas. Kansas Geological Survey Bulletin v. 127, p. 123-152.

Yarger, H.L., 1983, Regional interpretation of Kansas aeromagnetic data: Kansas Geological Survey, Geophysics Series 1, 35 p.

Yilmaz, O., 1987, Seismic data processing; S. M. Doherty, ed; in Series: Investigations in Geophysics, no. 2, Edwin B. Neitzel, series ed.: Society Exploration Geophysicists, Tulsa, OK, 526 p.

Youle, J.C., 1992, Sequence stratigraphy of the lower Middle Pennsylvanian and distribution of selected sandstones, eastern Hugoton embayment, southwestern Kansas: Unpublished Masters Thesis, University of Kansas, 205 p.

Zangerl, R., and Richardson, E.S., 1963, The paleoecologic history of two Pennsylvanian black shales: Chicago Natural History Museum, Fieldiana Geology Memoir, v. 4, 352 p.

APPENDIX A. CYCLOTHEM CONCEPT

Upper Pennsylvanian (Missourian) strata of the midcontinent United States are characterized by thin cyclical successions of carbonates and siliciclastic rocks. Cycles of sedimentation or cyclothems developed on shelf areas of the midcontinent generally have thin but widespread transgressive basal lithofacies overlain by thicker regressive strata (Figure A.1). These cyclothems are commonly separated from bounding strata by surfaces that are commonly associated with diagenetic and textural features indicative of subaerial weathering (Watney and Ebanks, 1978; Watney, 1980; Prather, 1981; Schutter and Heckel, 1985; Goebel et al., 1989). Variations in thickness, areal extent, and lithofacies in typical cyclothems suggest varying degrees of marine inundation of the craton (Heckel, 1980, 1984, 1986; Watney, 1984). Additional omission surfaces that define distinctive subcyclothemic sequences are commonly imbedded within many cyclothemic successions on the shelf.

Middle (Transgressive) Limestone

Using the nomenclature of Heckel (1977), the lowermost bed of the cyclothem is the middle or transgressive limestone (Figure A.1). The name middle limestone results from maintenance of R. C. Moore's (1936, 1949) nomenclatural scheme for Virgilian megacyclothems.

The middle limestone is a widespread transgressive deposit that is typically a few feet thick or less. These units were deposited in environments that ranged from the shoreline to below wavebase. Most preserved beds consist of subtidal marine wackestones. Middle limestone thickness ranges from relatively thick (50 ft [15 m]), to very thin, to absent. Normally, however, middle limestones are less than 3 ft (1 m) thick.

Core Shale

The core shale overlies the middle limestone in the typical Kansas cyclothem (Figure A.1). Core shales are typically thin, about 1-3 ft (0.3 0.9 m) and, like the middle limestones, are aerially extensive. Some core shales are black and organic rich (>4% carbon) and commonly contain phosphate nodules. The black core shales are readily recognizable in surface exposures and are frequently excellent subsurface markers due to their high natural gamma radioactivity. For example, the Hushpuckney and Stark shales in the lower Kansas City Group can be traced throughout the outcrop belt from Iowa and southward deep into siliciclastic cycles in the Arkoma basin south of Tulsa, OK. They also extend over 400 mi (640 km) to the west into western Kansas and eastern Colorado where they can be readily identified through their strong radioactive response on gamma-ray logs. Nevertheless, the black shales abruptly change to gray, fossiliferous shales along the upper shelf in northwestern Kansas and thin gray shales over the Central Kansas uplift, a long-term positive element.

Wanless (1964) used these black shales, which are also common to a number of Middle Pennsylvanian cyclothems, to physically correlate siliciclastic-dominated cyclothems in Illinois with equivalent, more

marine-dominated successions in the western midcontinent. Although biostratigraphy is now verifying some of these correlations, Wanless emphasized that a particular cyclothem could be distinguished through correlation of the core shale regardless of the variation in the remaining succession of sediments.

The origin of the black core shales has been vigorously debated. Heckel (1977) reemphasized the significance of the regional correlatability demonstrated by Wanless and stressed that this lateral continuity, coupled with the faunal composition and presence of nonskeletal phosphate, made the black shale the deepest-water deposit of the cyclothem. In the western craton, along the outcrop belt, the indigenous fauna is composed primarily of conodonts, ammonoids (from the southern exposures), and dissociated fish debris suggesting very slow sediment- accumulation rates. Minor elements such as uranium and various other metals are also abundant in the black shale along with phosphate. Heckel (1977, 1985, 1991) has proposed that the water column in which black shale accumulated contained a thermocline leading to quasi-estuarine circulation and upwelling, which accounts for the conspicuous phosphate. Water depths would necessarily be deep to accommodate formation of a long-term, stable thermocline.

Boardman et al. (1984) provide a paleoecologic model that relates faunal communities to dissolved oxygen, which is in turn related to a depth-defined bottom oxycline associated with vertical stratification resulting from the thermocline. Sufficient depths and stratification can result in anoxic bottom waters where sapropels typically accumulate. Accumulation rates would be slow and duration of black-shale deposition would be long in a deep, stratified water column.

In contrast, workers such as Zangerl and Richardson (1963), Merrill (1973), Maples (1986), Coveney and Martin (1983) and Coveney et al. (1991) have provided paleontologic and inorganic and organic geochemical evidence that supports that some black shales are of a shallow-water origin and rapidly deposited over a relatively short time.

The apparent controversies in interpreted depth, rate of sediment accumulation, and duration of black-shale deposition are addressed in Coveney et al. (1991). The correct interpretation of the magnitude of sea-level change associated with core shale is important with regard to process-response modeling of the cycle.

Upper (Regressive) Limestone

The upper or regressive limestone of Heckel (1977) is commonly the thickest bed within cyclothems on the carbonate platform (Figure A.1). This unit ranges from less than 10 ft (3 m) to more than 100 ft (30 m) in thickness. The upper limestone contains the major petroleum reservoirs of the Lansing and Kansas City groups.

Reservoirs occur in skeletal grainstone and oolitic facies, phylloid algal buildups, and structural and diagenetic traps created by fracturing and dissolution.

Lithofacies and early-diagenetic features of the upper limestones indicate a general shallowing-upward succession. Although the general Kansas cyclothem model of Heckel (1977) indicates a continuous gradual shallowing upward succession, observed facies successions and their correlation suggest fluctuations in water depth within an overall shoaling trend (Heckel, 1986). The relative importance of local (autogenic) controls, e.g., progradation and aggradation and subsequent local shallowing versus regional (allogenic) controls, such as eustatic sea level change, on the deposition of these generally complex shallowing- upward successions is another topic of intense interest and discussion. In general, individual upper limestones can be recognized and traced across widespread areas of the carbonate shelf, including into western Kansas, some 400 mi (640 km) west of the surface exposures.

Some upper limestones exhibit more obvious evidence for minor cycles than others, e.g., the Winterset Limestone, which is punctuated by thin, widespread shale beds, versus the more massively bedded Bethany Falls Limestone. Some of the internal beds and bounding surfaces within the upper limestones are interpreted to result from short-term events (e.g., storm deposits) or represent local aggradation and progradation processes with limited lateral extent. Other minor stratal units within the upper limestone are correlative over large distances and suggest an allogenic cause, e.g., shale- bounded packages within the Winterset Limestone extending over 50 mi (80 km) along the outcrop. This latter process appears to be important and common.

Outside Shale

The outside shale, the uppermost unit of the Kansas-type cyclothem, exhibits considerable variability among different cyclothems (Figure A.1). These stratal elements are locally thin or missing in southwestern Kansas due to an apparent lack of siliciclastic influx. Where siliciclastics were available, thicknesses of other outside shale units may be as much as 300 ft (91 m) in eastern Kansas. Thicker packages of shale, sandstone, and siltstone represent deltaic siliciclastic influx in shallow- marine conditions. These deltaic deposits contain invertebrate-rich horizons, thin limestones, channel sandstone, and paleosols. The platform deltaic deposits form broad aprons of mainly shale extending for tens of miles. Accordingly, outside shales of the lower Kansas City Group are typically thin, blocky mudstones with paleosol features, also common in the thin outside shales of central and southwestern Kansas. In southeastern Kansas outside shales become very thick and complex in character, preserving events that do not occur to the north suggesting notable changes in sediment accommodation.

Deltaic progradation and accumulation of thick outside shales occur when sufficient accommodation space is available. Deltaic influx on the northern shelf occurred late in a cycle while the shelf was still submerged. In some cases, siliciclastic detritus in the upper Kansas City and Lansing groups reached the east-central Kansas shelf prior to extensive subaerial exposure and paleosol development on the upper limestones. Relative sea level fell in late stages of deltaic sedimentation leading to local erosion and channeling of the deltaic wedges, occasionally downcutting into the underlying limestones. Concurrent with the channeling events, but more widespread, is the development of paleosols that are only now being recognized as significant bounding surfaces separating temporally distinct stratigraphic sequences. Evidence for subaerial exposure is much more apparent in outside shales without siliciclastic influx, e.g., the blocky mudstones, or on the surfaces of the upper limestone.

Widespread subaerial exposure is clearly evident in most outside shales and on the tops of many of the upper limestones (Watney and Ebanks, 1978; Schutter and Heckel, 1985; Goebel et al., 1989). In many cases the outside shale (at least the lower portion) is a paleosol capping the carbonate. Moreover, these paleosols can be traced across the northern carbonate shelf from Iowa to southeastern Kansas; they also are present westward in cores through the subsurface of western Kansas and southwestern Nebraska. Spatial trends of subaerial exposure have also been recognized on the shelf (Watney, 1980). Areas interpreted to be higher shelf locations generally exhibit evidence of more intense subaerial weathering and commonly early meteoric diagenesis (Watney and Ebanks, 1978; Watney, 1980; Heckel, 1983).

Current investigations in southern Kansas indicate that subaerial surfaces can be traced to conformable surfaces on the lower shelf and basin that show no evidence of exposure. When paleosols are present they provide a critical, temporal break in the sedimentary record analogous to a timing light. The paleosols are useful and necessary for temporal reconstruction to assess the impact of processes causing cyclicity. Problems remain in the distinction and correlation of these surfaces regionally, particularly in thick outside shale sections where paleosols are not easily recognized.

Causal Mechanisms for Cyclothem Development

Contrasting and widespread facies changes in cyclical sequences indicate a significant contribution from allogenic controls (Heckel, 1977; Watney, 1984, 1985a; Boardman and Malinky, 1985; Heckel, 1986). Glacial-eustatic control has been invoked most often by those who subscribe to allogenic causes for stratal cyclicity (Wanless and Shepherd, 1936; Wanless and Cannon, 1966; Crowell and Frakes, 1975; Heckel, 1977; Crowell, 1978; Denton and Hughes, 1983; Heckel, 1986; Crowley et al., 1987; Veevers and Powell, 1987). The analogue used in these arguments is the sea- level change associated with advance and retreat of Pleistocene

continental glaciers. These Pleistocene glacial advances and retreats produced high-frequency sea-level changes with magnitudes on the order of 330-500 ft (100-150 m), periodicity around 100,000 years, and rates of sea-level change around 10 m (33 ft)/thousand years (Ka) (Donovan and Jones, 1979).

Autogenic causes, due to internal feedback mechanisms that operated within the depositional system, are also argued to have produced these same cyclothemic strata, e.g., Duff and Walton (1962), Donaldson (1974), Ferm (1975), Brown (1972), and Galloway and Brown (1973). All of these studies dealt with strata dominated by deltaic sedimentation and heavily influenced by local (autogenic) sedimentary processes, thereby limiting the potential for correlation between individual delta systems. However, even in these areas of significant autogenic control, recent studies, e.g. by Brezinski, (1984), and Busch and Brezinski (1984) in the Upper Pennsylvanian strata of the Appalachians; West and Busch (1985), and Busch and West (1987) in the Lower Permian of Kansas, find distinct vertical variations in biotic diversity within relatively homogeneous lithologies, which may indicate temporally distinct sedimentary rocks that can be correlated over widespread areas. Boardman and Malinky (1985) recognize regional, interdeltaic genetic units defined by thin, darker marine shales on the eastern shelf of the Midland basin that are analogous to the core shales of the northern midcontinent. Boardman and Heckel (1989) have now correlated these Midland basin shales and their associated sedimentary packages with their equivalents in the northern midcontinent, strengthening the argument for a eustatic control that affected areas on an interbasinal scale. Brown (1989) has also invoked a eustatic component for the generation of Pennsylvanian and Lower Permian strata along the eastern shelf of the Midland basin.

The role of climate control on generation of cyclothems has been considered in the past, but without a recent analog model. Swann (1964) proposed a subtle climate-control hypothesis invoking changing precipitation to explain more complex carbonate-terrigenous clastic cyclothems of the Chesterian in the Illinois basin. Cecil et al. (1985) and Cecil (1990) proposed that repetitions in siliciclastic and chemical rocks is related to paleoclimate cycles probably operating in combination with other processes such as eustacy and tectonics. The basis of this conclusion is founded on studies of Recent environments thought to be analogous to conditions under which the Pennsylvanian cyclothems were deposited.

APPENDIX B.

RECOGNITION OF SEQUENCE-STRATIGRAPHIC COMPONENTS IN UPPER PENNSYLVANIAN CYCLOTHEMS

Introduction

The cyclothem model is limited in the ability to encompass the wide variation in these cycles of sedimentation. Examples of these complexities are expressed in the analog sites along the lower shelf where sediment accommodation space varies markedly resulting in extreme changes in facies and stratigraphy. Also for more accurate and precise reconstructions of the paleogeographic setting and as we step toward quantification, the temporal distinction that is sought through correlation of surfaces using sequence stratigraphic methods is essential. The time distinction is obtained through utilization of the regional unconformities that punctuate this stratigraphic succession.

Nevertheless, subsurface correlations of thin depositional sequences are hampered by limited means other than cores and possibly very high resolution seismic profiling to "see" the sequence boundaries (unconformities). Moreover, opportunities to have a study area that encompasses the full range of attributes of depositional sequence such as stratal geometries and systems tracts are usually not available. The surface exposures and near-surface has provided the constraints to comfortably apply sequence stratigraphic methods to these rocks -- 1) establish correlations of the lithofacies and genetic units to wireline logs; 2) provide stratal geometries along sharp change in depositional topography to permit the reconstruction of relative sea-level history and to develop a depositional model.

The black, radioactive shales, in addition to serving as excellent stratigraphic markers, are thought to represent significant time and wide demarkation in depositional environment. These shales are usually continuous elements and provide the means to establish initial correlations from which more detail can be sought.

Formal Definitions

The sedimentary cycles are ordered according to the range of time that each occurs. The ranges of time for each cycle that workers use varies. Those used in this report are from Goldhammer et al. (1993) (Table B.1).

Table B.1: CYCLE ORDERS (modified after Goldhammer et al., 1993)

Cycle Order	Duration (Ma)	Amplitude (meters)	Rise/Fall rates (m/ka)	Sequence terminology (Goldhammer et al., 1993)
1st order	>100		<0.01	
2nd order	10-100	50-100	0.01-0.03	Supersequence
3rd order	1-10	50-100	0.01-0.1	Sequence
4th order	0.1-1	1-150	0.4-5	Sequence, cycle, cyclothem
5th order	0.01-0.1	1-150	0.6-7	Parasequence, cycle

The depositional sequence is the fundamental unit of sequence stratigraphy defined as a genetically related succession of strata bounded by unconformity surfaces and their correlative conformities (Mitchum, 1977). The sequence boundaries are identified by an abrupt basinward shift in facies or change in parasequence stacking patterns (Van Wagoner, et al., 1990). Van Wagoner (1985) defines parasequence as "a relatively conformable succession of genetically related beds bounded by marine-flooding surfaces and their correlative surfaces". Parasequences stack into sets that delineate systems tracts within a depositional sequence. Sequence sets are groups of sequences that stack into similar progradational, aggradational, or retrogradational motifs and are analogous to systems tracts within a single depositional sequence (Mitchum and Van Wagoner, 1991). A composite sequence consists of lowstand, transgressive, and highstand sequence sets (Mitchum and Van Wagoner, 1991).

Although most sequence stratigraphers agree that the depositional sequence is the "fundamental unit of sequence stratigraphy" (Vail, et al., 1991), they disagree on its scaler properties. Vail et al. (1991) refer to the depositional sequence as a third-order cycle that ranges from 0.5 to 3 Ma in duration; however Mitchum and Van Wagoner (1991) and others (e.g., Posamentier et al., 1992) believe the sequence is scale independent.

For the purposes of this report a non-scaler sequence stratigraphic terminology is used. Despite estimated durations of between 0.25 and 0.5 Ma for the Pennsylvanian sequences, they possess all of the components of third-order depositional sequences. Furthermore, like cyclothems, these sequences serve as the fundamental stratigraphic unit in the Pennsylvanian. They are regionally correlative and capable of supplying temporally distinct stratigraphic frameworks for paleogeographic reconstructions and can be used to establish detailed facies relationships.

Sequence Stratigraphic Components (Genetic Units) of Pennsylvanian Cyclothems

Flooding Unit

The flooding unit is either absent or thin (zero to several 10 s of feet thick) with a sharp basal contact (Figure B.1). It is readily identified through vertical-sequence analysis in outcrop or core. The flooding unit commonly is succeeded by deeper marine strata. Lithologies include calcareous sandstones and siltstones with nearshore affinities (northwestern Kansas) and thin carbonate units that reflect deepening conditions, e.g., a generally shoal-water strata occur at the base and are overlain commonly by normal marine strata at the top that were likely deposited below normal and storm wave base. Clam borings, pyritization of skeletal debris, and preservation of small to moderate amounts of organic debris are common components of the carbonate-flooding units. The lower contact usually separates distinctly different depositional facies resulting in *facies dislocation*, e.g., a paleosol beneath a marine limestone. Carbonate buildups, although uncommon in this unit, are developed locally, e.g., Canville Limestone of Dennis cycle.

Widespread coals capped by invertebrate skeletal lag or limestone locally are characteristic of some flooding units. Marine sandstones and siltstones that compose the flooding unit also include reworking of underlying deposits or renewed detrital deposition. Whether erosion or deposition occurs during deepening was likely dependent on steepness of depositional slopes (energy level), climate, marine-circulation patterns, sediment supply, and rate of deepening. Estuarine deposits can be significant when siliciclastic sedimentation rates vs. rates of rise in sea level are high during rising sea level.

Results from studies of Holocene coastal sedimentation provide important analogues to the Pennsylvanian flooding units. The Holocene work suggests that at a certain threshold rate of deepening, effective carbonate sedimentation can decrease significantly (Neumann and Macintyre, 1985). Sedimentation does not keep up with rapidly increasing water depth, probably due, in part, to loss of opportunities for sediment progradation and aggradation, e.g., inundation of delta and estuary formation or rates of deepening exceeding effective carbonate-accumulation rate (Heckel, 1984).

Hallock and Schlager (1986), in their studies of Holocene carbonate settings, conclude that reefs and most carbonate- sediment-producing organisms flourish in nutrient-deficient systems. However, these organisms undergo significant reduction in sediment production during increasing nutrient supply, which often occurs during submergence of a carbonate shelf. Flooding is thought to produce a biotic crisis due to nutrient excess. While increased nitrate and phosphate would stimulate growth of some organisms, other more deleterious effects

apparently lead to net decreased sediment production, e.g., reduced water transparency limiting the depth range for some corals and calcareous algae, and consequently reduced sediment production.

Hallock and Schlager (1986) have identified criteria for recognizing changes in nutrient excess conditions in the sedimentary record: nondeposition (hiatal) surfaces, bioerosion such as clam borings, and reduced redox potential encouraging preservation of organic matter. The carbonate surface is commonly covered by fine-grained siliciclastics if conditions of nutrient excess persist. The net result is reduced sedimentation during flooding, contributing what is referred to as lag time. This is precisely what is observed in the Pennsylvanian strata.

The sensitivity of a carbonate platform to flooding is a function of local conditions. For example, the euphotic zone, below which reefs composed of zooxathellate corals will not survive, ranges from 170 m (561 ft) in the Gulf of Aqaba to 18 m (59 ft) around Barbados (Hallock and Schlager, 1986; fig. 17). The shallower the euphotic zone, the more susceptible the area is to diminished $CaCO_3$ accumulation during flooding events. Thus, in spite of the fact that short-term reef growth has been estimated at rates in excess of 10 m (33 ft)/Ka, environmental conditions must remain nearly constant while accommodation space must be increased in order for these rates to be maintained.

Neumann and Macintyre (1985) and Adey et al. (1977) further describe the widespread rapid drowning associated with the early Holocene eustatic rise due to glacial melting. Neumann and Macintyre (1985) suggest that the reefs were poisoned by their lagoons. Some reefs essentially give up during the rapid rise (~8m [26 ft]/ka) in sea level. Stratigraphic evidence noted by these workers for drowning includes bored hardgrounds, ferromanganese-oxide accumulations, phosphates, and glauconite separating neritic from overlying deeper water deposits. The nutrient influx and increased organic productivity led to reduced water clarity. This could effectively lead to a shallowing of the euphotic zone. Thus the euphotic zone, i.e. zone of carbonate production, could be dependent on the rate of sea level rise. Oscillatory sea level fluctuations in even shallow water could lead to retardation or termination of carbonate production.

The Pennsylvanian midcontinent seaway was a tropical inland sea with limited connection to the open ocean (Heckel, 1977). Conditions probably favored high nutrient supply during marine flooding due to freshwater runoff contributing terrestrial organic matter and inorganic compounds to the marine realm. The tendency for water stratification due to an equitable climate promoting a stable water column supports conditions of lowered oxygen and preservation of organic matter. For these reasons, the effective depth of the euphotic zone may have been shallow in the interior Pennsylvanian seaway and perhaps quite variable, especially in the areas of

detrital influx. Flooding units may be linked to the overlying condensed sections through the nutrient excess potentially created by the flooding process.

Condensed Section

Core shales in the midcontinent are similar to other condensed sections, often shales, that have been referred to as the starved-basin facies (Figure B.1) (Scholle et al., 1983; fig. 16). Organic-rich units are deposited under dysoxic to anoxic conditions. Black or gray shales can also result from rapid episodic changes in oxygen level due to organic productivity or water circulation. As suggested above, the condensed section may simply be represented by a diastemic surface such as a hardground. As in the case of the upper Virgilian strata, the black shale is lacking. Rather, the condensation in sedimentation in the upper Virgilian may be represented by a surface in a limestone or marine shale.

Dysoxic conditions result in accumulation of gray, dark-gray, or olive-green shales or siltstones. Anoxic conditions may result in the accumulation of black shales. Whereas the black shales are laminated, the gray shales are variably burrowed. These gray shales, albeit thin (<1 ft [0.3 m]), typically precede and succeed the black shale, if the latter is even developed, or are found laterally equivalent to a black shale.

Unlaminated gray or green fossiliferous siltstones and claystones are commonly deposited in landward positions or on bathymetrically higher elevations in positions equivalent to extensive black shales (Watney, 1984). The condensed sections are relatively thin, usually under 2 to 3 ft (0.6-0.9 m) in thickness. However, exceptions occur as the condensed section grades laterally to localities where suspension sedimentation was significant, such as in the Ouachita siliciclastic depositional sequences. Contacts with adjoining strata are usually abrupt, but gradations do occur with shale and carbonate lithologies. Most of the black shales on the upper carbonate-dominated shelf are regionally widespread.

Biota in the Upper Pennsylvanian black shales in the western midcontinent is limited to nektonic and nektobenthic organisms, abundant pelagic organisms, and rare benthic forms. Large amounts of conodonts and fish debris are common, but these shales generally lack benthic marine invertebrates. The microstratigraphy is complex as indicated by interlayered bioturbated zones, thin carbonate layers, and marked variations in minor elemental composition. Uranium concentrations in black shales ranges from <20 ppm to more than 250 ppm, accounting for most of the high natural gamma radiation emitted by black shales.

Nonskeletal phosphate (apatite) is common as assorted nodules and laminae in black shales. Abundant and diverse radiolarians, nautiloids, and fish debris have been found in the nodules in black shales in eastern Kansas

(Kidder, 1985). The source of the phosphate could be planktonic organisms, fecal material, or perhaps solution and suspension from river water.

Greatly reduced sedimentation rates for the condensed section are suggested by 1) commonly abundant phosphate, 2) high concentrations of normally sparse pelagic fossils, 3) horizontal orientation of clay minerals composing the shale (suggesting dilute suspension sedimentation; James, 1970), and 4) elevated concentrations of minor elements such as uranium.

The widespread nature of most of the black shales on the shelf and in the basin suggests that the shales represent uniform conditions developed synchronously such as in deep water, or in a time-transgressive manner during rapidly deepening conditions. While lithofacies such as sandstone and carbonates thin in a basinward direction, black shales persist across the shelf and into the basin. Black shales observed in the lower Missourian converge in the basin in areas of sediment starvation to form stacked condensed sections separated by very thin intervening dark, skeletal wackestones and gray shales and siltstones. A number of process models have been proposed to explain black-shale deposition, namely upwelling and quasi-estuarine circulation (Heckel, 1977), upwelling through Ekman transport (Parrish, 1982), halocline (Demaison and Moore's Black Sea model with freshwater influx, 1980, or basinal brine upwelling, Hite, 1978), and thermocline (Rossignol Strick, 1982; Heckel, 1985).

The dysoxic facies contain limited, but distinctive faunas that have been interpreted as an assemblage related to depth (Boardman et al., 1984). Biotic assemblages reflecting similar dysoxic conditions are commonly found in other Paleozoic shales. Perhaps these biotic zones may be affected by unfavorable water chemistry, or high organic-matter productivity, in addition to simple oxygen depletion due to water depth and isolation of the bottom water column, i.e. not necessarily depth controlled.

As previously stated, stratigraphic, sedimentologic, paleontologic, and geochemical evidence from a variety of settings supports *both* shallow- and deep-water origins of black shales. Accumulation of black shales is dependent on developing a prevailing bottom anoxia that is tied to the <u>rate</u> of the production of organic matter and preservation potential of organic matter versus amount of oxygenation of the water column or sediment. The higher the influx of organic matter, the more oxygen that will be consumed. Bottom stagnation may not be a prerequisite if abundant organic matter is available due to high organic productivity. Whereas favorable conditions for black- shale accumulation occurred frequently during the Pennsylvanian across the greater United States midcontinent, equivalent cyclothemic units on the Russian platform, although containing open-marine

carbonates, do not contain black shales. If water depths between the two shelves were similar, then water depth may not have been the only critical factor in generation of black shales.

Freshwater runoff flowing over the surface of marine waters that were flooding the shelf could provide limited, temporary stratification of the water column, particularly under tropical conditions. Input of large amounts of terrestrial organic matter and high nutrient supply could also be provided by runoff to generate abundant marine-organic matter. Woody-plant material has been found in both the Hushpuckney and Stark shales in eastern Kansas and Oklahoma, attesting to the input of terrestrial organic matter. Moreover, mixed terrestrial and marine macerals of organic matter occur in these shales (Hatch and Leventhal, 1985). Tropical conditions favoring thermal stratification would assist in developing a pycnocline. The epeiric sea in the midcontinent was only open to the ocean through a connection in the Dalhart basin in west Texas, thus limiting open exchange with normal oceanic waters. Basinal brines may also have formed in the Anadarko basin, possibly fed episodically by the influx of brines during lowstand shelf bypassing or during early flooding of the shelves that contained evaporites on the western craton, e.g., Minnelusa Formation of Wyoming and adjacent areas. A combination of different factors between locations likely may have facilitated preservation of organic matter during rising sea level. Rising water levels could have led to conditions favoring nutrient excess such as organic productivity and water stratification. Furthermore, the thickness of the bottom anoxic layer may have been variable, thus accounting for the loss of some black shales over topographic highs.

Detailed cm-scale analysis of a host of organic and metal concentrations in a core from the Stark Shale in the Dennis cycle in east central Kansas reveals considerably more variation than previously thought (Hatch and Leventhal, 1992). Redox conditions change rapidly and frequently vertically through the overall black shale including thin calcareous horizons containing carbonate skeletal remains. Bottom water conditions apparently fluctuated between mainly euxinic to intermittent oxidizing and dysoxic conditions. The stratal chemical signature resembles log profiles from the adjoining carbonates except for the greatly diminished thicknesses represented. Prior to being covered by the late regressive highstand deposit, the condensed section may incorporate changes in water chemistry in association with sea level fluctuation.

Three cores of the Hushpuckney Shale of the Swope cycle obtained along a shelf-to-basin transect in the southeastern Kansas analog area were similarly analyzed for this geochemical information. Preliminary results indicate that samples from the basinal Hushpuckney Shale show a simple profile building from dysoxic to euxinic back to dysoxic (Hatch, personal comm., 1993). In contrast, the shelf-based core has two euxinic intervals separated by a dysoxic zone. The bottom water during accumulation of the Hushpuckney Shale appears to have been interrupted by the oxidizing event because of the higher elevation of the shelf at this location. Landward and higher on the shelf the zones of oxidized shale may grade into carbonate units. The

Dennis cycle is punctuated by marine shales that have evidence that they downlap onto the Stark Shale in a basinward position.

The information in this shale may provide invaluable information about the nature of the cycles as more detailed microstratigraphic geochemical work is done. The condensed section may serve as an important seal for the reservoir as well as a likely source for some of the oil and gas.

Late Highstand Stratal Unit

This unit usually represents the thicker portion of the Pennsylvanian sedimentary sequences (Figure B.1). Lithofacies range from fluvial-deltaic sandstone, marine sandstones and shales, to shallow-water carbonates. Thicknesses of the late highstand carbonate-dominated units vary from a few feet to 10's of feet thick.

The generally shallowing-upward nature of the "regressive carbonate" is interrupted by minor cyclicity (Figure B.1). These minor cycles in themselves are usually shallowing-upwards units, either bounded by flooding surfaces or occasionally by subaerial exposure surfaces. The overall falling sea level is interrupted by both abrupt, minor rises in sea level and also abrupt falls in sea level. Rapid shallowing culminating in subaerial exposure on subtidal deposits is common. The regression appears to be forced by fall in sea level.

The late highstand unit is predominately carbonate in late Desmoinesian and Missourian strata in Kansas. This reference to late highstand reflects a <u>time later than the highstand deposition inferred for the condensed section</u> immediately underlying the carbonate. A <u>fall in sea level</u> is needed following the condensed section to reestablish photic conditions for carbonate sedimentation. The intervening time results in a <u>stratal hiatus</u> between the condensed section and the carbonate over most of the shelf. The facies successions at higher shelf locations suggest that the change from condensed section to carbonate was sooner and was more gradational in these areas, inferring a shorter time gap, if any, between to the two episodes of sedimentation. In general, carbonate sedimentation appears to be very episodic, occurring during times that the photic zone occupied various portions of the shelf.

Episodic nature is also suggested by the presence of major cycles that led to: 1) dislocation and isolation of reservoir facies in a field, 2) shifts in reservoir facies to other stillstand sites on the shelf. Facies analysis along on these reservoirs without resolution of the detailed stratigraphy will not be complete.

Depositional facies reflect a range of depositional environments that varies from subaerial, intertidal, to below storm-wave base. Basinal carbonates are argillaceous and commonly organic-rich; marine macrofossils and trace fossils are common to abundant.

Common facies of the late highstand deposit include:

1) clear-water marine carbonate

   i) low to moderate energy commonly phylloid algal wackestone or packstone ('mound rock') or crinoid- bryozoan-brachiopod wackestone; sedimentation rates are judged to be moderate to high, the latter during mound development

   ii) high energy bioclastic and oolitic grainstones; sedimentation rates interpreted as high as long as favorable conditions existed and accommodation space for accumulation was available.

2) Turbid-water and deeper water carbonate deposits

   i) argillaceous bioclastic mudstone and wackestones with dispersed silt and clay, macerals of organic matter, and wispy shale seams and microstylolites; sedimentation rates are judged to be low because of marginal conditions for carbonate accumulation; facies typically have undergone significant, apparently long- term compaction; porosity is typically low;

3) restricted, shallow-marine and clear-water carbonate sediment

   i) laminated, fenestral, mudcracked, stromatolitic lime mudstone and dolomicrite; sparsely fossiliferous, trace fossils common; sedimentation rates are interpreted as moderate to high as long as accommodation space was available.

Lowstand Siliciclastics

Late in the cycle when the shelf became subaerially exposed, siliciclastic sedimentation occurred occasionally along the lower shelf. Evidence suggests that siliciclastics bypassed the shelf and prograded down off the Ouachita tectonic front.

1) Northern carbonate-dominated shelf paleosols and rare valleys as evidence of subaerial exposure and incision of the shelf.
2) southeastern shelf (early Missourian) --fluvial and deltaic sandstones and shales with limited marine section; sedimentation rates are moderate to very high; significant topographic relief and clastic wedge development;

Paleosols and Other Evidence for Subaerial Exposure

Subaerial exposure and paleosol development are important in defining sequence boundaries (Figure B.1). Significant subaerial exposure, weathering, and paleosol development occurred over extensive areas of the shelf following deposition of the highstand unit or capping minor cycles within a sequence. Paleosols form a veneer

on top of depositional sequences on the shelf areas of most Missourian strata in western Kansas (Watney and Ebanks, 1978; Watney, 1984) and extend across much of eastern Kansas (Schutter and Heckel, 1985; Goebel et al., 1989). Early meteoric diagenesis consisting of both dissolution and cementation events is pervasive on the shelf, e.g., extensive dissolution of oolites produced broad expanses of oomoldic porosity in western Kansas (Watney, 1984). An improved understanding of the patterns and causes of cementation and dissolution events during diagenesis, such as the work of Goldstein et al. (1989, 1991), is an important component in developing a predictive model for porosity development associated with subaerial exposure.

In general, correlating subaerial-exposure surfaces is difficult. The lack of clear, definitive evidence of subaerial exposure may be due to spatial variations of processes involved in even a single weathering event, resulting in subtle, nondiagnostic products, or paleosols of complex origin containing mixed preservation features. Proximity of paleosols to the flooding unit of the overlying sequence leads to a high potential for their erosional truncation. However, evidence is sufficient to conclude that paleosols characteristically form extensive bounding (hiatal) surfaces over most sequences on the shelf. Recent coring shows that these hiatal surfaces merge with conformable surfaces in the basin or on lower parts of the shelves that were apparently still submerged during lowered sea levels. Heckel (1986) has identified such a relationship associated with the sequence boundary between the Wyandotte and Iola limestones in a mid-shelf and lower-shelf setting.

Subaerial exposure surfaces clearly separate younger sequences from older sequences, thus providing excellent temporal definition of the sequences.

Detrital-rich paleosols are composed of blocky mudstones. Weathering features are common in the upper portions of the underlying parent material on which these blocky mudstones are developed, e.g., dissolution channels and cavities in limestone. Missourian-age paleosols are both carbonate-rich, indicating carbonate accumulation due to a net moisture deficiency in the local soil environment, and more moist conditions with no conspicuous carbonate. Interpreting soils is complex in features to be recognized in the field and laboratory, in classification and nomenclature, and in assessing the relative contribution of potential agents responsible for the formation of the soil. Climate, local relief, vegetation, parent material, time, and multiple events all can affect the type of soil developed.

Many of the Pennsylvanian paleosols appear to have been affected by multiple stages of formation. Preservation probably favors only the more resistant components and those developed locally in the soil profile if erosion is significant. Also, subaerial exposure features are preferentially preserved in topographically low areas and may not be representative of the paleosol as a whole.

Diagnostic features commonly present in paleosols include

1) rhizoliths (rootlets);
2) ped surfaces in the blocky mudstones
3) color mottling or isolated horizons of color and textural variation in the mudstone due to differential oxidation and hydrolization of iron, and redistribution and formation of clay minerals (illuviation);
4) micritic carbonate nodules or casement around rhizoliths, or carbonate crusts (calcrete).

Paleosols rich in calcium carbonate are referred to as *caliche*, defined as a strataform to irregular deposit, formed primarily of calcium carbonate, with concretional, pisolitic, banded or massive structure that is formed in the soil or subsoil of arid and semiarid regions (Gonzalez Bonorino and Terruggi, 1952). Missourian sequences in northwestern Kansas are commonly capped by chalky caliches found in red paleosols or as laminated calcrete at the top or near the top and filling in the carbonates (Watney, 1980, 1984). Their abundance in western Kansas is indicative of drier conditions than in southeastern Kansas which fits with paleoclimatic reconstructions (Heckel, 1980). While varying from area to area, these paleosols appear to be shelfwide developments.

In contrast to caliche, the following are some of the identifying criteria for paleosols developed under moist, subaerial conditions, provided sufficient time has elapsed for soils to develop:

1) terra rossa (red residuum dissolved from carbonate dissolution);
2) paleokarst and solution piping, commonly plugged with clay of paleosol or wall-rock debris;
3) well-developed clayey soil profile exhibiting illuviation.

Some paleosols exhibit relationships of both wet and dry attributes. Dubois (1985) describes karsting as prevalent in topographically lower areas at the top of the Dennis cycle in southwestern Nebraska. Solution piping extends through the carbonate (>20 ft, 6 m). Proximity to the water table and greater residence time of water in the low areas are likely reasons for karsting. Topographically higher locations contain caliche paleosols indicative of locally drier conditions (Dubois, 1985).

DRUM LIMESTONE RESERVOIR ANALOG STUDY

APPENDIX C

OUTCROP DESCRIPTIONS

Key to lithologic symbols
(unless otherwise noted)

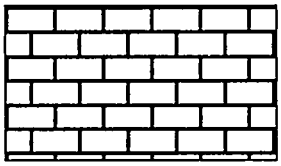

Skeletal oolitic grainstone

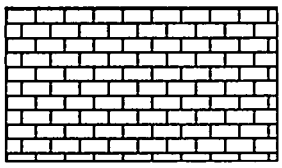

Skeletal wackestone, packstone and boundstone

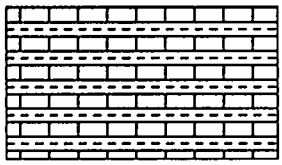

Interbedded carbonate mudstone and shale

Skeletal intraclastic grainstone to packstone

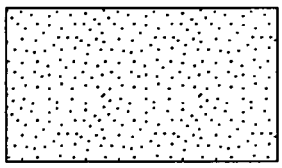

Sandstone

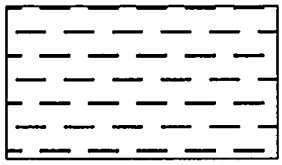

Shale

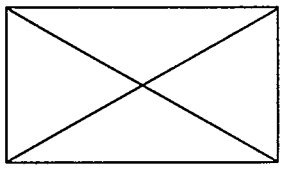

Covered

CHE-1

s edge of sw sw s 9, T. 32 S, R. 17 E
Cherryvale Quadrangle
Montgomery County

feet 5

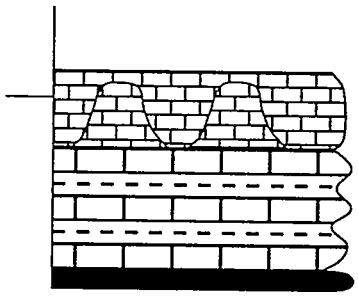

2' Stromatolitic limestone, fossiliferous wackestone to packstone between stromatolites.

3' Interbedded carbonate mudstone and shale.

2" Skeletal intraclastic grainstone to packstone.

LIB-2

sw sw sw s 25, T. 32 S, R. 16 E
Liberty Quadrangle
Montgomery County

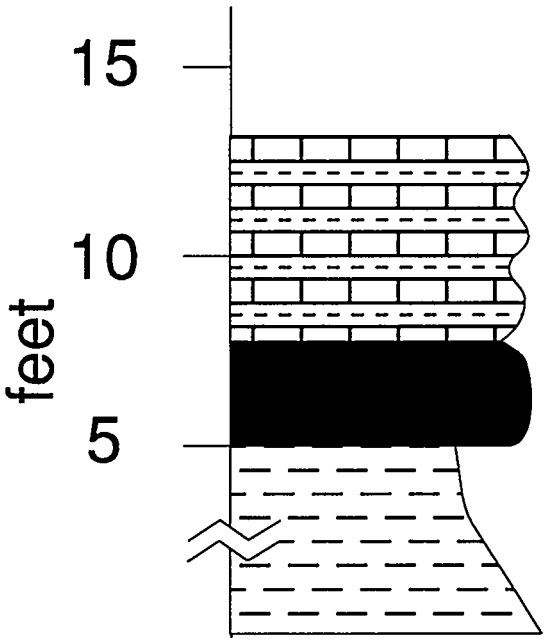

6' Interbedded carbonate mudstone and shale.

2'7" Skeletal intraclastic grainstone to packstone.

15' Shale.

LIB-3

1200 ft n of sw corner, s 31,T. 32 S, R. 17 E
Liberty Quadrangle
Montgomery County

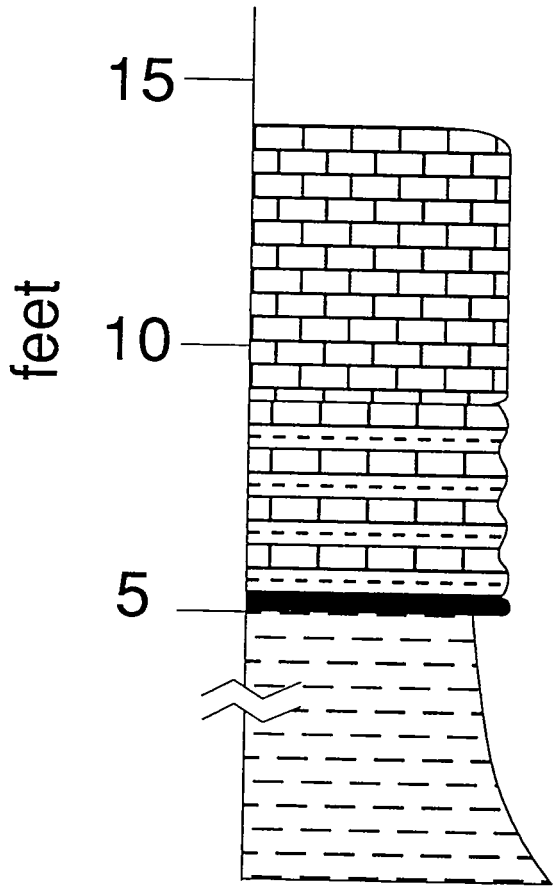

5' Skeletal oolitic grainstone.

4' Interbedded laminated carbonate mudstone and shale

4" Skeletal intraclastic grainstone

38' Gray shale.

LIB-4

s edge of sw s. 24, T. 32 S, R. 16 E
Liberty Quadrangle
Montgomery County

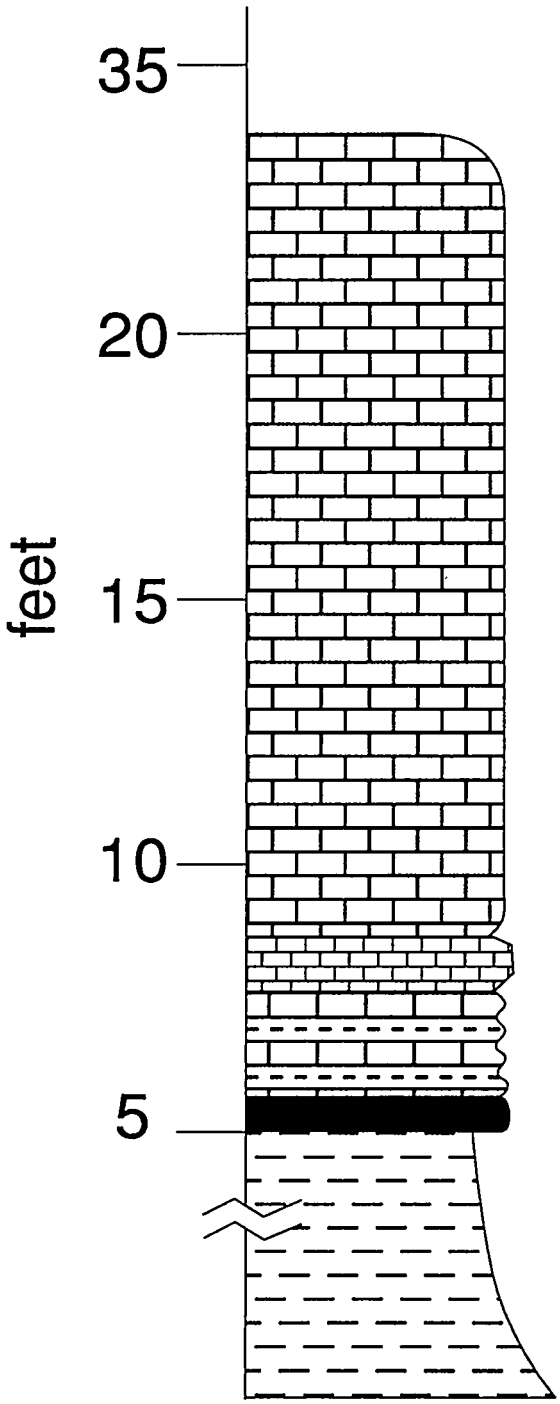

20' Skeletal oolitic grainstone.

1' Skeletal packstone and wackestone.

2'11" Interbedded laminated carbonate mudstone and shale

8" Skeletal intraclastic grainstone

32' Gray shale.

LIB-5

s edge of sw sw s. 29 T. 32 S, R. 17 E
and s edge of sw s. 30 T. 32 S, R. 17 E
Liberty Quadrangle
Montgomery County

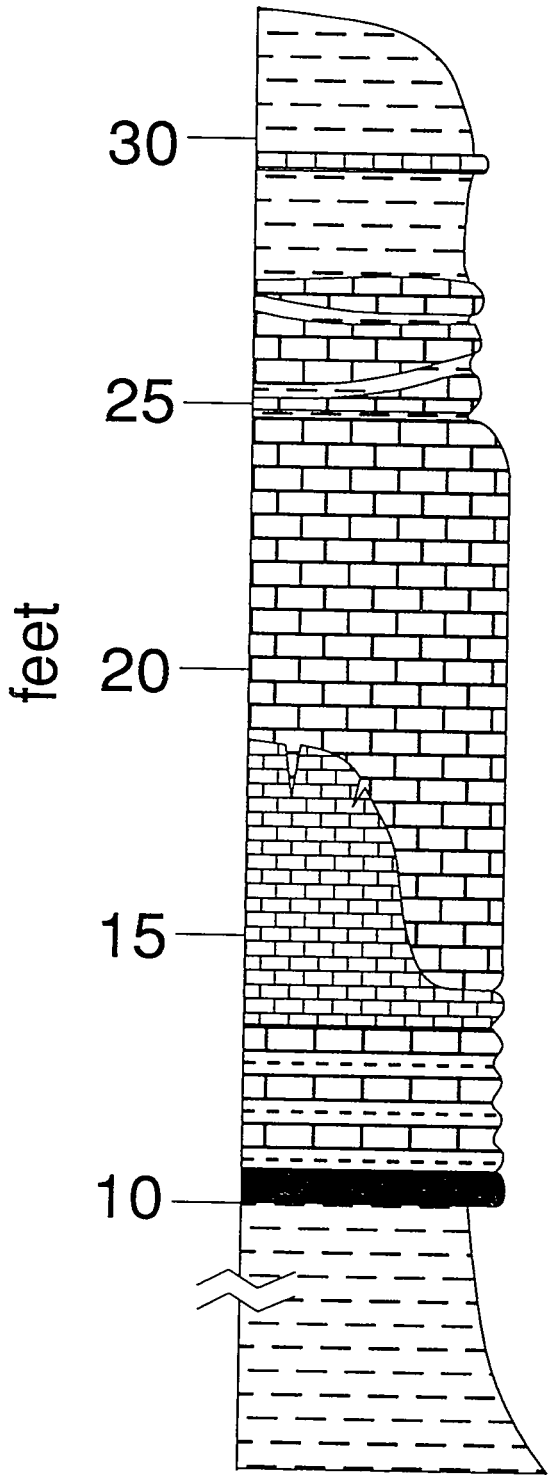

5' Silty shale with thin layers of fossiliferous packstone and cone-in-cone mudstone.

2'8" Interbedded skeletal oolitic grainstone and shale.

3'6" - 7' Skeletal oolitic grainstone.

5" - 5'5" Fossiliferous wackestone and boundstone. Laminated crust on upper surface.

1'-2'7" Interbedded laminated carbonate mudstone and shale.

5-10" Skeletal intraclastic grainstone.

10' Gray shale.

SYC-2

nw nw ne s. 10, T. 32 S, R 15 E.
Sycamore Quadrangle
Montgomery County

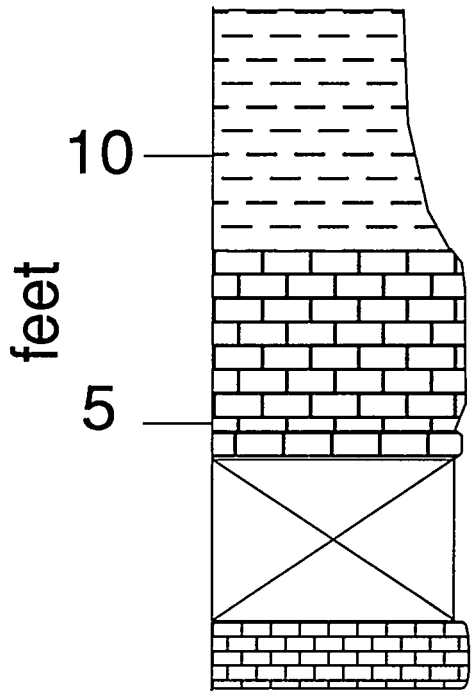

28' Interbedded sandstone and shale.

3'3" Skeletal oolitic grainstone.

6" Carbonate mudstone.

1'5" Fossiliferous wackestone.

HEARTLAND CEMENT CO. QUARRY

S 1/2 s 5 and nw s 4 T. 32 S, R. 15 E
Independence Quadrangle
Montgomery County

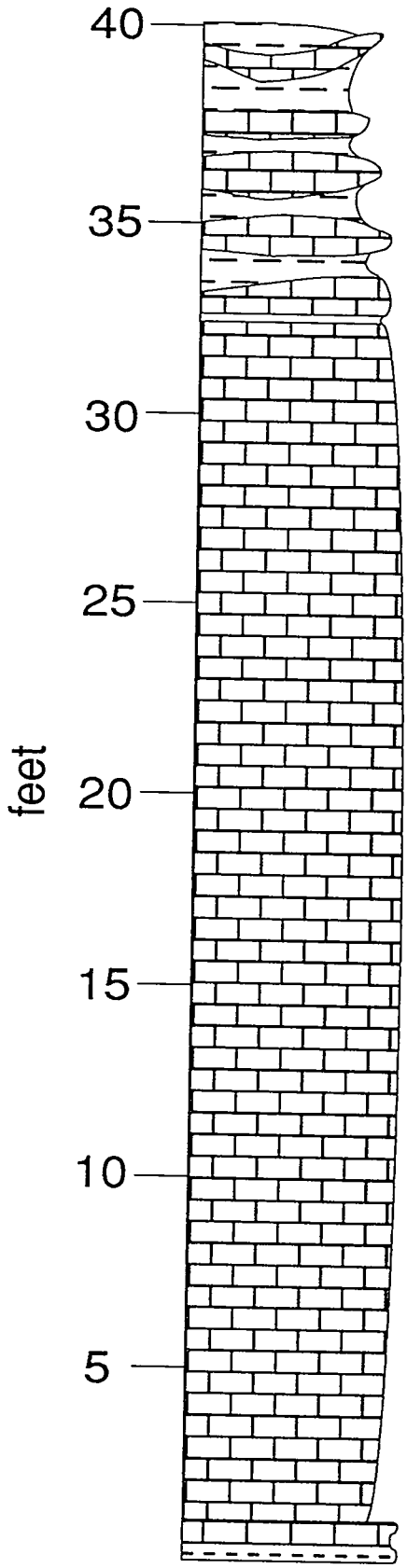

8' Interbedded skeletal oolitic grainstone and shale.

31' - 35' Skeletal oolitic grainstone.

1' Interbedded laminated carbonate mudstone and shale.

IND-1

nw sw sw s. 35, T. 32 S, R. 15 E
Independence Quadrangle
Montgomery County

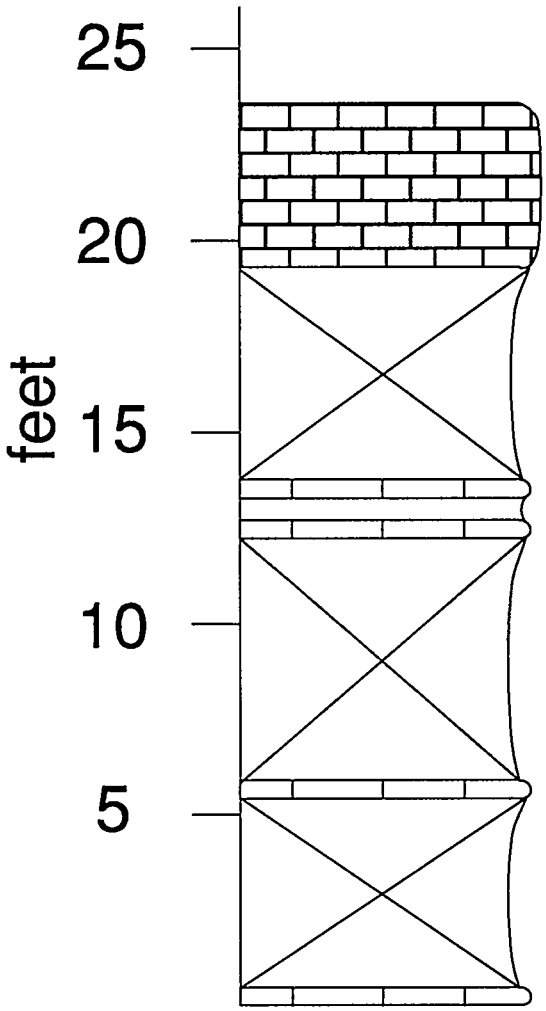

3' 7" Skeletal oolitic grainstone.

19' Mostly covered, isolated beds of micirite.

IND-2

nw sw sw s. 28, T. 33 S, R. 16 E
Independence Quadrangle
Montgomery County

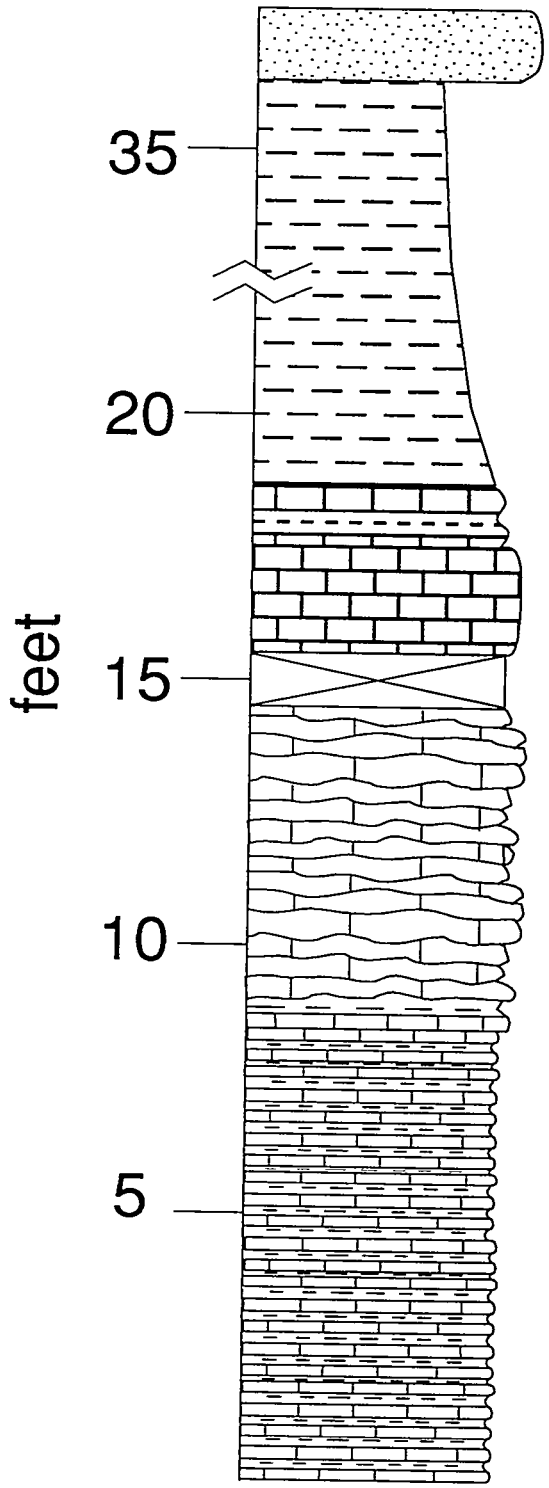

2' Micaceous sandstone.

17' Micaceous gray shale.

1'4" Interbedded shale and skeletal, oolitic grainstone. Shale interclasts.

2 ' Oolitic grainstone.

9' Interbedded shale seams and bioturbated carbonate mudstone

6' Interbedded laminated carbonate mudstone and shale

IND-4

sw sw nw s. 34 T. 33 S, R. 16 E
Independence Quadrangle
Montgomery County

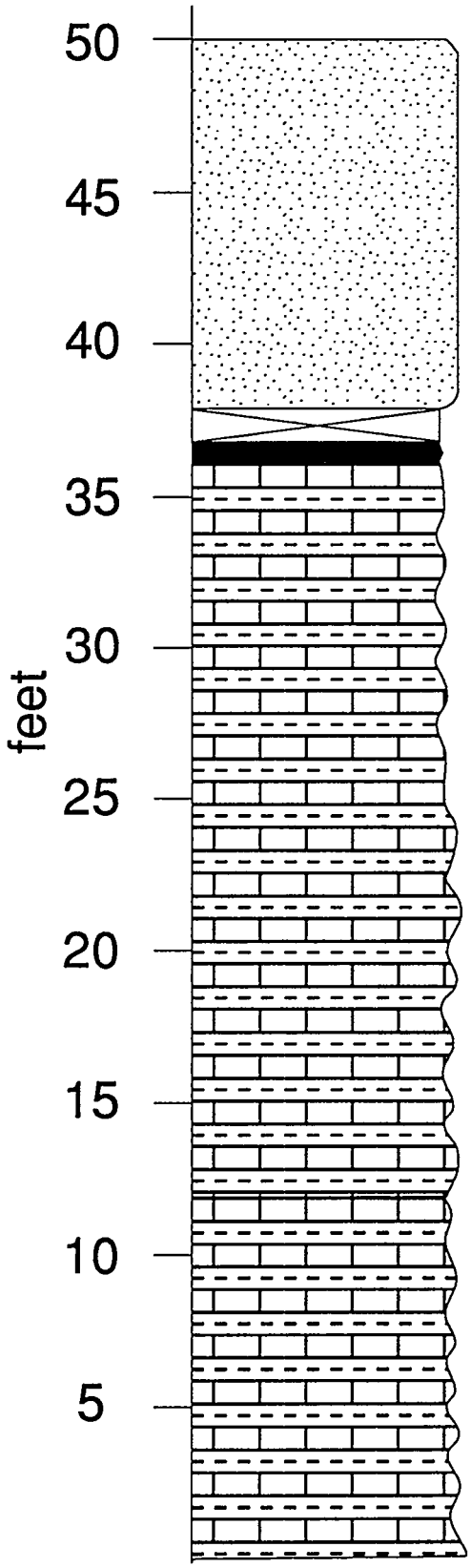

12' Micaceous sandstone.

4" Intracalstic limestone.

24' Interbedded limestone (mudstone) and shale.

12' Interbedded limestone and shale
Limestone, skeletal grainstone to wackestone.

IND-5

ne ne nw s. 33 T. 33 S, R. 16 E
Independence Quadrangle
Montgomery County

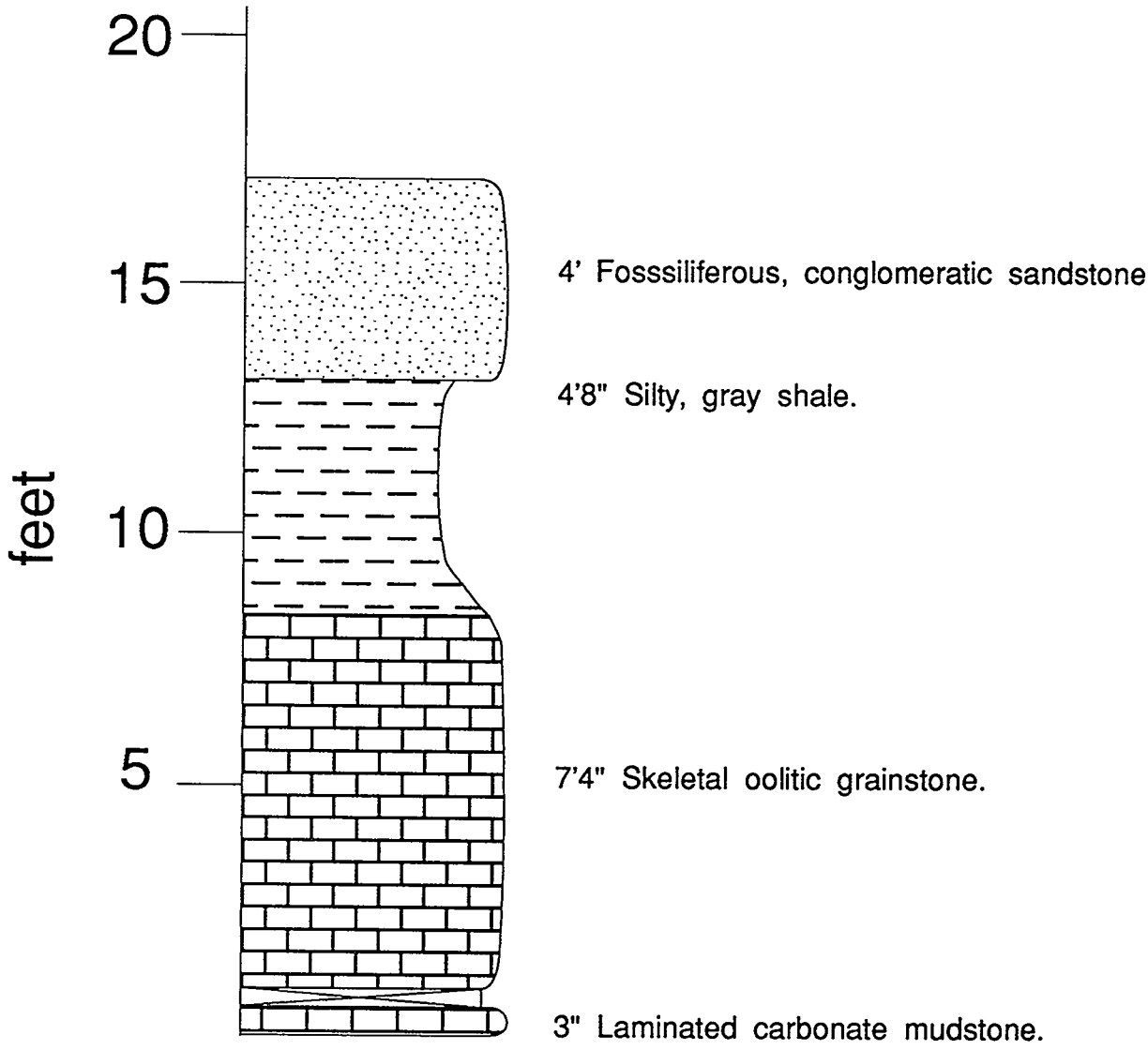

APPENDIX D

DETERMINATION OF PERMEABILITY

FROM DRILL STEM TESTS

DETERMINATION OF PERMEABILITY FROM DRILL STEM TESTS

By

Carel Otte

Production and Transportation Research Division

Research and Development Laboratories

The Pure Oil Company

Crystal Lake, Illinois

TABLE OF CONTENTS

	Page
Abstract	ii
Computing Permeability from Drill Stem Tests	iii
Introduction	1
Principles of a Drill Stem Test	2
Analysis of the Liquid Recovery During a Drill Stem Test	3
Examples	7
How To Do It	9
APPENDIX I	
Analysis of the Performance of an Ideal Well	11
A - Graphical Development	12
B - Mathematical Development	15
APPENDIX II	
Discussion of Basic Assumptions	19
Acknowledgments	21

LIST OF ILLUSTRATIONS

Figure 1 - Pressure-Time Relationship of a Drill Stem Test	2
Figure 2 - Diagram of Well Bore	11
Figure 3 - Diagram of Pressure-Time Chart of a Drill Stem Test	13
Figure 4 - Diagram of Pressure-Time Relationships During Overflow Conditions	20
Figure 5 - Abnormal Pressure-Time Relationship During Drill Stem Tests	20
Plate-1.00 - Average Pressure Driving Force for Permeability Studies	22
Plate-2.00 - Viscosity of Liquid Water	23
Plate-3.00 - Internal Volume of Drill Pipe	24
Plate-4.00 - Graph and Permeability Calculation Drill Stem Test, Wildcat No. 1	25
Plate-5.00 - Graph and Permeability Calculation Drill Stem Test, Wildcat No. 2	26

ABSTRACT

Permeability is a measure of the facility with which fluids can flow through a porous rock and is, therefore, an important property of a reservoir rock. In this paper the following formula:

$$k = 1.544 \times 10^6 \frac{Q\mu}{h(p_e - \bar{p})\Delta t}$$

is derived for calculating the average permeability of a formation from drill stem test data. In this formula the permeability, k, is expressed in millidarcys, Q is the volume of liquid that accumulates in the drill pipe expressed in barrels, μ the viscosity of the liquid in centipoises, h the thickness of the tested part of the formation in feet, Δt the duration of the test in minutes, p_e the Shut In Pressure in psi, and $\bar{p}$ an "average" pressure in psi, in magnitude between the Initial and Final Flow Pressures.

The thickness of the test interval, h, and the duration of the test, Δt, are directly available from drill stem test or scout reports. The volume of liquid in the drill stem, Q, and the viscosity of the liquid, μ, as a function of the bottom hole temperature, can be directly read from charts given with the report. Two methods are developed to determine the value of $(p_e - \bar{p})$, a graphical and a mathematical method. The graphical solution of $(p_e - \bar{p})$ requires the plot of the pressure versus time which is supplied with the report of a drill stem test. When only scout data are available, $(p_e - \bar{p})$ can be read from a chart, which expresses $(p_e - \bar{p})$ as a function of the Initial Flow Pressure, p_1, Final Flow Pressure, p_2, and the Shut In Pressure, p_e.

The derived formula is applicable only when the tested formation produces a single liquid: e.g., water or undersaturated oil. Two examples are worked out in detail.

Computing Permeability from Drill Stem Tests

$$\text{Permeability in Millidarcys} = 1.544 \times 10^6 \times \frac{\text{Barrels of liquid in drill stem} \times \text{Liquid viscosity in centipoises}}{\text{Thickness of tested interval in ft.} \times (\text{Shut In Pressure psi} - \text{"Average" pressure psi}) \times \text{Time in Min.}}$$

May be written:

$$K = 1.544 \cdot 10^6 \cdot \frac{Q\mu}{h(p_e - \bar{p})\ \Delta t}$$

In this equation, the term $(p_e - \bar{p})$ can be determined from the Time-Pressure graph given with the drill stem test report, or may be read from Pl-1.00 by using

$p_e - p_1$ = Shut In Pressure - Initial Flow Pressure

$p_e - p_2$ = Shut In Pressure - Final Flow Pressure

The other terms in the equation are directly available from the drill stem test reports or scout data.

A step by step outline of the procedure is given on pages 9 and 10 of Manual.

Symbols

K = permeability in millidarcys
Q = barrels of liquid in drill stem (Plate 3.00)
μ = viscosity in centipoise (Plate 2.00)
h = thickness of tested part of formations in ft.
p_e = Shut In Pressure in psi
p_1 = Initial Flow Pressure in psi
p_2 = Final Flow Pressure in psi
$\bar{p}$ = "Average pressure" in psi (Plate 1.00)
Δt = time in minutes.

INTRODUCTION

Permeability is one of the important properties of a formation, as it determines to a great degree whether the formation will make a satisfactory reservoir. Thus, it has become generally accepted practice throughout the petroleum industry, when developing a new discovery, to analyze core samples of the producing formation for their various physical properties and fluid content. The information obtained from these analyses aids in planning the optimum production schedule for new fields. The detailed knowledge of the permeability and its lateral variations within a formation has been proved to be also of considerable value to the exploration geologist, and has led to many new discoveries. Unfortunately, core data become generally available only after the new discoveries have been made and are of little use to the exploration geologist. When planning his exploration activities, the geologist usually relies on other, generally more qualitative, information regarding permeability characteristics.

In the following report a concise formula is derived for calculating rapidly and accurately average formation permeabilities. The formula utilizes drill stem test data that in any area are available from scout reports. Besides taking readings on three graphs, the entire calculation consists of multiplication and division of a total of seven terms. This operation should be handled rapidly on a common pocket slide rule. A step by step outline of the procedures to be followed is given on pages 9 and 10 of this paper.

As this method gives a permeability value that is an average for the tested interval, the results will be particularly useful when applied on a regional basis to establish lateral trends in permeability variations. If the geologist exercises care and judgment, the results should be applicable also in relatively restricted areas.

PRINCIPLES OF A DRILL STEM TEST

A drill stem test is a measure of the liquid content and productive capacity of a formation. The test is so designed that it can be run without previously casing the well. This feature makes the drill stem test so useful during the exploratory phase of a drilling program. A formation tester, which consists largely of a series of valves, is attached to the bottom of the drill pipe. At the time the drill pipe is run into the bore-hole for a formation test, the valves are closed and the drilling mud, that stands in the bore-hole, is prevented from entering the drill pipe. A packer is utilized which, when properly seated between the drill stem and the wall of the well, relieves the tested interval immediately below of the hydrostatic pressure of the overlying column of drilling mud. At the start of the actual test, certain valves are opened and the formation fluids are permitted to flow from the formation into the well bore, through the tester, into the drill pipe against the static pressure of the column of air above. The fluid entering the drill pipe is trapped by the system of valves in the tester, so that it can be withdrawn from the well with the drill pipe, examined and measured for volume. If the duration of the test is sufficiently long, the liquid rises in the drill pipe until equilibrium of pressure with that of the formation is attained. In case of high formation pressures, the liquid may reach the surface at which moment it will continue to flow at a steady rate.

A record of the variation in pressure throughout the period of the drill stem test is obtained by a pressure-recording device which is attached below the formation tester. Such a record is shown on Figure 1.

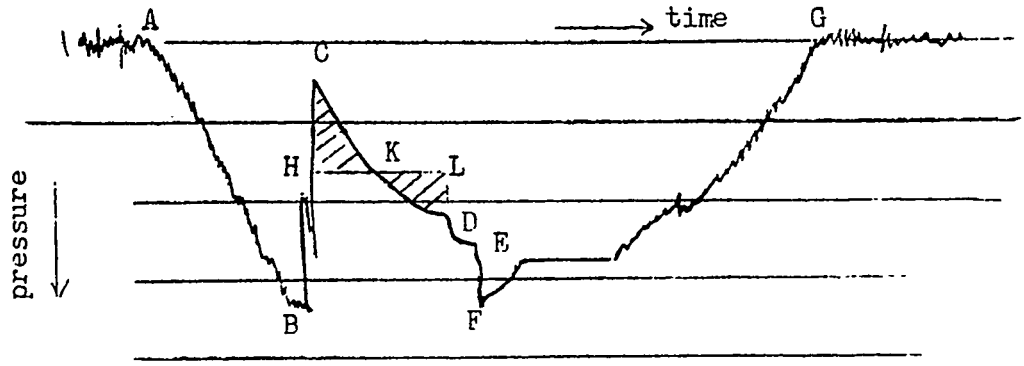

Figure 1. Pressure-Time Relationship of a Drill Stem Test

Portion AB of the graph indicates the pressure-increase as a result of the weight of the mud column while the tool is lowered in the well. At point B the packer is "set". At point C the valves are opened, the pressure on the recording device is essentially reduced to the static pressure of the atmosphere, and fluid is permitted to enter the drill pipe. Point D marks the end of the test, at which time the valves are closed. The curve between C and D is, therefore, the actual record of the variation of the pressure with time at the face of the rock in the well bore. The curve between D and E indicates the formation pressure build-up in the vicinity of the well after the valves are closed. Point E is, thus, a measure of the Shut In Pressure of the formation. The portions of the graph between points E, F and G indicate the changes in pressure that occur when the packer is released and the tester and recording device are pulled out of the hole.

ANALYSIS OF THE LIQUID RECOVERY DURING A DRILL STEM TEST

With the above "technical" principles in mind, it is possible to introduce the reader in a qualitative manner to the problem of fluid recovery during a drill stem test.

Everyone will readily agree that the total volume of liquid, Q, entering the well bore and the drill pipe will depend upon the permeability, k, of the formation; the larger the formation permeability, the greater the volume of liquid that enters the well bore during a certain length of time. Also, the volume of liquid will be proportional to the thickness of the tested interval, h, and the duration of the test, Δt. On the other hand, the volume of liquid varies inversely with the liquid viscosity, μ; greater viscosity will retard flow conditions. Finally, the quantity of liquid entering the well bore will be proportional to the driving force, e.g. the difference between the formation pressure, p_e, and the pressure, p,

at the face of the rock in the well bore. This latter quantity, p, is variable with time, and is very small at the start of the test. Inasmuch as the pressure, p, is an expression of the weight of the liquid column in the drill pipe its value will steadily increase as the test progresses. All the above terms can be brought into an equation as follows:

$$Q = f. \frac{kh(p_e - p)\Delta t}{\mu}$$, in which

f is a constant of proportionality. The terms can be rearranged to give an expression for the permeability, k:

$$k = \frac{1}{f} \frac{Q\mu}{h(p_e - p)\Delta t} \quad \text{.....(1)}$$

This formula is actually a restatement of Darcy's Law and applies to unidirectional flow such as occurs in a rock sample in the laboratory, or on a larger scale in a simple aquifer. As the present problem considers flow from all directions into a well bore, which is called "radial flow", another factor, must be inserted in the equation. This new factor takes into account the radius of the well bore, r_w, and the radius, r_e, at which the formation pressure, p_e, remains constant during the test and is not affected by the flow of liquid into the well bore. In this way, the equation becomes:

$$k = \frac{1}{f} \times \frac{\ln {}^{r_e}/_{r_w}}{2\pi} \times \frac{Q\mu}{h(p_e - p)\Delta t} \quad \text{.....(2)}$$

For a derivation of the new factor, $\frac{\ln {}^{r_e}/_{r_w}}{2\pi}$, the reader is referred to Muskat's text on the "Flow of Homogeneous Fluids" (Muskat, 1937 or 1946, pp 149-153). For a given well, the radii of the well and of the external boundary will be constant. As the permeability varies logarithmically with the ratio of r_e and r_w, large variations in those values are required to affect appreciably the total production of liquid. Thus, when making the following estimates, which are reasonable for average conditions, r_e = 500

feet, and $r_w = 1/4$ foot, no great errors in the permeability calculation will be introduced. Then, the term

$$\frac{\ln r_e/r_w}{2\pi} = \frac{\ln 500/1/4}{2\pi} = \frac{\ln 2000}{2\pi} = \frac{7.60}{6.28} = 1.21$$

In addition, by selecting the units in the metric system, the term, $\frac{1}{f}$, can be eliminated from the equation.

Equation (2) becomes

$$k = 1.21 \times \frac{Q\mu}{h(p_e - p)\Delta t} \quad \text{.....(3)}$$

In formula (3) k is expressed in darcys, Q in cm^3, h in cm, p_e and p in atmospheres, Δt in seconds and μ in centipoise. It is desirable to convert these to the engineering units, that are most commonly used in the petroleum industry.

$$1 \text{ barrel} = 159{,}000 \text{ cm}^3$$

$$1 \text{ foot} = 30.5 \text{ cm}$$

$$1 \text{ psi} = \frac{1}{14.7} \text{ atmosphere}$$

$$1 \text{ minute} = 60 \text{ seconds}$$

$$1 \text{ millidarcy} = \frac{1}{1000} \text{ darcy.}$$

Entering these conversion factors into equation (3)

$$k \text{ darcys} = 1.21 \times \frac{159{,}000\, Q\mu}{30.5h \times \frac{(p_e - p)}{14.7} \times 60\,\Delta t} = 1544 \frac{Q\mu}{h(p_e - p)\Delta t} \quad \text{or}$$

$$k \text{ millidarcys} = 1.544 \times 10^6 \frac{Q\mu}{h(p_e - p)\Delta t} \quad \text{.....(4)}$$

in which k is expressed in millidarcys, Q in barrels, μ in centipoise, h in feet, p_e and p in pounds per square inch and Δt in minutes.

Although equation (4) appears to be in finished form, it is not yet applicable for computing permeability. As was pointed out earlier, the value of pressure, p, varies with time. At the start of the test p is

small in comparison with the other pressures considered; thus the driving force (p_e-p) is large and the volume of liquid entering the well bore per unit time is large. Pressure p corresponds then to the Initial Flow Pressure. At the end of the test, p is larger, corresponds to the Final Flow Pressure, the driving force (p_e-p) is smaller and the rate of flow into the well bore is reduced. If a certain "average" value, $\bar{p}$, can be determined for the variable, p, that is in magnitude between the Initial and Final Flow Pressures in such manner that the total volume of liquid, Q, produced during the test is the same, then equation (4) can be utilized. Because of the type of flow conditions that exist, the "average" pressure, $\bar{p}$, is not a straight arithmetic mean of the Initial and Final Flow Pressures, for which reason the quotation marks are adopted. It can be selected with the aid of the time versus pressure curve in Figure 1. A point, K, is located on the curve CD in such a manner that the area enclosed by points CKH equals the area enclosed by points DKL. This can be done rapidly and relatively accurately by visual inspection. The pressure that corresponds to point K on the curve is the desired pressure, $\bar{p}$, which value can be read on the vertical scale. A proof, substantiating this derivation, is given in the appendix under the graphical method. Thus

$$k = 1.544 \times 10^6 \frac{Q\mu}{h(p_e - \bar{p})\Delta t} \quad \text{.....(5)}$$

In this equation the terms h and Δt are directly available from the drill stem test report. The volume of liquid, Q, and viscosity, μ, can be read from Charts F1-2.00 and F1-3.00, at the back of this report, when the height of the liquid level in the drill stem and the temperature are given. The term $(p_e - \bar{p})$ equals the Shut In Pressure minus the "average" pressure, which can be determined by the "equal-area method" from the pressure-time curve of the drill stem test report.

In case only scout data are available, which is in most instances, the term $(p_e - \bar{p})$ can be directly read from Chart P1-1.00, where $(p_e - \bar{p})$ is expressed in the Initial Flow Pressure, p_1, the Final Flow Pressure, p_2, and the Shut In Pressure, p_e. The derivation for the mathematical expression relating $\bar{p}$, p_1, p_2, and p_e is given in the appendix in the section of the mathematical method. However, at this stage, probably the reader appreciates qualitatively that somehow the "average" pressure, $\bar{p}$, must be dependent upon the Initial and Final Flow Pressures and Shut In Pressure, and that a mathematical relationship can be worked out. After this expression had been determined, Chart P1-1.00 was prepared for a range of values as an aid in permeability calculations.

In the next section and on Charts P1-1.00 and P1-5.00 two examples are worked out.

EXAMPLES

Case I

A. Graphical Method (Equal-Area Method):

Chart P1-4.00 indicates the charted pressure-time relationship of an actual drill stem test. The Shut In Pressure (SIP) is 2616 psi, Initial Flow Pressure (IFP) is 449 psi, and the Final Flow Pressure (FFP) is 2274 psi. By visual inspection, $\bar{p}$, is selected at 1600 psi, so that

$$\text{area } p_1 \text{ A } \bar{p} = \text{area } p_2 \text{ B } \bar{p}$$

thus,

$$(p_e - \bar{p}) = 2616 - 1600 = 1016 \text{ psi.}$$

The tested interval is 26 feet, which is the total depth, 6546 feet, minus the packer depth, 6520 feet. In case electric logs are available, it is possible to determine the presence of relatively impermeable zones, such as shale breaks, and the figure of the tested interval can be corrected for a corresponding amount.

The volume of liquid in the drill pipe is determined from Chart P1-3.00. Liquid height is 4500 feet (4140 feet of salt water and 360 feet of water cut mud), and as no further information is available on the drill pipe except its outside diameter of 4-1/2 inches, the more commonly used value, marked by an asterisk, is selected. Q is 62.8 barrels.

The viscosity of water varies considerably with temperature. At the given temperature of 140°F., μ = 0.467 centipoises, according to Chart P1-2.00. Thus the permeability is:

$$k = 1.544 \times 10^6 \frac{Q\mu}{h(p_e-\bar{p})\Delta t} = 1.544 \times 10^6 \times \frac{62.8 \times 0.467}{26 \times 1016 \times 90} =$$

19.1 millidarcys

B. Mathematical Method:

With the information from a scout report, and the aid of Chart P1-1.00, $(p_e-\bar{p})$ based on IFP, FFP and SIP can be determined. The determination of $(p_e-\bar{p})$ is as follows:

(SIP - IFP) or (p_e-p_1) = 2616 - 449 = 2167 psi

(SIP - FFP) or (p_e-p_2) = 2616 - 2274 = 342 psi

(p_e-p_1) is taken on the horizontal axis of Chart P1-1.00, (p_e-p_2) is interpolated from the set of curves, and $(p_e-\bar{p})$ is read on the vertical axis. In this instance $(p_e-\bar{p})$ = 990 psi. By this method the permeability, k, equals 19.6 millidarcys using equation (5).

Case II

Charts P1-1.00 and P1-5.00, exhibit a second example. The calculated permeability is 3.7 millidarcys.

HOW TO DO IT

The formula for computing permeability from drill stem test data is

$$k = 1.544 \times 10^6 \frac{Q \mu}{h(p_e - \bar{p}) \Delta t}$$

k = permeability in millidarcys

Q = volume of liquid in drill stem in barrels (Plate-3.00)

μ = viscosity of liquid in centipoises (Plate-2.00)

h = thickness of tested interval in feet

Δt = duration of the test in minutes

$p_e - \bar{p}$ = Shut In Pressure in psi - "Average" pressure in psi (Plate-1.00)

To determine the values to be substituted in the above equation, one proceeds as follows:

1) The thickness of the tested interval, h, is determined by deducting the packer depth from the total depth. This figure might be corrected if the number of feet of impermeable formation in the tested interval is known from an electric log.

2) The duration of the test, Δt, is directly given, and has to be expressed in minutes.

3) The volume of the liquid in the drill stem in barrels is determined with the aid of Plate-3.00, when the number of feet of liquid in the drill stem and size of the drill pipe are known.

4) Viscosity of liquid, μ, in centipoises can be read from Plate-2.00, when the bottom hole temperature is known. In case the temperature is not given with the scout report, an estimate can be made using the geothermal gradient of 1°F. per 100 feet of bore-hole. The surface temperature is considered at 80°F.

5) The pressure difference, or driving force, $(p_e - \bar{p})$ can be determined in two ways:

a) Graphical Method - A copy of the Drill Stem Test report is required. Determine the value of the "average" pressure, $\bar{p}$, by locating a point, k, on the pressure-time curve, CD, so that

area CKH = area DKL (Figure 1, Page 2)

Read the pressure, $\bar{p}$, on the vertical scale that corresponds to point, K.

The driving force, $p_e - \bar{p}$, is the difference between the Shut In Pressure, p_e, and the newly determined "average" pressure, $\bar{p}$.

b) Mathematical Method - This method can be used when scout data are available (see Plate-1.00). Determine difference of Shut In Pressure and Initial Flow Pressure, $(p_e - p_1)$.

Determine difference of Shut In Pressure and Final Flow Pressure, $(p_e - p_2)$.

Locate $(p_e - p_1)$ on horizontal scale of Plate-1.00.

Determine point of intersection of a vertical line through this point and the curve, $(p_e - p_2)$.

Read the corresponding value, $(p_e - \bar{p})$, of this point of intersection on the vertical scale.

The computation of the permeability, k, is now a simple operation of division and multiplication and can be done on a common pocket slide rule or worked out on paper.

APPENDIX I

Analysis of the Performance of an Ideal Well

The problem is one of flow in the unsteady state; i.e., one in which the pressures and flow velocities in the reservoir in the vicinity of the well bore are continuously changing. The accompanying diagram (Fig. 2) defines the pertinent variables associated with this problem.

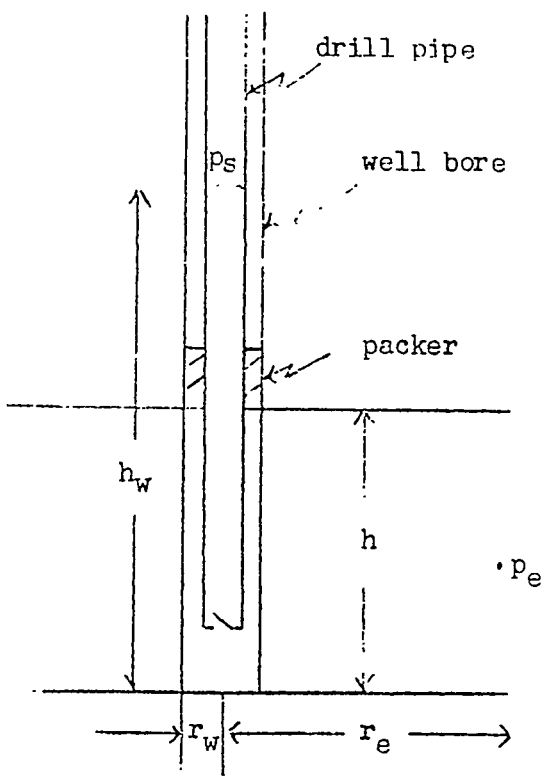

Figure 2. Diagram and Notations of Well Bore during a Drill Stem Test.

Notations

A = cross-sectional area of drill pipe

g = gravitational acceleration

h = tested interval

h_w = variable height of liquid in drill pipe

k = permeability

p_e = reservoir pressure of tested formati at radius r_e

p_s = static pressure above liquid column in drill pipe

p = variable pressure of tested formatio at the face of the rock in the well bore

Q = volume of liquid entering well bore

μ = viscosity of liquid

t = time

ρ = density of liquid

r_w = radius of well bore

r_e = distance from center of well bore to a point of constant pressure p_e in the reservoir

ln = natural logarithm

IFP = Initial Flow Pressure

FFP = Final Flow Pressure

SIP = Shut In Pressure

In order to set up the mathematical equations necessary to derive the performance of an ideal well, certain assumptions have been made. These are as follows:

1) The permeability, porosity, and formation thickness are uniform throughout that portion of the sand body that can be influenced by the well.

2) The velocity of fluid flow at any point is directly proportional to the pressure gradient.

3) The well bore is cylindrical, and penetrates completely the contributing part of the formation.

4) The liquid is incompressible.

5) Frictional losses of the fluid in the well bore and drill pipe are negligible.

6) The formation pressure remains constant for the duration of the test.

In most wells these assumptions are sufficiently reasonable to permit their use. In case of recovery of large quantities of oil and gas during the test, serious discrepancies might occur which would require drastic modification of the equations and make the results unwieldy for field use.

In the next few pages two methods are given to derive the basic formula for permeability calculations: (A) a graphical and (B), a mathematical method.

A - Graphical Development

A drill stem test measures the pressure, p, of the tested part of a formation at the face of the rock in the well bore. During the test, the liquid is permitted to enter the drill pipe and the pressure is a function of time under unsteady state flow conditions. If the test runs sufficiently long, the pipe fills to its equilibrium height with liquid, or else overflows. At the time overflow occurs the flow becomes steady state.

Figure 3 is a diagrammatic representation of the pressure-time chart obtained in an ideal drill stem test.

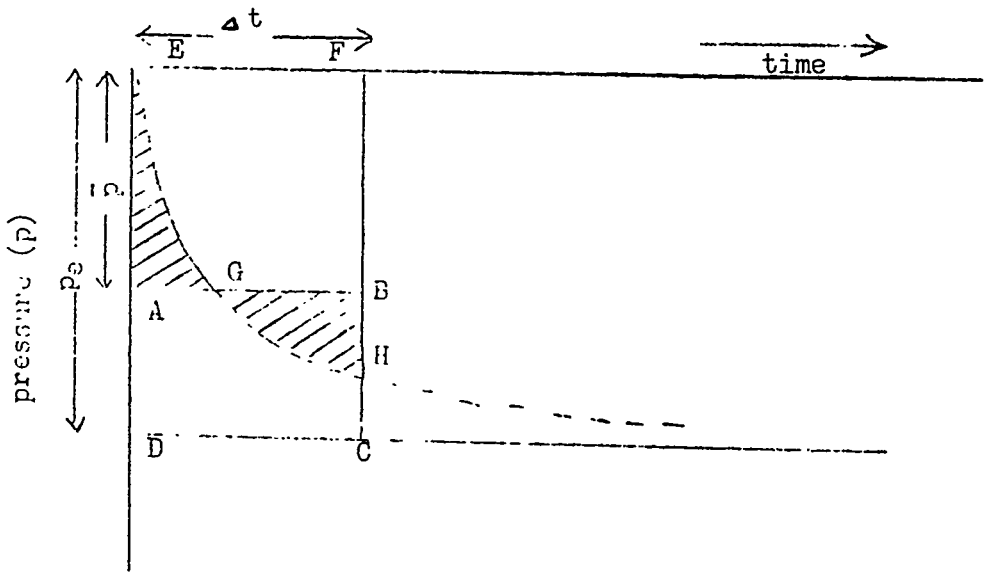

Figure 3. Diagram of Pressure-Time Chart of a Drill Stem Test.

At the time the tool is opened to start the test, point E on the diagram, the pressure at the face of the rock is essentially the static pressure of the atmosphere at that elevation. This pressure is generally small compared to the formation pressure, and this value can be neglected for present considerations. As a result of the pressure difference between formation pressure, p_e, and pressure at well bore, p, the liquid will flow into the well and rise in the drill pipe. The pressure at the well bore, p, is essentially equal to the liquid head maintained in the drill pipe. After sufficient time, equilibrium conditions will be reached and the pressure at the well bore (liquid head) will equal the formation pressure and correspond to the "Shut In Pressure" in a normal bottom hole pressure survey. With a very permeable formation, the liquid will accumulate very rapidly in the hole, the elapsed time will be short, and the pressure curve on Figure 3 will be steep. With a tight formation a shallow curve will be recorded.

Muskat (1937 or 1946, p. 150-154) in his text "The Flow of Homogeneous Fluids Through Porous Media" derived analytically the formula for radial flow per unit time (rate of flow) into a well, which is given by:

$$\frac{dQ}{dt} = \frac{2\pi kh}{\mu \ln r_e/r_w} (p_e - p) \quad \ldots\ldots\ldots\ldots\ldots\ldots\ldots (6)$$

The notation of the various terms are given on Figure 2.

In this equation the quantity of liquid, Q, the pressure, p, and the time, t, are variables. A plot of pressure versus time produces the curve in Figure 3. The other terms in the equation are dependent on local conditions and can vary from area to area. However, during a given drill stem test, they are taken to be constant.

Let $\frac{2\pi kh}{\mu \ln r_e/r_w} = C$. Then, the rate of flow is $\frac{dQ}{dt} = C(p_e - p)$

The amount of liquid that flows into the well bore during a small time increment, dt, is

$$dQ = C\ (p_e - p)\ dt$$

Thus, the total volume of liquid, Q, produced in time, Δt, is the summation of these small time increments, dt, or:

$$Q = C \int_0^{\Delta t} (p_e - p)\ dt = C\ (p_e \Delta t - \int_0^{\Delta t} p dt)$$

According to Figure 3, $p_e \Delta t$ is the area of rectangle EFCD and $\int_0^{\Delta t} p dt$ is the area bounded by EF, FH and the curve. Thus, the total quantity of liquid produced during time, Δt, is proportional to the area bounded by ED, DC, CH and the curve, EGH.

Muskat's formula can be maintained unchanged if a value, $\bar{p}$, can be selected on the curve of the variable, p, so that:

area EAG = area BHG (Shaded areas on Figure 3)

then, area EGHCD = area ABCD

and, area ABCD = area EFCD - area EFBA = $p_e \Delta t - \bar{p} \Delta t$, and

$Q = C\,(p_e - \bar{p})\,\Delta t$

thus, $$Q = \frac{2\pi kh}{\mu \ln r_e/r_w}\,(p_e - \bar{p})\,\Delta t \quad \text{.....(7)}$$

or, $$k = \frac{\ln r_e/r_w}{2\pi}\,\frac{Q\mu}{h(p_e - \bar{p})\,\Delta t} \quad \text{.....(8)}$$

When assuming again r_e = 500 feet, and r_w = 1/4 foot, formula (8) reduces to

$$k = 1.21 \times \frac{Q\mu}{h(p_e - \bar{p})\,\Delta t} \quad \text{.....(9)}$$

or expressed in engineering units:

$$k = 1.544 \times 10^6\,\frac{Q\mu}{h(p_e - \bar{p})\,\Delta t} \quad \text{.....(10)}$$

In an actual field test, as is demonstrated on Chart F1-4.00, the problem is reduced to selecting a value, $\bar{p}$, by the "equal-area method" between the Initial Flow Pressure, p_1, and the Final Flow Pressure, p_2.

B - Mathematical Development

From the earlier discussion on page 6, it is apparent that our main problem is to express the variable pressure, p, as a function of time.

According to Muskat's equation, the rate of flow of fluid through a porous medium in a radial system is expressed by

$$\frac{dQ}{dt} = \frac{2\pi kh}{\mu \ln r_e/r_w}\,(p_e - p) \quad \text{.....(11)}$$

The bottom hole pressure, or pressure at the face of the rock in the well bore, can be expressed by the following equation(notations on Fig.

$$p = \rho g\, h_w + p_s \quad \text{.....(12)}$$

The variation of pressure, p, with time is obtained by differentiating equation (2)

$$\frac{dp}{dt} = \rho g \frac{dh_w}{dt} \text{ or } \frac{1}{\rho g} \cdot \frac{dp}{dt} = \frac{dh_w}{dt} \quad \text{.....(13)}$$

At any time the volume of liquid, Q, in the drill pipe is the product of the height of the liquid column, h_w, and the cross-sectional area, A

$$Q = A\, h_w \quad \text{.....(14)}$$

Similarly, this equation may be differentiated to give the variation of the height of the liquid column, h_w, with time, t.

$$\frac{dQ}{dt} = A \frac{dh_w}{dt} \quad \text{.....(15)}$$

Equations (11), (13) and (15) when combined give:

$$\frac{dQ}{dt} = \frac{A}{\rho g} \cdot \frac{dp}{dt} = \frac{2\pi kh}{\mu \ln r_e/r_w} (p_e - p) \quad \text{.....(16)}$$

or

$$\frac{dp}{dt} = \frac{2\pi kh\rho g}{A\mu \ln r_e/r_w} (p_e - p) \quad \text{.....(17)}$$

or

$$\frac{dp}{(p_e - p)} = \frac{2\pi kh\rho g}{A\mu \ln r_e/r_w} dt \quad \text{.....(18)}$$

This differential equation expresses the pressure, p, as a function of time. Integrated between two values of the pressure, e.g., the Initial Flow Pressure, p_1, and the Final Flow Pressure, p_2, the expression becomes:

$$\left[-\ln (p_e - p)\right]_{p_1}^{p_2} = \left[\frac{2\pi kh\rho g}{A\mu \ln r_e/r_w} t\right]_{o}^{\Delta t} \quad \text{.....(19)}$$

$$\ln \frac{p_e - p_1}{p_e - p_2} = \frac{2\pi kh\rho g}{A\mu \ln r_e/r_w} \Delta t \quad \text{.....(20)}$$

Also

$$(p_e - p_1) - (p_e - p_2) = p_2 - p_1 \quad \text{.....(21)}$$

Divide equation (21) by equation (20), then:

$$\frac{(p_e - p_1) - (p_e - p_2)}{\ln \frac{p_e - p_1}{p_e - p_2}} = \frac{p_2 - p_1}{\frac{2\pi kh\rho g}{A\mu \ln r_e/r_w} \Delta t} \quad \text{.....(22)}$$

The first part of equation (22) is, by definition, the logarithmic mean of (p_e-p); or,

$$\ln \text{mean } (p_e-p) = \frac{(p_e-p_1) - (p_e-p_2)}{\ln \frac{p_e-p_1}{p_e-p_2}} \quad \ldots\ldots\ldots\ldots\ldots\ldots(23)$$

Also, p_2-p_1 is equal to the liquid head maintained in the drill pipe, as those values represent the initial pressure and the final pressure, e.g., the Initial and Final Flow Pressures at the face of the rock in the well bore.

$$p_2-p_1 = \rho g\, h_w \quad \ldots\ldots\ldots\ldots\ldots\ldots\ldots\ldots\ldots\ldots\ldots\ldots(24)$$

Equations (22), (23) and (24) when combined give:

$$\ln \text{mean } (p_e-p) = \frac{\rho g\, h_w}{\frac{2\pi kh\rho g}{A\mu \ln r_e/r_w}\Delta t} = \frac{A\, h_w \mu \ln r_e/r_w}{2\pi kh\, \Delta t} \quad \ldots\ldots(25)$$

As $Ah_w = Q$, the volume of liquid in the drill pipe, the equation becomes:

$$\ln \text{mean } (p_e-p) = \frac{\ln r_e/r_w}{2\pi} \cdot \frac{Q\mu}{kh\,\Delta t} \quad \ldots\ldots\ldots\ldots\ldots\ldots(26)$$

The terms can be rearranged to produce an expression for permeability, k,

$$k = \frac{\ln r_e/r_w}{2\pi} \cdot \frac{Q\mu}{h\,[\ln \text{mean } (p_e-p)]\Delta t} \quad \ldots\ldots\ldots\ldots\ldots(27)$$

Comparison of equation (27) with equation (8), that was derived by the graphical method, shows

$$(p_e-\bar{p}) = \ln \text{mean } (p_e-p)$$

or according to equation (23):

$$(p_e-\bar{p}) = \frac{(p_e-p_1) - (p_e-p_2)}{\ln \frac{p_e-p_1}{p_e-p_2}} \quad \ldots\ldots\ldots\ldots\ldots\ldots\ldots(28)$$

This method defines the "average" pressure, $\bar{p}$, mathematically and with equation (28) permits a direct calculation of $p_e-\bar{p}$ from the three known pressures, Initial Flow Pressure (IFP) = p_1, Final Flow Pressure (FFP) = p_2,

and the Shut In Pressure (SIP) = p_e. These values are readily available from scout data and thus, for calculation of the permeability, a copy of the drill stem test with graph is not required. In addition, by means of equation (28) a set of curves can be plotted, as are shown on Chart P1-1.00 for a range of values of IFP, FFP and SIP, from which $(p_e - \bar{p})$ can be easily determined.

APPENDIX II

In order to facilitate the analytical treatment of this problem, some basic assumptions had to be made which were reasonable within the practical and rather restricted scope of the problem. However, attention should be focused on several other factors that affect the accuracy of the final results.

1 — Earlier it was stated that the variation in the ratio of external boundary radius to well radius does not affect appreciably the final result. Hence, any reasonable assumption for r_o and r_w can be made without fear of introducing large uncertainties in the estimates for Q. For a variation from 4 inches to 10 inches in the diameter of the hole, or a corresponding variation in external boundary diameter, the maximum deviation from the previously assumed value ($\ln 500/ 1/4 = \ln 2000$) is only 6.7%.

2 — The viscosity of liquid water varies with temperature. The chart on P1-2.00 was plotted for fresh water. However, in many an instance the produced formation water will contain appreciable amounts of dissolved solids. The liquid viscosity at 25°C. for a solution of NaCl of 35,000 ppm, which corresponds to sea water, is about 5.5 per cent higher than that of fresh water. Because of this relatively low figure, and in order not to complicate the computation unduly, no further allowances have been made for this type of effect on liquid viscosity. It might be added that in a given geologic province usually the composition of the formation water is relatively constant. Therefore, all computed permeabilities within a certain province, although in error, will be affected to the same degree by this simplificatic

3 — It should be emphasized that the term Q, the volume of liquic only applies to the liquid in the drill stem. The mathematical treatment does not take into consideration the volume of liquid that in a few instance

flows on the surface into a stock tank. In the case overflow does occur, it is necessary to determine the time of overflow. This value might be obtained from the original drill stem test report. When a well overflows a steady state flow condition has been reached and pressure is constant from thereon. The plot of pressure versus time should show a sharp break at this point. (Figure 4)

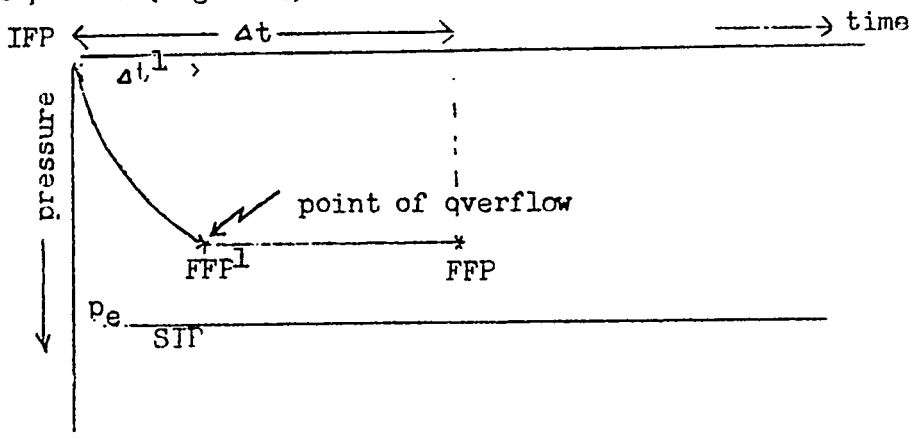

Figure 4. Diagram of Pressure-Time Relationships During Overflow Conditions.

If point, FFP, marks the end of the test, Δt, the time, Δt^1, that corresponds to point, FFP^1, should be entered into the equation for computing permeability.

4 — The mathematical derivation applies to ideal flow conditions; however, in many instances deviations from the ideal pressure build-up curve occur. Creation of a mud block might be one example. An anamolous pressure-time relationship, as is indicated on Figure 5, is not exceptional.

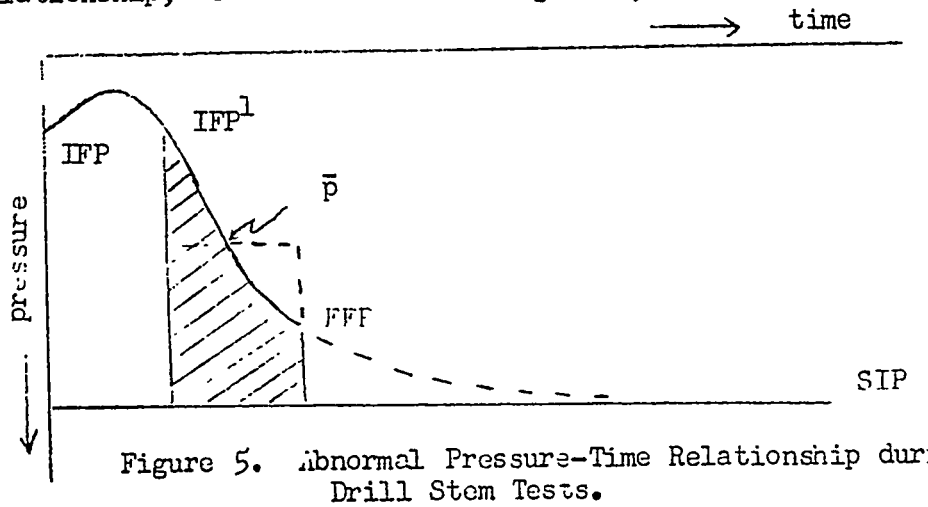

Figure 5. Abnormal Pressure-Time Relationship during Drill Stem Tests.

In the instances where deviations occur, more correct answers will be obtained for the permeability if the graphical method is employed. In this particular example a revised value of the Initial Flow Pressure is utilized to determine $(p_e - \bar{p})$. The value for IFP^1 can be read from the graph. Also, Q, the volume of liquid in the drill pipe, is corrected by a factor that is the ratio of the shaded area under the curve to the entire area under the curve. The determination of $p_e - \bar{p}$ is then routine and one proceeds by either method outlined above.

When care is taken the visual graphical estimates yield relatively accurate results.

5 — In the strictest sense, the formula for computation of permeability only applies to incompressible fluids. For all practical purposes, water fulfills this requirement. However, in case oil is produced with no major escape of gas during the test, in other words a single-phase product, the formula might still be useful. In that case it becomes necessary to determine a different viscosity value, giving proper regard to type of crude oil produced and temperature of the formation. Viscosity Chart P1-2.00 is then of no further use.

ACKNOWLEDGMENTS

This paper is a more elaborate treatment of a method originally outlined by Mr. Clifford A. Balster, of the Rocky Mountain Producing Division of The Pure Oil Company. Drs. George Thodos and L. F. Stutzman, of Northwestern University, are largely responsible for the analytical treatment of the problem. Messrs. Karl A. Mygdal and Norman L. Thomas of the Chicago Geological Department of The Pure Oil Company critically read the manuscript and made many helpful suggestions.

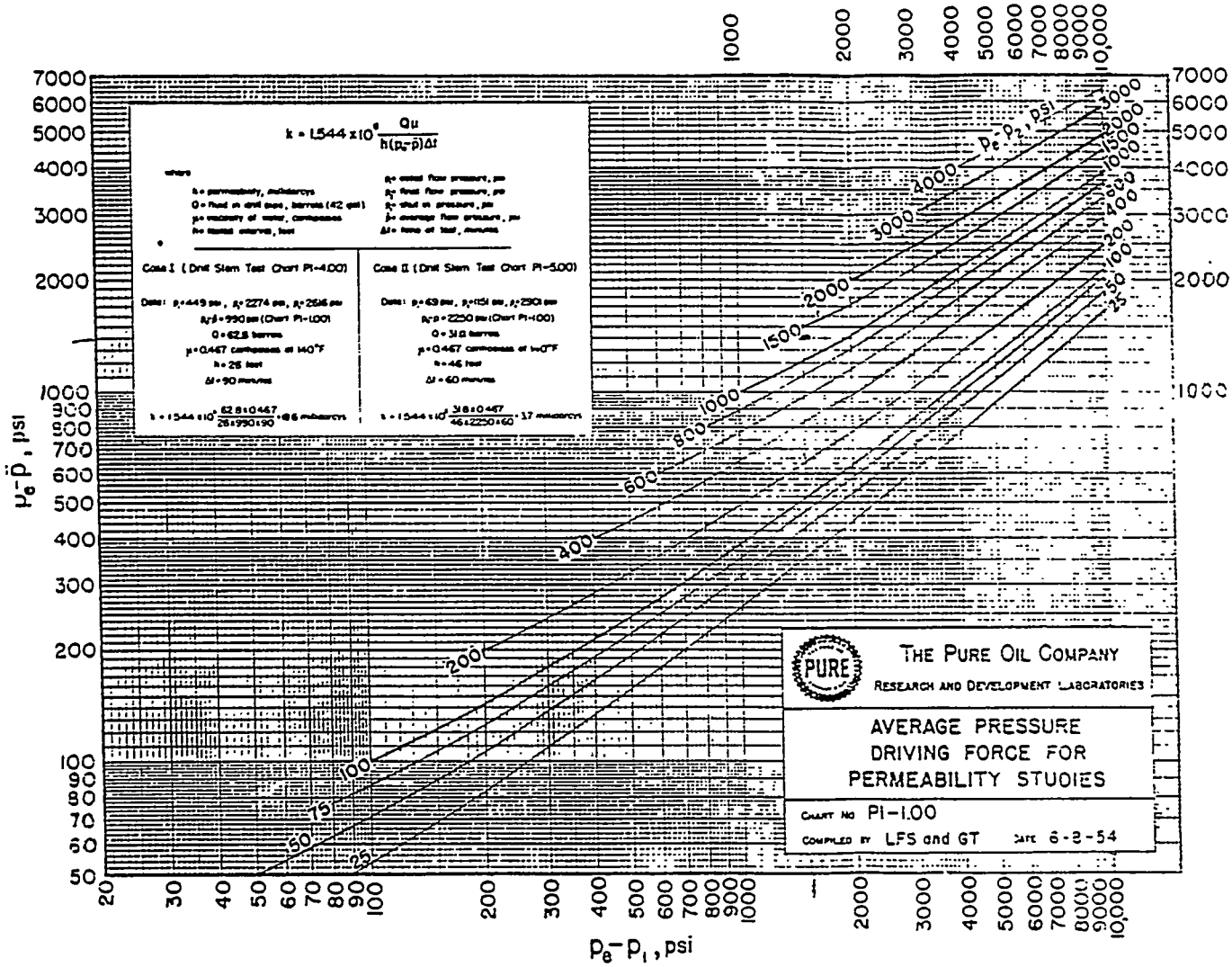
$k = 1.544 \times 10^{6} \frac{Q\mu}{h(p_e - \bar{p})\Delta t}$
where
h = permeability, millidarcys
Q = fluid in drill pipe, barrels (42 gal)
μ = viscosity of water, centipoises
h = tested interval, feet
p_e = initial flow pressure, psi
p_i = final flow pressure, psi
p_s = shut in pressure, psi
$\bar{p}$ = average flow pressure, psi
Δt = time of test, minutes
Case I (Drill Stem Test Chart PI-4.00)
Data: p_e = 449 psi, p_i = 2274 psi, p_s = 2516 psi
$p_s - \bar{p}$ = 990 psi (Chart PI-1.00)
Q = 62.8 barrels
μ = 0.467 centipoises at 140°F
h = 26 feet
Δt = 90 minutes
$k = 1.544 \times 10^{6} \frac{62.8 \times 0.467}{26 \times 990 \times 90} = 8.6$ millidarcys
Case II (Drill Stem Test Chart PI-5.00)
Data: p_e = 63 psi, p_i = 1151 psi, p_s = 2301 psi
$p_s - \bar{p}$ = 2250 psi (Chart PI-1.00)
Q = 31.0 barrels
μ = 0.467 centipoises at 140°F
h = 46 feet
Δt = 60 minutes
$k = 1.544 \times 10^{6} \frac{31.0 \times 0.467}{46 \times 2250 \times 60} = 1.7$ millidarcys
$p_e - p_i$, psi
$p_e - \bar{p}$, psi
THE PURE OIL COMPANY
RESEARCH AND DEVELOPMENT LABORATORIES
AVERAGE PRESSURE
DRIVING FORCE FOR
PERMEABILITY STUDIES
CHART NO PI-1.00
COMPILED BY LFS and GT
DATE 6-2-54

THE PURE C COMPANY
RESEARCH AND DEVELO LABORATORIES

INTERNAL VOL E OF DRILL PIPE

CHART NO. PI-3.00
COMPILED BY LFS and GT DATE 6-10-54

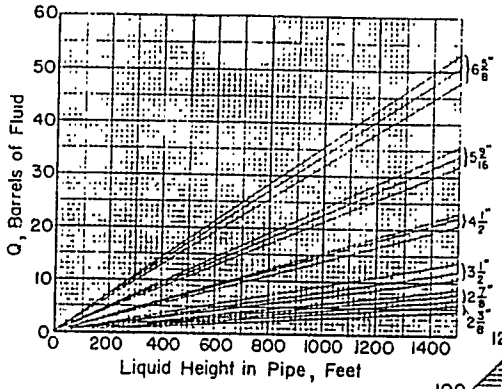

Internal Volume of API Drill Pipe
with API Tool Joints
(Zaba and Doherty)

* Commonly Used

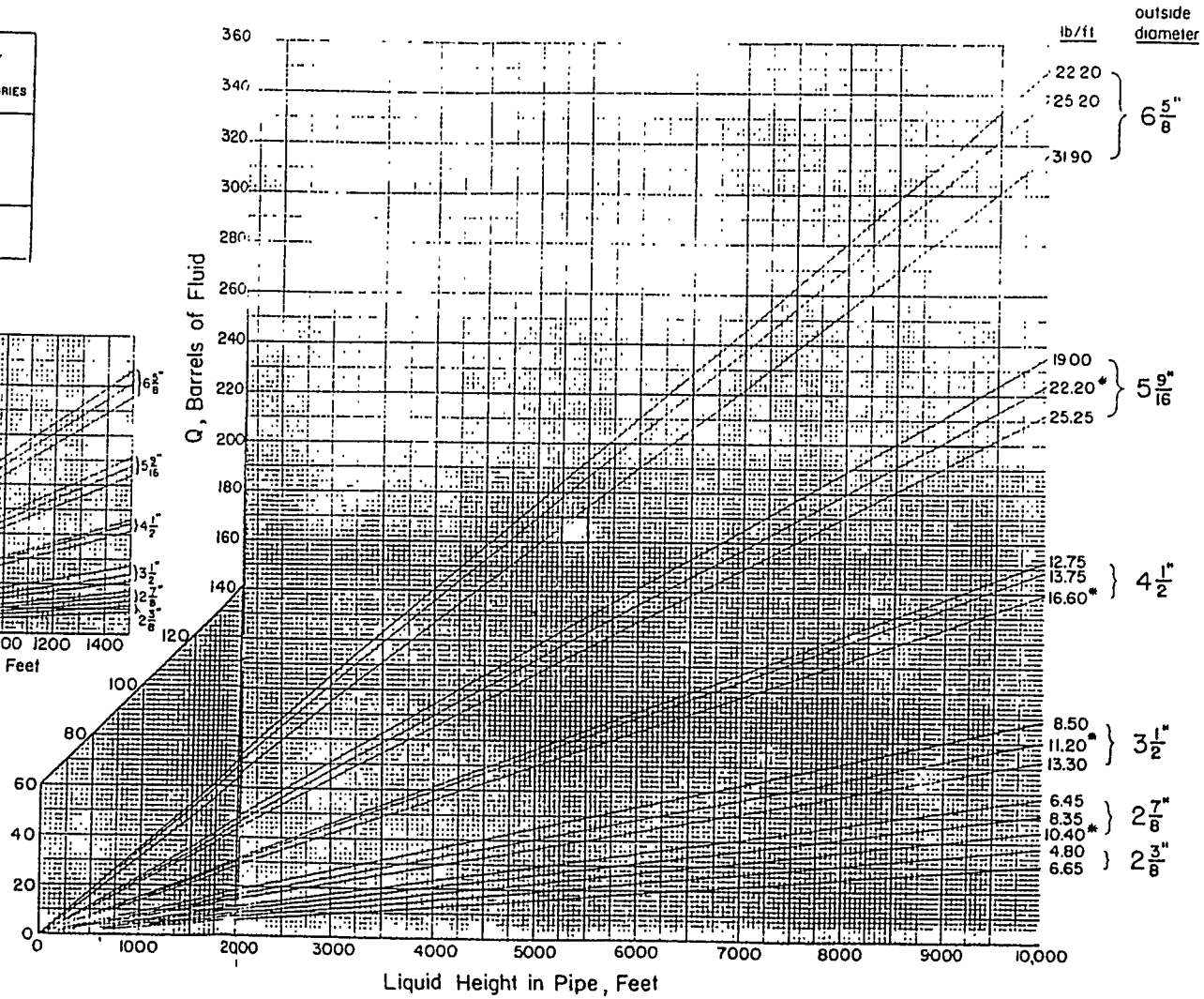

ATTACHMENTS

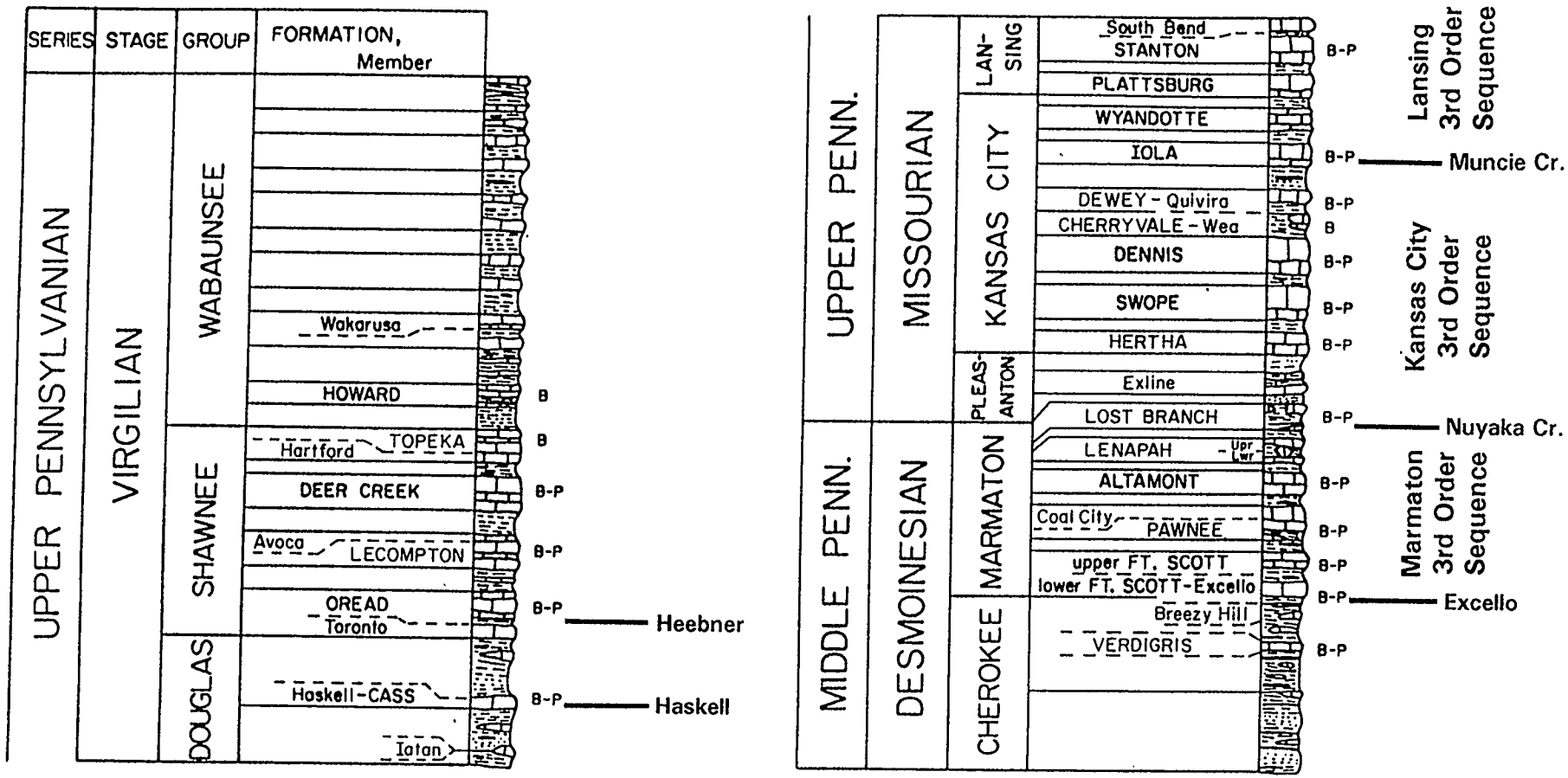

Figure I.1. Stratigraphic section of Middle and Upper Pennsylvanian in Kansas adapted from Heckel (1991). Each formation corresponds roughly to a single cyclothem. Positions of widespread phosphatic black shales are delimited by "B-P", black shales by "B". In addition to formal stratigraphic nomenclature, a new subdivision of 3rd-order sequences is identified in this report. These third-order sequences are distinguished by name -- Marmaton, Kansas City, and Lansing and major bounding marine markers -- Excello Shale, Nuyaka Creek Shale, and Muncie Creek Shale. The Heebner and Haskell shales are both noted because upper boundary of the Lansing 3rd-order appears to be transitional between them.

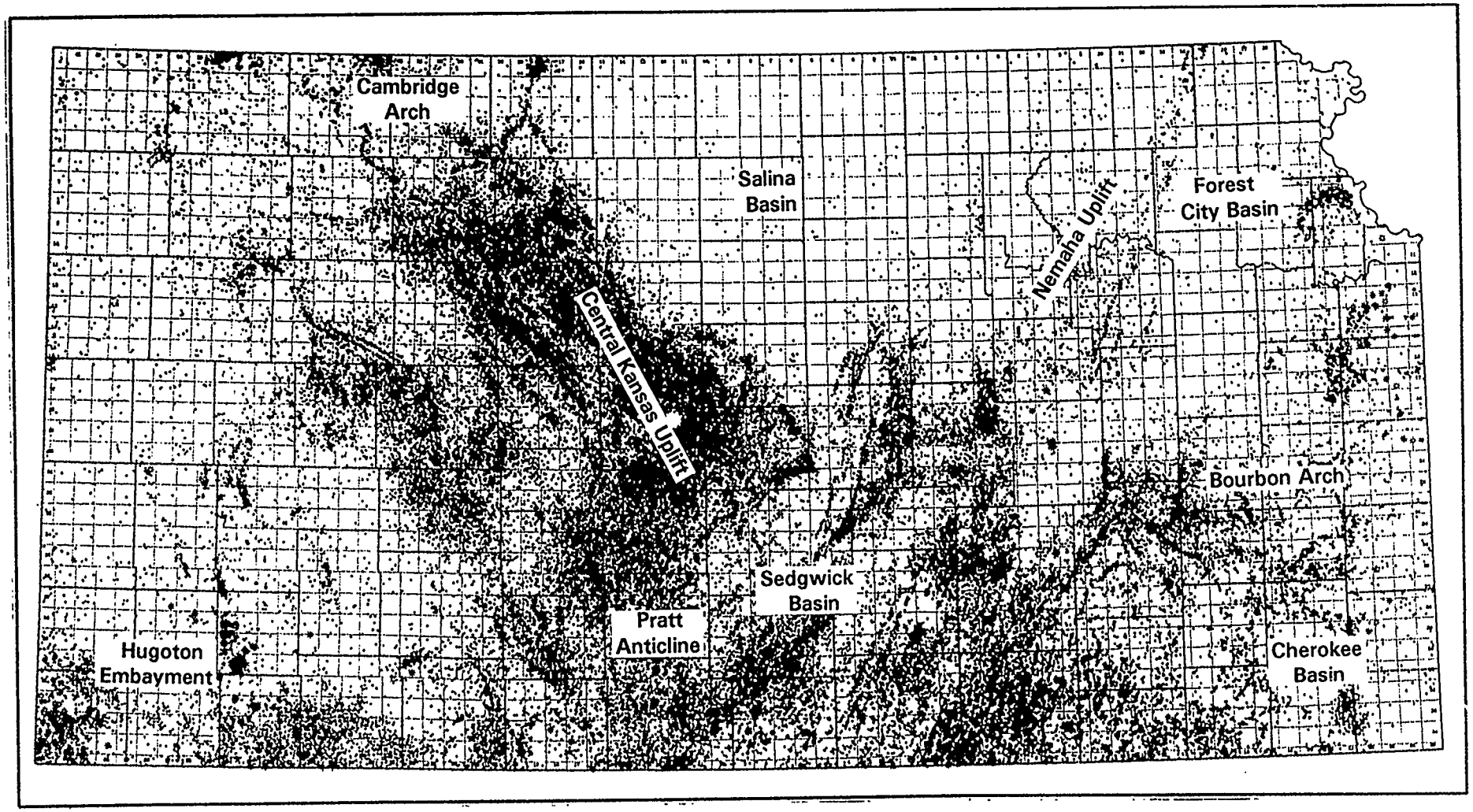

Figure I.2. Wells penetrating and producing from the Lansing-Kansas City (LKC) in Kansas. Darker wells are producing from LKC. Lighter wells are dry penetrations.

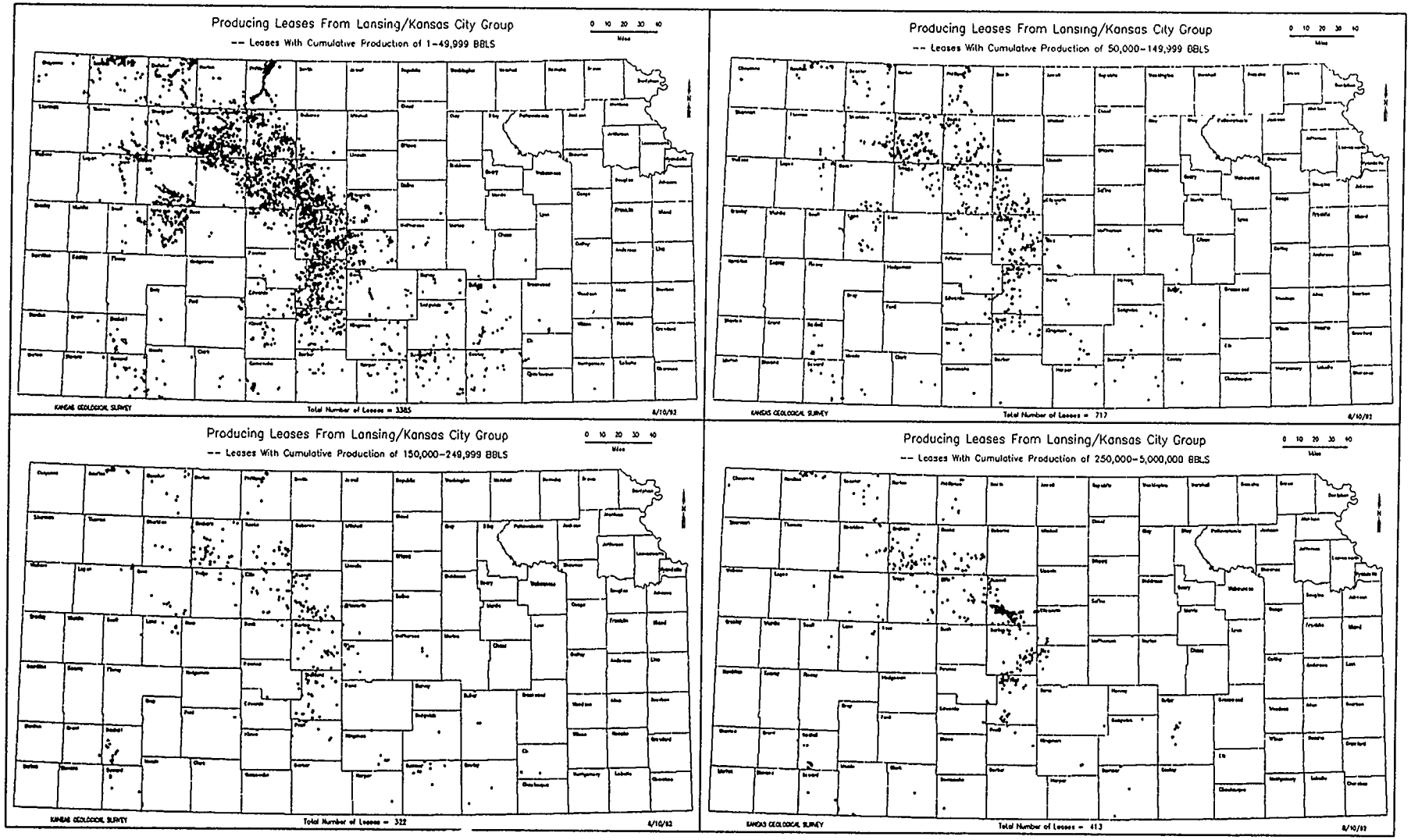

Figure I.3. Distribution of single pay leases from LKC by cumulative production (by Beene and Wong, Kansas Geological Survey, 1992). Included are leases that realized production during period between 1965 and present. Total lease count is 4839. Median cumulative production per lease is 29,011 barrels. Mean cumulative production per lease is 98,214. Total production for this group of leases is 475 million barrels.

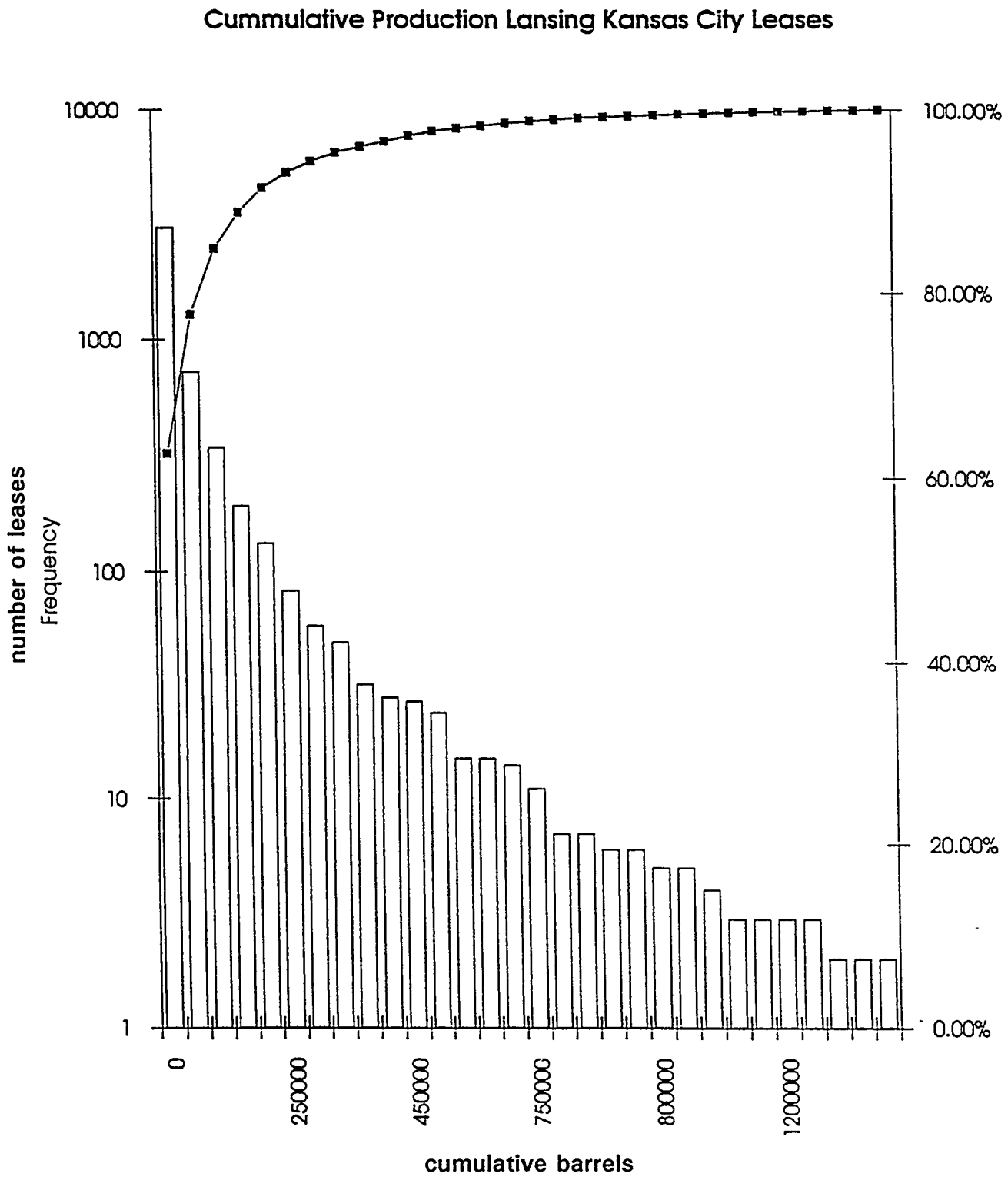

Figure I.4. Cumulative frequency distribution of production of single pay leases producing from LKC in Kansas during the period 1965 to present.

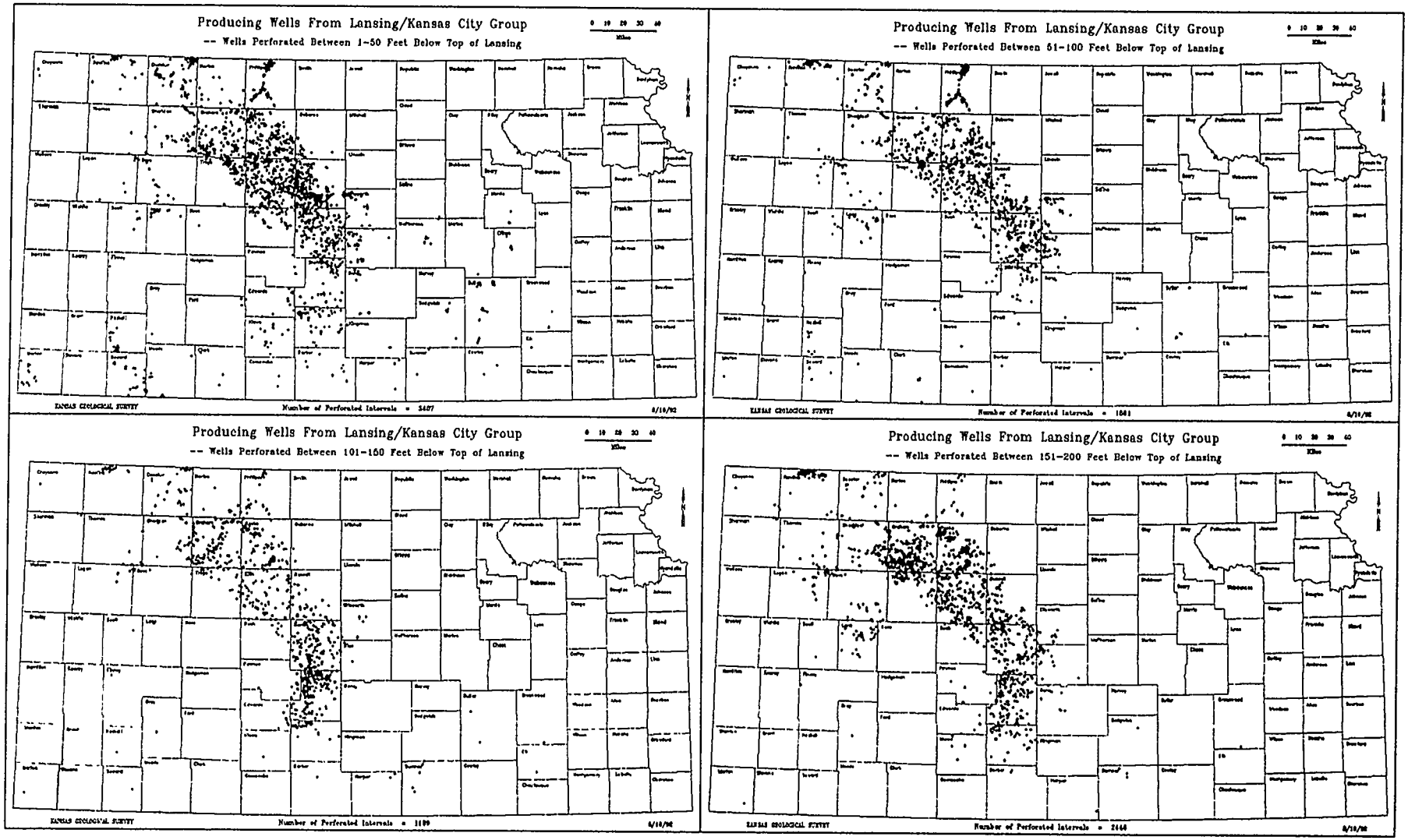

Figure I.5. Depth of perforated interval below the top of the Lansing Group for wells producing from LKC.

a

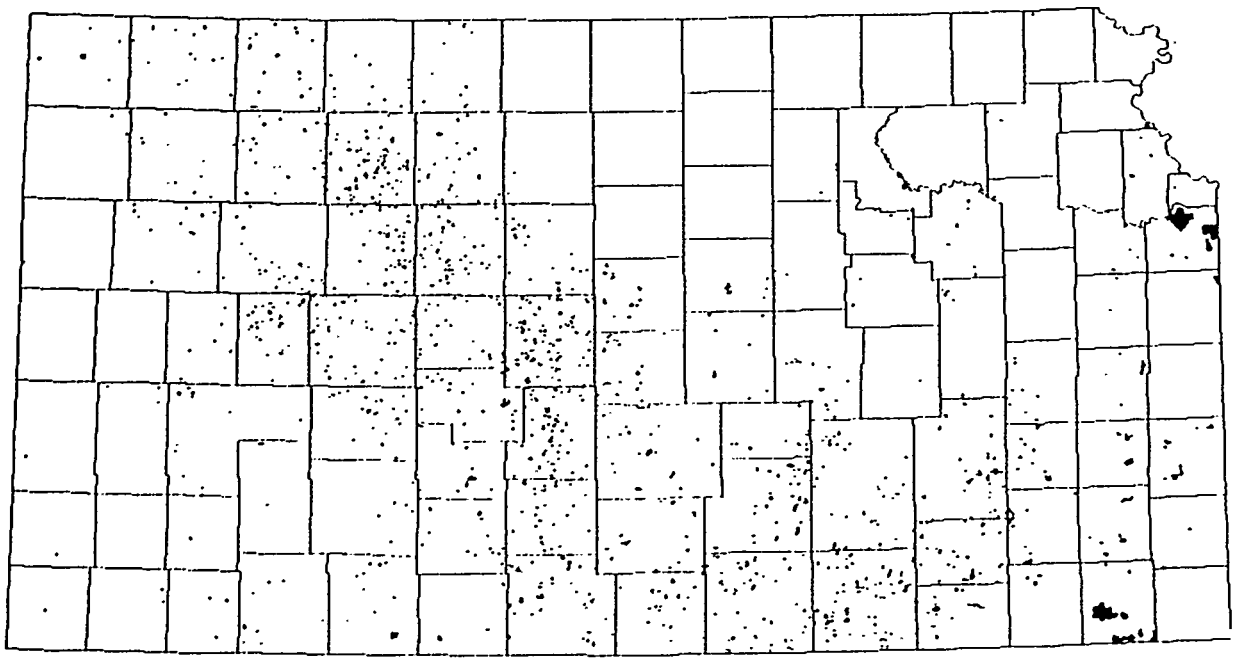

b

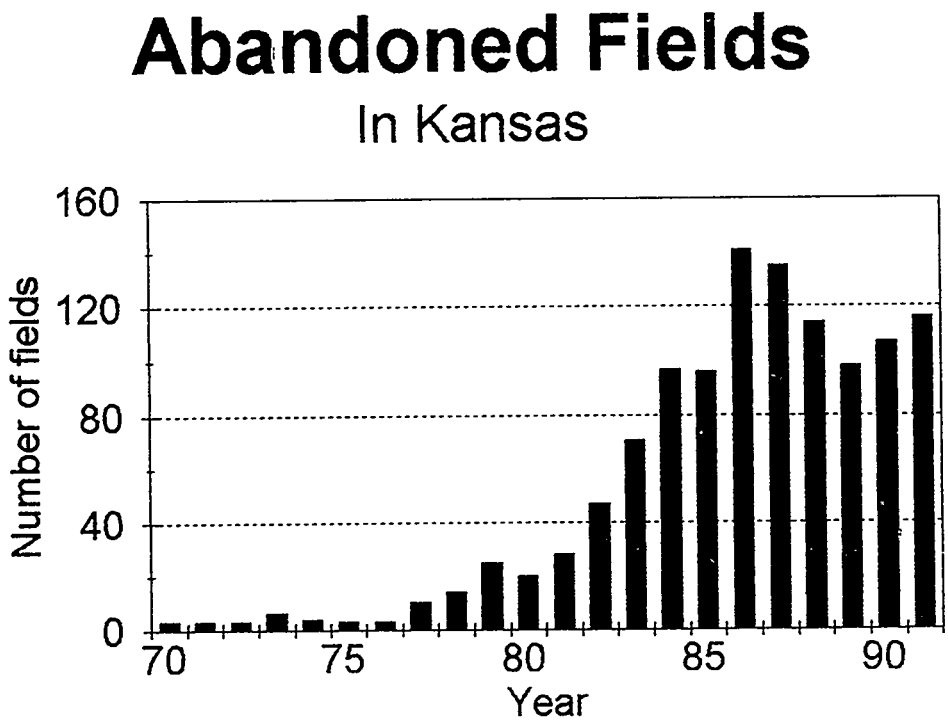

Figure I.6. a) Preliminary map showing oil fields in Kansas that have had no reported production for 1989 and 1990 (considered abandoned). (prep. by G. Ross, Ks. Geol. Survey, 1992). b) Number of oil fields abandoned in Kansas by year (from D. Beene, 1992).

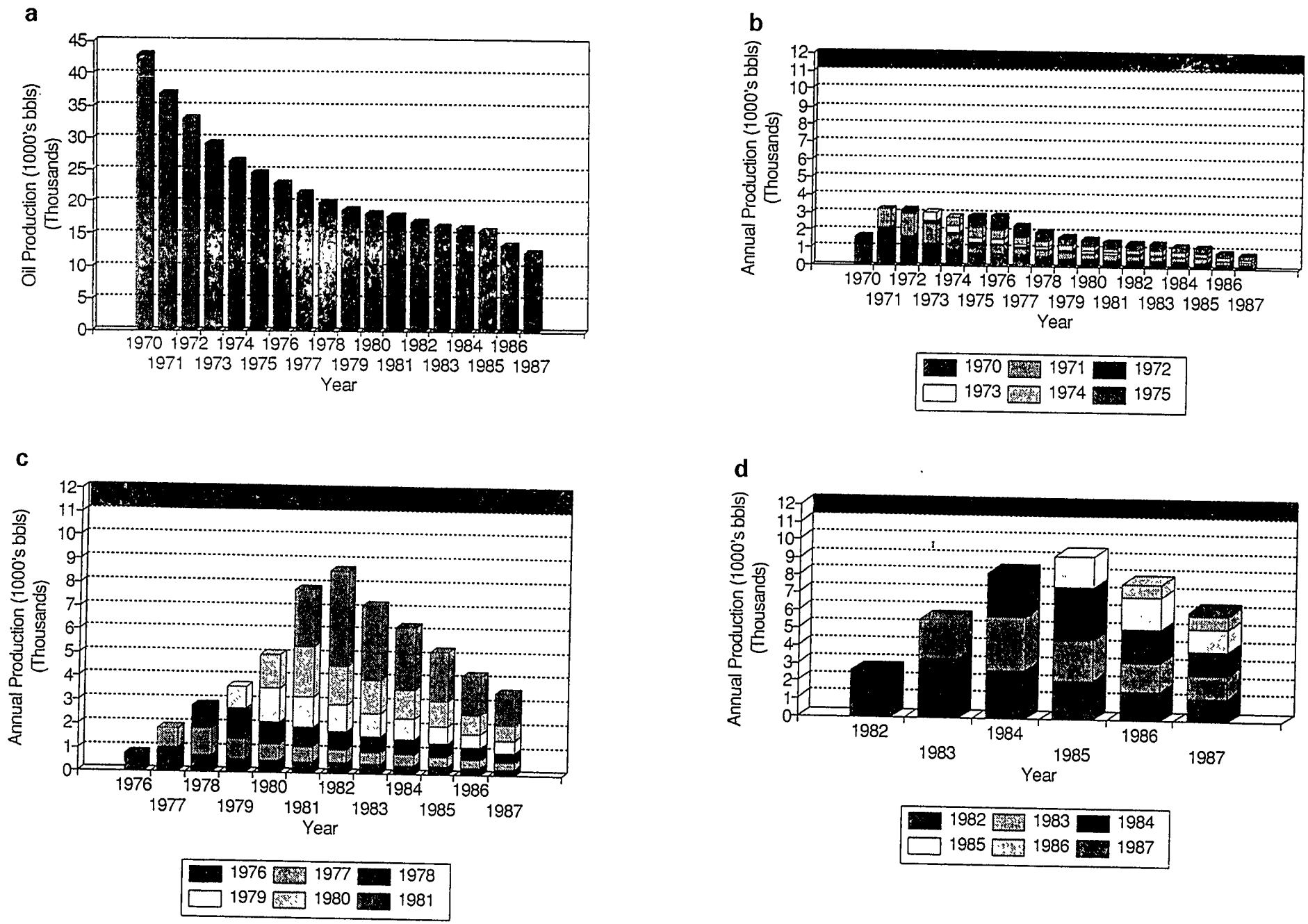

Figure I.7. Crude oil production plots for leases on the Central Kansas uplift showing performance of new leases added each year since 1970 compared to performance of leases placed on production before 1970: a) pre-1970 leases, b) new leases during 1970-1975, c) new leases during 1976-1981, d) new leases during 1982-1987. Information prepared by D. Collins, Kansas Geological Survey, 1991.

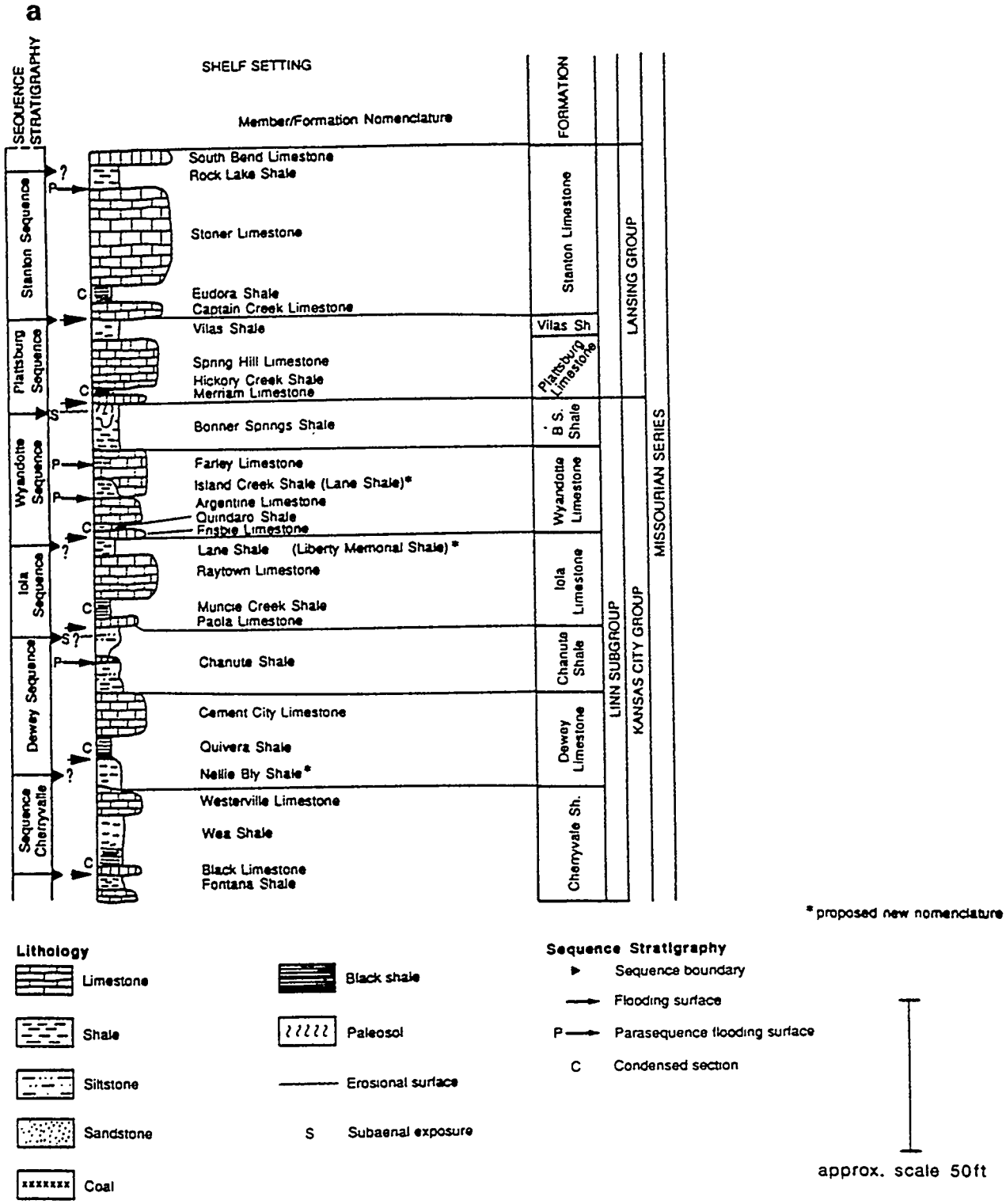

Figure I.8. Detailed stratigraphic chart for Lansing-Kansas City in Kansas including formal stratigraphic nomenclature and sequence stratigraphic information. Note especially Dewey, Cherryvale, Dennis, Swope, Hertha, and Pleasanton sequences. These are 4th-order depositional sequences bounded by unconformities (see symbol legend). Section divided into a), b), and c). C) shows the siliciclastic basinal equivalent of carbonate-dominated Hertha and Swope sequences on the shelf developed in southern Kansas.

b

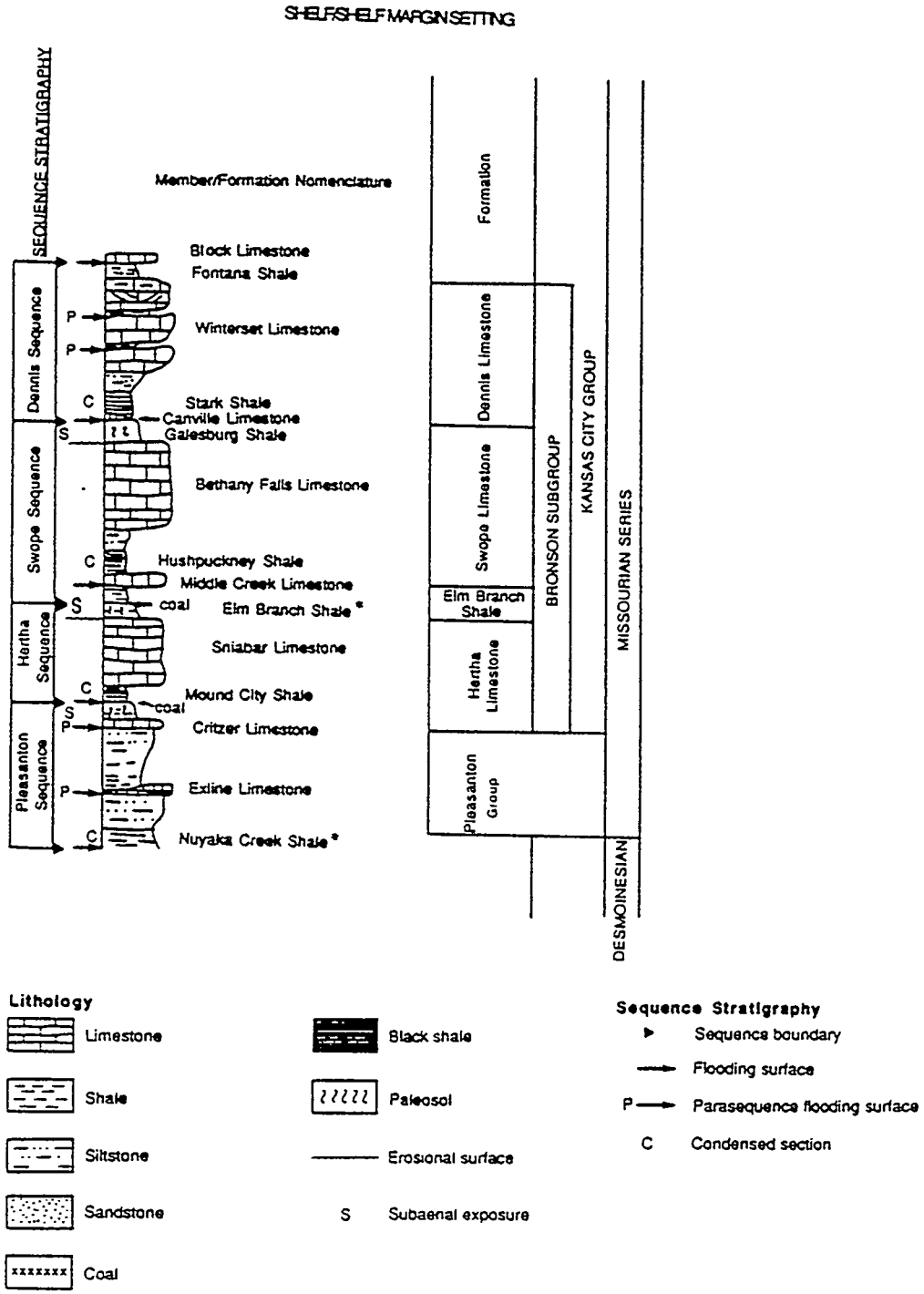

Figure I.8 (b). Continuation of Figure I.8.

C

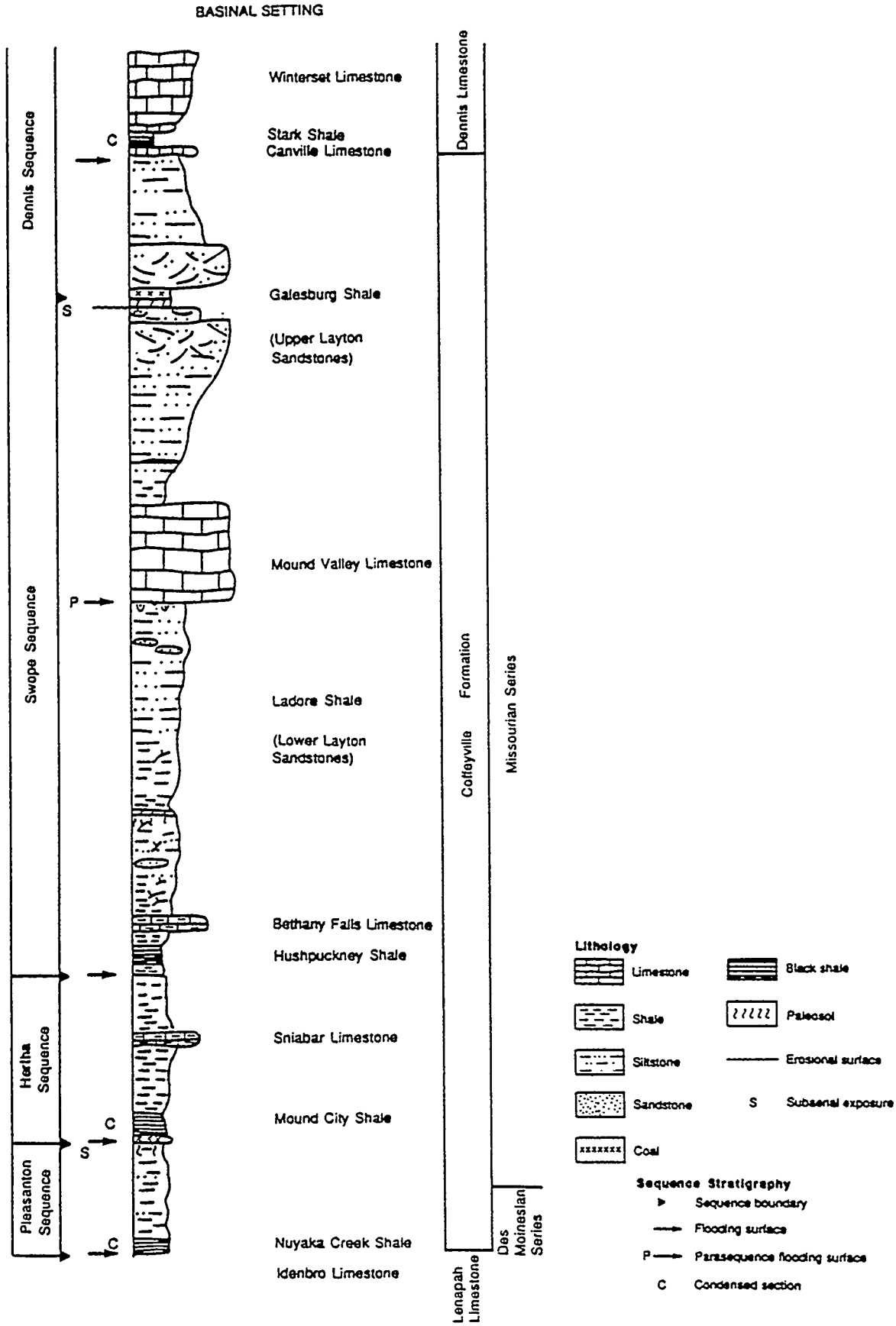

Figure I.8 (c). Continuation of Figure I.8.

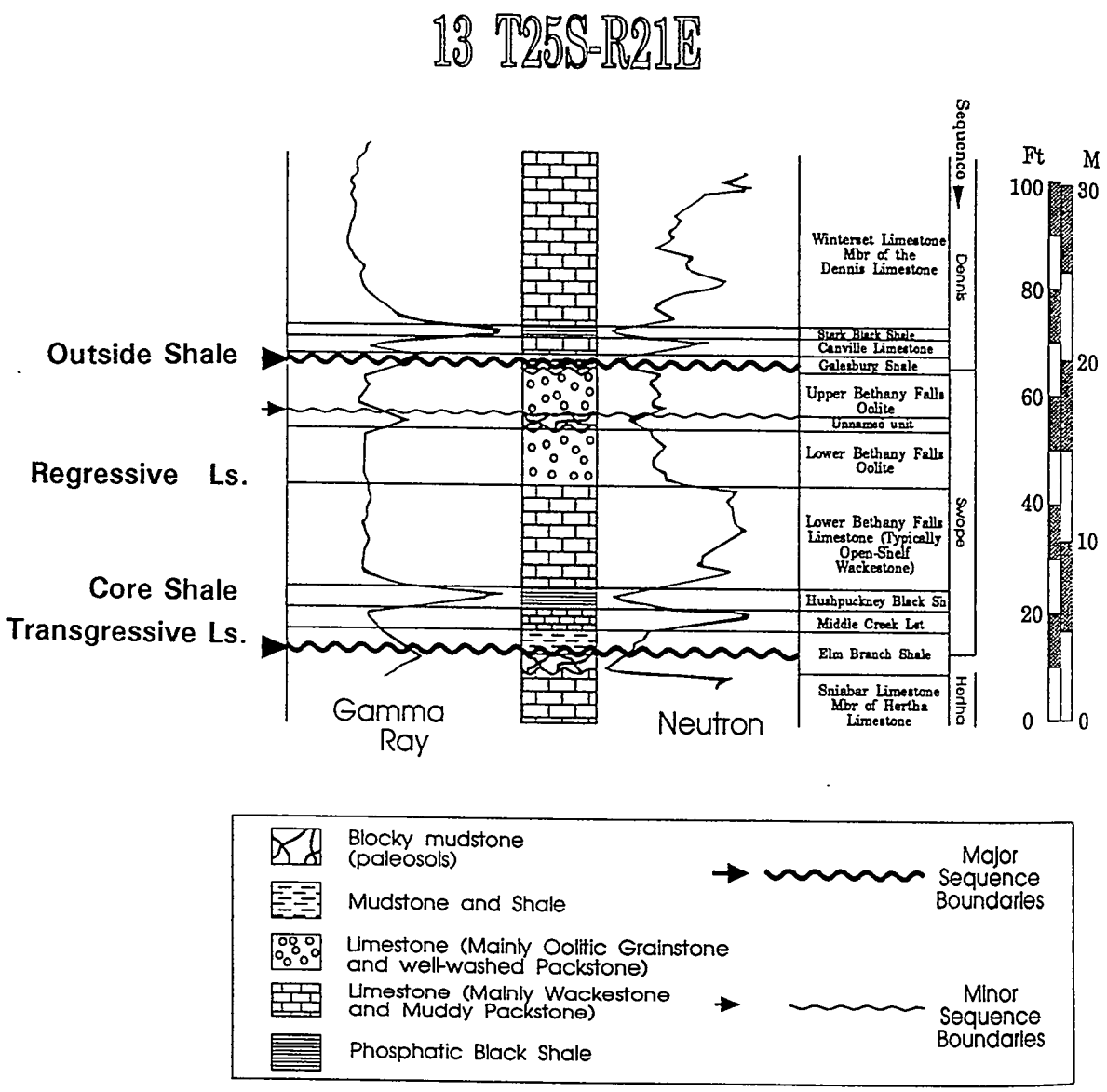

Figure I.9. Wireline log/core of portion of Hertha through Dennis formations from southeastern Kansas with identification of cyclothem components -- transgressive limestone (Middle Creek Limestone), core shale (Hushpuckney Shale), regressive limestone (Bethany Falls Limestone), outside shale (Galesburg Shale).

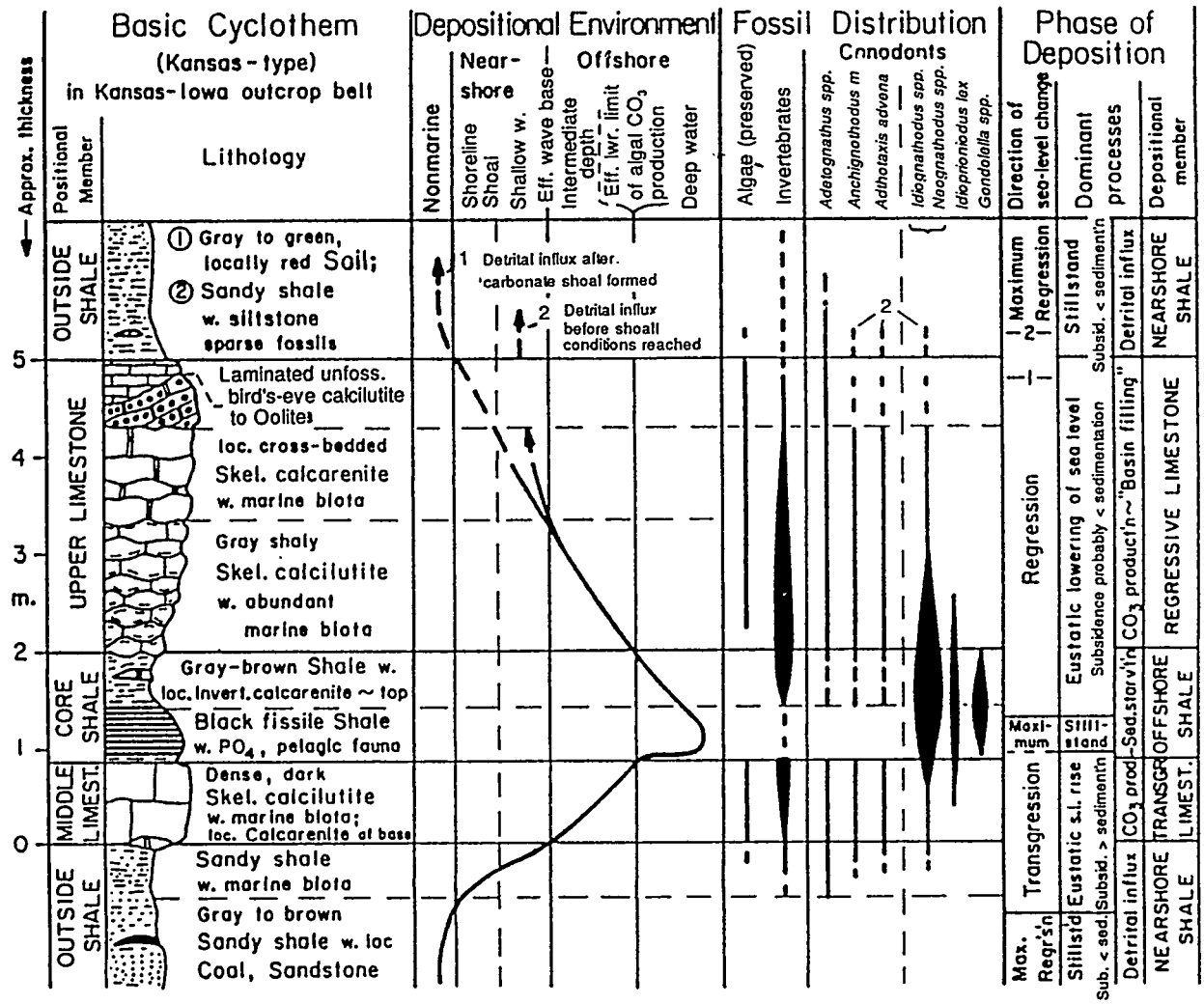

Figure I.10. Basic Kansas cyclothem characterizing carbonate-dominated strata in the northern Midcontinent shelf (from Heckel, 1977).

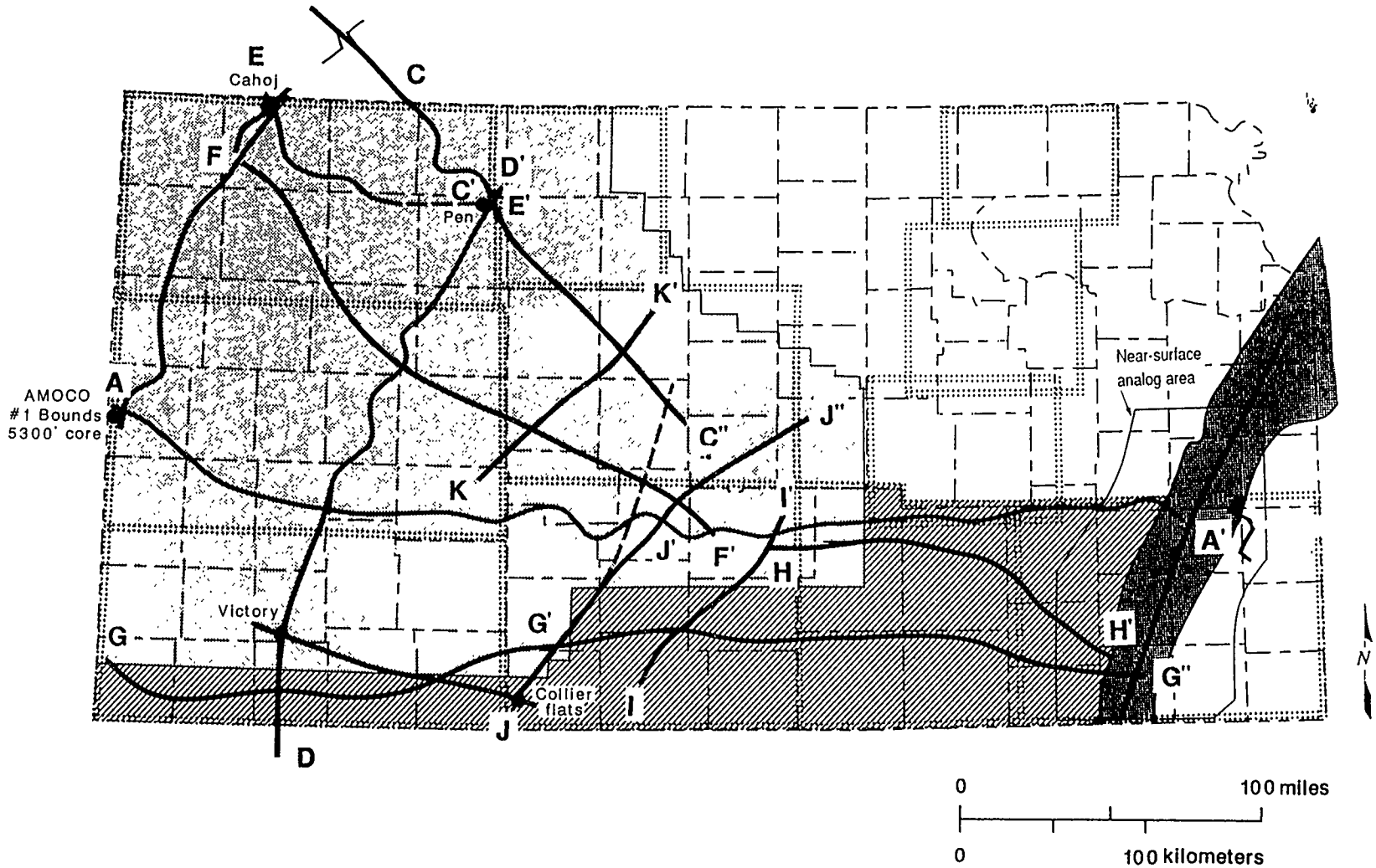

Figure I.11. Project map. Blocked shaded area and near-surface analog area are covered by sequence datasets developed in this project and linked for regional mapping. Analog study sites and oil fields that were examined are shown. Index lines are shown for regional surface-to-basement wireline log cross sections.

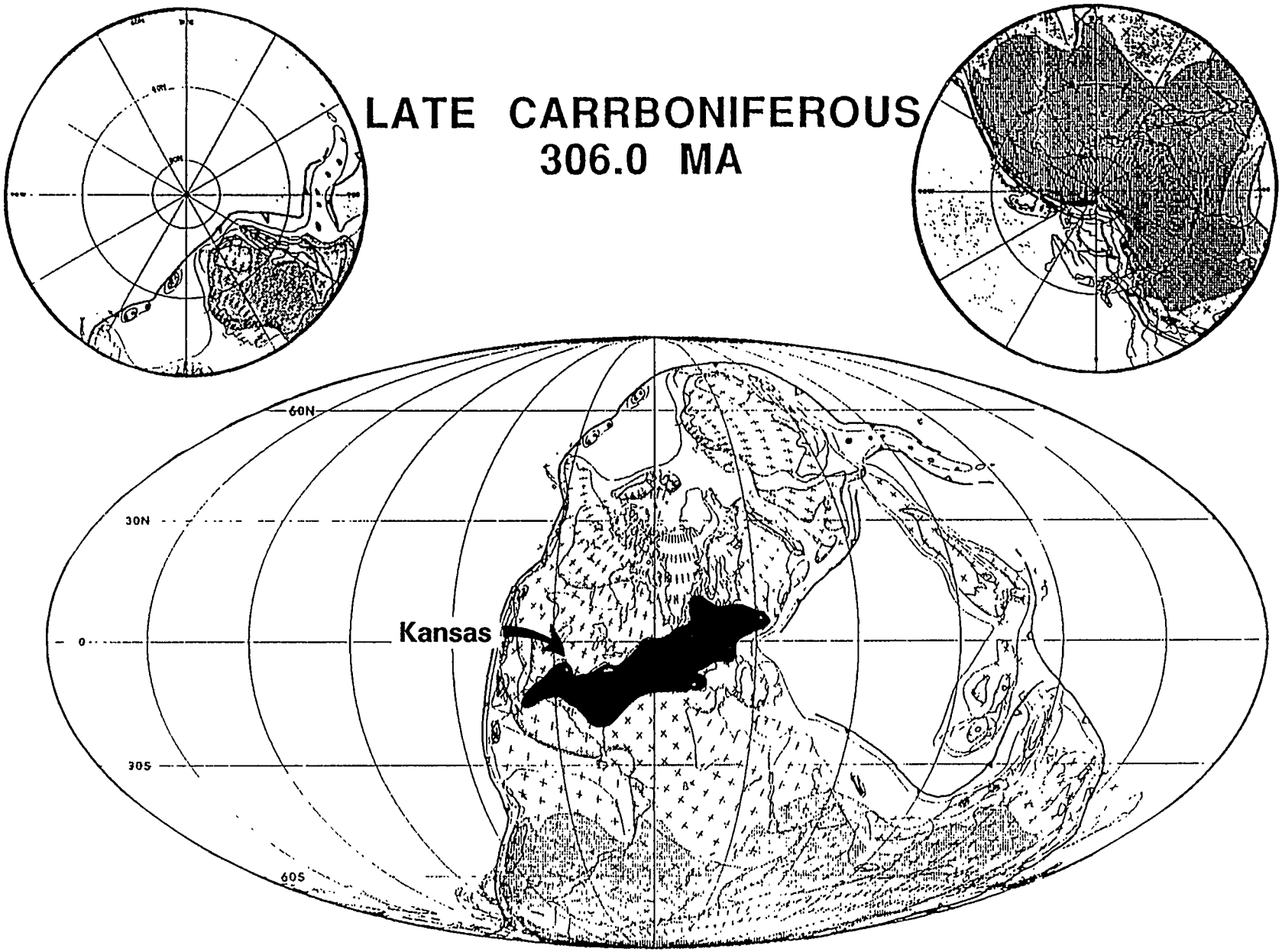

Figure I.12. Late Carboniferous paleogeography showing global siting of Kansas lying north of an active tectonic zone (including Ouachita mountains), shown here as the black region corresponding to suture of Laurasia and Gondwana to form the supercontinent, Pangea (modified from Scotese and Golonka, 1992).

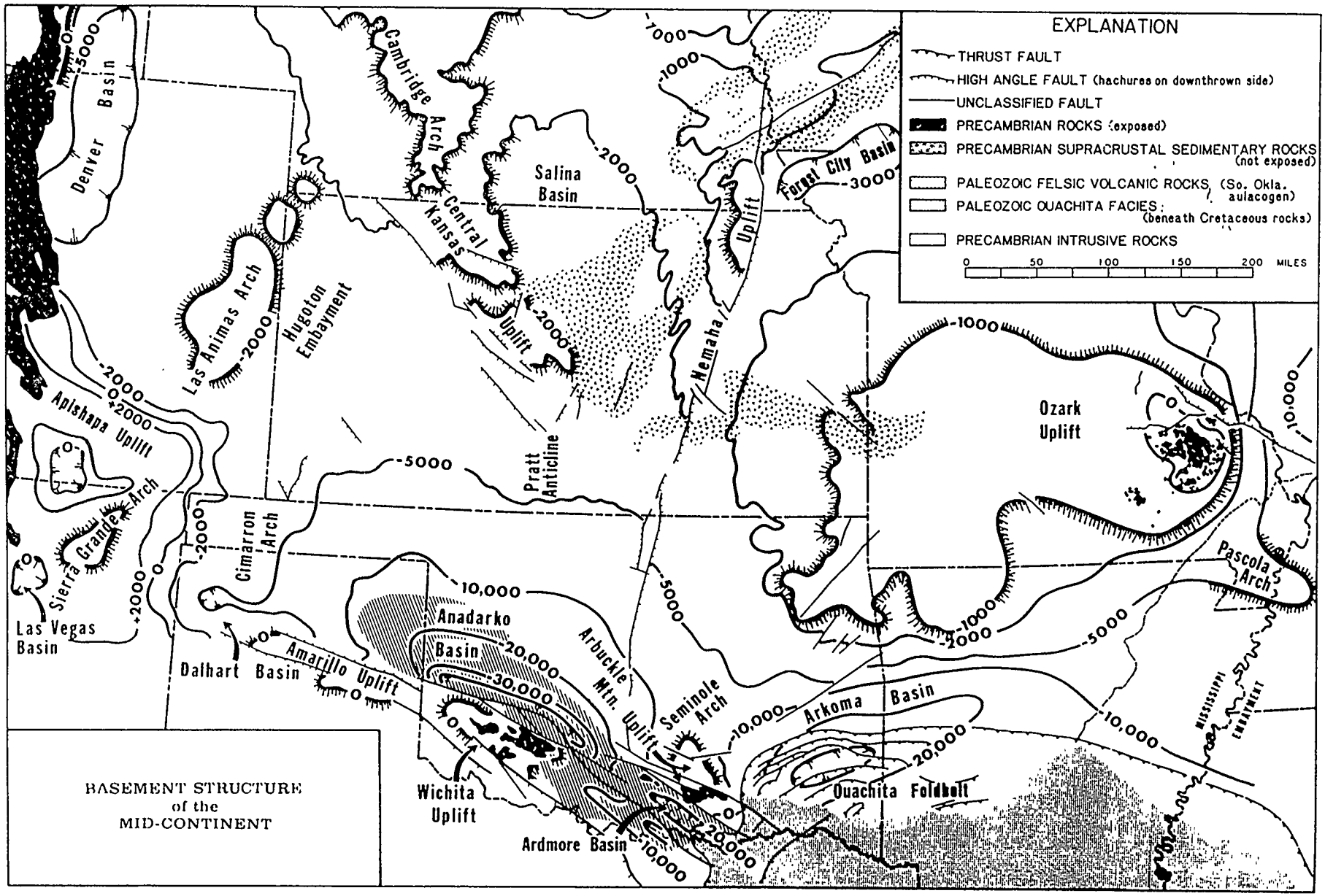

Figure I.13. Basement structure of the Midcontinent (from Rascoe and Adler, 1983).

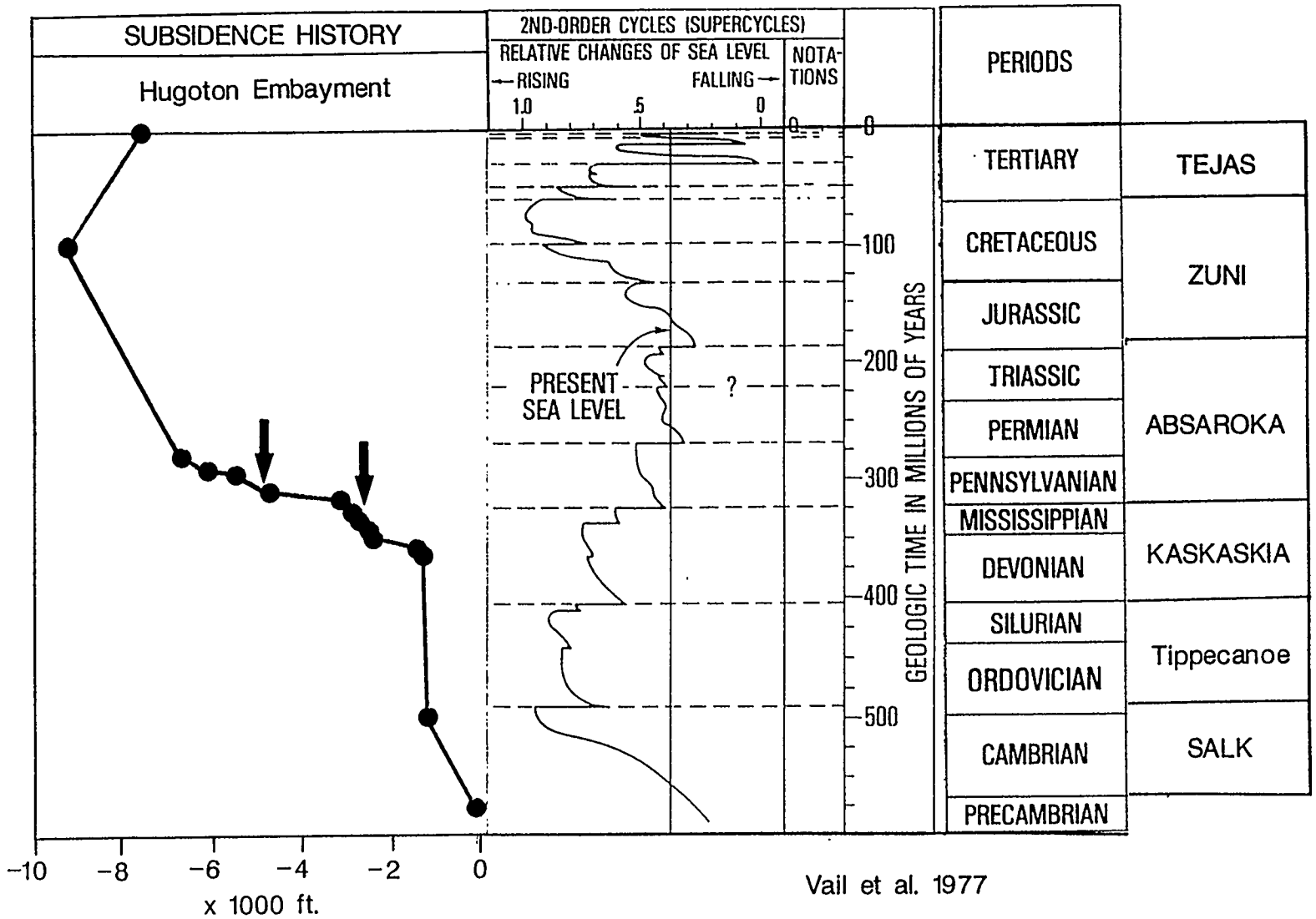

Figure I.14. Subsidence plot of basement versus time for well in Hugoton embayment in southwest Kansas accompanied by coastal onlap curve of Vail et al. (1977). Sloss (1963) cratonic sequences are identified on the right margin. Arrows on subsidence plot identify Pennsylvanian through Missourian Stage interval.

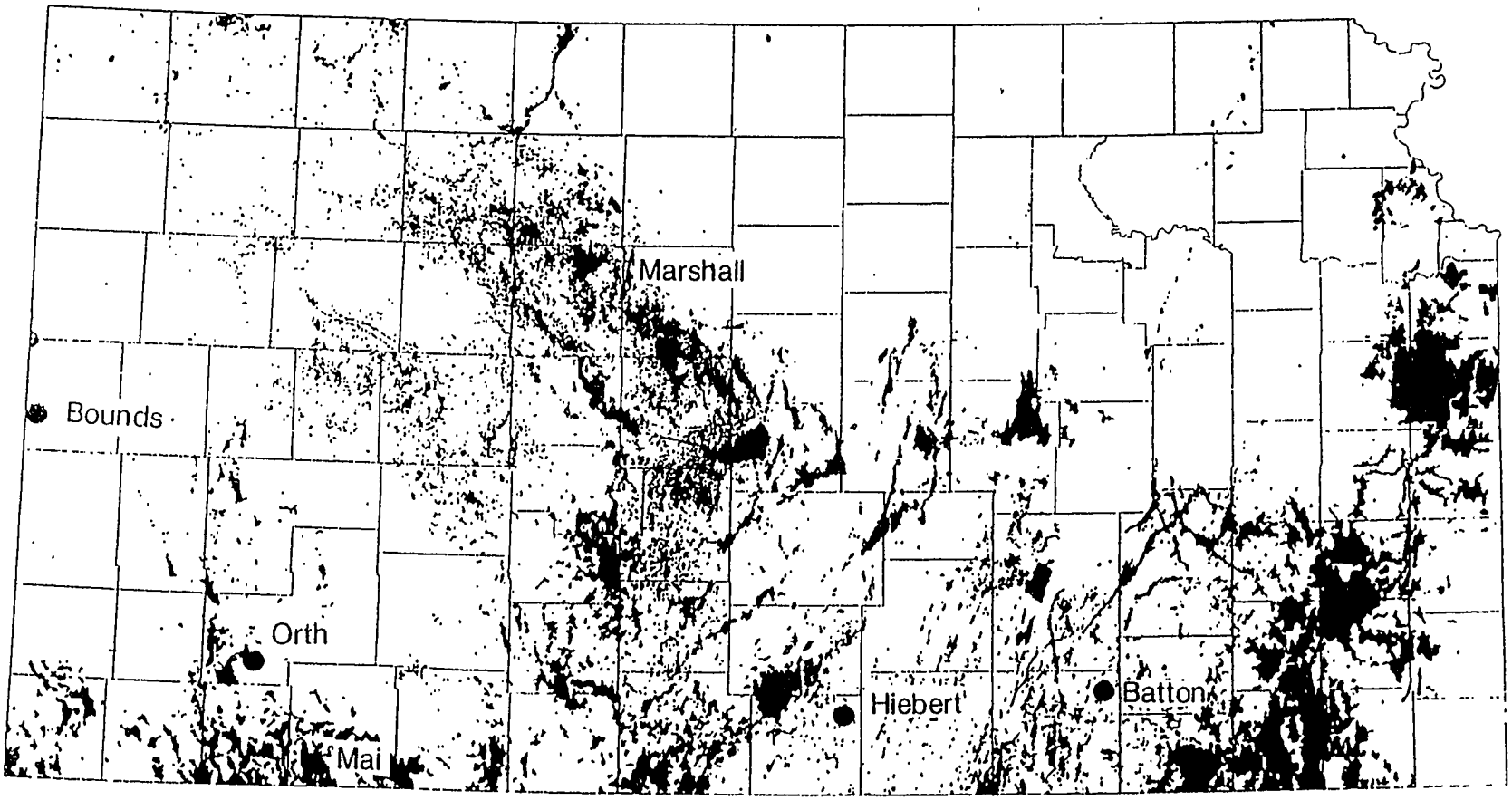

SUBSIDENCE STUDY

Figure I.15. Wells used in backstripped (decompaction) subsidence analysis.

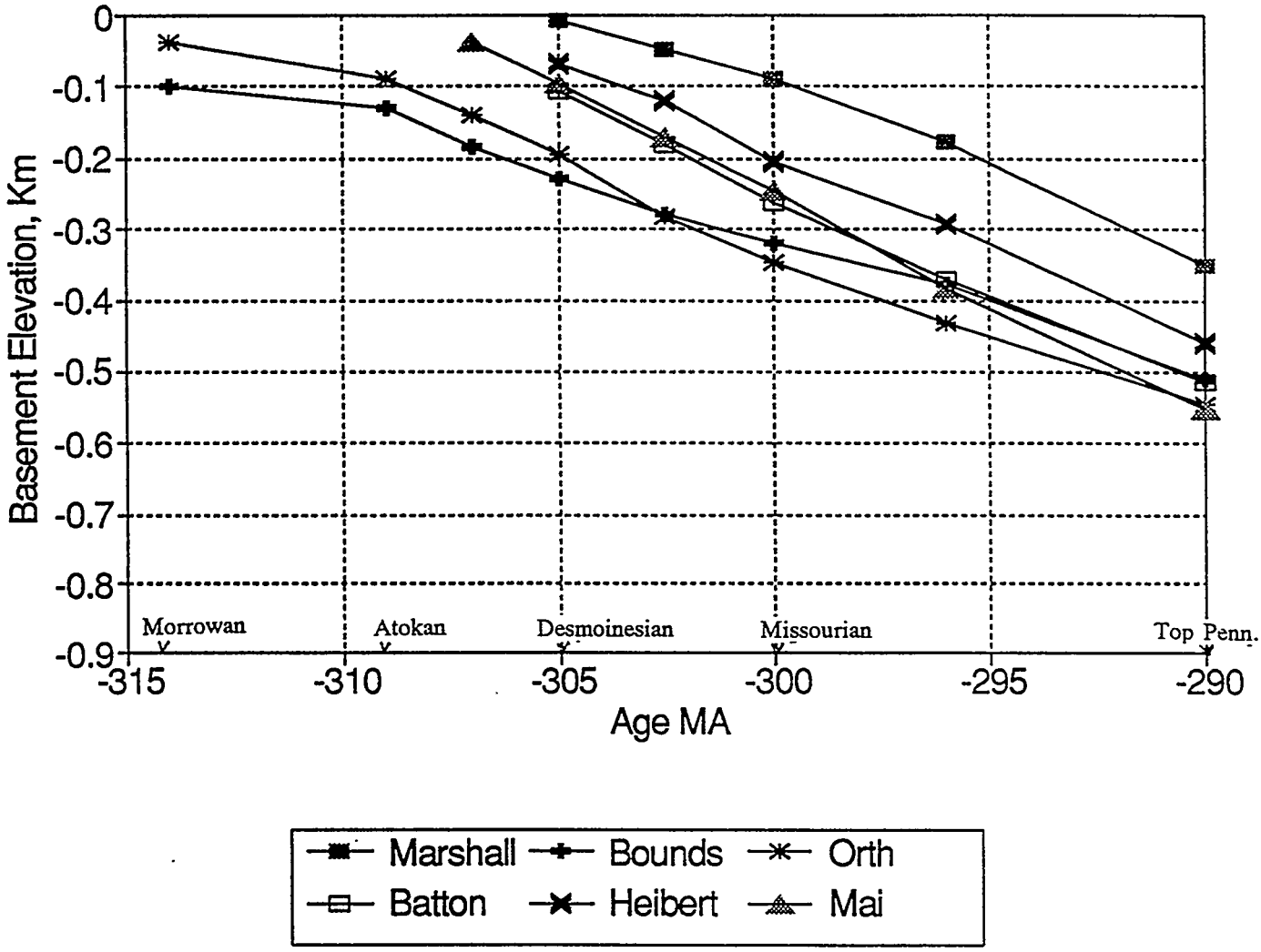

Figure I.16. Basement depth vs. time plot for six wells (shown on map in Figure I.15) using backstripping technique. Shape of curve is convex upward indicative of foreland basin-type subsidence.

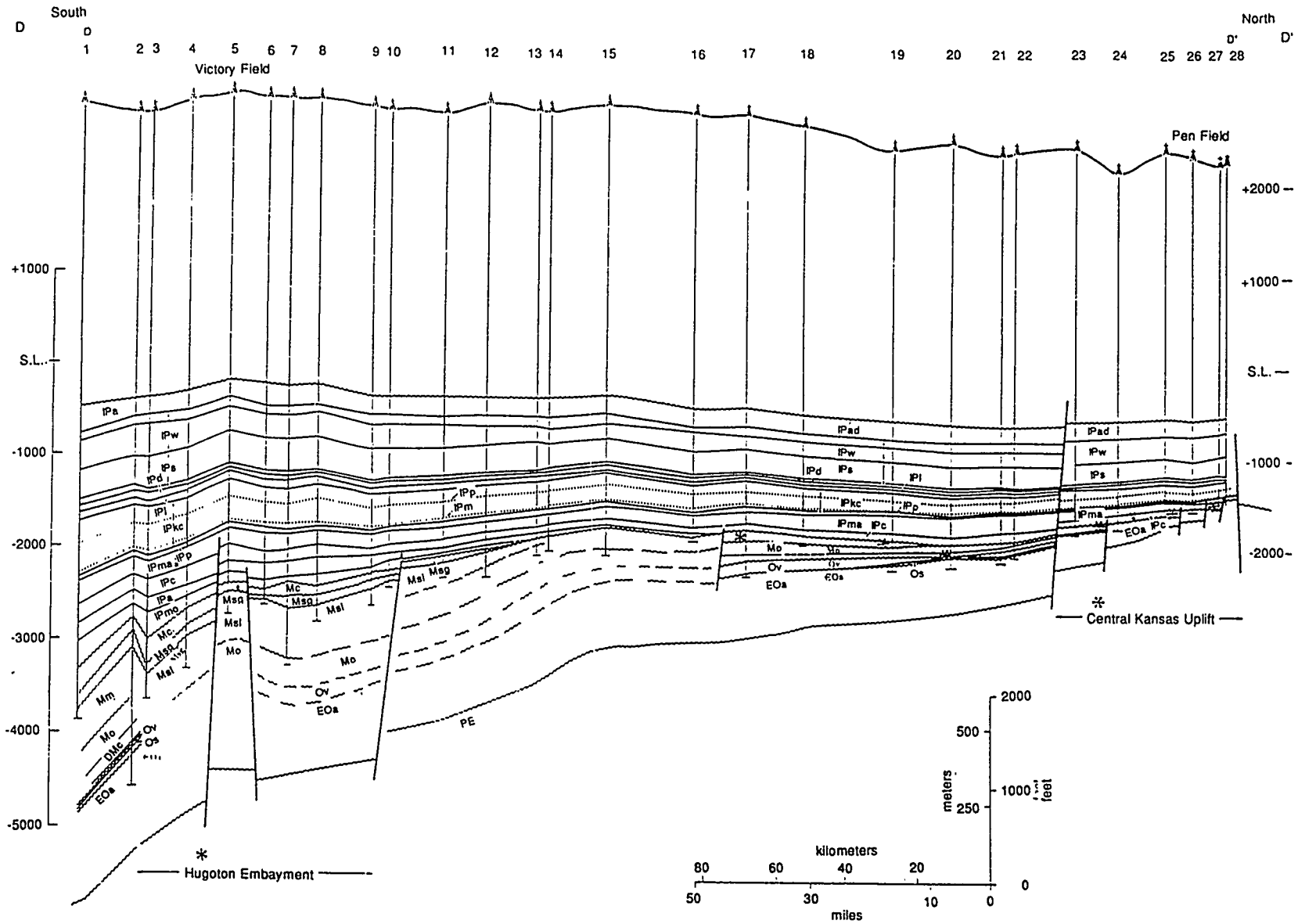

Figure I.17. South-to-north regional structural cross section D-D' prepared from well logs. Section extends from the northern margin of the Anadarko basin (lower shelf) to Central Kansas uplift (upper shelf). Note the locations of two of the field studies, Victory field in the south and Pen field on the north. Index for section is found in Figure I.11. Detailed discussion of can be found in section Subtask 2 B in this report

LITHOFACIES -- MARMATON GROUP

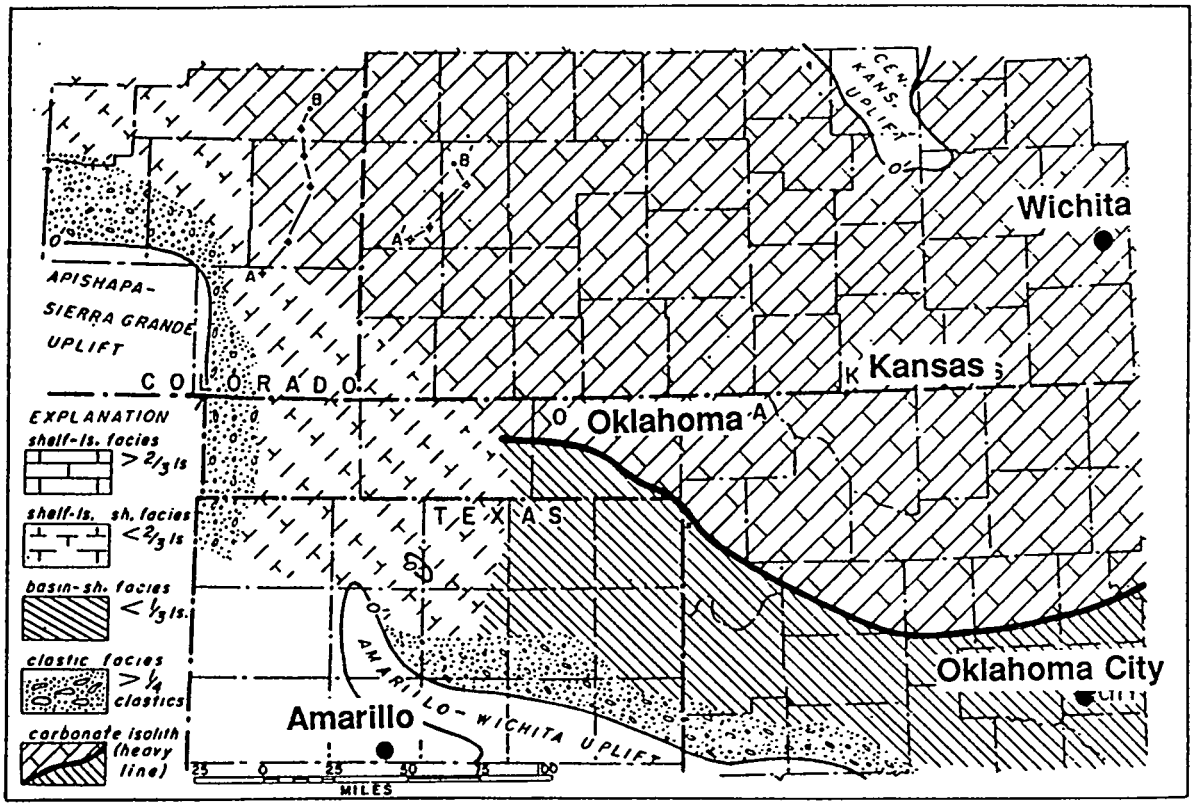

Rascoe (1962)

0 200
KM

Figure I.18. Lithofacies map of Marmaton Group (modified from Rascoe, 1962).

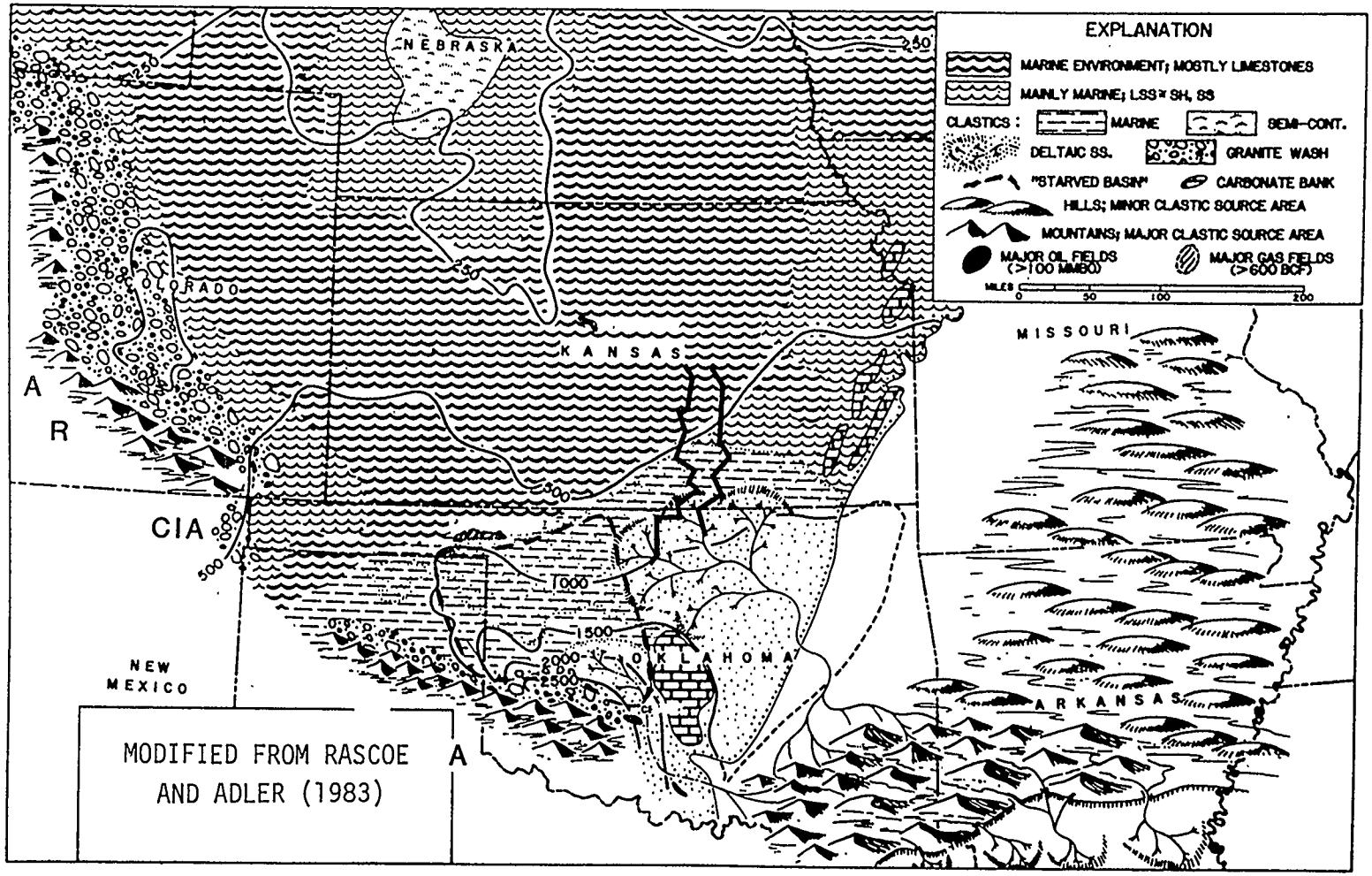

Figure I.19. Lithofacies and paleogeography of Missourian in the Midcontinent showing average conditions during this period. Dashed line in Anadarko basin indicates area of predominately deep water conditions base on work of Kumar and Slatt (1984). Map modified from Rascoe and Adler (1983). Note index lines identifying locations of cross sections shown in Figures I.24 and I.25.

LITHOFACIES -- DEWEY, CHERRYVALE, DENNIS, SWOPE, HERTHA (KANSAS CITY GROUP, MISSOURIAN)

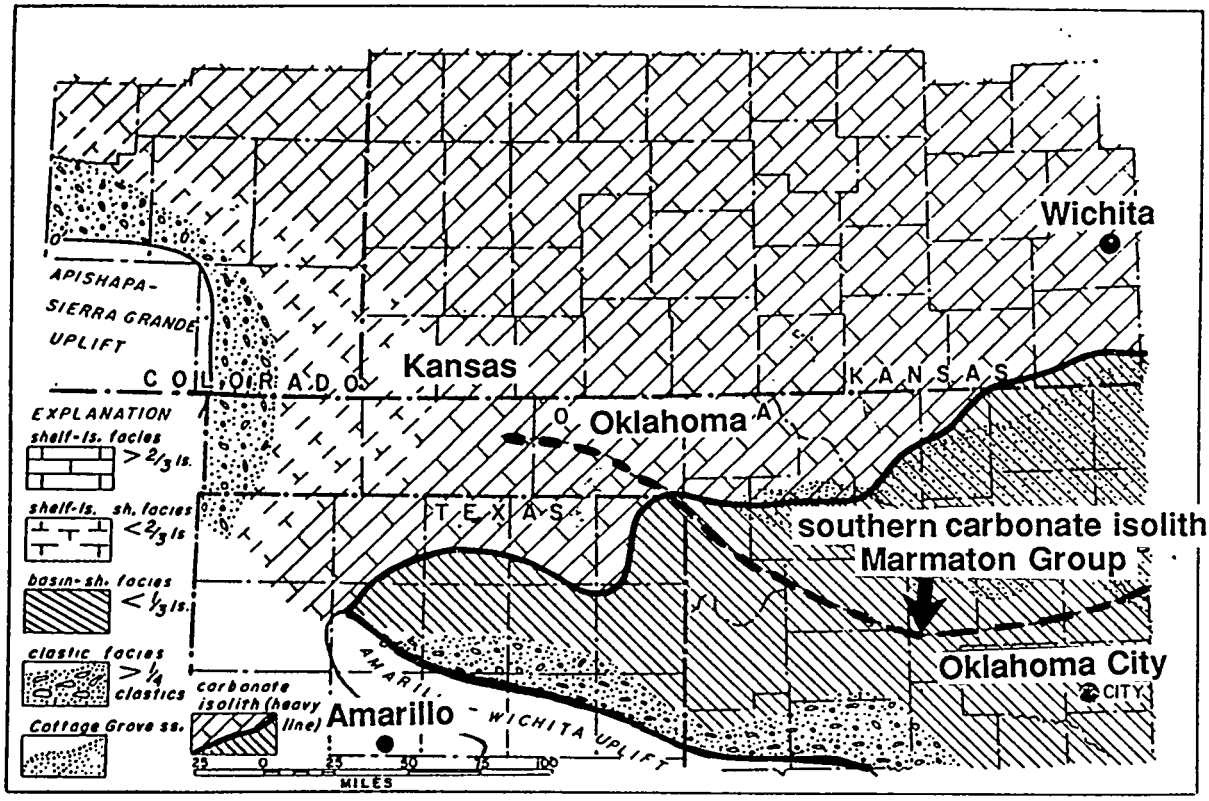

Rascoe (1962)

0 200
KM

Figure I.20. Dominant lithofacies of interval from Dewey to Hertha formation in Kansas City Group for southwestern Kansas and western Oklahoma (from Rascoe, 1962). Shelf margin with interpreted topographic relief follows carbonate-basinal shale boundary. Previous shelf margin of Marmaton Group is shown. Interval corresponds to 3rd-order sequence.

LITHOFACIES -- STANTON, PLATTSBURG, WYANDOTTE, IOLA
(UPPER LANSING GROUP, UPPER MISSOURIAN)

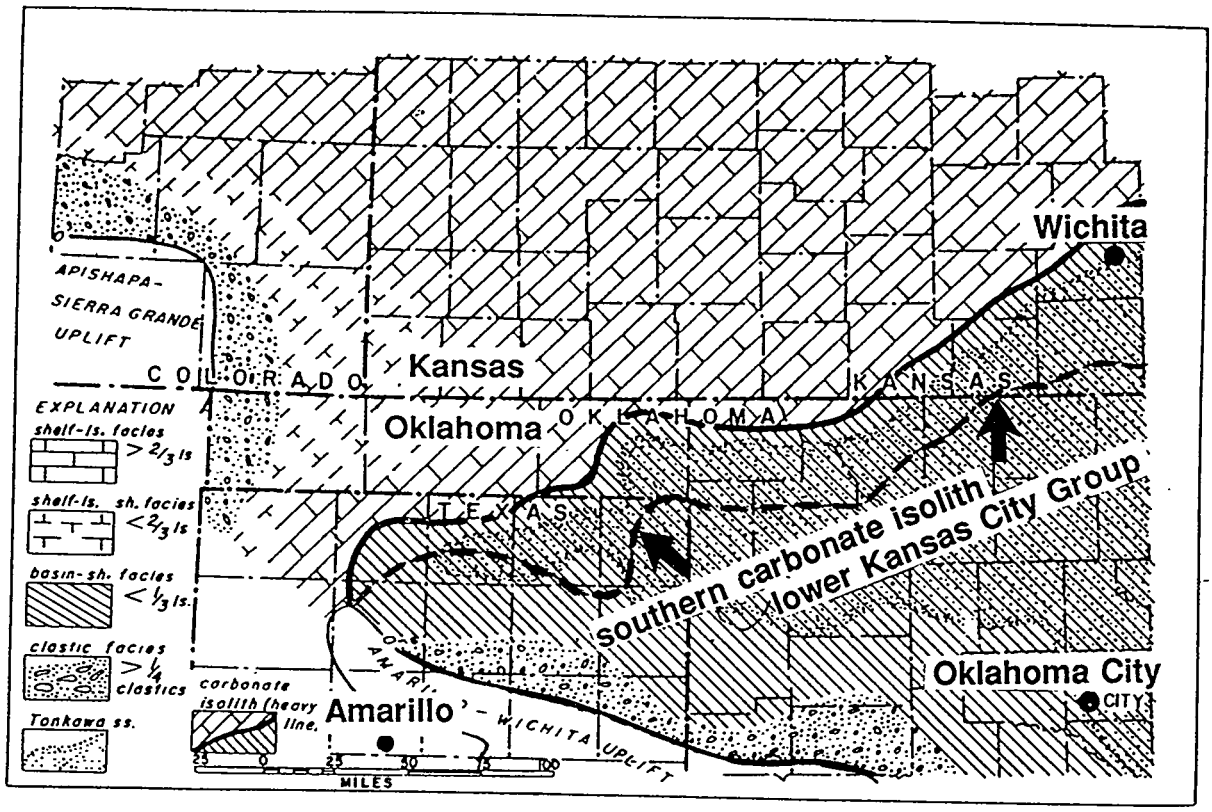

Rascoe (1962)

0 200
KM

Figure I.21. Lithofacies map of interval from Stanton Limestone through Iola Limestone showing southern carbonate margin for this interval and previous Kansas City section.

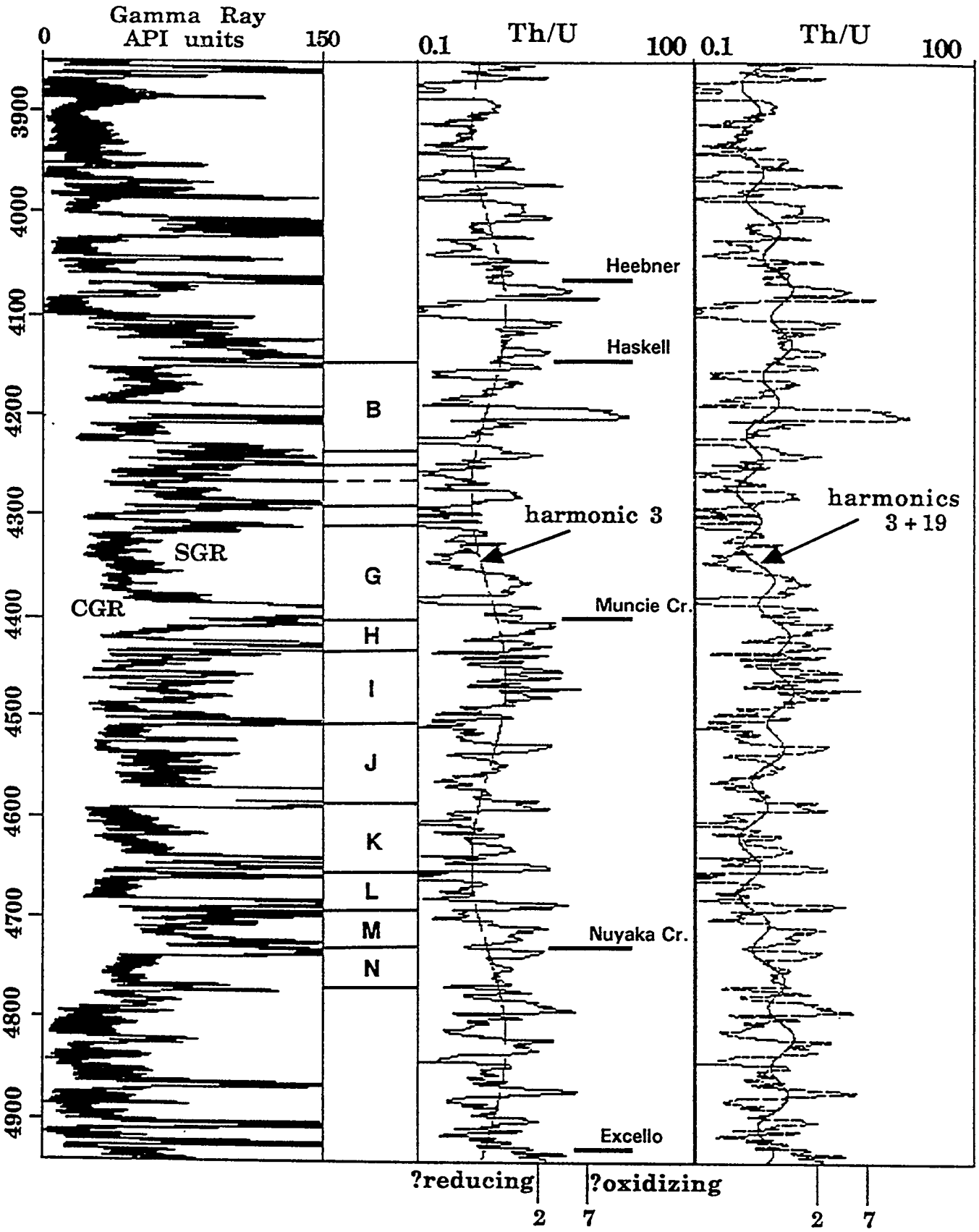

Figure I.22. Well log from Amoco Cox #A-4 in Victory field, Haskell County, Kansas for the interval including the Heebner Shale to the Excello Shale interval. Gamma ray and Th/U ratio with Th/U ratio fit by two dominant Fourier harmonics. Short cycle of 50-feet corresponds to 4th-order depositional sequences. The longer cycle of 350-foot corresponds to 3rd-order cycles (bundles of 4th-order). Cycles can be traced across the Kansas shelf. This project is described in Subtask 3.B.

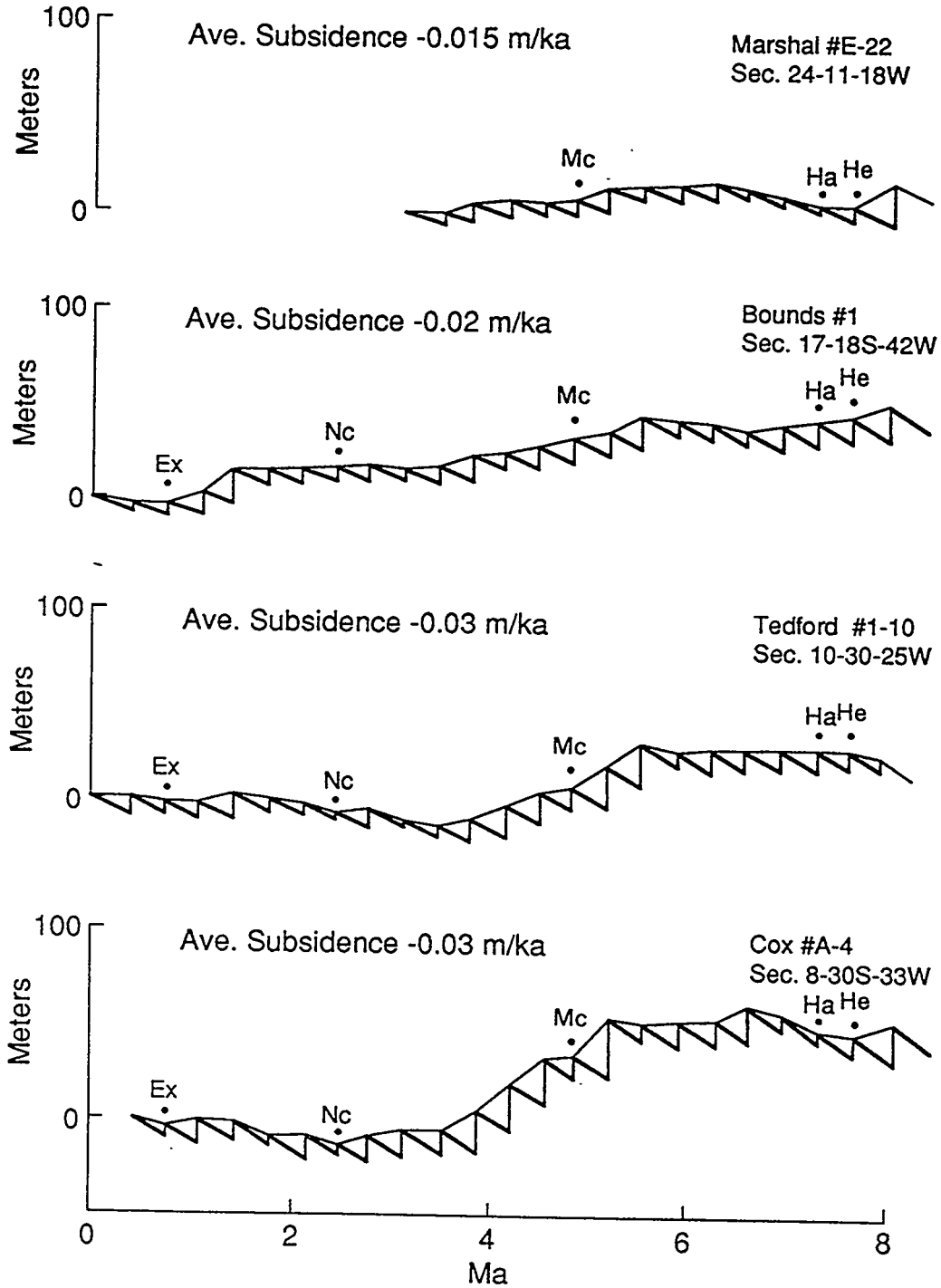

Figure I.23. Fischer plots for selected wells located in western Kansas. Plots provide estimate of sediment accommodation vs. time. Upper surface of connected triangle is a measure of relative elevation of depositional surface. Triangles are plotted for each 4th-order cycle evenly spaced along time axis (350 thousand years [ka] each in duration). Vertical axis of each triangle is measured thickness from well logs. Diagonal line of each triangle reflects calculated subsidence for a particular location on the shelf. Plot originally developed by A. Fischer (Fischer, 1964). The Fischer plot is further discussed in Subtask 4.B.

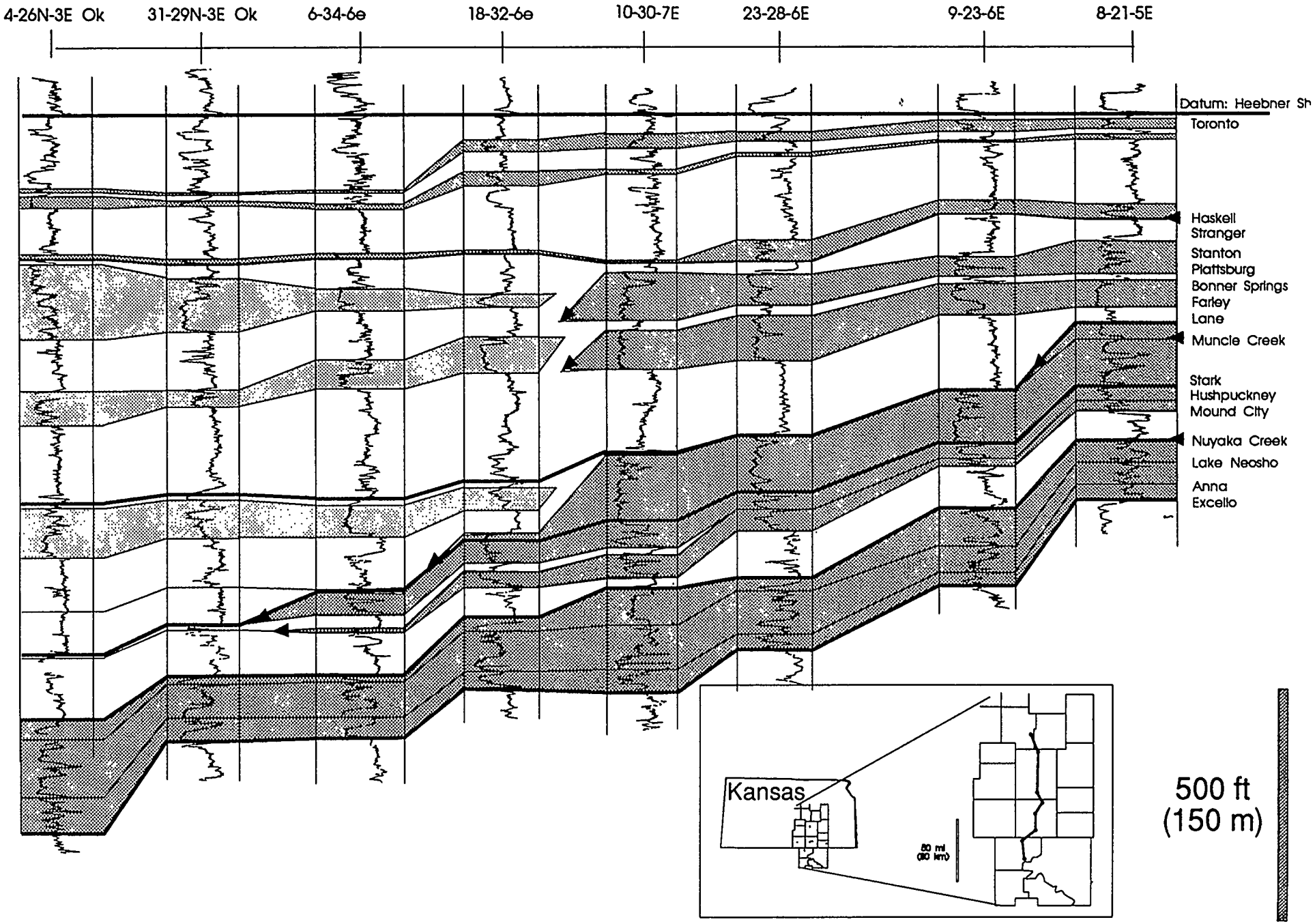

Figure I.24. South-to-north regional stratigraphic cross section datumed on the Heebner Shale for the Middle and Upper Pennsylvanian interval running approximately 125 miles (200 km) from northern Oklahoma to central Kansas (see Figure I.19). Gamma ray log traces and correlations of wells selected from regional sequence stratigraphic database showing shelf (right) to basin (left) transition where carbonate-dominated section gives way to siliciclastic rich section. Major continuous marine markers bounding 3rd-order cycles correspond to marked changes in shelf margin. Sandstones are interpreted as lowstand deposits based on analogies with the analog areas in surface exposures and shallow subsurface. Dark screen = limestone; light screen = sandstone; white = shale and thin sandstone.

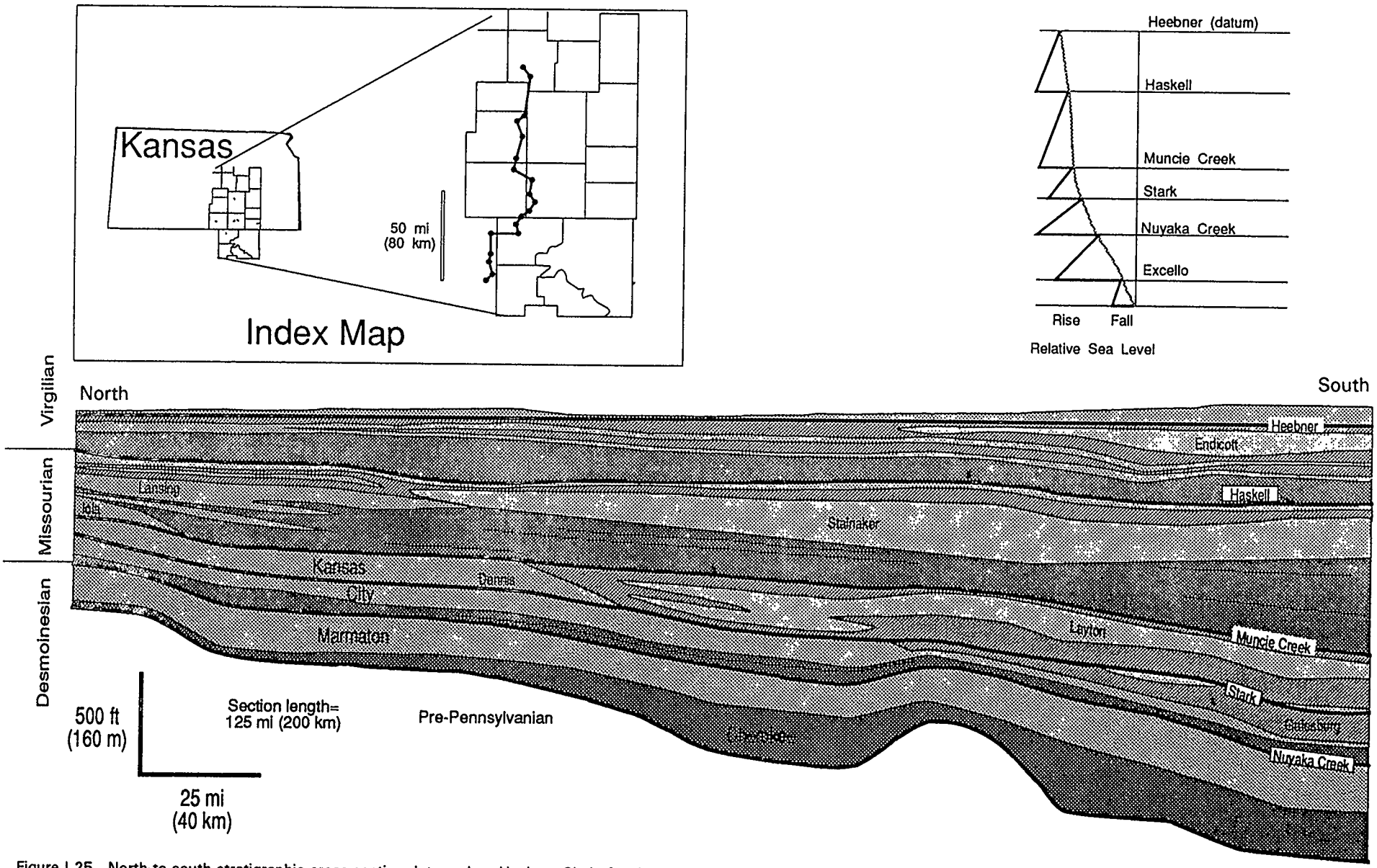

Figure I.25. North-to-south stratigraphic cross section datumed on Heebner Shale for the stratigraphic interval from the base of the Pennsylvanian to the top of the Oread Limestone. Cross section is approximately 125 mi.(200 km)long (see Figure I.19). Section is approximately 20 miles west and parallel to the gamma ray log cross section in Figure I.24. Section is a re-interpretation of a wireline log section prepared by Lukert (1948). Interpretation is assisted by use of wireline log database using gamma ray neutron-density logs that permit lithologic interpretation. Furthermore, stratigraphic model developed from near-surface analog study provided framework to support correlation development. The continuous marine shale markers delineate major changes to the shelf margin as indicated in Figure I.23. Relative sea-level curve is depicted in inset based on a framework of the marine markers.

Modified from original cross-section of Lukert (1948)

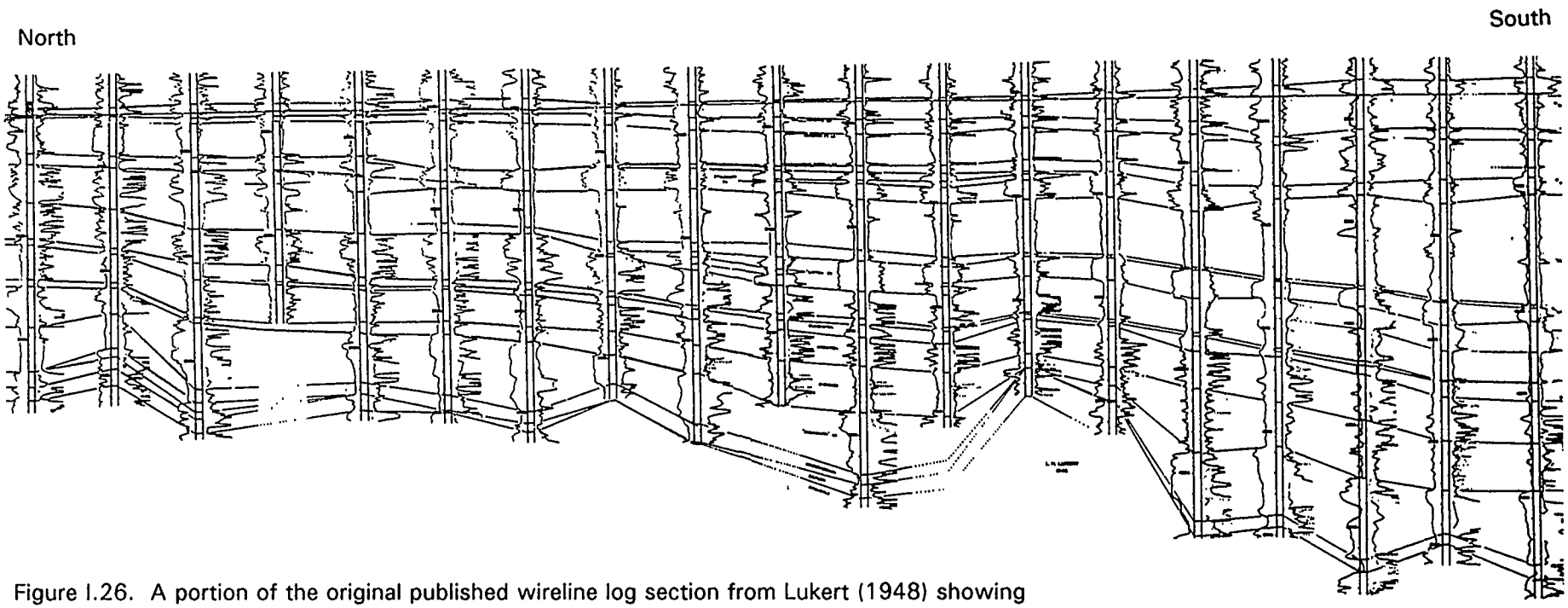

Figure I.26. A portion of the original published wireline log section from Lukert (1948) showing framework correlations. Basic correlations have not changed, only more detail has been added, including identification of marine shale markers based on nearby gamma ray log control.

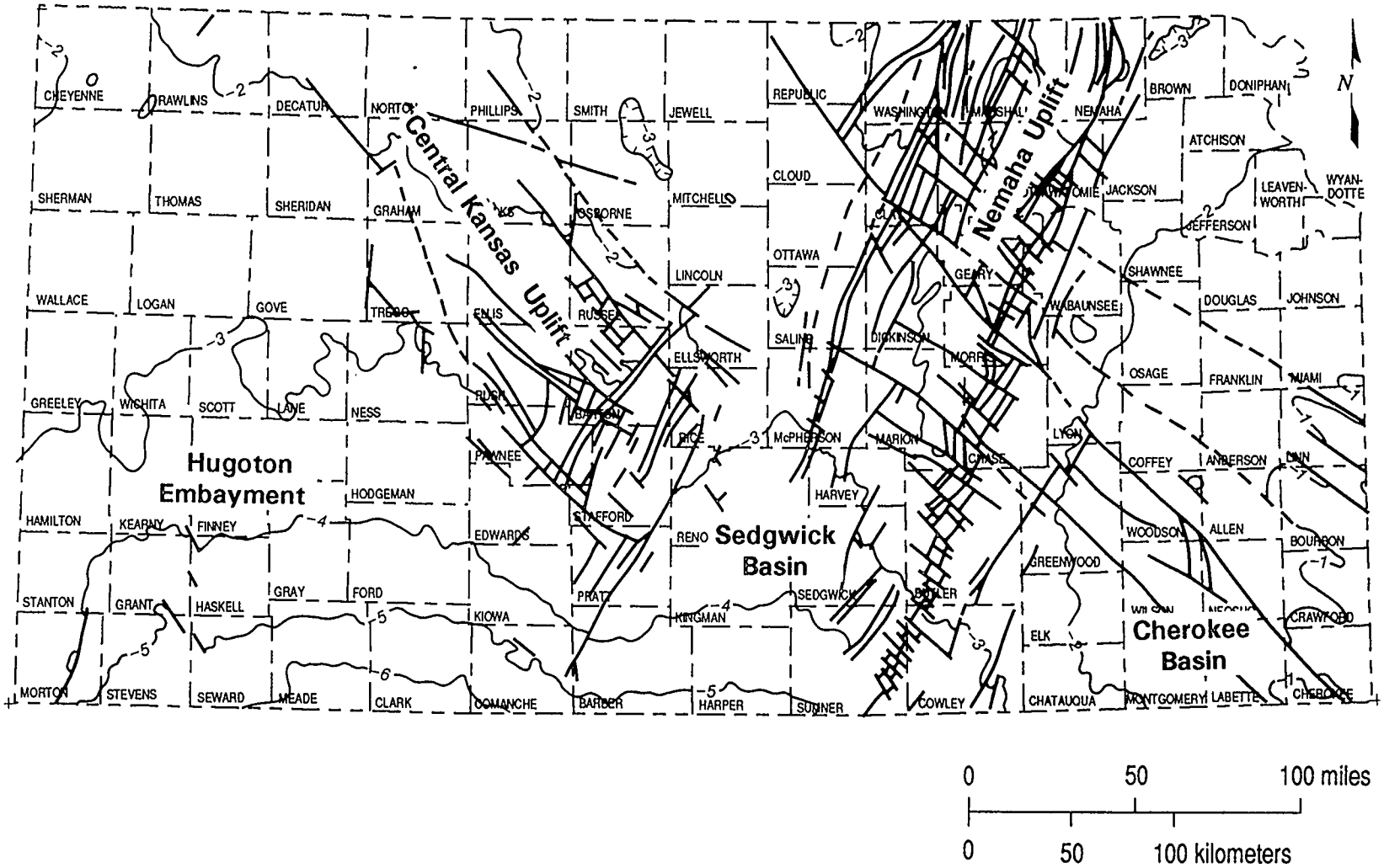

Figure I.27. Generalized Precambrian basement map of Kansas prepared by D. Baars.

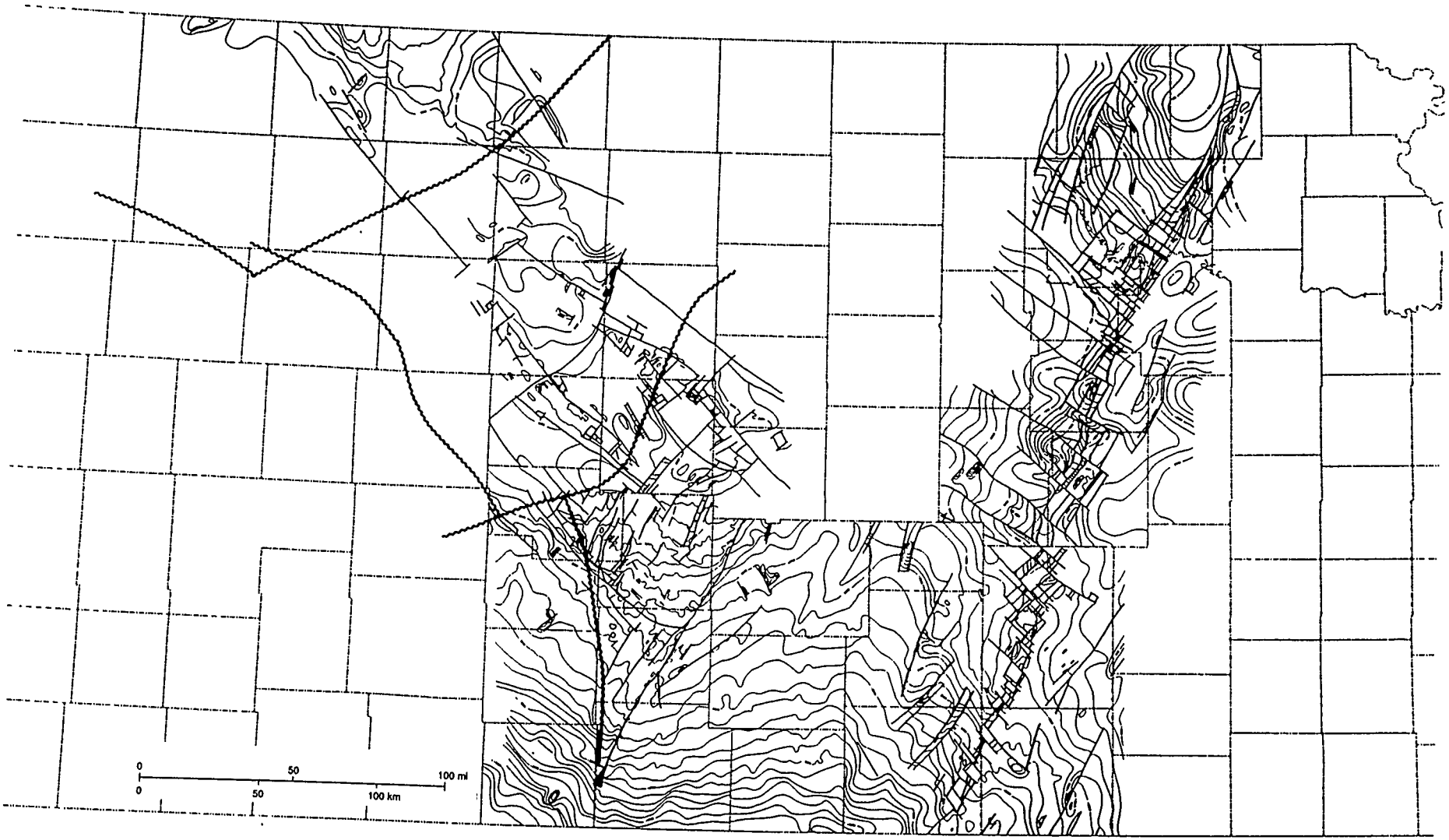

Figure I.28. Digitized contoured surface of "basement" in Kansas including configuration of Precambrian to the north and Cambro-Ordovician Arbuckle Group, overlying basement, in southern Kansas. Heavier wavy lines denote boundaries of regional shelf elements derived from statistical spatial analysis of Pennsylvanian isopach data.

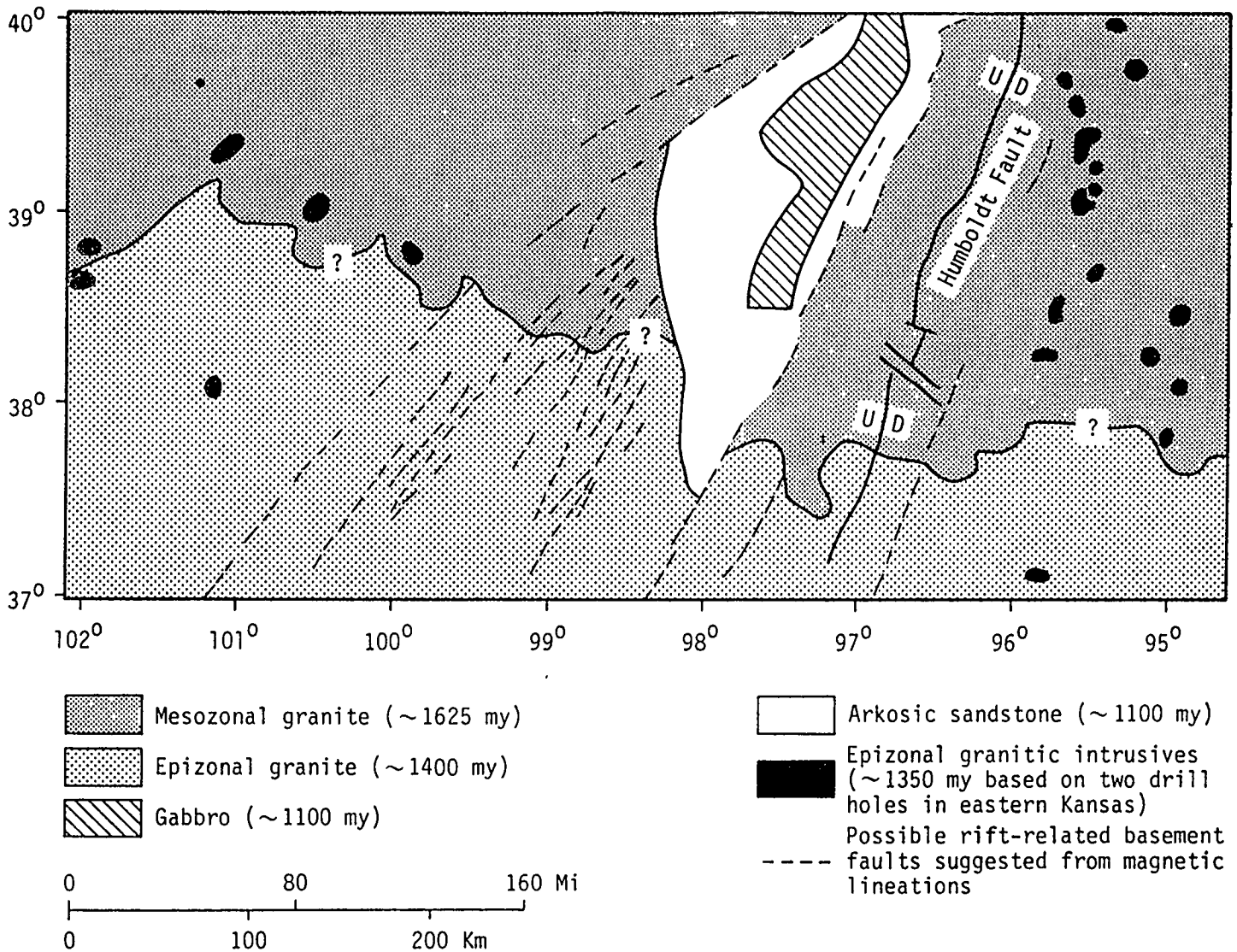

Figure I.29. Geology of the Precambrian surface based on combined lithologic, age, and magnetic and gravity signatures (from Yarger, 1983, after Bickford et al., 1981).

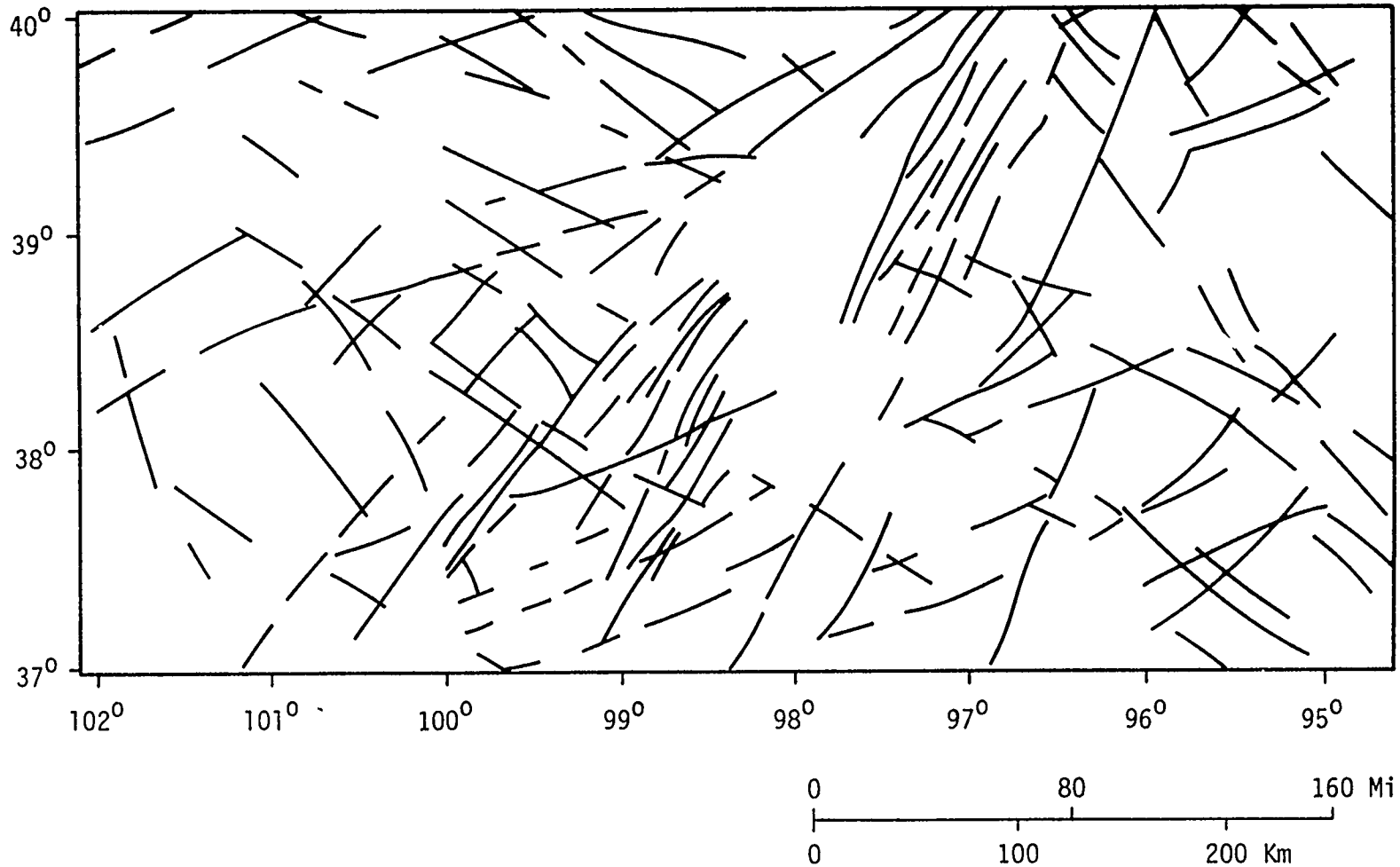

Figure I.30. Lineaments derived from magnetic maps from Yarger (1983).

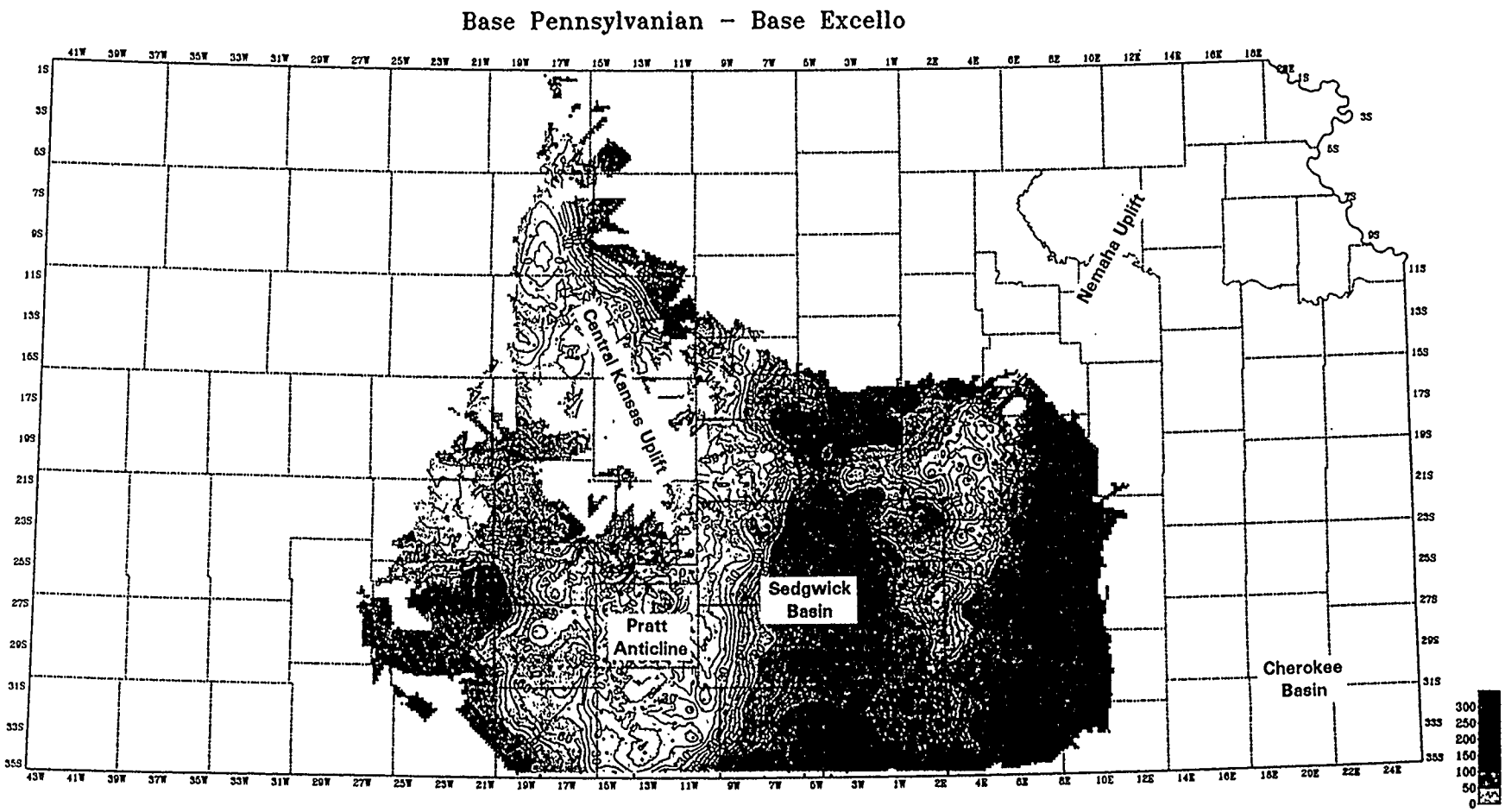

KANSAS GEOLOGICAL SURVEY

Figure I.31. Isopach of base of Pennsylvanian to base of Excello Shale from regional stratigraphic databases. Contour interval is 10 feet. Shaded interval is 50 feet. County outlines shown (counties indexed in Figure I.27). Every two townships and ranges are labeled along borders. Distance between them is 12 miles. Gridded and contoured using kriging option with SURFACE III. Missing contours in northwest portion of mapped area reflects zero thickness for interval over Central Kansas uplift.

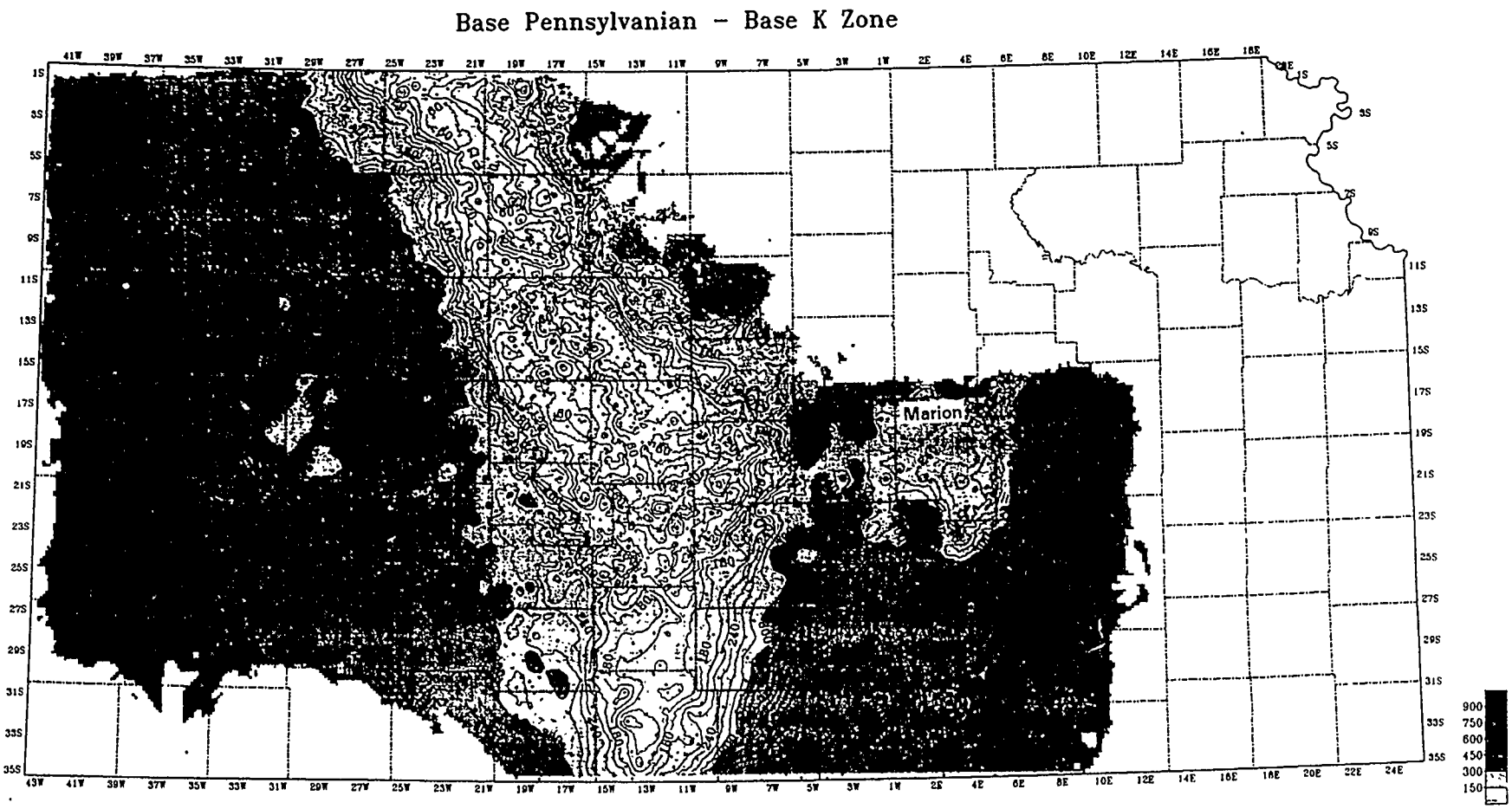

KANSAS GEOLOGICAL SURVEY

Figure I.32. Isopach of base of Pennsylvanian to base of the Swope cycle (K Zone) from linked regional stratigraphic databases. Contour interval is 20 feet. Shaded interval is 150 feet. County outlines shown (counties indexed in Figure I.27). Every two townships and ranges are labeled along borders. Distance between them is 12 miles. Gridded and contoured using kriging option with SURFACE III.

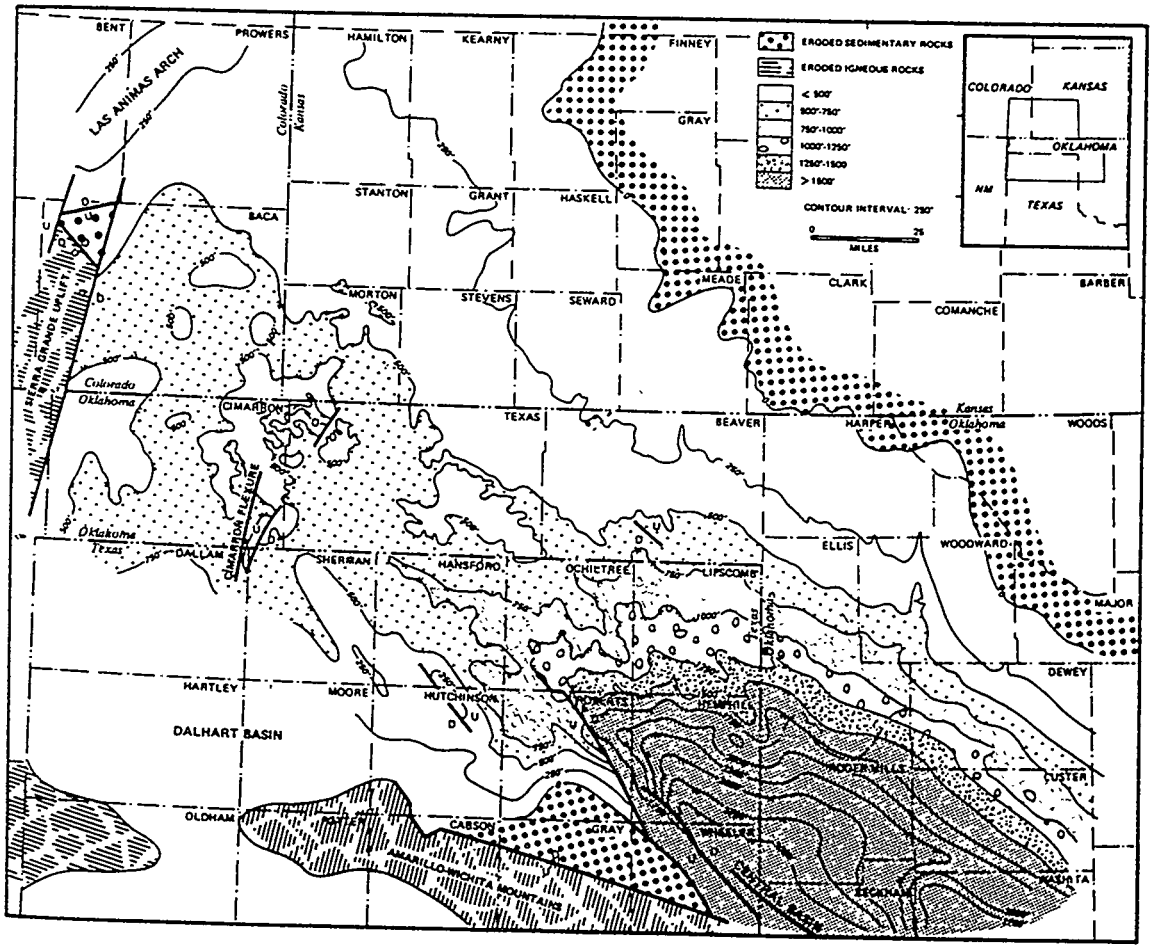

Figure I.33. Isopach map of the total Morrow in the Anadarko and southern Hugoton Embayment (Swanson, 1979).

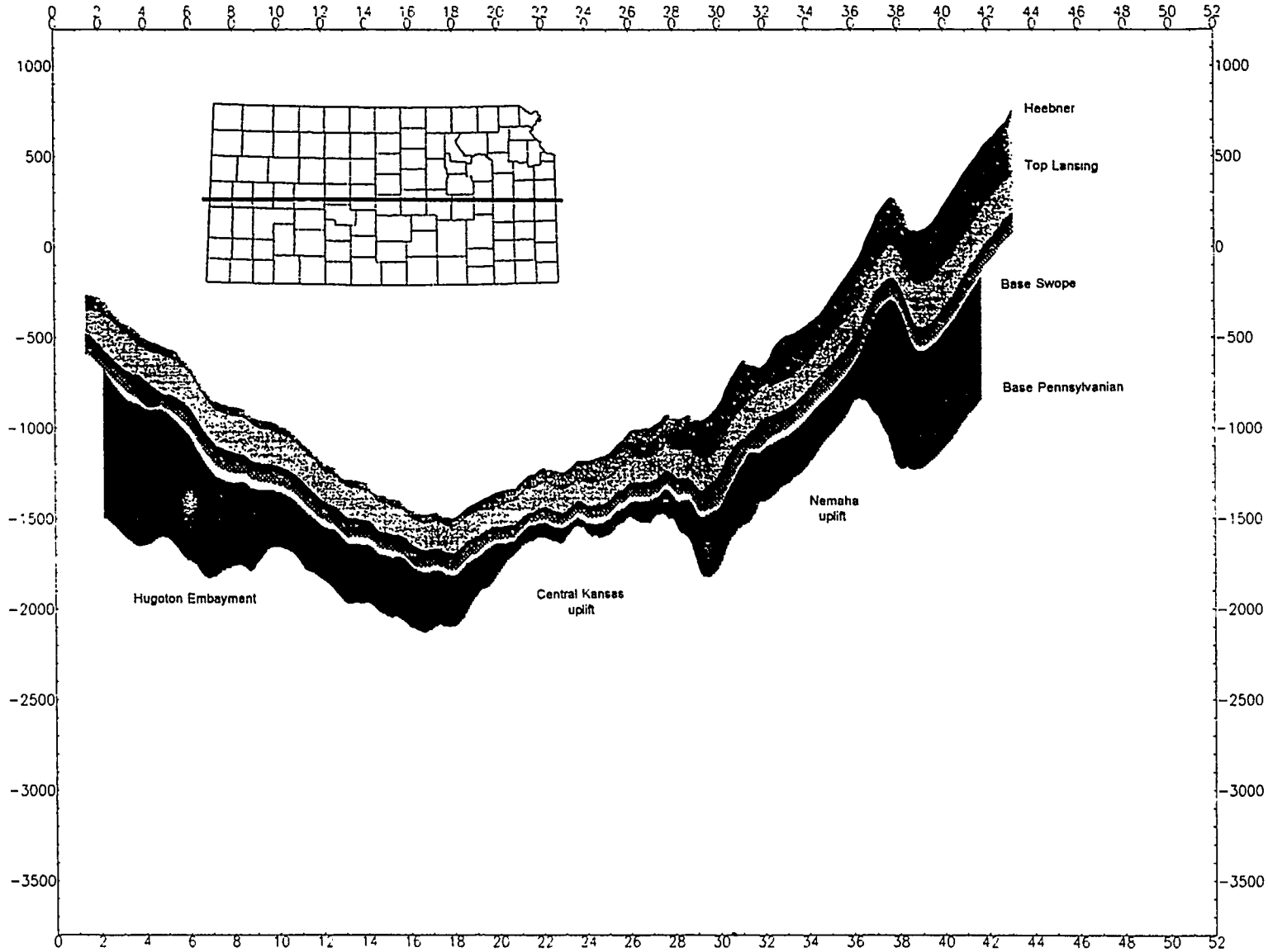

Figure I.34. Structural cross section of interval from Heebner Shale to base of Pennsylvanian. Elevation in feet. Location shown in inset map.

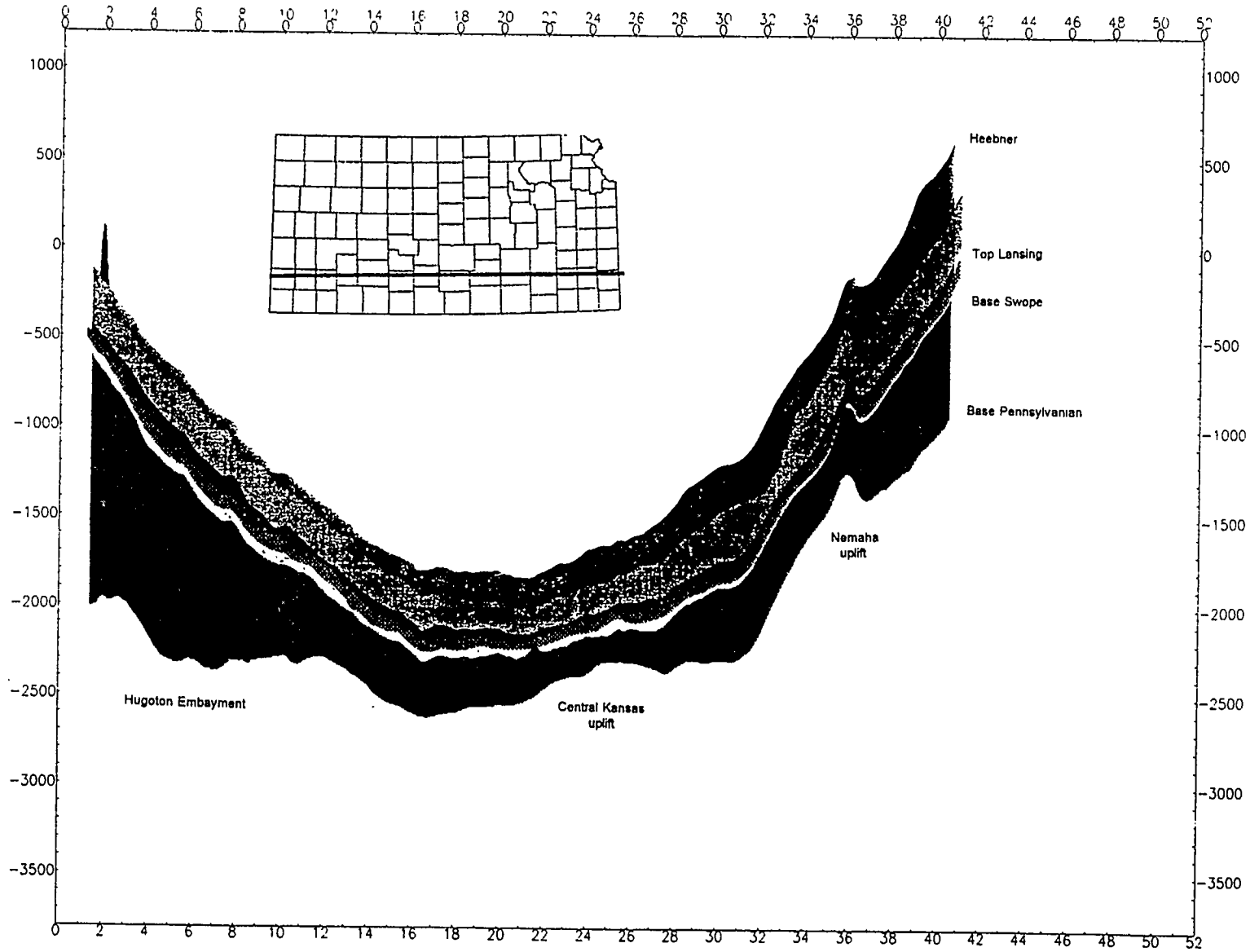

Figure I.35. Structural cross section of interval from Heebner Shale to base of Pennsylvanian. Elevation in feet. Location shown in inset map.

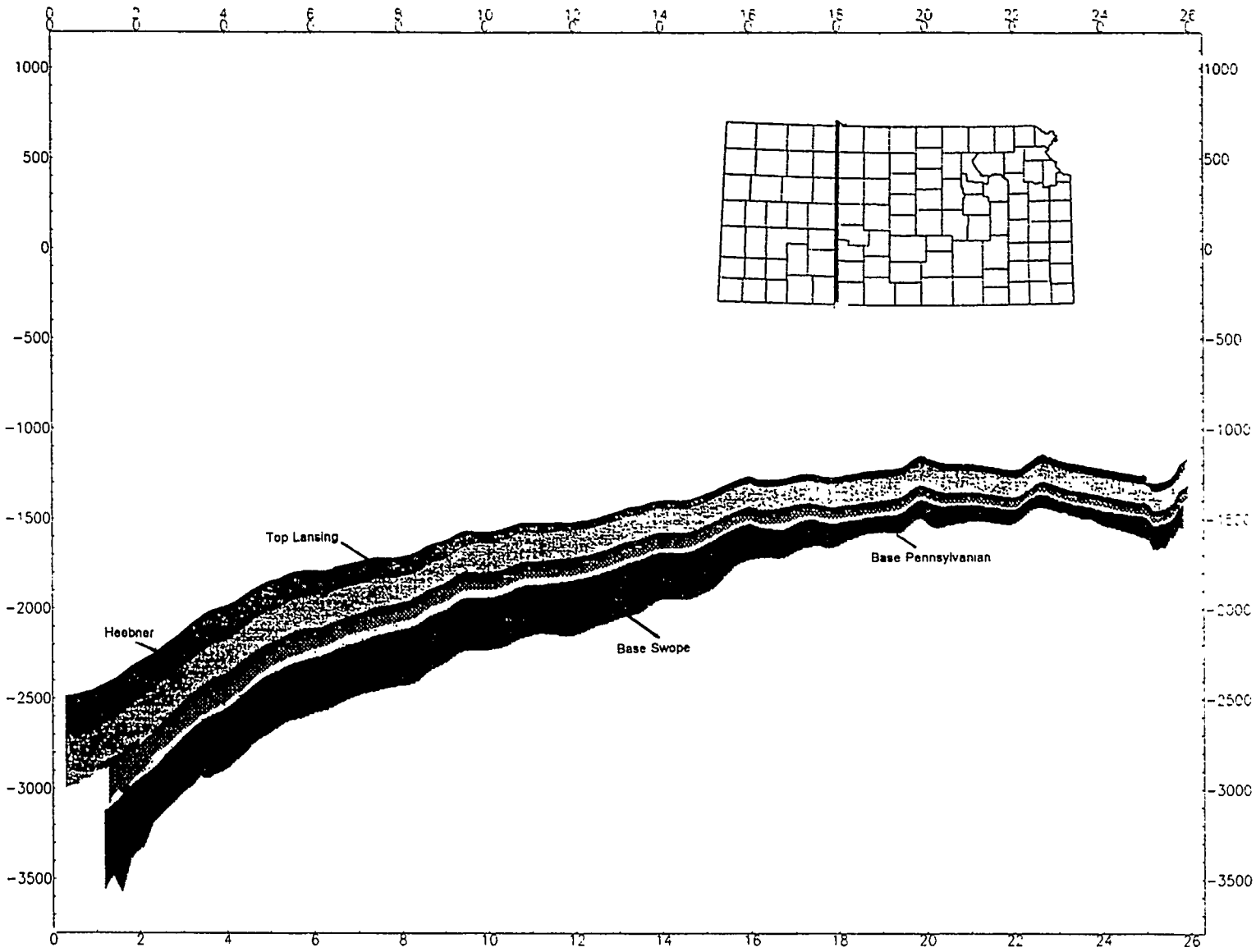

Figure I.36. Structural cross section of interval from Heebner Shale to base of Pennsylvanian. Elevation in feet. Location shown in inset map.

Structure Map : Top of Lansing

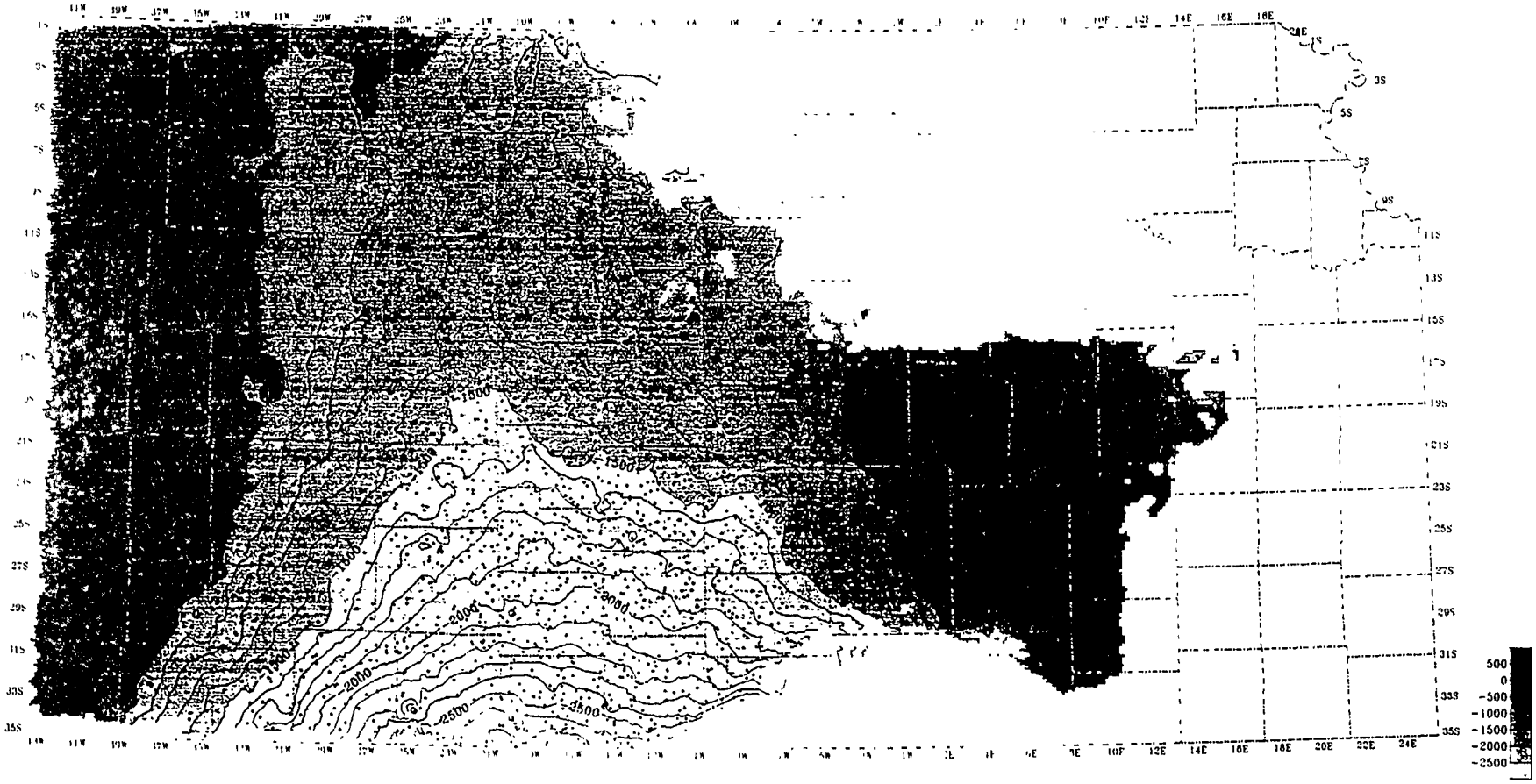

Figure I.37. Structural contour map on the top of the Lansing Group. Countour interval is 100 feet. Distance between townships and ranges labeled on side is 6 miles (10 km).

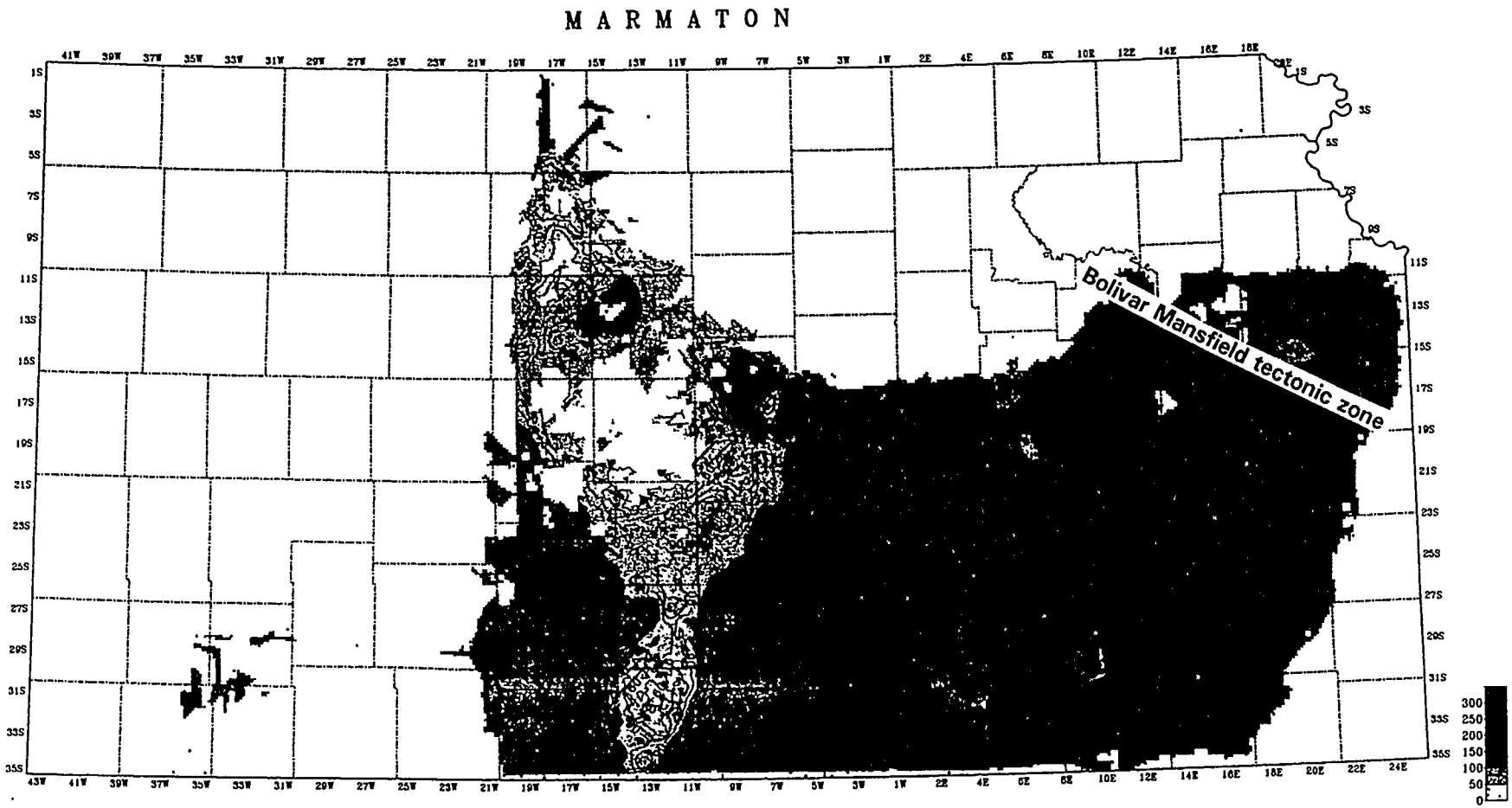

KANSAS GEOLOGICAL SURVEY

Figure I.38. Isopach of the Marmaton 3rd-order sequence (Excello Shale to Nuyaka Creek Shale) from regional stratigraphic databases. Contour interval is 10 feet. Shaded interval is 50 feet. County outlines shown (counties indexed in Figure I.27). Every two townships and ranges are labeled along borders. Distance between them is 12 miles. Gridded and contoured using kriging option with SURFACE III. Missing contours in northwest portion of mapped area reflects zero thickness for interval over Central Kansas uplift.

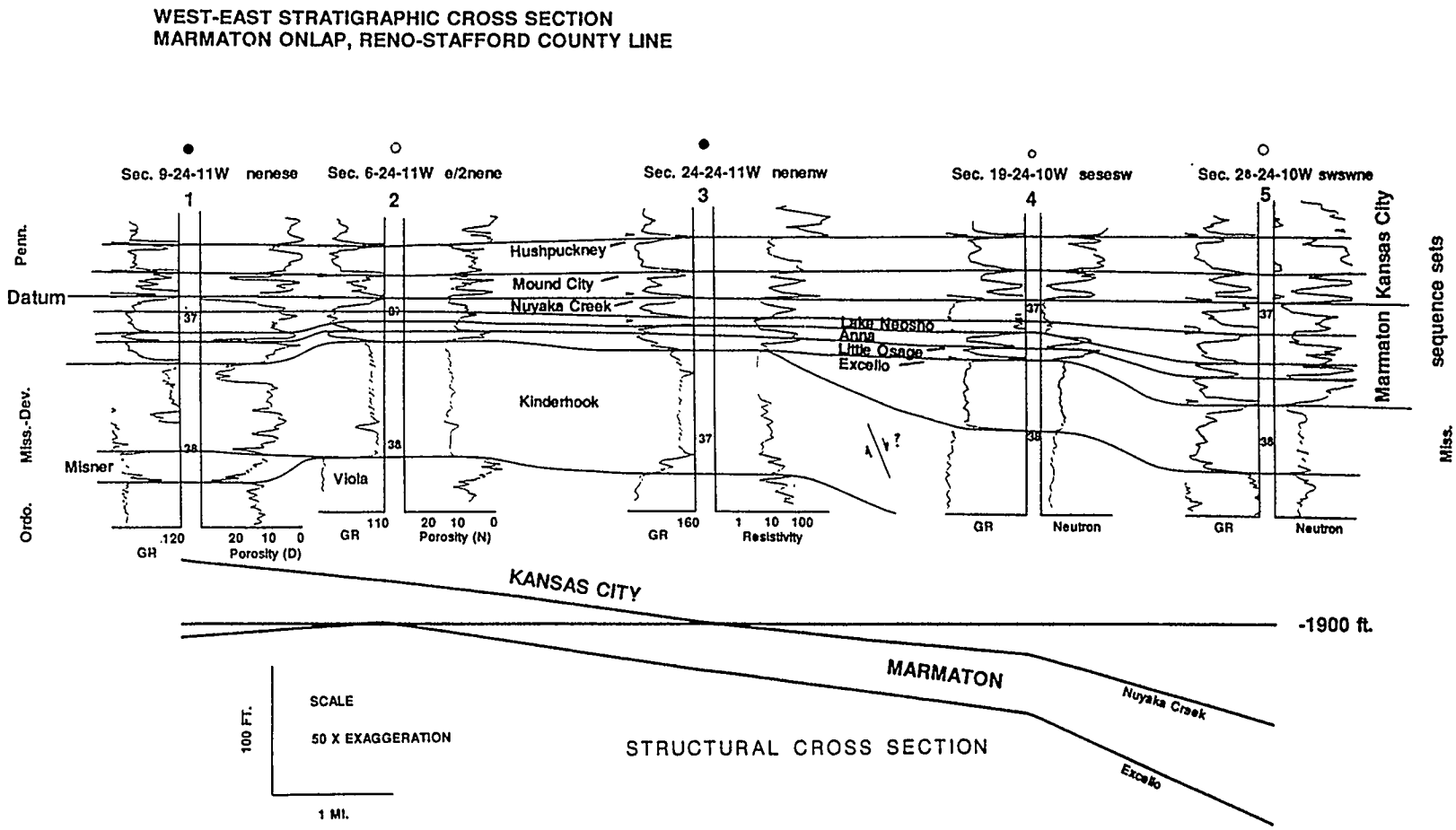

Figure I.39. Wireline log (GR-porosity) stratigraphic and structural cross sections along southern edge of Central Kansas Uplift for lowermost Pennsylvanian onlap over basal Pennsylvanian unconformity. Datum is Nuyaka Creek Shale. Marmaton 3rd-order sequence is first Pennsylvanian units to cover the uplift following the unconformity. Earliest cycles of Marmaton are most complete with well developed black shales and limestones. Upper cycles are thinner with loss of black shale and limestone. Nuyaka Creek Shale is the initiation of Kansas City 3rd-order sequence whose more uniform cycle thicknesses reflect reduced topographic relief.

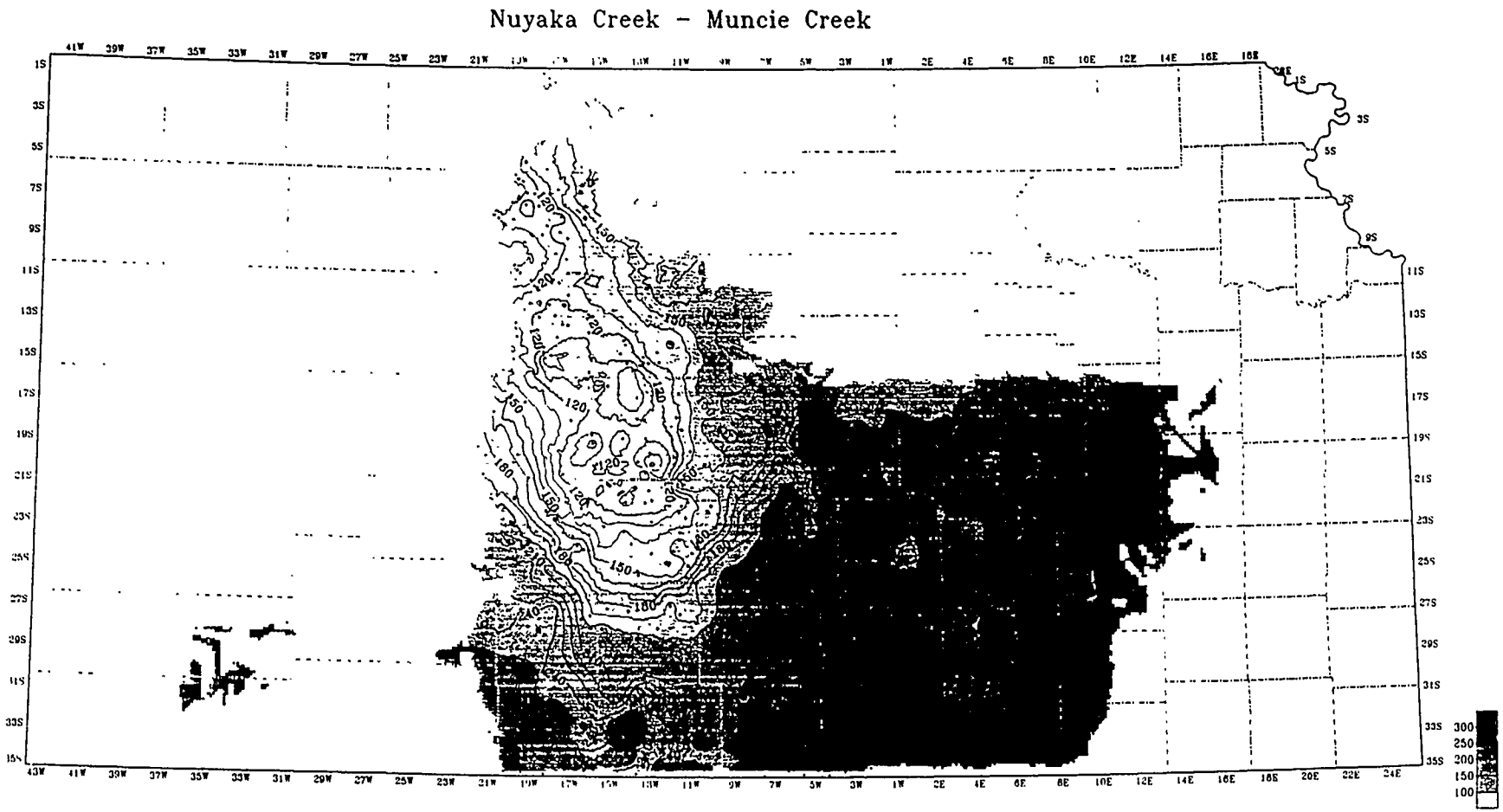

Figure I.40. Isopach of Nuyaka Creek Shale to the Muncie Creek Shale from regional stratigraphic databases. Contour interval is 10 feet. Shaded interval is 50 feet. County outlines shown (counties indexed in Figure I.27). Every two townships and and ranges are label along borders. Distance between them is 12 miles (19 km). Gridded and contoured using kriging option with SURFACE III.

Base K - Base Muncie Creek

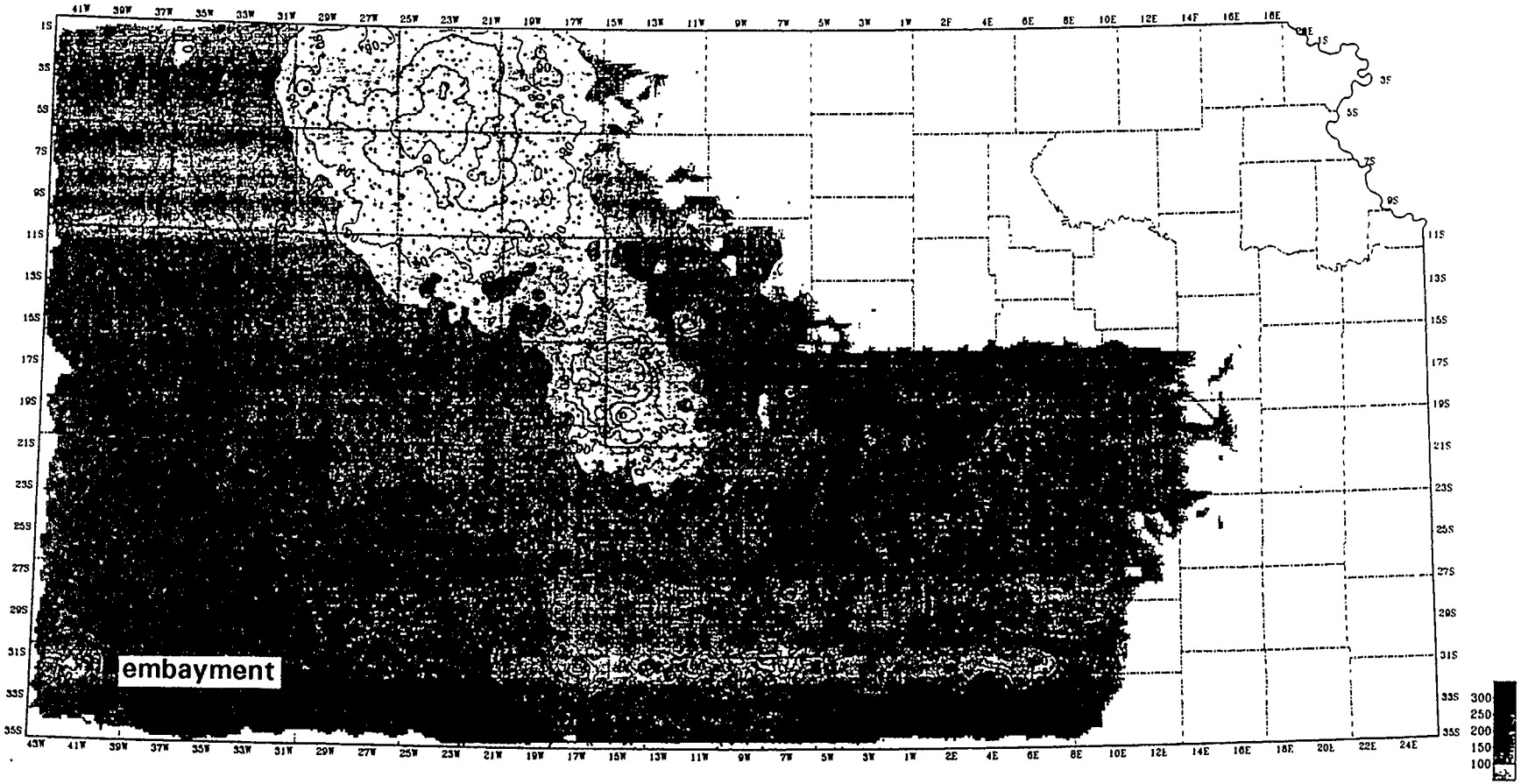

KANSAS GEOLOGICAL SURVEY

Figure I.41. Isopach of base of Swope (K zone) sequence to base of Muncie Creek Shale from regional stratigraphic databases. Contour interval is 10 feet. Shaded interval is 50 feet. County outlines shown (counties indexed in Figure I.27). Every two townships and ranges are labeled along borders. Distance between them is 12 miles. Gridded and contoured using kriging option with SURFACE III.

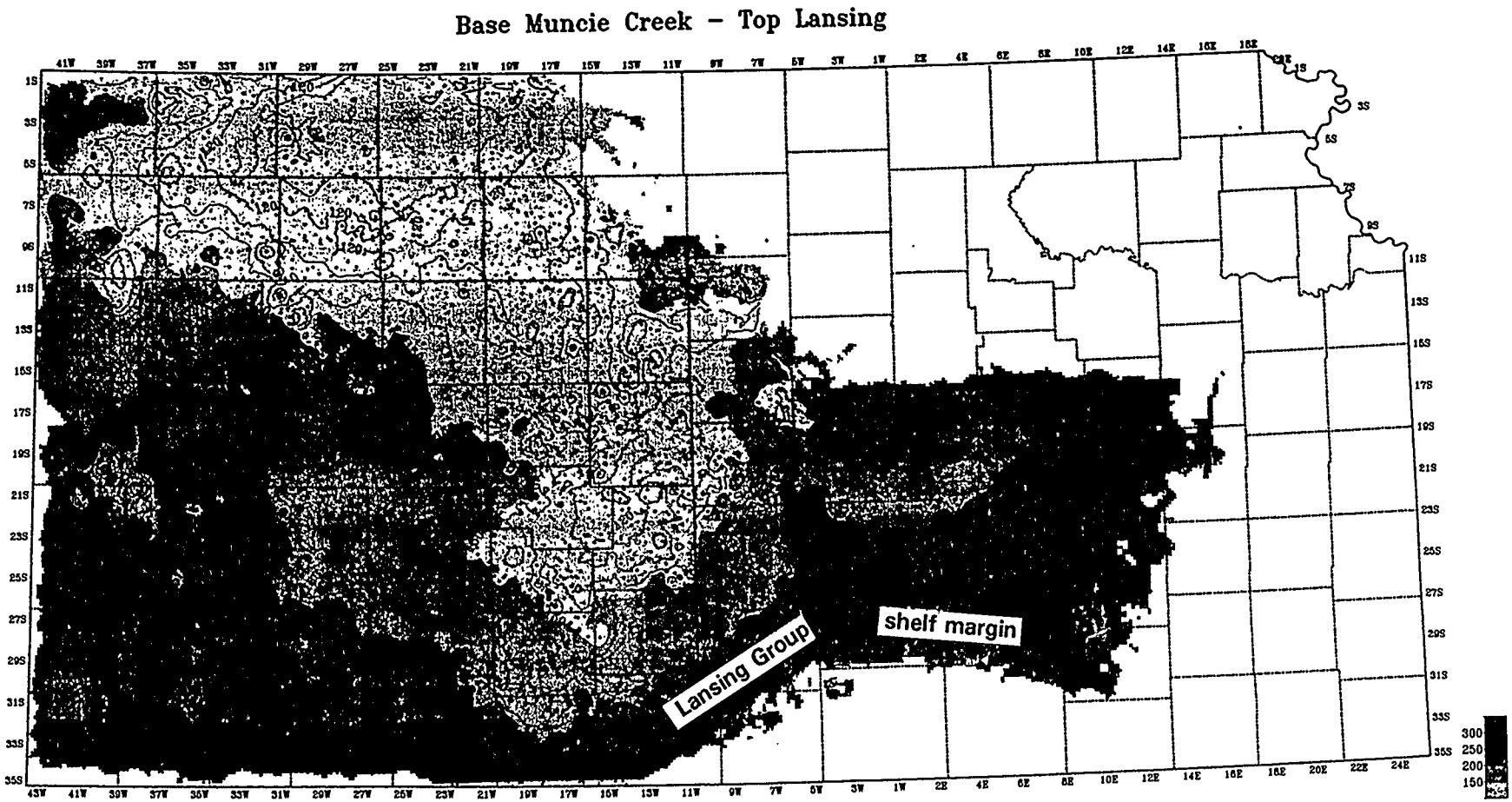

KANSAS GEOLOGICAL SURVEY

Figure I.42. Isopach of base Muncie Creek to top of Lansing from regional stratigraphic databases. Contour interval is 10 feet. Shaded interval is 50 feet. County outlines shown (counties indexed in Figure I.27). Every two townships and ranges are labeled along borders. Distance between them is 12 miles. Gridded and contoured using kriging option with SURFACE III.

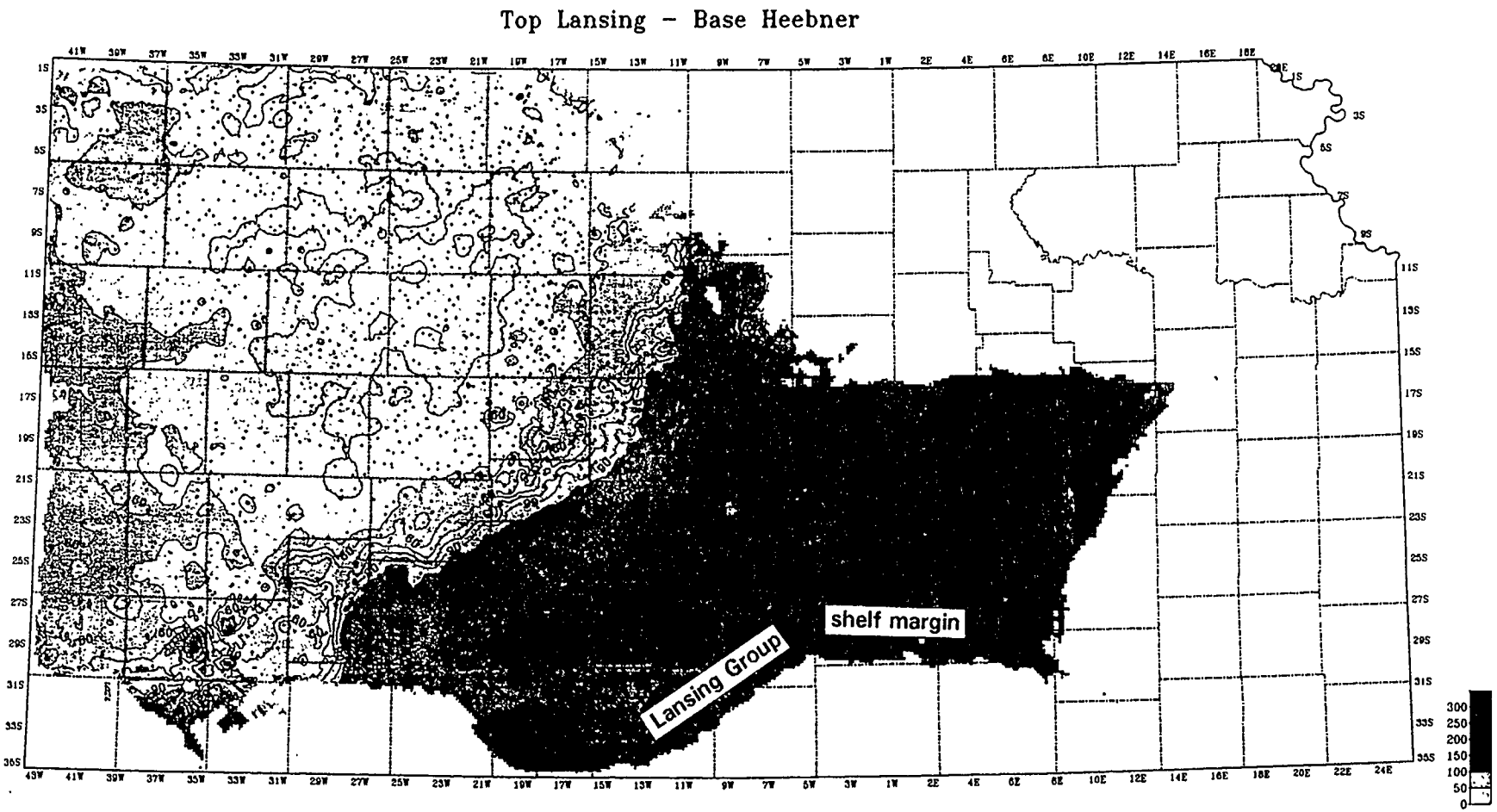

KANSAS GEOLOGICAL SURVEY

Figure I.43. Isopach of top of Lansing to base of Heebner Shale from regional stratigraphic databases. Contour interval is 10 feet. Shaded interval is 50 feet. County outlines shown (counties indexed in Figure I.27). Every two townships and ranges are labeled along borders. Distance between them is 12 miles. Gridded and contoured using kriging option with SURFACE III.

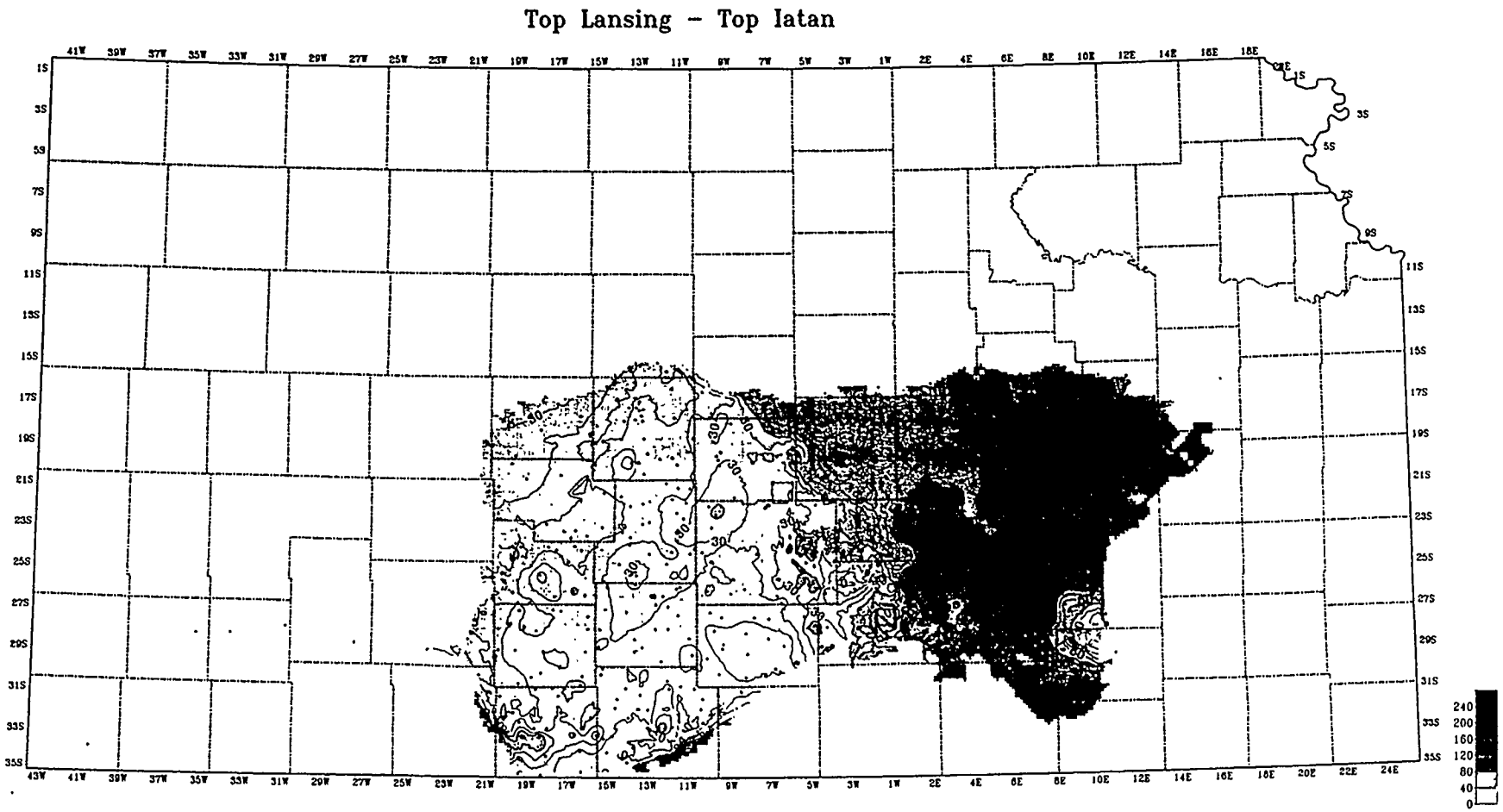

KANSAS GEOLOGICAL SURVEY

Figure I.44. Isopach of top of Lansing to base of Haskell Limestone (commonly correlated and recognized as Iatan in subsurface) from regional stratigraphic databases. Contour interval is 10 feet. Shaded interval is 40 feet. County outlines shown (counties indexed in Figure I.27). Every two townships and ranges are labeled along borders. Distance between them is 12 miles. Gridded and contoured using kriging option with SURFACE III.

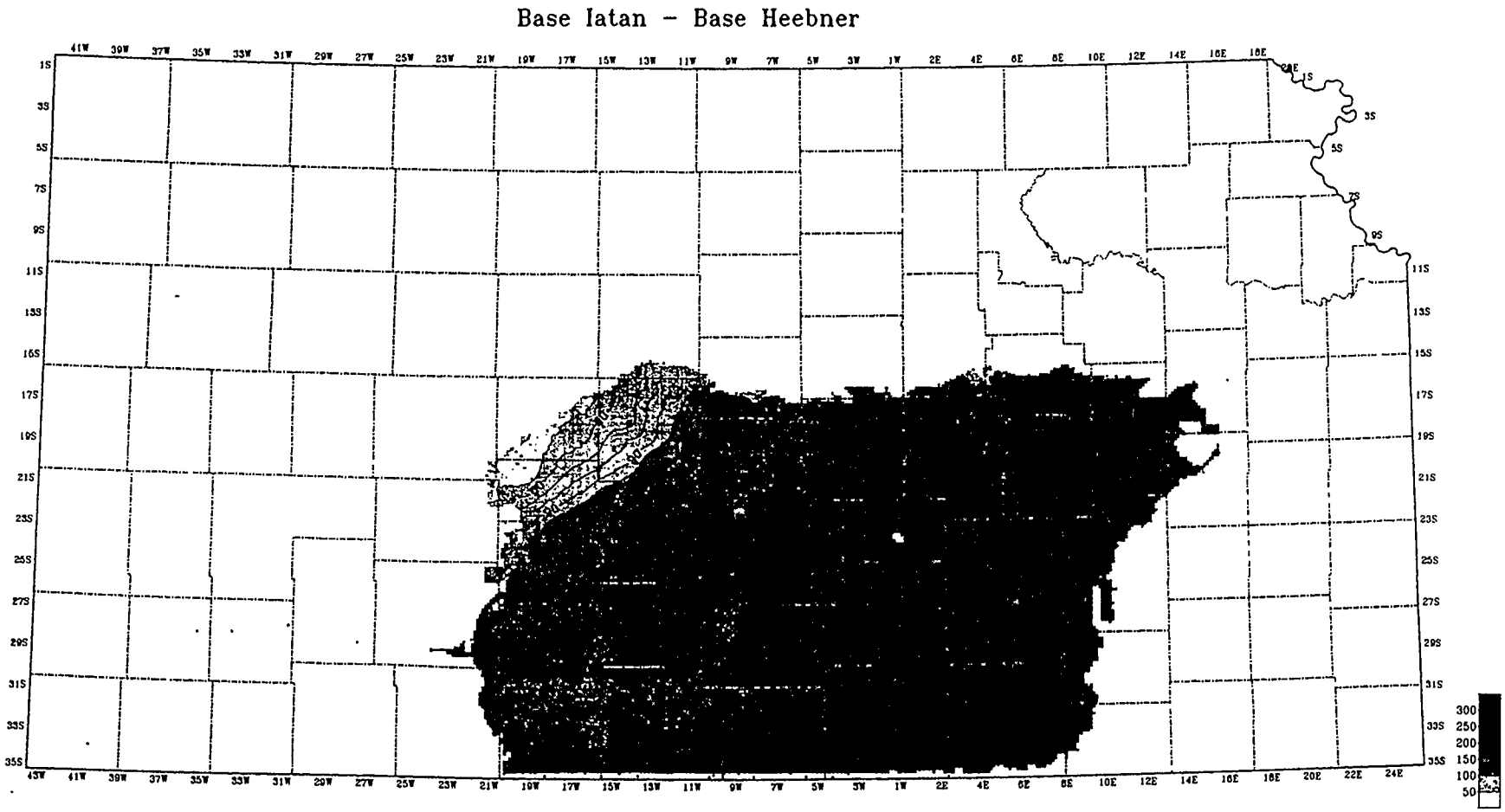

KANSAS GEOLOGICAL SURVEY

Figure I.45. Isopach of base of Haskell Limestone (commonly referred to as Iatan in subsurface) to base of Heebner Shale from regional stratigraphic databases. Contour interval is 10 feet. Shaded interval is 50 feet. County outlines shown (counties indexed in Figure I.27). Every two townships and ranges are labeled along borders. Distance between them is 12 miles. Gridded and contoured using kriging option with SURFACE III.

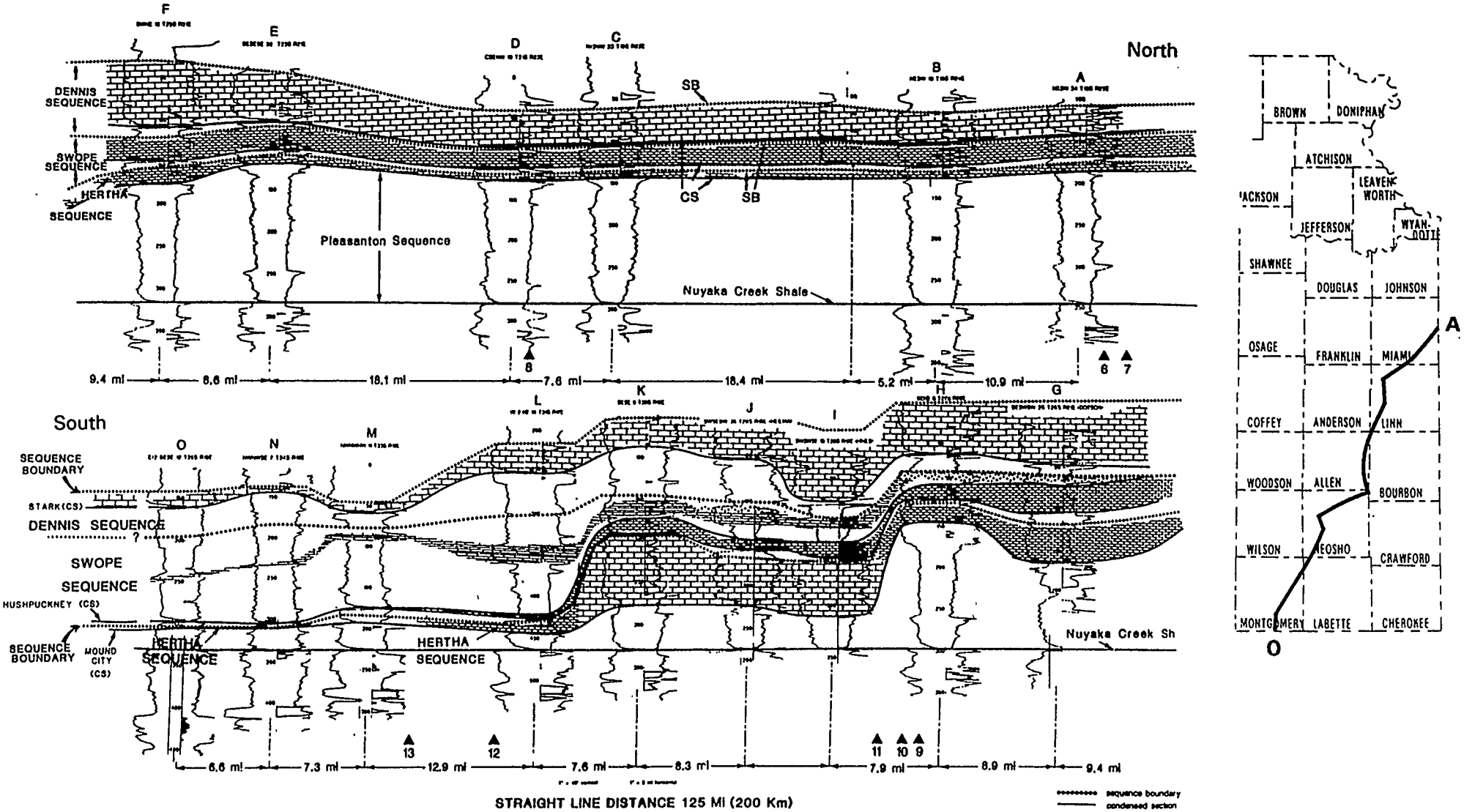

Figure I.46. Regional south-to-north stratigraphic cross section extending from Oklahoma line to 50 mi. south of Kansas City. Pleasanton Group and lower portion of Kansas City Group are shown. Datum is Nuyaka Creek Shale (base of Kansas City 3rd-order cycle). Southern half of section (lower portion of the section) is basin-to-shelf transition, here representing basinward lateral accretion of 4th-order depositional sequences. Cross section is located in proximity of surface and near-surface analog studies (Figure I.11).

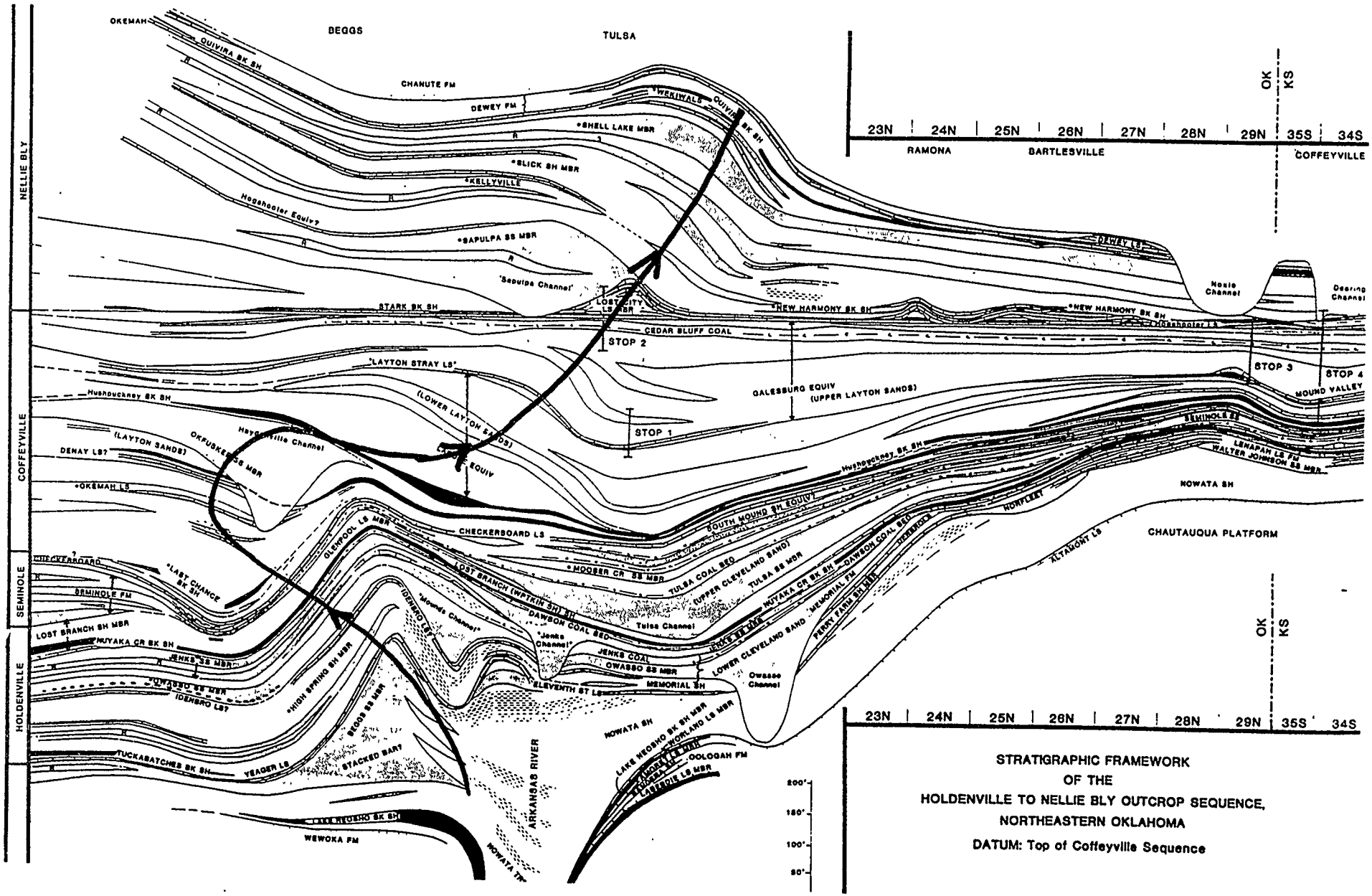

Figure I.47. South-to-north stratigraphic cross section from eastern Oklahoma to north of the Kansas state line for the uppermost Desmoinesian and lower Missourian siliciclastic-rich section derived from Ouachita Mountains (Figure I.19). Section is datumed on the Stark Shale of Dennis sequence prepared from surface sections by Bennison in Watney et al.(1989). Clinoforms reflecting the siliciclastic shelf margin are highlighted by the line with arrows moving southward through Nuyaka Creek (landward stepping or drowning) and stepping northward (basinward) during the Swope through Dewey sequence equivalent that parallels events described on the carbonate-dominated Kansas shelf.

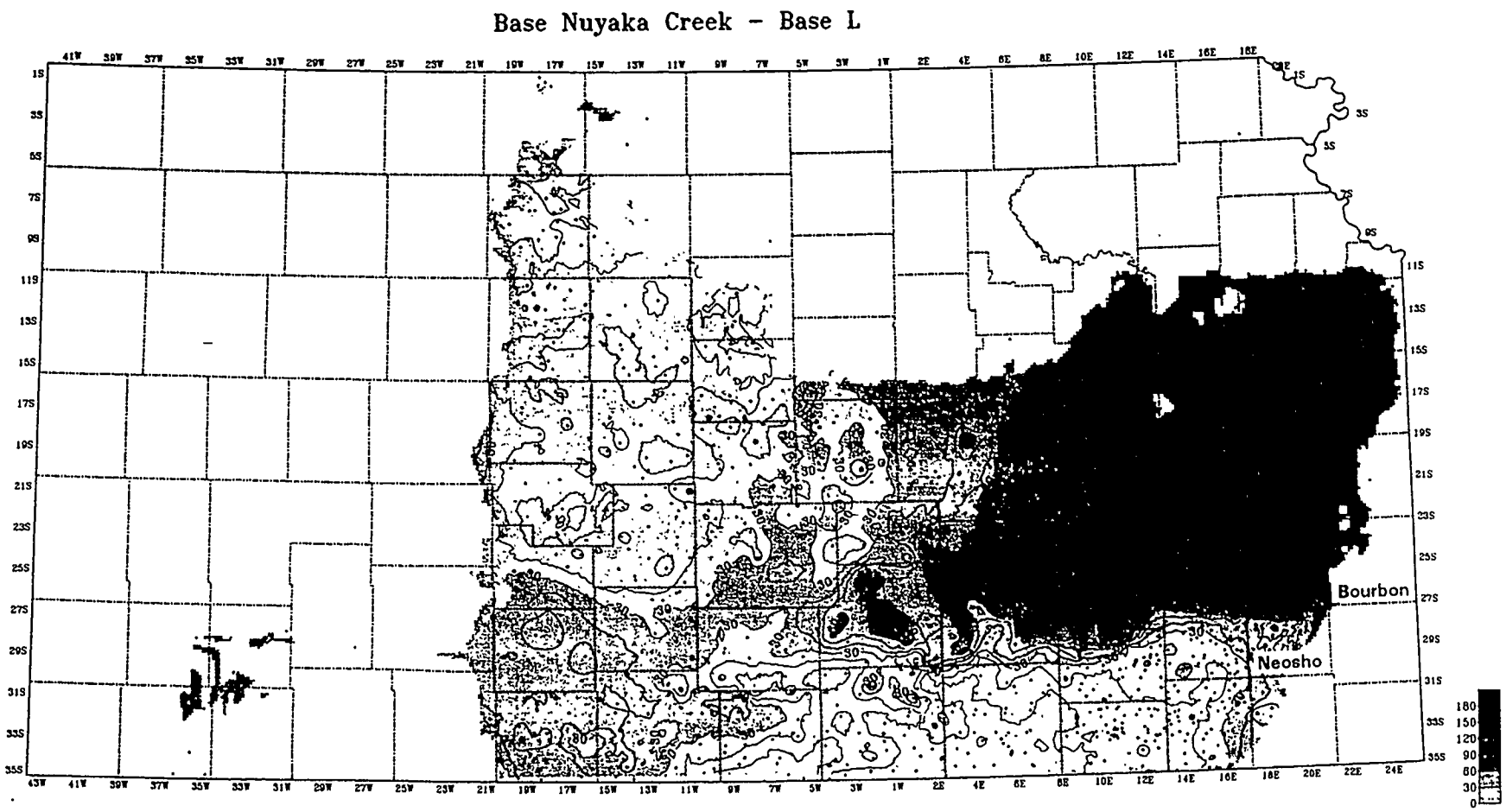

KANSAS GEOLOGICAL SURVEY

Figure I.48. Base of Nuyaka Creek Shale to base of Hertha (L zone)(Pleasanton sequence) from linked regional stratigraphic databases. Contour interval is 10 feet. Shaded interval is 20 feet. County outlines shown (counties indexed in Figure I.27). Every two townships and ranges are labeled along borders. Distance between them is 12 miles. Gridded and contoured using kriging option with SURFACE III.

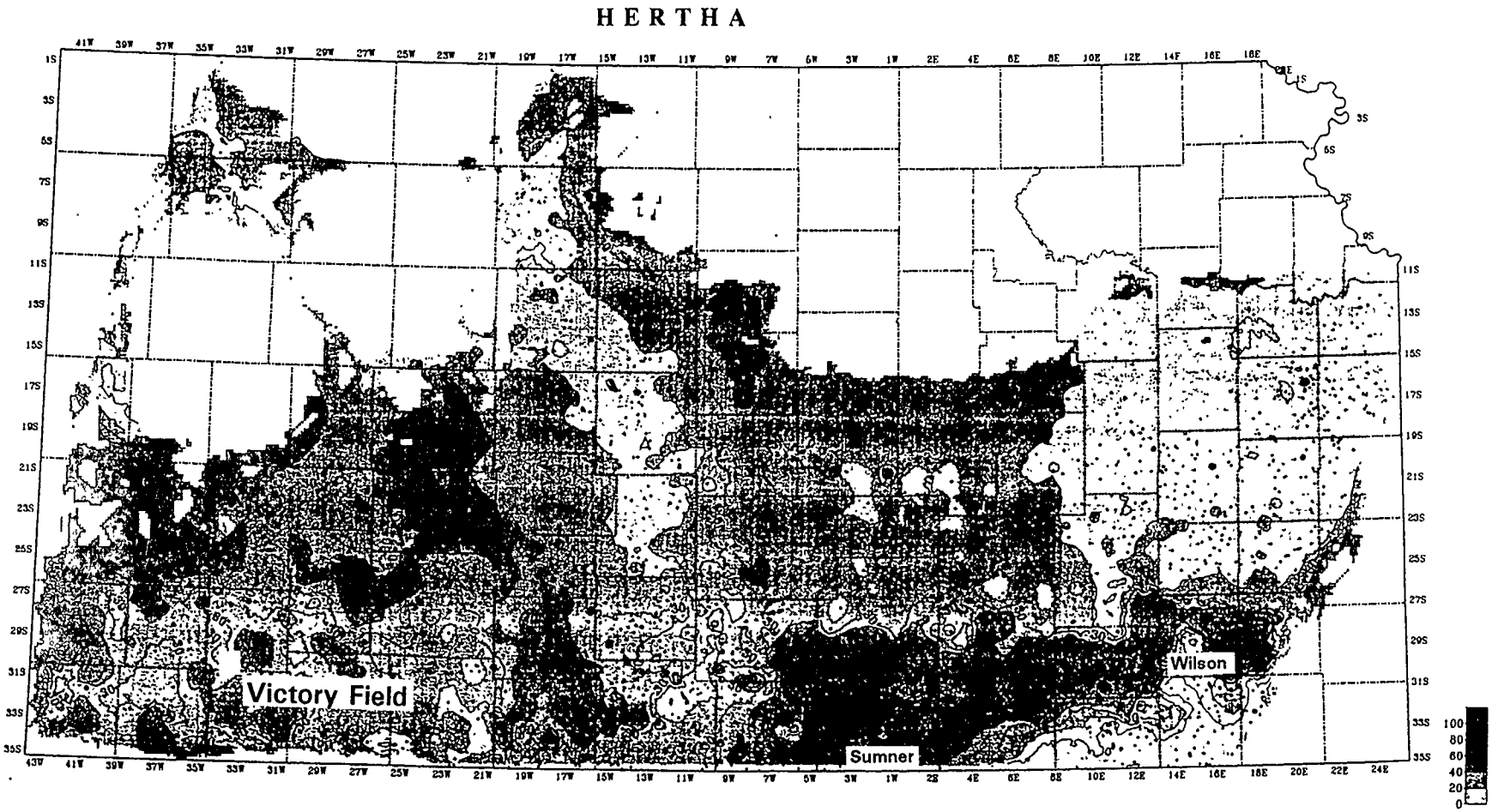

KANSAS GEOLOGICAL SURVEY

Figure I.49. Isopach of Sniabar sequence from linked regional stratigraphic databases. Contour interval is 10 feet. Shaded interval is 20 feet. County outlines shown (counties indexed in Figure I.27). Every two townships and ranges are labeled along borders. Distance between them is 12 miles. Gridded and contoured using kriging option with SURFACE III.

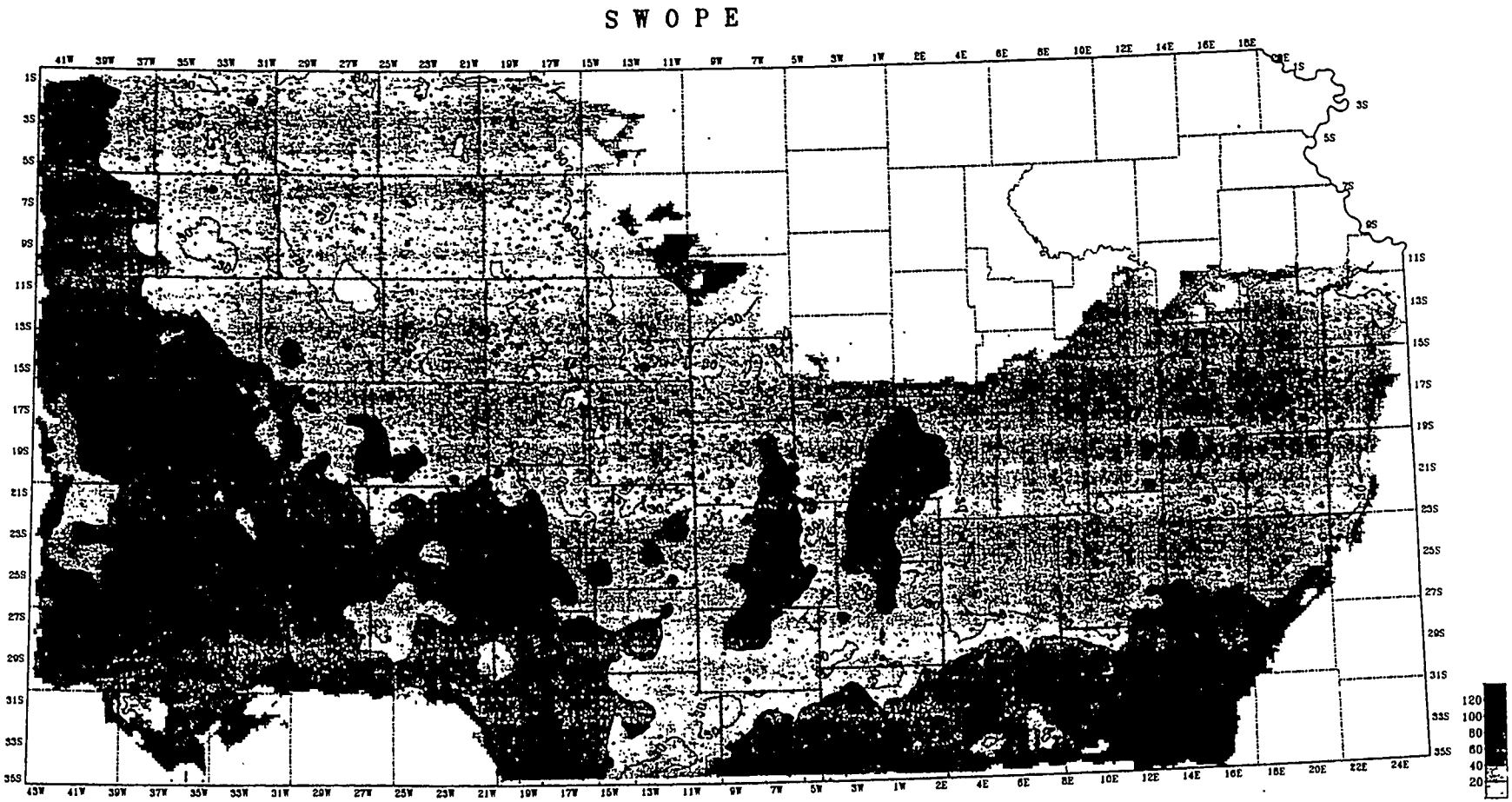

KANSAS GEOLOGICAL SURVEY

Figure I.50. Isopach of Swope sequence from linked regional stratigraphic databases. Contour interval is 10 feet. Shaded interval is 20 feet. County outlines shown (counties indexed in Figure I.27). Every two townships and ranges are labeled along borders. Distance between them is 12 miles. Gridded and contoured using kriging option with SURFACE III.

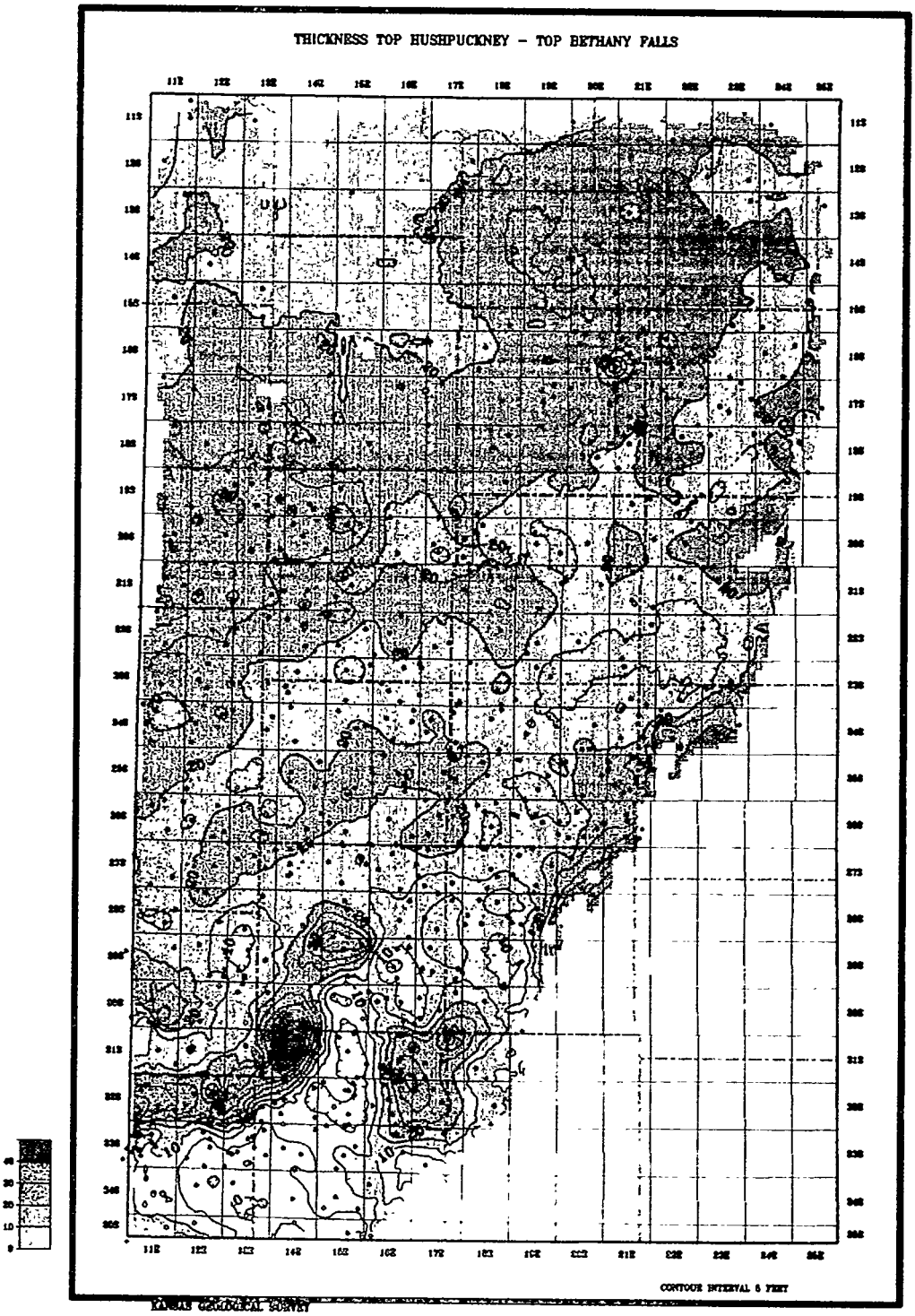

Figure I.51. Isopach of Bethany Falls Limestone in surface and near-surface analog area in southeast Kansas. Map includes county and township lines (6 mi. square).

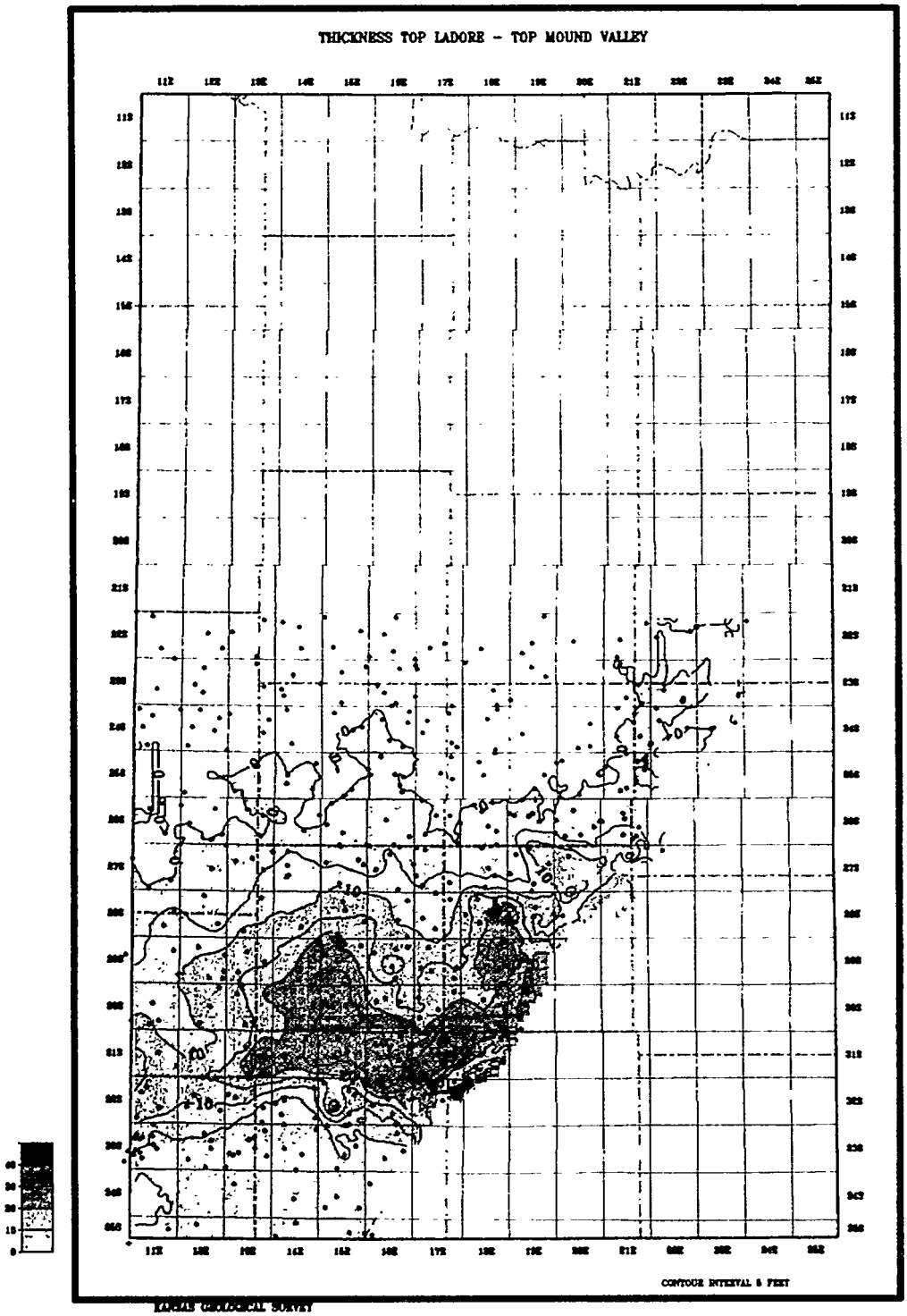

Figure I.52. Isopach of Mound Valley Limestone in surface and near-surface analog area in southeast Kansas. Map includes county and township lines (6 mi. square).

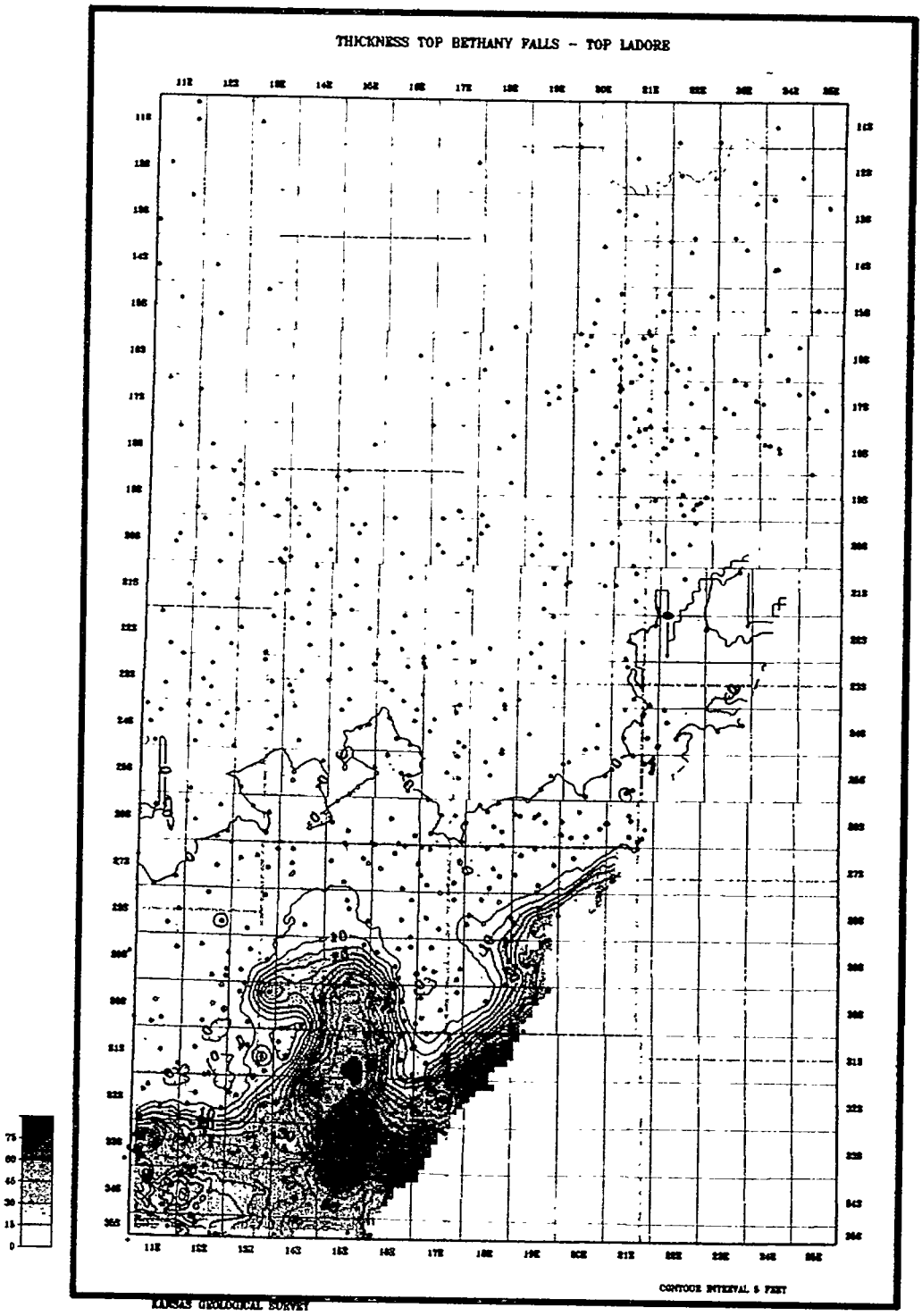

Figure I.53. Isopach of Ladore Shale in surface and near-surface analog area in southeast Kansas. Map includes county and township lines (6 mi. square).

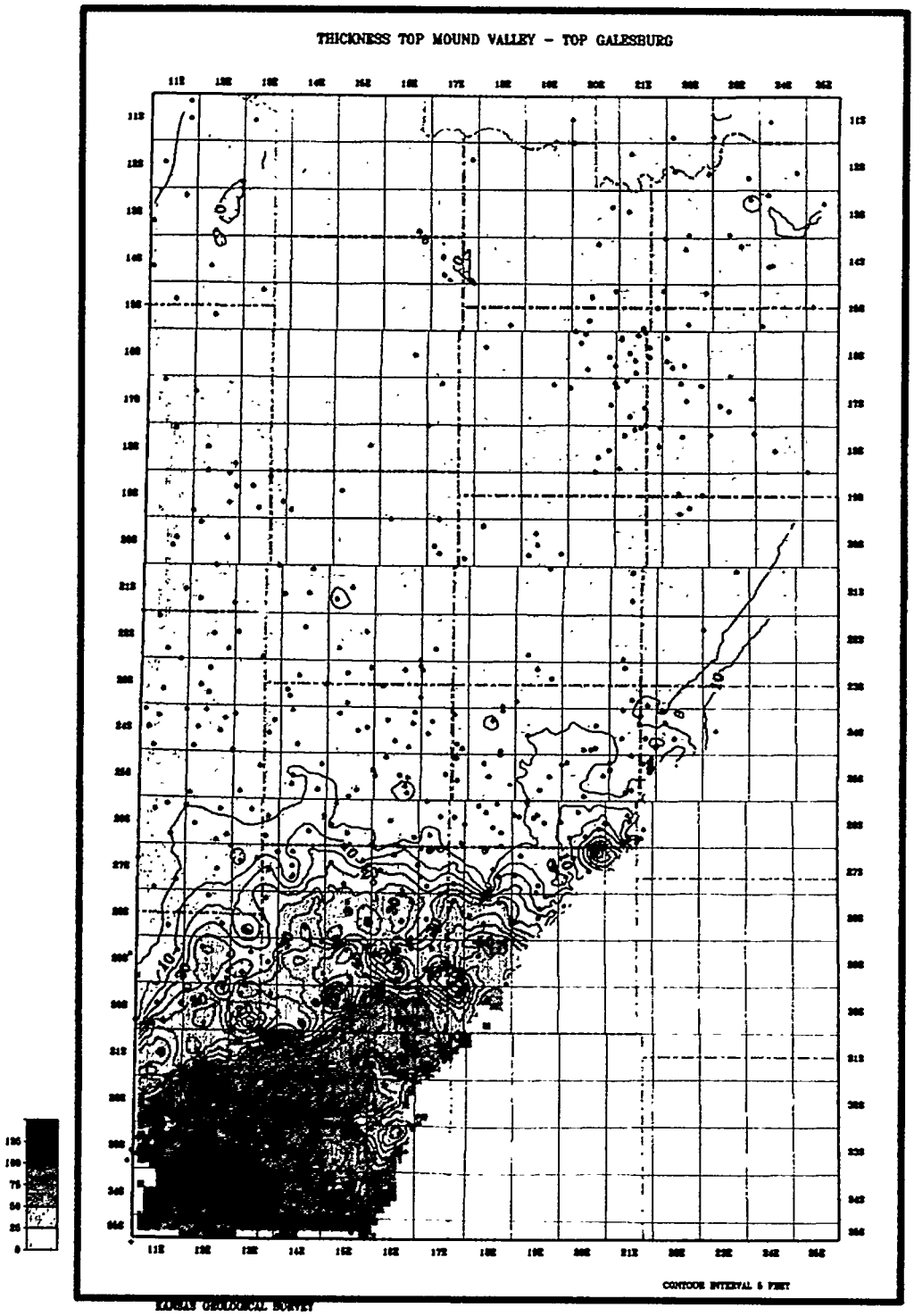

Figure I.54. Isopach of Galesburg Shale in surface and near-surface analog area in southeast Kansas. Map includes county and township lines (6 mi. square).

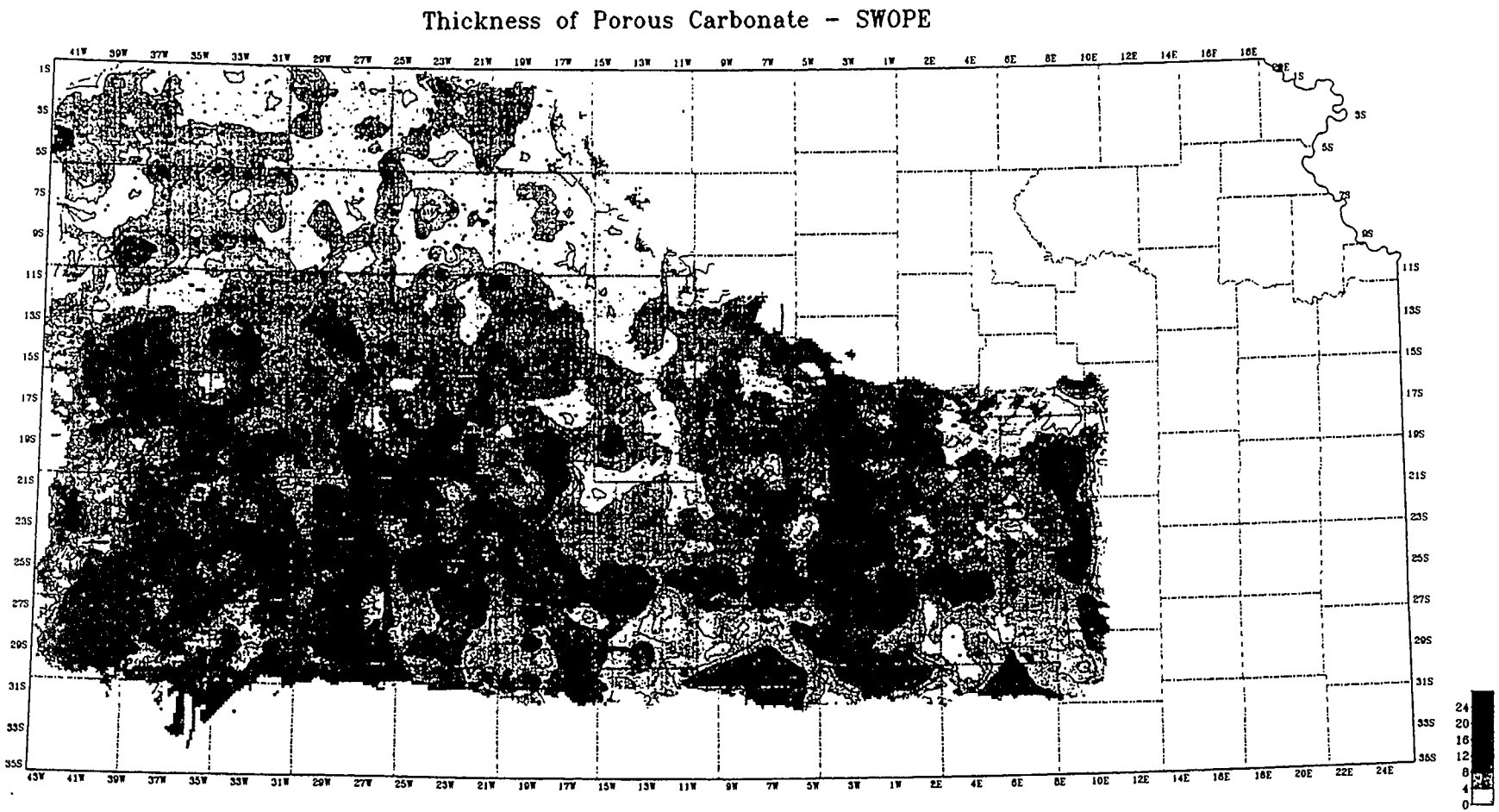

KANSAS GEOLOGICAL SURVEY

Figure I.55. Isochore map of the thickness of porous carbonate above 8% percent porosity in the Swope sequence (Bethany Falls Limestone) from linked regional stratigraphic databases. Contour interval is 2 feet. Shaded interval is 4 feet. County outlines shown (counties indexed in Figure I.27). Every two townships and ranges are labeled along borders. Distance between them is 12 miles. Gridded and contoured using kriging option with SURFACE III.

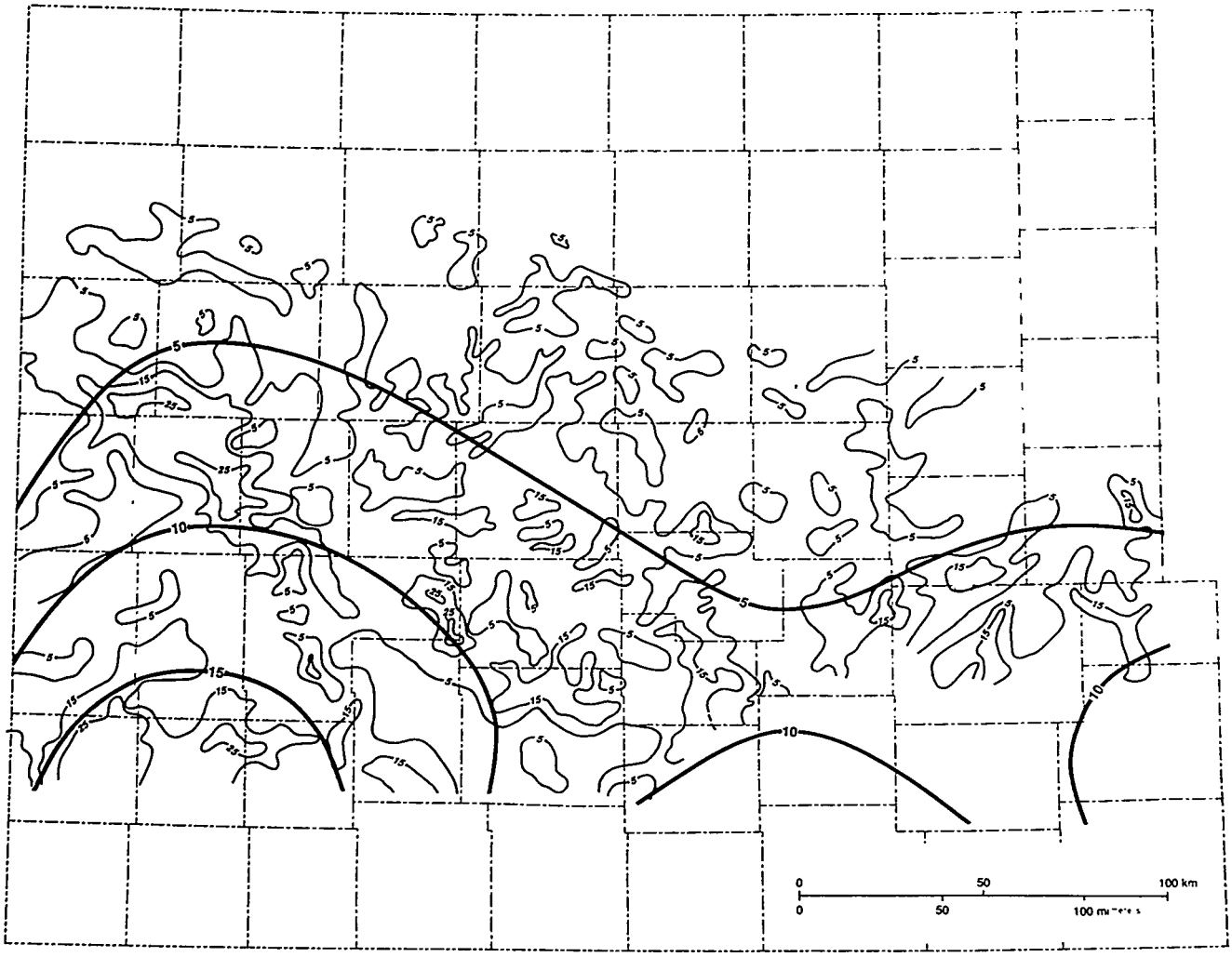

INDEX MAP

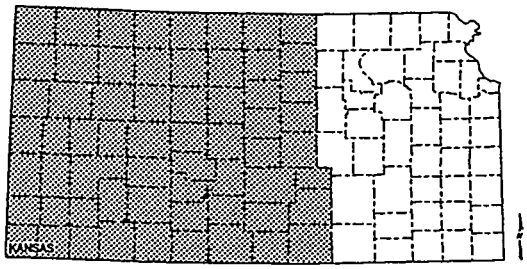

Figure I.56. Hand contoured isochore map of the thickness of porous carbonate in the Swope sequence (Bethany Falls Limestone). Contour interval equals 5 feet. Heavy contours are 4th-order polynomial trend surface contours fit to the Swope interval thickness.

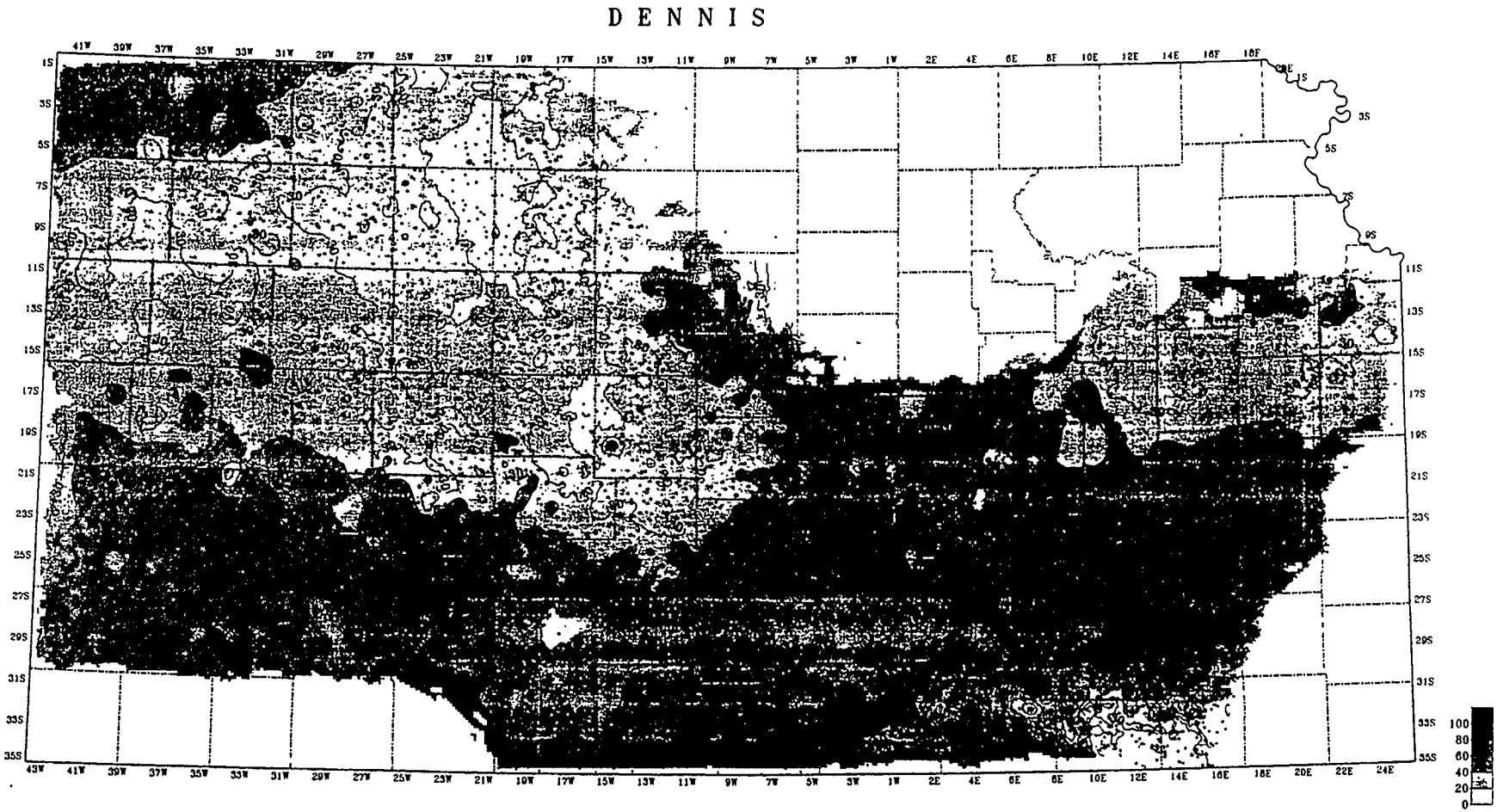

KANSAS GEOLOGICAL SURVEY

Figure I.57. Isopach of the Dennis sequence from linked regional stratigraphic databases. Contour interval is 10 feet. Shaded interval is 20 feet. County outlines shown (counties indexed in Figure I.27). Every two townships and ranges are labeled along borders. Distance between them is 12 miles. Gridded and contoured using kriging option with SURFACE III.

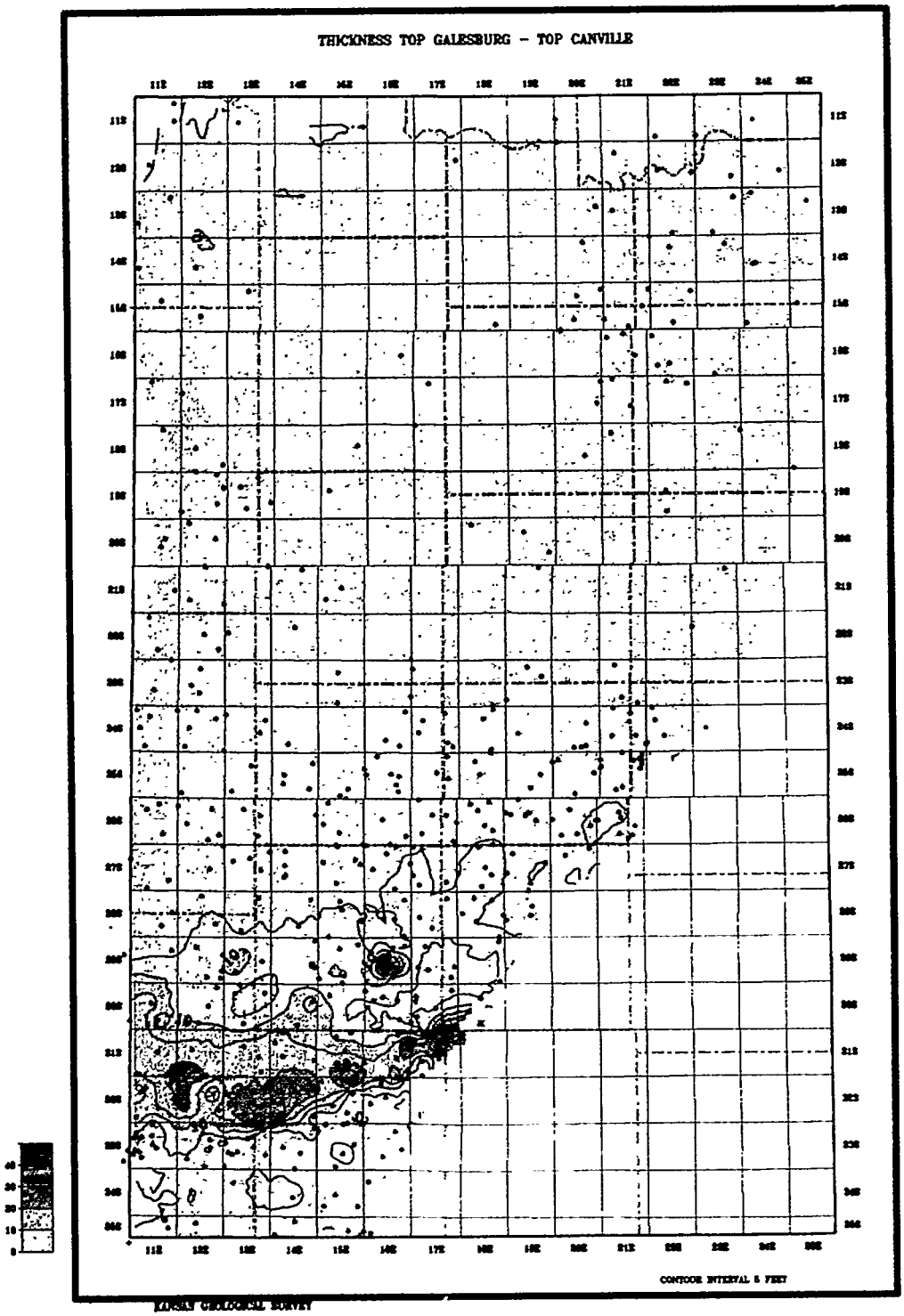

Figure I.58. Isopach of the Canville Limestone in the analog area in eastern Kansas. Unit is the transgressive limestone (flooding unit) of the Dennis sequence.

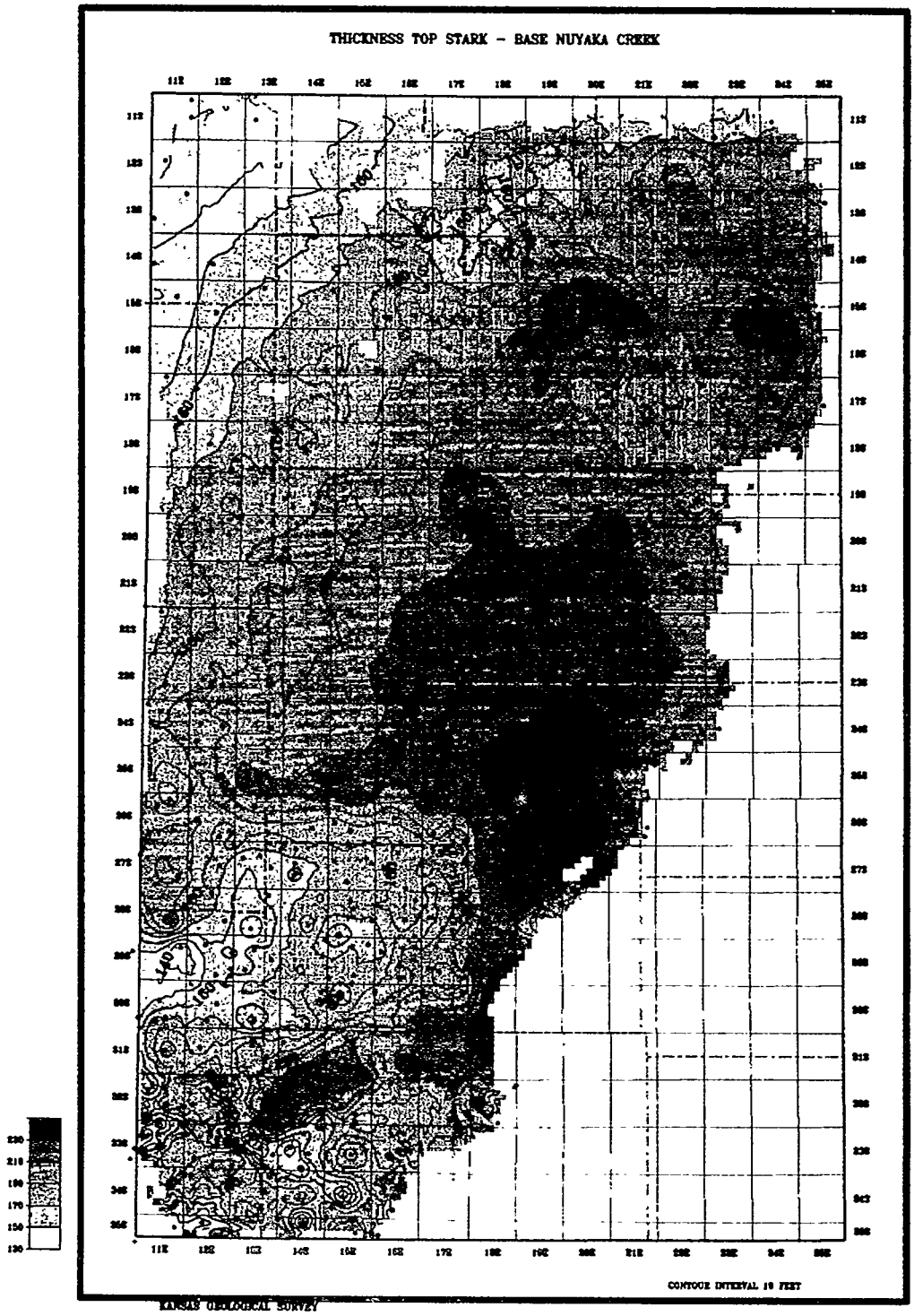

Figure I.59. Isopach of the interval from the Nuyaka Creek Shale to the Stark Shale in the surface and near-surface analog area in southeastern Kansas showing more uniform thickness pattern than that of individual sequences included in the interval (Pleasanton, Hertha, Swope) (see cross section in Figure I.39). Reflects infilling of shelf margin during the interval. Stark Shale deposition is interpreted to be a time of minor backstepping of the carbonate shelf margin in southeastern Kansas (regional cross sections in Figures I.24 and I.25) while equivocal evidence for backstepping is indicated on western shelf. This may be localized tectonic event within the Kansas City 3rd-order cycle.

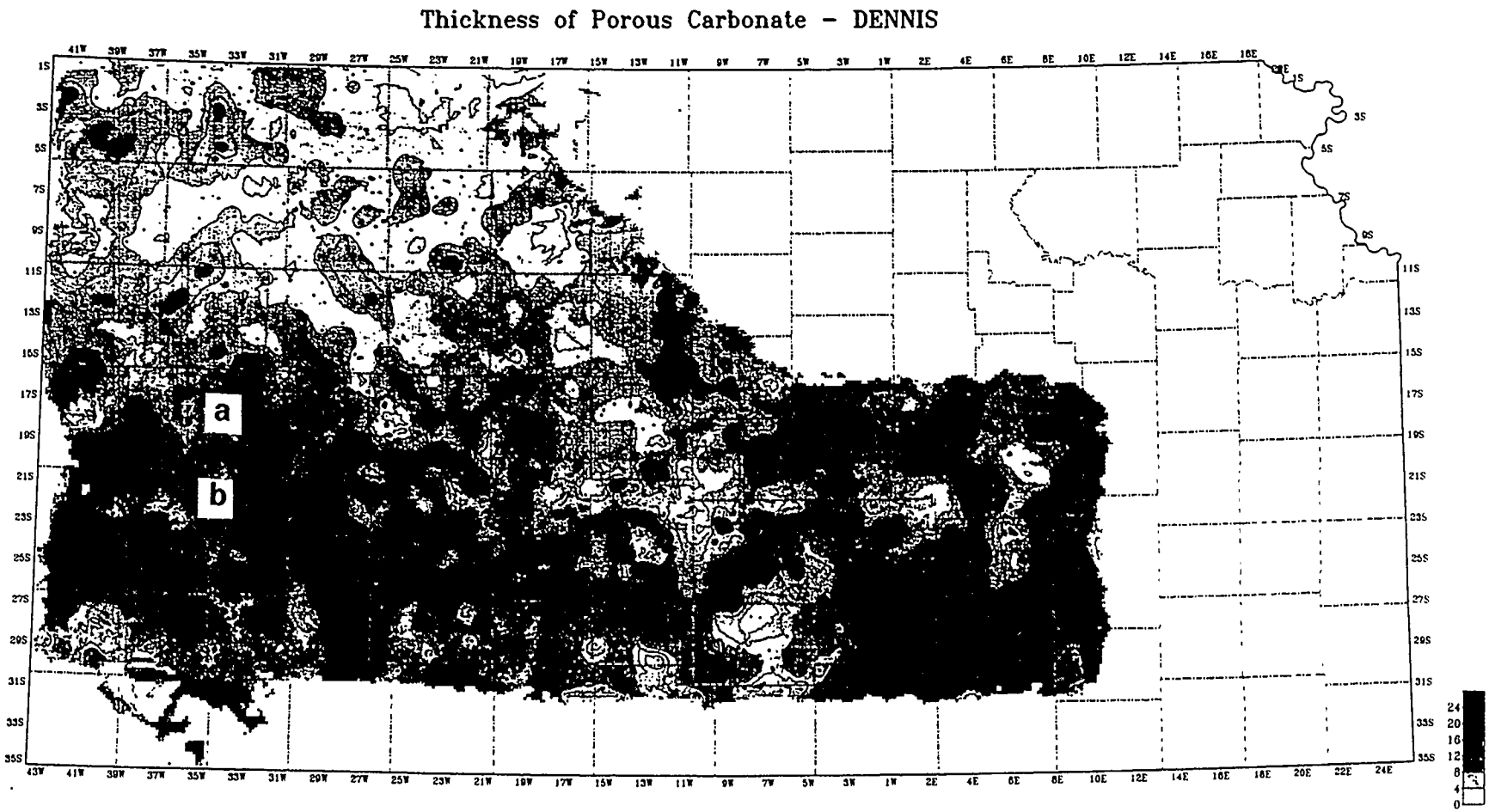

KANSAS GEOLOGICAL SURVEY

Figure I.60. Isochore of thickness of porous carbonate in Dennis sequence (Winterset Limestone) with porosity in excess of 8% from linked regional stratigraphic databases. Contour interval is 2 feet. Shaded interval is 4 feet. County outlines shown (counties indexed in Figure I.27). Every two townships and ranges are labeled along borders. Distance between them is 12 miles. Gridded and contoured using kriging option with SURFACE III. a -- updip lobate porosity; b -- secondary line of lobate porosity discussed in text.

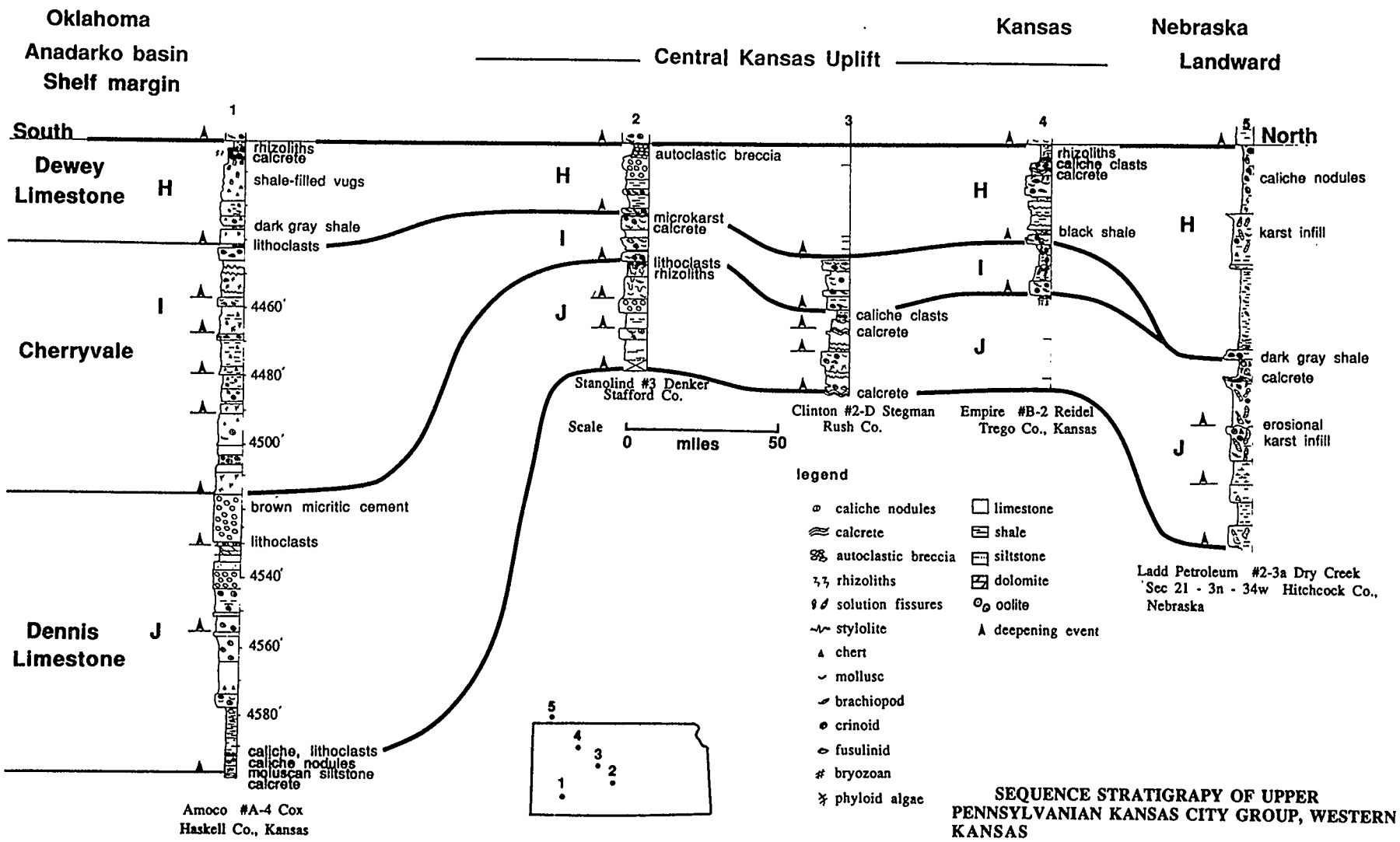

Figure I.61. South-to-north stratigraphic cross section of Dewey, Cherryvale, and Dennis sequences based on core descriptions including the Amoco #A-4 Cox well on the south end of the section. Datum is Muncie Creek Shale, top of the Kansas City 3rd-order cycle. Note multiple cyclicity and thickness variation in the Dennis and Cherryvale and the thin uniform nature of the Dewey sequence characterized by intense subaerial weathering along its upper surface (from Watney et al., 1991).

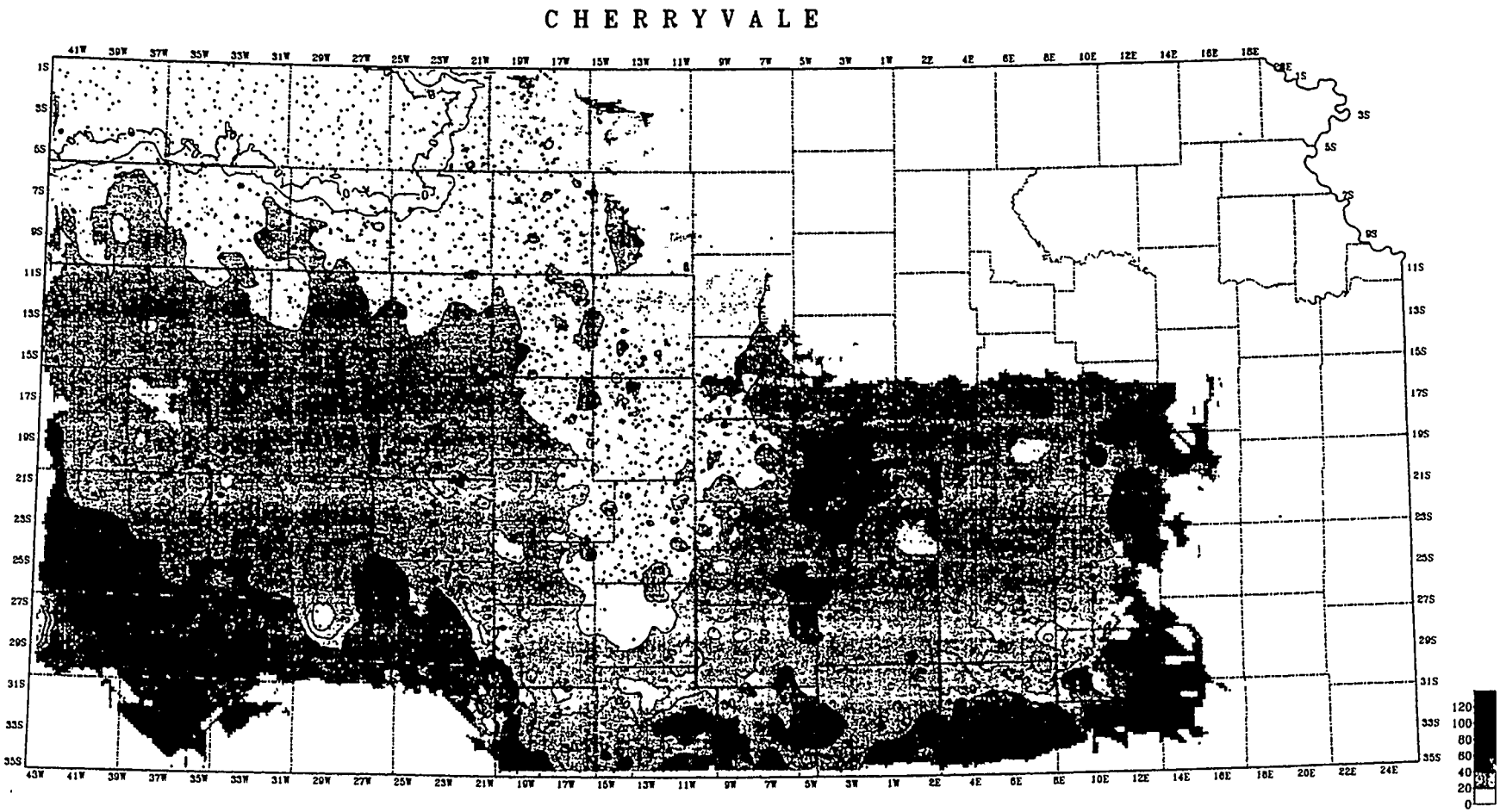

KANSAS GEOLOGICAL SURVEY

Figure I.62. Isopach of the Cherryvale sequence from linked regional stratigraphic databases. Contour interval is 10 feet. Shaded interval is 20 feet. County outlines shown (counties indexed in Figure I.27). Every two townships and ranges are labeled along borders. Distance between them is 12 miles. Gridded and contoured using kriging option with SURFACE III.

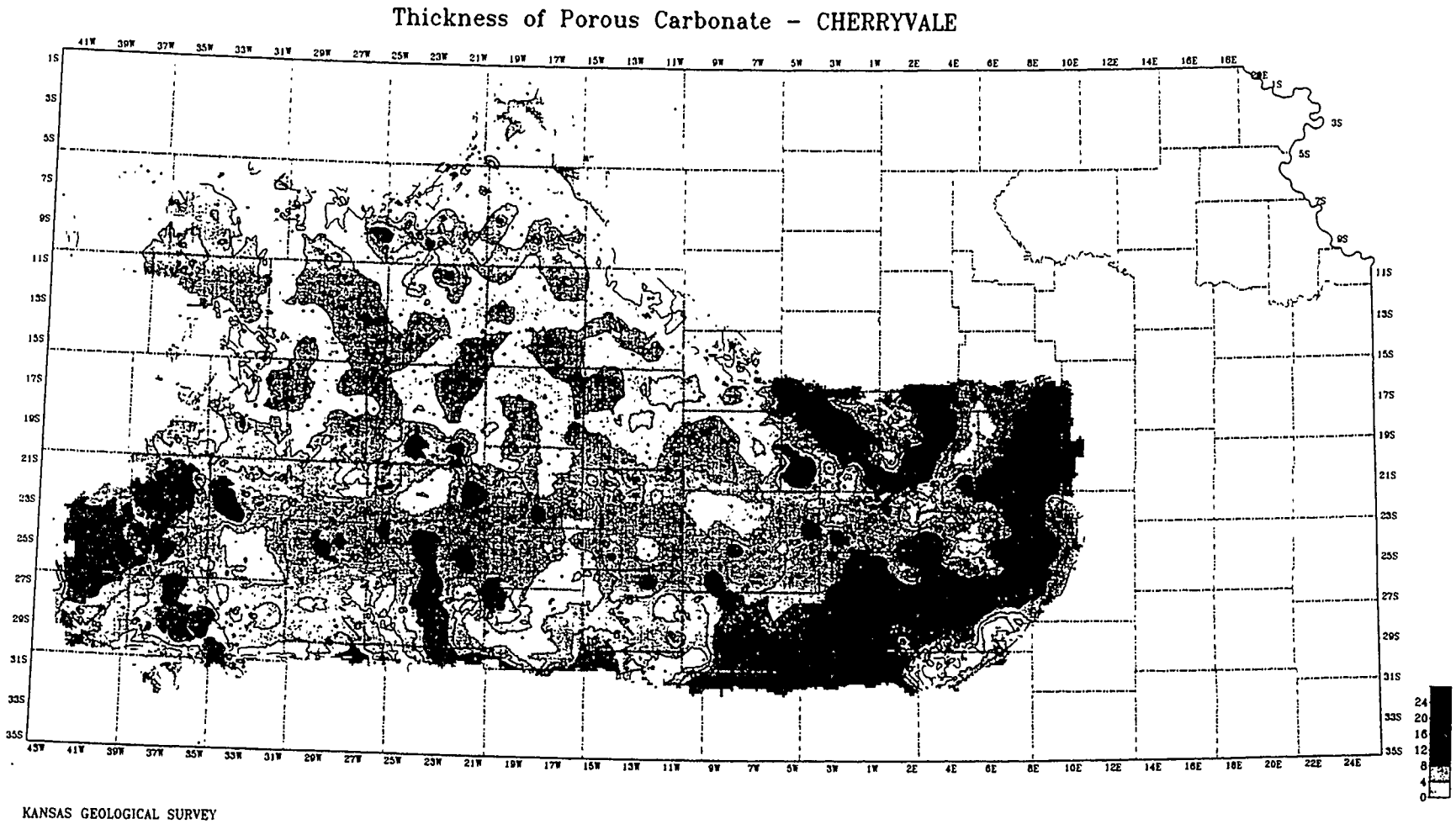

Figure I.63. Isochore map of thickness of porous carbonate in the Cherryvale sequence (Westerville or Drum limestone equivalents) from linked regional stratigraphic databases. Contour interval is 2 feet. Shaded interval is 4 feet. County outlines shown (counties indexed in Figure I.27). Every two townships and ranges are labeled along borders. Distance between them is 12 miles. Gridded and contoured using kriging option with SURFACE III.

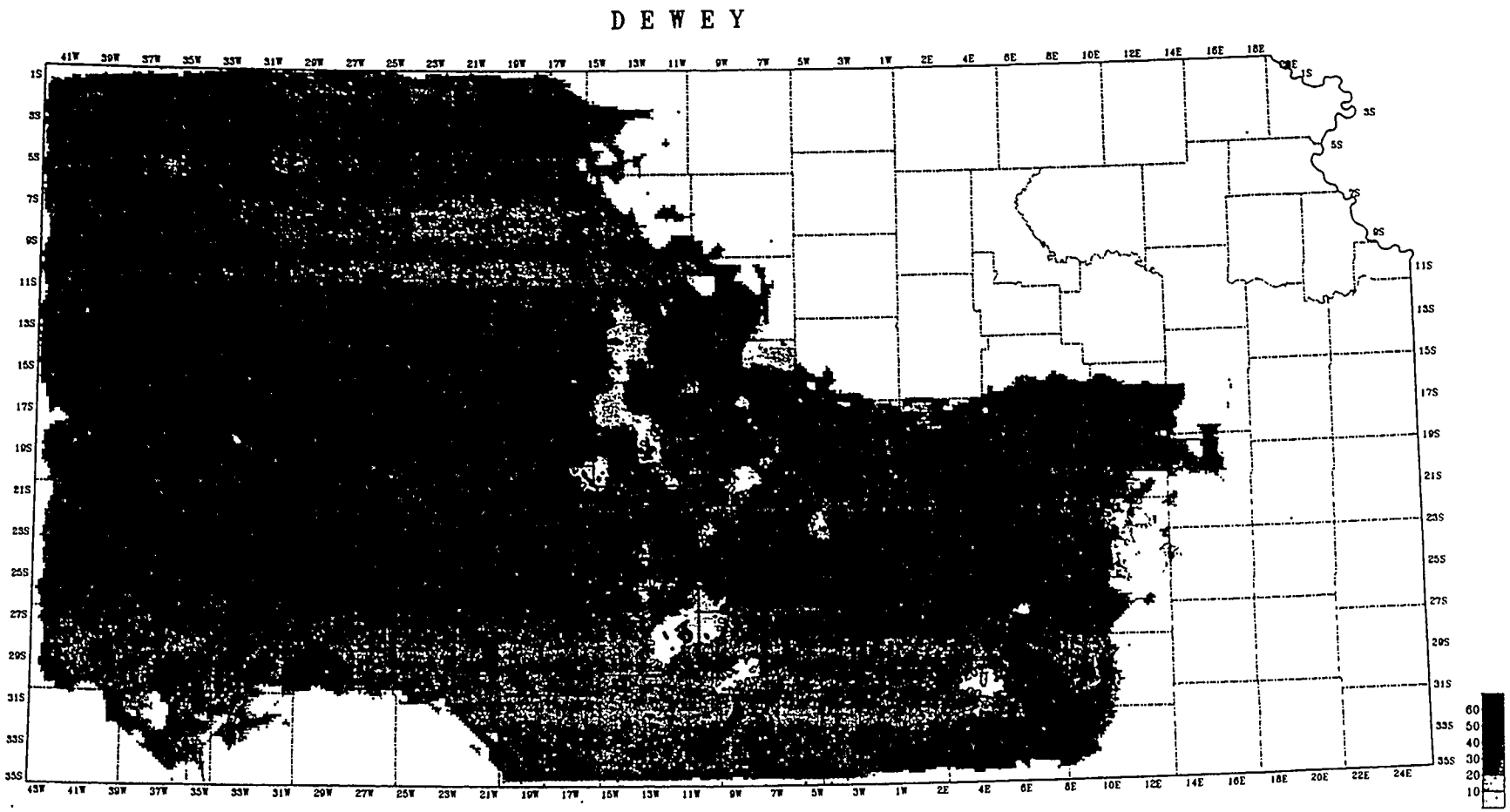

KANSAS GEOLOGICAL SURVEY

Figure I.64. Isopach of thickness of the Dewey sequence from linked regional stratigraphic databases. Contour interval is 10 feet. Shaded interval is 10 feet. County outlines shown (counties indexed in Figure I.27). Every two townships and ranges are labeled along borders. Distance between them is 12 miles. Gridded and contoured using kriging option with SURFACE III. Shelf configuration is interpreted to be much more uniform than previous sequence in Kansas City 3rd-order cycle.

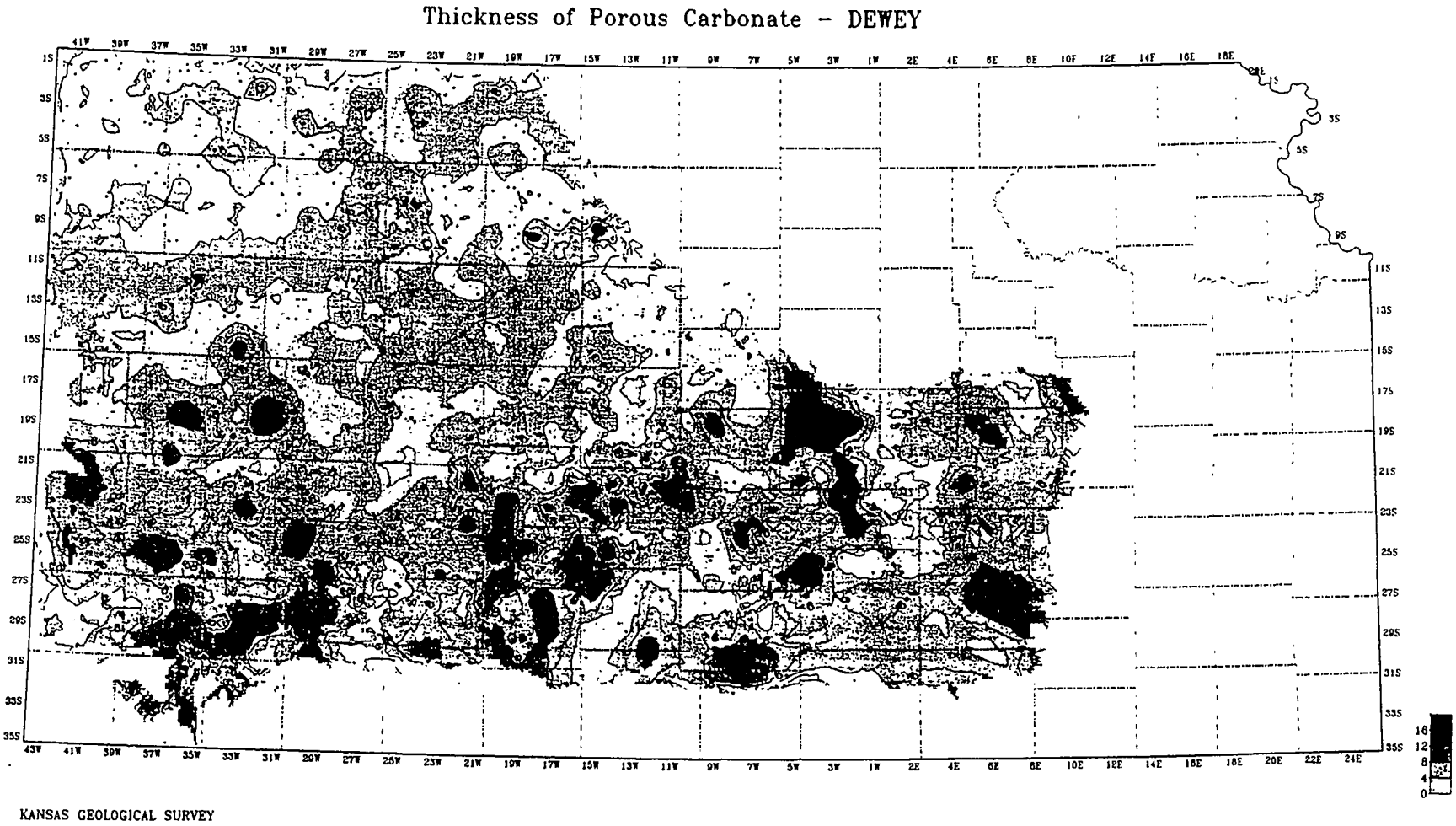

Figure I.65.. Isochore map of thickness of porous carbonate in excess of 8% in the Dewey sequence (Cement City Limestone) from linked regional stratigraphic databases. Contour interval is 2 feet. Shaded interval is 4 feet. County outlines shown (counties indexed in Figure I.27). Every two townships and ranges are labeled along borders. Distance between them is 12 miles. Gridded and contoured using kriging option with SURFACE III.

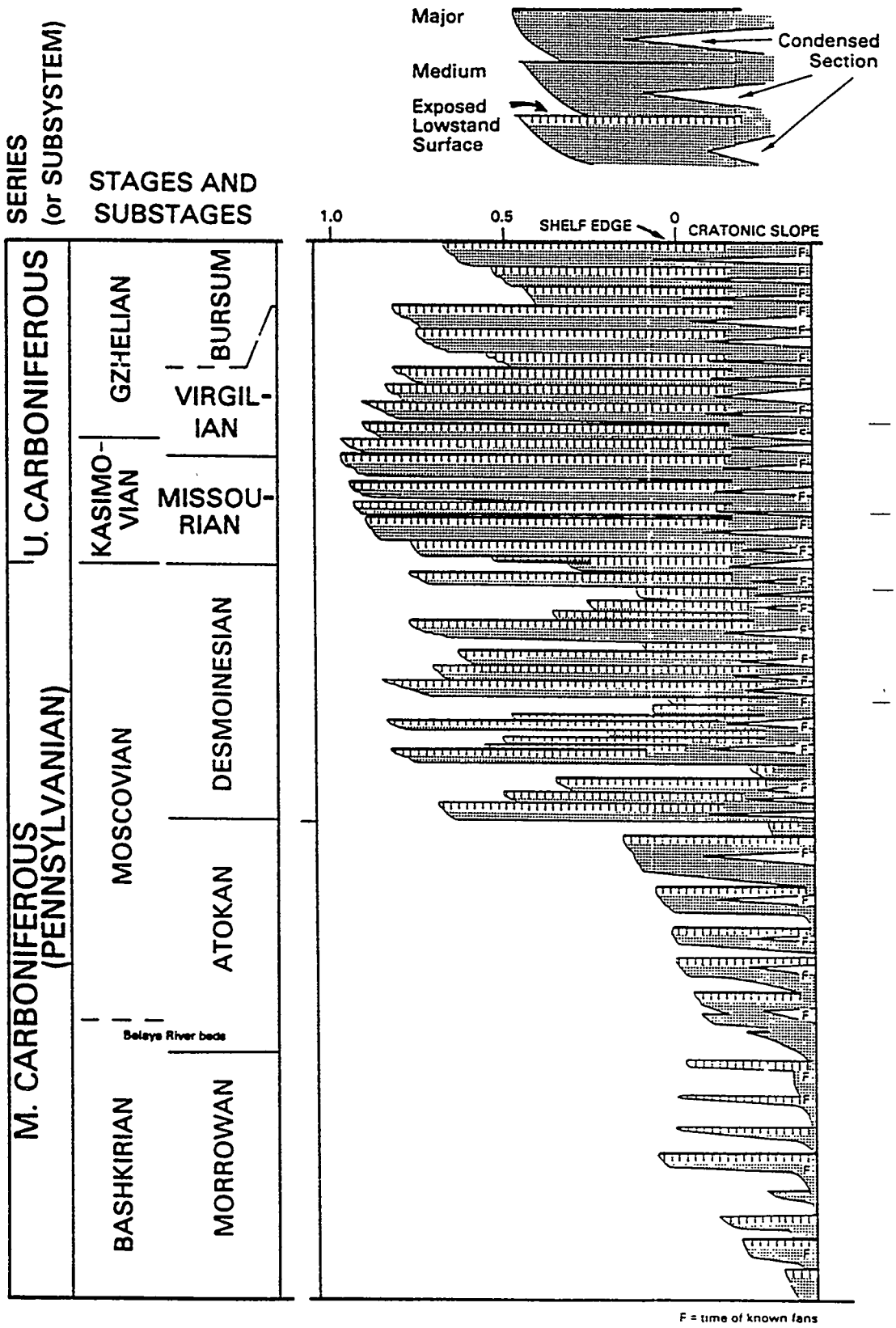

Ross and Ross, 1987

Figure I.66. Relative changes in coastal onlap for Middle and Upper Carboniferous modified from Ross and Ross (1987).

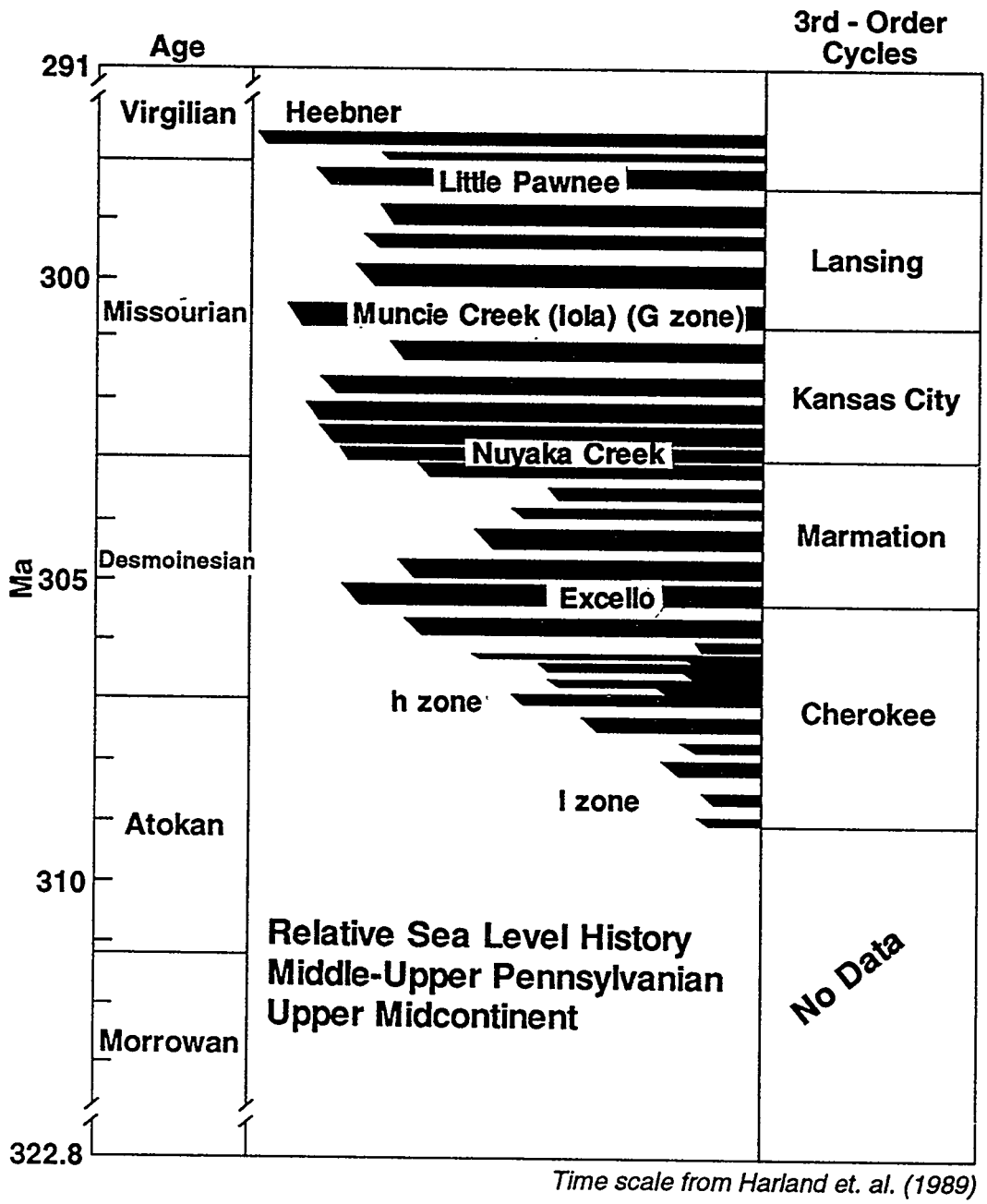

Figure I.67. Relative sea level chart for Midcontinent region for this study and Youle (1992). Black bars represent relative innundation of individual 4th-order (cyclothem scale) sequences (landward to left and basinward to right).

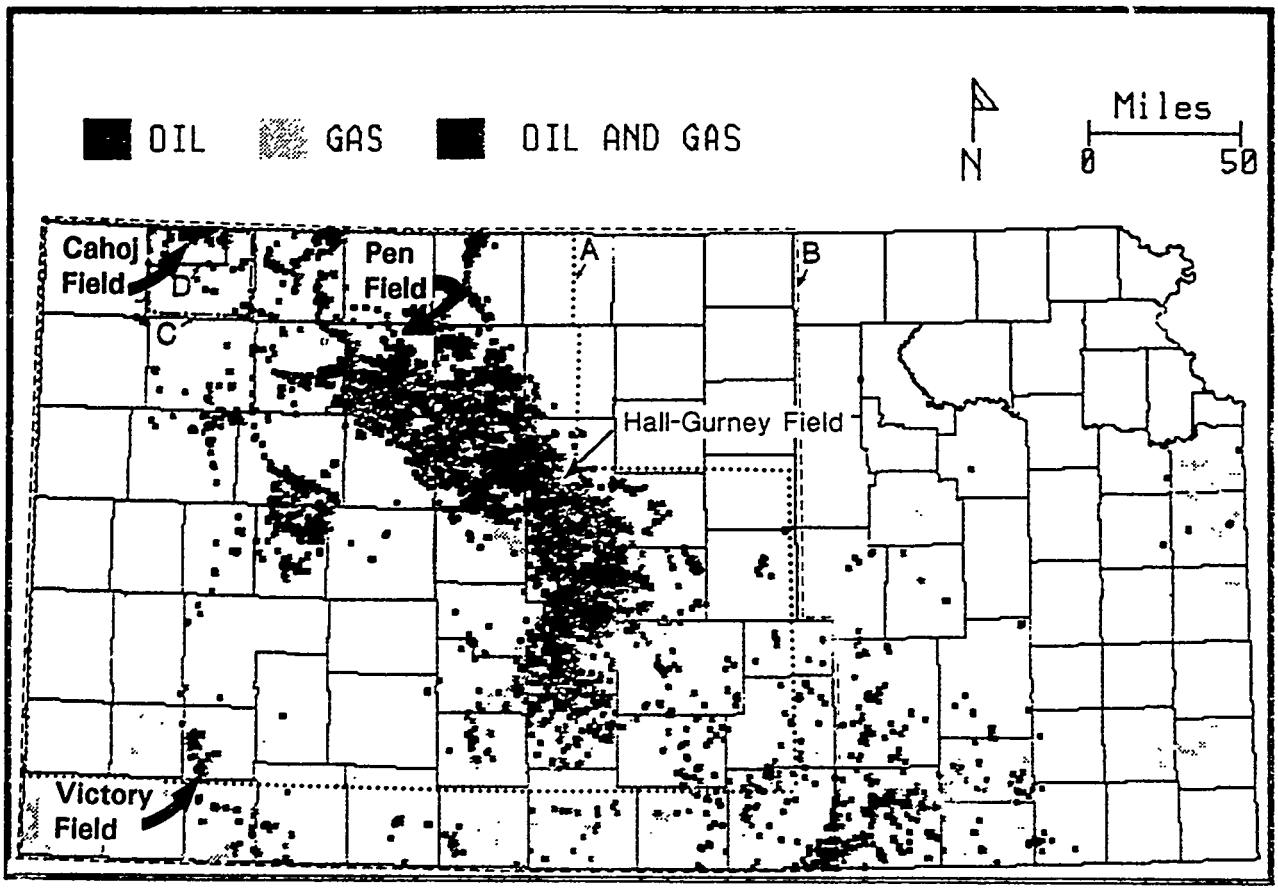

Figure 1.A.1. Map showing leases producing oil and gas from the Missourian (LKC) in Kansas with location of Cahoj, Pen, and Victory fields.

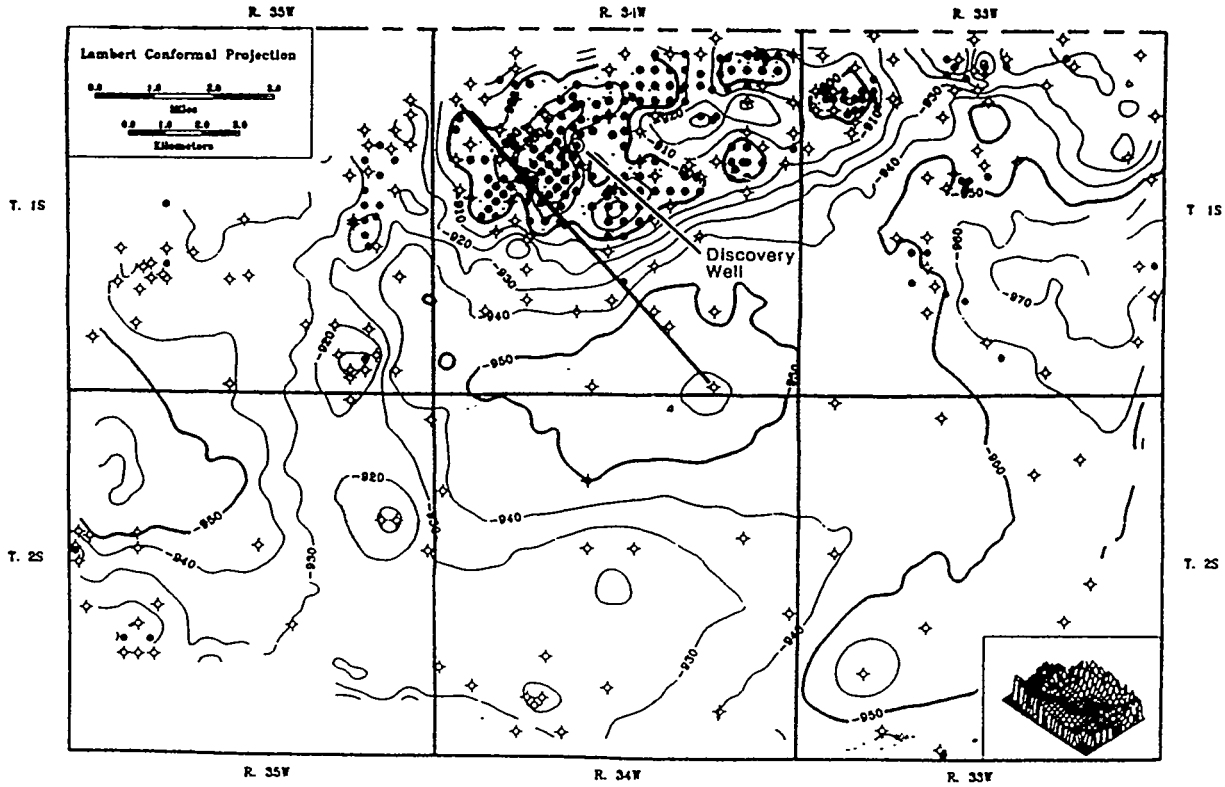

Figure 1.A.2. Structure contour map of the top of Lansing Group in the Cahoj field area from Watney et al., 1992. Contour interval = 10 feet. Squares are townships, 6 mi. on a side.

CAHOJ OIL FIELD

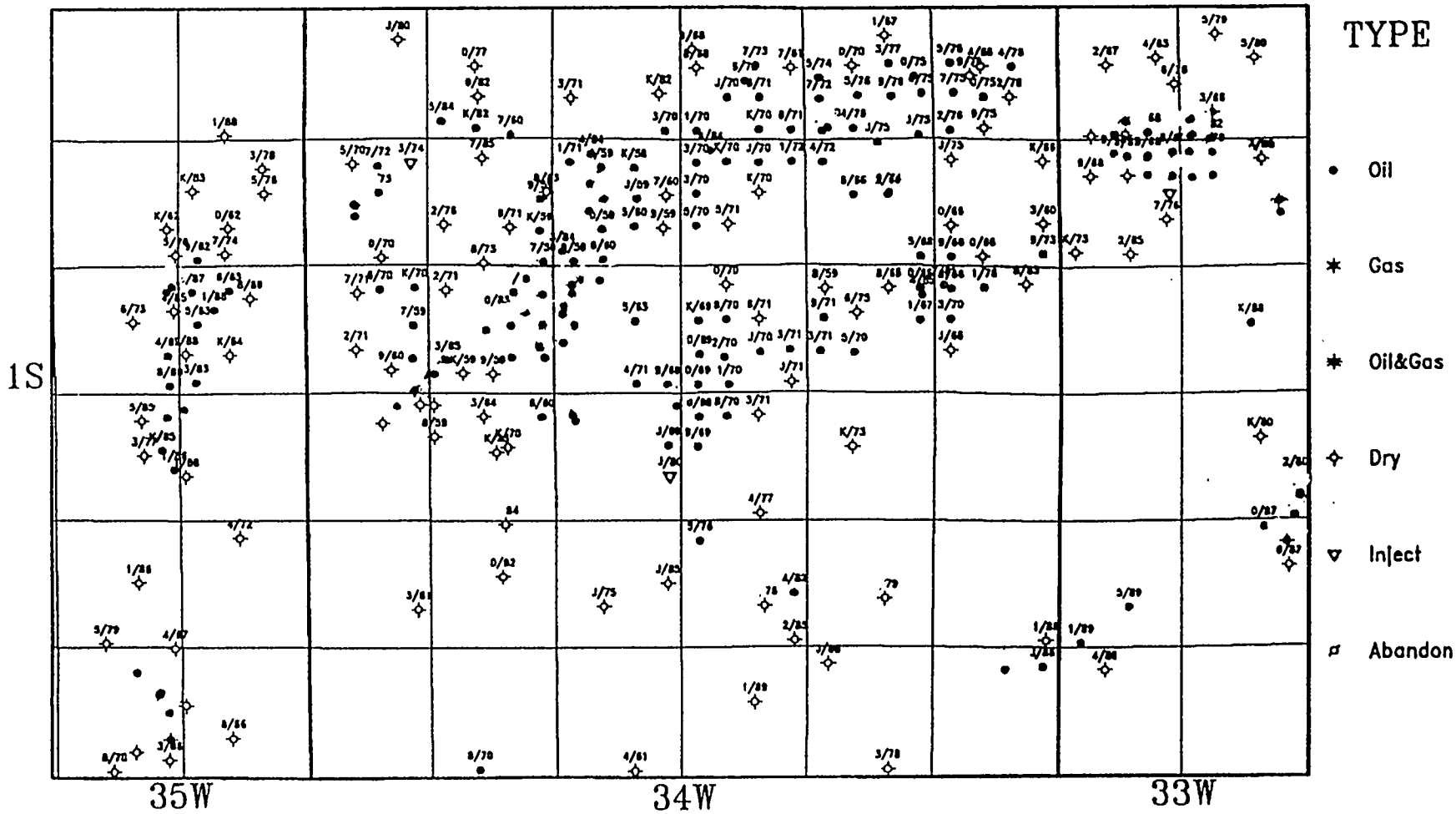

Figure 1.A.3. Map of Cahoj field area showing completion dates on wells. Higher squares are sections, 1 mi. on a side.

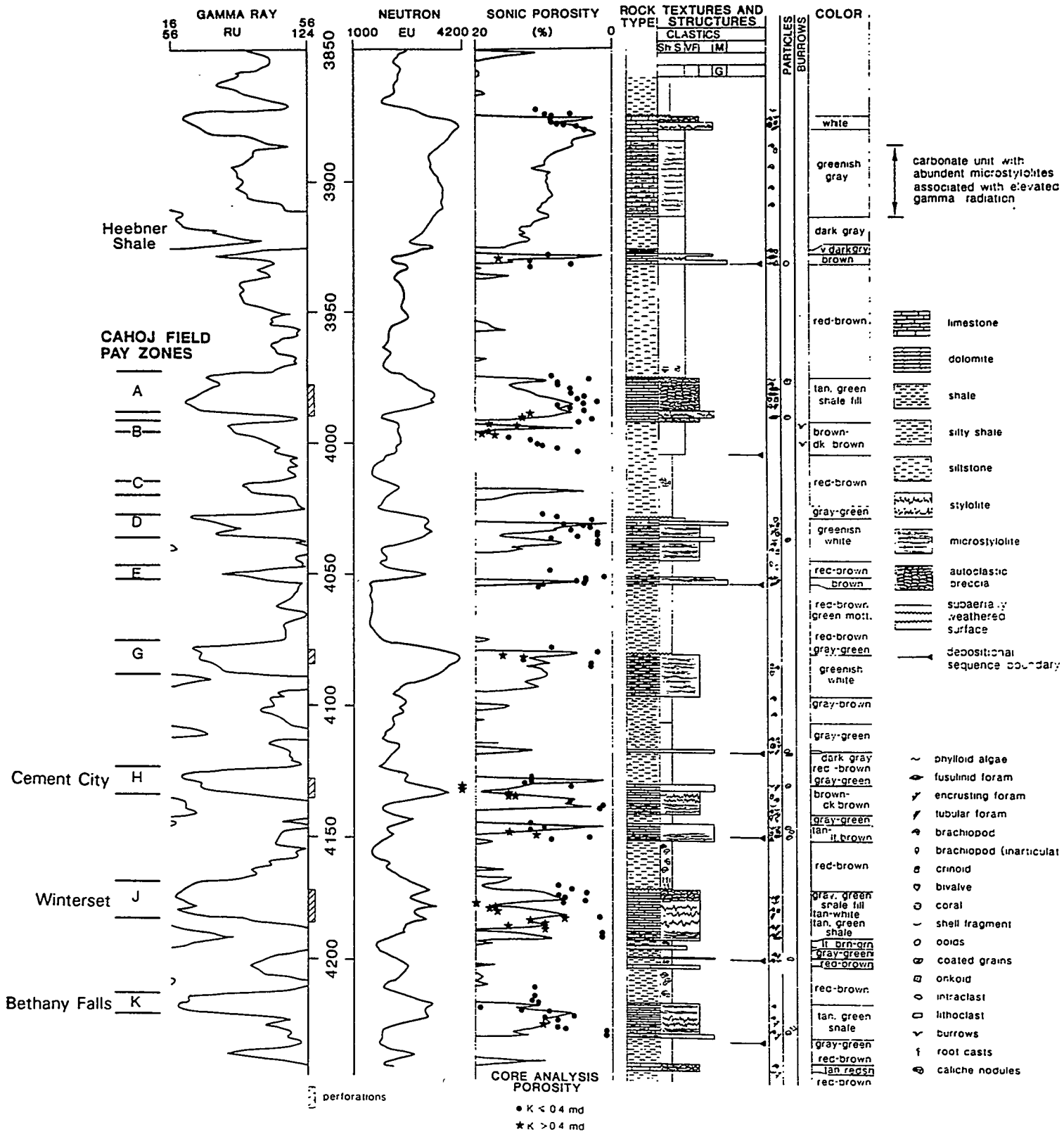

Figure 1.A.4. Combination well log, core analysis, and rock description for continuously cored well, Skelly #1 Bartosovsky located in Section 9-T.1S., R.34W. Subsurface nomenclature applied to zones. Zones of particular interest are the H, J, and K zones corresponding to the Cement City Limestone of the Dewey sequence, the Winterset Limestone of the Dennis sequence, and the Bethany Falls Limestone of the Swope sequence. Zones are much thinner than at Victory field.

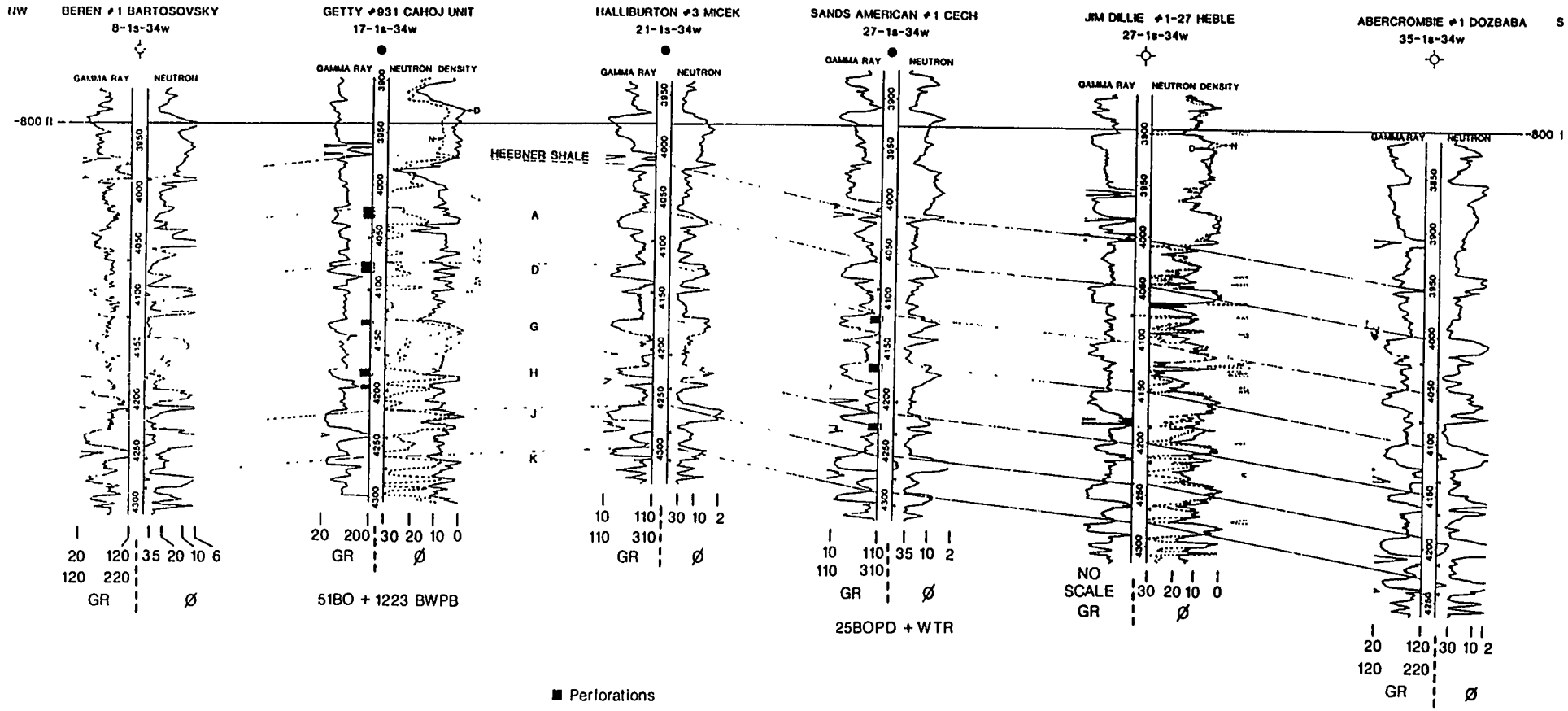

Figure 1.A.5. Structural wireline log cross section indexed in Figure 1.A.2 showing LKC interval with subsurface letter nomenclature applied to zones (from Watney et al., 1992).

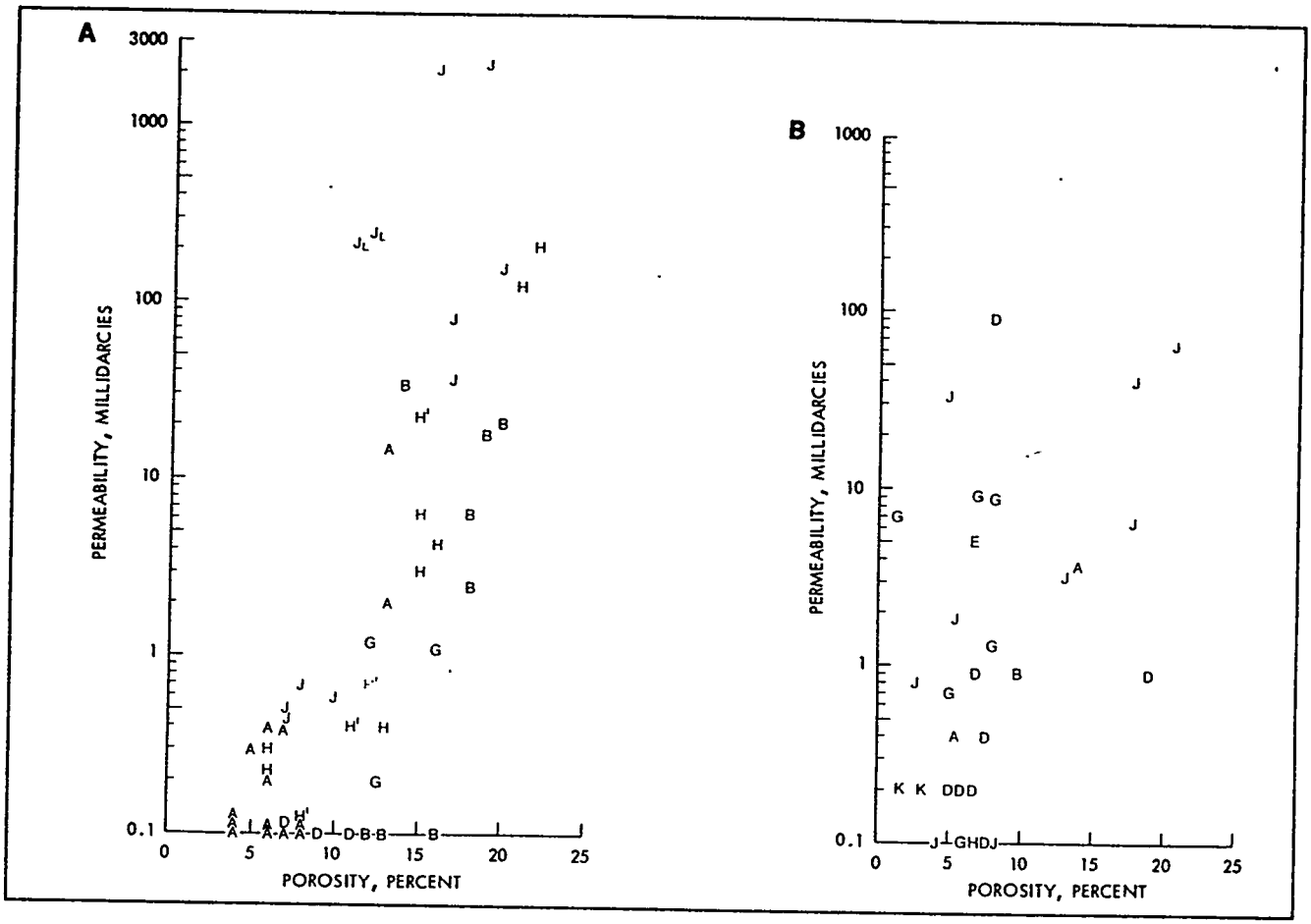

Figure 1.A.6. Porosity-permeability cross plots for (A) Skelly Bartosovsky #1 (Sec. 9, T.1S., R.34W) in Cahoj field compared with (B) Conoco Adell L-KC Unit #409 (Sec. 2, T.6S, R.27W) in Sheridan County. The Conoco well is located 50 mi. southeast of Cahoj field on the Adell anticline on the western edge of the Central Kansas uplift.

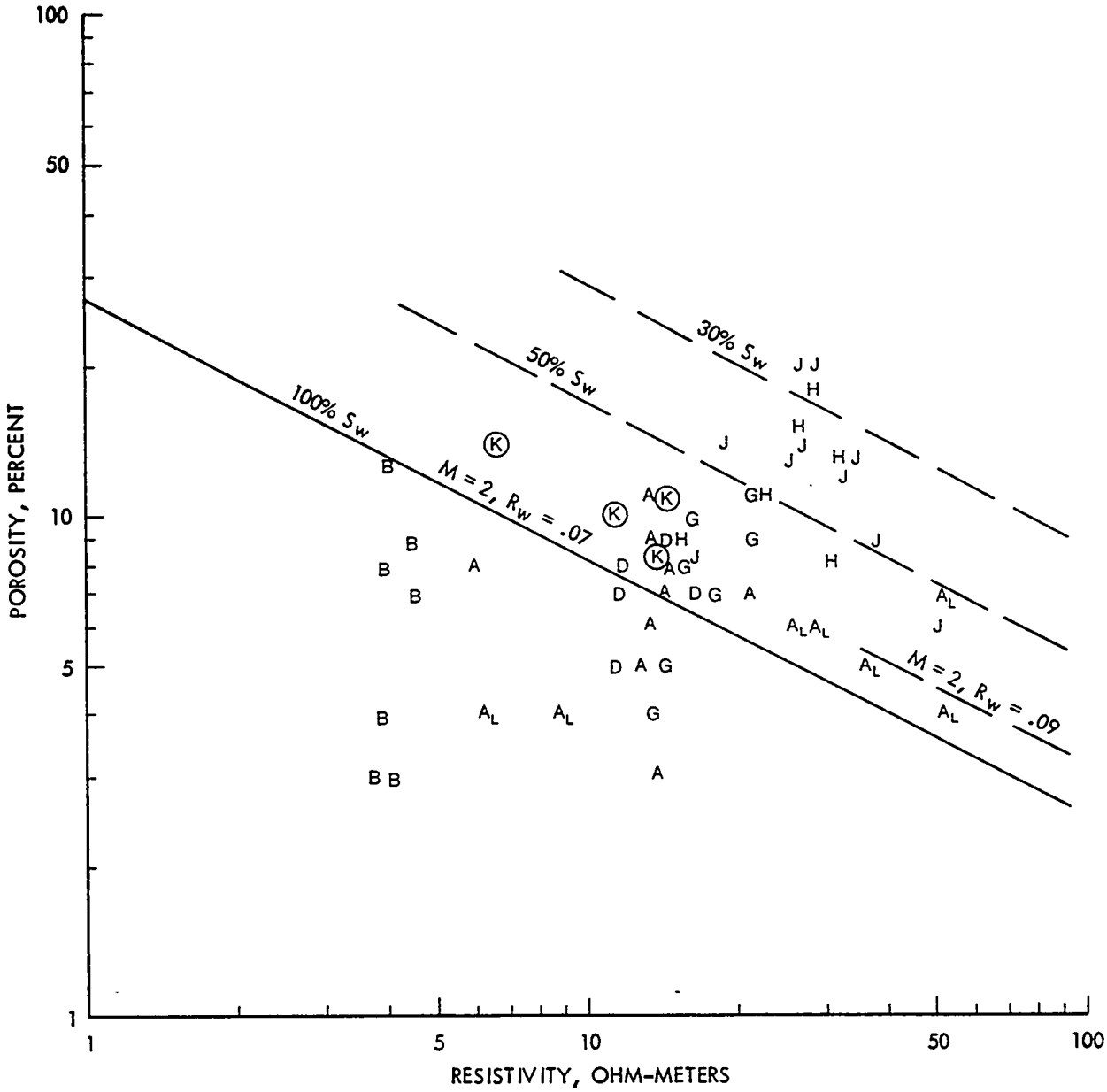

Figure 1.A.7. Log-log plot of induction resistivity vs. shale-corrected sonic porosity for porous zones of Skelly Bartosovsky #1. This is a Pickett plot that is compared with the "Super" Pickett plot approach developed in the study of Victory field (Figure 6.65). Drill stem test results by zone: J -- 3360' oil, SIP 1305-1280#, FP 160-1250#, SWB 144 BO/2 hrs.; H -- 2249' gas + 1880' oil, SIP 1305-1250#, FP 135-745#, SWB 132 BO/2 hrs.; A -- 320' gas, 160' oil, SIP 1280-1120#m /FP 50-80#, SWB 122 BO/2 hrs.; D -- 5' mud with specks oil, SIP 130-0#, FP 0-0#; K -- 60' muddy saltwater with specks oil, SIP 1330-1120#, FP 0-0#.

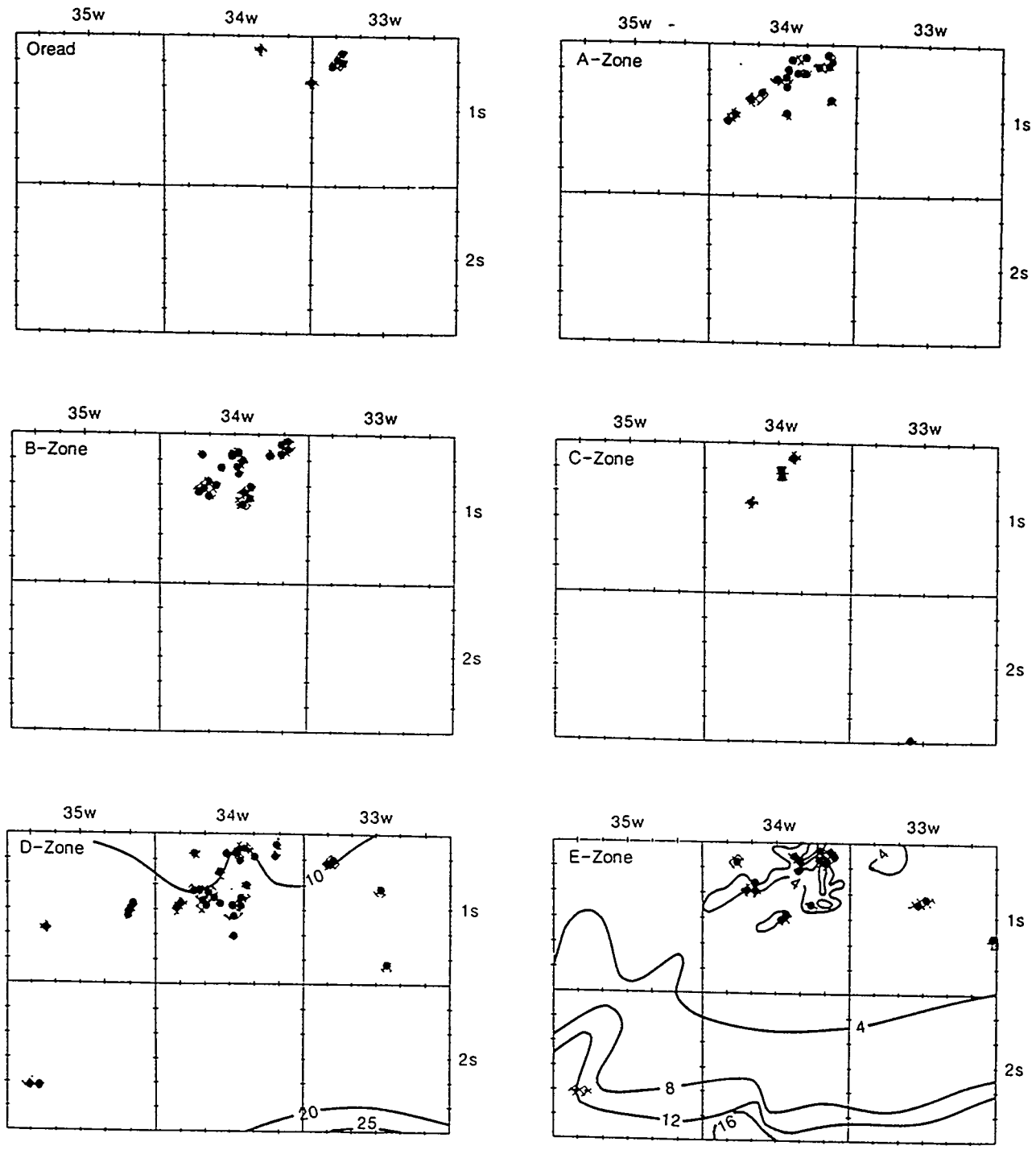

Figure 1.A.8. Map of perforated wells by zone for upper zones in LKC for same six township areas shown in Figure 1.A.2. Many wells have production from multiple zones. Isopach contours shown for D and E zones. See Figure 1.A.4 for key to letter nomenclature.

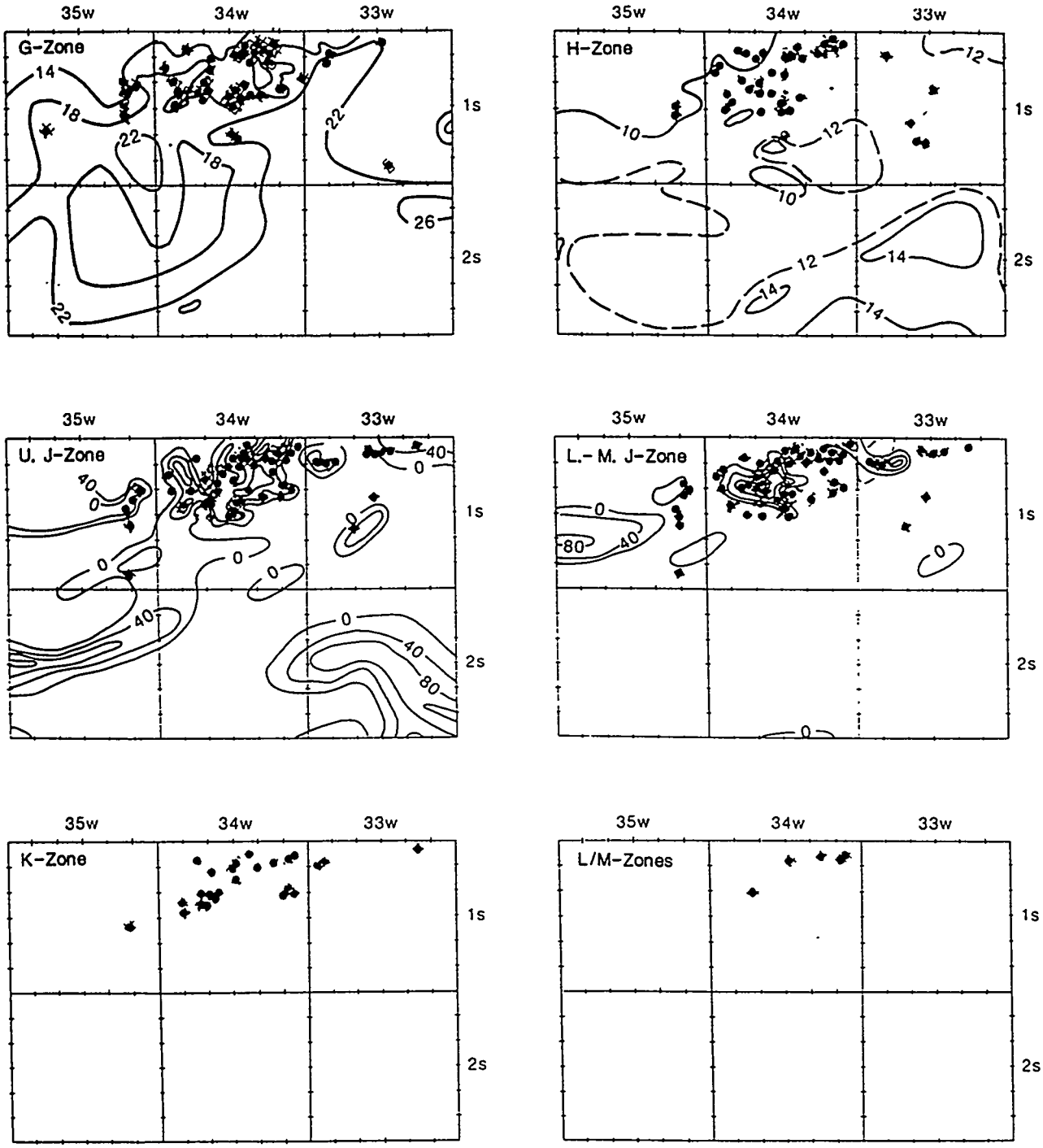

Figure 1.A.9. Map of perforated wells by zone for lower zones in LKC. Isopach contours shown for G and H zones, and porosity-feet contours for J zone. Note upper and lower porosity development in the J zone, very common in LKC fields, including Pen field.

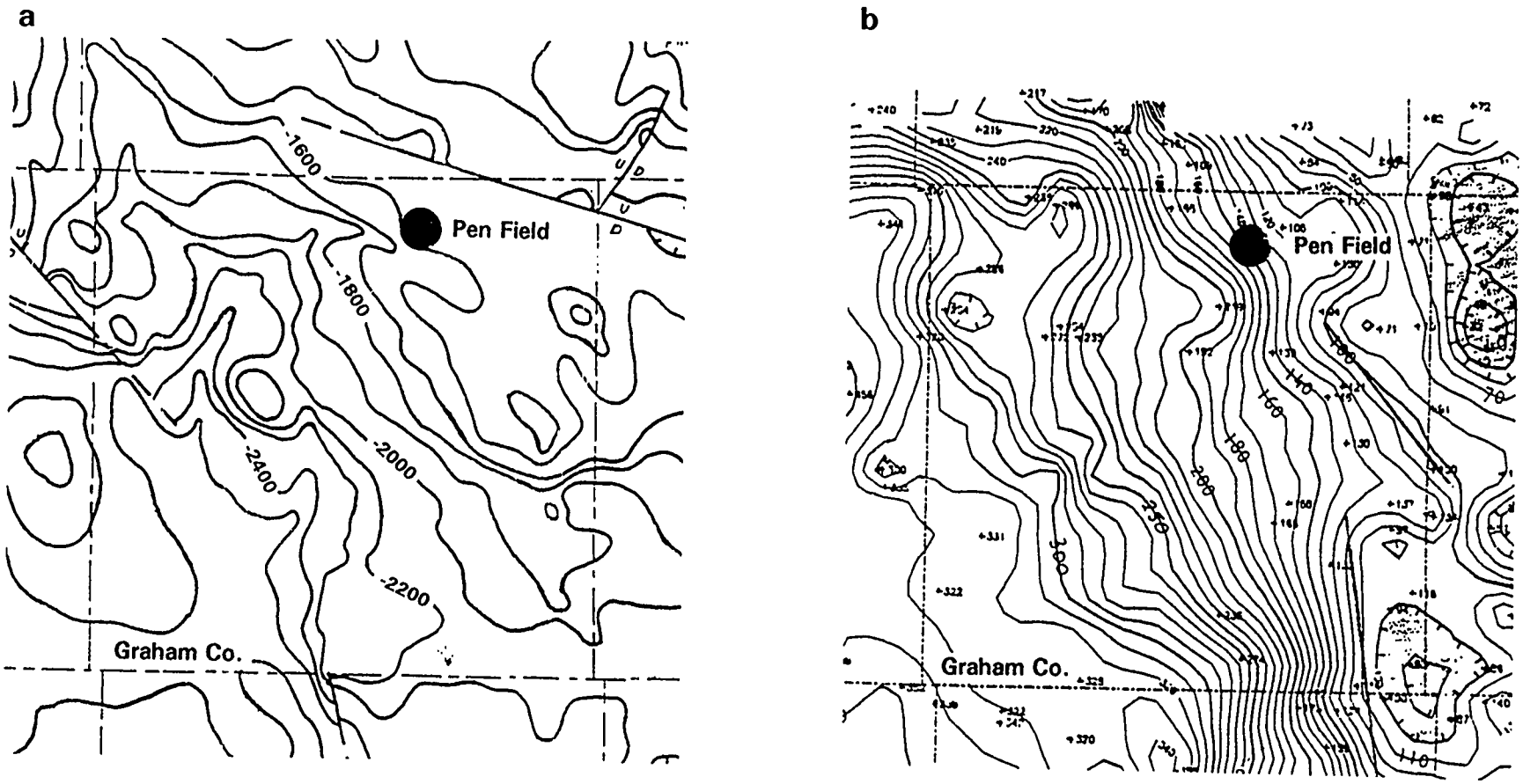

Figure 1.A.10. Two maps are shown for the same Graham County area. Map a): Dot shows location of Pen field on hand-drawn structure map of Precambrian basement (from Cole, 1976); b) Computer drawn map of isopach interval from base of Pennsylvanian to base Swope sequence (more detailed view of regional map shown in Figure I.32) showing Pennsylvanian thinning onto Cambridge arch.

PEN OIL FIELD

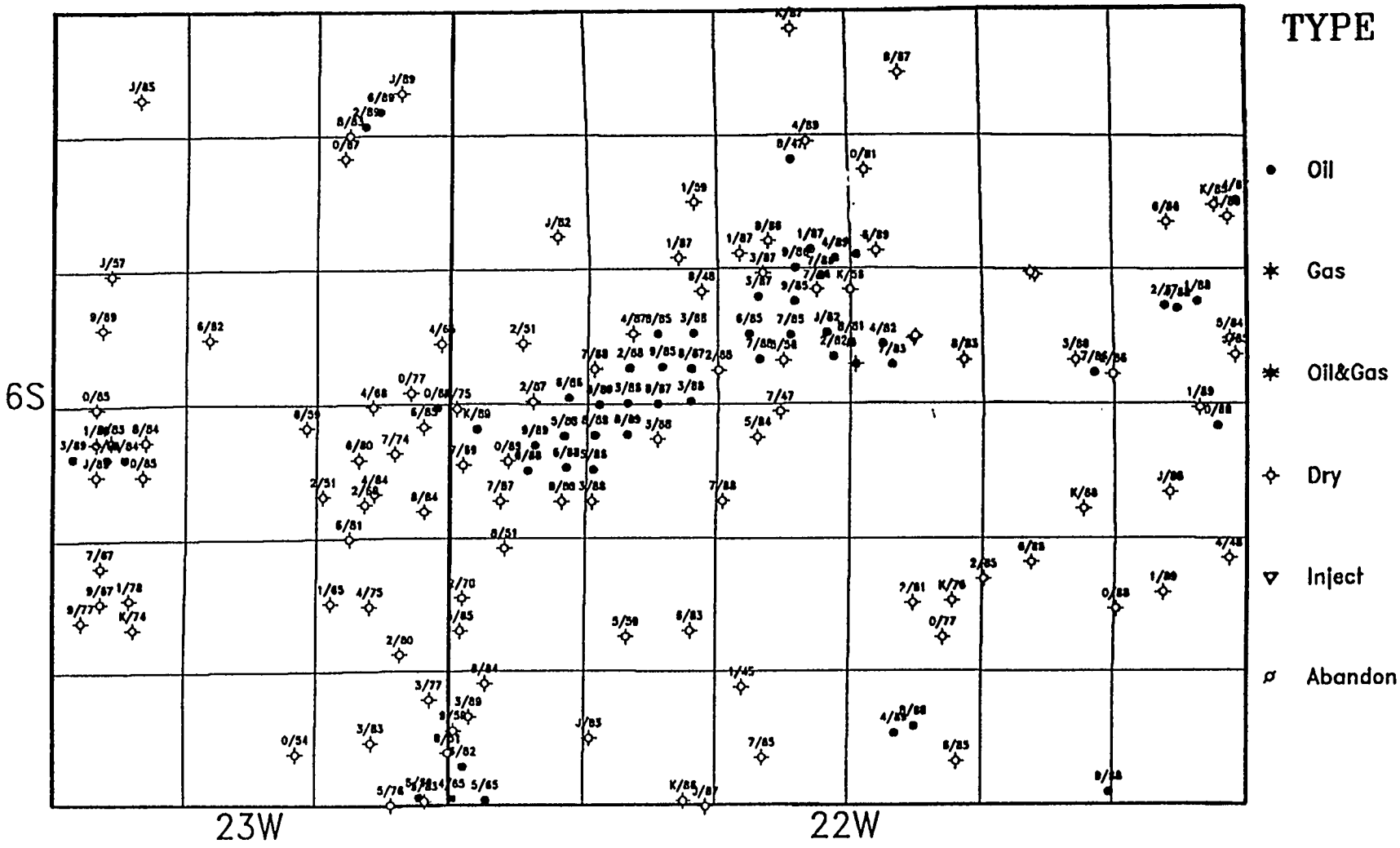

Figure 1.A.11. Production status and completion dates for wells in Penn field.

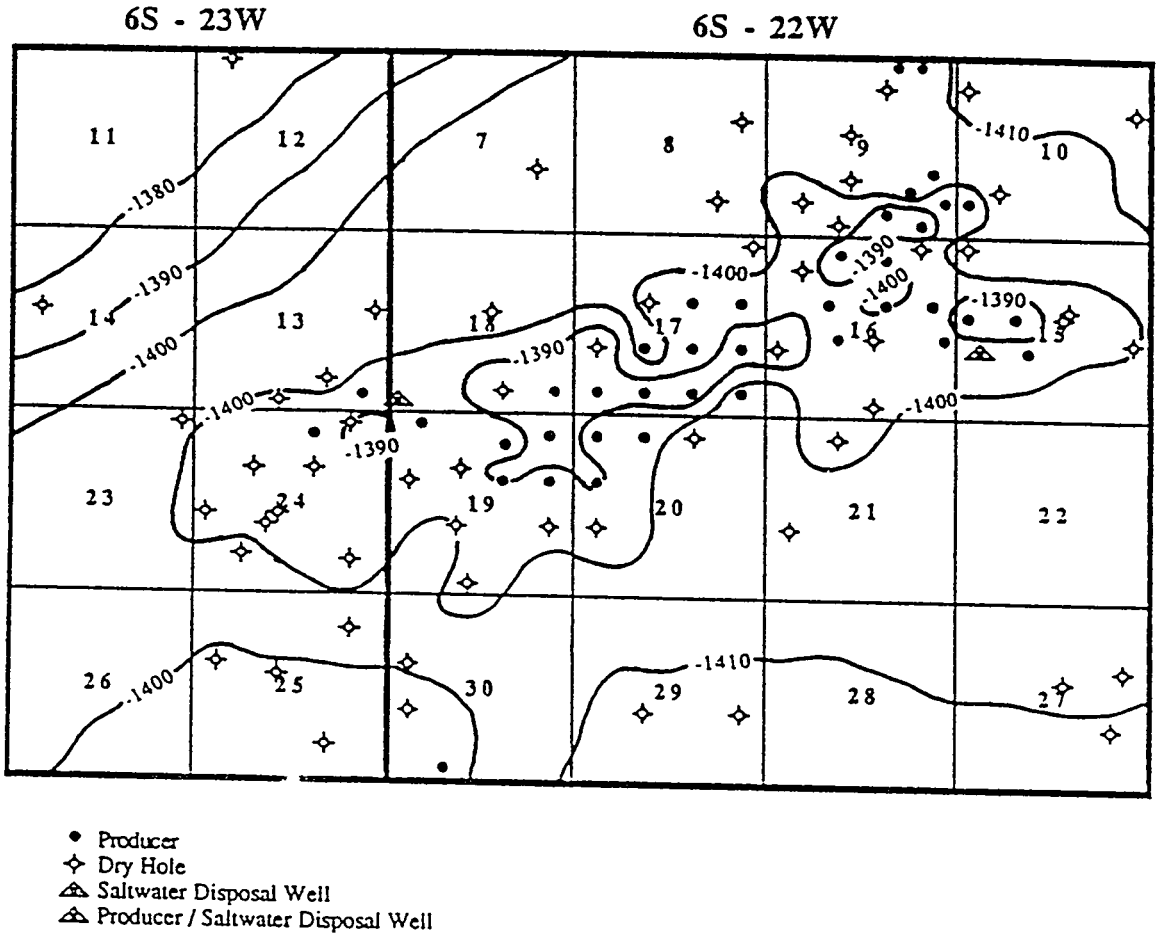

Figure 1.A.12. Structure contour map of the top of the J zone (Winterset Limestone of the Dennis sequence) at Pen field. Contour interval = 10 ft. All depths in feet below sea level (from Phares, 1991).

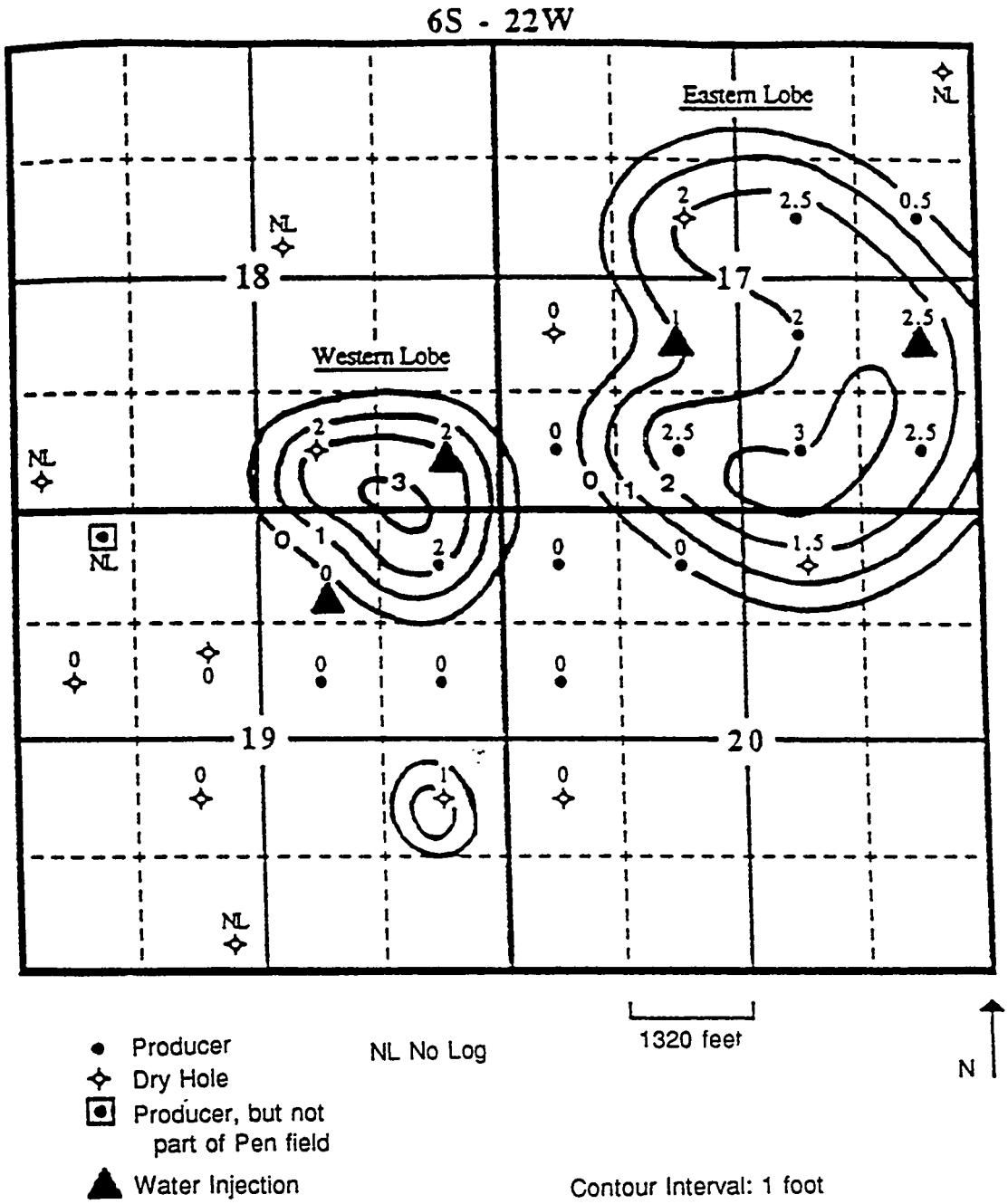

Figure 1.A.13. Isopach map of the grainstone interval of the I zone (from Phares, 1991).

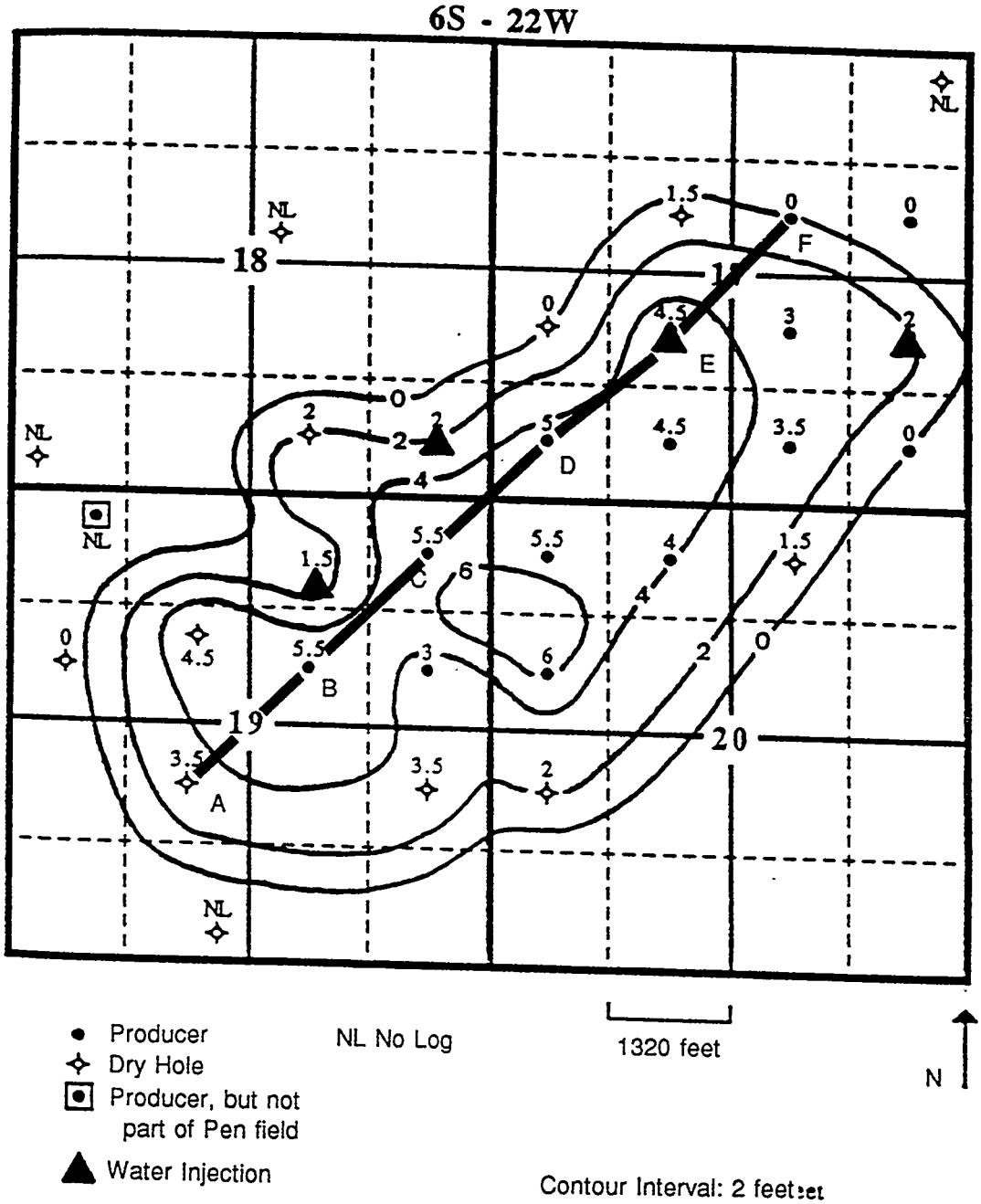

Figure 1.A.14. Isopach map of the grainstone interval of the J zone (from Phares, 1991). Index line for cross section shown in Figure 1.A.16.

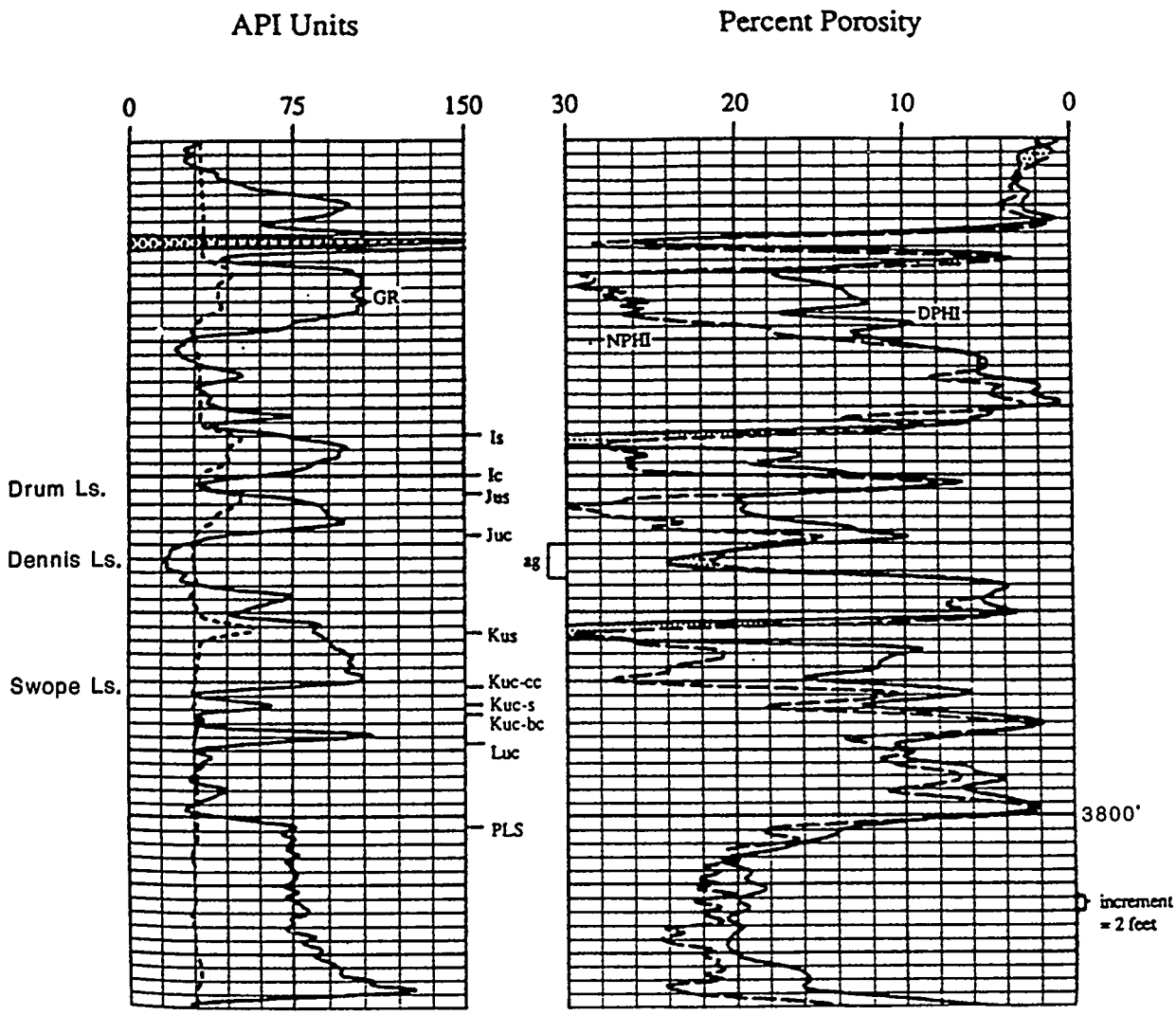

Figure 1.A.15. Gamma ray neutron-density log of Bethell #5 located in SW SW Sec. 17, T.6S., R.22W.

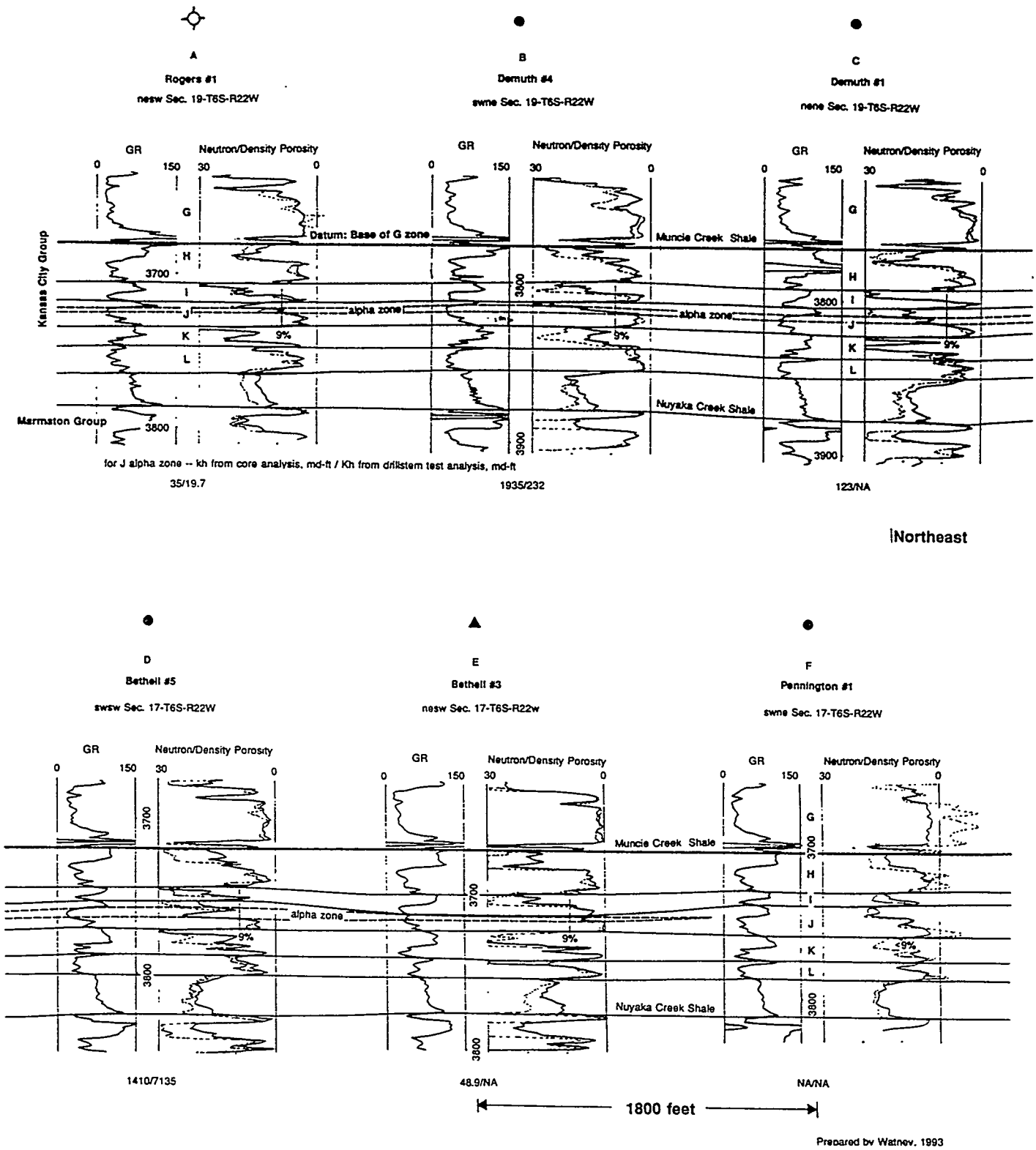

Figure 1.A.16. Stratigraphic wireline log cross section indexed in Figure 1.A.14 showing distribution of LKC zones in Pen field, in particular, the location of the upper "alpha" producing interval of the J zone.

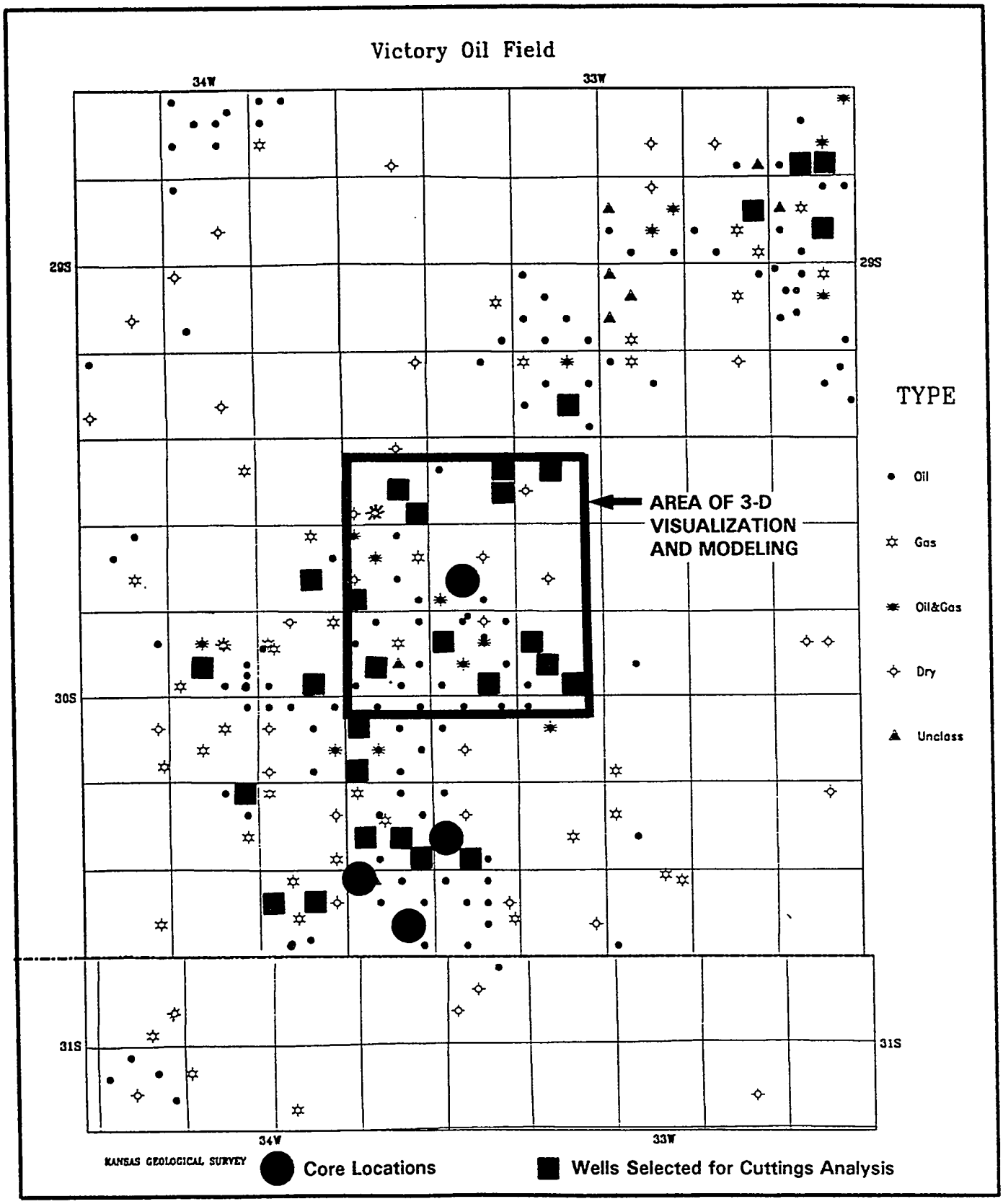

Figure 1.A.17. Base map of Victory field, Haskell County, Kansas showing the area of investigation and sub-projects including 3-D visualization and modeling (reported in Subtask 5.C) and petrographic description of cuttings and cores (Subtask 6). Iatan, Stanton, Dewey, Swope, and Sniabar sequences were analyzed for all wells using "Super" Pickett plot.

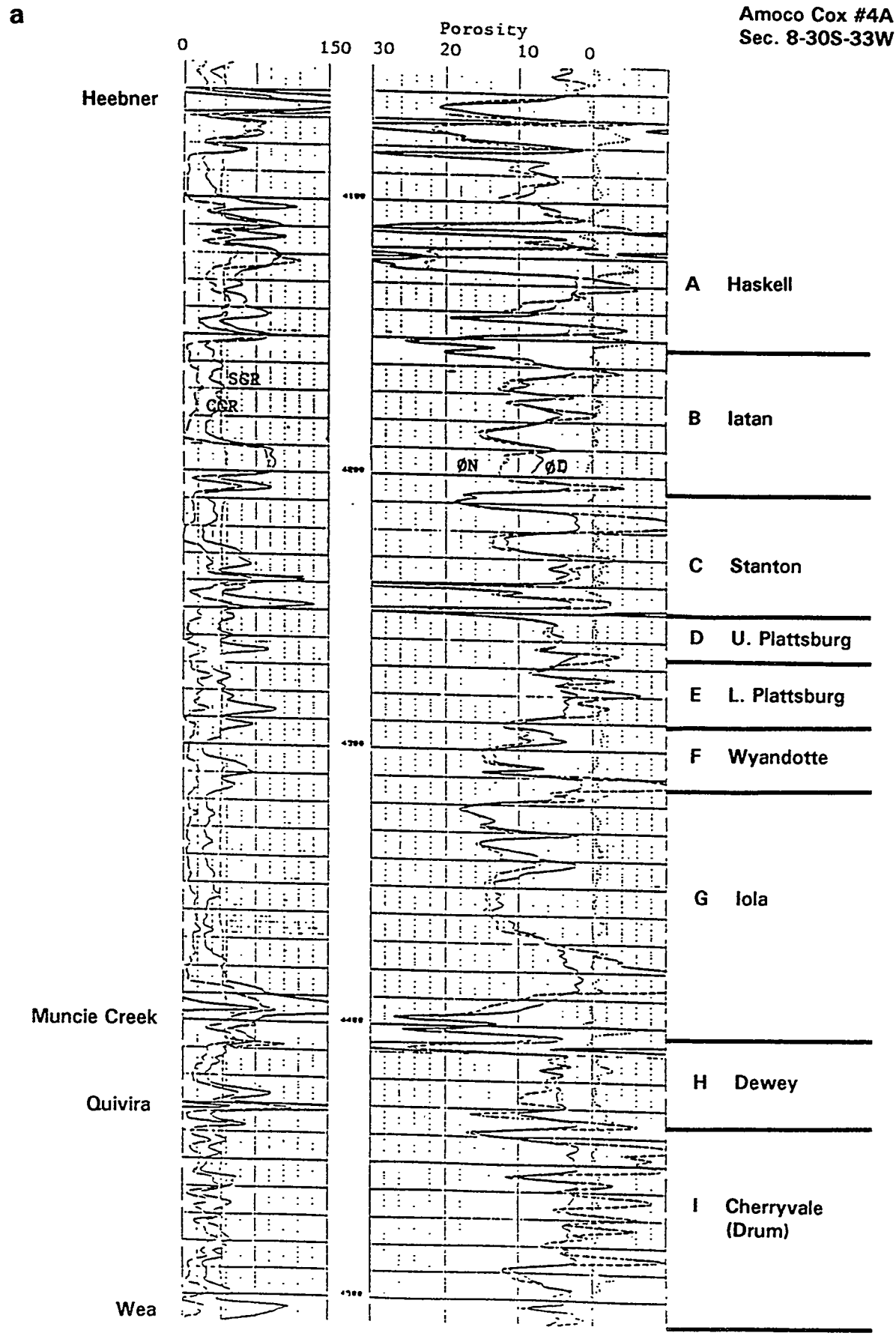

Figure 1.A.18 (a). Gamma ray neutron-density porosity log of Amoco Cox #A-4 well from Victory field marked with sequence boundaries and sequence nomenclature. Major marine shale markers are labeled on left axis.

b

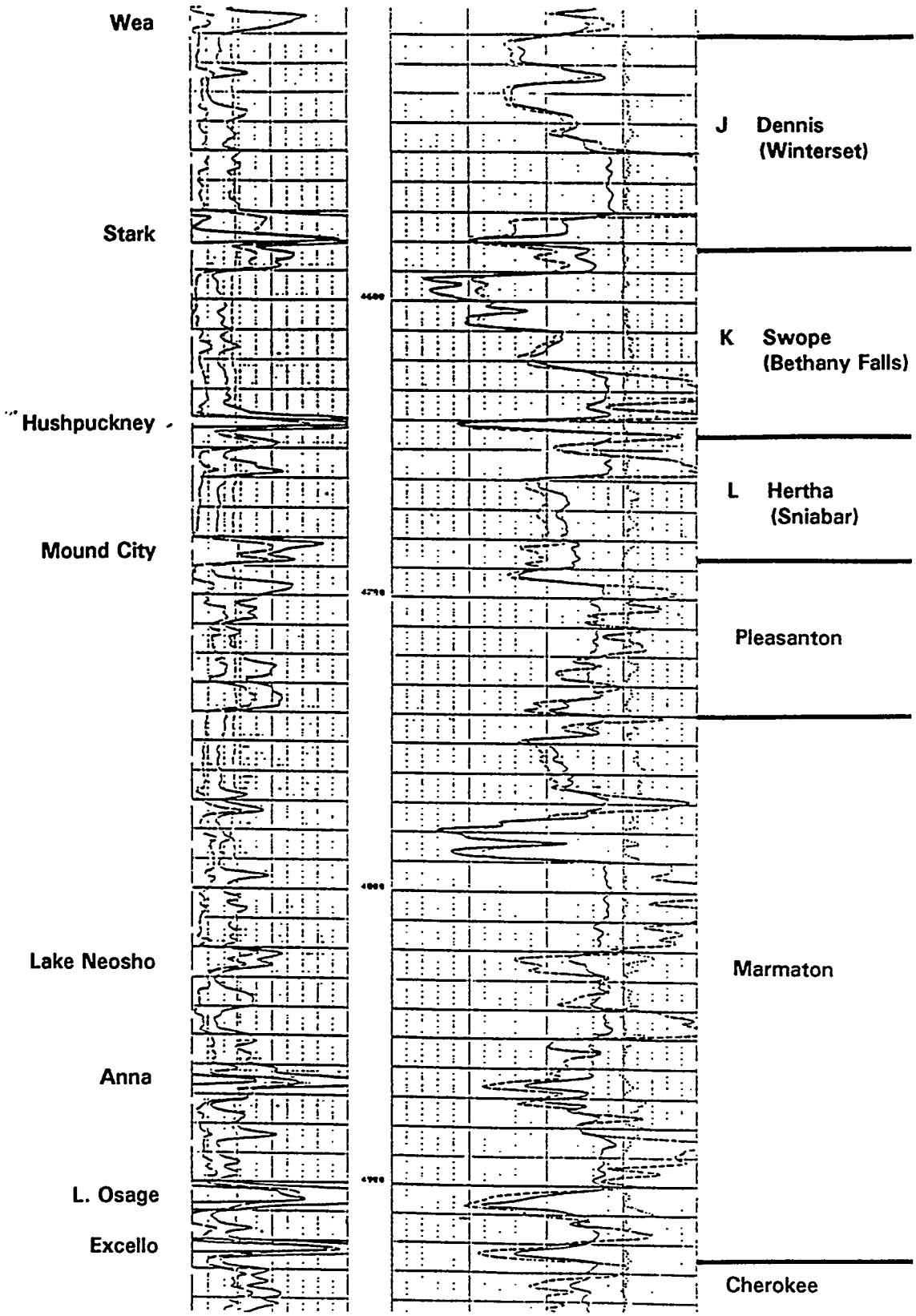

Figure 1.A.18 (b). Continuation of Figure 1.A.18 (a).

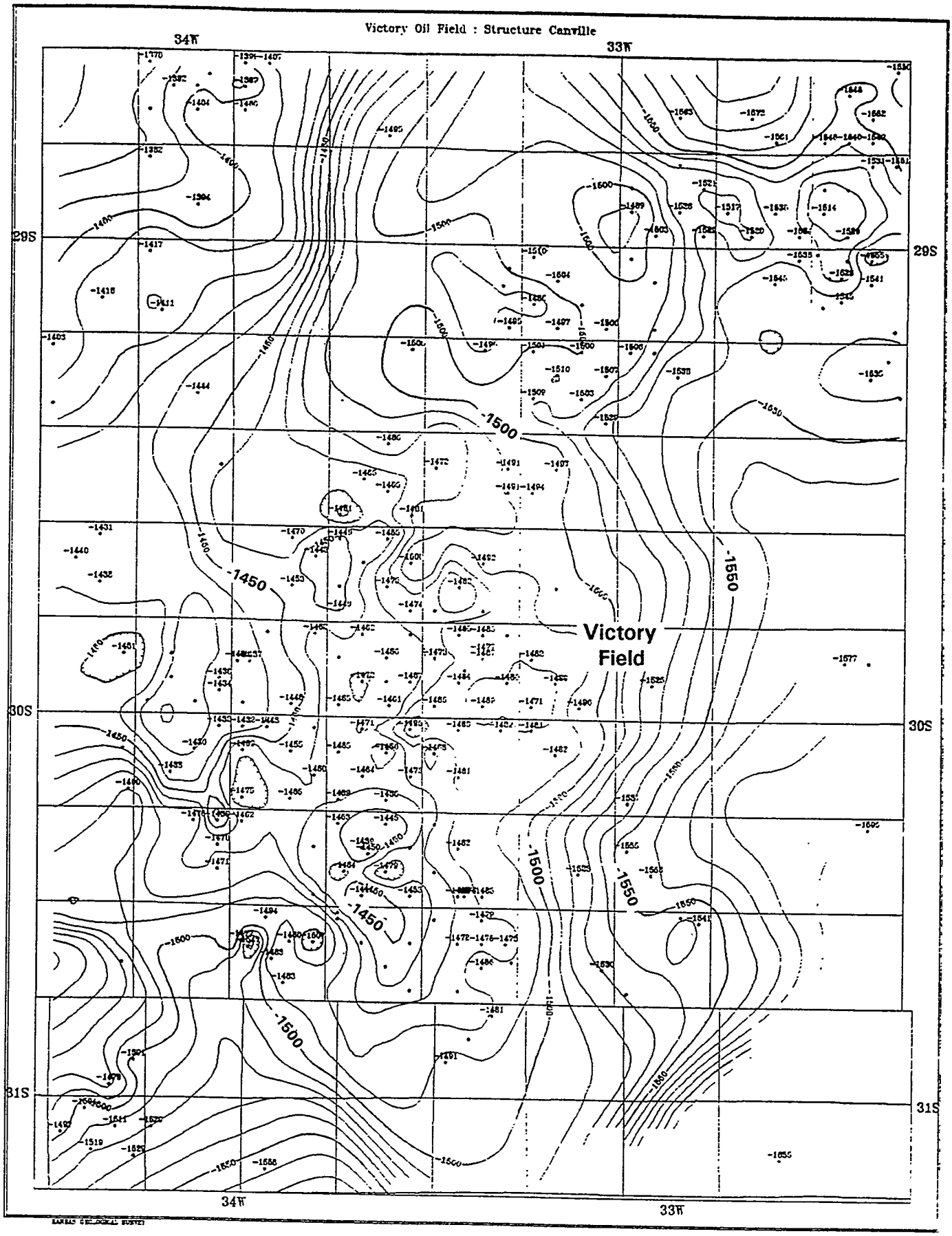

Figure 1.A.19. Structure contour map of base of Canville Limestone immediately overlying Bethany Falls reservoir. Contour interval is 10 ft. Squares are section lines, 1 mi.on a side.

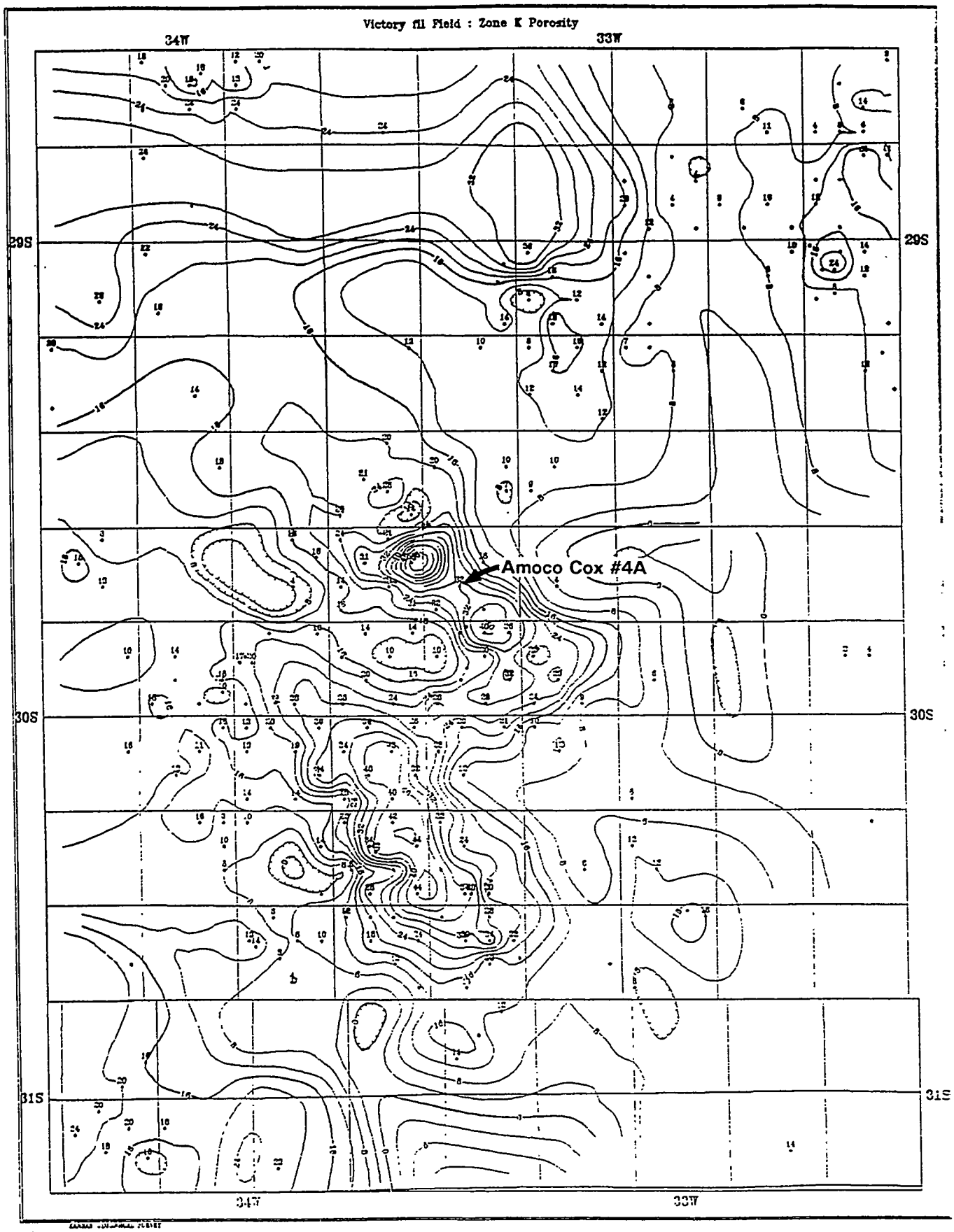

Figure 1.A.20. Thickness of porous carbonate (>8%) in Bethany Falls Limestone in the Victory field area. Contour interval is 4 ft. Squares are section lines, 1 mi. on a side.

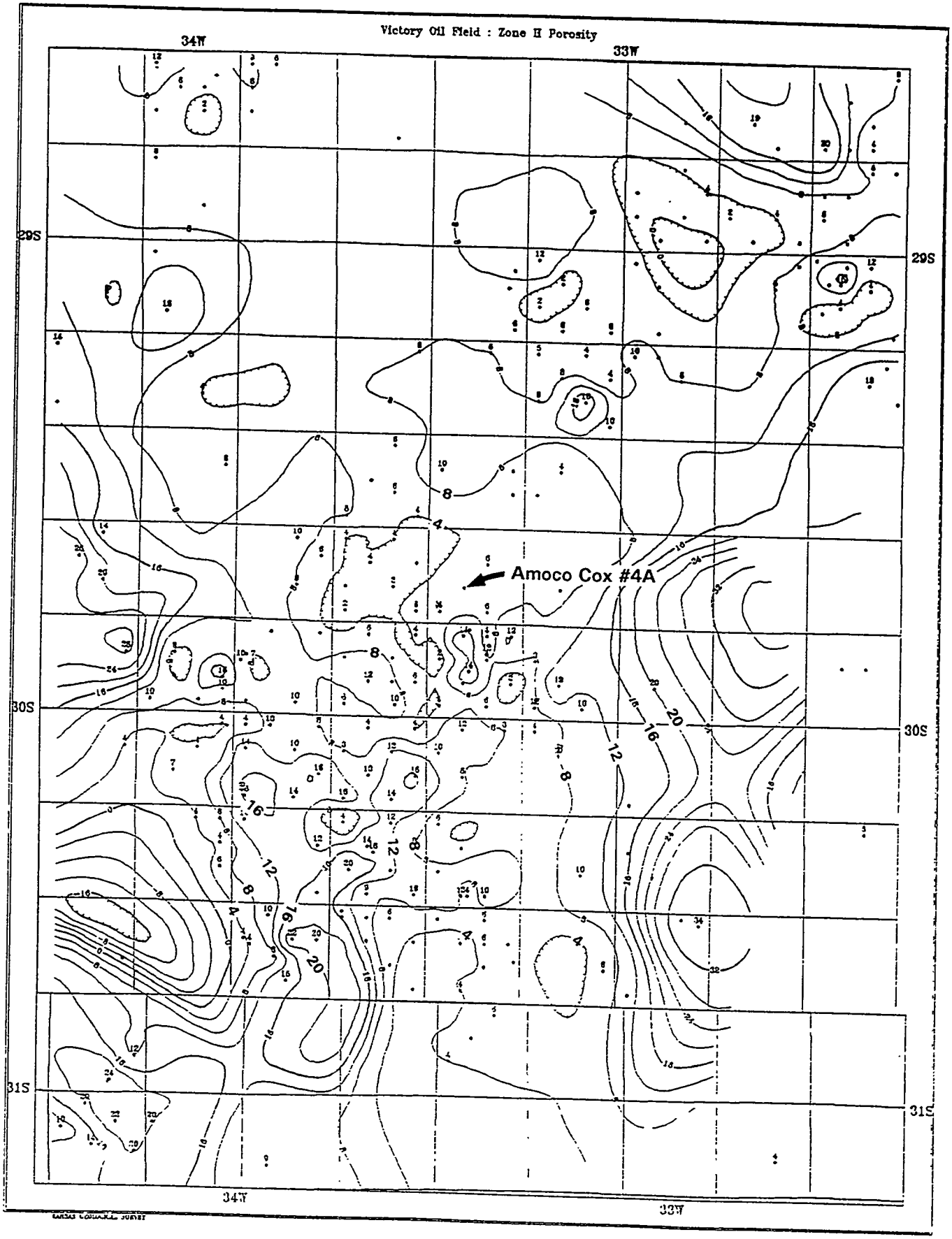

Figure 1.A.21. Thickness of porous carbonate (>8%) in Dewey Limestone in the Victory field area. Contour interval is 4 ft. Squares are section lines, 1 mi. on a side.

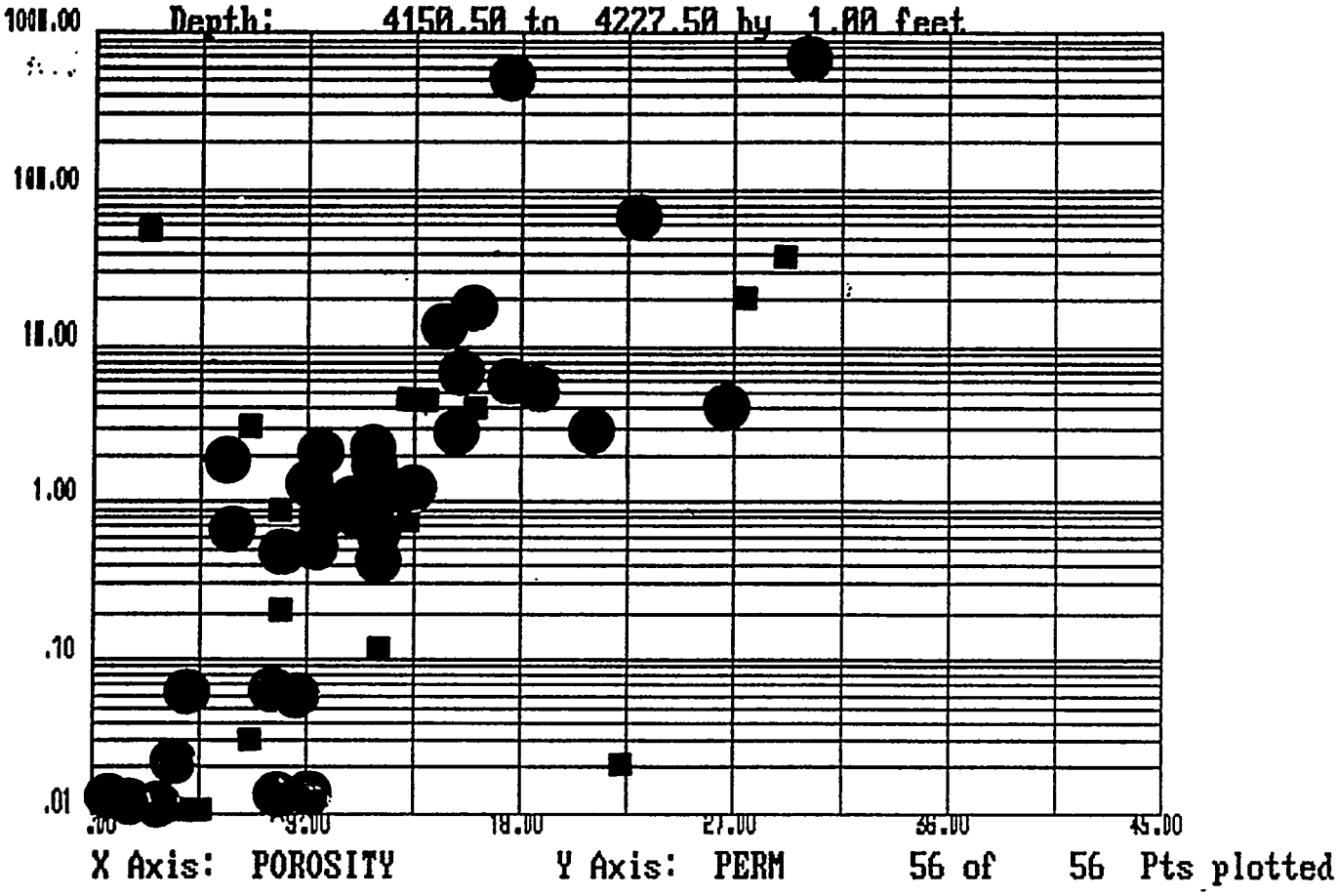

Figure 1.A.22. Porosity-permeability cross plot for Iatan Limestone from the Amoco Cox #A-4 core. Dots identify samples with water saturations <50%. Effective porosity is above 8% in this grainstone with interparticle porosity.

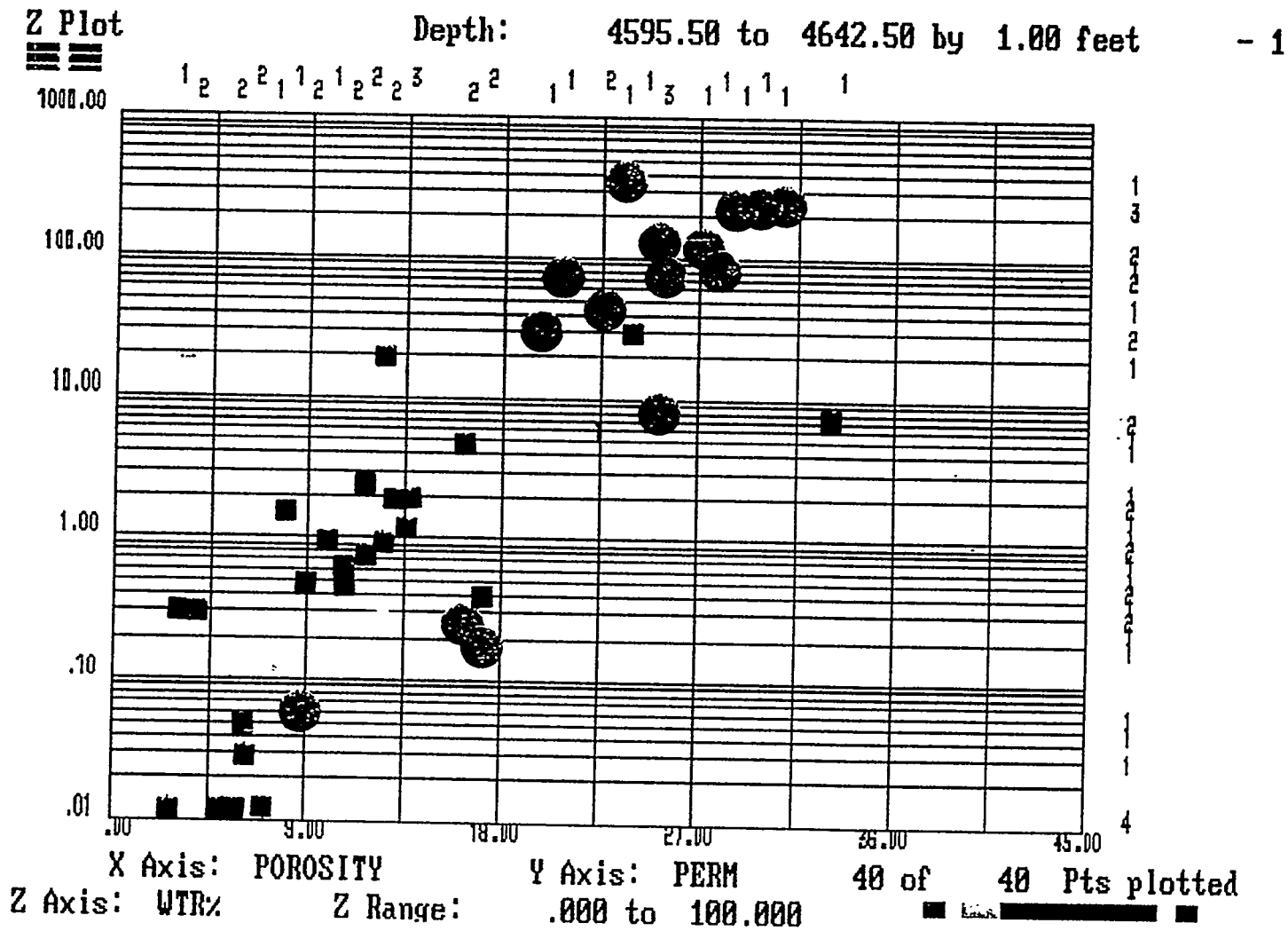

Figure 1.A.23. Porosity-permeability cross plot for Bethany Falls Limestone from the Amoco Cox #A-4 core. Dots identify samples with water saturations <50%. Effective porosity appears to be much higher than 8% in this oomoldic reservoir.

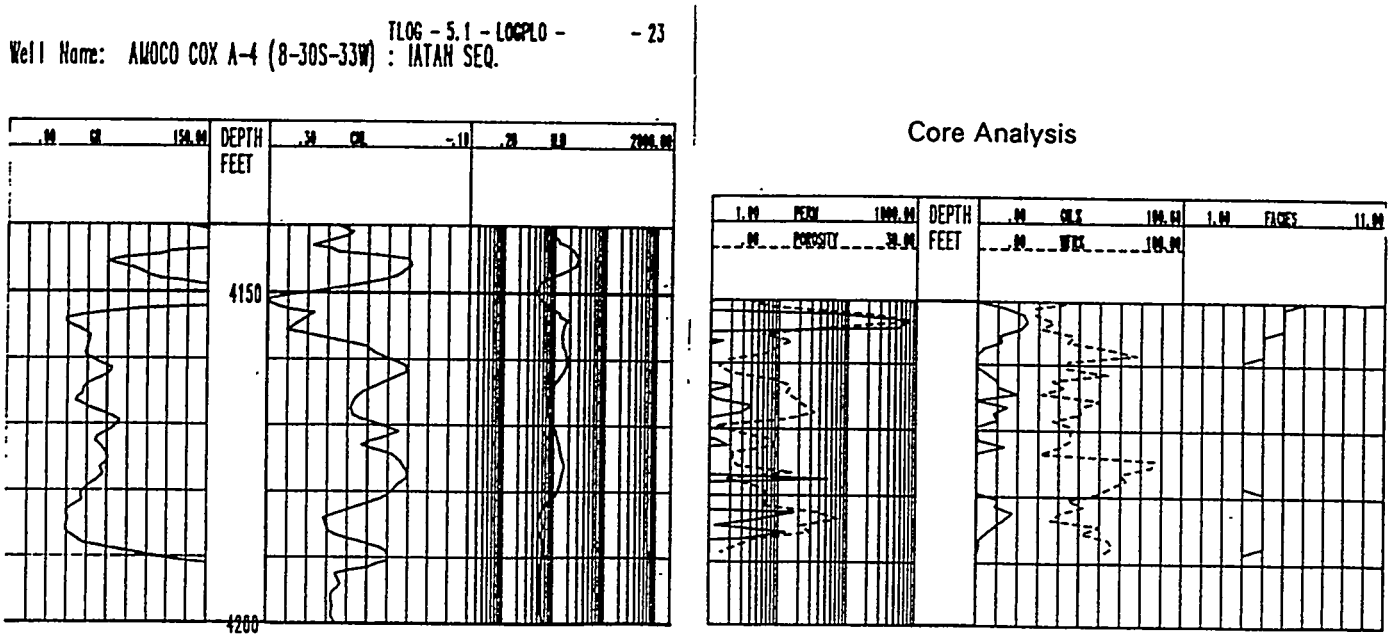

KEY FOR FACIES

1--BLACK SHALE
2--GRAY-GREEN SHALE
3--ARGILLACEOUS LIME WACKESTONE
3.5--DARK WACKESTONE
4--LIME WACKESTONE
4.5--MUDSTONE
5--LIME PACKSTONE
6--LIME GRAINSTONE
7--SILTY/SANDY SHALE
8--ARGILLACEOUS SANDSTONE
9--CLEAN SANDSTONE
10--COAL
11--PALEOSOL

Figure 1.A.24. Log and core analysis profile through the Iatan reservoir. Pay is fine intergranular and intercrystalline porosity. Permeability developed at top of limestone in grainstone. Tracks from left to right include gamma ray (GR), compensated neutron porosity (CNL), deep induction log (ILD), permeability (PERM) on log scale, porosity in same track on linear scale, oil saturations (OIL%), water saturation (WTR%), and facies from core description.

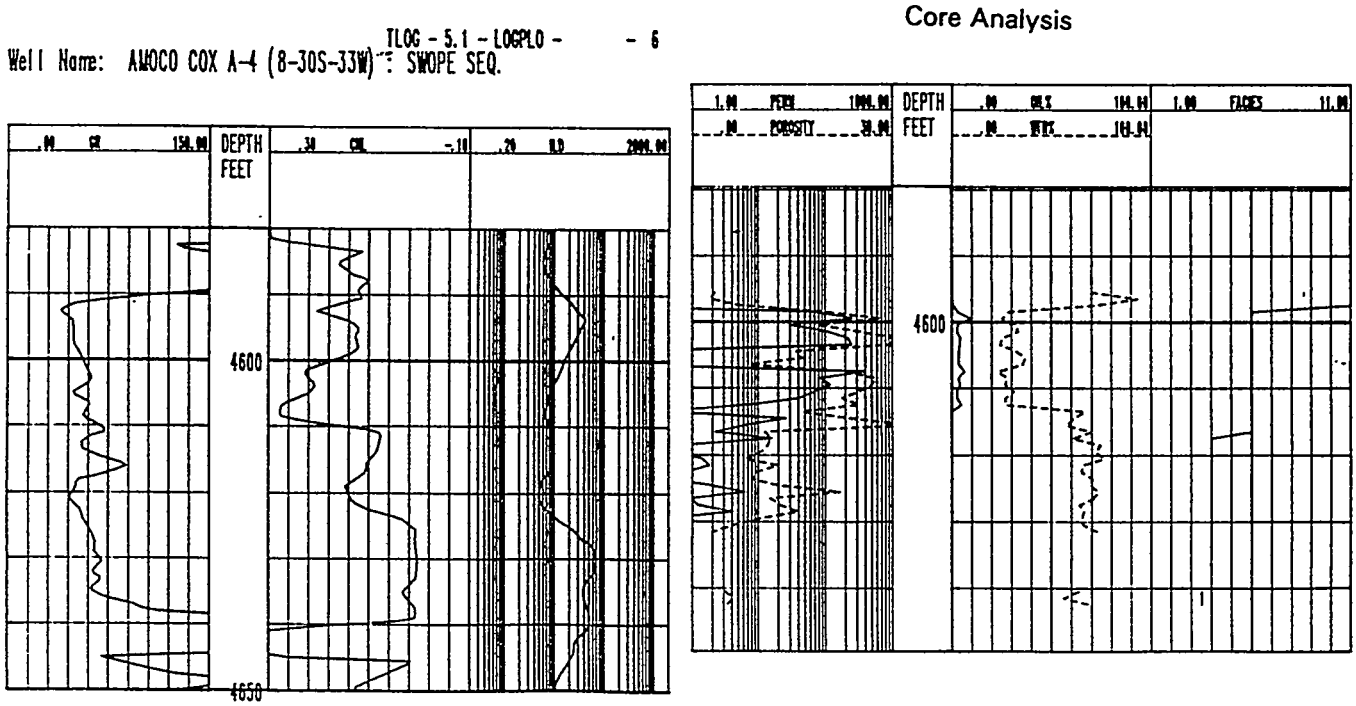

KEY FOR FACIES

1--BLACK SHALE
2--GRAY-GREEN SHALE
3--ARGILLACEOUS LIME WACKESTONE
3.5--DARK WACKESTONE
4--LIME WACKESTONE
4.5--MUDSTONE
5--LIME PACKSTONE
6--LIME GRAINSTONE
7--SILTY/SANDY SHALE
8--ARGILLACEOUS SANDSTONE
9--CLEAN SANDSTONE
10--COAL
11--PALEOSOL

Figure 1.A.25. Log and core analysis profile through the Bethany Falls reservoir. Pay is oomoldic porosity as in Figure 1.A.24.

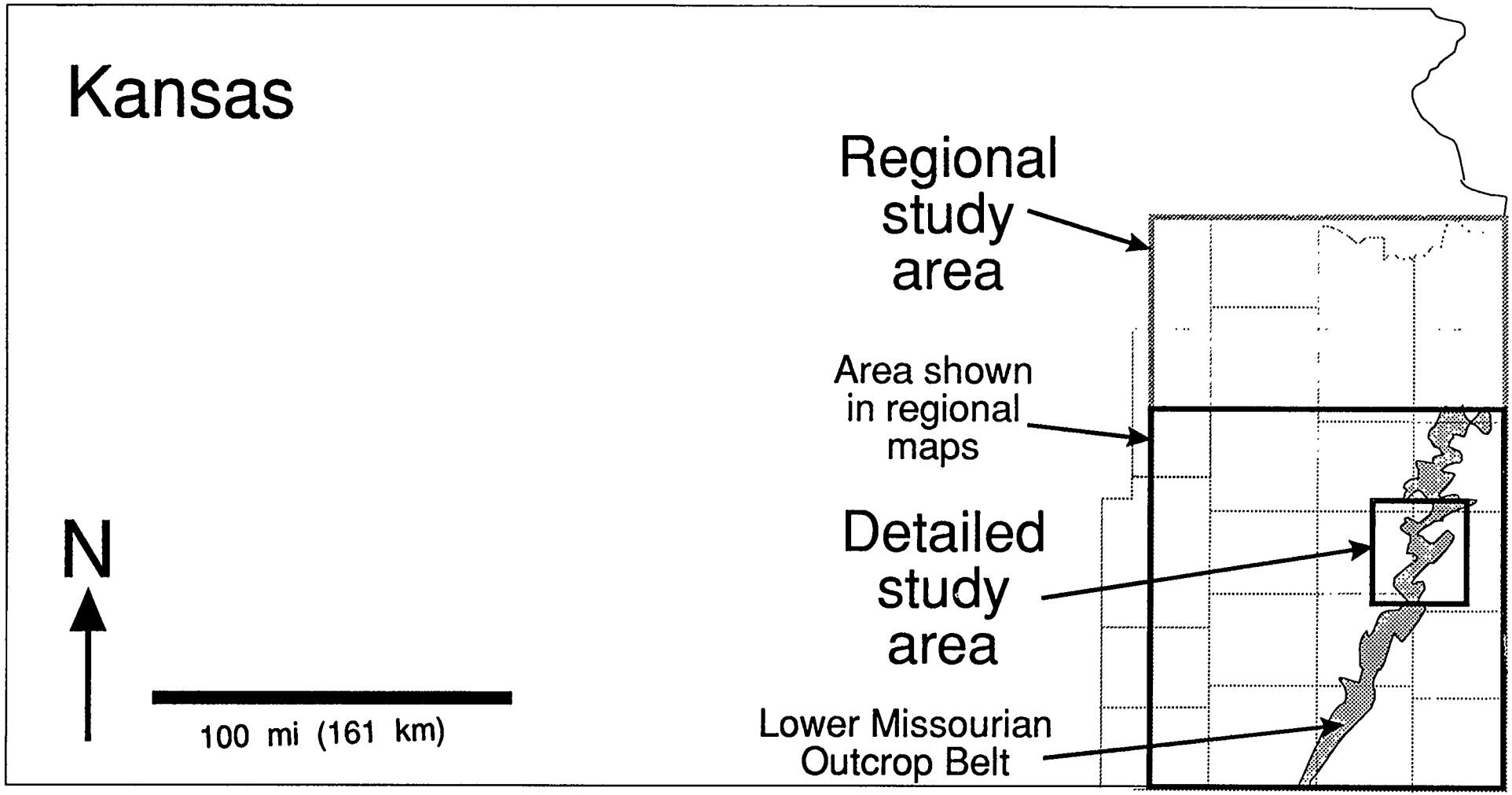

Figure 2.A.1.1. Map of Kansas showing the locations of the regional and detailed study areas examined in the analog study. Note that the area covered in the regional isopach maps (e.g. Figure 2.A.1.3) is larger than the area shown in the other regional maps (e.g. Figure 2.A.1.8).

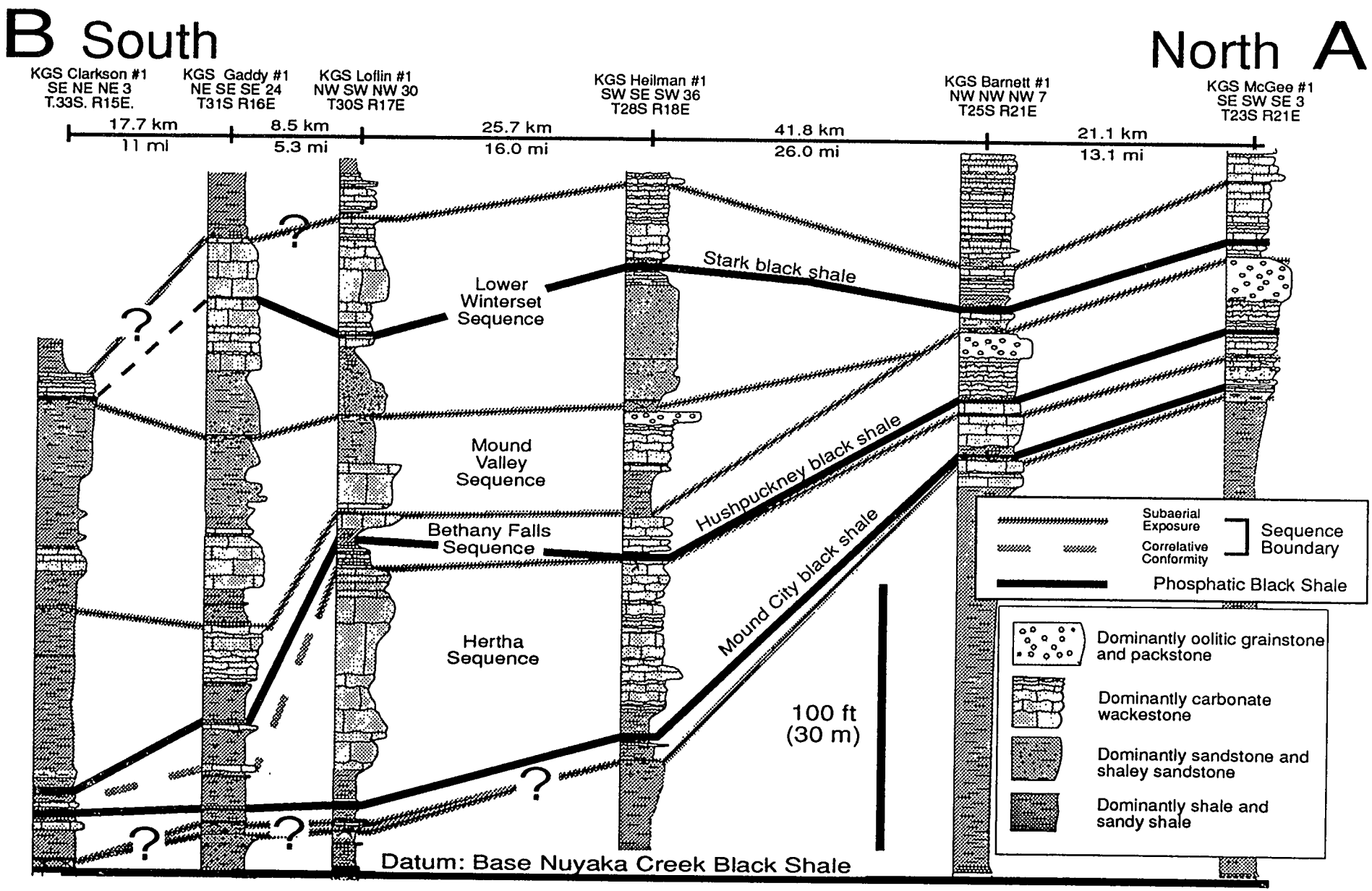

Figure 2.A.1.2. North-south core cross-section of the study interval just west of the outcrop belt in eastern Kansas (for location see Figure 2.A.1.9). Note the southward thinning in the interval between the Nuyaka Creek and Mound City black shales (essentially the "Pleasanton interval" discussed in the text) and the associated thickening of the Hertha sequence. Stratigraphic markers just below the interval shown here tend to parallel the Nuyaka Creek, supporting the inference that the Pleasanton thinning reflects paleotopography.

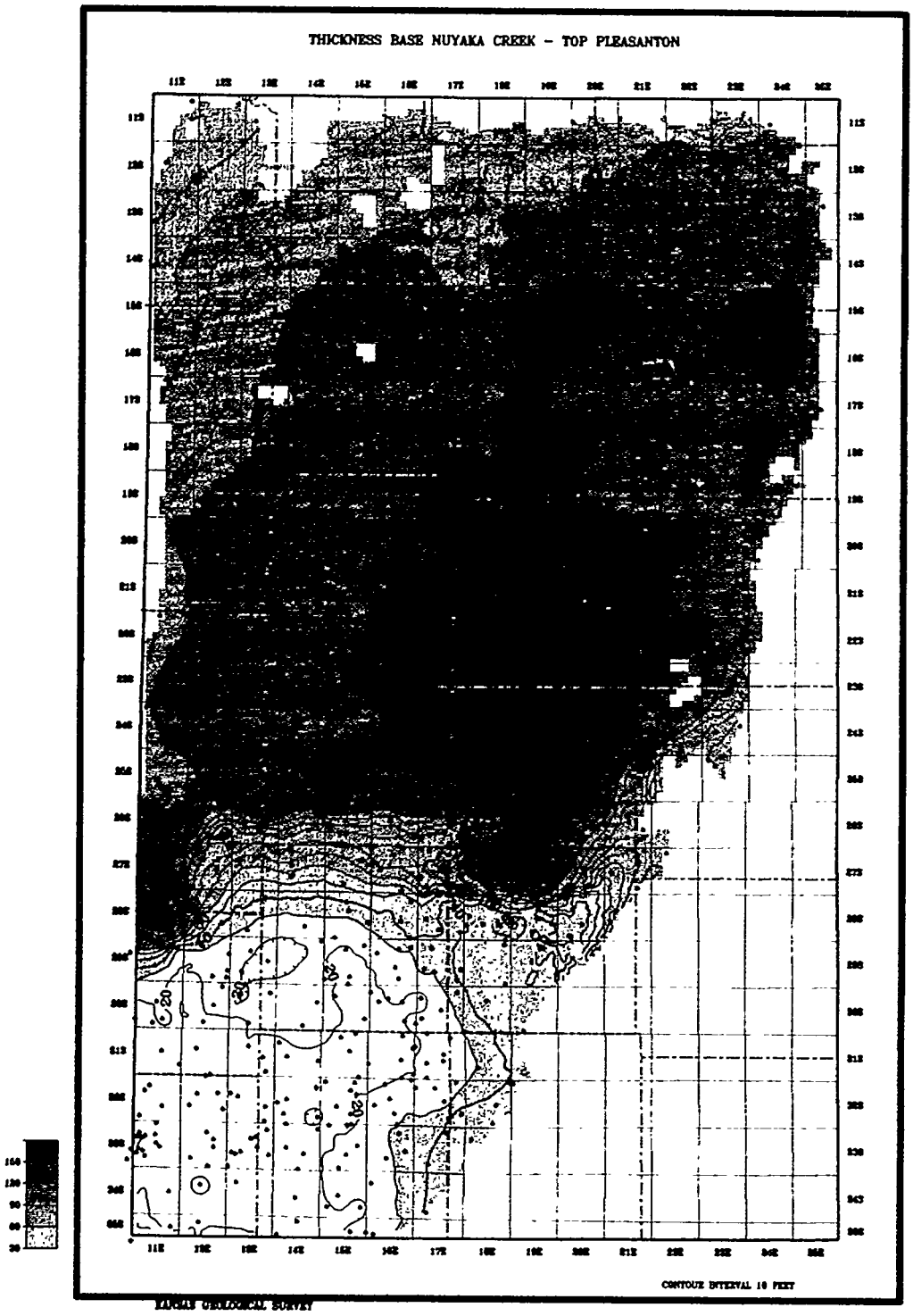

Figure 2.A.1.3. Isopach map of the Pleasanton interval across the regional study area. The thickest area (the "Pleasanton platform") occurs in the east-central portion of the area, and is represented by the darkest shades of gray. In these areas the Pleasanton is over 160 ft (49 m) thick. Areas of closely spaced contour lines to the southwest, south, and southeast of the areas of thick Pleasanton indicate the location of the Pleasanton slope.

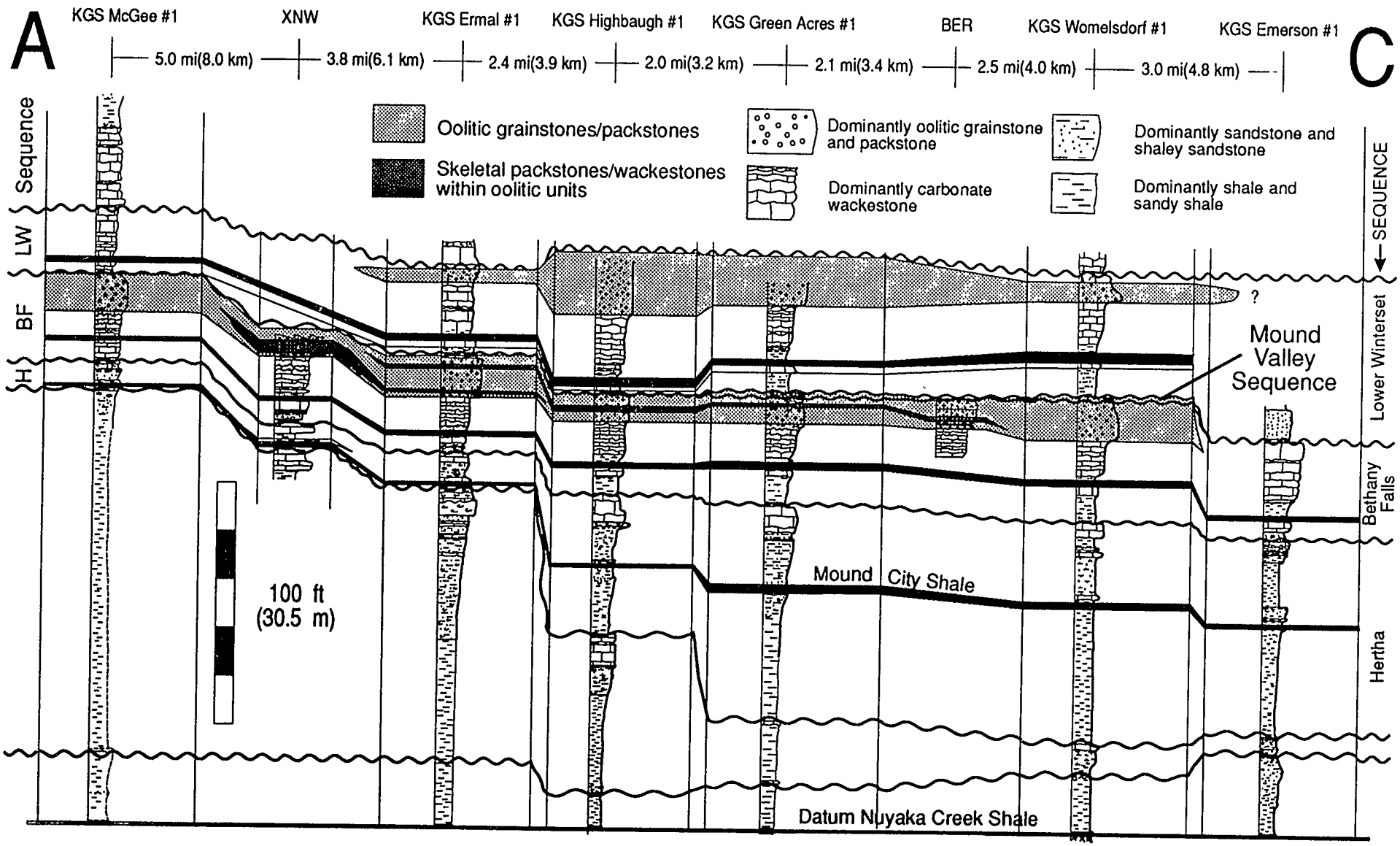

Figure 2.A.1.4. Cross section showing the four depositional sequences in the study interval along the southeastern margin of the Pleasanton platform. For location see fig. 2.A.1.9.

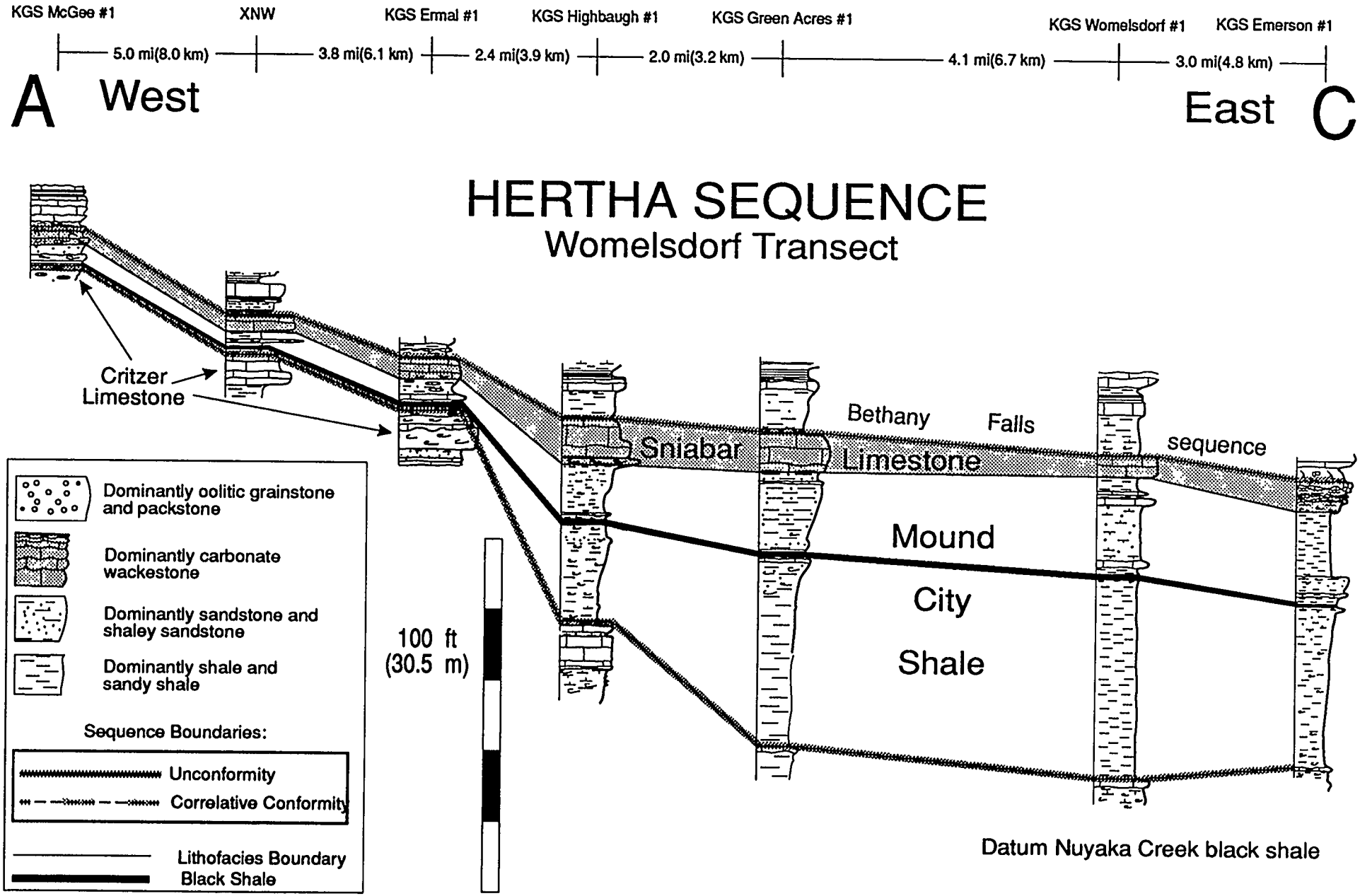

Figure 2.A.1.5. West-to-east cross section of the Hertha sequence across the east flank of the Pleasanton slope. Note that in this area the thickening of the sequence is almost entirely within the Mound City Shale rather than the Sniabar Limestone (compare with Figure 2.A.1.6).

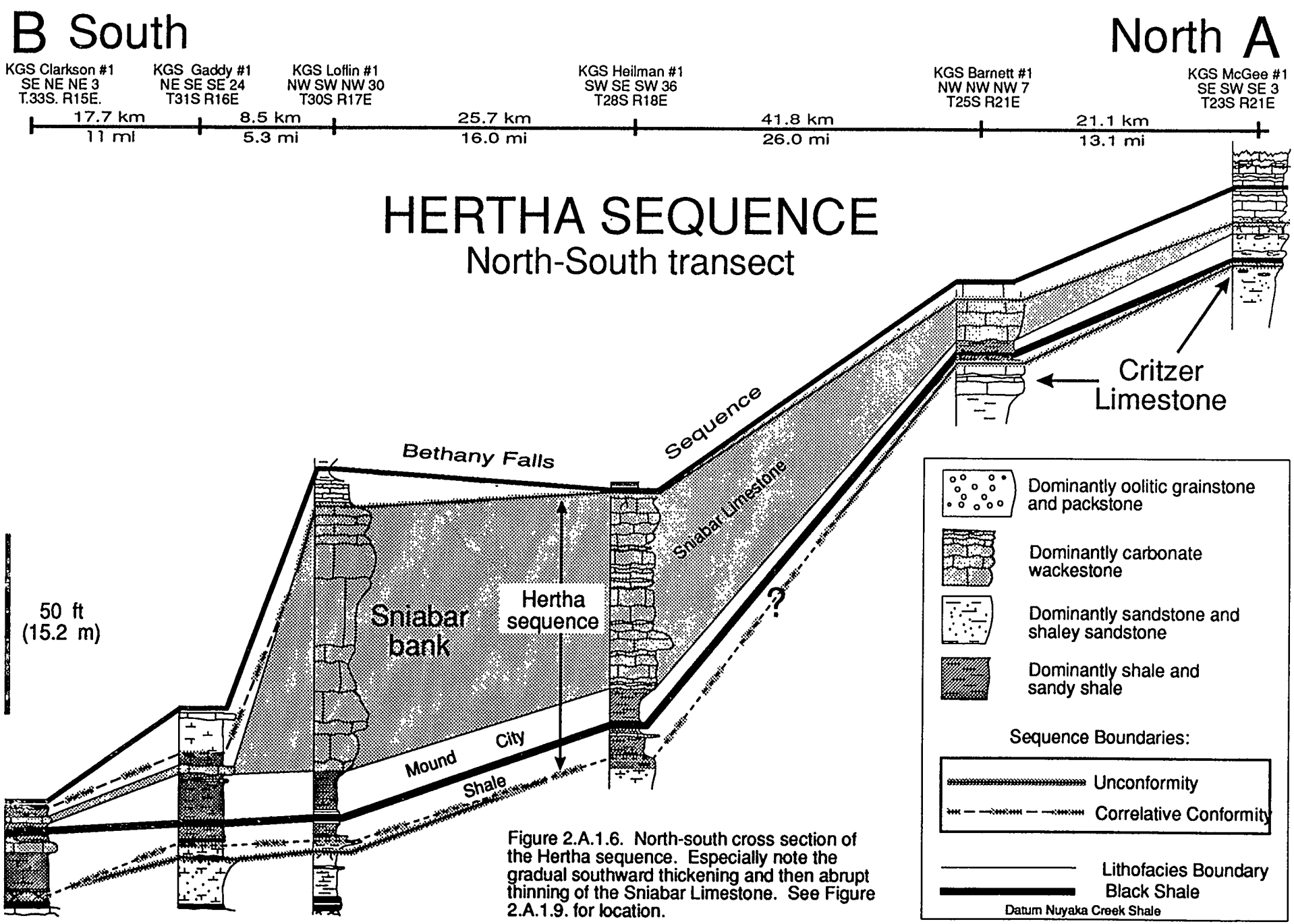

Figure 2.A.1.6. North-south cross section of the Hertha sequence. Especially note the gradual southward thickening and then abrupt thinning of the Sniabar Limestone. See Figure 2.A.1.9. for location.

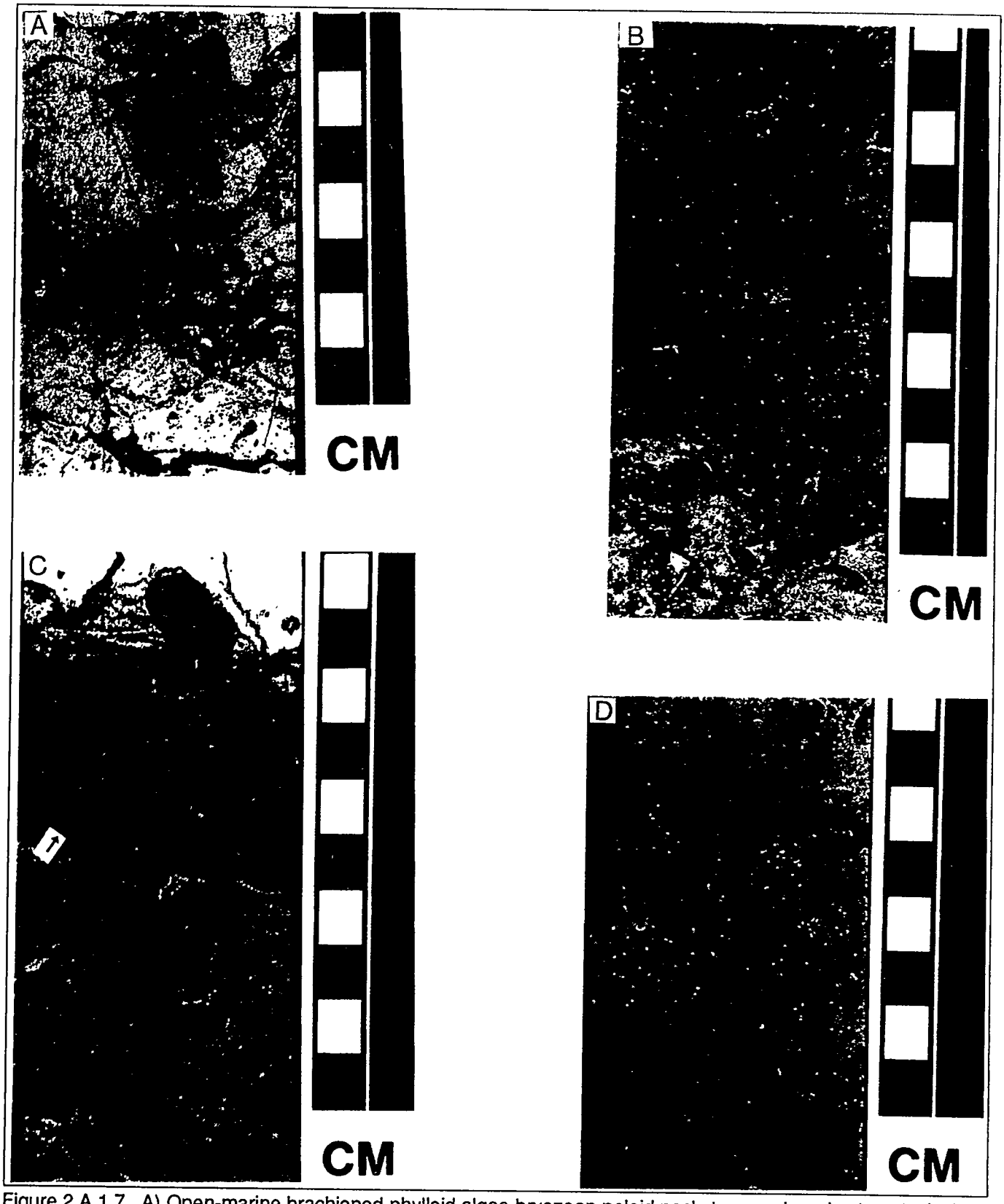

Figure 2.A.1.7. A) Open-marine brachiopod-phylloid algae-bryozoan-peloid packstone and wackestone typical of the lower Sniabar Limestone. KGS Larson #1, 120 ft. B) Skeletal-peloidal packstone characteristic of the upper Sniabar Limestone. These grainier lithofacies (compare to A) reflect the higher-energy conditions that prevailed during deposition of the upper part of the unit. KGS Larson #1, 112 ft. C) Uppermost Sniabar Limestone. Abundant spar-filled root traces (small dark areas), laminated crusts (arrow), and rounded intra/lithoclasts (near top) all are evidence of the subaerial exposure zone that marks the upper Hertha sequence boundary. KGS Larson #1, 110 ft. D) Skeletal-peloidal wackestone/packstone typical of the Middle Creek Limestone. KGS Larson #1, 99 ft 6 in.

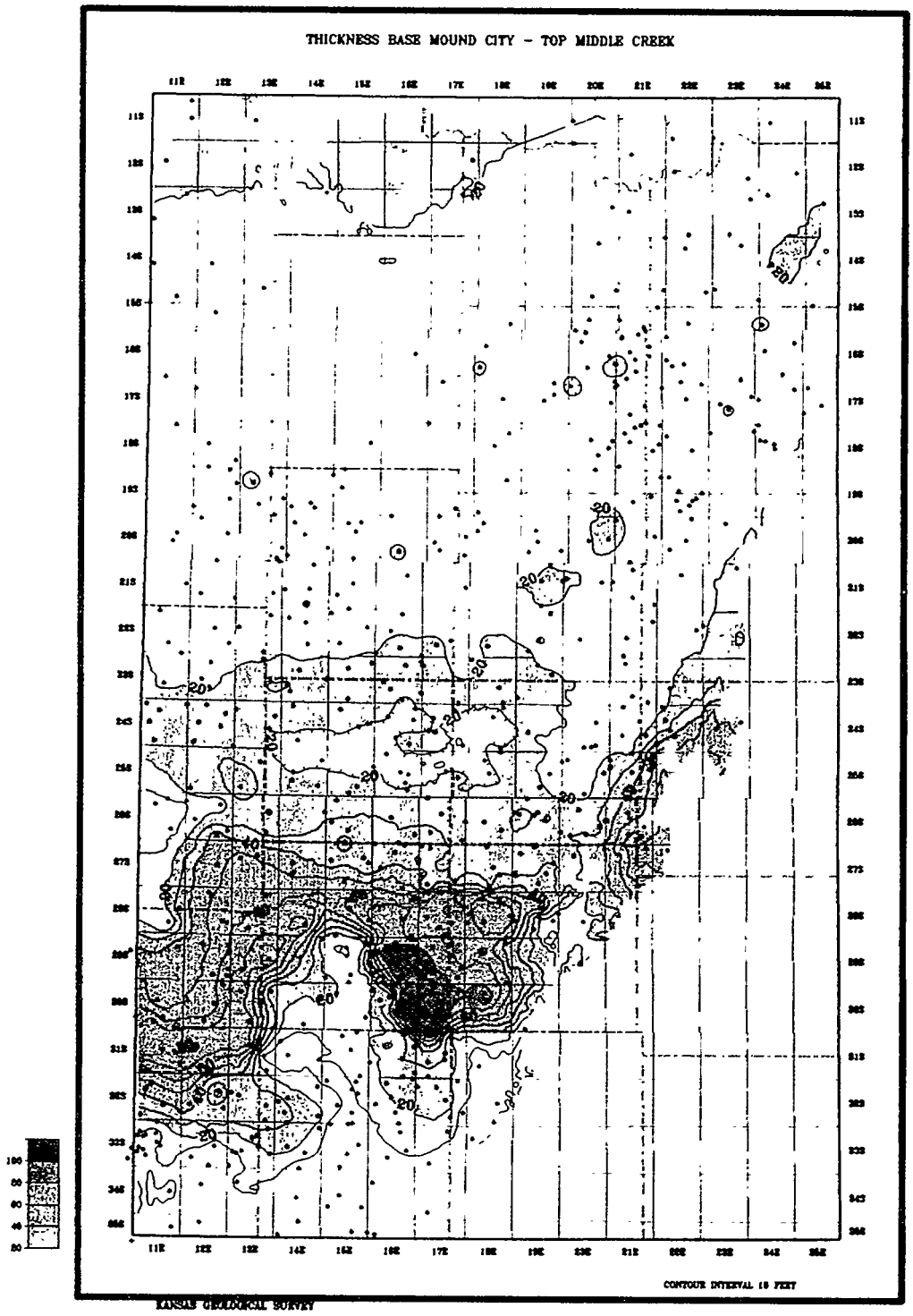

Figure 2.A.1.8. Isopach map of the interval from the base of the Mound City black shale to the top of the Middle Creek Limestone. This map shows the approximate thickness of the Sniabar Limestone across the regional study area. The Sniabar bank complex is shown in darker shades of gray in the southern part of the area.

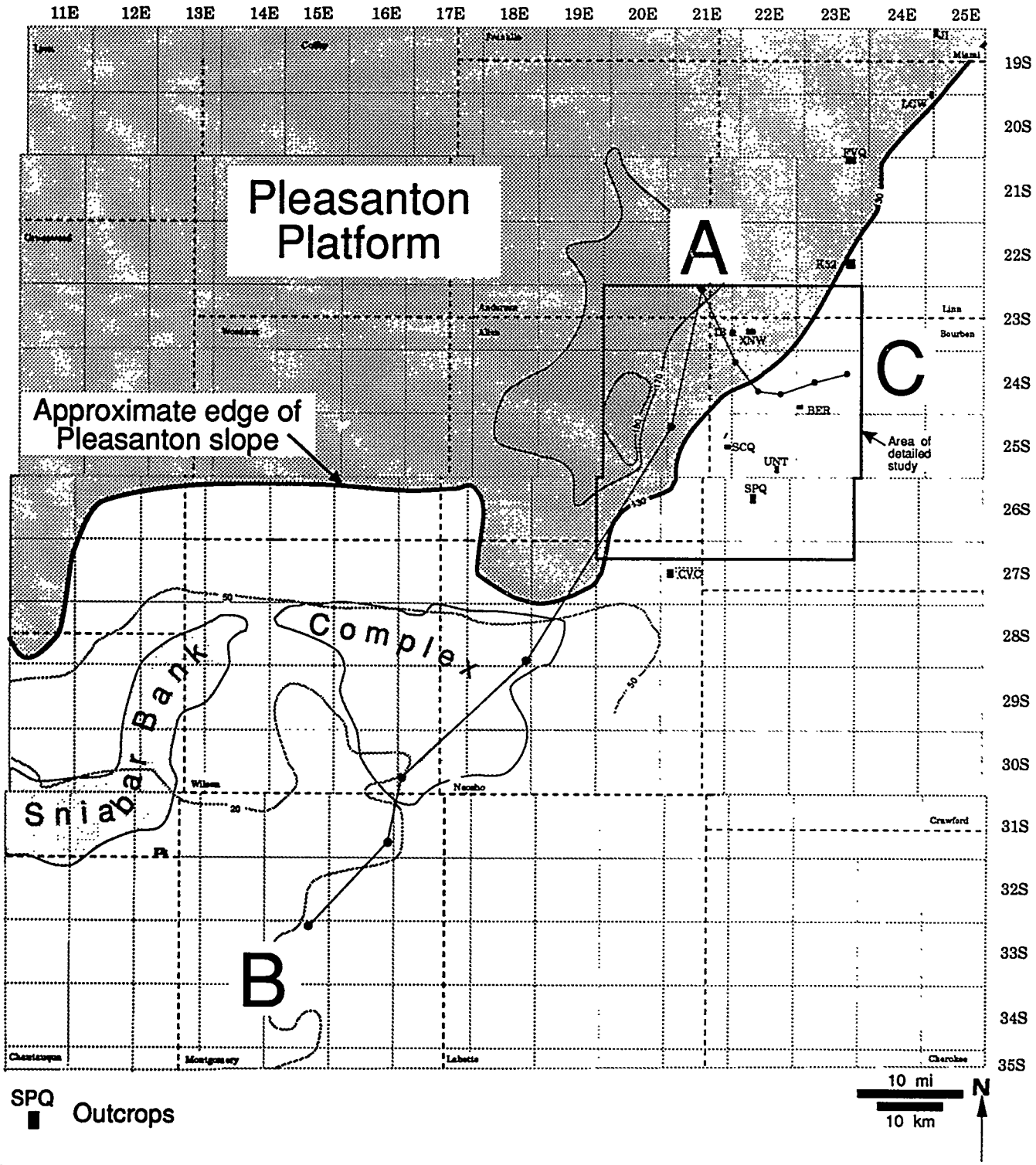

Figure 2.A.1.9. Map of the southern part of the study area showing the locations of the Pleasanton platform and the Sniabar bank complex. Locations of the cross sections shown in Figures 2.A.1.2, 4, and 5 shown also.

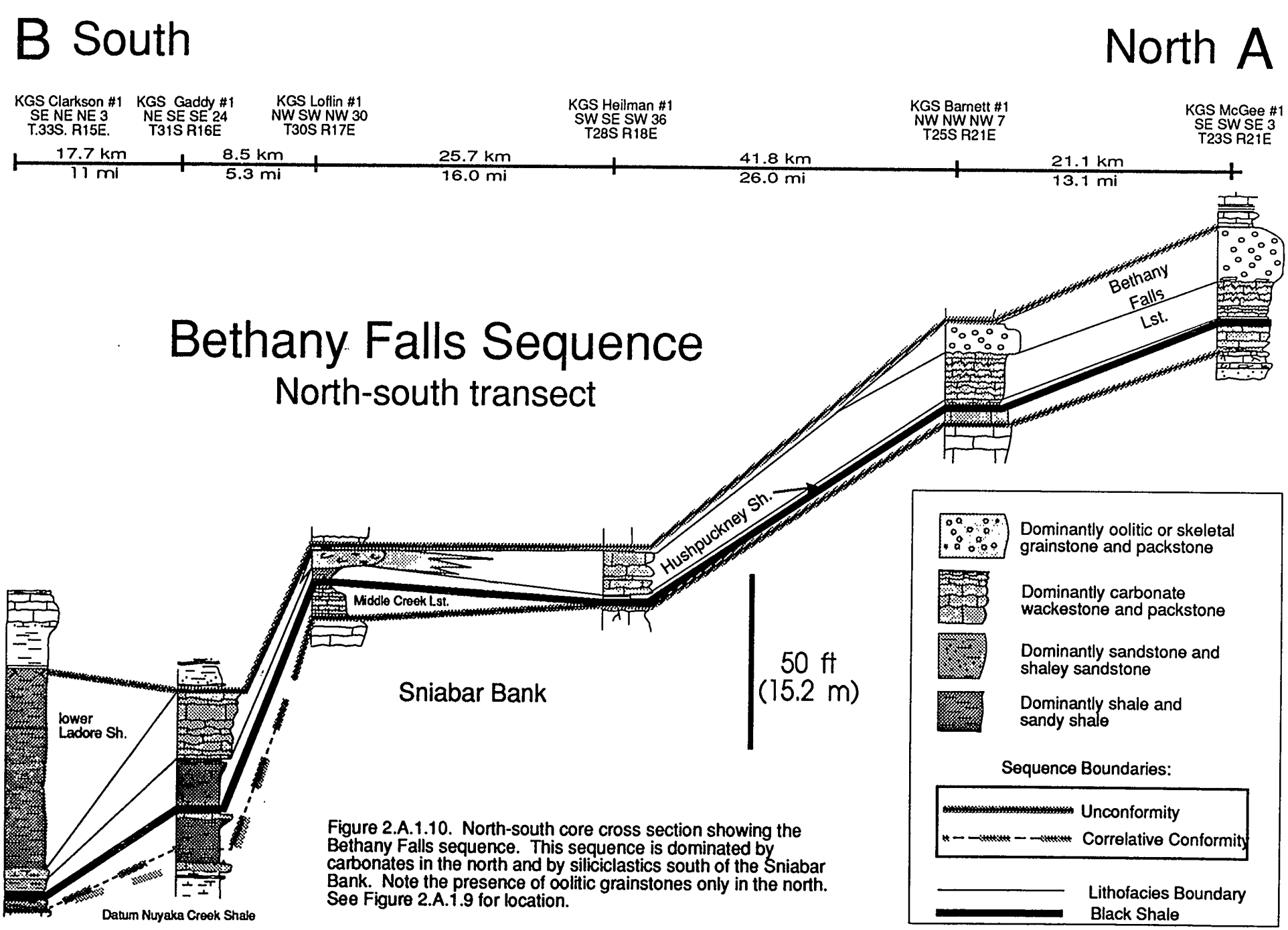

Figure 2.A.1.10. North-south core cross section showing the Bethany Falls sequence. This sequence is dominated by carbonates in the north and by siliciclastics south of the Sniabar Bank. Note the presence of oolitic grainstones only in the north. See Figure 2.A.1.9 for location.

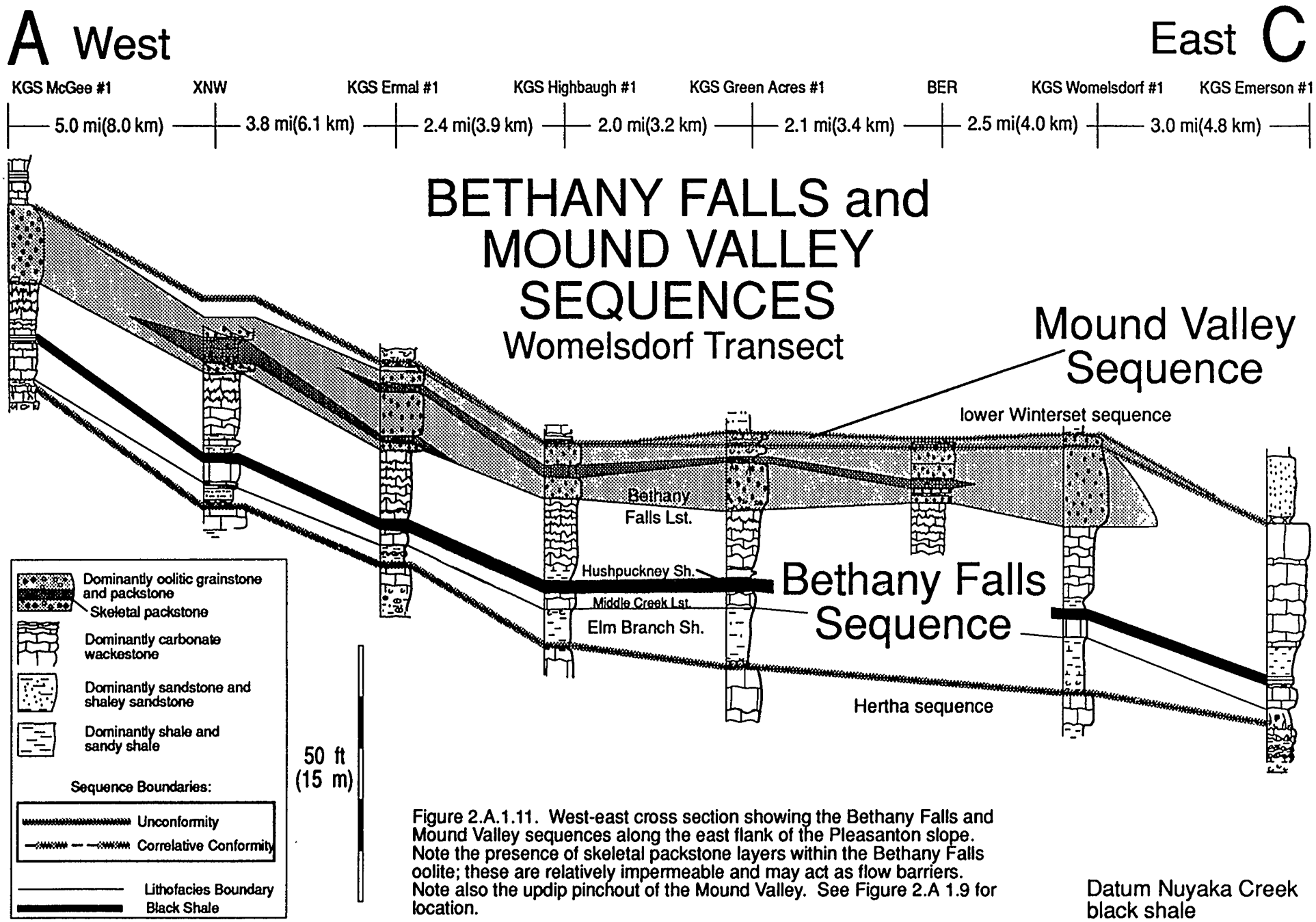

Figure 2.A.1.11. West-east cross section showing the Bethany Falls and Mound Valley sequences along the east flank of the Pleasanton slope. Note the presence of skeletal packstone layers within the Bethany Falls oolite; these are relatively impermeable and may act as flow barriers. Note also the updip pinchout of the Mound Valley. See Figure 2.A 1.9 for location.

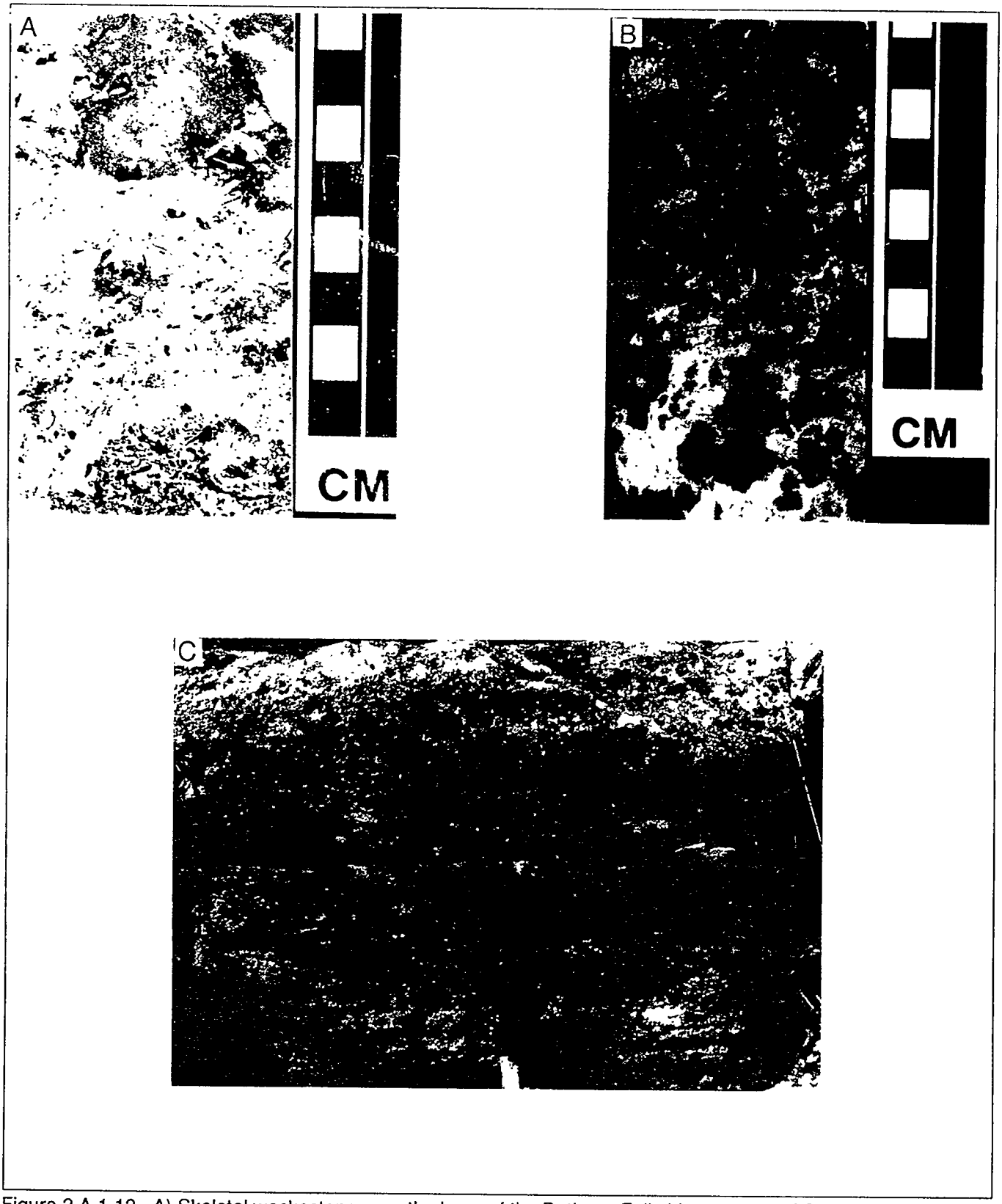

Figure 2.A.1.12. A) Skeletal wackestone near the base of the Bethany Falls Limestone. KGS Larson #1, 93 ft 6 in. B) Mottled skeletal-peloidal packstone less than 6 in (15 cm) below the Bethany Falls grainstone. KGS Larson #1, 78 ft. C) Cross-stratified ooid grainstone in an outcrop of the upper Bethany Falls Limestone. Location XNW.

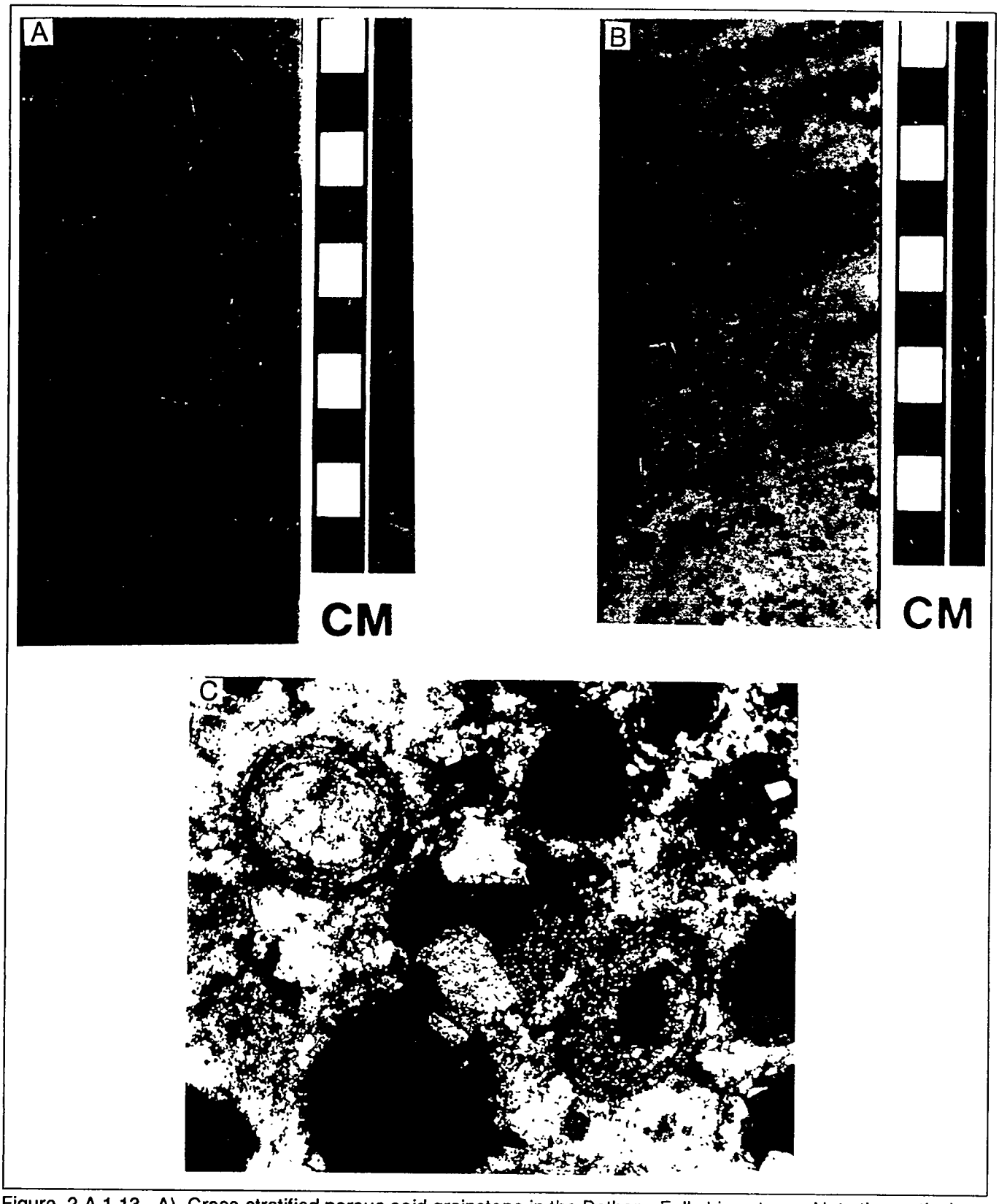

Figure 2.A.1.13. A) Cross-stratified porous ooid grainstone in the Bethany Falls Limestone. Note the vertical burrow or root trace disrupting bedding in the center of the core slab. KGS Larson #1, 72 ft 5 in. B) Cross-stratified, oil-stained ooid grainstone in the upper Bethany Falls Limestone. Note the preferential staining along certain beds/laminae, suggesting that effective permeability varies at a scale of centimeters. KGS Larson #1, 64 ft. C) Photomicrograph of porous ooid grainstone from the upper Bethany Falls Limestone. Note the partial occlusion of some oomolds (dark, circular areas) by saddle dolomite (rhombic crystals). KGS Woodward #3, 73 ft 4 in.

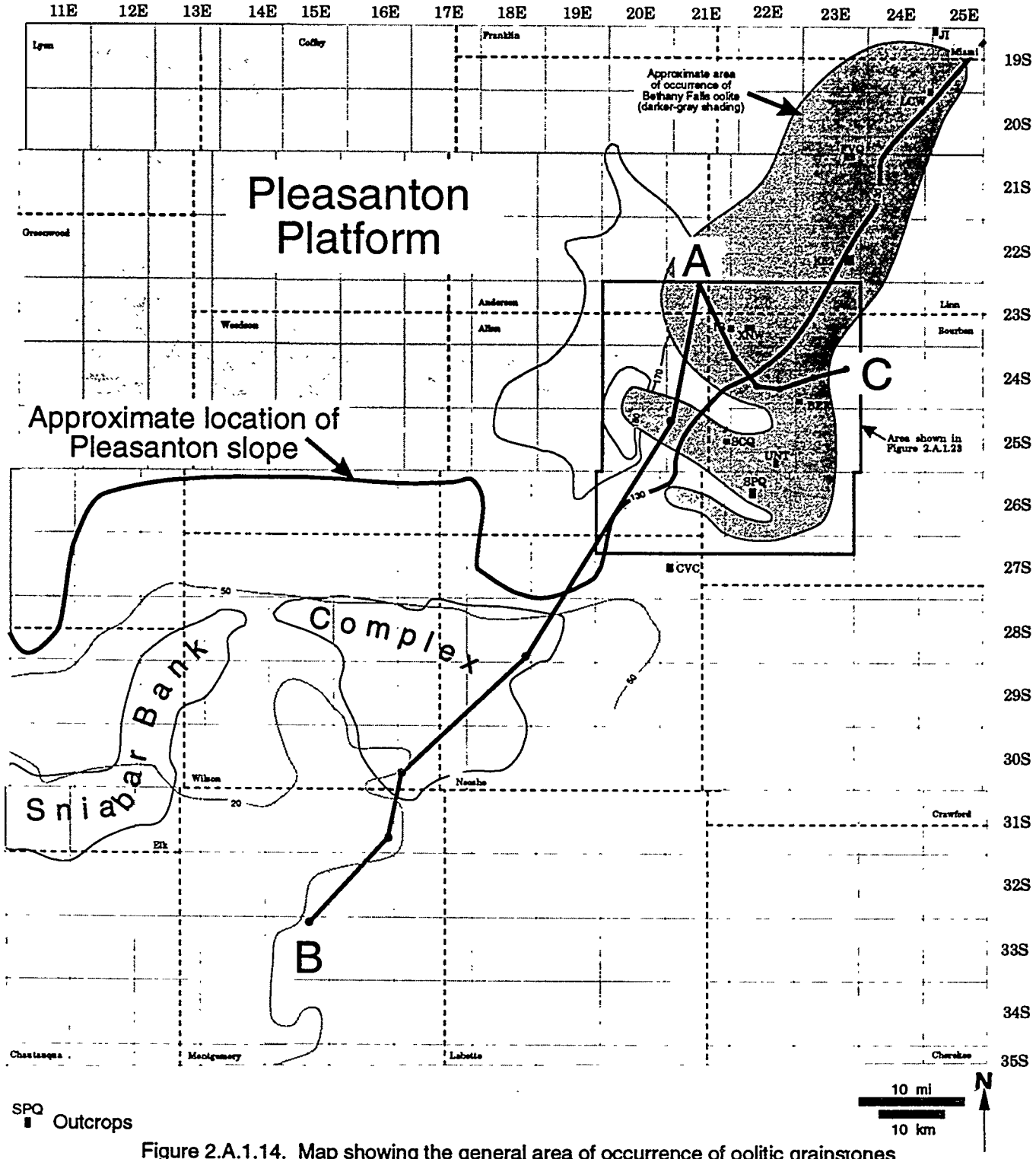

Figure 2.A.1.14. Map showing the general area of occurrence of oolitic grainstones in the Bethany Falls Limestone (gray-shaded area in northeast). This area of oolite is associated with the east flank of the Pleasanton platform, and is discussed more fully in the section describing the detailed study area (small box in northeast).

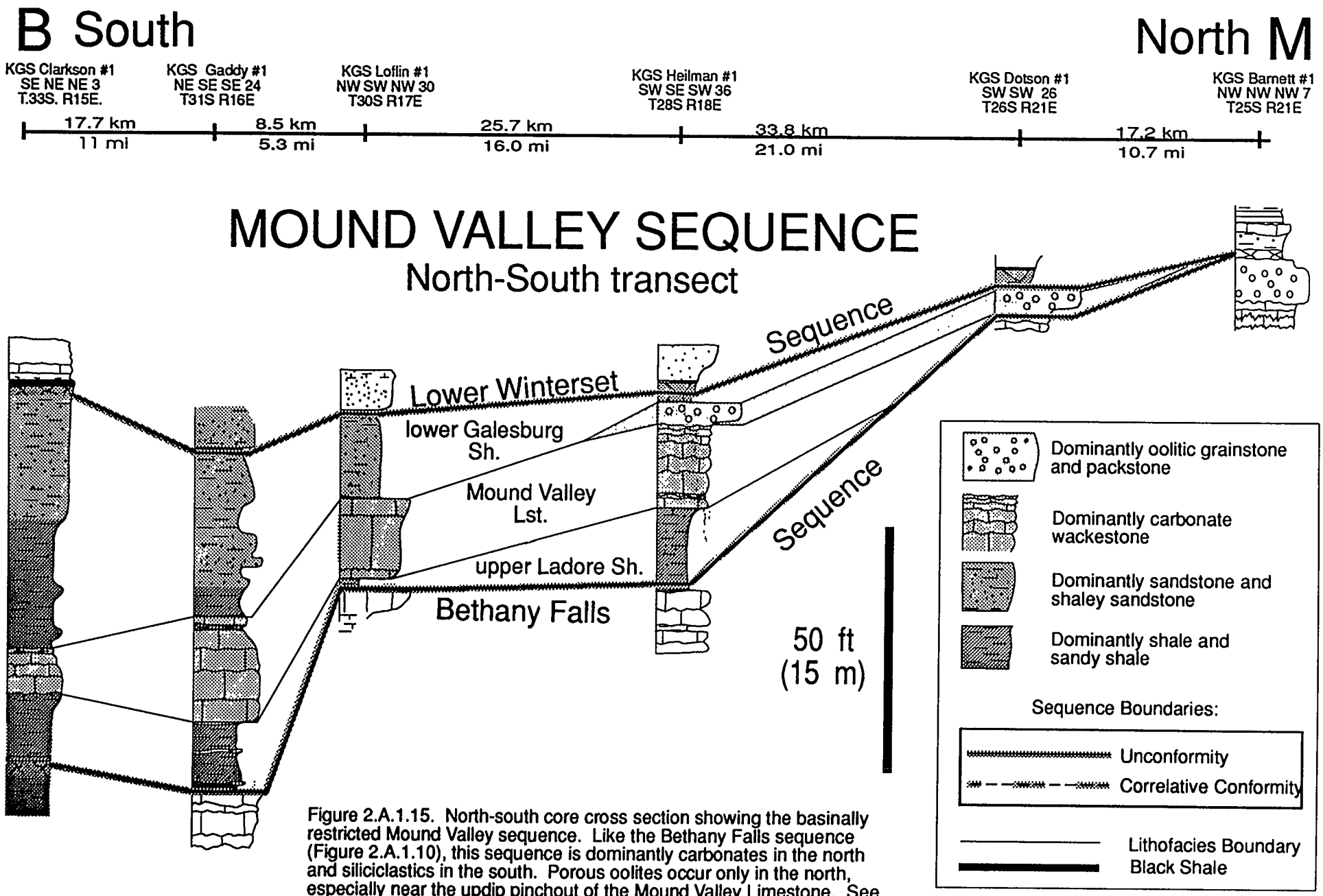

Figure 2.A.1.15. North-south core cross section showing the basinally restricted Mound Valley sequence. Like the Bethany Falls sequence (Figure 2.A.1.10), this sequence is dominantly carbonates in the north and siliciclastics in the south. Porous oolites occur only in the north, especially near the updip pinchout of the Mound Valley Limestone. See Figure 2.A.1.16 for location.

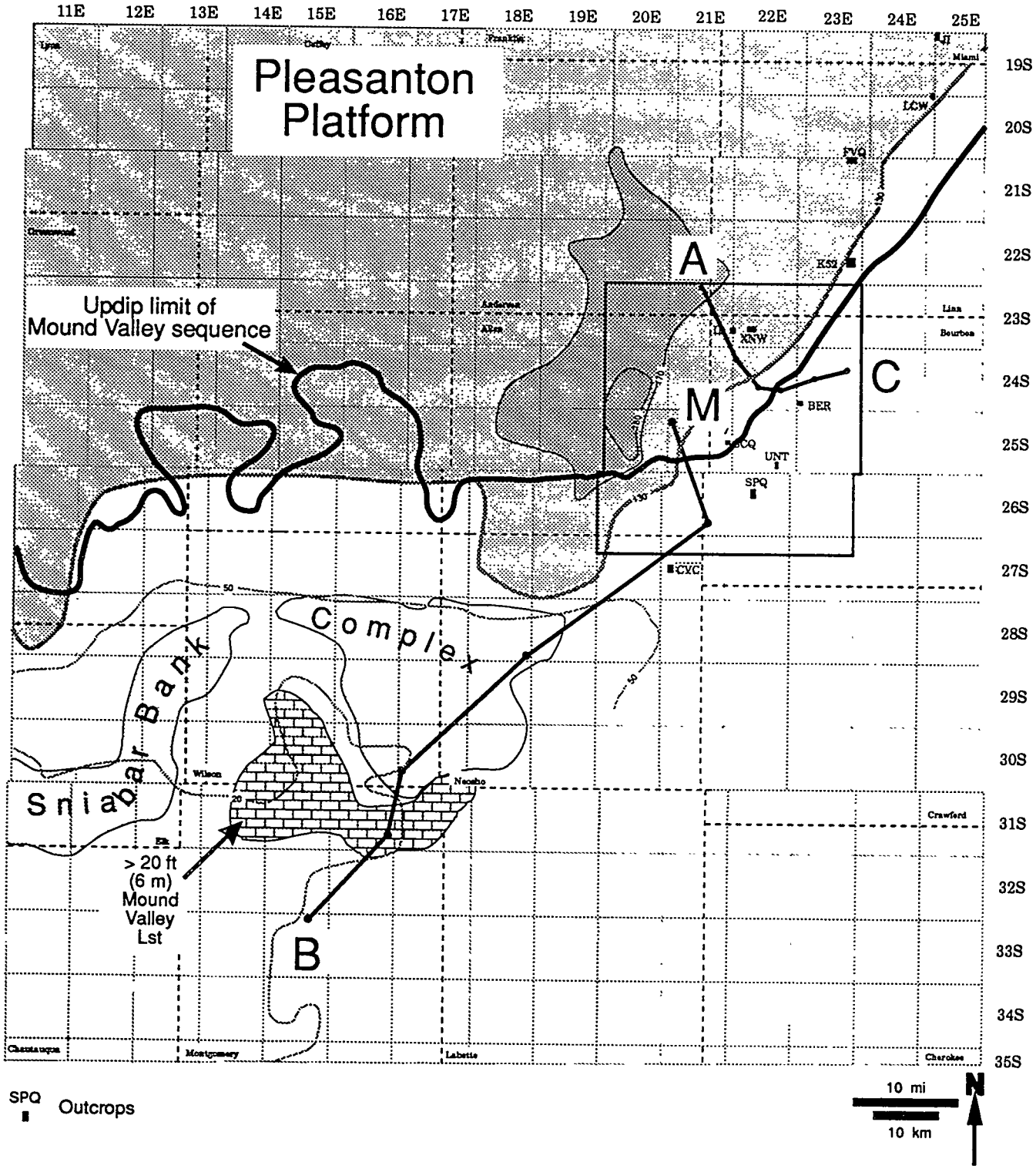

Figure 2.A.1.16. Map showing the occurrence of thick Mound Valley Limestone (brick pattern) just basinward of the underlying Sniabar bank complex. Note that the updip limit of the Mound Valley Limestone (solid black line) generally corresponds to the edge of the Pleasanton platform.

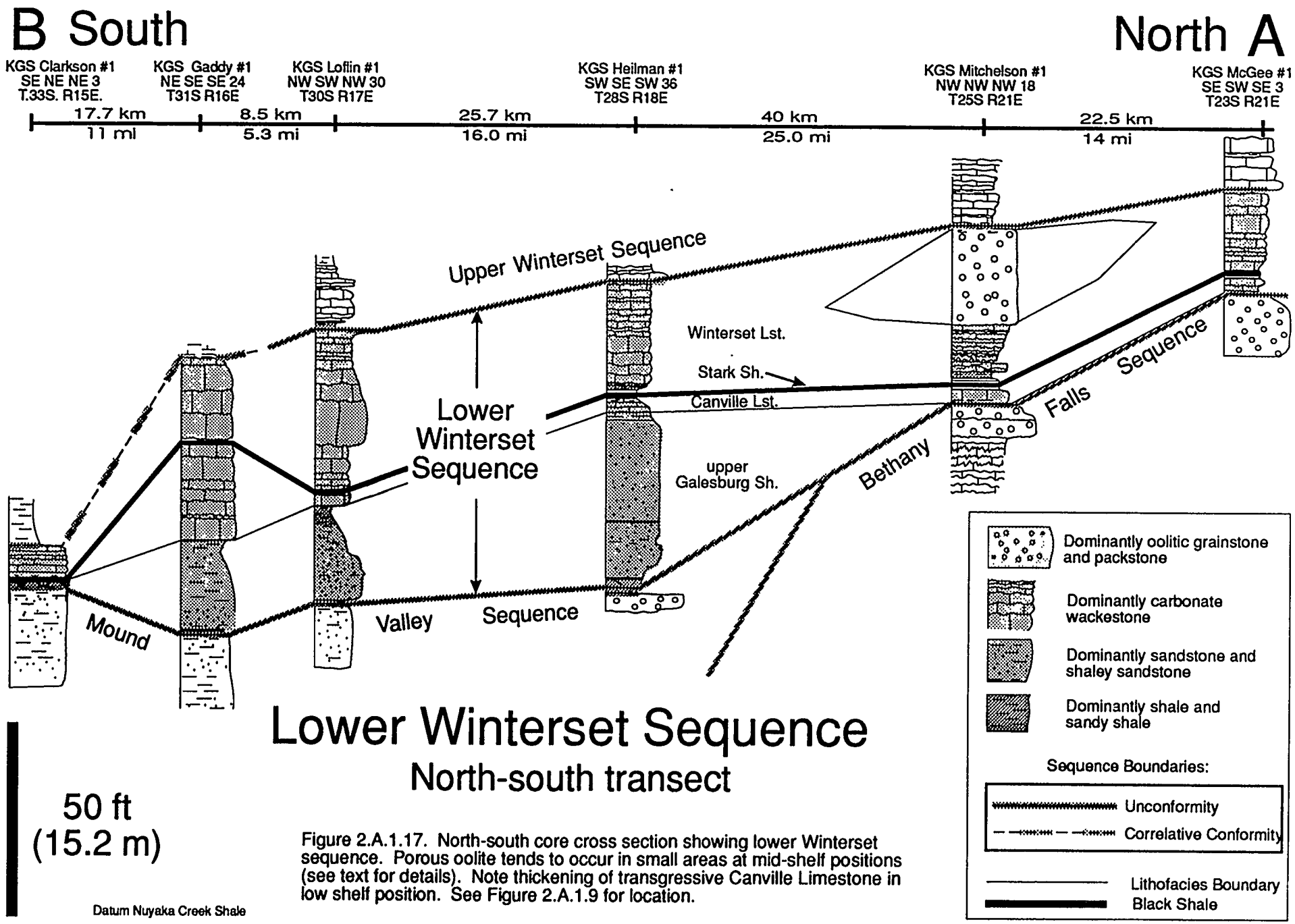

Lower Winterset Sequence

North-south transect

Figure 2.A.1.17. North-south core cross section showing lower Winterset sequence. Porous oolite tends to occur in small areas at mid-shelf positions (see text for details). Note thickening of transgressive Canville Limestone in low shelf position. See Figure 2.A.1.9 for location.

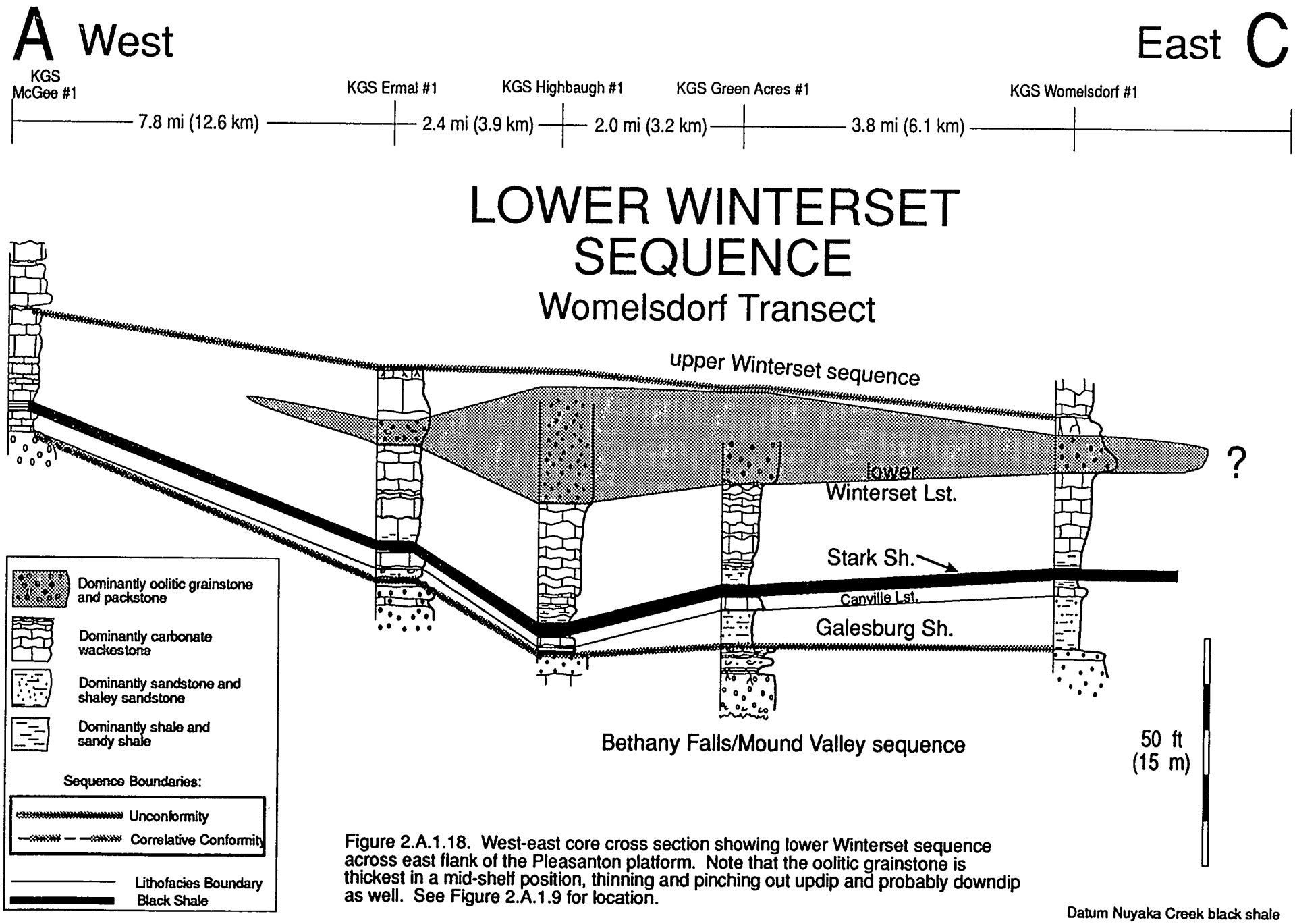

Figure 2.A.1.18. West-east core cross section showing lower Winterset sequence across east flank of the Pleasanton platform. Note that the oolitic grainstone is thickest in a mid-shelf position, thinning and pinching out updip and probably downdip as well. See Figure 2.A.1.9 for location.

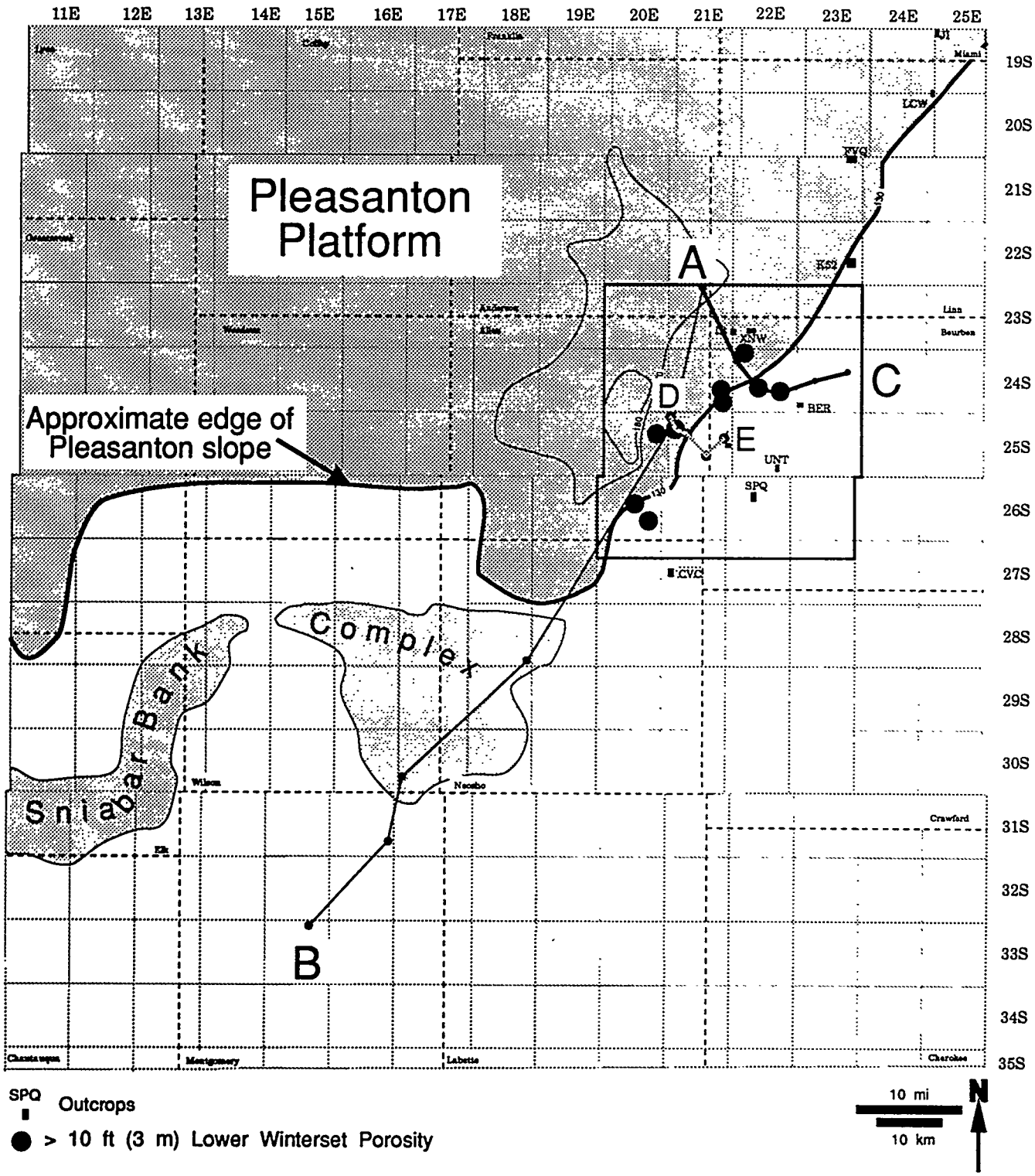

Figure 2.A.1.19. Map showing occurrences of >10 ft (3 m) of porous carbonate in the Winterset Limestone portion of the lower winterset sequence. Note that this porosity is closely associated with the edge of the Pleasanton platform.

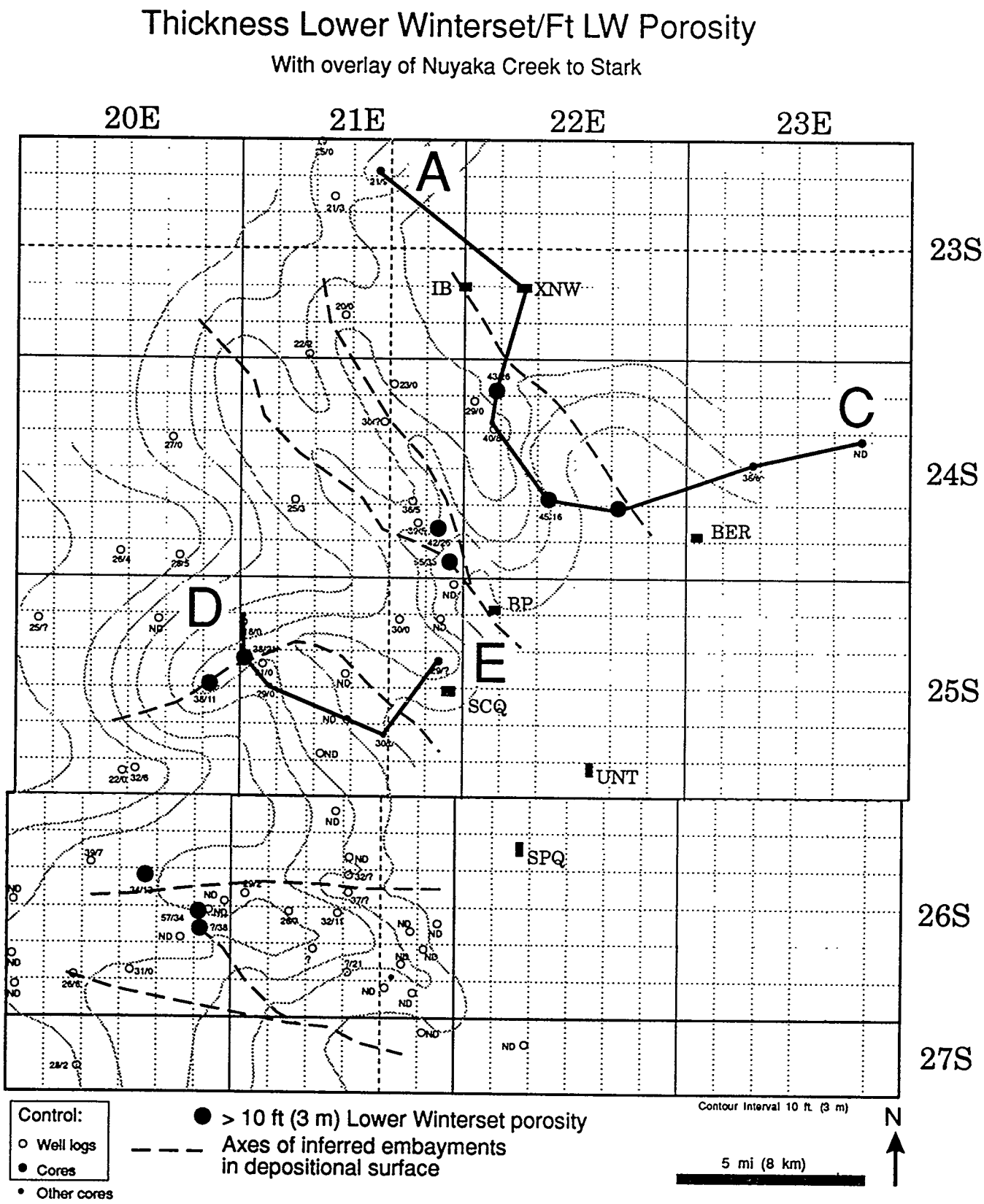

Figure 2.A.1.20. Map of detailed study area showing locations of >10 ft (3 m) of porosity development (large dots) in lower Winterset sequence overlain on an isopach of the Nuyaka Creek black shale-to-Stark black shale interval. This porosity tends to occur in association with distinct linear zones of thin Nuyaka Creek-to-Stark that are interpreted to reflect embayments or small valleys in the pre-lower winterset surface. See text for details.

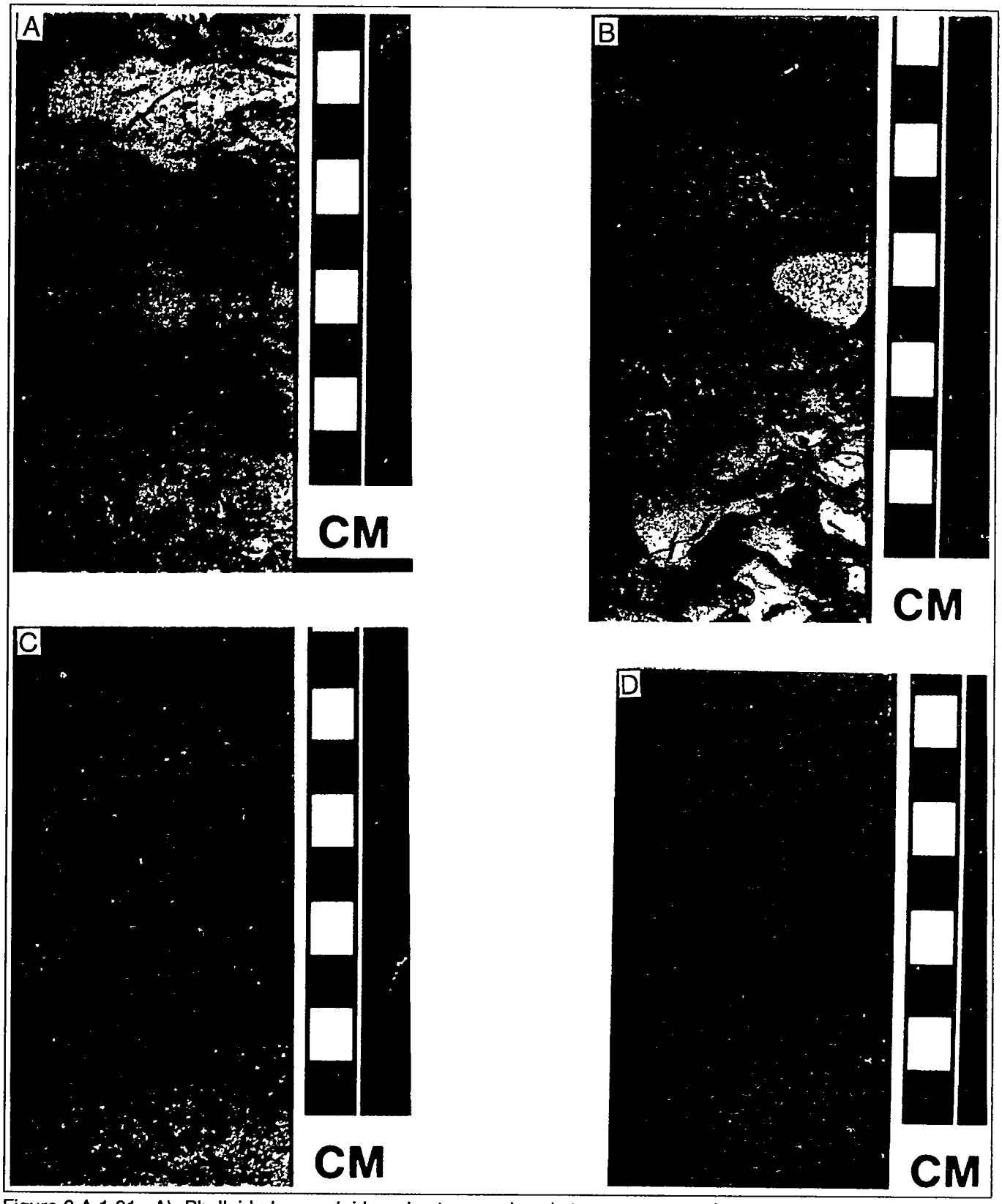

Figure 2.A.1.21. A) Phylloid-algae-peloid wackestone and packstone representative of much of the lower Winterset Limestone. KGS Larson #1, 31 ft. B) Abrupt contact between skeletal packstone/wackestone (below) and ooid-skeletal grainstone (above) in the lower Winterset Limestone. Such contacts may reflect an abrupt lowering of relative sea-level, or may simply represent erosional scouring of the muddy bottom as high-energy conditions impinged on an area during steady sea-level fall. KGS Larson #1, 29 ft. C) An example of non-porous lower Winterset ooid-skeletal grainstone. KGS Larson #1, 27 ft. D) Non-porous lower Winterset ooid-skeletal grainstone a few cm below the sequence boundary. The lighter patches are siliciclastic marine muds derived from the flooding unit above the sequence boundary that have been worked down into the grainstone by burrowers. KGS Larson #1, 21 ft 6 in.

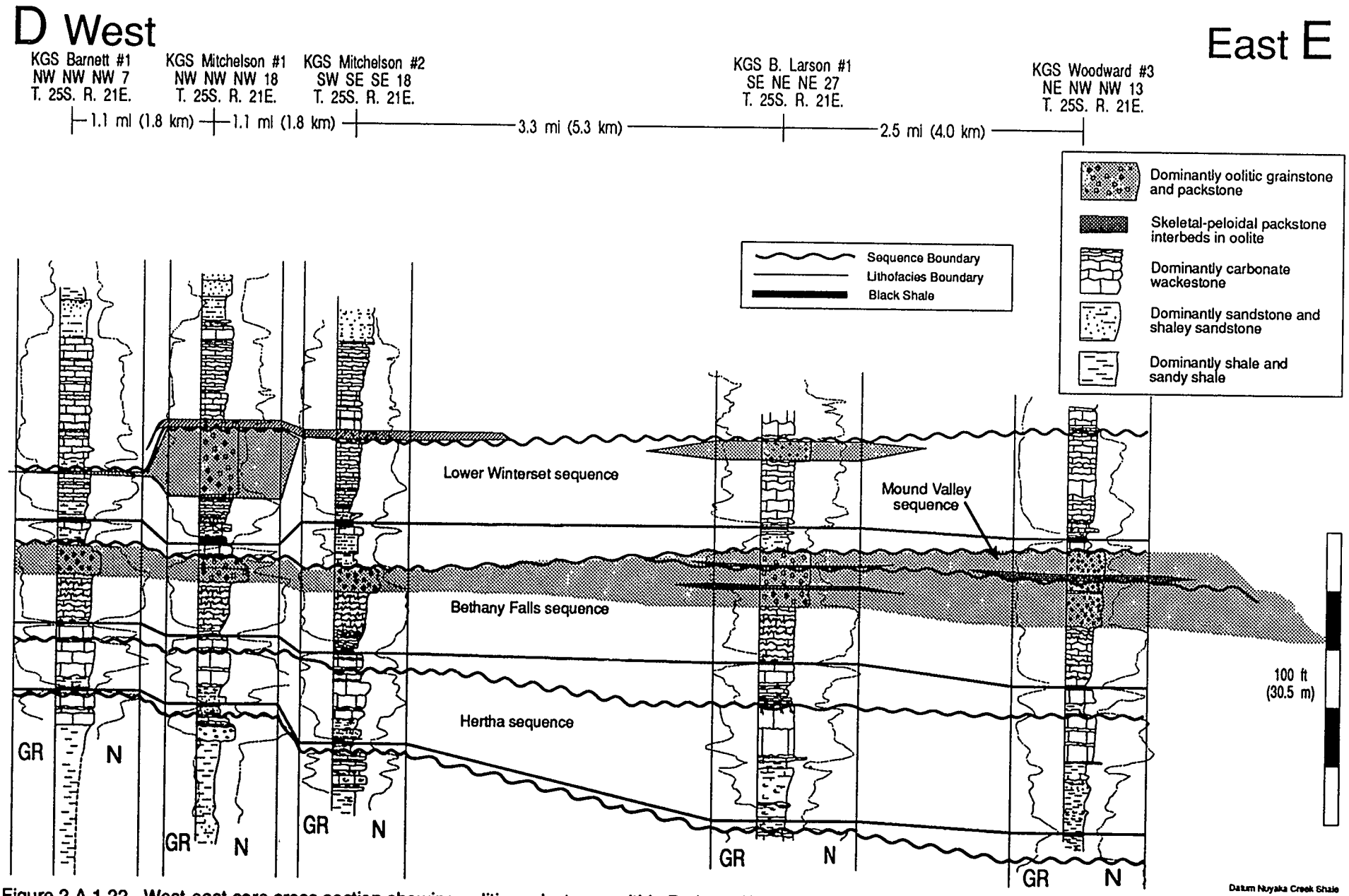

Figure 2.A.1.22. West-east core cross section showing oolitic grainstones within Bethany Falls, Mound Valley, and lower winterset sequences. Note the areally restricted nature of the lower winterset grainstones as compared to those in the Bethany Falls. Note also the presence of packstone interbeds within the Bethany Falls and between the Mound Valley and Bethany Falls. See Figures 2.A.1.19 and 20 for location. GR=gamma-ray log; N=neutron log.

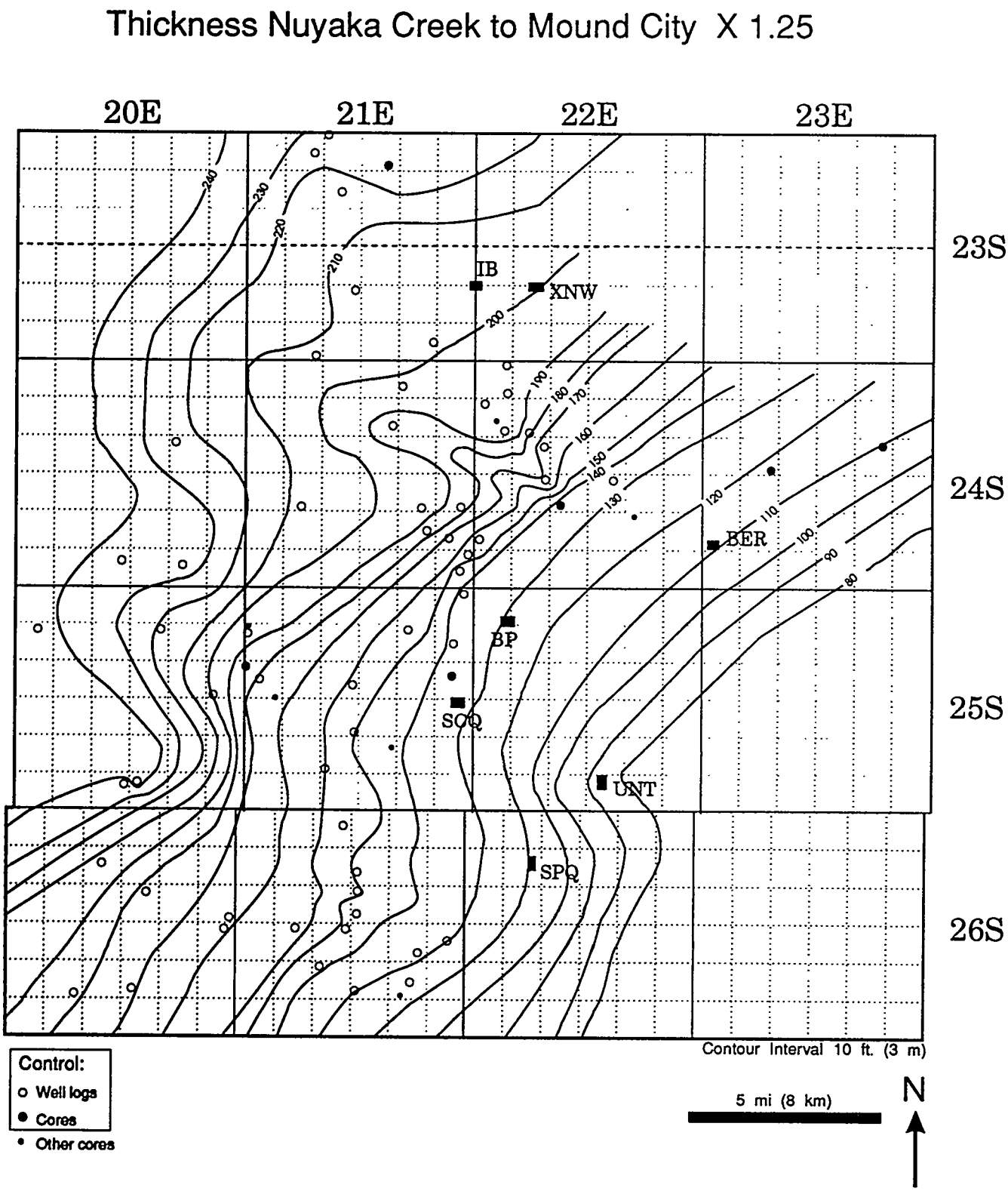

Figure 2.A.1.23. Isopach map of the interval from the base of the Nuyaka Creek black shale to the base of the Mound City black shale in the detailed study area. This shale-dominated interval has been decompacted by 25%, primarily to accentuate the configuration of the slope; there is little information available regarding the decompaction through time of such lithologies. This is the eastward- and southeastward-dipping "Pleasanton slope" that affected deposition of the overlying sequences (see text).

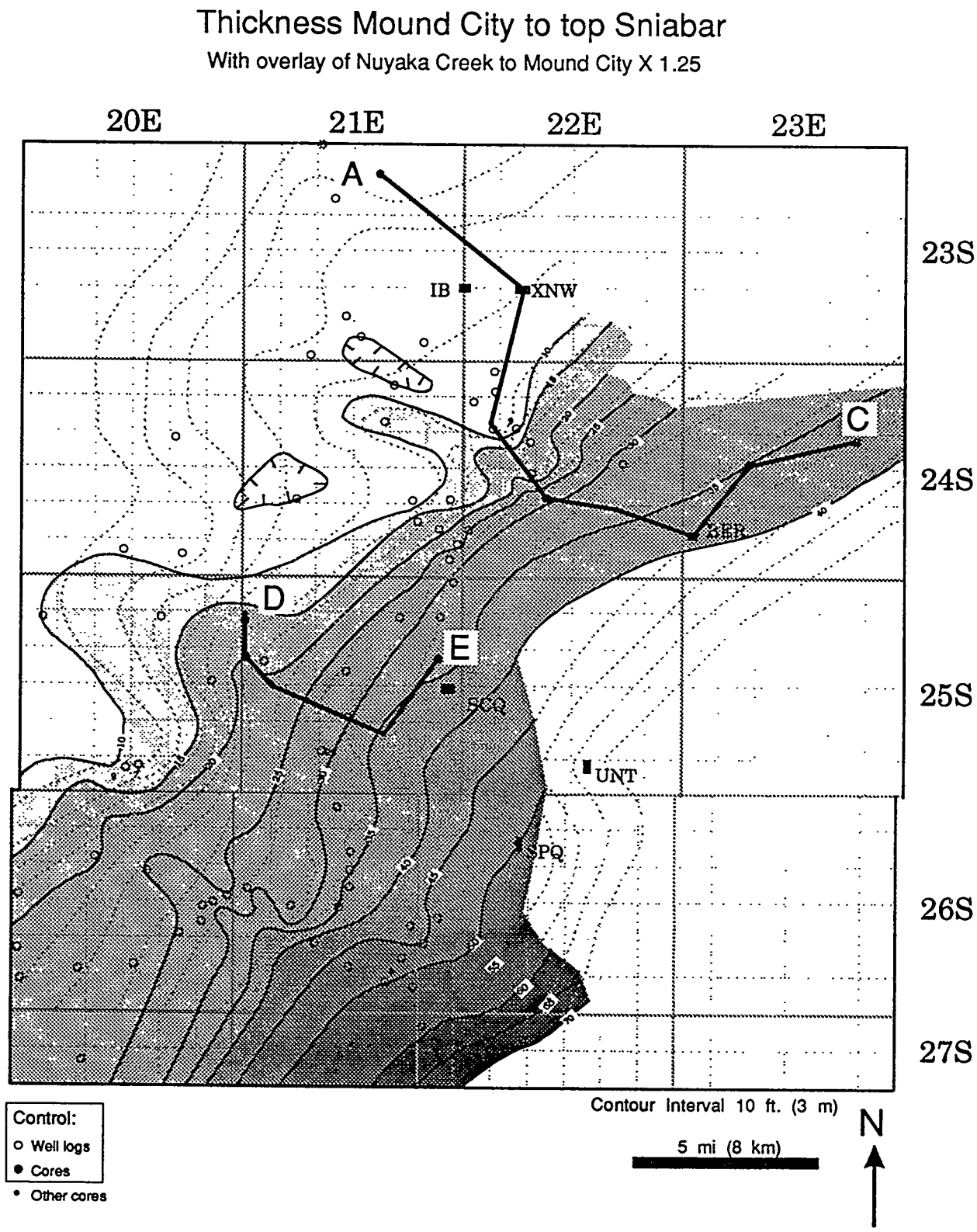

Figure 2.A.1.24. Isopach map of the interval from the Mound City black shale facies to the top of the Sniabar Limestone (shaded) in the detailed study area. Note that this interval thickens eastward and southeastward in association with thinning of the underlying Pleasanton interval (light-gray contours). Also see cross sections (Figures 2.A.1.5, 22).

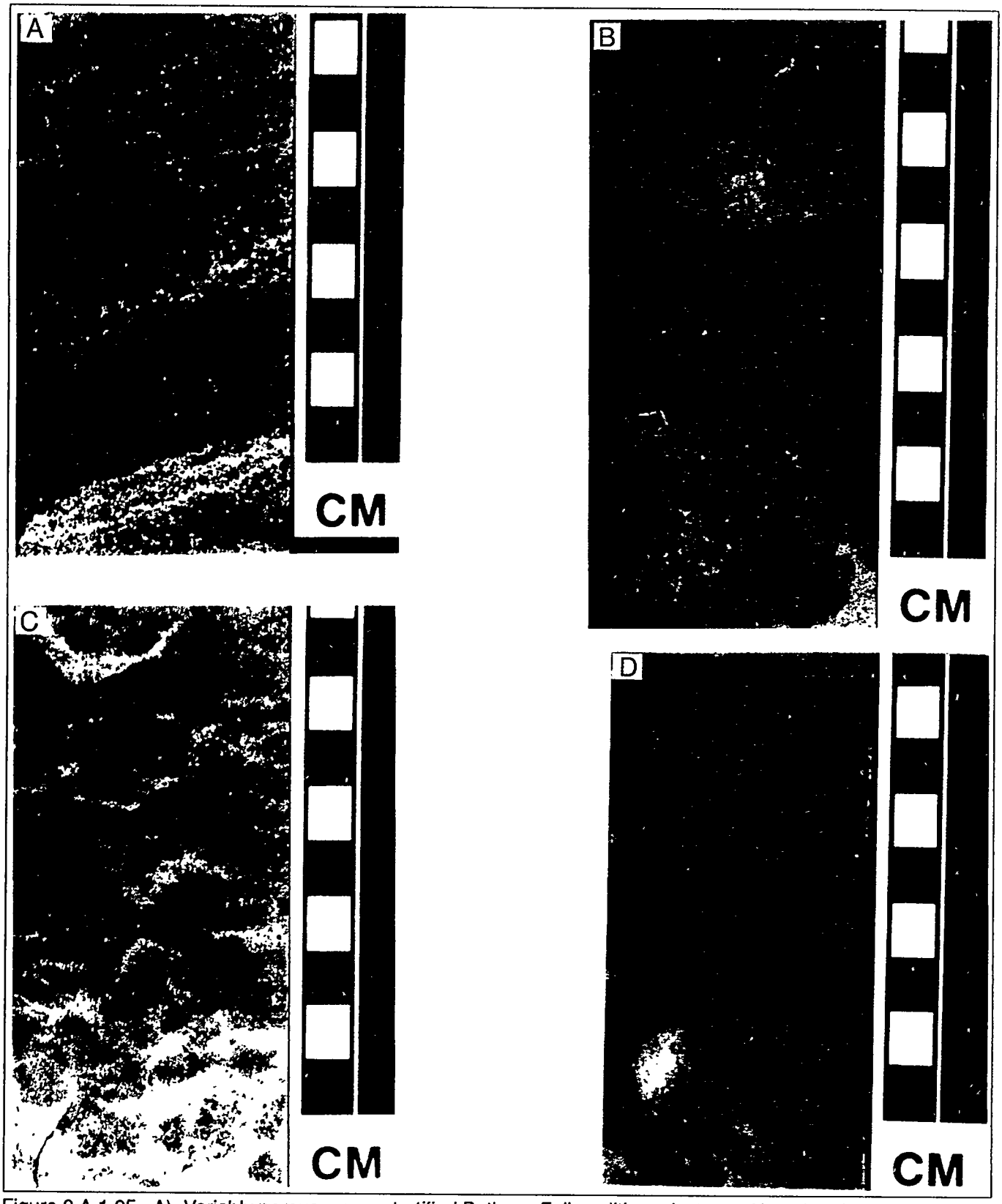

Figure 2.A.1.25. A) Variably porous, cross-stratified Bethany Falls oolitic grainstone. Note that the best porosity in this sample is associated with the relatively coarse-grained bed near the center of the photograph. KGS Woodward #3, 80 ft. B) Oil-stained Bethany Falls oolitic grainstone. This pattern of staining is an indication of the scale of porosity and permeability variations in this unit. KGS Larson #1, 64 ft 8 in. C) Impermeable, low-porosity peloidal-skeletal packstone that commonly occurs as interbeds within the oolites. These muddy, low-energy deposits may be local facies within the oolite tracts, but the presence of laterally equivalent paleosols and negative carbon isotope excursions at the bases of some of these units suggests that they are flooding units associated with regional sea-level rises (see text). KGS Woodward #3, 67 ft 6 in. D) Another example of a possible flooding unit within the Bethany Falls Limestone (see C). This sample has a porosity of about 12% and a permeability of less than 1 md. KGSLarson #1, 71 ft.

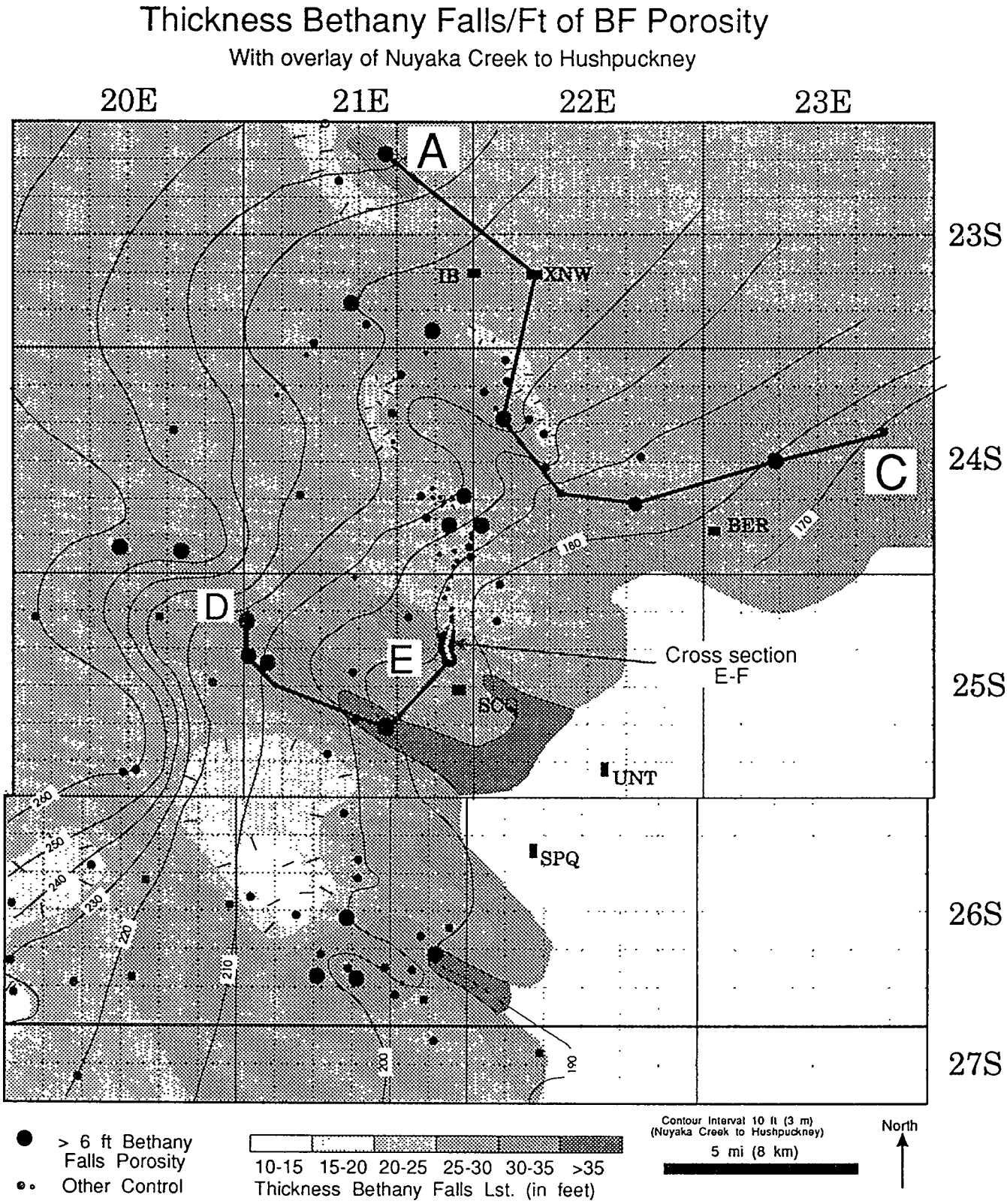

Figure 2.A.1.26. Thickness of the Bethany Falls Limestone (shaded) overlain on the thicknêss of the underlying Nuyaka Creek black shale to Hushpuckney black shale interval (solid contour lines). The large black dots correspond to locations where there is more than 6 ft (1.8 m) of porosity in the Bethany Falls. Note that there is a positive correlation between thickness and porosity. There is also a correlation between areas of thick and porous Bethany Falls and subtle thins in the underlying interval; these thins are inferred to have been embayments in the pre-Bethany Falls surface (see text).

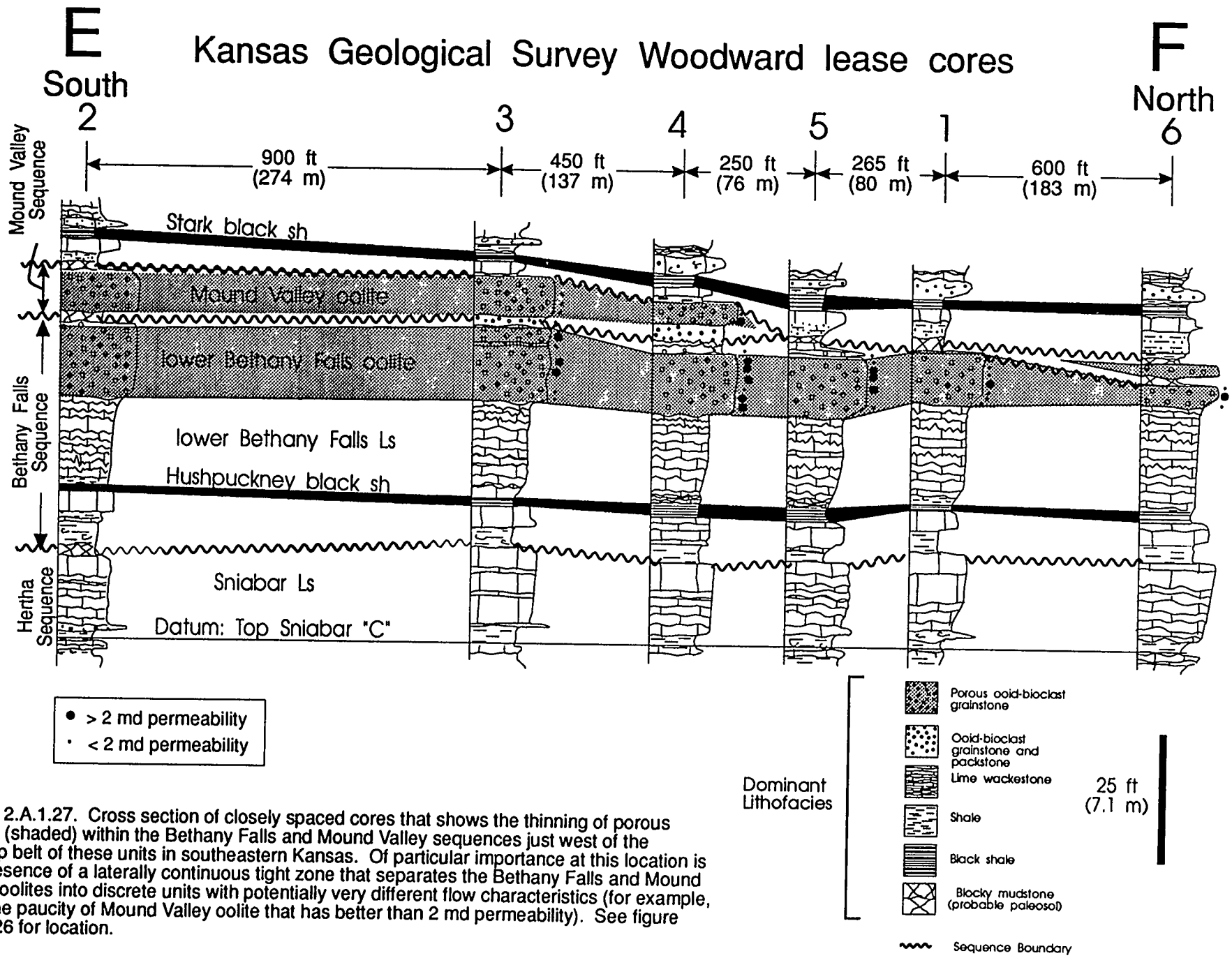

Figure 2.A.1.27. Cross section of closely spaced cores that shows the thinning of porous oolites (shaded) within the Bethany Falls and Mound Valley sequences just west of the outcrop belt of these units in southeastern Kansas. Of particular importance at this location is the presence of a laterally continuous tight zone that separates the Bethany Falls and Mound Valley oolites into discrete units with potentially very different flow characteristics (for example, note the paucity of Mound Valley oolite that has better than 2 md permeability). See figure 2.A.1.26 for location.

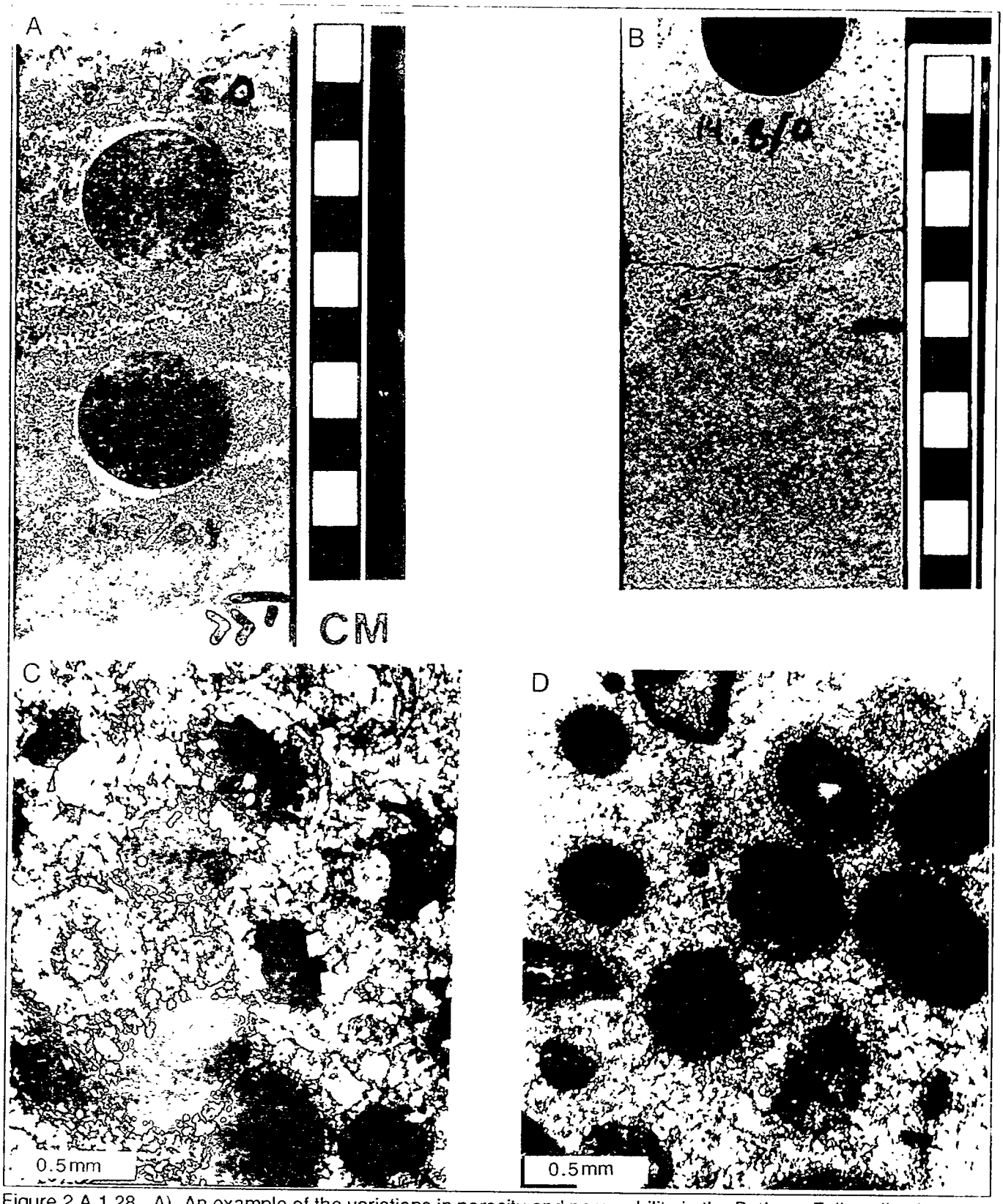

Figure 2 A.1.28. A) An example of the variations in porosity and permeability in the Bethany Falls oolite that can occur over very short vertical distances. The upper plug yielded a porosity of 20.9% and a permeability value of 5.0 md, while corresponding values in the lower plug were 15.7% and 0.4 md. KGS Woodward #3, 77 ft. B) Typical Mound Valley grainstone. This sample has a porosity of 14.8% and no measurable permeability. KGS Woodward #3, 61 ft 10 in. C) Photomicrograph of oomoldic Bethany Falls Limestone similar to that shown in the upper part of A (above). KGS Woodward #3, 73 ft 4 in. D) Photomicrograph of oomoldic Mound Valley Limestone similar to that shown in B (above). KGS Woodward #3, 64 ft 5 in.

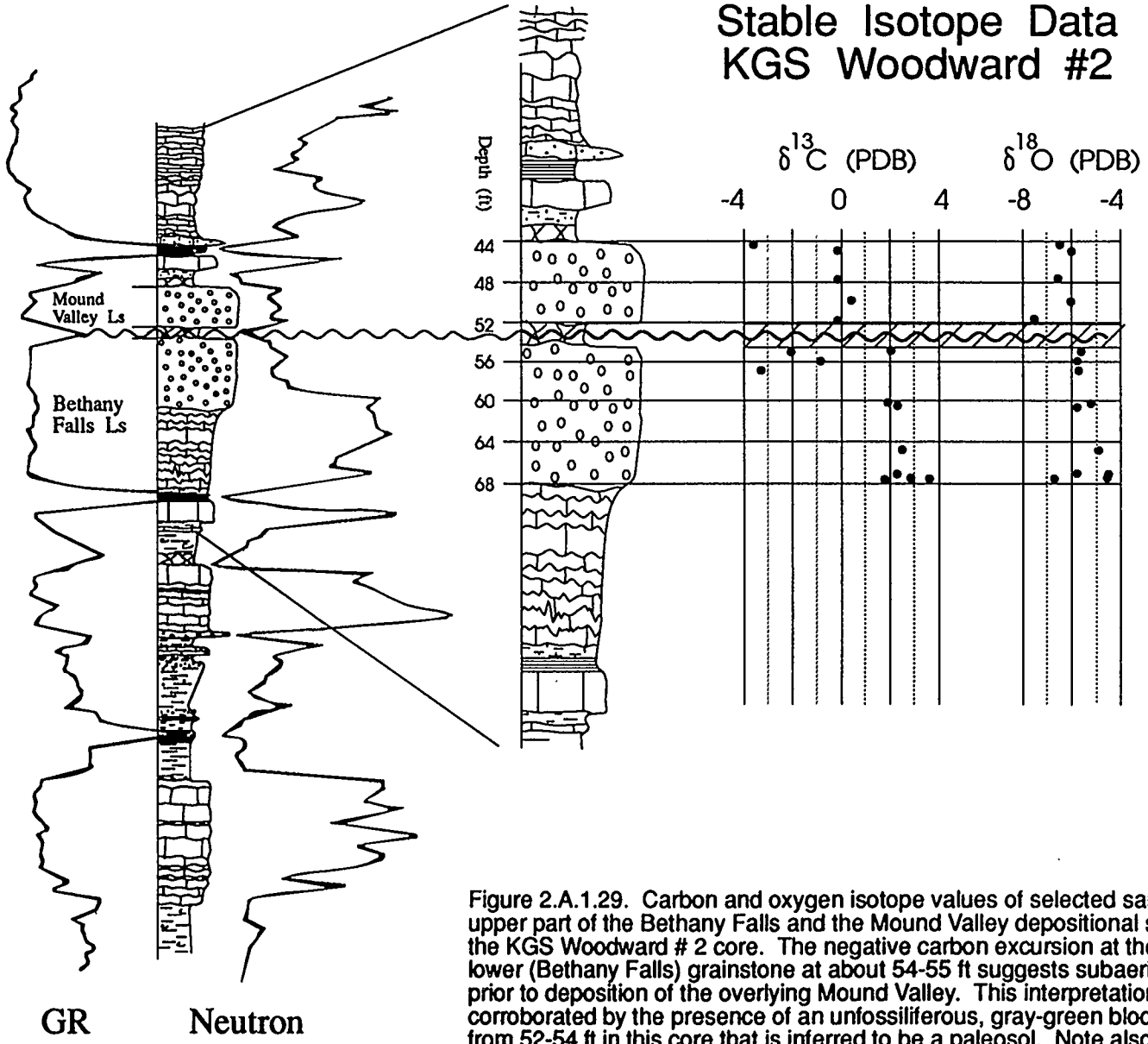

Figure 2.A.1.29. Carbon and oxygen isotope values of selected samples of the upper part of the Bethany Falls and the Mound Valley depositional sequences in the KGS Woodward # 2 core. The negative carbon excursion at the top of the lower (Bethany Falls) grainstone at about 54-55 ft suggests subaerial exposure prior to deposition of the overlying Mound Valley. This interpretation is corroborated by the presence of an unfossiliferous, gray-green blocky mudstone from 52-54 ft in this core that is inferred to be a paleosol. Note also the negative carbon excursion at the top of the Mound Valley oolite just below the upper paleosol.

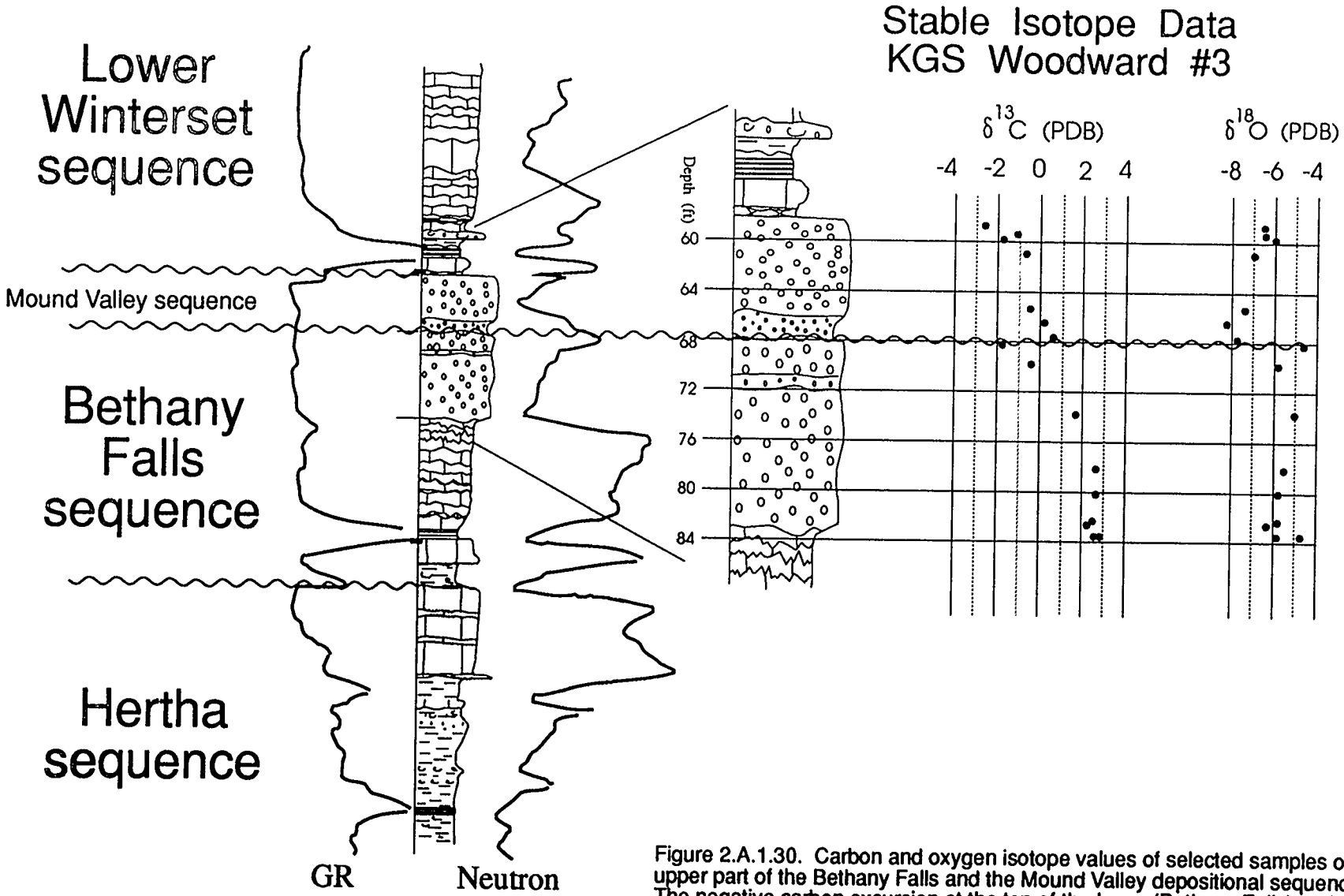

Figure 2.A.1.30. Carbon and oxygen isotope values of selected samples of the upper part of the Bethany Falls and the Mound Valley depositional sequences. The negative carbon excursion at the top of the lower (Bethany Falls) grainstone at about 68 ft suggests subaerial exposure prior to deposition of the overlying Mound Valley. This is important because there is little petrographic evidence of subaerial exposure at this horizon in this core, and the two grainstones could easily be considered to belong to the same sequence. Note also the negative carbon excursion at the top of the Mound Valley oolite just below the paleosol.

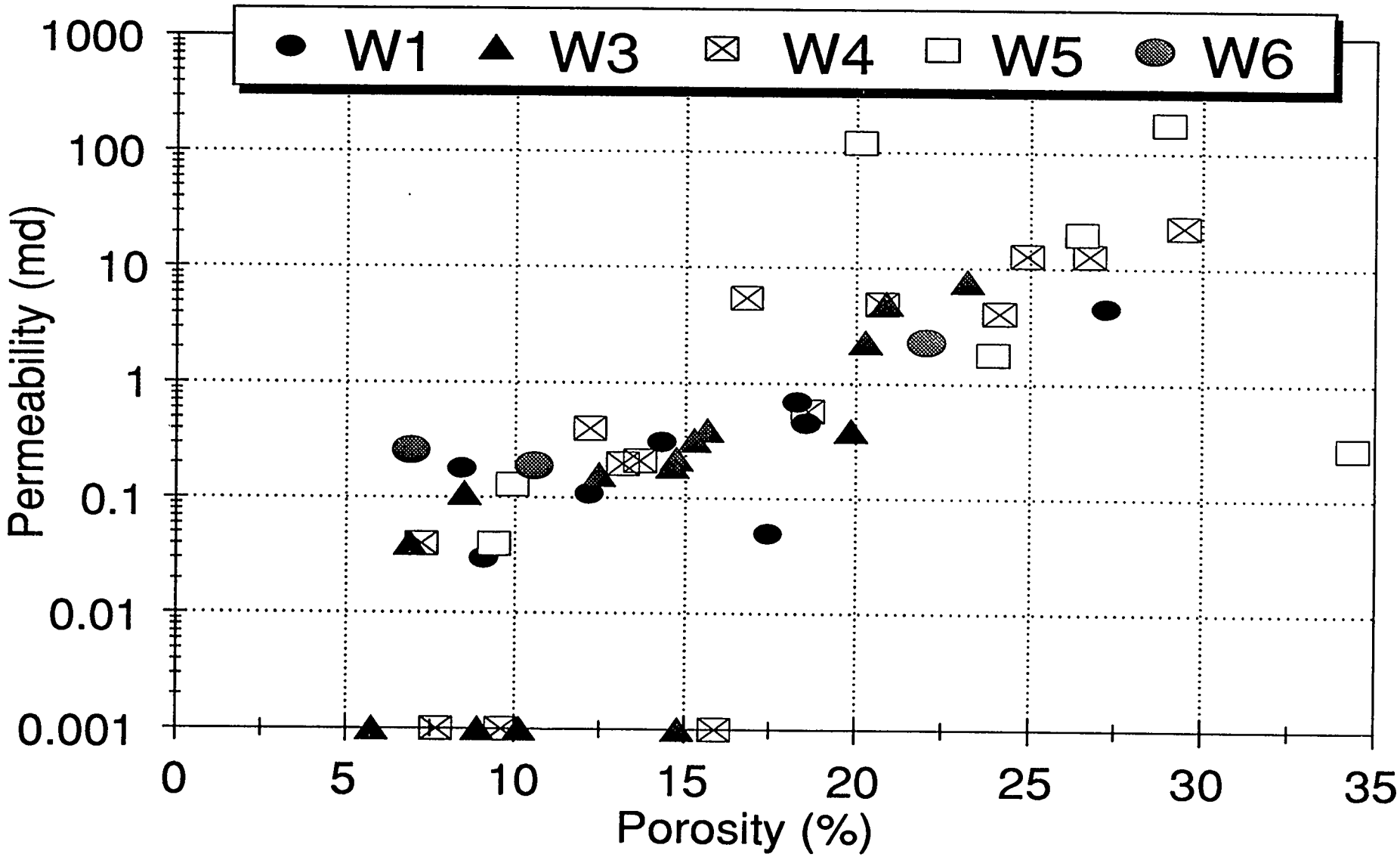

Figure 2.A.1.31. Plot showing the porosity and permeability values for the Bethany Falls and Mound Valley oolites in the Woodward transect cores (see Figure 2.A.1.27). Note that at about 20% porosity the permeabilities are generally greater than 1 md, whereas below 20% porosity, the permeabilities are almost all less than 1 md. This relationship is essentially the same as that found in the Bethany Falls in Victory Field in southwestern Kansas (discussed earlier in this report). The very low permeabilities are almost all from the Mound Valley Limestone.

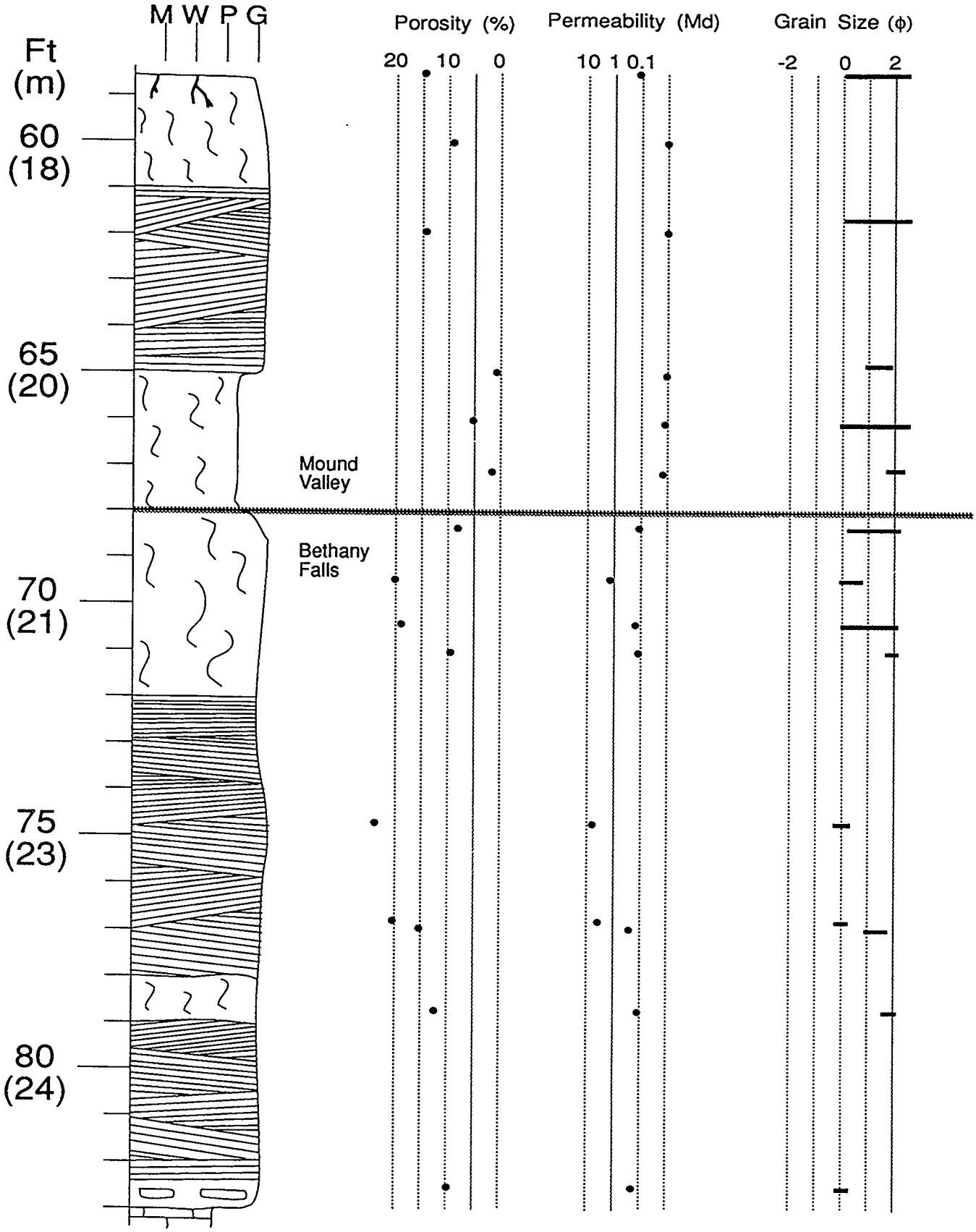

Figure 2.A.1.32. Porosity and permeability values and estimated grain size ranges within the Bethany Falls and Mound Valley limestones, KGS Woodward #3 core (see Figure 2.A.1.27 for location in transect). Lithofacies are primarily cross-stratified ooid-skeletal grainstones, with skeletal-peloidal packstones also present.

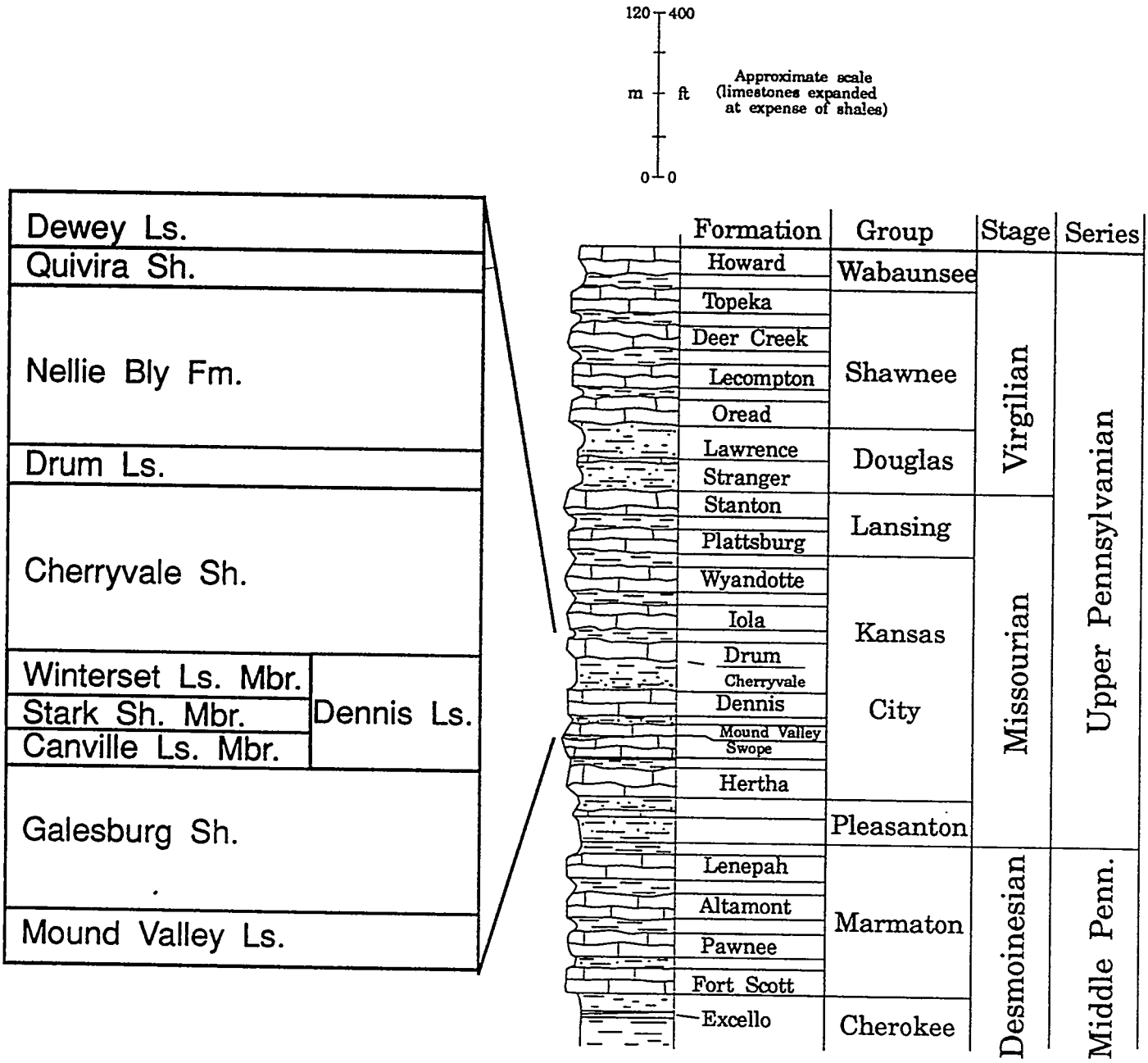

Figure 2.A.2.1. Scematic diagram of the stratigraphy in the study area. Modified from Heckel (1977).

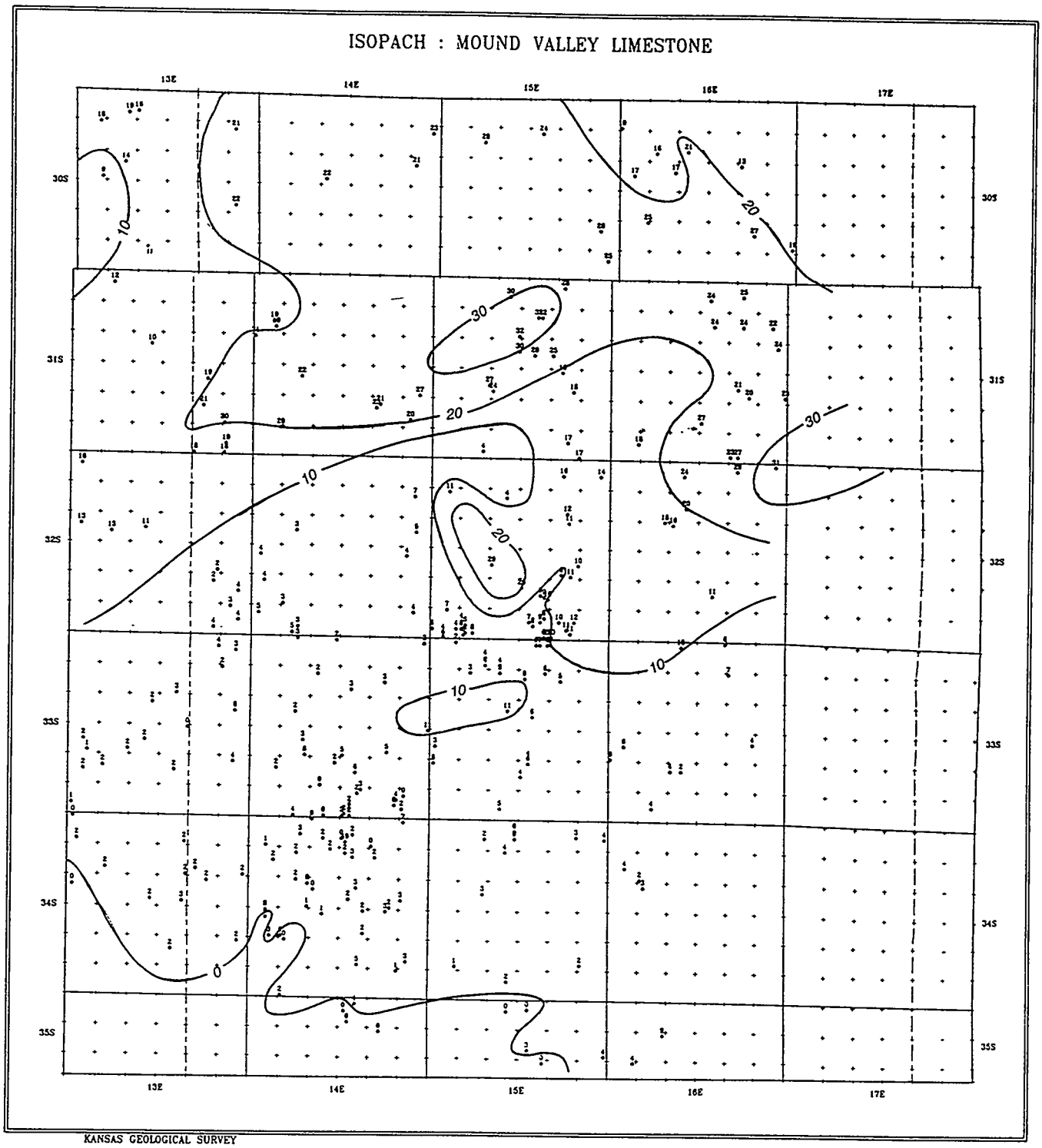

Figure 2.A.2.2. Isopach map of the Mound Valley Limestone in the study area. Dots indicate control points. Contour Interval is 10 ft.

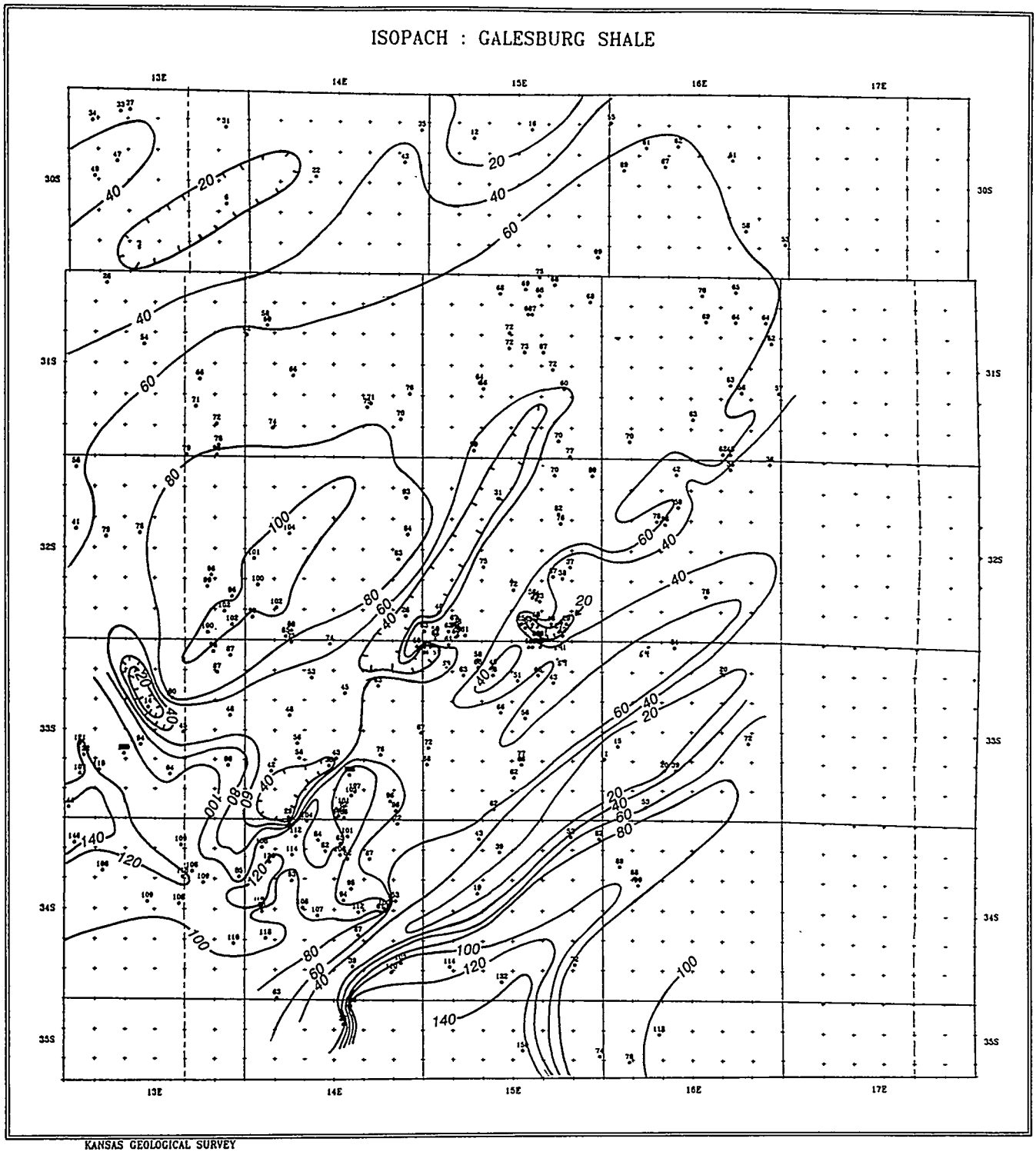

Figure 2.A.2.3. Isopach map of the Galesburg Shale in the study area. Dots indicate control points. Contour Interval is 20 ft.

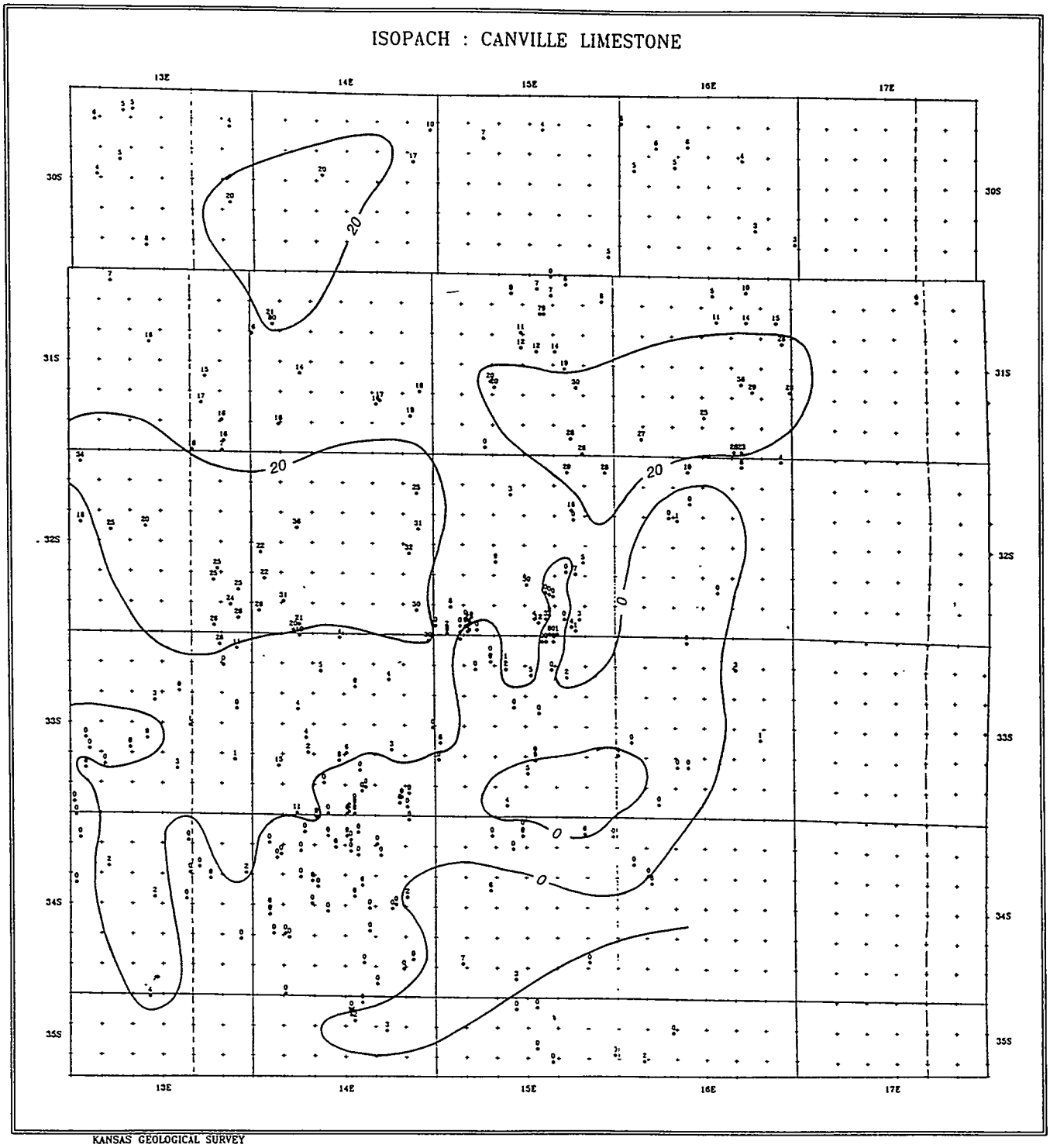

Figure 2.A.2.4. Isopach map of the Canville Limestone in the study area. Dots indicate control points. Contour Interval is 20 ft.

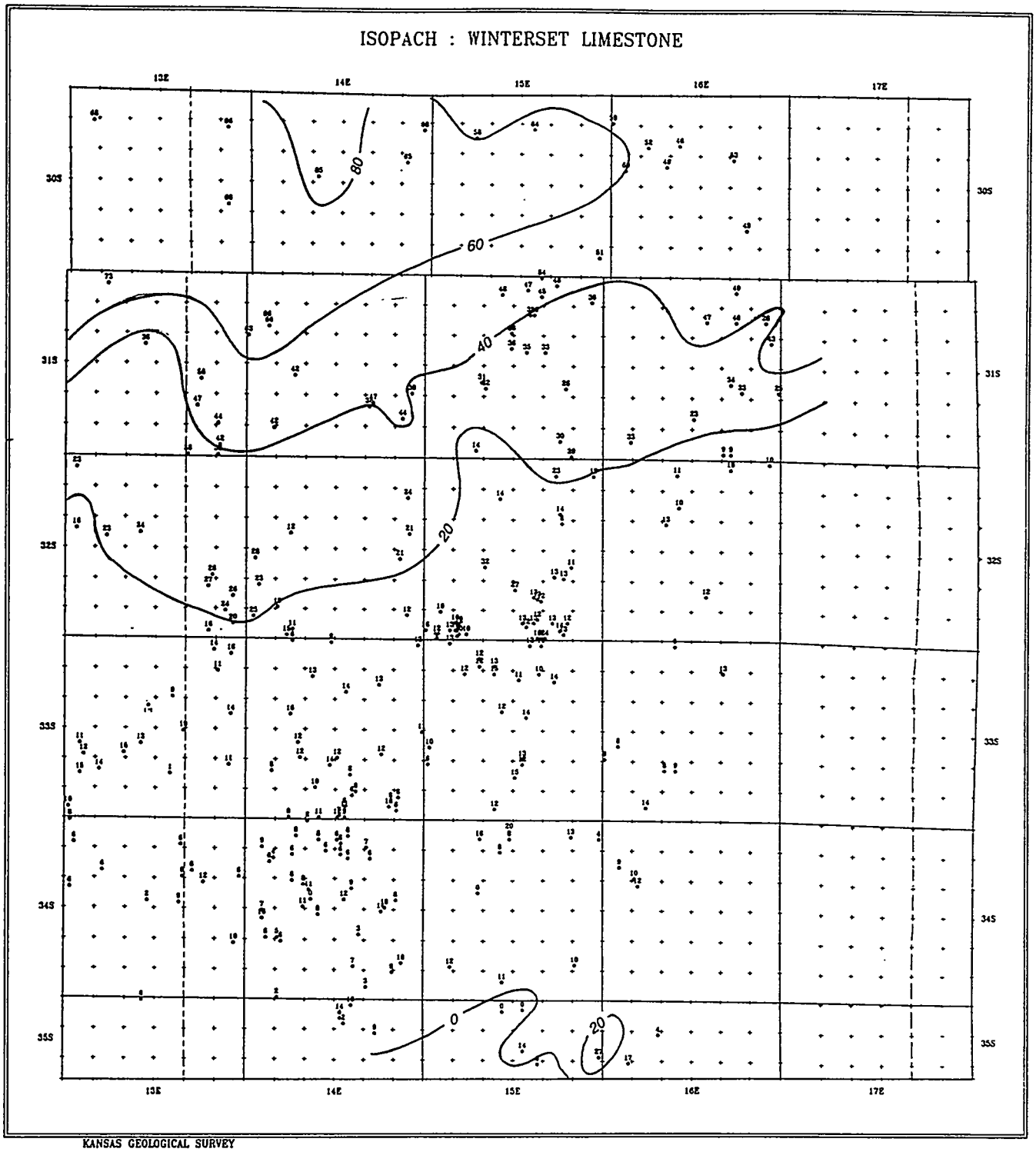

Figure 2.A.2.5. Isopach map of the Winterset Limestone in the study area. Dots indicate control points. Contour Interval is 20 ft.

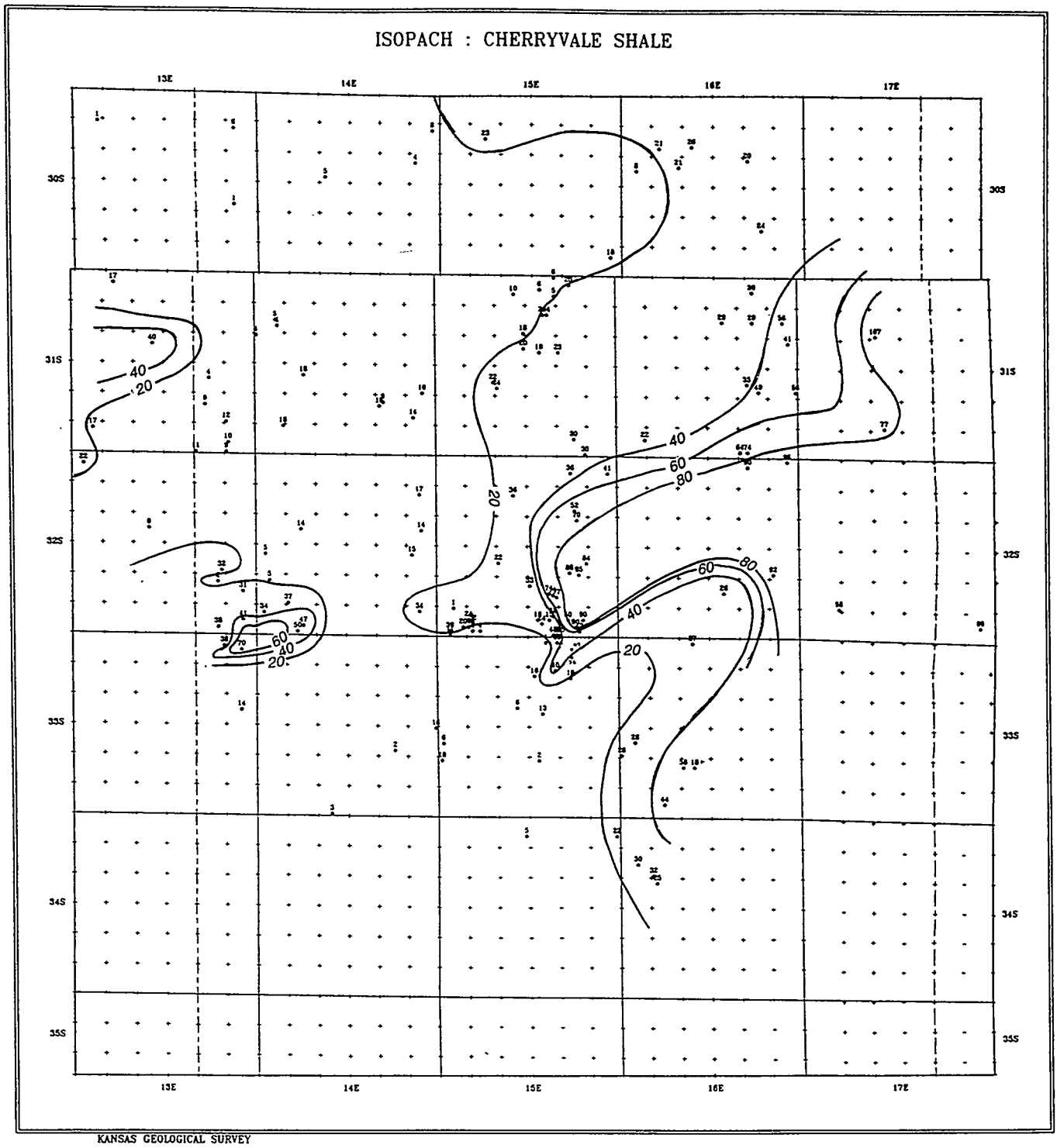

Figure 2.A.2.6. Isopach map of the Cherryvale Shale in the study area including the interbedded limestone and shale facies. The thick lobe in the southeast portion of the map is largely due to thick interbedded limestone and shale facies. Dots indicate control points. Contour Interval is 20 ft.

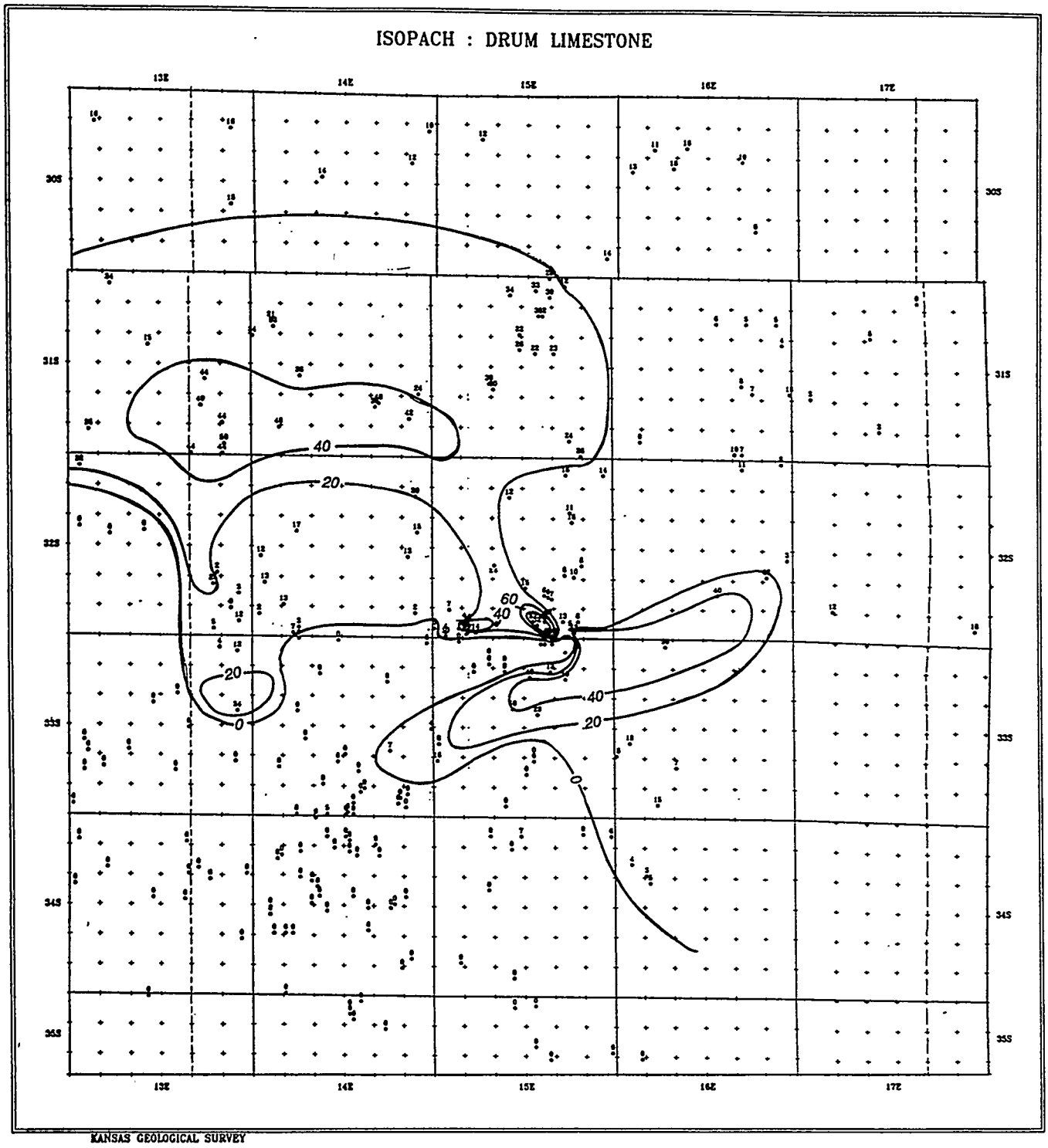

Figure 2.A.2.7. Isopach map of the Drum Limestone in the study area not including the interbedded limestone and shale facies. Dots indicate control points. Contour Interval is 20 ft.

A

B

Figure 2.A.2.8. A. Photograph of interbedded limestone and shale facies below the oolite in the Drum Limestone at location IND-2. Upper beds in photograph are bioturbated. Note hammer at left for scale. B. Photograph of the contact between the lowest limestone bed of the Drum Limestone (above hammer) and the underlying Cherryvale Shale at location LIB-5. The contact may be erosional at this location.

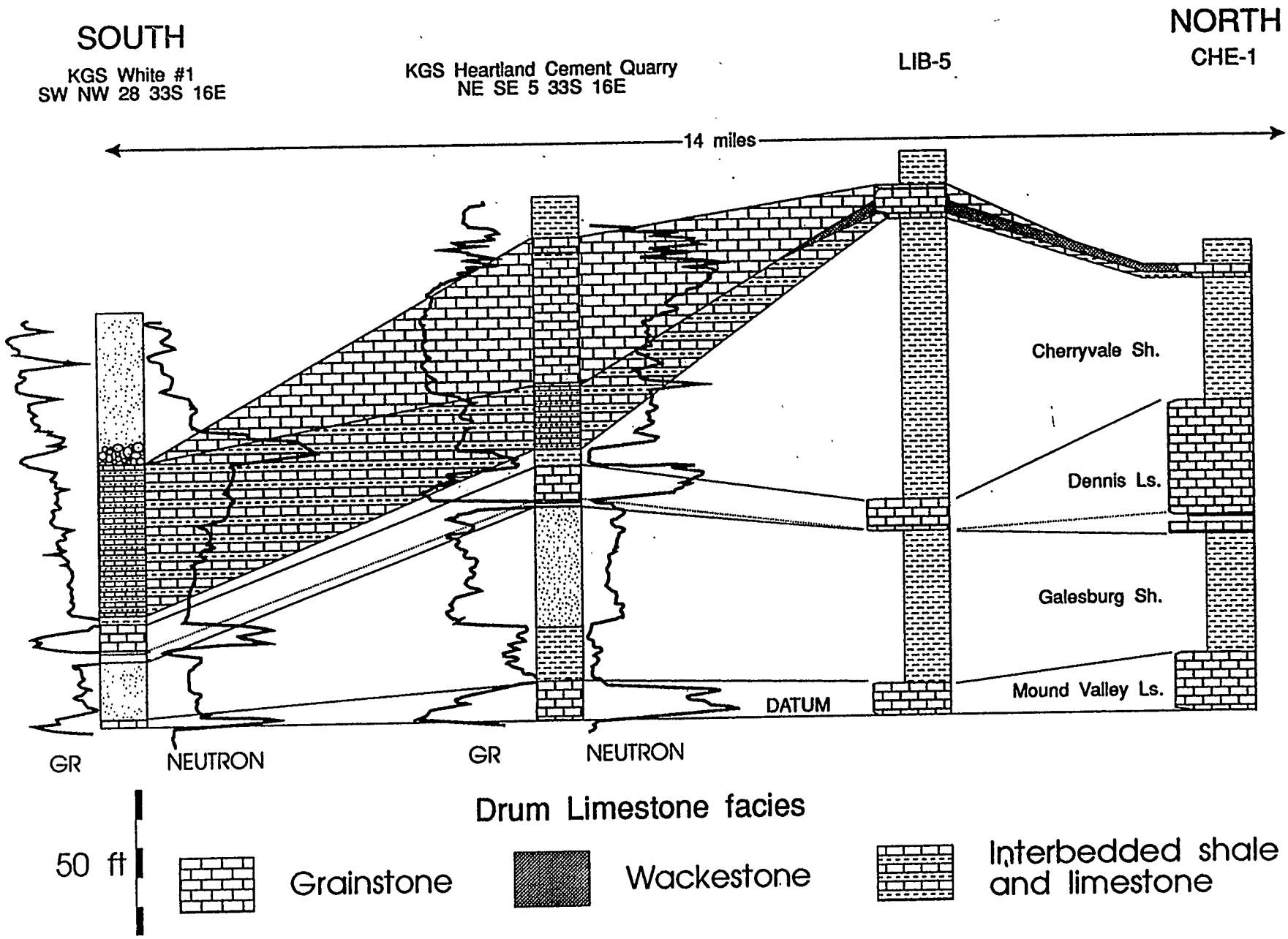

Figure 2.A.2.9. Cross section of the Drum Limestone along the outcrop belt. The KGS White #1 core is adjacent to outcrop location IND-2. See Appendix C for outcrop locations.

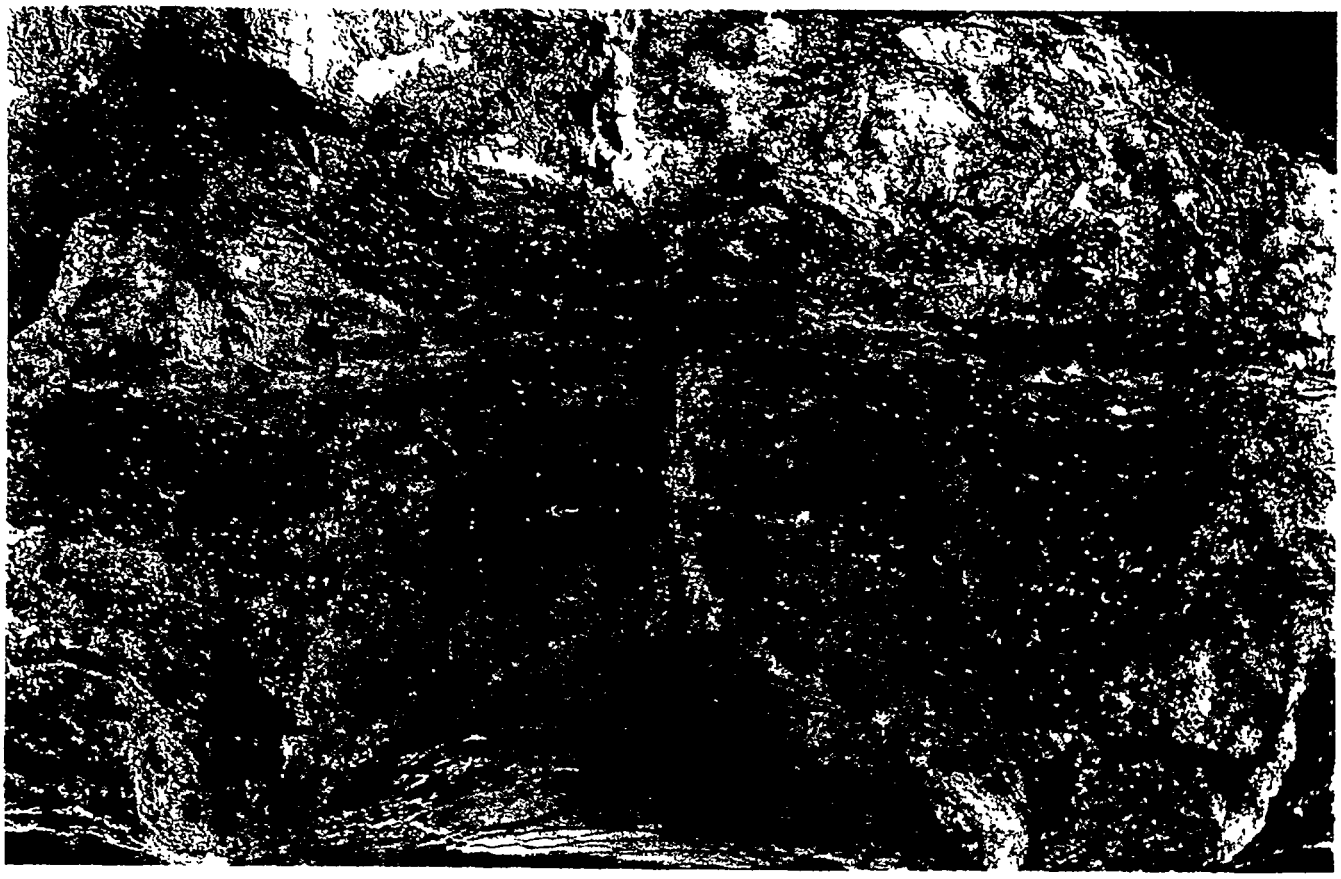

Figure 2.A.2.10. Photograph of cross sections through stromatolites from location CHE-1. Thickness of interval in photograph is 2 ft. Stromatolites photographed on overturned block, but are presented in presumed original orientation.

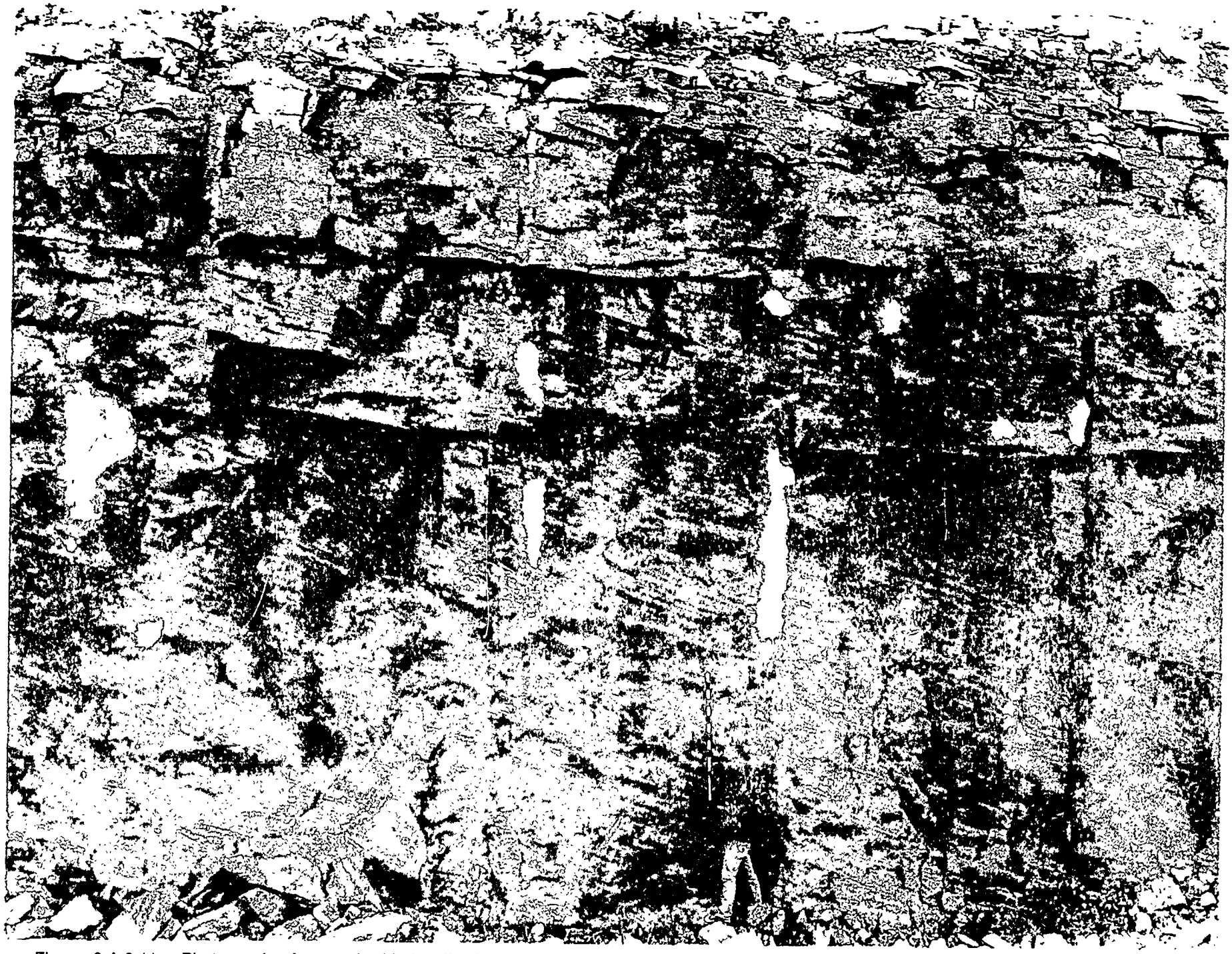

Figure 2.A.2.11. Photograph of cross bedded oolite in the Drum Limestone in the Heartland Cement Quarry. Quarry high wall is oriented west-north-west (see Fig. 2.A.2.12). Staff is 2 meters long.

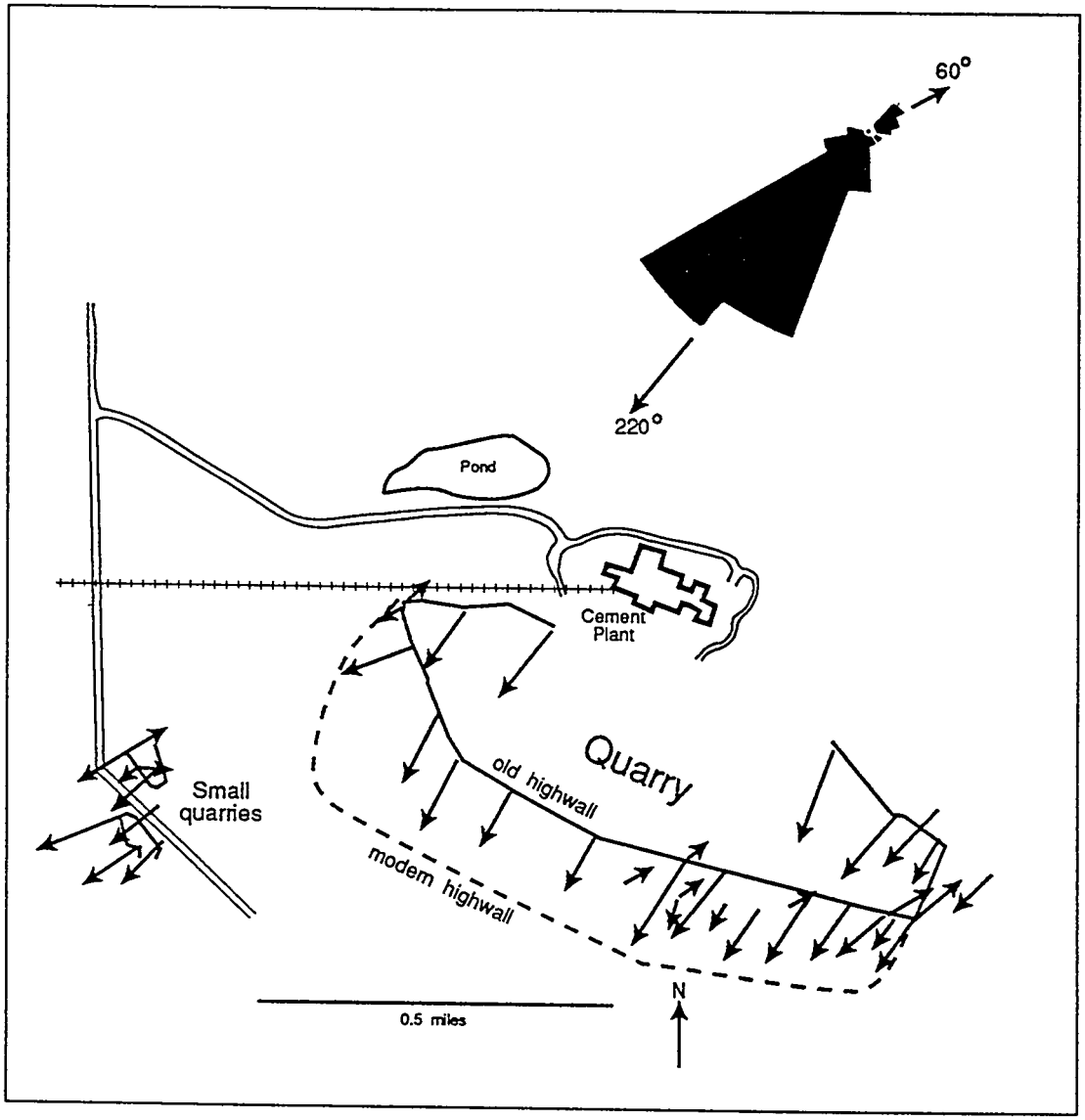

Figure 2.A.2.12. Map of the Heartland Cement Quarry showing cross bed directions from Hämblin (1969). Arrows indicate individual cross bed measurements.

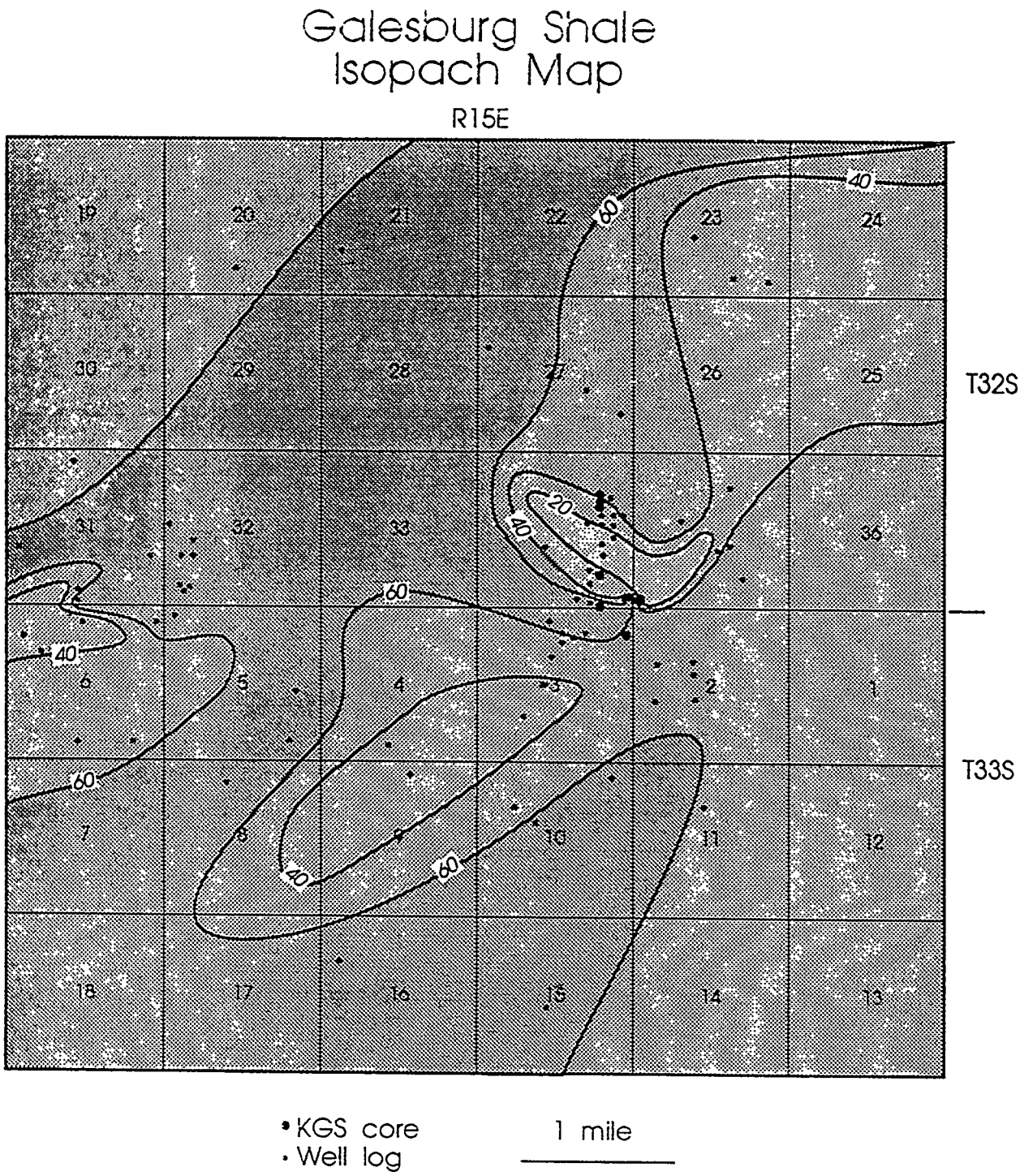

Figure 2.A.2.13. Isopach map of the Galesbug Shale in a portion of the study area in central Montgomery County. Thicknesses are in feet.

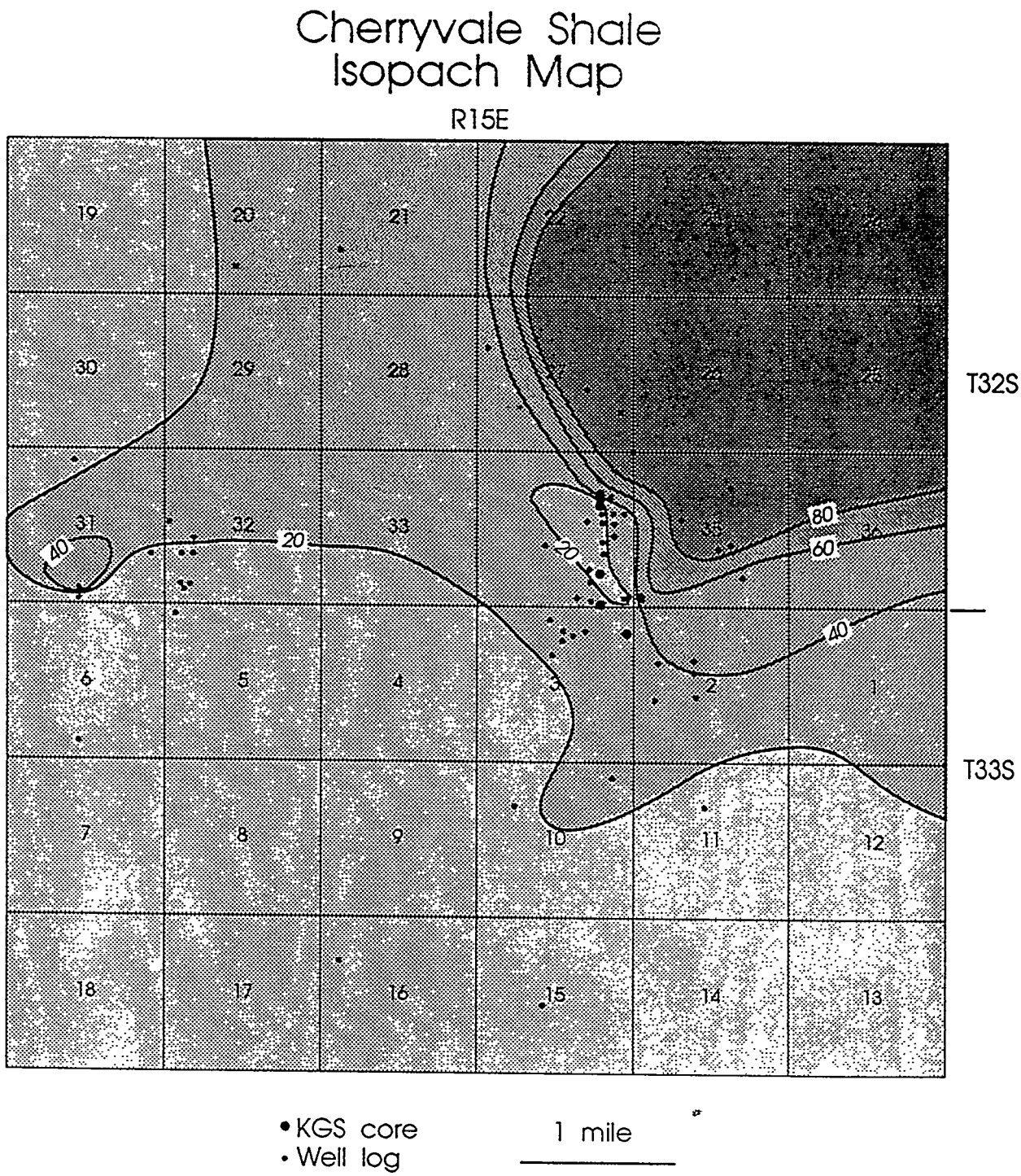

Figure 2.A.2.14. Isopach map of the Cherryvale Shale in a portion of the study area in central Montgomery County. Thicknesses are in feet.

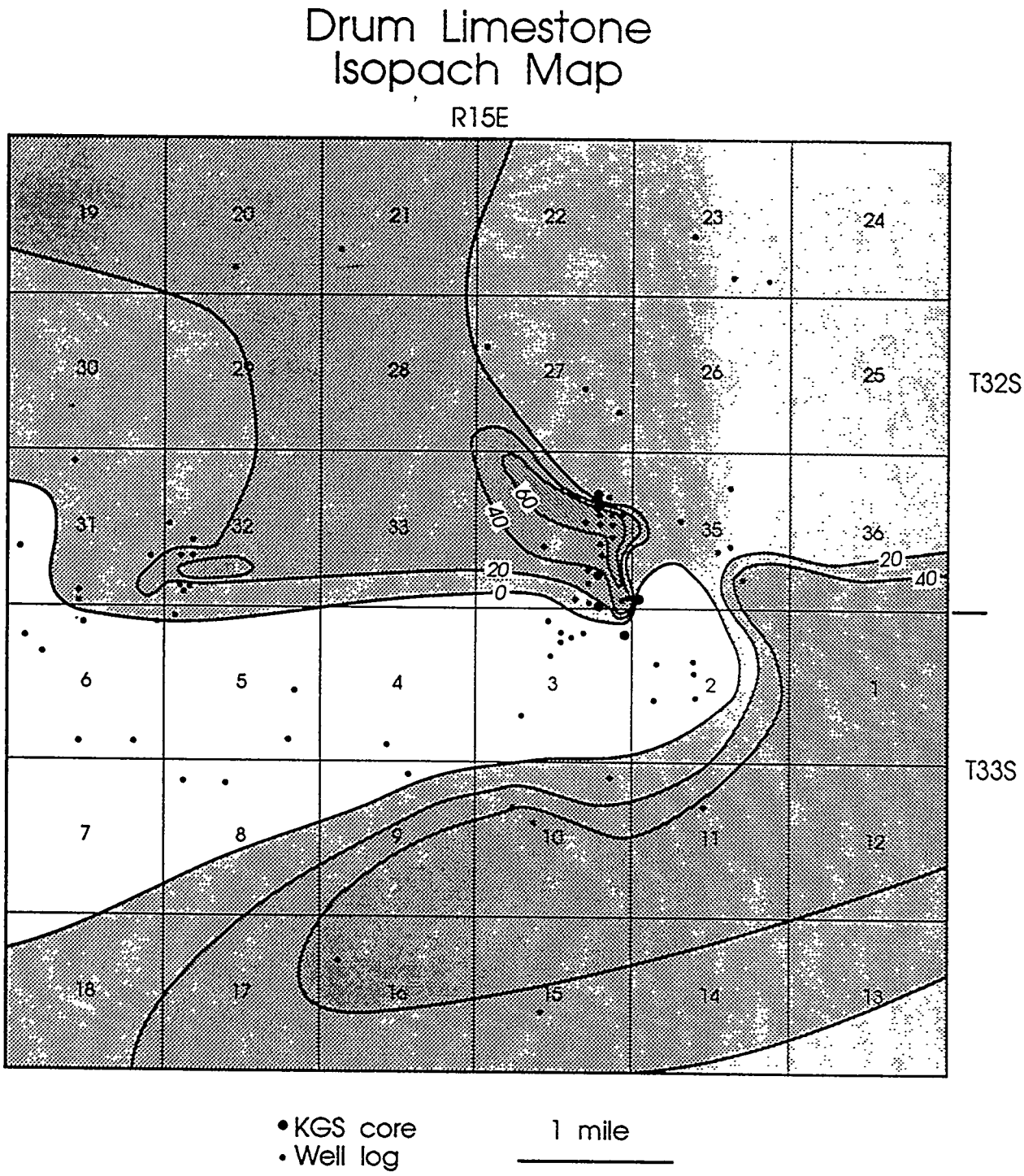

Figure 2.A.2.15. Isopach map of the Drum Limestone in a portion of the study area in central Montgomery County. Thicknesses are in feet.

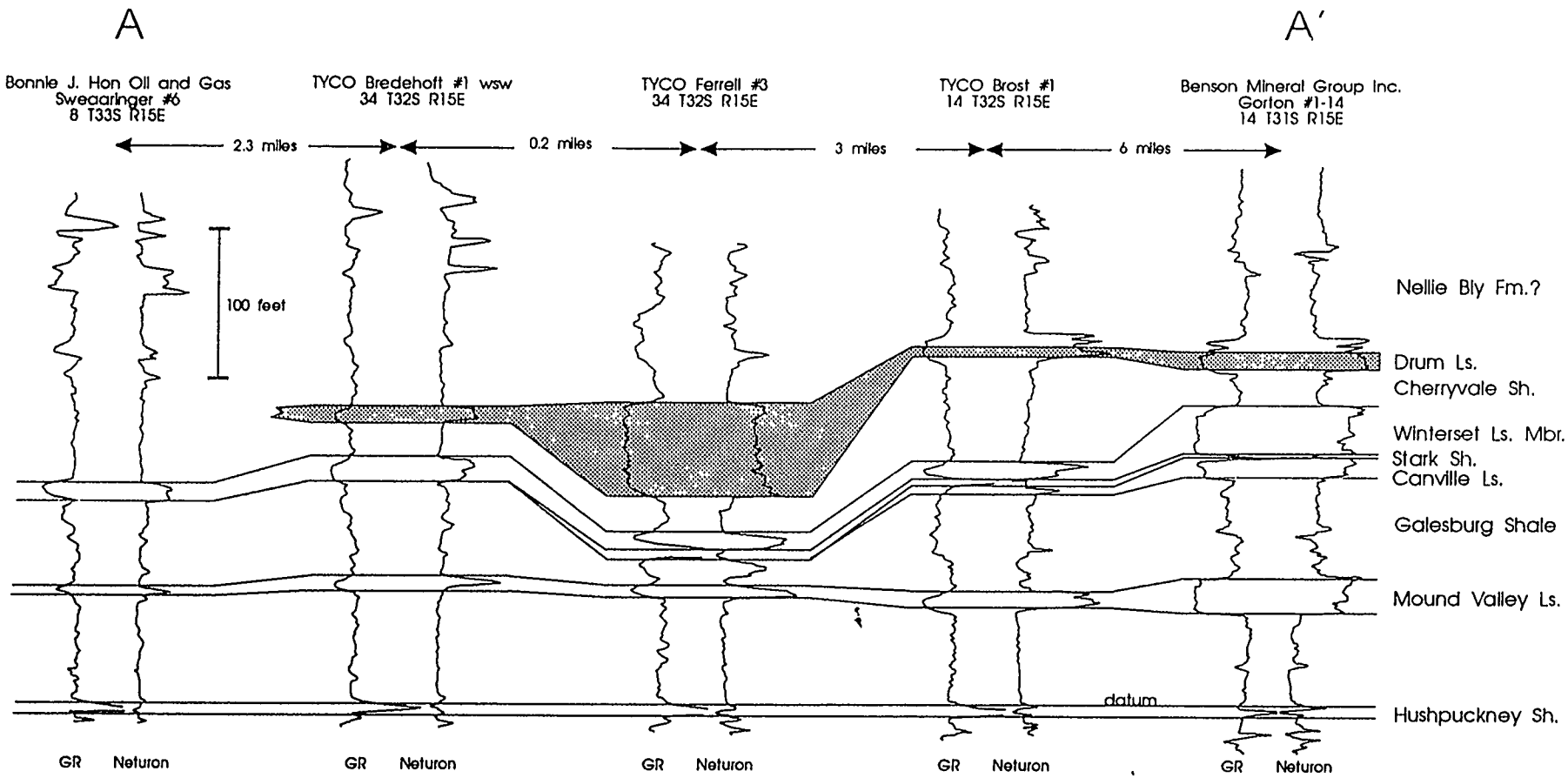

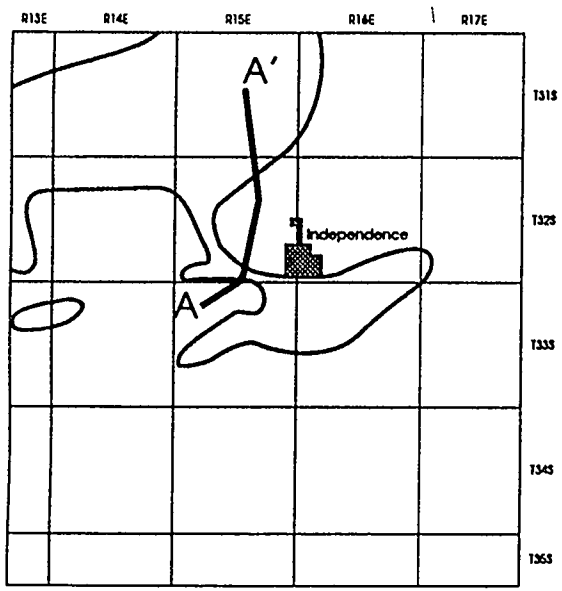

Figure 2.A.2.16. Cross section showing relationship between the Drum Limestone and related units. Note that the thickest Winterset Limestone, Cherryvale Shale, and Drum Limestone are in successively more southerly positions. Reference map of Montgomery County shows the 20 ft isopach line for the Drum Limestone.

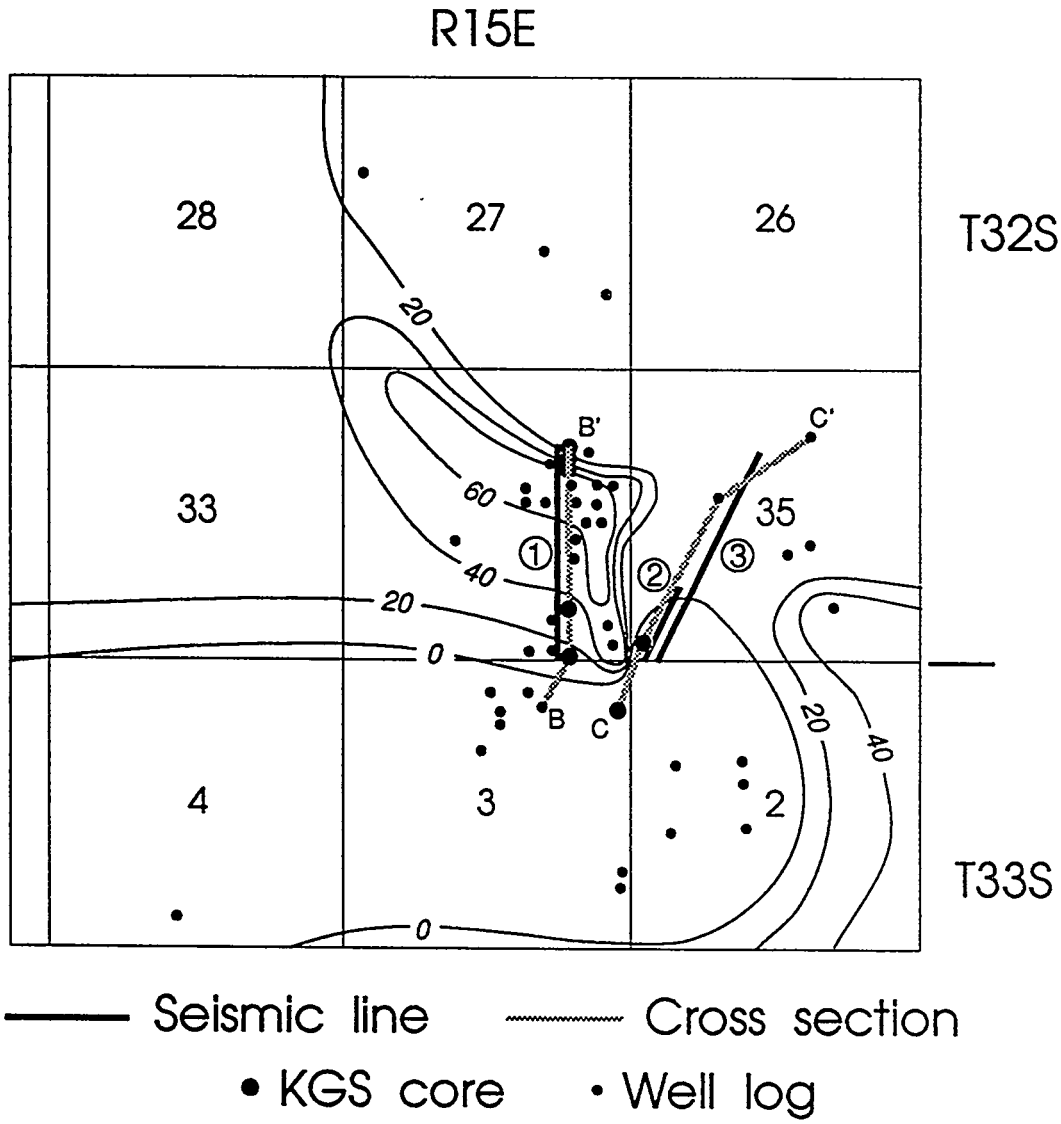

Figure 2.A.2.17. Map of seismic lines and adjacent coring transects. Circled numbers identify seismic lines referred to in text. Map is 3.2 miles wide.

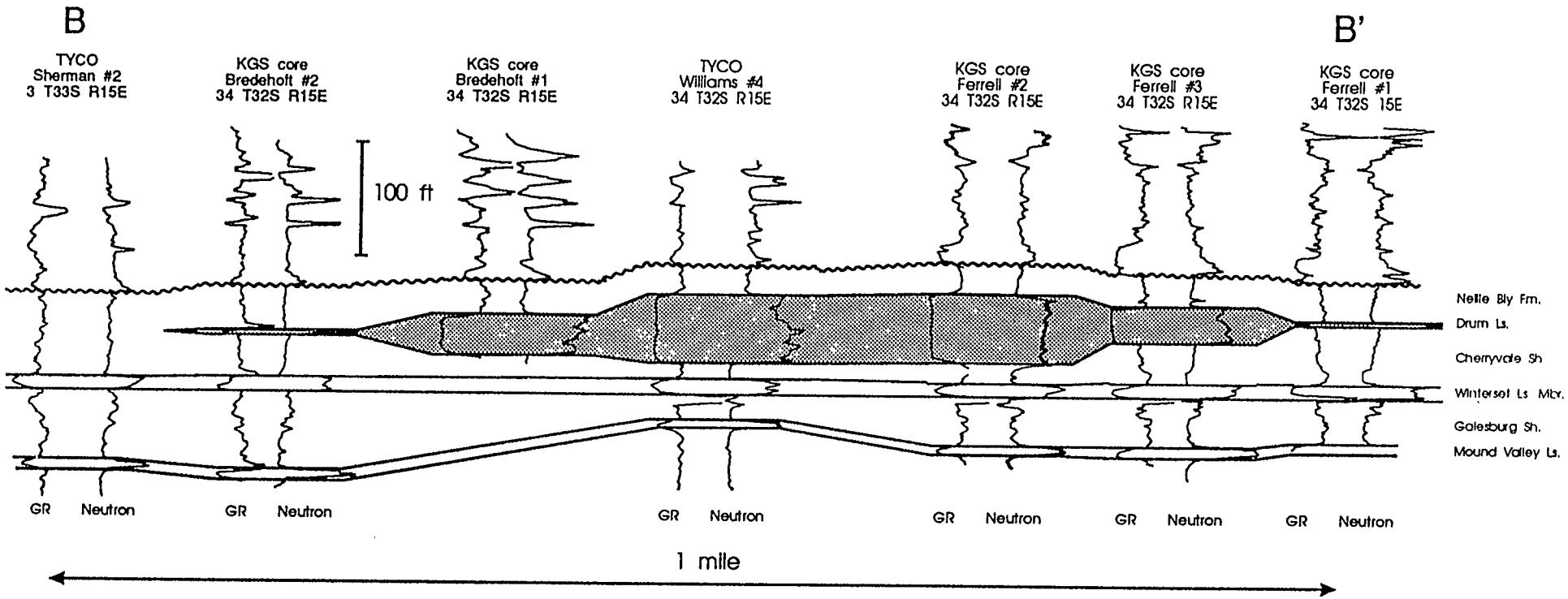

Figure 2.A.2.18. Cross section adjacent to seismic line 1. Refer to Fig. 2.A.2.17 for location of section.

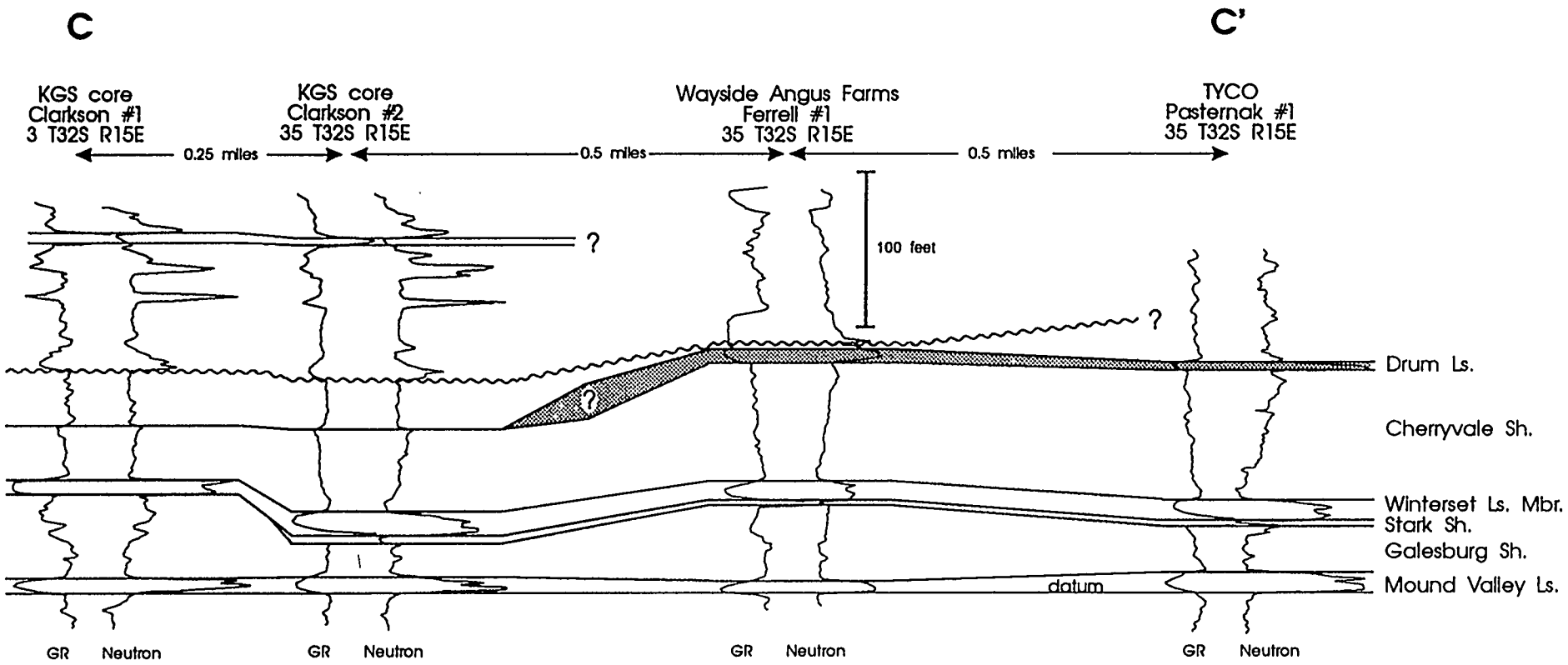

Figure 2.A.2.19. Cross section adjacent to seismic lines 2 and 3. The Drum Limestone oolite is aparently not developed in this location. Refer to Fig. 2.A.2.17 for location of section.

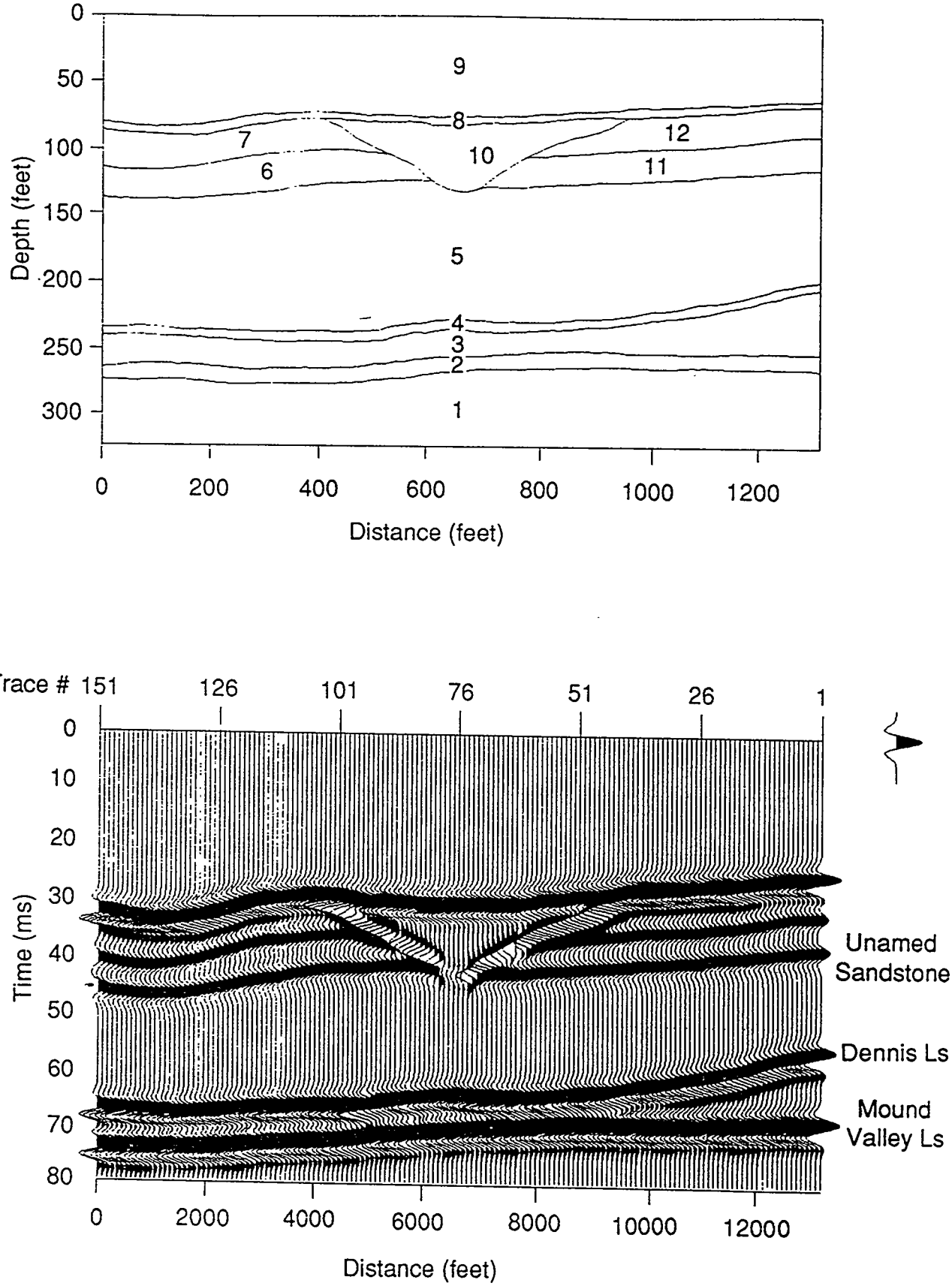

Figure 2.A.2.20. Geologic model (A) and synthetic seismogram (B) for line 2. Units of the geologic model are: 1, Ladore Shale; 2, Mound Valley Limestone; 3, Galesburg Shale; 4, Dennis Limestone; 5, Cherryvale Shale and Nellie Bly Formation; 6 and 11, unnamed sandstone; 7 and 12 shale, 8, shale; 10 shale-filled channel. Top of 8 is ground surface.

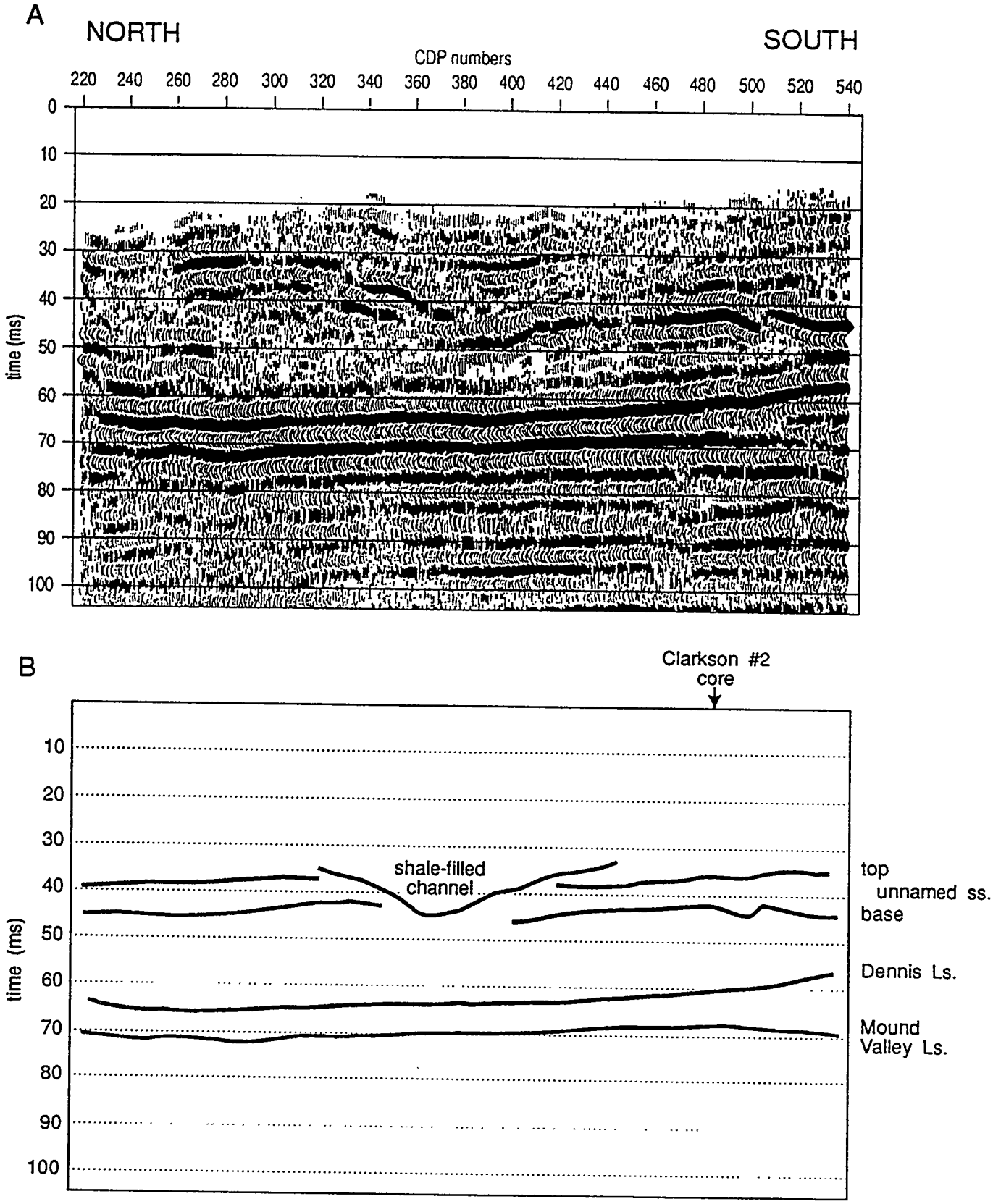

Figure 2.A.2.22. High resolution seismic line 2 (A) and interpretation (B). Length of seismic line is approximately 0.25 miles (0.4 km).

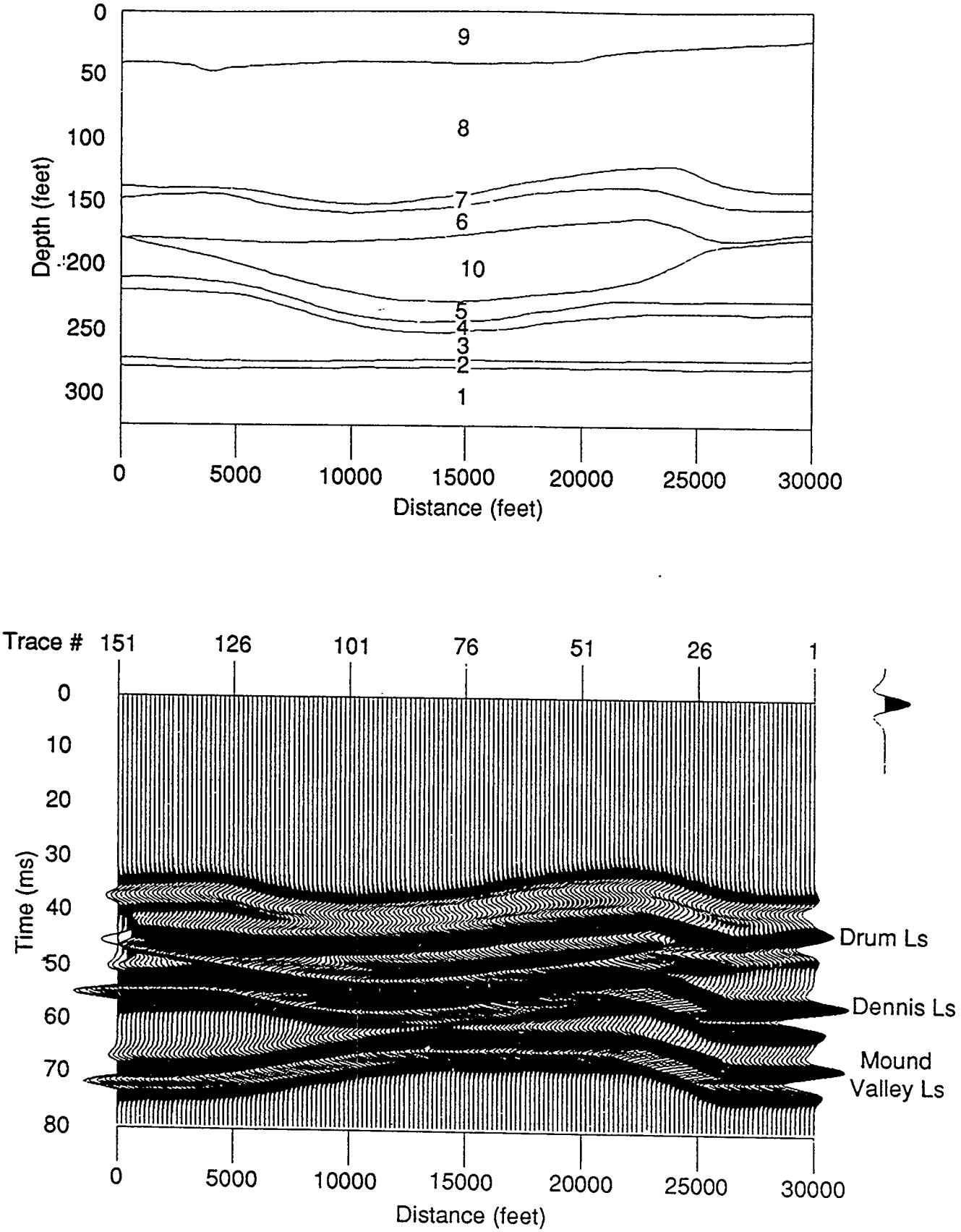

Figure 2.A.2.21. Geologic model (A) and synthetic seismogram (B) for line 1. Units of the geologic model are: 1, Ladore Shale; 2, Mound Valley Limestone; 3, Galesburg Shale; 4, Dennis Limestone; 5, Cherryvale Shale; 6, shale in Nellie Bly Formation; 7, unnamed sandstone; 8, shale; 10, Drum Limestone. Top of unit 8 is ground surface

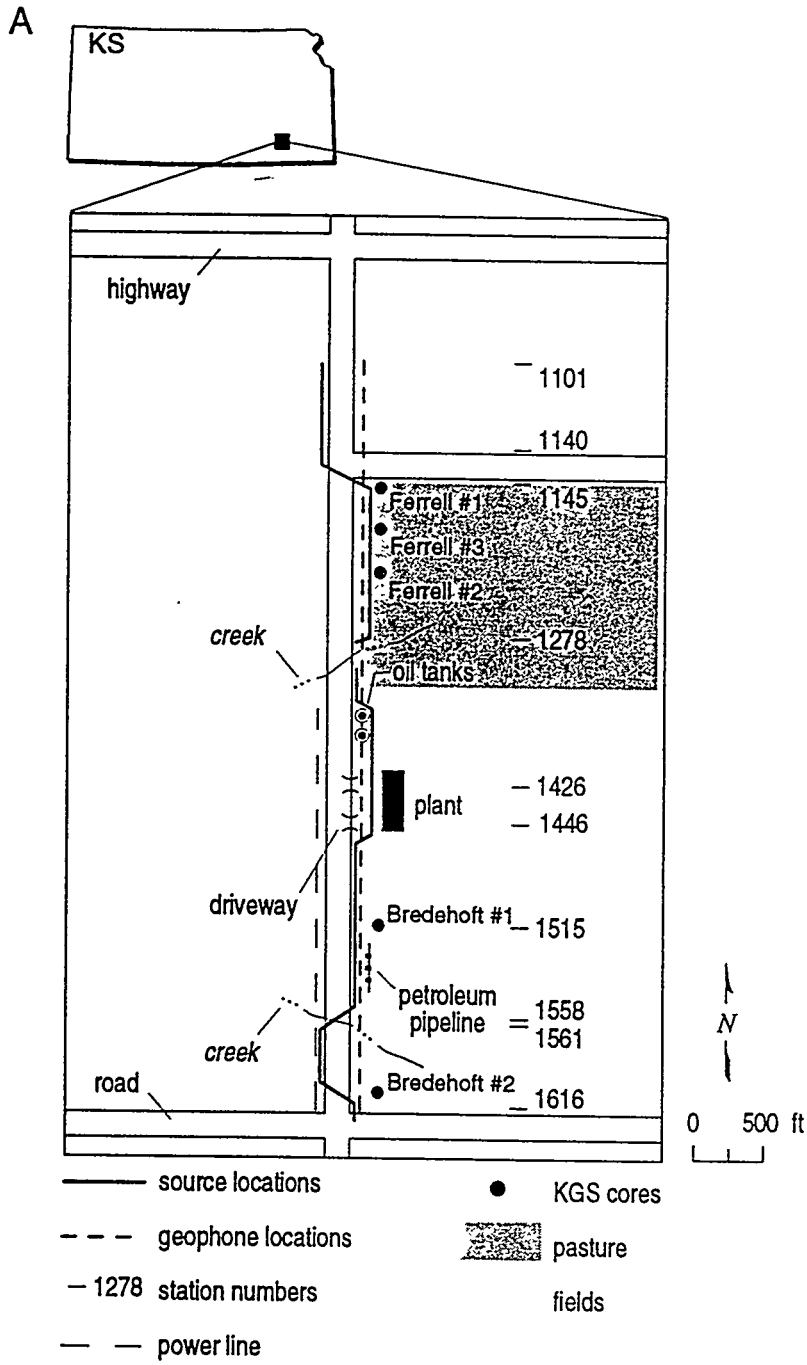

Figure 2.A.2.23. Seismogram of line 1. A. Location of seismic line showing location of KGS cores obtained along the transect. See also Figs. 2.A.2.17 and 2.A.2.18. B. Processed seismic line 1. C. Interpreted seismic line 1. B and C on next page.

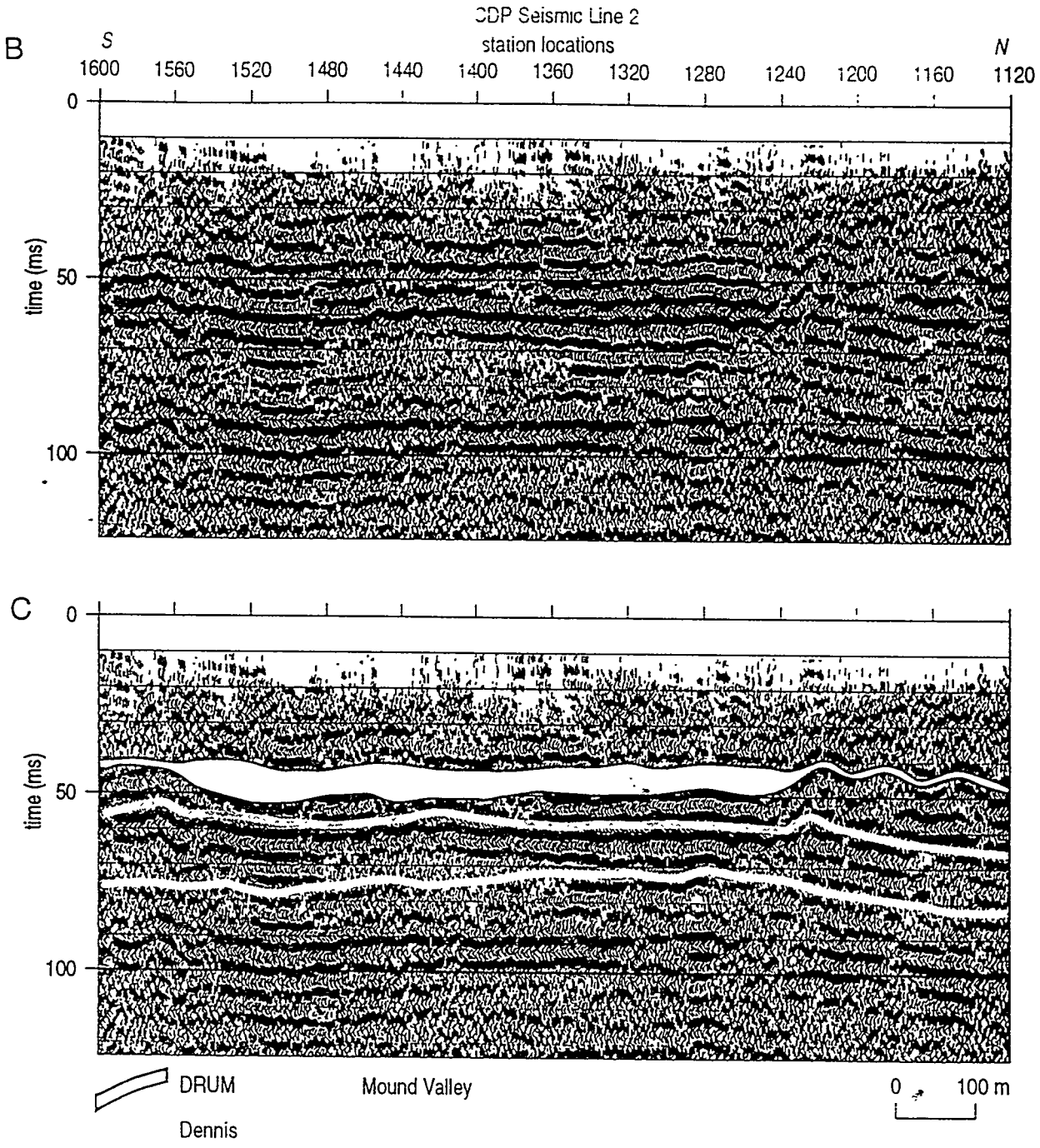

Figure 2.A.2.23. Continued.

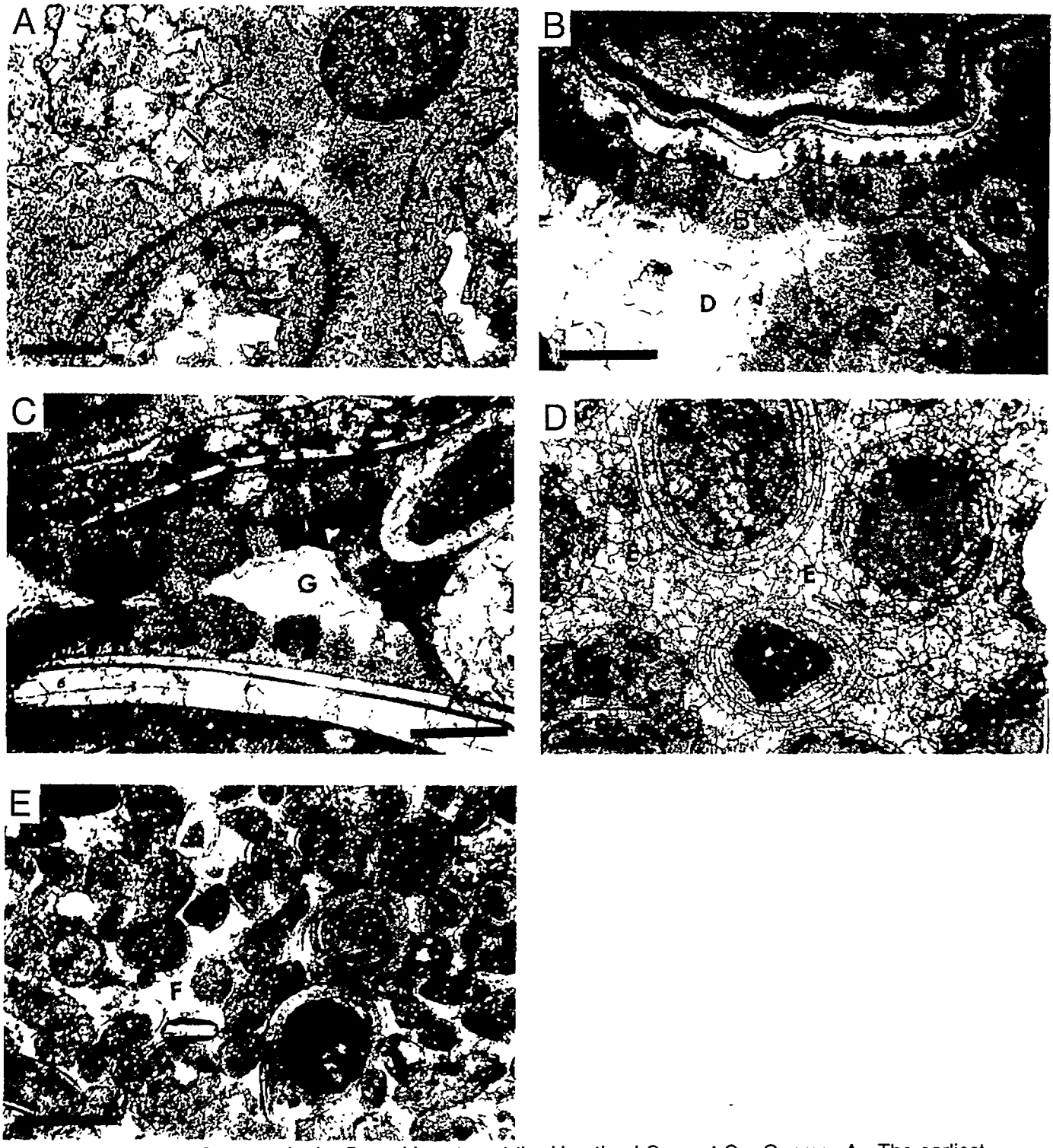

Figure 2.A.2.24. Cements in the Drum Limeston at the Heartland Cement Co. Quarry. A. The earliest cement is isopachous bladed calcite. Scale is 200 µm. B and C show isopachous, originally fibrous cement. Scales are 1 mm. D. Medium crystallin clear, equant calcite is the most common cement in the Drum Limestone oolite. Scale is 200 µm. E. Compacted grainstone from the uppermost Drum Limestone. All the cement is ferroan calcite. Scale is 1 mm. Cement key: A, isopachous bladed calcite; B, Isopachous cloudy, bladed to equant calcite; D, coarse crystalline, clear, equant calcite; E, medium crystalline, clear, equant calcite; F, coarse, equant, clear, ferroan calcite; G, baroque, ferroan dolomite. P, porosity.

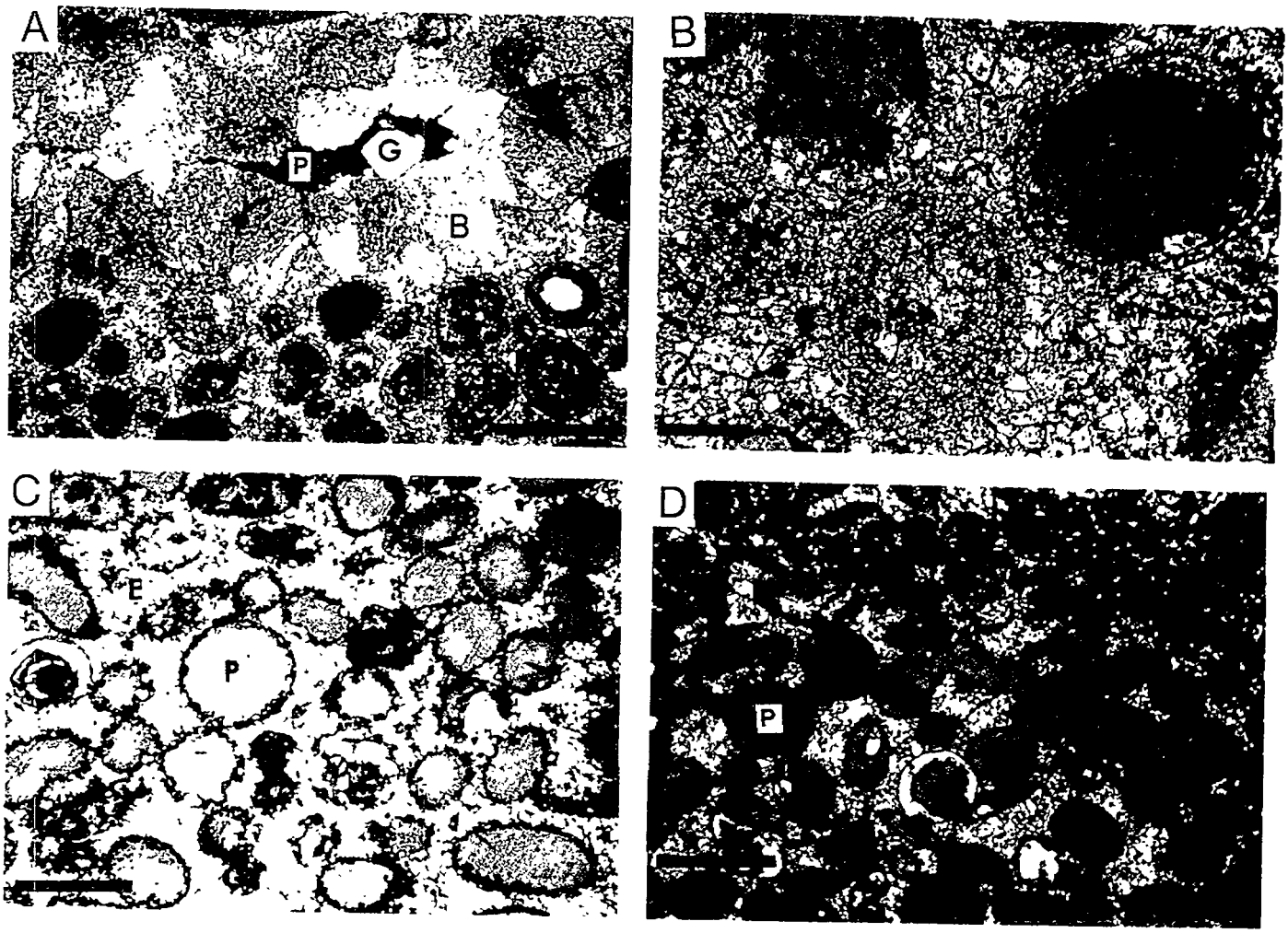

Figure 2.A.2.25. Porosity in the Drum Limestone at the Heartland Cement Co. Quarry. A. Primary porosity. Scale is 1 mm. B - D, secondary oomoldic porosity. B, isolated oomolds and highly altered ooids (center and middle left). Scale is 200 μm. C. Sample in which most ooids are dissolved, but few molds are connected. Scale is 1 mm. D. Partial crushing of oomolds dramatically increased permeability in lower portion of photomicrograph, and nearly complete crushing has reduced permeability in upper portion of photomicrograph. Scale is 1 mm. See Fig. 2.A.2.24 for key to cement types.

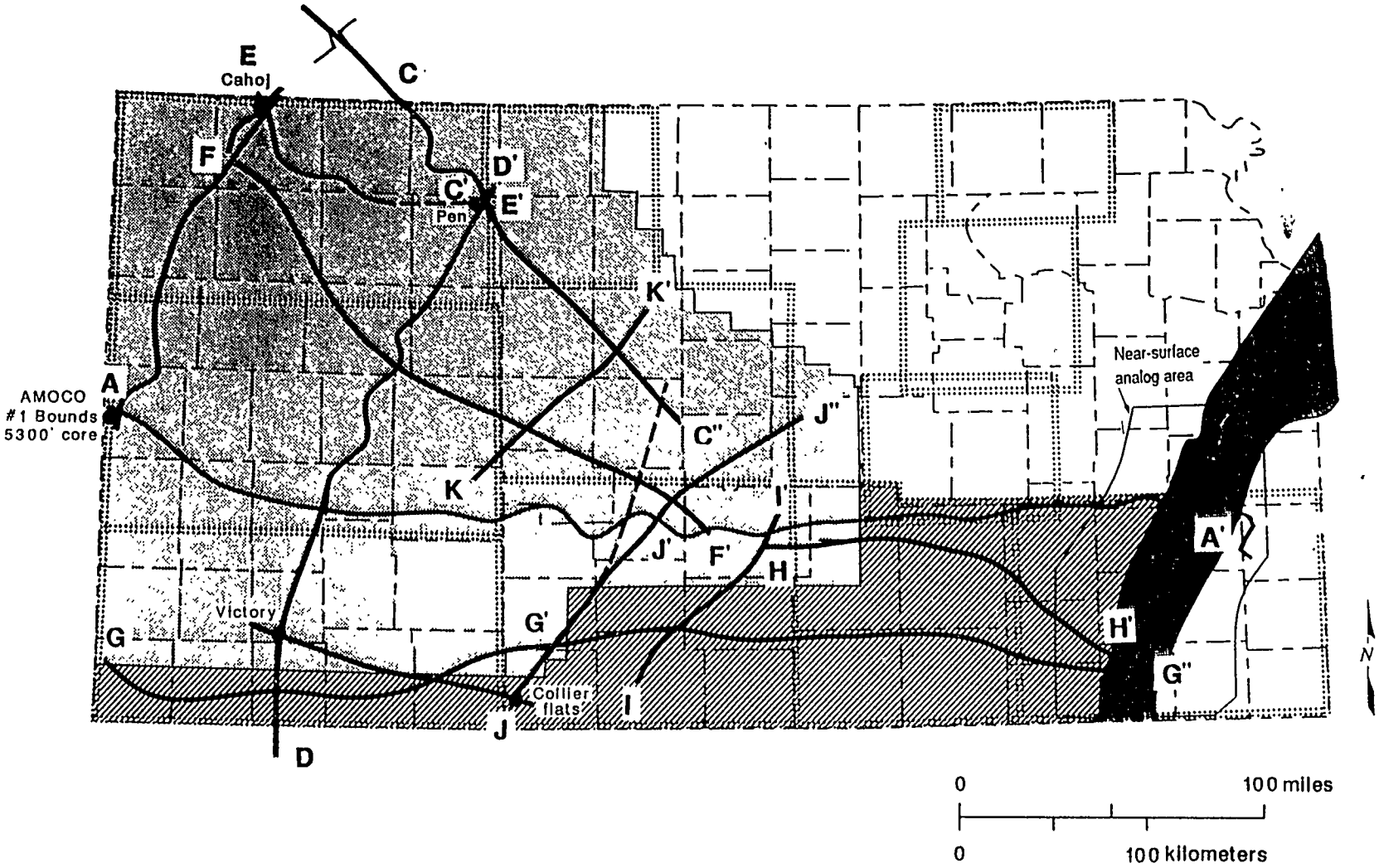

Figure 2.B.1.1. Base map for project showing location of cross sections. Those discussed here are A-H, D-D', G-G', and G'-G".

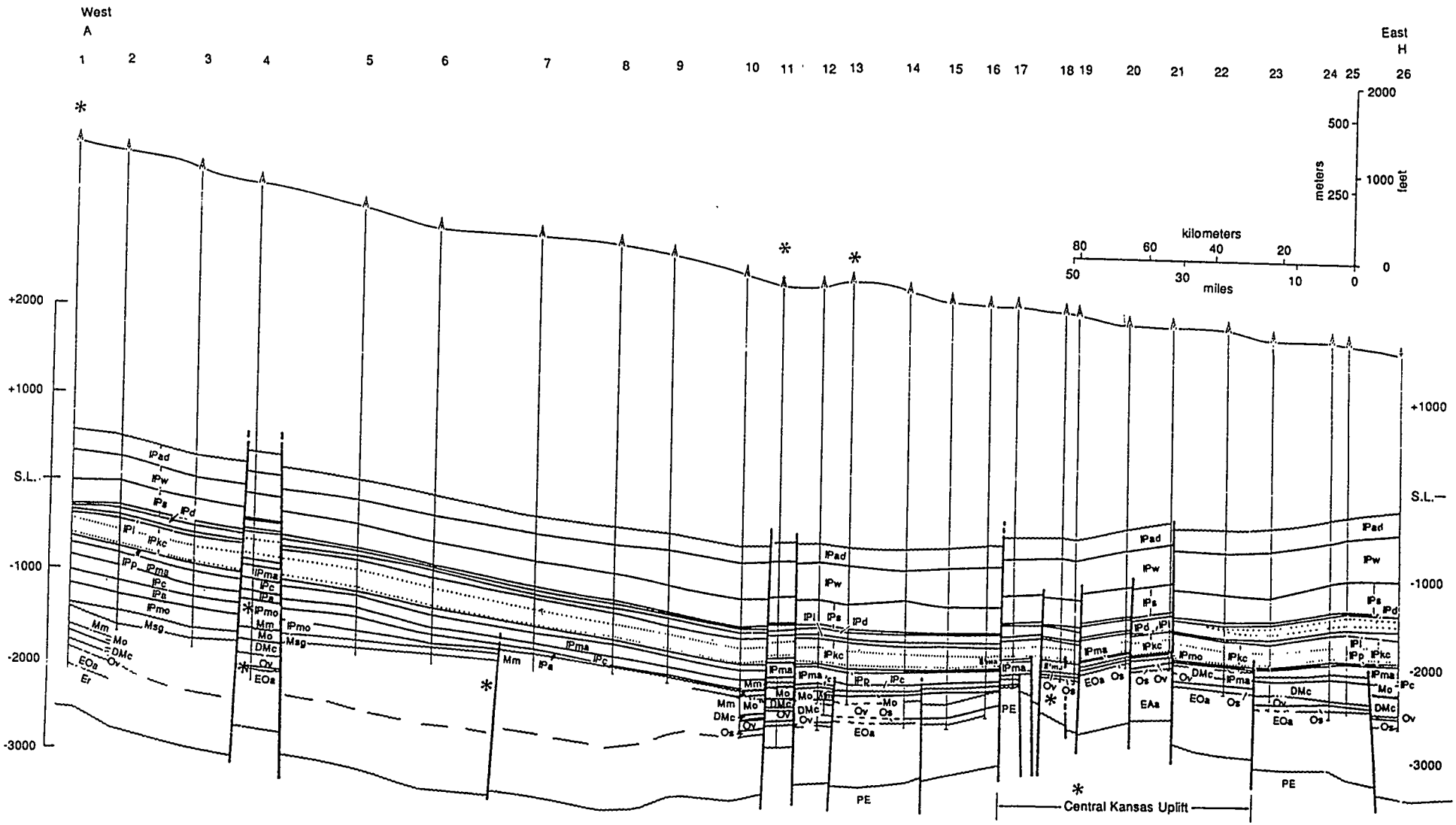

Figure 2.B.1.2. West-to-east regional structural cross section A-H prepared from wireline logs. Section extends across southwest Kansas unto the Central Kansas uplift. Index map is Figure 2.B.1.1. Key to symbols is Figure 2.B.1.6.

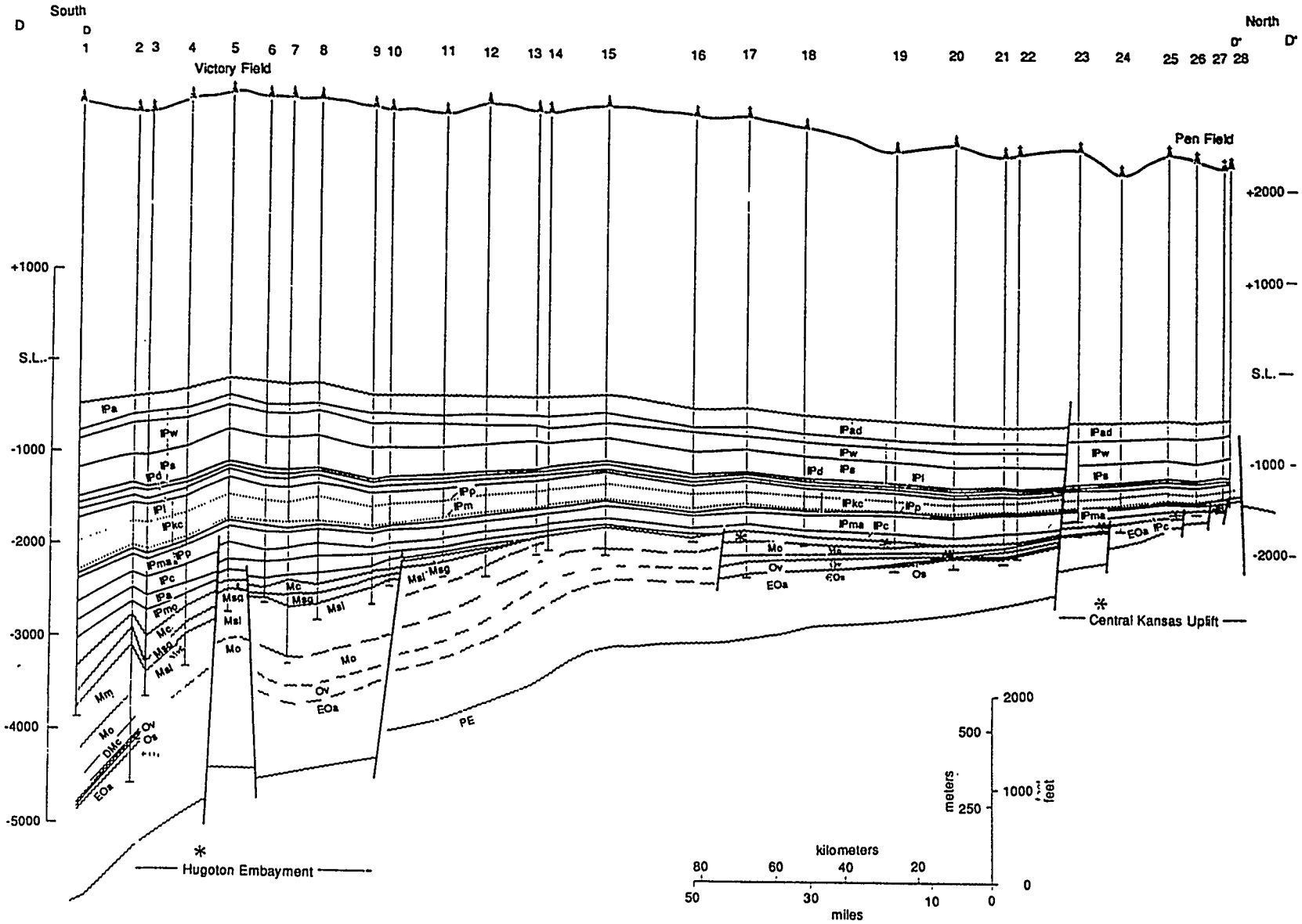

Figure 2.B.1.3. South-to-north regional structural cross section D-D' prepared from wireline logs. Section extends from the northern margin of the Anadarko basin (lower shelf) unto the Central Kansas uplift (upper shelf). Index map is Figure 2.B.1.1. Key to symbols is Figure 2.B.1.6.

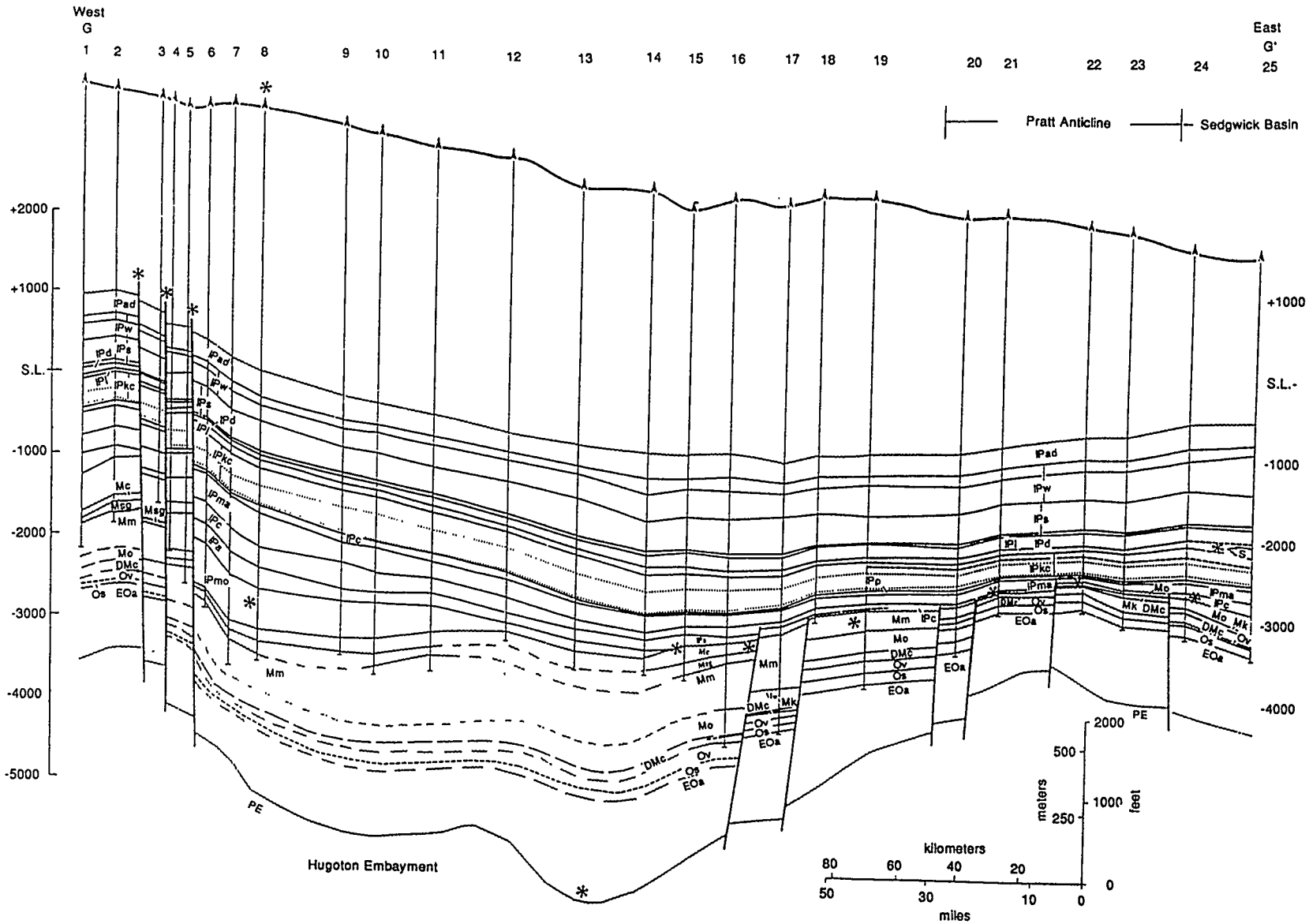

Figure 2.B.1.4. West-to-east structural cross section G-G' prepared from wireline logs. Section extends along the Oklahoma border of southwestern Kansas in the Hugoton embayment eastward to the Pratt anticline. Index map is Figure 2.B.1.1. Key to symbols is Figure 2.B.1.6.

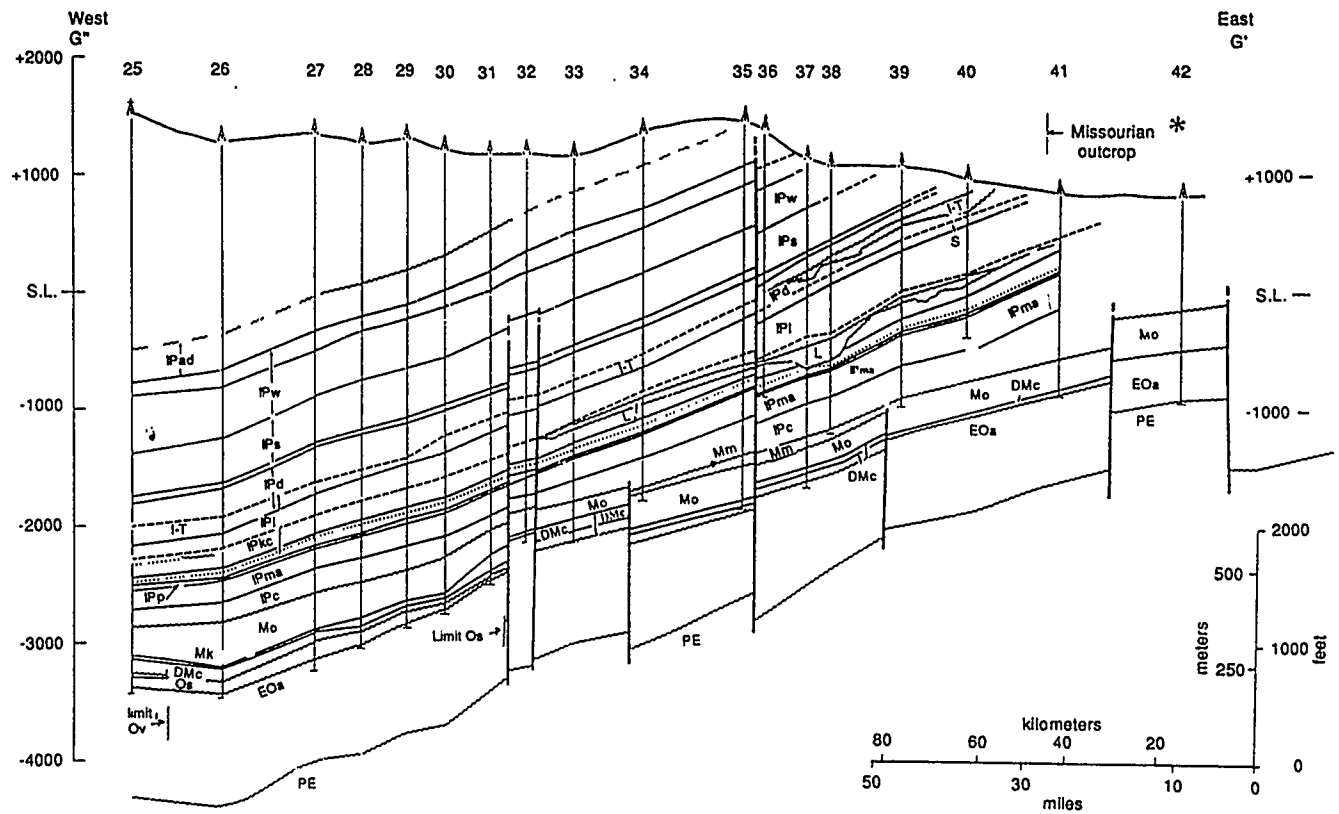

Figure 2.B.1.5. West-to-east regional structural cross section G'-G" prepared from wireline logs. Section is an eastward continuation of the section in Figure 2.B.1.4, extending through the Sedgwick basin, across the narrow Nemaha uplift (at well #32), and to the outcrop of the Missourian strata. Index map is Figure 2.B.1.1. Key to symbols is Figure 2.B.1.6.

Key to abbreviations used in cross sections

	Pennsylvanian System	
	Virgilian Series	
ℙad		Admire Group
ℙw		Waubansee Group
ℙs		Shawnee Group
ℙd		Douglas Group
I		Ireland sandstone interval
T		Tonganoxie sandstone interval
	Missourian Series	
ℙl		Lansing Group
S		Stalnaker sandstone interval
ℙkc		Kansas City Group
L		Layton sandstone interval
ℙp		Pleasanton Group
	Desmoinesian Series	
ℙma		Marmaton Group
ℙc		Cherokee
	Atokan Series	
ℙa		Atokan Group
ℙmo	Morrowan Series	
		Kearny Formation
	Mississippian System	
Mc	Chesterian Series	
		unnamed unit
Msg		Ste. Genevieve Limestone
Mm	Meramecian Series	
Msl		St. Louis Limestone
		Salem Limestone
		Warsaw Limestone
Mo	Osagian Series	
Mk	Kinderhookian Series	
	Devonian System	
DMc	Chattanooga Series	
	Silurian System	

Figure 2.B.1.6. Key to abbreviations used in cross sections.

	Ordovician System
	Upper Ordovician Series
	Middle Ordovician Series
Ov	Viola Limestone
Os	Simpson Group
	Lower Ordovician Series
€Oa	Arbuckle Group
	Cambrian System
	Upper Cambrian Series
	Eminence Dolomite
	Bonneterre Dolomite
€r	Reagan Sandstone
P€	Precambrian Erathem
	Rice Series
	Igneous and metamorphic complex

(*) asterisk donotes location accompanied by discussion in text

Figure 2.B.1.6. Continued.

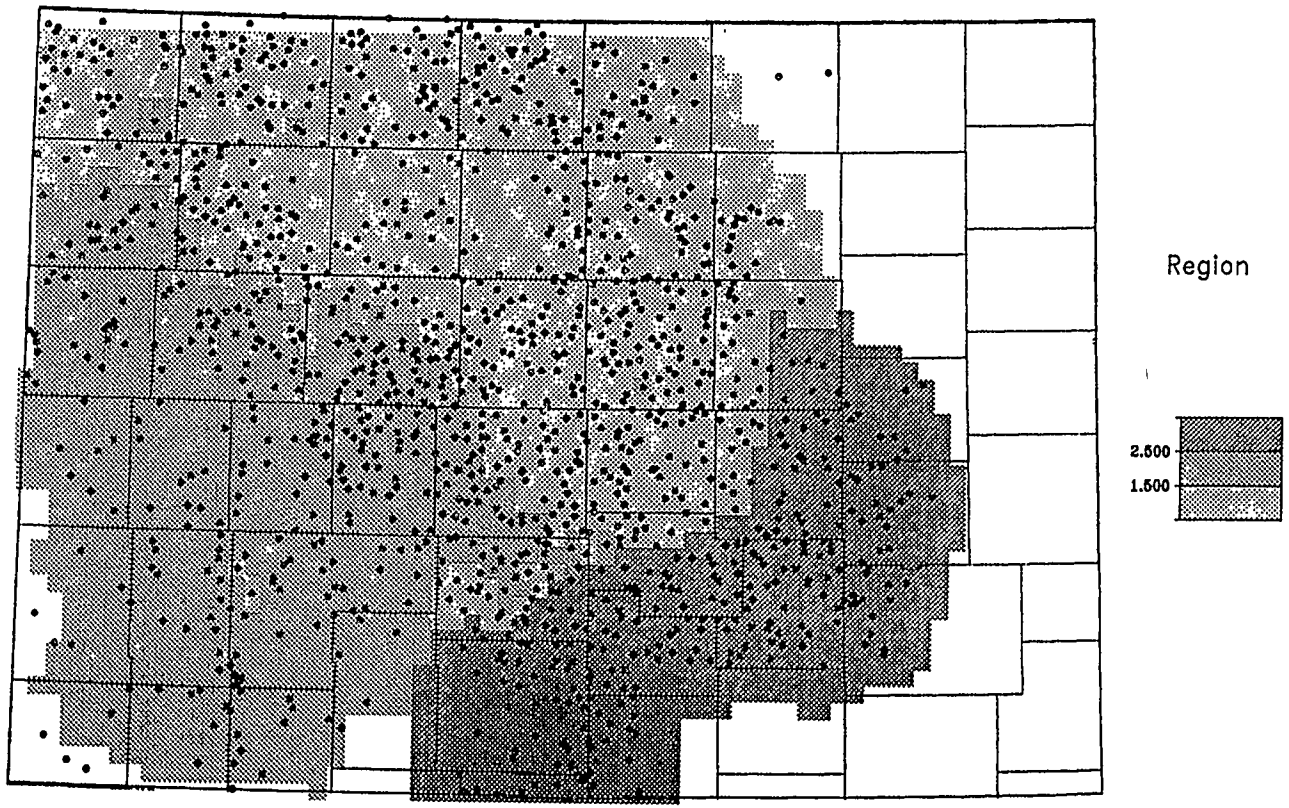

3-Category Regionalization
Thickness of 9 Pennsylvanian Stratigraphic Intervals

Regionalization of the Western Kansas Shelf

Figure 2.B.2.1. Three-class regionalization for 9 Pennsylvanian interval thicknesses listed in text.

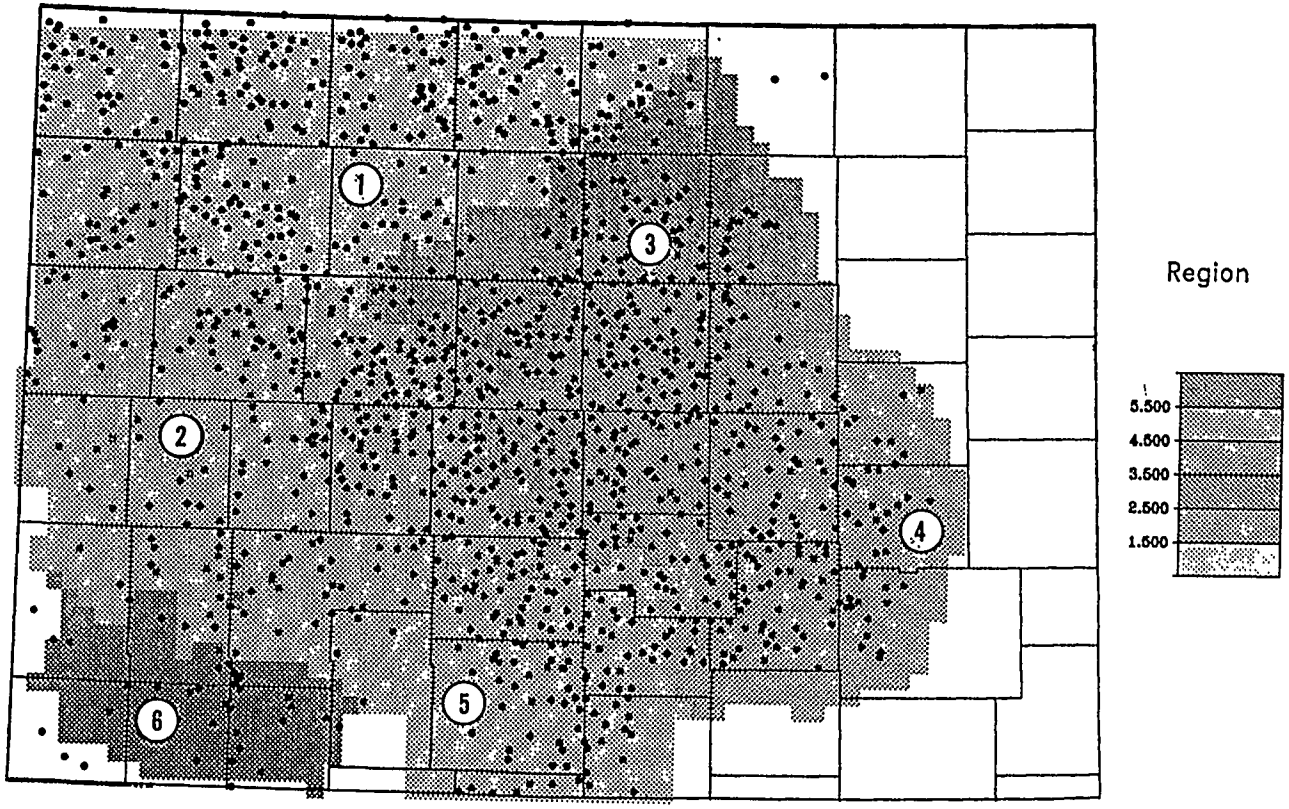

6-Category Regionalization
Thickness of 9 Pennsylvanian Stratigraphic Intervals

Regionalization of the Western Kansas Shelf

Figure 2.B.2.2. Six-class regionalization for 9 Pennsylvanian interval thicknesses.

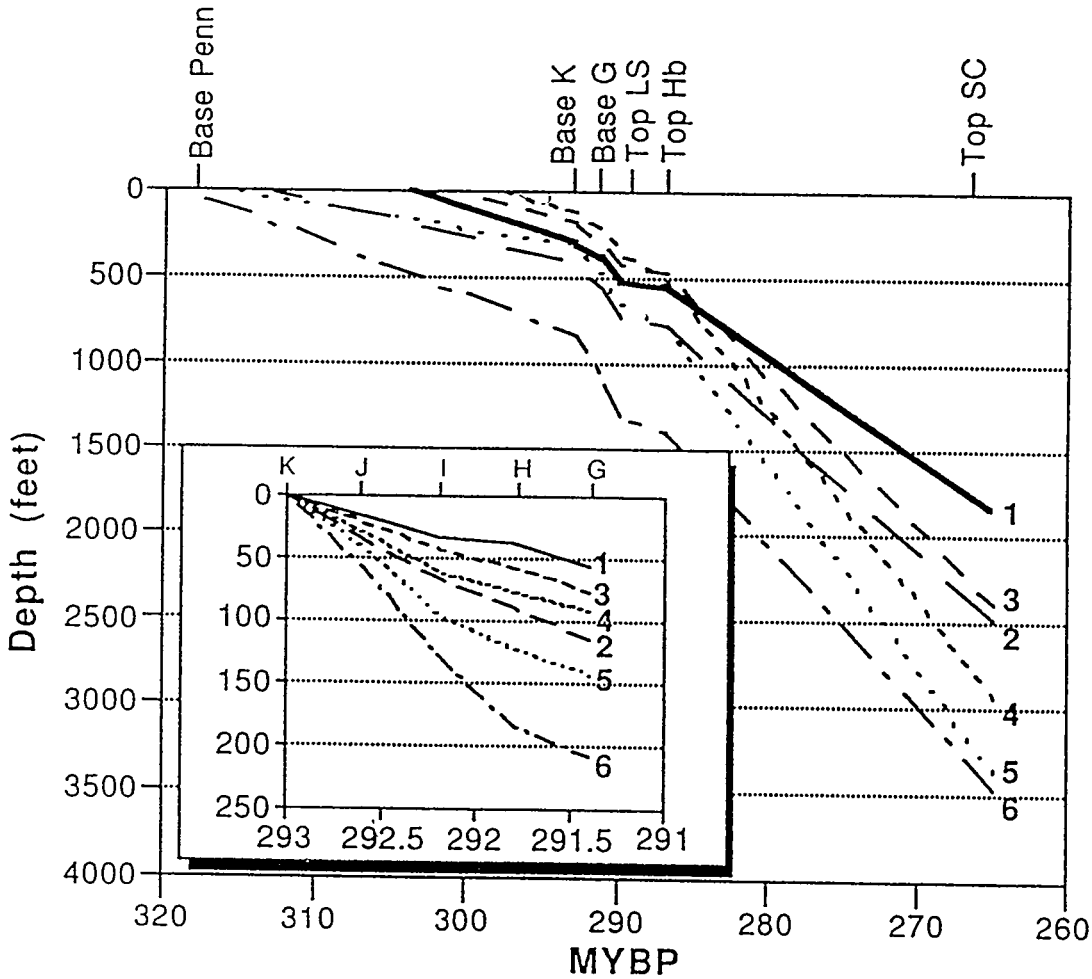

Figure 2.B.2.3. Subsidence curves for 6 areas classified in Figure 2.B.2.2 revealing similar trends, but varying rates of subsidence. Curves are numbered according to area shown in Figure 2.B.2.2.

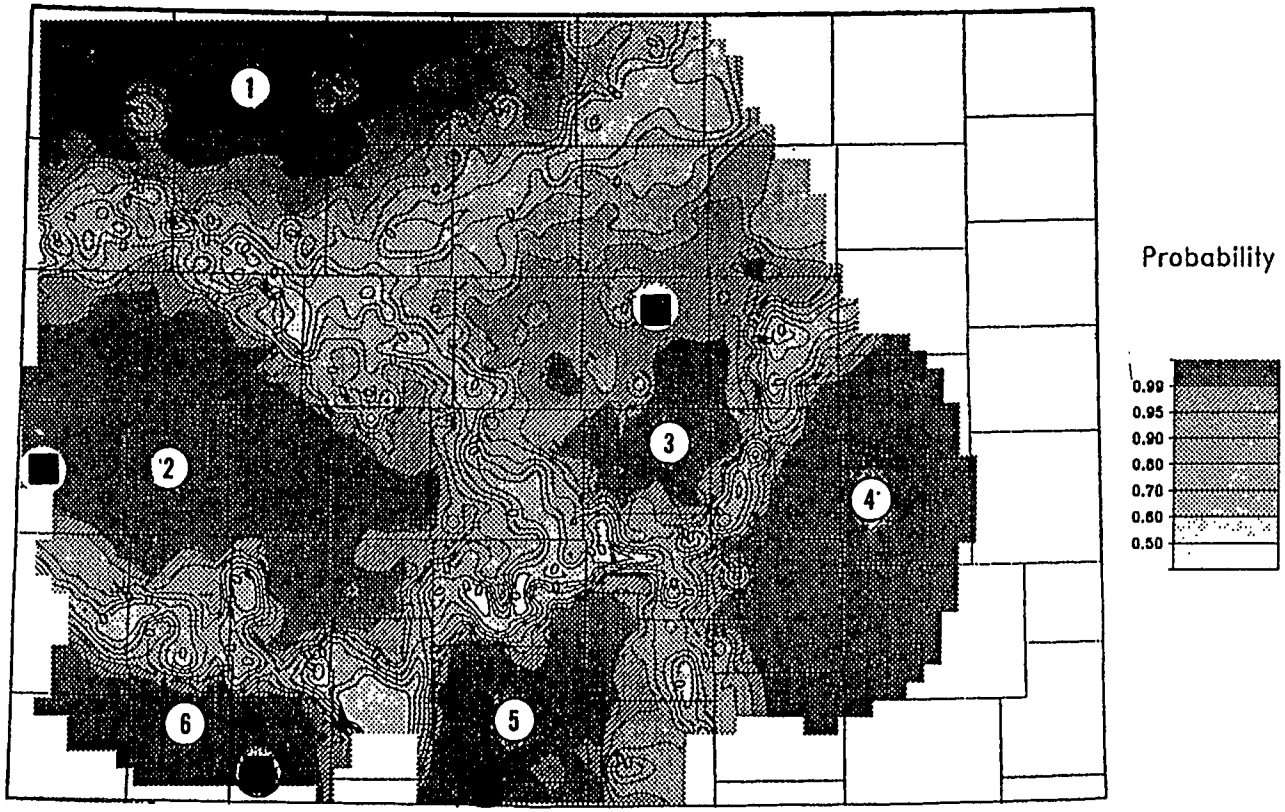

Probability of Correct Classification
6-Category Regionalization Based on Thickness

Regionalization of the Western Kansas Shelf

Figure 2.B.2.4. Probability of correct classification for 6-class regionalization. Black squares identify locations of backstripped subsidence analysis.

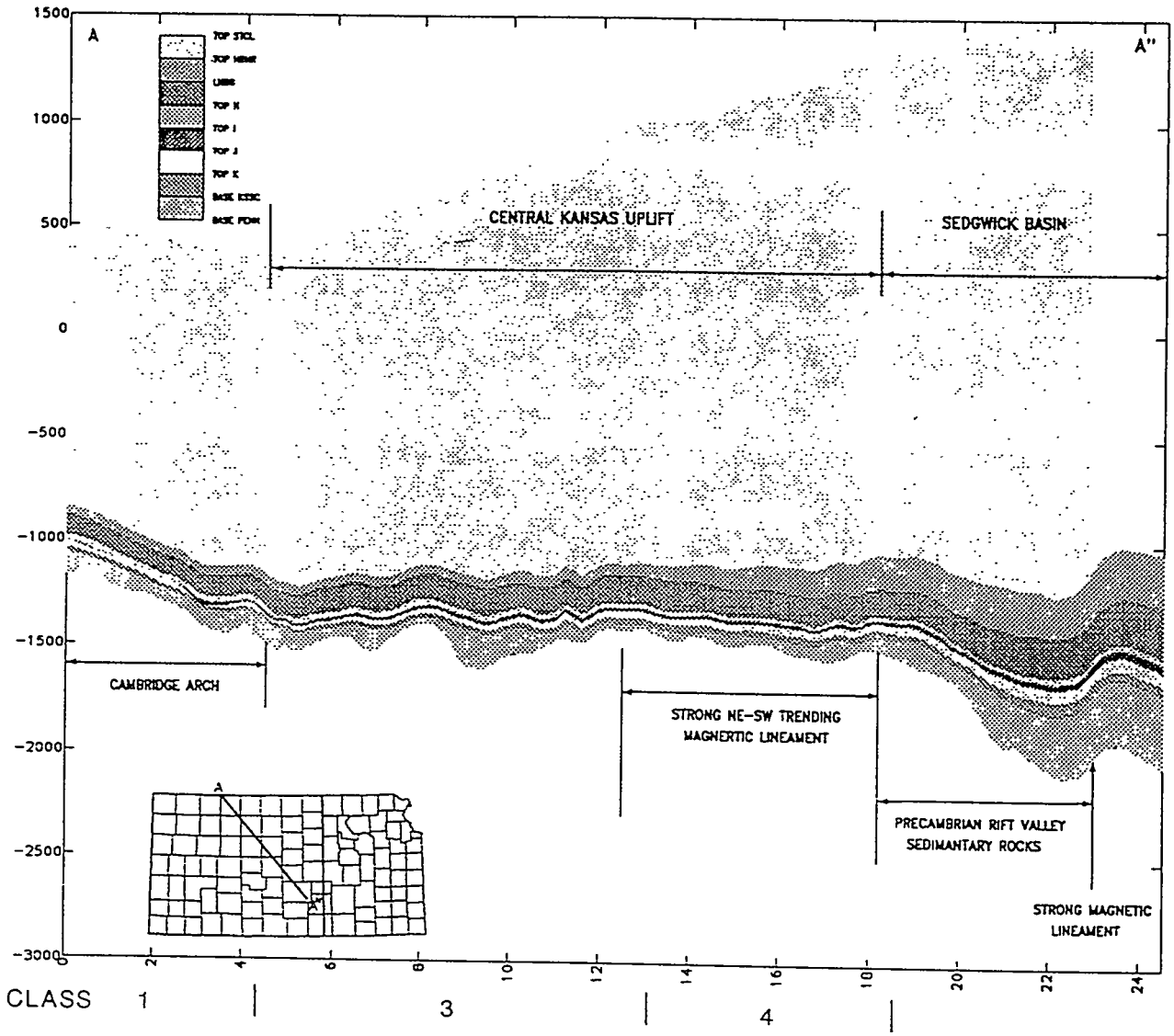

Figure 2.B.2.5. Northwest-to-southeast structural cross section along Central Kansas uplift utilizing 10 stratigraphic horizons used in regionalization. Section is keyed to class number as found in Figure 2.B.2.2 and prominent structural and basement features intersecting the cross section.

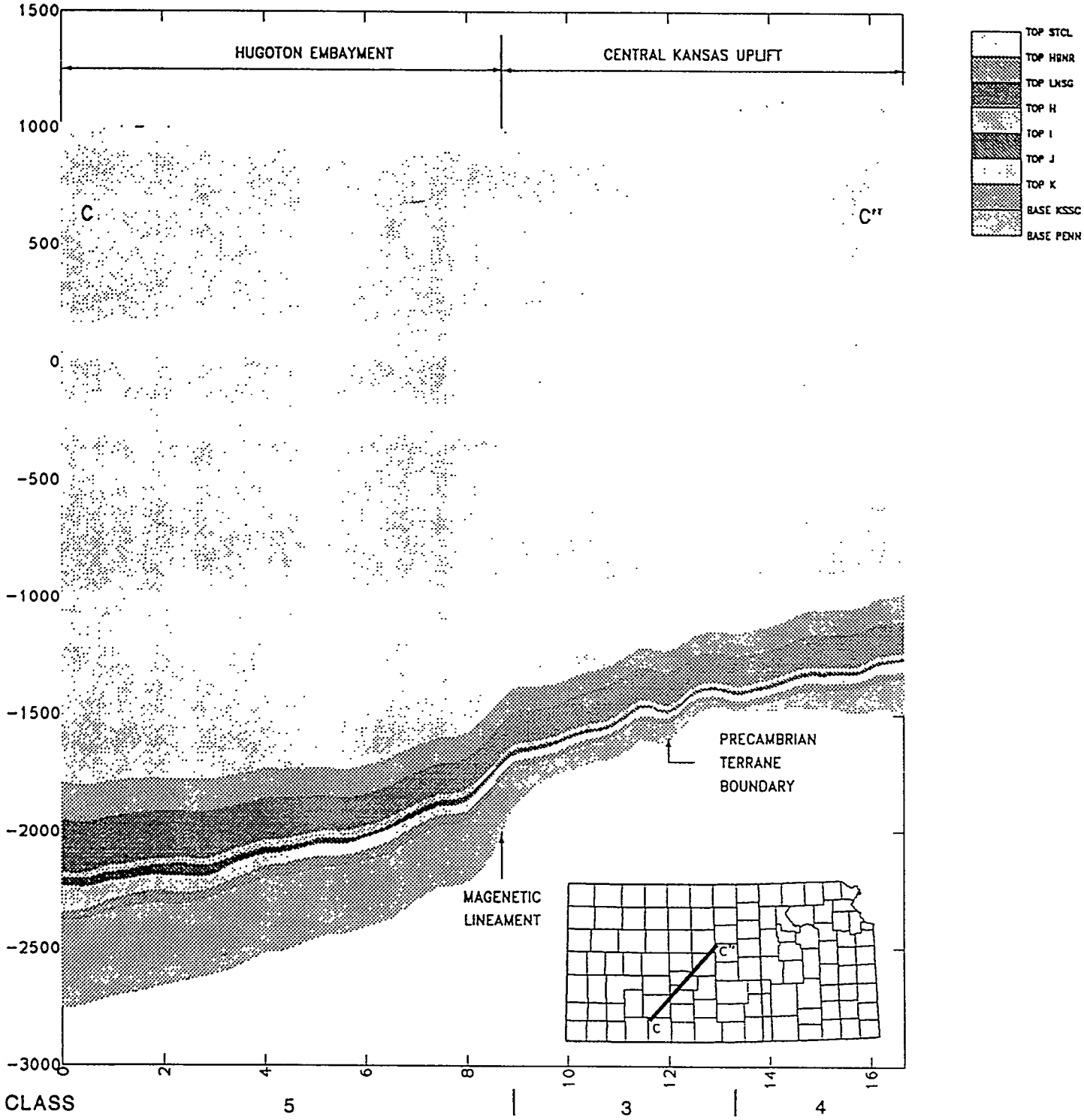

Figure 2.B.2.6. Southwest-to-northeast structural cross section from the Hugoton embayment unto the Central Kansas uplift utilizing 10 stratigraphic horizons used in regionalization. Section is keyed to class number as found in Figure 2.B.2.2 and prominent structural and basement features intersecting the cross section.

Amoco #1 Rebecca Bounds Sec. 17-18S-42W Greeley Co., Kansas

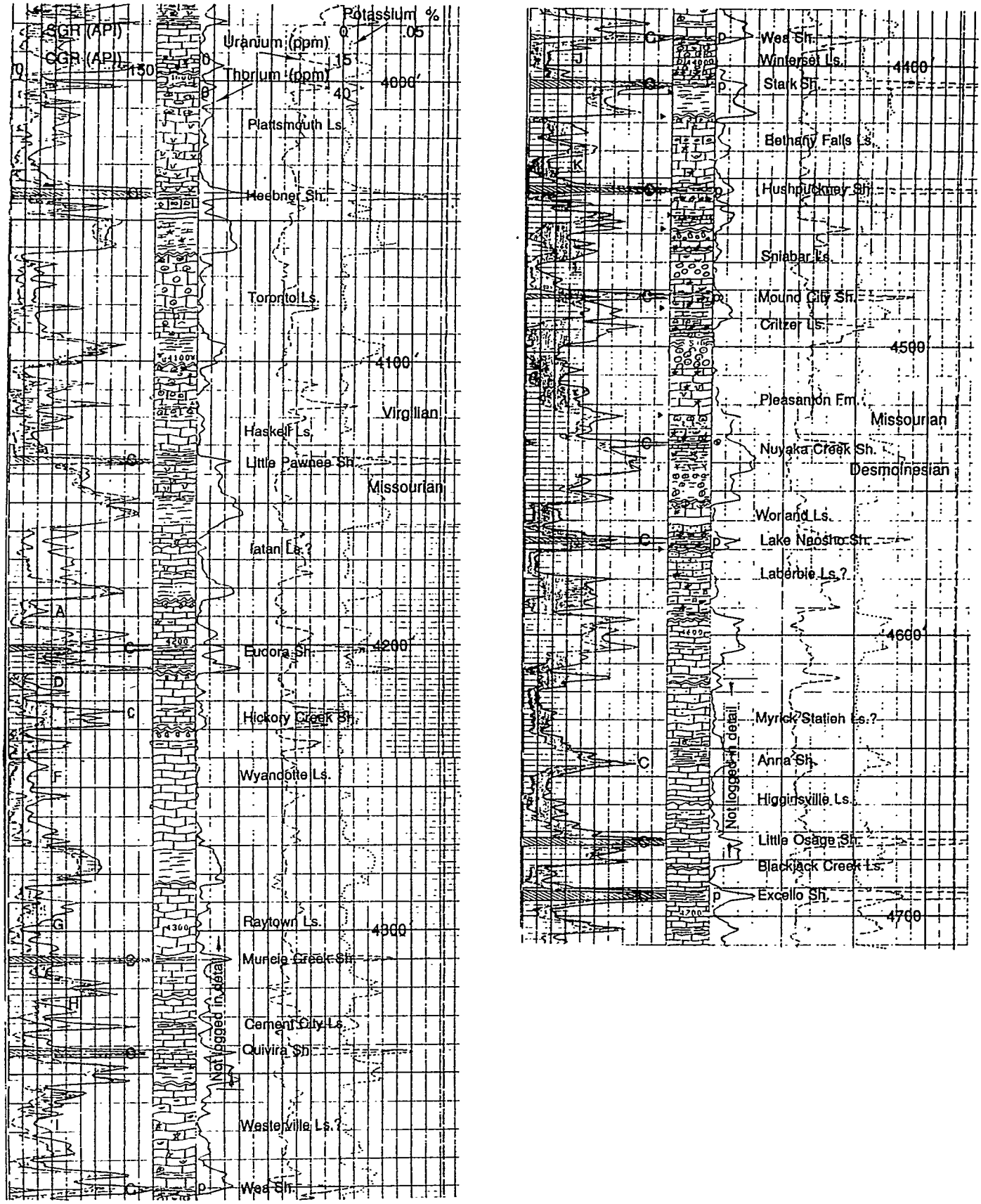

Figure 3.A.1. Gamma ray, uranium, thorium, potassium log for Amoco #1 Rebecca Bounds core from Section 17, T.18S.R42W, Greeley County, Kansas. Major marine marker shales correlated through conodont biostratigraphic analysis are indicated.

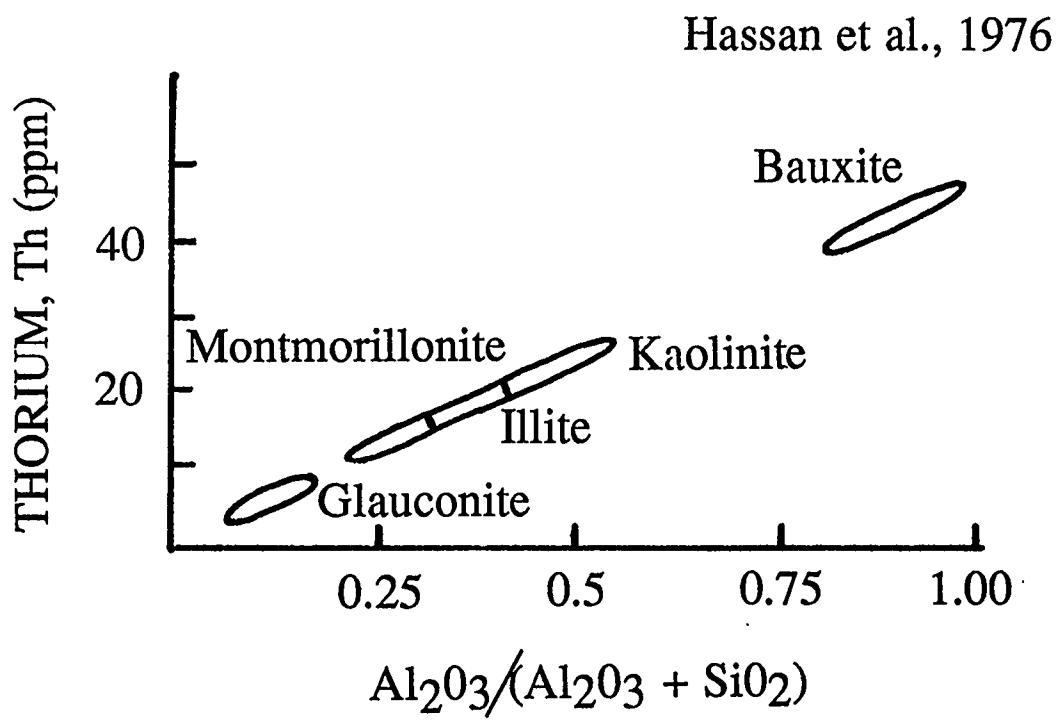

Figure 3.B.1. Thorium vs. alumina percent for various aluminosilicates (from Hassan et al., 1976).

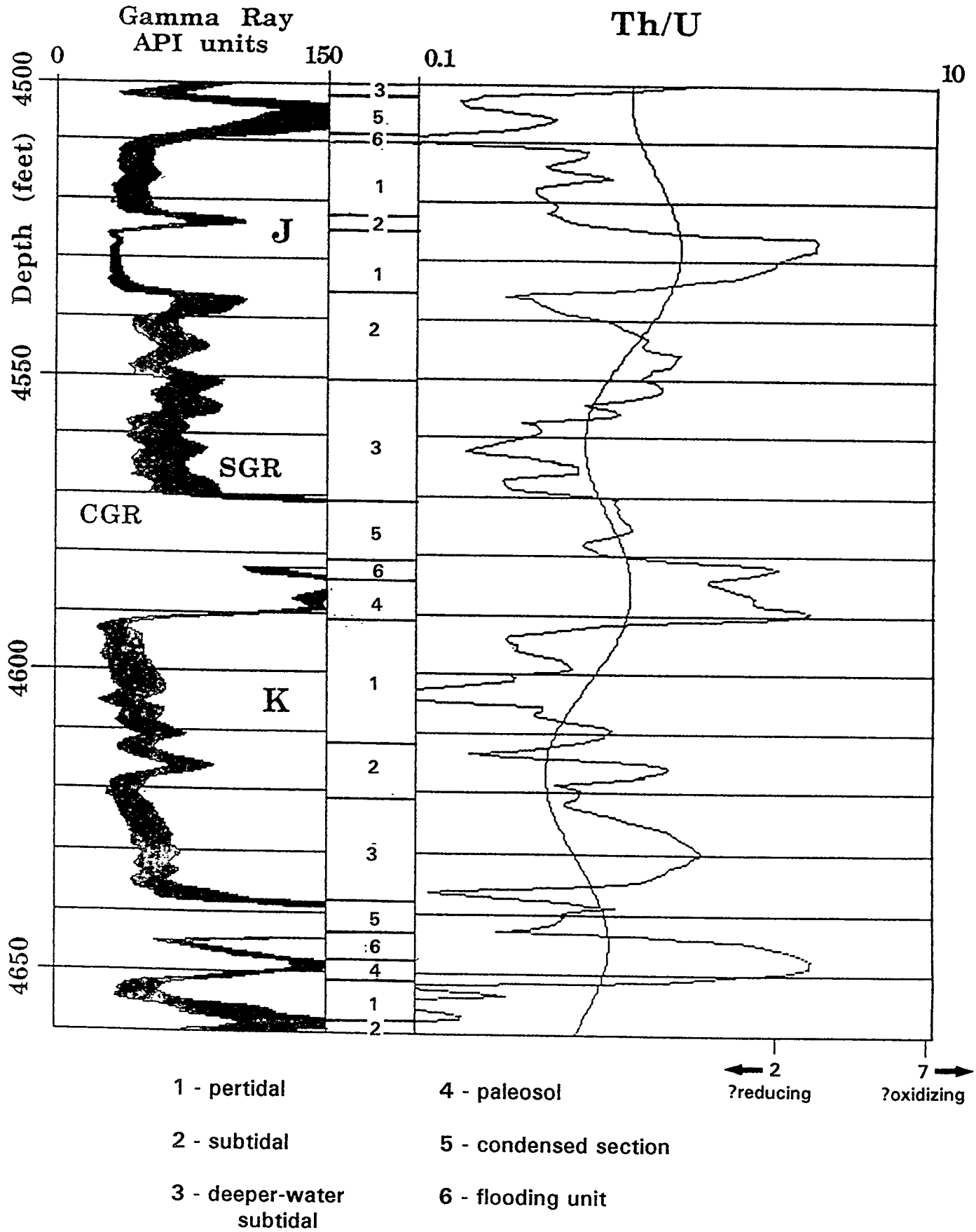

Figure 3.B.2. Gamma ray and Th/U ratio plotted for Amoco Cox #A-4 core in Victory field showing facies vs. log response. Th/U ratio is fit with a two-harmonic Fourier analysis curve discussed in text.

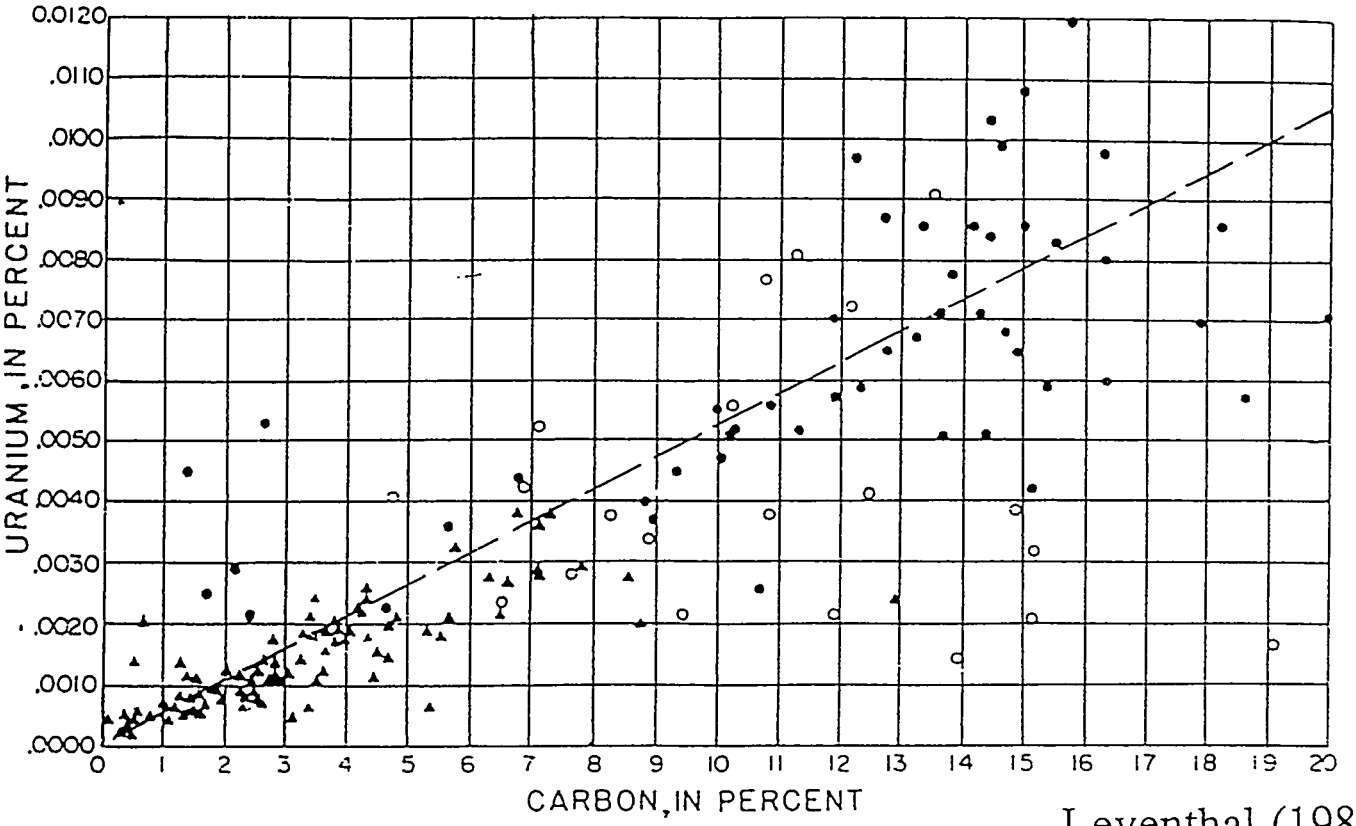

Leventhal (1981)

Figure 3.B.3. Uranium vs. organic carbon in sedimentary rocks (from Levanthal, 1981).

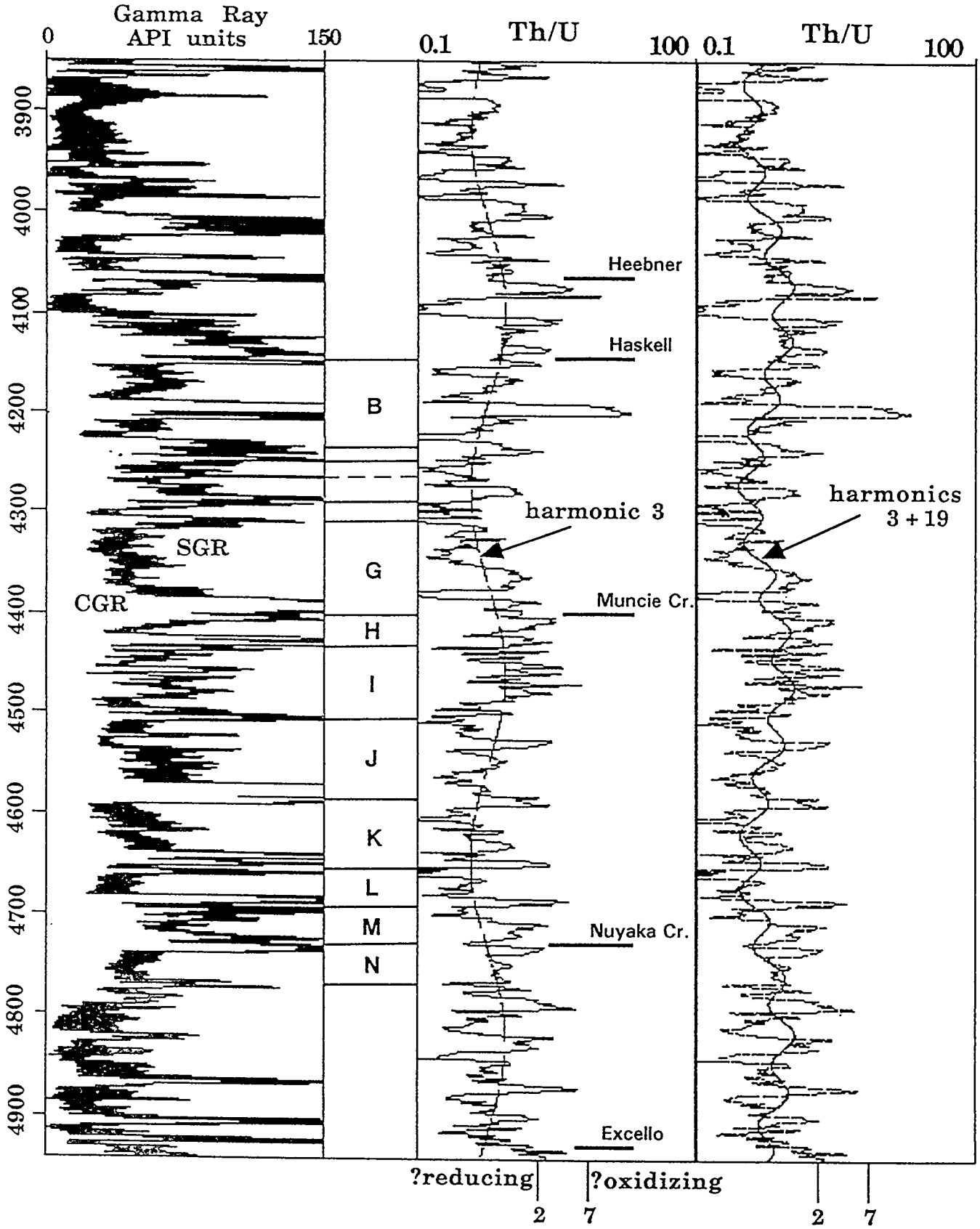

Figure 3.B.4. Gamma ray, Th/U ratio, and two Fourier harmonics of Th/U ratio for Amoco Cox #A-4 core for interval from Heebner Shale to Excello Shale.

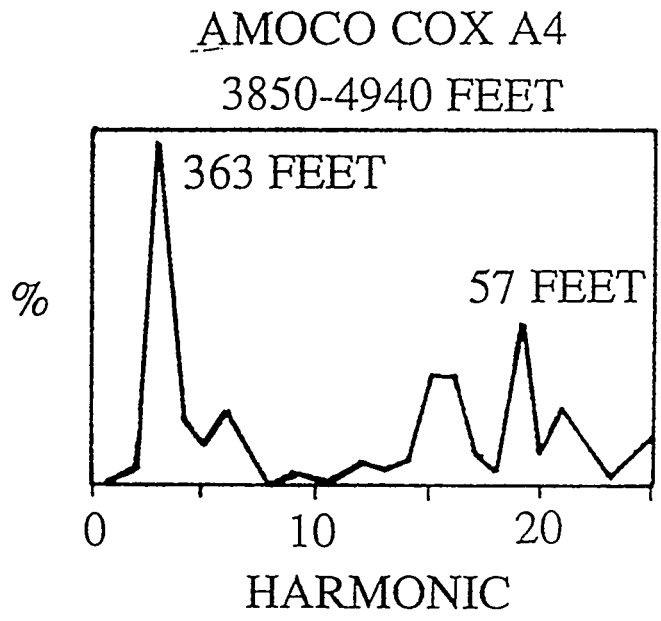

Figure 3.B.5. Power spectrum obtained from Fourier analysis of Th/U ratio from Amoco Cox #A-4.

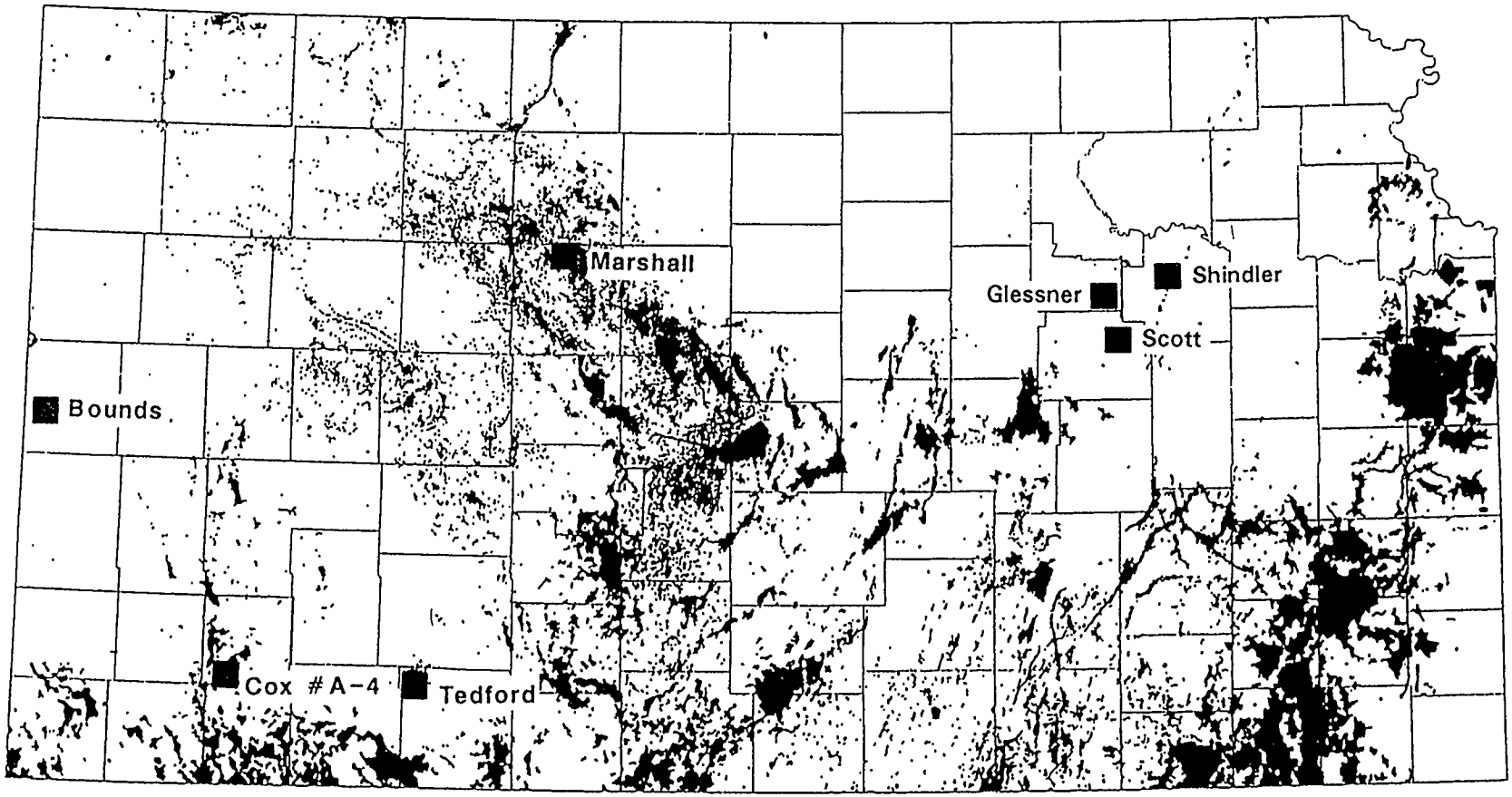

Th/U STUDY

Figure 3.B.6. Oil fields map of Kansas with locations of wells used in expanded Th/U ratio analysis.

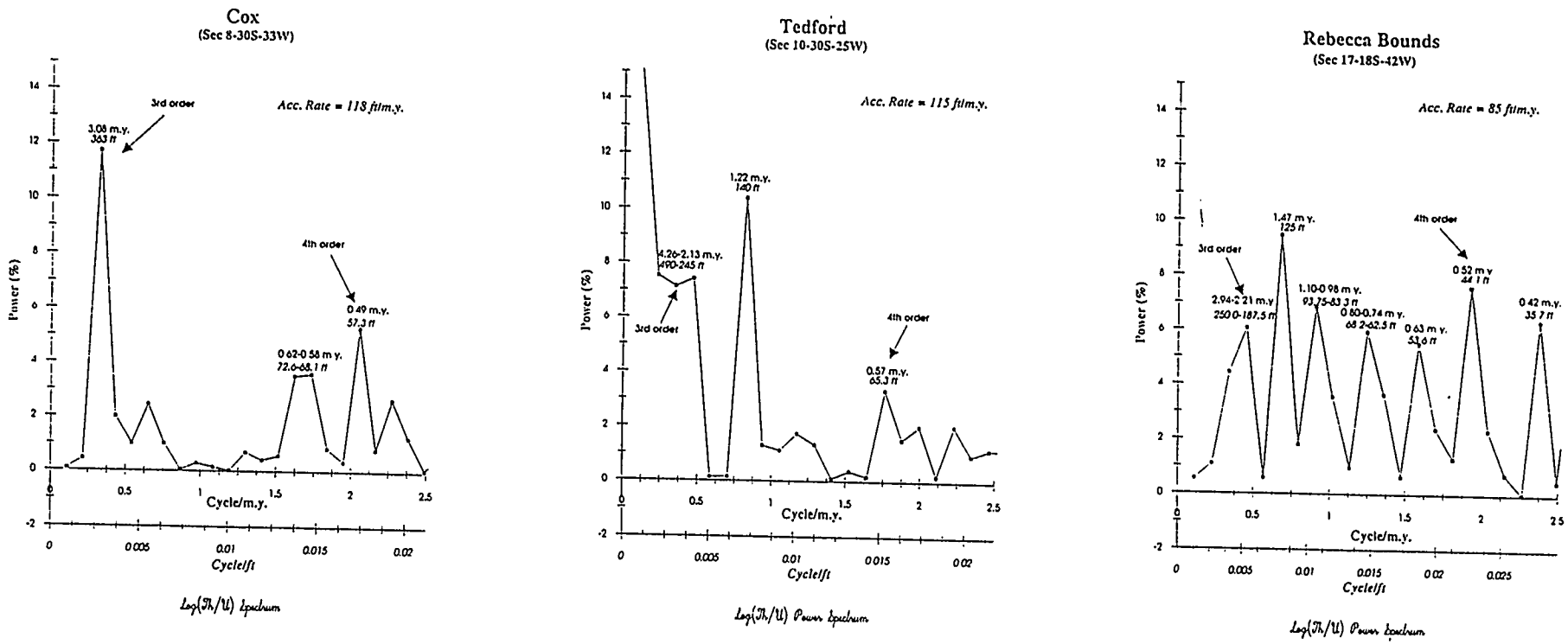

Figure 3.B.7(a). Power spectra for Th/U ratio data for six wells identified on the map in Figure 3.B.6. Interval used in analysis is Heebner Shale to Excello Shale. Presentation of spectra includes both cycle/ft and cycle/m.y. (million years). Cycle/m.y. is based on a long term accumulation rate equal to thickness/time represented in a well.

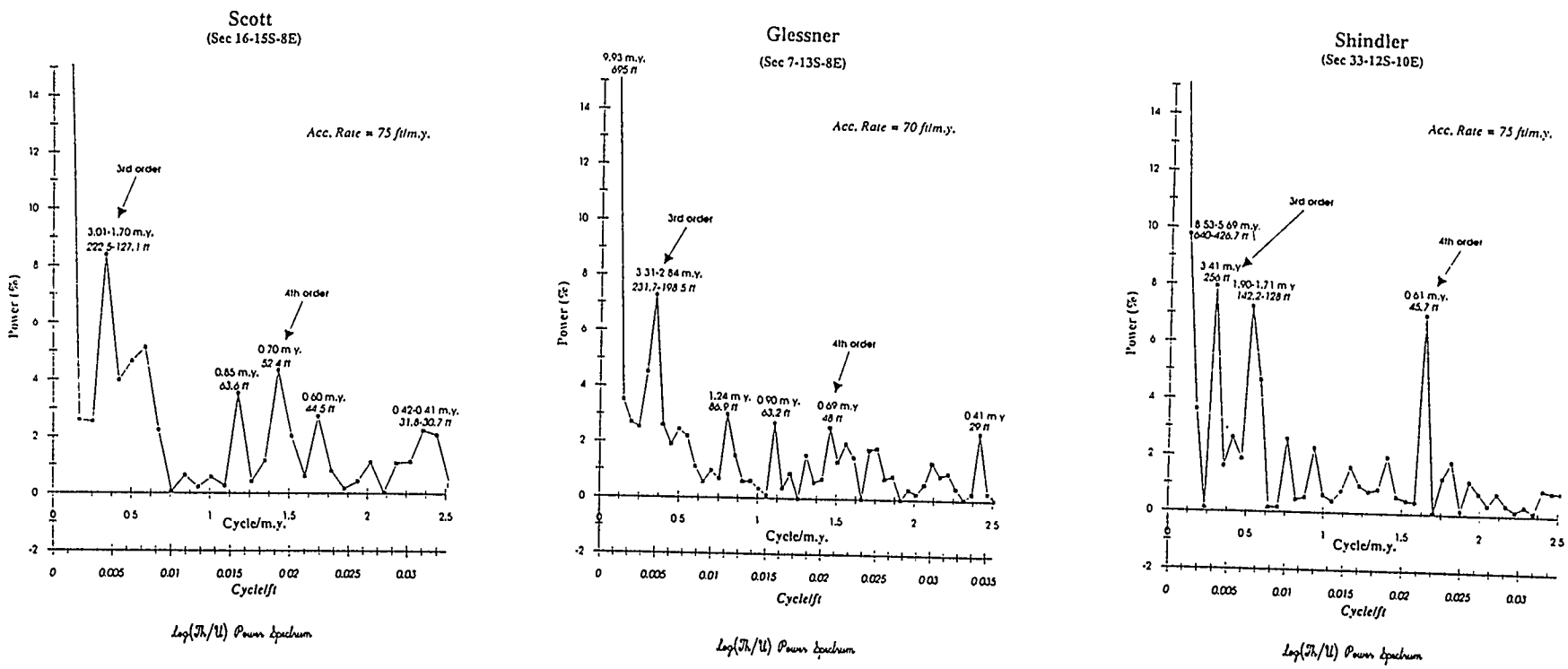

Figure 3.B.7(b). Continuation of power spectra from Figure 3.B.7(a).

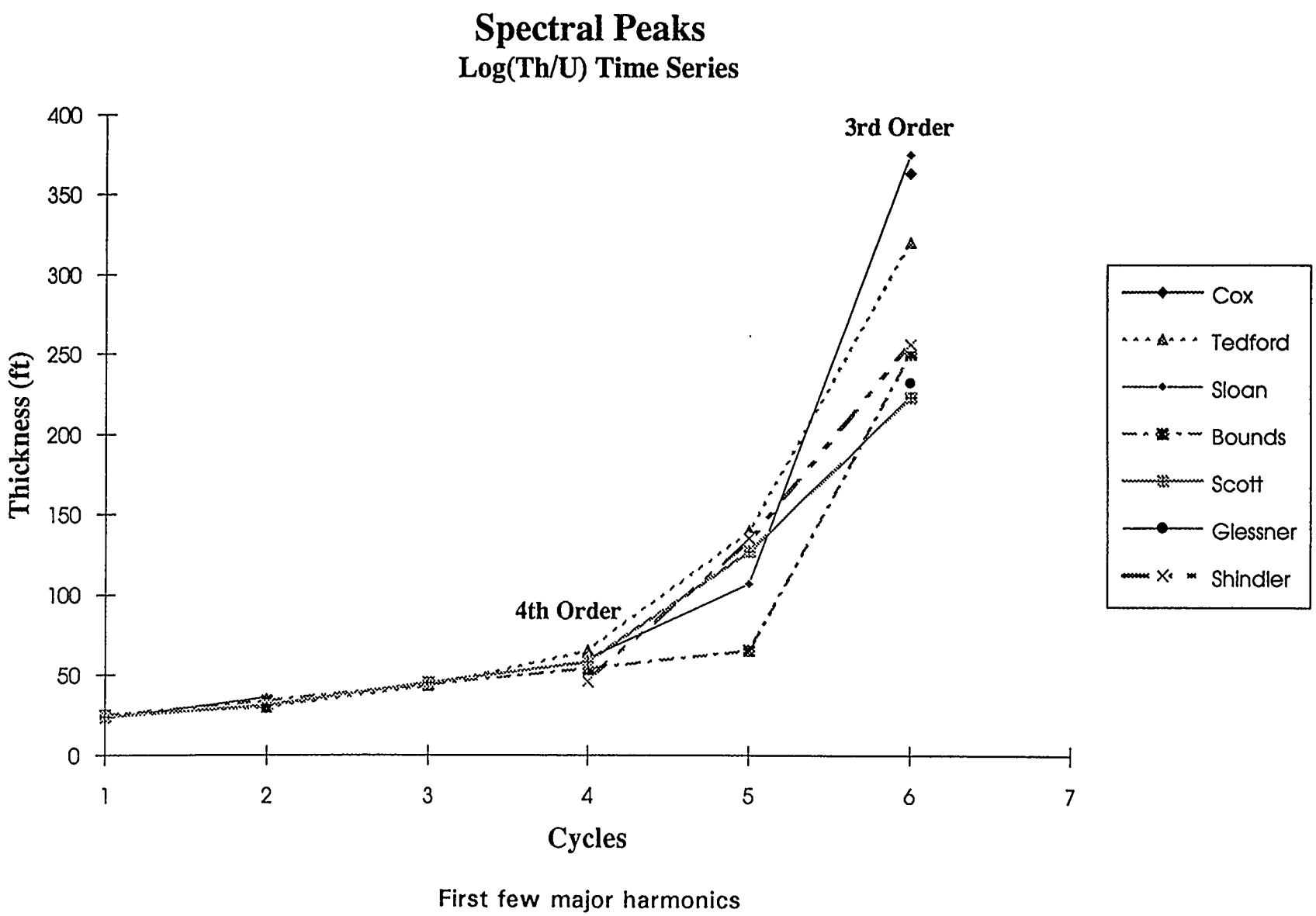

Figure 3.B.8. Plot of harmonic number (cycle) for major peaks vs. thickness of cycles for seven wells distributed across the Kansas shelf.

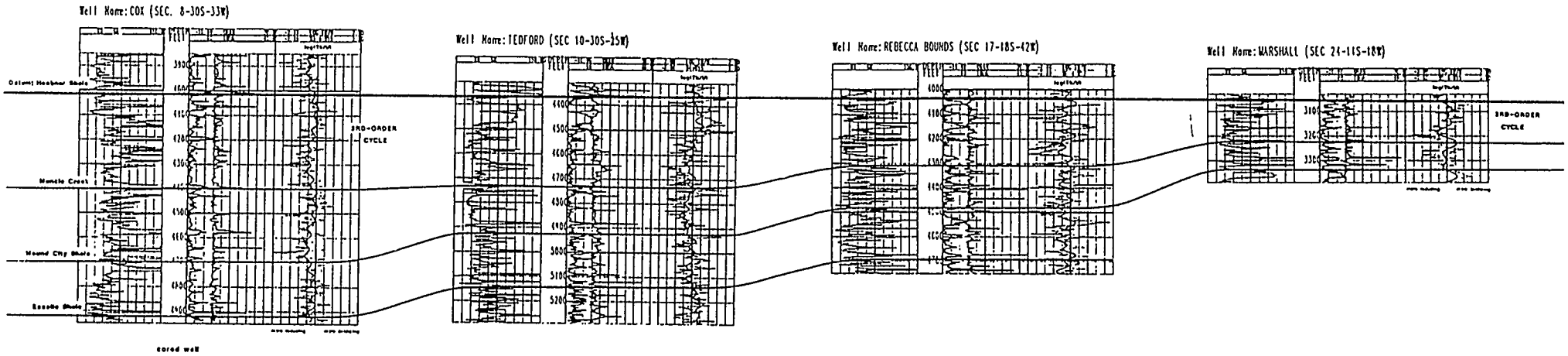

Figure 3.B.9(a). Cross sections linking wells used in the Th/U analysis presented as logs of the gamma ray, original Th and U concentrations, the Th/U ratios, and the 3rd- and 4th-order harmonics. Correlation lines connect the boundaries of the 3rd-order cycles.

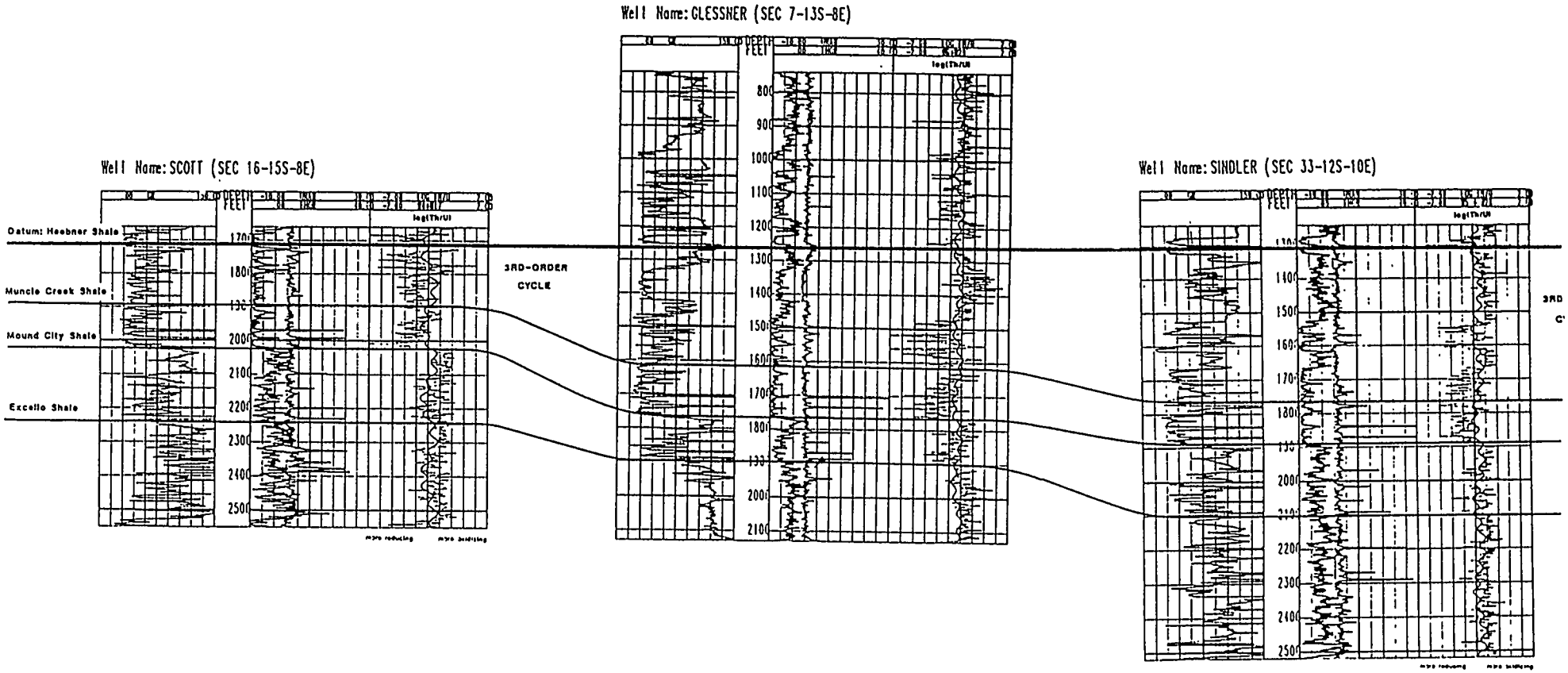

Figure 3.B.9(b). Continuation of Figure 3.B.9(a).

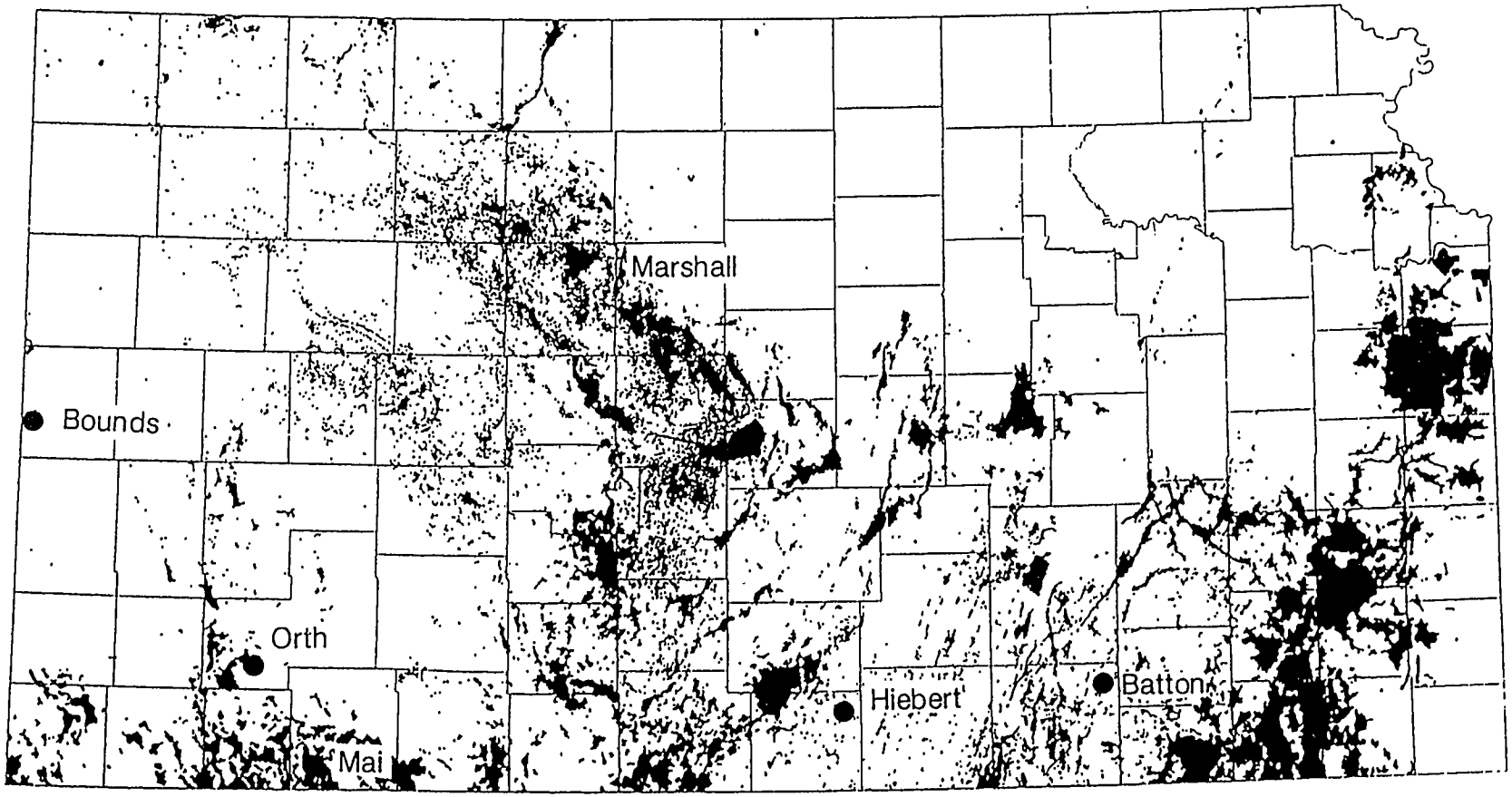

SUBSIDENCE STUDY

Figure 4.A.1. Oil fields map of Kansas showing wells used in backstripping (decompaction) subsidence analysis.

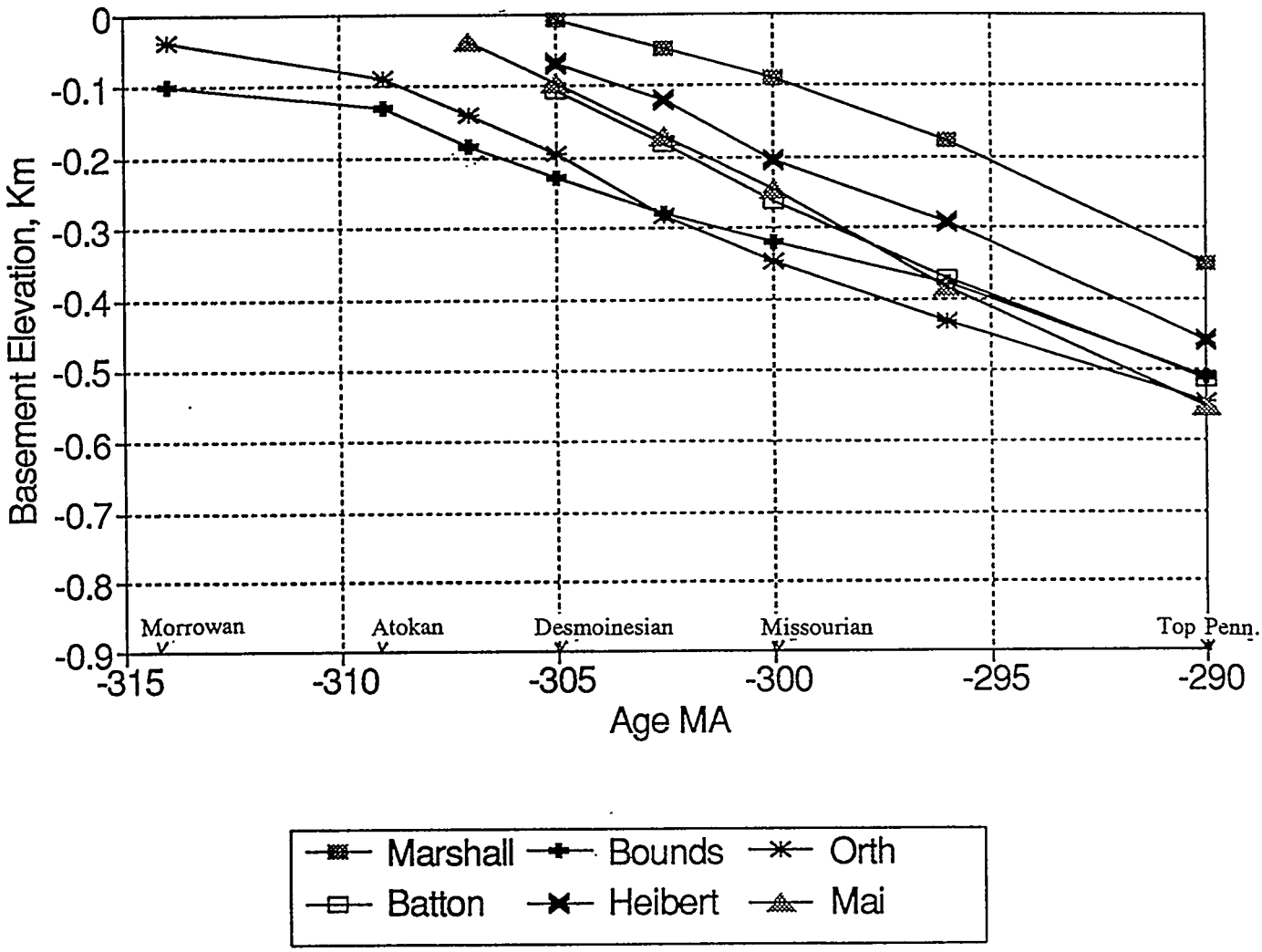

Figure 4.A.2. Basement depth vs. time plot for six wells using backstripping.

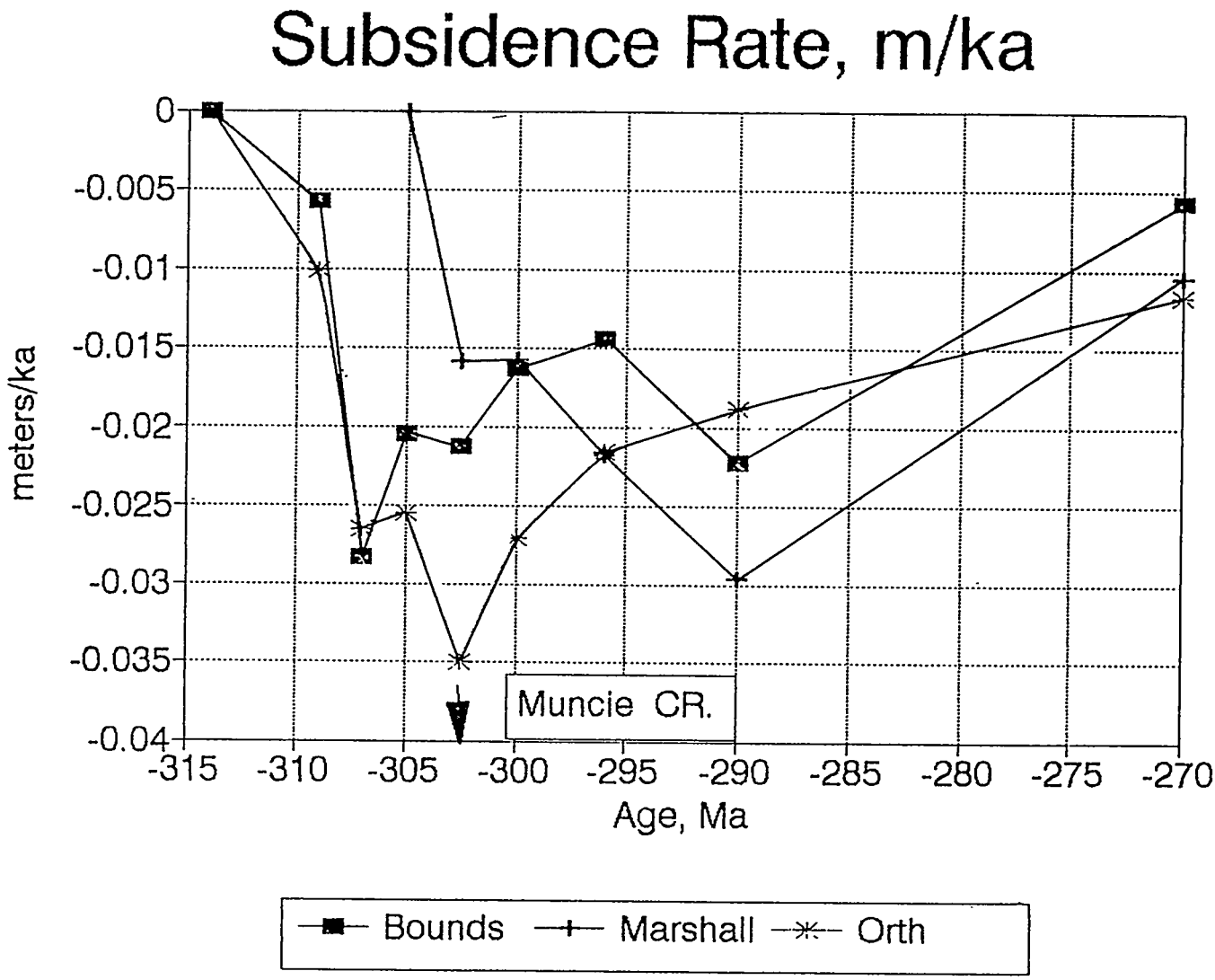

Figure 4.A.3. Subsidence rates in m/ka (meters/1000 years) vs. age of strata. Lines connect points for each well. Initial point of each well on left is invalid.

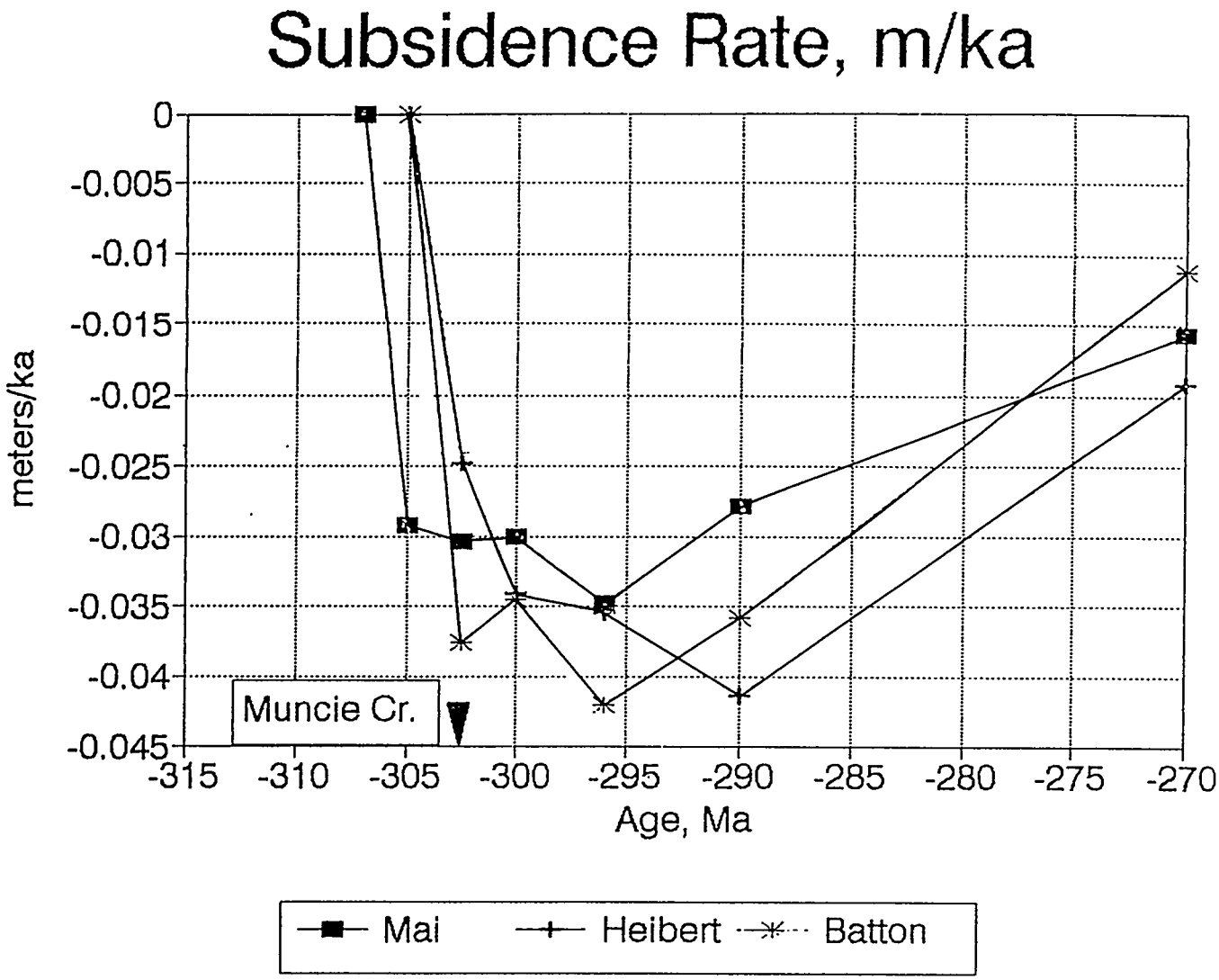

Figure 4.A.4. Same as Figure 4.A.3.

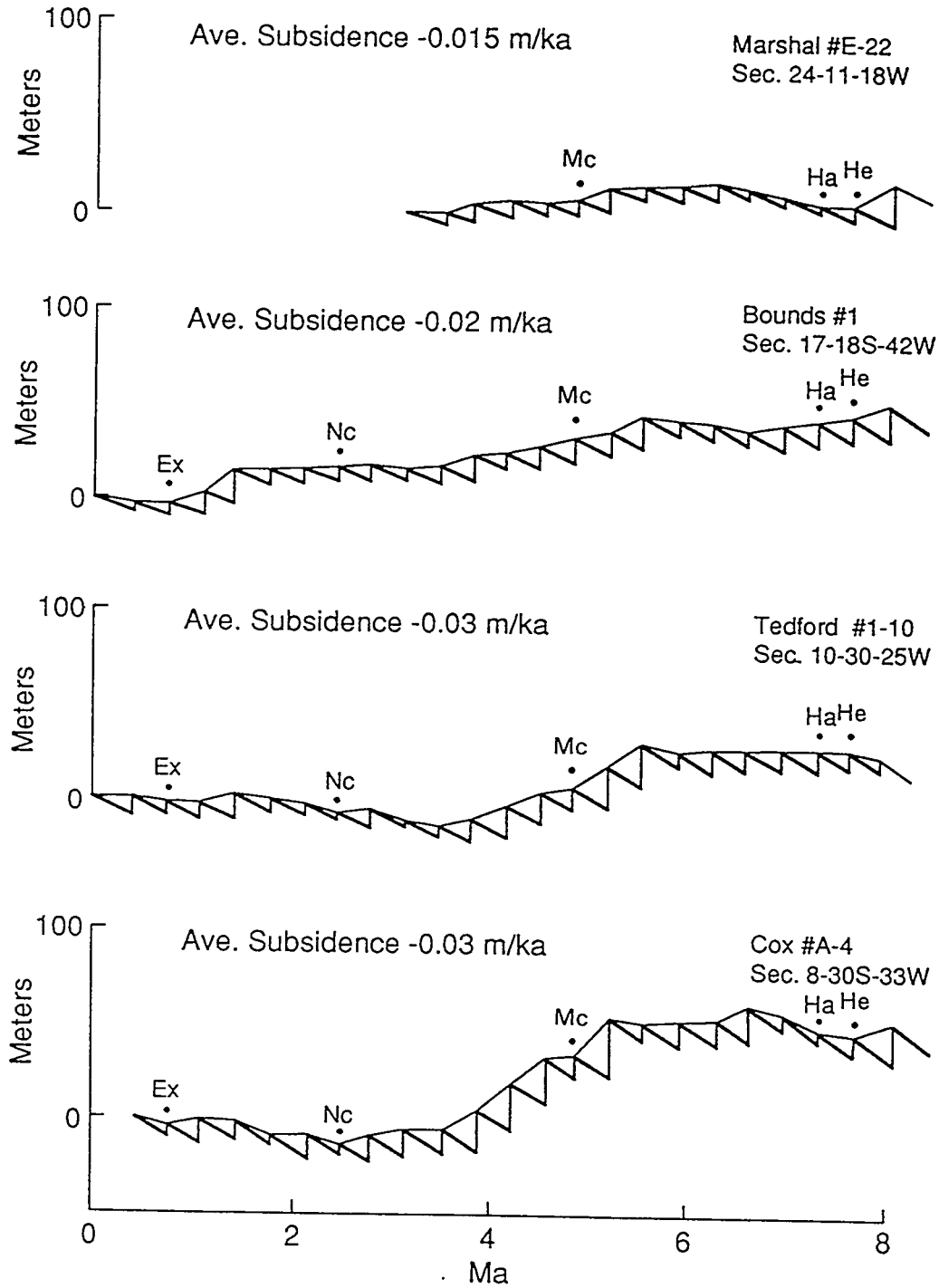

Figure 4.B.1. Fischer accommodation plots for wells in western Kansas. Time (Ma, millions of years) vs. thickness of 4th-order depositional sequences. Duration of 4th-order cycles set at 350 ka (thousand years). Subsidence applied determined from backstripping.

DOE PROJECT DATABASE MANAGEMENT PROGRAM (DOE.EDT)

Design Goal: The DOE.EDT is designed to handle all the database operations involved in the DOE Project. It provides an user-friendly working environment for data entry, modification, selection, projection, and printing, on each and between databases. The program also permits exchange of information.

Functions:

1. Data input.
2. Data modification.
3. Data search and selection.
4. Sorting.
5. Map projection.
6. Base map (land-grid) generation.
7. Printing a hard copy of database.

Utility Programs involved:

1. Form-utitlity.
2. Pl _support.lb
3. Sort/Merge.
4. Leo.cvt
5. Projct.

Database format:

Each well entry has a common title field which includes location, API #, well name, longitude, latitude, and surface elevation (see record format sheet for each database).

Correlation Keys:

1. API # (primary key).
2.. Location, well name, etc (secondary keys).

Figure 5.A.1. DOE project database management program.

DOE PROJECT DATABASES & DATA SETS

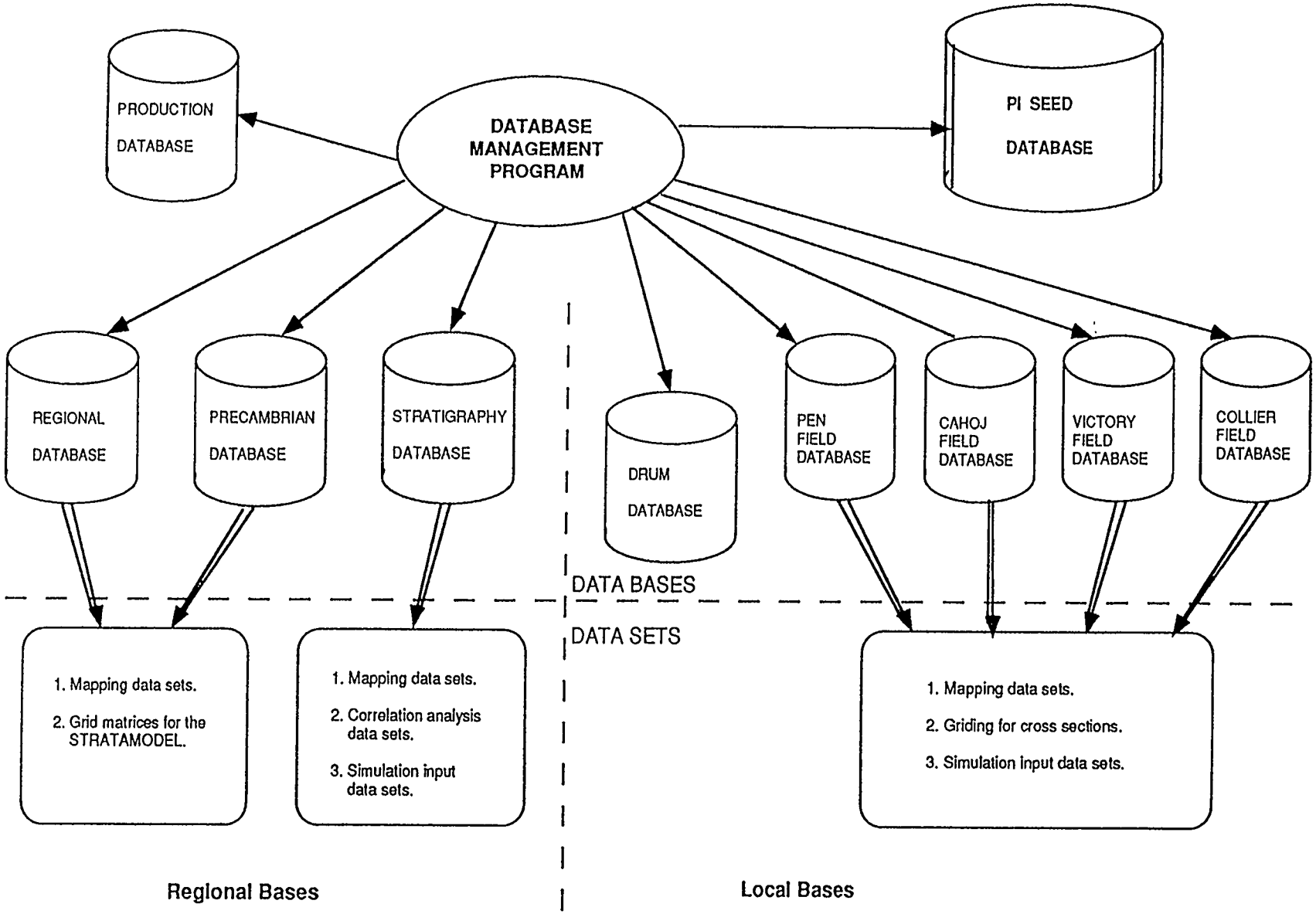

Figure 5.A.2. DOE project databases and data sets.

COMPUTER OPERATIONS IN DOE PROJECT

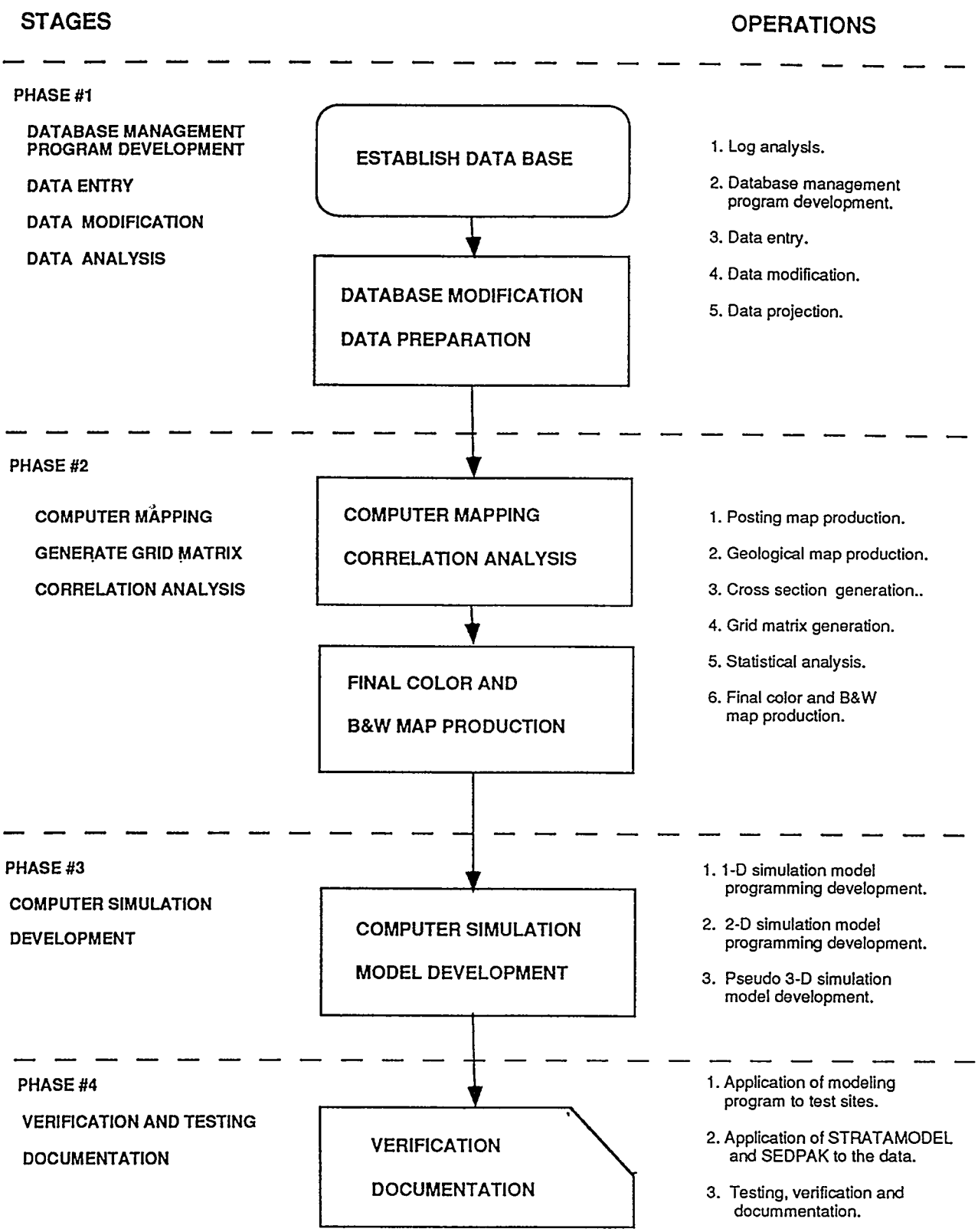

Figure 5.A.3. Computer Operations in DOE Project.

STRUCTURE DIAGRAM OF DOE.EDT

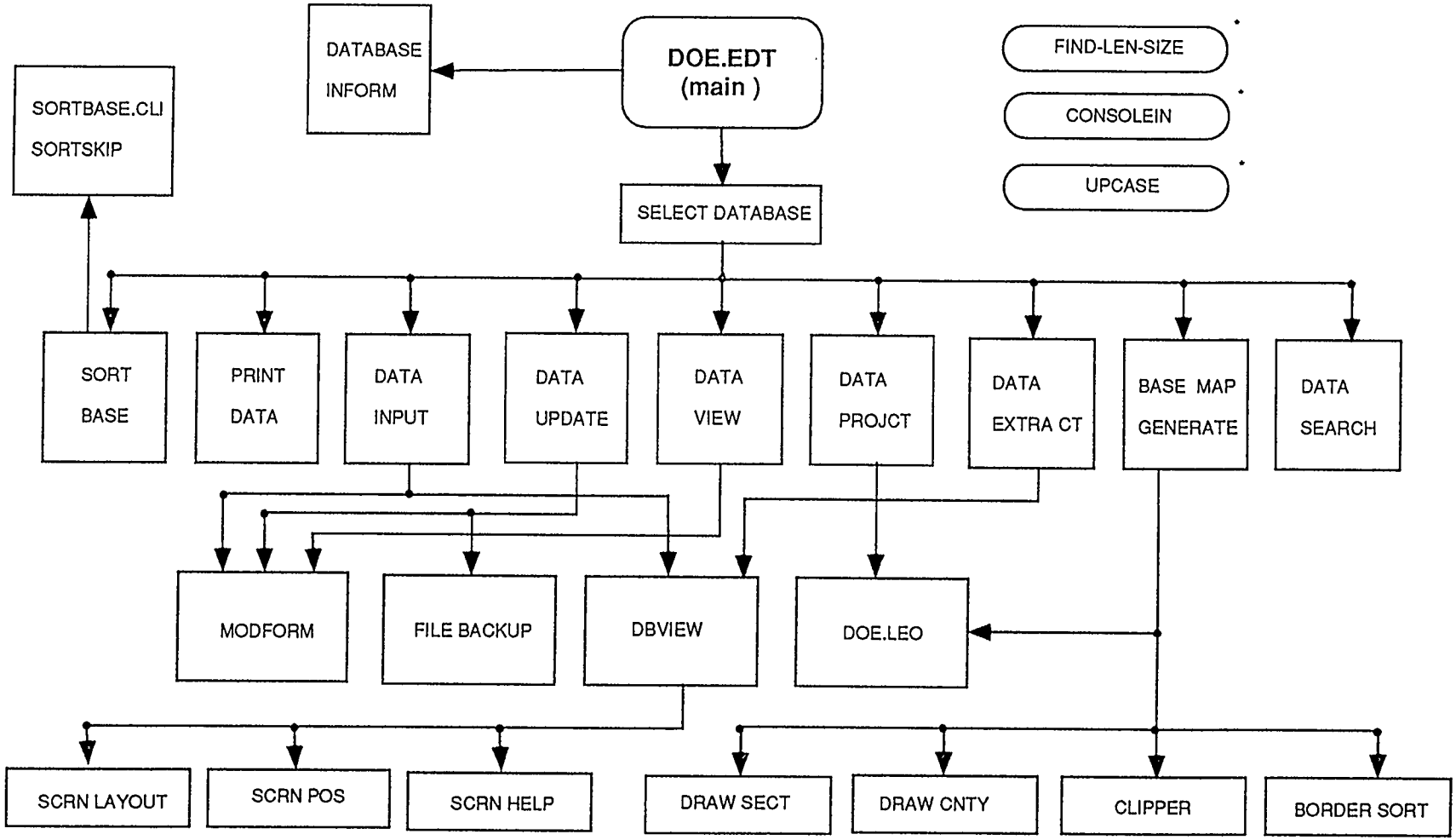

NOTE :

1. '*' indicates utility routine that is used by most modules.
2. The program must be linked with :UTIL:GIMMAP.LEOCVT, :UTIL:GIMMAP.PROJCT, UTILLIB.LB, and FORM77.

Figure 5.A.4. Structure Diagram of DOE.EDT.

```
0  << MOU'S  SEQUENCE DATABASE:   KANSAS-CITY  (LYNN'S)      >> INPUT DATA FORM

==============================================================================================
|      | RECORD HEADER :
|
|  1   |  WELL-ID     SPOT-LOC     SEC  TWN     RNG  E/W  CNTY  LONGITUDE   LATITUDE
|      | [        ]  [        ]  [  ] [  ][ ] [  ] [ ]  [  ] [         ] [         ]
|      |  --------    --------    --   --  -   --   -    --   ---------   ---------
|
|  2   |    API-NUMBER          OPERATOR-NAME          WELL-NUM       LEASER-NAME
|      | [              ] [                        ][           ][                  ]
|      |  --------------   ------------------------   -----------   -------------------
|
|  3   |                   FINAL-STATUS COMP-DATE   FM-@-TD  TOTAL-DEPTH   SURF-ELEV
|      |                       [  ]      [    ]    [       ]  [     ]      [     ]
|      |                        --        ----      -------    -----        -----
|
~~~~~~~~~~~~~~~~~~~~~~~~~~~~~~~~~~~~~~~~~~~~~~~~~~~~~~~~~~~~~~~~~~~~~~~~~~~~~~~~~~~~~~~~~~~~~~~~
|      | DATUMS :
|
|  4   |     LOG-TYPE  SCALE    B/HBNR IATAN  LANSG  BASE/G DEWEY  BASE/H POR.-H
|      |     (      )  (    )   (    ) (    ) (    ) (    ) (    ) (    ) (    )
|      |      ------    ----     ----   ----   ----   ----   ----   ----   ----
|      |                  ^
|  5   |  M.GR-H  TOP/I  BASE/I POR.-I M.GR-I TOP/J  BASE/J POR.-J M.GR-J  TOP/K
|      |  (     ) (    ) (    ) (    ) (    ) (    ) (    ) (    ) (    ) (    )
|      |    ----   ----   ----   ----   ----   ----   ----   ----   ----   ----
|
|  6   |  BASE/K  POR.-K M.GR-K TOP/L  BASE/L M.GR-L B/NUYA B/LAKE B/ANNA M.GR-ANNA
|      |  (     ) (    ) (    ) (    ) (    ) (    ) (    ) (    ) (    ) (    )
|      |    ----   ----   ----   ----   ----   ----   ----   ----   ----   ----
|
|  7   |   B/EXCL M.GR-E VSHALE B/PENN STALNA B/STAL EXTRA1 EXTRA2 EXTRA3
|      |  (     ) (    ) (    ) (    ) (    ) (    ) (    ) (    ) (    )
|      |    ----   ----   ----   ----   ----   ----   ----   ----   ----
|
|      |    TOTAL LENGTH   :    289  CHARACTERS
==============================================================================================
      012345678901234567890123456789012345678901234567890123456789012345678901234567890123456789
```

Figure 5.A.5. Database form.

Flow Chart Showing Logic of Quantitative Model

This diagram illustrates the logic involved in the "deposition" of sediment at a given location at each time step.

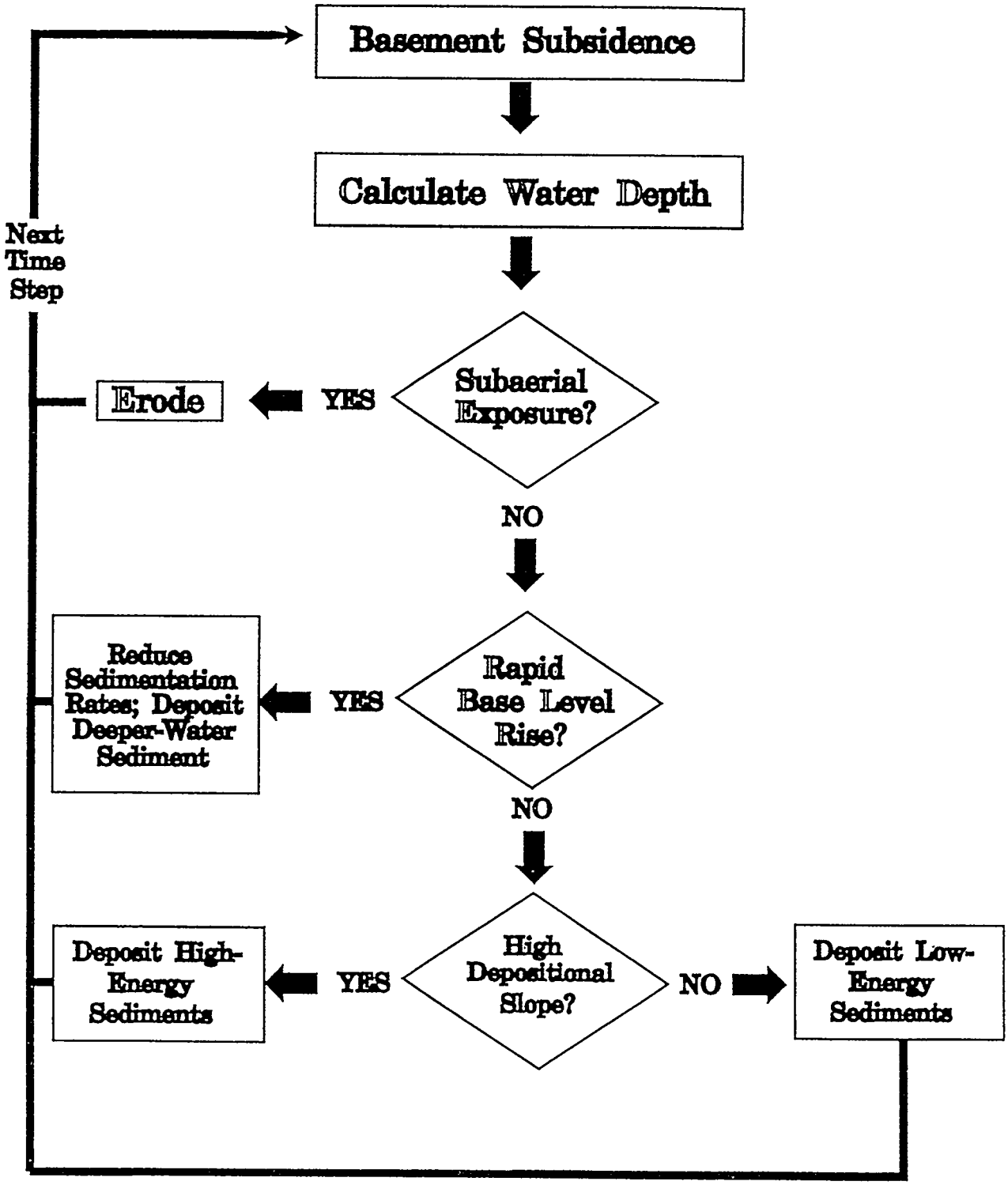

Figure 5.B.1. Flow chart showing logic of quantitative model.

a

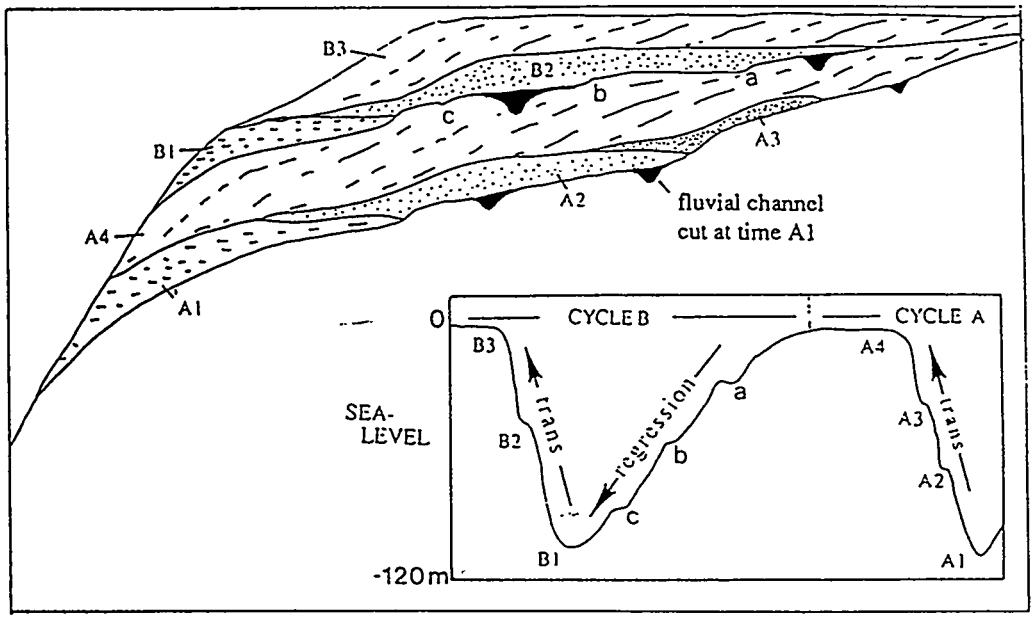

- rapid progradation on flatter shelf
- generally good preservation,
- erosion only locally significant

b

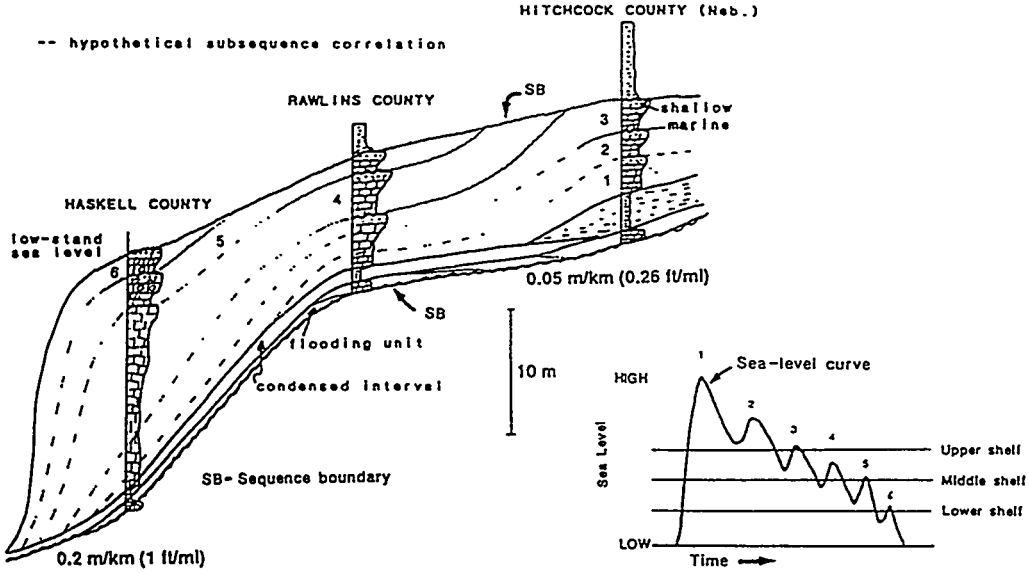

Figure 5.B.2. (a) Conceptual model of Quaternary coastal sedimentation in the Pacific region responding to two cycles of eustatic rise (from Carter et al., 1986). Flooding units (A1, A2, A3, B1, B2), condensed sections (diastemic marine surface separating flooding units and highstand deposits), and prograding highstand deposits characterize each cycle. Each cycle is bounded by subaerial exposure and limited erosion on the upper shelf. (b) Conceptual model of Lansing-Kansas City carbonate shelf cycle. Minor cycles punctuate the large 4th-order sequence.

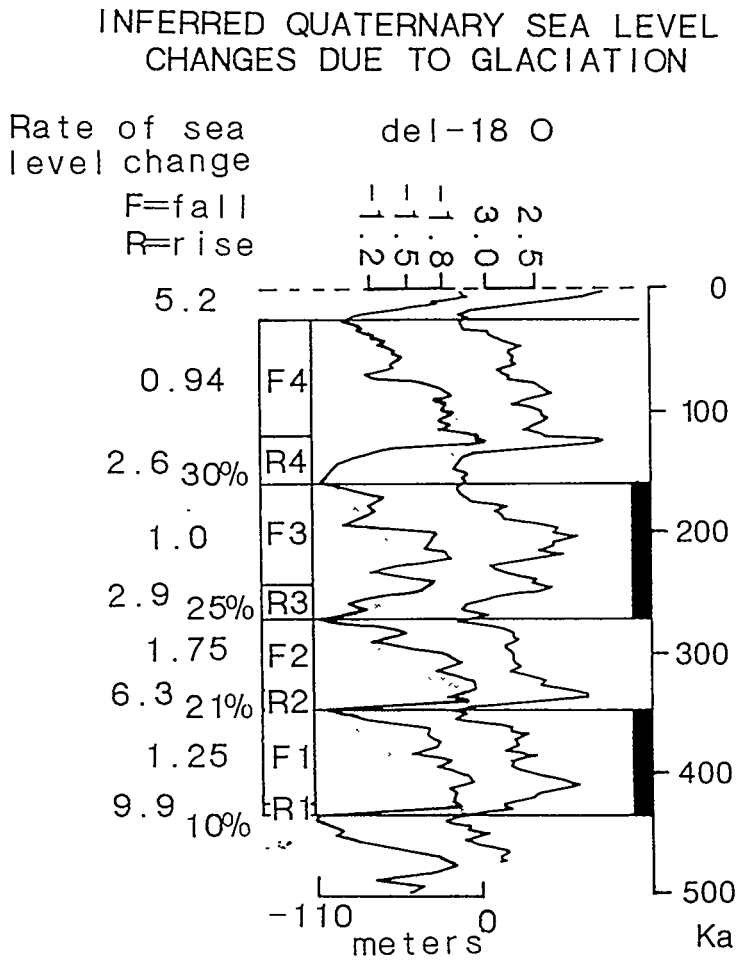

Figure 5.B.3. Quaternary-age oxygen isotope record for two deep sea cores obtained from the Caribbean (Denton and Hughes, 1983). Rates of rise and fall in m/ka on left side.

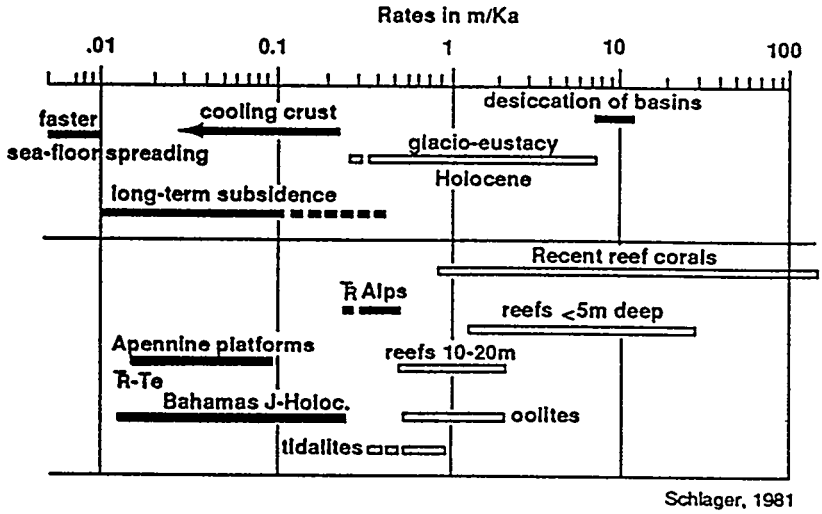

Figure 5.B.4. Subsidence and sediment accumulation (Schlager, 1981).

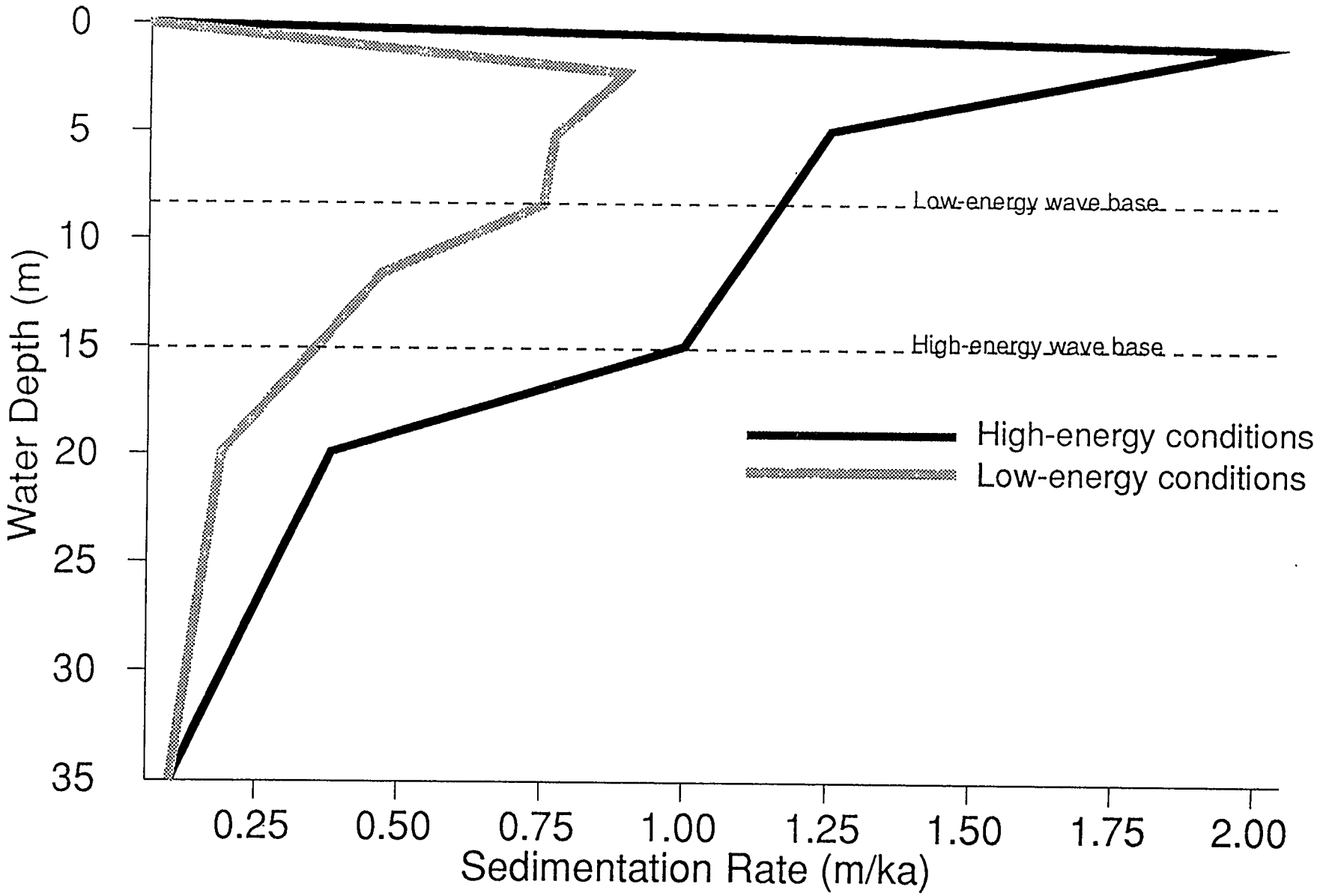

Figure 5.B.5. Carbonate sedinment accumulation rate vs. water depth used in 2-D model.

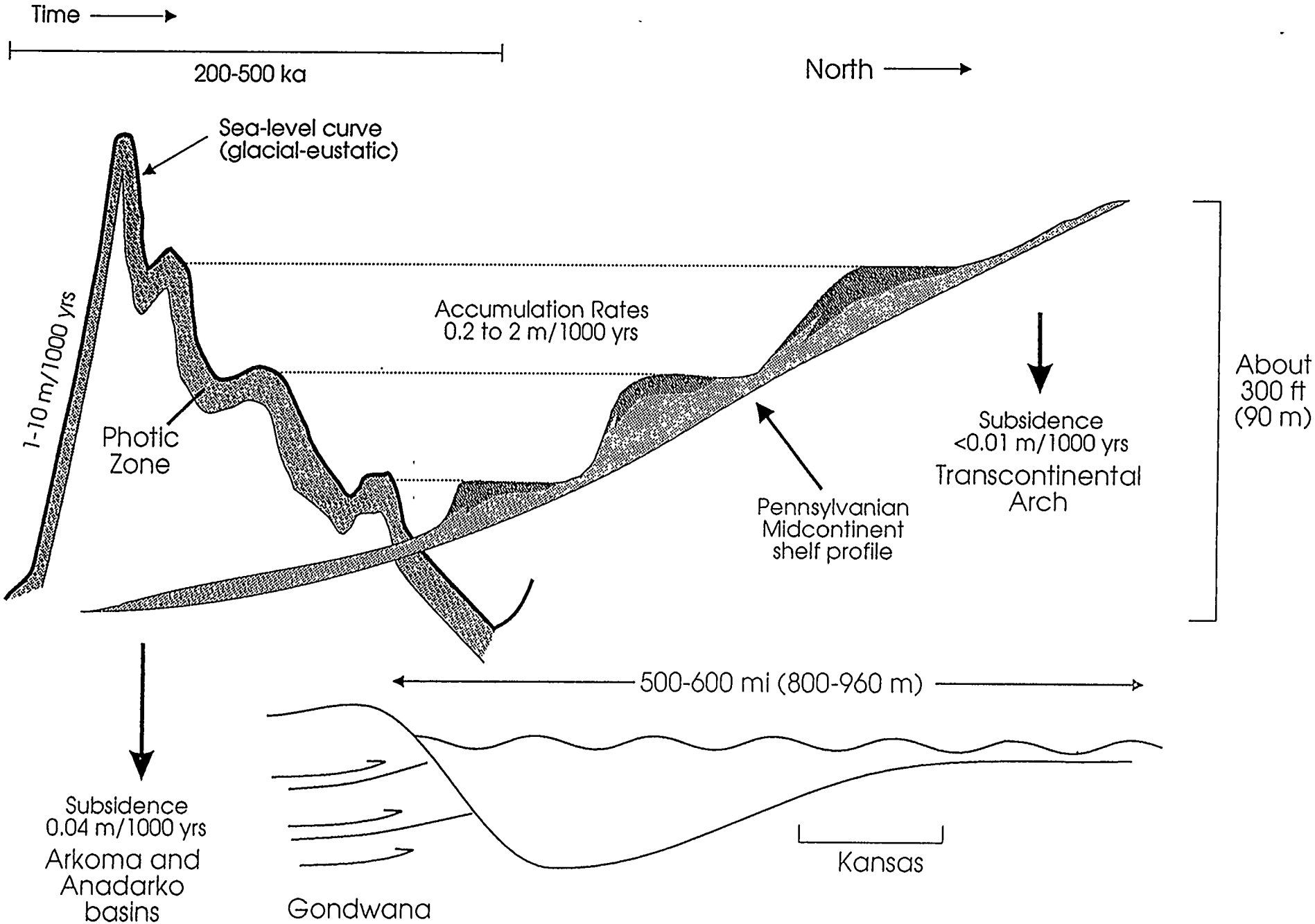

Figure 5.B.6. Conceptual model graphically depicting processes influencing development of an 4th-order sequences.

Amoco #A-4 Cox Haskell County, Kansas

FACIES	TOP	BOTTOM	CYCLE
2	4120	4125.5	A
4	4125.5	4129	
3	4129	4134	
5	4134	4141	
2	4141	4141.5	
4	4141.5	4147	
7	4147	4151	B
6	4151	4155	
5	4155	4159	
4	4159	4179.5	
5	4179.5	4188	
4	4188	4189	
2	4189	4189.5	
4	4189.5	4190.5	
7	4190.5	4201	
5	4201	4203.5	
11	4203.5	4207	
6	4207	4212	
4.5	4212	4228	
4	4228	4233	
3.5	4233	4239	
2	4239	4240	
7	4240	4243	
4	4243	4248	
3.5	4248	4249	
11	4249	4250	D
5	4250	4251	
4	4251	4265	
2	4265	4265.5	
4	4265.5	4274	
3.5	4274	4276	
2	4276	4278.5	
3	4278.5	4279	
4	4279	4284.5	
2	4284.5	4285	
4	4285	4286.5	E
5	4286.5	4291	
11	4291	4291.5	
5	4291.5	4296	F1
4.5	4296	4300	
4	4300	4308.5	
6	4308.5	4310.5	
2	4310.5	4311	
4	4311	4316	F2
2	4316	4317.5	
4	4317.5	4319	
6	4319	4321	
4.5	4321	4341	G
5	4341	4368	
4	4368	4380	

FACIES	TOP	BOTTOM	CYCLE
3.5	4380	4392	
2	4392	4396	
1	4396	4401	
2	4401	4405.5	
3.5	4405.5	4411.5	
11	4411.5	4413	H
4.5	4413	4416	
4	4416	4429	
3	4429	4436	
1	4436	4437	
4	4437	4441.5	
7	4441.5	4442.5	I
6	4442.5	4446	
4	4446	4457	
6	4457	4460	
4	4460	4468	
5	4468	4470	
3	4470	4474	
4	4474	4478	
4	4478	4480	
3	4480	4488	
4	4488	4491	
4	4491	4496	
3	4496	4498.5	
4	4498.5	4500	
5	4500	4505.5	
4	4505.5	4503	
3	4503	4506	
3.5	4506	4507	
5	4507	4508.5	
3.5	4508.5	4515	
6	4515	4529	J
3.5	4529	4530.5	
4.5	4530.5	4533	
5	4533	4535	
6	4535	4543	
4	4543	4550	
6	4550	4551	
4	4551	4556	
3.5	4556	4574	
3	4574	4577.5	
1	4577.5	4587	
7	4587	4593	
11	4593	4597.5	K
6	4597.5	4617	
4	4617	4638	
3.5	4638	4646	
1	4646	4650	
5	4650	4657	
11	4657	4659	L

FACIES	TOP	BOTTOM	CYCLE
4	4659	4663	
6	4663	4685	
4	4685	4688	
1	4688	4688.5	
7	4688.5	4695.5	
6	4695.5	4701	M
5	4701	4705.5	
4	4705.5	4710	
3	4710	4713.5	
2	4713.5	4714.5	
3	4714.5	4734	
7	4734	4736	
3	4736	4743	
5	4743	4744	
11	4744	4747.5	EX
4	4747.5	4748.5	
5	4748.5	4757	
6	4757	4776.5	
5	4776.5	4780	
3	4780	4781	
11	4781	4783	LOST B.
6	4783	4791.5	
4	4791.5	4792.5	
2	4792.5	4794	
6	4794	4799	ALT

KEY FOR FACIES

1--BLACK SHALE
2--GRAY-GREEN SHALE
3--ARGILLACEOUS LIME WACKESTONE
3.5--DARK WACKESTONE
4--LIME WACKESTONE
4.5--MUDSTONE
5--LIME PACKSTONE
6--LIME GRAINSTONE
7--SILTY/SANDY SHALE
8--ARGILLACEOUS SANDSTONE
9--CLEAN SANDSTONE
10--COAL
11--PALEOSOL

Figure 5.B.7. Facies classification used in "gamma" inverse modeling procedure.

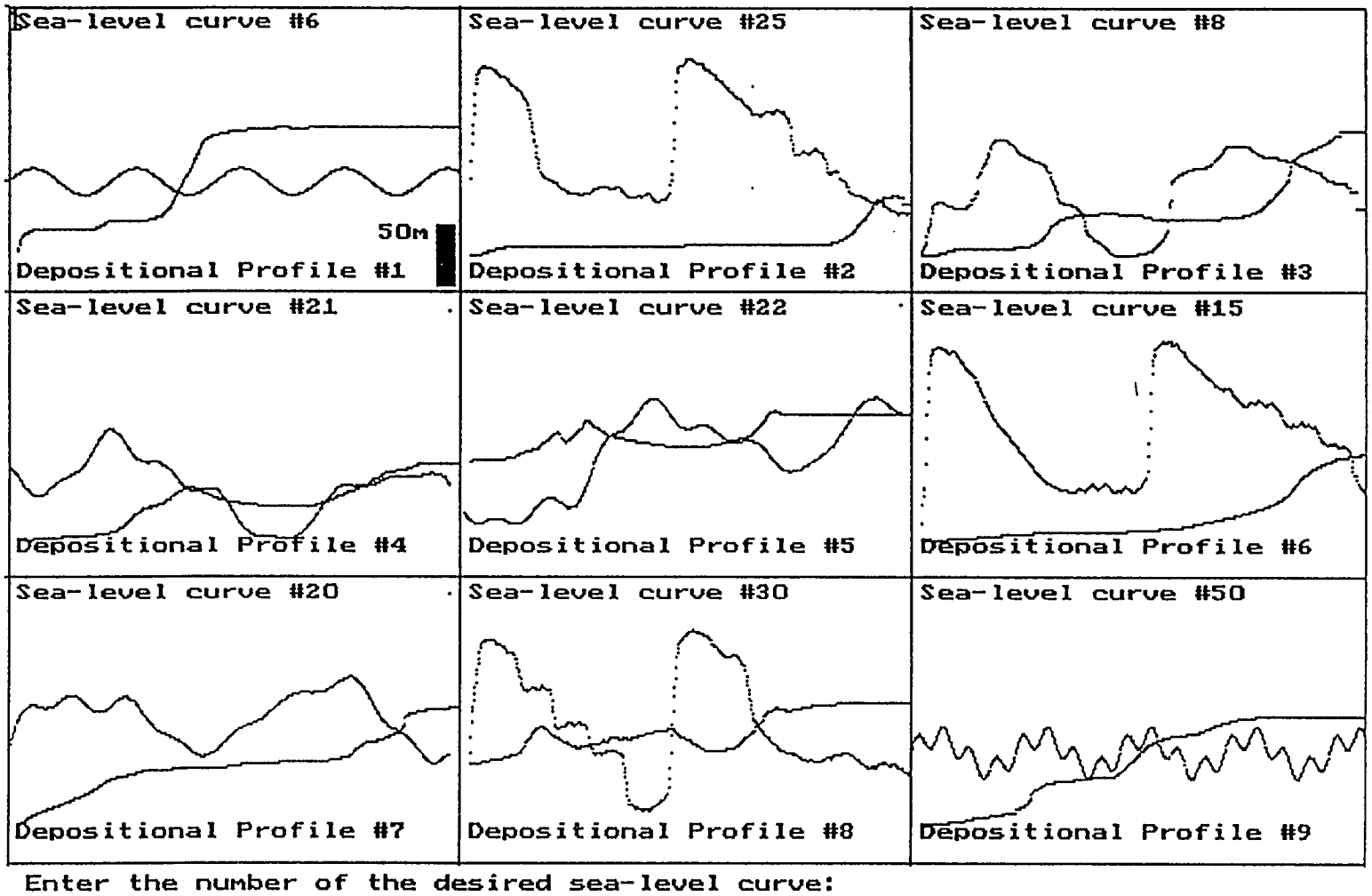

Figure 5.B.8. Menu screen showing choices when running the 2-D model.

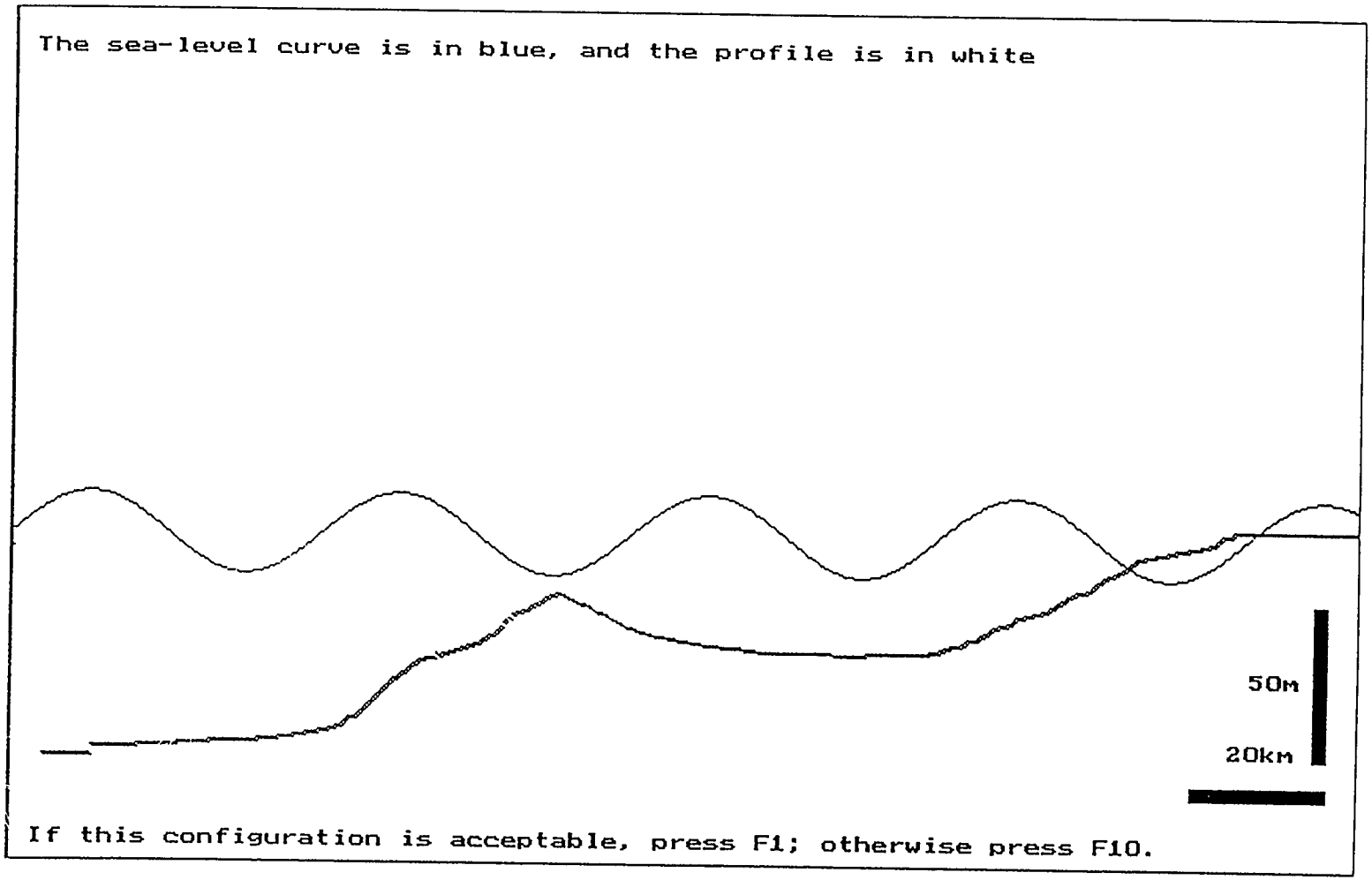

Figure 5.B.9. Curve/profile shown at large scale.

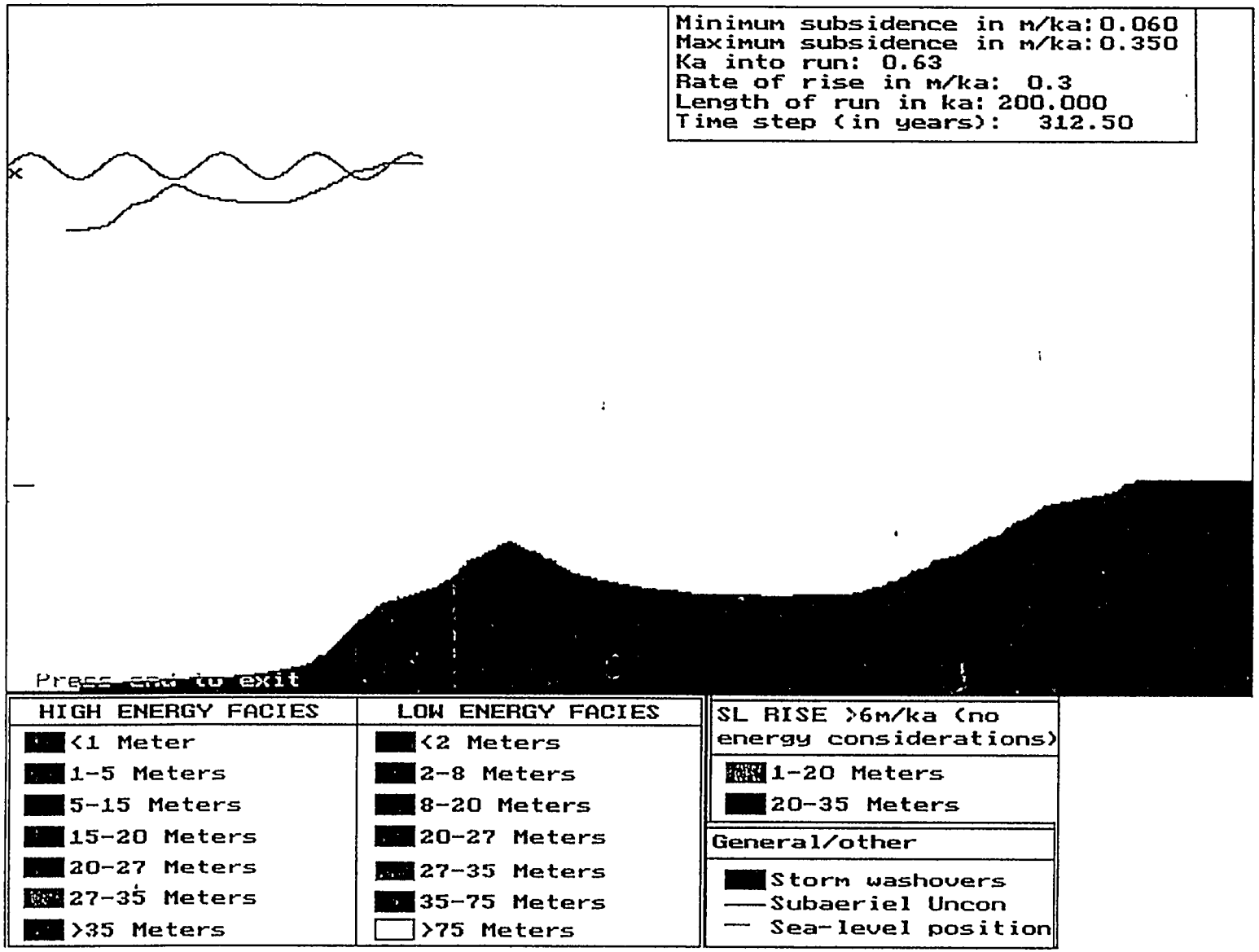

Figure 5.B.10. Screen showing profile selected with reduced version in upper left hand corner of screen.

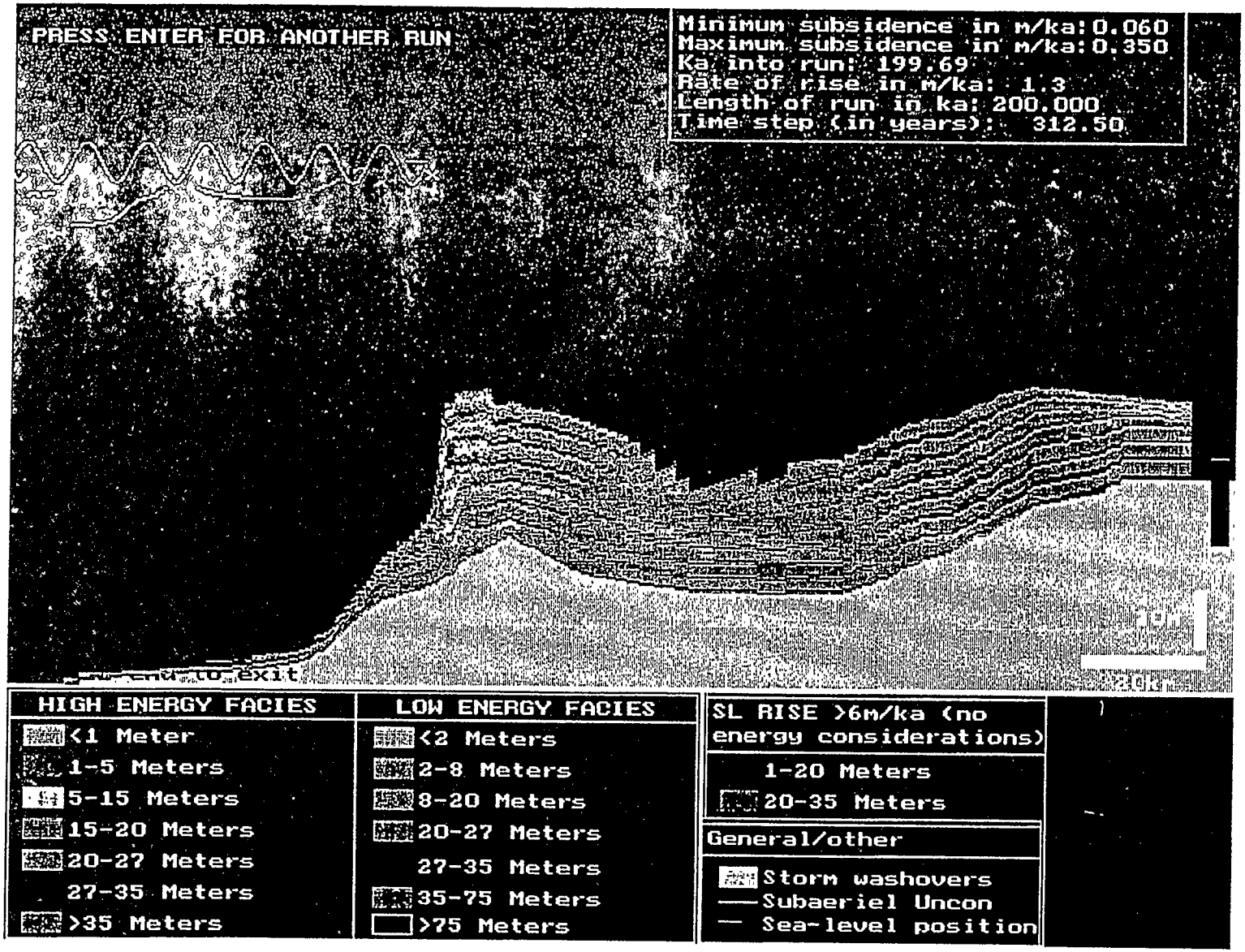

Figure 5.B.11. Example screen of finished model run.

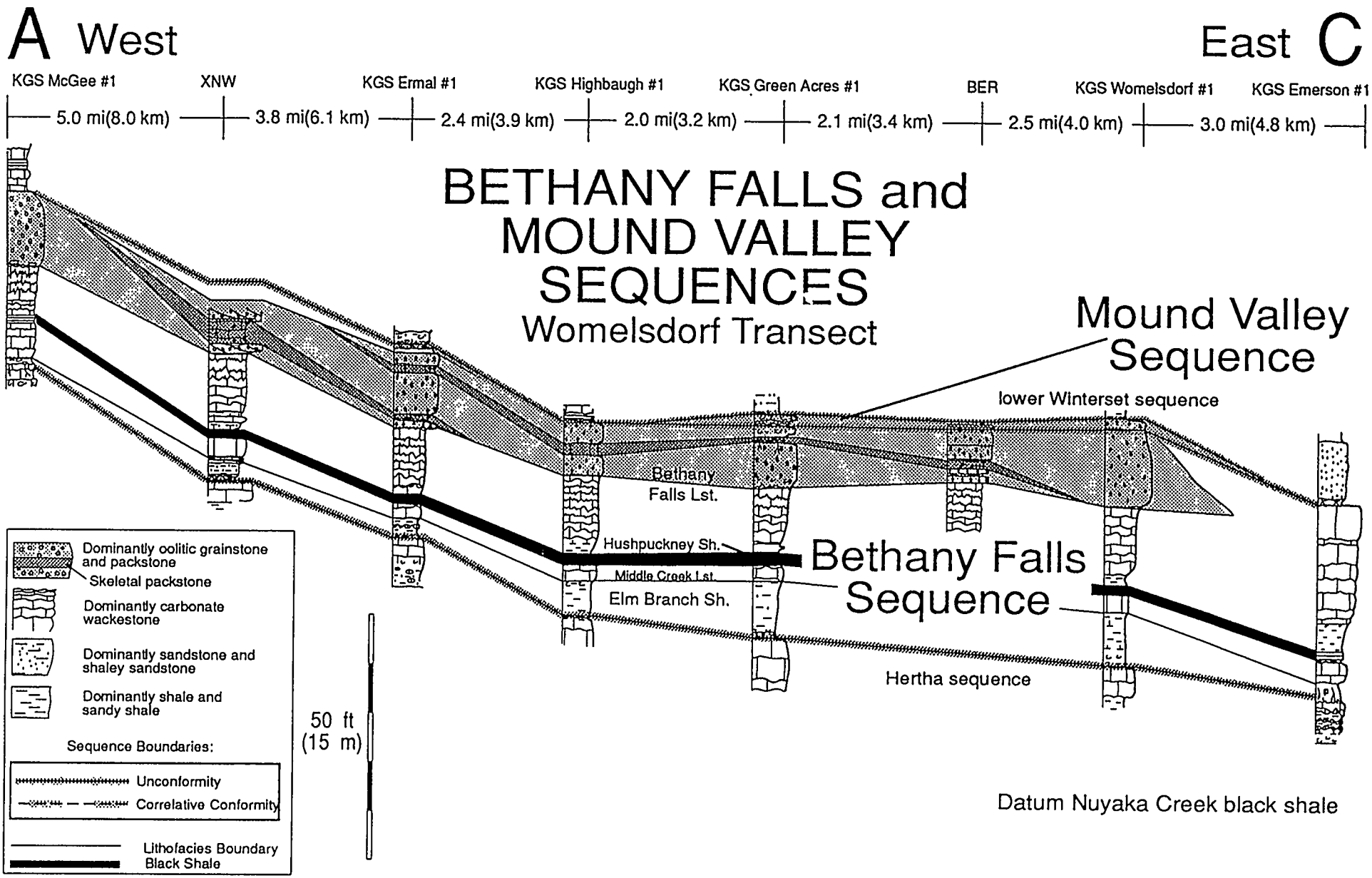

Figure 5.B.12. Diagrammatic core and outcrop cross section of the Bethany Falls and Mound Valley sequences in the southeastern Kansas analog area. This section shows three discrete oolie pods developed at different elevations on the Pleasanton slope.

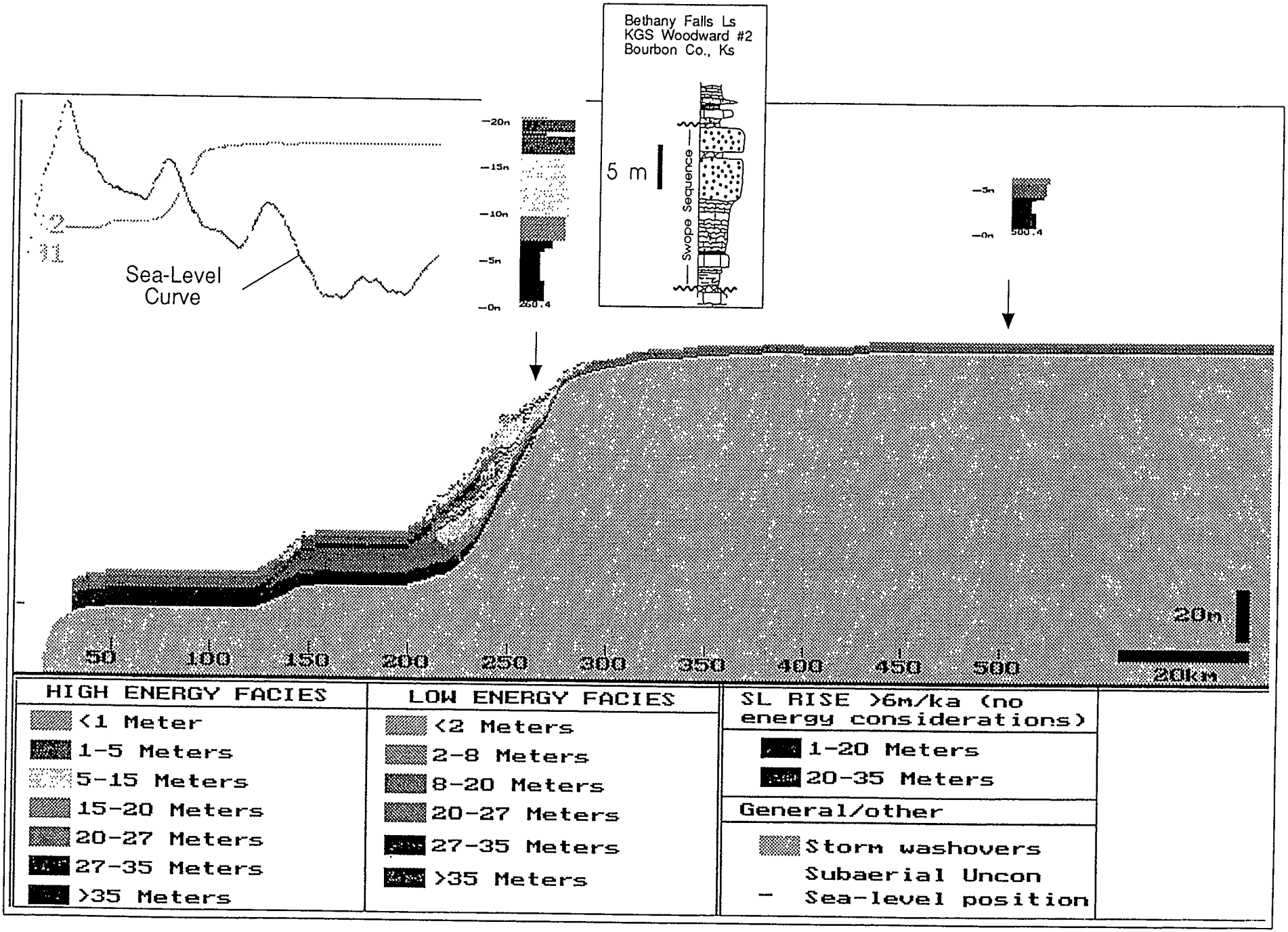

Figure 5.B.13. Two-dimensional stratigraphic simulation developed around sedimentation of the Swope sequence on an inclined slope created by the Pleasanton clastic wedge (analog study area in southeastern Kansas) (see cross section in Figure I.39). Note simulated stratigraphic columns in contrasting settings on slope and upper shelf. Actual stratigraphic column from Swope containing oolites is shown as inset next to synthetic column.

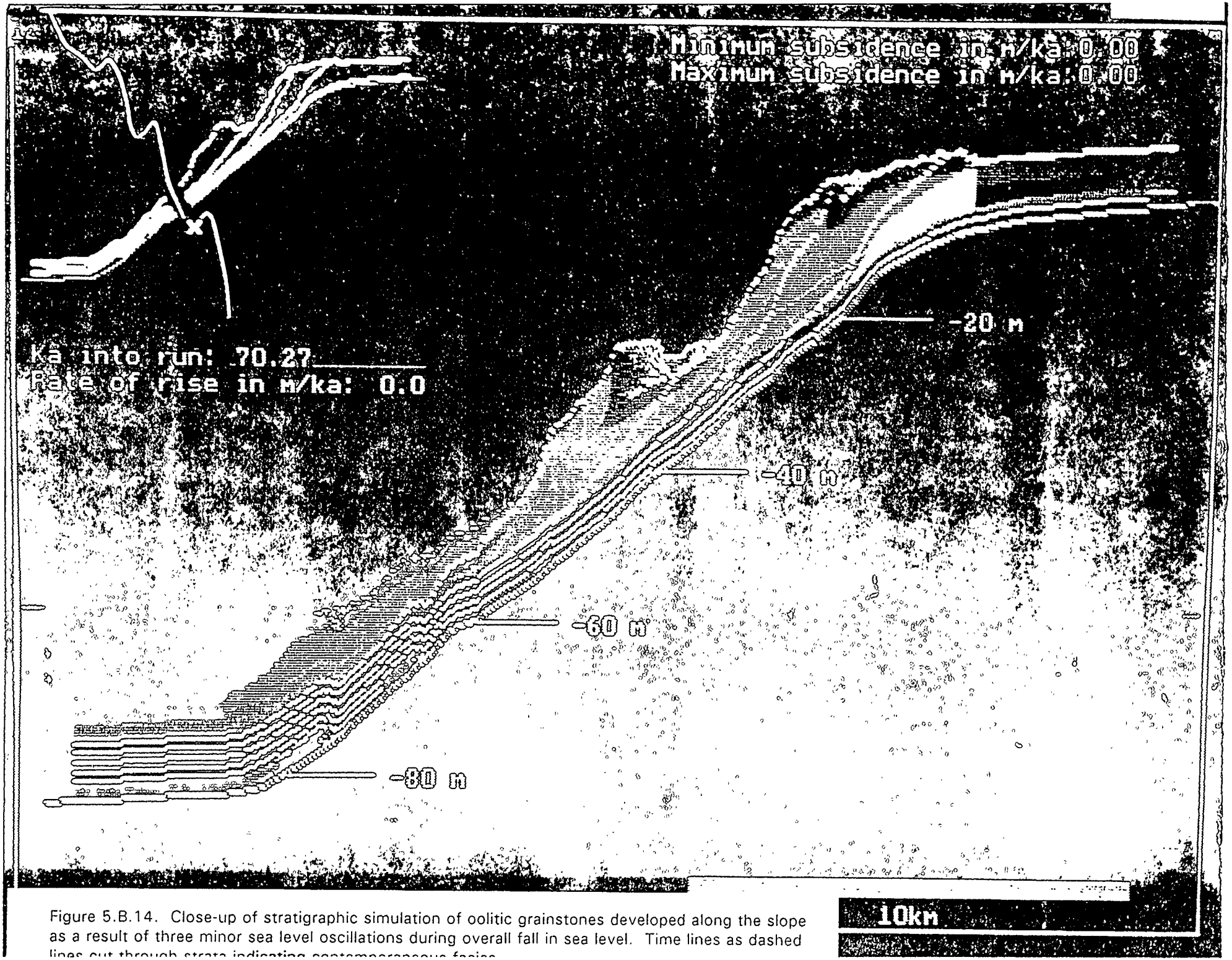

Figure 5.B.14. Close-up of stratigraphic simulation of oolitic grainstones developed along the slope as a result of three minor sea level oscillations during overall fall in sea level. Time lines as dashed lines cut through strata indicating contemporaneous facies.

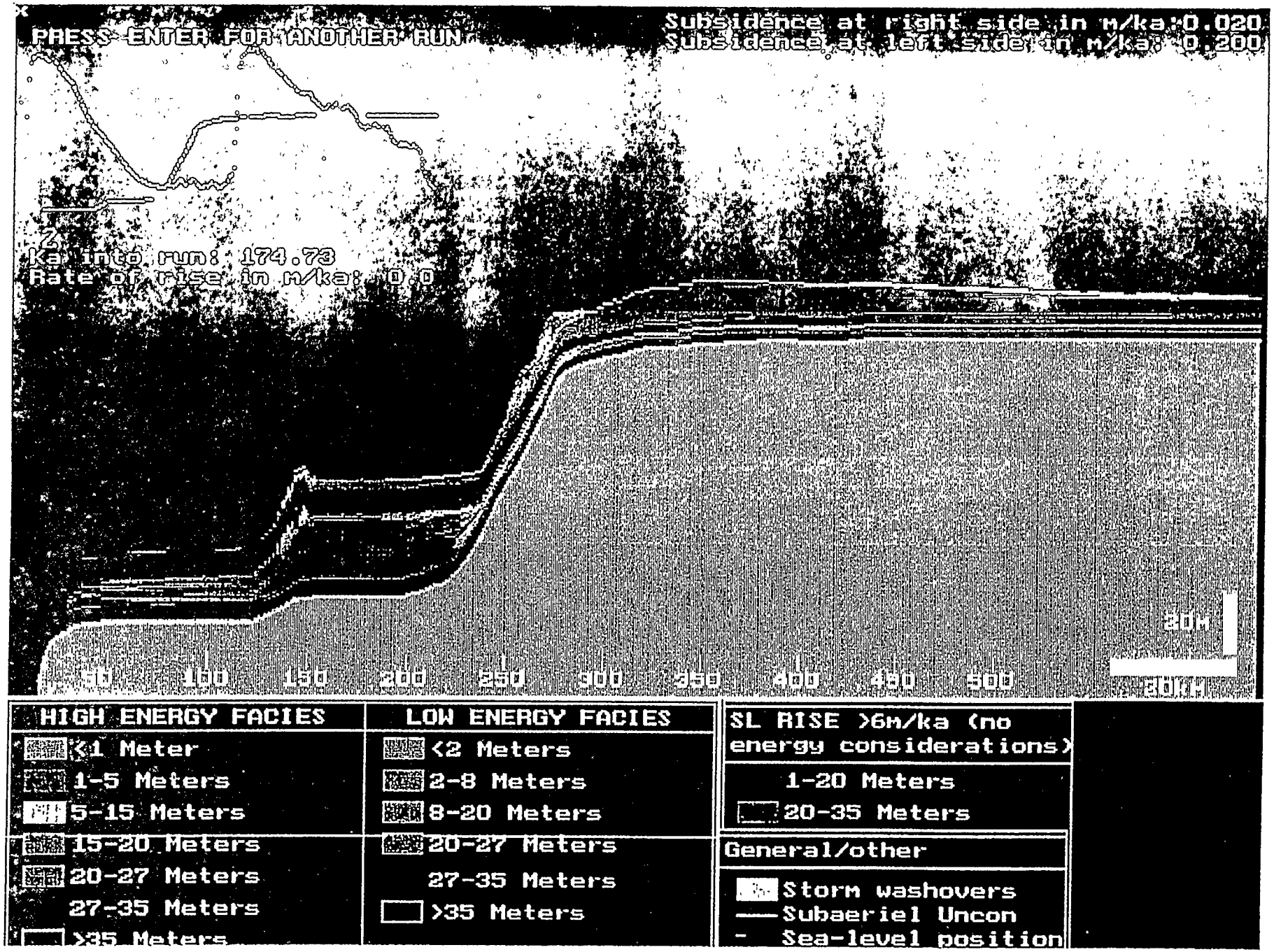

Figure 5.B.15. Two-dimensional model of Hertha and Swope sequences deposited over Pleasanton shelf-to-basin setting in eastern Kansas analog area. The Hertha bank developed down slope and the Swope oolite developed upslope, analogous to actual geometries. More detail is generated than can be shown on the screen image, consequently the generation of stratigraphic columns was developed to increase resolution of selected columns of pixels.

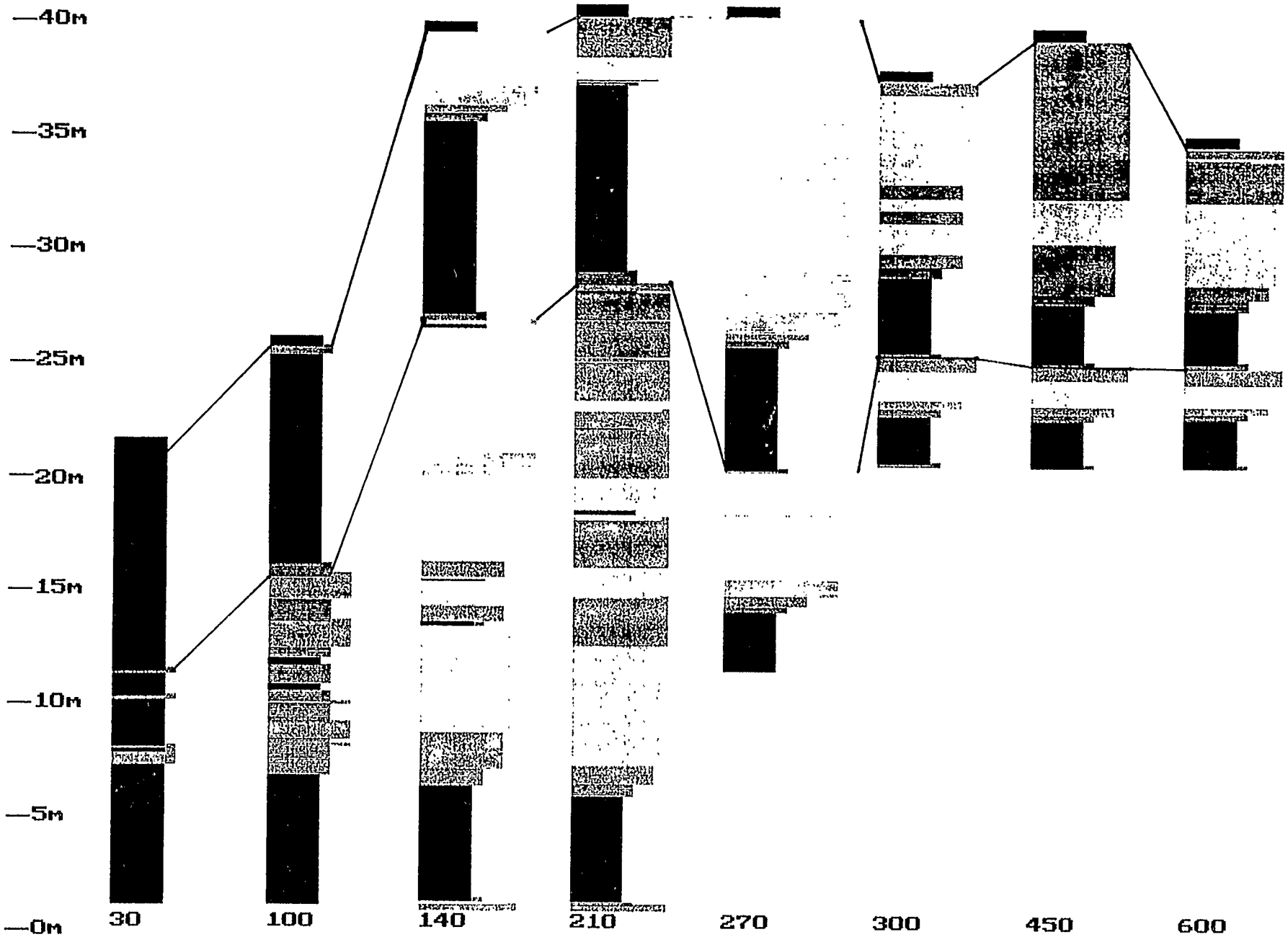

Figure 5.B.16. High-resolution output of the two-dimensional model produced by storing pixel information on facies and replotting the information as full stratigraphic columns. The 4th-order Hertha and Swope sequences displayed in Figure 5.B.15 are shown. Light toned facies are oolites reflecting slope position. Condensed sections are narrow black facies.

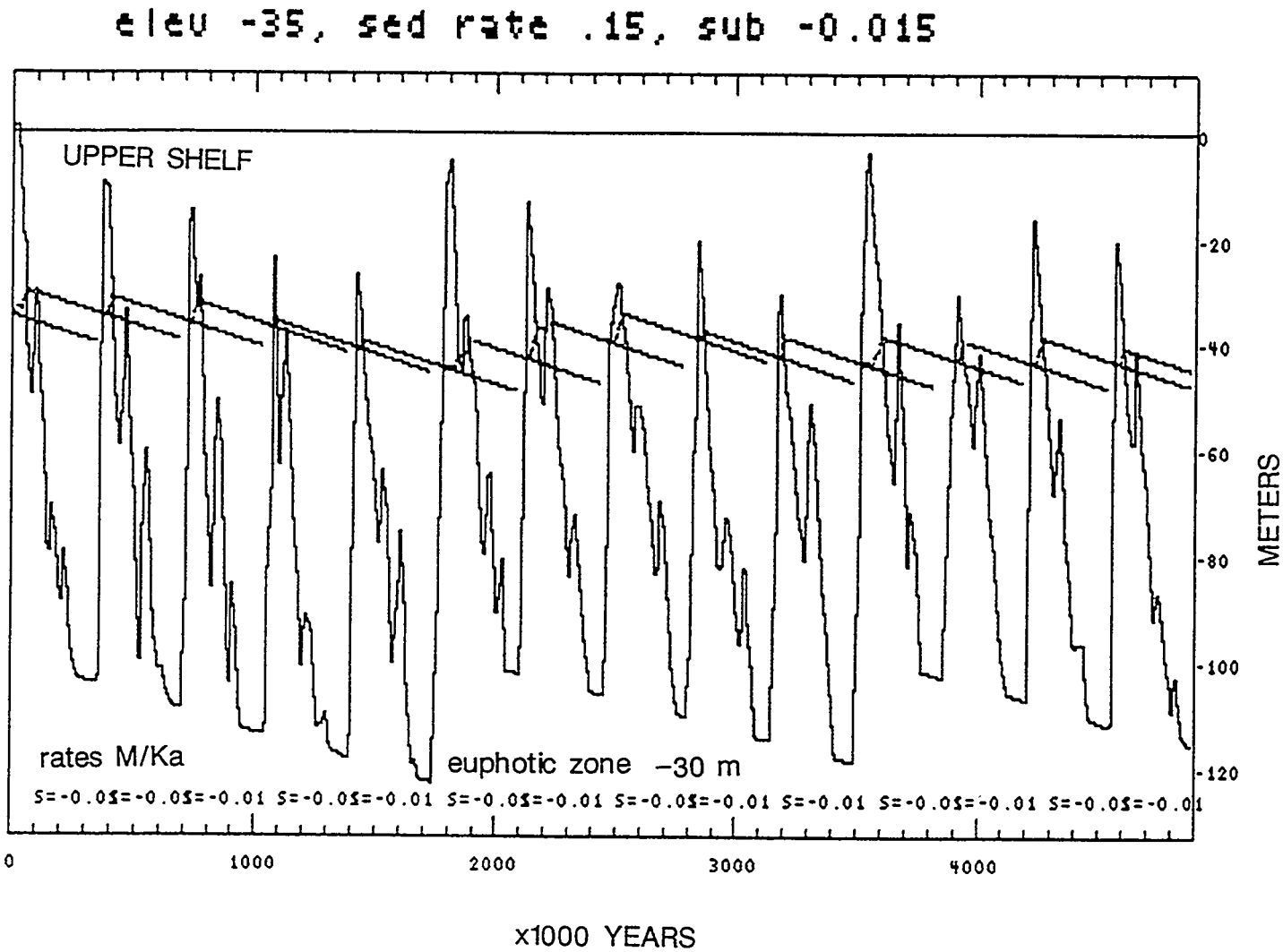

Figure 5.B.17. One-dimensional stratigraphic model showing interaction of 4th- and 3rd-order sea-level change. Inclined line segments at each 4th-order sea level cycle represent initial and ending sediment surfaces for each 4th-order cycle. This upper shelf presentation is defined by a high elevation relative to other sites on the shelf (-35 m, below maximum modeled sea level elevation), slow subsidence (-0.015 m/ka), and slower sediment accumulation rate (0.15 m/ka). Carbonate sedimentation terminates below water depths of 30 m (base of photic zone). The difference between the sea level curve and sediment surface is water depth, or the extent of emergence, as is often the case on the upper shelf. The net result of this high shelf position is production of thin 4th-order sedimentary sequences. These fourth-order cycles are thicker at initial stages of each 3rd-order cycle (bundles of 4th-order cycles).

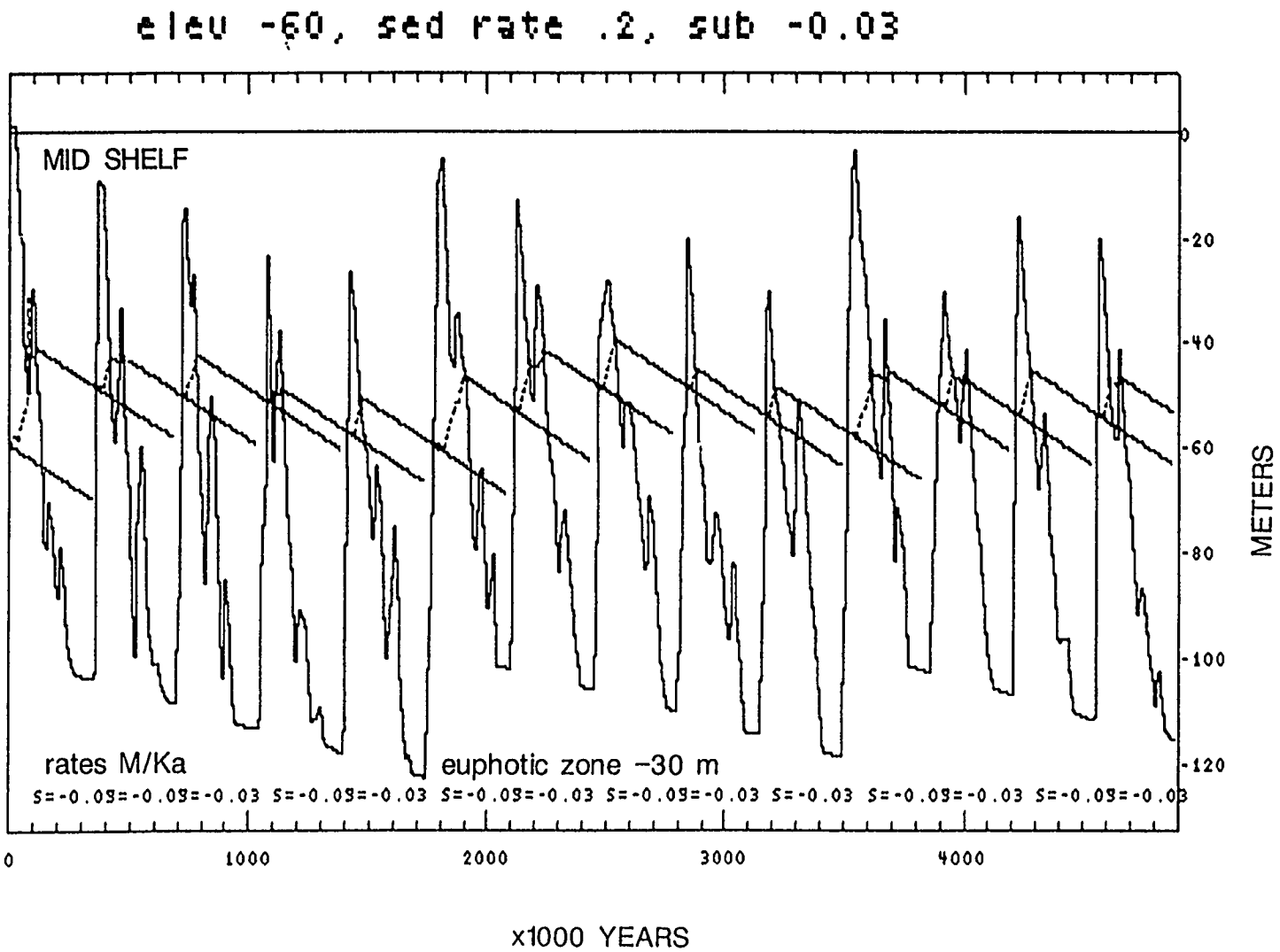

Figure 5.B.18. One-dimensional model at mid-shelf position with same sea level curve, decreased initial surface elevation, increased subsidence, and sediment accumulation rate producing noticeably thicker cycles.

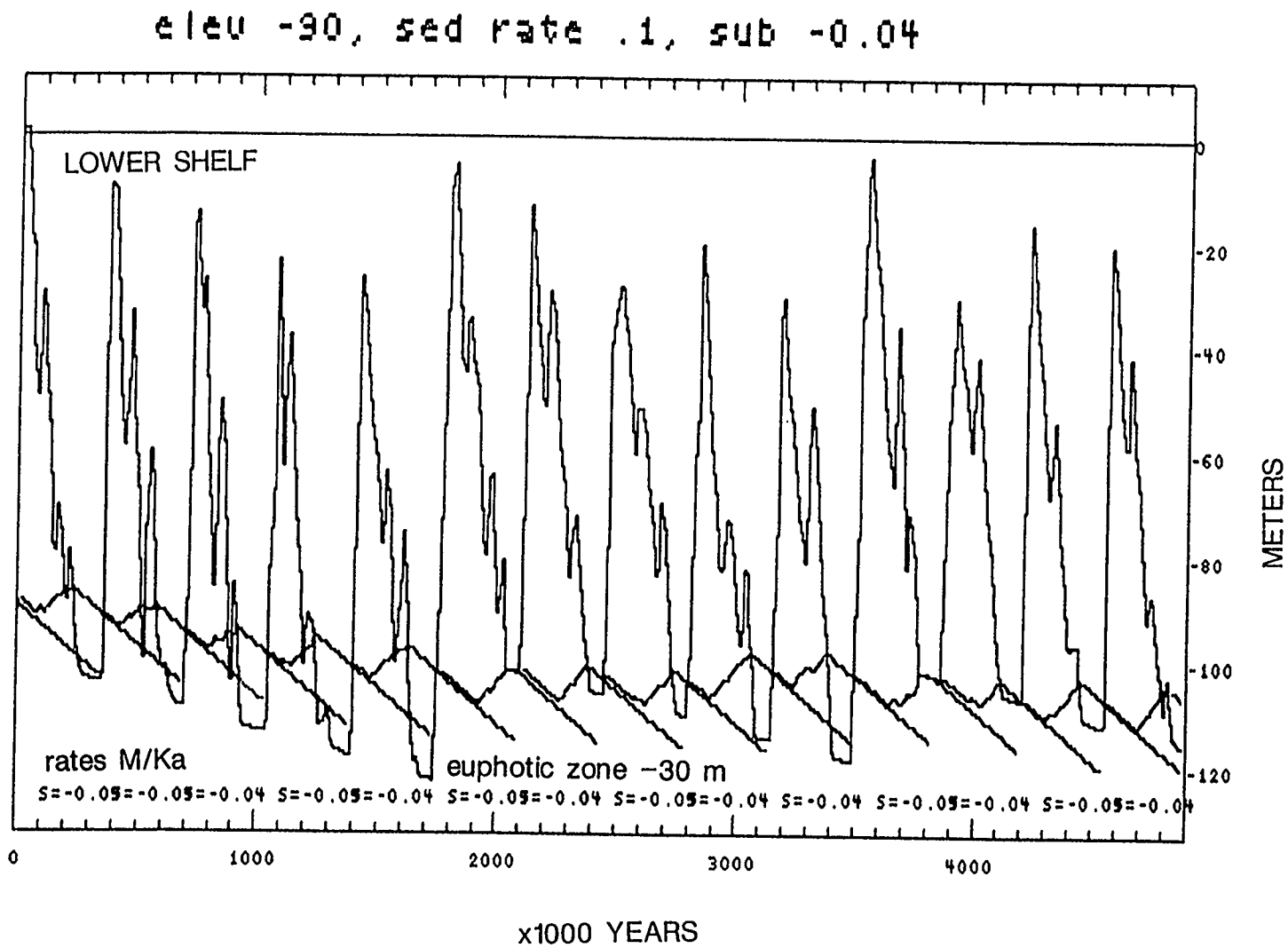

Figure 5.B.19. One-dimensional model at lower shelf position. Thicknesses of cycles are similar to the mid-shelf model. More time is spent in sediment starved conditions (>30 m water depth) during the duration of the lower shelf model, in contrast to more prolonged episodes of subaerial exposure in the upper shelf model.

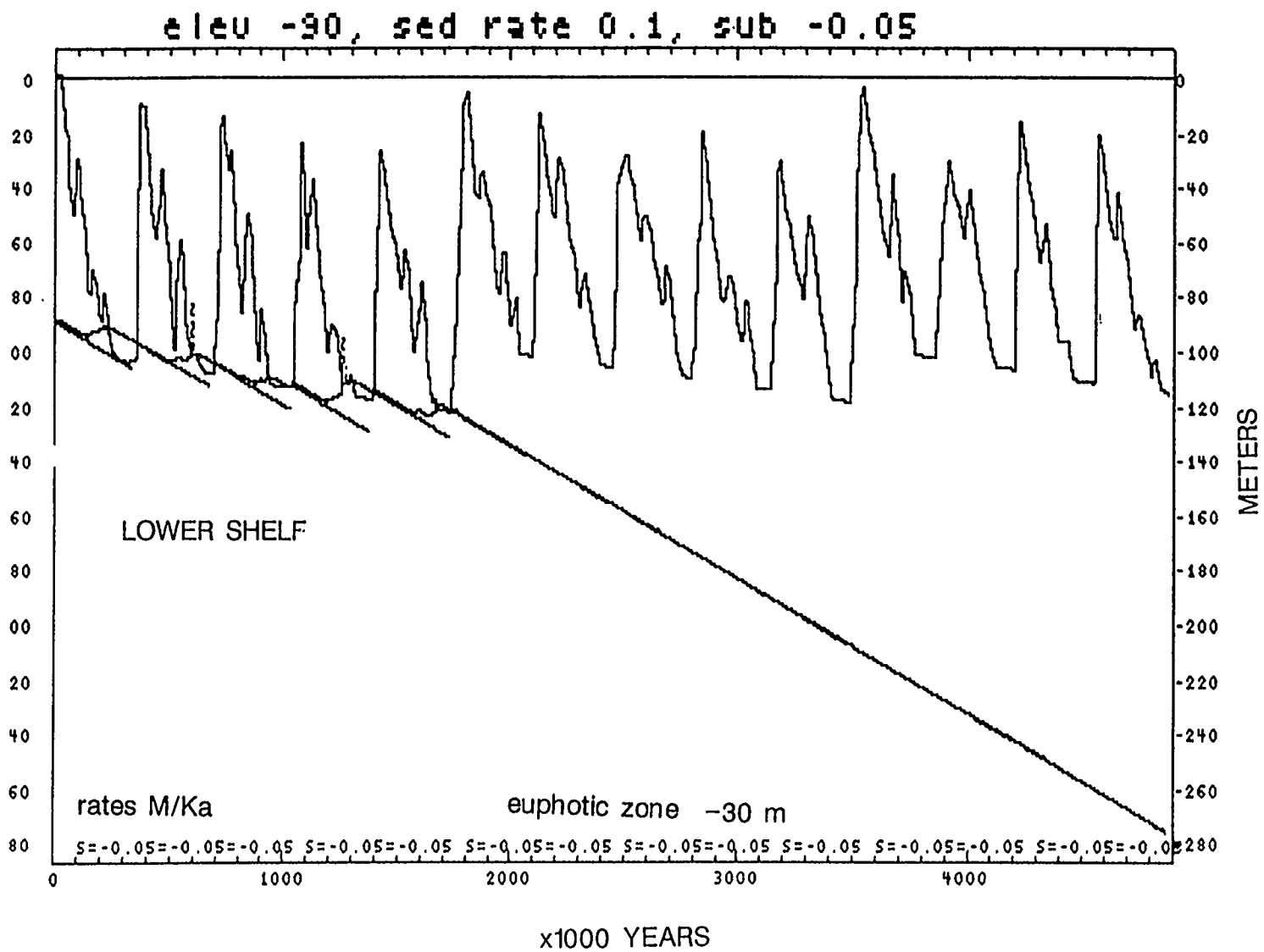

Figure 5.B.20. Lower shelf 1-D model where position has been drowned during a 3rd-order sea level rise of 20 m.

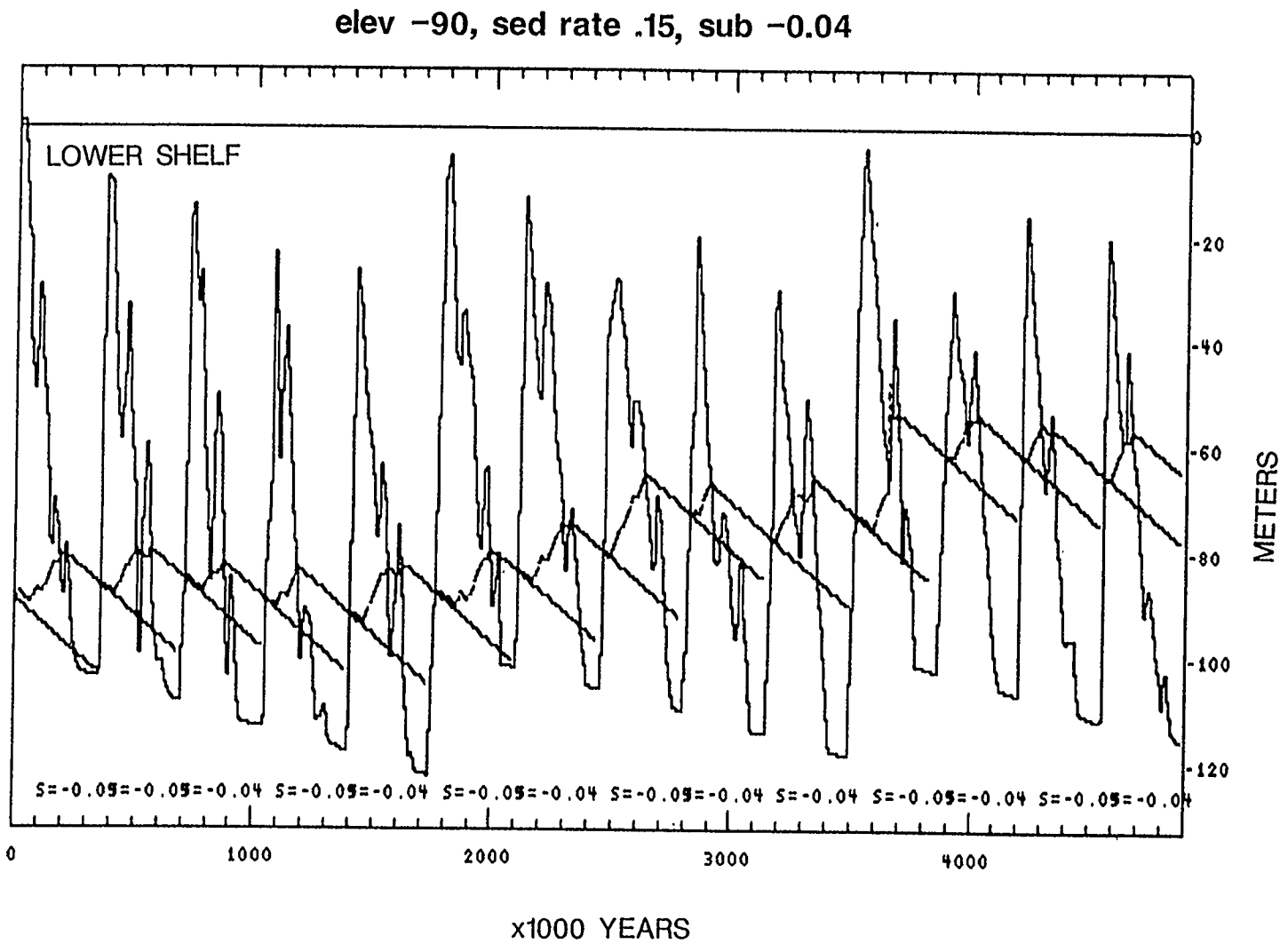

Figure 5.B.21. Lower shelf scenario where decreased sediment accumulation rate and lower subsidence result in a progressive rise in the sediment surface elevation through the course of the model run.

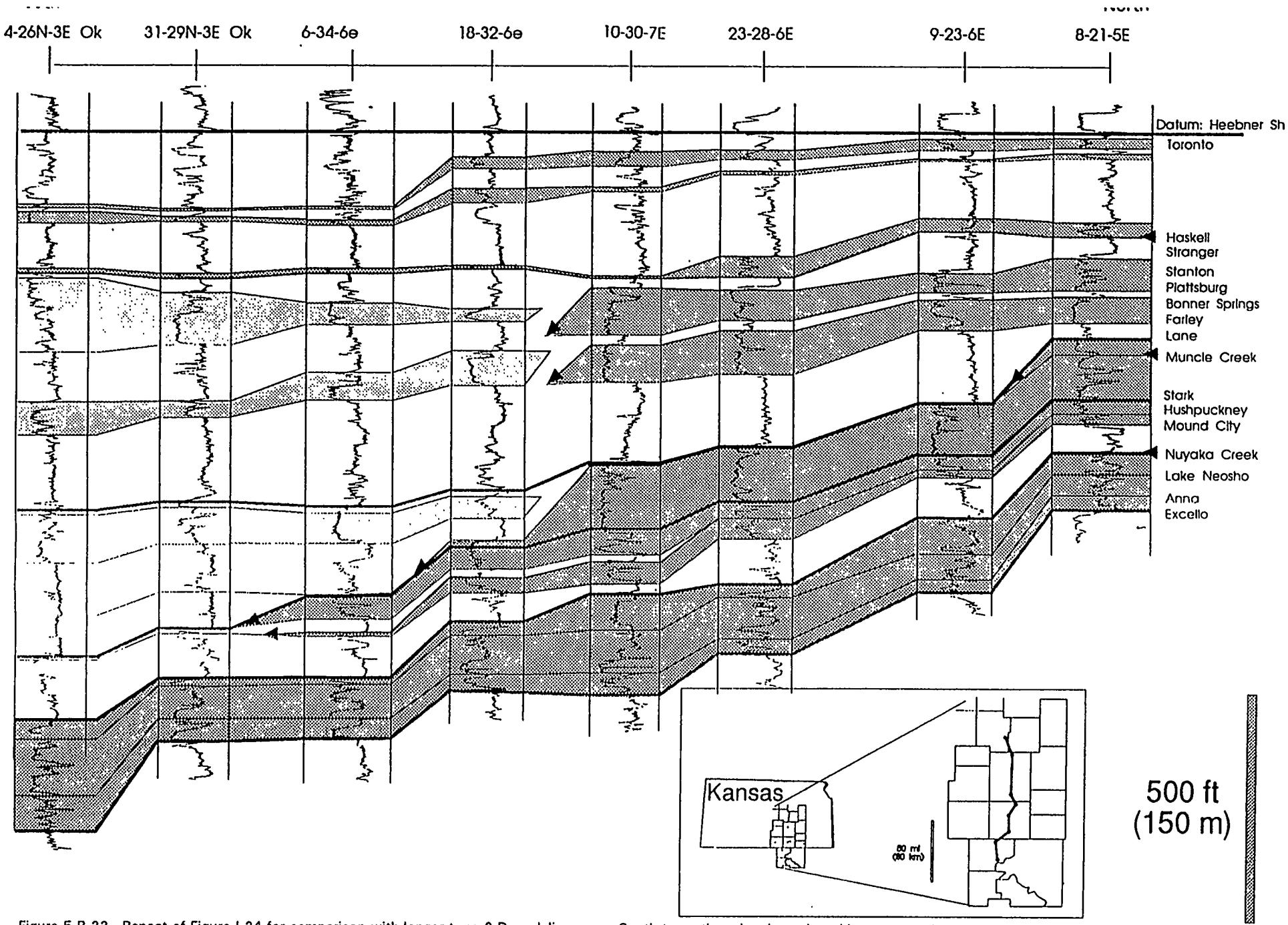

Figure 5.B.22. Repeat of Figure I.24 for comparison with longer-term 2-D modeling runs. South-to-north regional stratigraphic cross section datumed on the Heebner Shale for the Middle and Upper Pennsylvanian interval running approximately 125 miles (200 km) from northern Oklahoma to central Kansas. Gamma ray log traces and correlation of wells selected from regional sequence stratigraphic database showing shelf (right) to basin (left) transition where carbonate-dominated section gives way to siliciclastic rich section. Major thoroughgoing marine markers bounding 3rd-order cycles correspond to marked changes in the shelf margin. Sandstones are interpreted as lowstand deposits based on analogies with the surface and shallow subsurface analog areas. Dark screen = limestone; light screen = sandstone; white = shale and thin sandstone.

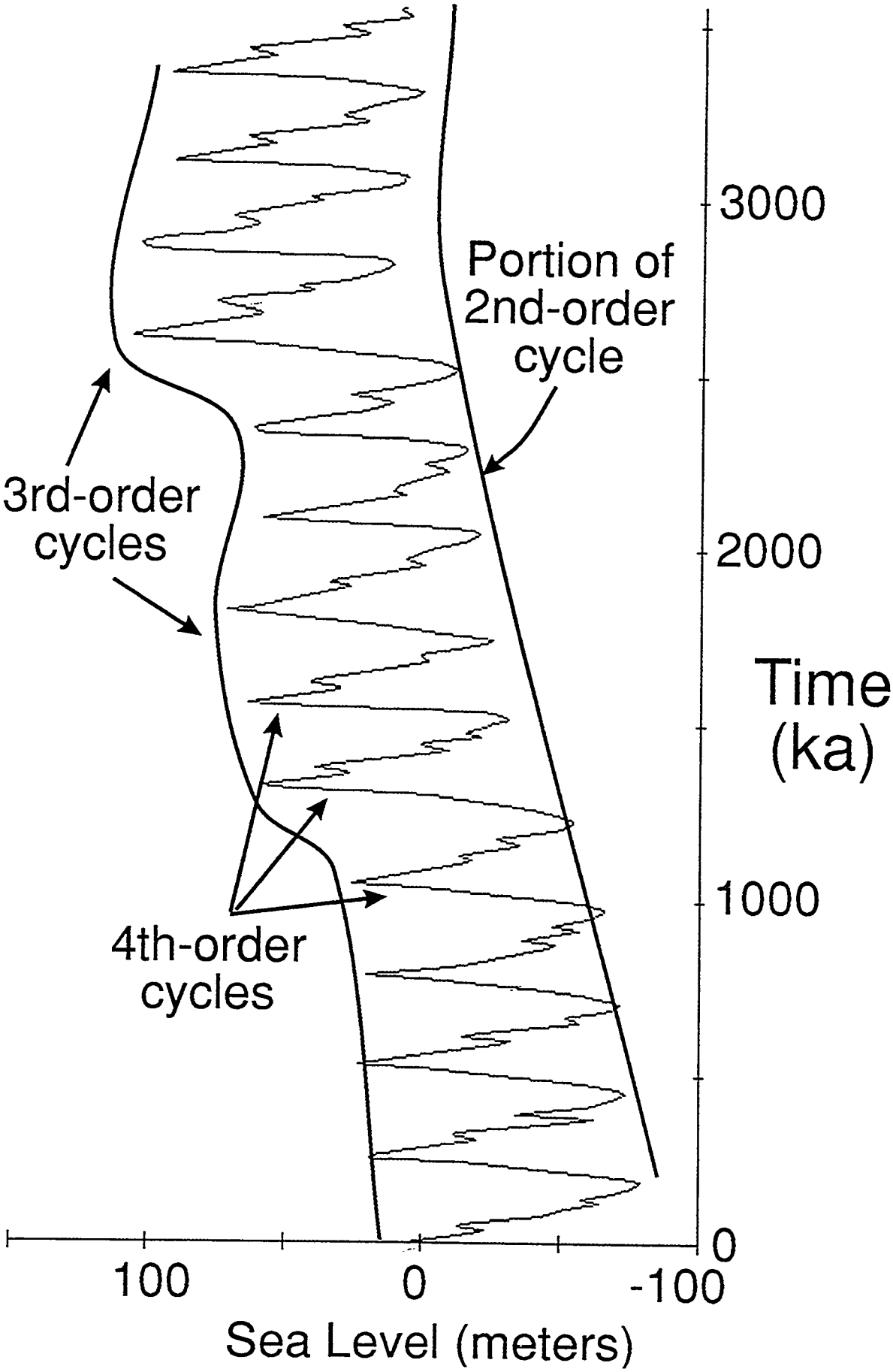

Figure 5.B.23. Sea-level curve used in long-term 2-D computer simulation. Curve includes composite 3rd- and 4th-order cycles based on relative sea level history as estimated from cross sections, Th/U ratio, and Fischer accommodation plots.

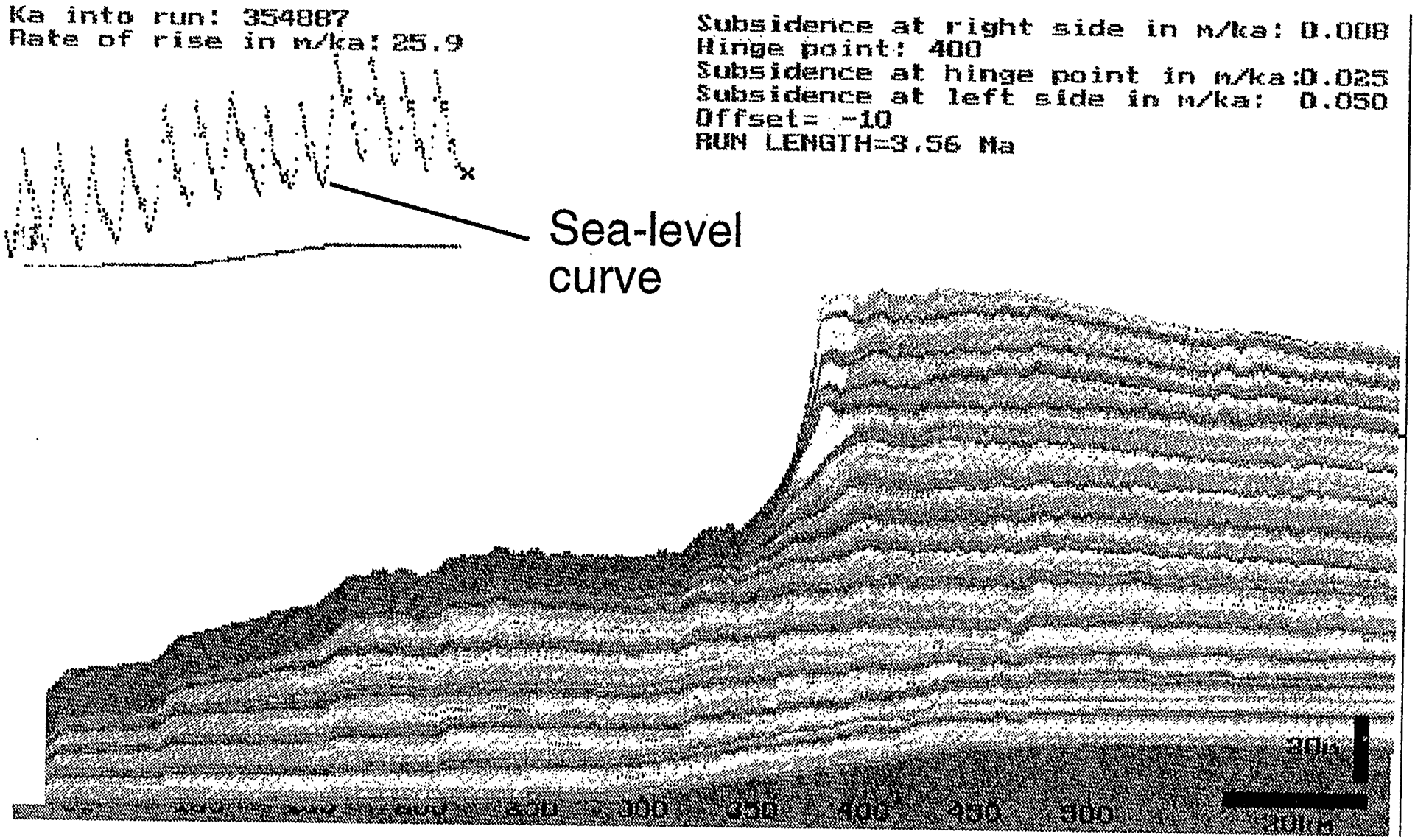

Figure 5.B.24. Lareg time and distance 2-D simulation model run to test sea-level curve shown in Figure 5.B.23. This run uses 2nd-, 3rd-, and 4th-order cyclicity abd subsidence rates comparable to those derived from this study, with a hinge zone located at the 400-km mark of this 600-km-long profile. The simulated stratigraphic framework closely resembles the internal and external stratigraphic framework of the Marmaton, Kansas City, and Lansing 3rd-order cycles as disussed in the text. Compare to the log section shown in figure 5.B.22.

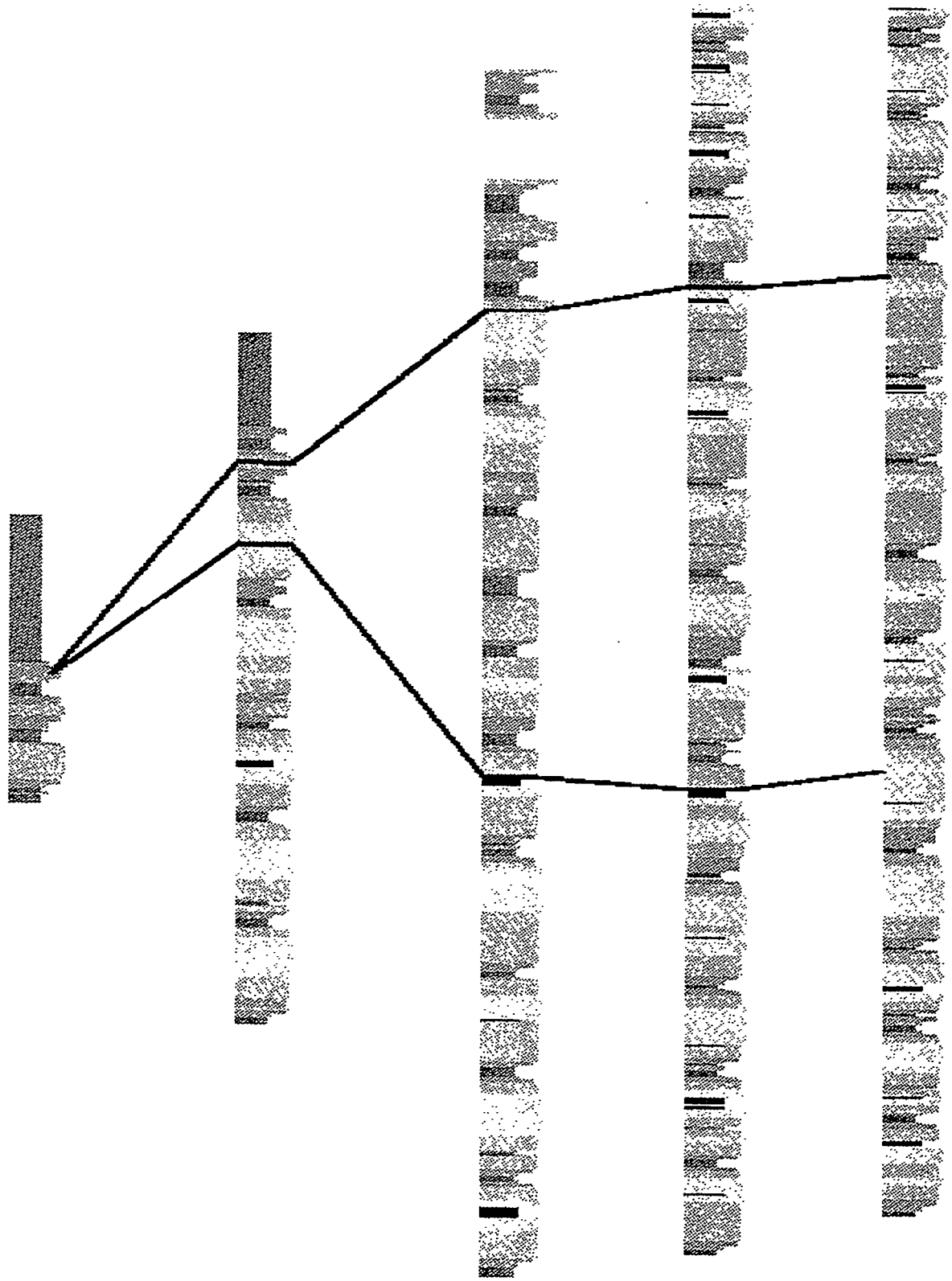

Figure 5.B.25. Selected stratigraphic columns generated along profile shown in figure 5.B.24. Lines connect 3rd-order sequence boundaries.

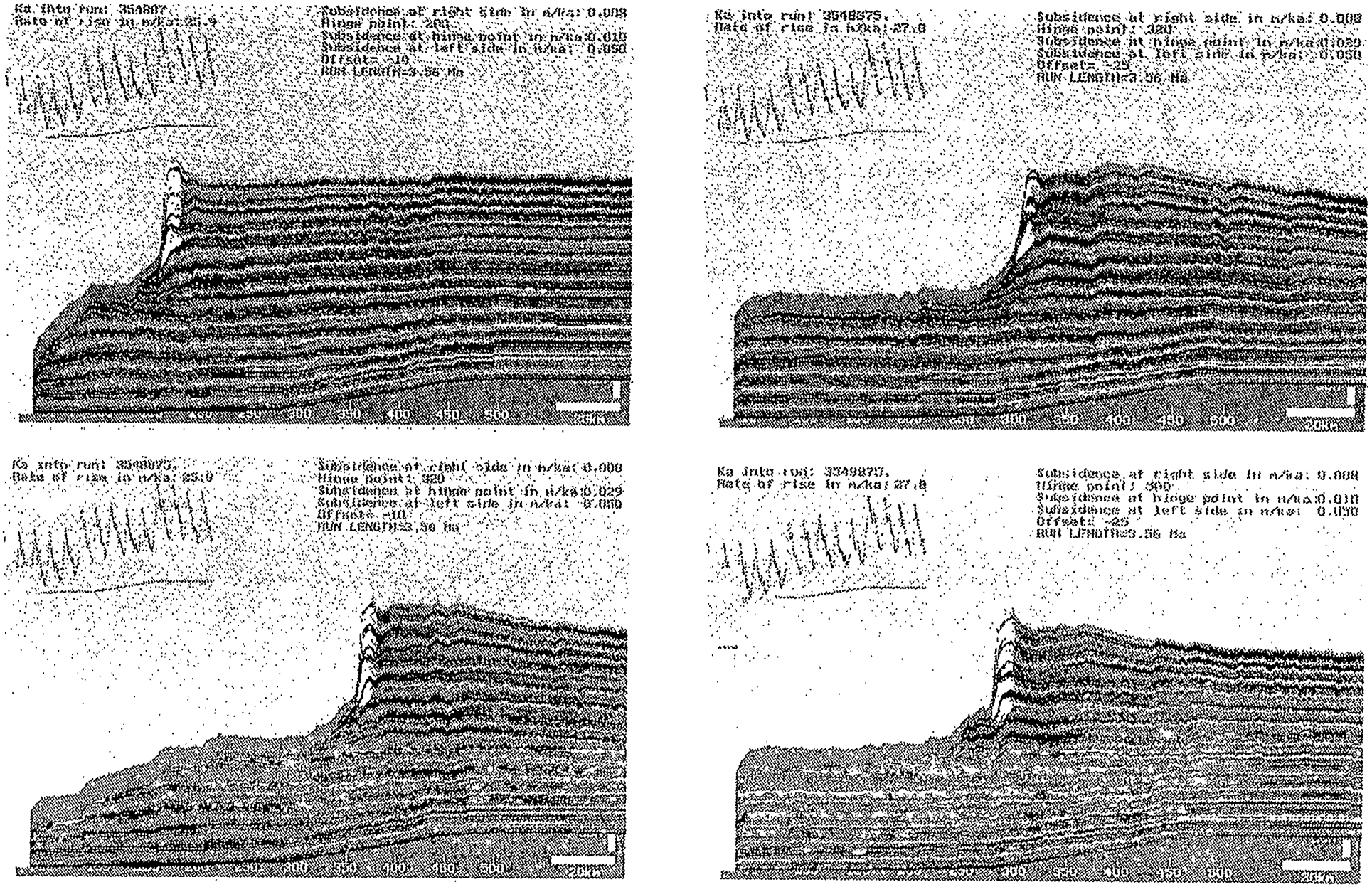

Figure 5.B.26. Four additional stratigraphic simulation scenarios for same initial shelf profile, varying one parameter while holding other parameters constant.

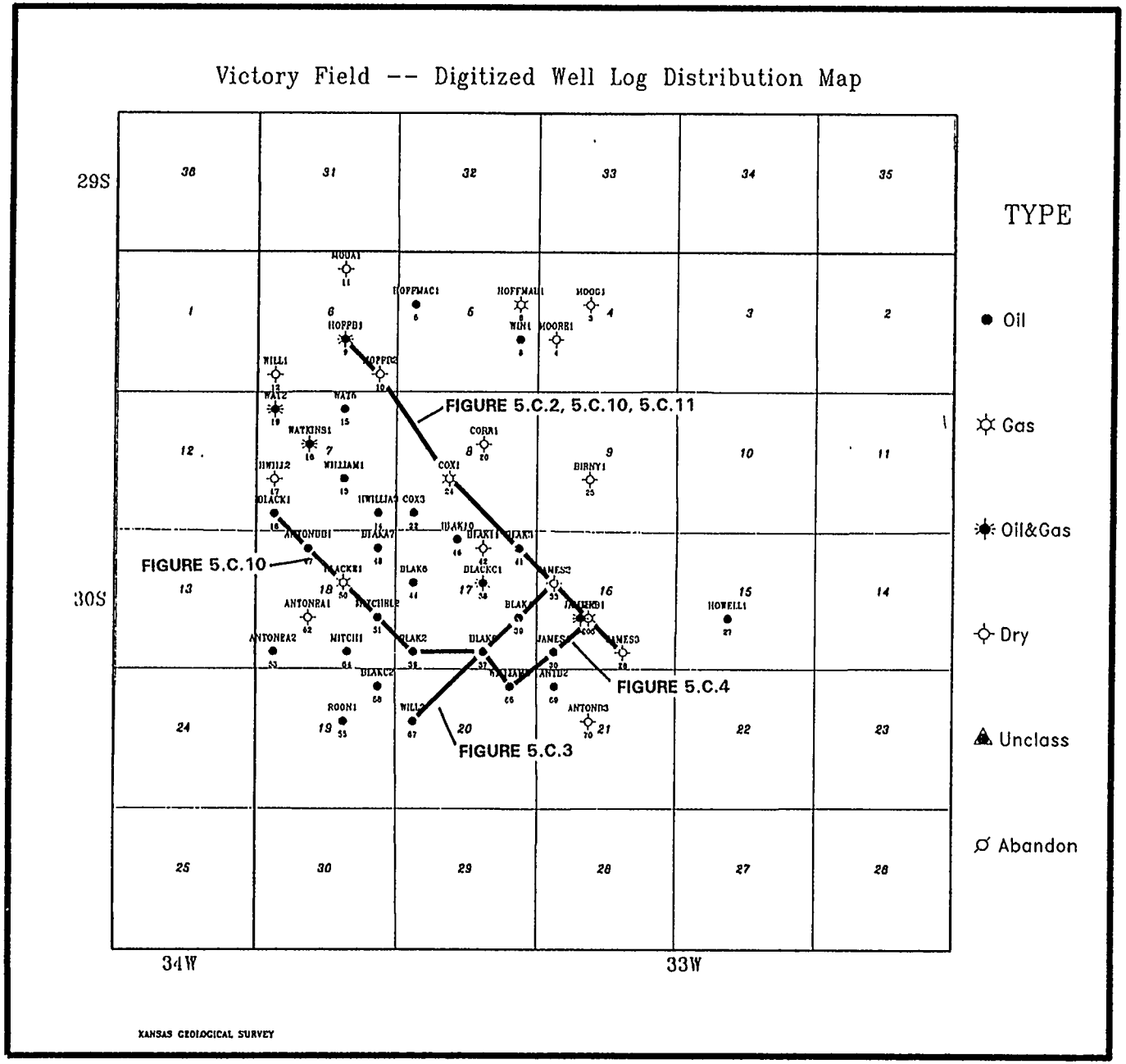

Figure 5.C.1. Index map of Victory field showing wells included in digitizing.

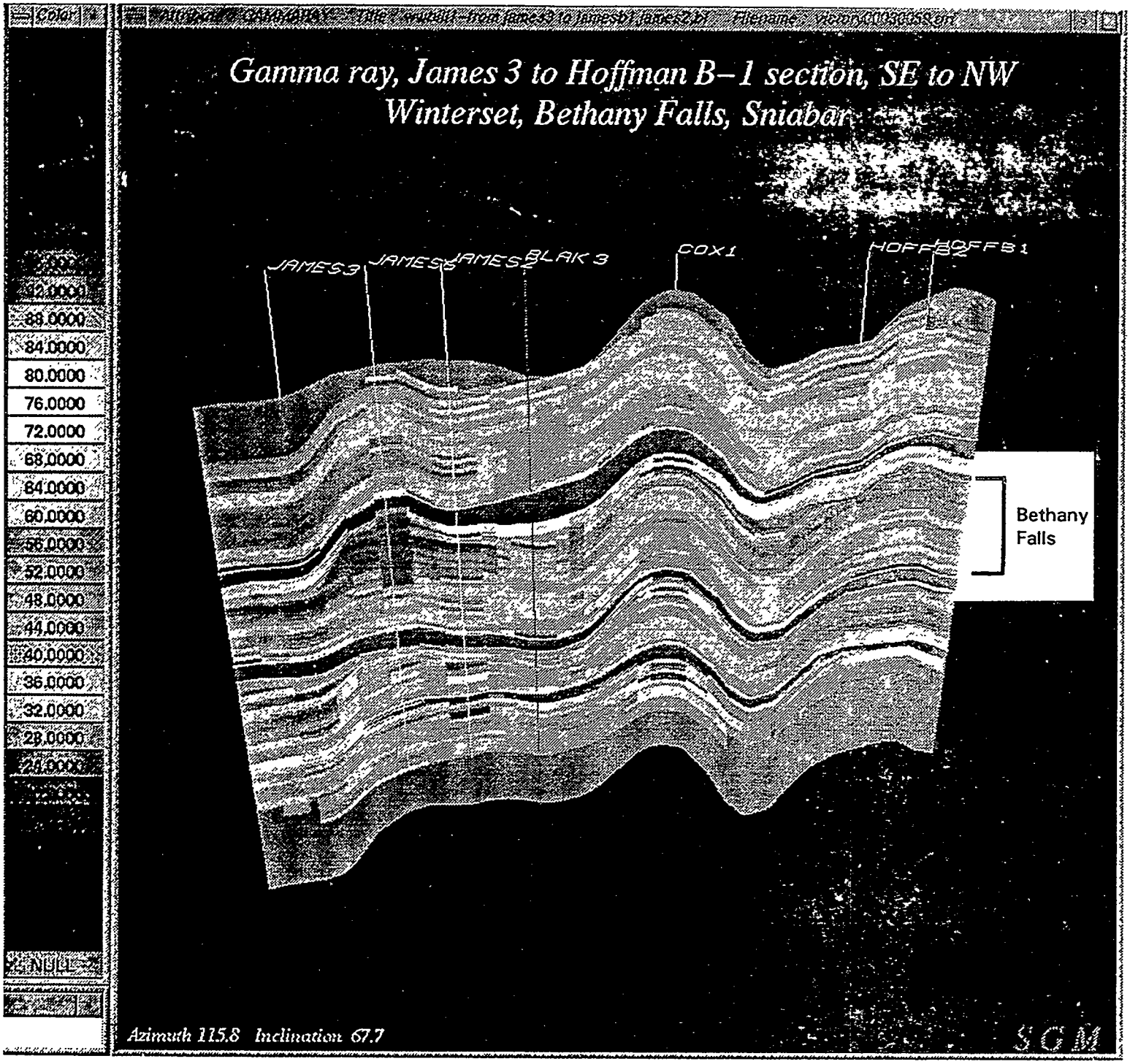

Figure 5.C.2. Southeast-to-northwest computer-constructed gamma ray cross section between wells as labeled on base map in Figure 5.C.1. Structural datumed section runs from Nuyaka Creek Shale at the base to lower Dennis Sequence at the top. Three higher radioactive marine shales are visible in this gray level presentation. Bethany Falls Limestone is below the first radioactive shale. Constructed with Stratamodel™ software.

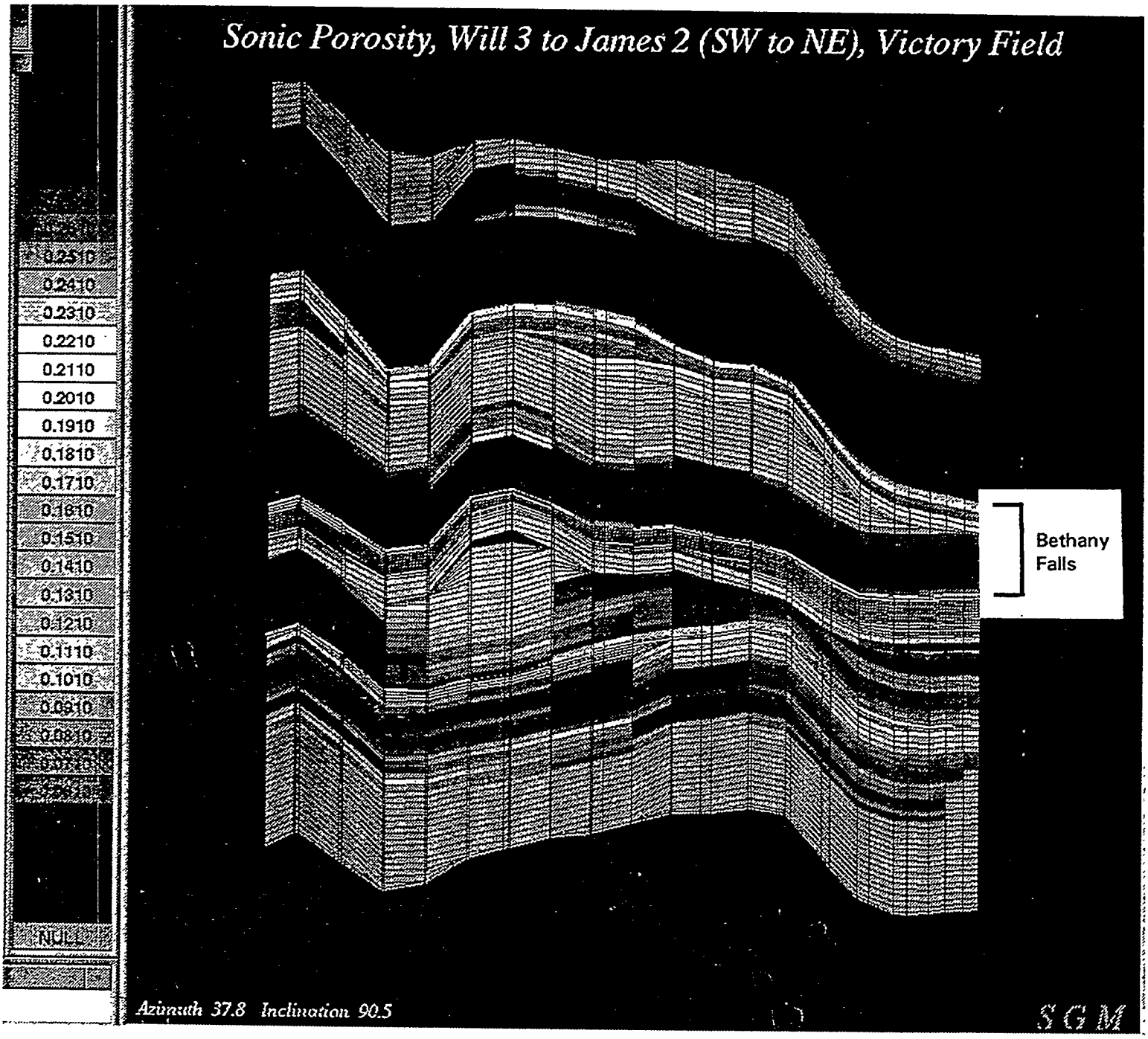

Figure 5.C.3. Southwest-to-northeast structural cross section showing sonic porosity between Will #3 and James #2 wells indexed in Figure 5.C.1. Bethany Falls Limestone interval is labeled. Cells are shown, including 2 ft. layers through the Bethany Falls Limestone. Truncation model in the Bethany Falls makes cells parallel to the base and truncated at the top. Higher porosity at the top is oolitic grainstone thinning markedly to the northeast. Constructed with Stratamodel™ software.

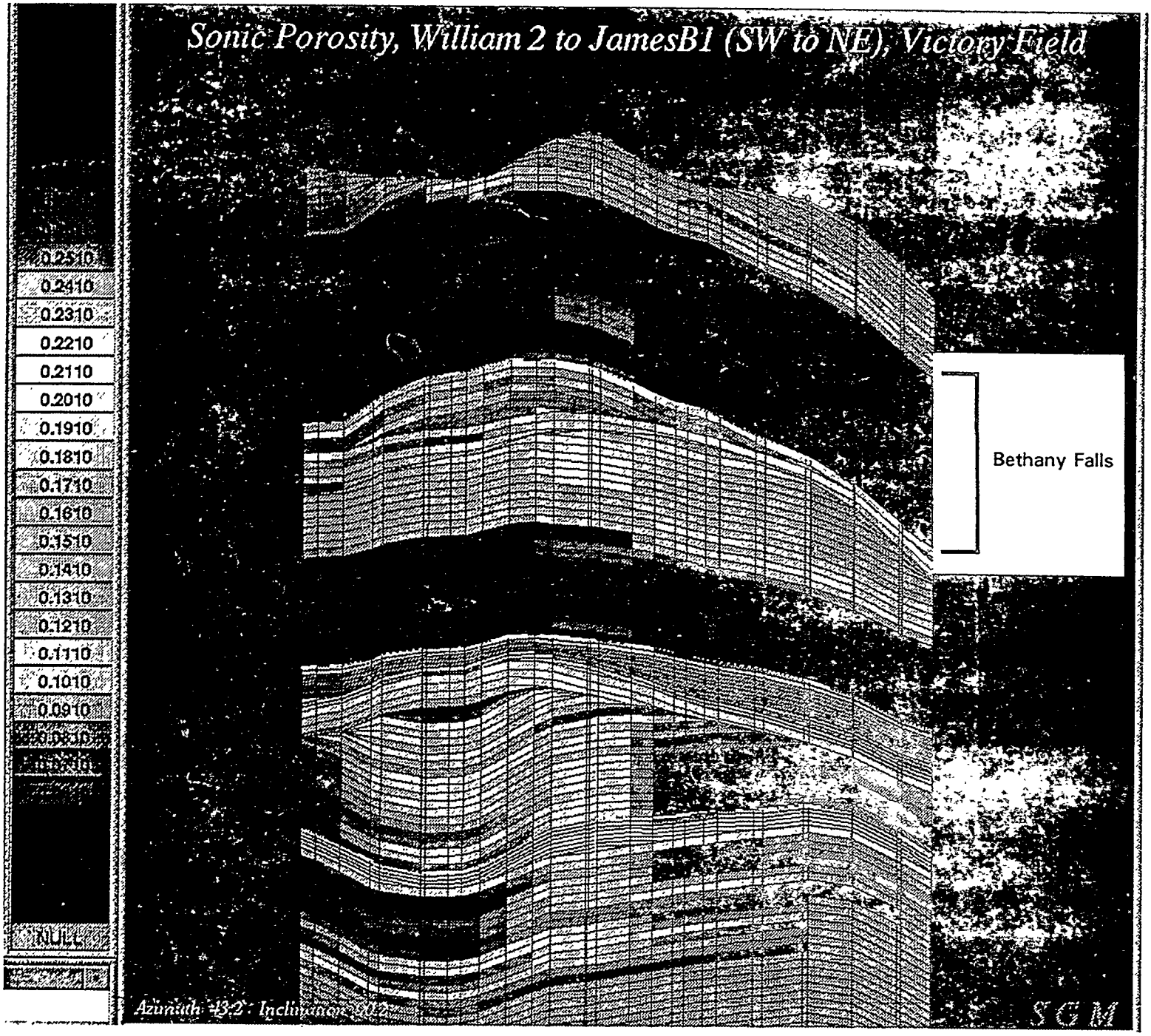

Figure 5.C.4. Southwest-to-northeast structural cross section showing sonic porosity between William #2 and James #B1 wells indexed in Figure 5.C.1. Bethany Falls Limestone interval is labeled. Constructed with Stratamodel™ software.

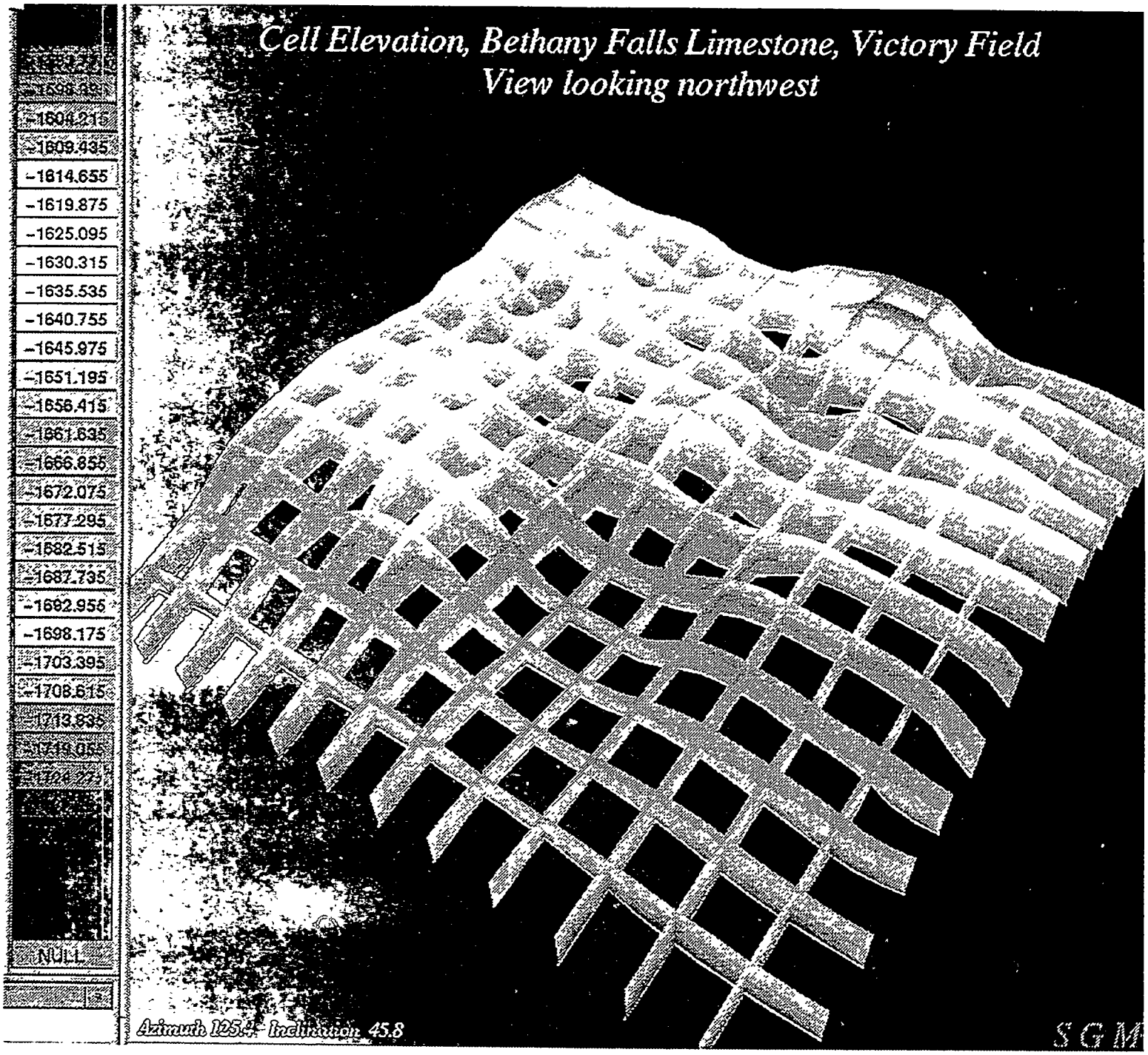

Figure 5.C.5. 3-D panel looking northwest showing elevation of cells in the Bethany Falls interval. Constructed with Stratamodel™ software.

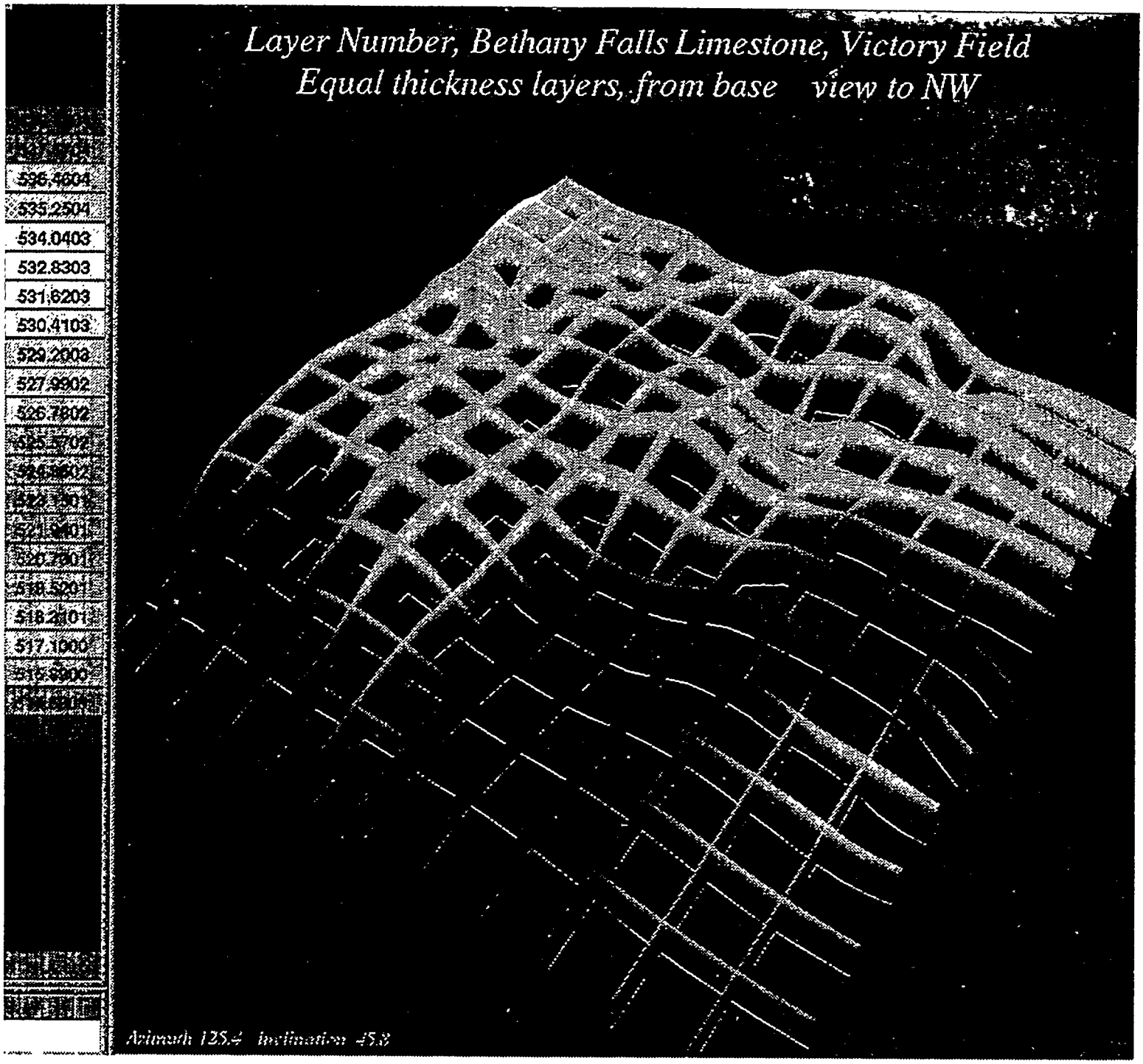

Figure 5.C.6. 3-D panel showing layer numbers for the Bethany Falls interval. Higher elevations as seen in Figure 5.C.5 correspond to areas with additional layers. Layers added from the top in the section occupied by porous oolitic grainstone. Panel configured as a structural elevation indicating close correspondence between all three elements.

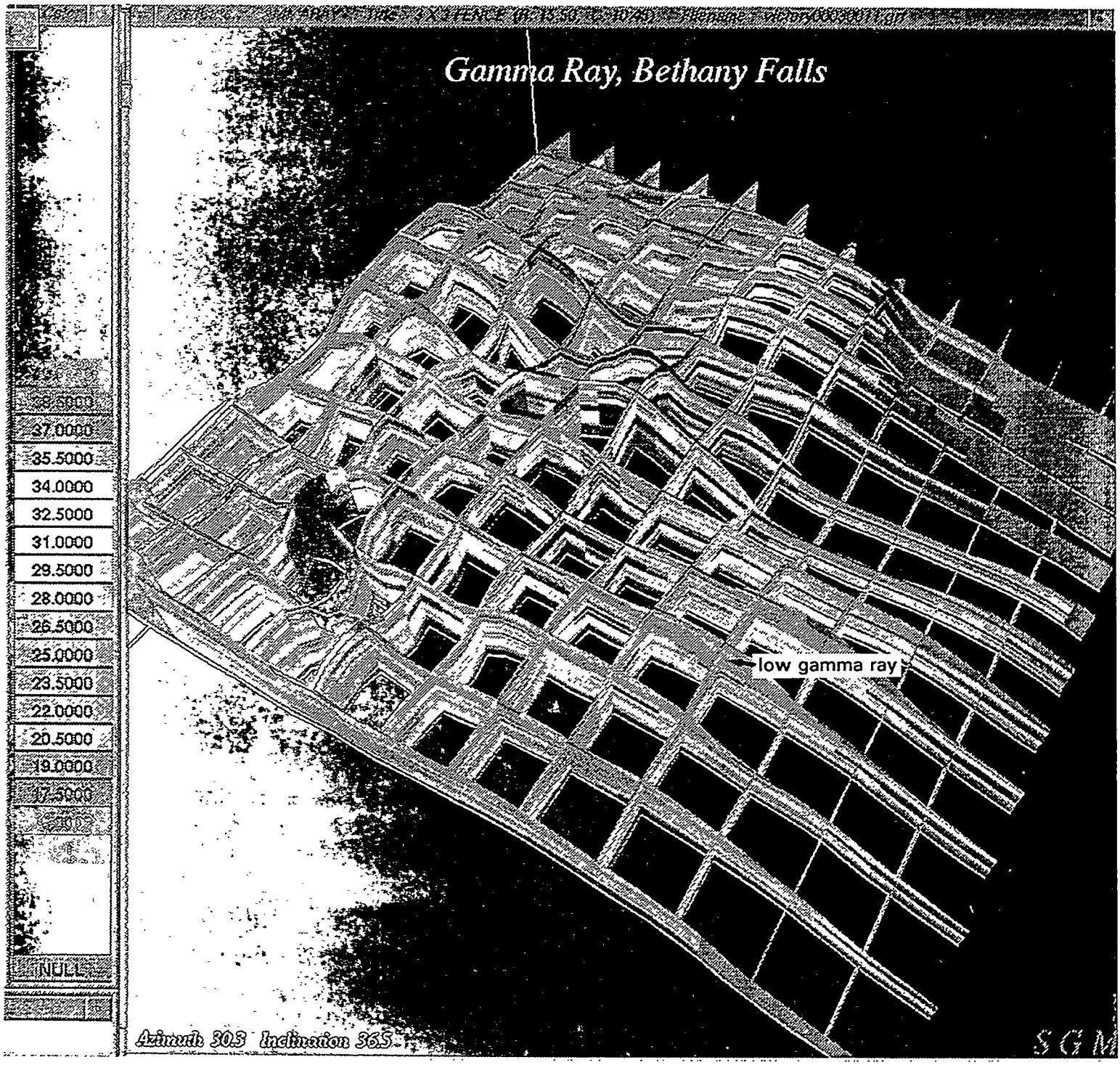

Figure 5.C.7. 3-D panel, again looking northwest, showing the gamma ray for the Bethany Falls Limestone interval. Cleaner gamma ray at the top corresponds closely with occurrence of oolites. Color (or gray scale) in this case can be made very sensitive to small changes as indicated by gray level bar on left. Of particular interest is low gamma ray area at top of Bethany Falls in southeast portion of panel. This area is not currently productive, but appears to have potential.

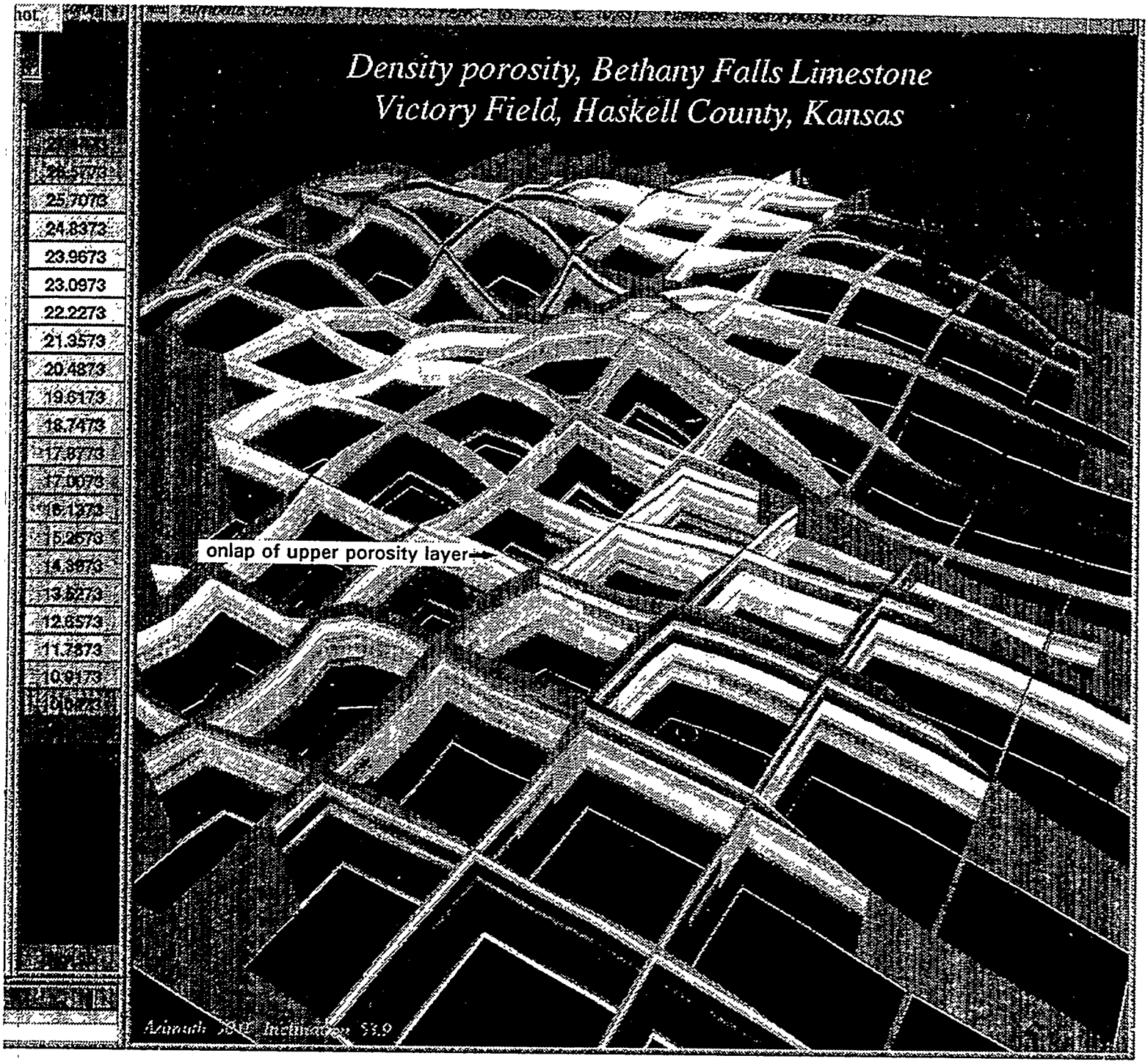

Figure 5.C.8. 3-D panel with same orientation as above displaying density porosity for the Bethany Falls Limestone. Edges of panel with no data are blank. Area in southeast shows distinct layering of porosity that laps out unto the structure.

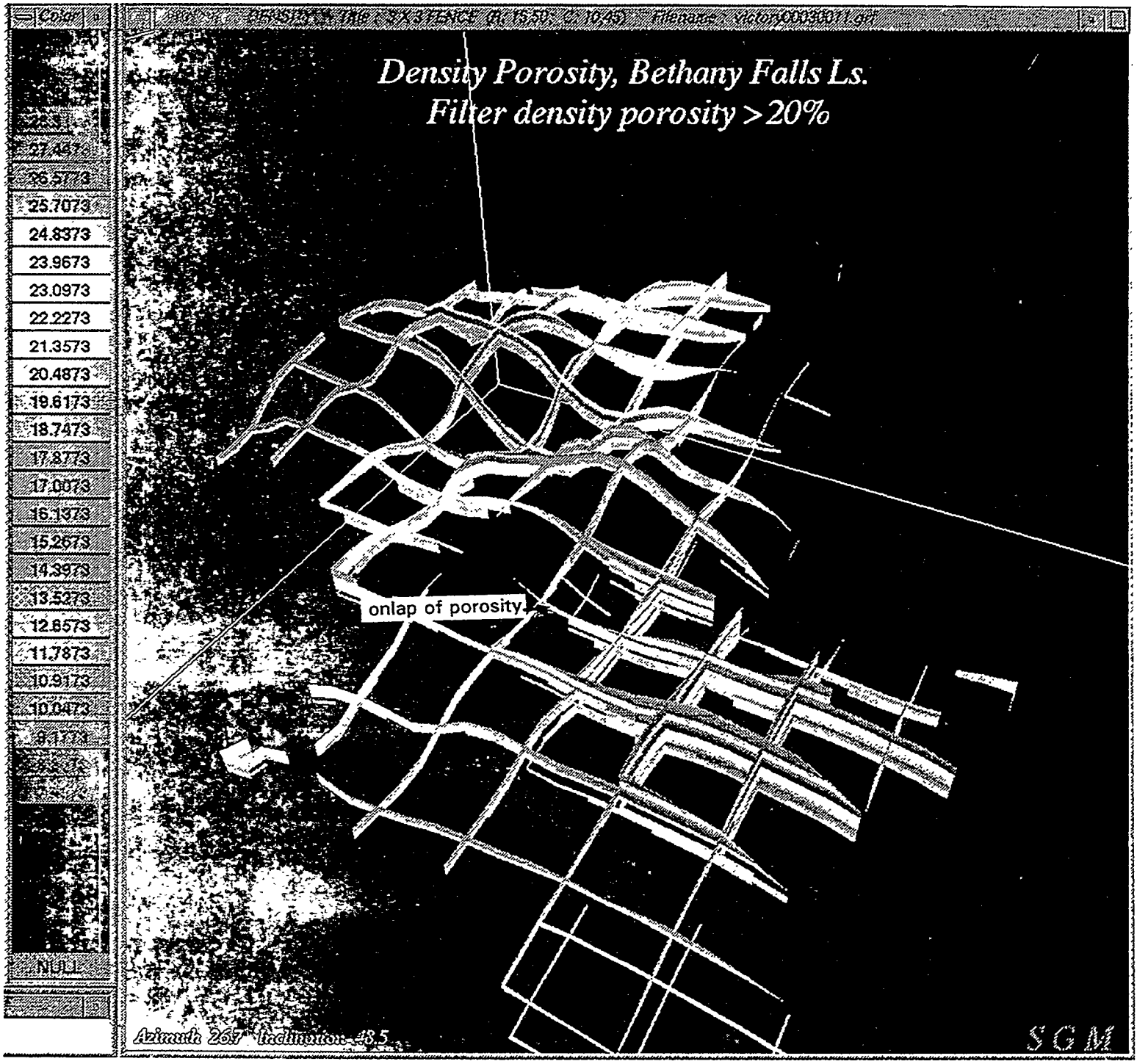

Figure 5.C.9. 3-D panel of density porosity in the Bethany Falls Limestone filtered to show only porosity above 20%. Note updip onlap of upper porosity layers in the southeast.

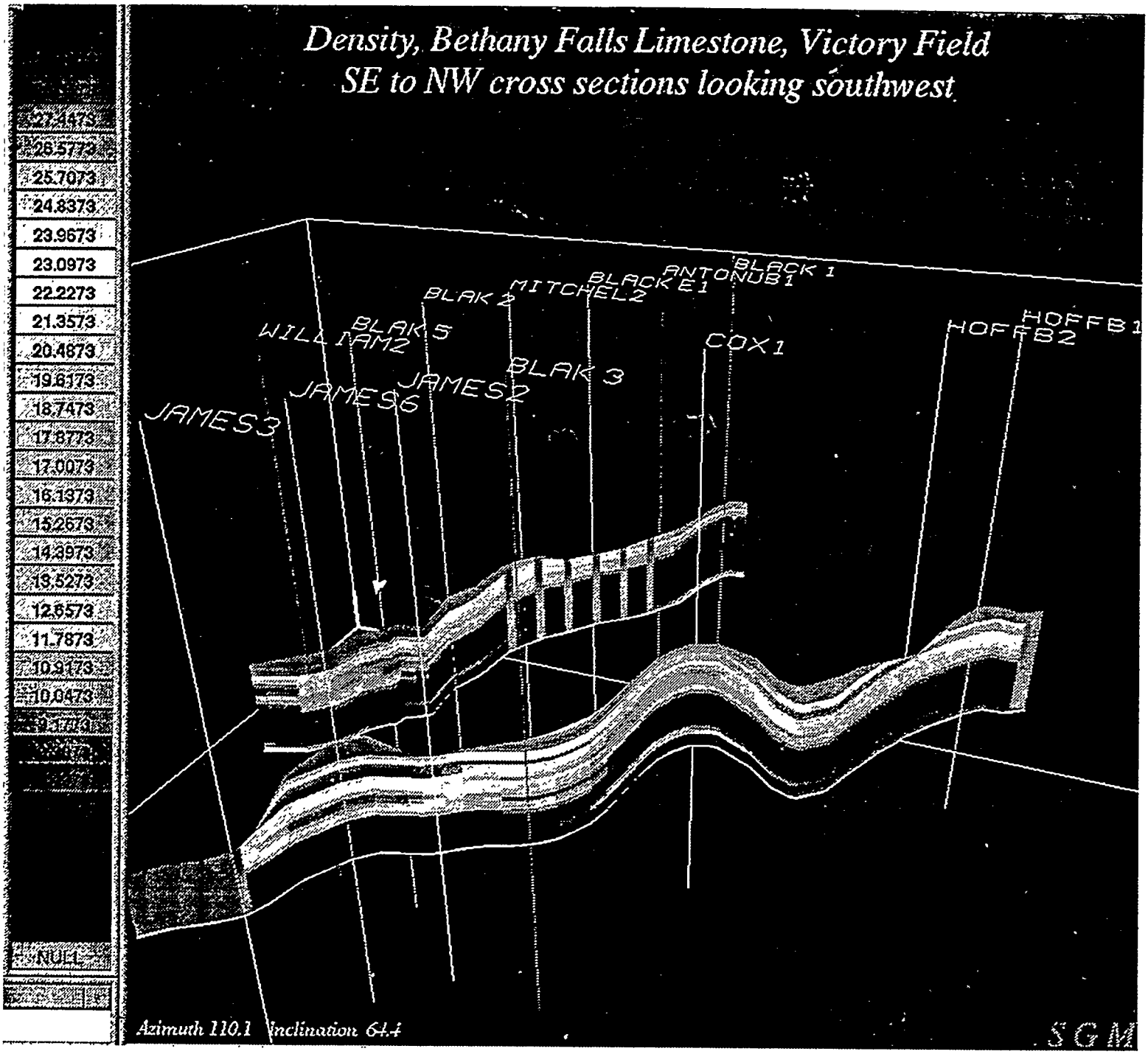

Figure 5.C.10. Two parallel southeast-to-northwest structural cross sections showing density porosity in the Bethany Falls Limestone. Sections are indexed on map in Figure 5.C.1. Porosity onlaps are previously noted.

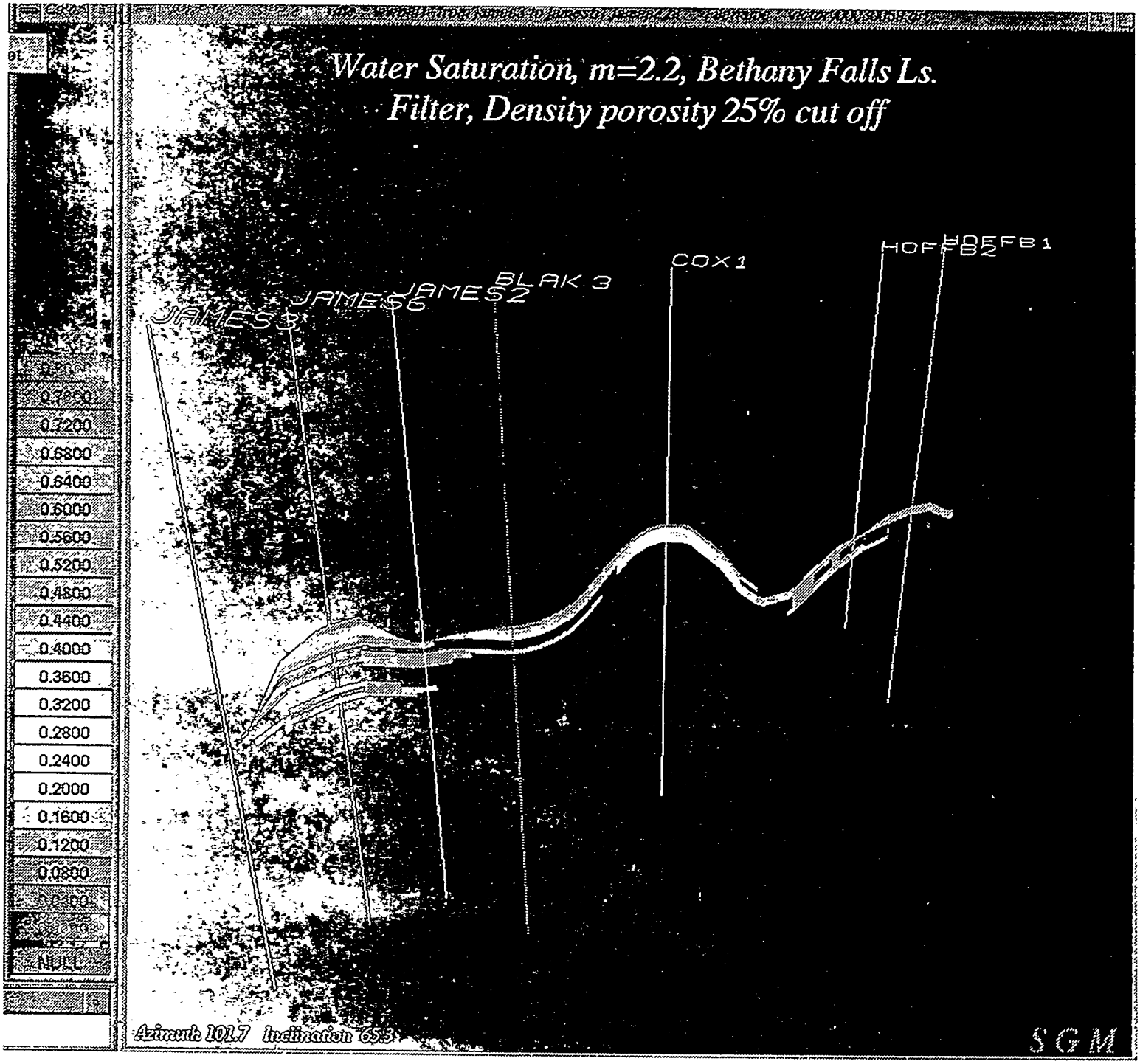

Figure 5.C.11. Water saturation calculated with cementation exponent of 2.2 for Bethany Falls Limestone filtered with density porosity cutoff of 25%. Cox #1 (twin to A-4 Cox) location is a producing well from the Bethany Falls at saturations below 0.22 Sw. Similar water saturations are indicated at the James #S-6 location, which is behind pipe. "Super" Pickett plots indicate this to be a prospective recompletion site in the Bethany Falls Limestone.

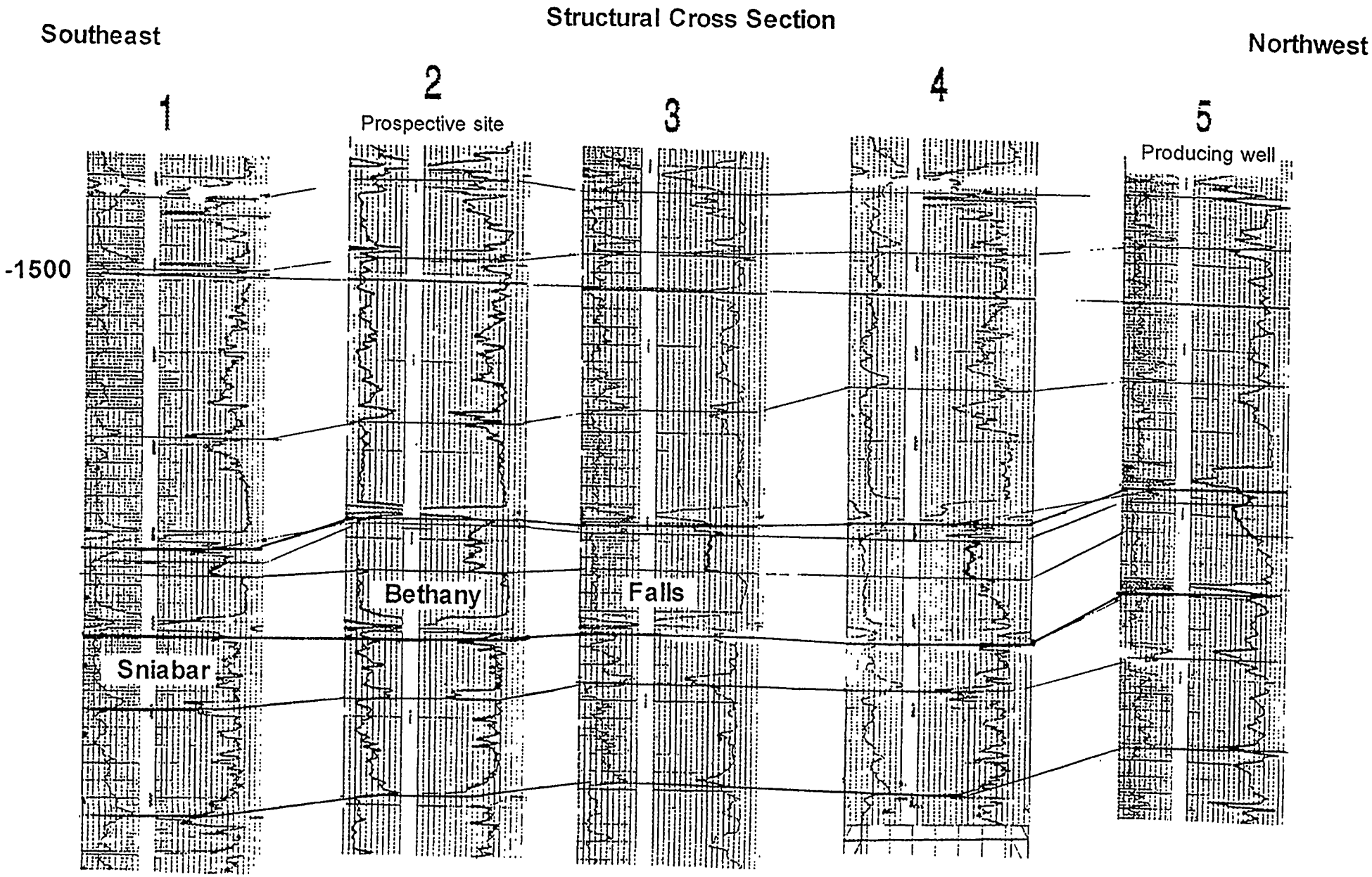

Figure 5.C.12. Conventional well log cross section in the same location as the cross section in Figure 5.C.11 demonstrating difficulties in recognizing porosity pinchouts between prospective sites and updip producing locations because porosity cutoffs are high.

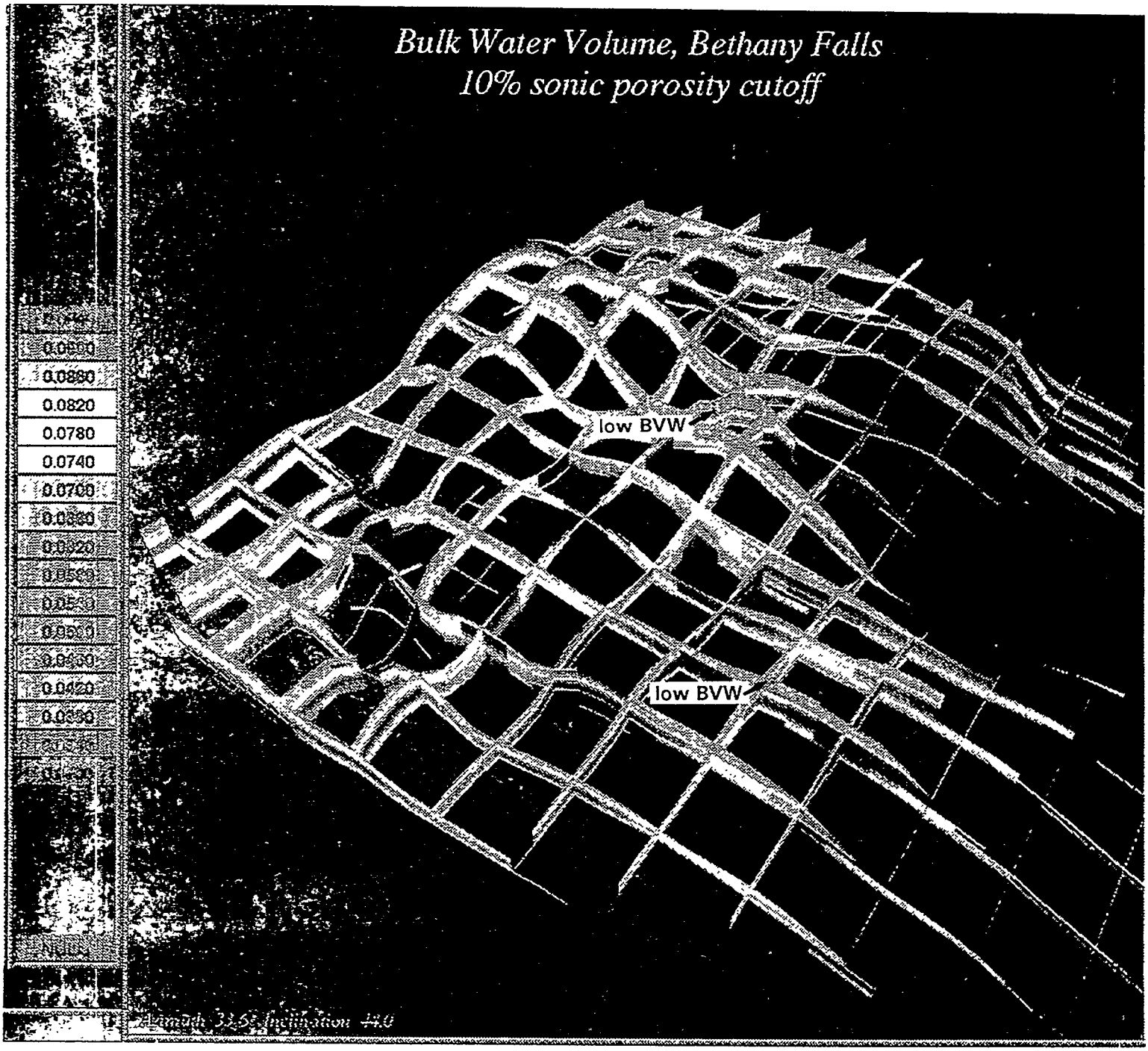

Figure 5.C.13. 3-D panel of calculated bulk water volume (BVW) for the Bethany Falls Limestone using sonic porosity, filtered at 10% sonic porosity cutoff using a range defined as significant from the "Super" Pickett plot work (0.02 to 0.08). Areas of low BVW correlate closely to areas of prospective reservoir identified using "Super" Pickett plots (see Figure 6.62)

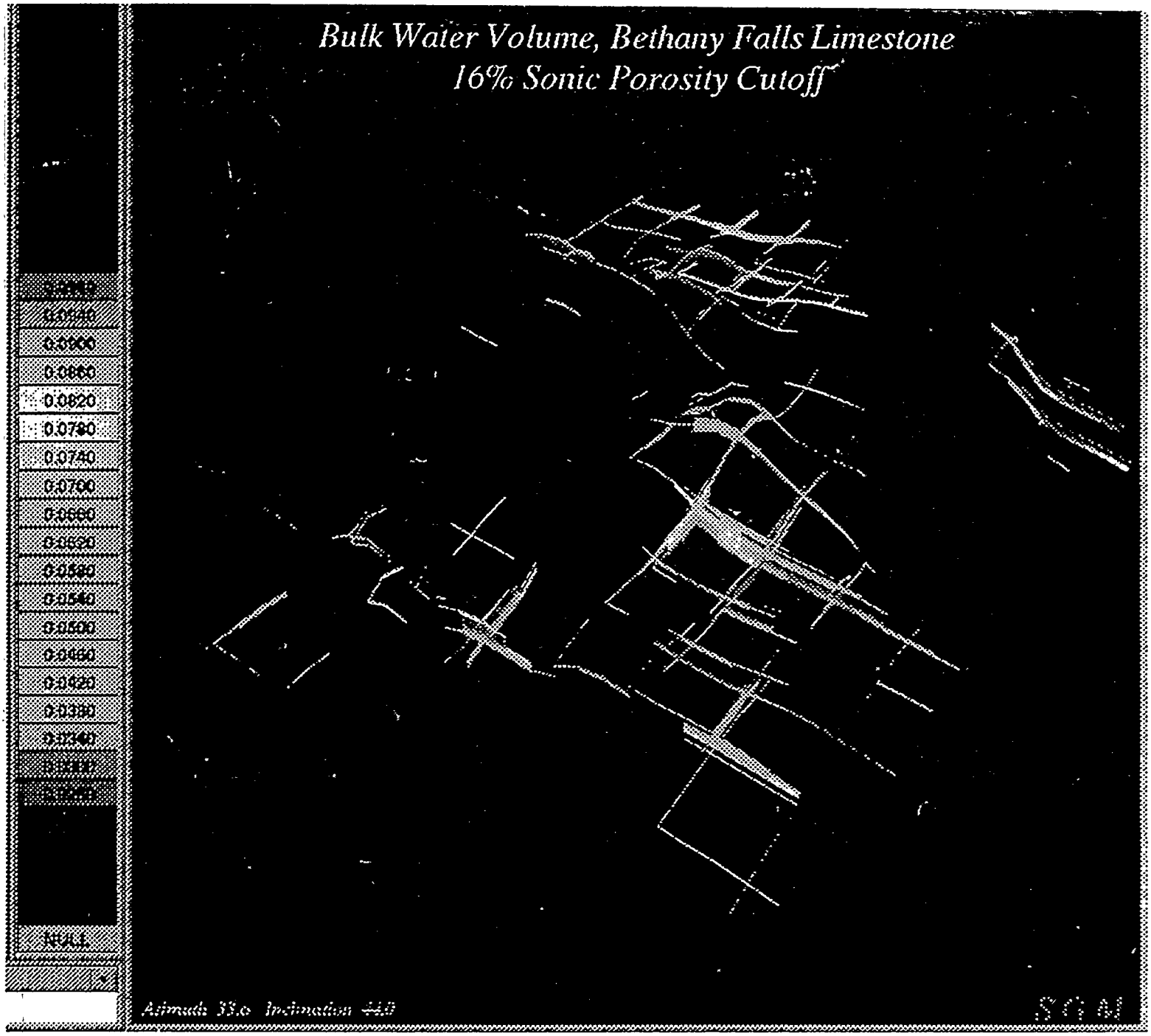

Figure 5.C.14. 3-D panel of calculated BVW for Bethany Falls Limestone using sonic porosity, filtered at 16% sonic porosity, indicating the southeast flank is prospective.

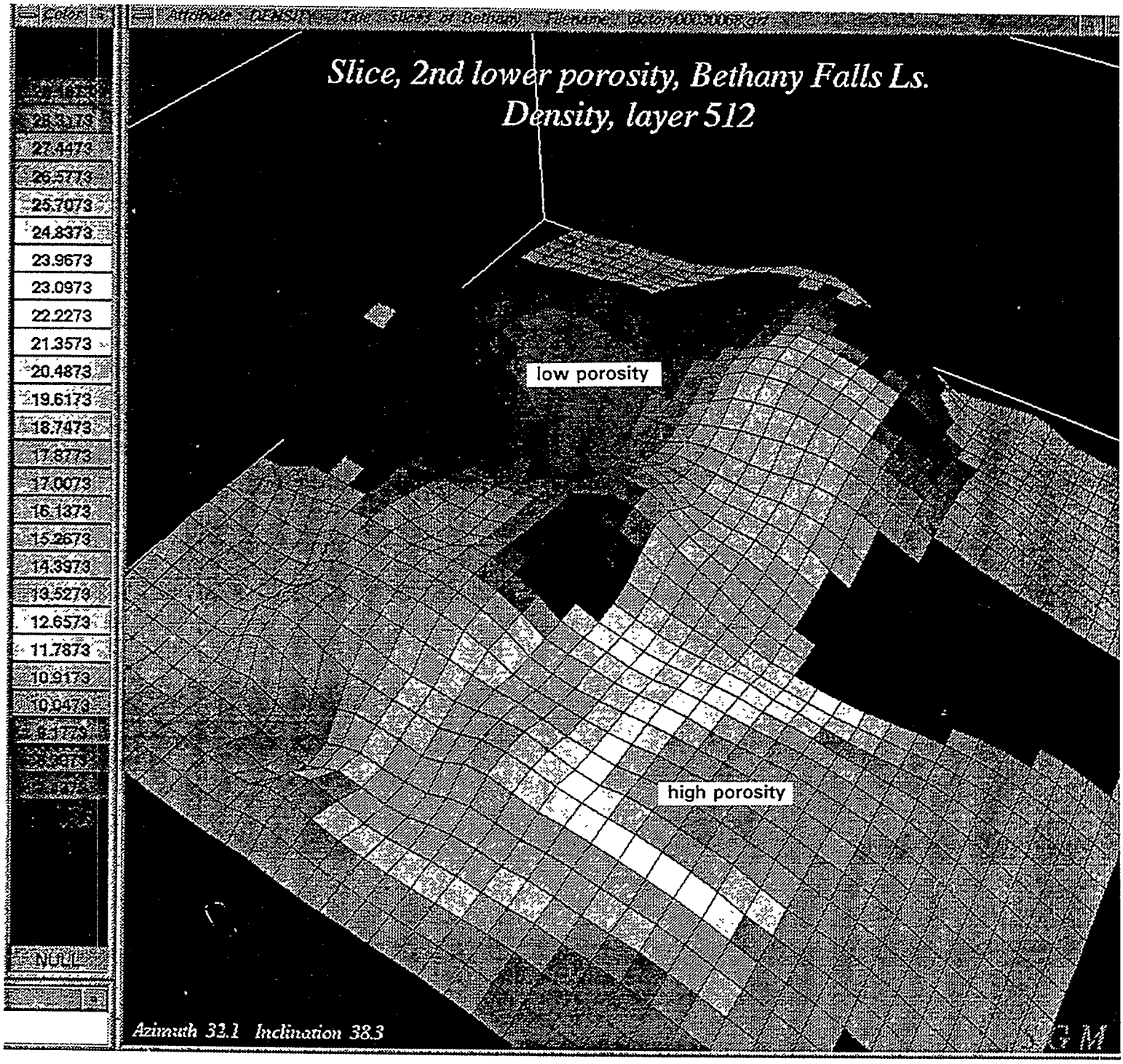

Figure 5.C.15. Slice map of density porosity in view looking northwest showing layer from the lower porosity zone lapping up onto higher portion of field.

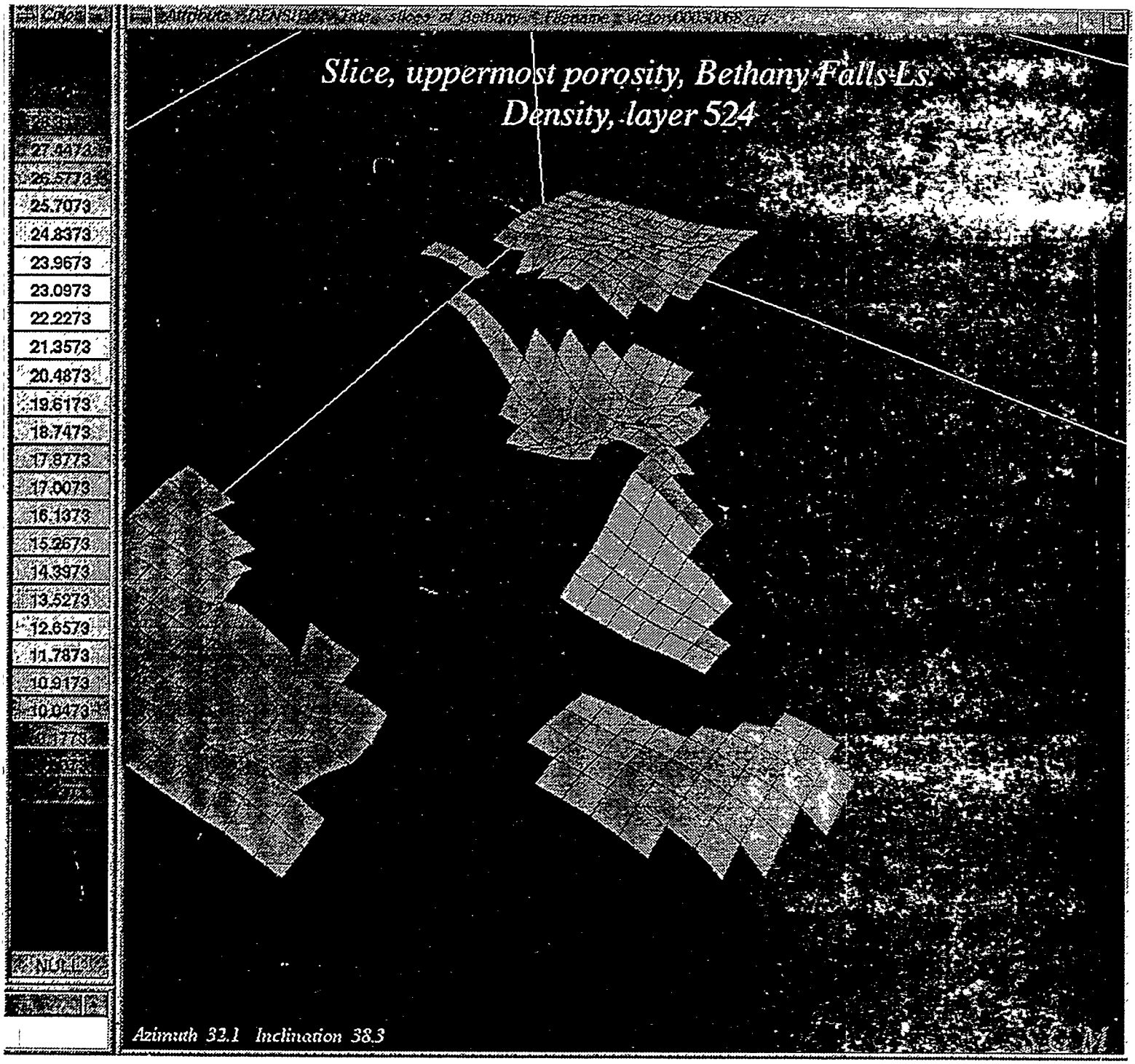

Figure 5.C.16. Slice map of density porosity for the layer from the uppermost porosity in the Bethany Falls Limestone in view looking northwest. This layer is best developed along the edges of the structure indicating an offlap relationship. This is very analogous to relationships observed in the Drum and Bethany Falls analog sites.

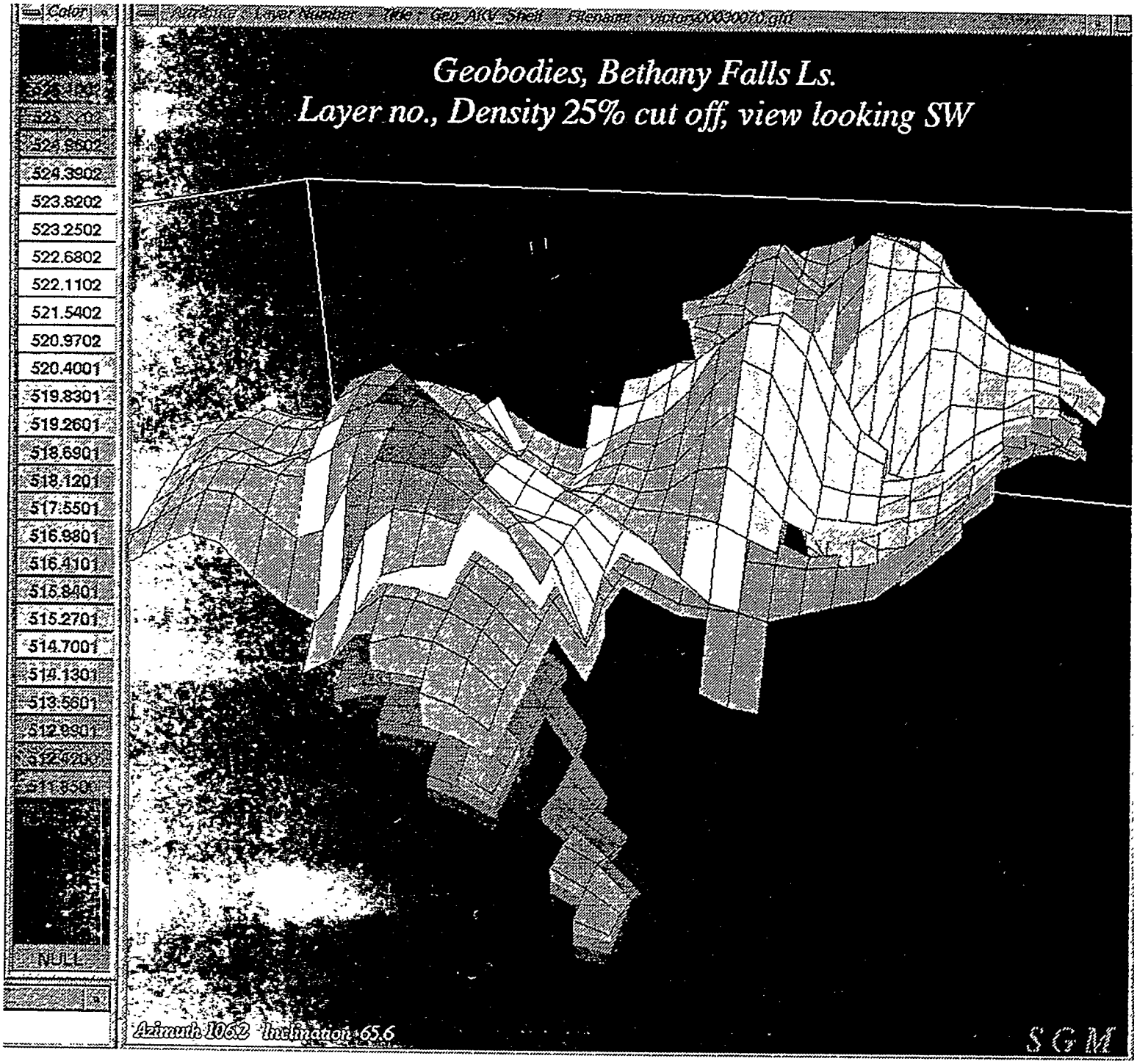

Figure 5.C.17. Geobody of connected volume of the Bethany Falls reservoir using density porosity with 25% cutoff. This view is looking southwest showing layer numbers. Lateral discontinuities are noted on this gray scale presentation, although much more apparent on the color presentation.

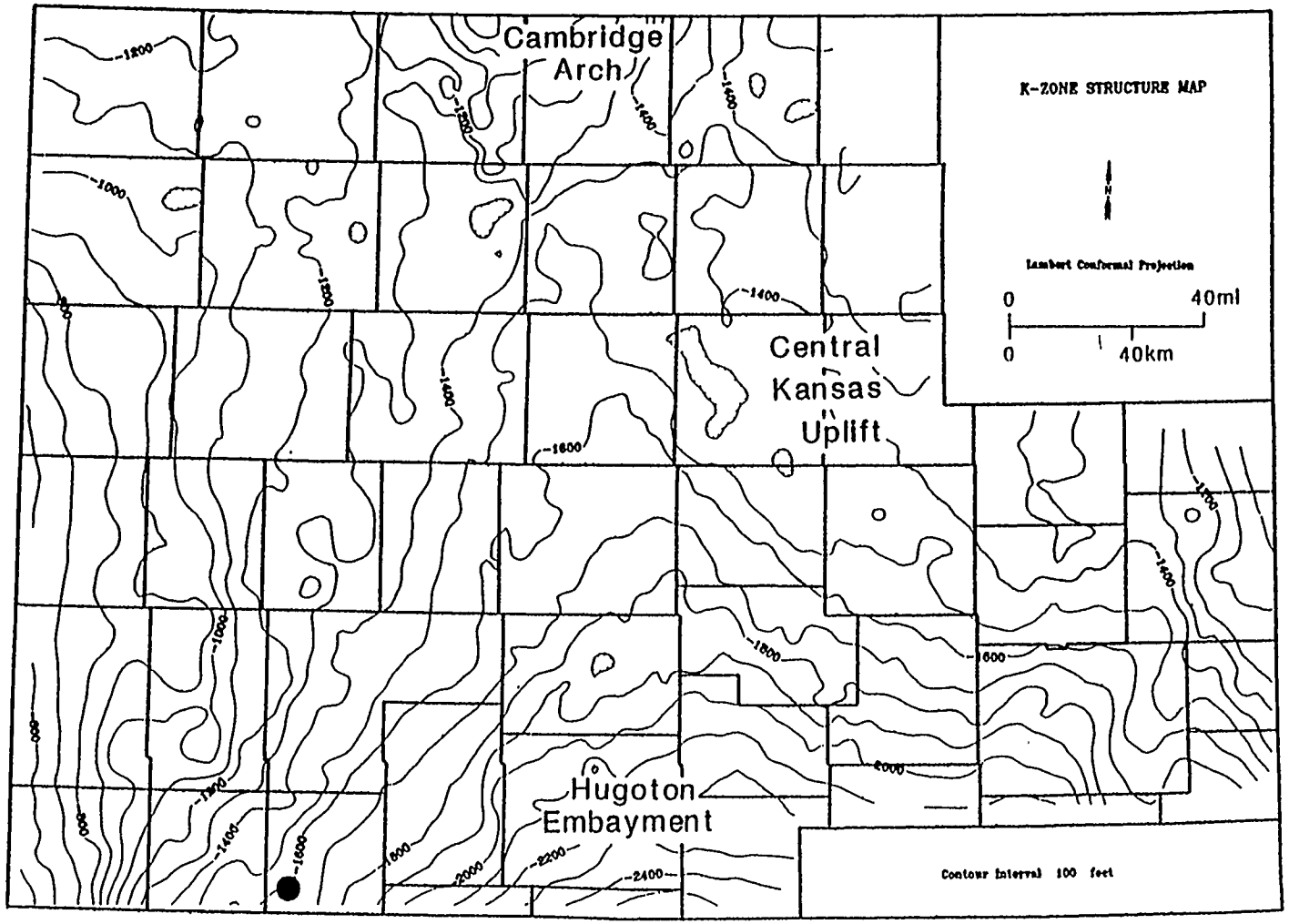

Figure 6.1. Structure map of the K-zone (Swope sequence) in the northern portion of the Hugoton Embayment in western Kansas showing very low dips. Black circle is the approximate location of the Victory-Northeast Lemon Fields.

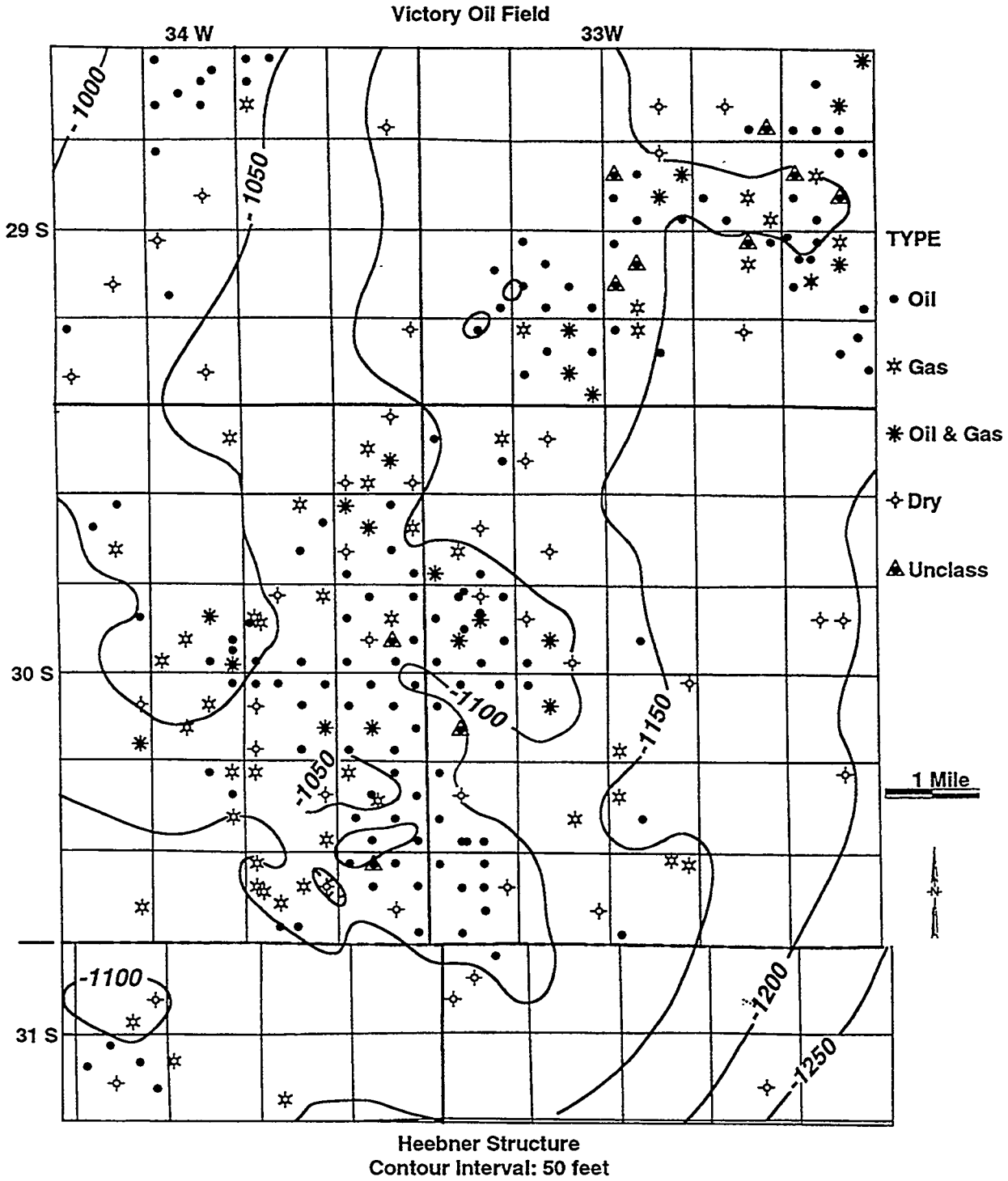

Figure 6.2. Structure map of the Heebner Shale in the Victory-Northeast Lemon Fields. Regional dip is about 50 feet per mile.

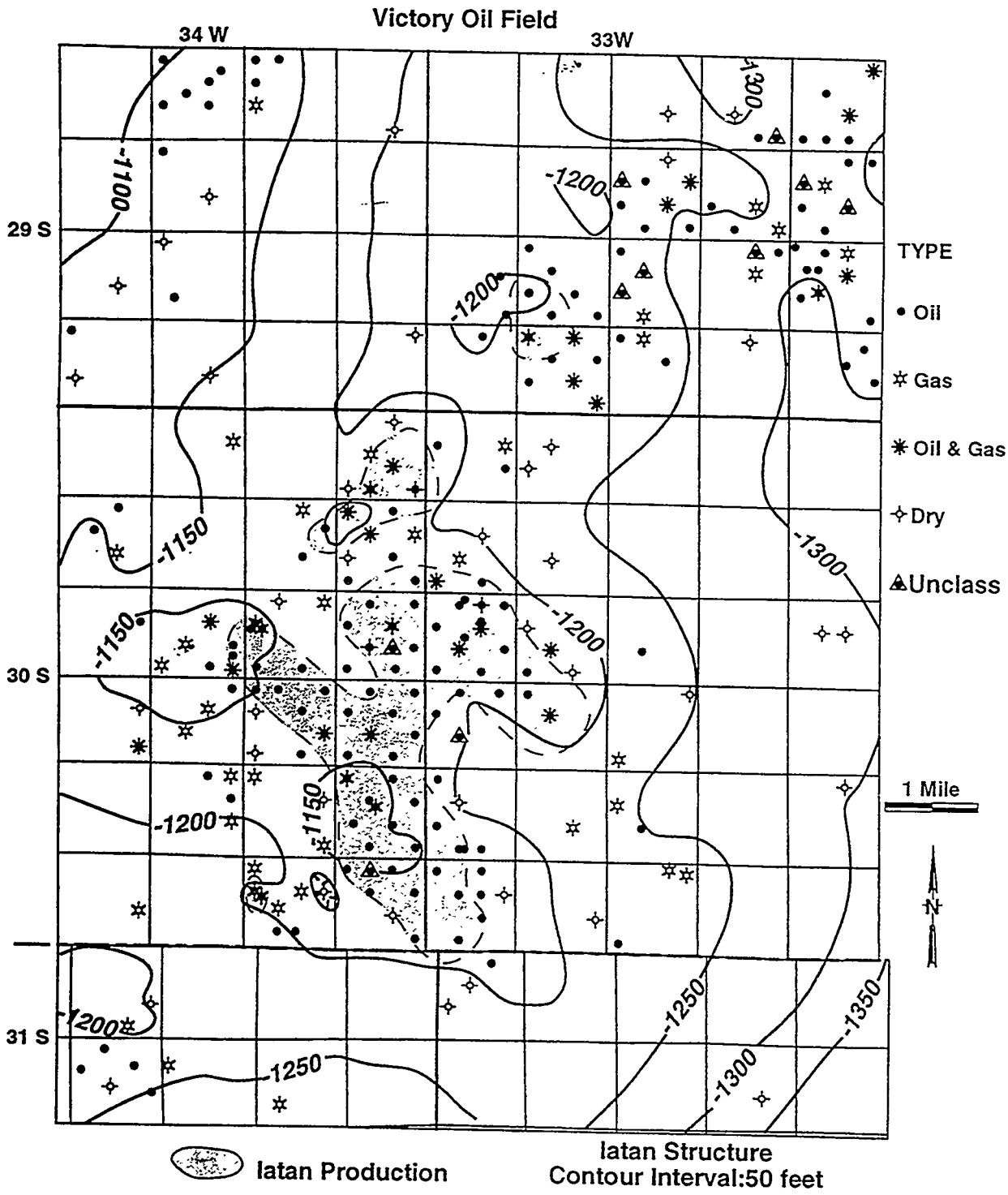

Figure 6.3. Structure map of the Iatan Limestone. Iatan production (shaded) in Victory Field is along gentle anticlines.

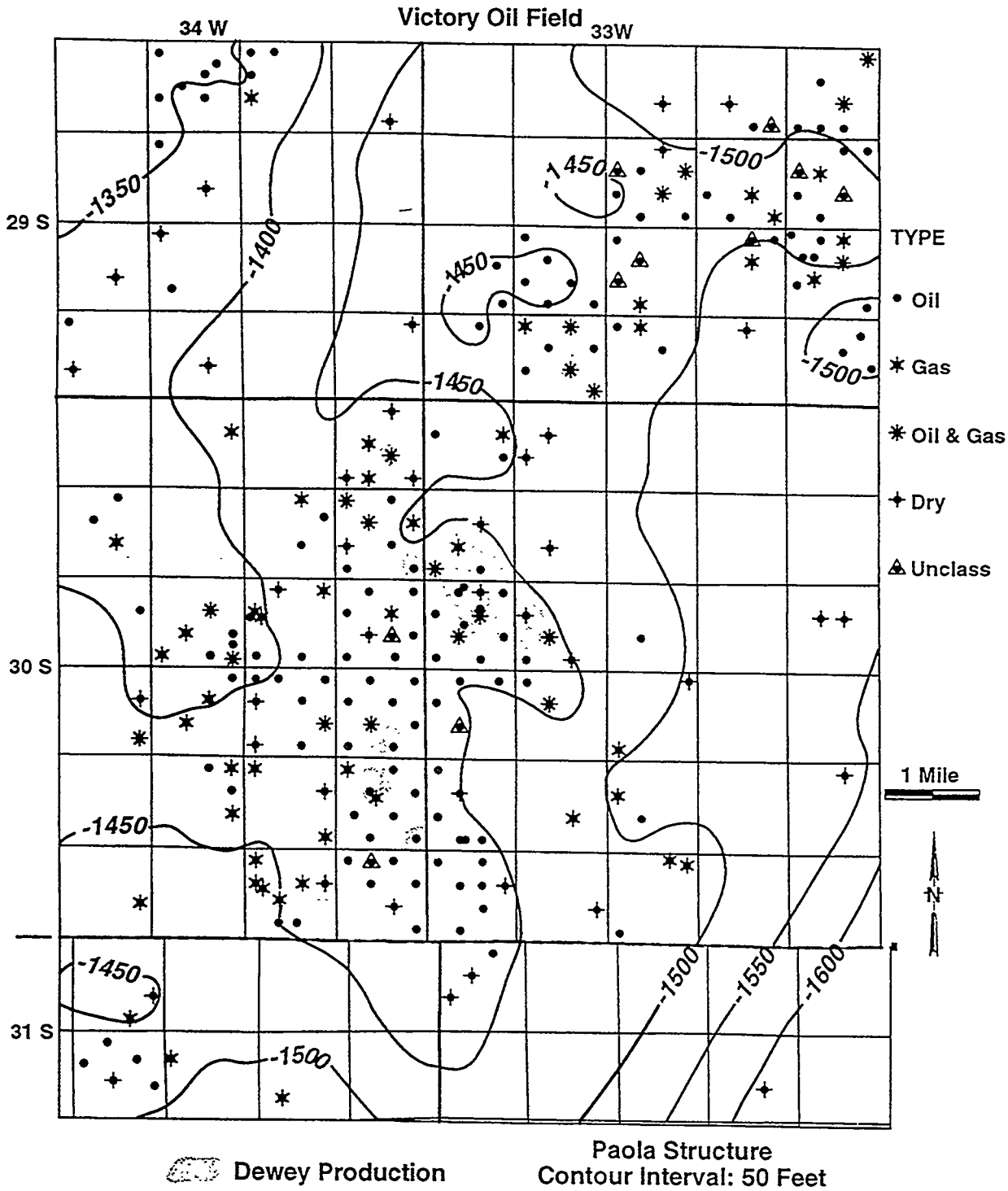

Figure 6.4. Structure map of the Paola Limestone. Dewey production (shaded) is on the gentle southeast plunging anticlines.

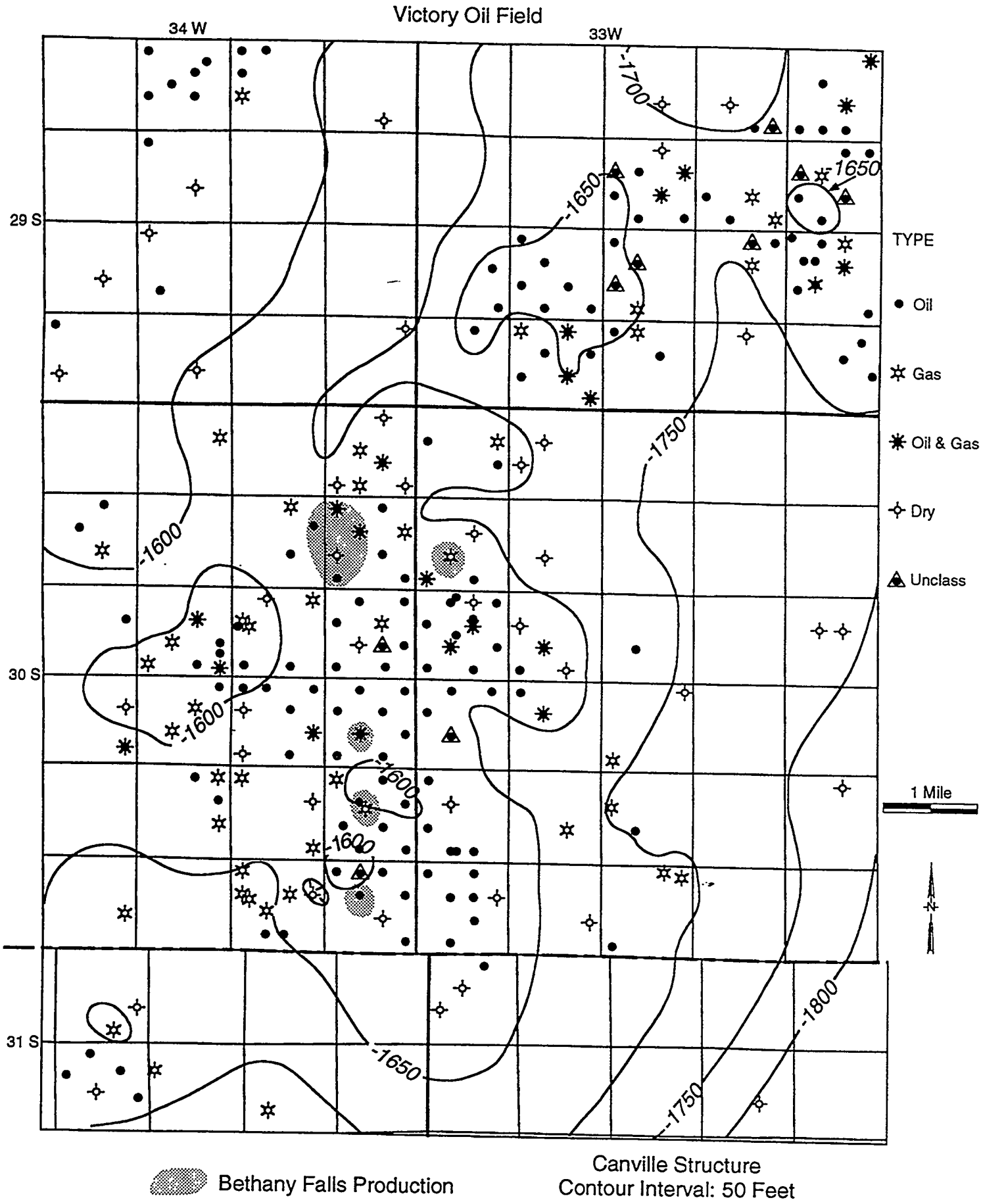

Figure 6.5. Structure map of the Canville Limestone. Bethany Falls production (shaded) is only present in Victory Oil Field on a broad southeast plunging anticline.

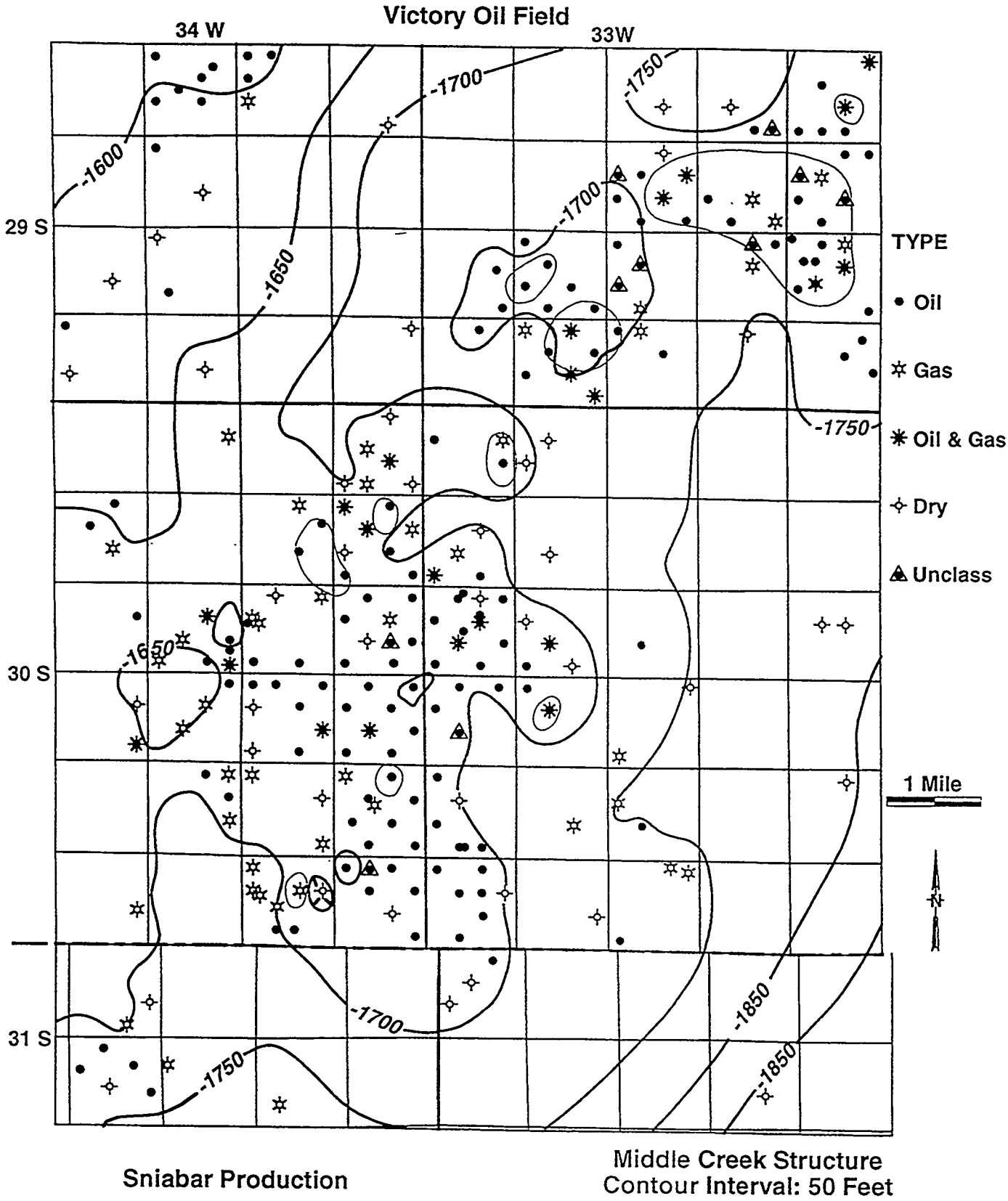

Figure 6.6. Structure map of the Middle Creek Limestone. Sniabar production (shaded) is not on the anticlinal trend at the Victory Field, but is located on a gentle flattening, off-structure.

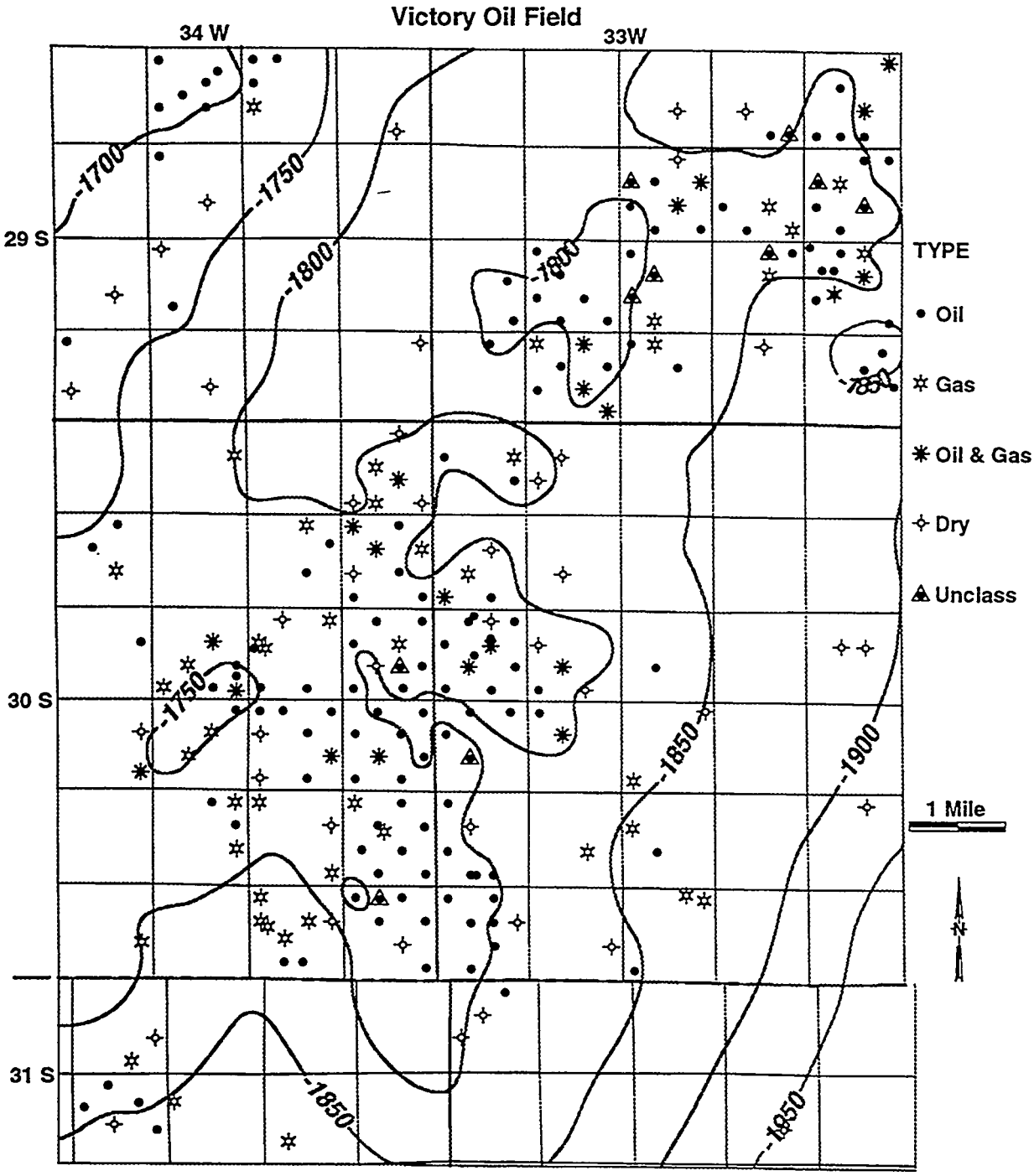

Nuyaka Structure
Contour Interval: 50 Feet

Figure 6.7. Structure map of the Nuyaka Creek Shale.

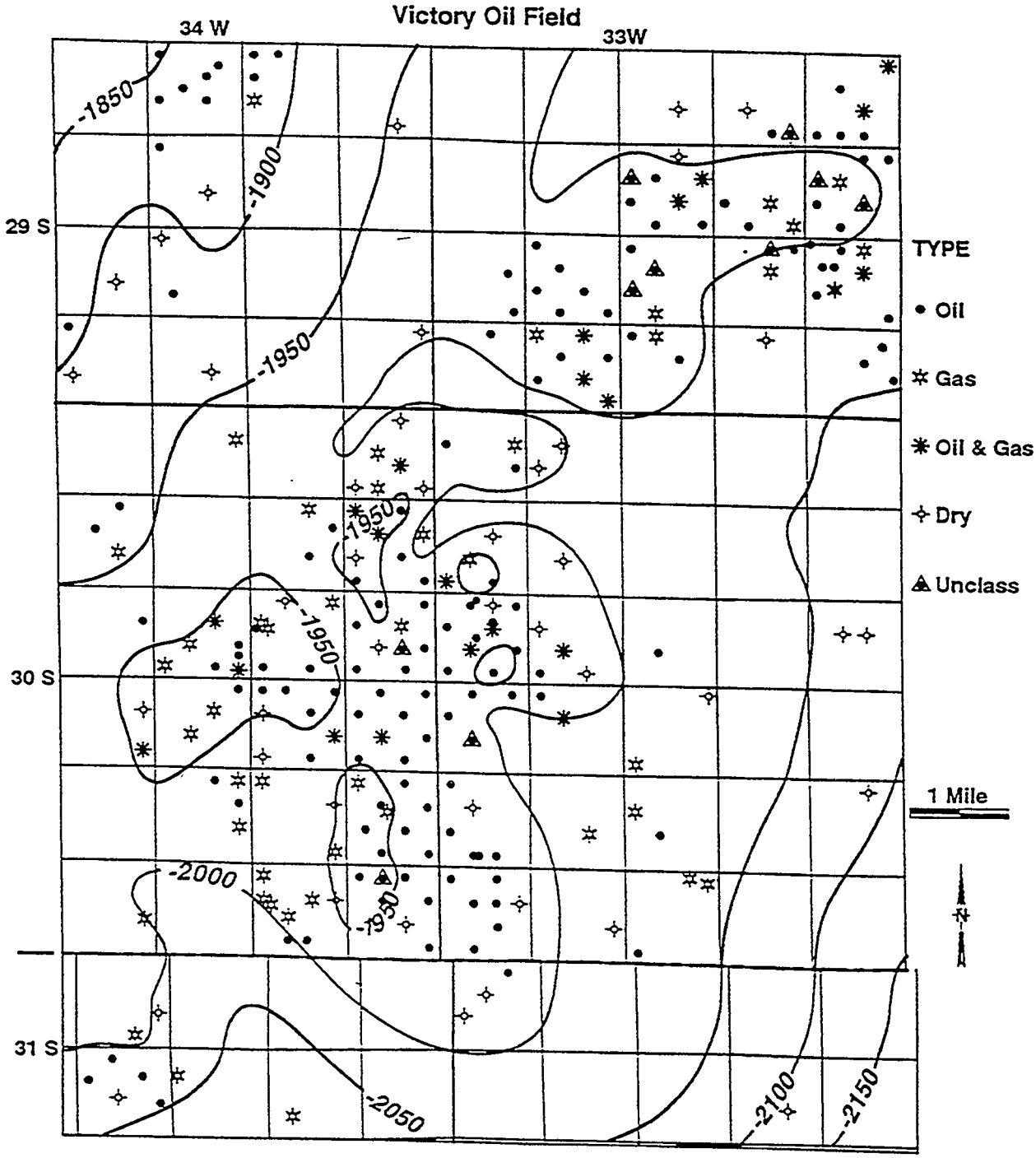

Excello Structure
Contour Interval: 50 Feet

Figure 6.8. Structure map of the Excello Shale.

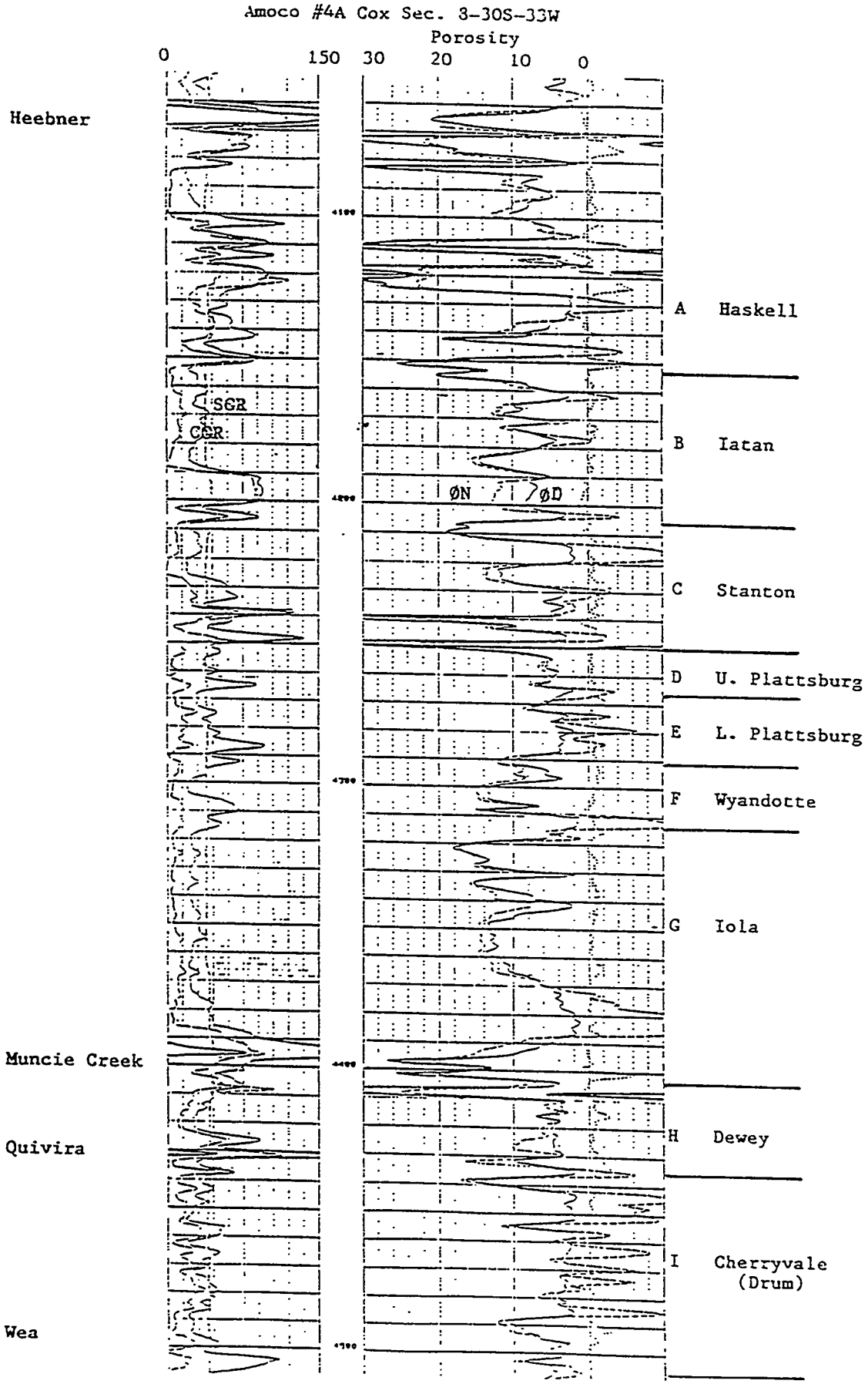

Figure 6.9. 'Type-section' log Victory-Northeast Lemon Fields (4050-4500'), Amoco A-4 Cox (Sec. 8-T30N-R33W).

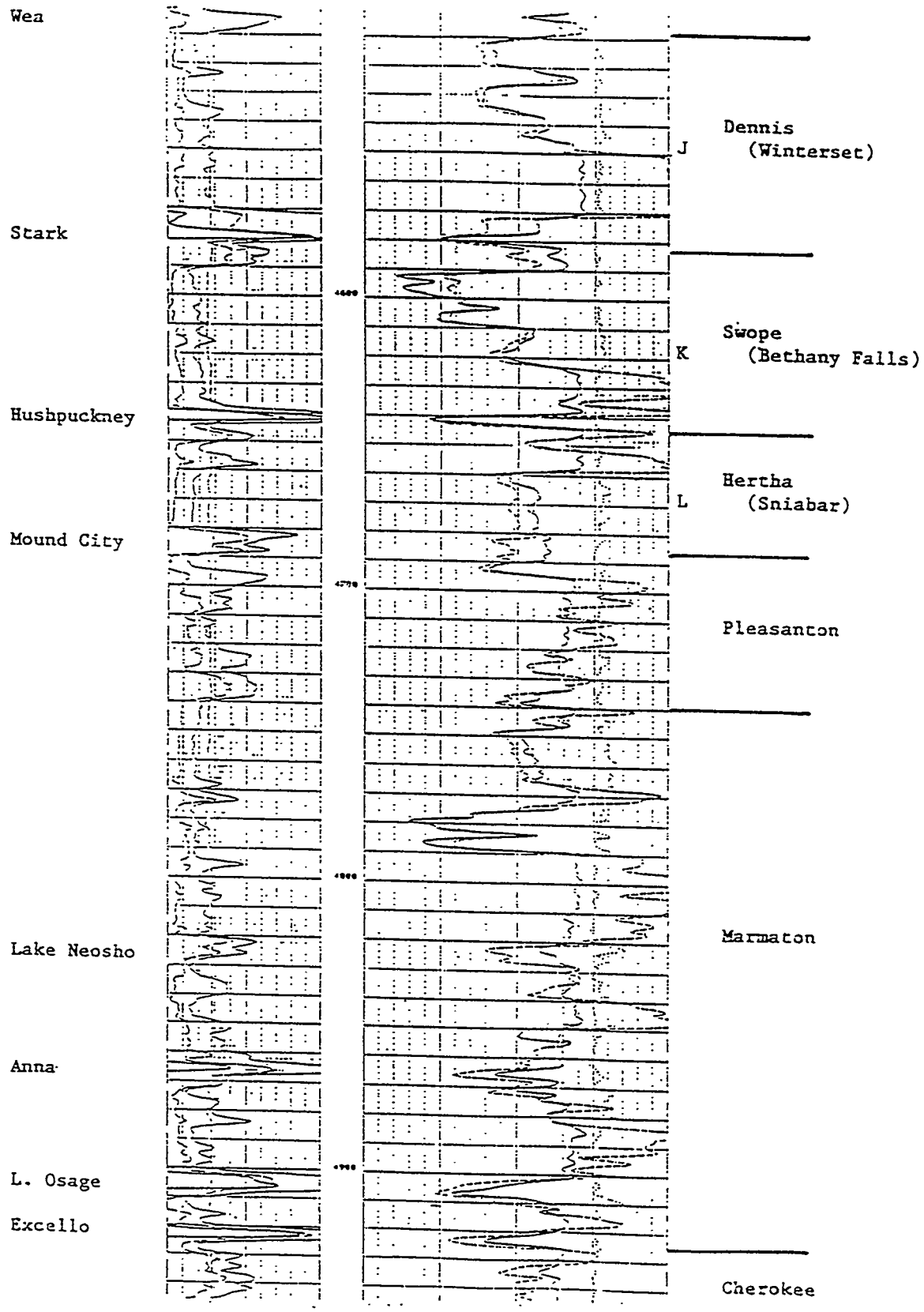

Figure 6.10. Type-section log Victory-Northeast Lemon Fields (4500-4950'), Amoco A-4 Cox (Sec. 8-T30N-R33W).

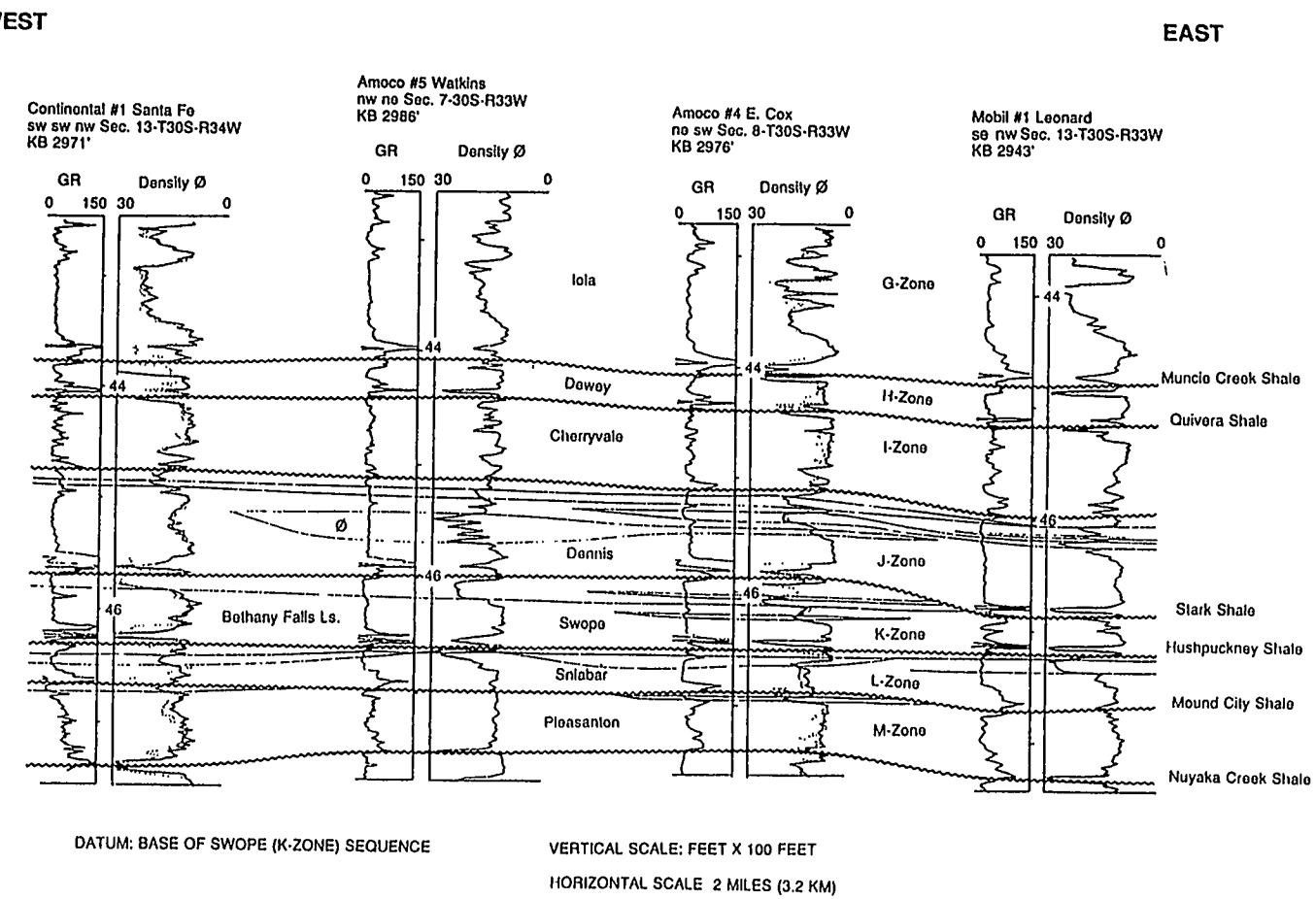

Figure 6.11. West-east gamma ray-density log cross section from Wea Shale of Cherryvale sequence to Nuyaka Creek Shale.

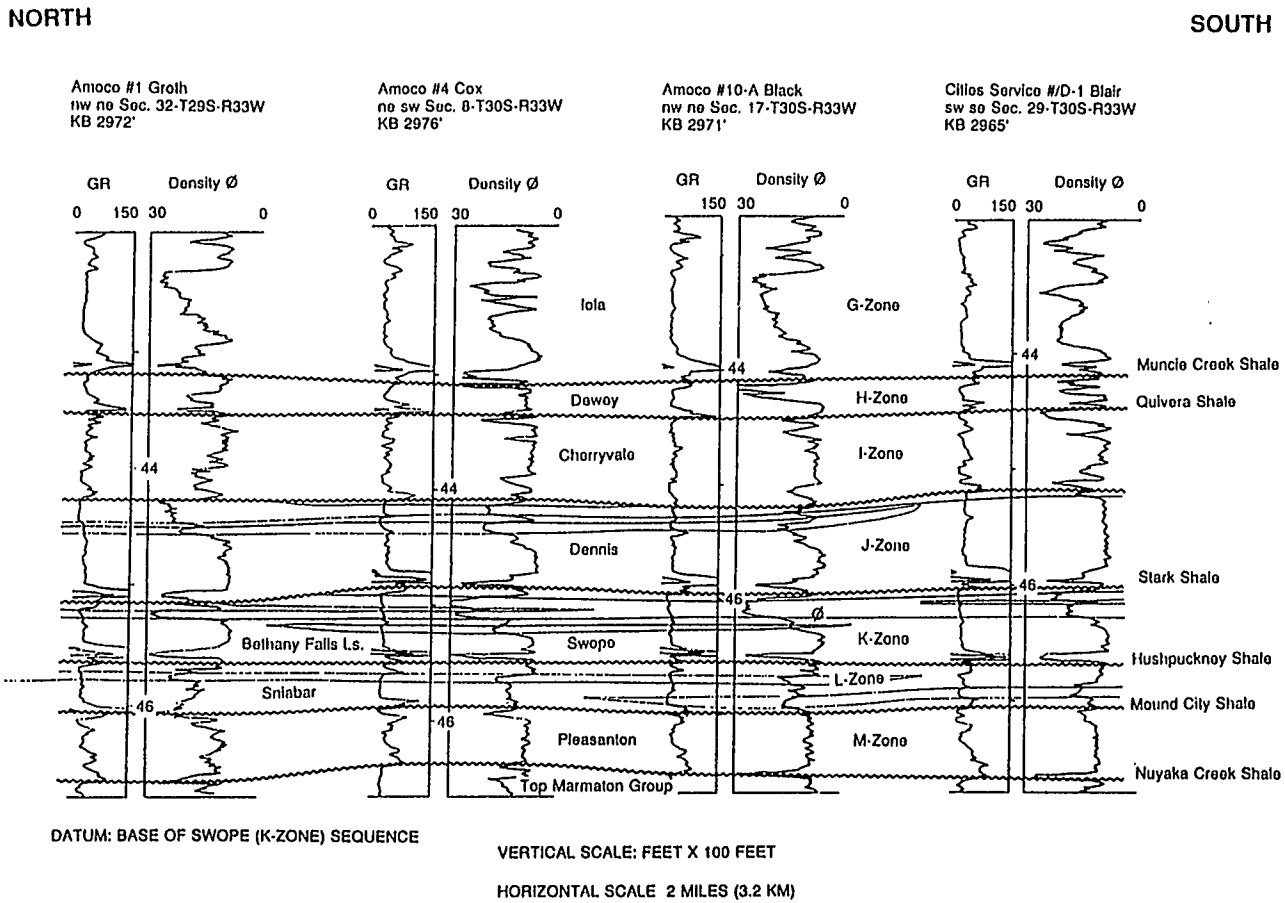

Figure 6.12. North-south gamma ray-density log cross section from Wea Shale of Cherryvale sequence to Nuyaka Creek Shale.

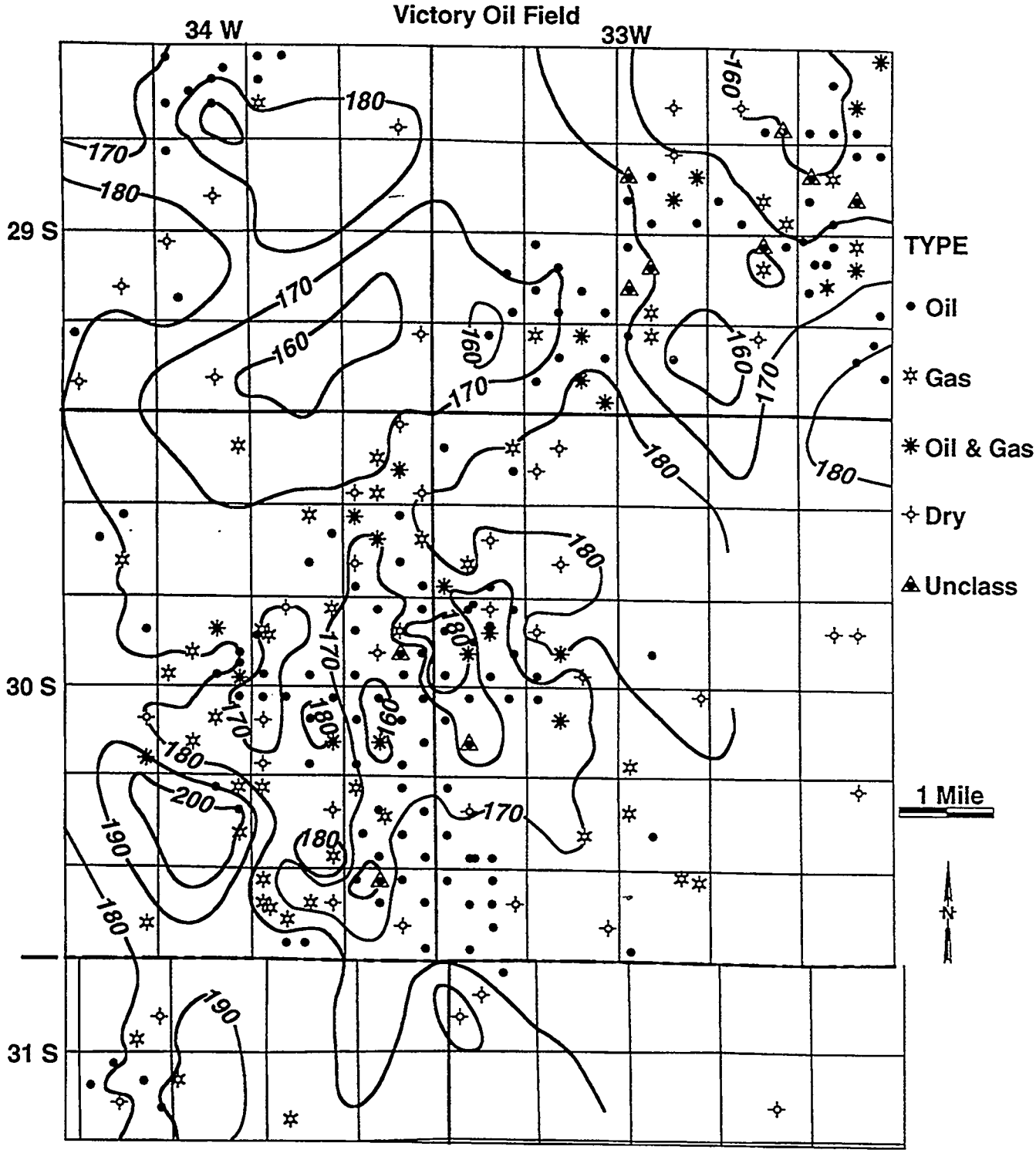

Excello - Nuyaka Isopach
Contour Interval: 10 Feet

Figure 6.13. Isopach of Excello-Nuyaka Creek interval (Marmaton Group). Thickness is relatively consistent with no observable pattern.

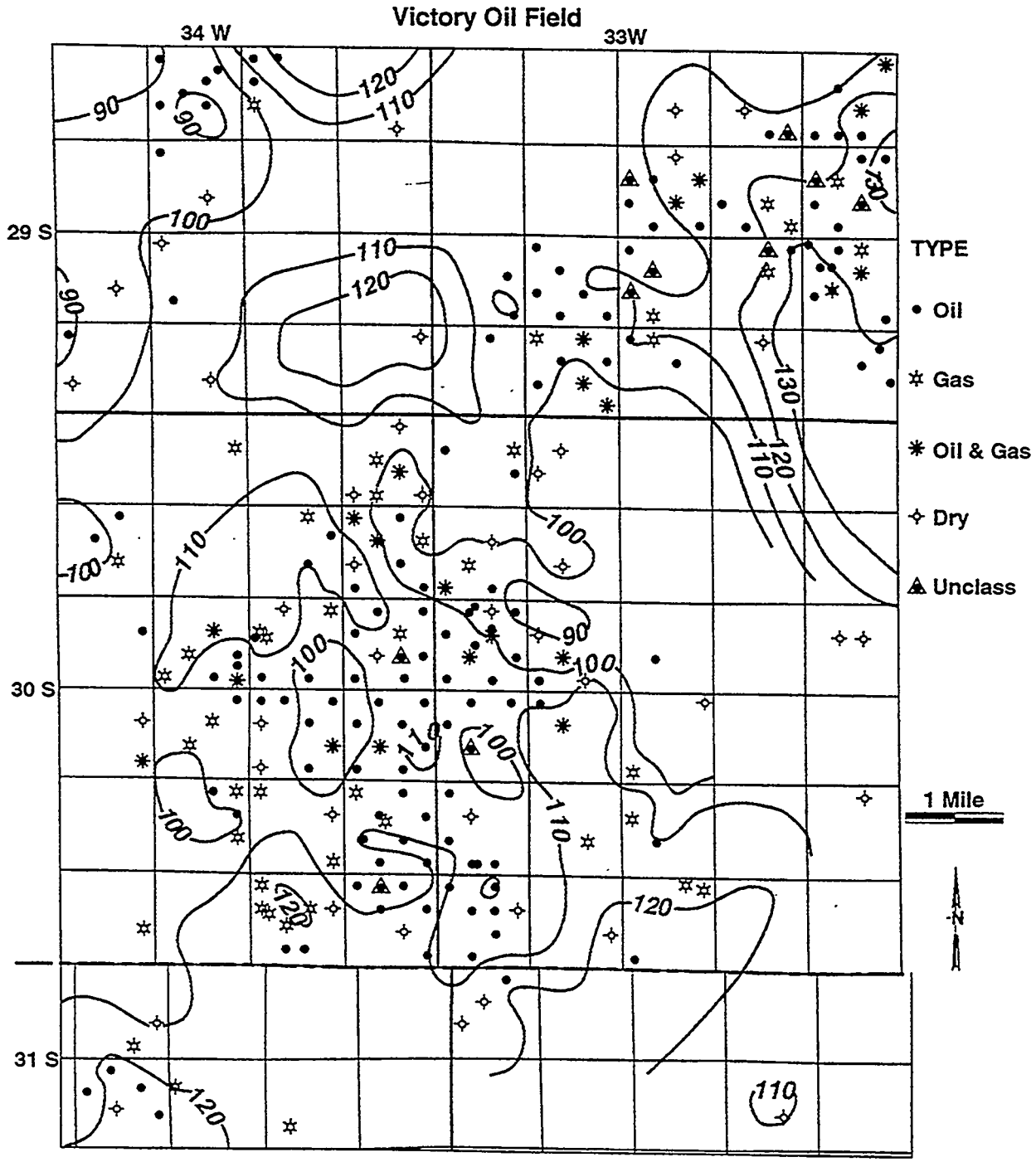

Nuyaka - Hushpuckney Isopach
Contour Interval: 10 Feet

Figure 6.14. Isopach of Nuyaka Creek-Hushpuckney interval (L and M sequences). Thickness is relatively consistent except for thick area of the Northeast Lemon Field due to a thick Sniabar oolitic shoal.

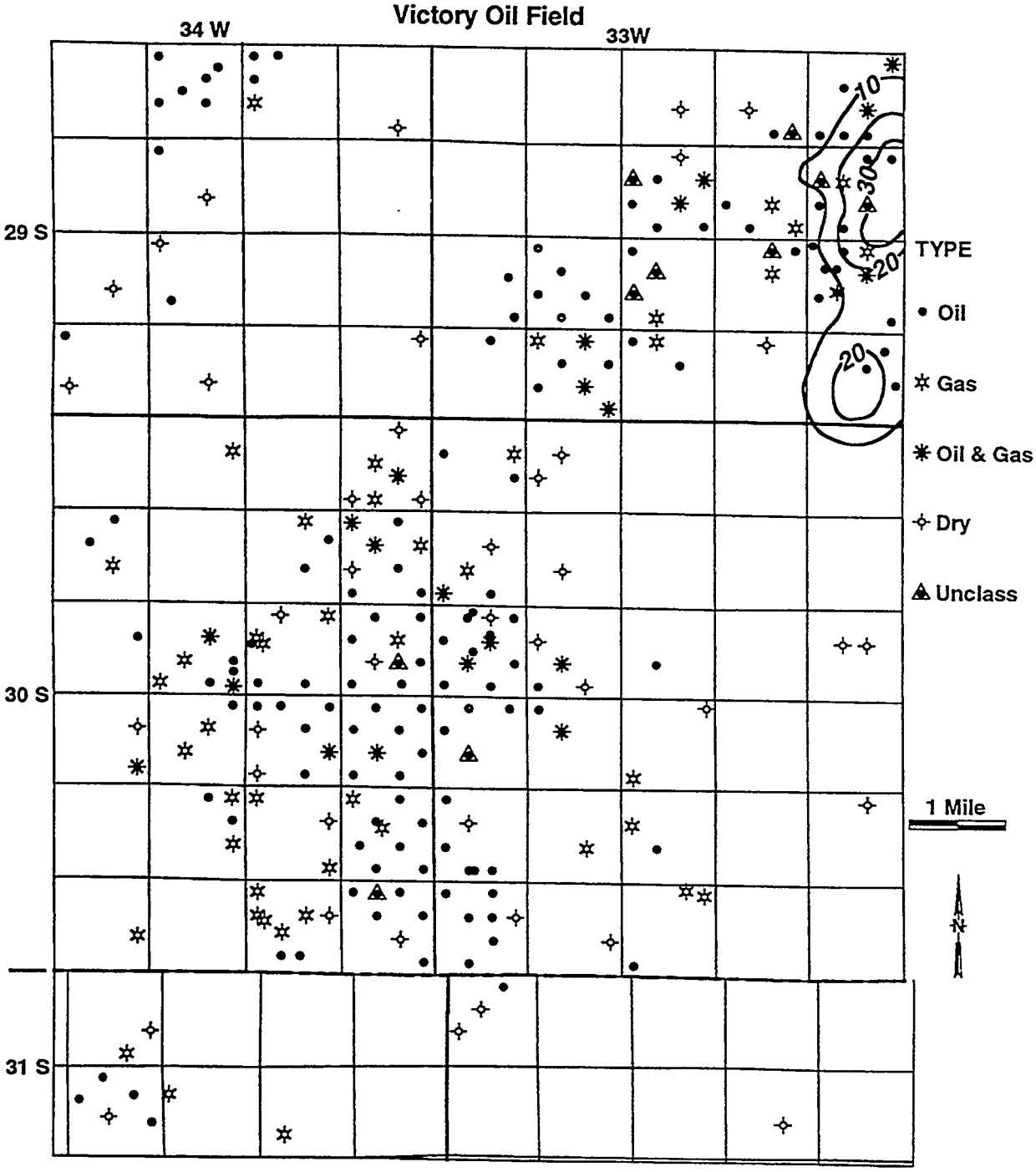

Exline - Feet of Porosity> 8%
Contour Interval: 10 Feet

Figure 6.15. Exline Limestone. Feet of porosity greater than 8%, which is anomalous as compared to the area of study where porosity in the Exline is thin to absent.

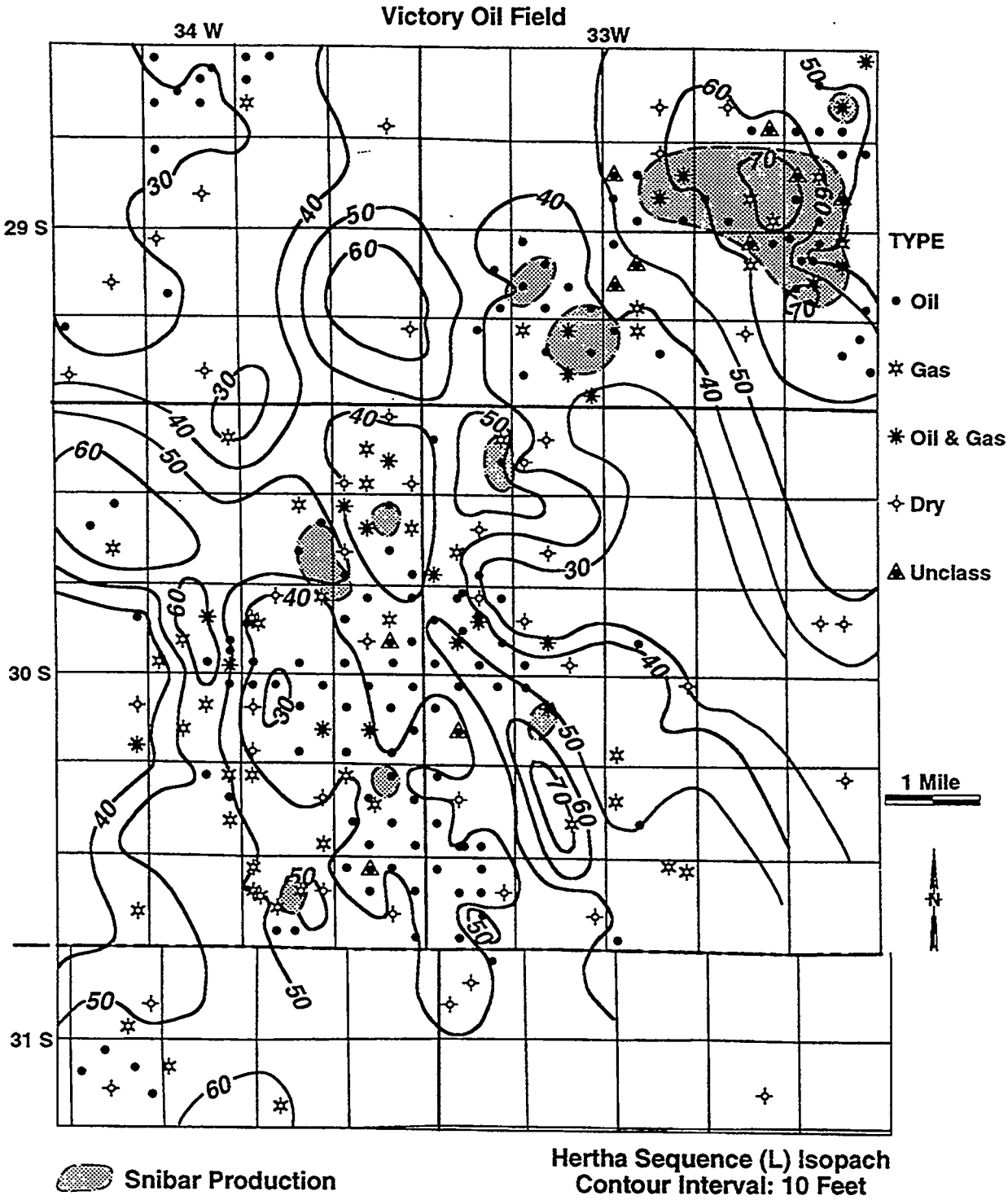

Figure 6.16. Isopach of the Hertha sequence (L). Anomalous thickness and extent in the Northeast Lemon area is cause for excellent oil production from the Sniabar Limestone.

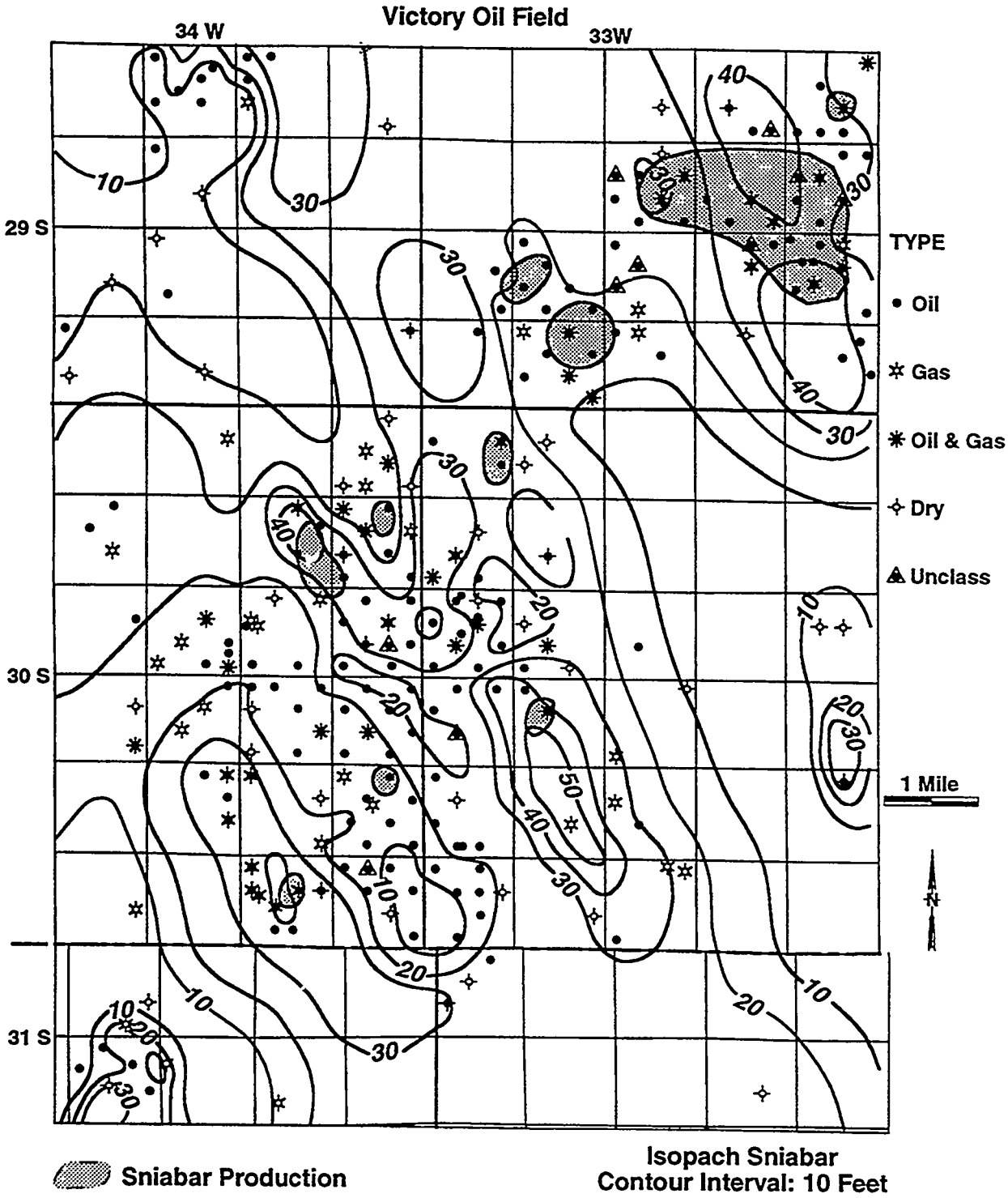

Figure 6.17. Isopach of the Sniabar Limestone illustrating southeast-northwest trending oolitic shoals. Shaded areas are Sniabar producing areas.

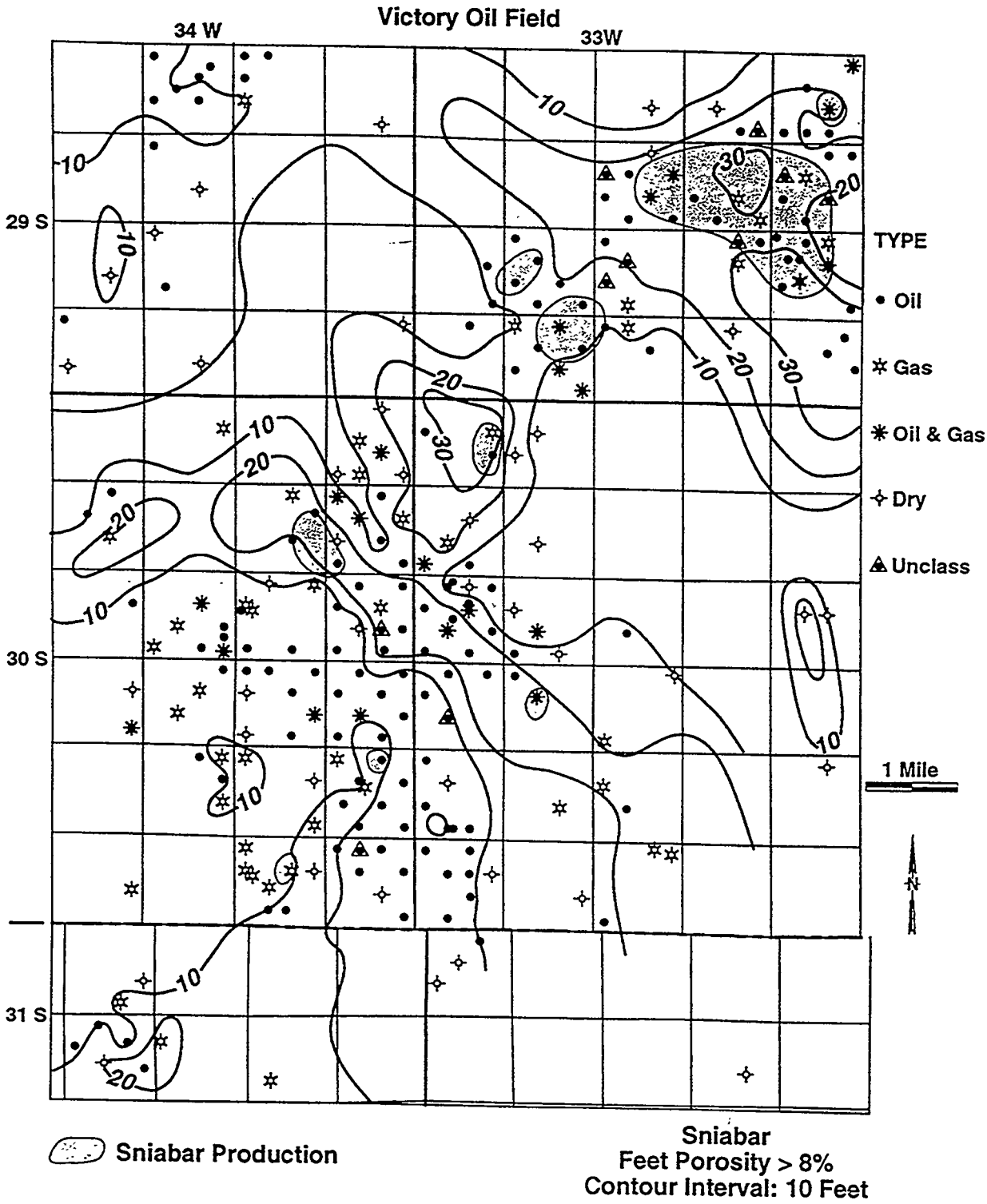

Figure 6.18. Sniabar Limestone. Feet of porosity greater than 8%.

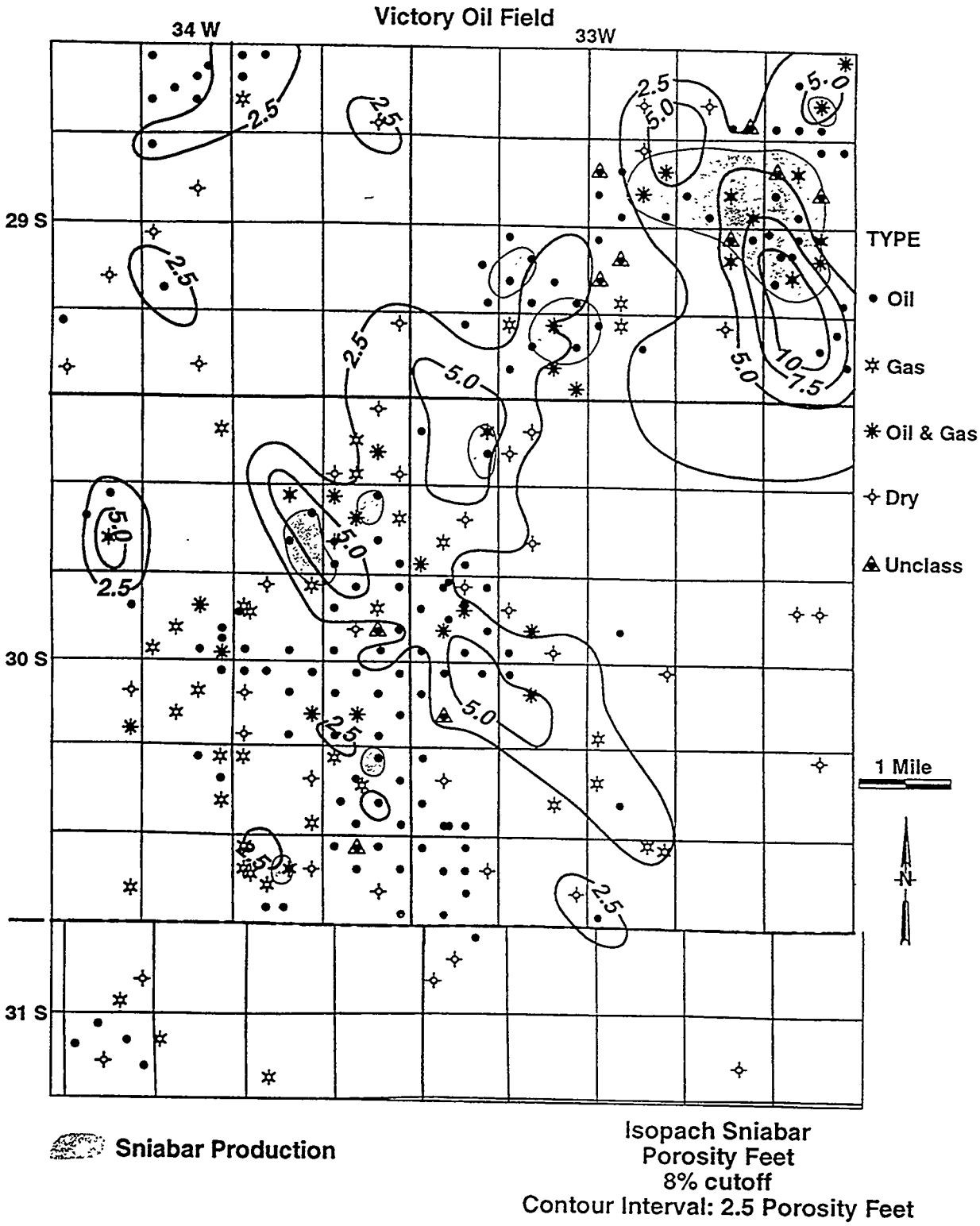

Figure 6.19. Sniabar Limestone. Porosity feet 8% cutoff. The Sniabar oil production (shaded) is primarily along the southeast-northwest trending oolite shoals with thick well developed porosity.

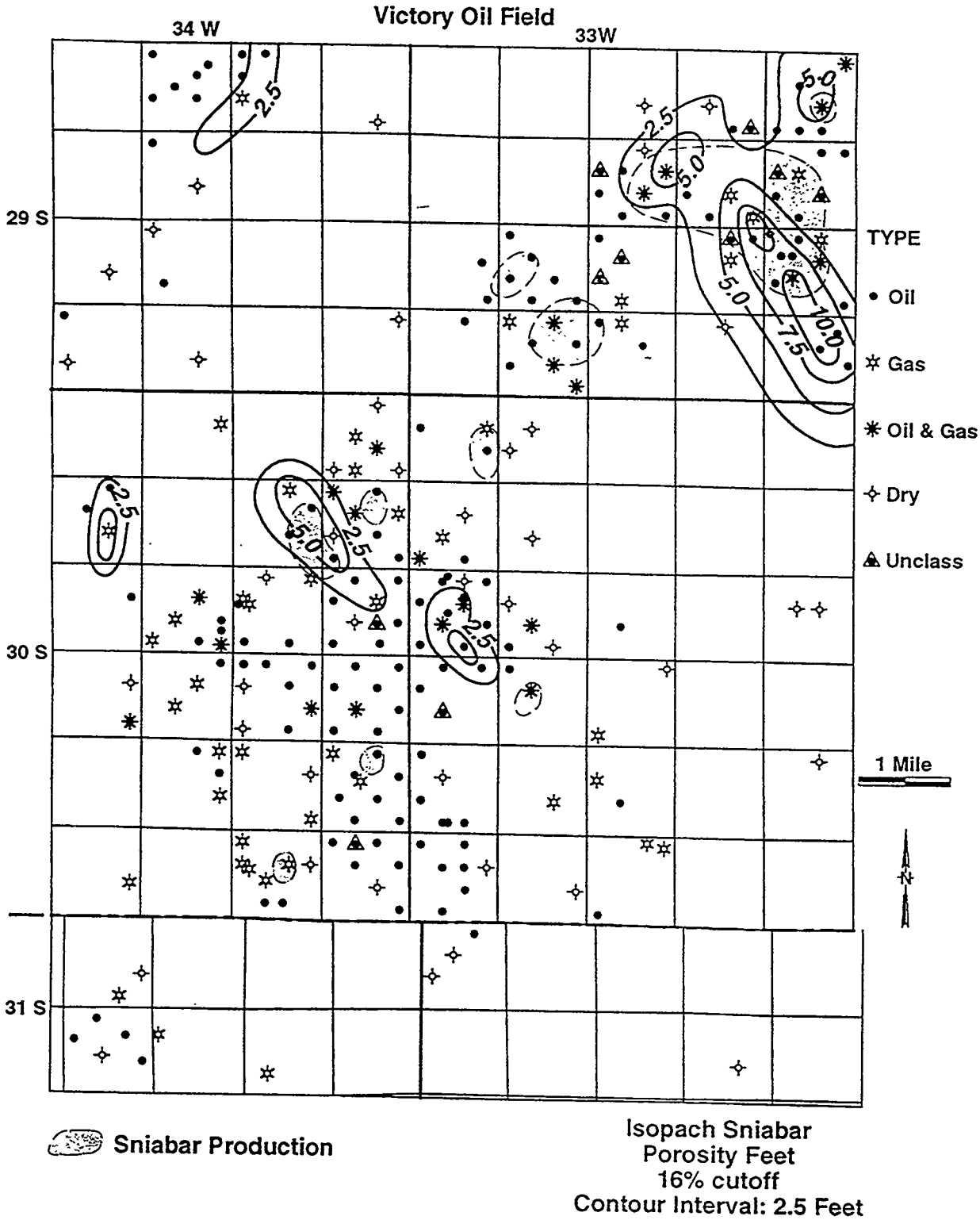

Figure 6.20. Sniabar Limestone. Porosity feet 16% cutoff. Note similarity to map with 8% cutoff indicating that the average porosity is greater than 16%.

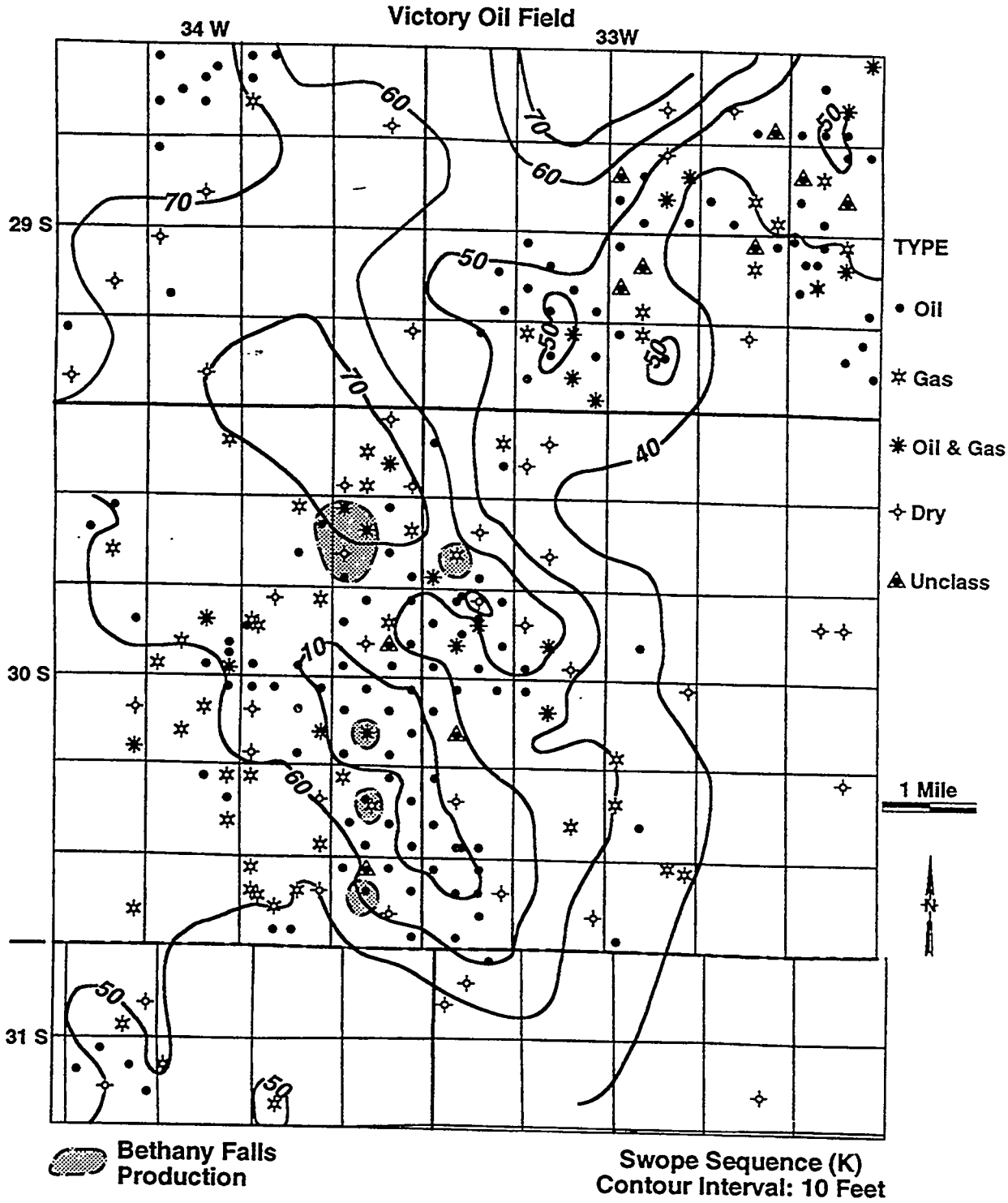

Figure 6.21. Isopach Swope sequence (K).

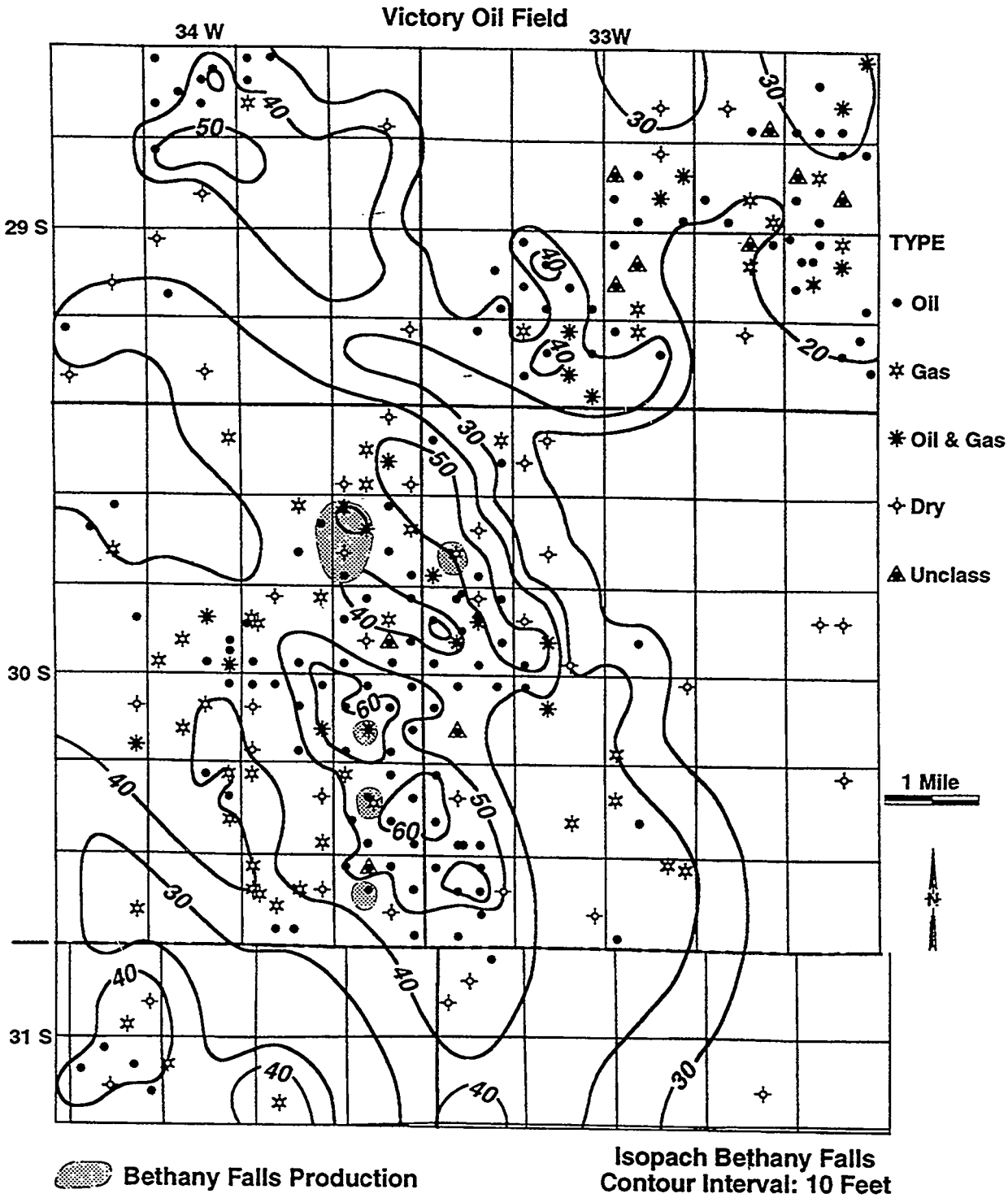

Figure 6.22. Isopach Bethany Falls Limestone illustrating southeast-northwest trending oolite shoals with 30-40 feet of buildup. Oil/gas production (shaded) is principally from these oolite shoals.

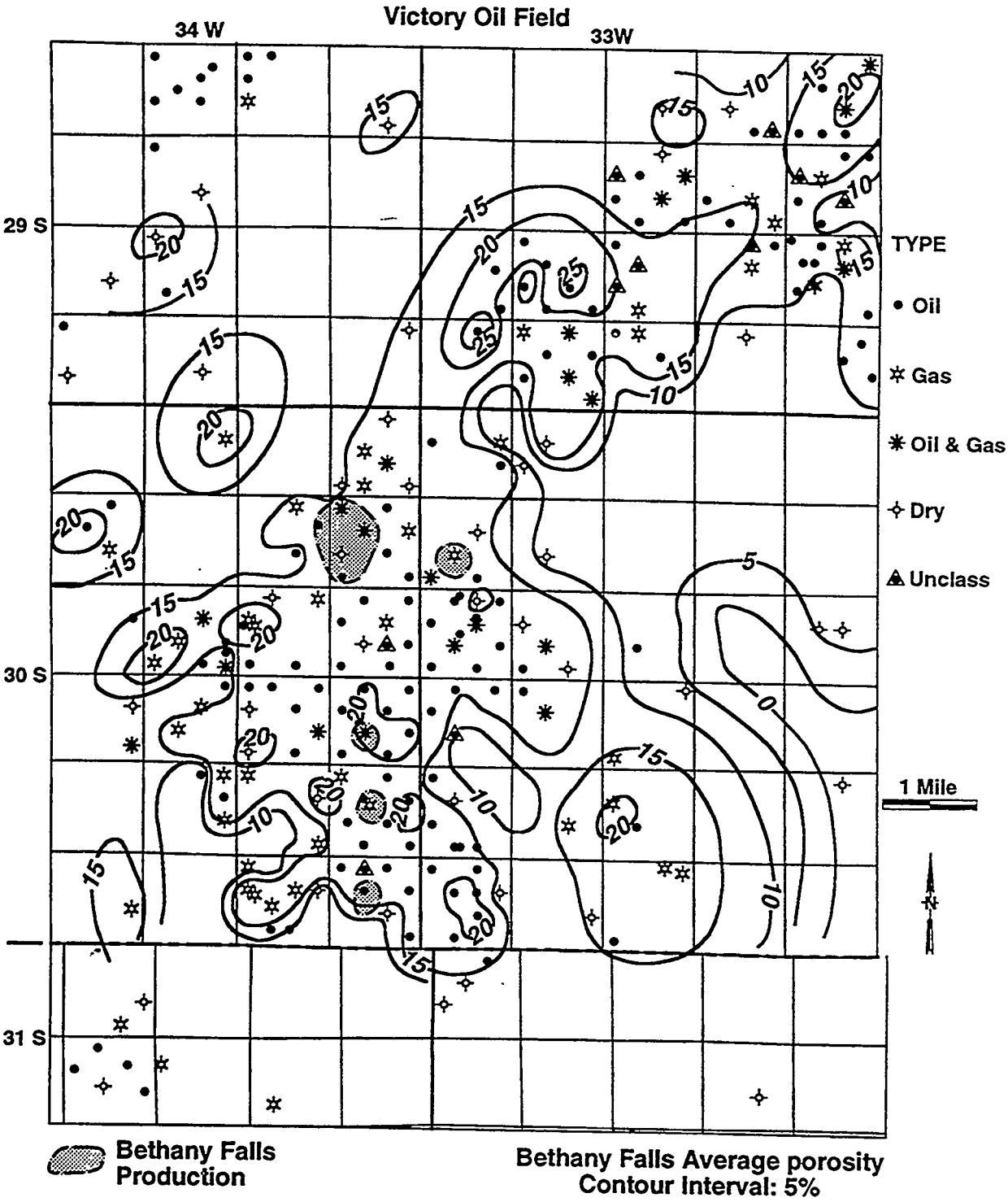

Figure 6.23. Average porosity Bethany Falls Limestone. Within the area of oolite development, the porosity is relatively consistent at about 20%.

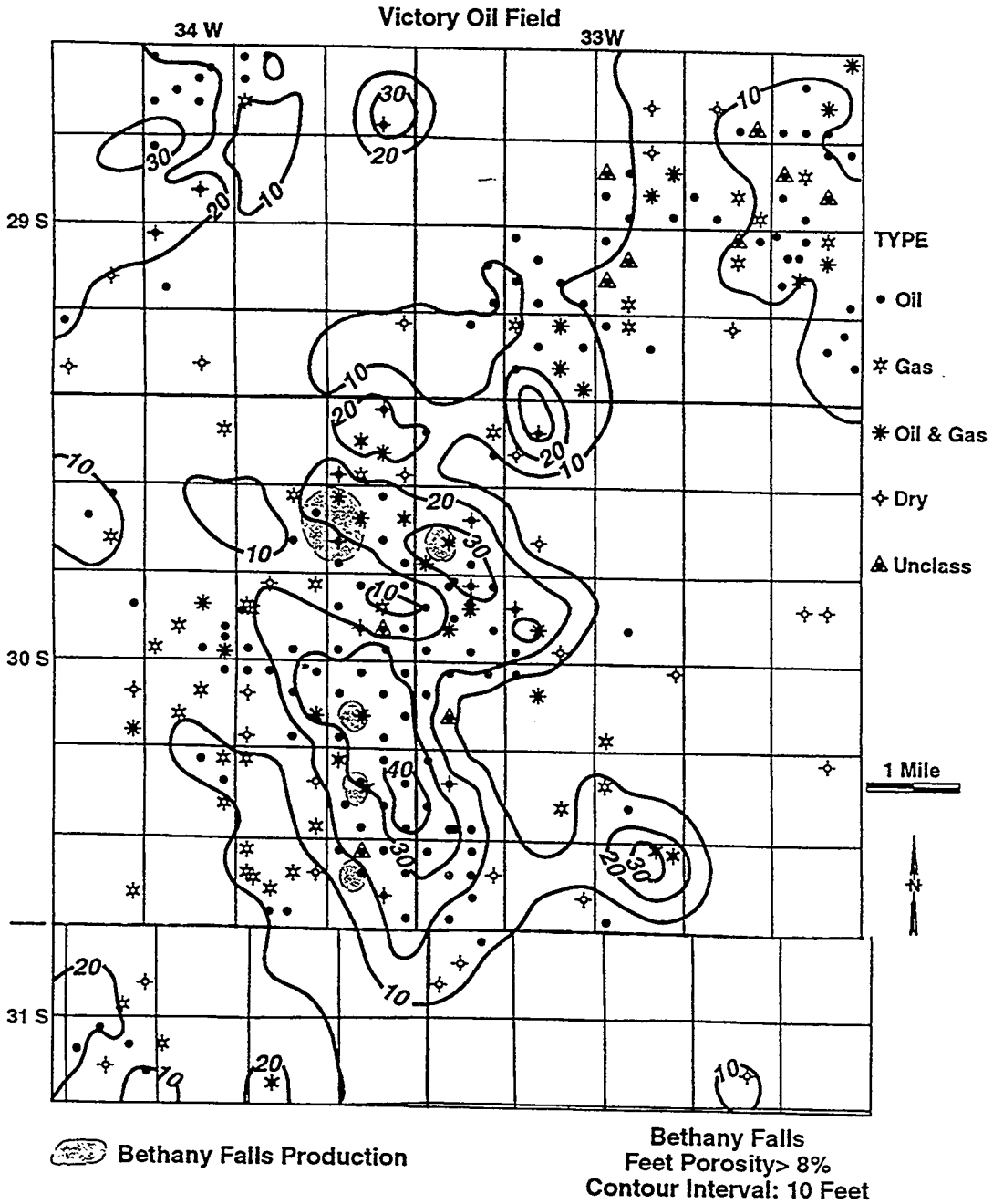

Figure 6.24. Bethany Falls Limestone. Feet of porosity greater than 8%. Note similarity with isopach of the Bethany Falls Limestone.

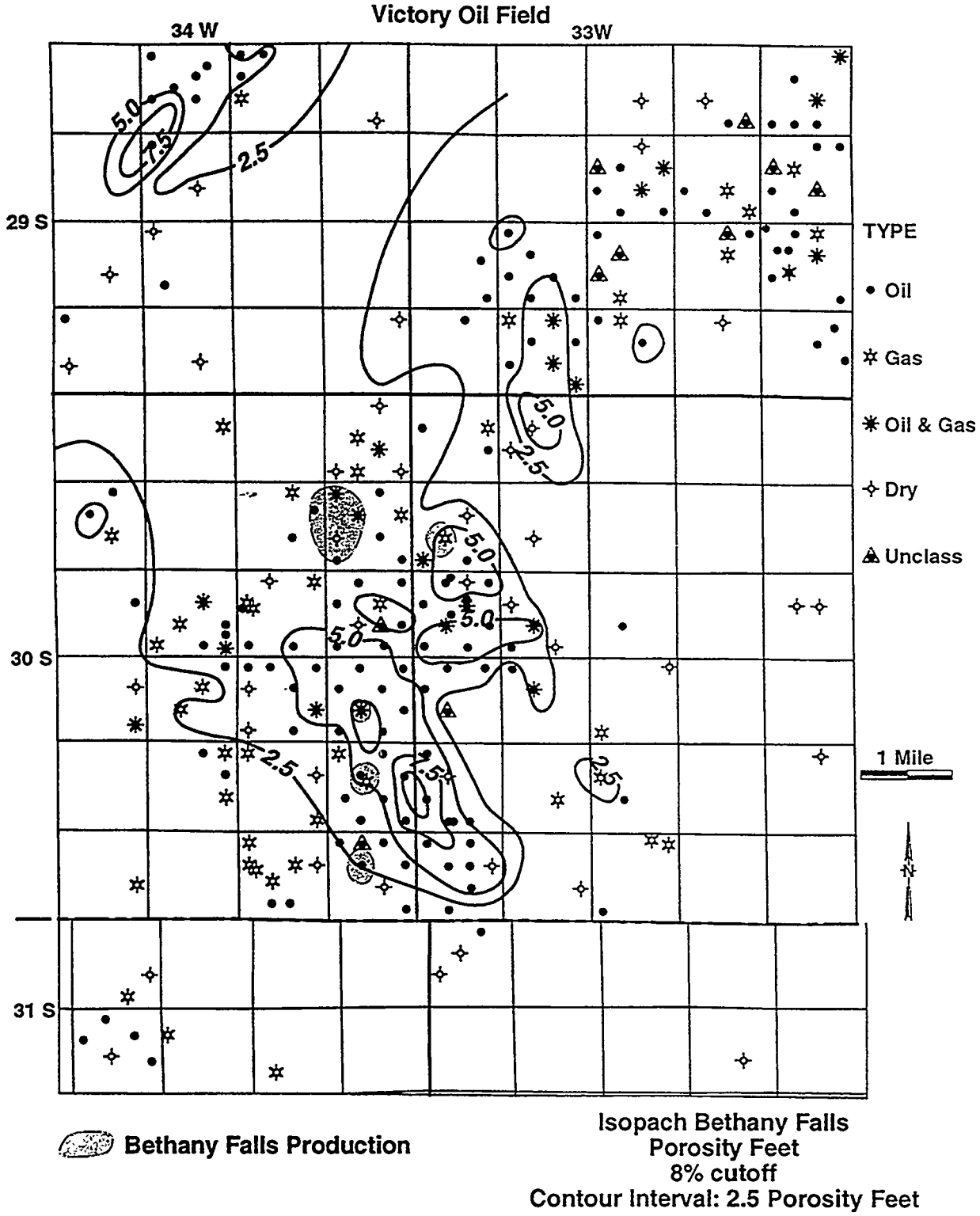

Figure 6.25. Bethany Falls Limestone. Porosity feet 8% cutoff. Note similarity to map using 16% cutoff.

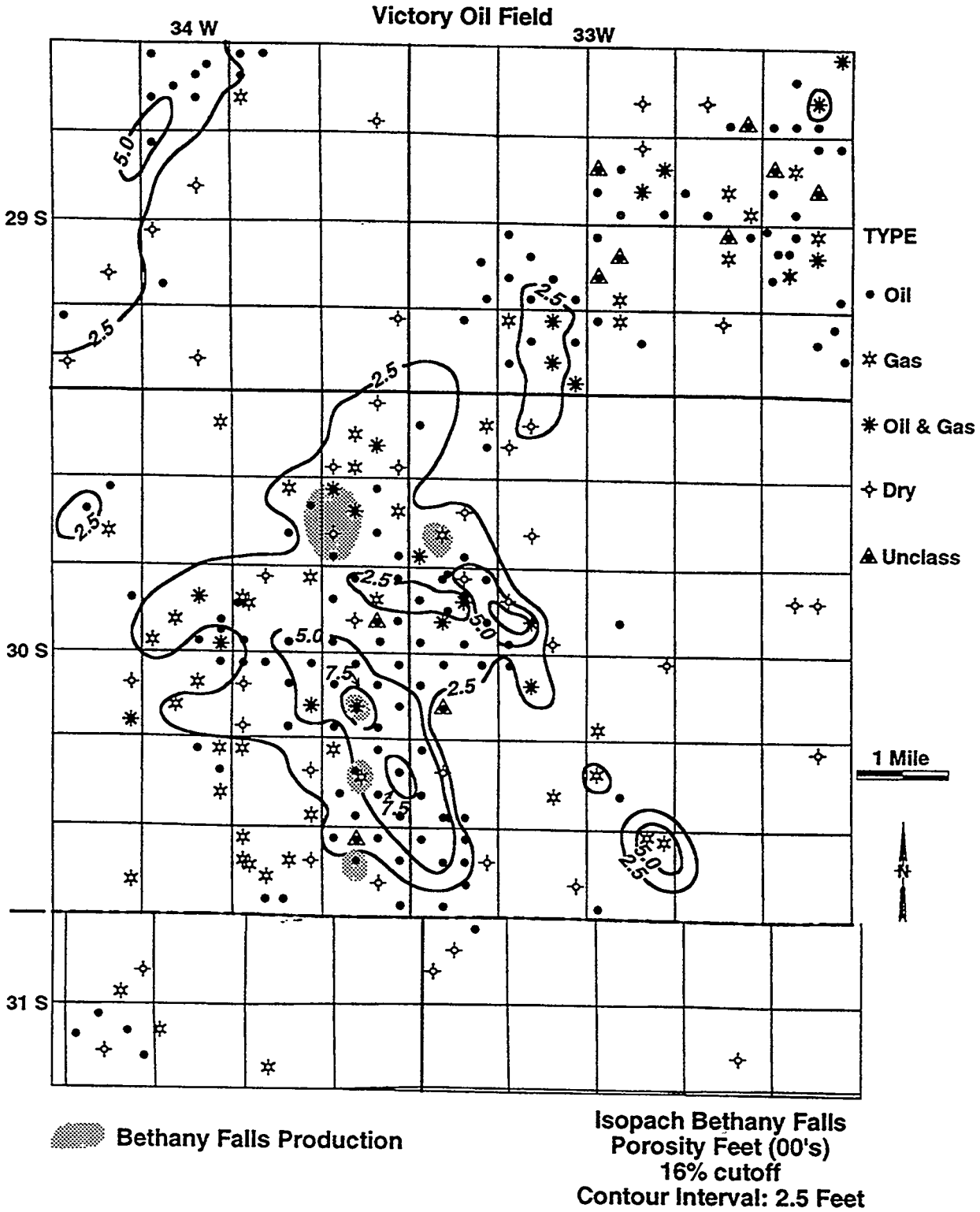

Figure 6.26. Bethany Falls Limestone. Porosity feet 16% cutoff. Similarity to map using 8% cutoff indicates that the average porosity is consistently above 16%.

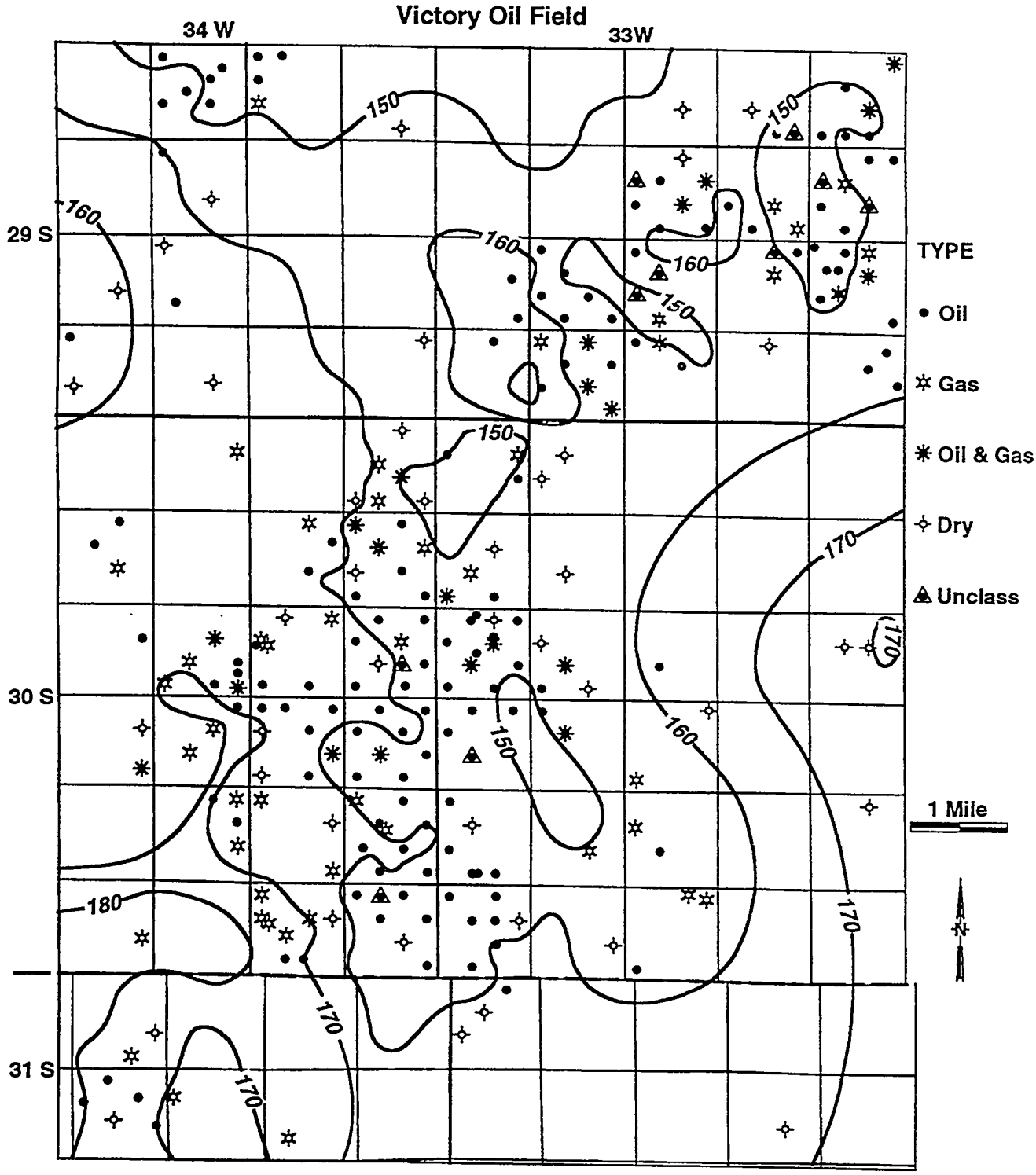

Isopach Galesburg Shale - Quivira Shale (I+J)
Contour Interval: 10 Feet

Figure 6.27. Isopach Galesburg Shale to Quivera Shale (I and J sequences). Note uniformity in thickness.

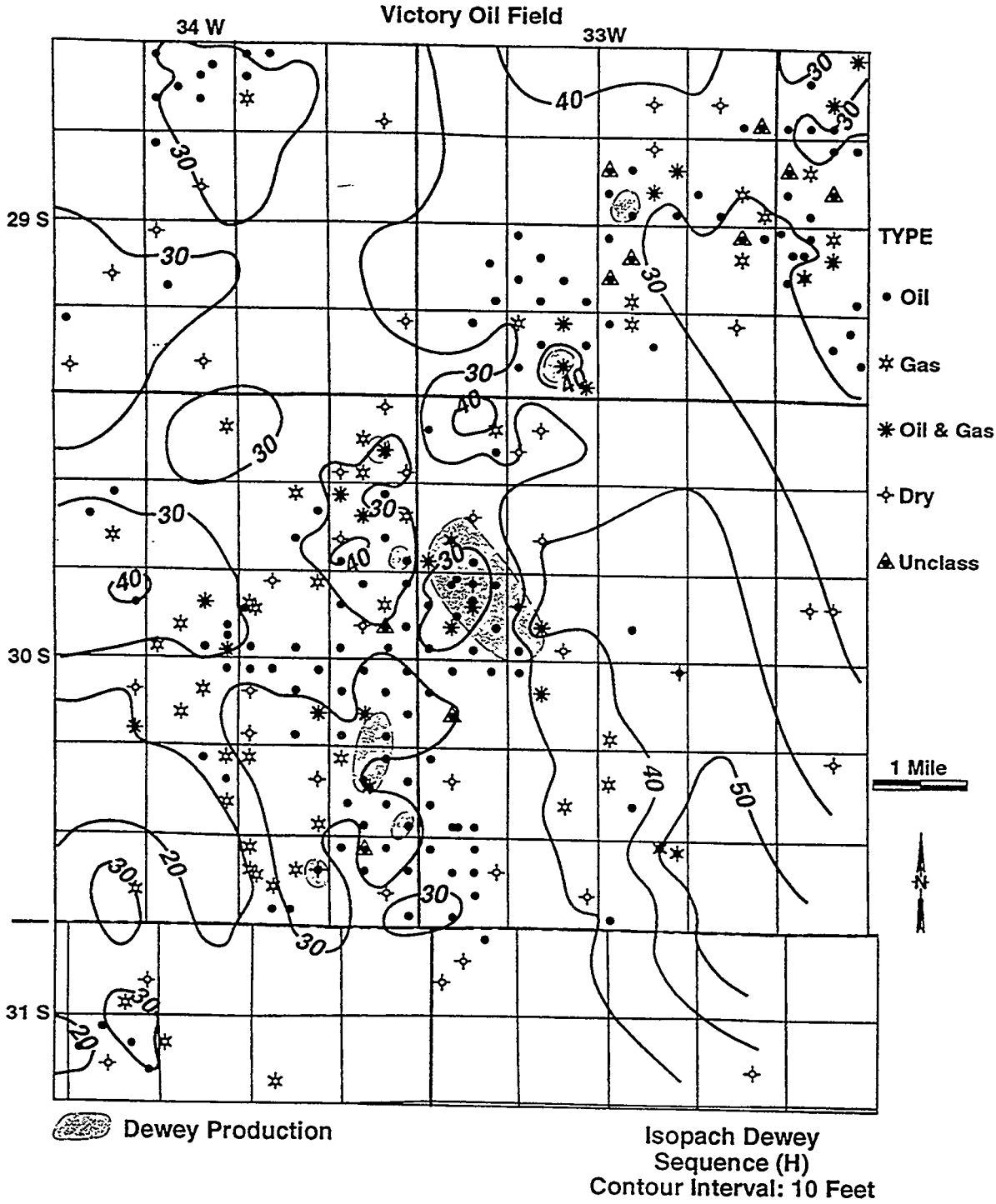

Figure 6.28. Isopach Dewey sequence (H). Note uniformity in thickness except for southeast corner where the sequence increases significantly.

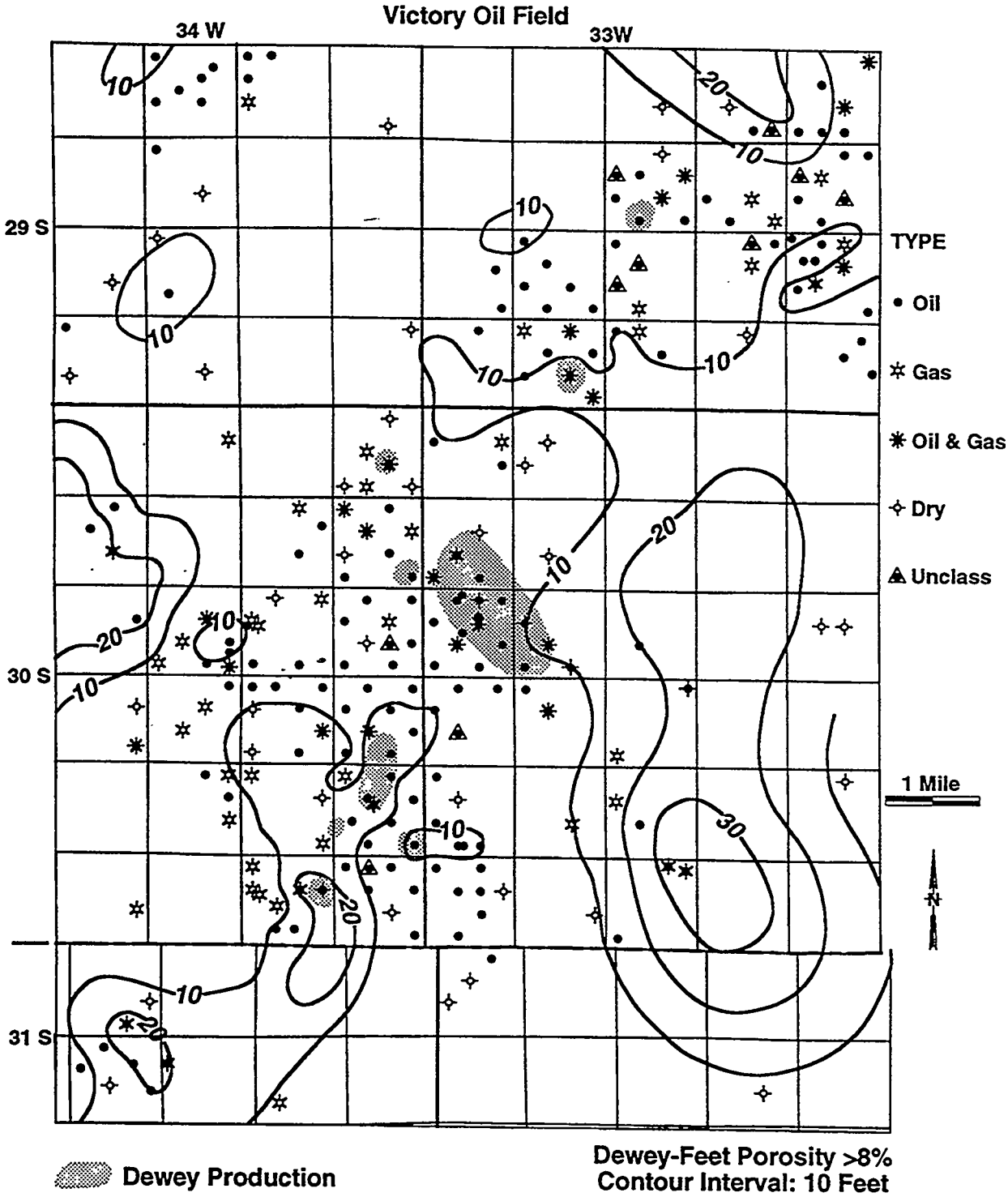

Figure 6.29. Dewey Limestone. Feet of porosity greater than 8%. Thick porosity development in southeast corner of map is indicator of an oolitic development downslope from earlier grainstone buildups as a result of a relative lowering of sea level.

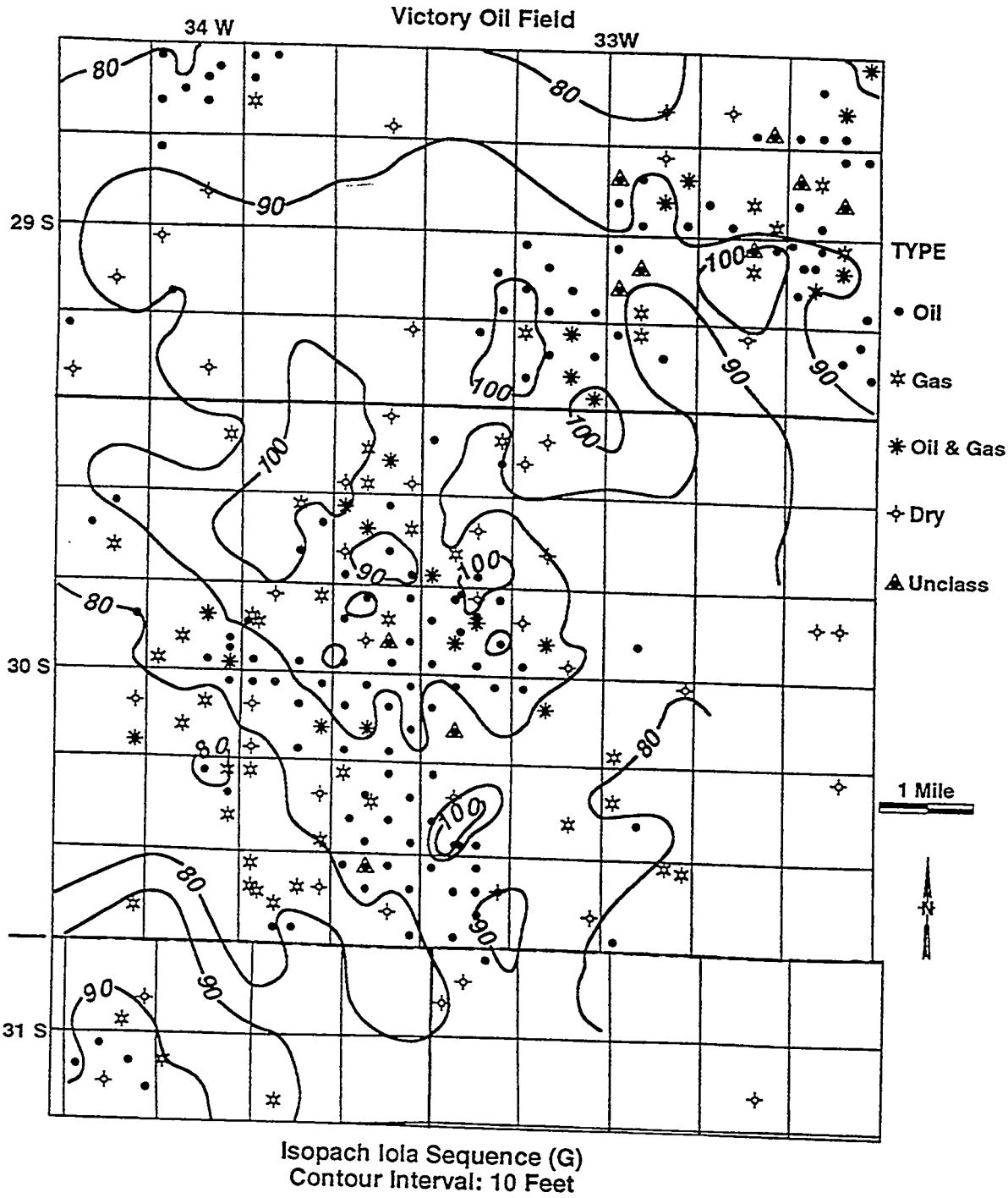

Figure 6.30. Isopach of Iola sequence (G). Note relative uniformity in thickness.

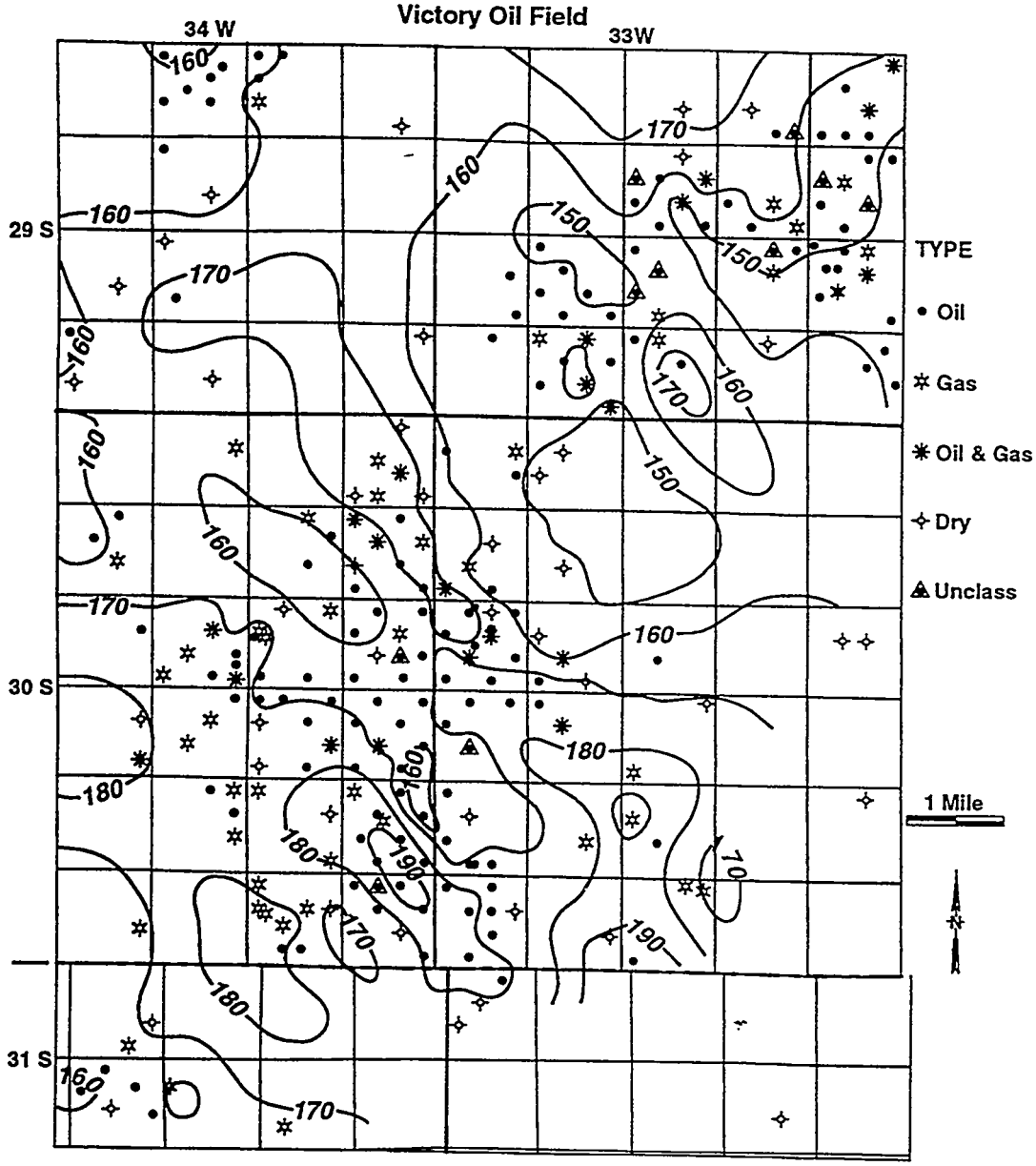

Figure 6.31. Isopach Iatan Limestone to Lane Shale (B through F sequences). Interval is composite of five sequences subdivided by unconformities. The upper two sequences, Iatan (B) and Stanton (C) are oil productive.

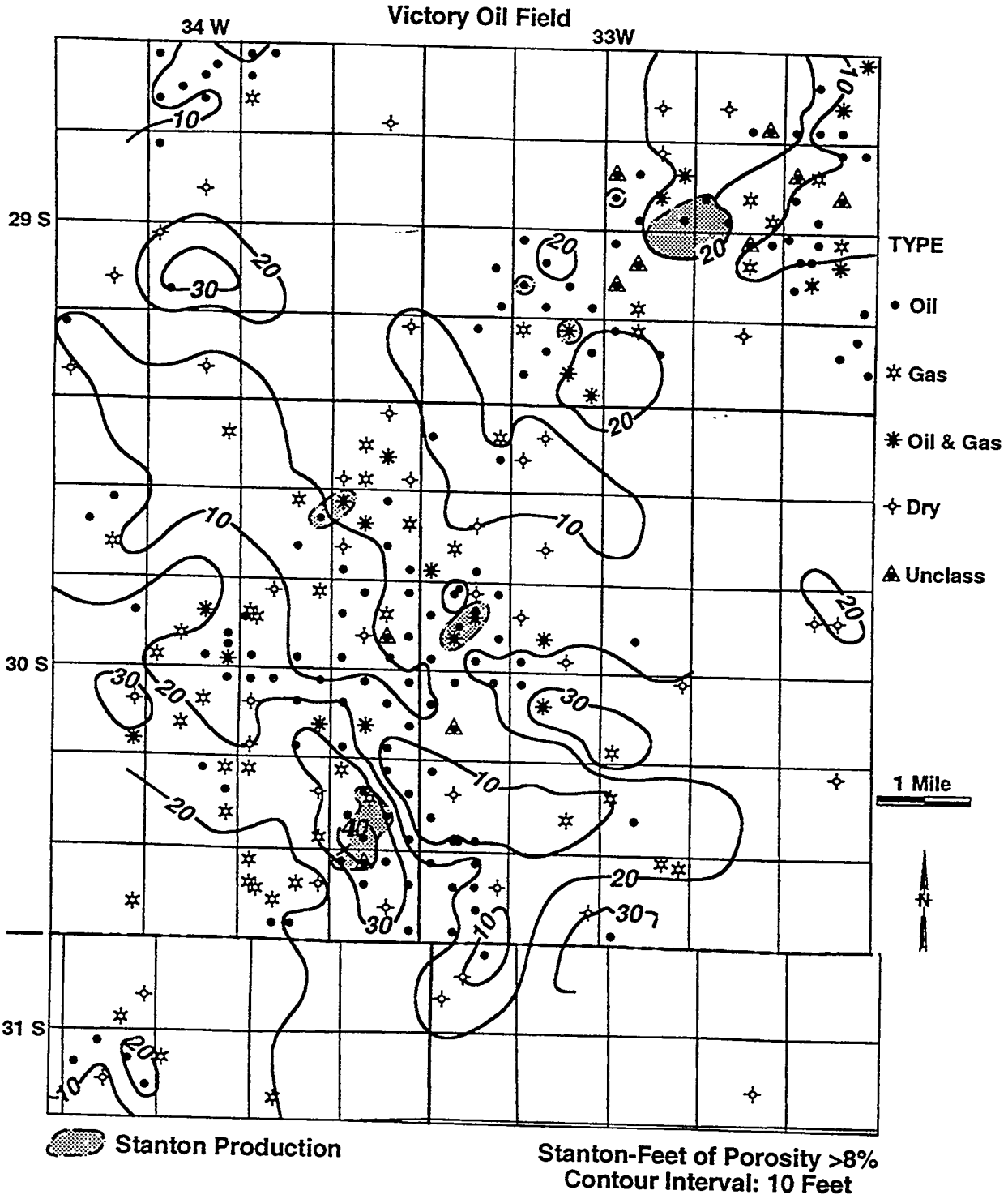

Figure 6.32. Stanton Limestone. Feet of porosity greater than 8%. The 40 feet of porosity contour in the southern part of the map indicates an oolitic grainstone shoal that has been productive.

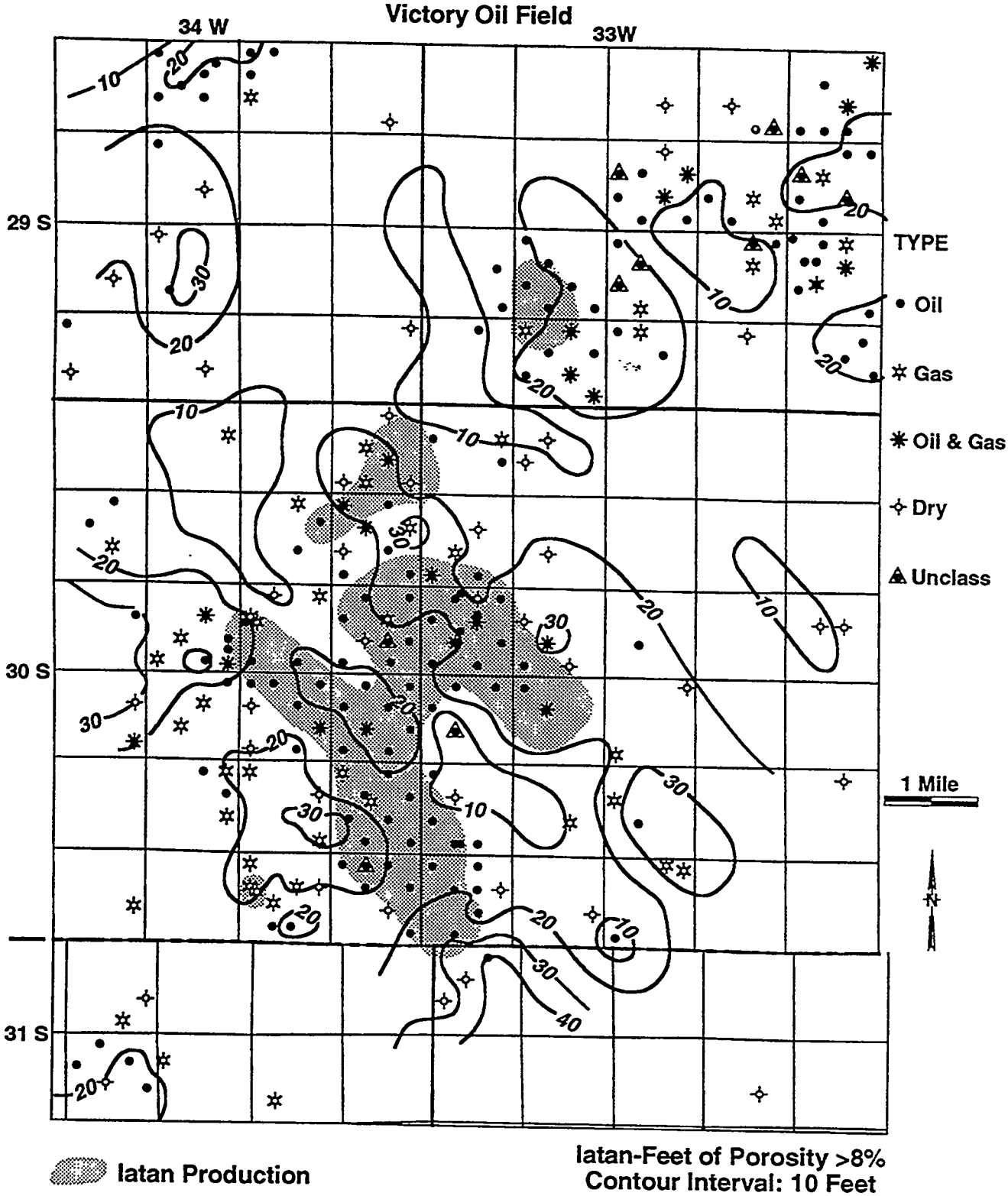

Figure 6.33. Iatan Limestone. Feet of porosity greater than 8%. This interval represents the most extensive producing reservoir (shaded) in the Victory Field. The production is from bioclastic limestone with intercrystalline-intergranular porosity.

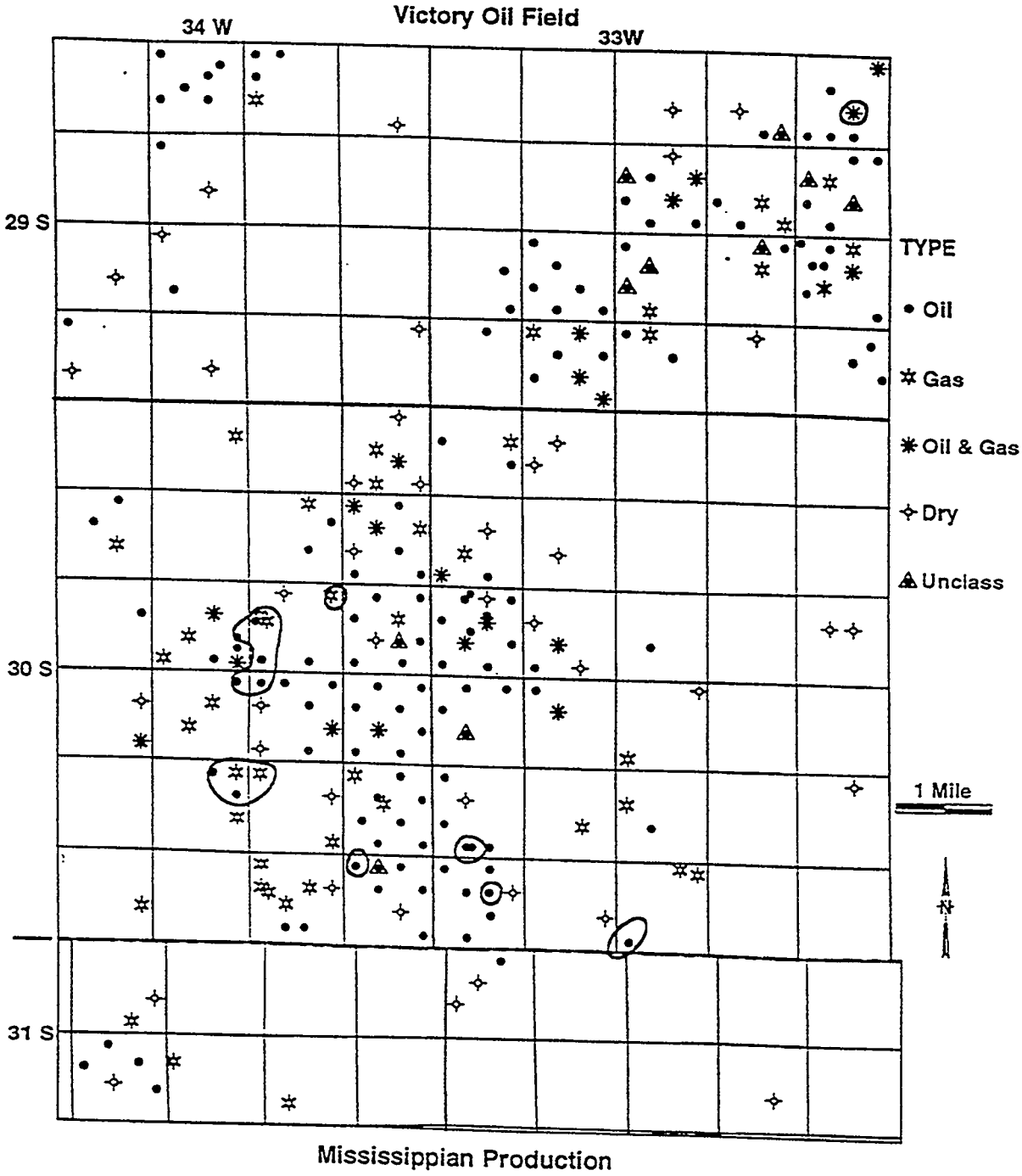

Figure 6.34. Mississippian limestone production.

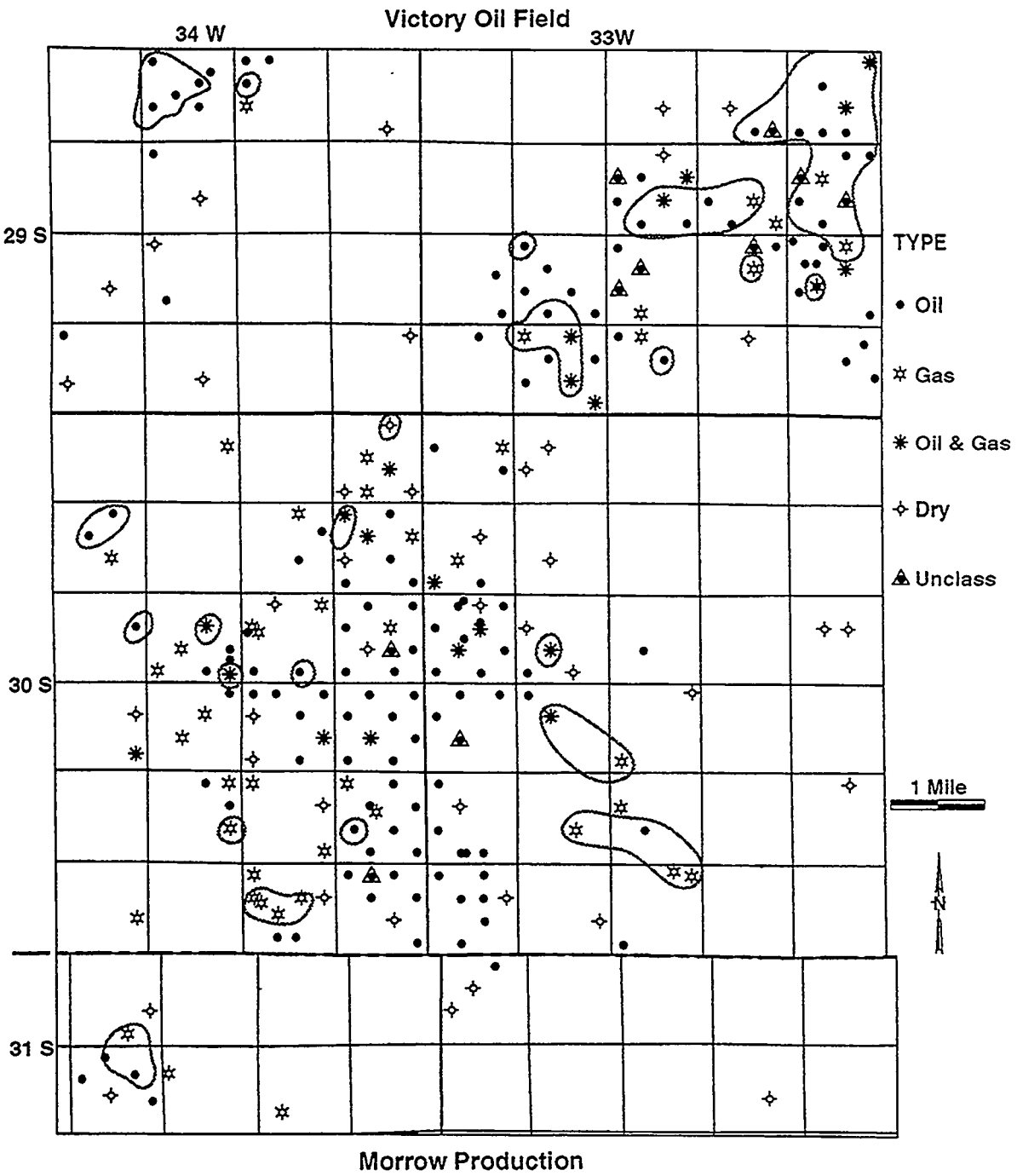

Figure 6.35. Pennsylvanian Morrow sandstone production.

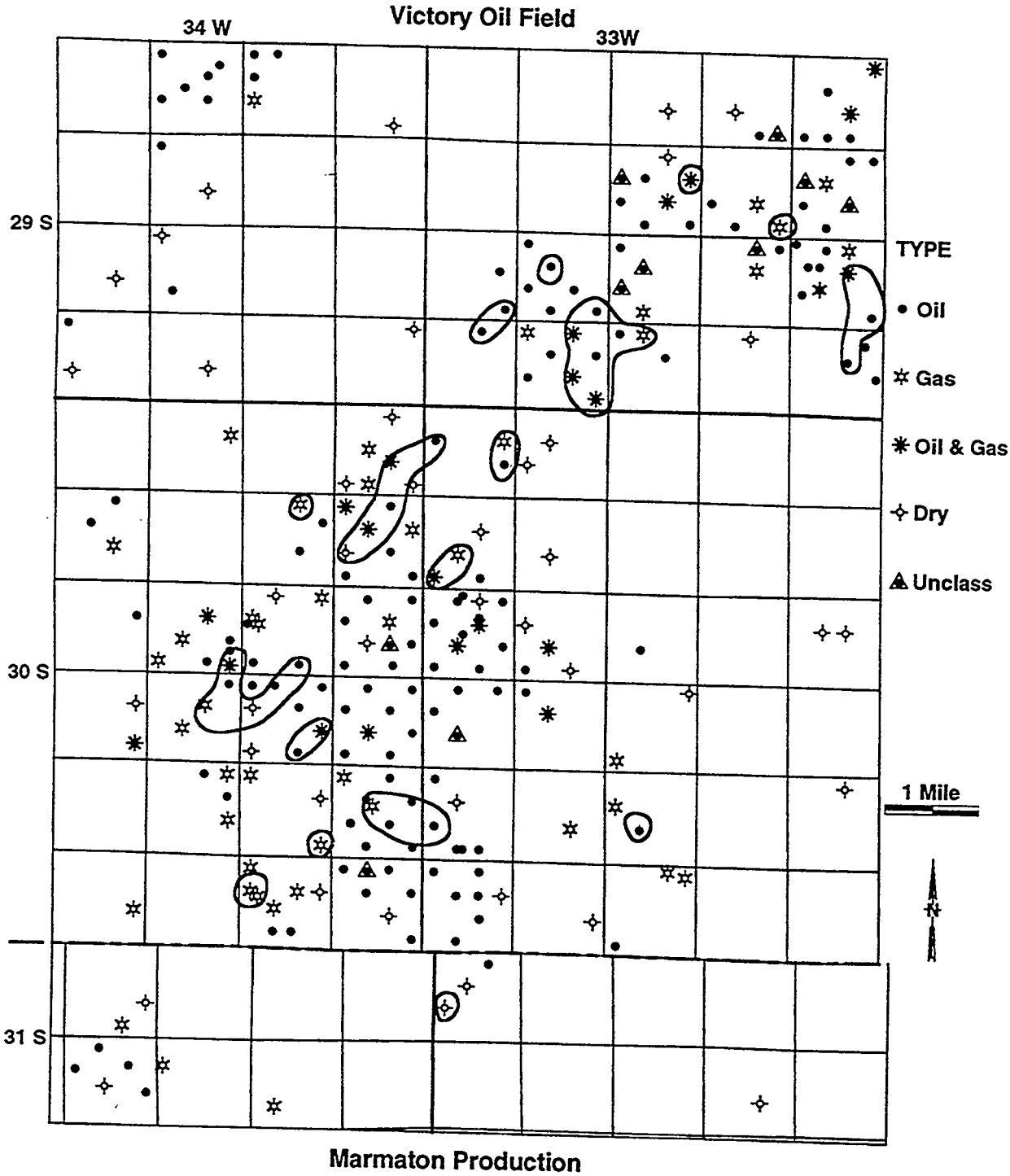

Figure 6.36. Pennsylvanian Marmaton limestone production.

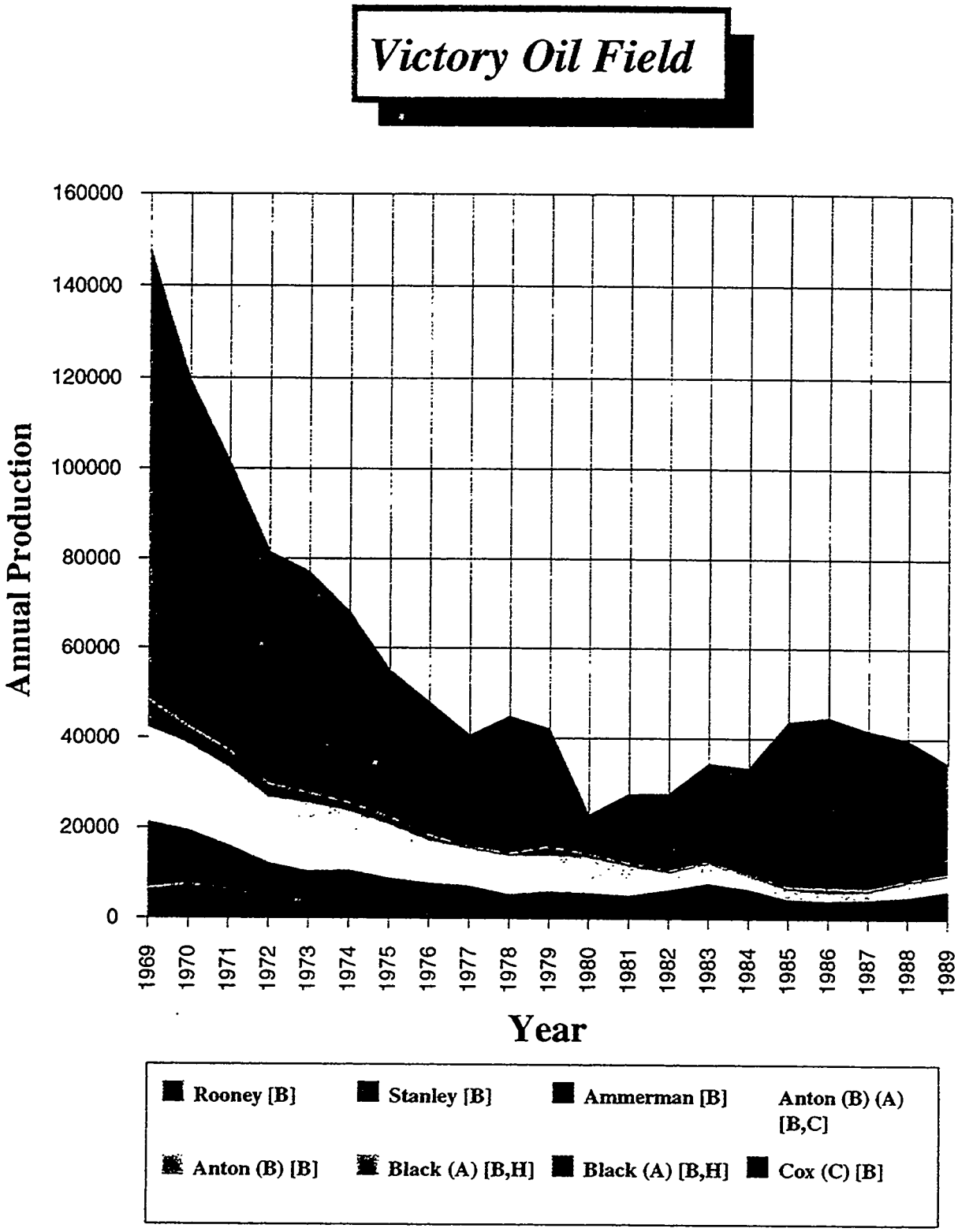

Figure 6.37. Lansing-Kansas City limestone lease production decline curves in the Victory Field. Letter in parenthesis indicates productive sequence.

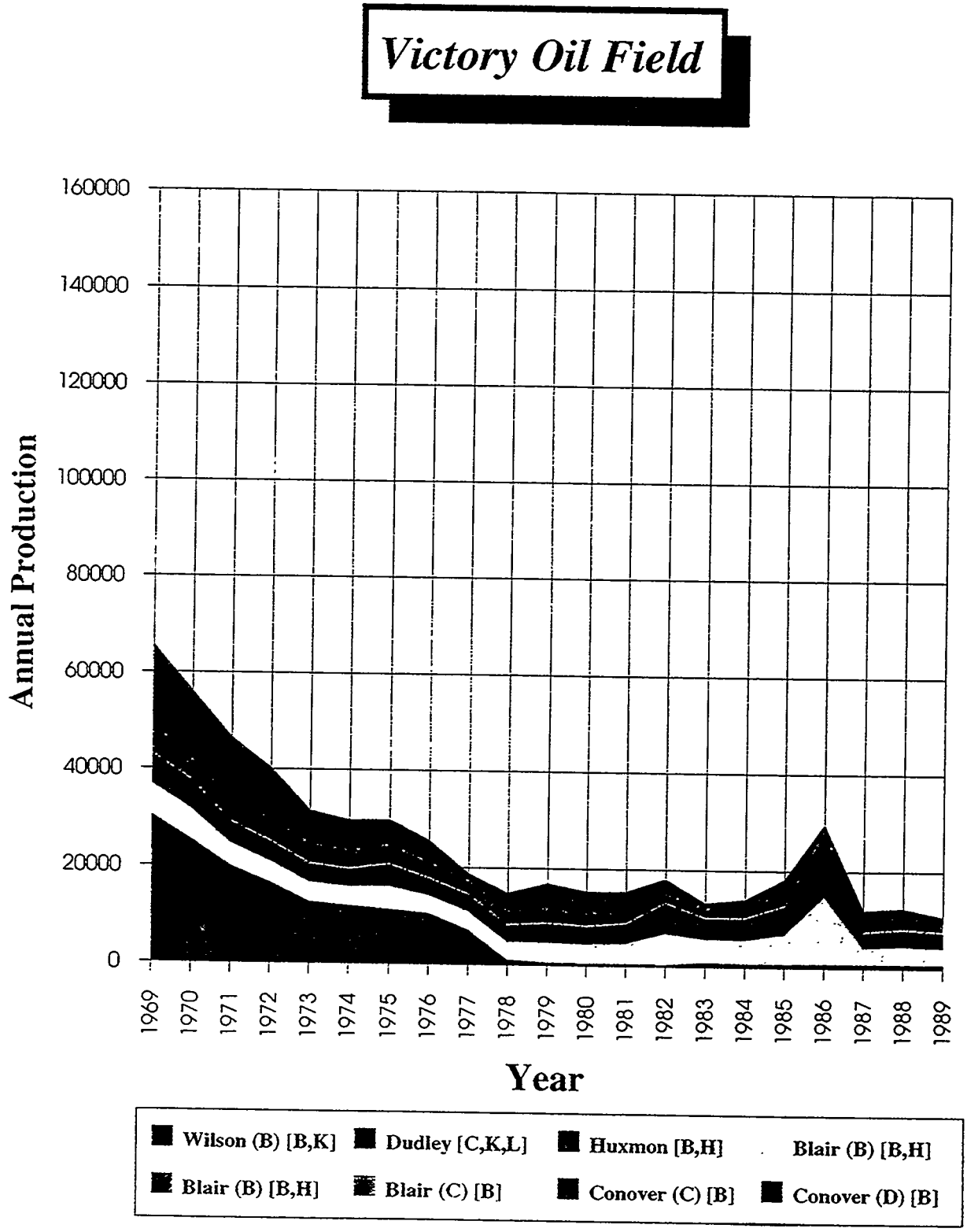

Figure 6.38. Lansing-Kansas City limestone lease production decline curves in the Victory Field. Letter in parenthesis indicates productive sequence.

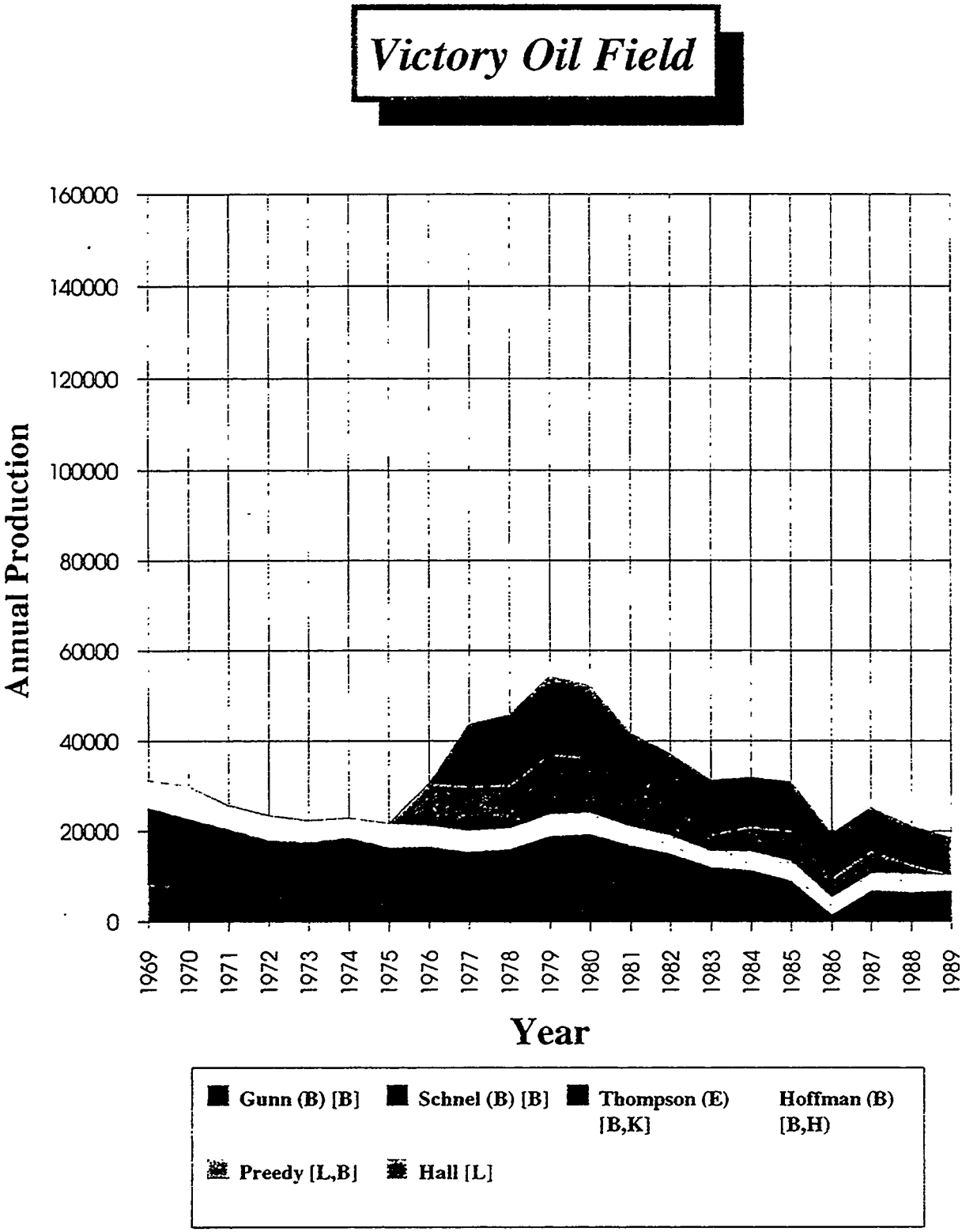

Figure 6.39. Lansing-Kansas City limestone lease production decline curves in the Victory Field. Letter in parenthesis indicates productive sequence.

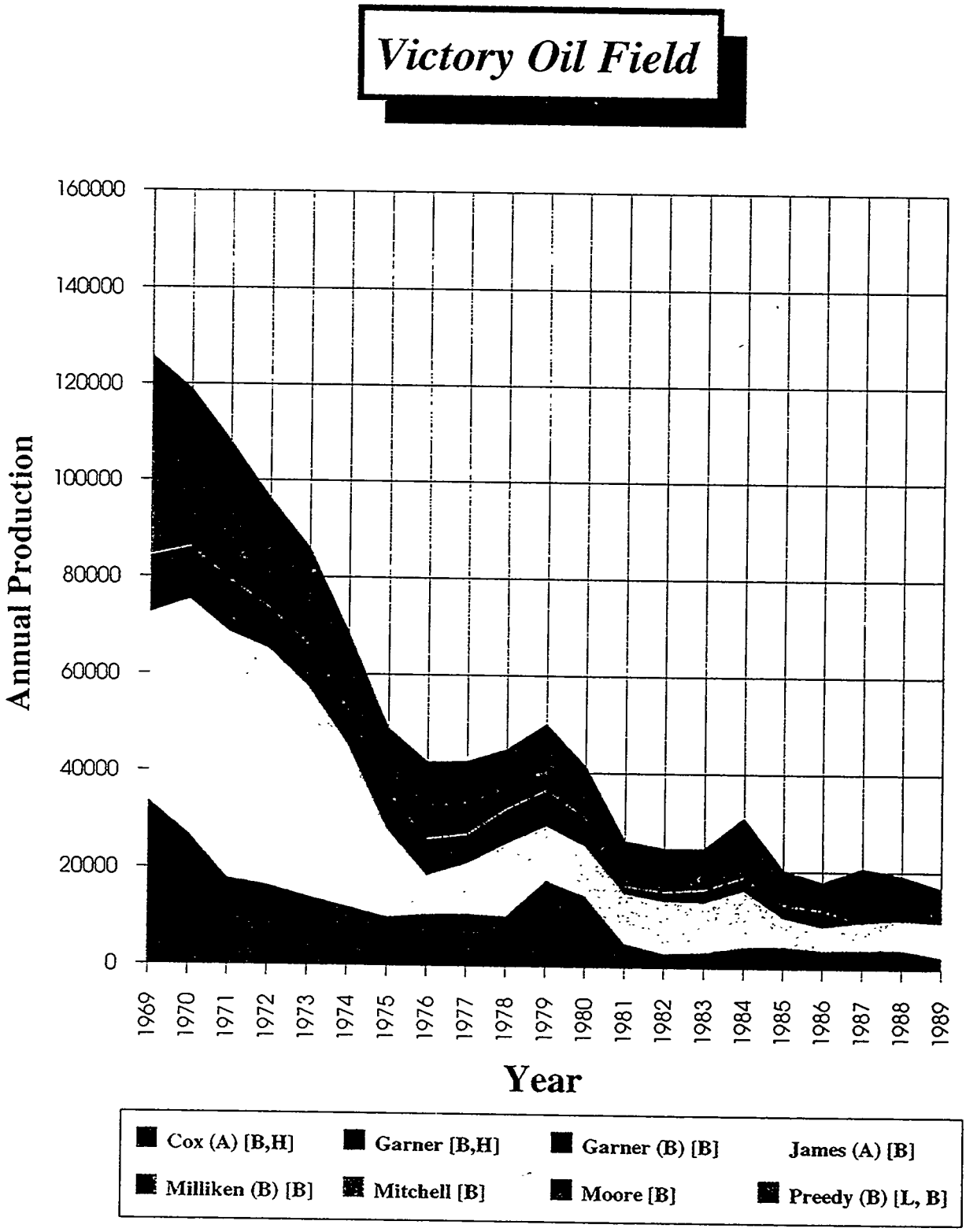

Figure 6.40. Lansing-Kansas City limestone lease production decline curves in the Victory Field. Letter in parenthesis indicates productive sequence.

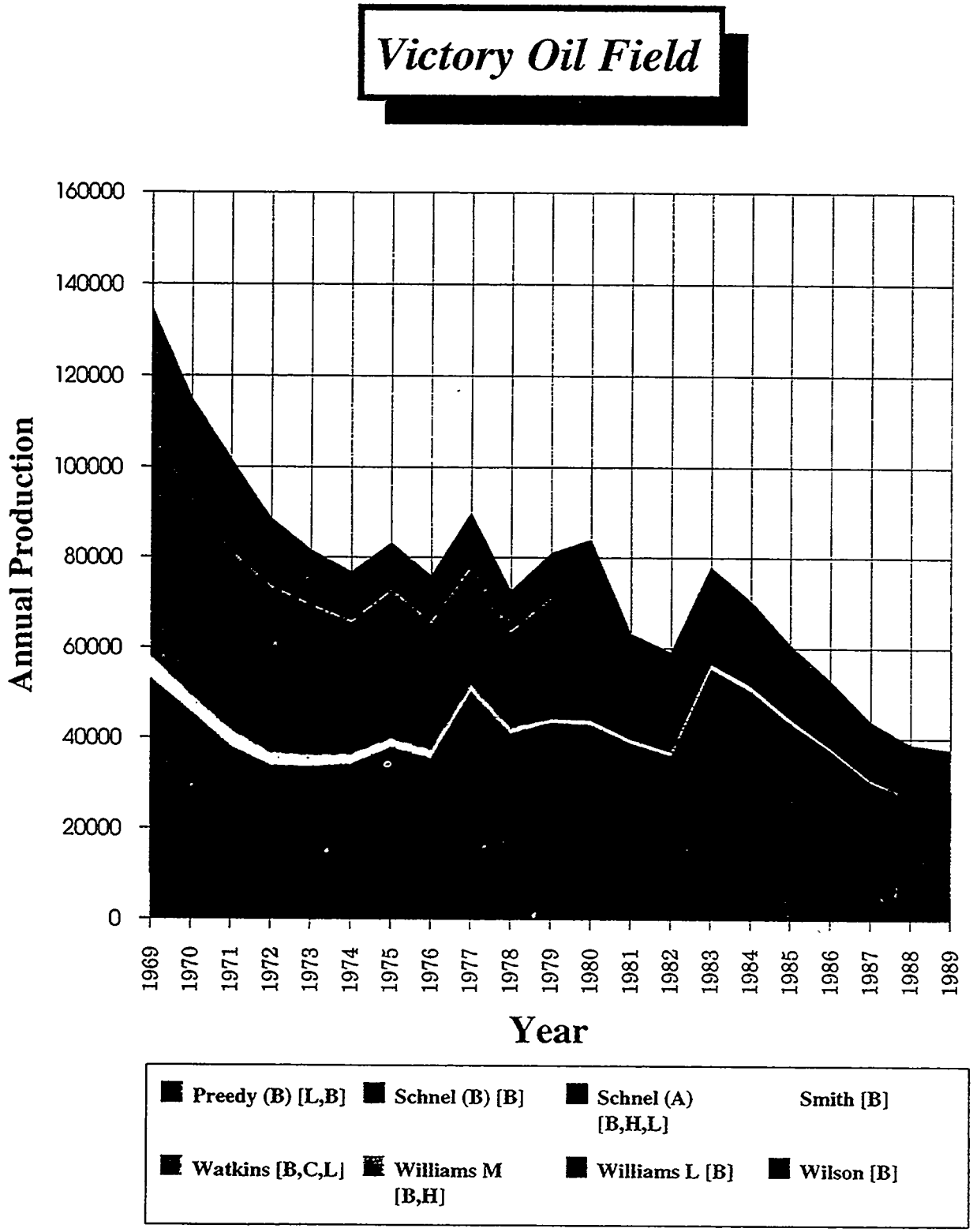

Figure 6.41. Lansing-Kansas City limestone lease production decline curves in the Victory Field. Letter in parenthesis indicates productive sequence.

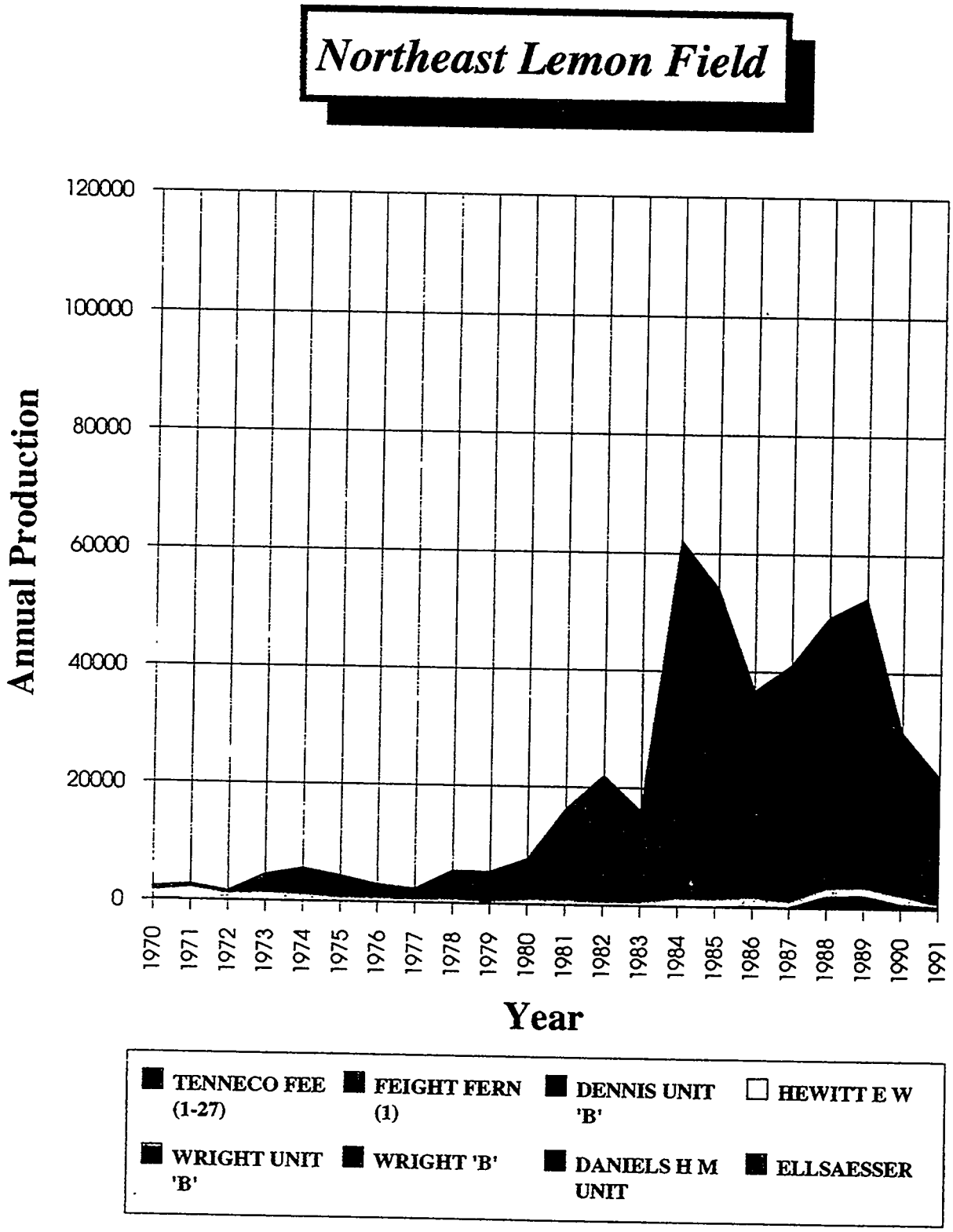

Figure 6.42. Lansing-Kansas City limestone lease production decline curves in the Northeast Lemon Field. Numbers in parentheses indicate the well number.

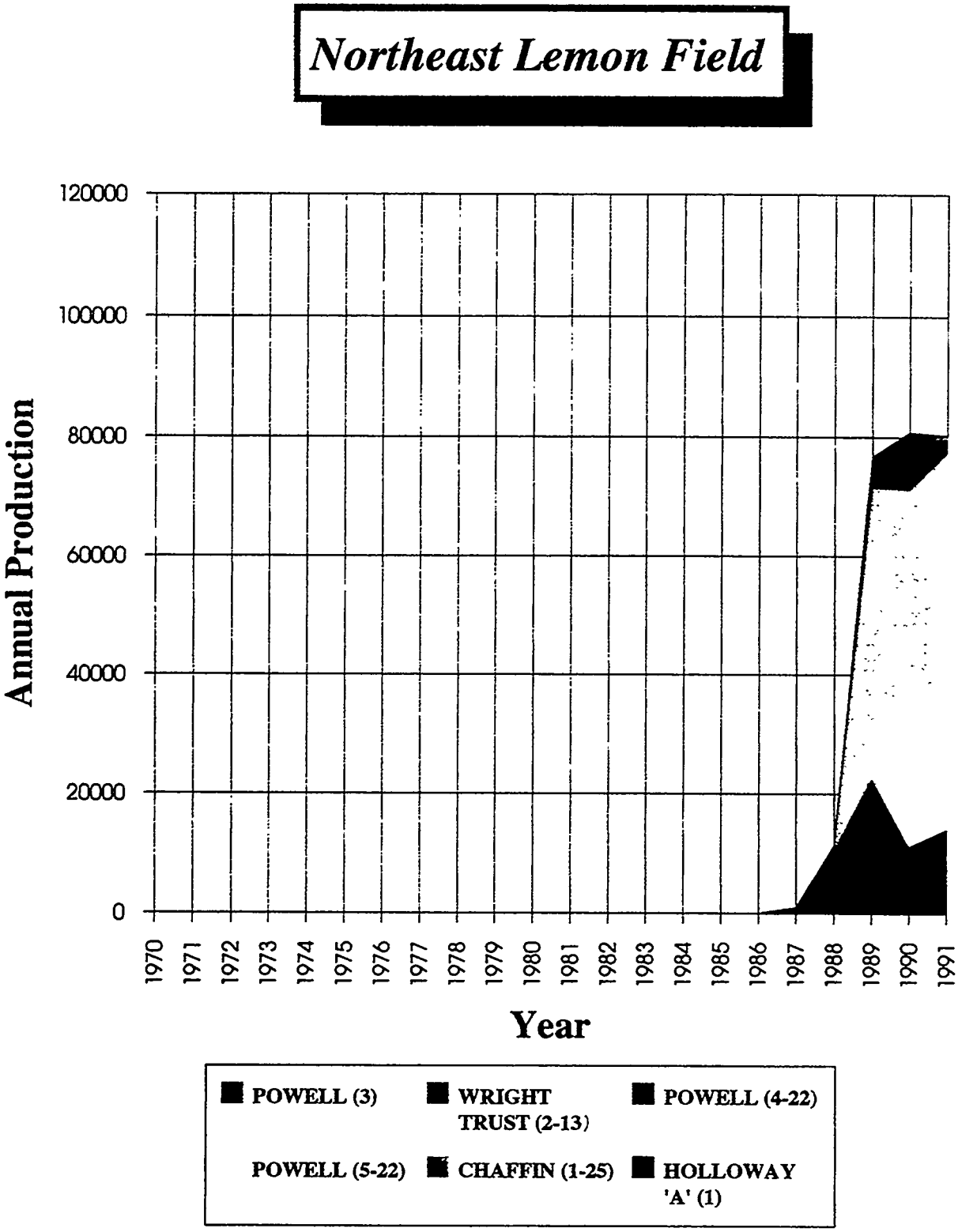

Figure 6.43. Lansing-Kansas City limestone lease production decline curves in the Northeast Lemon Field. Numbers in parentheses indicate the well number.

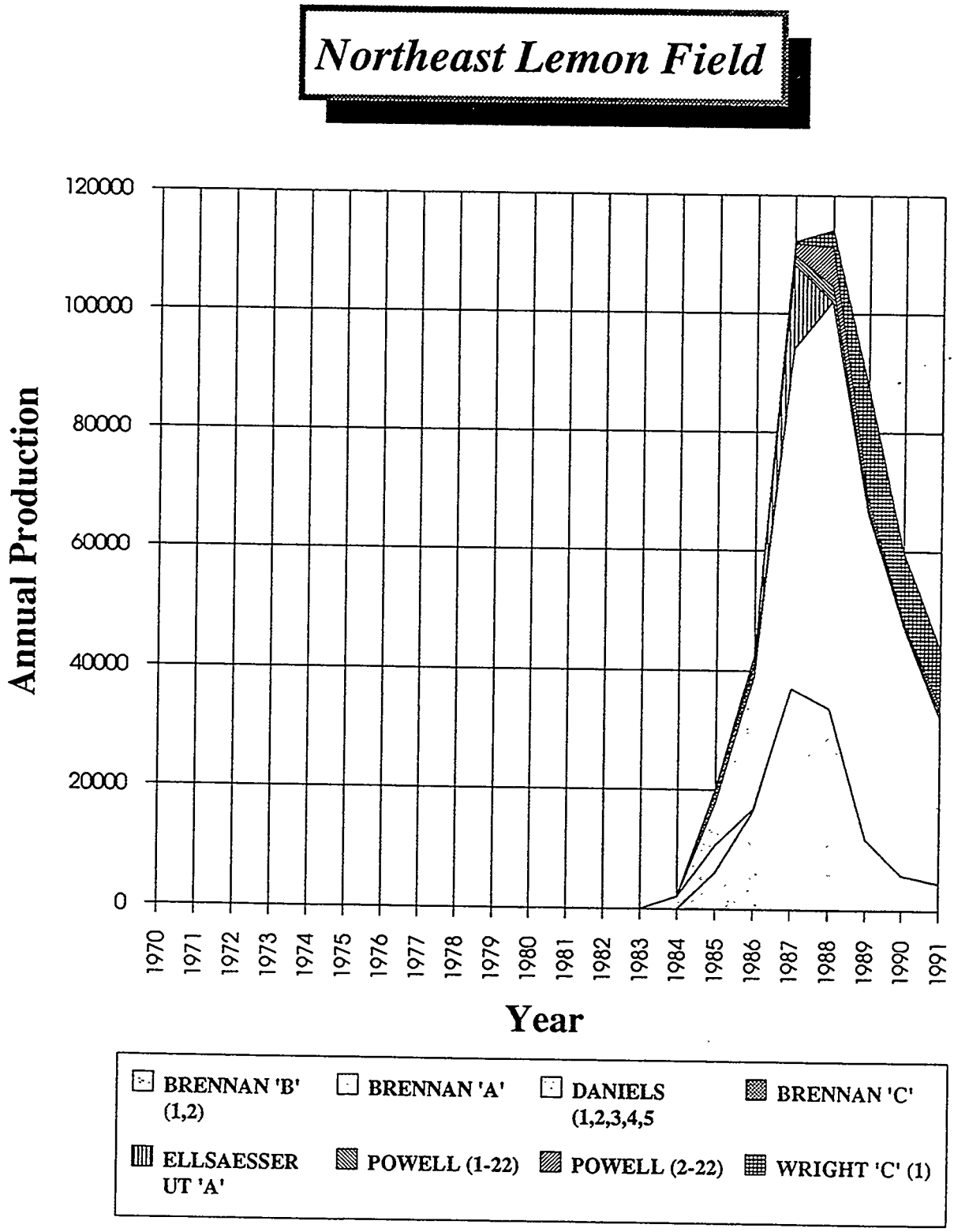

Figure 6.44. Lansing-Kansas City limestone lease production decline curves in the Northeast Lemon Field. Numbers in parentheses indicate the well number.

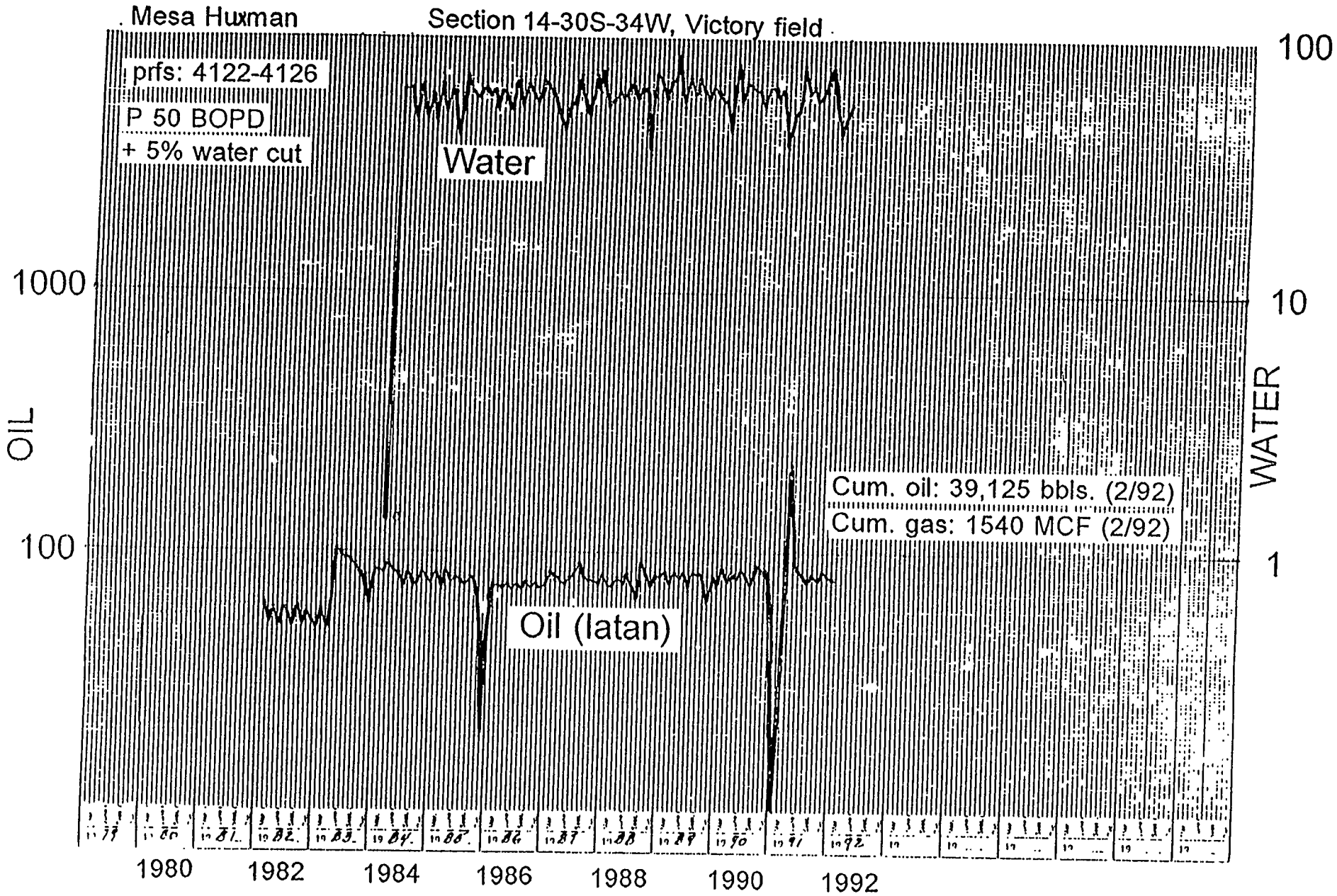

Figure 6.45. Iatan Limestone production decline curve from the Mesa #7 Huxman, Victory Field. The well was completed in 1966 for 56 barrels of oil and 5% salt water. As shown, the well made little to no water until 1983. Since 1982, the well has produced about 80 barrels of oil per month.

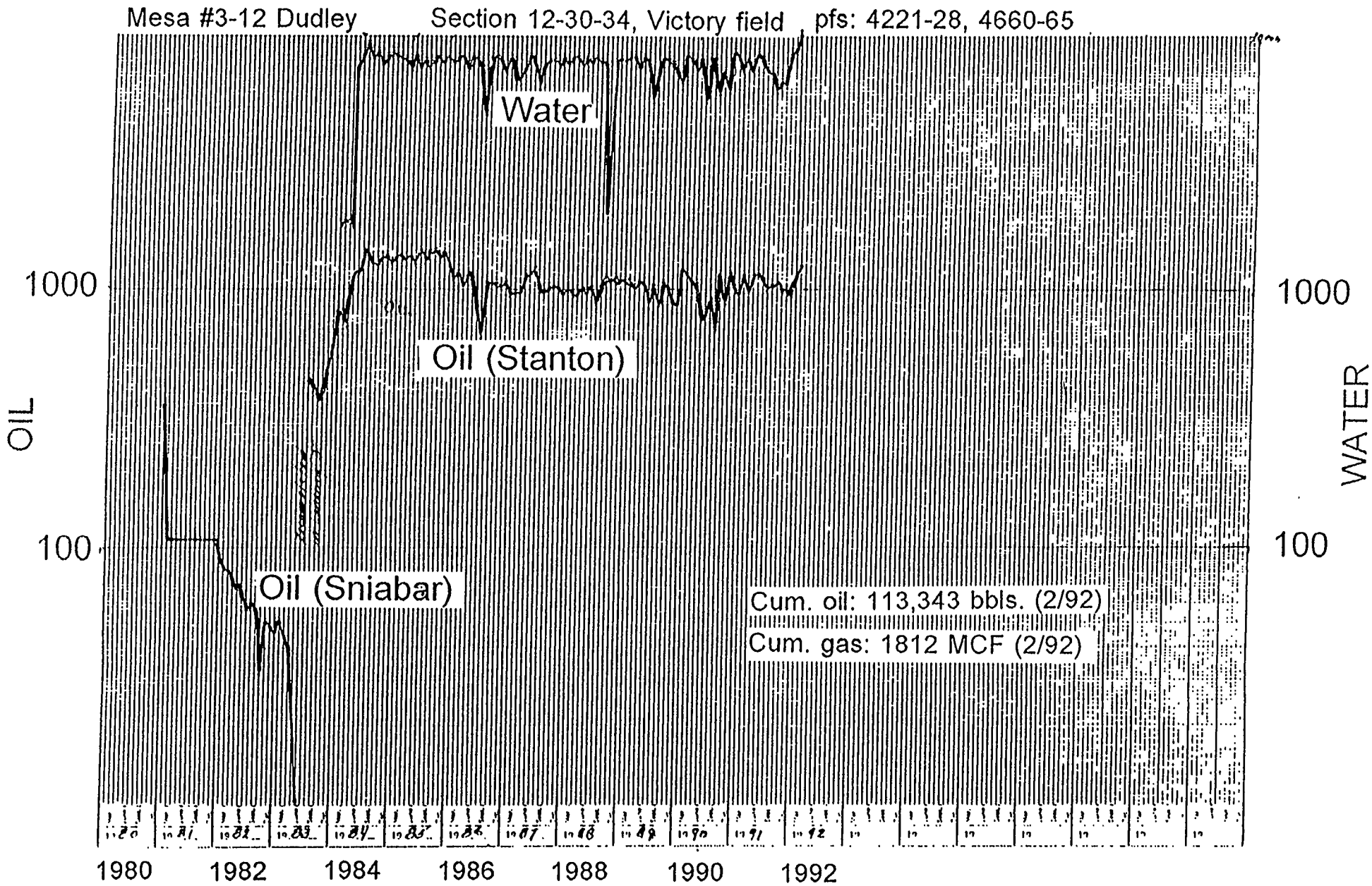

Figure 6.46. Stanton Limestone production decline curve from the Mesa #3-12 Dudley, Victory Field. The well was originally completed in 1980 from the Sniabar Limestone for 35 barrels of oil and 80 barrels of salt water per day. It was recompleted in 1983 from the Stanton Limestone. It has averaged 1000 barrels of oil production per month with no apparent decline. This could indicate a water drive, at least in the Stanton Limestone.

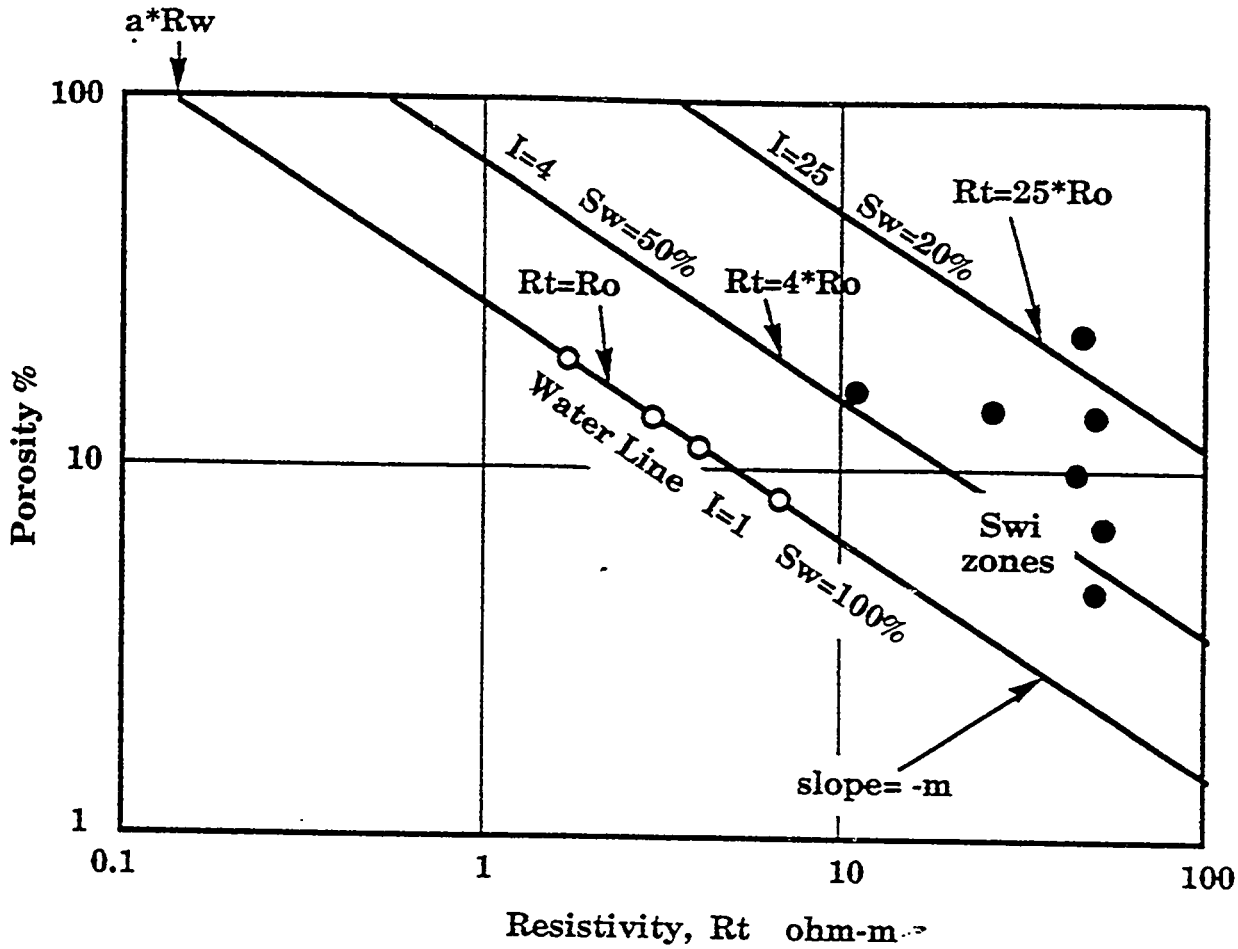

Figure 6.47. Principles of Pickett (resistivity vs. porosity) crossplot Swi is irreducible water value; I is resistivity index, Ro is resistivity of reservoir when 100% filled with water; and Sw is water saturation of reservoir.

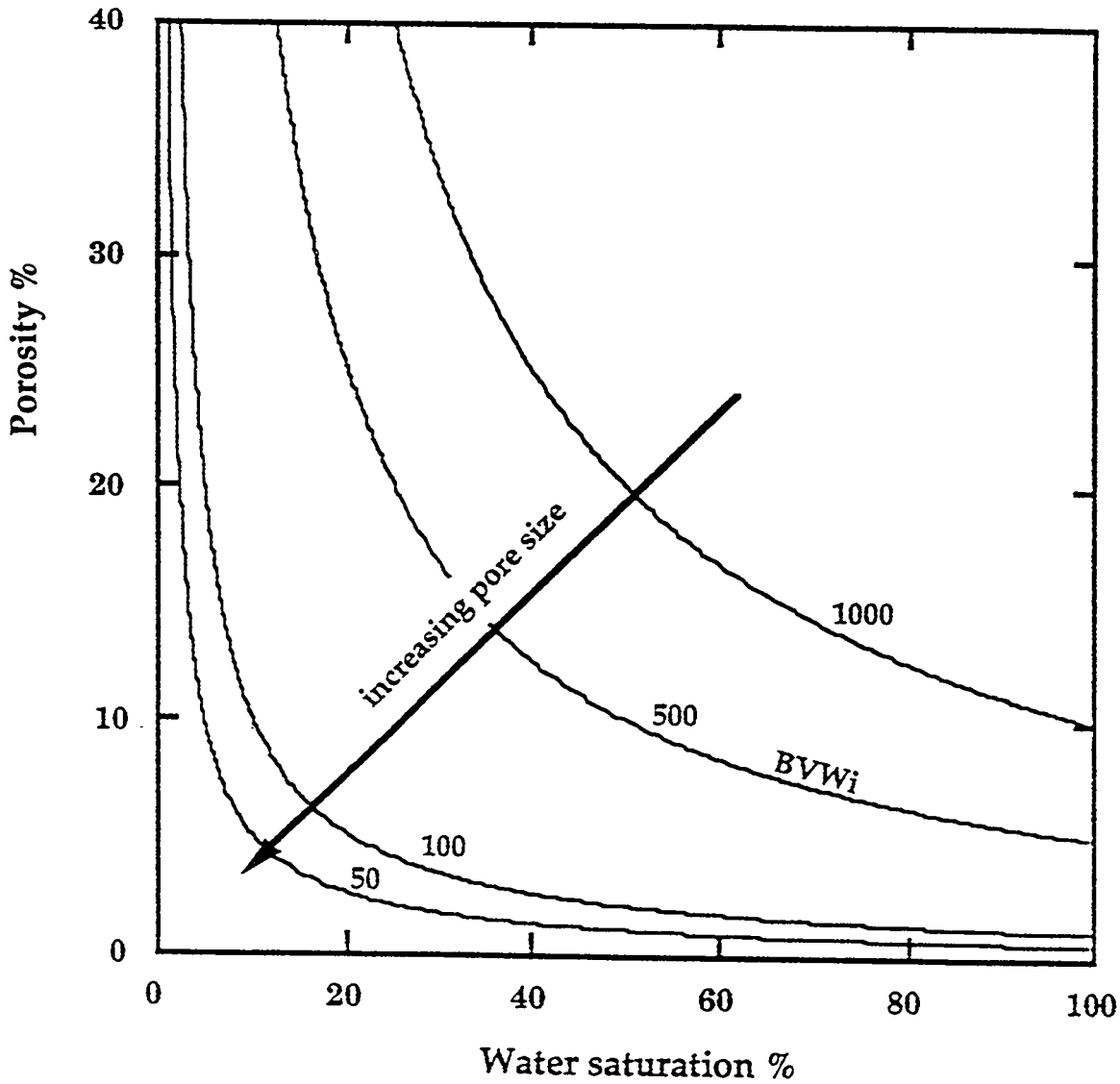

Figure 6.48. Plot of water saturation (Sw) versus porosity (phi) to determine bulk water volume (BVW) hyperbolic curves on a linear plot. The BVW numbers are in Buckle's numbers; that is phi vs. Sw with no decimal places.

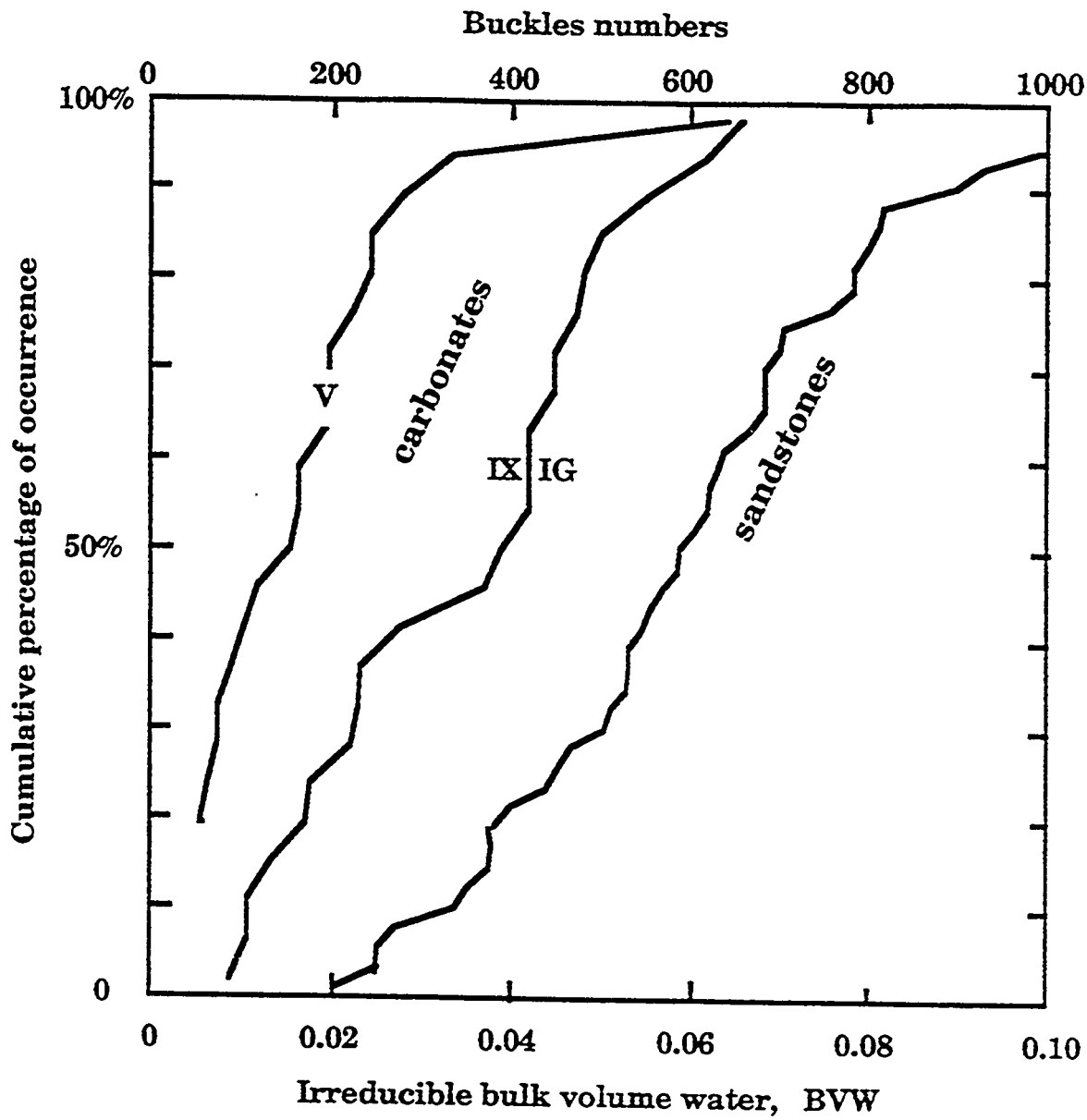

Figure 6.49. Cumulative frequency plots of irreducible bulk volume water (or Buckle's number) for carbonate reservoirs with vuggy porosity (V) and intercrystalline/intergranular porosity (IX-IG), and sandstone reservoirs. Carbonate data from Chilingar et al. (1972); sandstone data from Bond (1978).

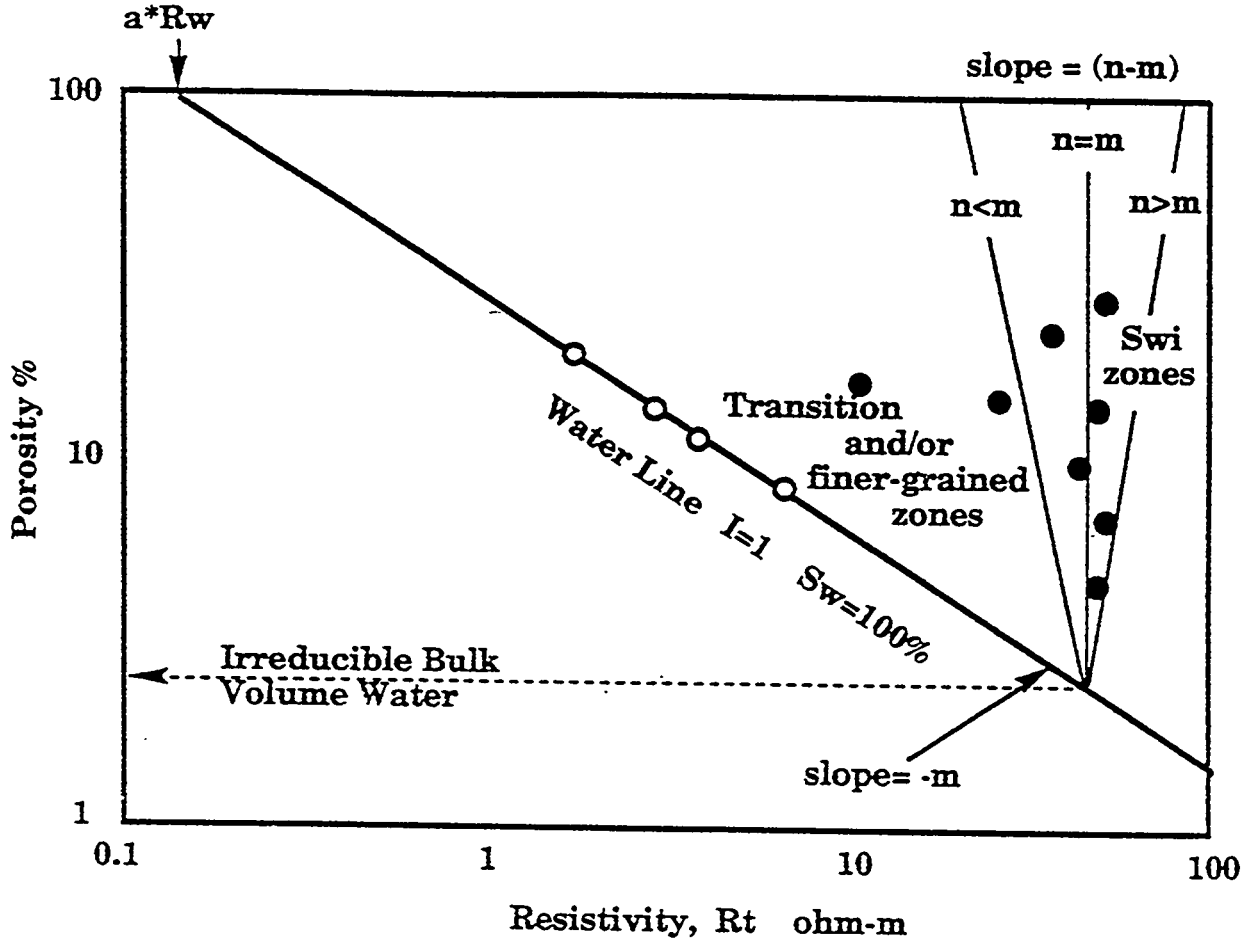

Figure 6.50. Location of irreducible bulk volume water trend on Pickett plot. Various relationships of saturation exponent (n) and cementation factor (m).

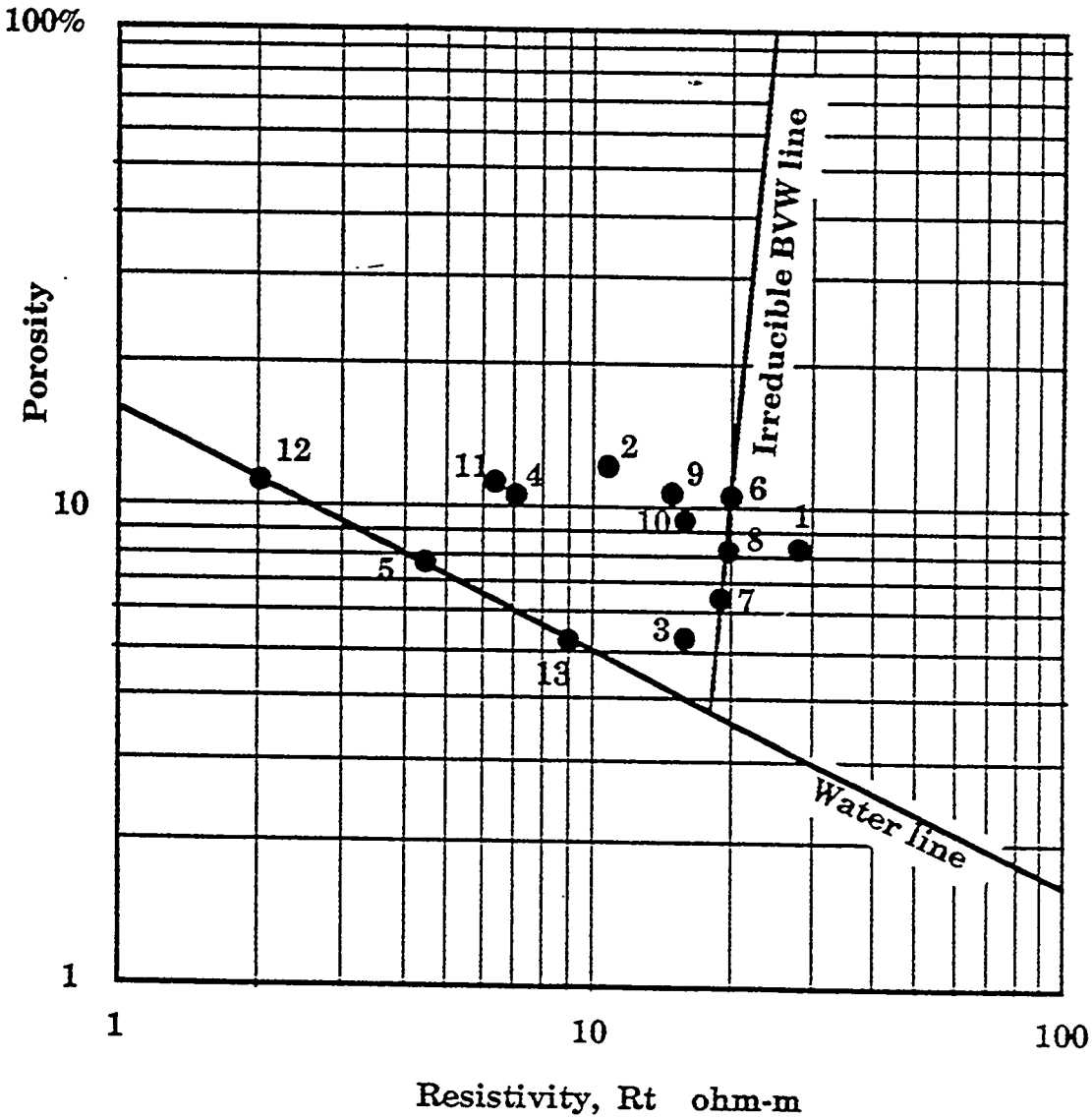

Figure 6.51. Pickett plot of limestone zone data from a well from south Texas indexed with water and irreducible bulk volume water lines (data from Fertl, 1979).

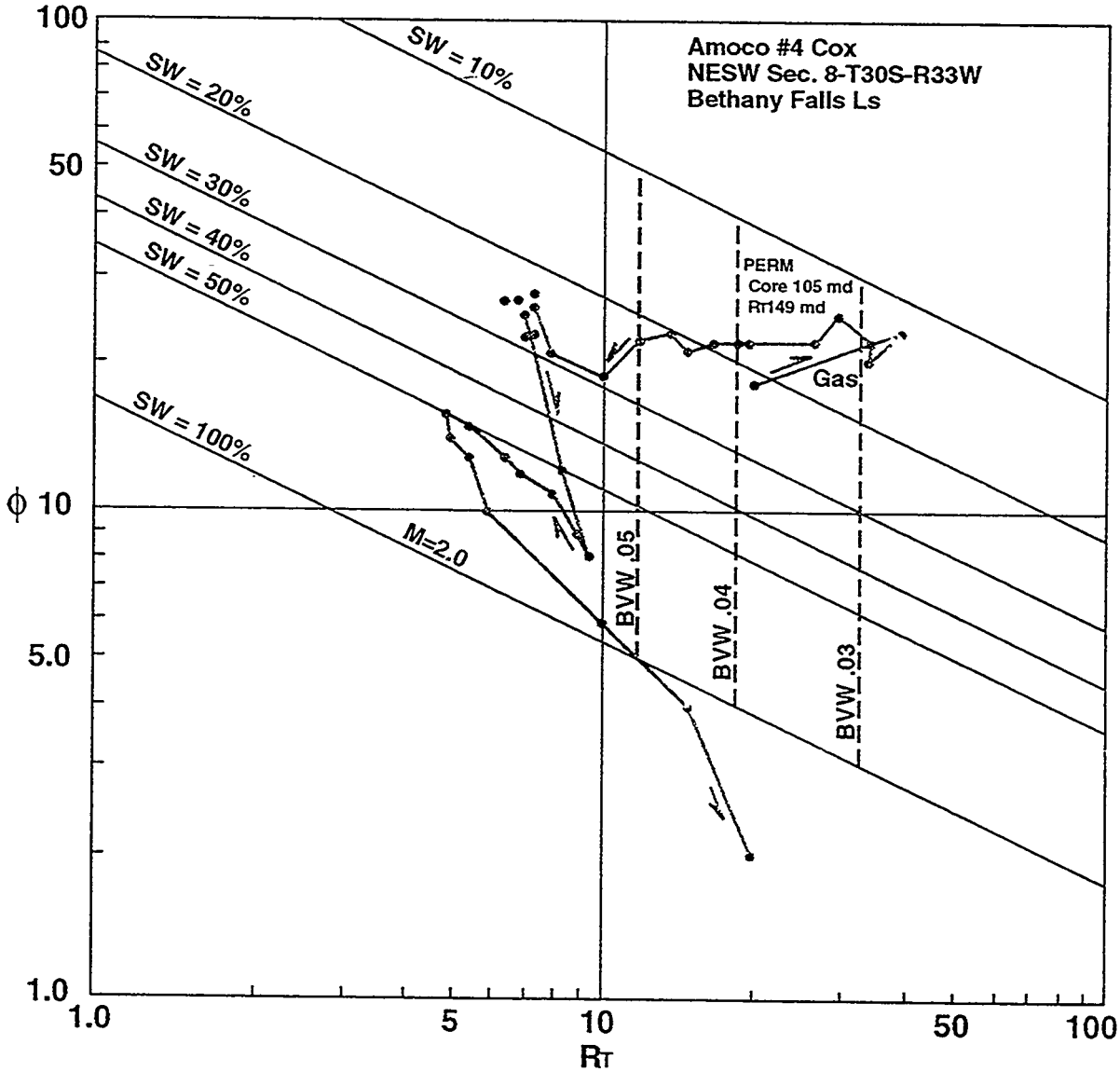

Figure 6.52. "Super" Pickett crossplot of Bethany Falls Limestone, Victory Field, Amoco #A-4 Cox. Completed as gas well.

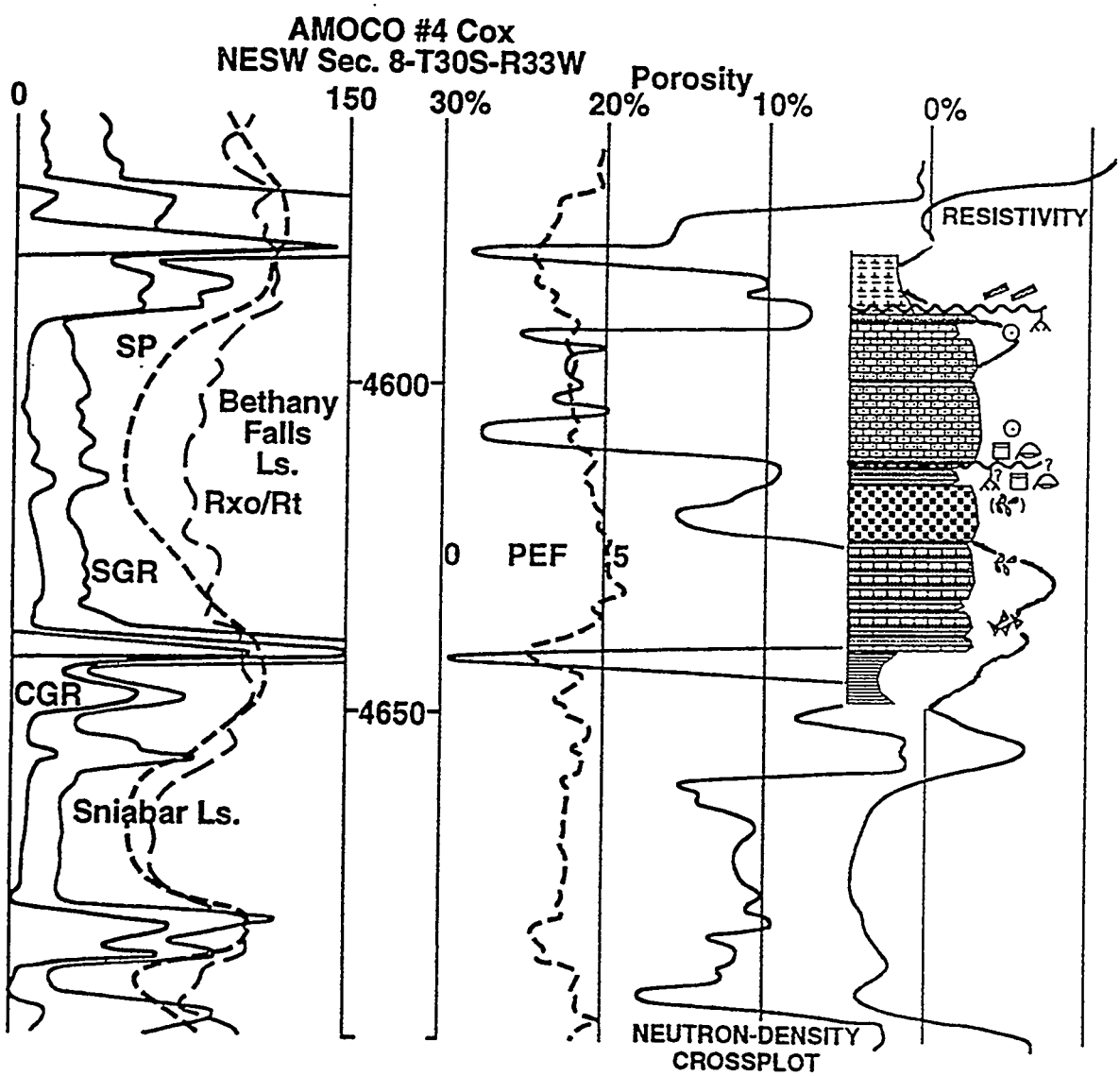

Figure 6.53. Log of Amoco #A-4 Cox in Bethany Falls and Sniabar Limestone intervals. Gas production from 4591-4600 feet.

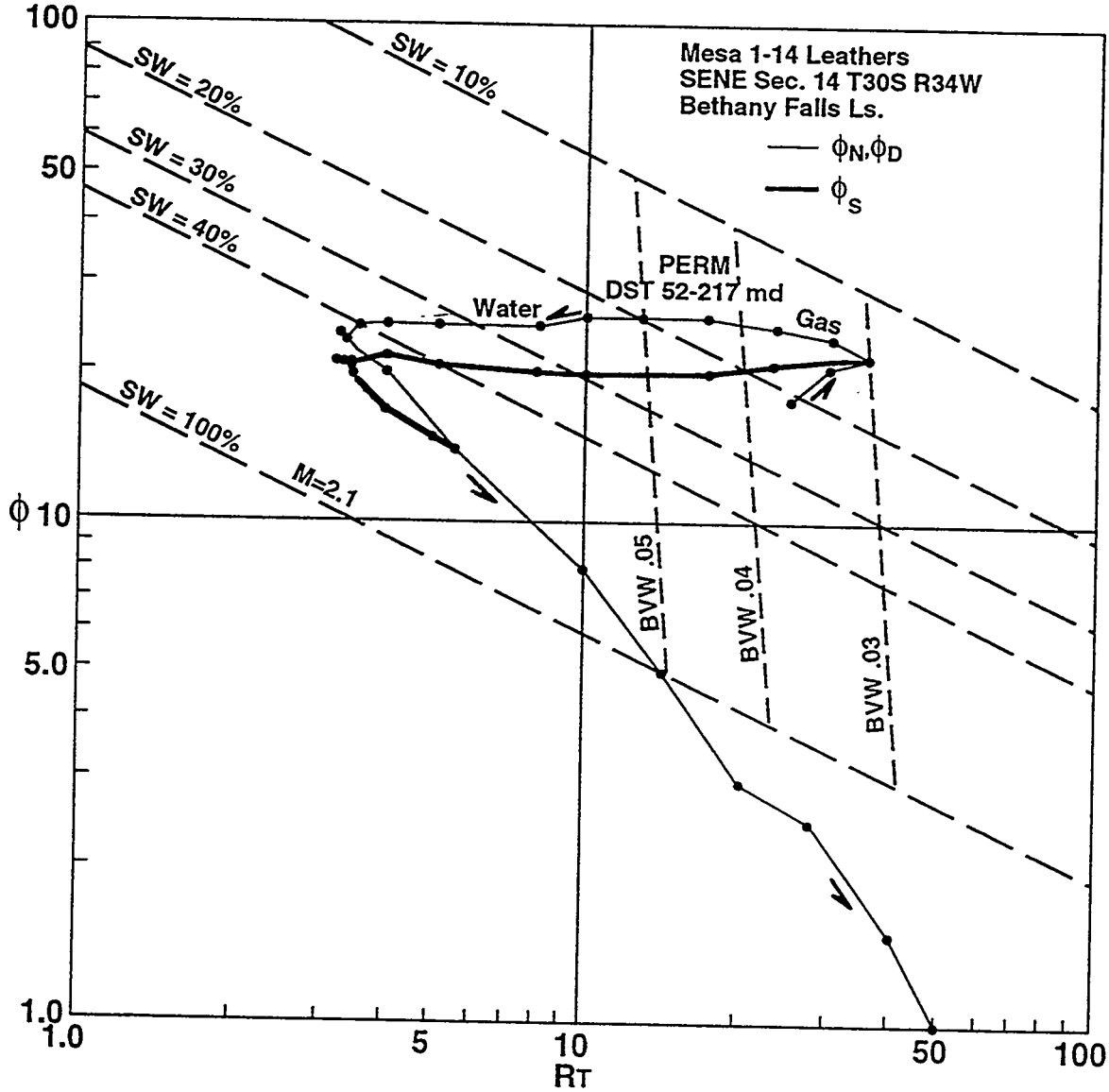

Figure 6.54. "Super" Pickett crossplot Bethany Falls Limestone, Victory Field, Mesa #1-14 Leathers well. DST from 4556-90 had gas to surface with 2321 feet of salt water recovery. The upper curve is a density-neutron crossplot value while the lower curve from the sonic log.

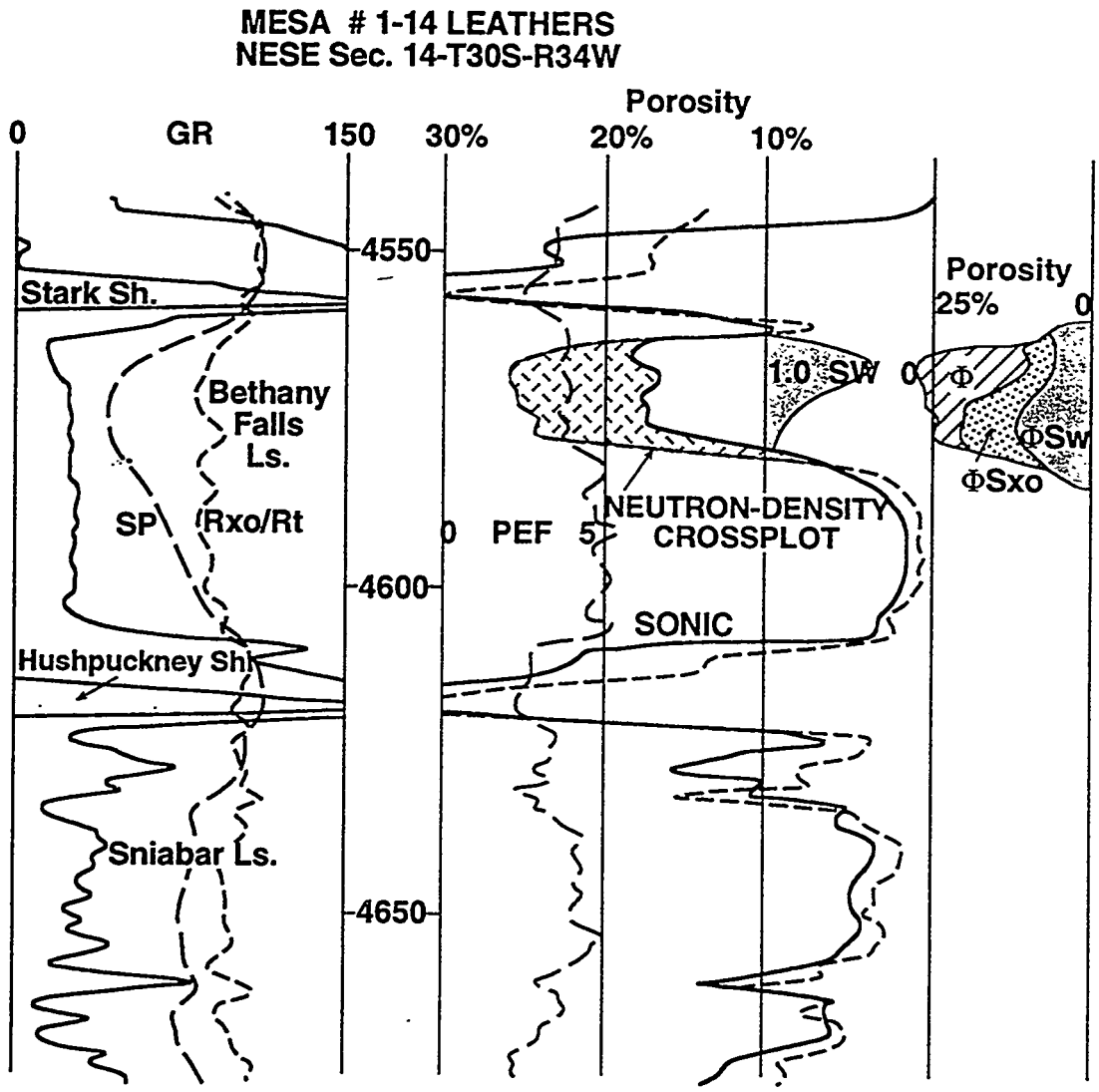

Figure 6.55. Log Mesa #1-14 Leathers, Bethany Falls and Sniabar Limestones. Shaded curves from left to right are gas effect from density-neutron log, water saturation (Sw), and porosity values (phi total, phi residual oil, phi water or BVW.

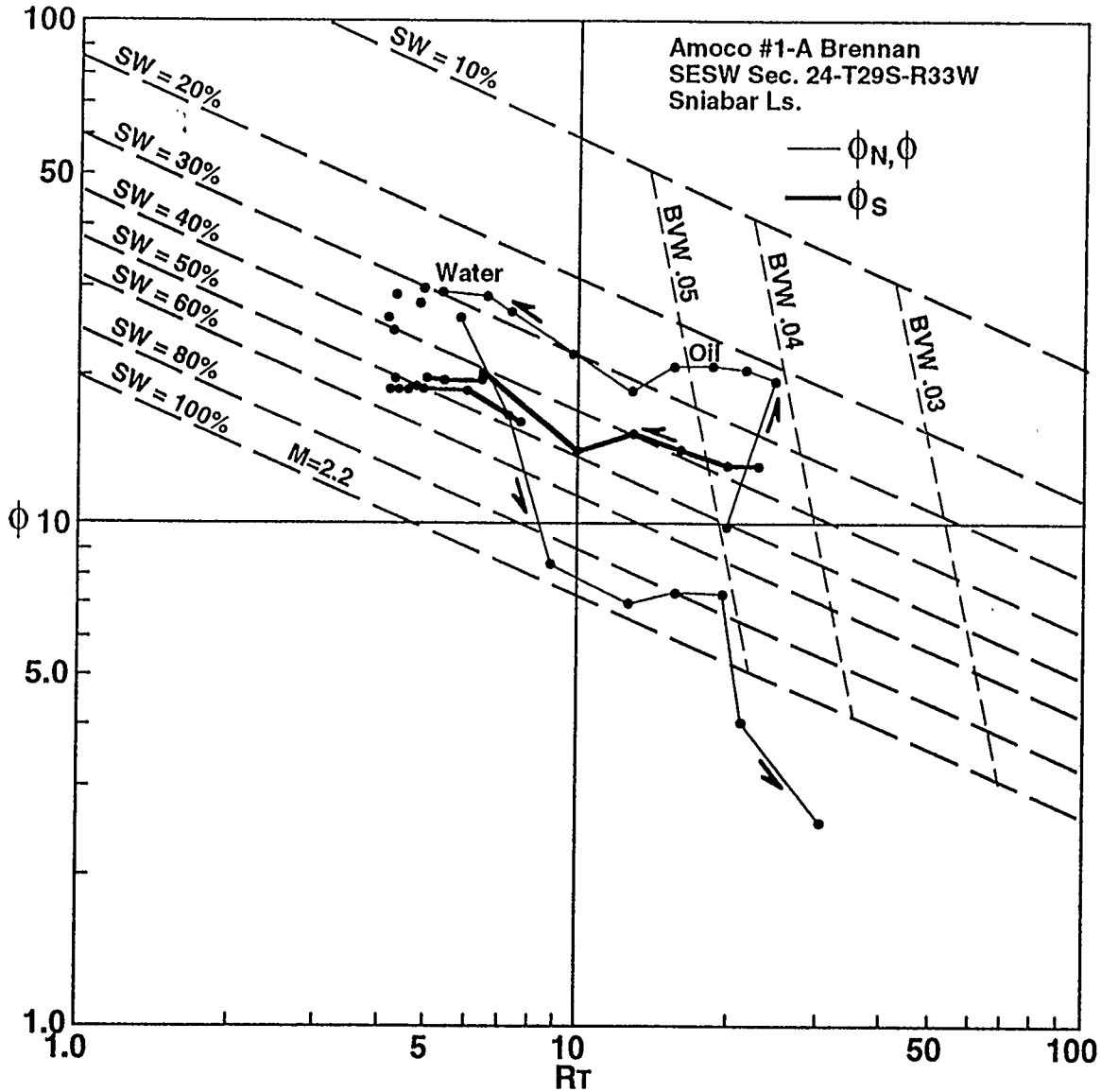

Figure 6.56. "Super" Pickett crossplot, Sniabar Limestone, Northeast Lemon Field, Amoco #1-A Brennan. Completed as an oil well from 4650-60 feet for 126 barrels of oil per day, 71 MCF gas, and 191 barrels of water per day. The upper curve is a density-neutron value while the lower curve is a sonic value.

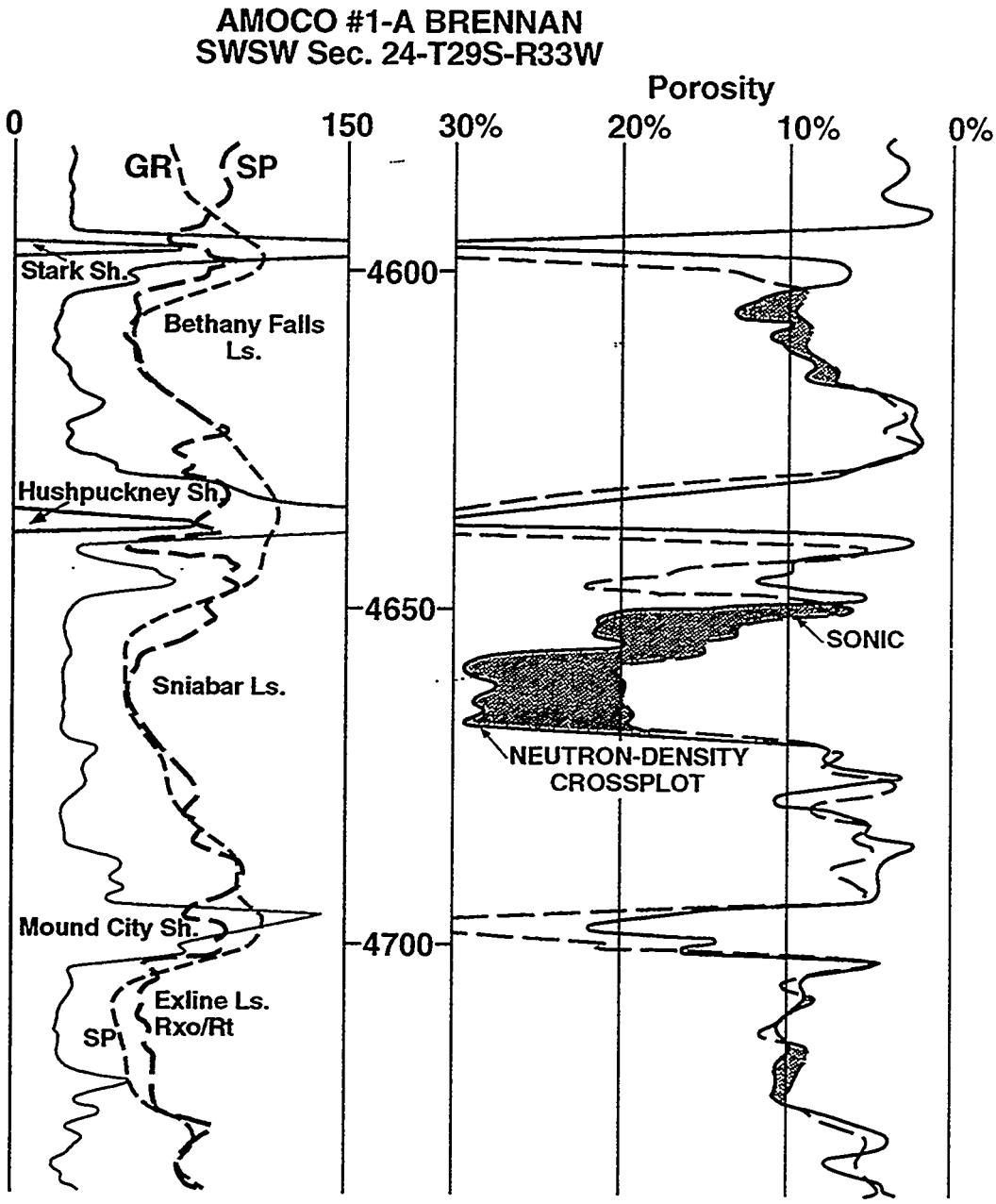

Figure 6.57. Log of Amoco #1-A Brennan in the Bethany Falls and Sniabar Limestones. Shaded curves are the gas effect from density-neutron log. Shift at about 4655 feet is to a better oomoldic porosity, but which is also water productive (Figure 6.56).

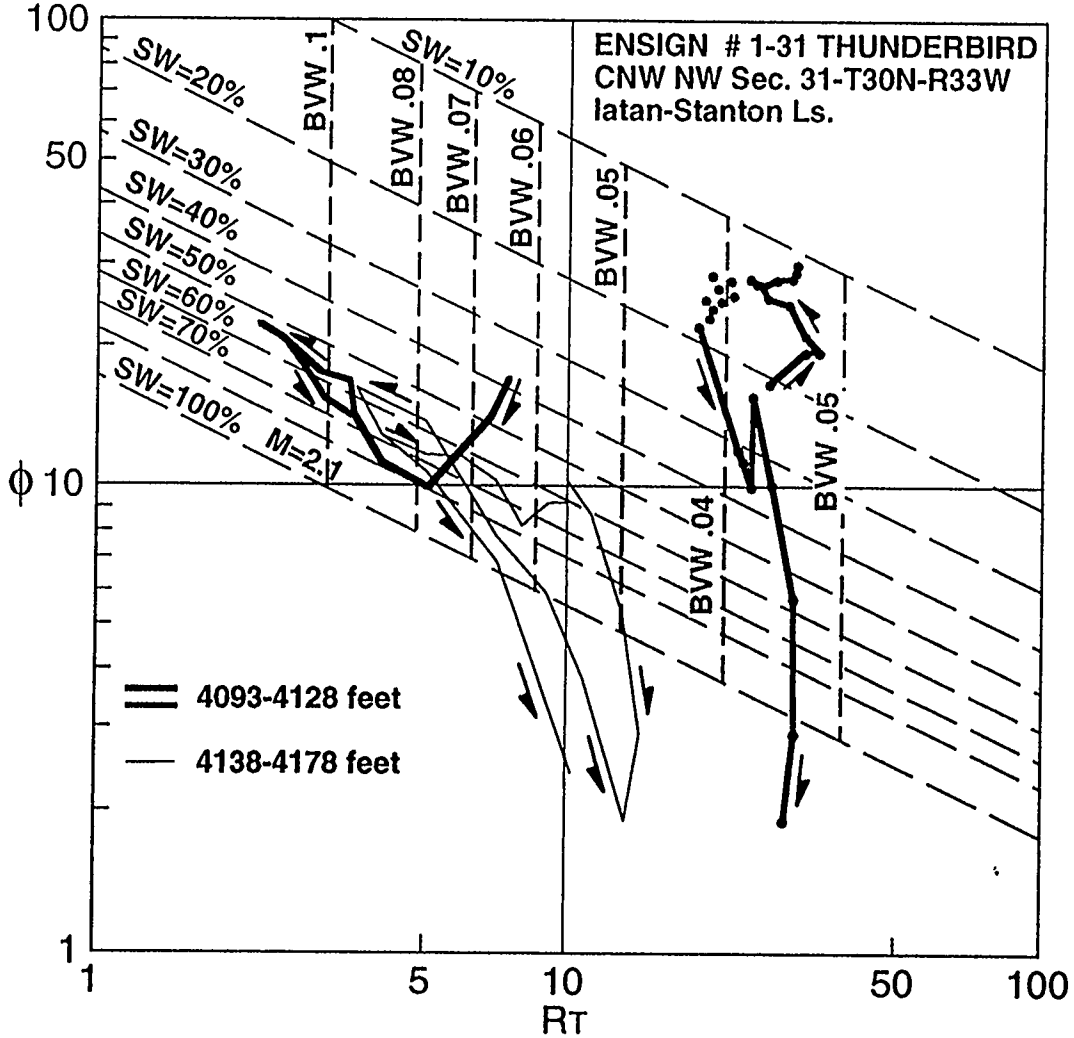

Figure 6.58. "Super" Pickett crossplot in the Iatan and Stanton Limestones, Victory Field, Ensign #1-31 Thunderbird. Very little data available on this test, Stanton Limestone crossplot on right indicates high porosity (20-30%), low BVW (0.04), low Sw (10-20%), and good indication of Swi (0.04). The Iatan Limestone crossplot on left indicates moderate porosity (10-20%), high BVW (0.06-0.1), high Sw (60%), and no indication of being at Swi. Differences is texture and porosity type.

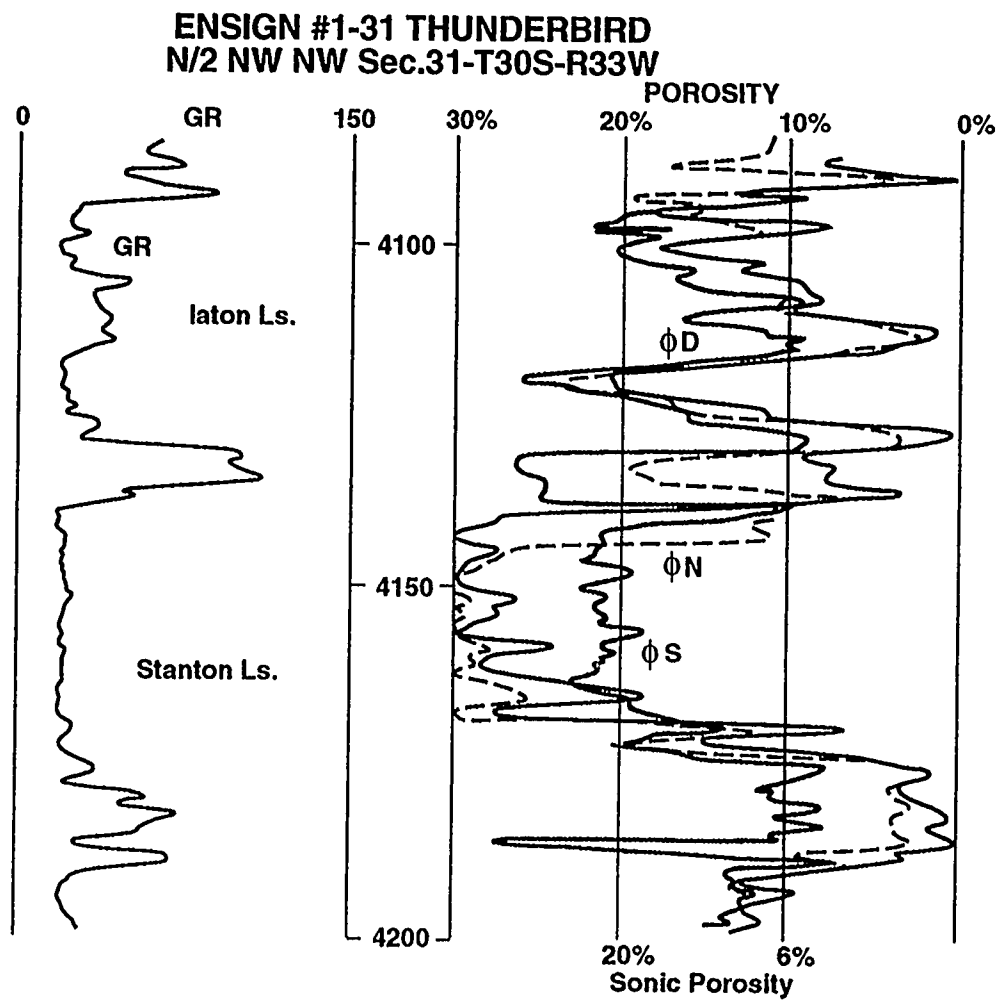

Figure 6.59. Log Ensign #1-31 Thunderbird in the Iatan and Stanton Limestones, Victory Field. Separation between density and neutron curves is gas effect (4140') and separation between neutron or density and sonic is secondary porosity. Twin well to north completed as Iatan and Stanton producer.

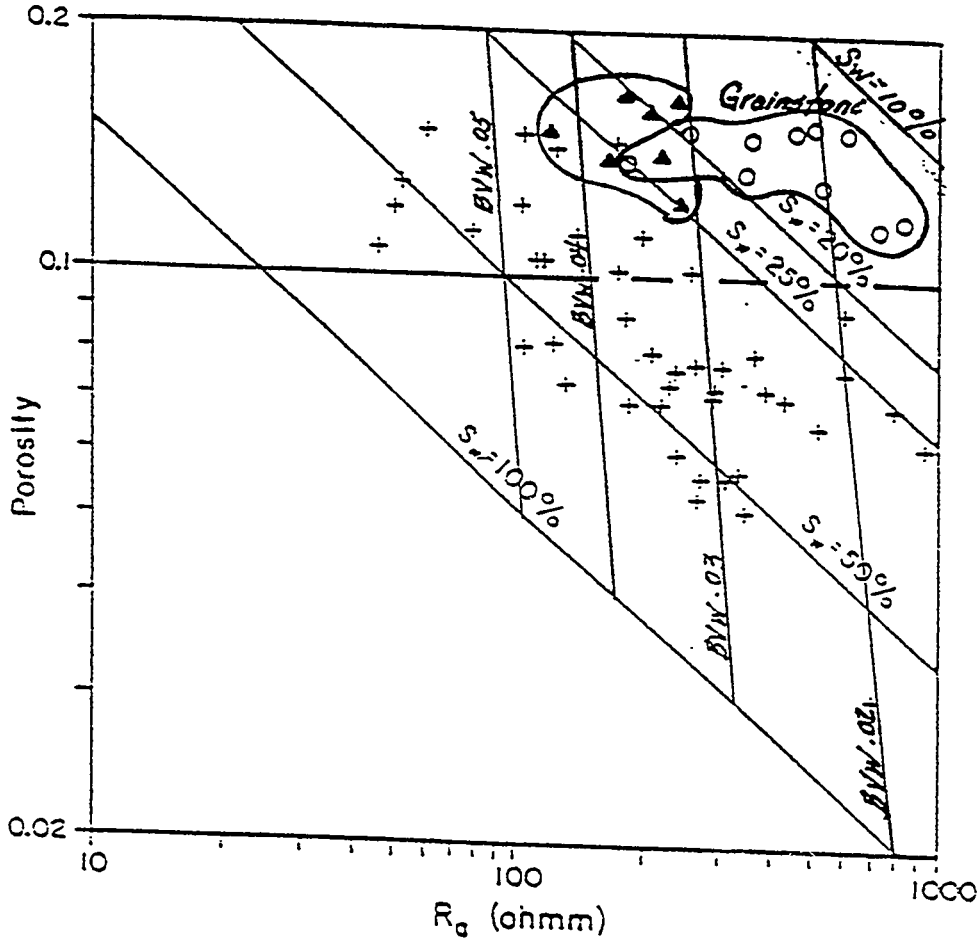

EXPLANATION

- ○ Intergranular between 180μm grains
- ÷ Intercrystalline between 50μm crystals
- ▲ Mixed intergranular and intercrystalline

Pickett plot for Mobil University 1535 showing the relationship between water saturation and the pore families

Figure 6.60.

From Beboud, et al 1987

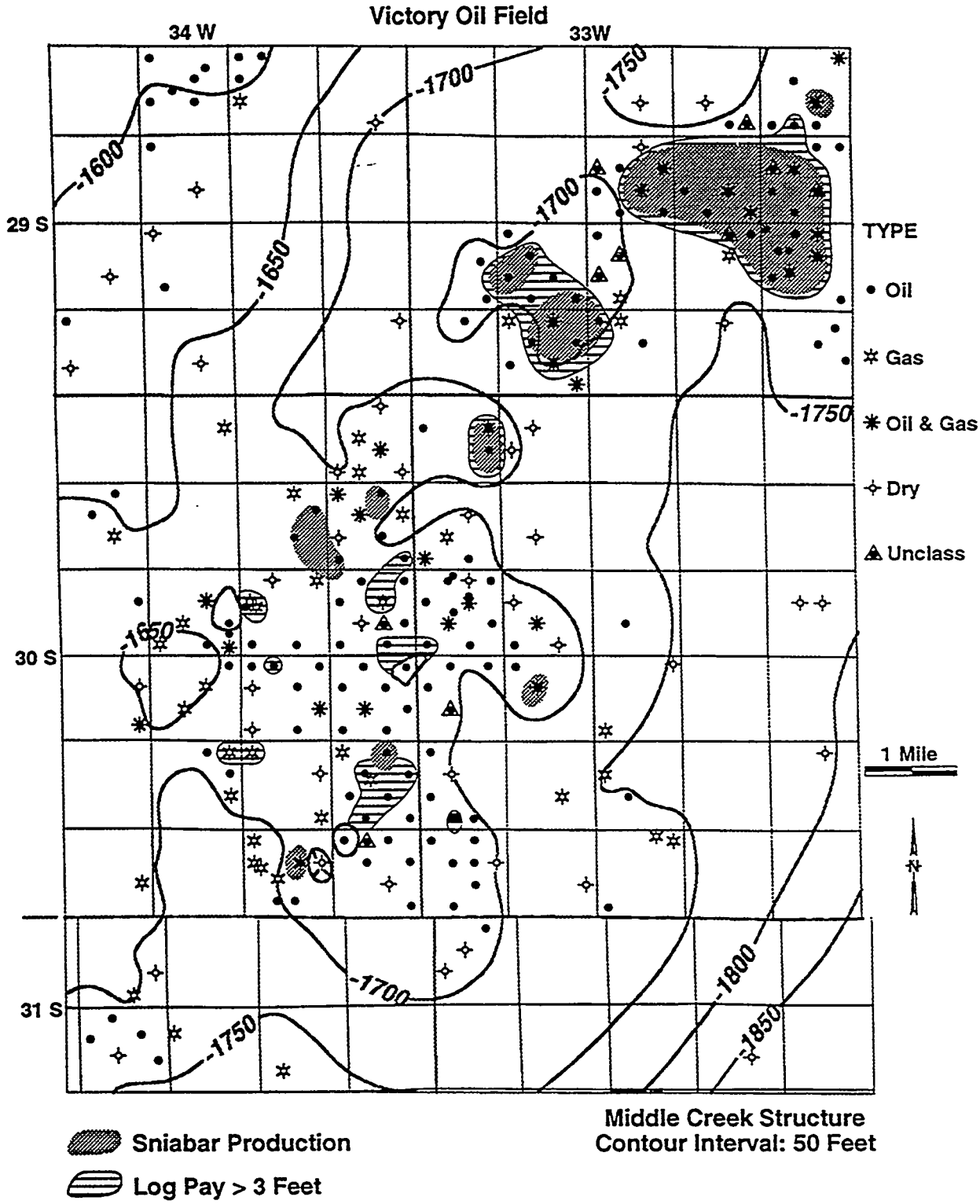

Figure 6.61. Sniabar Limestone potential producing area in the Victory-Northeast Lemon Fields. Horizontal pattern is area that includes Sniabar pay thickness greater than three feet as determined by "Super" Pickett crossplots.

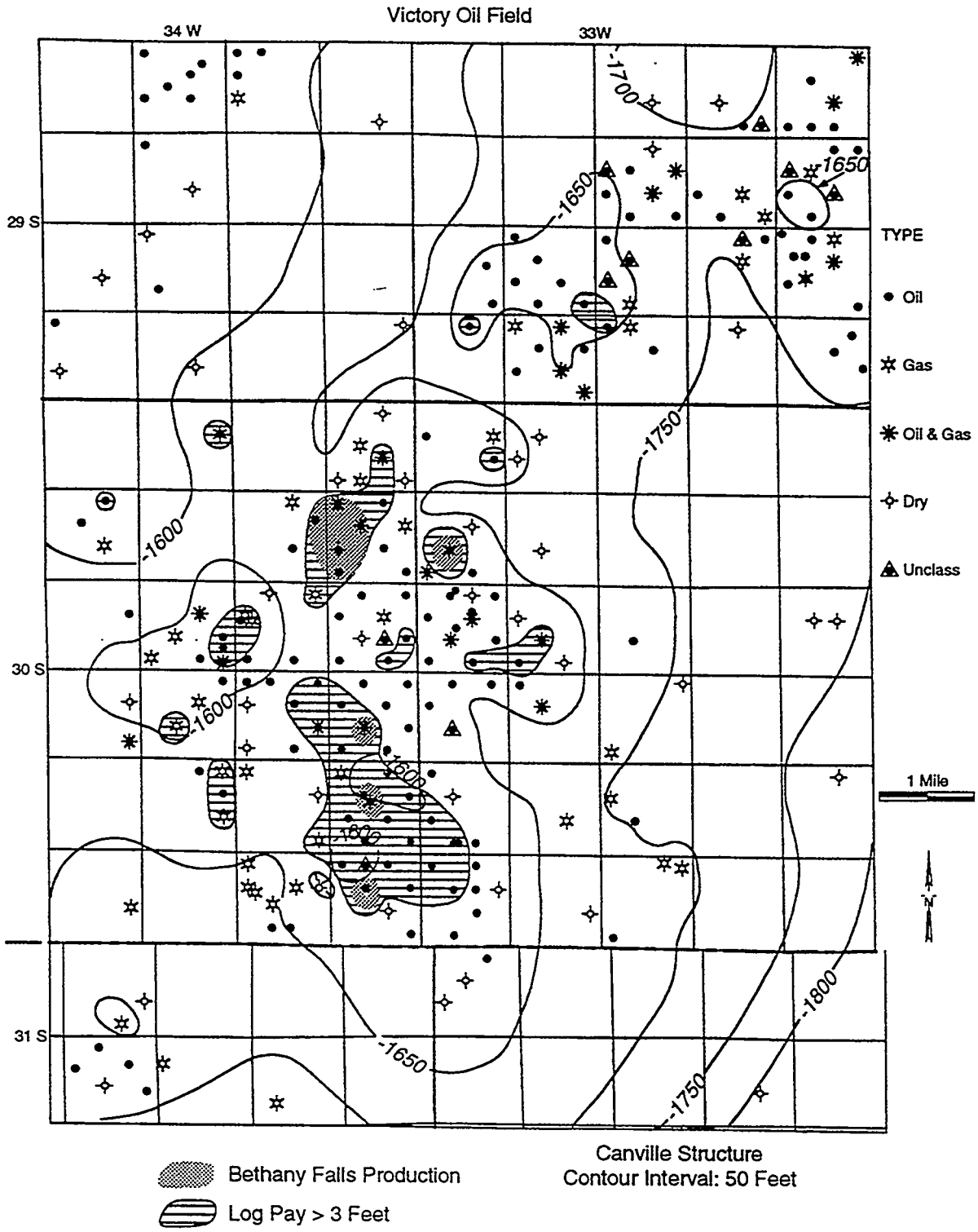

Figure 6.62. Bethany Falls Limestone potential producing area in the Victory Field area. Horizontal pattern is area that includes Bethany Falls pay thickness greater than three feet as determined by "Super" Pickett crossplot.

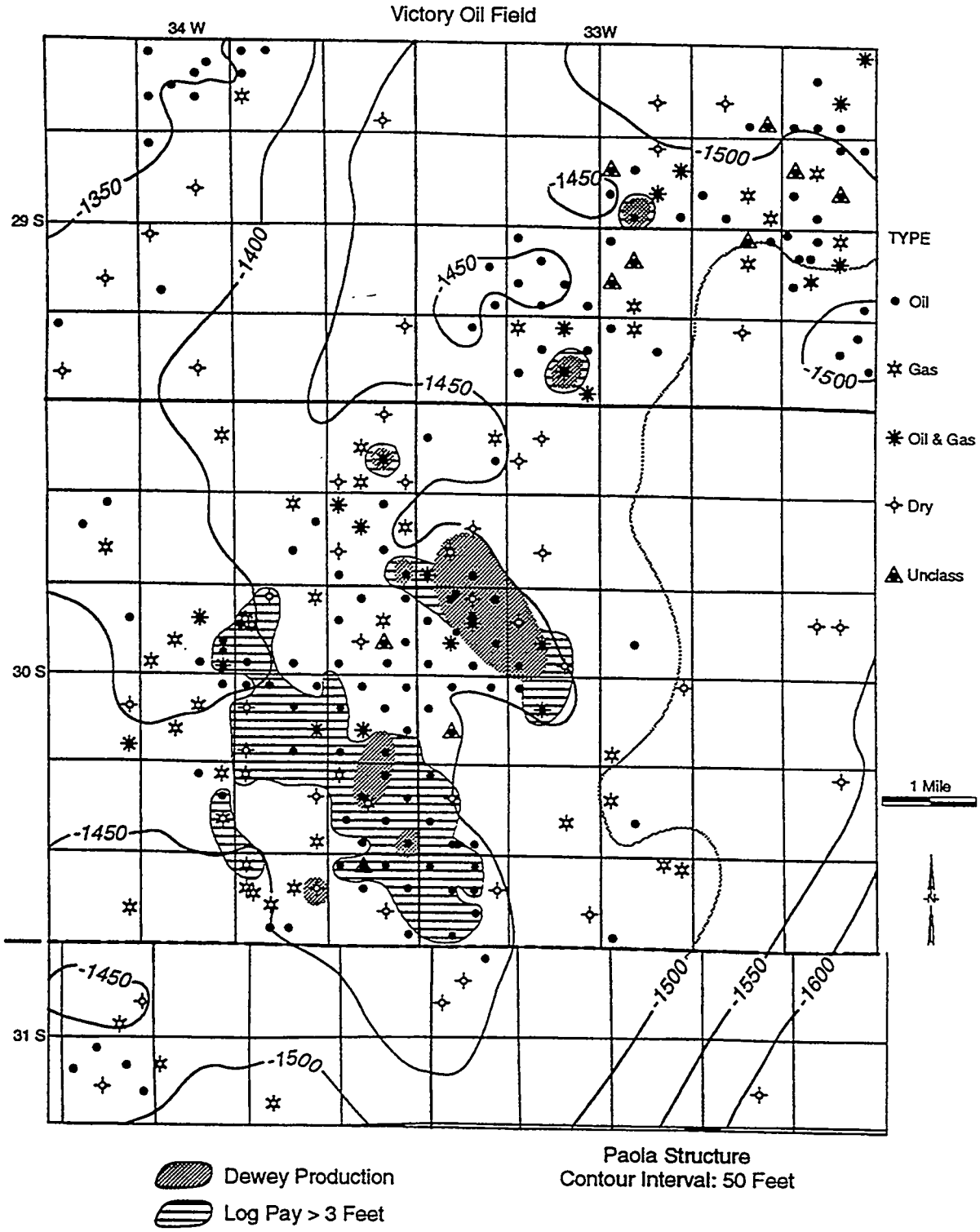

Figure 6.63. Dewey Limestone potential producing area in Victory field. Horizontal pattern is area that includes Dewey pay thickness greater than three feet as determined by "Super" Pickett crossplot.

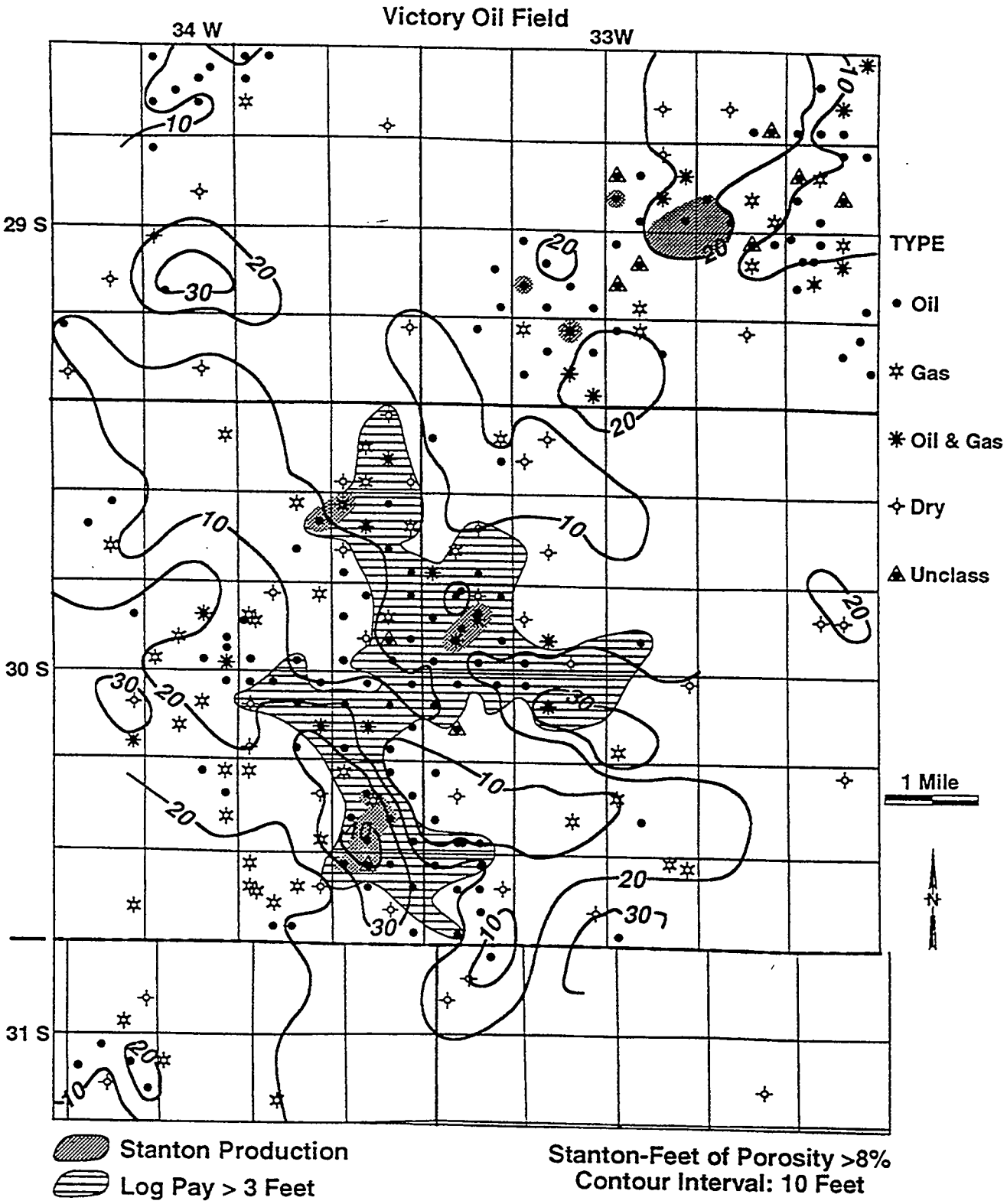

Figure 6.64. Stanton Limestone potential producing area in the Victory Field area. Horizontal pattern is area that includes Dewey pay thickness greater than three feet as determined by "Super" Pickett crossplot.

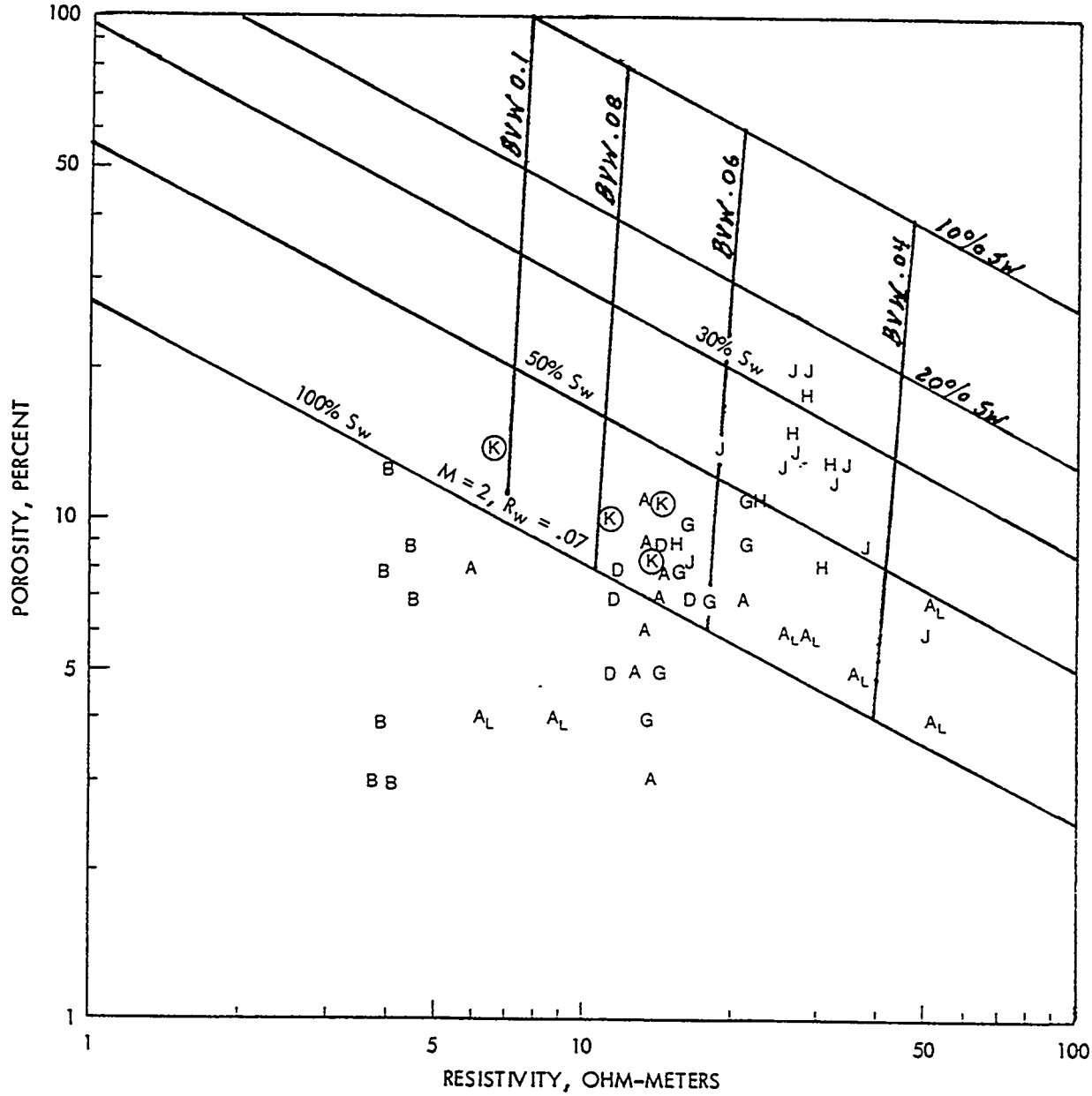

FIGURE . Log-log plot of induction well log resistivity versus shale-corrected sonic porosity for porous zones of Skelly Bartosovsky #1. Data points determined on a per-foot basis. Carbonate intervals are labeled accordingly. The solid heavy line is the R_o (water wet) line with slope, m (cementation exponent), equal to 2, and with an intercept of 100 percent porosity at 0.07 ohm-m ($= R_w$), determined by calculating R_w from SP deflection in porous, water-wet zones. Sonic log porosity was corrected for shale effects with a Dresser-Atlas nomograph (p. 7-1 of Log Interpretation) using the gamma-ray response. The points labeled "B" represent the sandstone-siltstone unit immediately below the A-Zone. The circled K values represent water-wet points.
plot.

DRILL STEM TEST RESULTS (BY ZONE)

ZONE	RESULTS
J	3360′ oil, SIP: 1305-1280#, FP: 160-1250# SWB 144 BO/2 hrs.
H	2249′ gas + 1880′ oil, SIP: 1305-1250#, FP: 135-745#, SWB 132 BO/2 hrs.
A	320′ gas, 160′ oil, SIP: 1280-1120#, FP: 50-80#, SWB 122 BO/2 hrs.
G	3 gallons water/hr. with show oil
D	5′ mud with specks oil, SIP: 130-0#, FP: 0-0#
K	60′ muddy saltwater with specks oil, SIP: 1330-1120#, FP: 0-0#

ABBREVIATIONS

SIP: shut-in-pressure (initial and final)
FP: flowing pressure (initial and final)
SWB: swabbed

Figure 6.65. Pickett crossplot, multi-reservoirs, Cahoj Field. Revised from Watney (1980), showing reservoir characteristics in nearly all reservoirs in field.

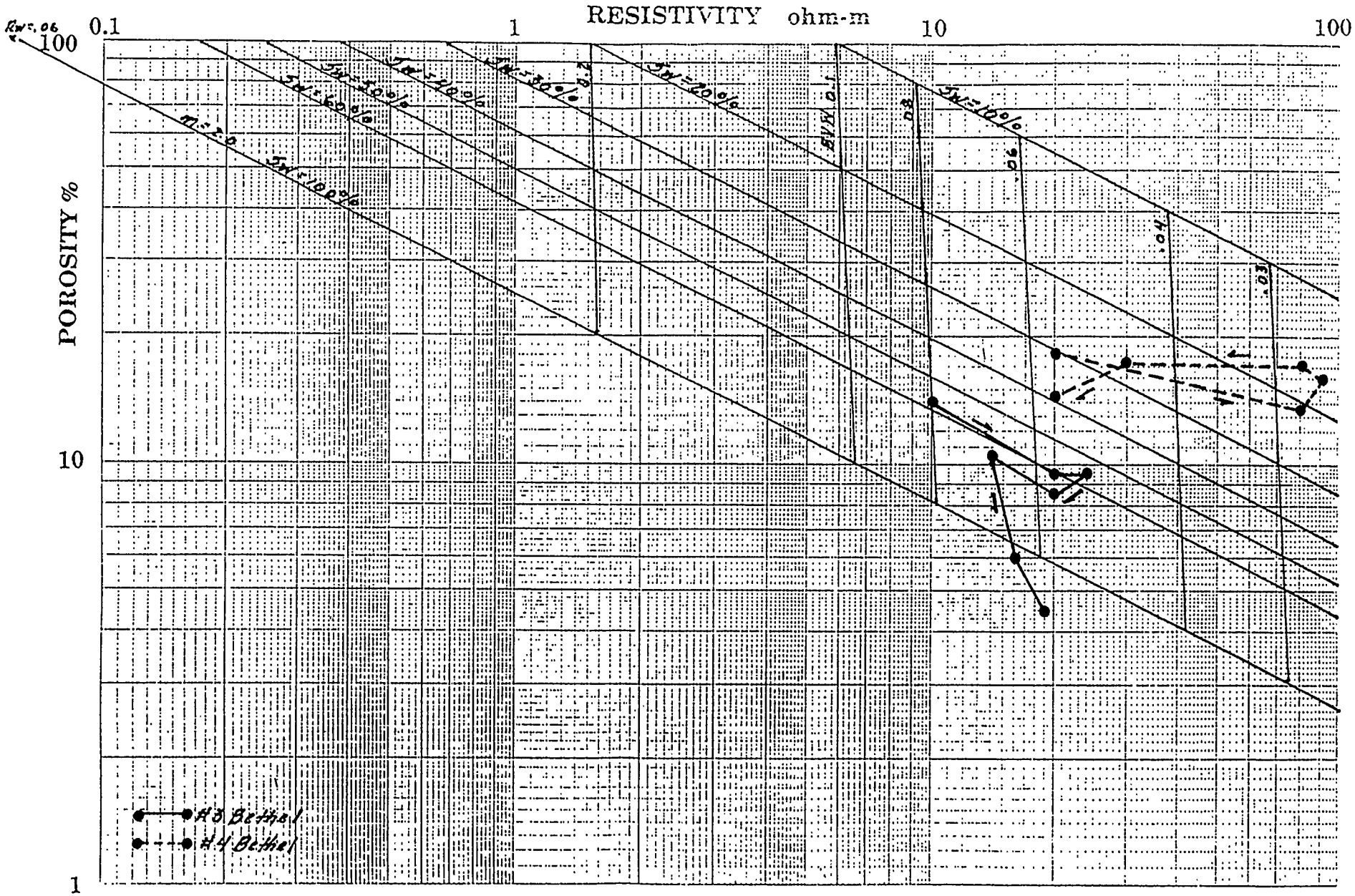

Figure 6.66. "Super" Pickett crossplot J zone, Pen Field, Pan Canadian #3 and #4 Bethell. Two crossplots illustrate different pore types in same reservoir.

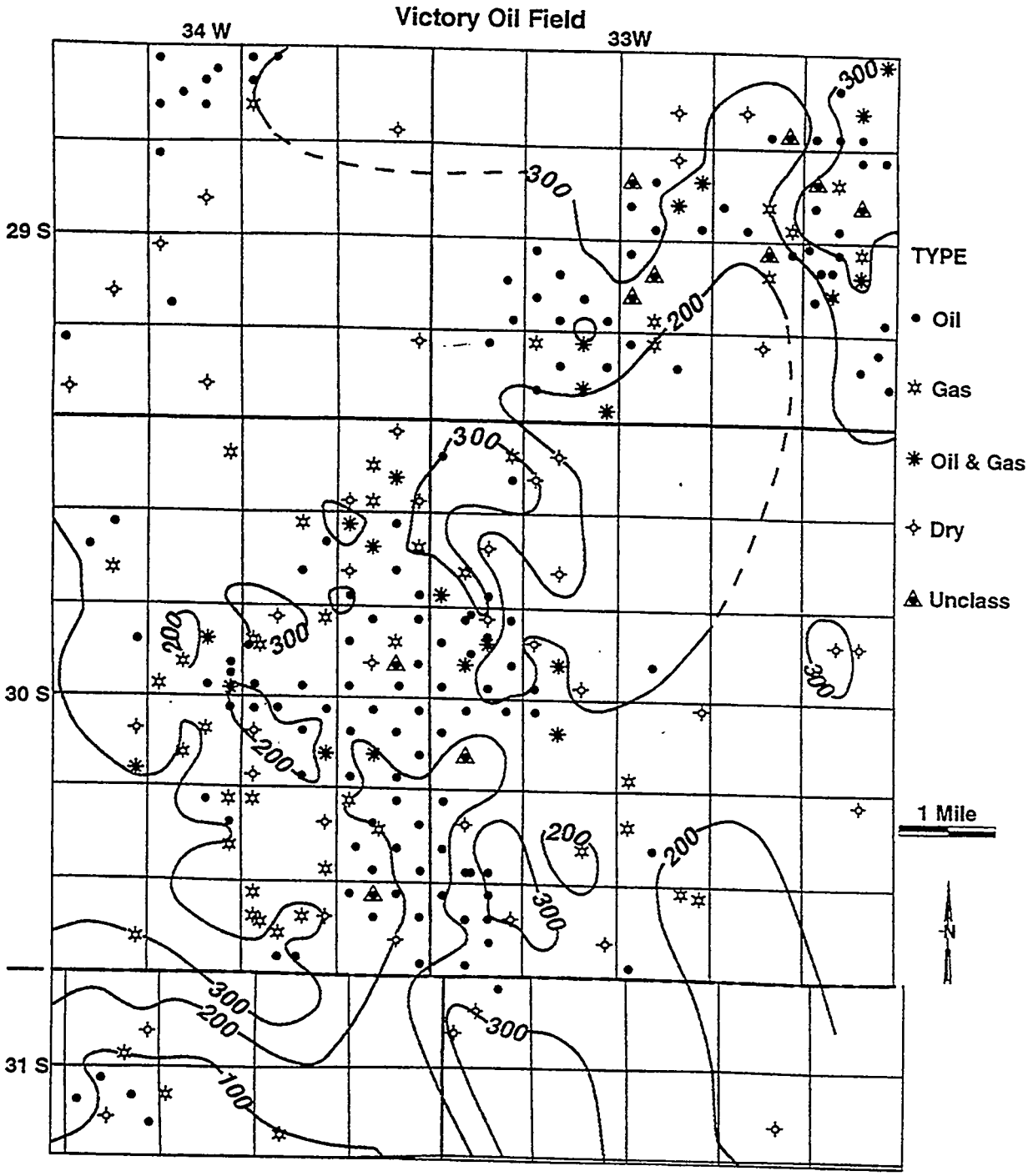

Maximum Gamma Ray - Hushpuckney
Contour Interval: 100 GAPI Units

Figure 6.67. Maximum gamma ray in Hushpuckney Shale.

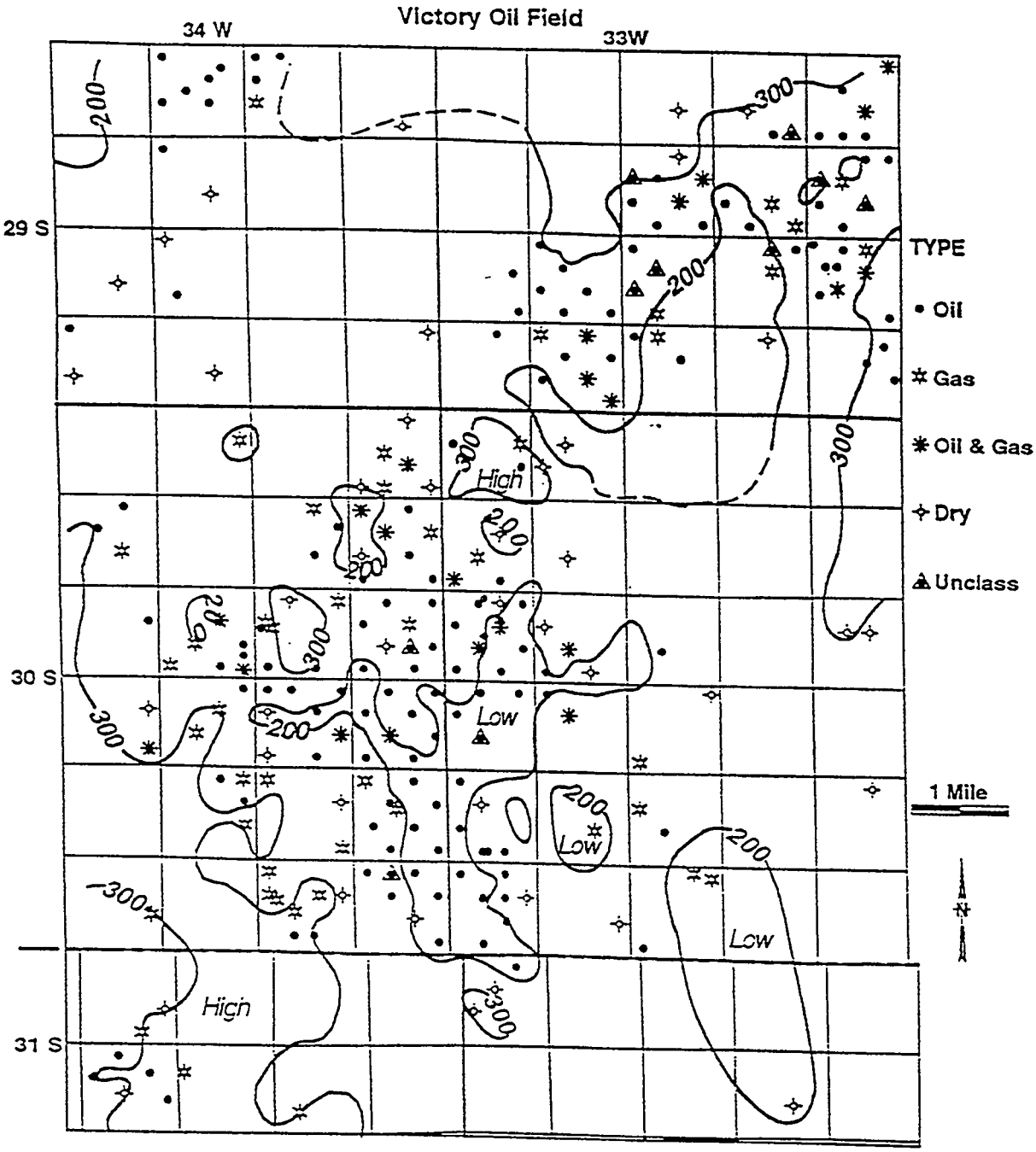

Maximum Gamma Ray
Stark Shale
Contour Interval: 100 Feet

Figure 6.68. Maximum gamma ray in Stark Shale.

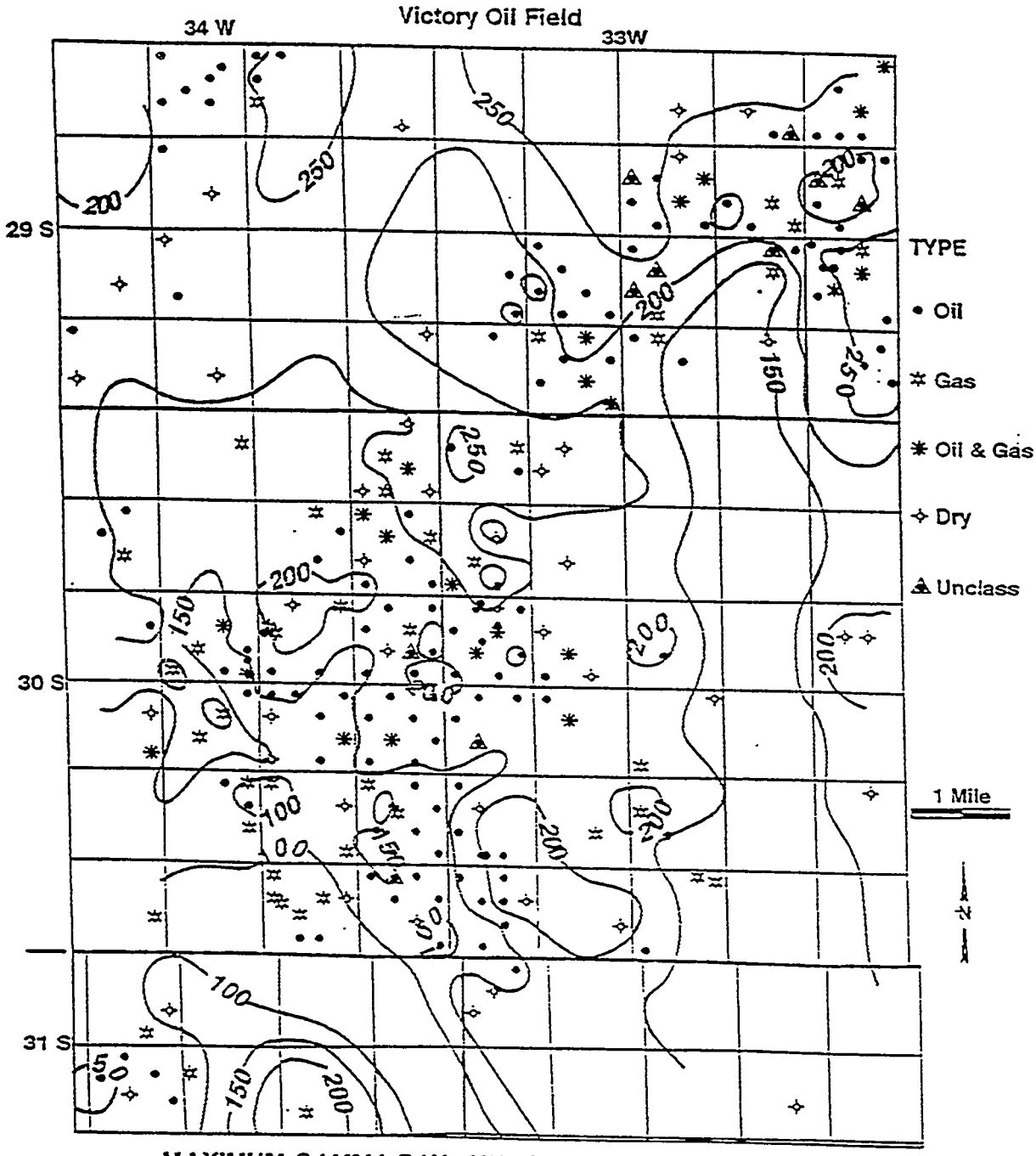

Figure 6.69. Maximum gamma ray in Muncie Creek Shale.

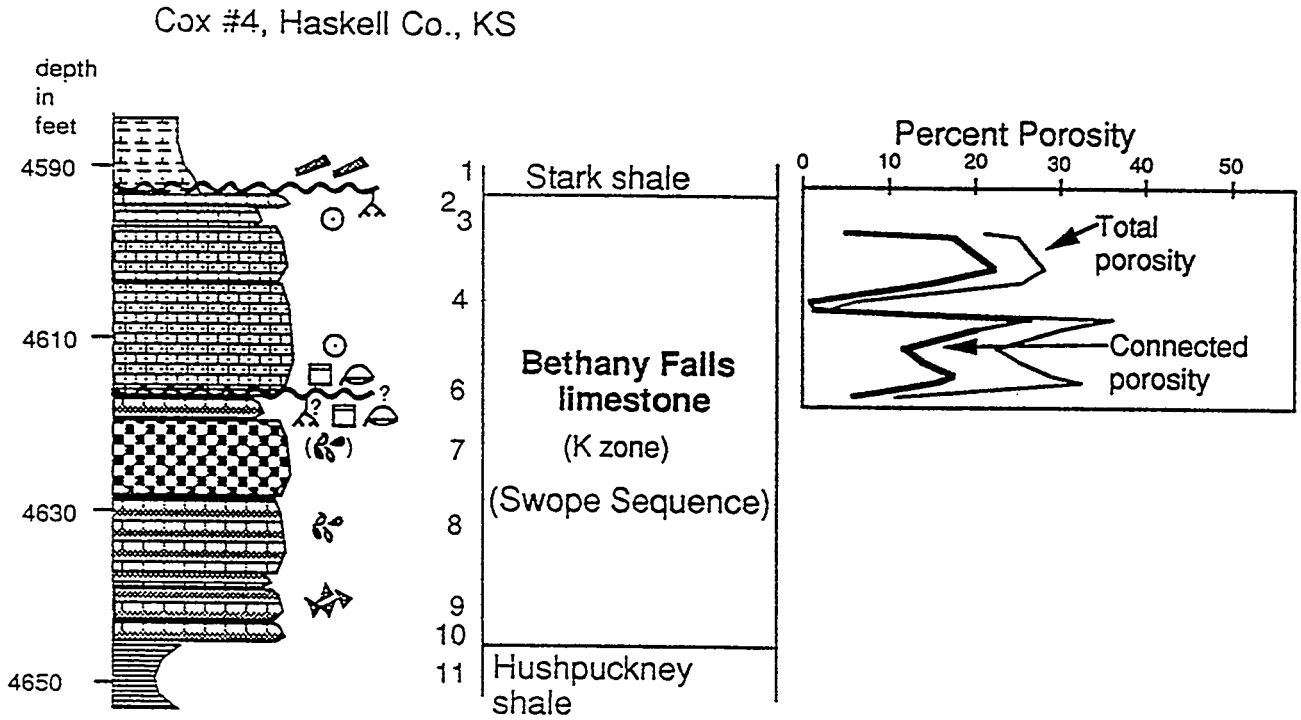

1. Calcareous shale with reworked clasts from the underlying paleosol.
2. Argillaceous lime mudstone with abundant rhizoliths.
3. Ooid packstone, poorly cemented.
4. Ooid grainstone with abundant oomoldic porosity .
5. Echinoderm grainstone grading downward to echinoderm packstone, and at its base, containing a few reworked clasts from the underlying bed (paleosol?).
6. Paleosol? - diagenetically altered lime mudstone that contains areas with a soil-like granular fabric.
7. Skeletal wackestone with subdued mottling.
8. Lime mudstone with well-developed mottling, some mottles have angular forms that resemble an autoclastic breccia; some horizons have a granular fabric.
9. Lime mudstone with well-developed, autoclastic breccia.
10. Broadly-wavy laminated lime mudstone, pyritic zones.
11. Shale; black.

Explanation

- wackestone
- calcareous shale
- lime mudstone
- packstone
- grainstone
- shale
- subaerial exposure surface
- lithoclasts
- rhizoliths
- ooids
- echinoderms
- brachiopods
- autoclastic breccia
- ( ) subdued
- mottled

Figure 6.70. Stratigraphic description of the Bethany Falls Limestone in Victory Field.

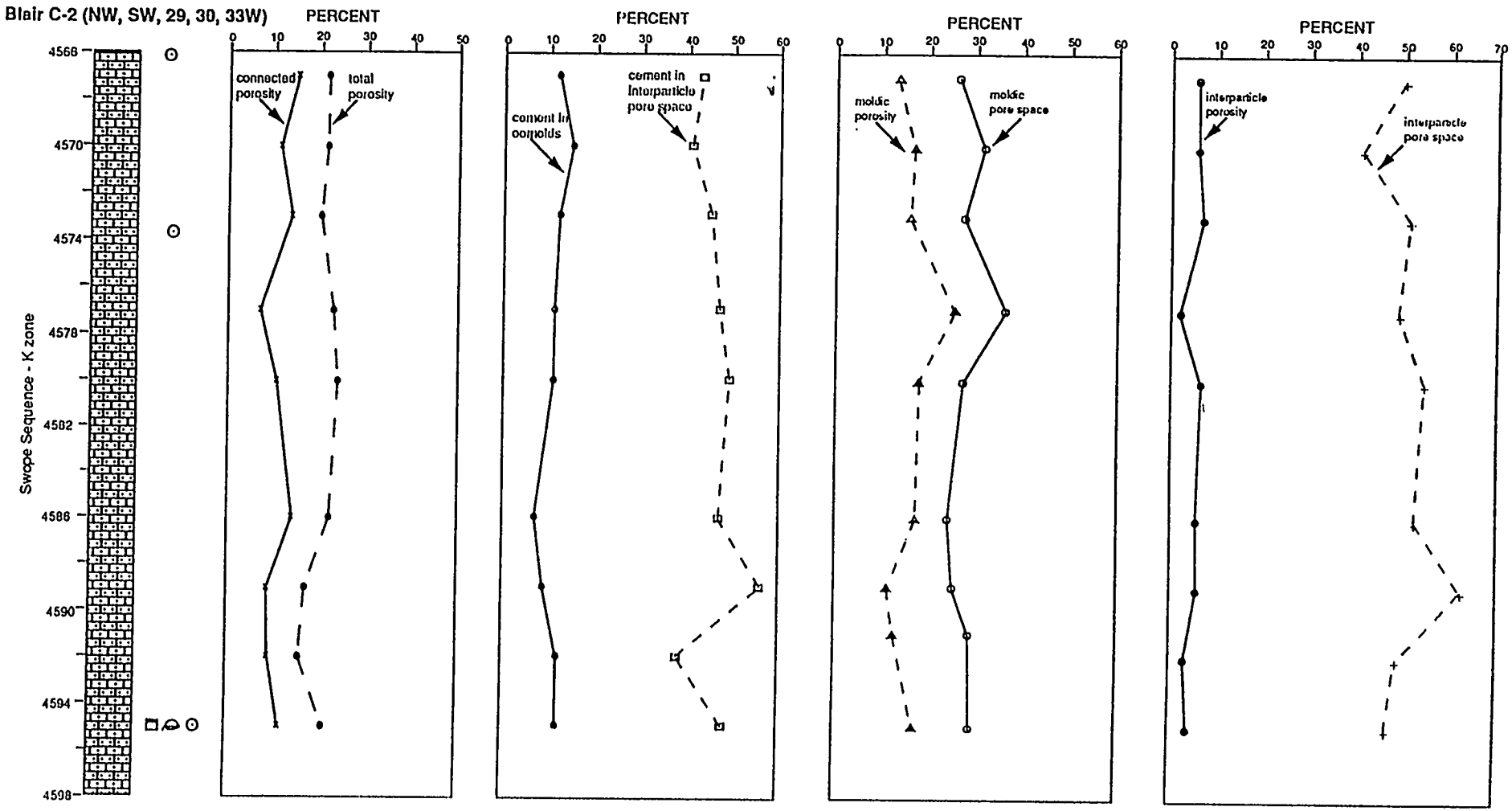

grainstone

ooid

echinoderm

brachiopod

Total porosity: interparticle + moldic + fracture + vuggy porosity.

Connected porosity: Total porosity minus isolated moldic pores.

Cement: equant calcite and minor baroque dolomite.

Estimate of percents based on point counts of thin sections (500 points).

Moldic pore space: cement filled and extant pores.

Moldic porosity: mostly oolitic grains.

Interparticle pore space: cement filled + extant pores.

Interparticle porosity: porosity between grains..

Figure 6.71. Stratigraphic distribution of diagenetic aspects of the grainstone in the Bethany Falls Limestone at the Blair 'C' No. 2 well.

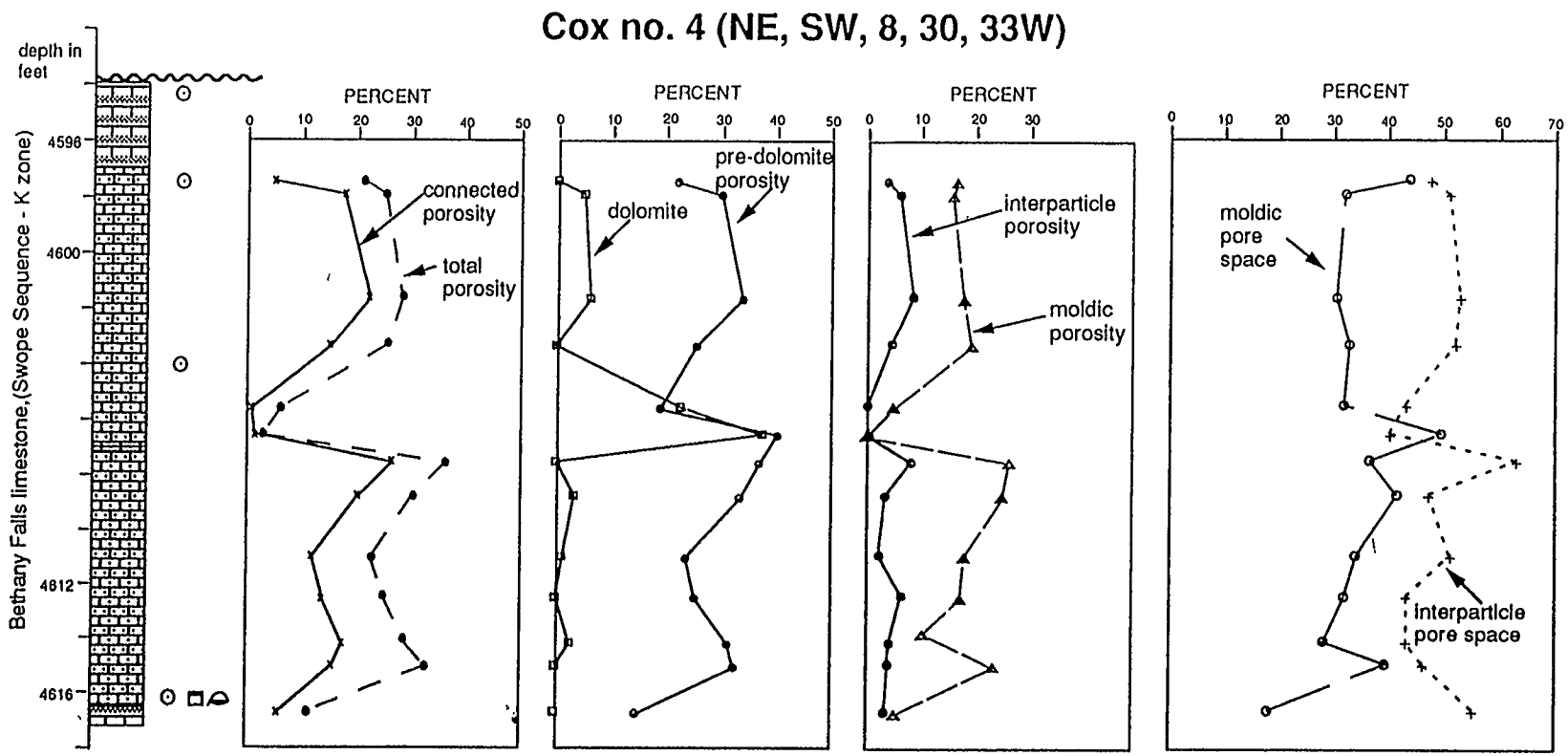

lime mudstone

grainstone

ooid

echinoderm

brachiopod

Total porosity: Interparticle + moldic + fracture + vuggy porosity.

Connected porosity: Total porosity minus isolated moldic pores.

Dolomite: baroque dolomite.

Pre-dolomite porosity: interparticle + moldic porosity + dolomite.

Interparticle pore space: cement filled + extant pores.

Interparticle porosity: porosity between grains..

Moldic pore space: cement filled + extant molds of ooids.

Moldic porosity: mostly oolitic grains affected.

Estimate of percents based on point counts of thin sections (500 points).

Figure 6.72. Stratigraphic distribution of diagenetic aspects of grainstone in the Bethany Falls Limestone at the Cox No. A-4 well.

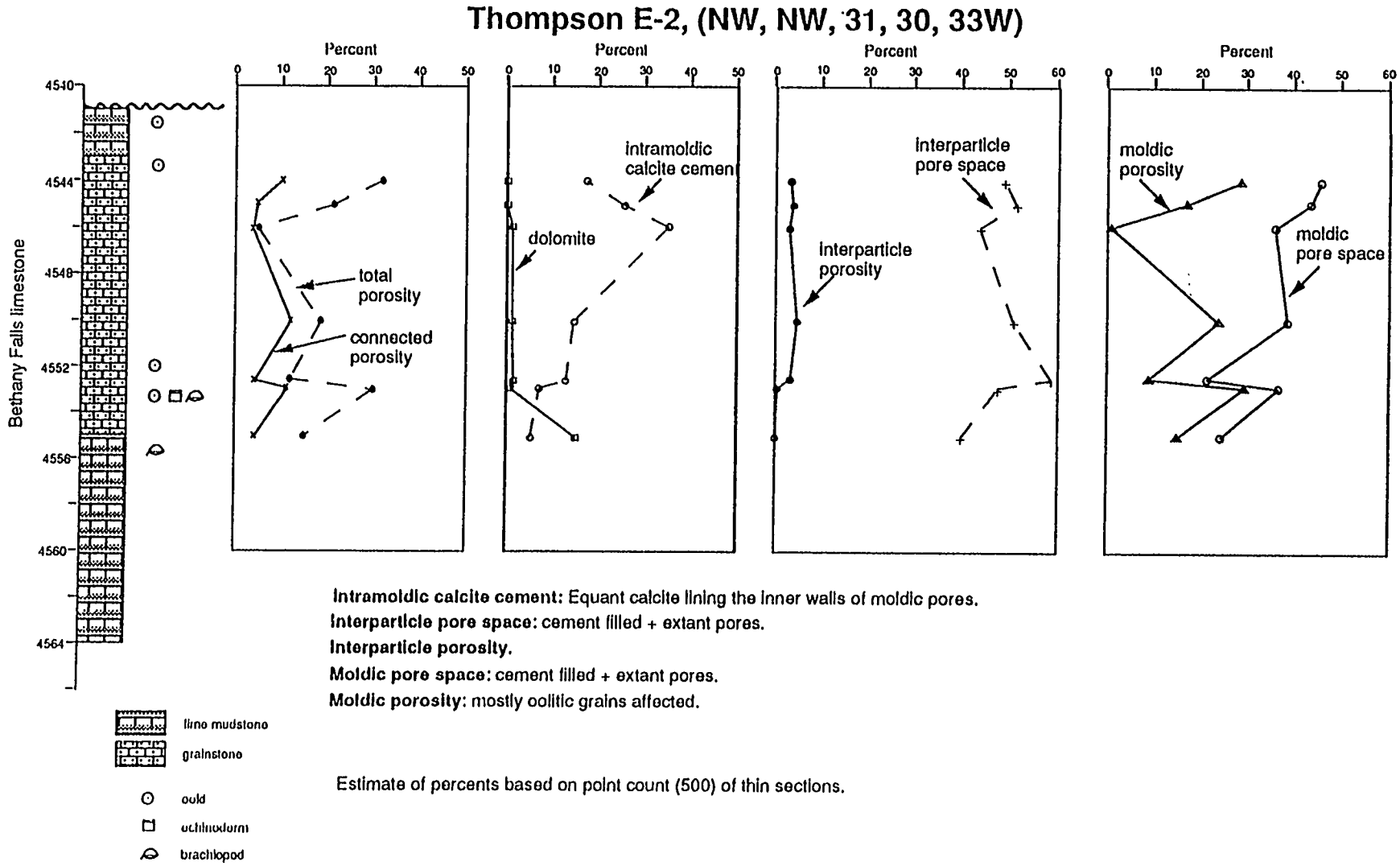

Intramoldic calcite cement: Equant calcite lining the inner walls of moldic pores.
Interparticle pore space: cement filled + extant pores.
Interparticle porosity.
Moldic pore space: cement filled + extant pores.
Moldic porosity: mostly oolitic grains affected.

Estimate of percents based on point count (500) of thin sections.

Figure 6.73. Stratigraphic distribution of diagenetic aspects of grainstone in the Bethany Falls Limestone at the Thompson 'E' No. 2 well.

Stage 1: Growth of equant calcite spar in isopachous rims on ooid grains. This process can result in nearly complete loss of interparticle porosity.

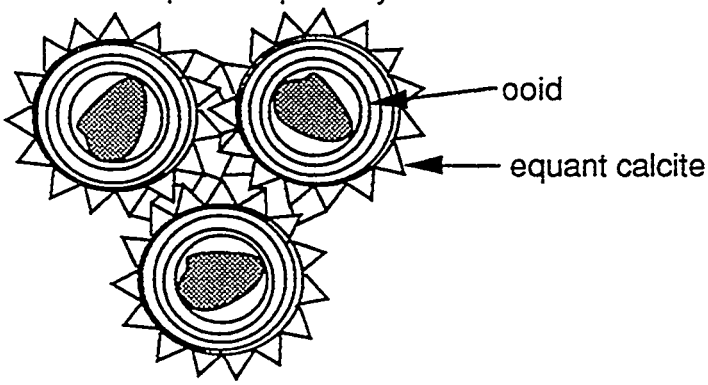

Stage 2: Dissolution of oolitic grains = oomoldic porosity. These pore are, in large part, isolated from other pores by the remaining ooid walls and the calcite cement in the interparticle porosity.

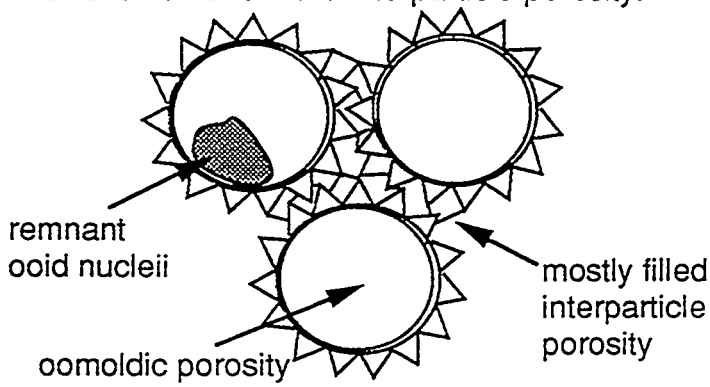

Stage 3: Continued dissolution of carbonate grains and early calcite cements leading to the creation of connected porosity.

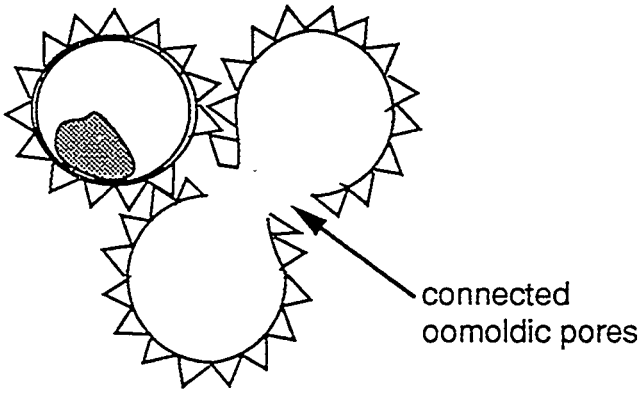

Stage 4: Growth of equant calcite spar on inner walls of moldic ooids. This stage further decreases the opportunity for pore connections to exist.

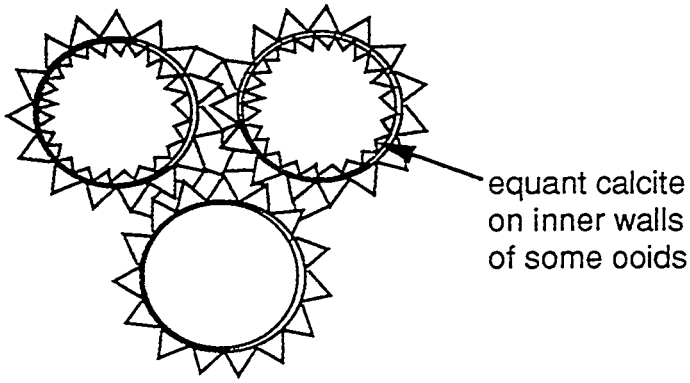

Stage 5: Slight crushing of some oomolds to form connections between pores.

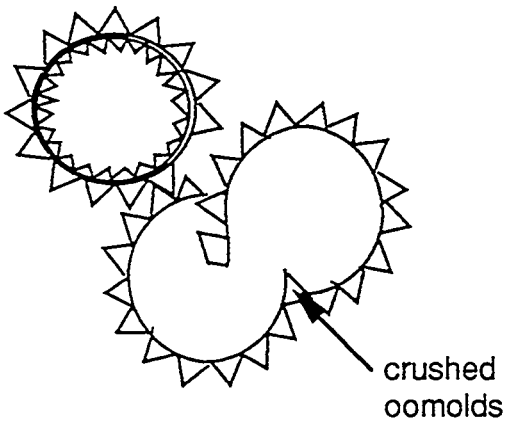

Stage 6: Continued growth of carbonate cements,ferroan calcite and baroque dolomite, during burial. Such cements can completely occlude the remaining porosity.

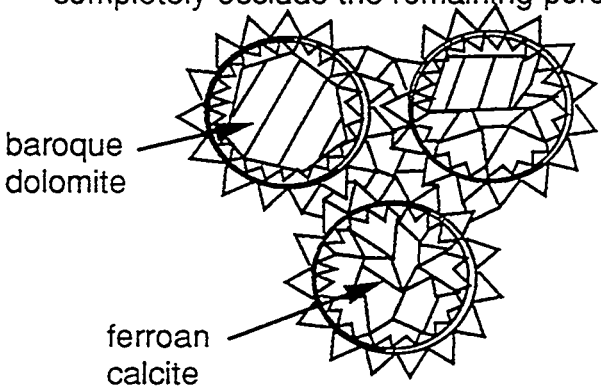

Diagenesis of the grainstones can be divided into six stages. Meteoric waters, introduced during early subaerial exposure, were active during stages 1 - 3. Stages 4, 5, and 6 occurred during burial.

Figure 6.74. Porosity evolution of grainstone in the Bethany Falls Limestone, Victory Field.

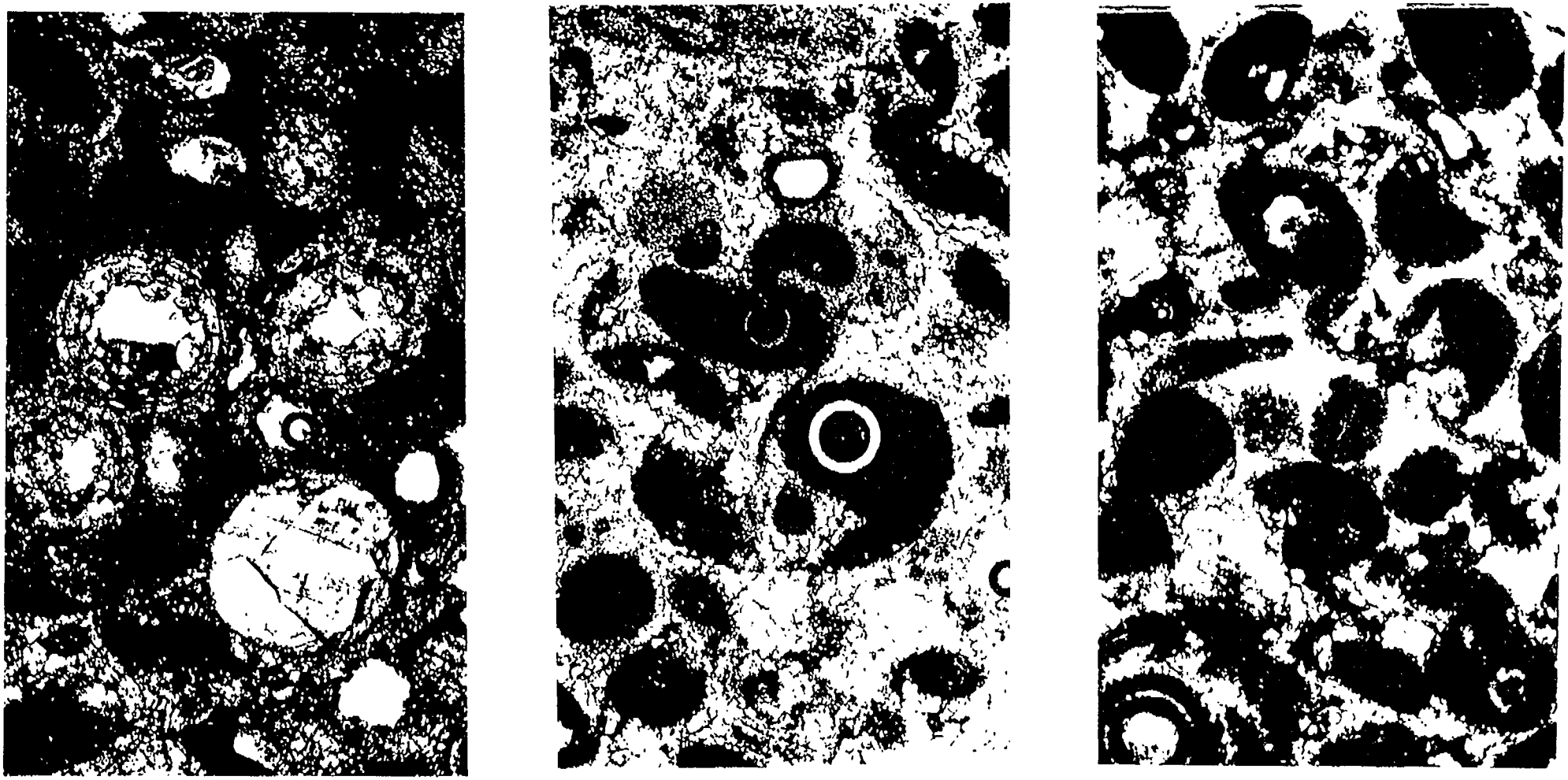

Figure 6.75. Bethany Falls photomicrographs of thin sections (4x). Cities Service #C-2 Blair, Sec. 29-T30S-R33W. Dark areas are porosity.

a. 4570' Stage 5: Increased permeability by crushing (porosity=30%, permeability=5md)
b. 4577' Stage 5: Increased permeability by crushing
c. 4570' Stage 6: Baroque dolomite cement. White areas are porosity not penetrated by epoxy

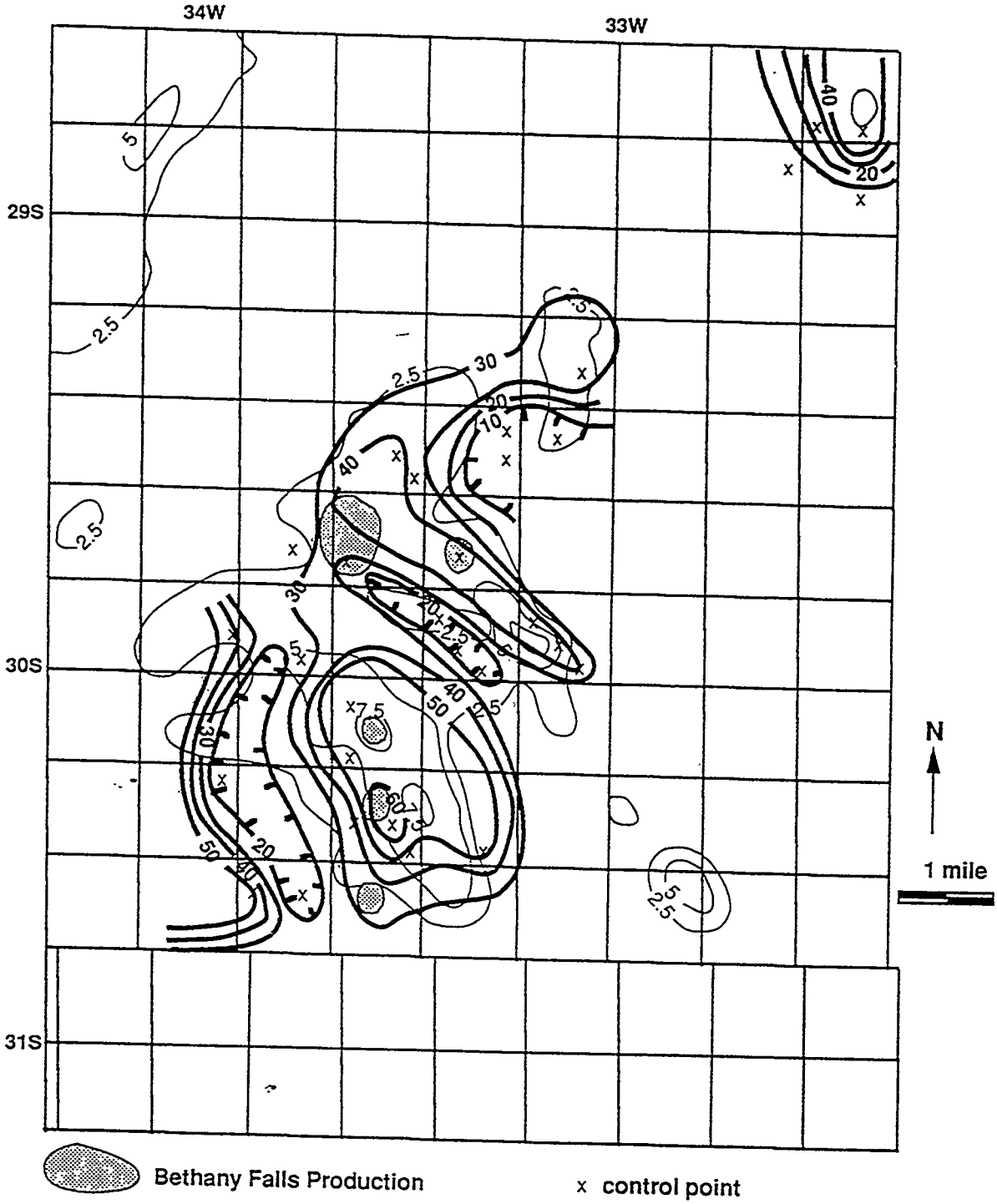

Light contours are Bethany Falls porosity feet greater than 16%. Heavy contours are percent fully porous (type C) ooid grainstone. Based on low power, reflected light studies of well cuttings.
n = 30 wells. Contour interval 10%.

Figure 6.76. Distribution of effective porosity in the Bethany Falls Limestone. Based on studies using low power, reflected light microscopy.

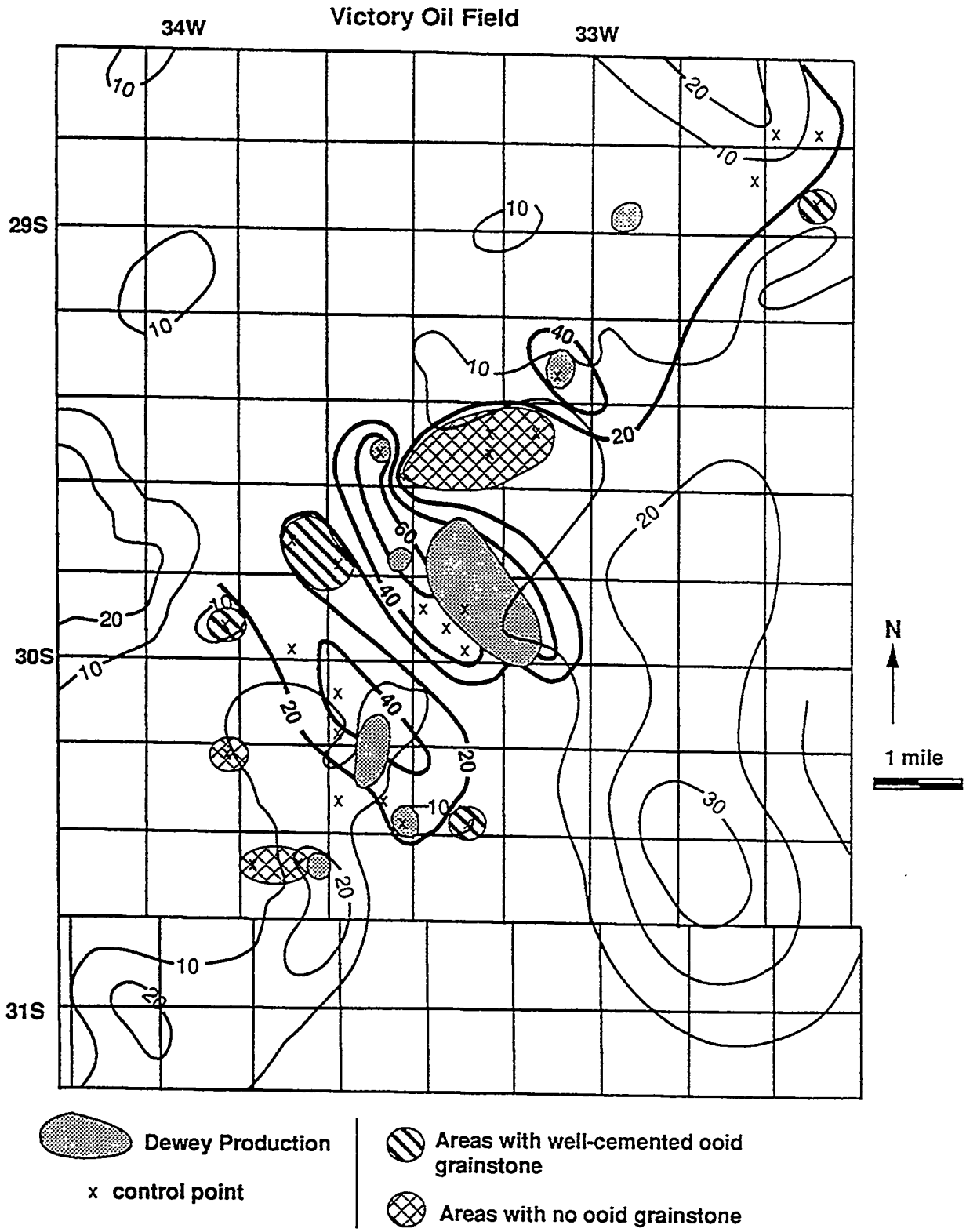

Light contours are Dewey feet porosity greater than 8%. Heavy contours are percent fully-porous ooid grainstone: from low power reflected light studies of well cuttings.
n = 27 wells. Contour interval 20%.

Figure 6.77. Distribution of effective porosity in the Dewey Limestone. Based on studies using low power, reflected light microscopy.

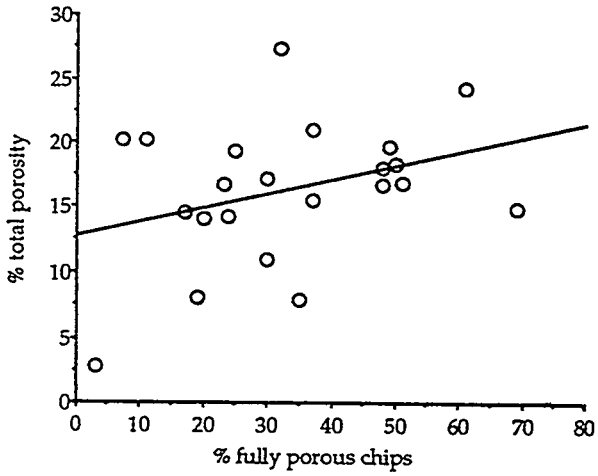

null hypothesis: $r = 0$

$t = r((n-2)/(1-r^2))^{1/2}$

$y = .108x + 12.739$, $r2 = .118$
$n = 22$
$t = 1.636$
a significant correlation at the 80% probability level.

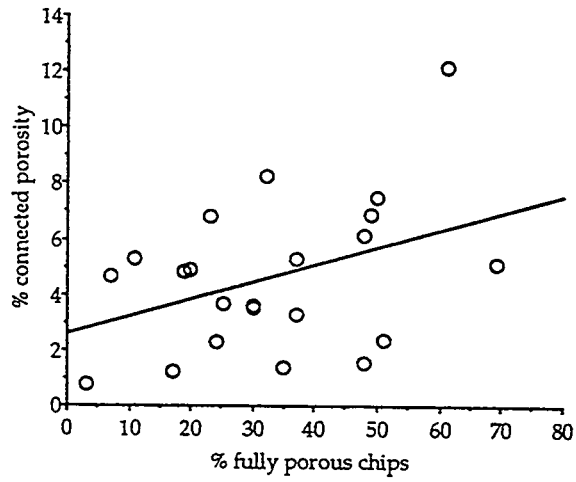

$y = .062x + 2.566$, $r2 = .16$
$n = 22$
$t = 1.952$
a significant correlation at the 90% probability level.

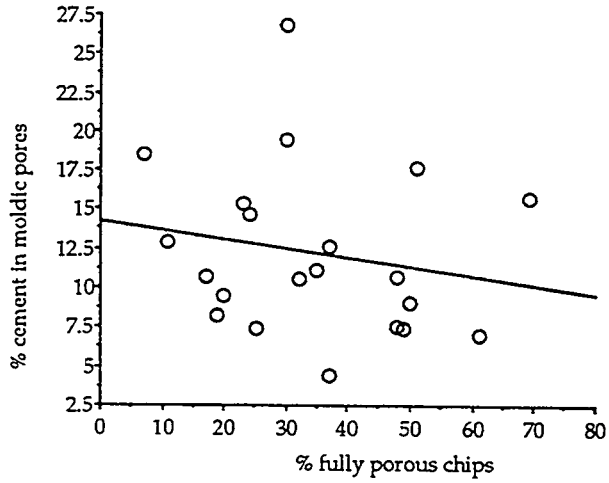

$y = -.059x + 14.273$, $r2 = .033$
$n = 21$
$t = 0.805$
a significant correlation at the 50% probability level.

Figure 6.78. Comparison of petrographic studies of thin sections of cuttings versus assessments of pore fabrics using low power, reflected light microscopy.

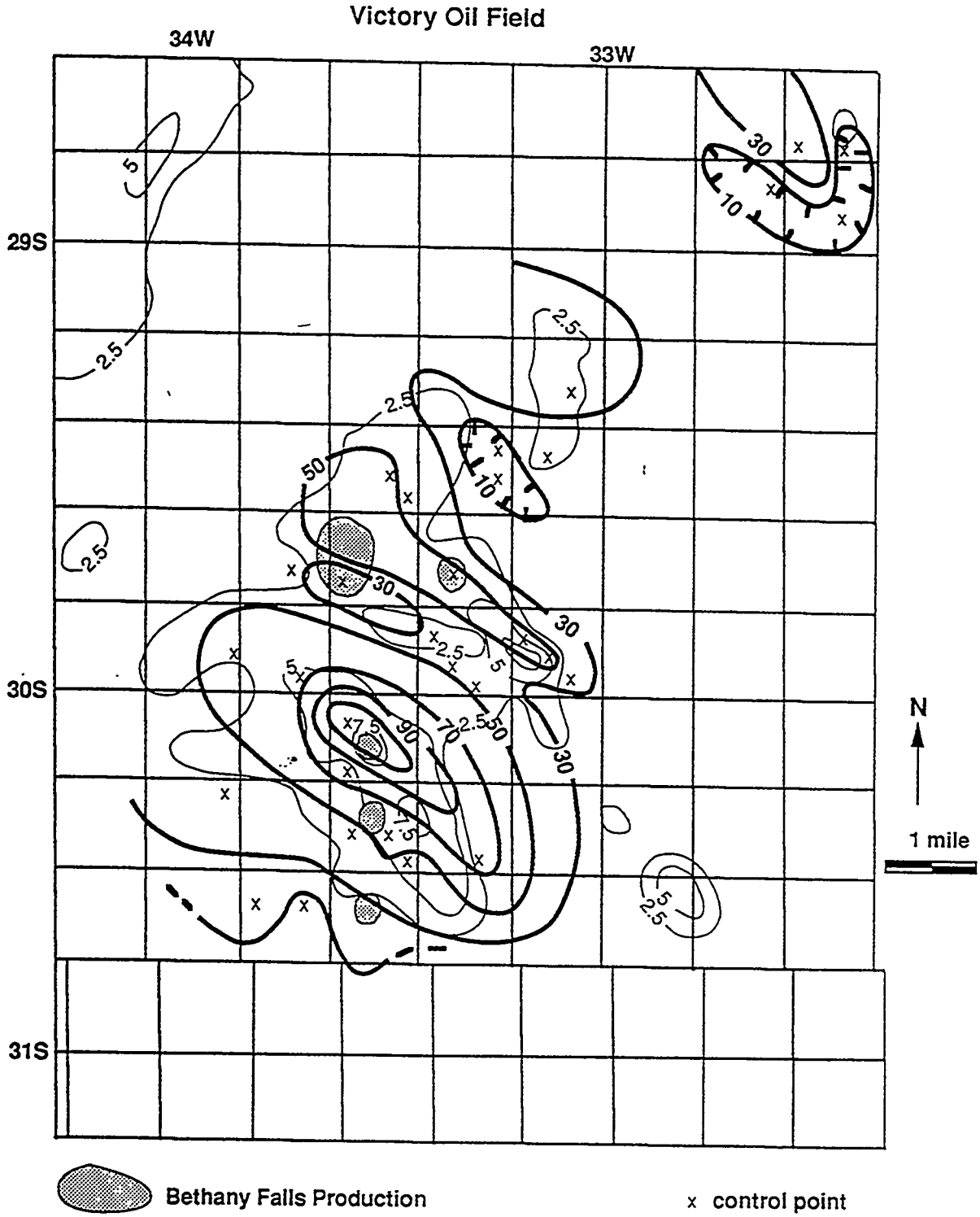

Light contours are Bethany Falls porosity feet greater than 16%. Heavy contours are percent effective porosity x 10. Based on point counts of thin sections of well cuttings.
n = 27 wells. Contour interval 20%.

Figure 6.79. Distribution of petrographically defined effective porosity in the Bethany Falls Limestone. Based on point counts of thin sections of cuttings.

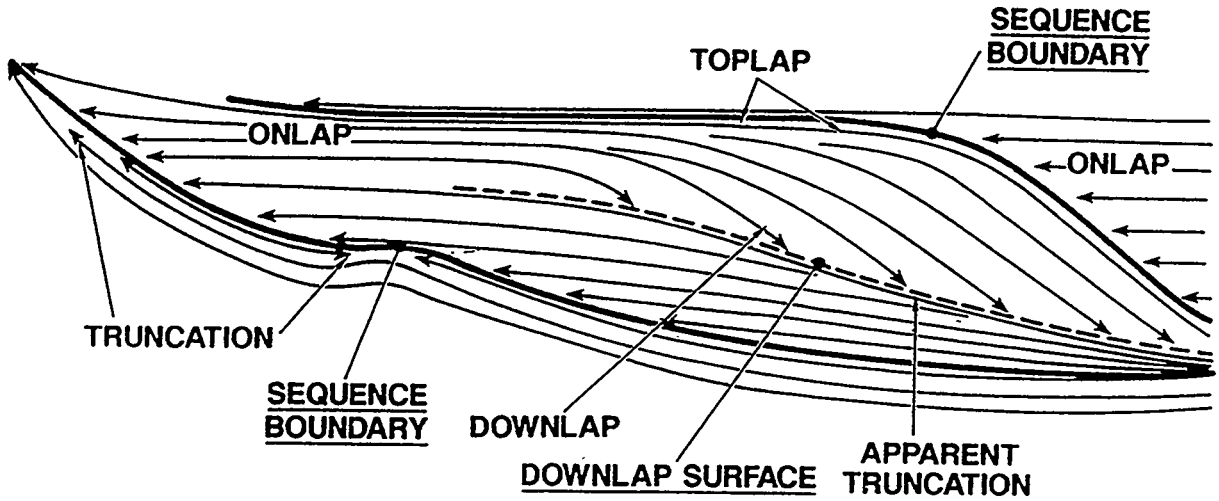

Figure B.1 (b). Types of discontinuites in a depositional sequence (from Vail, 1987).

☆U.S. GOVERNMENT PRINTING OFFICE: 1994 - 660-029/00055

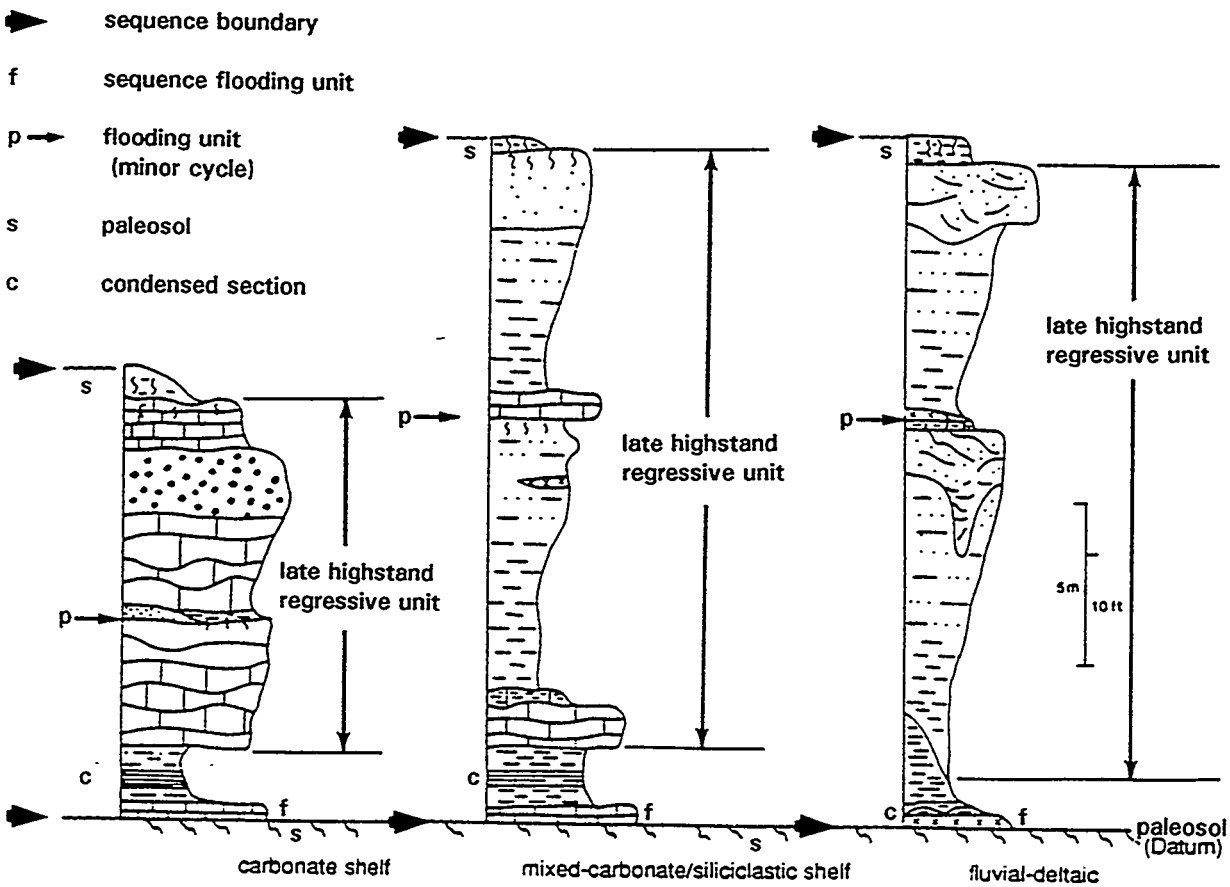

Figure B.1 (a). Vertical profiles of selected types of depositional sequences observed in Pennsylvanian strata of the Midcontinent. Simple shallowing-upward sections shown. Modified from Watney, et al., 1989.

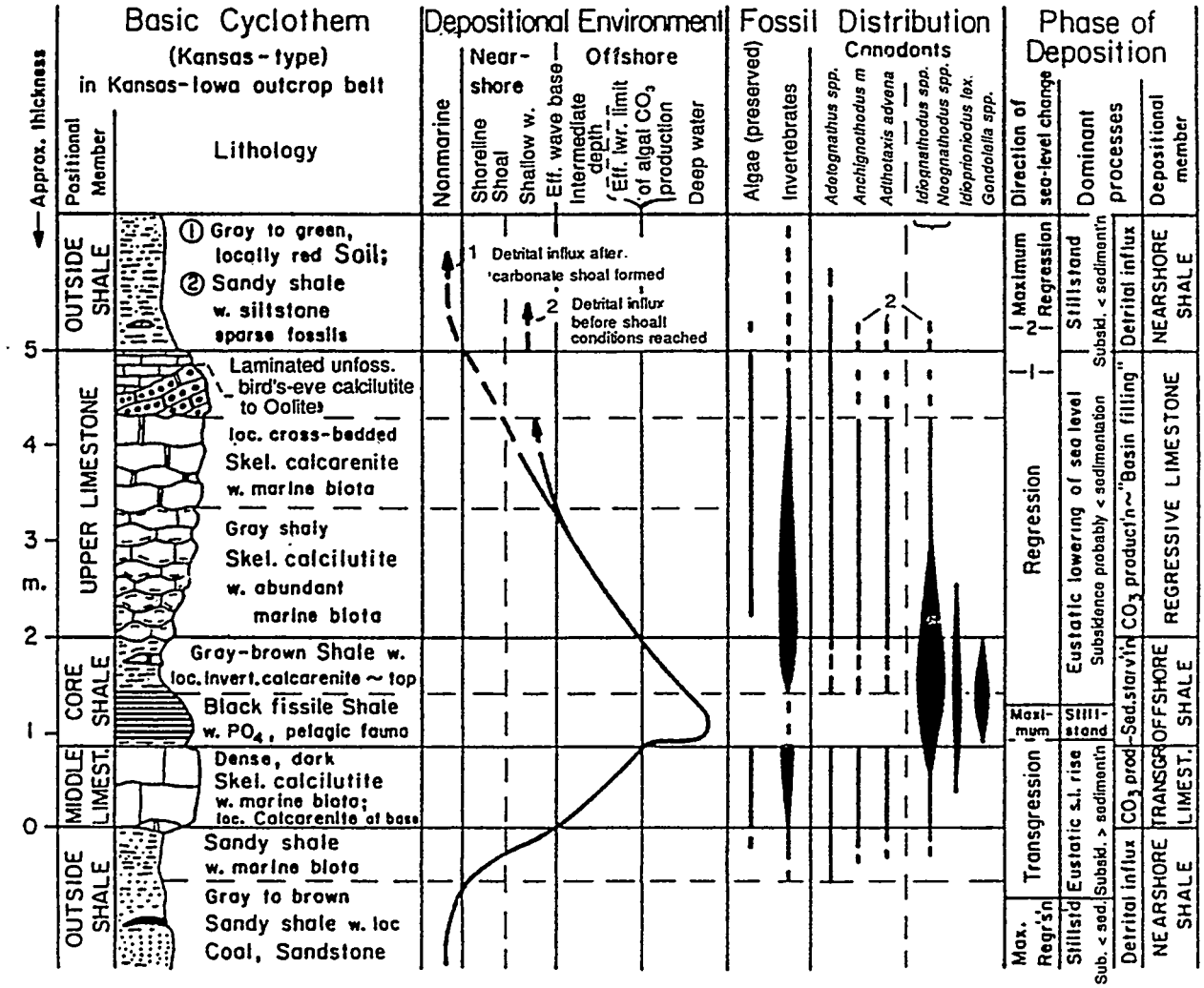

Figure A.1. Basic Kansas cyclothem. Modified from Heckel, 1989.

Chip evaluation: Comparison of thin section and cuttings observations. Victory Field, Haskell Co., KS

Well no.	depth ft.	tot. por.	eff. por.	sec. por. occlusion	%A	%B	%C
V1	4210-20	14.8	5.7	20.9			
V1	4640-50B	11.6	2.8	20.8	0.	31.	69.
V1	4640-50C	24.5	11.7	11.2			
V2	4190-00	22.1	7.5	9.4			
V3	4230-30	19.1	7.2	10.3			
V3	4650-60	8.0	4.8	10.7	37.	44.	19.
V4	4230-40	16.8	4.9	18.7			
V5	4650-60	11.0	3.6	32.4	16.	54.	30.
V5	4670-80	7.8	1.4	17.8	23.	42.	35.
V5	4680-90	13.4	1.2	22.5			
V6	4190-00	14.5	3.4	19.1			
V6	4610-20	24.3	12.2	7.0	17.	22.	61.
V7	4180-90	21.4	4.9	22.5			
V7	4610-20	27.4	8.3	13.8	4.	64.	32.
V10	4235-40	25.6	9.1	5.9			
V10	4620	19.4	3.7	7.4	0.	75.	25.
V10	4645	21.0	5.3	7.5	0.	63.	37.
V11	4232	18.5	3.7	11.0			
V11	4650-55B	14.0	3.8	12.9	7.	44.	49.
V11	4650-55C	16.8	2.4	14.8			
V11	4655-60	19.7	6.9	9.4	3.	60.	37.
V12	4630-40	20.1	4.7	18.5	14.	79.	7.
V12	4640-50	17.2	3.5	19.4	14.	56.	30.
V12	4650–60	20.1	5.3	12.9	11.	79.	11.
V13	4641	16.9	2.4	17.9	11.	38.	51.
V14	4588B	17.9	6.4	17.5	1.	49.	50.
V14	4588C	18.6	6.9	6.1			
V17	4600-10	16.7	6.8	15.3	6.	71.	23.
V17	4610-20	14.7	3.3	8.4			
V19	4690-00	9.4	2.6	16.9			
V20	4604	14.3	2.3	14.7	5.	71.	24.
V20	4600-10	14.6	1.2	10.7	0.	83.	17.
V21	4651B	12.8	3.9	7.4	0.	80.	20.
V21	4651C	15.5	5.8	10.7			
V24	4637	16.7	1.5	7.5	2.	50.	48.
V24	4690	13.5	2.8	11.7			
V25	4675	10.1	2.0	18.2			
V26	4570	2.8	0.8	2.8	53.	44.	3.
V27	4580-90B	15.3	4.2	13.5	0.	52.	48.
V27	4580-90C	20.9	8.0	7.5			

%A - fully cemented ooid grst.
%B - partly porous ooid grst. Secondary pores have cement
%C - fully porous ooid grst. Secondary pores lack cement.

Table 6.11 Comparison of point count data and data from reflected light studies of cuttings in oolitic grainstones in Victory Field.

Victory Field - thin sections of cuttings. percents from point count

Well no.	depth ft.	unit	MO (iso)	MO (con)	BP	frac.	cal (BP,WP)	cal (MO)	dol (MO)	dol (BP)	qtz (MO)	qtz (BP)	clay (MO)	grains	mud	tot. por.	eff. por.	sec. por. occlusion	tot. pts.	no. of chips and lithology
V1	4210-20	Stanton	9.1	2.7	3.0	0.0	40.4	18.6	0.0		2.3	0.0	0.0	23.9	0.0	14.8	5.7	20.9	264	4 oold, 3 pel, 3 skel-oold
V1	4640-50B	Bethany Falls	8.8	1.4	1.4	0.0	45.9	20.3	0.0	0.0	0.5	0.0	0.0	21.7	0.0	11.6	2.8	20.8	217	oold grst.
V1	4640-50C	Bethany Falls	12.8	5.9	5.3	0.5	42.0	11.2	0.0	0.0	0.0	0.0	0.0	21.2	1.1	24.5	11.7	11.2	188	oold grst.
V2	4190-00	Stanton	14.6	1.3	6.2	0.0	60.0	8.4	0.0	0.0	1.0	0.0	0.0	8.5	0.0	22.1	7.5	9.4	308	7 oold, 5 skel grst.
V3	4230-30	Stanton	11.9	1.2	6.0	0.0	41.6	8.7	0.0	0.0	1.6	0.0	0.0	26.6	2.4	19.1	7.2	10.3	252	6 oold, 5 skel, 1oold-skel grst.
V3	4650-60	Bethany Falls	3.2	1.6	2.8	0.4	30.4	8.3	0.0	0.0	2.4	0.0	0.0	46.2	4.7	8.0	4.8	10.7	253	8 oold, 15 skel grst.
V4	4230-40	Stanton	11.9	1.7	3.2	0.0	40.0	16.1	0.0	0.0	2.6	0.0	0.0	16.1	8.4	16.8	4.9	18.7	310	19 oold, 2 skel-pel grst
V5	4650-60	Sniabar	7.4	0.8	2.8	0.0	39.7	26.8	0.0	0.0	5.6	0.0	0.0	16.9	0.0	11.0	3.6	32.4	284	17 oold, 3 skel grst.
V5	4670-80	Sniabar.	6.4	0.1	1.3	0.0	43.0	11.1	0.0	0.0	6.7	0.0	0.0	31.4	0.0	7.8	1.4	17.8	297	13 oold, 15 skel grst.
V5	4680-90	Sniabar	12.2	0.6	0.6	0.0	36.0	15.2	0.3	0.0	7.0	0.0	0.0	28.1	0.0	13.4	1.2	22.5	288	18 oold, 3 skel grst.
V6	4190-00	Stanton	11.1	0.0	3.4	0.0	48.9	15.3	0.0	0.0	3.8	0.0	0.0	17.5	0.0	14.5	3.4	19.1	262	12 oold, 1 skel grst
V6	4610-20	Bethany Falls	12.1	1.8	10.0	0.4	40.4	7.0	0.0	0.0	0.0	0.0	0.0	28.3	0.0	24.3	12.2	7.0	272	17 oold, 13 skel-oold grst.
V7	4180-90	Stanton	16.5	0.6	4.3	0.0	43.9	18.0	0.3	0.0	3.0	0.0	1.2	12.2	0.0	21.4	4.9	22.5	328	14 oold grst.
V7	4610-20	Bethany Falls	19.1	6.2	2.1	0.0	47.1	10.6	0.9	0.0	2.3	0.0	0.0	11.7	0.0	27.4	8.3	13.8	341	oold, 2 skel-oold grst.
V10	4235-40	Stanton	16.5	1.6	7.5	0.0	42.5	3.9	0.4	0.0	1.6	0.0	0.0	26.0	0.0	25.6	9.1	5.9	254	8 oold, 1 pel grst.
V10	4620	Bethany Falls	15.7	0.6	3.1	0.0	49.2	7.1	0.0	0.0	0.0	0.0	0.3	22.5	1.5	19.4	3.7	7.4	325	8 oold grst. 1skel pkst.
V10	4645	Bethany Falls	15.7	0.9	4.4	0.0	50.5	4.4	0.0	0.0	3.1	0.0	0.0	19.7	1.3	21.0	5.3	7.5	319	9 oold, 2 skel-oold grst. 1 skel pkst.
V11	4232	Stanton	14.8	0.7	3.0	0.0	51.7	10.7	0.0	0.0	0.3	1.7	0.0	16.8	0.3	18.5	3.7	11.0	298	12 oold, 2 skel-oold grst.
V11	4650-55B	Bethany Falls	10.2	1.5	2.3	0.0	56.1	9.5	1.5	0.0	1.1	0.0	0.8	14.0	3.0	14.0	3.8	12.9	264	oold grst.
V11	4650-55C	Bethany Falls	14.4	0.7	1.7	0.0	52.6	12.0	1.4	0.0	1.4	0.0	0.0	15.1	0.7	16.8	2.4	14.8	291	oold grst.
V11	4655-60	Bethany Falls	12.8	2.5	4.4	0.0	59.6	7.4	0.0	0.0	2.0	0.0	0.0	11.3	0.0	19.7	6.9	9.4	203	oold grst.
V12	4630-40	Bethany Falls	15.4	0.9	3.8	0.0	38.2	13.5	4.4	0.0	0.6	4.7	0.0	16.9	1.6	20.1	4.7	18.5	319	7 oold, 1 skel, 1 oold-skel grst.
V12	4640-50	Bethany Falls	13.7	1.3	2.2	0.0	38.8	6.2	13.2	4.4	0.0	1.8	0.0	16.6	1.8	17.2	3.5	19.4	227	12 oold, 4 skel grst. 1 dolomite
V12	4650-60	Bethany Falls	14.8	2.4	2.9	0.0	43.8	3.8	8.6	0.0	0.5	1.4	0.0	20.4	1.4	20.1	5.3	12.9	210	12 oold, 3 skel grst.
V13	4641	Bethany Falls	14.5	0.8	1.6	0.0	46.7	9.8	3.9	0.0	3.9	5.1	0.3	13.4	0.0	16.9	2.4	17.9	255	13 oold, 4 skel grst.
V14	4588B	Bethany Falls	11.5	2.3	4.1	0.0	47.5	17.0	0.0	0.0	0.0	0.0	0.5	16.6	0.5	17.9	6.4	17.5	217	8 oold, 2 oold-skel grst
V14	4588C	Bethany Falls	11.7	2.0	4.9	0.0	57.1	6.1	0.0	0.0	0.0	0.8	0.0	16.6	0.8	18.6	6.9	6.1	247	oold grst.
V17	4600-10	Bethany Falls	9.9	1.8	4.5	0.5	52.3	10.8	4.5	1.4	0.0	0.0	0.0	13.8	0.5	16.7	6.8	15.3	222	6 oold, 3 pel, 2 skel grst.
V17	4610-20	Bethany Falls	11.4	1.7	1.3	0.3	56.7	6.4	0.0	0.0	2.0	3.4	0.0	16.8	0.0	14.7	3.3	8.4	298	9 oold, 4 pel grst.
V19	4690-00	Sniabar	6.8	1.3	1.3	0.0	46.8	3.0	13.9	0.4	0.0	0.0	0.0	26.5	0.0	9.4	2.6	16.9	237	oold grst.
V20	4604	Bethany Falls	12.0	0.0	1.9	0.4	57.9	14.3	0.0	0.4	0.4	1.9	0.0	10.8	0.0	14.3	2.3	14.7	259	oold grst
V20	4600-10	Bethany Falls	13.4	0.6	0.6	0.0	51.4	10.1	0.6	0.0	0.0	2.8	0.0	20.1	0.6	14.6	1.2	10.7	179	6 oold, 4 pel grst.
V21	4651B	Bethany Falls	8.9	1.2	2.7	0.0	54.0	6.2	0.0	0.0	0.9	3.0	0.3	22.8	0.0	12.8	3.9	7.4	337	8 oold, 9 pel grst.
V21	4651C	Bethany Falls	9.7	3.9	1.9	0.0	47.4	9.7	0.0	0.0	1.0	5.0	0.0	20.4	1.0	15.5	5.8	10.7	103	4 oold grst.
V24	4637	Bethany Falls	15.2	0.9	0.6	0.0	43.1	5.1	0.9	0.0	1.5	7.7	0.0	22.0	3.0	16.7	1.5	7.5	336	11 oold, 7 skel grst.
V24	4690	Sniabar	10.7	0.9	1.9	0.0	39.0	9.8	1.9	0.0	0.0	0.0	0.0	35.8	0.0	13.5	2.8	11.7	214	6 oold grst.
V25	4675	Bethany Falls	8.1	0.7	1.3	0.0	37.2	10.4	6.8	0.0	1.0	1.0	0.0	30.6	2.9	10.1	2.0	18.2	307	15 oold, 3 pel grst.
V26	4570	Bethany Falls	2.0	0.0	0.8	0.0	38.4	2.8	0.0	0.0	0.0	4.0	0.0	50.8	1.2	2.8	0.8	2.8	248	12 oold, 8 pel-oold grst.
V27	4580-90B	Bethany Falls	11.1	1.1	3.1	0.0	39.4	11.1	0.8	0.0	0.8	2.5	0.8	24.9	4.4	15.3	4.2	13.5	360	10 oold, 2 pel-oold grst.
V27	4580-90C	Bethany Falls	12.9	5.0	3.0	0.0	47.9	6.9	0.0	0.0	0.3	3.3	0.3	19.0	1.4	20.9	8.0	7.5	363	oold grst.

Table 6.10 Summary of point count data from cuttings samples of reservoir grainstone in Victory Field.

Dewey: cuttings porosity evaluation

Well no.	depth	%A	%B	%C	n
V1	4400-20	16	59	25	20
V2	4400-40	9	55	36	47
V3	4400-40	2	47	51	327
V4	4445	0	53	47	45
V5	4400-10	25	75	0	3
V6	4410-40	6	31	63	52
V7	4410-30	2	53	45	85
V9	4400-40	21	50	29	24
V10	no oold grst.				0
V11	4442	18	21	61	39
V12	4430-50	25	75	0	8
V13	no oold grst.				0
V14	4410-35	10	84	6	31
V15	no oold grst.				
V16	no oold grst.				
V17	4400-10	12	51	37	85
V18	4410-50	52	37	11	46
V19	no oold grst.				
V20	4400-10	64	36	0	50
V21	4460-70	21	58	21	24
V22	no oold grst.				
V23	no oold grst.				
V24	4450-60	24	52	24	29
V25	4420-30	43	38	19	21
V26	no oold grst.				
V27	4380-00	30	58	12	93

%A - fully cemented oold grst.
%B - partly porous oold grst. Secondary pores have cement
%C - fully porous oold grst. Secondary pores lack cement.
n - number of grains counted

Table 6.9 Evaluation of porosity classes in the Dewey Limestone in wells from Victory Field.

Semi-qualitative examination of porosity in well cuttings - Bethany Falls

Well no.	depth ft.	%A	%B	%C	n		avg %A	avg %B	avg %C	total n
V1	4630-40	0	25	75	48	V1	0.0	28.0	72.0	83.0
V1	4640-50	0	31	69	35					
V2	4600-10	4	48	48	85	V2	4.0	48.0	48.0	85.0
V3	4650-60	37	44	19	56	V3	36.0	41.0	18.0	79.0
V3	4660-70	35	48	17	23					
V4	4638	32	34	32	88	V4	32.0	34.0	32.0	88.0
V5	4650-60	16	54	30	67	V5	20.0	45.0	35.0	214.0
V5	4660-70	23	38	39	64					
V5	4670-80	23	42	35	83					
V6	4610-20	17	22	61	59	V6	14.0	27.0	59.0	197.0
V6	4620-30	11	32	57	138					
V7	4600-10	0	31	69	42	V7	2.0	47.5	50.5	70.0
V7	4610-20	4	64	32	28					
V8	4610-20	30	55	15	44	V8	30.5	55.5	14.0	114.0
V8	4620-30	31	56	13	70					
V10	4620	0	75	25	20	V10	0.0	69.0	31.0	44.0
V10	4645	0	63	37	24					
V11	4650-55	4	60	36	114	V11	4.5	55.5	40.0	295.0
V11	4655-60	5	51	44	181					
V12	4630-40	14	79	7	28	V12	13.0	71.0	16.0	91.0
V12	4640-50	14	56	30	36					
V12	4650--60	11	79	11	27					
V13	4641	11	38	51	45	V13	11.0	38.0	51.0	45.0
V14	4588	1	49	50	46	V14	1.0	49.0	50.0	46.0
V15	4630-40	8	58	33	81	V15	8.0	58.0	33.0	81.0
V17	4600-10	6	71	23	31	V17	5.5	71.0	23.5	120.0
V17	4610-20	5	71	24	89					
V20	4604	5	71	24	42	V20	2.5	77.0	20.5	41.0
V20	4600-10	0	83	17	12					
V21	4651	0	80	20	64	V21	0.0	80.0	20.0	64.0
V22	no ooid grst.									
V23	4600-20	44	66	0	18	V23	34.0	64.0	7.0	124.0
V23	4620-40	24	62	14	106					
V24	4637	2	50	48	63	V24	2.0	50.0	48.0	63.0
V25	4625	75	25	0	73	V25	75.0	25.0	0.0	73.0
V26	4570	53	44	3	143	V26	53.0	44.0	3.0	143.0
V27	4580-90	0	52	48	50	V27	0.0	52.0	48.0	50.0
V28	4620-30	10	48	42	92	V28	4.4	51.8	43.8	517.0
V28	4630-40	2	40	58	94					
V28	4640-50	2	57	41	101					
V28	4650-60	4	47	49	129					
V28	4660-70	4	67	29	101					
V29	4640-50	13	63	24	40	V29	43.8	33.0	23.2	114.0
V29	4650-60	47	40	13	15					
V29	4660-70	50	21	29	14					
V29	4670-80	66	17	17	24					
V29	4680-90	43	24	33	21					
V30	4650-60	4	58	38	84	V30	7.7	52.0	40.0	235.0
V30	4660-70	7	50	43	74					
V30	4670-80	12	49	39	77					

%A - fully cemented ooid grst.
%B - partly porous ooid grst. Secondary pores have cement
%C - fully porous ooid grst. Secondary pores lack cement.

Table 6.8 Evaluation of porosity classes in the Bethany Falls in wells from Victory Field.

Victory Field well locations

well no.	location	well name
V1	NW.SE.30.30.33W	Schneilbacher no. 1
V2	SE.SE.30.30.33W	Schneilbacher no. 2
V3	SW.SE.17.30.33W	Black no. 5
V4	NW.SE.33.29.33W	Miller G. U. 'I' no. 1
V5	SE.NW.4.30.33W	Moore G. U. 'G' no. 1
V6	SW.NW.19.30.33W	Wilson no. 3
V7	SW.SW.19.30.33W	Ammerman no. 2
V8	SW.NW.17.30.33W	Black 'A' no. 6
V9	SW.NW.17.30.33W	Black 'A' no. 9
V10	SE.SE.6.30.33W	Hoffman 'B' no. 2
V11	NW.SE.6.30.33W	Hoffman 'B' no. 1
V12	NE.NE.26.30.34W	Blair no. 1
V13	SW.NW.36.30.34W	Ungles 'A' no. 2
V14	SE.SW.29.30.33W	Blair 'C' no. 1
V15	SE.SW.30.30.33W	Schneilbacher 'B' no. 2
V16	NE.SW.17.30.33W	Black G. U. 'F' no. 1
V17	SW.SE.13.30.34W	Stanely no. 2
V18	NW.SE.12.30.34W	Fromong no. 2
V19	NE.SE.5.30.33W	winsted no. 1
V20	SW.SW.7.30.33W	Black no. 1
V21	SE.SW.13.29.33W	Wright Trust no. 1
V22	SE.NE.5.30.33W	Hoffman 'D' no. 1
V23	SW.SW.NE.36.30.34W	Fair no. 2-36
V24	SW.SE.13.29.33W	Wright Trust no. 5
V25	NW.SE.24.29.33W	Brennan no. 1-24
V26	SE.NE.23.29.33W	wright Trust no. 1-23
V27	NE.SW.14.30.34W	Huxman no. 12-14
V28	C.SW.NW.16.30.33W	James no. 2
V29	W1/2.NE.SW.16.30.33W	James no. 6
V30	SW.SE.16.30.33W	James no. 3

Table 6.7 Location of wells in studies of cuttings in Victory Field.

Conover 'D' no. 2

percents from point count

eff. por. = tot. porosity - MO iso.

depth ft.	MO iso	MO con	BP	frac.	vug	cal. BP,WP	cal. MO	dol MO	dol. BP	chert repl.	qtz	bit MO	grains	mud	tot. por.	eff. por.	tot. pts.	lith.	unit
4164 cp	18.0	3.8	2.9	0.0	0.9	57.4	10.2	0.0	0.0	0.0	0.0	0.0	6.8	0.0	25.6	7.6	451.00	oold grst.	Stanton
4173 cp	21.5	4.4	4.2	0.0	0.0	39.1	6.1	0.7	0.0	0.0	0.0	2.2	21.8	0.0	30.1	8.6	409.00	oold grst.	Stanton
4179 cp	14.8	1.8	2.2	0.2	0.0	45.4	6.7	0.0	0.0	0.0	0.6	3.7	20.2	4.2	19.0	4.2	492.00	oold pkst.	Stanton
4585	4.0	0.0	2.4	0.0	0.0	41.0	5.4	39.6	0.0	0.0	0.0	0.0	7.6	0.0	6.4	2.4	500.00	oold grst.	Bethany Falls
4591	7.6	3.4	5.0	0.0	0.2	41.0	8.2	3.0	0.6	2.8	1.0	0.0	25.0	2.2	16.2	8.6	500.00	oold pkst.	Bethany Falls

Table 6.6 Summary of point count data from the Conover 'D' No. 2 well, Victory Field

Blair 'C' no. 2

ft. depth	MOIso	MOcon	BP	frac.	vug	WP	BP,WP cal.	MO cal.	MO dol.	BP dol.	rep. chert	cem. qtz.	blt.	grain	mud	tot. por.	eff. por.	tot. pts.	lith.	unit
	percents from point count																			
4393 cp	3.4	0.0	2.0	0.0	0.0	0.0	31.1	2.0	2.5	1.4	0.0	0.2	2.5	40.7	14.2	5.4	2.0	444	skel-pel pkst.	Drum
4399 cp	3.5	1.2	0.2	0.0	0.0	0.0	7.5	4.4	3.7	1.6	0.0	0.0	0.2	34.0	43.7	4.9	1.4	429	oold wkst.	Drum
4567	5.4	9.0	6.3	0.0	0.0	0.2	43.9	10.0	2.2	0.0	0.0	0.0	0.0	23.0	0.0	20.9	15.5	521	oold grst.	Bethany Falls
4570	9.8	6.4	5.4	0.0	0.0	0.0	40.6	15.2	0.2	0.0	0.4	0.0	3.0	19.0	0.0	21.6	11.8	500	oold grst.	Bethany Falls
4577	19.8	5.4	1.8	0.0	0.0	0.0	47.0	10.8	0.6	0.0	0.0	0.0	1.4	13.2	0.0	27.0	7.2	500	oold grst.	Bethany Falls
4580	12.8	4.6	6.4	0.0	0.0	0.0	48.6	9.6	1.2	0.0	0.0	0.4	2.2	14.2	0.0	24.0	11.0	500	oold grst.	Bethany Falls
4586 cp	8.2	9.0	5.4	0.0	0.0	0.0	47.2	6.2	0.6	0.0	0.6	0.0	2.6	20.0	0.0	22.6	14.4	500	oold grst.	Bethany Falls
4589	7.8	3.4	5.6	0.0	0.0	0.0	56.6	7.6	0.8	0.0	0.0	0.0	5.6	12.6	0.0	16.8	9.0	500	oold grst.	Bethany Falls
4592	6.8	5.8	3.0	0.0	0.6	0.0	42.8	11.6	1.0	0.0	0.0	0.0	6.2	22.2	0.0	16.2	9.4	500	oold grst.	Bethany Falls
4595	8.8	8.0	3.8	0.2	0.0	0.0	41.4	9.6	1.2	0.0	0.0	0.0	3.6	23.4	0.0	20.8	12.0	500	oold grst.	Bethany Falls

cp - capillary pressure test sample.

Table 6.5 Summary of point count data from the Blair 'C' No. 2 well, Victory Field

Thompson 'E' no. 2 eff. por. = tot. porosity - MO iso. cp = capillary pressure samples
percents from point count

depth ft.	MO (iso)	MO (con)	BP	frac.	vug	WP	cal. (BP)	cal. (MO)	dol (MO)	dol (BP)	chert rep.	qtz. (MO)	Blt MO	Blt. BP	clay MO	grain	mud	tot. por.	eff. por.	tot. pts.	lith.	unit
4098	0.6	7.4	9.2	0.0	0.0	1.0	19.6	0.0	0.0	0.0	0.4	0.2	0.0	0.0	0.4	30.8	30.6	18.2	17.6	500	foram pkst.	Iatan
4102	0.4	2.0	9.8	0.0	3.8	0.8	20.6	0.0	0.0	0.0	0.0	0.0	0.0	0.0	0.0	43.4	19.2	16.8	16.4	500	skel pkst.	Iatan
4105	1.0	0.8	1.2	0.4	0.0	0.0	3.0	3.0	7.6	8.8	0.0	0.2	0.0	0.0	0.0	0.6	73.4	3.4	2.4	500	bivalve wkst.	Iatan
4105 cp	0.0	0.0	7.0	0.0	0.0	0.0	33.2	0.0	0.0	0.0	0.0	0.0	0.0	0.0	0.0	40.2	20.0	7.0	7.0	500	skel. pkst.	Iatan
4116	0.8	0.0	0.8	0.0	0.0	0.0	7.2	0.2	0.0	0.0	16.8	0.2	0.0	0.0	0.0	4.6	69.4	1.6	0.8	503	echin. wkst.	Iatan
4117	0.2	3.0	18.0	0.0	0.0	0.0	12.2	0.2	0.0	0.0	0.2	0.0	0.0	0.0	0.0	58.2	8.0	21.2	21.0	500	skel grst.	Iatan
4128	0.0	0.2	0.8	0.0	0.0	0.0	30.2	0.0	0.0	0.6	0.0	0.0	0.0	0.0	0.0	48.8	19.4	1.0	1.0	500	echin. pkst.	Iatan
4142	1.2	0.8	19.2	0.0	0.0	0.0	43.6	3.6	0.0	0.0	0.0	0.0	0.0	0.0	0.0	31.0	0.6	21.2	20.0	501	skel. grst.	Stanton
4146 cp	11.6	1.5	4.7	0.0	0.2	0.0	55.0	3.4	0.0	0.0	0.0	0.0	1.1	1.5	1.3	19.9	0.0	18.0	6.4	473	oold grst.	Stanton
4148	12.0	11.0	5.6	0.0	0.4	0.2	52.0	1.4	0.0	0.0	0.0	0.6	0.0	0.0	0.0	11.0	5.8	29.2	17.2	500	oold grst	Stanton
4149 cp	8.5	7.4	7.5	0.2	0.0	0.0	41.8	2.7	0.0	0.0	0.0	0.0	3.1	2.5	2.7	26.3	0.0	23.6	15.1	517	oold grst.	Stanton
4155	19.4	12.8	5.2	0.0	0.2	0.2	41.0	3.0	0.0	0.0	0.0	0.6	0.0	0.0	0.0	13.2	4.4	37.6	18.2	500	oold grst.	Stanton
4158 cp	19.3	2.0	3.7	0.0	0.0	0.0	37.2	8.7	0.0	0.0	0.0	1.0	0.0	0.0	1.8	25.8	0.0	25.0	5.7	492	oold grst.	Stanton
4356	8.0	9.0	7.3	0.0	0.0	0.0	57.0	5.3	0.6	0.0	0.0	0.0	0.0	0.0	0.0	11.0	0.0	24.3	16.3	300	oold grst.	Drum
4360	4.3	5.2	1.8	0.0	7.5	0.0	42.0	3.2	0.0	0.0	0.0	0.0	0.0	0.0	0.0	25.5	10.5	18.8	14.5	400	skel grst.	Drum
4360 cp	0.6	0.0	3.2	0.6	0.6	0.0	49.7	1.5	0.2	0.0	0.0	0.0	3.2	0.0	0.0	30.0	9.9	5.0	4.4	475	pel. pkst.	Drum
4361	3.8	0.8	2.0	0.0	14.2	0.0	45.8	0.4	0.0	0.0	0.0	0.4	0.0	0.0	0.2	32.4	0.0	20.8	17.0	503	pel. grst	Drum
4363	0.0	0.0	0.0	0.7	0.0	0.0	17.7	0.0	0.0	0.0	0.0	0.0	0.0	0.0	0.0	12.6	69.0	0.7	0.7	300	skel. wkst.	Drum
4368	6.0	2.4	1.0	0.0	0.0	0.0	42.2	8.2	0.6	0.0	0.2	0.2	0.0	0.0	0.0	31.0	8.2	9.4	3.4	500	pel-oold pkst	Drum
4368 cp	0.9	0.0	1.8	0.0	0.0	0.0	22.4	11.3	0.4	0.0	0.0	0.0	0.0	0.7	0.0	54.2	8.2	2.7	1.8	450	pel-oold pkst.	Drum
4544	21.8	7.0	3.2	0.0	0.0	0.0	46.0	17.0	0.0	0.0	0.0	0.2	0.0	0.0	0.0	4.8	0.0	32.0	10.2	501	oold grst.	Bethany Falls
4545	16.4	1.4	3.8	0.0	0.0	0.0	48.4	25.6	0.0	0.0	0.0	0.0	0.0	0.0	0.0	3.6	0.8	21.6	5.2	500	oold grst.	Bethany Falls
4546	1.0	0.2	2.8	0.0	1.0	0.0	40.7	35.0	0.0	0.8	0.0	0.0	0.0	0.0	0.0	18.5	0.0	2.5	2.0	508	oold grst.	Bethany Falls
4548 cp	7.2	2.1	4.9	0.2	0.0	0.0	39.8	6.9	1.6	0.0	0.0	0.0	9.7	1.4	0.2	25.3	0.7	14.4	7.2	432	oold grst.	Bethany Falls
4550	16.4	7.6	4.6	0.0	0.0	0.0	50.6	14.6	0.0	1.2	0.0	0.0	0.0	0.0	0.0	5.0	0.0	28.6	12.2	4550	oold grst.	Bethany Falls
4552.5	7.4	1.4	3.2	0.0	0.0	0.0	55.8	13.0	0.0	1.6	0.0	0.0	0.0	0.0	0.0	15.8	1.8	12.0	4.6	500	oold-skel pkst.	Bethany Falls
4553	18.6	11.1	0.4	0.0	0.0	0.0	44.0	6.6	0.2	0.0	0.0	0.4	0.0	0.0	0.0	18.7	0.0	30.1	11.5	494	oold grst.	Bethany Falls
4554 cp	13.4	6.0	3.5	0.0	0.0	0.0	43.5	4.6	10.4	0.0	0.0	0.2	4.4	0.2	0.7	12.9	0.0	22.9	9.5	432	oold grst.	Bethany Falls
4555	10.4	4.6	0.3	0.0	0.0	0.0	39.3	5.4	0.0	13.5	4.9	0.0	0.0	0.0	0.0	21.0	0.3	15.3	4.9	326	oold grst.	Bethany Falls

4130 arenaceous lime mdst.
4139 pyritiferous bivalve wkst.
4140 bivalve wkst.
4363 skel. wkst.
4536 fusulinid wkst.
4555 lime mdst; fusulinids echinoderms, bivalves.
4556 bryozoan wkst.;+echinoderms, gastropods, brachs.
4564 lime mdst.; echinoderms, 1-2 mm spheres of silica in clusters

Table 6.4 Summary of point count data from the Thompson 'E' No. 2 well, Victory Field

Cox no. 4 Amoco eff. por. = tot. porosity - MO Iso. percents from point count

depth ft	MO Iso.	MO con.	BP	frac.	vug	BP,WP cal.	MO cal.	MO dol.	rep. chert	cem. qtz.	bit.	auth. clay	grains	mud	tot. por.	eff. por.	tot. pts.	lithology	unit
4151.4	2.6	0.4	1.0	0.0	0.0	22.4	8.0	16.7	0.0	0.0	0.0	0.0	48.8	0.0	4.0	1.4	510	skel. grst.	Iantan
4152.5	4.5	3.4	10.4	0.0	0.0	15.8	2.6	0.2	0.0	0.0	0.0	0.0	62.4	0.0	18.3	15.0	508	skel-pel grst.	Iantan
4180.4	0.6	0.4	1.5	0.3	0.0	17.4	1.7	1.0	14.4	0.0	0.0	0.0	44.4	17.4	2.5	2.2	541	echin pkst.	Stanton
4209	8.8	0.6	7.4	0.0	0.0	26.2	17.4	0.2	0.0	0.0	4.8	0.2	7.4	0.4	16.8	8.0	500	oold grst.	Stanton
4597.6	16.8	0.8	3.8	0.2	0.0	43.6	18.6	0.4	0.6	0.2	1.0	0.0	14.0	0.0	21.6	4.8	500	oold grst.	Bethany Falls
4597.9	7.4	9.4	6.6	0.0	1.6	44.2	7.6	5.0	0.4	0.0	0.4	0.0	17.4	0.0	25.0	17.6	500	oold grst.	Bethany Falls
4601.3	5.4	13.2	9.2	0.2	0.0	43.6	4.0	6.2	0.2	0.0	2.8	0.0	15.0	0.0	28.0	22.6	500	oold grst.	Bethany Falls
4603.2	10.0	10.4	5.0	0.4	0.0	47.0	5.2	0.4	0.2	0.0	1.4	1.0	19.0	0.0	25.8	15.8	500	oold grst.	Bethany Falls
4605.5	5.4	0.8	0.4	0.0	0.0	47.8	5.4	22.6	0.6	0.0	1.2	0.2	15.6	0.0	6.6	1.2	500	oold grst.	Bethany Falls
4606.5	1.2	0.0	0.6	0.0	1.0	39.0	3.4	37.4	0.0	0.0	5.4	0.4	11.6	0.0	2.8	1.6	500	oold grst.	Bethany Falls
4607.5	10.4	17.2	8.6	0.2	0.4	50.2	1.0	0.4	0.0	0.0	0.4	0.6	10.6	0.0	36.8	26.4	500	oold grst.	Bethany Falls
4608.7	10.0	16.2	4.0	0.0	0.0	42.6	4.4	3.4	0.0	0.0	1.0	0.0	18.2	0.0	30.2	20.2	500	oold grst.	Bethany Falls
4611	10.6	8.6	3.2	0.0	0.0	48.2	6.0	1.2	0.0	0.2	0.8	0.0	21.2	0.0	22.6	12.0	500	oold grst.	Bethany Falls
4612.5	11.2	7.2	6.8	0.0	0.0	36.2	5.6	0.4	0.0	0.0	0.6	0.0	30.4	1.6	25.2	14.0	500	oold grst.	Bethany Falls
4614.2	11.2	13.4	4.4	0.0	0.0	38.4	4.8	2.4	0.0	0.2	0.2	0.0	25.0	0.0	29.0	17.8	500	oold grst.	Bethany Falls
4615	16.5	11.3	4.6	0.0	0.0	41.9	4.2	0.0	0.0	0.4	0.2	0.0	20.8	0.0	32.4	15.9	504	oold grst.	Bethany Falls
4616.7	4.4	2.0	4.2	0.2	0.0	41.8	4.4	0.0	0.0	1.6	0.0	0.0	33.1	7.8	11.4	6.6	507	skel pkst.	Bethany Falls

Table 6.3 Summary of point count data from the Cox No. A-4 well, Victory Field